VOLUME 28 / NUMBER 20
OCTOBER 23, 1990
ACC. NOS. N90-25933 TO N90-26789

STAR

AN ABSTRACT JOURNAL

Scientific and Technical Aerospace Reports

PRODUCED BY THE
SCIENTIFIC AND TECHNICAL
INFORMATION
DIVISION

NASA

NATIONAL AERONAUTICS AND SPACE ADMINISTRATION

WHAT YOU CAN DO FOR *STAR*

All users of this abstract service are urged to forward reports to be considered for announcement in *STAR*. This will aid NASA in its efforts to provide the fullest possible coverage of all scientific and technical publications that might support aeronautics and space research and development. If you have prepared relevant reports (other than those that you will transmit to NASA, DOD, or DOE through the usual contract- or grant-reporting channels), please send them for consideration to the NASA Scientific and Technical Information Facility, P.O. Box 8757, BWI Airport, MD 21240.

Reprints of journal articles, book chapters, and conference papers are also welcome. These will be considered for announcement in *STAR's* companion journal, *International Aerospace Abstracts*.

You may specify a particular source to be included in a report announcement if you wish; otherwise the report will be placed on public sale at the National Technical Information Service. Copyrighted publications will be announced but not distributed or sold.

PURCHASE OF *STAR*

The semimonthly issues are available to registered users on annual subscription from the NASA Scientific and Technical Information Facility, ATTN: Registration Services, P.O. Box 8757, BWI Airport, MD 21240. *STAR* is publicly available on annual subscription from the Superintendent of Documents, U.S. Government Printing Office, Washington, DC 20402.

PUBLISHED BY:

UNITED STATES GOVERNMENT
NATIONAL AERONAUTICS AND SPACE ADMINISTRATION
SCIENTIFIC AND TECHNICAL INFORMATION DIVISION
Scientific and Technical Aerospace Reports, Volume 28, is prepared by the NASA Scientific and Technical Information Facility operated for the National Aeronautics and Space Administration by RMS Associates.

The Administrator of the National Aeronautics and Space Administration has determined that the publication of this periodical is necessary in the transaction of the public business required by law of this agency. Use of funds for printing this periodical has been approved by the Director of the Office of Management and Budget through March 22, 1991.

US ISSN 0036-8741

Scientific and Technical Aerospace Reports (STAR) is issued twice a month and contains abstracts and indexes of meeting papers, conference proceedings, and unlimited distribution reports that have been added to the NASA Scientific and Technical Information Database during the preceding period. These citations may also be accessed online via NASA/RECON or via AIAA's Aerospace Database (File 108) through Dialog Information Services, Inc.

STAR subject coverage includes all aerospace-related areas that will help NASA achieve its mission. Material is gathered from all over the world and includes significant input from many countries under exchange and access agreements.

Consult the indexes at the back of this volume to help zero in on what you are looking for. These include:

Subject Index
Personal Author Index
Corporate Source Index
Contract Number Index
Report/Accession Number Index

STAR's companion abstract journal *International Aerospace Abstracts* should be used if you are looking for references to periodicals, books, and published meeting papers or conference proceedings.

Questions and comments should be addressed to:

NASA Scientific and Technical Information Facility
User Services
P.O. Box 8757
BWI Airport, MD 21240
301-621-0150

VOLUME 28 NUMBER 20 / OCTOBER 23, 1990

TABLE OF CONTENTS

AERONAUTICS

Includes aeronautics (general); aerodynamics; air transportation and safety; aircraft communications and navigation; aircraft design, testing and performance; aircraft instrumentation; aircraft propulsion and power; aircraft stability and control; and research and support facilities (air).

For related information see also *Astronautics.*

01 AERONAUTICS (GENERAL) 2801

02 AERODYNAMICS 2801

Includes aerodynamics of bodies, combinations, wings, rotors, and control surfaces; and internal flow in ducts and turbomachinery.

For related information see also *34 Fluid Mechanics and Heat Transfer.*

03 AIR TRANSPORTATION AND SAFETY 2804

Includes passenger and cargo air transport operations; and aircraft accidents.

For related information see also *16 Space Transportation* and *85 Urban Technology and Transportation.*

04 AIRCRAFT COMMUNICATIONS AND NAVIGATION 2806

Includes digital and voice communication with aircraft; air navigation systems (satellite and ground based); and air traffic control.

For related information see also *17 Space Communications, Spacecraft Communications, Command and Tracking* and *32 Communications and Radar.*

05 AIRCRAFT DESIGN, TESTING AND PERFORMANCE 2806

Includes aircraft simulation technology.

For related information see also *18 Spacecraft Design, Testing and Performance* and *39 Structural Mechanics.* For land transportation vehicles see *85 Urban Technology and Transportation.*

06 AIRCRAFT INSTRUMENTATION 2809

Includes cockpit and cabin display devices; and flight instruments.

For related information see also *19 Spacecraft Instrumentation* and *35 Instrumentation and Photography.*

07 AIRCRAFT PROPULSION AND POWER 2809

Includes prime propulsion systems and systems components, e.g., gas turbine engines and compressors; and onboard auxiliary power plants for aircraft.

For related information see also *20 Spacecraft Propulsion and Power, 28 Propellants and Fuels,* and *44 Energy Production and Conversion.*

08 AIRCRAFT STABILITY AND CONTROL 2813

Includes aircraft handling qualities; piloting; flight controls; and autopilots.

For related information see also *05 Aircraft Design, Testing and Performance.*

09 RESEARCH AND SUPPORT FACILITIES (AIR) 2814

Includes airports, hangars and runways; aircraft repair and overhaul facilities; wind tunnels; shock tubes; and aircraft engine test stands.

For related information see also *14 Ground Support Systems and Facilities (Space).*

ASTRONAUTICS

Includes astronautics (general); astrodynamics; ground support systems and facilities (space); launch vehicles and space vehicles; space transportation; space communications, spacecraft communications, command and tracking; spacecraft design, testing and performance; spacecraft instrumentation; and spacecraft propulsion and power.

For related information see also *Aeronautics.*

12 ASTRONAUTICS (GENERAL) 2815

For extraterrestrial exploration see *91 Lunar and Planetary Exploration.*

13 ASTRODYNAMICS 2816

Includes powered and free-flight trajectories; and orbital and launching dynamics.

14 GROUND SUPPORT SYSTEMS AND FACILITIES (SPACE) 2817

Includes launch complexes, research and production facilities; ground support equipment, e.g., mobile transporters; and simulators.

For related information see also *09 Research and Support Facilities (Air).*

15 LAUNCH VEHICLES AND SPACE VEHICLES 2817

Includes boosters; operating problems of launch/space vehicle systems; and reusable vehicles.

For related information see also *20 Spacecraft Propulsion and Power.*

16 SPACE TRANSPORTATION 2818

Includes passenger and cargo space transportation, e.g., shuttle operations; and space rescue techniques.

For related information see also *03 Air Transportation and Safety* and *18 Spacecraft Design, Testing and Performance.* For space suits see *54 Man/System Technology and Life Support.*

17 SPACE COMMUNICATIONS, SPACECRAFT COMMUNICATIONS, COMMAND AND TRACKING N.A.

Includes telemetry; space communications networks; astronavigation and guidance; and radio blackout.

For related information see also *04 Aircraft Communications and Navigation* and *32 Communications and Radar.*

18 SPACECRAFT DESIGN, TESTING AND PERFORMANCE **2820**

Includes satellites; space platforms; space stations; spacecraft systems and components such as thermal and environmental controls; and attitude controls.

For life support systems see *54 Man/System Technology and Life Support.* For related information see also *05 Aircraft Design, Testing and Performance, 39 Structural Mechanics,* and *16 Space Transportation.*

19 SPACECRAFT INSTRUMENTATION **2823**

For related information see also *06 Aircraft Instrumentation* and *35 Instrumentation and Photography.*

20 SPACECRAFT PROPULSION AND POWER **2823**

Includes main propulsion systems and components, e.g. rocket engines; and spacecraft auxiliary power sources.

For related information see also *07 Aircraft Propulsion and Power, 28 Propellants and Fuels, 44 Energy Production and Conversion,* and *15 Launch Vehicles and Space Vehicles.*

CHEMISTRY AND MATERIALS

Includes chemistry and materials (general); composite materials; inorganic and physical chemistry; metallic materials; nonmetallic materials; propellants and fuels; and materials processing.

23 CHEMISTRY AND MATERIALS (GENERAL) **2825**

24 COMPOSITE MATERIALS **2826**

Includes physical, chemical, and mechanical properties of laminates and other composite materials.

For ceramic materials see *27 Nonmetallic Materials.*

25 INORGANIC AND PHYSICAL CHEMISTRY **2829**

Includes chemical analysis, e.g., chromatography; combustion theory; electrochemistry; and photochemistry.

For related information see also *77 Thermodynamics and Statistical Physics.*

26 METALLIC MATERIALS **2832**

Includes physical, chemical, and mechanical properties of metals, e.g., corrosion; and metallurgy.

27 NONMETALLIC MATERIALS **2836**

Includes physical, chemical, and mechanical properties of plastics, elastomers, lubricants, polymers, textiles, adhesives, and ceramic materials.

For composite materials see *24 Composite Materials.*

28 PROPELLANTS AND FUELS **2841**

Includes rocket propellants, igniters and oxidizers; their storage and handling procedures; and aircraft fuels.

For related information see also *07 Aircraft Propulsion and Power, 20 Spacecraft Propulsion and Power,* and *44 Energy Production and Conversion.*

29 MATERIALS PROCESSING **2841**

Includes space-based development of products and processes for commercial application.

For biological materials see *55 Space Biology.*

ENGINEERING

Includes engineering (general); communications and radar; electronics and electrical engineering; fluid mechanics and heat transfer; instrumentation and photography; lasers and masers; mechanical engineering; quality assurance and reliability; and structural mechanics.

For related information see also *Physics.*

31 ENGINEERING (GENERAL) **2842**

Includes vacuum technology; control engineering; display engineering; cryogenics; and fire prevention.

32 COMMUNICATIONS AND RADAR **2844**

Includes radar; land and global communications; communications theory; and optical communications.

For related information see also *04 Aircraft Communications and Navigation* and *17 Space Communications, Spacecraft Communications, Command and Tracking.* For search and rescue see *03 Air Transportation and Safety,* and *16 Space Transportation.*

33 ELECTRONICS AND ELECTRICAL ENGINEERING **2857**

Includes test equipment and maintainability; components, e.g., tunnel diodes and transistors; microminiaturization; and integrated circuitry.

For related information see also *60 Computer Operations and Hardware* and *76 Solid-State Physics.*

34 FLUID MECHANICS AND HEAT TRANSFER **2860**

Includes boundary layers; hydrodynamics; fluidics; mass transfer and ablation cooling.

For related information see also *02 Aerodynamics* and *77 Thermodynamics and Statistical Physics.*

35 INSTRUMENTATION AND PHOTOGRAPHY **2865**

Includes remote sensors; measuring instruments and gauges; detectors; cameras and photographic supplies; and holography.

For aerial photography see *43 Earth Resources and Remote Sensing.* For related information see also *06 Aircraft Instrumentation* and *19 Spacecraft Instrumentation.*

36 LASERS AND MASERS **2866**

Includes parametric amplifiers.

For related information see also *76 Solid-State Physics.*

37 MECHANICAL ENGINEERING **2869**

Includes auxiliary systems (nonpower); machine elements and processes; and mechanical equipment.

38 QUALITY ASSURANCE AND RELIABILITY **2873**

Includes product sampling procedures and techniques; and quality control.

39 STRUCTURAL MECHANICS **2874**

Includes structural element design and weight analysis; fatigue; and thermal stress.

For applications see *05 Aircraft Design, Testing and Performance* and *18 Spacecraft Design, Testing and Performance.*

GEOSCIENCES

Includes geosciences (general); earth resources and remote sensing; energy production and conversion; environment pollution; geophysics; meteorology and climatology; and oceanography.

For related information see also *Space Sciences.*

42 GEOSCIENCES (GENERAL) **N.A.**

43 EARTH RESOURCES AND REMOTE SENSING **2878**

Includes remote sensing of earth resources by aircraft and spacecraft; photogrammetry; and aerial photography.

For instrumentation see *35 Instrumentation and Photography.*

44 ENERGY PRODUCTION AND CONVERSION **2880**

Includes specific energy conversion systems, e.g., fuel cells; global sources of energy; geophysical conversion; and windpower.

For related information see also *07 Aircraft Propulsion and Power, 20 Spacecraft Propulsion and Power,* and *28 Propellants and Fuels.*

45 ENVIRONMENT POLLUTION **2883**

Includes atmospheric, noise, thermal, and water pollution.

46 GEOPHYSICS **2887**

Includes aeronomy; upper and lower atmosphere studies; ionospheric and magnetospheric physics; and geomagnetism.

For space radiation see *93 Space Radiation.*

47 METEOROLOGY AND CLIMATOLOGY **2889**

Includes weather forecasting and modification.

48 OCEANOGRAPHY **2891**

Includes biological, dynamic, and physical oceanography; and marine resources.

For related information see also *43 Earth Resources and Remote Sensing.*

LIFE SCIENCES

Includes life sciences (general); aerospace medicine; behavioral sciences; man/system technology and life support; and space biology.

51 LIFE SCIENCES (GENERAL) **2891**

52 AEROSPACE MEDICINE **2898**

Includes physiological factors; biological effects of radiation; and effects of weightlessness on man and animals.

53 BEHAVIORAL SCIENCES **2899**

Includes psychological factors; individual and group behavior; crew training and evaluation; and psychiatric research.

54 MAN/SYSTEM TECHNOLOGY AND LIFE SUPPORT **2899**

Includes human engineering; biotechnology; and space suits and protective clothing.

For related information see also *16 Space Transportation.*

55 SPACE BIOLOGY **N.A.**

Includes exobiology; planetary biology; and extraterrestrial life.

MATHEMATICAL AND COMPUTER SCIENCES

Includes mathematical and computer sciences (general); computer operations and hardware; computer programming and software; computer systems; cybernetics; numerical analysis; statistics and probability; systems analysis; and theoretical mathematics.

59 MATHEMATICAL AND COMPUTER SCIENCES (GENERAL) **2902**

60 COMPUTER OPERATIONS AND HARDWARE **2903**

Includes hardware for computer graphics, firmware, and data processing.

For components see *33 Electronics and Electrical Engineering.*

61 COMPUTER PROGRAMMING AND SOFTWARE **2905**

Includes computer programs, routines, algorithms, and specific applications, e.g., CAD/CAM.

62 COMPUTER SYSTEMS **2911**

Includes computer networks and special application computer systems.

63 CYBERNETICS **2914**

Includes feedback and control theory, artificial intelligence, robotics and expert systems.

For related information see also *54 Man/System Technology and Life Support.*

64 NUMERICAL ANALYSIS **2916**

Includes iteration, difference equations, and numerical approximation.

65 STATISTICS AND PROBABILITY **2920**

Includes data sampling and smoothing; Monte Carlo method; and stochastic processes.

66 SYSTEMS ANALYSIS **2922**

Includes mathematical modeling; network analysis; and operations research.

67 THEORETICAL MATHEMATICS **N.A.**

Includes topology and number theory.

PHYSICS

Includes physics (general); acoustics; atomic and molecular physics; nuclear and high-energy physics; optics; plasma physics; solid-state physics; and thermodynamics and statistical physics.

For related information see also *Engineering.*

70 PHYSICS (GENERAL) **2922**

For precision time and time interval (PTTI) see *35 Instrumentation and Photography;* for geophysics, astrophysics or solar physics see *46 Geophysics, 90 Astrophysics,* or *92 Solar Physics.*

71 ACOUSTICS 2923
Includes sound generation, transmission, and attenuation.
For noise pollution see *45 Environment Pollution.*

72 ATOMIC AND MOLECULAR PHYSICS 2924
Includes atomic structure, electron properties, and molecular spectra.

73 NUCLEAR AND HIGH-ENERGY PHYSICS 2925
Includes elementary and nuclear particles; and reactor theory.
For space radiation see *93 Space Radiation.*

74 OPTICS 2926
Includes light phenomena and optical devices.
For lasers see *36 Lasers and Masers.*

75 PLASMA PHYSICS 2928
Includes magnetohydrodynamics and plasma fusion.
For ionospheric plasmas see *46 Geophysics.* For space plasmas see *90 Astrophysics.*

76 SOLID-STATE PHYSICS 2929
Includes superconductivity.
For related information see also *33 Electronics and Electrical Engineering* and *36 Lasers and Masers.*

77 THERMODYNAMICS AND STATISTICAL PHYSICS 2933
Includes quantum mechanics; theoretical physics; and Bose and Fermi statistics.
For related information see also *25 Inorganic and Physical Chemistry* and *34 Fluid Mechanics and Heat Transfer.*

SOCIAL SCIENCES

Includes social sciences (general); administration and management; documentation and information science; economics and cost analysis; law, political science, and space policy; and urban technology and transportation.

80 SOCIAL SCIENCES (GENERAL) 2934
Includes educational matters.

81 ADMINISTRATION AND MANAGEMENT 2934
Includes management planning and research.

82 DOCUMENTATION AND INFORMATION SCIENCE 2935
Includes information management; information storage and retrieval technology; technical writing; graphic arts; and micrography.
For computer documentation see *61 Computer Programming and Software.*

83 ECONOMICS AND COST ANALYSIS 2937
Includes cost effectiveness studies.

84 LAW, POLITICAL SCIENCE AND SPACE POLICY 2937
Includes NASA appropriation hearings; aviation law; space law and policy; international law; international cooperation; and patent policy.

85 URBAN TECHNOLOGY AND TRANSPORTATION 2939
Includes applications of space technology to urban problems; technology transfer; technology assessment; and surface and mass transportation.
For related information see *03 Air Transportation and Safety, 16 Space Transportation,* and *44 Energy Production and Conversion.*

SPACE SCIENCES

Includes space sciences (general); astronomy; astrophysics; lunar and planetary exploration; solar physics; and space radiation.
For related information see also *Geosciences.*

88 SPACE SCIENCES (GENERAL) N.A.

89 ASTRONOMY 2940
Includes radio, gamma-ray, and infrared astronomy; and astrometry.

90 ASTROPHYSICS 2941
Includes cosmology; celestial mechanics; space plasmas; and interstellar and interplanetary gases and dust.
For related information see also *75 Plasma Physics.*

91 LUNAR AND PLANETARY EXPLORATION 2942
Includes planetology; and manned and unmanned flights.
For spacecraft design or space stations see *18 Spacecraft Design, Testing and Performance.*

92 SOLAR PHYSICS 2950
Includes solar activity, solar flares, solar radiation and sunspots.
For related information see *93 Space Radiation.*

93 SPACE RADIATION 2950
Includes cosmic radiation; and inner and outer earth's radiation belts.
For biological effects of radiation see *52 Aerospace Medicine.* For theory see *73 Nuclear and High-Energy Physics.*

GENERAL

Includes aeronautical, astronautical, and space science related histories, biographies, and pertinent reports too broad for categorization; histories or broad overviews of NASA programs.

99 GENERAL 2951

Note: N.A. means that no abstracts were assigned to this category for this issue.

SUBJECT INDEX I-1
PERSONAL AUTHOR INDEX I-61
CORPORATE SOURCE INDEX I-69
CONTRACT NUMBER INDEX I-81
REPORT/ACCESSION NUMBER INDEX .. I-85
APPENDIX—ABOUT STAR A-1

TYPICAL CITATION AND ABSTRACT

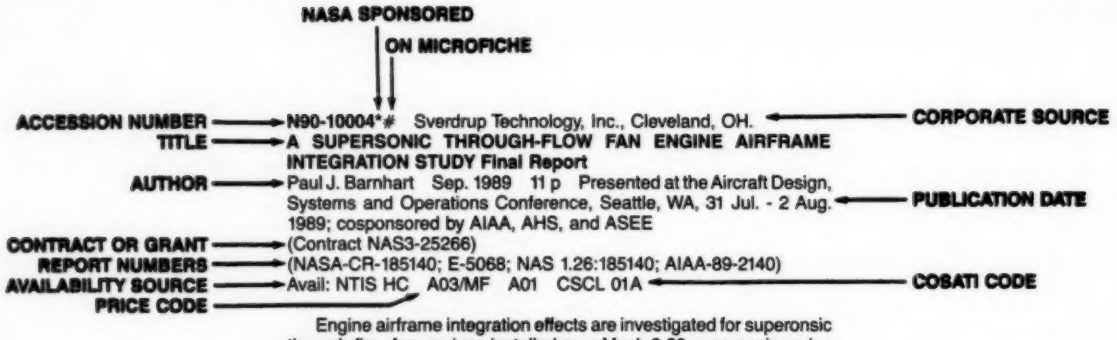
NASA SPONSORED
ON MICROFICHE
ACCESSION NUMBER
N90-10004*# Sverdrup Technology, Inc., Cleveland, OH.
CORPORATE SOURCE
TITLE
A SUPERSONIC THROUGH-FLOW FAN ENGINE AIRFRAME INTEGRATION STUDY Final Report
AUTHOR
Paul J. Barnhart Sep. 1989 11 p Presented at the Aircraft Design, Systems and Operations Conference, Seattle, WA, 31 Jul. - 2 Aug. 1989; cosponsored by AIAA, AHS, and ASEE
PUBLICATION DATE
CONTRACT OR GRANT
(Contract NAS3-25266)
REPORT NUMBERS
(NASA-CR-185140; E-5068; NAS 1.26:185140; AIAA-89-2140)
AVAILABILITY SOURCE
Avail: NTIS HC A03/MF A01 CSCL 01A
COSATI CODE
PRICE CODE

Engine airframe integration effects are investigated for superonsic through-flow fan engines installed on a Mach 3.20 supersonic cruise vehicle. Six different supersonic through-flow fan engine installations covering the effects of engine size, nacelle contour, nacelle placement, and approximate bypass plume effects are presented. The different supersonic through-flow fan installations are compared with a conventional turbine bypass engine configuration on the same basic airframe. The supersonic through-flow fan engine integrations are shown to be comparable to the turbine bypass engine configuration on the basis of installed nacelle wave drag. The supersonic through-flow fan engine airframe integrated vehicles have superior aerodynamic performance on the basis of maximum lift-to-drag ratio than the turbine bypass engine installation over the entire operating Mach number range from 1.10 to 3.20. When approximate bypass plume modeling is included, the supersonic through-flow fan engine configuration shows even larger improvements over the turbine bypass engine configuration. Author

VOLUME 28 NUMBER 20 / OCTOBER 23, 1990

Scientific and Technical Aerospace Reports

A Semimonthly Publication of the National Aeronautics and Space Administration

01 AERONAUTICS (GENERAL)

N90-25933*# National Aeronautics and Space Administration. Ames Research Center, Moffett Field, CA.
RESEARCH AT NASA'S NFAC WIND TUNNELS
H. Kipling Edenborough Jun. 1990 9 p Presented at the 27th International Session of the Japan Society for Aeronautical and Space Sciences (JSASS) Aircraft Symposium, Fukuoka, Japan, 18-19 Oct. 1989
(NASA-TM-102827; A-90170; NAS 1.15:102827) Avail: NTIS HC A02/MF A01 CSCL 01B

The National Full-Scale Aerodynamics Complex (NFAC) is a unique combination of wind tunnels that allow the testing of aerodynamic and dynamic models at full or large scale. It can even accommodate actual aircraft with their engines running. Maintaining full-scale Reynolds numbers and testing with surface irregularities, protuberances, and control surface gaps that either closely match the full-scale or indeed are those of the full-scale aircraft help produce test data that accurately predict what can be expected from future flight investigations. This complex has grown from the venerable 40- by 80-ft wind tunnel that has served for over 40 years helping researchers obtain data to better understand the aerodynamics of a wide range of aircraft from helicopters to the space shuttle. A recent modification to the tunnel expanded its maximum speed capabilities, added a new 80- by 120-ft test section and provided extensive acoustic treatment. The modification is certain to make the NFAC an even more useful facility for NASA's ongoing research activities. A brief background is presented on the original facility and the kind of testing that has been accomplished using it through the years. A summary of the modification project and the measured capabilities of the two test sections is followed by a review of recent testing activities and of research projected for the future. Author

02 AERODYNAMICS

Includes aerodynamics of bodies, combinations, wings, rotors, and control surfaces; and internal flow in ducts and turbomachinery.

For related information see also *34 Fluid Mechanics and Heat Transfer.*

N90-25934*# Case Inst. of Tech., Cleveland, OH. Dept. of Mechanical and Aerospace Engineering.
INTERACTIVE CALCULATION PROCEDURES FOR MIXED COMPRESSION INLETS Final Technical Report
Eli Reshotko Mar. 1983 7 p
(Grant NAG3-140)
(NASA-CR-186581; NAS 1.26:186581) Avail: NTIS HC A02/MF A01 CSCL 01A

The proper design of engine nacelle installations for supersonic aircraft depends on a sophisticated understanding of the interactions between the boundary layers and the bounding external flows. The successful operation of mixed external-internal compression inlets depends significantly on the ability to closely control the operation of the internal compression portion of the inlet. This portion of the inlet is one where compression is achieved by multiple reflection of oblique shock waves and weak compression waves in a converging internal flow passage. However weak these shocks and waves may seem gas-dynamically, they are of sufficient strength to separate a laminar boundary layer and generally even strong enough for separation or incipient separation of the turbulent boundary layers. An understanding was developed of the viscous-inviscid interactions and of the shock wave boundary layer interactions and reflections. Author

N90-25935 Toronto Univ. (Ontario). Inst. for Aerospace Studies.
PREDICTION OF TWO-DIMENSIONAL TIME-DEPENDENT GASDYNAMIC FLOWS FOR HYPERSONIC STUDIES
D. F. Hawken (Viatec Resource Systems, Inc., Toronto, Ontario) and J. J. Gottlieb Mar. 1990 45 p
(UTIAS-335; ISSN-0082-5255) Copyright Avail: Issuing Activity

Work on the development of an efficient and accurate computer code for the prediction of hypersonic flows within model hypersonic inlets is reported, and numerical results for some test problems are presented. The finite difference technique and total variation diminishing (TVD) scheme are summarized with Roe's approximate Riemann solver, which are incorporated into the code, in order to predict nonstationary planar and axisymmetric flows with steep shocks and thin slip streams on 2-D grids having multiple connected domains. Author

N90-25936# National Aeronautical Lab., Bangalore (India). Computational and Theoretical Fluid Dynamics Div.
FLIGHT TESTING OF A NATURAL LAMINAR FLOW AIRFOIL USING GLIDERS
P. Ramamoorthy Mar. 1990 11 p
(NAL Proj. FM-8-208)
(PD-CF-9005) Avail: NTIS HC A03/MF A01

A proposed flight test program to conduct pressure measurements and flow visualization on Natural Laminar Flow (NLF) airfoils using gliders is described. Author

N90-25937# Wichita State Univ., KS. National Inst. for Aviation Research.
PREDICTION METHODOLOGIES FOR NONLINEAR AERODYNAMIC CHARACTERISTICS OF CONTROL SURFACES M.S. Thesis
Brian P. Lee Jun. 1990 201 p
(NIAR-90-17) Avail: NTIS HC A10/MF A02

As airplane performance demands increase it will be necessary to understand and make use of aerodynamic characteristics well into the nonlinear operating range. There is a large body of parametric test data available which addresses a variety of significant features and their aerodynamic consequences. Historically, a number of efforts have been mounted to assimilate this data and reduce it to a form useful for design. Three of these are examined in light of their principal independent variable sets and their ability to model a variety of specific configurations. It is postulated that inadequacies in previous attempts to generalize this data resulted from both the linear model formulation and the lack of sufficient computing power to permit more sophisticated techniques. Recent advances in computing power and data reduction methods now provide the ability to address very large nonlinear multi-dimensional problems in a timely manner. The ability of one of these methods to digest a large subset of the test data

and extract salient features in model form is demonstrated. The resulting model demonstrates sensitivity to fundamentally significant independent variables, and produces significant improvements in fidelity at off-zero incidence and control deflections, yet retains a form which is readily linearized about a given condition for use in small perturbation stability analysis. The nonlinear model form is also shown to provide significantly more insight into off design characteristics than previous linear formulations. Author

N90-25938*# National Aeronautics and Space Administration. Langley Research Center, Hampton, VA.
EFFECT OF TAIL SIZE REDUCTIONS ON LONGITUDINAL AERODYNAMIC CHARACTERISTICS OF A THREE SURFACE F-15 MODEL WITH NONAXISYMMETRIC NOZZLES
Mark C. Frassinelli (Air Force Wright Aeronautical Labs., Wright-Patterson AFB, OH.) and George T. Carson, Jr. Washington Aug. 1990 59 p
(NASA-TP-3036; L-16800; NAS 1.60:3036) Avail: NTIS HC A04/MF A01 CSCL 01A

An investigation was conducted in the Langley 16-Foot Transonic Tunnel to determine the effects of horizontal and vertical tail size reductions on the longitudinal aerodynamic characteristics of a modified F-15 model with canards and 2-D convergent-divergent nozzles. Quantifying the drag decrease at low angles of attack produced by tail size reductions was the primary focus. The model was tested at Mach numbers of 0.40, 0.90, and 1.20 over an angle of attack of -2 degree to 10 degree. The nozzle exhaust flow was simulated using high pressure air at nozzle pressure ratios varying from 1.0 (jet off) to 7.5. Data were obtained on the baseline configuration with and without tails as well as with reduced horizontal and/or vertical tail sizes that were 75, 50, and 25 percent of the baseline tail areas. Author

N90-25939*# Vigyan Research Associates, Inc., Hampton, VA.
EFFECTS OF FOREBODY GEOMETRY ON SUBSONIC BOUNDARY-LAYER STABILITY
Simha S. Dodbele Washington NASA Aug. 1990 20 p Presented at the 5th International Conference on Numerical Methods in Laminar and Turbulent Flow, Montreal, Quebec, 6-10 Jul. 1987 Previously announced in IAA as A88-30509
(Contract NAS1-17919)
(NASA-CR-4314; NAS 1.26:4314) Avail: NTIS HC A03/MF A01 CSCL 01A

As part of an effort to develop computational techniques for design of natural laminar flow fuselages, a computational study was made of the effect of forebody geometry on laminar boundary layer stability on axisymmetric body shapes. The effects of nose radius on the stability of the incompressible laminar boundary layer was computationally investigated using linear stability theory for body length Reynolds numbers representative of small and medium-sized airplanes. The steepness of the pressure gradient and the value of the minimum pressure (both functions of fineness ratio) govern the stability of laminar flow possible on an axisymmetric body at a given Reynolds number. It was found that to keep the laminar boundary layer stable for extended lengths, it is important to have a small nose radius. However, nose shapes with extremely small nose radii produce large pressure peaks at off-design angles of attack and can produce vortices which would adversely affect transition. Author

N90-25940*# Purdue Univ., West Lafayette, IN.
AN UNSTEADY LIFTING SURFACE METHOD FOR SINGLE ROTATION PROPELLERS Final Report
Marc H. Williams Washington NASA Jul. 1990 62 p
(Grant NAG3-499)
(NASA-CR-4302; E-5428; NAS 1.26:4302) Avail: NTIS HC A04/MF A01 CSCL 01A

The mathematical formulation of a lifting surface method for evaluating the steady and unsteady loads induced on single rotation propellers by blade vibration and inflow distortion is described. The scheme is based on 3-D linearized compressible aerodynamics and presumes that all disturbances are simple harmonic in time. This approximation leads to a direct linear integral relation between the normal velocity on the blade (which is determined from the blade geometry and motion) and the distribution of pressure difference across the blade. This linear relation is discretized by breaking the blade up into subareas (panels) on which the pressure difference is treated as approximately constant, and constraining the normal velocity at one (control) point on each panel. The piece-wise constant loads can then be determined by Gaussian elimination. The resulting blade loads can be used in performance, stability and forced response predictions for the rotor. Mathematical and numerical aspects of the method are examined. A selection of results obtained from the method is presented. The appendices include various details of the derivation that were felt to be secondary to the main development in Section 1. Author

N90-25941# Sandia National Labs., Albuquerque, NM.
WIND TUNNEL STUDY OF WAKE DOWNWASH BEHIND A 6 PERCENT SCALE MODEL B1-B AIRCRAFT
James H. Strickland, Eden L. Tadios, and David A. Powers May 1990 86 p
(Contract DE-AC04-76DP-00789)
(DE90-011783; SAND-90-0008) Avail: NTIS HC A05/MF A01

Parachute system performance issues such a turnover and wake recontact may be strongly influenced by velocities induced by the wake of the delivering aircraft, especially if the aircraft is maneuvering at the time of parachute deployment. The effect of the aircraft on the parachute system is a function of the aircraft size, weight, and flight path. In order to provide experimental data for validation of a computer code to predict aircraft wake velocities, a test was conducted in the NASA 14 by 22 ft wind tunnel using a 5.78 percent model of the B-1B strategic bomber. The model was strut mounted through the top of its fuselage by a mechanism which was capable of pitching the model at moderate rates. In this series of tests, the aircraft was pitched at 10 deg/sec from a cruise angle of attack of 5.3 deg to an angle of attack of 11 deg in order to simulate a 2.2g pullup. Data were also taken for the subsequent pitch down sequence back to the cruise angle of attack. Instantaneous streamwise and vertical velocities were measured in the wake at a number of points using a hot wire anemometer. These data were reduced to the form of downwash coefficients which are a function of the aircraft angle of attack time history. Unsteady effects are accounted for by use of a wake convection lag-time correlation. DOE

N90-25942# Institut Franco-Allemand de Recherches, Saint-Louis (France).
AERODYNAMIC LOADS AND BLADE VORTEX INTERACTION NOISE PREDICTION
M. Schaffar, J. Haerting, and P. Gnemmi 1989 16 p Presented at 15th European Rotorcraft Forum, Amsterdam, Netherlands, 12-15 Sep. 1989
(ISL-PU-310/89; ETN-90-97024) Avail: NTIS HC A03/MF A01

The vortex lattice method is described and applied in order to predict the aerodynamic loads on a thin two-bladed rotor. A local conformal mapping for each position in span is used to transform the thin rotor into a thick one. The pressure coefficients obtained for the thick rotor are fed into an acoustic code which is based on the Ffowcs-Williams-Hawkings equation. The results obtained with this method show the importance of the rotor and flight parameters; they are compared with results found in the literature for a two-bladed rotor in hovering and advancing. The comparison shows a good agreement and shows that the cut-off length for limiting the instabilities from the Biot and Savart law must be chosen carefully. ESA

N90-25943*# Kansas Univ. Center for Research, Inc., Lawrence. Flight Research Lab.
IDENTIFICATION OF AERODYNAMIC MODELS FOR MANEUVERING AIRCRAFT Semiannual Status Report
Suei Chin and C. Edward Lan Aug. 1990 51 p
(Grant NAG1-1087)
(NASA-CR-186630; NAS 1.26:186630; KU-FRL-872-1) Avail: NTIS HC A04/MF A01 CSCL 01A

Due to the requirement of increased performance and

maneuverability, the flight envelope of a modern fighter is frequently extended to the high angle-of-attack regime. Vehicles maneuvering in this regime are subjected to nonlinear aerodynamic loads. The nonlinearities are due mainly to three-dimensional separated flow and concentrated vortex flow that occur at large angles of attack. Accurate prediction of these nonlinear airloads is of great importance in the analysis of a vehicle's flight motion and in the design of its flight control system. A satisfactory evaluation of the performance envelope of the aircraft may require a large number of coupled computations, one for each change in initial conditions. To avoid the disadvantage of solving the coupled flow-field equations and aircraft's motion equations, an alternate approach is to use a mathematical modeling to describe the steady and unsteady aerodynamics for the aircraft equations of motion. Aerodynamic forces and moments acting on a rapidly maneuvering aircraft are, in general, nonlinear functions of motion variables, their time rate of change, and the history of maneuvering. A numerical method was developed to analyze the nonlinear and time-dependent aerodynamic response to establish the generalized indicial function in terms of motion variables and their time rates of change. Author

N90-25944*# Boeing Commercial Airplane Co., Seattle, WA.
APPLICATION OF LAMINAR FLOW CONTROL TO SUPERSONIC TRANSPORT CONFIGURATIONS Final Report, Oct. 1987 - Dec. 1988
P. G. Parikh and A. L. Nagel Jul. 1990 191 p
(Contract NAS1-15325)
(NASA-CR-181917; NAS 1.26:181917) Avail: NTIS HC A09/MF A01 CSCL 01A

The feasibility and impact of implementing a laminar flow control system on a supersonic transport configuration were investigated. A hybrid laminar flow control scheme consisting of suction controlled and natural laminar flow was developed for a double-delta type wing planform. The required suction flow rates were determined from boundary layer stability analyses using representative wing pressure distributions. A preliminary design of structural modifications needed to accommodate suction through a perforated titanium skin was carried out together with the ducting and systems needed to collect, compress and discharge the suction air. The benefits of reduced aerodynamic drag were weighed against the weight, volume and power requirement penalties of suction system installation in a mission performance and sizing program to assess the net benefits. The study showed a feasibility of achieving significant laminarization of the wing surface by use of a hybrid scheme, leading to an 8.2 percent reduction in the cruise drag. This resulted in an 8.5 percent reduction in the maximum takeoff weight and a 12 percent reduction in the fuel burn after the inclusion of the LFC system installation penalties. Several research needs were identified for a resolution of aerodynamics, structural and systems issues before these potential benefits could be realized in a practical system. Author

N90-25945*# National Aeronautics and Space Administration. Ames Research Center, Moffett Field, CA.
A BRIEF REVIEW OF SOME MECHANISMS CAUSING BOUNDARY LAYER TRANSITION AT HIGH SPEEDS
M. E. Tauber Jun. 1990 12 p
(NASA-TM-102834; A-90186; NAS 1.15:102834) Avail: NTIS HC A03/MF A01 CSCL 01A

In high speed flight, the state of the boundary layer can strongly influence the design of vehicles through its effect on skin friction drag and aerodynamic heating. The major mechanisms causing boundary layer transition on high speed vehicles are briefly reviewed and some empirical relations from the unclassified literature are given for the transition Reynolds numbers. Author

N90-25946*# National Aeronautics and Space Administration. Lewis Research Center, Cleveland, OH.
EULER ANALYSIS COMPARISON WITH LDV DATA FOR AN ADVANCED COUNTER-ROTATION PROPFAN AT CRUISE
Christopher J. Miller and Gary G. Podboy Aug. 1990 23 p Presented at the 8th Applied Aerodynamics Conference, Portland, OR, 20-22 Aug. 1990; sponsored in part by AIAA
(NASA-TM-103249; E-5676; NAS 1.15:103249; AIAA-90-0438)
Avail: NTIS HC A03/MF A01 CSCL 01A

A fine mesh Euler solution of the F4/A4 unducted fan (UDF) model flowfield is compared with laser Doppler velocimeter (LDV) data taken in the NASA Lewis 8- by 6-Foot Supersonic Wind Tunnel. The comparison is made primarily at one axial plane downstream of the front rotor where the LDV particle lag errors are reduced. The agreement between measured and predicted velocities in this axial plane is good. The results show that a dense mesh is needed in the centerbody stagnation region to minimize entropy generation that weakens the aft row passage shock. The predicted radial location of the tip vortex downstream of the front rotor agrees well with the experimental results but the strength is overpredicted. With 40 points per chord line, the integrated performance quantities are nearly converged, but more points are needed to resolve passage shocks and flow field details. Author

N90-25947# Advisory Group for Aerospace Research and Development, Neuilly-Sur-Seine (France). Fluid Dynamics Panel.
TECHNICAL EVALUATION REPORT ON THE FLUID DYNAMICS PANEL SYMPOSIUM ON COMPUTATIONAL METHODS FOR AERODYNAMIC DESIGN (INVERSE) AND OPTIMIZATION
Preston A. Henne and J. W. Slooff, ed. (National Aerospace Lab., Amsterdam, Netherlands) Apr. 1990 16 p Symposium held in Loen, Norway, 22-23 May 1989
(AGARD-AR-267; ISBN-92-835-0557-3) Copyright Avail: NTIS HC A03/MF A01; Non-NATO Nationals requests available only from AGARD/Scientific Publications Executive

The papers presented at the symposium are reviewed as a whole. Strengths and weaknesses are identified for many of the contributions as each is reviewed. The reviewer closes with some general comments. The 23 papers presented at the Meeting have been collected in AGARD-CP-463. Author

N90-25948*# National Aeronautics and Space Administration. Lewis Research Center, Cleveland, OH.
TWO-DIMENSIONAL EULER AND NAVIER-STOKES TIME ACCURATE SIMULATIONS OF FAN ROTOR FLOWS
A. A. Boretti (Fiat Research Center, Orbassano, Turin, Italy) Jul. 1990 22 p
(NASA Order C-99066-G)
(NASA-TM-102402; E-5155; NAS 1.15:102402; ICOMP-89-29)
Avail: NTIS HC A03/MF A01 CSCL 01A

Two numerical methods are presented which describe the unsteady flow field in the blade-to-blade plane of an axial fan rotor. These methods solve the compressible, time-dependent, Euler and the compressible, turbulent, time-dependent, Navier-Stokes conservation equations for mass, momentum, and energy. The Navier-Stokes equations are written in Favre-averaged form and are closed with an approximate two-equation turbulence model with low Reynolds number and compressibility effects included. The unsteady aerodynamic component is obtained by superposing inflow or outflow unsteadiness to the steady conditions through time-dependent boundary conditions. The integration in space is performed by using a finite volume scheme, and the integration in time is performed by using k-stage Runge-Kutta schemes, k = 2,5. The numerical integration algorithm allows the reduction of the computational cost of an unsteady simulation involving high frequency disturbances in both CPU time and memory requirements. Less than 200 sec of CPU time are required to advance the Euler equations in a computational grid made up of about 2000 grid during 10,000 time steps on a CRAY Y-MP computer, with a required memory of less than 0.3 megawords. Author

N90-25949# National Aerospace Lab., Tokyo (Japan).
SPACE PLANE MODEL FOR VISUAL MEASUREMENT OF AERODYNAMIC HEATING
Mitunori Watanabe Aug. 1989 21 p In JAPANESE

(DE90-505514; NAL-TM-608; ISSN-0452-2982) Avail: NTIS (US Sales Only) HC A03/MF A01

Space plane models (300 mm in length) were fabricated with electroformed molds. High heat resistant epoxy resin (STYCAST) was used for a model material, and the glossy models superior in heat resistance, heat insulation and rigidity were obtained, as well as a prospect for low cost production of several models with the same accuracy. While errors of the model were + or - 1 percent in thickness of a fuselage and -0.3 mm in mean thickness of a main wing, errors due to the mold were -1 percent and -0.1 mm, respectively. The mold error was mainly dependent on the machining accuracy of a positive mold, and thermal deformation in a burning process for molding. A three-dimensional instrument and numerical control machine tool had the potential of enhancing the machining accuracy considerably. On the other hand, a split mold with a back stiffening plate and the use of smaller amounts of mold releasing agent had the potential of reducing thermal deformation. DOE

N90-25950# National Aerospace Lab., Amsterdam (Netherlands). Fluid Dynamics Div.

EXPERIMENTAL STUDY ON VORTEX AND SHOCK WAVE DEVELOPMENT ON A 65 DEG DELTA WING

A. Elsenaar and K. A. Buetefisch 20 May 1988 14 p Presented at IUTAM Symposium Transsonicum 3, Goettingen, Fed. Republic of Germany, 24-27 May 1988

(NLR-MP-88033-U; ETN-90-97186) Avail: NTIS HC A03/MF A01

The analysis of the transonic flow over a 65 degrees delta wing at Mach equal to 0.85 is presented. Pressure data, flow visualizations and laser Doppler anemometry flow field measurements are used. It is argued that shock waves and shock induced separations can induce primary and secondary vortices. Near the symmetry plane another shock is observed that seems to interact in a very abrupt way with vortex break down. ESA

N90-25951# National Aerospace Lab., Amsterdam (Netherlands). Fluid Dynamics Div.

COMPUTATION OF VISCOUS AERODYNAMIC CHARACTERISTICS OF 2-D AIRFOILS FOR HELICOPTER APPLICATIONS

R. Houwink, J. A. vanEgmond, and P. A. vanGelder 9 Jan. 1988 19 p Presented at 14th European Rotorcraft Forum, Milan, Italy, 20-23 Sep. 1988

(NLR-MP-88052-U; ETN-90-97189) Avail: NTIS HC A03/MF A01

A computer code, used for the prediction of quasi-steady and unsteady aerodynamic characteristics of rotor blade section in oscillatory and linear pitching motions is presented. The code, named ULTRAN-5, is based on unsteady transonic small perturbation theory, coupled in strong interaction with an unsteady version of Green's lag-entrainment method for a turbulent boundary layer. Results are compared with experimental data for the NACA0012 airfoil and for actual rotor blade sections. Provided that the stall behavior is not dominated by leading edge separation, an accurate prediction of quasi-steady and unsteady airfoil characteristics up to stall conditions is obtained. ESA

N90-25952# National Aerospace Lab., Amsterdam (Netherlands). Fluids Dynamics Div.

THE ROLE OF COMPUTATIONAL FLUIDS DYNAMICS IN MISSILE AERODYNAMICS

H. W. M. Hoeijmakers 31 Dec. 1988 66 p Presented at Missile Aerodynamics Conference, Monterey, CA, 31 Oct. - 2 Nov. 1988

(NLR-MP-88072-U; ETN-90-97194) Avail: NTIS HC A04/MF A01

The application of computational fluid dynamics method in the analysis of aerodynamic characteristics of missile configurations is reviewed. The flow about geometrically complex configurations is analyzed for a range of the flight parameters. The flow can be dominated by vortical flow structures which at higher speed interact with shock waves. The capability of computational procedures to simulate missile aerodynamics is described. The advantages and disadvantages of using flow models of various levels of approximation are underlined. ESA

N90-25953# Royal Aerospace Establishment, Farnborough (England).

FORMATION OF DESIGN ENVELOPE CRITERION IN TERMS OF DETERMINISTIC SPECTRAL PROCEDURE

J. G. Jones 17 Jan. 1990 15 p

(RAE-TM-SS-9; BR113195; ETN-90-97066) Copyright Avail: NTIS HC A03/MF A01

An existing design envelope approach to meeting aircraft limit load requirements for flight in continuous turbulence, using power spectral methods, is reformulated in a manner which makes no distinction between linear and non-linear aircraft response. Computational techniques for implementing the new procedure in applications to nonlinear aircraft are discussed and compared with existing simulation methods. ESA

N90-25954*# Eloret Corp., Palo Alto, CA.

EXPERIMENTAL AEROTHERMODYNAMIC RESEARCH OF HYPERSONIC AIRCRAFT Final Technical Report, 1 Mar. 1986 - 31 Jul. 1990

Joseph W. Cleary 23 Aug. 1990 17 p

(Contract NCC2-416)

(NASA-CR-186903; NAS 1.26:186903) Avail: NTIS HC A03/MF A01 CSCL 01A

Wind tunnel tests were conducted to establish a benchmark experimental data base for a genetic hypersonic aircraft vehicle. Comprehensive measurements were made at Mach 7 to give flow visualization, surface pressure, surface convective heat transfer, and flow field Pitot pressure for a delta platform all-body vehicle. The tests were conducted in the NASA/Ames 3.5-Foot Hypersonic Wind Tunnel at Reynolds numbers sufficient to give turbulent flow. Comparisons are made of the experimental results with computational solutions of the flow by an upwind parabolized Navier-Stokes code developed at Ames. Good agreement of experiment with solutions by the code is demonstrated. Author

N90-25955# Air Force Systems Command, Wright-Patterson AFB, OH. Foreign Technology Div.

EFFECT OF VORTEX GENERATORS ON THE AERODYNAMIC WING CHARACTERISTICS AND BODY OF REVOLUTION

A. M. Mkhitaryan, S. A. Lukashuk, V. D. Trubenok, and V. Ya. Fridland 3 May 1990 24 p Transl. into ENGLISH from Gidroaerodinamika Nesushchikh Poverkhnostey (Kiev, USSR, Naukova Dumka), 1966 p 254-263

(AD-A222813; FTD-ID(RS)T-0266-90) Avail: NTIS HC A03/MF A01 CSCL 01/1

The results are presented of experimental investigations of the effect of vortex generators on the aerodynamic characteristics of streamlined bodies. Qualitative results are obtained corrobating the possibility of stabilizing the intact flow over a wing at large angles of attack. The results of an experiment on the flow over bodies of revolution with vortex generators are presented. GRA

03 AIR TRANSPORTATION AND SAFETY

Includes passenger and cargo air transport operations; and aircraft accidents.

For related information see also *16 Space Transportation* and *85 Urban Technology and Transportation.*

N90-25956# Wichita State Univ., KS. Inst. for Aviation Research.

COMPUTATIONAL CRASH DYNAMICS. PROJECT 1.2: COMPUTATIONAL CRASH DYNAMICS ANALYSIS Final Report

Walter J. Horn and Dan L. Christmore Oct. 1989 75 p

(Contract DTFA03-96-C-00041)

(IAR-89-19) Avail: NTIS HC A04/MF A01

The purpose of this research effort was to develop an analytical

capability to predict the crashworthiness characteristics of composite aircraft. A literature survey of crashworthiness research work indicated that the computer code, KRASH, was probably the best suited for information. The code is a hybrid and thus requires a great deal of input data that is typically generated by structural tests. In an effort to make this code useful at the preliminary design stage, modifications were investigated which could be incorporated into KRASH so that the crashworthiness of the vehicle could be evaluated without the requirement for structural testing. A finite element method was investigated for inclusion in the code to generate the nonlinear stiffness matrix for the beam elements in KRASH. Recommendations are presented for the modification of the computer code to accommodate the nonlinear analysis of the vehicle. A preliminary assessment of the effect of composite materials on the crashworthiness of aircraft structures was conducted using the KRASH code. The influence of composite material mechanical properties such as anisotropy, ultimate strength, torsional stiffness and nonlinearity on the dynamic response was investigated. Very minor influence on the vehicle responses were observed for the range of parameters investigated. Author

N90-25957*# National Aeronautics and Space Administration. Langley Research Center, Hampton, VA.
AN OVERVIEW OF THE JOINT FAA/NASA AIRCRAFT/GROUND RUNWAY FRICTION PROGRAM
Thomas J. Yager Feb. 1989 16 p Submitted for publication
(NASA-TM-103486; NAS 1.15:103486) Avail: NTIS HC A01/MF A01 CSCL 01C

There is a need for information on runways which may become slippery due to various forms and types of contaminants. Experience has shown that since the beginning of all weather aircraft operations, there have been landing and aborted takeoff incidents and/or accidents each year where aircraft have either run off the end or veered off the shoulder of low friction runways. NASA Langley's Landing and Impact Dynamics Branch is involved in several research programs directed towards obtaining a better understanding of how different tire properties interact with varying pavement surface characteristics to produce acceptable performance for aircraft ground handling requirements. One such effort, which was jointly supported by not only NASA and the FAA but by several aviation industry groups including the Flight Safety Foundation, is described. Author

N90-25958# General Accounting Office, Washington, DC. Resources, Community, and Economic Development Div.
AVIATION SAFETY: CONDITIONS WITHIN THE AIR TRAFFIC CONTROL WORK FORCE. FACT SHEET FOR CONGRESSIONAL REQUESTERS
Apr. 1989 131 p
(GAO/RCED-89-113FS; B-222217) Avail: NTIS HC A07/MF A01; also available from GAO, Gaithersburg, MD HC first five copies are free, additional copies $2.00

The complete 1988 questionnaire responses of air traffic controllers, supervisors, and facility managers (the air traffic work force) are compared with those of the air traffic control work force survey done in 1985. The 1985 questions were replicated, and new ones were added. The survey and scope of and methodology are described and the responses to each question are summarized for the air route traffic control centers, which control flights between airports and over oceanic routes; the largest terminals; and the overall combined responses of centers and terminals. The questions and responses address a variety of air traffic issues facing the Federal Aviation Administration (FAA), including, among others, work load, staffing, overtime, training, morale, and system safety. The perceptions of the air traffic work force on these subjects have changed little since the 1985 survey. J.P.S.

N90-25959# General Accounting Office, Washington, DC. Resources, Community, and Economic Development Div.
AVIATION SAFETY: SERIOUS PROBLEMS CONTINUE TO TROUBLE THE AIR TRAFFIC CONTROL WORK FORCE. REPORT TO CONGRESSIONAL REQUESTERS
Apr. 1989 59 p
(GAO/RCED-89-112; B-222217) Avail: NTIS HC A04/MF A01; also available from GAO, Gaithersburg, MD HC first five copies free, additional copies $2.00

Federal Aviation Administration (FAA) air traffic controllers, supervisors, and managers were surveyed to determine how they feel about their working conditions. This updates a similar study done in 1985. Eighty-four facilities were surveyed on various issues including staffing adequacy, training of new controllers, morale, and safety of the air traffic control system. Five thousand ninty-eight out of six thousand four hundred sixty-nine questionnaires were returned. The Flight Safety Foundation, an independent international membership organization dedicated solely to the improvement of flight saftey, evaluated the questionnaire results and provided its views on safety. The Foundation concluded that the air traffic control system is not unsafe, remains essentially unchanged from 1985, and is less than desirable. FAA has planned or undertaken several nationwide initiatives to address work force concerns. These include plans for improving its recruitment and hiring techniques, revolutionizing the way it trains air traffic controllers, and using a pay demonstration project to attract personnel to hard-to-staff facilities. J.P.S.

N90-25960# Naval Postgraduate School, Monterey, CA.
AN ANALYSIS OF REQUIREMENTS FOR A P-3 WINDSHEAR TRAINING PROGRAM M.S. Thesis
Kevin Eugene White Dec. 1989 85 p
(AD-A222577) Avail: NTIS HC A05/MF A01 CSCL 01/2

A deficiency in the Navy's P-3 flight crew training curriculum was examined in the area of windshear and microburst survival and to analyze the requirements necessary for an effective training program. An analysis was conducted to identify training objectives, equate them to learning outcomes, and recommend media to support the training. The resulting media combination is presently available at each Fleet Replacement Squadron. Additional recommendations were made concerning training materials, costs and benefits, and windshear technology. Many of the procedures written in the P-3 NATOPS manual are the result of a major incident or the loss of lives. Information necessary to implement a training program and procedures that could possibly save an aircraft and its crew is provided. GRA

N90-25961# Flight Safety Foundation, Inc., Arlington, VA.
SECOND ANNUAL INTERNATIONAL CONFERENCE ON AGING AIRCRAFT
1989 262 p Conference held in Baltimore, MD, 3-5 Oct. 1989 Sponsored by FAA, Atlantic City, NJ
(AD-A222715; DOT/FAA/CT-89/35) Avail: NTIS HC A12/MF A02 CSCL 05/1

This document contains the formal presentations made at the 2nd Annual International Conference on Aging Aircraft. It includes status reports in the areas of transport and commuter aircraft certification, maintenance, research and development, the ATA/AIA airworthiness assurance task force and efforts by NASA. Also included are detailed presentations on the research and development efforts underway and planned in the areas of structural fatigue, loads, corrosion, nondestructive testing/inspection and human factors. GRA

04 AIRCRAFT COMMUNICATIONS AND NAVIGATION

Includes digital and voice communication with aircraft; air navigation systems (satellite and ground based); and air traffic control.

For related information see also *17 Space Communications, Spacecraft Communications, Command and Tracking* and *Communications and Radar.*

N90-25962# Air Force Geophysics Lab., Hanscom AFB, MA. Earth Sciences Div.
PROCEEDINGS OF THE SECOND SYMPOSIUM ON GPS APPLICATIONS IN SPACE, VOLUME 1 Environmental Research Papers
Christopher Jekeli, ed. 13 Feb. 1990 252 p Symposium held in Bedford, MA, 10-11 Oct. 1989
(AF Proj. 2309)
(AD-A219978; GL-TR-90-0032(1)-Vol-1; GL-ERP-1052-Vol-1)
Avail: NTIS HC A12/MF A02 CSCL 21/1

This collection of abstracts, papers, and presentation material constitutes the Proceedings of the Second Symposium on Global Positioning System (GPS) Applications in Space. Volume 1 covers the first two sessions: Space Missions with GPS, and Orbit Determination with GPS. Both the application of GPS to a variety of NASA and DOD space missions, as well as corresponding GPS receiver development were discussed at this symposium. Specific applications included orbit determination of the GPS satellites and low Earth orbiters, space navigation, and, in particular, attitude determination of space vehicles. GRA

N90-25963# Air Force Geophysics Lab., Hanscom AFB, MA.
PROCEEDINGS OF THE SECOND SYMPOSIUM ON GPS APPLICATIONS IN SPACE, VOLUME 2 Environmental Research Papers
Christopher Jekeli, ed. 13 Feb. 1990 316 p Symposium held in Bedford, MA, 10-11 Oct. 1989
(AF Proj. 2309)
(AD-A219979; GL-TR-90-0032(2)-Vol-2; GL-ERP-1052-Vol-2)
Avail: NTIS HC A14/MF A02 CSCL 17/7

This collection of abstracts, papers, and presentation material constitutes the Proceedings of the Second Symposium on GPS Applications in Space. Volume 2 covers the last two sessions: Attitude Determination with GPS, and Other Applications and Topics. Specific applications included orbit determination of the GPS satellites and low Earth orbiters, space navigation, and, in particular, attitude determination of space vehicles. GRA

N90-25964*# Ohio State Univ., Columbus. Cognitive Systems Engineering Lab.
ENROUTE FLIGHT PLANNING: THE DESIGN OF COOPERATIVE PLANNING SYSTEMS Final Report
Philip J. Smith, Chuck Layton, and Elaine McCoy (San Jose State Univ., CA.) Jul. 1990 153 p
(Contract NCC2-615; RF Proj. 767591/722399)
(NASA-CR-186797; NAS 1.26:186797) Avail: NTIS HC A08/MF A01 CSCL 17G

Design concepts and principles to guide in the building of cooperative problem solving systems are being developed and evaluated. In particular, the design of cooperative systems for enroute flight planning is being studied. The investigation involves a three stage process, modeling human performance in existing environments, building cognitive artifacts, and studying the performance of people working in collaboration with these artifacts. The most significant design concepts and principles identified thus far are the principle focus. Author

N90-25965# Technische Univ., Brunswick (Germany, F.R.). Fakultaet fuer Maschinenbau und Elektrotechnik.
THE DISTURBANCE PROCESSES ON THE DATA LINKS OF THE MODE-S AIR TRAFFIC CONTROL SYSTEM Ph.D. Thesis [DIE STORPROZESSE AUF DEN DATENSTRECKEN DES MODE-S-SYSTEMS DER FLUGSICHERUNG]
Frank Ziegler 1989 141 p In GERMAN
(ETN-90-96960) Avail: NTIS HC A07/MF A01

The influence of system-inherent disturbances on the behavior of both data links used in the mode-S air traffic control system was investigated. The characteristics of the uplink and downlink signals and the cyclic error correction code are outlined. A hardware model was developed because the present system exists only in a few test stations. The different disturbances were analyzed for the downlink as well as for the uplink signals. The probabilities for the occurrence of the important phenomena test error and signal breakdown were determined in the case of signal overlapping. ESA

05 AIRCRAFT DESIGN, TESTING AND PERFORMANCE

Includes aircraft simulation technology.

For related information see also *18 Spacecraft Design, Testing and Performance* and *39 Structural Mechanics.* For land transportation vehicles see *85 Urban Technology and Transportation.*

N90-25966*# Douglas Aircraft Co., Inc., Long Beach, CA. New Commercial Programs.
STUDY OF HIGH-SPEED CIVIL TRANSPORTS. SUMMARY Final Report
Washington NASA Aug. 1990 53 p
(Contract NAS1-18378)
(NASA-CR-4236; NAS 1.26:4236) Avail: NTIS HC A04/MF A01 CSCL 01C

A systems study to identify the economic potential for a high-speed commercial transport has considered technology, market characteristics, airport infrastructure, and environmental issues. Market forecasts indicate a need for high speed civil transport (HSCT) service in the 2000/2010 time frame conditioned on economic viability and environmental acceptability. Design requirements focused on a 300 passenger, 3 class service, and 6500 nautical mile range based on the accelerated growth of the Pacific region. Compatibility with existing airports was an assumed requirement. Mach numbers between 2 and 25 were examined in conjunction with the appropriate propulsion systems, fuels, structural materials, and thermal management systems. Aircraft productivity was a key parameter with aircraft worth, in comparison to aircraft price, being the airline-oriented figure of merit. Aircraft screening led to determination that Mach 3.2 (TSJF) would have superior characteristics to Mach 5.0 (LNG) and the recommendation that the next generation high-speed commercial transport aircraft use a kerosene fuel. The sensitivity of aircraft performance and economics to environmental constraints (e.g., sonic boom, engine emissions, and airport/community noise) was identified together with key technologies. In all, current technology is not adequate to produce viable HSCTs for the world marketplace. Specific technology requirements have been identified which was the prime objective of this study. National economic benefits are projected. Author

N90-25967*# Worcester Polytechnic Inst., MA.
FEASIBILITY STUDY FOR A MICROWAVE-POWERED OZONE SNIFFER AIRCRAFT, VOLUME 2
1990 203 p
(Contract NASw-4435)
(NASA-CR-186676; NAS 1.26:186676) Avail: NTIS HC A10/MF A02 CSCL 01C

Using 3-D design techniques and the Advanced Surface Design Software on the Computervision Designer V-X Interactive Graphics System, the aircraft configuration was created. The canard, tail, vertical tail, and main wing were created on the system using Wing Generator, a Computervision based program introduced in Appendix A.2. The individual components of the plane were created separately and were later individually imported to the master

database. An isometric view of the final configuration is presented. Author

N90-25968*# Notre Dame Univ., IN. Dept. of Aerospace and Mechanical Engineering.
THE SCREEM-J4D: A PROPOSAL IN RESPONSE TO A LOW REYNOLDS NUMBER STATION KEEPING MISSION Final Design Proposal
May 1990 154 p Sponsored in part by Boeing Commercial Airplane Co.
(Contract NASw-4435)
(NASA-CR-186664; NAS 1.26:186664) Avail: NTIS HC A08/MF A01 CSCL 01C

The Screem-J4D is a remotely piloted airplane that was designed to fly at a chord Reynold's number of 100,000 while performing figure-8 maneuvers in a restricted area. It has a high aspect ratio main wing with a conventional empennage giving it a sailplane appearance. A specifications table and three-view drawing is provided. The flight plan calls for ascent to cruise altitude at 20 ft and then perform three figure-8 turns around pylons. These pylons will be separated by fifty yards and stationed inside a sports facility. Once completed, the pilot is to make use of any remaining power by loitering before landing the plane. The propulsion system of the J4D consists of a propeller-electric motor combination with the prop mounted at the front of the fuselage. In order to provide sufficient lift for low speed travel, the J4D has an aspect ratio of 11.72 with an 8.2 inch mean chord. The wing consists of a spar and rib construction with Micafilm skin. A combination of directional and longitudinal control will enable the J4D to perform the figure-8 maneuvers. However, in order to avoid the construction and servo weight of ailerons, the rudder was designed to be over one-half the size of the vertical tail to insure that the proper roll motion could be attained. Author

N90-25969# Wichita State Univ., KS. Inst. for Aviation Research.
A NASA/UNIVERSITY/INDUSTRY CONSORTIUM FOR RESEARCH ON AIRCRAFT ICE PROTECTION
Glen W. Zumwalt Oct. 1989 9 p Presented at the 24th Annual Midwest Regional Conference, Wichita, KS, 22-24 Mar. 1989
(IAR-89-18) Avail: NTIS HC A02/MF A01

From 1982 through 1987, an unique consortium was functioning which involved government (NASA), academia (Wichita State Univ.) and twelve industries. The purpose was the development of a better ice protection systems for aircraft. The circumstances which brought about this activity are described, the formation and operation recounted, and the effectiveness of the ventue evaluated. Author

N90-25970*# Eloret Corp., Sunnyvale, CA.
TRANSATMOSPHERIC VEHICLE RESEARCH Final Technical Report, 1 Dec. 1985 - 31 May 1990
Henry G. Adelman and Jean-Luc Cambier 1 Jun. 1990 92 p
LIMITED REPRODUCIBILITY: More than 20% of this document may be affected by color photographs Original contains color illustrations
(Contract NCC2-388)
(NASA-CR-186705; NAS 1.26:186705) Avail: NTIS HC A05/MF A01; 15 functional color pages CSCL 01C

Research was conducted into the alternatives to the supersonic combustion ramjet (scramjet) engine for hypersonic flight. A new engine concept, the Oblique Detonation Wave Engine (ODWE) was proposed and explored analytically and experimentally. Codes were developed which can couple the fluid dynamics of supersonic flow with strong shock waves, with the finite rate chemistry necessary to model the detonation process. An additional study was conducted which compared the performance of a hypersonic vehicle powered by a scramjet or an ODWE. Engineering models of the overall performances of the two engines are included. This information was fed into a trajectory program which optimized the flight path to orbit. A third code calculated the vehicle size, weight, and aerodynamic characteristics. The experimental work was carried out in the Ames 20MW arc-jet wind tunnel, focusing on mixing and combustion of fuel injected into a supersonic airstream. Several injector designs were evaluated by sampling the stream behind the injectors and analyzing the mixture with an on-line mass spectrometer. In addition, an attempt was made to create a standing oblique detonation wave in the wind tunnel using hydrogen fuel. It appeared that the conditions in the test chamber were marginal for the generation of oblique detonation waves. Author

N90-25971*# California State Polytechnic Univ., Pomona.
GLOBAL SENTRY: NASA/USRA HIGH ALTITUDE RECONNAISSANCE AIRCRAFT DESIGN, VOLUME 2
Mona-Lisa Alexandru, Frank Martinez, Jim Tsou, Henry Do, Ashish Peters, Tom Chatsworth, Ye Yu, and Jaskiran Dhillon 1990 119 p
(Grant NGT-21-002-800)
(NASA-CR-186820-Vol-2; NAS 1.26:186820-Vol-2; ARO-446; ARO-463) Avail: NTIS HC A06/MF A01 CSCL 01C

The Global Sentry is a high altitude reconnaissance aircraft design for the NASA/USRA design project. The Global Sentry uses proven technologies, light-weight composites, and meets the R.F.P. requirements. The mission requirements for the Global Sentry are described. The configuration option is discussed and a description of the final design is given. Preliminary sizing analyses and the mass properties of the design are presented. The aerodynamic features of the Global Sentry are described along with the stability and control characteristics designed into the flight control system. The performance characteristics are discussed as is the propulsion installation and system layout. The Global Sentry structural design is examined, including a wing structural analysis. The cockpit, controls and display layouts are covered. Manufacturing is covered and the life cost estimation. Reliability is discussed. Conclusions about the current Global Sentry design are presented, along with suggested areas for future engineering work. Author

N90-25972*# National Aeronautics and Space Administration. Ames Research Center, Moffett Field, CA.
SYNTHESIS OF INDIVIDUAL ROTOR BLADE CONTROL SYSTEM FOR GUST ALLEVIATION Final Report
Ji C. Wang, Alphonse Y. Chu (San Jose State Univ., CA.), and Peter D. Talbot Jul. 1990 72 p
(Contract NCC2-267)
(NASA-TM-101886; NAS 1.15:101886) Avail: NTIS HC A04/MF A01 CSCL 01C

The utilization of rotor flapping in synthesizing an Individual Blade Control (IBC) system for gust alleviation is demonstrated. The objective is to illustrate and seek to improve Ham's IBC method. A sensor arrangement with two accelerometers mounted on the root and tip of a blade is proposed for estimating of flapping states for feedback control. Equivalent swash plate implementation of IBC is also deliberated. The study concludes by addressing the concept of general rotor states feedback, of which the IBC method is a special case. The blade flapping equation of motion is derived. Ham's original IBC method and a modified IBC scheme called Model Reference (MRIBC) are examined, followed by simulation study with ideal measurements and relative performances of the two methods. The practical aspects of IBC implementation are presented. Different configuration of sensors and their merits are considered. The realization of IBC using equivalent swash plate instead of direct actuator motion is discussed. It is shown that IBC is a particular case of rotor states feedback. The idea of general rotor states feedback is further elaborated. Finally, major conclusions are given. Author

N90-25973*# National Aeronautics and Space Administration. Hugh L. Dryden Flight Research Facility, Edwards, CA.
AN IN-FLIGHT INTERACTION OF THE X-29A CANARD AND FLIGHT CONTROL SYSTEM
Michael W. Kehoe, Lisa J. Bjarke, and Edward J. Laurie (Grumman Aerospace Corp., Bethpage, NY.) Apr. 1990 21 p Presented at the AIAA Dynamics Specialists Meeting, Long Beach, CA, 5-6

Apr. 1990
(NASA-TM-101718; H-1590; NAS 1.15:101718) Avail: NTIS HC A03/MF A01 CSCL 01C

Many of today's high performance airplanes use high gain, digital flight control systems. These sytems are liable to couple with the aircraft's structural dynamics and aerodynamics to cause an aeroservoelastic interaction. These interactions can be stable or unstable depending upon damping and phase relationships within the system. The details of an aeroservoelastic interaction experienced in flight by the X-29A forward-swept wing airplane. A 26.5-Hz canard pitch mode response was aliased by the digital sampling rate in the canard position feedback loop of the flight control system, resulting in a 13.5-Hz signal being commanded to the longitudinal control surfaces. The amplitude of this commanded signal increased as the wear of the canard seals increased, as the feedback path gains were increased, and as the canard aerodynamic loading decreased. The resultant control surface deflections were of sufficient amplitude to excite the structure. The flight data presented shows the effect of each component (structural dynamics, aerodynamics, and flight control system) for this aeroservoelastic interaction. Author

N90-25974# Technische Univ., Brunswick (Germany, F.R.). Fakultaet fuer Maschinenbau und Elektrotechnik.
A CONTRIBUTION TO THE IMPROVEMENT OF THE ACCURACY IN THE PARAMETER IDENTIFICATION OF NONLINEAR PROCESSES, BY EXAMPLE OF THE AIRCRAFT MOTION Ph.D. Thesis [EIN BEITRAG ZUR GENAUIGKEITSSTEIGERUNG BEI DER PARAMETERIDENTIFIZIERUNG NICHTLINEARER PROZESSE AM BEISPIEL DER FLUGZEUBEWEGUNG]
Karl-Oskar Proskawetz 1989 157 p In GERMAN
(ETN-90-96961) Avail: NTIS HC A08/MF A01

The parameter identification of nonlinear dynamic processes was studied taking by example the aircraft motion of the double motor research aircraft Dornier DO-28. A two-step maximum likehood output error method was developed as identification method. The first step uses the exactly known, kinematic correlations between the flight situation quantities to check the consistency of the measured data and allows estimation of the necessary corrections. In the second step an iterative nonlinear multipoint model was used to describe more exactly the local aerodynamic interferences. The results demonstrate the general applicability and efficiency of modern offline identification methods for parameter estimation of nonlinear dynamic processes. ESA

N90-25975# Technische Univ., Brunswick (Germany, F.R.). Fakultaet fuer Maschinenbau und Elektrotechnik.
THE APPLICABILITY OF SIMPLE HELICOPTER MODELS FOR FLIGHT MECHANICS STUDIES Ph.D. Thesis [DIE ANWENDBARKEIT EINFACHER HUBSCHRAUBERMODELLE FUER FLUGMECHANISCHE UNTERSUCHUNGEN]
Karl Liese 1989 166 p In GERMAN Sponsored by BMFT
(ETN-90-96962) Avail: NTIS HC A08/MF A01

Helicopter mathematical models of different complexity were developed for the multitude of flight-mechanical questions, and their application domain were determined. A simple model was developed that is representative of rotor dynamics, rotor blades impact motion as well as dynamic rotor flow. Starting from this model, simplified models of different complexity were generated. The model results show good agreement with those of other calculation methods and with flight test data. It is shown that a helicopter modeling with simplified rotor dynamics as a first order system covers a significantly broader frequency range than quasistationary methods. However, the applicability of rigid body models to control problems is questionable. ESA

N90-25976# Stuttgart Univ. (Germany, F.R.). Inst. fuer Computer-Anwendungen.
A CONTRIBUTION TO THE ECONOMIC, OPTIMAL DIMENSIONING, AND SHAPING OF AIRCRAFT STRUCTURES USING A DESIGN MODEL Ph.D. Thesis [EIN BEITRAG ZUR OEKONOMISCHEN, OPTIMALEN DIMENSIONIERUNG UND FORMGEBUNG ALLGEMEINER TRAGWERKE MIT HILFE EINES ENTWURFSMODELLS]
Peter Schmolz 1988 210 p In GERMAN
(ETN-90-96966) Avail: NTIS HC A10/MF A02

A method for the optimization of dimensions and shape of aircraft structures is presented. As target function for minimization the weight and the maximum stress can be chosen. The reduction of the optimization variables requires an optimization data structure independent of the finite element structure. The structure is divided into optimization substructures and design elements. Interpolation approaches are used in the dimension optimization to approximate the geometric data. For the shape optimization several imaging functions are used. A method for the economic calculation of the required re-analysis was deduced. The optimization concept is demonstrated by examples. ESA

N90-25977# Rolls-Royce Ltd., Derby (England).
STAGE 2 RE-ENGINING: THE ONLY WAY TO ACHIEVE A REAL STAGE 3 AIRCRAFT
M. J. T. Smith and K. Goddard 3 Nov. 1989 11 p Presented at the Royal Aeronautical Society Conference on Aircraft Ageing and Noise Problems: Consequences for the Aviation Industry, London, England, 3 Nov. 1989; sponsored by FFV Aerotech, Sweden
(PNR90636; ETN-90-97143) Copyright Avail: NTIS HC A03/MF A01

The re-engining of the Rolls-Royce Tay is discussed. Airport authorities in the U.S. and Europe insist that only stage 3 compliant aircraft are able to operate at night. The impact of this, and technical options available to make stage 2 aircraft meet stage 3 standards are considered. Noise reduction possibilities and hushkits are described. The Tay 650 and 670 engines are described and illustrated. Other benefits of re-engining are discussed. ESA

N90-25978# Costruzioni Aeronautiche Giovanni Agusta S.p.A., Cascina Costa (Italy). Div. Elicotteri.
AGUSTA METHODOLOGY FOR PITCH LINK LOADS PREDICTION IN PRELIMINARY DESIGN PHASE
Fabio Nannoni and Alessandro Stabellini 20 Sep. 1988 54 p In ENGLISH and ITALIAN Presented at 14th European Rotorcraft Forum, Milan, Italy, 20-23 Sep. 1988 Previously announced in IAA as A90-42465
(ETN-90-97270) Avail: NTIS HC A04/MF A01

The fast increase of static and torsional loads at the root of the blade is, sometimes, the first limit that a helicopter meets in forward flight at high speed. A good design must consider an analysis of this phenomenon which is very important in rotation control development and, above all, in performance estimation and handling qualities of the whole aircraft. The Agusta methodology for the estimation of these loads in the preliminary design is presented. ESA

N90-25979# Wright Research Development Center, Wright-Patterson AFB, OH. Analysis and Applications Branch.
PDWAP: A PRELIMINARY DESIGN AND WEIGHTS ANALYSIS PROGRAM FOR AEROSPACE VEHICLES Final Technical Report, Oct. 1987 - Dec. 1988
L. R. Carreiro Jan. 1990 90 p
(AF Proj. 3012)
(AD-A222614; WRDC-TR-90-2005) Avail: NTIS HC A05/MF A01 CSCL 22/4

This is the User's Manual and Formulation Report for the program PDWAP (Preliminary Design and Weights Analysis Program). The program runs XT/AT compatible microcomputers. It is designed to provide a complete vehicle size summary and weight statement based on very rudimentary user inputs, in a very short runtime (i.e., less than 3 minutes). The preliminary design

phase is based on current trends in hypersonic-aerospace vehicles. The weights analysis, based on the WAATS code, can be used separately, and can handle a wide range of vehicles, such as fighters, transport, boosters, shuttles, etc. The program is interactive and menu driven, providing results in minimum time and investment. GRA

06 AIRCRAFT INSTRUMENTATION

Includes cockpit and cabin display devices; and flight instruments.

For related information see also *19 Spacecraft Instrumentation* and *35 Instrumentation and Photography.*

N90-25980*# National Aeronautics and Space Administration, Washington, DC.
SPACE TRANSPORTATION AVIONICS TECHNOLOGY SYMPOSIUM. VOLUME 1: EXECUTIVE SUMMARY
Aug. 1990 24 p Symposium held in Williamsburg, VA, 7-9 Nov. 1989
(NASA-CP-3081; NAS 1.55:3081) Avail: NTIS HC A03/MF A01 CSCL 01D

The focus of the symposium was to examine existing and planned avionics technology processes and products and to recommend necessary changes for strengthening priorities and program emphases. Innovative changes in avionics technology development and design processes, identified during the symposium, are needed to support the increasingly complex, multi-vehicle, integrated, autonomous space-based systems. Key technology advances make such a major initiative viable at this time: digital processing capabilities, integrated on-board test/checkout methods, easily reconfigurable laboratories, and software design and production techniques. Author

N90-25981*# National Aeronautics and Space Administration. Langley Research Center, Hampton, VA.
QUALITATIVE EVALUATION OF A CONFORMAL VELOCITY VECTOR DISPLAY FOR USE AT HIGH ANGLES-OF-ATTACK IN FIGHTER AIRCRAFT
Denise R. Jones and James R. Burley, II Jun. 1990 11 p
(NASA-TM-102629; NAS 1.15:102629) Avail: NTIS HC A03/MF A01 CSCL 01D

A piloted simulation study was conducted to evaluate the utility of a display device designed to illustrate graphically and conformally the approximate location of a fighter aircraft's velocity vector. The display device consisted of two vertical rows of light emitting diodes (LED's) located toward the center of the cockpit instrument panel to each side of the control stick. The light strings provided a logical extension of the head up display (HUD) velocity vector symbol at flight path angles which exceeded the HUD field-of-view. Four test subjects flew a modified F/A-18 model with this display in an air-to-air engagement task against an equally capable opponent. Their responses to a questionnaire indicated that the conformal velocity vector information could not be used during the scenarios investigated due to the inability to visually track a target and view the lights simultaneously. Author

07 AIRCRAFT PROPULSION AND POWER

Includes prime propulsion systems and systems components, e.g., gas turbine engines and compressors; and onboard auxilliary power plants for aircraft.

For related information see also *20 Spacecraft Propulsion and Power, 28 Propellants and Fuels,* and *44 Energy Production and Conversion.*

N90-25982*# National Aeronautics and Space Administration. Lewis Research Center, Cleveland, OH.
PERFORMANCE OF A SUPERCHARGED DIRECT-INJECTION STRATIFIED-CHARGE ROTARY COMBUSTION ENGINE
Timothy A. Bartrand (Sverdrup Technology, Inc., Brook Park, OH.) and Edward A. Willis Apr. 1990 25 p Presented at the Joint Symposium on General Aviation Systems, Ocean City, NJ, 11-12 Apr. 1990; sponsored in part by AIAA and FAA
(NASA-TM-103105; E-5430; NAS 1.15:103105) Avail: NTIS HC A03/MF A01 CSCL 21E

A zero-dimensional thermodynamic performance computer model for direct-injection stratified-charge rotary combustion engines was modified and run for a single rotor supercharged engine. Operating conditions for the computer runs were a single boost pressure and a matrix of speeds, loads and engine materials. A representative engine map is presented showing the predicted range of efficient operation. After discussion of the engine map, a number of engine features are analyzed individually. These features are: heat transfer and the influence insulating materials have on engine performance and exhaust energy; intake manifold pressure oscillations and interactions with the combustion chamber; and performance losses and seal friction. Finally, code running times and convergence data are presented. Author

N90-25983# National Aerospace Lab., Tokyo (Japan).
MEASUREMENT OF VELOCITY AND TEMPERATURE PROFILES AT THE EXIT PLANE OF A TUBULAR GAS TURBINE COMBUSTOR
Suguru Tamaru and Kazuo Shimodaira Aug. 1989 19 p In JAPANESE
(DE90-505519; NAL-TM-609; ISSN-0452-2982) Avail: NTIS (US Sales Only) HC A03/MF A01

Velocity and temperature profiles at the exit plane of a tubular gas turbine combustor were measured in detail on an existing combustor. Those were measured under atmospheric conditions adjusted to have a design Mach number, because of difficulty under design specifications (pressure: 55 atm, temperature: 1600 K). Both velocity and temperature profile were slightly asymmetric due to a swirler, however, in non-combustion, the velocity profile was relatively uniform, and its radial profile showed a small peak on the side of a turbine blade hub, indicating large difference from the temperature profile. Each profile was slightly different between the case under a design temperature rise condition and the case under a design reference cross section velocity or liner pressure loss condition, even under the same Mach number. As compared with existing high pressure combustion test data measured on a half scale combustor, the temperature profiles were different each other. DOE

N90-25984# National Aerospace Lab., Tokyo (Japan).
DECAY OF SECONDARY FLOW AND THE ASSOCIATED LOSS VARIATION DOWNSTREAM OF AN ANNUAL TURBINE STATOR CASCADE
Atsumasa Yamamoto and Hiroyuki Nouse Apr. 1989 16 p Sponsored in part by Ministry of International Trade and Industry, Tokyo, Japan
(DE90-505520; NAL-TR-1021T; ISSN-0389-4010) Avail: NTIS (US Sales Only) HC A03/MF A01

Flows downstream of an annular turbine stator cascade were measured in detail at seven serial measuring planes, using a five-hole Pitot tube and total pressure probe, and the decay of secondary flows and variation of associated total loss were examined. The effects of rotation of a hub endwall and effects of secondary air injection from the hub end well on the secondary flow and the loss were also analyzed. The shape of wake downstream of the cascade was mainly affected by secondary vortices, and after inner vortex near the hub endwall made an endwall boundary layer thickness non-uniform, it dissipated quickly due to viscous friction with the endwall. After outer vortex was pushed inward, it decayed gradually downstream of the cascade. The rotation of the hub endwall induced outward secondary flows and reduced pressure losses there. A small amount of air injected from a hub endwall slit induced inward secondary flows and increased total pressure losses. DOE

N90-25985# Von Karman Inst. for Fluid Dynamics, Rhode-Saint-Genese (Belgium).
GAS TURBINE COMBUSTION, VOLUME 1
1990 407 p Lecture series held in Rhode-Saint-Genese, Belgium, 19-23 Feb. 1990
(VKI-LS-1990-02-Vol-1; ISSN-0377-8312; ETN-90-97001) Avail: NTIS HC A18/MF A03

Combustor types, preliminary design and performance aspects, fuel injection and ignition, combustor cooling and emissions are discussed. Subsonic and supersonic combustion flow modeling are described. Sample calculations and comparisons with experimental data are shown and discussed. The physical phenomena and interactions in turbulent flames are described. Various models for premixed and nonpremixed flames are reviewed. Combustion chemistry is discussed. Special attention is given to better understanding laminar and turbulent combustion as well as pollutant formation. The instrumentation techniques used to characterize air, droplet or particle velocity flow fields is discussed. The role of data processing equipment in interpreting the data is demonstrated. For individual titles, see N90-25986 through N90-25994.

N90-25986# Cranfield Inst. of Tech., Bedford (England). School of Mechanical Engineering.
COMBUSTION IN THE GAS TURBINE. PART 1: COMBUSTOR TYPES AND DESIGN
Riti Singh *In* VKI, Gas Turbine Combustion, Volume 1 1990 9 p (For primary document see N90-25985 20-07)
(CIT/SME/VKI/RS/1) Avail: NTIS HC A18/MF A03

The general design and performance of gas turbine engines are discussed. The performance requirements and the basic design features of a gas turbine combustion chamber are summarized. The types of combustion chamber and their relative merits are described. The reasons why tubular chambers are no longer specified for aeroengine designs are presented. The complex and heavy ducting needed between the compressor and the chambers and between the chambers and turbine makes tubular type engines both heavier and larger in diameter than tubo-annular or annular type combustion chambers. The advantages and disadvantages of the tubo-annular and annular type combustion chambers are presented. Illustrations of these combuster types are included. ESA

N90-25987# Cranfield Inst. of Tech., Bedford (England). School of Mechanical Engineering.
COMBUSTION IN THE GAS TURBINE. PART 2: PRELIMINARY DESIGN AND PERFORMANCE
Riti Singh *In* VKI, Gas Turbine Combustion, Volume 1 1990 17 p (For primary document see N90-25985 20-07)
(CIT/SME/VKI/RS/3) Avail: NTIS HC A18/MF A03

The function and sizing of combustion chamber components is addressed. Ways to determining the relative dimensions of diffuser, outer casing, and flame tube incorporating primary, intermediate and dilution zones are discussed. Formulas and diagrams used in calculating the dimensions of these various engine components are presented. Flame tube width and length are calculated. A detailed study of gas flow in the primary, intermediate and dilution zones of the flame tube is presented. ESA

N90-25988# Cranfield Inst. of Tech., Bedford (England). School of Mechanical Engineering.
COMBUSTION IN THE GAS TURBINE. PART 3: FUEL INJECTION, IGNITION AND STABILITY
Riti Singh *In* VKI, Gas Turbine Combustion, Volume 1 1990 13 p (For primary document see N90-25985 20-07)
(CIT/SME/VKI/RS/4) Avail: NTIS HC A18/MF A03

The basic role of the fuel injector in a gas turbine engine is summarized. A table comparing the properties of different types of fuel injectors is presented. The notion of designing for stability in fuel injection and combustion chamber design is discussed. Engine ignition, especially high altitude relight performance is discussed. The fundamental aspects of the ignition process are listed. Ways of improving ignition performance are listed. A table listing solutions to failure to light on ground or at altitude is presented. Factors affecting the stability of combustion chambers are discussed. ESA

N90-25989# Cranfield Inst. of Tech., Bedford (England). School of Mechanical Engineering.
COMBUSTOR COOLING ASPECTS
Riti Singh *In* VKI, Gas Turbine Combustion, Volume 1 1990 78 p (For primary document see N90-25985 20-07)
(CIT/SME/VKI/RS/5) Avail: NTIS HC A18/MF A03

Heat transfer processes in a gas turbine engine are discussed. Internal heat radiation and radiation from non luminous gases inside the engine is studied. The parts played by H2O, CO2 and N2 in the hydrocarbon flames are analyzed in detail. Radiation from luminous gases produced by the buildup of soot particles in the combustion chamber is discussed. When large buildup of soot particles occurs, severe radiant heating with its attendant problems of liner durability occurs. The influence of fuel composition on engine temperature is outlined. ESA

N90-25990# Cranfield Inst. of Tech., Bedford (England). School of Mechanical Engineering.
POLLUTANTS: PRODUCTION AND METHODS OF REDUCTION
Riti Singh *In* VKI, Gas Turbine Combustion, Volume 1 1990 60 p (For primary document see N90-25985 20-07)
(CIT/SME/VKI/RS/6) Avail: NTIS HC A18/MF A03

The various components of gas turbine engine exhausts are analyzed in terms of their role as pollutants. The engine emissions identified as offering the greatest potential threat to the stratosphere are water vapor, carbon dioxide, sulfur compounds and nitric oxides. The mechanisms of pollutant formation are described. The production of carbon monoxide and unburned hydrocarbons due to incomplete combustion is described. The influence of fuel properties, pressure and temperature on emissions is discussed. Methods of pollution reduction are presented. ESA

N90-25991# Imperial Coll. of Science and Technology, London (England). Fluids Section.
SUBSONIC COMBUSTOR FLOW MODELING: STATE OF THE ART OF CFD TECHNIQUES FOR REACTING AND COMBUSTING FLOW
J. J. McGuirk *In* VKI, Gas Turbine Combustion, Volume 1 1990 29 p (For primary document see N90-25985 20-07)
Avail: NTIS HC A18/MF A03

Gas turbine models of subsonic flows which give reasonable predictions at reasonable computing cost are reviewed. The ability to handle the complex geometry of practical combustors, to predict details of internal flow structure, and exit temperature pattern factors make such models more accurate than those used ten years before. Almost all model elements, however, need further improvement. The prediction of pollutant emissions, and accurate wall temperatures in particular, requires combustion model improvement. ESA

N90-25992# National Aeronautics and Space Administration. Langley Research Center, Hampton, VA.
SUPERSONIC COMBUSTOR MODELING
David W. Riggins, J. Philip Drummond, and Mark H. Carpenter *In* VKI, Gas Turbine Combustion, Volume 1 1990 95 p (For primary document see N90-25985 20-07)
Avail: NTIS HC A18/MF A03

The physical phenomena involved when a supersonic flow undergoes chemical reaction are discussed. Detailed physical models of convective and diffusive mixing, and finite rate chemical reaction in supersonic flow are presented. Numerical algorithms used to solve the equations governing these processes are introduced. Computer programs using these algorithms are used to analyze the structure of the reacting mixing layer. It is concluded that, as in subsonic flow, exothermic heat release in unconfined supersonic flows retards fuel/air mixing. Non mixing is shown to be a potential problem in reducing the efficiency of supersonic as well as subsonic combustion. Techniques for enhancing fuel/air mixing and combustion are described. ESA

N90-25993# Rouen Univ. (France). Faculte des Sciences.
TURBULENT COMBUSTION MODELING FOR TURBO-JET COMBUSTION CHAMBERS
R. Borghi *In* VKI, Gas Turbine Combustion, Volume 1 1990 42 p (For primary document see N90-25985 20-07)
Avail: NTIS HC A18/MF A03

The size of the combustion chamber and the operating conditions chosen are taken into account in developing turbulent combustion models for turbojet engines. Premixed and non premixed conditions are discussed in terms of their integration in turbulence models. Computation of flame length and global heat release during normal engine operating conditions is shown to be accurate within 10 to 20 percent provided that one is sure of the turbulence values used. The need for improvement in the prediction of chemical reactions, particularly the production of pollutants, is called for. ESA

N90-25994# Stuttgart Univ. (Germany, F.R.). Inst. fuer Technische Verbrennung.
CHEMISTRY OF COMBUSTION PROCESSES
J. Warnatz *In* VKI, Gas Turbine Combustion, Volume 1 1990 50 p Sponsored by BMFT, CEE, Fonds der Chemischen Industrie, and Max-Buchner-Stiftung (For primary document see N90-25985 20-07)
Avail: NTIS HC A18/MF A03

Typical combustion processes are considered with emphasis on the basic physics and chemistry of combustion processes. Homogeneous reaction systems, the structure of laminar flame fronts for both stationary and instationary flame propagation and pollutant formation chemistry are discussed. Transport models, temperature and pressure dependance of reaction rate coefficients and the multiscale character of reaction systems are reviewed. High and low temperature chemical reaction mechanisms are described. Simulation of laminar premixed one-dimensional and two-dimensional combustion is presented. The detailed chemistry of turbulent combustion is discussed. ESA

N90-25995# Von Karman Inst. for Fluid Dynamics, Rhode-Saint-Genese (Belgium).
GAS TURBINE COMBUSTION, VOLUME 2
1990 273 p Lecture series held in Rhode-Saint-Genese, Belgium, 19-23 Feb. 1990
(VKI-LS-1990-02-Vol-2; ISSN-0377-8312; ETN-90-97002) Avail: NTIS HC A12/MF A02

Combustion instrumentation designed to lower engine development and testing costs is described. Total and static pressure probes, low and high pressure thermocouples, holographic particle sizing and velocity systems and laser Doppler velocimeters are some of the instruments described. Supersonic and subsonic combustor testing are discussed in detail. Carbon slurry fuel spray characterization is described. Liquid-fuelled ramjet systems and concentric-dump ramburners are discussed. The history of hydrogen scramjet development and testing is described in detail. Supersonic mixing, fuel injector design and combustor diagnostics and performance are described. For individual titles, see N90-25996 through N90-25998.

N90-25996# United Technologies Research Center, East Hartford, CT. Aerothermal Technology Group.
COMBUSTION INSTRUMENTATION
Jan B. Kennedy *In* VKI, Gas Turbine Combustion, Volume 2 1990 90 p (For primary document see N90-25995 20-07)
Avail: NTIS HC A12/MF A02

A historical background of combustion instrumentation is presented. Thermocouples, dual sonic orifice probes, video cameras, holography, spray patternation, and other instrumentation used in engine testing are described. Phase discriminating sampling probes, planar mie scattering imaging and line of sight light diffraction particle sizers are discussed. Laser measuring instruments such as laser velocimeters and phase doppler particle analyzers are described. The use of exciplex fluorescence in engine testing is summarized. The importance of choosing the test instruments appropriate for a particular task is stressed. The choice of instrumentation which is very expensive and difficult to use is identified as one of the causes of engine development cost and time run-overs. ESA

N90-25997# United Technologies Research Center, East Hartford, CT. Propulsion Technology Group.
SUBSONIC COMBUSTOR TESTING
William T. Peschke *In* VKI, Gas Turbine Combustion, Volume 2 1990 75 p (For primary document see N90-25995 20-07)
Avail: NTIS HC A12/MF A02

The development of a subsonic carbon slurry fuelled gas turbine engine is described. The carbon slurry fuels may offer significant improvement in volume limited flight vehicle applications. Atomization characteristics of the fuel are determined using a Malvern droplet sizer based on the Fraunhofer light diffraction theory. Fuel spray patterns are documented by photographs using stroboscopic illumination with a twenty probe patternator rake. Three commercially available fuel injectors are tested. Flow visualization, flame spreading and stabilization, and testing procedure are described. The instrumentation used in the engine tests is described. The test results and lessons learned from the ramburner testing are outlined. ESA

N90-25998# United Technologies Research Center, East Hartford, CT. Propulsion Technology Group.
SUPERSONIC COMBUSTOR TESTING
William T. Peschke *In* VKI, Gas Turbine Combustion, Volume 2 1990 104 p (For primary document see N90-25995 20-07)
Avail: NTIS HC A12/MF A02

The history of hydrogen scramjet development efforts is described. Various issues in hydrogen scramjet development are given particular attention. These include supersonic mixing, fuel injector design, fuel injector orifice spacing, fuel injector orifice diameter, fuel jet penetration and pressure gradient effects. Progress made in these aspects of hydrogen scramjet development is summarized. A supersonic mixing and combustion experiment is described. Combustor diagnostics and combustor performance are discussed in detail. Key issues facing further development efforts are summarized. ESA

N90-25999# Rolls-Royce Ltd., Derby (England).
APPLICATION OF HIGH PERFORMANCE METALS IN GAS TURBINE ENGINES
P. J. Postans 17 Oct. 1989 15 p Presented at the Metals Fight Back, London, England, 17 Oct. 1989
(PNR90640; ETN-90-97145) Copyright Avail: NTIS HC A03/MF A01

The development and application of two high performance gas turbine engine materials, Iml834 and Udimet 720 are described. These typify current approaches to alloy and microstructural development, component design, manufacture and life assessment. They illustrate how metals continue to expand their applications. Iml834 is a titanium alloy designed to operate at 600 C continuously with short excursions to 650 C, and is aimed at disc and blade operations in high performance compressors. Udimet 720 is a high strength 675 to 700 C capability nickel superalloy developed for high performance turbine discs. Material properties including tensile and creep strengths are described. ESA

N90-26000# Rolls-Royce Ltd., Derby (England).
TOWARDS 2000: THE COMPOSITE ENGINE
D. Driver 11 Nov. 1989 16 p Presented at the Australian Aeronautical Conference 1989 on Research and Technology: The Next Decade, Melbourne, Australia, 9-11 Oct. 1989
(PNR90646; ETN-90-97147) Copyright Avail: NTIS HC A03/MF A01

By the turn of the century aeroengine gas turbine temperatures are likely to approach 2000 C; thrust-to-weight ratios could reach 20:1 and turbofan thrusts exceed 80,000 lbs. Such advances will only be achieved with novel aeroengine designs which incorporate the higher specific strengths of polymeric, metal-matrix, and ceramic reinforced composite materials. The current state of materials and processing development for this range of aeroengine composite

materials is reviewed. Conclusions are detailed. The designers and manufacturers face greater challenges than the materials developers. Three-dimensional design methodologies need to be developed to exploit the anisotropic nature of continuous/long fiber reinforced materials. ESA

N90-26001# Rolls-Royce Ltd., Derby (England). Theoretical Science Group.
PREDICTION OF ROTATING DISC FLOW AND HEAT TRANSFER IN GAS TURBINE ENGINES
John W. Chew Nov. 1989 17 p Presented at the 3rd International Symposium on Transport Phenomena and Dynamics of Rotating Machinery, Honolulu, Hawaii, Apr. 1990
(PNR90650; TSG0478; ETN-90-97148) Copyright Avail: NTIS HC A03/MF A01

Motivated by the need to improve design techniques for aeroengines considerable effort has been put into developing predictive techniques for rotating disc flow and heat transfer. Some notable recent advances are reviewed. The theoretical techniques employed include analytical solutions for laminar flow, momentum-integral methods for turbulent flow, and finite difference solutions of the Reynolds-averaged Navier-Stokes equations. Each of these methods is discussed and predictive capability is illustrated through comparisons with experimental data. ESA

N90-26002# Rolls-Royce Ltd., Derby (England). Aero-Engine Div.
PREDICTION AND MEASUREMENT OF ROTOR BLADE/STATOR VANE DYNAMIC CHARACTERISTICS OF A MODERN AERO-ENGINE AXIAL COMPRESSOR
R. J. Williams, K. L. Johal, H. A. Barton, and S. T. Elston 3 Apr. 1989 8 p Presented at the Modern Practice in Stress and Vibration Analysis, Liverpool, England, 3-5 Apr. 1989
(PNR90667; ETN-90-97152) Copyright Avail: NTIS HC A02/MF A01

Commercial pressures require ever more fuel efficient and light weight propulsion systems. Inevitably this results in an increased stage loading that can exacerbate vibration problems of stall flutter, acoustic resonance, and conventional mechanical resonances from the immediate upstream and downstream blade/vane rows. The design of a rotor and stator from design to engine validation is traced. The components are analyzed at design stage using finite element models and modified to give acceptable dynamic characteristics. The predicted and measured results are compared and the method of assessment described. ESA

N90-26003# Rolls-Royce Ltd., Derby (England).
THE IMPACT AND REQUIREMENTS OF NEW MATERIALS ON AEROENGINES
G. E. Kirk 1 Mar. 1989 15 p Presented at the Royal Aeronautical Society Conference on Aerospace Application of Advanced Materials, 1 Mar. 1989
(PNR90671; ETN-90-97155) Copyright Avail: NTIS HC A03/MF A01

Future engine requirements, the status of major candidate materials and the problems that need to be solved before these materials can be incorporated with confidence are reviewed. Conclusions include: a requirement exists to reduce manufacturing cost by lower raw material cost and improved process control; resin composites need increased temperature capability, improved impact and resistance, coatings for erosion resistance and better repair procedures; advanced glass, metal and ceramic composites need improvements in fiber technology, coatings, the control of fiber matrix interface, and advanced fabrication techniques. ESA

N90-26004# Rolls-Royce Ltd., Derby (England).
AIRCRAFT EXHAUST EMISSIONS: AN ENGINE MANUFACTURER'S PERSPECTIVE
D. M. Snape 5 Feb. 1990 24 p Presented at the ICAA Seminar, Brussels, Belgium, 5-7 Feb. 1990
(PNR90675; ETN-90-97156) Copyright Avail: NTIS HC A03/MF A01

Exhaust emissions from an aircraft gas turbine are studied. Estimated emissions deposited into the atmosphere per passenger for a typical journey by car and by aircraft are compared. For this consideration, the duty of the combustor is studied and emissions characteristics shown. Potential benefits of improved combustion are outlined. A summary of the current position illustrates that while it is difficult to justify economically the need for further work on smoke, hydrocarbons and carbon monoxide, further progress is desirable on oxides of nitrogen and possibly carbon dioxide. These are considered in detail. ESA

N90-26005# Rolls-Royce Ltd., Derby (England).
THE APPLICATION OF ENGINEERING CERAMICS IN GAS TURBINES
G. Syers 1 Mar. 1990 24 p Presented at the Hatfield Polytechnic Inst. of Mettallurgist Lecture, Hatfield, England, 28 Mar. 1990
(PNR90676; ETN-90-97157) Copyright Avail: NTIS HC A03/MF A01

The solution to problems concerning the supply of cooling air, for components whose temperatures increase with improved combustion in propulsion units, by the adoption of ceramic materials in either reinforced or monolithic forms is addressed. Ceramic materials offer a marked reduction in weight and the ability to operate at significantly higher temperatures than those currently experienced by the conventional superalloys without cooling. The use of ceramic materials in gas turbines has been investigated for a number of years. Investigations include microstructural engineering, materials characterization, manufacture and testing of experimental turbine blades, shroud rings and gas bearings etc. Aspects concerning these components are discussed. ESA

N90-26006# Deutsche Forschungsanstalt fuer Luft- und Raumfahrt, Goettingen (Germany, F.R.). Abt. Stabilitaet und Antwort.
STRUCTURAL ANALYSIS AND OPTIMIZATION OF A PROPFAN BLADE USING A FINITE ELEMENT METHOD
Rolf Lammering Dec. 1989 58 p In GERMAN; ENGLISH summary Report will be announced as translation (ESA-TT-1216)
(DLR-FB-90-01; ISSN-0171-1342; ETN-90-97012) Avail: NTIS HC A04/MF A01; DLR VB-PL-DO, Postfach 40 60 58, 5000 Cologne, Fed. Republic of Germany, 22.50 Deutsche marks

Algorithms applicable to finite element calculation of a propfan blade are presented. The blade is discretized as a shallow shell. Constitutive equations for isotropic and layered materials are implemented in the formulation of the finite elements. The quasi static deformations resulting from centrifugal forces as well as the eigenmodes and eigenfrequencies (as a function of rotational speed) are presented. Methods of mathematical optimization are used to minimize displacement at the tip of a propfan blade of composite material with six layers of equal thickness. Fiber orientation is used as a design variable. It is shown that deformation behavior is strongly influenced by fiber orientation. ESA

N90-26007# Royal Aerospace Establishment, Farnborough (England).
HANDBOOK OF UNCERTAINTY METHODOLOGY FOR ENGINE TESTING AT PYESTOCK (ENGLAND)
J. C. Ascough 8 Nov. 1989 68 p
(RAE-TM-P-1179; BR112839; ETN-90-97068) Copyright Avail: NTIS HC A04/MF A01

Measurements of aircraft gas turbine engine performance in the altitude test facility are subject to a small amount of uncertainty resulting from a combination of precision (or random) errors and bias (or systematic) errors. The limits of the precision errors can be readily calculated by statistical analysis of the results measured during the engine tests. Bias limits are not directy observable in the test results, but can be predicted by a comprehensive assessment or all possible sources of error, which are propagated to the test results. These methods can be difficult to comprehend and apply and a handbook was written as a guide, not only for engine test staff, but also for their customers who need to be

assured of the rigorous attention given to identifying and reducing measurement uncertainty. ESA

N90-26008# Alfa Romeo S.p.A., Naples (Italy).
TURBINE BLADE HEAT TRANSFER COEFFICIENT EVALUATION BY MODIFIED VERSION OF STAN5. COMPARISON WITH EXPERIMENTAL DATA
P. Dimartino, D. Carbone, and S. Colantuoni 1989 17 p Presented at Computers and Experiments in Mechanics Conference, Capri, Italy, 23-26 May 1989
(ETN-90-97283) Avail: NTIS HC A03/MF A01

The calculation of airfoil heat transfer coefficient with the accuracy required in gas turbine applications is investigated. STAN5 is a two-dimensional code developed for turbine heat transfer calculations. The purpose of the work is to improve the STAN5 code for use in heat transfer on turbine airfoil surfaces. The modifications carried out on the model used in the two-dimensional, finite difference boundary layer code are presented. The experimental activity performed on a cascade model for measuring the heat transfer on a blade is given. The comparison between predictions and experimental data of the heat transfer coefficients on the suction surface of the blade is performed. ESA

N90-26009*# National Aeronautics and Space Administration. Lewis Research Center, Cleveland, OH.
HOT GAS INGESTION CHARACTERISTICS AND FLOW VISUALIZATION OF A VECTORED THRUST STOVL CONCEPT
Albert L. Johns, George H. Neiner, Timothy J. Bencic, Joseph D. Flood, Kurt C. Amuedo, Thomas W. Strock, and Ben R. Williams (McDonnell Aircraft Co., Saint Louis, MO.) 1990 22 p Presented at the International Powered Lift Conference, London, England, 29-31 Aug. 1990; sponsored by Royal Aeronautical Society
(NASA-TM-103212; E-5623; NAS 1.15:103212) Avail: NTIS HC A03/MF A01 CSCL 21E

A 9.2 percent scale short takeoff and vertical landing (STOVL) hot gas ingestion model was designed and built by McDonnell Douglas Corporation (MCAIR) and tested in the NASA Lewis Research Center 9- by 15-Foot Low Speed Wind Tunnel (LSWT). Hot gas ingestion, the entrainment of heated engine exhaust into the inlet flow field, is a key development issue for advanced short takeoff and vertical landing aircraft. The Phase 1 test program, conducted by NASA Lewis and McDonnell Douglas Corporation, evaluated the hot ingestion phenomena and control techniques and Phase 2 test program which was conducted by NASA Lewis are both reported. The Phase 2 program was conducted at exhaust nozzles temperatures up to 1460 R and utilized a sheet laser system for flow visualization of the model flow field in and out of ground effects. Hot gas ingestion levels were measured for the several forward nozzle splay configurations and with flow control/lift improvement devices which reduced the hot gas ingestion. The model support system had four degrees of freedom, heated high pressure air for nozzle flow, and a suction system exhaust for inlet flow. The headwind (freestream) velocity for Phase 1 was varied from 8 to 90 kn, with primary data taken in the 8 to 23 kn headwind velocity range. Phase 2 headwind velocity varied from 10 to 23 kn. Results of both Phase 1 and 2 are presented. A description of the model, facility, a new model support system, and a sheet laser illumination system are also provided. Results are presented over a range of main landing gear height (model height) above the ground plane at a 10 kn headwind velocity. The results contain the compressor face pressure and temperature distortions, total pressure recovery, compressor face temperature rise, and the environmental effects of the hot gas. The environmental effects include the ground plane temperature and pressure distributions, model airframe heating, and the location of the ground flow separation. Results from the sheet laser flow visualization test are also shown. Author

08 AIRCRAFT STABILITY AND CONTROL

Includes aircraft handling qualities; piloting; flight controls; and autopilots.

For related information see also *05 Aircraft Design, Testing and Performance.*

N90-26010# National Aeronautical Lab., Bangalore (India). Flight Mechanics and Controls Div.
MODEL FOLLOWING CONTROL SYSTEM DESIGN: PRELIMINARY ATTAS IN-FLIGHT SIMULATION TEST RESULTS
Shyam Chetty and F. Henschel Feb. 1990 48 p
(PD-FC-9003) Avail: NTIS HC A03/MF A01

The preliminary Advanced Technologies Testing Aircraft System (ATTAS) inflight simulation flight test results of the model following flight control system are described. A major portion of the current effort was directed towards estimating the time delays in the various control loop segments and incorporating these estimates in the controller design process and ground simulation software. Author

N90-26011*# National Aeronautics and Space Administration. Lewis Research Center, Cleveland, OH.
H-INFINITY BASED INTEGRATED FLIGHT-PROPULSION CONTROL DESIGN FOR A STOVL AIRCRAFT IN TRANSITION FLIGHT
Sanjay Garg, Duane L. Mattern (Sverdrup Technology, Inc., Brook Park, OH.), Michelle M. Bright, and Peter J. Ouzts Aug. 1990 32 p Presented at the Guidance, Navigation and Control Conference, Portland, OR, 20-22 Aug. 1990; sponsored in part by AIAA
(NASA-TM-103198; E-5594; NAS 1.15:103198) Avail: NTIS HC A03/MF A01 CSCL 01C

Results are presented from an application of H-infinity control design methodology to a centralized integrated flight/propulsion control (IFPC) system design for a supersonic Short Take-Off and Vertical Landing (STOVL) fighter aircraft in transition flight. The overall design methodology consists of a centralized IFPC controller design with controller partitioning. Only the feedback controller design portion of the methodology is addressed. Design and evaluation vehicle models are summarized, and insight is provided into formulating the H-infinity control problem such that it reflects the IFPC design objectives. The H-infinity controller is shown to provide decoupled command tracking for the design model. The controller order could be significantly reduced by modal residualization of the fast controller modes without any deterioration in performance. A discussion is presented of the areas in which the controller performance needs to be improved, and ways in which these improvements can be achieved within the framework of an H-infinity based linear control design. Author

N90-26012# Advisory Group for Aerospace Research and Development, Neuilly-Sur-Seine (France). Guidance and Control Panel.
TECHNICAL EVALUATION REPORT ON THE GUIDANCE AND CONTROL PANEL 49TH SYMPOSIUM ON FAULT TOLERANT DESIGN CONCEPTS FOR HIGHLY INTEGRATED FLIGHT CRITICAL GUIDANCE AND CONTROL SYSTEMS
Bernard Chaillot (Direction des Recherches, Etudes et Techniques, Paris, France) May 1990 21 p Symposium held in Toulouse, France, 10-13 Oct. 1989
(AGARD-AR-281; ISBN-92-835-0559-X) Copyright Avail: NTIS HC A03/MF A01; Non-NATO Nationals requests available only from AGARD/Scientific Publications Executive

Twenty-three papers were presented at the Guidance and Control Panel 49th Symposium including the keynote address, covering the following headings; trends in integrated flight critical systems; advanced fault tolerant design concepts; system architectures, mechanization, and integration issues; high integrity software design methodologies and algorithms; and system validation, simulation, and flight test experience. Author

N90-26013*# Old Dominion Univ., Norfolk, VA. Dept. of Electrical and Computer Engineering.
GUIDANCE AND CONTROL STRATEGIES FOR AEROSPACE VEHICLES Final Report, period ending 31 Jul. 1990
Joseph L. Hibey and Desineni S. Naidu Aug. 1990 101 p
(Grant NAG1-736)
(NASA-CR-186878; NAS 1.26:186878) Avail: NTIS HC A06/MF A01 CSCL 01C

The first part of the report concerns broadly the summary of the work done in the areas of singular perturbations and time scales (SPaTS), aerobraking technology, guidance and aerocruise. The synergistic plane change problem connected with orbital transfer employing aeroassist technology, is addressed. The mission involves transfer from high Earth orbit to low Earth orbit with plane change being performed within the atmosphere. The complete mission consists of a deorbit phase, atmospheric phase, and finally reorbit phase. The atmospheric maneuver is composed of an entry mode, a cruise mode, and finally an exit mode. During the cruise mode, constant altitude and velocity are maintained by means of bank angle control with constant thrust or thrust control with constant bank angle. Comparisons between these two control strategies bring out some interesting features. Author

N90-26014# Loughborough Univ. of Technology (England). Dept. of Mathematical Sciences.
AN INVESTIGATION OF THE USE OF SINGULAR PERTURBATION METHODS AND MODAL CONTROL THEORY IN THE DERIVATION OR AIRCRAFT CONTROL SCHEMES
S. K. Spurgeon 1989 37 p
(MATHS-Rept-A-106; ETN-90-97122) Avail: NTIS HC A03/MF A01

Two techniques which extend control design philosophies based upon pole-placement are considered. Singular perturbation theory, to provide desirable asymptotic system behavior, and direct eigenstructure assignment, to specify the desired dynamic response of the system are used. The underlying theory behind these methods is described. The two design philosophies are compared. The development of an advanced longitudinal multi-mode scheme for a dynamically unstable aircraft is considered. ESA

N90-26015# Institut Franco-Allemand de Recherches, Saint-Louis (France).
MANEUVERING BY MEANS OF LATERAL JETS [STEUERUNG MITTELS SEITLICH AUSTRETENDER STRAHLEN]
K. W. Naumann 29 Dec. 1989 55 p In GERMAN Presented at CCG-Lehrgang B2.19 der Carl-Granz-Gessellschaft, Weil am Rhein, Fed. Republic of Germany, 21-24 Nov. 1988
(ISL-CO-255/88; ETN-90-97021) Avail: NTIS HC A04/MF A01

Piloting techniques by means of lateral jets during hypersonic flight are discussed. The jets cause important perturbations of the air flow around the vessel. These perturbations can increase or decrease the overall thrust. Methods of finding a compromise between favorable interactions, and parasitic effects decreasing the flight stability of the vessel are presented. The goal of the research is to provide engineers with appropriate methods and data for accurate calculation of piloting parameters. An extensive bibliography is included to help engineers in developing lateral jet guidance systems. ESA

N90-26016# Aeritalia S.p.A., Turin (Italy). Flight Test Dept.
AM-X HIGH INCIDENCE TRIALS, DEVELOPMENT AND RESULTS
G. Menso and B. Marchetto 1989 10 p Presented at 20th Society of Flight Test Engineers Annual Symposium, Reno, NV, 18-21 Sep. 1989
(ETN-90-97277) Avail: NTIS HC A02/MF A01

The activities carried out to investigate the high angle of attack/spin characteristics of the AM-X are described. Vertical wind tunnel and rotary balance facilities were used to collect all the information on aircraft behavior at stall, beyond stall, and in developed spin required to efficiently approach the flight test activity. A special training of the ground monitoring team and adequate use of the telemetry facilities allowed the efficient employment of flight time. Analysis of the test results allowed validation and identification of the aerodynamics model. Flight controls modifications useful to improve the aircraft behavior at high incidence are suggested. ESA

N90-26017*# North Carolina State Univ., Raleigh. Dept. of Mechanical and Aerospace Engineering.
LOW-SPEED WIND TUNNEL INVESTIGATION OF THE STATIC STABILITY AND CONTROL CHARACTERISTICS OF AN ADVANCED TURBOPROP CONFIGURATION WITH THE PROPELLERS PLACED OVER THE TAIL M.S. Thesis
Graham Scott Rhodes 1990 87 p
(Contract NCC1-123)
(NASA-CR-186900; NAS 1.26:186900) Avail: NTIS HC A05/MF A01 CSCL 01C

An exploratory wind tunnel investigation was performed in the 30 x 60 foot wind tunnel to determine the low speed static stability and control characteristics into the deep stall regime of an advanced turboprop aircraft with the propellers located over the horizontal tail. By this arrangement, the horizontal tail could potentially provide acoustic shielding to reduce the high community noise caused by the propeller blades. The current configuration was a generic turboprop model equipped with 1 foot diameter single rotating eight bladed propellers that were designed for efficient cruise operation at a Mach number of 0.8. The data presented is static force data. The effects of power on the configuration characteristics were generally favorable. An arrangement with the propellers rotating with the outboard blades moving down was found to have significantly higher installed thrust than an arrangement with the propellers rotating with the inboard blades moving down. The primary unfavorable effect was a large pitch trim change which occurred with power, but the trim change could be minimized with a proper configuration design. Author

N90-26018# Air Force Inst. of Tech., Wright-Patterson AFB, OH. School of Engineering.
ROBUSTNESS EVALUATION OF H2 AND H(INFINITY) CONTROL THEORY AS APPLIED TO A TRANSPORT AIRCRAFT M.S. Thesis
Randy L. Robinson Mar. 1990 119 p
(AD-A222795; AFIT/GAE/ENY/89D-30) Avail: NTIS HC A06/MF A01 CSCL 12/9

The purpose of this study was to evaluate the performance and stability robustness of a lateral autopilot designed for a transport aircraft using H2 and H(Infinity) control theory. The intent was to design a controller that met performance and robustness specifications over a range of flight conditions. First, a control structure to be used in designing the autopilot was developed. Once this was accomplished, it was formulated into the small gain problem. Controllers were then developed using H2 and H(Infinity) control theory. The final task involved evaluating the controllers developed in a closed loop simulation. GRA

09 RESEARCH AND SUPPORT FACILITIES (AIR)

Includes airports, hangars and runways; aircraft repair and overhaul facilities; wind tunnels; shock tubes; and aircraft engine test stands.

For related information see also *14 Ground Support Systems and Facilities (Space).*

N90-26019*# MCAT Inst., Moffett Field, CA.
SUPERSONIC WIND TUNNEL NOZZLES: A SELECTED, ANNOTATED BIBLIOGRAPHY TO AID IN THE DEVELOPMENT OF QUIET WIND TUNNEL TECHNOLOGY Final Report
Stephen W. D. Wolf Washington Jul. 1990 82 p
(Contract NCC2-604)
(NASA-CR-4294; A-90163; NAS 1.26:4294) Avail: NTIS HC A05/MF A01 CSCL 14B

This bibliography, with abstracts, consists of 298 citations arranged in chronological order. The citations were selected to be

helpful to persons engaged in the design and development of quiet (low disturbance) nozzles for modern supersonic wind tunnels. Author, subject, and corporate source indexes are included to assist with the location of specific information. Author

N90-26020# Wright Research Development Center, Wright-Patterson AFB, OH.
WRIGHT RESEARCH AND DEVELOPMENT CENTER TEST FACILITIES HANDBOOK
Margaret B. Skujins Jan. 1990 309 p
(AD-A222582; AD-E951478; WRDC-TR-90-0001) Avail: NTIS HC A14/MF A02 CSCL 14/2

This handbook contains a listing of Wright Research and Development Center facilities located at Wright-Patterson AFB OH. Facilities included are those of the Materials, Aero Propulsion and Power, Avionics, Flight Dynamics, and Electronic Technology laboratories and the Signature Technology, Technology Exploitation, and Cockpit Integration directorates. Documented listings include information on facility type, capabilities, instrumentation, availability and POC. GRA

12 ASTRONAUTICS (GENERAL)

For extraterrestrial exploration see *91 Lunar and Planetary Exploration.*

N90-26021# General Accounting Office, Washington, DC. National Security and International Affairs Div.
SPACE EXPLORATION: COST, SCHEDULE, AND PERFORMANCE OF NASA'S MARS OBSERVER MISSION. FACT SHEET FOR THE CHAIRMAN, SUBCOMMITTEE ON SCIENCE, TECHNOLOGY, AND SPACE, COMMITTEE ON COMMERCE, SCIENCE, AND TRANSPORTATION, US SENATE
Harry R. Finley May 1988 22 p
(GAO/NSIAD-88-137FS; B-230525) Avail: NTIS HC A03/MF A01; also available from GAO, Gaithersburg, MD HC first five copies free, additional copies $2.00

The Mars Observer mission is the first in a series of planned planetary missions based on a low-cost approach to spacecraft and mission design. The mission's objective is to explore the geology, topography, and climatology of Mars. After a 1-year transit to Mars, the spacecraft is expected to assume a low-altitude polar orbit and to repetitively map the surface and atmosphere of Mars every 59 days for 687 days, which is 1 year on Mars. The mission was originally scheduled to be launched in 1990 and to be completed in 1993. However, NASA decided in April 1987 to delay the launch until 1992 because too many planetary missions were scheduled during the first 2 years of the shuttle's return to service and because of fiscal year 1987 funding constraints. At the start of the project in fiscal year 1985, NASA estimated the total cost of the mission at $292.5 million. In October 1987, the cost estimate was $513.8 million. The estimate rose principally due to additional costs related to future mission studies, engineering and technical assistance in evaluating proposals, communications band development, support for two altimeters, and, after the Challenger accident, replanning the mission and expanding its scope. The initial mission objectives are expected to be fully achieved. In addition, the mission is scheduled to be expanded in several areas. France is supplying an instrument for improving the magnetic field measurements, and NASA has decided to test deep space communications frequencies and equipment on this mission. Furthermore, NASA plans to have the spacecraft take photographs that will be made available to the public because of the increased interest in Mars exploration. J.P.S.

N90-26022# General Accounting Office, Washington, DC. National Security and International Affairs Div.
SPACE EXPLORATION: COST, SCHEDULE, AND PERFORMANCE OF NASA'S MAGELLAN MISSION TO VENUS. FACT SHEET FOR THE CHAIRMAN, SUBCOMMITTEE ON SCIENCE, TECHNOLOGY, AND SPACE, COMMITTEE ON COMMERCE, SCIENCE, AND TRANSPORTATION, US SENATE
Harry R. Finley May 1988 22 p
(GAO/NSIAD-88-130FS; B-230525) Avail: NTIS HC A03/MF A01; also available from GAO, Gaithersburg, MD HC first five copies free, additional copies $2.00

The Magellan mission is intended to investigate the origin and evolution of Venus. The launch date for this mission was originally set for April 1988, and it was scheduled to end in April 1989. Since then the launch date has changed twice. At the start of the project in fiscal year 1984, NASA estimated the project's total cost at $294.6 million, assuming that the spacecraft would be launched by the shuttle in April 1988 and would use a Centaur upper stage to provide propulsion into an interplanetary trajectory. In October 1987, the mission cost estimate was increased about $219 million to $513.5 million, which was a result of launch delays adopting to a new upper stage, accommodating a new trajectory, and problems with the development of the mission's major scientific instrument. The Magellan mission is described, its cost is estimated, its schedule chronicled, and its performance predicted. The mission's objective to map at least 70 percent of the Venus surface is expected to be achieved. J.P.S.

N90-26023# General Accounting Office, Washington, DC. National Security and International Affairs Div.
SPACE EXPLORATION: COST, SCHEDULE, AND PERFORMANCE OF NASA'S ULYSSES MISSION TO THE SUN. FACT SHEET FOR THE CHAIRMAN, SUBCOMMITTEE ON SCIENCE, TECHNOLOGY, AND SPACE, COMMITTEE ON COMMERCE, SCIENCE, AND TRANSPORTATION, US SENATE
Harry R. Finley May 1988 27 p
(GAO/NSIAD-88-129FS; B-230525) Avail: NTIS HC A03/MF A01; also available from GAO, Gaithersburg, MD HC first five copies free, additional copies $2.00

The Ulysses mission, previously known as the International Solar Polar Mission, is a joint NASA/ESA project. It is the first and only planned mission to observe the remote polar region of the sun. Its objective is to study the three-dimensional structure and dynamics of the solar chromosphere and corona, heliosphere, and interstellar medium, to provide a better understanding of the effects of solar activity on the earth's weather and climate. As originally conceived, the mission was to use two spacecrafts: one developed by NASA and one developed by ESA, and more than 200 scientists from 65 universities and research centers in 13 countries. Because of budget reductions, NASA canceled its spacecraft resulting in the elimination of about one-half of the science instruments to be flown and about 80 U.S. and European investigators from the project, the opportunity to perform simultaneous observations in both solar hemispheres and stereoscopic observations from two vantage points in the heliosphere, and the ability to perform white light, x ray, and ultraviolet measurements of various coronal phenomena. A unique aspect of this mission is that it will be the first solar exploration to use an out-of-ecliptic trajectory. Previous solar studies have been limited to solar observations in the ecliptic plane where solar wind phenomena is very complex and difficult to understand. Since the project's inception, the launch date has been delayed three times. The original mission objective will not be fully achieved, primarily due to the cancellation of the NASA spacecraft. J.P.S.

N90-26024# General Accounting Office, Washington, DC. Information Management and Technology Div.
SPACE PROGRAM: SPACE DEBRIS A POTENTIAL THREAT TO SPACE STATION AND SHUTTLE
Stephen A. Schwartz, Ronald W. Beers, Colleen M. Phillips, and Yvette Ramos Apr. 1990 38 p
(GAO/IMTEC-90-18; B-237832) Avail: NTIS HC A03/MF A01; also available from GAO, Gaithersburg, MD HC first five copies free, additional copies $2.00

Experts estimate that more than 3.5 million man-made objects are orbiting the earth. These objects - space debris - include whole and fragmentary parts of rocket bodies and other discarded equipment from space missions. About 24,500 of these objects are 1 centimeter across or larger. A 1-centimeter man-made object travels in orbit at roughly 22,000 miles per hour. If it hit a spacecraft,

it would do about the same damage as would a 400-pound safe traveling at 60 miles per hour. The Government Accounting Office (GAO) reviews NASA's plans for protecting the space station from debris, the extent and precision of current NASA and Defense Department (DOD) debris-tracking capabilities, and the extent to which debris has already affected shuttle operations. GAO recommends that the space debris model be updated, and that the findings be incorporated into the plans for protecting the space station from such debris. GAO further recommends that the increased risk from debris to the space shuttle operations be analyzed. J.P.S.

N90-26025# General Accounting Office, Washington, DC. National Security and International Affairs Div.
SPACE EXPLORATION: COST, SCHEDULE, AND PERFORMANCE OF NASA'S GALILEO MISSION TO JUPITER. FACT SHEET FOR THE CHAIRMAN, SUBCOMMITTEE ON SCIENCE, TECHNOLOGY, AND SPACE, COMMITTEE ON COMMERCE, SCIENCE, AND TRANSPORTATION, US SENATE
Harry R. Finley May 1988 34 p
(GAO/NSIAD-88-138FS; B-230525) Avail: NTIS HC A03/MF A01

The objectives of the Galileo mission are to investigate the chemical composition and physical state of Jupiter's atmosphere and satellites and to study the structure and physical dynamics of Jupiter's magnetosphere, that is its magnetic field. The launch date, originally scheduled for January 1982, has been delayed by over 7 years. Under previous launch schedules, the shortest cruise time - the amount of time it takes a spacecraft to reach its destination - to Jupiter was 26 months; now, under the current launch schedule, the cruise time to Jupiter, will be 72 months, an increase of almost 4 years. At the start of the project in fiscal year 1978, NASA estimated its total cost at $410.1 million. In October 1987, the cost estimate was $1,362.5 million. The increase in the cost estimate was primarily due to Shuttle launch delays, changes to the upper stage, which provides the propulsion for interplanetary trajectory, and the Challenger accident. According to the project staff, this mission is expected to exceed its initial objectives. The launch delays and the extended cruise time have allowed NASA to expand the scope of the scientific investigations and to add or enhance scientific instruments. J.P.S.

N90-26026*# Maryland Univ., College Park. Dept. of Aerospace Engineering.
PROJECT EXODUS Final Report, 23 Jan. - 14 May 1990
Rodney Bryant, comp. and ed., Jennifer Dillon, comp. and ed., George Grewe, comp. and ed., Jim McMorrow, comp. and ed., Craig Melton, comp. and ed., Gerald Rainey, comp. and ed., John Rinko, comp. and ed., David Singh, comp. and ed., and Tzu-Liang Yen, comp. and ed. May 1990 200 p
(Grant NGT-21-002-800)
(NASA-CR-186836; NAS 1.26:186836; ENAE-412; UM-AERO-90-28) Avail: NTIS HC A09/MF A02 CSCL 22A

A design for a manned Mars mission, PROJECT EXODUS is presented. PROJECT EXODUS incorporates the design of a hypersonic waverider, cargo ship and NIMF (nuclear rocket using indigenous Martian fuel) shuttle lander to safely carry out a three to five month mission on the surface of Mars. The cargo ship transports return fuel, return engine, surface life support, NIMF shuttle, and the Mars base to low Mars orbit (LMO). The cargo ship is powered by a nuclear electric propulsion (NEP) system which allows the cargo ship to execute a spiral trajectory to Mars. The waverider transports ten astronauts to Mars and back. It is launched from the Space Station with propulsion provided by a chemical engine and a delta velocity of 9 km/sec. The waverider performs an aero-gravity assist maneuver through the atmosphere of Venus to obtain a deflection angle and increase in delta velocity. Once the waverider and cargo ship have docked the astronauts will detach the landing cargo capsules and nuclear electric power plant and remotely pilot them to the surface. They will then descend to the surface aboard the NIMF shuttle. A dome base will be quickly constructed on the surface and the astronauts will conduct an exploratory mission for three to five months. They will return to Earth and dock with the Space Station using the waverider. Author

N90-26027*# Maryland Univ., College Park. Dept. of Aerospace Engineering.
TERRAPIN TECHNOLOGIES MANNED MARS MISSION PROPOSAL Report, 23 Jan. - 14 May 1990
Michael Amato, Heather Bryant, Rodney Coleman, Chris Compy, Patrick Crouse, Joe Crunkleton, Edgar Hurtado, Eirik Iverson, Mike Kamosa, and Lauri Kraft, ed. and comp. et al May 1990 208 p
(Grant NGT-21-002-800)
(NASA-CR-186838; NAS 1.26:186838; ENAE-412; UM-AERO-90-27) Avail: NTIS HC A10/MF A02 CSCL 22A

A Manned Mars Mission (M3) design study is proposed. The purpose of M3 is to transport 10 personnel and a habitat with all required support systems and supplies from low Earth orbit (LEO) to the surface of Mars and, after an eight-man surface expedition of 3 months, to return the personnel safely to LEO. The proposed hardware design is based on systems and components of demonstrated high capability and reliability. The mission design builds on past mission experience, but incorporates innovative design approaches to achieve mission priorities. Those priorities, in decreasing order of importance, are safety, reliability, minimum personnel transfer time, minimum weight, and minimum cost. The design demonstrates the feasibility and flexibility of a Waverider transfer module. Author

13 ASTRODYNAMICS

Includes powered and free-flight trajectories; and orbital and launching dynamics.

N90-26028*# National Aeronautics and Space Administration. Marshall Space Flight Center, Huntsville, AL.
FORBIDDEN TANGENTIAL ORBIT TRANSFERS BETWEEN INTERSECTING KEPLERIAN ORBITS
Rowland E. Burns Jul. 1990 53 p
(NASA-TP-3031; NAS 1.60:3031) Avail: NTIS HC A04/MF A01 CSCL 22A

The classical problem of tangential impulse transfer between coplanar Keplerian orbits is addressed. A completely analytic solution which does not rely on sequential calculation is obtained and this solution is used to demonstrate that certain initially chosen angles can produce singularities in the parameters of the transfer orbit. A necessary and sufficient condition for such singularities is that the initial and final orbits intersect. Author

N90-26029# GKSS-Forschungszentrum Geesthacht (Germany, F.R.). Inst. fuer Physik.
ATMOSPHERIC CORRECTION OF THEMATIC MAPPING MEASUREMENTS ABOUT SEABEDS OF THE GERMAN BAY [ATMOSPHAERENKORREKTUR VON THEMATIC MAPPER-MESSUNGEN UEBER WATTENGEBEITEN DER DEUTSCHEN BUCHT]
O. Krueger 17 Nov. 1989 106 p In GERMAN; ENGLISH summary Original contains color illustrations
(GKSS-89/E/47; ISSN-0344-9629; ETN-90-96970) Copyright Avail: NTIS HC A06/MF A01

Data from Thematic Mapper, a scanning radiometer on board the Earth surface observing satellite LANDSAT 5, are simulated with a radiative transfer model. The transfer code, the matrix-operator-method (Fischer, 1983), is applied to data from different Earth surfaces. On the basis of Gordon's method for atmospheric correction over water, an algorithm was developed to correct for the influence of aerosols, air molecules and atmospheric trace gases on Thematic Mapper data from measurements over land surfaces. The optical thickness of a cloud-free atmosphere was therefore varied for different aerosoltypes and surface reflectances. ESA

N90-26219*# Jet Propulsion Lab., California Inst. of Tech., Pasadena. Tracking Systems and Applcations Section.
A REDUCED-DYNAMIC TECHNIQUE FOR PRECISE ORBIT DETERMINATION
S. C. Wu, T. P. Yunck, and C. L. Thornton *In its* The Telecommunications and Data Acquisition Report 15 May 1990 p 13-25 (For primary document see N90-26217 20-32)
Avail: NTIS HC A10/MF A02 CSCL 22A

14 GROUND SUPPORT SYSTEMS AND FACILITIES (SPACE)

Includes launch complexes, research and production facilities; ground support equipment, e.g., mobile transporters; and simulators.

For related information see also *09 Research and Support Facilities (Air).*

N90-26030*# National Aeronautics and Space Administration. Lewis Research Center, Cleveland, OH.
NATIONAL SPACE TEST CENTERS, LEWIS RESEARCH CENTER FACILITIES
Ronald R. Roskilly 1990 7 p Proposed for presentation at the Space Programs and Technologies Conference, Huntsville, AL, 25-27 Sep. 1990; sponsored by AIAA
(NASA-TM-103187; E-5570; NAS 1.15:103187; AIAA-90-3593)
Avail: NTIS HC A02/MF A01 CSCL 14B

The Lewis Research Center, NASA, presently has a number of test facilities that constitute a significant national space test resource. It is expected this capability will continue to find wide application in work involving this country's future in space. Testing from basic research to applied technology, to systems development, to ground support will be performed, supporting such activities as Space Station Freedom, the Space Exploration Initiative, Mission to Planet Earth, and many others. The major space test facilities at both Cleveland and Lewis' Plum Brook Station are described. Primary emphasis is on space propulsion facilities; other facilities of importance in space power and microgravity are also included. Author

15 LAUNCH VEHICLES AND SPACE VEHICLES

Includes boosters; operating problems of launch/space vehicle systems; and reusable vehicles.

For related information see also *20 Spacecraft Propulsion and Power.*

N90-26031# Sandia National Labs., Albuquerque, NM.
GUIDANCE AND TARGETING FOR THE STRATEGIC TARGET SYSTEM
John E. White 20 Nov. 1989 10 p Presented at the 1990 Guidance, Navigation, and Control Conference, Portland, OR, 20-22 Aug. 1990
(Contract DE-AC04-76DP-00789)
(DE90-005239; SAND-89-2928C; CONF-900861-1) Avail: NTIS HC A02/MF A01

Guidance algorithms and targeting procedures for the Strategic Target System (STARS) launch vehicle are described. The STARS vehicle is a three stage booster, based partly upon retired Polaris A3 missile assets, which is intended to support development and testing of the Strategic Defense Initiative by delivering target payloads to the vicinity of the Kwajalein Atoll. STARS will be launched from the Kauai Test Facility located on Kauai, Hawaii. The STARS guidance objective is to deliver payloads to a prescribed target location with maximum accuracy at intercontinental ballistic missile velocities. The guidance problem is complicated by the fact that all three stages lack thrust termination or other velocity control mechanisms, and by range safety requirements for one or more out-of-plane turns. Mission objectives are achieved with a combination of guidance algorithms. The original Polaris guidance is used during the atmospheric ascent phase. The powered-explicit-guidance used by the Space Shuttle is later employed to execute an out-of-plane turn and to place the third stage as closely as possible into the desired coast trajectory. Third stage targeting is a modified Lambert procedure formulated to eliminate the target miss due to off-nominal ascent phase performance. Active guidance is also used during the third stage burn to maximize the delivery accuracy. DOE

N90-26032*# National Aeronautics and Space Administration. Langley Research Center, Hampton, VA.
ORBITER UTILIZATION AS AN ACRV
Jonathan N. Cruz, Michael L. Heck, Renjith R. Kumar, Daniel D. Mazanek (Analytical Mechanics Associates, Inc., Hampton, VA.), and Patrick A. Troutman Jun. 1990 101 p
(NASA-TM-102700; NAS 1.15:102700) Avail: NTIS HC A06/MF A01 CSCL 22B

Assuming that a Shuttle Orbiter could be qualified to serve long duration missions attached to Space Station Freedom in the capacity as an Assured Crew Return Vehicle (ACRV), a study was conducted to identify and examine candidate attach locations. Baseline, modified hardware, and new hardware design configurations were considered. Dual simultaneous Orbiter docking accommodation were required. Resulting flight characteristics analyzed included torque equilibrium attitude (TEA), microgravity environment, attitude controllability, and reboost fuel requirements. The baseline Station could not accommodate two Orbiters. Modified hardware configurations analyzed had large TEA's. The utilization of an oblique docking mechanism best accommodated an Orbiter as an ACRV. Author

N90-26033*# Draper (Charles Stark) Lab., Inc., Cambridge, MA.
TRAJECTORY OPTIMIZATION FOR AN ASYMMETRIC LAUNCH VEHICLE M.S. Thesis - MIT
Jeanne Marie Sullivan Jun. 1990 125 p
(Contract NAS9-18147)
(NASA-CR-185630; NAS 1.26:185630; CSDL-T-1062) Copyright Avail: NTIS HC A06/MF A01 CSCL 22B

A numerical optimization technique is used to fully automate the trajectory design process for an symmetric configuration of the proposed Advanced Launch System (ALS). The objective of the ALS trajectory design process is the maximization of the vehicle mass when it reaches the desired orbit. The trajectories used were based on a simple shape that could be described by a small set of parameters. The use of a simple trajectory model can significantly reduce the computation time required for trajectory optimization. A predictive simulation was developed to determine the on-orbit mass given an initial vehicle state, wind information, and a set of trajectory parameters. This simulation utilizes an idealized control system to speed computation by increasing the integration time step. The conjugate gradient method is used for the numerical optimization of on-orbit mass. The method requires only the evaluation of the on-orbit mass function using the predictive simulation, and the gradient of the on-orbit mass function with respect to the trajectory parameters. The gradient is approximated with finite differencing. Prelaunch trajectory designs were carried out using the optimization procedure. The predictive simulation is used in flight to redesign the trajectory to account for trajectory deviations produced by off-nominal conditions, e.g., stronger than expected head winds. Author

N90-26034# National Aerospace Lab., Tokyo (Japan).
PERFORMANCE EVALUATION OF LE-7 HIGH PRESSURE PUMPS
Makoto Yoshida, Kenjiro Kamijo, and Ryuji Nagao Jun. 1989 10 p In JAPANESE; ENGLISH summary
(DE90-505523; NAL-TR-1031; ISSN-0389-4010) Avail: NTIS (US Sales Only) HC A02/MF A01

As a part of the development of the large high pressure liquid oxygen/liquid hydrogen (LOX/H2) engine (LE-7) of the large launch vehicle H-II, to evaluate the performance of large flow rate high delivery pressure cryogenic pumps, an efficiency and head similar

to a polytropic efficiency and head for gas compressors were proposed as the evaluation index of pumps for compressible hydrogen. The defined efficiency and head were obtained by accumulating adiabatic heads between two isobars in close proximity to each other in a compression stroke, under the assumption, liquid was compressed at an equal adiabatic efficiency in the region between two isobars. As the relation among delivery pressure, the number of isobars and the difference between the adiabatic and defined efficiency was calculated, there were extremely large efficiency differences in liquid hydrogen. The defined efficiency and head were fairly close to the test data of the LE-7 cryogenic pumps. DOE

N90-26035# Aeritalia S.p.A., Turin (Italy). Space Systems Group.
IRIS SYSTEM AND FUTURE APPLICATION TO EXPANDABLE LAUNCHERS
Luigi Bussolino, Franco Varesio, Giovanni Rum, and Claudio Portelli (Italian Space Agency, Rome.) 1989 9 p Presented at 40th IAF Conference, Malaga, Spain, 7-13 Oct. 1989 Previously announced in IAA as A90-13375
(IAF-89-212; ETN-90-97272) Avail: NTIS HC A02/MF A01

The Italian Research Interim Stage (IRIS) is described. It consists of a Shuttle upper stage system designed to inject light payloads up to 900 kg mass from the Shuttle circular parking orbit into a geostationary transfer orbit. A summary of the information included in the IRIS user's manual provides users with the necessary performance data, environment and interfaces for their payloads. A review of the status of the project is presented. The first flight unit will be launched in Aug. 1991. ESA

16 SPACE TRANSPORTATION

Includes passenger and cargo space transportation, e.g., shuttle operations; and space rescue techniques.

For related information see also *03 Air Transportation and Safety* and *18 Spacecraft Design, Testing and Performance.* For space suits see *54 Man/System Technology and Life Support.*

N90-26036*# National Aeronautics and Space Administration. Langley Research Center, Hampton, VA.
THE EFFECT OF INTERPLANETARY TRAJECTORY OPTIONS ON A MANNED MARS AEROBRAKE CONFIGURATION
Robert D. Braun, Richard W. Powell, and Lin C. Hartung Washington Aug. 1990 79 p
(NASA-TP-3019; L-16661; NAS 1.60:3019) Avail: NTIS HC A05/MF A01 CSCL 22B

Manned Mars missions originating in low Earth orbit (LEO) in the time frame 2010 to 2025 were analyzed to identify preferred mission opportunities and their associated vehicle and trajectory characteristics. Interplanetary and Mars atmospheric trajectory options were examined under the constraints of an initial manned exploration scenario. Two chemically propelled vehicle options were considered: (1) an all propulsive configuration, and (2) a configuration which employs aerobraking at Earth and Mars with low lift/drag (L/D) shapes. Both the interplanetary trajectory options as well as the Mars atmospheric passage are addressed to provide a coupled trajectory simulation. Direct and Venus swingby interplanetary transfers with a 60 day Mars stopover are considered. The range and variation in both Earth and Mars entry velocity are also defined. Two promising mission strategies emerged from the study: (1) a 1.0 to 2.0 year Venus swingby mission, and (2) a 2.0 to 2.5 year direct mission. Through careful trajectory selection, 11 mission opportunities are identified in which the Mars entry velocity is between 6 and 10 km/sec and Earth entry velocity ranges from 11.5 to 12.5 km/sec. Simulation of the Earth return aerobraking maneuver is not performed. It is shown that a low L/D configuration is not feasible for Mars aerobraking without substantial improvements in the interplanetary navigation system. However, even with an advanced navigation system, entry corridor and aerothermal requirements restrict the number of potential mission opportunities. It is also shown that for a large blunt Mars aerobrake configuration, the effects of radiative heating can be significant at entry velocities as low as 6.2 km/sec and will grow to dominate the aerothermal environment at entry velocities above 8.5 km/sec. Despite the additional system complexity associated with an aerobraking vehicle, the use of aerobraking was shown to significantly lower the required initial LEO weight. In comparison with an all propulsive mission, savings between 19 and 59 percent were obtained depending upon launch date. Author

N90-26037# Astron Research and Engineering, Santa Monica, CA.
VIBRATION TEST PROCEDURES FOR ORBITER SIDEWALL-MOUNTED PAYLOADS, PHASE 1 Final Report
Allan G. Piersol, Pritchard H. White, Emma G. Wilby, John F. Wilby, and P. J. Hipol Nov. 1988 204 p
(Contract F04701-87-C-0010)
(AD-A220773; Rept-7114-01-Phase-1) Avail: NTIS HC A10/MF A02

Mechanical vibration tests of payloads mounted on the Space Shuttle Vehicle (SSV) cargo bay sidewall are currently performed in compliance with USAF Space Division Document SD-CF-0206, which specifies an acceleration level at the inputs to the payload. This procedure does not take into account the loading of the sidewall structure by the payload where the payload apparent weight becomes large. The result is potentially severe overtesting of payloads at their resonance frequencies where payload damage is most likely. A new mechanical vibration test procedure was developed that takes into account the mounting point impedance of the sidewall structure, and allows a well defined reduction of notching of the input acceleration levels at payload resonances based upon an input force limit to the payload. The validity and practicality of the procedure was demonstrated by experiments on a simulated OASIS payload with an adaptive payload carrier (APC). A complete vibration tests specification detailing the procedure is presented. GRA

N90-26038# Astron Research and Engineering, Santa Monica, CA.
VIBRATION TEST PROCEDURES FOR ORBITER SIDEWALL-MOUNTED PAYLOADS, PHASE 2 Final Report, period ending Jan. 1989
Allan G. Piersol, Pritchard H. White, Emma G. Wilby, and John F. Wilby 1 Feb. 1989 160 p
(Contract F04701-87-C-0010)
(AD-A220774; Rept-7114-02-Phase-2) Avail: NTIS HC A08/MF A01

Mechanical vibration tests of payloads mounted on the Space Shuttle Vehicle (SSV) cargo bay sidewall are currently performed in compliance with the USAF Space Division. This procedure does not take into account the loading of the sidewall structure by the payload at the resonance frequencies of the payload where the payload apparent weight becomes large. The result is potentially severe overtesting of payloads at their resonance frequencies where payload damage is most likely. The recommended testing procedure is reviewed. Also discussed are the source apparent weight functions and the experimental studies (test set-up, instrumentation, calibration, data analysis, and exploratory tests and results). B.G.

N90-26039*# Pennsylvania State Univ., University Park. Dept. of Aerospace Engineering.
PRELIMINARY SUBSYSTEM DESIGNS FOR THE ASSURED CREW RETURN VEHICLE (ACRV), VOLUME 1 Final Report
Jun. 1990 589 p Presented at the 1990 Annual Summer Conference, Cleveland, OH, 11-15 Jun. 1990
(Contract NASw-4435)
(NASA-CR-186677-Vol-1; NAS 1.26:186677-Vol-1) Avail: NTIS HC A25/MF A04 CSCL 22B

A series of design studies is presented concerning the Assured Crew Return Vehicle (ACRV) for Space Station Freedom. Four alternate designs are presented for the ACRV braking and landing system. Options presented include: ballistic and lifting body

reentries; the use of high-lift, high-payload aerodynamic decelerators, as well as conventional parachutes; landing systems designed for water landings, land landings, or both; and an aerial recovery system. All four design options presented combine some or all of the above attributes, and all meet performance requirements established by the ACRV Program Office. Two studies of ACRV growth options are also presented. Use of the ACRV or a similarly designed vehicle in several roles for possible future space missions is discussed, along with the required changes to a basic ACRV to allow it to perform these missions optimally. The outcome of these studies is a set of recommendations to the ACRV Program Office describing the vehicle characteristics of the basic ACRV which lend themselves most readily to be adapted for use in other missions. Finally, the impacts on the design of the ACRV due to its role as a medical emergency vehicle were studied and are presented. The use of the ACRV in this manner will impact its shape, internal configuration, and equipment.

Author

N90-26040*# National Aeronautics and Space Administration. John F. Kennedy Space Center, Cocoa Beach, FL.

DEBRIS/ICE/TPS ASSESSMENT AND PHOTOGRAPHIC ANALYSIS FOR SHUTTLE MISSION STS-31R

Gregory N. Katnik, Scott A. Higginbotham, and J. Bradley Davis Jun. 1990 172 p Original contains color illustrations

(NASA-TM-102790; NAS 1.15:102790) Avail: NTIS HC A08/MF A01; 68 functional color pages CSCL 22B

A Debris/Ice/Thermal Protection System (TPS) assessment and photographic analysis was conducted for Space Shuttle Mission STS-31R. Debris inspections of the flight elements and launch pad are performed before and after launch. Ice/frost conditions on the External Tank are assessed by the use of computer programs, nomographs, and infrared scanner data during cryogenic loading of the vehicle followed by on-pad visual inspection. High speed photography is analyzed after launch to identify ice/debris sources and evaluate potential vehicle damage and/or in-flight anomalies. The debris/ice/TPS conditions and photographic analysis of Mission STS-31R, is presented along with their overall effect on the Space Shuttle Program.

Author

N90-26041# General Accounting Office, Washington, DC. National Security and International Affairs Div.

SPACE TRANSPORTATION: NASA HAS NO FIRM NEED FOR INCREASINGLY COSTLY ORBITAL MANEUVERING VEHICLE

Charles Rey and James Morrison Jul. 1990 32 p

(GAO/NSIAD-90-192; B-239570) Avail: NTIS HC A03/MF A01; also available from GAO, Gaithersburg, MD HC first five copies free, additional copies $2.00

The General Accounting Office's (GAO) findings on the Orbital Maneuvering Vehicle (OMV) are described. It was to be a multipurpose space tug used to transport satellites from the space shuttle to other orbits, reboost them when their orbits decayed, retrieve and return them to the shuttle when they malfunctioned, and control their reentry into the atmosphere when their useful lives expired. Subsequent OMV enhancements would enable it to refuel satellites in orbit, perform in-orbit satellite repairs, and rescue out-of-control satellites. The OMV was to operate initially from the shuttle's cargo bay but would ultimately operate from the Space Station Freedom. OMV was designed to be a free-flying, remotely controlled propulsion stage about 15 feet in diameter and 6 feet thick, that would be carried into orbit inside the shuttle's cargo bay. Once separated from the shuttle, the OMV would be remotely controlled by astronauts working at consoles on earth. GAO found that a firm requirement for the OMV to accomplish the scheduled missions does not exist. Also the estimated cost has greatly increased while the OMV's capabilities have significantly decreased. GAO recommended that the OMV program be terminated, which NASA did following the receipt of GAO's draft report.

J.P.S.

N90-26042*# Virginia Polytechnic Inst. and State Univ., Blacksburg. Dept. of Aerospace and Ocean Engineering.

PROJECT LOCOST: LASER OR CHEMICAL HYBRID ORBITAL SPACE TRANSPORT

Alan Dixon, Alicia Kost, Gregory Lampshire, Rob Larsen, Bob Monahan, and Geoff Wright 19 Jun. 1990 115 p

(Grant NGT-21-002-800)

(NASA-CR-186822; NAS 1.26:186822) Avail: NTIS HC A06/MF A01 CSCL 22B

A potential mission in the late 1990s is the servicing of spacecraft assets located in GEO. The Geosynchronous Operations Support Center (GeoShack) will be supported by a space transfer vehicle based at the Space Station (SS). The vehicle will transport cargo between the SS and the GeoShack. A proposed unmanned, laser or chemical hybrid orbital space transfer vehicle (LOCOST) can be used to efficiently transfer cargo between the two orbits. A preliminary design shows that an unmanned, laser/chemical hybrid vehicle results in the fuel savings needed while still providing fast trip times. The LOCOST vehicle receives a 12 MW laser beam from one Earth orbiting, solar pumped, iodide Laser Power Station (LPS). Two Energy Relay Units (ERU) provide laser beam support during periods of line-of-sight blockage by the Earth. The baseline mission specifies a 13 day round trip transfer time. The ship's configuration consist of an optical train, one hydrogen laser engine, two chemical engines, a 18 m by 29 m box truss, a mission-flexible payload module, and propellant tanks. Overall vehicle dry mass is 8,000 kg. Outbound cargo mass is 20,000 kg, and inbound cargo mass is 6,000 kg. The baseline mission needs 93,000 kg of propellants to complete the scenario. Fully fueled, outbound mission mass is 121,000 kg. A regeneratively cooled, single plasma, laser engine design producing a maximum of 768 N of thrust is utilized along with two traditional chemical engines. The payload module is designed to hold 40,000 kg of cargo, though the baseline mission specifies less. A proposed design of a laser/chemical hybrid vehicle provides a trip time and propellant efficient means to transport cargo from the SS to a GeoShack. Its unique, hybrid propulsion system provides safety through redundancy, allows baseline missions to be efficiently executed, while still allowing for the possibility of larger cargo transfers.

Author

N90-26043# Idaho National Engineering Lab., Idaho Falls.

ACOUSTO-OPTIC SIGNATURE ANALYSIS FOR INSPECTION OF THE ORBITER THERMAL PROTECTION TILE BONDS

J. G. Rodriguez, D. M. Tow, and B. A. Barna 1989 14 p Presented at the 2nd Conference on Non-Destructive Evaluation for Aerospace Requirements, Huntsville, AL, 22-24 Aug. 1989

(Contract DE-AC07-76ID-01570)

(DE90-013089; EGG-M-89242; CONF-8908160-3) Avail: NTIS HC A03/MF A01

The goal of this research is to develop a viable NDE technique for the inspection of orbiter thermal protection system (TPS) tile bonds. Phase 2, discussed here, concentrated on developing an empirical understanding of the bonded and unbonded vibration signatures of acreage tiles. Controlled experiments in the laboratory have provided useful information on the dynamic response of TPS tiles. It has been shown that several signatures are common to all the pedigree tiles. This degree of consistency in the tile-SIP (strain isolation pad) dynamic response proves that an unbond can be detected for a known tile and establish the basis for extending the analysis capability to arbitrary tiles for which there are no historical data. The field tests of the noncontacting laser acoustic sensor system, conducted at Kennedy Space Center (KSC), investigated the vibrational environment of the Orbiter Processing Facility (OPF) and its effect on the measurement and analysis techniques being developed. The data collected showed that for orbiter locations, such as the body flap and elevon, the data analysis scheme, and/or the sensor, will require modification to accommodate the ambient motion. Several methods have been identified for accomplishing this, and a solution is seen as readily achievable. It was established that the tile response was similar to that observed in the laboratory. Of most importance, however, is that the field environment will not affect the physics of the dynamic response that is related to bond condition. All of this information is fundamental to any future design and development of a prototype system.

DOE

17 SPACE COMM., SPACECRAFT COMM., COMMAND & TRACKING

Includes telemetry; space communications networks; astronavigation and guidance; and radio blackout.

For related information see also *04 Aircraft Communications and Navigation* and *32 Communications and Radar.*

N90-26221*# Jet Propulsion Lab., California Inst. of Tech., Pasadena. Navigation Systems Section.
APPLICATIONS OF DIFFERENT DESIGN METHODOLOGIES IN NAVIGATION SYSTEMS AND DEVELOPMENT AT JPL
S. W. Thurman *In its* The Telecommunications and Data Acquisition Report 15 May 1990 p 39-49 (For primary document see N90-26217 20-32)
Avail: NTIS HC A10/MF A02 CSCL 17G

18 SPACECRAFT DESIGN, TESTING AND PERFORMANCE

Includes satellites; space platforms; space stations; spacecraft systems and components such as thermal and environmental controls; and attitude controls.

For life support systems see *54 Man/System Technology and Life Support.* For related information see also *05 Aircraft Design, Testing and Performance, 39 Structural Mechanics,* and *16 Space Transportation.*

N90-26044*# Arizona Univ., Tucson.
AUTONOMOUS SPACE PROCESSOR FOR ORBITAL DEBRIS Final Report, 1989 - 1990
Kumar Ramohalli, David Campbell, Micky Marine, Mohamad Saad, Daniel Bertles, and Dave Nichols 1990 101 p Presented at the Universities Space Research Association Summer Conference, Cleveland, OH, 12-15 Jun. 1990
(Contract NASw-4435)
(NASA-CR-186691; NAS 1.26:186691) Avail: NTIS HC A06/MF A01 CSCL 22B

Advanced designs are being continued to develop the ultimate goal of a GETAWAY special to demonstrate economical removal of orbital debris utilizing local resources in orbit. The fundamental technical feasibility was demonstrated in 1988 through theoretical calculations, quantitative computer animation, a solar focal point cutter, a robotic arm design and a subcase model. Last year improvements were made to the solar cutter and the robotic arm. Also performed last year was a mission analysis which showed the feasibility of retrieve at least four large (greater than 1500 kg) pieces of debris. Advances made during this reporting period are the incorporation of digital control with the existing placement arm, the development of a new robotic manipulator arm, and the study of debris spin attenuation. These advances are discussed.
Author

N90-26045*# Longhorn Satellite Co., Austin, TX.
TEXSTAR: THE ALL-TEXAS EDUCATIONAL SATELLITE SYSTEM
7 May 1990 79 p
(Contract NASw-4435)
(NASA-CR-186654; NAS 1.26:186654; RFP-ASE274L-S90)
Avail: NTIS HC A05/MF A01 CSCL 22B

Longhorn Satellite Company (LSC) has designed Texstar, and educational satellite communications system which will be considered as a means of equalizing the distribution of educational resources throughout the state of Texas. Texstar will be capable of broadcasting live lectures and documentaries in addition to transmitting data from a centralized receiving-transmitting station. Included in the design of Texstar is the system and subsystem design for the satellite and the design of the ground stations. The launch vehicle used will be the Texas-built Conestoga 421-48. The Texstar system incorporates three small satellites in slightly inclined geosynchronous orbits. Due to the configuration and spacing of these satellites, the system will be accessed as if it were one large, geostationary satellite. Texstar is shown to be a viable option to the educational crisis in the state of Texas.
Author

N90-26046*# Harris Corp., Melbourne, FL. Government Aerospace Systems Div.
DESIGN AND IMPLEMENTATION OF ROBUST DECENTRALIZED CONTROL LAWS FOR THE ACES STRUCTURE AT MARSHALL SPACE FLIGHT CENTER Final Report, 30 Jan. 1989 - 40 Apr. 1990
Emmanuel G. Collins, Jr., Douglas J. Phillips, and David C. Hyland Washington Jul. 1990 76 p
(Contract NAS1-18872)
(NASA-CR-4310; NAS 1.26:4310) Avail: NTIS HC A05/MF A01 CSCL 22B

Many large space system concepts will require active vibration control to satisfy critical performance requirements such as line-of-sight accuracy. In order for these concepts to become operational it is imperative that the benefits of active vibration control be practically demonstrated in ground based experiments. The results of the experiment successfully demonstrate active vibration control for a flexible structure. The testbed is the Active Control Technique Evaluation for Spacecraft (ACES) structure at NASA Marshall Space Flight Center. The ACES structure is dynamically traceable to future space systems and especially allows the study of line-of-sight control issues.
Author

N90-26047*# Boeing Aerospace Co., Huntsville, AL.
PLANNING FOR SPACE STATION FREEDOM LABORATORY PAYLOAD INTEGRATION
Harvey J. Willenberg and Larry P. Torre 1989 15 p Presented in Nashville, TN, 5-10 Mar. 1989
(Contract NAS8-50000)
(NASA-CR-186751; NAS 1.26:186751) Avail: NTIS HC A03/MF A01 CSCL 22B

Space Station Freedom is being developed to support extensive missions involving microgravity research and applications. Requirements for on-orbit payload integration and the simultaneous payload integration of multiple mission increments will provide the stimulus to develop new streamlined integration procedures in order to take advantage of the increased capabilities offered by Freedom. The United States Laboratory and its user accommodations are described. The process of integrating users' experiments and equipment into the United States Laboratory and the Pressurized Logistics Modules is described. This process includes the strategic and tactical phases of Space Station utilization planning. The support that the Work Package 01 Utilization office will provide to the users and hardware developers, in the form of Experiment Integration Engineers, early accommodation assessments, and physical integration of experiment equipment, is described. Plans for integrated payload analytical integration are also described.
Author

N90-26048*# Alabama Univ., Huntsville.
[LITERATURE CONCERNING CONTROL AND DISPLAY TECHNOLOGY APPLICABLE TO THE ORBITAL MANEUVERING VEHICLE (OMV)]
24 Jul. 1990 168 p
(Grant NAG8-706)
(NASA-CR-186790; NAS 1.26:186790) Avail: NTIS HC A08/MF A01 CSCL 22B

A review is presented of the literature concerning control and display technology that is applicable to the Orbital Maneuvering Vehicle (OMV), a system being developed by NASA that will enable the user to remotely pilot it during a mission in space. In addition to the general review, special consideration is given to virtual image displays and their potential for use in the system, and a preliminary partial task analysis of the user's functions is also presented.
Author

N90-26049*# Illinois Univ., Urbana-Champaign. Dept. of Aeronautical and Astronautical Engineering.
NASA/USRA UNIVERSITY ADVANCED DESIGN PROGRAM AT THE UNIVERSITY OF ILLINOIS FOR THE 1989-1990 ACADEMIC YEAR Final Report
Andrew Koepke and Kenneth Sivier 29 Jun. 1990 32 p
(Grant NGT-21-002-800)
(NASA-CR-186829; NAS 1.26:186829) Avail: NTIS HC A03/MF A01 CSCL 22B

The University's design project, the Unmanned Probe to Pluto, is reviewed. Forty-two students divided into seven groups, participated in the program. A presentation, prepared by three students and a graduate teaching assistant for the program's summer conference, summarized the project results. Author

N90-26050*# Minnesota Univ., Minneapolis. Dept. of Aerospace Engineering and Mechanics.
WINGED CARGO RETURN VEHICLE. VOLUME 1: CONCEPTUAL DESIGN NASA/USRA Advanced Design Project
2 Jun. 1990 270 p
(Grant NGT-21-002-800)
(NASA-CR-186823; NAS 1.26:186823) Avail: NTIS HC A12/MF A02 CSCL 22B

The Advanced Design Project (ADP) allows an opportunity for students to work in conjunction with NASA and other aerospace companies on NASA Advanced Design Projects. The following volumes represent the design report: Volume 1 Conceptual Design; Volume 2 Wind Tunnel Tests; Volume 3 Structural Analysis; and Volume 4 Water Tunnel Tests. The project chosen by the University of Minnesota in conjunction with NASA Marshall Space Flight Center for this year is a Cargo Return Vehicle (CRV) to support the Space Station Freedom. The vehicle is the third generation of vehicles to be built by NASA, the first two being the Apollo program, and the Space Shuttle program. The CRV is to work in conjunction with a personnel launch system (PLS) to further subdivide and specialize the vehicles that NASA will operate in the year 2000. The cargo return vehicle will carry payload to and from the Space Station Freedom (SSF). Author

N90-26051*# Virginia Polytechnic Inst. and State Univ., Blacksburg. Dept. of Aerospace Engineering.
PROJECT SPARC: SPACE-BASED AEROASSISTED REUSABLE CRAFT
May 1990 155 p
(Grant NGT-21-002-800)
(NASA-CR-186816; NAS 1.26:186816) Avail: NTIS HC A08/MF A01 CSCL 22B

Future United States' space facilities include a Space Station in low Earth orbit (LEO) and a Geosynchronous Operations Support Center, or GeoShack, in geosynchronous orbit (GEO). One possible mode of transfer between the two orbits is an aerobraking vehicle. When traveling from GEO to LEO, the Earth's atmosphere can be used to aerodynamically reduce the velocity of the vehicle, which reduces the amount of propulsive change in velocity required for the mission. An aerobrake is added to the vehicle for this purpose, but the additional mass increases propellant requirements. This increase must not exceed the amount of propellant saved during the aeropass. The design and development of an aerobraking vehicle that will transfer crew and cargo between the Space Station and GeoShack is examined. The vehicle is referred to as Project SPARC, a SPace-based Aeroassisted Reusable Craft. SPARC consists of a removable 45 ft diameter aerobrake, two modified Pratt and Whitney Advanced Expander Engines with a liquid oxygen/liquid hydrogen propellant, a removable crew module with a maximum capacity of five, and standard sized payload bays providing a maximum payload capacity of 28,000 lbm. The aerobrake, a rigid, ellipsoidally blunted elliptical cone, provides lift at zero angle-of-attack due to a 73 deg rake angle, and is covered with a flexible multi-layer thermal protection system. Maximum dry mass of the vehicle without payload is 20,535 lbm, and the maximum propellant requirement is 79,753 lbm at an oxidizer to fuel ratio of 6/1. Key advantages of SPARC include its capability to meet mission changes, and its removable aerobrake and crew module. Author

N90-26052*# Minnesota Univ., Minneapolis. Dept. of Aerospace Engineering and Mechanics.
BICONIC CARGO RETURN VEHICLE WITH AN ADVANCED RECOVERY SYSTEM. VOLUME 1: CONCEPTUAL DESIGN NASA/USRA Advanced Design Project
2 Jun. 1990 231 p
(Grant NGT-21-002-800)
(NASA-CR-186520; NAS 1.26:186520) Avail: NTIS HC A11/MF A02 CSCL 22B

The conceptual design of the biconic Cargo Return Vehicle (CRV) is presented. The CRV will be able to meet all of the Space Station Freedom (SSF's) resupply needs. Worth note is the absence of a backup recovery chute in case of Advanced Recovery System (ARS) failure. The high reliability of ram-air parachutes does not warrant the penalty weight that such a system would create on successful missions. The CRV will launch vertically integrated with an Liquid Rocket Booster (LRB) vehicle and meets all NASA restrictions on fuel type for all phases of the mission. Because of the downscaled Orbital Maneuvering Vehicle (OMV) program, the CRV has been designed to be able to transfer cargo by docking directly to the Space Station Freedom as well as with OMV assistance. The CRV will cover enough crossrange to reach its primary landing site, Edwards Airforce Base, and all secondary landing sites with the exception of one orbit. Transportation back to KSC will be via the Boeing Super Guppy. Due to difficulties with man-rating the CRV, it will not be used in a CERV role. A brief summary of the CRV's specifications is given. Author

N90-26053*# Virginia Polytechnic Inst. and State Univ., Blacksburg. Aerospace Senior Design Team.
THE AEROBRAKING SPACE TRANSFER VEHICLE
Glen Andrews, Brian Carpenter, Steve Corns, Robert Harris, Brian Jun, Bruce Munro, Eric Pulling, Amrit Sekhon, Walt Welton, and A. Jakubowski Apr. 1990 116 p
(Grant NGT-21-002-800)
(NASA-CR-186819; NAS 1.26:186819) Avail: NTIS HC A06/MF A01 CSCL 22B

With the advent of the Space Station and the proposed Geosynchronous Operation Support Center (GeoShack) in the early 21st century, the need for a cost effective, reusable orbital transport vehicle has arisen. This transport vehicle will be used in conjunction with the Space Shuttle, the Space Station, and GeoShack. The vehicle will transfer mission crew and payloads between low earth and geosynchronous orbits with minimal cost. Recent technological advances in thermal protection systems such as those employed in the Space Shuttle have made it possible to incorporate and aerobrake on the transfer vehicle to further reduce transport costs. The research and final design configuration of the aerospace senior design team from VPISU, working in conjunction with NASA, are presented. The topic of aerobraking and focuses on the evolution of an Aerobraking Space Transfer Vehicle (ASTV), is addressed. Author

N90-26054*# National Aeronautics and Space Administration. Lewis Research Center, Cleveland, OH.
COMPARISON OF CURRENTS PREDICTED BY NASCAP/LEO MODEL SIMULATIONS WITH ELEMENTARY LANGMUIR-TYPE BARE PROBE MODELS FOR AN INSULATED CABLE CONTAINING A SINGLE PINHOLE
Joel T. Galofaro Jul. 1990 39 p Original contains color illustrations
(NASA-TM-102486; E-5095; NAS 1.15:102486) Avail: NTIS HC A03/MF A01; 9 functional color pages CSCL 22B

The behavior of a defect in the insulation of a short biased section of cable in a Low Earth Orbit (LEO) space environment was examined. Such studies are of the utmost importance for large space power systems where great quantities of cabling will be deployed. An insulated probe containing a pinhole was placed into a hypothetical high speed LEO plasma. The NASA Charging

Analyzer Program (NASCAP/LEO) was used to explore sheath growth about the probe as a function of applied voltage and to predict I-V behavior. A set of independent current calculations using Langmuir's formulations for concentric spheres and coaxial cylinders were also performed. The case of concentric spheres was here extended to include the case of concentric hemispheres. Several simple Langmuir-type models were then constructed to bracket the current collected by the cable. The space-charge sheath radius and impact parameters were used to determine the proper current regime. I-V curves were plotted for the models and comparisons were made with NASCAP/LEO results. Finally, NASCAP/LEO potential contours and surface cell potential plots were examined to explain interesting features in the NASCAP/LEO I-V curve. Author

N90-26055*# National Aeronautics and Space Administration. Lewis Research Center, Cleveland, OH.

BACKGROUND, CURRENT STATUS, AND PROGNOSIS OF THE ONGOING SLUSH HYDROGEN TECHNOLOGY DEVELOPMENT PROGRAM FOR THE NASP

R. L. DeWitt, T. L. Hardy, M. V. Whalen, G. P. Richter, and T. M. Tomsik 1990 16 p Presented at the 8th World Hydrogen Energy Conference, Honolulu, HI, 22-27 Jul. 1990; sponsored by Hawaii Natural Energy Inst.

(NASA-TM-103220; E-5634; NAS 1.15:103220) Avail: NTIS HC A03/MF A01 CSCL 22B

Among the Hydrogen Projects at the NASA Lewis Research Center (NASA LeRC), is the task of implementing and managing the Slush Hydrogen (SLH2) Technology Program for the United States' National AeroSpace Plane Joint Program Office (NASP JPO). The objectives of this NASA LeRC program are to provide verified numerical models of fluid production, storage, transfer, and feed systems and to provide verified design criteria for other engineered aspects of SLH2 systems germane to a NASP. The pursuit of these objectives is multidimensional, covers a range of problem areas, works these to different levels of depth, and takes advantage of the resources available in private industry, academia, and the U.S. Government. A summary of the NASA LeRC overall SLH2 program plan, is presented along with its implementation, the present level of effort in each of the program areas, some of the results already in hand, and the prognosis for the effort in the immediate future. Author

N90-26056* National Aeronautics and Space Administration, Washington, DC.

TECHNOLOGY FOR LARGE SPACE SYSTEMS: A BIBLIOGRAPHY WITH INDEXES (SUPPLEMENT 22)

Jul. 1990 274 p

(NASA-SP-7046(22); NAS 1.21:7046(22)) Avail: NTIS HC A12 CSCL 22B

This bibliography lists 1077 reports, articles, and other documents introduced into the NASA Scientific and Technical Information System between July 1, 1989 and December 31, 1989. Its purpose is to provide helpful information to the researcher or manager engaged in the development of technologies related to large space systems. Subject areas include mission and program definition, design techniques, structural and thermal analysis, structural dynamics and control systems, electronics, advanced materials, assembly concepts, and propulsion. Author

N90-26057# Institut National Polytechnique, Grenoble (France). Unite Genie Materiel.

HEAVY ION TESTS ON PROGRAMMABLE VLSI Ph.D. Thesis [TEST AUX IONS LOURDS DE VLSI PROGRAMMABLES]

Antoine Provost-Grellier 1989 175 p IN FRENCH; ENGLISH summary

(ETN-90-97254) Avail: NTIS HC A08/MF A01

The natural radiative environment in space was shown to induce anomalies in satellite borne microelectronics. The qualification strategies which allow choice of the less vulnerable circuits are defined. The upset phenomenon is one of the most critical radiative effects on integrated circuits. Different test strategies are shown for programmable integrated circuits. An experimental test equipment was developed and a test methodology approach was validated by experiments using different heavy ion simulators. ESA

N90-26058# Aeritalia S.p.A., Turin (Italy). Space Systems Group.

LONG CYCLE PRESSURIZED LOGISTICS MODULE: AN ITALIAN CONTRIBUTION TO THE SPACE STATION FREEDOM LOGISTICS SCENARIO

Ernesto Vallerani, Luciano Basile, and Giovanni Rum (Italian Space Agency, Rome.) 1989 11 p Presented at 40th IAF Congress, Malaga, Spain, 7-13 Oct. 1989 Previously announced in IAA as A90-13299

(IAF-89-083; ETN-90-97278) Avail: NTIS HC A03/MF A01

The candidate solution for the presence of the Long Cycle Pressurized Logistics Module (LCPLM) within the Freedom Station scenario is presented. It offers advantages for logistics operations management.The LCPLM can be considered user friendly for all the pressurized elements of the Freedom Station and allows use of temporary storage space and increases work space combined with the ability to cycle payloads. Commonality with other Freedom Station pressurized elements reduce the cost and risks of the LCPLM design/development. The need to organize the Freedom Station logistics scenario and to minimize the up/down load for payload maintenance/servicing is evident. The LCPLM represents a suitable means of dealing with these critical areas. ESA

N90-26059# Aeritalia S.p.A., Turin (Italy). Space Systems Group.

PERSPECTIVE FEATURES OF THE TETHERED SYSTEMS FOR SPACE APPLICATIONS

Carlo Buongiorno (Italian Space Agency, Rome.) and Ernesto Vallerani 1989 13 p Previously announced in IAA as A90-13249

(ETN-90-97279) Avail: NTIS HC A03/MF A01

Some of the possible new applications beyond the tethered missions already manifested are reviewed. Particular emphasis is given to the International Space Station Scenario. Applications of the tethered systems as supporting tools in the field of the reentry technology research are addressed. A tethered system deployed from the Space Station provides a cleaner and safer environment for particularly sensitive experiments. The management of the Station center of gravity, by controlling its vertical position at low frequencies or in DC mode, allow the minimization of the microgravity levels within the laboratory module. The choice of the characteristics of the tethered system can improve the performance of the Station attitude control system by augmenting the stabilizing effect. ESA

N90-26060# Aeritalia S.p.A., Turin (Italy). Space Systems Group.

POSSIBLE APPLICATIONS OF TETHERED SYSTEMS TO MARS EXPLORATION MISSIONS

Franco Bevilacqua and Stefano Cesare 1989 15 p Previously announced in IAA as A90-13568

(IAF-89-489; ETN-90-97280) Avail: NTIS HC A03/MF A01

Some possible applications of tethers to the Mars exploration mission, both manned and unmanned, are discussed. An analysis concerning the sizing of a tether system for generating artificial gravity inside a spaceship was performed. A preliminary evaluation of the system dynamical stability and the overall vehicle configuration is performed. The behavior of a carrier-tether-probe system orbiting in the Martian middle atmosphere is investigated. Simplified models to assess the lowest altitude towards which the tethered probe can be deployed to perform atmospheric measurements are developed. A description of the ideas for the use of tethered systems for sampling the surface of Martian satellites and performing aerobreaking maneuvers is presented. ESA

N90-26061*# Astro Aerospace Corp., Carpinteria, CA.

STRUCTURES FOR REMOTELY DEPLOYABLE PRECISION ANTENNAS Final Report

John M. Hedgepeth 16 Jan. 1989 55 p
(Contract NAS1-18567)
(NASA-CR-182065; NAS 1.26:182065; AAC-TN-1154) Avail: NTIS HC A04/MF A01 CSCL 22B

There is a need for completely deployable large antenna reflectors capable of efficiently handling millimeter-wave electromagnetic radiation. The structural concepts and technologies that are appropriate to fully automated deployment of dish-type antennas with solid reflector surfaces were studied. First, the structural requirements are discussed. Then, existing concepts for fully deployable antennas are described and assessed relative to the requirements. Finally, several analyses are presented that evaluate the effects of beam steering and segmented reflector design on the accuracy of the antenna. Author

N90-26062# Lockheed Missiles and Space Co., Palo Alto, CA. Space Sciences Lab.
VIKING DATA ANALYSIS Final Technical Report, Aug. 1986 - Mar. 1990
J. M. Quinn 25 May 1990 59 p
(Contract N00014-86-C-0159; AF Proj. 4143)
(AD-A222609) Avail: NTIS HC A04/MF A01 CSCL 04/1

The polar orbiting Swedish research satellite, Viking, obtained extensive data on auroral zone phenomena. Data from the Viking Hot Plasma Experiment have been analyzed to investigate auroral acceleration and the transport of plasma between the ionosphere and magnetosphere. A detailed statistical study was made of the relative location of ionospheric ion acceleration with respect to various magnetospheric plasma boundary signatures. The results indicate that the ion acceleration occupies a much wider latitudinal extent of the auroral zone than is expected by many current models; and that the regions of ion acceleration are ordered by, and move with, several magnetospheric plasma boundaries. Multi-spacecraft analyses of transverse ion acceleration broadband low-frequency waves have been performed and indicate that this mechanism is an important factor in transporting plasma into the magnetosphere. GRA

N90-26712# European Space Agency, Paris (France).
TECHNICAL CHARACTERISTICS AND FUNCTIONS OF DIFFERENT TYPES OF SPACE STATIONS [LES CARACTERISTIQUES TECHNIQUES ET LES FONCTIONS DES DIVERS TYPES DE STATIONS SPATIALES]
J.-J. Dordain *In its* Manned Space Station: Legal Aspects Jan. 1990 p 19-2 In FRENCH (For primary document see N90-26711 20-84)
Copyright Avail: NTIS HC A10/MF A02; also available from EPD, ESTEC, Noordwijk, Netherlands, 40 Dutch guilders

N90-26714# Societe Francaise de Droit Aerien et Spatial, Blere.
DAMAGE RESPONSIBILITY AND LIABILITY IN SPACE STATIONS [LA RESPONSABILITE POUR DOMMAGES DANS LE CAS DES STATIONS SPATIALES]
M. Bourely *In* ESA, Manned Space Stations: Legal Aspects Jan. 1990 p 35-42 In FRENCH (For primary document see N90-26711 20-84)
Copyright Avail: NTIS HC A10/MF A02; also available from EPD, ESTEC, Noordwijk, Netherlands, 40 Dutch guilders

19 SPACECRAFT INSTRUMENTATION

For related information see also *06 Aircraft Instrumentation* and *35 Instrumentation and Photography.*

N90-26063*# Sverdrup Technology, Inc., Brook Park, OH.
A RESISTANCE STRAIN GAGE WITH REPEATABLE AND CANCELLABLE APPARENT STRAIN FOR USE TO 800 C Final Report
Jih-Fen Lei Jul. 1990 10 p Presented at the Spring Conference on Experimental Mechanics, Albuquerque, NM, 4-6 Jun. 1990; sponsored in part by the Society for Experimental Mechanics, Inc.
(Contract NAS3-25266)
(NASA-CR-185256; E-5577; NAS 1.26:185256) Avail: NTIS HC A02/MF A01 CSCL 22B

A temperature compensated static strain gage, which is fabricated from palladium-13w/o chromium (Pd13Cr) alloy and a platinum (Pt) compensator, is being developed and was tested over a temperature range to 800 C at NASA-Lewis. The PdCr compensated strain gage has significantly lower apparent strain to 800 C than other high temperature strain gages. The PdCr compensated gage is protected from oxidation by a flame-sprayed alumina-4w/o zirconia overcoating. Test results to 800 C indicate apparent strain variations of less than 300 micro-epsilon and reproducibility between thermal cycles within 50 micro-epsilon. Apparent strain of the coated PdCr compensated gage can be predicted and cancelled due to its reproducibility and low value. Author

20 SPACECRAFT PROPULSION AND POWER

Includes main propulsion systems and components, e.g., rocket engines; and spacecraft auxilliary power sources.

For related information see also *07 Aircraft Propulsion and Power, 28 Propellants and Fuels, 44 Energy Production and Conversion,* and *15 Launch Vehicles and Space Vehicles.*

N90-26064*# Thiokol Corp., Brigham City, UT. Space Operations.
RSRM-9 (360L009): BALLISTICS MASS PROPERTIES Final Report
Albert S. Drendel and M. C. Richards 20 Mar. 1990 37 p
(Contract NAS8-30490)
(NASA-CR-183944; NAS 1.26:183944; TWR-17548-10) Avail: NTIS HC A03/MF A01 CSCL 21H

The propulsion performance and reconstructed mass properties data from Thiokol's RSRM-9 motors which were assigned to the STS-36 launch are presented. The SRM propellant, TP-H1148, is a composite type solid propellant, formulated of polybutadiene acrylic acid acryonitrile terpolymer binder (PBAN), epoxy curing agent, ammonium perchlorate oxidizer and aluminum powder fuel. A small amount of burning rate catalyst (iron oxide) was added to achieve the desired propellant burn rate. The propellant evaluation and raw material information for the RSRM-9 are included. The propellant grain design consists of four segments. There is a forward segment with an eleven point star with a transition into a tapered circular perforated (CP) configuration. There are two center segments that result in a double tapered CP configuration and an aft segment with a triple taper CP configuration and a cutout for the partially submerged nozzle. The ballistic performance presented is based on the Operational Flight Instrumentation (OFI) 12.5 sample per second pressure data for the steady state and tail off portion of the pressure trace. No high sample rate pressure gauges, Development Flight Instrumentation (DFI), were used on this flight and therefore no ignition data is presented. Author

N90-26065*# National Aeronautics and Space Administration. Lewis Research Center, Cleveland, OH.
MARS IN SITU PROPELLANTS: CARBON MONOXIDE AND OXYGEN IGNITION EXPERIMENTS
Diane L. Linne, James Roncace (Sverdrup Technology, Inc., Brook Park, OH.), and Mary F. Groth Jul. 1990 13 p Presented at the 26th Joint Propulsion Conference, Orlando, FL, 16-18 Jul. 1990; sponsored in part by AIAA, SAE, ASME, and ASEE
(NASA-TM-103202; E-5607; NAS 1.15:103202; AIAA-90-1894)
Avail: NTIS HC A03/MF A01 CSCL 21I

Carbon monoxide and oxygen were tested in a standard spark-torch igniter to identify the ignition characteristics of this potential Mars in situ propellant combination. The ignition profiles were determined as functions of mixture ratio, amount of hydrogen added to the carbon monoxide, and oxygen inlet temperature. The experiments indicated that the carbon monoxide and oxygen

combination must have small amounts of hydrogen present to initiate reaction. Once the reaction was started, the combustion continued without the presence of hydrogen. A mixture ratio range was identified where ignition occurred, and this range varied with the oxygen inlet temperature. Author

N90-26066# General Accounting Office, Washington, DC. National Security and International Affairs Div.

SPACE SHUTTLE: FOLLOW-UP EVALUATION OF NASA'S SOLID ROCKET MOTOR PROCUREMENT. REPORT TO THE CHAIRMAN, COMMITTEE ON GOVERNMENT OPERATIONS, HOUSE OF REPRESENTATIVES

Harry R. Finley et al May 1989 50 p
(GAO/NSIAD-89-89; B-223785) Avail: NTIS HC A03/MF A01; also available from GAO, Gaithersburg, MD HC first five copies free, additional copies $2.00

Solid rocket motors provide most of the thrust needed for lift-off and during initial phases of shuttle flight. Morton Thiokol, Incorporated, has been the sole supplier of these motors since it won the contract in 1973. The Fiscal Year 1988 NASA Authorization Act required the NASA Administrator to issue a request for proposals for competitive development of an advanced motor by the time the President submits the fiscal year 1990 NASA budget request. The Act further directs the Administrator to consider constructing a government-owned, contractor-operated production facility and providing for a dual source of supply for the advanced motor. NASA issued the request for proposals for advanced solid rocket motor development in August 1988. As part of the program, new motor manufacturing facilities are to be constructed on government property. GAO finds that NASA's Acquisition Plan for the advanced solid rocket motor provides for full and open competition in the initial contract award and protects NASA's option to compete future contracts for advanced motor production, but does not guarantee continued competition. NASA will continue to purchase Thiokol's redesigned motors during the transition to the advanced motor program. Steps have been taken to enhance quality assurance and reduce industrial safety hazards at Thiokol's motor manufacturing plant. The Air Force Plant Representative Office, which monitors Thiokol's performance for NASA, and NASA, both believe that quality assurance has improved and that Thiokol management needs to devote more attention to industrial safety. GAO agrees, but believes that NASA needs to improve its monitoring of Thiokol's safety program. J.P.S.

N90-26067*# Thiokol Corp., Brigham City, UT. Space Operations.

FLIGHT MOTOR SET 360L007 (STS-33R) Final Report

Diane Garecht Jun. 1990 166 p
(Contract NAS8-30490)
(NASA-CR-183979; NAS 1.26:183979; TWR-17546-1) Avail: NTIS HC A08/MF A01 CSCL 21H

Flight motor set 360L007 was launched as part of NASA space shuttle mission STS-33R. As with all previous redesigned solid rocket motor launches, overall motor performance was excellent. There were no debris concerns for either motor. Both motors exhibited unbonds on one factory joint weatherseal. All ballistics contract end item specification parameters were verified, with the exception of ignition interval and rise rates. Ignition interval and rise rates could not be verified due to the elimination of developmental flight instrumentation from fourth flight and subsequent, but the low sample rate data that were available showed nominal propulsion performance. All ballistic and mass property parameters closely matched the predicted values and were well within the required contract end item specification levels that could be assessed. All 108 Ground Environment Instrumentation (GEI) measurements performed properly throughout the prelaunch phase. Evaluation of the GEI measurements again verified thermal model analysis data and showed agreement with predicted environmental effects. No launch commit criteria thermal violations occurred. All joint heaters operated normally, but a high voltage reading was noted on the left hand aft heater, which was immediately determined to be a voltage sensor error and not a heater anomaly due to no current increase. Postflight inspection again verified superior performance of the insulation, phenolics, metal parts, and seals. Postflight evaluation indicated both nozzles performed as expected during flight. All combustion gas was contained by insulation in the field and case-to-nozzle joints. Author

N90-26068*# National Aeronautics and Space Administration. Lewis Research Center, Cleveland, OH.

AEOLIAN REMOVAL OF DUST FROM RADIATOR SURFACES ON MARS

James R. Gaier, Marla E. Perez-Davis, Sharon K. Rutledge, and Deborah Hotes (Cleveland State Univ., OH.) Aug. 1990 15 p Presented at the AIChE Summer National Meeting, San Diego, CA, 19-22 Aug. 1990
(NASA-TM-103205; E-5547; NAS 1.15:103205) Avail: NTIS HC A03/MF A01 CSCL 10B

Simulated radiator surfaces made of arc-textured Cu and Nb-1 percent-Zr and ion beam textured graphite and C-C composite were fabricated and their integrated spectral emittance characterized from 300 to 3000 K. A thin layer of aluminum oxide, basalt, or iron (III) oxide dust was then deposited on them, and they were subjected to low pressure winds in the Martian Surface Wind Tunnel. It was found that dust deposited on simulated radiator surfaces may or may not seriously lower their integrated spectral emittance, depending upon the characteristics of the dust. With Al2O3 there is no appreciable degradation of emittance on a dusted sample, with basaltic dust there is a 10 to 20 percent degradation, and with Fe2O3 a 20 to 40 percent degradation. It was also found that very high winds on dusted highly textured surfaces can result in their abrasion. Degradation in emittance due to abrasion was found to vary with radiator material. Arc-textured Cu and Nb-1 percent Zr was found to be more susceptible to emittance degradation than graphite or C-C composite. The most abrasion occurred at low angles, peaking at the 22.5 deg test samples. Author

N90-26069*# National Aeronautics and Space Administration. Lewis Research Center, Cleveland, OH.

ESTIMATION OF MINORITY CARRIER DIFFUSION LENGTHS IN InP/GaAs SOLAR CELLS

R. K. Jain and D. J. Flood 1990 10 p Presented at the 2nd International Conference on Indium Phosphide and Related Materials, Denver, CO, 23-25 Apr. 1990; sponsored in part by IEEE Lasers and Electro-Optics Society and IEEE Electron Device Society
(NASA-TM-103213; E-5624; NAS 1.15:103213) Avail: NTIS HC A02/MF A01 CSCL 10A

Minority carrier diffusion length is one of the most important parameters affecting the solar cell performance. An attempt is made to estimate the minority carrier diffusion lengths is the emitter and base of InP/GaAs heteroepitaxial solar cells. The PC-1D computer model was used to simulate the experimental cell results measured at NASA Lewis under AMO (air mass zero) spectrum at 25 C. A 16 nm hole diffusion length in the emitter and a 0.42 micron electron diffusion length in the base gave very good agreement with the I-V curve. The effect of varying minority carrier diffusion lengths on cell short current, open circuit voltage, and efficiency was studied. It is also observed that the front surface recombination velocity has very little influence on the cell performance. The poor output of heteroepitaxial cells is caused primarily by the large number of dislocations generated at the interfaces that propagate through the bulk indium phosphide layers. Cell efficiency as a function of dislocation density was calculated and the effect of improved emitter bulk properties on cell efficiency is presented. It is found that cells with over 16 percent efficiencies should be possible, provided the dislocation density is below 10(exp 6)/sq cm. Author

N90-26070*# National Aeronautics and Space Administration. Lewis Research Center, Cleveland, OH.

DIGITAL FILTERING OF PLUME EMISSION SPECTRA

George C. Madzsar Jul. 1990 13 p Presented at the 26th Joint Propulsion Conference, Orlando, FL, 16-18 Jul. 1990;

sponsored in part by AIAA, ASME, SAE, and ASEE
(NASA-TM-103135; E-5478; NAS 1.15:103135; AIAA-90-1994)
Avail: NTIS HC A03/MF A01 CSCL 21H

Fourier transformation and digital filtering techniques were used to separate the superpositioned spectral phenomena observed in the exhaust plumes of liquid propellant rocket engines. Space shuttle main engine (SSME) spectral data were used to show that extraction of spectral lines in the spatial frequency domain does not introduce error, and extraction of the background continuum introduces only minimal error. Error introduced during band extraction could not be quantified due to poor spectrometer resolution. Based on the atomic and molecular species found in the SSME plume, it was determined that spectrometer resolution must be 0.03 nm for SSME plume spectral monitoring. Author

N90-26071*# National Aeronautics and Space Administration. Lewis Research Center, Cleveland, OH.
PRELIMINARY PLUME CHARACTERISTICS OF AN ARCJET THRUSTER
David H. Manzella, Francis M. Curran, Roger M. Myers, and Dieter M. Zube (Stuttgart Univ., Germany, F.R.) 1990 16 p Presented at the 21st International Electric Propulsion Conference, Orlando, FL, 18-20 Jul. 1990; sponsored by AIAA, DGLR, and JSASS
(NASA-TM-103241; E-5659; NAS 1.15:103241; AIAA-90-2645)
Avail: NTIS HC A03/MF A01 CSCL 21H

An experimental investigation of a low power arcjet plume was conducted using emission spectroscopy. A laboratory model arcjet incorporating a segmented anode was run on simulated hydrazine at a flow rate of 5 x 10(exp -5) kg/s. The complete visible spectrum measured in the exit plane of the arcjet showed the presence of N2, N2(+), NH, and H. Radial intensity profiles for the H alpha, H sub beta, and the NH A(sup 3)Pi yields X(sup 3)Sigma(0,0) transitions at four different axial locations were measured. These line of sight intensity measurements, spaced 0.05 mm apart, were deconvoluted to give the radial intensity distribution using an inverse Abel transformation. The ratio between the intensities from the H sub alpha and H sub beta transitions indicated a non-Boltzmann energy distribution between excited states in the plume. Axial intensity profiles taken on center line indicated the decay rate of excited states in the plume. An electron number density of 2 x 10(exp 13)/cu cm at the exit plane was determined based on Stark broadening of the H sub beta line. Rotational temperatures of 750 K, 1750 K, and 2500 K were determined for N2, N2(+), and NH respectively. The results demonstrate that the location of the current attachment on the anode has a measurable effect on the electronically excited species in the plume and that dissociation is the dominant frozen flow loss mechanism in low power arcjets. Author

N90-26072# National Aerospace Lab., Tokyo (Japan).
HARD START PROBLEM OF THE APOGEE ENGINE FOR THE ETS-6
Masahiro Sato, Kazuo Kusaka, Makoto Tadano, Hiroshi Miyajima, and Hideyuki Kobayashi Oct. 1989 18 p In JAPANESE; ENGLISH summary
(DE90-505525; NAL-TR-1036; ISSN-0389-4010) Avail: NTIS (US Sales Only) HC A03/MF A01

On the nitrogen tetroxide/hydrazine bipropellant apogee engine for the geostationary engineering test satellite (ETS-6), a hard start problem encountered during high altitude combustion simulation tests was reported as well as its possible solution. Since the hard start was observed only in altitude tests, never in sea-level tests, it was analyzed with relation to combustion pressures, fuel mixing ratios or operation delay times of a bipropellant valve. The hard start was, as a result, caused by a large amount of propellant accumulated in an engine combustion chamber due to a longer ignition delay time. As the relation between the hard start and ignition timing was tested, the hard start in vacuum environment was sufficiently suppressed by adopting oxidizer-lead of 50 to 100 ms. Based on the test verification, the bipropellant valve design was altered from the fuel-lead type to oxidizer-lead one. DOE

N90-26073*# National Aeronautics and Space Administration. Lyndon B. Johnson Space Center, Houston, TX.
METHODS AND APPARATUS FOR PROVIDING REAL-TIME CONTROL OF A GASEOUS PROPELLANT ROCKET PROPULSION SYSTEM Patent Application
Brian G. Morris, inventor (to NASA) 26 Jan. 1990 33 p
(NASA-Case-MSC-21542-1; NAS 1.71:MSC-21542-1; US-Patent-Appl-SN-470480) Avail: NTIS HC A03/MF A01 CSCL 21H

The new and improved methods and apparatus disclosed provide effective real-time management of a spacecraft rocket engine powered by gaseous propellants. Real-time measurements representative of the engine performance are compared with predetermined standards to selectively control the supply of propellants to the engine for optimizing its performance as well as efficiently managing the consumption of propellants. A priority system is provided for achieving effective real-time management of the propulsion system by first regulating the propellants to keep the engine operating at an efficient level and thereafter regulating the consumption ratio of the propellants. A lower priority level is provided to balance the consumption of the propellants so significant quantities of unexpended propellants will not be left over at the end of the scheduled mission of the engine. NASA

23 CHEMISTRY AND MATERIALS (GENERAL)

N90-26074*# National Aeronautics and Space Administration. Lewis Research Center, Cleveland, OH.
THE CHEMICAL EFFECTS OF THE MARTIAN ENVIRONMENT ON POWER SYSTEM COMPONENT MATERIALS: A THEORETICAL APPROACH
Marla E. Perez-Davis and James R. Gaier Aug. 1990 13 p Presented at the AIChE Summer National Meeting, San Diego, CA, 19-22 Aug. 1990
(NASA-TM-103203; E-5608; NAS 1.15:103203) Avail: NTIS HC A03/MF A01 CSCL 07C

In the foreseeable future, an expedition may be undertaken to explore the planet Mars. Some of the power source options being considered for such a mission are photovoltaics, regenerative fuel cells and nuclear reactors. In addition to electrical power requirements, environmental conditions en route to Mars, in the planetary orbit and on the Martian surface must be simulated and studied in order to anticipate and solve potential problems. Space power systems components such as photovoltaic arrays, radiators, and solar concentrators may be vulnerable to degradation in the Martian environment. Natural characteristics of Mars which may pose a threat to surface power systems include high velocity winds, dust, ultraviolet radiation, large daily variation in temperature, reaction to components of the soil, atmosphere and atmospheric condensates as well as synergistic combinations. Most of the current knowledge of the characteristics of the Martian atmosphere and soil composition was obtained from the Viking 1 and 2 missions in 1976. A theoretical study is presented which was used to assess the effects of the Martian atmospheric conditions on the power systems components. A computer program written at NASA-Lewis for combustion research that uses a free energy minimization technique was used to calculate chemical equilibrium for assigned thermodynamic states of temperature and pressure. The power system component materials selected for this study include: silicon dioxide, silicon, carbon, copper, and titanium. Combinations of environments and materials considered include: (1) Mars atmosphere with power surface material, (2) Mars atmosphere and dust component with power surface material, and (3) Mars atmosphere and hydrogen peroxide or superoxide or superoxide with power system material. The chemical equilibrium calculations were performed at a composition ratio (oxidant to reactant) of 100. The temperature for the silicon dioxide material and silicon, which simulate photovoltaic cells, were 300 and 400 K; for carbon, copper and titanium, which simulate radiator surfaces, 300, 500,

and 1000 K. All of the systems were evaluated at pressures of 700, 800, and 900 Pa, which stimulate the Martian atmosphere.
Author

N90-26075*# National Aeronautics and Space Administration. Langley Research Center, Hampton, VA.
PROCEEDINGS OF THE LDEF MATERIALS DATA ANALYSIS WORKSHOP
Bland A. Stein, comp. and Philip R. Young, comp. Jul. 1990 289 p Workshop held at Cocoa Beach, FL, 13-14 Feb. 1990
(NASA-CP-10046; NAS 1.55:10046) Avail: NTIS HC A13/MF A02 CSCL 07A

The 5-year, 10-month flight of the Long Duration Exposure Facility (LDEF) greatly enhanced the potential value of most LDEF materials, compared to the original 1-year flight plan. NASA recognized this potential by forming the LDEF Space Environmental Effects on Materials Special Investigation Group in early 1989 to address the expanded opportunities available in the LDEF structure and on experimental trays, so that the value of all LDEF materials to current and future space missions would be assessed and documented. The LDEF Materials Data Analysis Workshop served as one step toward the realization of that responsibility and ran concurrently with activities surrounding the successful return of the spacecraft to the NASA Kennedy Space Center. A compilation of visual aids utilized by speakers at the workshop is presented. Session 1 summarized current information on analysis responsibilities and plans and was aimed at updating the workshop attendees: the LDEF Advisory Committee, Principle Investigators, Special Investigation Group Members, and others involved in LDEF analyses or management. Sessions 2 and 3 addressed materials data analysis methodology, specimen preparation, shipment and archival, and initial plans for the LDEF Materials Data Base. A complementary objective of the workshop was to stimulate interest and awareness of opportunities to vastly expand the overall data base by considering the entire spacecraft as a materials experiment.
Author

24 COMPOSITE MATERIALS

Includes physical, chemical, and mechanical properties of laminates and other composite materials.
For ceramic materials see *27 Nonmetallic Materials*.

N90-26076*# National Aeronautics and Space Administration. Langley Research Center, Hampton, VA.
STRAIN ENERGY RELEASE RATE ANALYSIS OF DELAMINATION IN A TAPERED LAMINATE SUBJECTED TO TENSION LOAD
S. A. Salpekar, I. S. Raju, and T. K. OBrien (Army Aviation Systems Command, Hampton, VA.) Mar. 1990 51 p
(NASA-TM-102592; AVSCOM-TM-90-B-003; NAS 1.15:102592)
Avail: NTIS HC A04/MF A01 CSCL 11D

A tapered composite laminate subjected to tension load was analyzed using the finite-element method. The glass/epoxy laminate has a (+ or - 45)sub 3 group of plies dropped in three distinct steps, each 20 ply-thicknesses apart, thus forming a taper angle of 5.71 degrees. Steep gradients of interlaminar normal and shear stress on a potential delamination interface suggest the existence of stress singularities at the points of material and geometric discontinuities created by the internal plydrops. The delamination was assumed to initiate at the thin end of the taper on a -45/+45 interface and the delamination growth was simulated in both directions, i.e., along the taper and into the thin region. The strain-energy-release rate for a delamination growing into the thin laminate consisted predominantly of mode I (opening) component. For a delamination growing along the tapered region, the strain-energy-release rate was initially all mode I, but the proportion of mode I decreased with increase in delamination size until eventually total G was all mode II. The total G for both delamination tips increased with increase in delamination size, indicating that a delamination initiating at the end of the taper will grow unstably along the taper and into the thin laminate simultaneously.
Author

N90-26077*# National Aeronautics and Space Administration. Langley Research Center, Hampton, VA.
BUCKLING AND POSTBUCKLING BEHAVIOR OF SQUARE COMPRESSION-LOADED GRAPHITE-EPOXY PLATES WITH CIRCULAR CUTOUTS
Michael P. Nemeth Washington Aug. 1990 33 p Presented at the 8th DOD/NASA/FAA Conference on Fibrous Composites in Structural Design, Norfolk, VA, 28-30 1989
(NASA-TP-3007; L-16777; NAS 1.60:3007) Avail: NTIS HC A03/MF A01 CSCL 11D

An experimental study of the postbuckling behavior of square compression-loaded graphite-epoxy plates and isotropic plates with a central circular cutout is presented. Results are presented for unidirectional (0 sub 10)s and (90 sub 10)s plates, (0/90 sub 5)s plates, and for aluminum plates. Results are also presented for (+ or - O sub 6)s angle-ply plates for values of O = 30, 46, and 60 degrees. The experimental results indicate that the change in axial stiffness of a plate at buckling is strongly dependent upon cutout size and plate orthotropy. The presence of a cutout gives rise to an internal load distribution that changes, sometimes dramtically, as a function of cutout size coupled with the plate orthotropy. In the buckled state, the role of orthotropy becomes more significant since bending in addition to membrane orthotropy is present. Most of the plates with cutouts exhibited less postbuckling stiffness than the corresponding plate without a cutout, and the postbuckling stiffness decreased with increasing cutout size. However, some of the highly orthotropic plates with cutouts exhibited more postbuckling stiffness than the corresponding plate without a cutout.
Author

N90-26078# Wichita State Univ., KS. Inst. for Aviation Research.
EROSION MECHANISMS IN COMPOSITE MATERIALS AND RIPPLE FORMATION MECHANISM IN EROSION Ph.D. Thesis
Youssef Adel Ballout Dec. 1988 139 p
(IAR-89-4-Pt-1) Avail: NTIS HC A07/MF A01

The general mechanisms involved in the solid particle erosion of fully a aligned glass fiber reinforced epoxy composite are investigated. The solid particle erosion rates of the composite were obtained by using an air-blast type system. Experiments were carried out to analyze the effect of the sharp Al2O3 erodent particle size, velocity, angle of impact, glass fiber orientation, and fiber/matrix weight ratio. The erosion characteristics of S-glass and epoxy resin were also investigated. Surface morphology of eroded samples was investigated by optical and scanning electron microscopy, both at steady-state erosion and single-impact events. Based on these activities, the essential data for erosion processes and mechanisms were provided. The fully aligned fiber composite showed a great dependence of the erosion rates on the impact angle and fiber orientation with maximum and relative minimum erosion rates varying with the changing fiber orientation. The S-glass impacted by sharp Al2O3 particles showed a bilinear relationship of logarithmic erosion rate in function of logarithmic normal velocity, and a linear relationship when S-glass is impacted by spherical glass beads. The epoxy resin showed a semi-ductile type of erosion behavior. The erosion rates of the composite were found to follow more closely an inverse rule of mixture. Erosion mechanisms based on the erosion characteristics of S-glass and epoxy resin are suggested. A mechanism of solid particle erosion of fully aligned glass fiber reinforced epoxy composite is proposed based on the combined mechanisms of the composite components and, the macrostructural geometrical constraints imposed by the fiber-matrix system.
Author

N90-26079# Wichita State Univ., KS. Inst. for Aviation Research.
EROSION MECHANISMS IN COMPOSITE MATERIALS AND RIPPLE FORMATION MECHANISM IN EROSION Ph.D. Thesis
Youssef Adel Ballout Dec. 1988 123 p
(IAR-89-4-Pt-2) Avail: NTIS HC A06/MF A01

The formation of Ripples on pure Al and Al-12Si alloy surfaces was investigated. Sharp polyhedral Al2O3 and spherical glass beads were used as erodent particles accelerated in an air blast type system. The experimental variables were erodent particle shape, angle of impact, abrasive particle mixture, sample surface topology, and tangential velocity vector. Scanning electron and optical microscopy used to study the morphology of impacted surfaces showed the well developed ripple formation on Al-12Si with beads used as abrasives. As the fraction of Al2O3 sharp particles was increased, the ripple formation on Al-12Si diminished. Geometric instabilities changing the surface topology of target material were introduced. The geometric instabilities act as initiation sites for accelerated and relatively large ripples. A new laboratory technique was utilized to control the relative tangential velocity of the erodent particles with respect to the target sample by placing it on a velocity controlled rotating disk. With this new technique, it was possible to form ripples at normal angles of impact and to avoid ripple formation at oblique angles of impact. An investigation of the surface morphology of the eroded samples provided evidence for a mechanism of ripple formation based on material displacement instead of material removal. Author

N90-26080*# National Aeronautics and Space Administration. Langley Research Center, Hampton, VA.
CARBON-CARBON COMPOSITES: EMERGING MATERIALS FOR HYPERSONIC FLIGHT
Howard G. Maahs [1989] 18 p Submitted for publication
(NASA-TM-103472; NAS 1.15:103472) Avail: NTIS HC A03/MF A01 CSCL 11D

An emerging class of high temperature materials called carbon-carbon composites are being developed to help make advanced aerospace flight become a reality. Because of the high temperature strength and low density of carbon-carbon composites, aerospace engineers would like to use these materials in even more advanced applications. One application of considerable interest is as the structure of the aerospace vehicle itself rather than simply as a protective heat shield as on Space Shuttle. But suitable forms of these materials have yet to be developed. If this development can be successfully accomplished, advanced aerospace vehicles such as the National Aero-Space Plane (NASP) and other hypersonic vehicles will be closer to becoming a reality. A brief definition is given of C-C composites. Fabrication problems and oxidation protection concepts are examined. Applications of C-C composites in the Space Shuttle and in advanced hypersonic vehicles as well as other applications are briefly discussed.
Author

N90-26081# Wyoming Univ., Laramie. Dept. of Mechanical Engineering.
VITREOUS JOINING OF SIC FIBER REINFORCED SIC COMPOSITES
Dennis N. Coon Dec. 1989 69 p Submitted for publication
Prepared for Edgerton, Germeshausen and Grier, Inc., Idaho Falls, ID
(Contract DE-AC07-76ID-01570)
(DE90-012951; EGG-MS-8933) Avail: NTIS HC A04/MF A01

Glass in the MgO--Li2O--Al2O3--SiO2 system were developed to as brazing materials to join SiC fiber reinforced SiC composites. These glass materials will melt and flow at temperatures ranging from 1000 to 1200 C, and are chemically compatible with SiC. The glass transition temperature and melting temperature can be altered by adjusting the MgO:Li2O ratio. The glasses exhibited viscous deformation at their glass transition temperatures, 490 to 725 C. The glasses were devitrified to develop crystalline phases based on beta (prime)-spodumene, beta (prime)-eucryptite, or a beta (prime)-spodumene-beta(prime)-eucryptite solid solution. Glass-ceramics, prepared by thermal treatment, exhibited no viscous deformation to temperature as high as 785 C, and exhibited improved strength as the test temperature was increased. Joints were prepared by painting the composite surface with a slurry of the glass powder suspended in water. Joining temperature, joining time, glass composition, amount of joining glass, and post-joining heat treatments were the variables examined. Larger quantities of joining glass and shorter joining times were observed to improve joint strength. The addition of niobium oxide to the glass also improved joint strength. The niobium oxide also stabilizes the glass/composite interface at temperatures less than 1200 C.
DOE

N90-26082*# National Aeronautics and Space Administration. Langley Research Center, Hampton, VA.
THE INFLUENCE OF MICROSTRUCTURE ON THE TENSILE BEHAVIOR OF AN ALUMINUM METAL MATRIX COMPOSITE
Michael J. Birt (Analytical Services and Materials, Inc., Hampton, VA.) and W. Steven Johnson Jul. 1990 29 p
(NASA-TM-102694; NAS 1.15:102694) Avail: NTIS HC A03/MF A01 CSCL 11D

The relationship between tensile properties and microstructure of a powder metallurgy aluminum alloy, 2009 was examined. The alloy was investigated both unreinforced and reinforced with 15 v/o SiC whiskers or 15 v/o SiC particulate to form a discontinuous metal matrix composite (MMC). The materials were investigated in the as-fabricated condition and in three different hot-rolled sheet thicknesses of 6.35, 3.18, and 1.8 mm. Image analysis was used to characterize the morphology of the reinforcements and their distributions within the matrix alloy. Fractographic examinations revealed that failure was associated with the presence of microstructural inhomogeneities which were related to both the matrix alloy and to the reinforcement. The results from these observations together with the matrix tensile data were used to predict the strengths and moduli of the MMC's using relatively simple models. The whisker MMC could be modeled as a short fiber composite and an attempt was made to model the particulate MMC as a dispersion/dislocation hardened alloy. Author

N90-26083*# National Aeronautics and Space Administration. Langley Research Center, Hampton, VA.
DAMAGE STATES IN LAMINATED COMPOSITE THREE-POINT BEND SPECIMENS: AN EXPERIMENTAL-ANALYTICAL CORRELATION STUDY Interim Report No. 79
J. Michael Starbuck, Zafer Guerdal, Marek-Jerzy Pindera (Virginia Univ., Charlottesville.), and Clarence C. Poe Jul. 1990 357 p
(Grant NAG1-343)
(NASA-TM-101800; NAS 1.15:101800; CCMS-90-06; VPI-E-90-11)
Avail: NTIS HC A16/MF A02 CSCL 11D

Damage states in laminated composites were studied by considering the model problem of a laminated beam subjected to three-point bending. A combination of experimental and theoretical research techniques was used to correlate the experimental results with the analytical stress distributions. The analytical solution procedure was based on the stress formulation approach of the mathematical theory of elasticity. The solution procedure is capable of calculating the ply-level stresses and beam displacements for any laminated beam of finite length using the generalized plane deformation or plane stress state assumption. Prior to conducting the experimental phase, the results from preliminary analyses were examined. Significant effects in the ply-level stress distributions were seen depending on the fiber orientation, aspect ratio, and whether or not a grouped or interspersed stacking sequence was used. The experimental investigation was conducted to determine the different damage modes in laminated three-point bend specimens. The test matrix consisted of three-point bend specimens of 0 deg unidirectional, cross-ply, and quasi-isotropic stacking sequences. The dependence of the damage initiation loads and ultimate failure loads were studied, and their relation to damage susceptibility and damage tolerance of the mean configuration was discussed. Damage modes were identified by visual inspection of the damaged specimens using an optical microscope. The four fundamental damage mechanisms identified were delaminations, matrix cracking, fiber breakage, and crushing. The correlation study between the experimental results and the analytical results were performed for the midspan deflection, indentation, damage modes, and damage susceptibility. Author

N90-26084# Carborundum Co., Niagara Falls, NY. Structural Ceramics Div.
SYNTHESIS OF HIGH PURITY SINTERABLE SILICON CARBIDE POWDER
W. D. Boecker, B. L. Mehosky, R. S. C. Rogers, R. S. Storm, and V. Venkateswaran Nov. 1989 277 p Prepared for ORNL, TN
(Contracts DE-AC05-84OR-21400; ORNL-86X-00214C)
(DE90-012029; ORNL/Sub-84-00214/1) Avail: NTIS HC A13/MF A02

High purity, submicron silicon carbide powders were produced via gas phase synthesis using a hydrogen/argon plasma. Two test facilities were constructed, a bench-scale unit and a larger pilot scale reactor. Three candidate silicon sources were evaluated:silicon tetrachloride (SiCl4), dimethyldichlorosilane (CH3)2SiCl2), and methyltrichlorosilane (CH3SiCl3). Product powders were evaluated on the basis of pressureless sinterability, surface area, agglomeration, particle size distribution, phase distribution and chemistry. Three commercial powders, Starck A10, Starck B10, and Carborundum submicron alpha silicon carbide, were also evaluated for comparison to the product powders. Powders were reproducibly synthesized at a rate of one pound per hour for standard run times of five hours. Product powders exhibited chemical and physical properties equal to or exceeding the commercial powders evaluated. In limited attempts to pressureless sinter the product powders, densities of 91 percent of theoretical were obtained with as-produced powder. Post-processing permitted densities in excess of 97 percent of theoretical. X ray diffraction of the product indicates that the product powders are primarily beta poly-types, with traces of alpha present. Increased production rates to a target level of seven pounds per hour were not possible due to current transients produced by the pilot scale power supply. Extensive unsuccessful efforts to reduce or eliminate the transients are described. Low recovered product yields resulted from a failure of a product collection filter that was not discovered until the completion of the project. DOE

N90-26085# National Aerospace Lab., Tokyo (Japan).
PROBABILISTIC APPROACH TO THE CERTIFICATION FOR FATIGUE DURABILITY OF COMPOSITE STRUCTURES
Toshiyuki Shimokawa Jun. 1989 16 p
(DE90-505521; NAL-TR-1029T; ISSN-0389-4010) Avail: NTIS (US Sales Only) HC A03/MF A01

Probabilistic approach to the certification for the fatigue durability of composite structures was systematically discussed, and the approach, the combination of scatter factors of a fatigue life and fatigue strength was used, was proposed, as well as equations to express the mutual relationship between the scatter factors and the combination of both factors. Moreover, calculation examples of the scatter factors were also given on the basis of the scatter parameters of the fatigue life and strength obtained from the test results of carbon/epoxy laminate specimens. Because of a small amount of specimens, the test results were used to estimate only central tendencies of the fatigue life, and a log-normal and two-parameter Weibull distribution were used for the life. Those of the strength were also determined under the same assumption. As the scatter factors were compared on the basis of the scatter parameters derived from three matching methods, those were strongly dependent on the selection of the matching methods. DOE

N90-26086# National Aerospace Lab., Tokyo (Japan).
STUDY ON FAILURE MODES OF BORON FIBER REINFORCED ALUMINUM COMPOSITE MATERIALS BY AE METHOD, PART 2
Yasushi Sofue and Akinori Ogawa Jun. 1989 13 p In JAPANESE; ENGLISH summary
(DE90-505522; NAL-TR-1030-Pt-2; ISSN-0389-4010) Avail: NTIS (US Sales Only) HC A03/MF A01

The failure modes of boron fiber reinforced aluminum composite materials were examined by the power spectrum analysis of AE waves. The 6061 aluminum alloy was used as a matrix, and four types of specimens such as a unidirectionally fiber reinforced composite material were prepared for tensile tests. In boron fiber breakage, power spectra indicated high peaks in the low frequency range from 100 to 200 kHz, and in fiber breakage of composite materials, AE waves continued occasionally for 3.84 ms or more due to the friction between a matrix and fibers. In 6061 aluminum alloy, AE waves were different between tensile and shear fracture, showing a short damping time in tensile fracture and a long time in shear, independently of small amplitudes in both fractures. The power spectra of the alloy indicated high peaks in the high frequency range from 400 to 900 kHz, and AE waves continued for only 64 microsec or less extremely short compared with those in fiber breakage. DOE

N90-26087# Rolls-Royce Ltd., Derby (England). Manufacturing Technology.
METAL MATRIX COMPOSITES AND POWDER PROCESSING FOR AERO-ENGINE APPLICATIONS
D. Driver 3 Jul. 1989 26 p Presented at the BNF 7th International Conference on the Materials Revolution through the 90's, Oxford, England, 3-5 Jul. 1989
(PNR90617; ETN-90-97135) Copyright Avail: NTIS HC A03/MF A01

Engineering opportunities and processing implications for composites offering potential in aeroengines are addressed, with particular emphasis on metal matrix composites. Compressor disc and blade applications, and fiber and matrix characteristics are discussed. High temperature metal matrix composites and powder processing are considered. The exploitation of metal matrix composites offers particular advantages for stiffness-critical applications while powder processing provides the potential for near net shape components which, when coupled with microstructural control, gives extended component lives. ESA

N90-26088# University of Southern California, Los Angeles.
COMPOSITE MATERIALS WITH IMPROVED PROPERTIES IN COMPRESSION: SYNTHESIS OF 3-METHYLENE-1,1-DICHLOROSILACYCLOBUTANE AND 1,1-DICHLOROSILACYCLOPENT-3-ENE Interim Report
R. Damrauer, A. Laporterie, G. Manuel, Y. T. Park, and R. Simon 9 May 1990 12 p
(Contract N00014-89-J-1961)
(AD-A222615) Avail: NTIS HC A03/MF A01 CSCL 07/3

Silacyclobutanes have played an important role in the development of modern silicon chemistry. For example, silacyclobutanes serve as precursors to carbon-silicon double bonded intermediates silenes as well as to pentacoordinate silicon anions in the gas phase. Silacyclobutanes also undergo facile ring opening polymerization. Despite the importance of this ring system, surprisingly few functionalized silacyclobutanes and silacyclobutenes have been prepared. GRA

N90-26089# Virginia Univ., Charlottesville. Dept. of Materials Science.
INVESTIGATION OF THERMO-MECHANICAL EFFECTS IN SILICON CARBIDE WHISKER/Al ALLOY COMPOSITES Final Report, 1 Mar. 1985 - 31 Aug. 1989
F. E. Wawner, Jr. and R. D. Schueller Jun. 1990 78 p
(Contract N00014-85-K-0179)
(AD-A222635; UVA/525398/MS90/104) Avail: NTIS HC A05/MF A01 CSCL 11/6

This program deals with determining factors that influence strength, ductility, and elongation to failure in SiC whisker/Al alloy composites. Specifically, a microstructural study was made in an attempt to define extrinsic and intrinsic factors that control fracture and thus influence properties. One of the more important products from SiC/Al composites has been the rolled sheet. The response of the material to secondary processing and thermo-mechanical treatment is of utmost importance with respect to material quality. The present study emphasizes microstructural-mechanical property characterization of the rolled material. GRA

N90-26090# Illinois Univ., Urbana.
THE EFFECT OF INTERFACIAL CHARACTERISTICS ON THE MECHANICAL PERFORMANCE OF CERAMIC-CERAMIC COMPOSITES Final Report, Jul. 1986 - Dec. 1989
Joseph Homeny and Sherman D. Brown Feb. 1990 10 p
(Contract DAAL03-86-K-0121)
(AD-A223031; ARO-23421.12-MS) Avail: NTIS HC A02/MF A01 CSCL 11/4

The research reported addresses several of the critical issues in the field of ceramic fiber (whisker) / ceramic matrix composites. The overall goal was to understand the complex relationships between processing, interfacial microstructure, and mechanical properties in order to engineer the overall performance of the composites. The composite systems of interest were: (1) SiC whisker / Al2O3 matrix composites, (2) beta-Si3N4 whisker / Si3N4 matrix composites, and (3) SiC continuous fiber / lithium-aluminosilicate matrix composites. GRA

25 INORGANIC AND PHYSICAL CHEMISTRY

Includes chemical analysis, e.g., chromatography; combustion theory; electrochemistry; and photochemistry.

For related information see also *77 Thermodynamics and Statistical Physics.*.

N90-26091 New South Wales Univ., Kensington (Australia).
MASS SPECTROMETRY OF POLY(METHYL METHACRYLATE)S OF LOW MOLECULAR WEIGHT Ph.D. Thesis Abstract Only
Wilbert Winston Hope Oct. 1988 3 p
Avail: Issuing Activity

Low molecular weight (less than 2000 microns) poly (methyl methacrylate) with unsaturated endgroup oligomers was synthesized using cobalt tetraphenyl porphyrin as the catalyst for chain transfer to monomer. The fully saturated oligomers were obtained with subsequent hydrogenation. Field desorption characteristics of the two types of poly (methyl methacrylate)s were investigated using a large double focussing mass spectrometer. High performance liquid chromatograph was employed to isolate saturated and unsaturated endgroup oligomers from the respective poly (methyl methacrylate) sample. Tetramethyl 2,4,5,7-tetramethyloctane 2,4,5,7-tetracarboxyl (TOTC) a methyl methacrylate tetramer with a head-to-head link at the 4 to 5 position, was also investigated. A comparison of the field desorption mass spectra of the saturated and the unsaturated endgroup tetramers and TOTC, snowed the head-to-head link to be comparatively weak. Spontaneous and collision-induced decompositions (CID) of the methyl methacrylate oligomeric ions, produced by field desorption of the individual oligomers, were investigated using mass analyzed ion kinetic energy (MIKE) technique. A Fourier transform ion cyclotron resonance (FT/ICR) mass spectrometer was also employed to analyze the methyl methacrylate oligomers. Author

N90-26092# National Aeronautical Lab., Bangalore (India). Materials Science Div.
PRESSURE DEPENDENCE OF THERMOELECTRIC POWER OF HIGH T(SUB c) 123 COMPOUND
Sheela Ramasesha and A. K. Singh Jan. 1990 15 p
(NAL Proj. MT-0-181)
(PD-MT-9001) Avail: NTIS HC A03/MF A01

Thermoelectric powers (TEP) of two YBa2Cu3O(7-delta) compounds (with delta = 0.17 and 0.21) were measured as a function of quasi-hydrostatic pressure up to 9 GPa at 300 K on samples with low porosity. In both cases TEP decreases with increasing pressure, at a rate approx. 0.8 microVK(-1)(GPa). The data obtained under hydrostatic pressure up to 3 GPa are in good agreement with those under quasi-hydrostatic pressure. The TEP of both compositions is found to decrease linearly at a rate 0.8 microVK(-1)(GPa) above 1.5 GPa. Author

N90-26093*# SRI International Corp., Menlo Park, CA. Molecular Physics Lab.
ROTATIONAL AND TRANSLATIONAL EFFECTS IN COLLISIONS OF ELECTRONICALLY EXCITED DIATOMIC HYDRIDES
David R. Crosley (Ruhr Univ., Bochum, Germany, F.R.) 22 Dec. 1988 42 p Submitted for publication Sponsored by NSF; ARO; DOE; GRI; AFWAL; and AFOSR
(Contract NAS1-16956)
(NASA-CR-186770; NAS 1.26:186770; MP-88-279) Avail: NTIS HC A03/MF A01 CSCL 07D

Collisional quenching and vibrational energy proceed competitively with rotational energy transfer for several excited states of the diatomic radicals OH, NH, and CH. This occurs for a wide variety of molecular collision partners. This phenomenon permits the examination of the influence of rotational motion on the collision dynamics of these theoretically tractable species. Measurements can also be made as a function of temperature, i.e., collision velocity. In OH (sup 2 sigma +), both vibrational transfer and quenching are found to decrease with an increase in rotational level, while quenching decreases with increasing temperature. This behavior indicates that for OH, anisotropic attractive forces govern the entrance channel dynamics for these collisions. The quenching of NH (sup 3 pi sub i) by many (although not all) collision partners also decreases with increasing rotational and translational energy, and NH (sup 1 pi) behaves much like OH (sup 2 sigma +). However, the quenching of CH (sup 2 delta) appears to decrease with increasing rotation but increases with increasing temperature, suggesting in this case anisotropic forces involving a barrier or repulsive wall. Such similarities and differences should furnish useful comparisons with both simple and detailed theoretical pictures of the appropriate collision dynamics. Author

N90-26094*# National Aeronautics and Space Administration. Langley Research Center, Hampton, VA.
SUPERSONIC REACTING INTERNAL FLOW FIELDS
J. Philip Drummond [1989] 82 p Submitted for publication
(NASA-TM-103480; NAS 1.15:103480) Avail: NTIS HC A05/MF A01 CSCL 21B

The national program to develop a trans-atmospheric vehicle has kindled a renewed interest in the modeling of supersonic reacting flows. A supersonic combustion ramjet, or scramjet, has been proposed to provide the propulsion system for this vehicle. The development of computational techniques for modeling supersonic reacting flow fields, and the application of these techniques to an increasingly difficult set of combustion problems are studied. Since the scramjet problem has been largely responsible for motivating this computational work, a brief history is given of hypersonic vehicles and their propulsion systems. A discussion is also given of some early modeling efforts applied to high speed reacting flows. Current activities to develop accurate and efficient algorithms and improved physical models for modeling supersonic combustion is then discussed. Some new problems where computer codes based on these algorithms and models are being applied are described. Author

N90-26095*# Aerojet Technical Systems Co., Sacramento, CA. Propulsion Div.
CARBON DEPOSITION MODEL FOR OXYGEN-HYDROCARBON COMBUSTION. TASK 6: DATA ANALYSIS AND FORMULATION OF AN EMPIRICAL MODEL Final Report, Apr. 1989 - May 1990
Darby B. Makel and Sanders D. Rosenberg May 1990 82 p
(Contract NAS8-34715)
(NASA-CR-183986; NAS 1.26:183986; KFY-FR) Avail: NTIS HC A05/MF A01 CSCL 21B

The formation and deposition of carbon (soot) was studied in the Carbon Deposition Model for Oxygen-Hydrocarbon Combustion Program. An empirical, 1-D model for predicting soot formation and deposition in LO2/hydrocarbon gas generators/preburners was derived. The experimental data required to anchor the model were identified and a test program to obtain the data was defined. In support of the model development, cold flow mixing experiments

using a high injection density injector were performed. The purpose of this investigation was to advance the state-of-the-art in LO2/hydrocarbon gas generator design by developing a reliable engineering model of gas generator operation. The model was formulated to account for the influences of fluid dynamics, chemical kinetics, and gas generator hardware design on soot formation and deposition. Author

N90-26096# Los Alamos National Lab., NM.
TEXTURE OF MATERIALS BY TIME-OF-FLIGHT NEUTRON DIFFRACTION
Robert B. VonDreele 1990 7 p Presented at the 14th Conference on Applied Crystallography, Cieszyn, Poland, 5-8 Aug. 1990 Submitted for publication
(Contract W-7405-eng-36)
(DE90-008968; LA-UR-90-1068; CONF-900884-1) Avail: NTIS HC A02/MF A01

Time-of-flight (TOF) neutron diffraction as performed at a spallation neutron source such as LANSCE offers special features that makes it potentially useful for the determination of the texture (preferred orientation, particle size and strain) of polycrystalline materials. DOE

N90-26097# Sandia National Labs., Albuquerque, NM.
THE EISI (ELEMENTAL AND INTERPLANAR SPACING INDEX) INDEX: A SEARCH/MATCH TOOL FOR ELECTRON DIFFRACTION PHASE ANALYSIS
M. J. Carr, V. L. Himes, A. D. Mighell, and R. Anderson (International Business Machines Corp., Hopewell Junction, NY.) 1990 4 p Presented at the 12th International Congress for Electron Microscopy, Seattle, WA, 12-18 Aug. 1990
(Contract DE-AC04-76DP-00789)
(DE90-010832; SAND-90-1203C; CONF-900877-3) Avail: NTIS HC A01/MF A01

The identification of unknown phases in the JCPDS-ICDD Powder Diffraction File (PDF) using diffraction data is a three-step process. First, the Search step rapidly screens the entire PDF to produce a list of candidate solutions that correspond to the unknown phase's d-spacings and chemistry. Second, the Match step examines closely every aspect of each phase in the candidate list, vs the unknown, to make the final identification. Third, the Decision step: Does the solution found make crystal-chemical-thermodynamic sense. A hindrance to the identification process for electron diffraction applications is that the PDF consists of x ray diffraction powder data. The present Elemental and Interplanar Spacing Index (EISI) book is based on the successful 1979 Max-d/Alphabetical Index rules, but with significantly enhanced capability, as it utilizes the combined NIST/Sandia/ICDD Database. The EISI is designed to be used independently as a searching tool. As a searching tool it provides a list of candidate phases for consideration as solutions to the unknown phase diffraction data. The EISI index was designed to assist the actual steps taken by an Analytical Electron Microscope (AEM) diffractionist when confronted with an unknown diffraction dataset: the assemblage and d-spacing searching of a microfile of data containing chemically correct phases. The construction of the NIST/Sandia/ICDD Database overcomes many of the disadvantages associated with searching x ray derived databases for solutions to electron diffraction problems. DOE

N90-26098*# National Aeronautics and Space Administration. Pasadena Office, CA.
REGENERATIVE Cu La ZEOLITE SUPPORTED DESULFURIZING SORBENTS Patent Application
Gerald E. Voecks, inventor (to NASA) and Pramod Sharma, inventor (to NASA) (Jet Propulsion Lab., California Inst. of Tech., Pasadena.) 12 Apr. 1990 21 p
(Contract NAS7-918)
(NASA-Case-NPO-17480-1-CU; NAS 1.71:NPO-17480-1-CU; US-Patent-Appl-SN-508386) Avail: NTIS HC A03/MF A01 CSCL 07D

Efficient, regenerable sorbents for removal of H2S from fluid hydrocarbons such as diesel fuel at moderate condition comprise a porous, high surface area aluminosilicate support, suitably a synthetic zeolite, and most preferably a zeolite having a free lattice opening of at least 6 Angstroms containing from 0.1 to 0.5 moles of copper ions, lanthanum ions or their mixtures. The sorbent removes sulfur from the hydrocarbon fuel in high efficiency and can be repetitively regenerated without loss of activity. NASA

N90-26099# Missouri Univ., Rolla. Dept. of Chemistry.
DYNAMICS OF MICELLAR OLIGOMERIC AND MONOMERIC SODIUM 10-UNDECENOATE Interim Report, Jan. - Jun. 1990
Robert J. Gambogi and Frank D. Blum 28 May 1990 26 p
(Contract N00014-88-K-0109)
(AD-A222570; UMR-FDB-16) Avail: NTIS HC A03/MF A01 CSCL 07/6

Multi-field carbon-13 Nuclear Magnetic Resonance longitudinal relaxation time measurement were used to probe the dynamics and structure of monomeric and oligomeric sodium 10-undecenoate in micellar solutions. Longitudinal relaxation data were fit to a two-state model for the spectral density function which utilizes as adjustable parameters a fast correlation time and an order parameter for each carbon atom, and an overall slow correlation time for the entire aggregate. This model was needed to explain the relaxation phenomena because of the anisotropic reorientation of the amphiphiles. The monomeric fast correlation profile indicated a motional gradient increasing towards the micellar core. Comparison of the fast correlation time profiles for monomer and oligomer revealed that the motional gradient found in the monomer was not present in the oligomer. Slow correlation times extracted from the two-state model indicate that the radii of the oligomeric micelles, approximated from the Debye-Stokes-Einstein equation, are slightly larger than the monomeric micelles; 10.6 versus 9.4 A, respectively. Radii calculated using self-diffusion coefficients also suggest a larger radius for the oligomeric micelles; 13.4 A for oligomeric micelles and 10.6 A for the monomeric micelles. The values determined for the micellar radii are less than that for the extended monomeric chain, 14.7 A. GRA

N90-26100# Ballistic Research Labs., Aberdeen Proving Ground, MD.
TEMPERATURE AND OH CONCENTRATIONS IN A SOLID PROPELLANT FLAME USING ABSORPTION TECHNIQUES
John A. Vanderhoff and Anthony J. Kotlar Apr. 1990 30 p Presented at the Army Science Conference, Durham, NC, 12-15 Jun. 1990
(DA Proj. 1L1-61102-AH-43)
(AD-A222591; AD-E951478; BRL-TR-3098) Avail: NTIS HC A03/MF A01 CSCL 21/9

Rotationally resolved absorption spectroscopy in the A-X (0,0) vibrational band system of OH around 306.4 nm was performed to determine the temperature and OH concentration in solid propellant flames. OH is sufficiently well characterized that the spectra can be least squares fitted under a variety of conditions. These conditions include the peculiarities of the experimental setup, instrument response parameters and absorption baseline, as well as the temperature and OH concentration. The multi-parameter least squares fit of the spectra gives values and statistical uncertainties for temperature, OH concentration, and other experimental design parameters. This technique was applied to a nitramine propellant flame burning in a windowed combustion vessel pressurized with 1.5 MPa nitrogen. A propellant feed mechanism coupled to the combustion vessel extended the data taking time such that good quality OH absorption spectra could be obtained for this transient event. Here the light source was an arc lamp and the detector a spectrometer with an intensified photodiode array. GRA

N90-26101# Purdue Univ., West Lafayette, IN. Dept. of Chemistry.
DYNAMICAL SOLVENT EFFECTS ON ELECTRON-TRANSFER PROCESSES: RECENT PROGRESS AND PERSPECTIVES
M. J. Weaver and G. E. McManis, III 1 May 1990 31 p
(Contract N00014-89-J-1452)

(AD-A222603; TR-97) Avail: NTIS HC A03/MF A01 CSCL 07/4

Recent advances in theoretical and experimental aspects of dynamic ' solvent effects in activated electron-transfer processes are discussed, along with future research prospects. The last decade has seen a remarkable upsurge of interest in the dynamical role of the solvent in liquid-state chemical processes. Along with the intrinsic importance of such phenomena in chemistry and biology, these activities have been fostered by substantial recent developments of both a theoretical and experimental nature. The central concept of solvent friction, whereby the collective solvent motion necessary to surmount the activation barrier slows the rate below that expected from transition state theory (TST), has spawned a myriad of theoretical treatments that attempt to describe the effective solvation dynamics. GRA

N90-26102# Jackson State Univ., MS. Dept. of Chemistry.
ELECTROCHEMICAL, IN SITU RAMAN SPECTROSCOPIC, AND CONDUCTIVITY STUDIES OF POLYPYRROLE INCORPORATING LARGE SIZE ANIONS: CONDUCTING NATURE OF REDUCED FORM Technical Report No. 3, Dec. 1989 - Nov. 1990
Chan S. Chan, Amar N. Singh, Zhisheng Sun, and Hiroyasu Tachikawa 21 May 1990 50 p Submitted for publication
(Contract N00014-89-J-1339; NIH-S06-GM-08047)
(AD-A222739; TR-3-ONR) Avail: NTIS HC A03/MF A01 CSCL 07/6

Polypyrrole (PPY) thin films doped with large size anions, such as tetrasulfonated metallophthalocyanines, tetrasulfornated copper porphyrin, polyvinyl sulfate, and poly(P-styrenesulfonate), have shown electrochemical activities of redox pairs in both aqueous and nonaqueous solutions at the negative potentials where the PPY is reduced to a neutral form. In situ Raman spectroscopy showed that the charge-transfer reactions of redox pairs took place at the surface of the reduced PPY thin films in the negative potential range. Cyclic voltammetric results indicated that the structurally rigid PPY films which were doped with large size anions demonstrated a considerable electrochemical conductivity when the PPY was reduced to a neutral form, although both ex-situ and in situ conductivity measurements of these films indicated that the electronic conductivity of the reduced form is generally several orders of magnitude smaller than that of the oxidized form. GRA

N90-26103# Indiana Univ., Bloomington. Dept. of Physics.
THE APPLICATION OF HREELS TO MODEL CATALYSTS: CO AND C2H4 ADSORPTION ON Pt/Al2O3
D. A. Hensley and L. L. Kesmodel 20 May 1990 27 p Sponsored in part by American Chemical Society
(Contract N00014-89-J-1775)
(AD-A222744; TR-2) Avail: NTIS HC A03/MF A01 CSCL 20/5

A model catalyst made by platinum vapor deposition onto a thin alumina film is investigated with transmission electron microscopy (TEM) and high resolution electron energy loss spectroscopy (HREELS). The preparation techniques are fully described, then the results of TEM analysis for platinum deposits from 0.3 monolayers to 1.7 monolayers are reported, for which clusters varying from 1.0 to 1.6 nanometers in diameter are observed. High resolution electron energy loss spectroscopy spectra are reported for the cases of carbon monoxide and ethylene adsorption onto the model. For the case of CO adsorption, it is shown that the catalyst is stable when heated to 500 K. For the case of ethylene adsorption, pi and di-sigma species are identified for adsorption at 165 K, but on warming to 325 K, ethylidyne is only observed for the larger platinum deposits. This is first HREELS observation of the ethylidyne species on alumina supported catalysts. GRA

N90-26104# California Univ., Berkeley. Dept. of Mechanical Engineering.
LIQUID FUELED RAMJET COMBUSTION INSTABILITY: ACOUSTICAL AND VORTICAL INTERACTIONS WITH BURNING SPRAYS Final Technical Report, 5 May 1985 - 30 Apr. 1988
W. A. Sirignano, R. Bhatia, and K. Molavi 15 May 1990 99 p
(Contract N00014-85-K-0658)
(AD-A222752) Avail: NTIS HC A05/MF A01 CSCL 21/4

A theoretical/computational study of liquid-fueled ramjet instability has been performed. The roles of droplet vaporization and spray combustion processes have been determined as rate-controlling factors on the performance and stability of combustors. The effects of vaporization, mixing, turbulent transport, and chemical kinetics were evaluated. The impact of variations in geometry, initial droplet size, equivalence ratio, and various numerical factors were determined. The study had four major components: individual droplet studies, a one-dimensional combustor analysis, a planar combustor study, and an axisymmetric study. A predictive capability was developed. Vaporization processes and droplet trajectories were found to affect performance and stability significantly. GRA

N90-26105# Utah Univ., Salt Lake City. Dept. of Chemistry.
CHEMICAL STRUCTURE AND KINETICS AT LIQUID/SOLID INTERFACES Report, 1 Jun. 1989 - 31 May 1990
Joel M. Harris 31 May 1990 11 p
(Contract N00014-89-J-1412)
(AD-A222766) Avail: NTIS HC A03/MF A01 CSCL 20/5

This program of research is to develop spectroscopic methods for exploring chemical structure and molecular dynamics at interfaces between dielectric solids and liquids. The research is carried out using fluorescence and vibrational spectroscopy from probe molecules where spectral and temporal differences in emission, absorption, or scattering provide information about the surface onto which they are adsorbed or bound. Studies focus on the interfacial chemistry of oxide surfaces (mostly silica) and derivatized silica in contact with liquids. The spectral and temporal response of probe molecules is used to observe differences in the chemical environment at the liquid-solid interface due to the presence of bound or adsorbed molecules. Time-resolution is also valuable in sorting out heterogeneous surface environments from differences in emission rate constants, adsorption rates, and reaction kinetics of probe molecules to solid surfaces are being measured using perturbation methods. GRA

N90-26764*# Catholic Univ. of America, Washington, DC. Dept. of Chemistry.
KINETICS AND THERMOCHEMISTRY OF POLYATOMIC FREE RADICALS: NEW RESULTS AND NEW UNDERSTANDINGS
David Gutman and Irene R. Slagle *In* NASA, Goddard Space Flight Center, First International Conference on Laboratory Research for Planetary Atmospheres May 1990 p 210-220 Sponsored in part by DOE and NSF (For primary document see N90-26744 20-91)
Avail: NTIS HC A21/MF A03 CSCL 07D

N90-26765*# Howard Univ., Washington, DC. Dept. of Chemistry.
THE HEAT OF FORMATION OF CN RADICALS AND RADIATIVE LIFETIMES OF THE A 1 SIGMA - STATE OF C2N2
Samuel A. Barts, Karen V. Pinnex, and Joshua B. Halpern *In* NASA, Goddard Space Flight Center, First International Conference on Laboratory Research for Planetary Atmospheres May 1990 p 221-226 Sponsored in part by DOE; Danforth Foundation; and Department of Education (For primary document see N90-26744 20-91)
(Grant NAG5-785)
Avail: NTIS HC A21/MF A03 CSCL 07D

N90-26774*# Cornell Univ., Ithaca, NY. Lab. for Planetary Studies.
LIQUID-VAPOR EQUILIBRIUM OF MULTICOMPONENT CRYOGENIC SYSTEMS
W. Reid Thompson, Jorge C. G. Calado (Instituto Superior Tecnico, Lisbon, Portugal), and John A. Zollweg *In* NASA, Goddard Space Flight Center, First International Conference on Laboratory Research for Planetary Atmospheres May 1990 p 303-326 (For primary document see N90-26744 20-91)
(Grant NAGw-1444)
Avail: NTIS HC A21/MF A03 CSCL 07D

N90-26775*# National Aeronautics and Space Administration. Ames Research Center, Moffett Field, CA.
OPTICAL CONSTANTS OF SOLID METHANE
Bishun N. Khare, W. R. Thompson, C. Sagan, E. T. Arakawa, C. Bruel, J. P. Judish, R. K. Khanna (Maryland Univ., College Park.), and J. B. Pollack *In* NASA, Goddard Space Flight Center, First International Conference on Laboratory Research for Planetary Atmospheres May 1990 p 327-339 (For primary document see N90-26744 20-91)
(Contract NGR-33-010-220; NGR-33-010-082; NAGw-637; DE-AC05-84OR-21400)
Avail: NTIS HC A21/MF A03 CSCL 07D

N90-26776*# Cornell Univ., Ithaca, NY. Lab. for Planetary Studies.
OPTICAL CONSTRAINTS OF KEROGEN FROM 0.15 TO 40 MICRONS: COMPARISON WITH METEORITIC ORGANICS
Bishun N. Khare, W. R. Thompson, C. Sagan, E. T. Arakawa, C. Meisse, and I. Gilmour (Chicago Univ., IL.) *In* NASA, Goddard Space Flight Center, First International Conference on Laboratory Research for Planetary Atmospheres May 1990 p 340-356 Sponsored in part by Norris (Kenneth T. and Eileen L.) Foundation (For primary document see N90-26744 20-91)
(Contract NAG9-52; NGR-33-010-101; DE-AC05-84OR-21400; NSF EAR-86-09218)
Avail: NTIS HC A21/MF A03 CSCL 07D

N90-26777*# National Aeronautics and Space Administration. Goddard Space Flight Center, Greenbelt, MD.
VAPOR PRESSURES OF ACETYLENE AT LOW TEMPERATURES
C. M. Masterson, John E. Allen, Jr., G. F. Kraus, and R. K. Khanna (Maryland Univ., College Park.) *In its* First International Conference on Laboratory Research for Planetary Atmospheres May 1990 p 357-362 (For primary document see N90-26744 20-91)
Avail: NTIS HC A21/MF A03 CSCL 07D

26 METALLIC MATERIALS

Includes physical, chemical, and mechanical properties of metals, e.g., corrosion; and metallurgy.

N90-26106# Aeronautical Research Labs., Melbourne (Australia). Dept. of Defence.
STATISTICAL TREATMENT OF SLOW STRAIN RATE DATA FOR ASSESSMENT OF HYDROGEN EMBRITTLEMENT IN LOW ALLOY HIGH STRENGTH STEEL
W. J. Pollock Apr. 1990 30 p
(ARL-MAT-R-122; AR-006-084; AD-A222732) Copyright Avail: NTIS HC A03/MF A01

Slow strain rate testing was used to quantify the degree of hydrogen embrittlement produced in high strength 4340 steel by plating processes and aircraft maintenance chemicals. The results of slow strain rate tests, conducted at a crosshead displacement rate of 2 x 10(exp-4)mm/s using samples of three notched tension specimens in various paint strippers, show that a mean fracture stress of 1850 MPa can be correlated with the pass/fail criterion for acceptability of paint strippers in an existing Standard Notched C-ring Test. Statistical analysis of the slow strain rate data allows criteria to be established which will ensure a 99 percent probability of identifying all paint strippers that fail the Notched C-ring Test. This analysis is also used to trade a series of products and processes in terms of their tendency to cause hydrogen embrittlement, and to identify environmental parameters that cause excessive scatter in hydrogen embrittlement tests. Criteria are also specified for acceptability of each heat treatment batch of 4340 steel specimens to ensure reproducibility of results obtained from slow strain rate tests. Author

N90-26107# Wichita State Univ., KS. Dept. of Mechanical Engineering.
A STUDY OF THE FATIGUE BEHAVIOR IN SCRATCHED SAMPLES OF Al-Li ALLOY (2090-T3) M.S. Thesis
Takao Toriyama Dec. 1989 58 p
(Contract DAAL03-87-G-0003)
(IAR-89-24) Avail: NTIS HC A04/MF A01

The Fatigue behavior of Al-Li alloy (2090-T3) with small surface generated scratches was investigated experimentally on a servohydraulic material testing machine. Small scratches were generated on the specimens which were then subjected to low cycle fatigue tests. These sets of experiments provided information on the relevant deformation and fracture parameters, in relation with depth of the scratch, scratch angle, and the radius of curvature at a tip of the scratch. All of scratch parameters were thought to have significant influence on fatigue life of Al-Li alloy (2090-T3). It was found that as the depth of the scratch becomes larger, the fatigue life decreases. However the scratch angle doesn't affect the fatigue life. The fracture surfaces were observed by using an scanning electron microscope. The fatigue tests and fractographs were analyzed to identify the responsible mechanism for the reduction of fatigue life comparing with modern theories of fatigue and fracture. Mechanism about the formation of microcracks at the scratch tip proposes to explain the results obtained. Author

N90-26108*# Auburn Univ., AL. Dept. of Mechanical Engineering.
HYDROGEN INDUCED FRACTURE CHARACTERISTICS OF SINGLE CRYSTAL NICKEL-BASED SUPERALLOYS Final Report, 19 Jun. 1989 - 18 Jun. 1990
Po-Shou Chen and Roy C. Wilcox 18 Jun. 1990 85 p
(Contract NAS8-38184)
(NASA-CR-183992; NAS 1.26:183992) Avail: NTIS HC A05/MF A01 CSCL 11F

A stereoscopic method for use with x ray energy dispersive spectroscopy of rough surfaces was adapted and applied to the fracture surfaces single crystals of PWA 1480E to permit rapid orientation determinations of small cleavage planes. The method uses a mathematical treatment of stereo pair photomicrographs to measure the angle between the electron beam and the surface normal. One reference crystal orientation corresponding to the electron beam direction (crystal growth direction) is required to perform this trace analysis. The microstructure of PWA 1480E was characterized before fracture analysis was performed. The fracture behavior of single crystals of the PWA 1480E nickel-based superalloy was studied. The hydrogen-induced fracture behavior of single crystals of the PWA 1480E nickel-based superalloy was also studied. In order to understand the temperature dependence of hydrogen-induced embrittlement, notched single crystals with three different crystal growth orientations near zone axes (100), (110), and (111) were tensile tested at 871 C (1600 F) in both helium and hydrogen atmospheres at 34 MPa. Results and conclusions are given. Author

N90-26109# Oak Ridge National Lab., TN. High Temperature Materials Lab.
OXIDATION AND SULFIDATION OF TYPE 310S STAINLESS STEEL AT ELEVATED TEMPERATURES
James S. Wolf (Clemson Univ., SC.) and O. Burl Cavin 1990 23 p Presented at the 29th International Symposium on High Temperature Oxidation and Sulfidation Processes, Hamilton, Ontario, 26-30 Aug. 1990

(Contract DE-AC05-84OR-21400)
(DE90-010149; CONF-900886-1) Avail: NTIS HC A03/MF A01

Specimens of Type 310S stainless steel in the forms of thin flat and bent sheet (ells) were exposed either to air or a sulfidizing atmosphere at temperatures near 900 C. An attempt was made to determine the relationships between: (1) the scale structure, (2) the rate of reaction, and (3) the mechanical stresses generated during exposure. The investigative techniques used included: room and elevated temperature x ray diffraction, optical and electron microscopy as well as optical determinations of specimen deformations. Protective and spall-resistant scales were formed in both atmospheres. All scales were composed of an inner sesquioxide and an outer spinel layer. Both the scale crystallinity and the surface topography were, however, grossly different in the two environments; including especially the presence of metallic particles found embedded in the scales of sulfidized specimens. The interaction of sulfur with the growth of oxide scales apparently alters their crystallinity, microstructure and stress state. It is suggested that the oxide grain boundary plays a role in this perturbed growth process and that, therefore, the control of oxide grain size may be one fruitful approach in the future development of alloys resistant to breakdown in sulfidizing atmospheres. DOE

N90-26110# Lawrence Livermore National Lab., CA.
THE ORIGIN OF POORLY CONDITIONED SUSCEPTIBILITY MATRIX WITHIN INVERSE CVM ALGORITHM IN THE CASE OF Pd(SUB 3)V: A COMPARISON TO THE CASE OF Ni(SUB 3)V
Francine Solal and Alphonse Finel (Office National d'Etudes et de Recherches Aerospatiales, Paris, France) 24 Apr. 1990 8 p Presented at the Spring Meeting of the Materials Research Society, San Francisco, CA, 16-20 Apr. 1990 Submitted for publication
(Contract W-7405-eng-48)
(DE90-012464; UCRL-JC-103666; CONF-900466-58) Avail: NTIS HC A02/MF A01

Transition metal alloys are interesting in order to test the Cluster Variation Method as a proper statistical model to describe order-disorder phenomena. In the case of such alloys electronic structure calculations all agree to predict short-ranged pairwise interactions as sufficient to account for phase diagrams and order-disorder properties in general. Performing Inverse CVM within the 13 to 14 points approximation, pair interactions were determined up to the fourth neighbors. In the process of determining these interactions, some difficulties were encountered, especially in the case of Pd3V where the experimental errors on the short range order parameters were dramatically enhanced through the Inverse CVM process, leading to poorly determined interactions. In particular to precise these interactions, had be used as supplementary informations i.e., the order-disorder transition temperature. It is emphasized that these problems are closely related to the nature of the system, namely to its high degeneracy (1), and not at all, for example, to the quality of the experimental data. Moreover, we would like to show that the parameter responsible for this high degeneracy, namely the (100) antiphase energy is determined with a good accuracy compared to the individual interactions. The case of Pd3V is compared to the Ni3V one, for which the degeneracy is lifted. DOE

N90-26111# Pennsylvania State Univ., University Park. Materials Research Lab.
TWIN BOUNDARIES, INTERFACES AND MODULATED STRUCTURES IN MARTENSITES Annual Progress Report No. 5, 1 Jul. 1989 - 30 Jun. 1990
Gerhard R. Barsch 15 Jan. 1990 19 p
(Contract DE-FG02-85ER-45214)
(DE90-012899; DOE/ER-45214/5) Avail: NTIS HC A03/MF A01

A comprehensive theoretical study with concurrent supporting experimental investigations is being carried out on coherent and semicoherent interfaces in ferroelastic martensites, including twin boundaries and twin bands, heterophase parent/product interfaces and inclusions, and transformation precursors. This work is motivated by the need for a new theoretical basis for investigating the martensite nucleation mechanism and for establishing the conditions for nonclassical nucleation. Soliton-like solutions of a dynamic Ginzburg-Landau continuum theory for ferroelastic martensites are being studied in order to determine the strain distribution, strain energy and dynamical behavior for various geometric configurations as a function of the material parameters, temperature and boundary conditions. Model parameters of the theory consist of the second and higher order elastic constants and the harmonic strain gradient coefficients in the parent phase. X ray measurements of the transformation strain versus temperature, and ultrasonic velocity and attenuation measurements on biaxially stressed crystals in In sub 1 minus x Tl sub x alloys for determining the second and higher order elastic constants in the single domain tetragonal state and for studying the morphology and the dynamic behavior of the martensite interfaces and transformation precursors are in progress. DOE

N90-26112# Sandia National Labs., Livermore, CA. Mechanics of Materials Div.
COMPENDIUM OF MATERIAL TEST RESULTS ON HY-130 AND Ti-3Al2V METALS IN SUPPORT OF UNITED STATES NAVY PROGRAMS Interim Report
John S. Korellis and Kenneth L. Lee Apr. 1990 41 p Sponsored in part by NSWC, White Oak, MD
(Contract DE-AC04-76DR-00789)
(DE90-011754; SAND-90-8217) Avail: NTIS HC A03/MF A01

This report documents the status of ongoing tests performed to construct a material database for use in structural analysis codes. Uniaxial tension and compression tests were performed to quantify isotropy and strain-rate dependence of stress-strain behavior at room temperature. Notched tensile tests were performed to support development of the damage portion of coupled flow-damage constitutive models. The above results, supplemented with a few elevated temperature tests, will be used to define all material constants in a constitutive model. Plate perforation tests were also performed, to be compared with model predictions. DOE

N90-26113# Yale Univ., New Haven, CT. Dept. of Mechanical Engineering.
MICROSTRUCTURAL DEPENDENCE OF THE CAVITATION DAMAGE FUNCTION IN FCC MATERIALS Progress Report, 1 Mar. 1989 - 28 Feb. 1990
Brent L. Adams 1990 7 p
(Contract DE-FG02-88ER-45355)
(DE90-012898; DOE/ER-45355/2) Avail: NTIS HC A02/MF A01

The experimental program over the past year has concentrated on establishing optimal testing conditions for creep testing, and on characterization of the starting microstructure of the high purity copper sheet. DOE

N90-26114# Lawrence Livermore National Lab., CA.
DENSIFICATION STUDIES OF REFRACTORY MATERIALS USING HOT ISOSTATIC PRESSING (HIP) AND TANTALUM CONTAINMENT
Clarence Hoenig, Ralph Otto, and William Stutler 27 Apr. 1990 9 p Presented at the 7th World Ceramics Congress and Satellite Symposia, Montecatini Terme, Italy, 24-30 Jun. 1990 Submitted for publication
(Contract W-7405-eng-48)
(DE90-013481; UCRL-102154; CONF-900634-2) Avail: NTIS HC A02/MF A01

Powders of crystalline rohmbohedral boron were HIP processed to near full density at 1500 to 1800 C and 206.8 MPa. At 1700 C, the densification of boron was independent of particle size in the range of less than 37 microns to 10 mm. At 1500 C, only the less than 37 microns powder reached near full density. Silicon and calcium impurities were found to segregate in the grain boundaries during densification. Results indicate that plastic yielding was to dominate densification mechanism. Boron nitride powder with 0.97 percent oxygen content was pressed to a density of

2.21 g/cu cm at 18000 C and 206.8 MPa. The density of high purity hot pressed graphite was increased by 15 percent to 2.10 g/cu cm at 2200 C and 206.8 MPa. These results show that refractory metal containers used in hot isostatic pressing significantly expand the availability of high density high purity materials.
DOE

N90-26115*# Alabama Univ., Birmingham. Dept. of Materials Engineering.
EFFECT OF BORON ON INTERGRANULAR HOT CRACKING IN Ni-Cr-Fe SUPERALLOYS CONTAINING NIOBIUM Final Report
R. G. Thompson 22 Jun. 1990 115 p
(Contract NAS8-38084)
(NASA-CR-186714; NAS 1.26:186714) Avail: NTIS HC A06/MF A01 CSCL 11F

Solidification mechanisms had a dominant influence on microfissuring behavior of the test group. Carbon modified the Laves formation significantly and showed that one approach to alloy design would be balancing carbide formers against Laves formers. Boron's strong effect on microfissuring can be traced to its potency as a Laves former. Boron's segregation to grain boundaries plays at best a secondary role in microfissuring.
Author

N90-26116# Iowa State Univ. of Science and Technology, Ames. Dept. of Materials Science.
SEARCHING FOR HEAVY FERMION MATERIALS IN Ce INTERMETALLIC COMPOUNDS Ph.D. Thesis
Jinke Tang Jan. 1990 144 p
(Contract W-7405-eng-82)
(DE90-011809; IS-T-1354) Avail: NTIS HC A07/MF A01

The low temperature heat capacity, magnetic susceptibility and electrical resistivity were studied for a series of Ce intermetallic compounds. No heavy fermion behavior was found in these compounds. CePtGa3 has a rounded peak at approx 1.7 K in its heat capacity, which is shifted to higher temperatures in magnetic fields approx. 6 K at 9.8 T. The origin of this peak is believed to be due to a spin glass type transition. CeCd11 has an unusual temperature dependence of its heat capacity which is due to a crystalline electric field (CEF) effect which occurs at an exceptionally low temperature. The CEF effect also plays an important role in CeGa2. Antiferromagnetic phase transitions were found in CeHg3, CeCd2, CeCd3 and CeNi12B6. Discussions on the low temperature behaviors of these and other Ce intermetallic compounds are given.
DOE

N90-26117# Oak Ridge National Lab., TN. Metals and Ceramics Div.
FORMATION OF CUBIC LI2 PHASES FROM Al3Ti AND Al3Zr BY TRANSITION METAL SUBSTITUTIONS FOR Al
C. J. Sparks, W. D. Porter, J. H. Schneibel, W. C. Oliver, and C. G. Golec (Purdue Univ., Hammond, IN.) 1990 6 p Presented at the Spring Meeting of the Materials Research Society, San Francisco, CA, 16-21 Apr. 1990
(Contract DE-AC05-84OR-21400)
(DE90-012288; CONF-900466-67) Avail: NTIS HC A02/MF A01

Alloys of Al(x)M(1-x)3Ti where M is V, Cr, Mn, Fe, Co, Nb, W, Fe + Ga or Fe + Ga + Mn were fabricated to form the LI(2) cubic phase, tested for ductility, and characterized by lattice parameter, microstructure, quantitative phase analysis, and phase composition. The elements V, Co, Nb, W, Fe + Ga and Fe + Ga + Mn are hereby newly found LI(2) formers in Al3Ti. Both x ray diffraction and microprobe analysis were used to identify the phases, their volume fractions and compositions. The amount of ternary addition found in the LI(2) cubic phase varied between 4 and 12 atomic percent. This amount of ternary addition decreased as the atomic radius of the elemental addition increased. Pettifor's Mendeleev number was a useful guide in the selection of elements to form the LI(2) phase but did not correlate strongly with the amount of the ternary addition. For the DO(23) phase of Al3Zr, the elements V, Mn, and Co were added to the list of Ni, Cu, Fe, and Cr as elements known to form the LI(2) phase. Little if any ductility was observed in these cubic LI(2) phases which readily cleaved with transgranular failure. To achieve ductility and toughness, more than transformation of these compositions from a lower to a higher symmetry crystal structure will be required.
DOE

N90-26118# Los Alamos National Lab., NM. Materials Science and Technology Div.
FORMATION OF TITANIUM-BORON SURFACE ALLOYS BY EXCIMER LASER MIXING
Thomas Roland Jervis, Michael Nastasi, Juha-Pekka Hirvonen, and Thomas G. Zocco 1990 5 p Presented at the 10th International Symposium on Boron, Borides, and Related Compounds, Albuquerque, NM, 27-30 Aug. 1990 Submitted for publication
(Contract W-7405-eng-36)
(DE90-013172; LA-UR-90-2009; CONF-900870-1) Avail: NTIS HC A01/MF A01

Scientist have formed a surface Ti-B alloy by excimer laser mixing of a single B layer on a Ti-6Al-4V alloy substrate. Rutherford backscattering spectroscopy indicates a uniform B:Ti ratio of approximately 0.7 in the surface layer. A Boron layer 60 nm thick resulted in an alloy layer approximately 200 nm thick. There is little indication, by either Auger electron spectroscopy or nuclear reaction analysis, of substantial oxygen incorporation in the surface alloy despite the fact that the processing was done in air. Transmission electron microscopy of the surface alloy shows a completely amorphous surface layer underlain by a martensitic structure.
DOE

N90-26119# Ames Lab., IA.
THE EFFECT OF MANGANESE ON THE ONSET OF THE STAGE 2 REACTION IN AN AUSTEMPERED DUCTILE IRON MATRIX M.S. Thesis
Kenneth Norman Hagen Feb. 1990 61 p
(Contract W-7405-eng-82)
(DE90-011804; IS-T-1476) Avail: NTIS HC A04/MF A01

Austempered ductile irons (ADIs) possess a unique combination of toughness and ductility plus high strength which make them attractive alternatives to other metal castings. ADIs can have tensile strengths up to 230 ksi with a 1 percent elongation and high hardness for wear resistant applications, or tensile strengths of approximately 150 ksi and elongations of 14 percent where a large amount of ductility is required. Austempering is a two step process: complete transformation to the austenite ((gamma)) phase; and a quench and hold in the temperature range of 270 to 420 C for some time followed by cooling to room temperature. This quench must be sufficiently rapid to avoid formation of pearlite or ferrite if the best mechanical properties are to be obtained. The results are presented of a number of experiments aimed at determining the effect of Mn on the length of the Stage 1 reaction. (austenite decomposes into bainitie ferrite and high carbon austenite). A basic knowledge of the effects of Mn will yield a more complete understanding of the austempering process for the normal case and also when microsegregation is present. The onset time for Stage 2 (high carbon austenite decomposes into bainitic ferrite plus carbides) in ductile irons is a critical parameter because of the associated degradation of the mechanical properties which result from carbide formation.
DOE

N90-26120# Rolls-Royce Ltd., Derby (England).
MICROSTRUCTURAL DESIGN FOR FATIGUE CRACK GROWTH RESISTANCE IN Ni-BASE ALLOY
J. M. Kendall, L. Grabowski, and K. E. King (Cambridge Univ., England) 21 Mar. 1989 26 p Sponsored by Science Research Council, England; British Gas PLC; and Fellowship of Engineering, Westminister, England
(PNR90632; ETN-90-97141) Copyright Avail: NTIS HC A03/MF A01

In gamma prime strengthened Ni-base disc alloys control of processing and heat treatment can be used to vary microstructural parameters for both the matrix and the precipitates. The effects of such changes are reviewed for long and for microstructurally

short cracks. If inherent defect sizes can be controlled by the alloy production route to values well below current NDI (Non Destructive Inspection) limits, there will be need to consider short crack growth behavior in alloy design. Fatigue life integrations are used to compare predictions from long crack data with combinations of long and short crack growth rates, for fine, coarse and mixed (or necklace) grain microstructures. The results emphasize the importance of the transition crack length between short and long crack behavior, and its dependence on microstructure. Both long and short crack propagation resistance need to be included in alloy design for aeroengine disc applications. ESA

N90-26121# Royal Aerospace Establishment, Farnborough (England).
SMALL CRACK GROWTH AND ITS INFLUENCE IN NEAR ALPHA-TITANIUM ALLOYS
M. C. Hardy 27 Jun. 1989 33 p
(RAE-TM-P-1171; BR112079; ETN-90-97067) Copyright Avail: NTIS HC A03/MF A01

Small fatigue cracks are known to propagate at rates much greater than large cracks in the same material at an equivalent crack driving force. The small crack problem and the reasons for its existence are clarified. Some recent models, incorporating large scale plasticity, crack closure and micro-structural dissimilitude, are introduced. Small crack behavior in near alpha-titanium alloys is examined. ESA

N90-26122# Royal Aerospace Establishment, Farnborough (England).
HIGH TEMPERATURE MULTIAXIALE CREEP TESTING OF NIMONIC 115
L. W. Candler 16 Jan. 1990 14 p Presented at 4th International Conference on Creep and Fatigue of Engineering Materials and Structures, Swansea, England, 1-6 Apr. 1990
(RAE-TM-P-1182; BR113062; ETN-90-97069) Copyright Avail: NTIS HC A03/MF A01

Materials in present day gas turbine components are known to operate under complex stress situations. In recent years much effort has been devoted to quantified the state of stress in multi-axial geometries and to studying the deformation and rupture mechanism involved, but little attention was paid to the practical aspects of multiaxial testing and to understanding the material behavior under complex stress states. A high temperature multiaxial testing facility, commissioned using the nickel based alloy Nimonic 115, is described and the difficulties associated with this technique for testing are highlighted. ESA

N90-26123# Office National d'Etudes et de Recherches Aerospatiales, Paris (France).
STRUCTURES AND MECHANICAL PROPERTIES OF NEAR-BETA TITANIUM ALLOYS TiV10Fe2Al3 AND TiV10Cu3Al3 Ph.D. Thesis - Paris VI Univ.
Marie-Helene Campagnac 1989 105 p In FRENCH; ENGLISH summary Report will also be announced as translation (ESA-TT-1200)
(ONERA-NT-1989-3; ISSN-0078-3781; ETN-90-97260) Avail: NTIS HC A06/MF A01

Near-beta titanium alloys are attractive for aircraft structural applications. Both alloys have a similar beta-transus around 800 C. The phase is preserved after quenching to room temperature in TiV10Fe2Al3, whereas TiV10Cu3Al3 undergoes complete transformation to orthorhombic alpha two prime martensite. The age-hardening reactions were investigated in these two alloys in the 300 to 525 C temperature range using transmission electron microscopy and x ray analysis. The alpha phase precipitates in TiV10Fe2Al3 either from isothermal omega particles or directly from the beta matrix, depending on the aging temperature. In the case of TiV10Cu3Al3, the phase transformations involve the reversion of alpha two prime and beta followed by the precipitations of omega and alpha phases. In both alloys, no isothermal omega is observed above 375 C and grain boundary alpha phase appears at 525 C. Only the Burgers oriented alpha phase is present. The intermetallic compound Ti2Cu is formed in the alpha phase of the TiV10Cu3Al3 alloy. These microstructural investigations show that the morphology and the distribution of the alpha phase can be controlled by varying heat treatments. The effect of double solution treatment, two step aging treatment, rate of heating to the ageing temperature on tensile strength, ductility and fracture toughness is examined and the properties of the two alloys are compared. ESA

N90-26124# David Taylor Research Center, Bethesda, MD. Dept. of Ship Materials Engineering.
DAMPING CAPACITY OF ALUMINUM 6061-INDIUM ALLOYS Research and Development Report, Oct. 1987 - Feb. 1989
C. R. Wong, O. Diehm, and D. C. VanAken (Michigan Univ., Ann Arbor.) Jan. 1990 27 p
(AD-A222802; DTRC/SME-89/111) Avail: NTIS HC A03/MF A01 CSCL 11/6

Monotectic Al-6061 alloys containing between 0 and 5.2 volume percent indium and pure indium samples were fabricated. Each sample was characterized by metallographic and analytical electron microscopy and the damping capacity and storage modulus were measured. The model proposed by L.G. Nielsen was used to calculate the damping capacity and storage modulus of the alloys using the damping capacity and storage modulus of the constituents. The damping capacity of the Al-6061-T6 alloy was increased with increasing indium content. The Nielsen model gave a good first approximation of the damping capacity and storage modulus of the alloys. GRA

N90-26125# Dayton Univ., OH. Research Inst.
FRACTURE TOUGHNESS AND FAILURE MECHANISMS IN COMMERCIAL 2091 Al-Li SHEET AT CRYOGENIC TEMPERATURES Interim Report, Jul. 1988 - Dec. 1989
Kumar V. Jata and John J. Ruschau 9 Mar. 1990 46 p
(Contract F33615-88-C-5437; AF Proj. 2418)
(AD-A222803; UDR-TR-90-04; WRDC-TR-90-4013) Avail: NTIS HC A03/MF A01 CSCL 11/6

Strength-toughness relationships in 2091 Al-Li (Aluminum-Lithium) alloy in the T3 temper were examined at ambient, liquid nitrogen and liquid helium temperatures as a function of sheet orientation and product form (sheet thickness). Commercially available 1.6 millimeters (0.063 inch) and 3.6 millimeters (0.144 inch) thick sheets in the T3 temper were examined, with both alloy sheets exhibiting increasing yield strength but decreasing tensile elongation and toughness at cryogenic temperatures in all orientations. This behavior is in contrast with the observation of enhanced strength and toughness in longitudinal and transverse orientations (L-T and T-L) and certain heat treatment tempers of 2090 and 8090 Al-Li; alloys at cryogenic temperatures. It is also noted that in the present 2091 sheets where the triaxial state of stress is expected to be low, through thickness delaminations are prevalent at cryogenic temperatures due to weak short transverse properties. GRA

N90-26126# Cummins Engine Co., Inc., Columbus, IN.
EFFECT OF CASTING PROCEDURES AND DIESEL ENGINE ENVIRONMENT ON THE BEHAVIOR OF ALUMINUM TITANATE Final Report, Oct. 1987 - Dec. 1989
R. J. Stafford, J. W. Cogburn, and T. M. Yonushonis Apr. 1990 91 p
(Contract DAAL04-87-C-0085; DA Proj. 1L1-62105-AH-84)
(AD-A223079; MTL-TR-90-20) Avail: NTIS HC A05/MF A01 CSCL 11/6

The purpose of this report is to document the final results and conclusions of work on the behavior of aluminum titanate materials in a diesel engine environment. The work was conducted in three phases. Phase 1 covered investigation of material properties and microstructures of aluminum titanate materials from three different manufacturers. Phase 2 consisted of testing and evaluation of the material properties and microstructure, of each of the materials, after environmental exposures. Phase 3 work involved investigation of casting procedures to produce a cast-in-place exhaust port. Temperature profiles were recorded

and different external compliant layers and core sand compositions were examined. The aluminum titanate material from the three different manufacturers showed significant differences in strength, stability and thermophysical properties. One material was low density with low strength, modulus and conductivity. The second material exhibited degradation to alpha-Al2O3 after aging at temperatures greater than 1000 C. The third material had very high strength as-received but showed a strength loss of up to 40 percent after aging. However, the strength for this material after aging remained greater than the as-received strength of the other two materials. The casting studies showed that cast-in-place ports can be produced. The most promising results were seen when the core sand composition was 50 percent SiC/50 percent Fe.
GRA

27 NONMETALLIC MATERIALS

Includes physical, chemical, and mechanical properties of plastics, elastomers, lubricants, polymers, textiles, adhesives, and ceramic materials.

For composite materials see *24 Composite Materials*.

N90-26127 New South Wales Univ., Kensington (Australia). Dept. of Ceramic Engineering.
THE INTERACTION OF POLYMERIC MATERIALS WITH CERAMIC SURFACES WITH SPECIAL REFERENCE TO THE BEHAVIOUR OF BIOCERAMICS Ph.D. Thesis Abstract Only
William W. L. Ching Nov. 1988 4 p
Avail: Issuing Activity

The discovery that bioceramics are tolerable by the body has led to a demand for better understanding of ceramic/tissue interactions. Silicon nitride and calcium hydroxyapatite are two ceramic materials of great biological interest; the former for its inertness and excellent mechanical strength, and use as a possible alternative to surgical metal alloys, and the latter for its similar chemical composition to that of natural bone, as well as its resorbable property. Methods to produce each type of the ceramic implants in a porous form were investigated. Since pore size and interlinkage among pores play such an important role in tissue penetration and bone ingrowth, samples were prepared with different pore sizes, which were controlled. Although larger pores are needed for better bone growth, too many of them would weaken the physical strength. Therefore an optimum pore size is a critical factor in the design of ceramic implants for potential prothetic devices. A total of over thousand small ceramic compacts were produced and tested for their apparent porosities, bulk densities, compressive strength, and tensile strength, before they were placed into the morphological assessment, in which the effects of ceramic compacts on bone marrow cells and their differentiation, when grown in victro and in vivo, were studied. Results show that silicon nitride should be considered as a potentially permanent ceramic for use in bone reconstructure, and calcium hydroxyapatite as a resorbable ceramic for short-term bone repairs. Author

N90-26128*# Georgia Inst. of Tech., Atlanta. School of Mechanical Engineering.
SOIL STABILIZATION MAT FOR LUNAR LAUNCH/LANDING SITE
Amy L. Acord, Mark W. Cohenour, Daniel Ephraim, Dennis Gochoel, and Jefferson G. Roberts Mar. 1990 71 p
(Contract NASw-4435)
(NASA-CR-186690; NAS 1.26:186690; TEX-4312; ME-4182)
Avail: NTIS HC A04/MF A01 CSCL 11E

Facilities which are capable of handling frequent arrivals and departures of spaceships between Earth and a lunar colony are necessary. The facility must be able to provide these services with minimal interruption of operational activity within the colony. The major concerns associated with the space traffic are the dust and rock particles that will be kicked up by the rocket exhaust. As a result of the reduced gravitation of the Moon, these particles scatter over large horizontal distances. This flying debris will not only seriously interrupt the routine operations of the colony, but could cause damage to the equipment and facilities surrounding the launch site. An approach to overcome this problem is presented. A proposed design for a lunar take-off/landing mat is presented. This proposal goes beyond dealing with the usual problems of heat and load resistances associated with take-off and landing, by solving the problem of soil stabilization at the site. Through adequate stabilization, the problem of flying debris is eliminated.
Author

N90-26129*# National Aeronautics and Space Administration. Langley Research Center, Hampton, VA.
CONDENSATION POLYIMIDES
P. M. Hergenrother New York, NY VCH Publishers, Inc. Feb. 1989 47 p
(NASA-TM-103467; NAS 1.15:103467) Avail: NTIS HC A03/MF A01 CSCL 11C

Polyimides belong to a class of polymers known as polyheterocyclics. Unlike most other high temperature polymers, polyimides can be prepared from a variety of inexpensive monomers by several synthetic routes. The glass transition and crystalline melt temperature, thermooxidative stability, toughness, dielectric constant, coefficient of thermal expansion, chemical stability, mechanical performance, etc. of polyimides can be controlled within certain boundaries. This versatility has permitted the development of various forms of polyimides. These include adhesives, composite matrices, coatings, films, moldings, fibers, foams and membranes. Polymides are synthesized through both condensation (step-polymerization) and addition (chain growth polymerization) routes. The precursor materials used in addition polyimides or imide oligomers are prepared by condensation method. High molecular weight polyimide made via polycondensation or step-growth polymerization is studied. The various synthetic routes to condensation polyimides, structure/property relationships of condensation polyimides and composite properties of condensation polyimides are all studied. The focus is on the synthesis and chemical structure/property relationships of polyimides with particular emphasis on materials for composite application.
Author

N90-26130*# National Aeronautics and Space Administration. Langley Research Center, Hampton, VA.
FRACTURE TOUGHNESS OF POLYIMIDE FILMS
J. A. Hinkley and S. L. Mings (AS&M, Inc., Hampton, VA.) [1989] 14 p Submitted for publication
(NASA-TM-103473; NAS 1.15:103473) Avail: NTIS HC A03/MF A01 CSCL 11C

Two aromatic polyimides and an aromatic polyamide-imide were tested in single edge notched tension. Fracture toughnesses, normalized to 25 micron film thickness ranged from 1.65 to 5.4 MPa m sup 1/2. LARC-TPI, a thermoplastic polyimide, showed evidence of crazing ahead of a growing crack whereas the other materials formed a shear yielded zone. Author

N90-26131*# National Aeronautics and Space Administration. Langley Research Center, Hampton, VA.
CHARACTERIZATION OF A THERMALLY IMIDIZED SOLUBLE POLYIMIDE FILM
Philip R. Young. Judith R. J. Davis, A. C. Chang, and John N. Richardson (Analytical Services and Materials, Inc., Hampton, VA.) 1989 24 p Submitted for publication
(Contracts NAS1-18000; NAS1-18599)
(NASA-TM-103484; NAS 1.15:103484) Avail: NTIS HC A03/MF A01 CSCL 11C

A soluble aromatic poly(amic acid) film was converted to a soluble polyimide by staging at 25 deg intervals to 325 C and characterized at each interval by several analytical methods. The behavior observed was consistent with an interpretation that a reduction occurred in molecular weight of the poly(amic acid) during the initial stages of cure before the ultimate molecular weight was achieved as a polyimide. This interpretation was supported by the results of solution viscosity, gel permeation chromatography, low angle laser light scattering photometry and infrared spectroscopy

analysis. The results serve to increase the fundamental understanding of how polyimides are thermally formed from poly(amic acids). Author

N90-26132*# National Aeronautics and Space Administration. Lewis Research Center, Cleveland, OH.
DETERMINATION OF THE STRESS DISTRIBUTIONS IN A CERAMIC: TENSILE SPECIMEN USING NUMERICAL TECHNIQUES
M. G. Jenkins, M. K. Ferber, V. J. Tennery (Oak Ridge National Lab., TN.), and J. A. Salem 1990 8 p Presented at the ASME International Conference on Computers in Engineering, Boston, MA, 5-9 Aug. 1990
(Contract DE-AC05-84OR-21400)
(NASA-TM-101914; NAS 1.15:101914; DE90-010499; CONF-900837-2) Avail: NTIS HC A02/MF A01 CSCL 11C

Finite element analyses (FEA) were used to determine the stress distributions in a ceramic, tensile specimen with two types of button-head gripping systems. The FEA revealed stress raisers at both the button-head and the transition from the gage section to the shank. However, the stress field within the bulk of the gage section is uniform and uniaxial. The stress ratio, k(sub t), between the button-head and gage section stresses varied from 0.35 to 0.72 for the tapered collet or the straight collet systems, respectively. Previous empirical tests confirm these results whereby, the tapered collet system, compared to the straight collet system, sustained over twice the average load before failure at the button-head. DOE

N90-26133# Sandia National Labs., Albuquerque, NM.
WEAR MECHANISMS OF AMORPHOUS CARBON AND ZIRCONIA COATINGS ON RIGID DISK MAGNETIC RECORDING MEDIA
M. T. Dugger, Y.-W. Chung, B. Bhushan, and W. Rothschild (International Business Machines Corp., Rochester, MN.) 1990 33 p Presented at the Joint STLE-ASME Tribology Conference, Toronto, Ontario, 7-10 Oct. 1990
(Contract DE-AC04-76DP-00789)
(DE90-011053; SAND-90-1314C; CONF-901071-4) Avail: NTIS HC A03/MF A01

Examination of the durability of zirconia-coated rigid disks in various environments reveals a sensitivity to the presence of water vapor during sliding. Vacuum and dry air yield contact durabilities of 300 to 400 m, while in 50 percent relative humidity air the contact life increases to about 20 km. The durability of amorphous carbon-coated disks was also found to be more sensitive to the presence of moisture than to oxygen. The dominant factors affecting wear are believed to be oxidation of metallic debris and interaction of the overcoat layer with water vapor. Tests with ferrite read/write sliders on carbon-coated disks suggest that the pin-on-disc test is a valid simulation of the tribological behavior of this system. Carbon film thickness measurements indicate that the carbon film remains intact without appreciable thinning until the point of failure. DOE

N90-26134# Sandia National Labs., Albuquerque, NM.
EVOLUTION OF STRUCTURE AND VISCOELASTICITY IN DIETHANOLAMINE-CURED EPOXY
Douglas Adolf and James E. Martin Jun. 1990 30 p
(Contract DE-AC04-76DP-00789)
(DE90-011256; SAND-90-0217) Avail: NTIS HC A03/MF A01

As a crosslinking polymer cures, dramatic changes in molecular architecture occur. These structural changes in turn affect the viscoelastic behavior of the material. At a critical extent of reaction (the gel point), the polymer undergoes a transition from a viscous liquid to an elastic solid. The evolution of structure and viscoelasticity was monitored in the most common epoxy encapsulant used at Sandia, diethanolamine cured Epon 828. The structure evolves according to percolation theory, and the viscoelasticity evolves according to the dynamic scaling theory for branched polymers. DOE

N90-26135# Sandia National Labs., Albuquerque, NM.
RESISTIVITY, ADHESIVE STRENGTH, AND RESIDUAL STRESS MEASUREMENTS OF THIN FILM METALLIZATIONS ON SINGLE CRYSTAL QUARTZ
P. T. Vianco, W. R. Conley, and J. K. G. Panitz 1990 28 p Presented at the 44th Annual Freuency Control Symposium, Baltimore, MD, 23-25 May 1990
(Contract DE-AC04-76DP-00789)
(DE90-011902; SAND-90-0117C; CONF-9005202-1) Avail: NTIS HC A03/MF A01

Resistivity, adhesive strength, and residual stress measurements were made of the thin films, 450 A Cr/1800 A Au and 450 A Mo/1800 A Au deposited on optically polished, z-plate single crystal quartz surfaces. The films were analyzed after deposition and following annealing at 380 or 450 C for 30 min in either air or vacuum. The resistivity of the Cr/Au film increased by 1090 and 1780 percents after vacuum annealing at 380 and 450 C, respectively. These increases were reduced when 1000 A of Ni or Mo were introduced as barrier layers between the Cr and Au to prevent interdiffusion of the two layers. The resistivity of the Mo/Au films remained unchanged after all annealing exposures. The Cr/Au, Cr/Mo/Au, and Cr/Ni/Au films had adhesion strengths of 41 to 70 MPa in both the as-deposited and annealed conditions. The adhesive strength of the Mo/Au metallization was 23 to 31 MPa except after the 450 C air anneal where the value dropped to zero. The residual stress of the as-deposited Cr/Au film was 170 MPa (tensile) but became compressive at -120 to -250 MPa after annealing. The Mo/Au metallization was deposited with a zero stress value that also became compressive at -140 to -180 MPa. DOE

N90-26136# Oak Ridge National Lab., TN. Metals and Ceramics Div.
TENSILE STRENGTH MEASUREMENT TECHNIQUES FOR STRUCTURAL CERAMICS
V. J. Tennery 1 Jun. 1990 15 p
(Contract DE-AC05-84OR-21400)
(DE90-012193; ORNL/FTR-3630) Avail: NTIS HC A03/MF A01

The traveler visited Japan to discuss research results on structural ceramics at the Government Industrial Research Institute, Nagoya; to review IEA research plans at the Japan Fine Ceramics Center, Nagoya; to tour the Kyocera ceramic manufacturing complex and the corporate research and development laboratory at Kokubu; to attend the annual meeting of the Japan Fine Ceramics Association (JFCA) and accept the International Prize for Mr. A. A. Chesnes of the U.S. Department of Energy in Tokyo; to visit staff of the Ministry of International Trade and Industry (MITI) and of the Agency of Industrial Science and Technology (AIST) in Tokyo; to make a technical presentation to JFCA and MITI staff on fracture analysis results from IEA Annex II research in Tokyo; and to visit the Mechanical Engineering Laboratory of the AIST at Tsukuba. DOE

N90-26137# Montana State Univ., Bozeman. Dept. of Physics.
NMR AND OPTICAL STUDIES OF PIEZOELECTRIC POLYMERS Annual Report, 1 Apr. 1989 - 31 Mar. 1990
V. Hugo Schmidt 1990 6 p
(Contract DE-FG06-87ER-45292)
(DE90-012459; DOE/ER-45292/11) Avail: NTIS HC A02/MF A01

The work done to date includes NMR, Brillouin scattering and neutron scattering studies of piezoelectric polymers, some applied research with polymer-dispersed liquid crystals, and reanalysis of the elastic theory of nematic liquid crystals. DOE

N90-26138# Oak Ridge National Lab., TN. Metals and Ceramics Div.
MECHANICAL PROPERTIES OF SILICA COATINGS
Kenneth D. Cornett, B. D. Fabes (Arizona Univ., Tucson.), and W. C. Oliver 1990 6 p Presented at the Spring Meeting of the Materials Research Society, San Francisco, CA, 16-21 Apr. 1990

(Contracts DE-AC05-84OR-21000; DE-AC05-76OR-00033)
(DE90-012721; CONF-900466-62) Avail: NTIS HC A02/MF A01

Silica coatings with as-deposited densities ranging from approximately 50 to 100 percent were deposited on sapphire substrates by electron beam evaporation and sol-gel techniques. The shrinkage, hardness, and etch rates of the coatings were measured after various heat treatments. Differences in shrinkage indicated that hardness was not controlled by bulk porosity alone. Most films exhibited a surface crust that was significantly harder, and etched more slowly than the interior of the sample. It is proposed that the differences in mechanical and chemical behavior are caused by Si-O network reorganization starting at the film/air interface. DOE

N90-26139# Oak Ridge National Lab., TN. Metals and Ceramics Div.
MECHANICAL PROPERTIES OF COATINGS AND INTERFACES
B. D. Fabes (Arizona Univ., Tucson.) and W. C. Oliver 1990 6 p Presented at the Spring Meeting of the Materials Research Society, San Francisco, CA, 16-21 Apr. 1990
(Contracts DE-AC05-84OR-21000; DE-AC05-76OR-00033)
(DE90-012726; CONF-900466-61) Avail: NTIS HC A02/MF A01

Silica Coatings of various thickness, hardnesses, and interface integrities were deposited on sapphire substrates using sol-gel techniques. The mechanical properties of the coatings were examined using a mechanical properties microprobe. The observed changes in hardness with indentation depth are explained on the basis of a model of the indentation sequence, in which three separate stages of the indentation process are described. In the first stage, the properties of the coating alone are probed: in the second stage, as the plastic field associated with the indenter extends beyond the coating into the substrate, the properties of the substrate begin to appear; and in the third stage, where the indenter penetrates into the substrate, the composite hardness is dominated by that of the substrate, although the properties of the coating are still apparent. DOE

N90-26140# Idaho National Engineering Lab., Idaho Falls.
REAL-TIME MONITORING OF CERAMIC SINTERING WITH LASER ULTRASONICS
K. L. Telschow 1990 8 p Presented at the 4th International Symposium on Nondestructive Characterization of Materials, Anapolis, MD, 11-14 Jun. 1990
(Contracts DE-AC07-76ID-01570; BM-J034035)
(DE90-012960; EGG-M-89513; CONF-9006209-1) Avail: NTIS HC A02/MF A01

A Fabry-Perot Doppler interferometer that directly measures elastic waves from rough, optically diffuse, surfaces of materials has been constructed at the Idaho National Engineering Laboratory (INEL). This apparatus, coupled with a pulsed laser for elastic wave generation, is currently being used for real-time monitoring of the sintering of zinc oxide. From the ultrasonic propagation measurements, actual densities and shrinkage values can be calculated as the material sinters; the algorithm requires previous knowledge of the ultrasonic velocity dependence on density and assumptions concerning the method of shrinkage in the material. DOE

N90-26141# Idaho National Engineering Lab., Idaho Falls.
LASER ULTRASONIC MEASUREMENTS ON CERAMIC MATERIALS WITH ROUGH SURFACES
J. B. Walter and K. L. Telschow 1990 5 p Presented at the Conference on Nondestructive Evaluation of Modern Ceramics, Columbus, OH, 9-12 Jul. 1990
(Contracts DE-AC07-76ID-01570; BM-J0134035)
(DE90-012961; EGG-M-89514; CONF-900736-1) Avail: NTIS HC A01/MF A01

At the Idaho National Engineering Laboratory, noncontacting ultrasonic measurements are being made on materials while they are being processed at elevated temperatures. These materials have rough surfaces, typical of those encountered during processing. A pulsed laser is used for generation of elastic waves and a laser Doppler interferometer for detection. Processes being studied are the fabrication of silicon carbide fiber reinforced silicon carbide (SiC--SiC) by chemical vapor infiltration (CVI) and the sintering of zinc oxide (ZnO). For SiC-SiC produced by CVI, the velocity and wave amplitude of elastic waves propagating through the sample have been found to depend on the porosity and on the fiber-matrix interface bond strength. Surface waves on this material are affected by the density of the near surface layer, which can be substantially greater than that of the interior for many CVI processes. Data are also presented for the sintering of ZnO, where the laser ultrasonic method is used to monitor density and shrinkage in real time. DOE

N90-26142*# Cleveland State Univ., OH. Dept. of Civil Engineering.
EXTENSION OF A NONINTERACTIVE RELIABILITY MODEL FOR CERAMIC MATRIX COMPOSITES Final Report
Stephen F. Duffy, Robert C. Wetherhold, and Lalit K. Jain (State Univ. of New York, Buffalo.) Aug. 1990 10 p
(Contract NCC3-89; NAG3-862)
(NASA-CR-185267; E-5621; NAS 1.26:185267) Avail: NTIS HC A02/MF A01 CSCL 11C

Developments in the processing of high temperature ceramic composites demand innovative and progressive design protocols that adequately predict the thermal and mechanical behavior of these materials. The focus here is the extension of a reliability model for orthotropic ceramic composites. The approach chosen to describe failures leads to a noninteractive formulation of reliability that is phenomenological. This particular criterion, which was constructed using tensorial invariant theory, allows six potential failure modes to emerge. Author

N90-26143# Sandia National Labs., Albuquerque, NM.
QUANTITATIVE CONFIRMATION OF DIFFUSION-LIMITED OXIDATION THEORIES
Kenneth T. Gillen and Roger L. Clough 1990 9 p Presented at the 200th American Chemical Society National Meeting, Washington, DC, 26-31 Aug. 1990
(Contract DE-AC04-76DP-00789)
(DE90-012997; SAND-90-0826C; CONF-900802-3) Avail: NTIS HC A02/MF A01

Diffusion-limited (heterogeneous) oxidation effects are often important for studies of polymer degradation. Such effects are common in polymers subjected to ionizing radiation at relatively high dose rate. To better understand the underlying oxidation processes and to aid in the planning of accelerated aging studies, it would be desirable to be able to monitor and quantitatively understand these effects. In this paper, we briefly review a theoretical diffusion approach which derives model profiles for oxygen surrounded sheets of material by combining oxygen permeation rates with kinetically based oxygen consumption expressions. The theory leads to a simple governing expression involving the oxygen consumption and permeation rates together with two model parameters (alpha) and (beta). To test the theory, gamma-initiated oxidation of a sheet of commercially formulated ethylene propylene diene monomer (EPDM) rubber was performed under conditions which led to diffusion-limited oxidation. Profile shapes from the theoretical treatments are shown to accurately fit experimentally derived oxidation profiles. In addition, direct measurements on the same EPDM material of the oxygen consumption and permeation rates, together with values of (alpha) and (beta) derived from the fitting procedure, allow us to quantitatively confirm for the first time the governing theoretical relationship. DOE

N90-26144# Sandia National Labs., Albuquerque, NM.
FRACTAL STRUCTURE AND FRACTAL TIME IN SILICA SOL-GELS
James E. Martin and Jess Wilcoxon 1990 13 p Presented at the Spring Meeting of the Materials Research Society, San Francisco, CA, 16-21 Apr. 1990

(Contract DE-AC04-76DP-00789)
(DE90-013197; SAND-89-2795C; CONF-900466-68) Avail: NTIS HC A03/MF A01

Near the gel point, light scattering studies of silica sol-gels reveal fractal clusters whose size diverges as a power law, in accord with the predictions of percolation theory. More surprising is the appearance of a fractal time description of the dynamics of these clusters. This novel dynamics has recently been revealed by quasielastic light scattering from the density fluctuations that occur at the sol-gel transition. Since the relaxation of fluctuations in these branched polymer systems is self-similar, decay processes occur on all time scales (fractal time), and average decay times diverge. An interpretation of this observation will be presented that relies on a length-scale-dependent viscosity and the geometrical self-similarity of the sol-gel transition. The scattering theory is extended to the calculation of time- and frequency-dependent viscoelastic properties, as well as mechanical properties such as the shear modulus, steady state creep compliance, and viscosity. The viscoelastic predictions are found to be in good agreement with experimental data. DOE

N90-26145# Sandia National Labs., Albuquerque, NM.
SHORT-RANGE STRUCTURE OF FLUORINE-MODIFIED PHOSPHATE GLASS
Z. A. Osborne, R. K. Brow, and D. R. Tallant 1990 11 p Presented at the SPIE's International Symposium on Optical and Optoelectronic Applied Science and Engineering and Exhibit, San Diego, CA, 8-13 Jul. 1990
(Contract DE-AC04-76DP-00789)
(DE90-013494; SAND-89-2787C; CONF-900756-9) Avail: NTIS HC A03/MF A01

Raman and x ray photoelectron spectroscopy are used to characterize the effects of fluorine incorporation on the short range structures of several simple phosphate glasses. Fluorine depolymerizes the chain structure of NaPO sub 3 by replacing bridging POP bonds with terminal PF species. In aluminophosphate glasses with small fluorine contents, fluorine is primarily associated with aluminum. When the fluorine to aluminum ratio exceeds three, the number of Al-F bonds are maximized and significant numbers of P-F bonds form. DOE

N90-26146# Sandia National Labs., Albuquerque, NM.
ONE-DIMENSIONAL SIGMA-CONJUGATED POLYSILYLENES: SCIENCE AND TECHNOLOGY
John M. Zeigler 1990 30 p Presented at the Symposium on Electroresponsive Polymeric Materials, Midland, TX, 10 May 1990
(Contract DE-AC04-76DP-00789)
(DE90-012902; SAND-90-1620C; CONF-9005231-1) Avail: NTIS HC A03/MF A01

The electronic and photochemical properties of polysilylenes were studied, with particular emphasis on the many resemblances in the electronic properties of polysilylenes to those of the familiar pi-conjugated polymers. In this context, the term sigma-conjugation appears herein, as it is almost universally prevalent in the field. However, the use of this term should only be interpreted to suggest a correspondence in the electronic properties with those of pi-conjugated materials. No direct correspondence in electronic interactions at the atomic level is implied. In fact, the theoretical underpinnings of the mechanism of electron delocalization in sigma-bonded systems remain incomplete, at best. The systematic name polysilylene is used in place of the equivalent and widely used term polysilane. In this context, these terms are intended to refer to polydiorganosilylenes, i.e., silicon backbones having substituents other than hydrogen. Moreover, since, with the exception of the commercial use of the intractable polydimethylsilylene as a precursor to beta-SiC fibers, the overwhelming majority of the interest in the field is in soluble polysilylenes, the discussion here will be of that greatly predominant group of the materials which are fully tractable and processible. DOE

N90-26147# Central Research Inst. of Electric Power Industry, Tokyo (Japan). Energy and Environment Lab.
EVALUATION OF FRACTURE STRENGTH PROPERTIES OF SILICON CARBIDE CERAMICS UNDER CYCLIC/STATIC AXIAL LOADING AT ULTRA-HIGH TEMPERATURE
Terutaka Fujioka, Takashi Ogata, Masaaki Matsubara, and Akihito Nitta May 1989 29 p In JAPANESE; ENGLISH summary
(DE90-503402; CRIE-T-88081) Avail: NTIS (US Sales Only) HC A03/MF A01

Ceramics materials for high temperature structures such as silicon carbide or silicon nitride, are expected as elemental materials for gas turbines for coal gasification combined-cycle power plants, which are needed high efficiency due to high temperature operation. Because of their brittleness, however, some strength evaluations of ceramics are required to make them practicable as structure materials. In this study, two types of testing machine, enable to perform difficult axial loading tests, include tension-compression cyclic loading test, at 1300 centigrade ultra-high temperature, were developed. And cyclic/static axial loading tests of atmospheric sintered silicon carbide ceramics were conducted at 1300 centigrade ultra-high temperature. Based on the test results, elucidation of the fracture strength properties was performed from a viewpoint of statistics and fracture mechanics. Some interesting phenomena on the development of evaluation method were found such as first observation of cyclic effects on fatigue fracture property, which have been made light of so far. DOE

N90-26148# Central Research Inst. of Electric Power Industry, Tokyo (Japan).
DEVELOPMENT OF CERAMIC FIBER TYPE COMBUSTOR: IMPROVEMENT OF COMBUSTOR AND COMBUSTION TEST RESULTS
Tadashi Hisamatsu, Noriyuki Mori, Isao Yuri, and Toshio Abe May 1989 26 p In JAPANESE; ENGLISH summary
(DE90-503441; CRIE-W-88037) Avail: NTIS (US Sales Only) HC A03/MF A01

Improvement of combustor and combustion test under normal pressure were conducted, based on the results of its manufacture for experimental purpose and the study obtained until now, on ceramic fiber type combustor utilized to turbine, and applicability of ceramic fiber to combustor liner was studied. As a result, it was found that this combustor was capable to be safely and efficiently burned under a load combustion of 2 to 3 times higher than that of existing combustor, and simultaneously showed extremely superior thermal insulation effectiveness. Therefore, it was considered that much advantage was found in the application of ceramic fiber to the combustor liner. However local separation due to embrittlement of fiber layer surface located on near swirler under high temperature, was not prevented. In order to apply ceramic fiber to gas turbine combustor which requires high reliability, it was considered that development of high heat resistance materials, and of new heat resistant construction so that high temperature gas do not directly contact to the fiber, were required. DOE

N90-26149# Central Research Inst. of Electric Power Industry, Tokyo (Japan).
DEVELOPMENT OF CERAMIC HYBRID COMBUSTOR: DESIGN AND COMBUSTION TEST RESULTS
Tadashi Hisamatsu, Toshio Abe, Noriyuki Mori, Isao Yuri, Toshio Mimaki, Hiroshi Miyata, Lazumi Iwai, Takashi Machida, Kimiaki Nakakado, and Katsuo Wada May 1989 34 p In JAPANESE; ENGLISH summary
(DE90-503442; CRIE-W-88038) Avail: NTIS (US Sales Only) HC A03/MF A01

Result of combustion test, air allocation, and liner construction of a gas turbine combined combustor were described. The combustor liner was hybrid construction in which honeycomb ceramic tile and ceramic fiber were fixed to the inside of metal wall by ceramic bolts. By the result of the manufacture for experimental purpose of the liner for 20 MW combustor of 1300 C in temperature, it was found that the liner was about 1/6 lighter in weight than that of engagement type ceramic liner and was

easily assembled. In order to reduce conversion ratio from NH3 included in fuel into NO(x), air was allocated so that the initial combustion region became rich fuel. It was clarified that combustion efficiency decreased with increasing combustion intensity, and was increased with increasing pressure. While, the combustion efficiency reached to about 100 percent even under much load combustion of 2 to 3 times higher than that of existing combustor. The conversion ratio from NH3 into NO(x) was about 40 percent under high pressure, and capable to be burned under low NO(x) condition. DOE

N90-26150# Rolls-Royce Ltd., Derby (England).
UNDERSTANDING SILICA BINDERS
D. Mills 21 Mar. 1989 11 p
(PNR90625; ETN-90-97138) Copyright Avail: NTIS HC A03/MF A01

A model is developed with the aim of better understanding binders used in slurries for producing ceramic shell moulds. With this knowledge, the model can provide better use of silica binders. The main fact that these binders are temperamental and highly sensitive to misuse emerges. Contamination from both the atmosphere and impurities in the filler can cause problems. An interesting point noted is that the finest particles of the refractory fillers are of colloidal size, so the model can explain the rheology of slurries. ESA

N90-26151# Technische Univ., Delft (Netherlands). Faculty of Aerospace Engineering.
TIME TEMPERATURE RELATIONS DURING RUBBER FORMING CONTINUOUS FIBER REINFORCED THERMOPLASTICS
L. G. Meyers Dec. 1989 37 p
(LR-620; ETN-90-97182) Avail: NTIS HC A03/MF A01

Preliminary tests which were carried out in order to determine the cooling speeds of CFRTP (Carton Fiber Reinforced Thermoplastics) appeared to be rather high, which might become a problem when a large reconsolidation process during the pressing phase is obligated. However, several heat-saving measurements are mentionable and can be taken to tune the cooling ratio in such a way that optimum material properties with respect to optimum production cycle times are obtained. The test setup needs to be altered. The use of an automated data acquisition system is recommended to ease further experiments with respect to this subject. ESA

N90-26152# Technische Univ., Eindhoven (Netherlands).
MODELLING OF THE PROCESSING OF INCOMPATIBLE POLYMER BLENDS Ph.D. Thesis
Petrus Henricus Mari Elemans 1989 218 p Sponsored by DSM
(ETN-90-97211) Avail: NTIS HC A10/MF A01

Desired properties of a blend depend on the resulting morphology. The parameters governing the blending process are studied. A computational model is proposed for the two important continuous mixers: the corotating twin-screw extruder and the co-kneader. Detailed studies of deformation and breakup processes of droplets in well defined flow fields can be incorporated in the practical model if the time effects during the different stages are taken into account. Several non-equilibrium morphologies as obtained blends of the model system polyethylene/polystyrene are discussed. Stability of morphologies, coupling of modeling, experimental results and conclusions are included. ESA

N90-26153# Research Inst. of National Defence, Stockholm (Sweden). Dept. of Weapon Systems, Effects, and Protection.
RENEWED AGING CONTROL OF ADHESION OF INHIBITOR ON THE GAS GENERATOR CHARGES FOR RB 24
Roland Sanden Feb. 1990 16 p
(FOA-C-20780-2.1; ISSN-0347-3694; ETN-90-97099) Avail: NTIS HC A03 /MF A01

A strong decrease of the shear stress occurs during the first 7 to 8 years and then a gradually slower decrease with aging time. Gas generators for the RB 24, Sidewinder missile were tested, with regard to the adhesion of inhibitor on the charges. The inhibitor adhesion seems to have stabilized at an acceptable level and there is at present no reason to fear too low an adhesion in the next few years. A renewed test is recommended in 5 years. ESA

N90-26154# Institut National des Sciences Appliquees, Lyon (France).
INFLUENCE OF THE MANUFACTURING CONDITIONS ON THE MICROSTRUCTURE AND MECHANICAL PROPERTIES OF THE SILICON NITRIDE Ph.D. Thesis [INFLUENCE DES CONDITIONS D'ELABORATION SUR LA MICROSTRUCTURE ET LES PROPPRIETES MECANIQUES DU NITRURE DE SILICIUM]
Christian Olagnon 1990 144 p In FRENCH
(ISAL-90-0008; ETN-90-97261) Avail: NTIS HC A07/MF A01

The barbotine casting technique allows complex configurations and suitable distribution of powders to be obtained. High density sintering products can be obtained under low pressures. The technique is applied to the manufacturing of silicon nitride and the fabrication parameters are investigated. The obtaining of high density composite materials depends on the optimization of the powdering and sintering procedures as well as on the fiber's dimensions. The reinforcing mechanisms are analyzed from the microstructure and mechanical properties. Comparison with monolithic materials is carried out. ESA

N90-26155# Ballistic Research Labs., Aberdeen Proving Ground, MD.
A COMPUTATIONAL STUDY OF THE EFFECTIVENESS OF COATING MATERIALS FOR KE PROJECTILE FINS SUBJECTED TO THE COMBINED EFFECTS OF INBORE AND AERODYNAMIC HEATING Final Report, May - Aug. 1988
Frank D. Sturek, Walter B. Sturek, and Earl N. Ferry, Jr. Apr. 1990 39 p
(DA Proj. 1L1-62618-AH-80)
(AD-A222595; AD-E951478; BRL-MR-3831) Avail: NTIS HC A03/MF A01 CSCL 11/3

The objective was to examine the inbore and free flight aerodynamic heating of aluminum fins used on large l/d kinetic energy (KE) projectiles. Numerical computations were used to to examine the effectiveness of two coating materials for thermal protection of the aluminum fins. A comparison of the predicted unsteady thermal response to the combined effects of inbore and free flight aerodynamic heating was made between a fin coated with the current aluminum oxide coating and a fin coated with a new silicon/fiber mixture. The silicon/fiber coating was found to provide substantially improved thermal protection compared to the standard aluminum oxide coating. A fin coated with the silicon/fiber material was predicted to not reach melt temperature throughout a simulated 3.0 second flight. In comparison, a fin coated with aluminum oxide was predicted to reach melt temperature after less than 1.0 second of flight. GRA

N90-26156# Washington Univ., Seattle. Dept. of Materials Science and Engineering.
THE CATALYTIC SYNTHESIS OF INORGANIC POLYMERS FOR HIGH TEMPERATURE APPLICATIONS AND AS CERAMIC PRECURSORS
Jeffrey A. Rahn, Richard M. Laine, and Zhi-Fan Zhang Dec. 1989 10 p Presented at the MRS Meeting, Boston, MA, Dec. 1989 Submitted for publication
(Contract N00014-88-K-0305)
(AD-A222620) Avail: NTIS HC A02/MF A01 CSCL 07/6

Polysilsesquioxanes, -(RSi(O)1.5)x(-), exhibit many properties that are potentially quite useful for industrial applications. These properties include high temperature stability (approx. 600 deg C in Oxygen); good adhesion and, liquid crystal-like behavior for some derivatives. Moreover, polymethylsilsesquioxane has been used successfully as a precursor for the fabrication of carbon fiber/black glass (SiO2/SiC/C) composites and black glass fibers. Current methods of preparation depend on hydrolysis of RSiCl3 or

RSi(OR)3. Unfortunately, this approach leads to several products that are difficult to purify because polysilsesquioxanes exhibit a great propensity for forming gels. GRA

N90-26157# Cincinnati Univ., OH. Dept. of Materials Science and Engineering.
MOLECULAR STRUCTURE OF INTERPHASES BETWEEN DGEBA/BTDA ADHESIVES AND SILVER SUBSTANCES USING SURFACE-ENHANCED RAMAN SCATTERING
W. H. Tsai, J. T. Young, and F. J. Boerio 1 Jun. 1990 29 p Submitted for publication
(Contract N00014-89-J-1590)
(AD-A222750; TR-7) Avail: NTIS HC A03/MF A01 CSCL 07/6

Surface-enhanced Raman scattering (SERS) was used for the non-destructive characterization of interphases between epoxy/anhydride adhesive systems and silver substrates. Normal Raman spectra of benzophenone tetra-carboxylic dianhydride (BTDA) were characterized by strong bands near 1785 and 1860/cm that were assigned to the anhydride groups, a strong band near 1690/cm that was assigned to the benzophenone C=O stretching mode, and by a strong band near 1620/cm that was attributed to vibration and to the benzophenone C=O stretching mode were prominent in the SERS spectra of BTDA but the bands related to the anhydride group were missing, indicating that the anhydride groups were hydrolyzed at the silver surface to form carboxylate groups. GRA

N90-26158# Massachusetts Inst. of Tech., Cambridge. Dept. of Chemistry.
POLYMERIC ALUMINASILAZANE PRECURSORS FOR ALUMINOSILICON NITRIDE
Dietmar Seyferth and Gregor Brodt 4 May 1990 9 p Submitted for publication Sponsored in part by NSF and von Humboldt (Alexander) Foundation
(Contract N00014-82-K-0322)
(AD-A222755; Rept-32) Avail: NTIS HC A02/MF A01 CSCL 07/6

The reaction of trimethylaluminum with the cyclic oligomers obtained by ammonolysis of methyldichlorosilane results in evolution of methane and formation of soluble, cross-linked aluminasilazanes. Pyrolysis of the products in a stream of argon gives a good yield of black aluminosilicon carbonitride, while pyrolysis in a stream of ammonia results in formation of white aluminosilicon nitride. GRA

N90-26159# California Inst. of Tech., Pasadena.
DEVELOPMENT OF MICROENCAPSULATION TECHNIQUES Final Report, 15 Mar. 1987 - 24 Mar. 1990
John D. Baldeschwieler May 1990 4 p
(Contract DAAL03-87-K-0044)
(AD-A223032; ARO-23967.5-CH) Avail: NTIS HC A01/MF A01 CSCL 13/4

Surfactant vesicles are small, spherical shell-like structures composed of bilayers of surfactant molecules which can be used to contain an aqueous solution. Since a variety of materials can be encapsulated in such vesicles, they are ideal vehicles for many different applications. The advantages of vesicle formulations involve protection from the environment, sustained release, and targeted delivery of vesicle contents. Such potential for phospholipid vesicles as chemical delivery systems, and possibly many other roles has motivated a significant effort towards improving their properties. The primary objectives for much of the current research in this area have therefore been to obtain enhanced membrane stability (mechanical and chemical) and decreased or controlled vesicle fusion and permeability. Major progress toward these ends has been made by the introduction of polymerizable lipid analogues and to a lesser extent with the formation of polymer coated vesicles. Studies have been made of the effects of disulfide polymerization and the incorporation of cholesterol derivatives on the structure and properties (permeability, stability, and size) of phospholipid vesicles. Studies have been initiated on the interaction of polymers with liposomes. GRA

28 PROPELLANTS AND FUELS

Includes rocket propellants, igniters, and oxidizers; their storage and handling procedures; and aircraft fuels.

For related information see also *07 Aircraft Propulsion and Power, 20 Spacecraft Propulsion and Power,* and *44 Energy Production and Conversion.*

N90-26160*# National Aeronautics and Space Administration. Lewis Research Center, Cleveland, OH.
PREDICTION OF THE ULLAGE GAS THERMAL STRATIFICATION IN A NASP VEHICLE PROPELLANT TANK EXPERIMENTAL SIMULATION USING FLOW-3D
Terry L. Hardy and Thomas M. Tomsik Jul. 1990 27 p
(NASA-TM-103217; E-5629; NAS 1.15:103217) Avail: NTIS HC A03/MF A01 CSCL 07D

As part of the National Aero-Space Plane (NASP) project, the multi-dimensional effects of gravitational force, initial tank pressure, initial ullage temperature, and heat transfer rate on the 2-D temperature profiles were studied. FLOW-3D, a commercial finite difference fluid flow model, was used for the evaluation. These effects were examined on the basis of previous liquid hydrogen experimental data with gaseous hydrogen pressurant. FLOW-3D results were compared against an existing 1-D model. In addition, the effects of mesh size and convergence criteria on the analytical results were investigated. Suggestions for future modifications and uses of FLOW-3D for modeling of a NASP tank are also presented. Author

29 MATERIALS PROCESSING

Includes space-based development of products and processes for commercial applications.

For biological materials see *55 Space Biology.*

N90-26161*# Alabama Univ., Huntsville. Dept. of Mechanical Engineering.
FLUID PHASE SEPARATION (FPS) EXPERIMENT FOR FLIGHT ON A SPACE SHUTTLE GET AWAY SPECIAL (GAS) CANISTER Final Report
Bruce Peters, Dennis Wingo, Mark Bower, Robert Amborski, Laura Blount, Alan Daniel, Bob Hagood, James Handley, Donald Hediger, and Lisa Jimmerson et al Jun. 1990 67 p
(Grant NGT21-002-800)
(NASA-CR-186830; NAS 1.26:186830) Avail: NTIS HC A04/MF A01 CSCL 22A

The separation of fluid phases in microgravity environments is of importance to environmental control and life support systems (ECLSS) and materials processing in space. A successful fluid phase separation experiment will demonstrate a proof of concept for the separation technique and add to the knowledge base of material behavior. The phase separation experiment will contain a premixed fluid which will be exposed to a microgravity environment. After the phase separation of the compound has occurred, small samples of each of the species will be taken for analysis on the Earth. By correlating the time of separation and the temperature history of the fluid, it will be possible to characterize the process. The experiment has been integrated into space available on a manifested Get Away Special (GAS) experiment, CONCAP 2, part of the Consortium for Materials Complex Autonomous Payload (CAP) Program, scheduled for STS-42. The design and the production of a fluid phase separation experiment for rapid implementation at low cost is presented. Author

N90-26162*# Worcester Polytechnic Inst., MA.
INTEGRATED SUPPORT STRUCTURE
Stephen D. Bruneau, John T. Campbell, and Christopher A. Struven 26 Apr. 1990 176 p Prepared in cooperation with Mitre Corp., McLean, VA
(Grant NGT-21-002-800)
(NASA-CR-186835; NAS 1.26:186835) Avail: NTIS HC A09/MF A01 CSCL 22A

This Major Qualifying Project is part of the Advanced Space

Design Program at WPI. The goal is to design a support structure for a NASA GetAway Special experimental canister. The payload integration, weight, volume, and structural integrity of the canister as specified by NASA guidelines were studied. The end result is a complete set of design drawings with interface drawings and data to specify the design and leave a base on which the next group can concentrate. Author

N90-26163*# National Aeronautics and Space Administration. Lewis Research Center, Cleveland, OH.
NEW FINDINGS AND INSTRUMENTATION FROM THE NASA LEWIS MICROGRAVITY FACILITIES
Howard D. Ross and Paul S. Greenberg May 1990 8 p Presented at the 2nd Workshop on Microgravity Experimentation, Ottawa, Ontario, 8-9 May 1990
(NASA-TM-103189; E-5575; NAS 1.15:103189) Avail: NTIS HC A02/MF A01 CSCL 22A

The study of fundamental combustion and fluid physics in a microgravity environment is a relatively new scientific endeavor. The microgravity environment enables a new range of experiments to be performed since: buoyancy-induced flows are nearly eliminated; normally obscured forces and flows may be isolated; gravitational settling or sedimentation is nearly eliminated; and larger time or length scales in experiments become permissible. Unexpected phenomena have been observed, with surprising frequency, in microgravity experiments, raising questions about the degree of accuracy and completeness of the classical understanding. An overview is provided of some new phenomena found through ground-based, microgravity research, the instrumentation used in this research, and plans for new instrumentation. Author

N90-26164# Aeritalia S.p.A., Turin (Italy). Space Systems Group.
BUBBLE, DROP AND PARTICLE UNIT (BDPU): A MULTI-USER MICROGRAVITY FACILITY
Saverio Lioy and Vanni Defilippi 1989 13 p Previously announced in IAA as A90-13533
(IAF-89-431; ETN-90-97281) Avail: NTIS HC A03/MF A01

The Bubble Drop and Particle Unit (BDPU) project is a multi-user, reusable Spacelab facility, designed as a modular payload. It is conceived to support scientific experiments under low gravity conditions concerning the dynamics of bubbles, drops and particles within optically transparent fluid matrices. The functional characteristics and design performances of the facility are described. The facility consists of the following subsystems: service module for data handling and crew interfacing; power supply module for power distribution to the system; basic experiment module to support and contain the experimental subsystems and the camera system; optical module to support the test container's diagnostic illumination systems and the test container itself during experimental phases only; video recorder module for recording of both video and thermographic images; standard test container: the core of the facility dedicated to contain the experimental fluid and support the stimuli/diagnostic equipment. ESA

31 ENGINEERING (GENERAL)

Includes vacuum technology; control engineering; display engineering; cryogenics; and fire prevention.

N90-26165*# Georgia Inst. of Tech., Atlanta. School of Mechanical Engineering.
SOIL EXPERIMENT Advanced Missions Space Design Program
Linton Hutcheson, Todd Butler, Mike Smith, Charles Cline, Steve Scruggs, and Nadim Zakhia Aug. 1987 158 p
(Grant NGT-21-002-080)
(NASA-CR-184927; NAS 1.26:184927; ME-4182) Avail: NTIS HC A08/MF A01 CSCL 13B

An experimental procedure was devised to investigate the effects of the lunar environment on the physical properties of simulated lunar soil. The test equipment and materials used consisted of a vacuum chamber, direct shear tester, static penetrometer, and fine grained basalt as the simulant. The vacuum chamber provides a medium for applying the environmental conditions to the soil experiment with the exception of gravity. The shear strength parameters are determined by the direct shear test. Strength parameters and the resistance of soil penetration by static loading will be investigated by the use of a static cone penetrometer. In order to conduct a soil experiment without going to the moon, a suitable lunar simulant must be selected. This simulant must resemble lunar soil in both composition and particle size. The soil that most resembles actual lunar soil is basalt. The soil parameters, as determined by the testing apparatus, will be used as design criteria for lunar soil engagement equipment. Author

N90-26166# Wichita State Univ., KS. Inst. for Aviation Research.
MECHANICAL PAINT REMOVAL TECHNIQUES FOR AIRCRAFT STRUCTURES
Joe P. Amro and Jorge E. Talia May 1990 20 p Presented at the 1990 AIAA/FAA Joint Symposium on General Aviation Systems
(NIAR-90-12) Avail: NTIS HC A03/MF A01

Paint removal by mechanical means, i.e., blasting, from aluminum structural aeronautical materials (2024-T3) was examined alone with the changes on the surface morphology introduced by the paint removal process. Three types of plastic particles were used in this research: Polyextra, Polyplus, and Type III. Scanning electron microscopy has shown that a potentially damaging surface morphology is formed on the surface of the structural material. Multiple microcracks or fissures generated by the stripping could reduce the life and/or change the engineering properties of the material. It was also found that aluminum material stripped using plastic media particles has a very rough surface that may affect the aerodynamic flow of an airplane. The number of microcracks and degree of surface roughness vary with the particle impact angle and velocity. To minimize or eliminate the damage done to the surface during the plastic particle stripping, it was necessary to change the blasting media to softer and smaller particles. Commercial wheat flour was selected for this purpose. With the substitution of these natural particles, the scanning electron microscopy observations of the stripped surface revealed no potential damage (microcracks or fissures) on the structural material, and the surface roughness was also reduced. Author

N90-26167*# National Aeronautics and Space Administration. Langley Research Center, Hampton, VA.
SIMULATED DYNAMIC RESPONSE OF A SERVOVALVE CONTROLLED HYDRAULIC ACTUATOR
Dale A. Babcock Jun. 1990 30 p
(NASA-TM-101644; NAS 1.15:101644) Avail: NTIS HC A03/MF A01 CSCL 13I

A general purpose math model of a servovalve controlled hydraulic actuator system is derived. The system consists of a linear actuator with unequal piston areas, a single stage servovalve, a gas charged hydraulic accumulator, and the interconnecting piping. The state equations are integrated using the Advanced Continuous Simulation Language (ACSL) for determining the system's dynamic response characteristics. Using this generalized hydraulic actuator system model, response characteristics were determined for various servovalve commands. Author

N90-26168* National Aeronautics and Space Administration. Marshall Space Flight Center, Huntsville, AL.
ELECTRODE CARRYING WIRE FOR GTAW WELDING Patent
Gene E. Morgan, inventor (to NASA) and Gerald E. Dyer, inventor (to NASA) 8 May 1990 5 p Filed 5 Dec. 1988 Supersedes N89-23738 (27 - 17, p 2420)
(NASA-Case-MFS-29491-1; US-Patent-4,924,053; US-Patent-Appl-SN-279677; US-Patent-Class-219-75; US-Patent-Class-219-136; Int-Patent-Class-B23K-9/24) Avail: US Patent and Trademark Office CSCL 13H

A welding torch for gas tungsten arc welding apparatus has a hollow tungsten electrode including a ceramic liner and forms the filler metal wire guide. The wire is fed through the tungsten electrode thereby reducing the size of the torch to eliminate clearance problems which exist with external wire guides. Since the wire is preheated from the tungsten more wire may be fed into the weld puddle, and the wire will not oxidize because it is always within the shielding gas.
Official Gazette of the U.S. Patent and Trademark Office

N90-26169# General Accounting Office, Washington, DC. National Security and International Affairs Div.
NASA PROJECT STATUS REPORTS: CONGRESSIONAL REQUIREMENTS CAN BE MET, BUT RELIABILITY MUST BE ENSURED
Frank Degnan, Karen L. Kemper, and Amy L. Manheim Jan. 1990 47 p
(GAO/NSIAD-90-40; B-237602) Avail: NTIS HC A03/MF A01; also available from GAO, Gaithersburg, MD HC first five copies free, additional copies $2.00

Congressional decisionmakers rely on reports in making difficult funding allocation choices. New criteria for biannual Project Status Reports are specified for NASA. A project is defined as meeting the NASA Budget Administration Manual's definition of project and estimated to cost $200 million or more to research and develop. Reports are to be prepared according to mutually agreed upon guidelines, and written as of March 15 and July 30. Following a project's new-start approval, the reports will begin the first March after the project's estimate reaches the cost threshold and end with the report following the project's completion. NASA needs to write its guidelines or specifying responsibilities for developing the reports to ensure that the Project Status Reports using the new criteria are reliable for cost, schedule, and performance information. Current guidance is informal and too vague to ensure accurate, timely, and verifiable information. J.P.S.

N90-26170*# National Aeronautics and Space Administration. Lewis Research Center, Cleveland, OH.
CRITICAL EVALUATION OF JET-A SPRAY COMBUSTION USING PROPANE CHEMICAL KINETICS IN GAS TURBINE COMBUSTION SIMULATED BY KIVA-2
H. L. Nguyen and S.-J. Ying (University of South Florida, Tampa.) Jul. 1990 21 p Presented at the 26th Joint Propulsion Conference, Orlando, FL, 16-18 Jul. 1990; sponsored in part by AIAA, SAE, ASME, and ASEE
(NASA-TM-103173; E-5551; NAS 1.15:103173) Avail: NTIS HC A03/MF A01 CSCL 21B

Jet-A spray combustion has been evaluated in gas turbine combustion with the use of propane chemical kinetics as the first approximation for the chemical reactions. Here, the numerical solutions are obtained by using the KIVA-2 computer code. The KIVA-2 code is the most developed of the available multidimensional combustion computer programs for application of the in-cylinder combustion dynamics of internal combustion engines. The released version of KIVA-2 assumes that 12 chemical species are present; the code uses an Arrhenius kinetic-controlled combustion model governed by a four-step global chemical reaction and six equilibrium reactions. Researchers efforts involve the addition of Jet-A thermophysical properties and the implementation of detailed reaction mechanisms for propane oxidation. Three different detailed reaction mechanism models are considered. The first model consists of 131 reactions and 45 species. This is considered as the full mechanism which is developed through the study of chemical kinetics of propane combustion in an enclosed chamber. The full mechanism is evaluated by comparing calculated ignition delay times with available shock tube data. However, these detailed reactions occupy too much computer memory and CPU time for the computation. Therefore, it only serves as a benchmark case by which to evaluate other simplified models. Two possible simplified models were tested in the existing computer code KIVA-2 for the same conditions as used with the full mechanism. One model is obtained through a sensitivity analysis using LSENS, the general kinetics and sensitivity analysis program code of D. A. Bittker and K. Radhakrishnan. This model consists of 45 chemical reactions and 27 species. The other model is based on the work published by C. K. Westbrook and F. L. Dryer. Author

N90-26171*# Cincinnati Univ., OH.
COMPUTER SIMULATION OF GEAR TOOTH MANUFACTURING PROCESSES Final Report
Dimitri Mavriplis and Ronald L. Huston Feb. 1990 53 p Sponsored in part by AVSCOM, Cleveland, OH.
(Grant NsG-3188; DA Proj. 1L1-62209-A-47-A)
(NASA-CR-185200; NAS 1.26:185200; AVSCOM-TM-90-C-003)
Avail: NTIS HC A04/MF A01 CSCL 13I

The use of computer graphics to simulate gear tooth manufacturing procedures is discussed. An analytical basis for the simulation is established for spur gears. The simulation itself, however, is developed not only for spur gears, but for straight bevel gears as well. The applications of the developed procedure extend from the development of finite element models of heretofore intractable geometrical forms, to exploring the fabrication of nonstandard tooth forms. Author

N90-26172*# National Aeronautics and Space Administration. Lewis Research Center, Cleveland, OH.
ANALYSIS OF A MARS-STATIONARY ORBITING MICROWAVE POWER TRANSMISSION SYSTEM
Kenwyn J. Long Jul. 1990 22 p
(NASA-TM-101344; E-4367; NAS 1.15:101344) Avail: NTIS HC A03/MF A01 CSCL 20N

To determine the feasibility of providing efficient RF power transmission from a Mars-stationary orbit to the surface of the planet, an assessment was made focussing on RF propagation in the 2.45- to 300-GHz range. The proposed orbiting system configuration provides for power generation by either photovoltaic array or nuclear reactor, the conversion of the dc output to RF, and subsequent propagation of RF energy from the orbiting array to the Martian surface. On the planet, a rectenna array will convert RF to dc power to be distributed for planetary power needs. Total efficiency of the energy conversion chain from dc to RF in orbit through RF to dc on the planetary surface was derived for several representative frequencies in the range of study. Tradeoffs between component efficiency and transmitting antenna requirements were considered for each of these frequencies. Rectenna element power density thresholds and desired received power levels were used to determine receiving antenna criteria. Recommendations are presented for research into developing technologies which may afford enhanced viability of the proposed microwave power transmission system. Author

N90-26173# European Space Agency, Paris (France).
MATERIALS AND STRUCTURES FOR 2000 AND BEYOND: AN ATTEMPTED FORECAST BY THE DLR MATERIALS AND STRUCTURES DEPARTMENT
Carl-Jochen Winter, Martin Mailaender, Heinrich Bergmann, Hans Foersching, Wolfgang Bunk, Gerhard Grueninger, and Berndt Feuerbacher May 1990 85 p Transl. into ENGLISH of Werkstoffe und Bauweisen fuer 2000 und Danach: Ein Versuch des DLR-Forschungsbereichs Werkstoffe und Bauweisen (Stuttgart, Fed. Republic of Germany, DFVLR), Feb. 1989 p 1-82 Original language document was announced as N89-25358 Previously announced as N90-18609 Revised
(ESA-TT-1154-Rev; DFVLR-MITT-89-02-Rev; ETN-90-97357)
Avail: NTIS HC A05/MF A01; original German version available from DFVLR, VB-PL-DO, Postfach 90 60 58, 5000 Cologne 90, Fed. Republic of Germany, 20.50 DM

The following forecasts were attempted on 21 to 22 Oct. 1988: to estimate what challenges the next 15 years might bring, and what would be the consequences for the direction and methodology of work, and for the organization of the institutes and of the research department. Building on the basis of the current position and of the discussions, the views of the five institutes, namely those for aeroelasticity, advanced design and manufacturing technology, space simulation, structural mechanics and materials

research, on the future, are presented. A summary drawn up, and derived action guidelines, are given. ESA

N90-26174# Rolls-Royce Ltd., Derby (England).
MANUFACTURING CONTROL: A BASIS FOR ANALYSIS
N. Bugg 24 Nov. 1989 35 p Submitted for publication
(PNR90639; ETN-90-97144) Copyright Avail: NTIS HC A03/MF A01

The application of elementary control theory to manufacturing systems demonstrating how the organization of basic shop-floor logistics can be optimized prior to the introduction of computer technology is explored. A control structure is introduced and applied to manufacturing systems, breaking the problem into its constituent parts in such a way that the advantages of improved control technology become more apparent and more readily implementable. ESA

N90-26175# National Aerospace Lab., Amsterdam (Netherlands). Informatics Div.
INFERENCE AND CONTROL MECHANISMS IN NEXT 2.0
P. J. Kat 13 Oct. 1988 11 p In DUTCH; ENGLISH summary Presented at AI Toepassingen 1988 Conferentie, The Hague, Netherlands, 14-16 Nov. 1988
(NLR-MP-88062-U; ETN-90-97191) Avail: NTIS HC A03/MF A01

The inference and control mechanisms of NEXT 2.0 (NLR Engineering X-pert system Toolkit) are discussed. It contains a hybrid knowledge representation of frames, production rules and tasks, and an inference and control mechanism based on an agenda principle. The separation of inference and control, in both knowledge representation and actual reasoning, enables flexible expert systems to be developed in a convenient way. ESA

N90-26176*# National Aeronautics and Space Administration. Pasadena Office, CA.
MULTICOMPONENT GAS SORPTION JOULE-THOMSON REFRIGERATOR Patent Application
Jack Jones, inventor (to NASA), S. Walter Petrick, inventor (to NASA), and Steven Bard, inventor (to NASA) (Jet Propulsion Lab., California Inst. of Tech., Pasadena.) 28 Jun. 1990 14 p (Contract NAS7-918)
(NASA-Case-NPO-17569-1-CU; NAS 1.71:NPO-17569-1-CU; US-Patent-Appl-SN-545236) Avail: NTIS HC A03/MF A01 CSCL 13B

The present invention relates to a cryogenic Joule-Thomson refrigeration capable of pumping multicomponent gases with a single stage sorption compressor system. Alternative methods of pumping a multicomponent gas with a single stage compressor are disclosed. In a first embodiment, the sorbent geometry is such that a void is defined near the output of the sorption compressor. When the sorbent is cooled, the sorbent primarily adsorbs the higher boiling point gas such that the lower boiling point gas passes through the sorbent to occupy the void. When the sorbent is heated, the higher boiling point gas is desorbed at high temperature and pressure and thereafter propels the lower boiling point gas out of the sorption compressor. A mixing chamber is provided to remix the constituent gases prior to expansion of the gas through a Joule-Thomson valve. Other methods of pumping a multicomponent gas are disclosed. For example, where the sorbent is porous and the low boiling point gas does not adsorb very well, the pores of the sorbent will act as a void space for the lower boiling point gas. Alternatively, a mixed sorbent may be used where a first sorbent component physically adsorbs the high boiling point gas and where the second sorbent component chemically absorbs the low boiling point gas. NASA

N90-26177# Coast Guard, Groton, CT. Marine Fire and Safety Research Staff.
TESTING OF FLAME SCREENS AND FLAME ARRESTERS AS DEVICES DESIGNED TO PREVENT THE PASSAGE OF FLAME (DPPF) INTO TANKS CONTAINING FLAMMABLE ATMOSPHERES ACCORDING TO AN IMO STANDARD Final Report
John H. Dyer, Robert C. Richards, and C. D. Wolverton, Jr. Oct. 1989 123 p
(AD-A222566; USCG-MFSRD-74; USCG-M-3-90) Avail: NTIS HC A06/MF A01 CSCL 13/12

Devices to Prevent the Passage of Flame (DPPF) include flame arresters, flame screens and pressure/vacuum valves which are used in venting systems on storage tanks and tanker vessels transporting flammable or combustible liquids. DPPFs are intended to prevent the propagation of flame into enclosed spaces containing explosive vapors/air mixtures. Flashback and endurance burn tests are described which are used to determine compliance of DPPFs to International Maritime Organization (IMO) Standard, MSC/Circ. 373, Standards for the Design, Testing and Locating of Devices to Prevent the Passage of Flame into Cargo Tanks in Tankers. Data is presented of flashback and endurance burn tests conducted on four (4) flame screen arrangements and ten (10) arresters. GRA

32 COMMUNICATIONS AND RADAR

Includes radar; land and global communications; communications theory; and optical communications.

For related information see also *04 Aircraft Communications and Navigation* and *17 Space Communications, Spacecraft Communications, Command and Tracking.* For search and rescue see *03 Air Transportation and Safety,* and *16 Space Transportation.*

N90-26178# Advisory Group for Aerospace Research and Development, Neuilly-Sur-Seine (France). Electromagnetic Wave Propagation Panel.
PROPAGATION EFFECTS AND CIRCUIT PERFORMANCE OF MODERN MILITARY RADIO SYSTEMS WITH PARTICULAR EMPHASIS ON THOSE EMPLOYING BANDSPREADING
Dec. 1989 422 p In ENGLISH and FRENCH Symposium held in Paris, France, 17-21 Oct. 1988
(AGARD-CP-442; ISBN-92-835-0511-5) Copyright Avail: NTIS HC A18/MF A03; Non-NATO Nationals requests available only from AGARD/Scientific Publications Executive

The importance of understanding radio wave propagation increases as radar and communication systems become increasingly complex. Signal processing for modern systems can be realized in software. The recent development of such signal processors is radically changing the engineering approach to designing communications equipment. Advanced realizations for tactical communications in modern armies, now include digital transmission, voice and data capability and ECM resistant systems. Various techniques are needed to enhance security of communications and to improve resistance to jamming. The state-of- the-art in development of present day radio communication systems; the role and the need for radio propagation research; the assessed effects of propagation on existing systems and proposed improvements for new systems to meet operational requirements are examined. For individual titles, see N90-26179 through N90-26208.

N90-26179# Communications Research Centre, Ottawa (Ontario).
AN OVERVIEW OF CANADIAN RADIO PROPAGATION/COMMUNICATIONS TECHNOLOGIES RESEARCH
J. S. Belrose, R. Bultitude, D. Clark, R. W. Jenkins, W. Lauber, G. Nourry, N. M. Serinken, and G. Venier *In* AGARD, Propagation Effects and Circuit Performance of Modern Military Radio Systems with Particular Emphasis on those Employing Bandspreading Dec. 1989 30 p (For primary document see N90-26178 20-32) Copyright Avail: NTIS HC A18/MF A03; Non-NATO Nationals requests available only from AGARD/Scientific Publications Executive

The Communications Research Center (CRC) has and is carrying out research in radio propagation and radio communications technologies. Some of this research is briefly

overviewed. The overview will begin with a brief tutorial on the characteristics of fading channels. Topics to be addressed include: characterization and simulation of the channel (HF and land mobile channels); simulation of the HF spread spectrum channel; broad band adaptive antennas; and coding and packet switching technologies (particularly for the HF channel). The subject of miniprocessors and radio will be briefly mentioned. B.G.

N90-26180# Hull Univ. (England). Dept. of Electronic Engineering.

A GLOBAL COMMON-USER SYSTEM FOR THE PROVISION OF HF PROPAGATION DATA

M. Darnell, J. Hague, and A. Chan *In* AGARD, Propagation Effects and Circuit Performance of Modern Military Radio Systems with Particular Emphasis on those Employing Bandspreading Dec. 1989 14 p (For primary document see N90-26178 20-32)

Copyright Avail: NTIS HC A18/MF A03; Non-NATO Nationals requests available only from AGARD/Scientific Publications Executive

The system design described comprises a world-wide network of HF transmitters and receivers designed to allow the collection of field strength and other propagation data. The primary objective of the system is to enable the effectiveness of HF propagation/noise prediction methods to be enhanced by means of real-time measurement data. Historically, control of HF broadcasts and communications was heavily dependent on off-line path predictions; however, the degree of precision associated with such propagation analysis is somewhat limited. Some use was also made of passive monitoring of known transmitters to update off-line models, but problems of transmitter identification and inappropriate signal formats limit the efficiency of this approach. For these reasons, a system was designed comprising a number of dedicated HF transmitters, sited in different parts of the world, and emitting signals with a defined format, unique to each site. Reception of the signals can take place at various levels of sophistication, depending on the requirements and resources of the users. Information about transmitter identification, signal strength, phase stability, fading, multipath structure, signal-to-noise ratio, noise/interference, and predicted error rates for digital traffic can all be extracted from the transmissions. The signals can be received and exploited by a range of users. Facilities for system evolution in response to user requirements are incorporated. The detailed design philosophy of the system, the implementation of a prototype system, and the results of trials carried out with the prototype system over a medium range skywave path are described. Problems of system deployment and global data collection and analysis are also discussed. B.G.

N90-26181# Centre National d'Etudes des Telecommunications, Lannion (France).

EXPERIMENTAL ANALYSIS OF THE HF LINKAGE [ANALYSE EXPERIMENTALE DE LIAISONS HF]

Y. M. LeRoux, R. Fleury, J. Menard, and J. P. Jolivet *In* AGARD, Propagation Effects and Circuit Performance of Modern Military Radio Systems with Particular Emphasis on those Employing Bandspreading Dec. 1989 9 p In FRENCH (For primary document see N90-26178 20-32)

Copyright Avail: NTIS HC A18/MF A03; Non-NATO Nationals requests available only from AGARD/Scientific Publications Executive

The improvement of the quality and reliability of decametric scale transmission through a better understanding of the mechanics of ionospheric wave propagation was attempted. Accordingly, an experimental characterization tool was prepared at CNET. This system is operational at about 650 km, located at midlatitude. It allows simultaneous measurement of on the one hand, the impulse channel response at a frequency of 10 KHz, with a response period of 10 ms, and on the other hand, at 50 KHz, with parameters of set time, attenuation, and instant phases relative to each mode or propagation path. Analysis of characteristics of noise and interference are possible. The system and the main functional modes are described. There are examples of the experiment results. An important conclusion is that from their performance, the analysis of the links give insufficient evidence of the real existing channel (Watterson type), to explain in its totality the conduction of the ionospheric wave propagation. A general model of the channel, based on a representation of a linear system varying in time, is in being validated. Transl. by E.R.

N90-26182# Institute for Telecommunication Sciences, Boulder, CO.

PROGRESS AND REMAINING ISSUES IN THE DEVELOPMENT OF A WIDEBAND HF CHANNEL MODEL AND SIMULATION

L. Vogler, J. Hoffmeyer, J. Lemmon, and M. Nesenbergs *In* AGARD, Propagation Effects and Circuit Performance of Modern Military Radio Systems with Particular Emphasis on those Employing Bandspreading Dec. 1989 20 p Sponsored in part by RADC (For primary document see N90-26178 20-32)

Copyright Avail: NTIS HC A18/MF A03; Non-NATO Nationals requests available only from AGARD/Scientific Publications Executive

Although high frequency (HF) communication systems were used for many decades, these systems are currently the subject of renewed interest, particularly in assessing the capabilities of the HF channel with regard to wideband (of the order of 12 to 1000 KHz) signals. This interest has generated a need for wideband HF channel propagation measurements and the development of wideband channel models and simulators. Recent work in wideband HF is briefly reviewed, some limitations of existing HF channel models discussed, on-going work at the Institute for Telecommunication Sciences in the development of a validated wideband HF channel model described, and key technical issues remaining in the development of this model are discussed. B.G.

N90-26183# Laboratoire d'Etude des Transmissions Ionospheriques, Cachan (France).

OPTIMAL SYNCHRONIZATION OF SPREAD SPECTRUM SEQUENCED BY NONTRANSFERABLE SWITCHING OPERATORS [SEQUENCES D'ETALEMENT A SYNCHRONISATION OPTIMALE PAR COMMUTATION D'OPERATEURS INCOMMUTABLES]

C. Goutelard *In* AGARD, Propagation Effects and Circuit Performance of Modern Military Radio Systems with Particular Emphasis on those Employing Bandspreading Dec. 1989 7 p In FRENCH (For primary document see N90-26178 20-32)

Copyright Avail: NTIS HC A18/MF A03; Non-NATO Nationals requests available only from AGARD/Scientific Publications Executive

One of the main problems in spread spectrum transmission lies in the difficulty of acquiring of synchronization of spread spectrum sequencing. The procedure is based on the correlation of the long sequences necessary for the large number of operations considered nontransferable in the classical method. Meanwhile, there are the sequences in which the switching operations are possible, which reduces the number of operations, alleviates the complexity of decoders, and assures with maximum security, synchronization in minimum time. The mathematical limits that must be respected in sequencing in order to obtain the switchability of the operators are defined and a sequencing structure is proposed. A series of sequences is given as an example. Transl. by E. R.

N90-26184# British Telecom Research Labs., Ipswich (England).

RADIO CHANNEL MEASUREMENT AND MODELLING FOR FUTURE MOBILE RADIO SYSTEMS

E. Guerdenli and P. W. Huish *In* AGARD, Propagation Effects and Circuit Performance of Modern Military Radio Systems with Particular Emphasis on those Employing Bandspreading Dec. 1989 11 p (For primary document see N90-26178 20-32)

Copyright Avail: NTIS HC A18/MF A03; Non-NATO Nationals requests available only from AGARD/Scientific Publications Executive

Digital mobile radio systems will require planning methods that provide accurate predictions of signal strength, distortion, and interference for situations ranging from very small cells in dense urban locations to large rural cells. Topographic and land usage

data bases will find increasing use to enhance the accuracy of prediction models. The implications of these issues are discussed and the work in progress at British Telecommunications Research Laboratories on land mobile radio propagation modeling and wide-band channel measurements is presented. B.G.

N90-26185# Thomson-CSF, Gennevilliers (France).
BROADBAND ANALYSIS OF GROUND WAVE PROPAGATION AT A50 TO 400 MHz [ANALYSE LARGE BANDE DE LA PROPAGATION DES ONDES DE SOL DANS LA BANDE 150-400 MHZ]
D. Sorais *In* AGARD, Propagation Effects and Circuit Performance of Modern Military Radio Systems with Particular Emphasis on those Employing Bandspreading Dec. 1989 11 p In FRENCH (For primary document see N90-26178 20-32)
Copyright Avail: NTIS HC A18/MF A03; Non-NATO Nationals requests available only from AGARD/Scientific Publications Executive

Broadband ground wave propagation is studied in a semirural geographic area by measuring the complex impulse response from a fixed and a mobile station. The distribution of the main statistical estimators is presented for 150, 250, and 400 MHz. The analysis of multipaths is presented and the identification of their physical causes is shown by the location of their particular measurement. Transl. by E.R.

N90-26186# Forschungsinstitut der Deutschen Bundespost, Darmstadt (Germany, F.R.).
MEASUREMENT AND SIMULATION OF WIDESPREAD MOBILE RADIO CHANNEL CHARACTERISTICS
Rudolf Werner Lorenz *In* AGARD, Propagation Effects and Circuit Performance of Modern Military Radio Systems with Particular Emphasis on those Employing Bandspreading Dec. 1989 7 p (For primary document see N90-26178 20-32)
Copyright Avail: NTIS HC A18/MF A03; Non-NATO Nationals requests available only from AGARD/Scientific Publications Executive

The general model of the transmission characteristics in mobile radio is derived. It is shown which abstractions are necessary to come up with the wide-sense stationary uncorrelated scattering (WSSUS) model. This model, well known from troposcatter propagation, is valid in mobile radio only for small vehicle travel distances. Nevertheless, the WSSUS model proved to be ideal for system test performance in mobile radio. The reasons are explained. A frequency-selective fading simulator recently developed in France and Germany is described, which is based on the WSSUS model and proved to be a very suitable tool for hardware test of mobile radio equipment. The key dates of mobile radio channel characteristics standardized by COST 207 are briefly presented. B.G.

N90-26187# Institut National des Sciences Appliquees, Rennes (France). Laboratoire Structures Rayonnantes.
ESTIMATION OF THE IMPULSE RESPONSE OF A BROADBAND MOBILE RADIO CHANNEL IN SUBURBIA AT 910 MHz [ESTIMATION DE LA REPONSE IMPULSIONNELLE DU CANAL RADIOMOBILE LARGE BANDE EN SITE SUBURBAIN A 910 MHZ]
M. Salehudin, G. ElZein, J. J. Bai, A. Daniel, and J. Citerne *In* AGARD, Propagation Effects and Circuit Performance of Modern Military Radio Systems with Particular Emphasis on those Employing Bandspreading Dec. 1989 9 p In FRENCH (For primary document see N90-26178 20-32)
Copyright Avail: NTIS HC A18/MF A03; Non-NATO Nationals requests available only from AGARD/Scientific Publications Executive

A method is presented for the estimation of impulse response of a broadband radio channel, in UHF, beginning with the parameters relating to the environment. It covers the relative position of the transmitter to that of the mobile radio. These transmitters are distributed randomly in a homogeneous environment and function like a secondary source of waves emitting only one beam in the direction of the receiver. The environmental parameters are drawn, beginning with the existing topographic map sections. The height of the transmitters, conducting a 3-D geometric model, is introduced by an effective bistatic radar section. The radar determines the reflectance of the transmitters. Comparison of the results of the estimation which was drawn from the measurement of the actual channel was given a functional form by use of the paths of intervals of a known delay. This shows agreement in suburban areas. Transl. by E.R.

N90-26188# CyberCom Corp., Arlington, VA.
WIDEBAND CHARACTERIZATION OF FOREST PROPAGATION CHANNELS
Allan Schneider, Frederick J. Altman, and Kevin Lackey (Army Communications-Electronics Command, Fort Monmouth, NJ.) *In* AGARD, Propagation Effects and Circuit Performance of Modern Military Radio Systems with Particular Emphasis on those Employing Bandspreading Dec. 1989 14 p (For primary document see N90-26178 20-32)
Copyright Avail: NTIS HC A18/MF A03; Non-NATO Nationals requests available only from AGARD/Scientific Publications Executive

Wideband propagation measurements within the frequency band 200 to 2000 MHz were made through a coniferous forest of Douglas fir at Fort Lewis, Washington, and through a deciduous forest of red maple in Coventry, Connecticut. Measurements were repeated at Fort Lewis in successive years following thinning of the forest, and twice within the same year at Coventry, before and after the autumn fall of leaves. These field measurements utilized wideband impulse-response measurements to characterize the UHF wideband forest propagation channel. The effort relied upon the U.S. Army's Wideband Propagation Measurement System (WPMS), a self-contained, mobile, automated, wideband propagation data acquisition and recording system. This measurement program was closely coupled to an anlytic effort to develop a UHF forest propagation model suitable for predicting the transmission loss and delay spread experienced by a radiowave propagating through the forest. Both measured and predicted values of transmission loss and delay spread are reviewed as they relate to distance, antenna height, frequency, polarization, and biophysical forest parameters. Concepts bearing on the analysis and interpretation of the measured data are discussed, and conclusions drawn relating to communication system deployment in forests. B.G.

N90-26189# Centre National d'Etudes des Telecommunications, Issy-les-Moulineaux (France).
IN-BAND AMPLITUDE DISPERSION ON A MICROWAVE LINK
Y. K. Li (China Research Inst. of Radiowave Propagation, Xinxiang.), P. Gole, and M. Sylvain *In* AGARD, Propagation Effects and Circuit Performance of Modern Military Radio Systems with Particular Emphasis on those Employing Bandspreading Dec. 1989 13 p (For primary document see N90-26178 20-32)
Copyright Avail: NTIS HC A18/MF A03; Non-NATO Nationals requests available only from AGARD/Scientific Publications Executive

Statistical results of in-band amplitude dispersion on a microwave link during 1985 with diversity reception in France are represented. The large time extent of the data base allowed an analysis of the seasonal variations of in-band amplitude dispersion distributions. Worst-month distributions are also presented for each channel. Idealized switch diversity is investigated with the decision criterion of in-band amplitude dispersion. It was found that the potential improvement due to the space diversity technique in terms of the reduction in amplitude dispersion was remarkable. The frequency correlation coefficient of received amplitudes and powers in the summer of 1985 was computed on the experimental data base. Comparisons between experimental results and theoretical results were made for the two non-diversity channels for the summer period of 1985. Author

N90-26190# Hull Univ. (England). Dept. of Electronic Engineering.
A DIGITAL METEOR-BURST COMMUNICATION (MBC) PROPAGATION PATH SIMULATOR
K. Watson *In* AGARD, Propagation Effects and Circuit Performance of Modern Military Radio Systems with Particular Emphasis on those Employing Bandspreading Dec. 1989 15 p (For primary document see N90-26178 20-32)
Copyright Avail: NTIS HC A18/MF A03; Non-NATO Nationals requests available only from AGARD/Scientific Publications Executive

An MBC propagation path simulator which was developed is discussed and the specification of this simulator is contrasted with that of a typical HF simulator. A discussion of how the simulator was implemented and how it is to be employed then follows. Finally, there is included a brief discussion of a few concepts which are to be investigated using the simulator. The final aim of the research is to produce an MBC system which makes more efficient use of the available capacity than previously reported systems. B.G.

N90-26191# Organisatie voor Toegepast Natuurwetenschappelijk Onderzoek, The Hague (Netherlands). Physics and Electronics Lab.
MAN-MADE NOISE IN A MILITARY ENVIRONMENT
K. S. Kho and P. A. vanderVis *In* AGARD, Propagation Effects and Circuit Performance of Modern Military Radio Systems with Particular Emphasis on those Employing Bandspreading Dec. 1989 7 p (For primary document see N90-26178 20-32)
Copyright Avail: NTIS HC A18/MF A03; Non-NATO Nationals requests available only from AGARD/Scientific Publications Executive

Over the last few years the laboratory was involved in studies concerning the design of future radio systems and of electronic support measures (ESM). Within the ESM-scope special attention is paid to direction finding (DF), as it offers a powerful means of locating enemy transmitters. Because environmental noise may seriously confine the range of reliable operation of both systems, the availablilty of relevant data is of crucial importance. Attention is given to noise in the lower end of the VHF band, i.e., between 30 and 90 MHz. Statistics on atmospheric and galactic noise may be found in CCIR Report 322, and CCIR Report 258-3 provides information about man-made noise for areas described as urban, suburban, or industrial, etc., the military environment is (understandably) not mentioned. As it goes without saying that military equipment must above all work well in wartime, there is an obvious need to gather information on what is to be expected if it comes to the worst. Because a better way of filling this information gap was not found, measurements were performed during military maneuvers, by making use of Certain Strike, a large scale NATO exercise in Europe in September 1987. The idea was supported by the Royal Netherlands Army (RNLA). The 4th division of the 1st NL corps hosted the team in Germany. B.G.

N90-26192# Communications Research Centre, Ottawa (Ontario). Dept. of Communications.
A NARROWBAND TACTICAL COMMUNICATION SYSTEM FOR THE VHF AND UHF MOBILE RADIO BANDS
L. Boucher, Y. Jolly, and J. H. Lodge *In* AGARD, Propagation Effects and Circuit Performance of Modern Military Radio Systems with Particular Emphasis on those Employing Bandspreading Dec. 1989 14 p Sponsored by National Defence Headquarters (For primary document see N90-26178 20-32)
Copyright Avail: NTIS HC A18/MF A03; Non-NATO Nationals requests available only from AGARD/Scientific Publications Executive

A description of the research effort, performed in accordance with a National Defense (DND) sponsored Research Program, is presented. Goals fixed for the program aim at achieving good quality, encryptable voice communications in the VHF and UHF mobile bands within a channel spacing of about 3 kHz. A review of the desirable performance objectives of a land-mobile tactical voice communications system is presented, and the design strategy suggested to achieve this performance is described. Implementation includes the use of techniques such as frequency domain digital signal processing of single sideband speech, speech bandwidth reduction, and linear modulation. A study, and in some cases experimental evaluation, on promising bandwidth reduction techniques was done, and a method, called the dynamic frequency band extraction technique, was developed for this application. With this technique, a good voice quality is obtained by dynamically saving only about 1200 Hz of the original 3000 Hz voice spectrum. Taking into account the extra bandwidth required by the data, the frequency domain filtering, and the pulse shaping of the discrete-time samples, and using a highly linear power amplifier, the RF channel spacing of the modulated signal is expected to be approx. of 2.5 kHz. Author

N90-26193# Hull Univ. (England). Dept. of Electronic Engineering.
CHANNEL SELECTION AND CONTROL PROCEDURES IN AN AUTOMATIC HF SYSTEM
J. Hague *In* AGARD, Propagation Effects and Circuit Performance of Modern Military Radio Systems with Particular Emphasis on those Employing Bandspreading Dec. 1989 13 p Sponsored by Science and Engineering Research Council (For primary document see N90-26178 20-32)
Copyright Avail: NTIS HC A18/MF A03; Non-NATO Nationals requests available only from AGARD/Scientific Publications Executive

Conventional HF systems rely on a combination of human operators and off-line propagation prediction programs to determine an optimum operating frequency in what is a time-varying medium. Both these methods suffer drawbacks in that the rapidly varying nature of many HF paths lead to greatly reduced performance, since the system is unable to respond to the changing state of the medium. An automatic HF system is described which is intended to overcome many of the drawbacks associated with conventional methods of control. By utilizing cheap, amateur-grade equipment coupled with simple antenna systems, the system is able to carry data on one channel while assessing the usability of other channels assigned to that particular system. Measurements taken on alternative channels (probing channels) are compared with those of the current channel. The best channel currently available at each end of the link is then relayed to the other end by means of a robust data header on the user data channel. Thus each end of the link will always be transmitting on the optimum channel. In order to assess the usability of the channel, some means of real time channel evaluation (RTCE) is needed, both on the user's data and probing channels. The overall architecture of the automatic HF system is discussed and the methods of channel assessment performed detailed. A description of a variable-redundancy coding scheme utilized by the system is also given, since this enables the system to optimize the data throughout. Finally, a performance of various aspects of the system over an HF path are given. B.G.

N90-26194# Manchester Coll. of Science and Technology (England). Dept. of Electrical Engineering and Electronics.
AN EXPERIMENTAL MEDIUM SPEED WIDEBAND MODEM
Alastair N. Brydon and Geoffrey F. Gott *In* AGARD, Propagation Effects and Circuit Performance of Modern Military Radio Systems with Particular Emphasis on those Employing Bandspreading Dec. 1989 10 p Sponsored by Royal Signals and Radar Establishment, England (For primary document see N90-26178 20-32)
Copyright Avail: NTIS HC A18/MF A03; Non-NATO Nationals requests available only from AGARD/Scientific Publications Executive

An experimental high frequency (HF) modem which uses chirp signals swept across a voice channel bandwidth is discussed. The modem is able to adaptively excise interference from other HF users, and has inherent tolerance to frequency selective fading and additive white Gaussian noise. A number of experimental chirp signal formats were incorporated so as to achieve data transmission at rates of 75, 150, 300, and 600 bits per second, and error correction via interleaved Golay (23,12,3) code is included. The

principles behind the experimental formats are outlined, and how they performed during 156 hours of tests over a 125 km HF sky-wave link is indicated. B.G.

N90-26195# Norwegian Defence Research Establishment, Kjeller. Div. for Electronics.

CORA: A DIRECT SEQUENCE SPREAD SPECTRUM RADIO FOR VOICE AND DATA

T. Thorvaldsen *In* AGARD, Propagation Effects and Circuit Performance of Modern Military Radio Systems with Particular Emphasis on those Employing Bandspreading Dec. 1989 18 p (For primary document see N90-26178 20-32)

Copyright Avail: NTIS HC A18/MF A03; Non-NATO Nationals requests available only from AGARD/Scientific Publications Executive

For many years the ordinary FM radio (e.g., the VRC 12 family) was the workhorse in military forces throughout the world. This type of radio has some advantages; it is relatively simple and cheap, it has a low power consumption as a man-pack, and an excellent voice quality. Since the modulation type and details are known by everyone, however, the messages are easily intercepted and even rebroadcasted in order to fool the enemy. Age is also becoming an important argument for introducing a new radio generation on the market. Radios operating in the military VHF band 30 to 88 MHz are discussed. The requirements for such a radio will of course vary from country to country. The most important requirements are given. B.G.

N90-26196# Hull Univ. (England). Dept. of Electronic Engineering.

MULTIPLE-ACCESS TECHNIQUES FOR COMMUNICATION OVER DISPERSIVE RADIO CHANNELS

M. Darnell and B. Honary (Warwick Univ., Coventry, England) *In* AGARD, Propagation Effects and Circuit Performance of Modern Military Radio Systems with Particular Emphasis on those Employing Bandspreading Dec. 1989 p 16 Sponsored by Science and Engineering Research Council, England (For primary document see N90-26178 20-32)

Copyright Avail: NTIS HC A18/MF A03; Non-NATO Nationals requests available only from AGARD/Scientific Publications Executive

Conventional multiple-user/multiple-access techniques are reviewed which were employed on various types of radio channels. These techniques are time-division multiple access (TDMA), frequency-division multiple-access (FDMA), and code-division multiple-access (CDMA). Attention is turned to CDMA-type systems which appear to offer promise of reliable operation over dispersive radio paths. First consider the use of completely uncorrelated, as opposed to near-correlated, code sets. In practical CDMA systems designed to date, the latter class of codes was used. It is shown that completely uncorrelated sets have distinct advantages (particularly for packet data operations). Secondly, collaborative coding techniques are used to permit simultaneous transmission by several users sharing a common channel, with overall transmission rates in excess of that achievable with TDMA. The performance of three new collaborative coding multiple-access (CCMA) schemes, each with two users, under Gaussian noise conditions are described. Author

N90-26197# Thomson-CSF, Gennevilliers (France). Div. Telecommunications.

A VERSATILE INTEGRATED BLOCK CODES ENCODER-DECODER

P. A. Laurent *In* AGARD, Propagation Effects and Circuit Performance of Modern Military Radio Systems with Particular Emphasis on those Employing Bandspreading Dec. 1989 10 p In FRENCH; ENGLISH summary (For primary document see N90-26178 20-32)

Copyright Avail: NTIS HC A18/MF A03; Non-NATO Nationals requests available only from AGARD/Scientific Publications Executive

A new Very Large Scale Integrated (VLSI) circuit which is designed to perform encoding and decoding of almost all Reed-Solomon and BCH codes (including generalized BCH) using symbol sizes from 1 to 8 bits. It is fully programmable by many standard microprocessors which consider it like any other more common co-processor. Its architecture allows a high bit rate and a great flexibility. The interfacing protocol is optimized for minimizing time constraint (mail boxes) and limiting programming effort: no advanced knowledge of codes is required to use it. Author

N90-26198# Laboratoire d'Etude des Transmissions Ionospheriques, Cachan (France).

MINIMIZATION OF THE COST OF INFORMATION TRANSFER IN HF SPREAD SPECTRUM TRANSMISSION [MINIMISATION DU COUT DE TRANSFERT DE L'INFORMATION DANS LES TRANSMISSIONS HF A ETALEMENT DE SPECTRE]

C. Goutelard and J. Caratori *In* AGARD, Propagation Effects and Circuit Performance of Modern Military Radio Systems with Particular Emphasis on those Employing Bandspreading Dec. 1989 12 p In FRENCH (For primary document see N90-26178 20-32)

Copyright Avail: NTIS HC A18/MF A03; Non-NATO Nationals requests available only from AGARD/Scientific Publications Executive

The spread spectrum is a well known technique with certain forms of HF because of the dispersivity of the channel and, more importantly, interference. The limits imposed by these channels and their effects on the signal are analyzed. The characteristics of the interference noise are determined by a series of measurements which are analyzed statistically. The effects of the limits due to the channel and interference are taken into account to help explain the different strategies possible. It is then shown that it is possible to minimize the cost of data transmission determined by the amount of energy used for the transmission of a Shannon of Information, as in the case of a perfect or semiperfect spread spectrum. A comparison of the different strategies is made. The choice is affected by the complexity of effective operation allowed by the detection. Transl. by E.R.

N90-26199# Hull Univ. (England). Dept. of Electronic Engineering.

NEW SYNCHRONISATION TECHNIQUES APPLICABLE TO MULTI-TONE TRANSMISSION SYSTEMS

M. Darnell and B. Honary (Warwick Univ., Coventry, England) *In* AGARD, Propagation Effects and Circuit Performance of Modern Military Radio Systems with Particular Emphasis on those Employing Bandspreading Dec. 1989 8 p (For primary document see N90-26178 20-32)

Copyright Avail: NTIS HC A18/MF A03; Non-NATO Nationals requests available only from AGARD/Scientific Publications Executive

The synchronization techniques are applicable to both narrowband, multiple frequency shift keyed (MFSK) digital transmission systems and wideband frequency hopping systems. The techniques do not require specific synchronization overheads to be incorporated into the transmissions, but operate using the normal traffic signal formats. It is required that digital signal processing be employed at the receiver for the procedures to be effective. Three distinct synchronization methods are discussed: modulation-derived synchronization; code-derived synchronization; and combined modulation- and code-derived synchronization. B.G.

N90-26200# Telecommunications Radioelectriques et Telephoniques, Le Plessis-Robinson (France).

SYNCHRONIZATION OF FREQUENCY SHIFT TRANSMISSION AND THE EFFECT OF OVERSAMPLING [SYNCHRONISATION DES TRANSMISSIONS EN EVASION DE FREQUENCE EFFET DU SURECHANTILLONNAGE]

J. P. VanUffelen *In* AGARD, Propagation Effects and Circuit Performance of Modern Military Radio Systems with Particular Emphasis on those Employing Bandspreading Dec. 1989 8 p In FRENCH (For primary document see N90-26178 20-32)

Copyright Avail: NTIS HC A18/MF A03; Non-NATO Nationals

requests available only from AGARD/Scientific Publications Executive

There are numerous communications necessary for the establishment of the synchronization of the receiver as related to the message received. In the course of initialization, several phases are defined: (1) The synchronization sequence over the frequency in the case of communication using frequency shifts; (2) The synchronization where the network goal is defined by the instant of message arrival and refinding the network again; (3) The synchronization of symbols sometimes called synchronization bits, which allows the definition of the instant of decision; and (4) The synchronization of the carrier in the case of coherent demodulation. One can also consider code synchronization in the case of encoded communications and synchronization of spread spectrum sequence for transmissions of this type. Herein, the main interest is in the synchronization and the sequence shift frequency and its impact on symbol synchronization. Transl. by E.R.

N90-26201# Marconi Secure Radio Systems Ltd., Portsmouth (England).

NEW APPROACHES FOR RAPID SYNCHRONISATION FREQUENCY HOPPERS

A. D. Bisset *In* AGARD, Propagation Effects and Circuit Performance of Modern Military Radio Systems with Particular Emphasis on those Employing Bandspreading Dec. 1989 20 p (For primary document see N90-26178 20-32)

Copyright Avail: NTIS HC A18/MF A03; Non-NATO Nationals requests available only from AGARD/Scientific Publications Executive

The analysis and simulation of a typical synchronization protocol employed in a medium rate frequency hopper, specifically under poor signal conditions are described in detail. Bit slippage within the initial synchronization frame was identified as the major source of reduced performance of synchronization protocols. A set of performance curves is presented to enable the dependence on correlation threshold, and the ultimate receive probability for a given protocol, to be evaluated. The dependence on bit synchronizer phase locked loop (PLL) bandwidth was simulated, indicating that major improvement was possible at limit signal conditions. However, this was off-set by a reduced performance for better signal conditions. An effective solution to such a problem can be achieved by employing a combined bit and frame synchronizer. Simulation results for such a technique are also presented for comparison. B.G.

N90-26202# Center for Remote Sensing, McLean, VA.

EFFECTS OF IONOSPHERIC MODIFICATION ON SYSTEM PERFORMANCE

Suman Ganguly *In* AGARD, Propagation Effects and Circuit Performance of Modern Military Radio Systems with Particular Emphasis on those Employing Bandspreading Dec. 1989 11 p (For primary document see N90-26178 20-32)

Copyright Avail: NTIS HC A18/MF A03; Non-NATO Nationals requests available only from AGARD/Scientific Publications Executive

Controlled ionospheric modification can be used for disrupting as well as facilitating communication and radar systems. After briefly describing the results achieved with the present day ionospheric modification facilities, a scenario is presented for the generation of strong and significant ionospheric modification. A few schemes are presented for the development of modern high power facilities using the state of the art technology and then the impact of such facilities on the system performance is described. Author

N90-26203# Rediffusion Radio Systems Ltd., Crawley (England).

HF SPREAD SPECTRUM, AN AUDIT OF THE POWER REQUIREMENTS AND LPI VULNERABILITY

C. S. denBrinker *In* AGARD, Propagation Effects and Circuit Performance of Modern Military Radio Systems with Particular Emphasis on those Employing Bandspreading Dec. 1989 9 p (For primary document see N90-26178 20-32)

Copyright Avail: NTIS HC A18/MF A03; Non-NATO Nationals requests available only from AGARD/Scientific Publications Executive

Electronic Countermeasures (ECM) and the response to ECM was widely introduced in frequency bands other than HF. The unique characteristics of HF generate a different set of problems. In this overview, the normal hygienic measures that can be adopted for communication are reviewed. Force fitting of trends in spectral occupancy has revealed that the power penalty to be paid for low error rate frequency hopping could be prohibitive. The arguments used here may shed new light on the differing views taken with respect to the VHF band, where the choice of location could influence the efficacy assessment. Parallel diversity over a restricted bandwidth appears to offer a low probability of intercept in the case of dense occupancy and thus negate the need for excessive frequency hopping powers. Author

N90-26204# Centre National d'Etudes des Telecommunications, Issy-les-Moulineaux (France).

COMBINED EFFECTS OF FAST AND SELECTIVE FADING ON PERFORMANCE OF PSK AND MSK WITH COHERENT DETECTION

Armand J. Levy *In* AGARD, Propagation Effects and Circuit Performance of Modern Military Radio Systems with Particular Emphasis on those Employing Bandspreading Dec. 1989 8 p (For primary document see N90-26178 20-32)

Copyright Avail: NTIS HC A18/MF A03; Non-NATO Nationals requests available only from AGARD/Scientific Publications Executive

Depending on the symbol rate and on the particular channel conditions, mobile radio communications can be affected by fast fading, by selective fading, or by both of them. In order to determine when each effect should be considered, the performance of PSK and MSK with coherent detection is theoretically evaluated in the presence of a fast and selective fading channel. A numerical method of analysis is derived for Gaussian Wide Sense Stationary Uncorrelated Scattering channel, taking into account the phase recovery error induced by the degraded channel. Results are presented for cases of practical interest. It appears that for some severe channel conditions, none of the fast and selective fading can be neglected. Author

N90-26205# Institut National des Sciences Appliquees, Rennes (France). Laboratoire Structures Rayonnants.

EXPERIMENTAL STUDY OF A DIGITAL MOBILE RADIO SPREAD SPECTRUM IN AN URBAN SITE [ETUDE EXPERIMENTALE D'UNE LIAISON NUMERIQUE RADIOMOBILE A ETALEMENT DE SPECTRE EN SITE URBAIN]

G. ElZein, M. Salehudin, A. Daniel, J. J. Bai, and J. Citerne *In* AGARD, Propagation Effects and Circuit Performance of Modern Military Radio Systems with Particular Emphasis on those Employing Bandspreading Dec. 1989 12 p In FRENCH (For primary document see N90-26178 20-32)

Copyright Avail: NTIS HC A18/MF A03; Non-NATO Nationals requests available only from AGARD/Scientific Publications Executive

The investigation and results of a digital mobile radio at 910 MHz, using the spread spectrum for immediate sequencing is reported. The use of this links is with a communication system or a measuring system for characterization of the urban mobile radio channel. Effective performance measurement, accomplished with good theoretical agreement, is obviously better than spread spectrum. Effective propagation measurement on the true linkage is shown from the spatial and temporal variations on the external signal reception and also on the instantaneous flutter fadings of the impulse response of channel transmissions. These measurements allow the termination of a statistical model of channel transmission and the improvement of the quality of the multipath linkage. Transl. by E.R.

N90-26206# Norwegian Defence Research Establishment, Kjeller.
PACKET RADIO NETWORK CONCEPTS FOR THE NORWEGIAN FIELD ARMY
Tore Berg, John Erik Rustad, and Ole Henrik Storen *In* AGARD, Propagation Effects and Circuit Performance of Modern Military Radio Systems with Particular Emphasis on those Employing Bandspreading Dec. 1989 26 p (For primary document see N90-26178 20-32)
Copyright Avail: NTIS HC A18/MF A03; Non-NATO Nationals requests available only from AGARD/Scientific Publications Executive

The Norwegian army has taken a very close look at the advantages in integrating weapon control systems, general CCIS, and tactical communication. All these services are provided by the communication area system TADKOM consisting of a nodal trunk part and a mobile radio part. The concept laid down for TADKOM is based on the idea of a unified system with decentralized net-control and where voice and data are integrated into one system. The mobile radio part of TADKOM is presented and what is identified as the most critical design issue is stressed. Author

N90-26207# Thomson-CSF, Gennevilliers (France).
EXPERIMENTATION OF A TRANSMISSION SYSTEM DATA PROCESSING BY METEOR BURSTS [EXPERIMENTATION D'UN SYSTEME DE TRANSMISSION DE DONNEES PAR CANAL METEORIQUE: THEOREME]
P. Sicila, D. Sorais, and F. Barrier *In* AGARD, Propagation Effects and Circuit Performance of Modern Military Radio Systems with Particular Emphasis on those Employing Bandspreading Dec. 1989 19 p In FRENCH (For primary document see N90-26178 20-32)
Copyright Avail: NTIS HC A18/MF A03; Non-NATO Nationals requests available only from AGARD/Scientific Publications Executive

A data transmission system was made using meteor burst theory. The project was accomplished in three phases. The first phase was with point to point links alternating between 2 stations 350 km apart, phases 2 and 3 were linked by broadcasting from a vehicle and air paths, respectively. The experiments were conducted at several powers (1 kW, 200, 100, and 50 W) in VHF and in fixed frequency range of 40 to 43 MHz. The model permits an effective measuring test of the opening and closing of the channel and the error rate as well as the message transmission. The measured mean flow is in the range of 100 to 185 characters/per sec with a maximum of 300 to 400 characters/sec.
Transl. by E.R.

N90-26208# Massachusetts Technological Lab., Inc., Bethesda, MD.
SYSTEM FACTORS TO BE CONSIDERED IN ASSESSING PROPAGATION EFFECTS ON MODERN DIGITAL SATELLITE COMMUNICATIONS SYSTEMS
D. J. Fang and H. Soicher (Army Communications-Electronics Command, Fort Monmouth, NJ.) *In* AGARD, Propagation Effects and Circuit Performance of Modern Military Radio Systems with Particular Emphasis on those employing Bandspreading Dec. 1989 12 p (For primary document see N90-26178 20-32)
(Contract DAAB07-88-C-A007)
Copyright Avail: NTIS HC A18/MF A03; Non-NATO Nationals requests available only from AGARD/Scientific Publications Executive

In the traditional approach of assessing system impact due to propagation anomalies, the primary effort is on the characterization of a propagation channel to the maximum extent possible. In such an approach, environmental parameters (which affect the channel transfer function) and the system parameters (which dictate the system performance) are largely uncoupled. For instance, the transfer function for an ionospheric scintillation channel is characterized by ionospheric irregularity parameters, irrespective of whether the communications system is digital or analog, with or without interleave/coding, in the prescence or absence of diversity. From assessing the system impact's viewpoint, the lack of coupling is acceptable to the conventional analog system (an 8 dB propagation degradation implies an 8 dB reduction of S/N irrespective of whether the system is AM or FM, single side band or double side band), but is not acceptable for the modern digital system (an 8 dB propagation degradation can imply 10(exp -3) BER for a QPSK system without coding but can also imply 10(exp -6) BER for the same system with coding and interleave). System factors to be considered in the assessment of propagation effects are outlined.The essence is to point out, for modern digital satellite communications systems, propagation assessment has to have proper system reference in order to provide readily useful conclusions for system engineers. Author

N90-26209# Department of the Army, Washington, DC.
CONTINUOUS ON-LINE LINK ERROR RATE DETECTOR Patent Application
Charles F. Wagner, Jr., inventor (to Army) and James A. Coleman, inventor (to Army) 19 Mar. 1990 21 p
(AD-D014510; US-Patent-Appl-SN-495553) Avail: NTIS HC A03/MF A01 CSCL 25/2

This invention relates generally to communications apparatus and more particularly to apparatus for continuously monitoring, determining, and displaying the error rate of a digital communications signal in a multi-channel radio link. Time division multiplex (TDM) multi-channel communication systems or networks are well known. Such systems are particularly useful in digital communication systems utilizing a frame pattern which consists of a plurality of binary signal bits which appear in a continuous data stream. In order to distinguish each frame in the data stream, one bit referred to as the framing bit, typically appears at the end of the frame and exhibits a predetermined same digital pattern unless there are errors in the data stream. Accordingly, the purpose of the framing bit is to provide a marker in the digital stream so that electronic hardware can identify the location of each frame. It is necessary for the communications hardware to know the end of a frame because the data position within the frame must be sorted and transferred to different destinations. Accordingly, it is an object of the present invention to improve the quality, maintainability and operability of time division multiplex communication systems without interruption or interference to the communications channels and without sacrificing channel capacity. GRA

N90-26210# Federal Aviation Administration, Atlantic City, NJ.
EQUIPMENT FEASIBILITY STUDY: VERY HIGH FREQUENCY COMMUNICATION EQUIPMENT (136-137 MEGAHERTZ)
James Aviles, Ed Lind, and Larry McMillen Jun. 1990 19 p
(DOT/FAA/CT-TN89/72) Avail: NTIS HC A03/MF A01

The feasibility of utilizing existing ground and airborne very high frequency (VHF) voice communication equipment for operation in the frequency range of 136 to 137 megahertz (MHz) was investigated. Existing general aviation databases were utilized and avionic transceiver manufactures consulted in an effort to estimate the numbers and capabilities of existing VHF communication transceivers to operate or be modified to operate up to 137 MHz. Information gathered for a sample of VHF communication transceivers manufactured over a certain time period was statistically projected to the entire general aviation population. Results indicate that: (1) Sixty-eight percent of the actual VHF communication transceivers will not cover the new band 136 to 137 MHz; and (2) Thirty-two percent of the actual VHF communication transceivers will cover the new band 136 to 137 MHz. Author

N90-26211 British Broadcasting Corp., Kingswood (England). Engineering Div.
ANTENNAS FOR PORTABLE VHF-FM RECEIVERS
R. D. C. Thoday 1990 12 p
(BBC-RD-1990/1) Copyright Avail: BBC, Kingswood Warren, Tadworth, Surrey, England

A number of compact antennas are described which have been considered as replacements for the standard whip antenna which

is normally fitted to VHF portable receivers. A comparison made of their characteristics shows that, of the antennas considered in the survey, the quarter-wave whip still provides the best sensitivity. However the normal-mode helix is a more convenient and compact antenna and is shown to perform better than a short whip of the same axial length. This antenna can be easily engineered to operate over the VHF band and has sufficient sensitivity for normal use. Author

N90-26212 British Broadcasting Corp., Kingswood (England). Engineering Div.
ELECTRIC FIELD STRENGTH METERS FOR THE HF, VHF, AND UHF BANDS
R. D. C. Thoday 1990 14 p
(BBC-RD-1990/3) Copyright Avail: BBC, Kingswood Warren, Tadworth, Surrey, England

The BBC has been deploying two of its own design of RF hazard meters since about 1964. These are used to ensure that levels of RF field can be measured and thus a safe operating regime can be maintained. The scales on the meters have been modified to reflect new guidance from the National Radiological Protection Board, and the meters have therefore needed to be recalibrated. The design and calibration methods used including independent certification by the National Physical Laboratory, are described. Author

N90-26213*# Virginia Polytechnic Inst. and State Univ., Blacksburg. Dept. of Electrical Engineering.
FEASIBILITY STUDY OF A SYNTHESIS PROCEDURE FOR ARRAY FEEDS TO IMPROVE RADIATION PERFORMANCE OF LARGE DISTORTED REFLECTOR ANTENNAS Semiannual Status Report
W. L. Stutzman and W. T. Smith Aug. 1990 251 p
(Grant NAG1-859)
(NASA-CR-186641; NAS 1.26:186641; EE-SATCOM-90-2) Avail: NTIS HC A12/MF A02 CSCL 20N

Surface errors on parabolic reflector antennas degrade the overall performance of the antenna. Space antenna structures are difficult to build, deploy and control. They must maintain a nearly perfect parabolic shape in a harsh environment and must be lightweight. Electromagnetic compensation for surface errors in large space reflector antennas can be used to supplement mechanical compensation. Electromagnetic compensation for surface errors in large space reflector antennas has been the topic of several research studies. Most of these studies try to correct the focal plane fields of the reflector near the focal point and, hence, compensate for the distortions over the whole radiation pattern. An alternative approach to electromagnetic compensation is presented. The proposed technique uses pattern synthesis to compensate for the surface errors. The pattern synthesis approach uses a localized algorithm in which pattern corrections are directed specifically towards portions of the pattern requiring improvement. The pattern synthesis technique does not require knowledge of the reflector surface. It uses radiation pattern data to perform the compensation. Author

N90-26214*# National Aeronautics and Space Administration. Langley Research Center, Hampton, VA.
A NEW TECHNIQUE IN THE GLOBAL RELIABILITY OF CYCLIC COMMUNICATIONS NETWORK
Jon A. Sjogren (Army Aviation Systems Command, Hampton, VA.) 1989 32 p Submitted for publication
(NASA-TM-103479; NAS 1.15:103479) Avail: NTIS HC A03/MF A01 CSCL 17B

The global reliability of a communications network is the probability that given any pair of nodes, there exists a viable path between them. A characterization of connectivity, for a given class of networks, can enable one to find this reliability. Such a characterization is described for a useful class of undirected networks called daisy-chained or braided networks. This leads to a new method of quickly computing the global reliability of these networks. Asymptotic behavior in terms of component reliability is related to geometric properties of the given graph. Generalization of the technique is discussed. Author

N90-26215# General Accounting Office, Washington, DC. Information Management and Technology Div.
SPACE OPERATIONS: NASA'S COMMUNICATIONS SUPPORT FOR EARTH ORBITING SPACECRAFT. REPORT TO CHAIRMAN, SUBCOMMITTEE ON SPACE SCIENCE AND APPLICATIONS, COMMITTEE ON SCIENCE, SPACE AND TECHNOLOGY, HOUSE OF REPRESENTATIVES
Samuel W. Bowlin et al Apr. 1989 34 p
(GAO/IMTEC-89-41; B-234056) Avail: NTIS HC A03/MF A01; also available from GAO, Gaithersburg, MD HC first five copies free, additional copies $2.00

NASA's plans to provide emergency backup communications support for earth orbiting spacecraft after the closing of four ground stations are examined. Backup support is needed when malfunctions in on-board systems occur and ground intervention is required. The number of spacecraft emergencies that have occurred over the past few years and the reliability of the space-based Tracking and Data Relay Satellite System (TDRSS) White Sands Ground Terminal are also investigated. Spacecraft project managers have expressed the view, based on their professional judgment, that the probability of loss or damage to spacecraft in an emergency, to small spacecraft missions in equatorial orbits, or to launches of expendable rockets would be extremely low, but no formal risk assessments on the ground station closings have been performed. There are no communications support plans for transmission of scientific data from NASA missions should the use of TDRSS be lost. The 11 to 23 earth orbiting spacecraft for which the Goddard Space Flight Center has been responsible have experienced 316 malfunctions that required emergency intervention, about 2.2 per spacecraft per year. Most of these resulted in little or no permanent damage to the spacecraft. White Sands has had numerous outages of the terminal that processes all TDRSS communications. During an outage, spacecraft that normally use TDRSS must rely on ground stations for all communications support. NASA is constructing a second TDRSS ground terminal that is to be opened in 1993. GAO recommends that risk analyses be performed, and support plans for launches of expendable vehicles and Small Explorer missions in equatorial orbits be developed before the four ground stations are closed. J.P.S.

N90-26216*# Jet Propulsion Lab., California Inst. of Tech., Pasadena.
A NOVEL MULTIRECEIVER COMMUNICATIONS SYSTEM CONFIGURATION BASED ON OPTIMAL ESTIMATION THEORY
R. Kumar 1 Feb. 1990 94 p Prepared in cooperation with California State Univ., Long Beach
(Contract NAS7-918)
(NASA-CR-186847; NAS 1.26:186847) Avail: NTIS HC A05/MF A01 CSCL 17B

A multireceiver configuration for the purpose of carrier arraying and/or signal arraying is presented. Such a problem arises for example, in the NASA Deep Space Network where the same data-modulated signal from a spacecraft is received by a number of geographically separated antennas and the data detection must be efficiently performed on the basis of the various received signals. The proposed configuration is arrived at by formulating the carrier and/or signal arraying problem as an optimal estimation problem. Two specific solutions are proposed. The first solution is to simultaneously and optimally estimate the various phase processes received at different receivers with coupled phase locked loops (PLLs) wherein the individual PLLs acquire and track their respective receivers' phase processes, but are aided by each other in an optimal manner. However, when the phase processes are relatively weakly correlated, and for the case of relatively high values of symbol energy-to-noise spectral density ratio, a novel configuration for combining the data modulated, loop-output signals is proposed. The scheme can be extended to the case of low symbol energy-to-noise case by performing the combining/detection process over a multisymbol period. Such a

configuration results in the minimization of the effective radio loss at the combiner output, and thus a maximization of energy per bit to noise-power spectral density ration is achieved. Author

N90-26217*# Jet Propulsion Lab., California Inst. of Tech., Pasadena.
THE TELECOMMUNICATIONS AND DATA ACQUISITION REPORT Progress Report, Jan. - Mar. 1990
E. C. Posner, ed. 15 May 1990 203 p
(Contract NAS7-918)
(NASA-CR-186852; JPL-TDA-PR-42-101; NAS 1.26:186852)
Avail: NTIS HC A10/MF A02 CSCL 17B

Archival reports on developments in programs managed by the JPL Office of Telecommunications and Data Acquisition (TDA) are provided. Topics covered include: DSN advanced systems (tracking and ground-based navigation; communications, space-craft-ground; and station control and system technology) and DSN systems implementation (capabilities for existing projects; capabilities for new projects; TDA program management and analysis; and Goldstone solar system radar). For individual titles, see N90-26218 through N90-26232.

N90-26218*# Jet Propulsion Lab., California Inst. of Tech., Pasadena. Tracking Systems and Applications Section.
GOLDSTONE INTRACOMPLEX CONNECTED ELEMENT INTERFEROMETRY
C. D. Edwards *In its* The Telecommunications and Data Acquisition Report 15 May 1990 p 1-12 (For primary document see N90-26217 20-32)
Avail: NTIS HC A10/MF A02 CSCL 17B

Interferometric observations of the radio source pair 3C 84 and OE 400 were made on the 21 km baseline between Deep Space Station (DSS) 13 and DSS 15 to explore the angular navigation potential of intracomplex connected element interferometry (CEI). The differential phase-delay observable formed from pairs of 3 minute scans exhibited a precision of 1 psec, while the actual scatter of the phase-delay residuals for eleven scans over the 90 minute observing session was about 10 psec, consistent with the expected few millimeter fluctuations in the wet tropospheric path delay. Fitting for the position of OE 400 relative to 3C 84 yielded an error ellipse with a semi-minor axis of 60 nrad. Given the short data arc in this experiment, the orthogonal direction in the plane of the sky is not well determined; however, a second baseline or a data arc spanning a larger fraction of the source mutual visibility window could provide simultaneous determination of both right ascension and declination. Examination of the phase-delay residuals supports the accuracy of the cycle ambiguity resolution. However, reliable phase ambiguity resolution will pose the most significant challenge to routine use of CEI for spacecraft tracking, particularly when the a priori spacecraft source position is not well known. Several approaches for ambiguity resolution are briefly outlined. Author

N90-26219*# Jet Propulsion Lab., California Inst. of Tech., Pasadena. Tracking Systems and Applications Section.
A REDUCED-DYNAMIC TECHNIQUE FOR PRECISE ORBIT DETERMINATION **c13**
S. C. Wu, T. P. Yunck, and C. L. Thornton *In its* The Telecommunications and Data Acquisition Report 15 May 1990 p 13-25 (For primary document see N90-26217 20-32)
Avail: NTIS HC A10/MF A02 CSCL 22A

Observations of the Global Positioning System (GPS) will enable a reduced-dynamic technique for achieving subdecimeter orbit determination of earth-orbiting satellites. With this technique, information on the transition between satellite states at different observing times is furnished by both a formal dynamic model and observed satellite positional change (which is inferred kinematically from continuous GPS carrier-phase data). The relative weighting of dynamic and kinematic information can be freely varied. Covariance studies show that in situations where observing geometry is poor and the dynamic model is good, the model dominates determination of the state transition; where the dynamic model is poor and the geometry strong, carrier phase governs the determination of the transition. When neither kinematic nor dynamic information is clearly superior, the reduced-dynamic combination of the two can substantially improve the orbit-determination solution. Guidelines are given here for selecting a near-optimal weighting for the reduced-dynamic solution, and sensitivity of solution accuracy to this weighting is examined. Author

N90-26220*# Jet Propulsion Lab., California Inst. of Tech., Pasadena. Navigation Systems Section.
INFORMATION CONTENT OF A SINGLE PASS OF PHASE-DELAY DATA FROM A SHORT BASELINE CONNECTED ELEMENT INTERFEROMETER
S. W. Thurman *In its* The Telecommunications and Data Acquisition Report 15 May 1990 p 26-38 (For primary document see N90-26217 20-32)
Avail: NTIS HC A10/MF A02 CSCL 17B

An analytic development of the information array obtained with a single tracking pass of phase-delay measurements made from a short baseline interferometer is presented. Phase-delay observations can be made with great precision from two antennas using a single, common distributed frequency standard, hence the name connected element. With the information array, closed-form expressions are developed for the error covariance in declination and right ascension. These equations serve as useful tools for analyzing the relative merits of candidate station locations for connected element interferometry (CEI). The navigation performance of a short baseline interferometer located at the Deep Space Network's (DSN's) Goldstone intracomplex is compared with that which is presently achievable using Very Long Baseline Interferometry (VLBI) over intercontinental baselines. The performance of an intracomplex pair of short baselines formed by three stations is also investigated, along with the use of a single baseline in conjunction with conventional two-way Doppler data. The phase-delay measurement accuracy and data rate used in the analysis are based on the expected performance of an experimental connected element system presently under construction at Goldstone. The results indicate that the VLBI system that will be used during the Galileo mission can determine the declination and right ascension of a distant spacecraft to an accuracy of 20 to 25 nrad, while the CEI triad system and the combination of CEI-Doppler system are both capable of 30 to 70 nrad performance. Author

N90-26221*# Jet Propulsion Lab., California Inst. of Tech., Pasadena. Navigation Systems Section.
APPLICATIONS OF DIFFERENT DESIGN METHODOLOGIES IN NAVIGATION SYSTEMS AND DEVELOPMENT AT JPL **c17**
S. W. Thurman *In its* The Telecommunications and Data Acquisition Report 15 May 1990 p 39-49 (For primary document see N90-26217 20-32)
Avail: NTIS HC A10/MF A02 CSCL 17G

The NASA/JPL deep space navigation system consists of a complex array of measurement systems, data processing systems, and support facilities, with components located both on the ground and on-board interplanetary spacecraft. From its beginings nearly 30 years ago, this system has steadily evolved and grown to meet the demands for ever-increasing navigation accuracy placed on it by a succession of unmanned planetary missions. Principal characteristics of this system are its capabilities and great complexity. Three examples in the design and development of interplanetary space navigation systems are examined in order to make a brief assessment of the usefulness of three basic design theories, known as normative, rational, and heuristic. Evaluation of the examples indicates that a heuristic approach, coupled with rational-based mathematical and computational analysis methods, is used most often in problems such as orbit determination strategy development and mission navigation system design, while normative methods have seen only limited use is such applications as the development of large software systems and in the design of certain operational navigation subsystems. Author

N90-26222*# Jet Propulsion Lab., California Inst. of Tech., Pasadena. Communications Systems Research Section.
INHOMOGENEOUS ELECTRIC FIELD EFFECTS IN A LINEAR RF QUADRUPLE TRAP **c33**
R. K. Melborne *In its* The Telecommunications and Data Acquisition Report 15 May 1990 p 51-60 (For primary document see N90-26217 20-32)
Avail: NTIS HC A10/MF A02 CSCL 09C

The exact potential corresponding to confining fields inside a linear rf quadrupole particle trap of finite length is presented. The analytic expressions for the trapping potential is derived by introducing a linear trap employing a relatively simple cylindrical geometry and solving Laplace's equation for the trap electrodes. The finite length of linear traps results in field distortion near the trap ends. An exact analytic determination of the fields is useful because the profile of the trapped ion cloud is highly dependent on the fields confining it. It is shown that near the ends of the trap, the effective potential arising from the rf fields acts to propel particles out of the trap, and further, that the addition of a dc bias generates an inhomogeneous in the trap that influences the particles both perpendicularly to and along the trap's long axis.
Author

N90-26223*# Jet Propulsion Lab., California Inst. of Tech., Pasadena. Communications Systems Research Section.
A STUDY OF THE INFLUENCE OF Hg(6(3)P2) POPULATION IN A LOW-PRESSURE DISCHARGE ON MERCURY ION EMISSION AT 194.2 nm **c72**
L. Maleki, B. J. Blasenheim, and G. R. Janik *In its* The Telecommunications and Data Acquisition Report 15 May 1990 p 61-72 (For primary document see N90-26217 20-32)
Avail: NTIS HC A10/MF A02 CSCL 20H

A low-pressure mercury-argon discharge, similar to the type existing in the mercury lamp for the trapped-ion standard, is probed with a new technique of laser spectroscopy to determine the influence of the Hg(6 3P(sub 2)) population on discharge emission. The discharge is excited with inductively coupled rf power. Variations in the intensity of emission lines in the discharge were examined as lambda = 546.1 nm light from a continuous wave (CW) laser excited the Hg(6 3P(sub 2)) to (7 3S (sub 1)) transition. The spectrum of the discharge viewed in the region of laser irradiation showed increased emission in lambda = 546.1, 435.8, 404.7, 253.7, and 194.2 nm lines. Other lines in Hg I exhibited a decrease in emission. When the discharge was viewed outside the region of laser irradiation, all lines exhibited an increased emission. Based on these results, it is concluded that the dominant mechanism for the excitation of higher lying levels of mercury is the the electron-impact excitation via the 3P(sub 2) level. The depopulation of this metastable is also responsible for the observed increase in the electron temperature when the laser irradiates the discharge. It is also concluded that the 3P(sub 2) metastable level of mercury does not play a significant role in the excitation of the 3P(sub 1/2) level of mercury ion.
Author

N90-26224*# Jet Propulsion Lab., California Inst. of Tech., Pasadena. Guidance and Control Section.
APPLICATION OF INERTIAL INSTRUMENTS FOR DSN ANTENNA POINTING AND TRACKING **c35**
D. B. Eldred, N. M. Nerheim, and K. G. Holmes *In its* The Telecommunications and Data Acquisition Report 15 May 1990 p 73-98 (For primary document see N90-26217 20-32)
Avail: NTIS HC A10/MF A02 CSCL 14B

The feasibility of using inertial instruments to determine the pointing attitude of the NASA Deep Space Network antennas is examined. The objective is to obtain 1 mdeg pointing knowledge in both blind pointing and tracking modes to facilitate operation of the Deep Space Network 70 m antennas at 32 GHz. A measurement system employing accelerometers, an inclinometer, and optical gyroscopes is proposed. The initial pointing attitude is established by determining the direction of the local gravity vector using the accelerometers and the inclinometer, and the Earth's spin axis using the gyroscopes. Pointing during long-term tracking is maintained by integrating the gyroscope rates and augmenting these measurements with knowledge of the local gravity vector. A minimum-variance estimator is used to combine measurements to obtain the antenna pointing attitude. A key feature of the algorithm is its ability to recalibrate accelerometer parameters during operation. A survey of available inertial instrument technologies is also given.
Author

N90-26225*# Jet Propulsion Lab., California Inst. of Tech., Pasadena. Ground Antenna and Facilities Engineering Section.
DESIGN AND PERFORMANCE ANALYSIS OF THE DSS-13 BEAM WAVEGUIDE ANTENNA
T. Veruttipong, W. Imbriale, and D. Bathker *In its* The Telecommunications and Data Acquisition Report 15 May 1990 p 99-113 (For primary document see N90-26217 20-32)
Avail: NTIS HC A10/MF A02 CSCL 17B

A new 34 m research and development antenna is currently being constructed prior to introducing beam waveguide (BWG) antennas and Ka-band (32 GHz) frequencies into the NASA/JPL Deep Space Network. The new 34 m antenna, fed with either a center or bypass BWG, will lose less than 0.2 dB (excluding surface root mean square and mirror misalignment losses), as compared with a standard-fed Cassegrain antenna a X- (8.4 GHz) and Ka-bands. The antenna is currently under construction and is scheduled to be completed July 1990. Phase 1 of the project is for independent X- and Ka-band receive-only tests. Phase 2 of the project is for simultaneous S- (2.3 GHz) and X-band or X- and Ka-band operation, and the design is currently under way.
Author

N90-26226*# Jet Propulsion Lab., California Inst. of Tech., Pasadena. Communications Systems Research Section.
A TWO-TELESCOPE RECEIVER DESIGN FOR DEEP SPACE OPTICAL COMMUNICATIONS **c74**
K. Shaik *In its* The Telecommunications and Data Acquisition Report 15 May 1990 p 114-120 (For primary document see N90-26217 20-32)
Avail: NTIS HC A10/MF A02 CSCL 20F

A two-telescope system for a deep space optical communication receiver is proposed. To substantially improve the overall receiver efficiency, the design reserves the large telescope for signal-detection purposes only. A small diffraction-limited telescope is introduced to accomplish the task of navigational tracking.
Author

N90-26227*# Jet Propulsion Lab., California Inst. of Tech., Pasadena. Tracking Systems and Applications Section.
PRELIMINARY ERROR BUDGET FOR AN OPTICAL RANGING SYSTEM: RANGE, RANGE RATE, AND DIFFERENCED RANGE OBSERVABLES **c74**
W. M. Folkner and M. H. Finger *In its* The Telecommunications and Data Acquisition Report 15 May 1990 p 121-135 (For primary document see N90-26217 20-32)
Avail: NTIS HC A10/MF A02 CSCL 20F

Future missions to the outer solar system or human exploration of Mars may use telemetry systems based on optical rather than radio transmitters. Pulsed laser transmission can be used to deliver telemetry rates of about 100 kbits/sec with an efficiency of several bits for each detected photon. Navigational observables that can be derived from timing pulsed laser signals are discussed. Error budgets are presented based on nominal ground stations and spacecraft-transceiver designs. Assuming a pulsed optical uplink signal, two-way range accuracy may approach the few centimeter level imposed by the troposphere uncertainty. Angular information can be achieved from differenced one-way range using two ground stations with the accuracy limited by the length of the available baseline and by clock synchronization and troposphere errors. A method of synchronizing the ground station clocks using optical ranging measurements is presented. This could allow differenced range accuracy to reach the few centimeter troposphere limit.
Author

N90-26228*# Jet Propulsion Lab., California Inst. of Tech., Pasadena. Communications Systems Research Section.
INITIAL RESULTS ON FAULT DIAGNOSIS OF DSN ANTENNA CONTROL ASSEMBLIES USING PATTERN RECOGNITION TECHNIQUES **c37**
P. Smyth and J. Mellstrom *In its* The Telecommunications and Data Acquisition Report 15 May 1990 p 136-151 (For primary document see N90-26217 20-32)
Avail: NTIS HC A10/MF A02 CSCL 13I

Initial results obtained from an investigation using pattern recognition techniques for identifying fault modes in the Deep Space Network (DSN) 70 m antenna control loops are described. The overall background to the problem is described, the motivation and potential benefits of this approach are outlined. In particular, an experiment is described in which fault modes were introduced into a state-space simulation of the antenna control loops. By training a multilayer feed-forward neural network on the simulated sensor output, classification rates of over 95 percent were achieved with a false alarm rate of zero on unseen tests data. It concludes that although the neural classifier has certain practical limitations at present, it also has considerable potential for problems of this nature. Author

N90-26229*# Jet Propulsion Lab., California Inst. of Tech., Pasadena. Ground Antenna and Facilities Engineering Section.
DSS 15, 45, AND 65 34-METER HIGH EFFICIENCY ANTENNA RADIO FREQUENCY PERFORMANCE ENHANCEMENT BY TILT ADDED TO THE SUBREFLECTOR DURING ELEVATION ANGLE CHANGES
M. S. Katow (Planning Research Corp., McLean, VA.) *In its* The Telecommunications and Data Acquisition Report 15 May 1990 p 152-163 (For primary document see N90-26217 20-32)
Avail: NTIS HC A10/MF A02 CSCL 20N

The focusing adjustments of the subreflectors of an az-el Cassegrainian antenna that uses only linear motions have always ended in lateral offsets of the phase centers at the subreflector's focus points at focused positions, which have resulted in small gain losses. How lateral offsets at the two focus points were eliminated by tilting the subreflector, resulting in higher radio frequency (RF) efficiencies at all elevation angles rotated from the rigging angles are described. Author

N90-26230*# Jet Propulsion Lab., California Inst. of Tech., Pasadena. Telecommunications Systems Section.
QPSK LOOP LOCK DETECTION IN THE ADVANCED RECEIVER
A. Mileant and S. Hinedi *In its* The Telecommunications and Data Acquisition Report 15 May 1990 p 164-178 (For primary document see N90-26217 20-32)
Avail: NTIS HC A10/MF A02 CSCL 20N

The Advanced Receiver (ARX 2) currently being developed uses a Costas crossover loop to acquire and track the phase of an incoming quadrature phase-shift-keyed (QPSK) signal. The performance is described for the QPSK lock detector to be implemented, taking into account the phase jitter in the tracking loop. Simulations are used to verify the results of the analysis. Author

N90-26231*# Jet Propulsion Lab., California Inst. of Tech., Pasadena. Software Product Assurance Section.
LONG-RANGE PLANNING COST MODEL FOR SUPPORT OF FUTURE SPACE MISSIONS BY THE DEEP SPACE NETWORK **c83**
J. S. Sherif, D. S. Remer (Harvey Mudd Coll., Claremont, CA.), and H. R. Buchanan *In its* The Telecommunications and Data Acquisition Report 15 May 1990 p 179-190 (For primary document see N90-26217 20-32)
Avail: NTIS HC A10/MF A02 CSCL 05C

A simple model is suggested to do long-range planning cost estimates for Deep Space Network (DSP) support of future space missions. The model estimates total DSN preparation costs and the annual distribution of these costs for long-range budgetary planning. The cost model is based on actual DSN preparation costs from four space missions: Galileo, Voyager (Uranus), Voyager (Neptune), and Magellan. The model was tested against the four projects and gave cost estimates that range from 18 percent above the actual total preparation costs of the projects to 25 percent below. The model was also compared to two other independent projects: Viking and Mariner Jupiter/Saturn (MJS later became Voyager). The model gave cost estimates that range from 2 percent (for Viking) to 10 percent (for MJS) below the actual total preparation costs of these missions. Author

N90-26232*# Jet Propulsion Lab., California Inst. of Tech., Pasadena. Telecommunications Science and Engineering Div.
RINGS OF EARTH DETECTED BY ORBITAL DEBRIS RADAR **c90**
R. Goldstein and L. Randolph *In its* The Telecommunications and Data Acquisition Report 15 May 1990 p 191-195 (For primary document see N90-26217 20-32)
Avail: NTIS HC A10/MF A02 CSCL 03B

Small particles moving at an orbital velocity of 7.6 kilometers per second can present a considerable hazard to human activity in space. For astronauts outside of the protective shielding of their space vehicles, such particles can be lethal. The powerful radar at NASA's Goldstone Deep Communications Complex was used to monitor such orbital debris. This radar can detect metallic objects as small as 1.8 mm in diameter at 600 km altitude. The results of the preliminary survey show a flux (at 600 km altitude) of 6.4 objects per square kilometer per day of equivalent size of 1.8 mm or larger. Forty percent of the observed particles appear to be concentrated into two orbits. An orbital ring with the same inclination as the radar (35.1 degrees) is suggested. However, an orbital band with a much higher inclination (66 degrees) is also a possibility. Author

N90-26233*# Arizona State Univ., Tempe. Telecommunications Research Center.
SCATTERING FROM COATED STRUCTURES AND ANTENNA PATTERN CONTROL USING IMPEDANCE SURFACES, PART A/B Semiannual Progress Report, 1 Feb. - 31 Jul. 1990
Constantine A. Balanis, Lesley A. Polka, and Kefeng Liu 1990 60 p
(Grant NAG1-562)
(NASA-CR-186871; NAS 1.26:186871) Avail: NTIS HC A04/MF A01 CSCL 20N

The scattering from coated, conducting structures, specifically the coated dihedral corner reflector configuration and the coated strip/plate configuration is examined. The formulation uses impedance-wedge Uniform Theory of Diffraction scattering coefficients to calculate the diffracted fields. A finite-thickness coating is approximated using the impedance boundary condition to arrive at an equivalent impedance for the coating. The formulation of the impedance wedge coefficients is outlined. Far-field, perfectly conducting approximations are discussed. Problems with the present dihedral corner reflector model for certain angles of incidence and observation are discussed along with a potentially rectifying modification. Also, the capacity to measure the electromagnetic properties of lossy materials was developed. The effects of using multiple material coatings on the radiation pattern of the horn antenna were studied. Numerous computations were devoted toward the inverse problem of synthesizing desired radiation patterns using the impedance surfaces. Stabilizing the equivalent sheet impedance using the linear control condition was attempted, and it was found to be a very difficult task. Author

N90-26234*# New York Univ., New York. Dept. of Applied Science.
FIGURE OF MERIT STUDIES OF BEAM POWER CONCEPTS FOR ADVANCED SPACE EXPLORATION
Gabriel Miller and Murali N. Kadiramangalam 1990 52 p
(Grant NAG3-1048)
(NASA-CR-186720; NAS 1.26:186720) Avail: NTIS HC A04/MF A01 CSCL 20N

Surface to surface, millimeter wavelength beam power systems for power transmission on the lunar base were investigated. Qualitative/quantitative analyses and technology assessment of 35, 110 and 140 GHz beam power systems were conducted. System characteristics including mass, stowage volume, cost and efficiency as a function of range and power level were calculated. A simple figure of merit analysis indicates that the 35 GHz system would be the preferred choice for lunar base applications, followed closely by the 110 GHz system. System parameters of a 35 GHz beam power system appropriate for power transmission on a recent lunar base concept studied by NASA-Johnson and the necessary deployment sequence are suggested. Author

N90-26235*# Chicago Univ., IL. Dept. of Electrical Engineering and Computer Science.
THEORY OF CIRCULAR DIELECTRIC WAVEGUIDE WITH ANISOTROPIC SHEET COVER M.S. Thesis
Jerome Thomas Kish 1990 46 p
(Grant NAG2-544)
(NASA-CR-186883; NAS 1.26:186883) Avail: NTIS HC A03/MF A01 CSCL 20N

A circular dielectric waveguide consisting of an isotropic core covered with a thin anisotropic sheet is considered. The sheet is represented as a jump immittance and Maxwell's equations are applied. Solution of the boundary value problem yields the characteristic equation, or dispersion relation, which is then solved numerically. The results are verified for the step-index fiber and circular, metallic waveguides. Finally, examples are included to investigate the effects of the anisotropic sheet. Author

N90-26236# Technische Univ., Berlin (Germany, F.R.). Fachbereich Physik.
VALIDITY DOMAIN OF THE SCALAR KIRCHHOFF AND RAYLEIGH-SOMMERFELD DIFFRACTION THEORIES IN THE NEAR FIELD OF SMALL PHASE OBJECTS: COMPARISON BETWEEN CALCULATION MODELS AND MICROWAVE MEASURE Ph.D. Thesis [GUELTIKEITSBEREICH DER SKALAREN BEUGUNGSTHEORIEN NACH KIRCHHOFF UND RAYLEIGH-SOMMERFELD IM NAHFELD KLEINER PHASENOBJEKTE: VERGLEICH VON MODELLRECHNUNGEN MIT MIKROWELLENMESSUNGEN]
Michael Totzeck 1989 172 p In GERMAN Sponsored by DFG
(ETN-90-96963) Avail: NTIS HC A08/MF A01

Phase and amplitude of the diffraction near fields of dielectric stripe objects with rectangular cross section were measured simultaneously and with high spatial resolution using a modified Mach-Zehnder interferometer for 3 cm microwaves. The measured diffraction fields were well approximated two-dimensionally and agree well with moment method calculations. The approximate calculations following Kirchhoff and Rayleigh-Sommerfeld show clear differences in the diffraction fields. The agreement with the measurements depends on the object dimensions. The differences between the diffraction theories are especially determined by the highest local frequencies which can still propagate. ESA

N90-26237# Stuttgart Univ. (Germany, F.R.). Inst. fuer Navigation.
TRACKING PERFORMANCE OF A COMBINED COSTAS/AFC-LOOP UNDER NOISY RAYLEIGH/RICIAN CHANNEL CONDITIONS WITH ADDITIVE GAUSSIAN NOISE JAMMING Ph.D. Thesis [TRACKINGVERHALTEN EINER ZUSAMMENGESETZTEN COSTAS/AFC-REGELSCHLEIFE UNTER RAYLEIGH/RICE'SCHEN KANALBEDINGUNGEN MIT ADDITIVER GAUSSSCHER RAUSCHSTOERUNG]
Achim Kleine 1988 170 p In GERMAN
(ETN-90-96964) Avail: NTIS HC A08/MF A01

Models were developed to investigate the tracking behavior of combined Costas/AFC (Automatic Frequency Control) feedback loops under Rayleigh/Rician fading conditions with additive Gaussian noise jamming. A general linearized tracking model was developed for land-mobile channels. The model can be used for the nonlinearized case with sinusoidal phase detection characteristic using a standard solution of the Fokker-Planck equation. A tracking analysis for Costas/AFC loops with coherent automatic gain control, and an accuracy analysis for interferometers equipped with Costas/AFC loops are treated as examples. The tracking model is the most inaccurate in the case of quasistationary channels. ESA

N90-26238# National Aerospace Lab., Amsterdam (Netherlands). Flight Div.
MOBILE SATELLITE COMMUNICATIONS FOR CIVIL AVIATION
T. H. M. Hagenberg 3 Nov. 1988 25 p Presented at Symposium on Future Navigation, Communication, and Surveillance Systems, Schiphol, Netherlands, 1 Dec. 1988
(NLR-MP-88066-U; ETN-90-97192) Avail: NTIS HC A03/MF A01

Both voice and data communication of high quality without the line-of-sight propagation restriction or poor reliability are needed. In order to overcome the present limitations, the application of satellite communication is considered. A satellite communication system architecture will be standardized in the near future. The foreseen satellite communication architecture for civil aviation is discussed. ESA

N90-26239# Technische Univ., Eindhoven (Netherlands). Faculty of Electrical Engineering.
IMPLEMENTATION OF AN ALGORITHM FOR TRAVELLING-WAVE-BASED DIRECTIONAL DETECTION
M. H. J. Bollen and G. A. P. Jacobs Jan. 1989 26 p
(EUT-89-E-214; ISBN-90-6144-214-1; ISSN-0167-9708; ETN-90-97198) Avail: NTIS HC A03/MF A01

Some concepts concerning the implementation of an algorithm for traveling-wave-based directional detection are given. Two new traveling-wave-based algorithms are proposed, supplementing the directional detection during non detectable situations. One algorithm concerns single-phase-reclosure. An integrated scheme for the fast protection of a double circuit line is proposed. Traveling-wave-based directional detection is part of that scheme. ESA

N90-26240# Technische Univ., Eindhoven (Netherlands). Telecommunication Div.
SOFTWARE SET-UP FOR DATA PROCESSING OF DEPOLARIZATION DUE TO RAIN AND ICE CRYSTALS IN THE OLYMPUS PROJECT
M. M. J. L. vandeKamp Apr. 1989 91 p
(EUT-89-E-218; ISBN-90-6144-218-4; ISSN-0167-9708; ETN-90-97202) Avail: NTIS HC A05/MF A01

In the Olympus project, measurements are performed concerning scintillation, attenuation and depolarization on a satellite to Earth path in the 10 to 30 GHz range. An advance investigation is made for the processing of the measurement results concerning depolarization due to rain and ice crystals. For the case of rain, different existing models for the relation between depolarization and attenuation are compared. A procedure is presented which tests the models using the measurement results. For the case of ice crystals, several existing models for the depolarization are presented. They cannot be tested directly. A procedure is presented which derives the statistics of some characteristic parameters. A software setup is presented which encloses the mentioned procedures, as well as some other operations on the measurement results. ESA

N90-26241# Technische Univ., Eindhoven (Netherlands). Group Electromagnetism and Circuit Theory.
TRANSMISSION, REFLECTION, AND RADIATION AT JUNCTION PLANES OF DIFFERENT OPEN WAVEGUIDES Ph.D. Thesis
Helena Maria deRuiter 1989 254 p
(ISBN-90-9002864-1; ETN-90-97213) Avail: NTIS HC A12/MF A02

The quantitative analysis of the discontinuity in the electromagnetic properties, at the junction of different cylindrical

open waveguides, is performed. The propagation of electromagnetic waves along a uniform (infinite) waveguide section and the interaction of waves at the junction plane are described. Integral representations are derived for the fields in a finite open waveguide section in terms of the transverse fields in the boundary planes, and for the fields in a semi-infinite section in terms of the transverse field in the terminal plane and the transverse incident field propagating towards the terminal plane. Systems of integral equations are established for the fields in the junction plane(s) of two (three) series-connected open waveguide sections. One of these systems of integral equations was selected and solved numerically. The transmission at the junction plane is computed for the series-connection of two waveguide sections. ESA

N90-26242# Technische Univ., Delft (Netherlands).
ELECTROMAGNETIC INVERSE SCATTERING OF BURIED OBJECTS Ph.D. Thesis
Johannes Maria deLaat 1990 173 p
(ETN-90-97216) Avail: NTIS HC A08/MF A01

The issues for solving an inverse scattering problem are studied. The inverse scattering problem concerns the identification of obstacles in a configuration from their scattering properties. How to perform the identification, the scattering properties of obstacles and how to arrive from the former to the latter need to be known. The essence of identification in the inverse scattering problem is shown, and the contribution of philosophy to a solution is indicated. A mathematical model is introduced for the scattering object in terms of known expansion functions with unknown parameters, that are to be determined. Numerical results are presented for a two-dimensional problem, in which an electric current line source illuminates a buried arbitrary cylindrical object. For this configuration, two specific types of inverse problems are discussed. The first one is denoted as the localization problem, which concerns the determination of the location of an object with a known orientation and material constitution. The second problem consists of determining the material constitution of an object with a known position. ESA

N90-26243# Pennsylvania Univ., Philadelphia. Dept. of Electrical Engineering.
THE VARIABLY TRIMMED MEAN CFAR DETECTOR FOR NONHOMOGENEOUS BACKGROUND M.S. Thesis Final Technical Report, Jul. 1988 - May 1989
Inci Ozgunes Tonguz and Saleem Kassam Apr. 1990 71 p
(Contract F30602-88-D-0027; AF-AFOSR-0052-87; AF Proj. 4506)
(AD-A222801; RADC-TR-90-27) Avail: NTIS HC A04/MF A01 CSCL 17/9

This thesis investigates the performance of various constant false alarm rate (CFAR) detectors in both stationary noise conditions and nonideal conditions caused by multiple targets and nonuniform clutter. In particular, we introduce a new scheme for CFAR detection and called the Variably Trimmed Mean (VTM) CFAR detector. We show that this detector is a CFAR detector in exponentially distributed as well as in more general clutter distributions. A closed form analytical expression for the false alarm probability in exponentially distributed homogeneous clutter is given. We also show that in the exponentially distributed clutter situation, this detector can be designed to yield performance characteristics that are better than those of the Order Statistic and Trimmed Mean CFAR detectors. GRA

N90-26244# Texas Univ., Austin.
INTERACTION OF ELECTROMAGNETIC SIGNALS WITH PARTICULATE CLOUDS M.A. Thesis
Jose Mario Pauda May 1990 79 p Sponsored by AFIT, Wright-Patterson AFB, OH
(AD-A222804; AFIT/CI/CIA-90-030) Avail: NTIS HC A05/MF A01 CSCL 20/14

A particulate cloud affects the ability of an electronic detector to receive an electromagnetic signal in two ways: by scattering light from the sun into the detector, thereby masking the signal, and by attenuating the signal itself. These effects are well studied in the Mie theory, which is summarized. The effect of the particle distribution in the cloud and the shape of the cloud on scattering and absorption problems is then analyzed. The results of this analysis and of the Mie theory are incorporated into a computer program which is included in the appendix. The graphs generated with the program can be used (in conjunction with information about the sunlight intensity and the detector's discriminating ability) to determine the effect of scattered light on the detection of the signal. We conclude the attenuation of the signal plays a relatively minor role in the ability of a detector to receive a signal affected by a cloud of particles. GRA

N90-26245# Air Force Inst. of Tech., Wright-Patterson AFB, OH. School of Engineering.
DIRECT-SEQUENCE SPREAD SPECTRUM SYSTEM M.S. Thesis
James P. Stephens 1 Jun. 1990 166 p
(AD-A223021; AFIT/GE/ENG/90J-2) Avail: NTIS HC A08/MF A01 CSCL 25/2

The purpose of this study is to construct and evaluate the performance of a direct-sequence spread spectrum (DSSS) system. The system, based upon a previously published design, uses a special type of injection-locked oscillator called a synchronous oscillator for code synchronization. The DSSS system was constructed in a manner that provides a test-bed for demonstrating spread spectrum principles and allows researchers to evaluate their own sub-system design concepts. The DSSS system, designed as a one-way link in the 420 to 450 MHz band, is constructed to operate in accordance with Federal Communications Commission rules and regulations pertaining to the Amateur Radio Service (Part 97). Unlike conventional DSSS systems which combine digital data with a pseudorandom (PN) code sequence, the system described here directly modulates an FM modulated carrier with the PN code sequence. GRA

N90-26246# Wright Research Development Center, Wright-Patterson AFB, OH.
ELECTRONIC WARFARE TECHNOLOGY: TRENDS AND VISIONS
Kenneth Helberg, Tony White, Kevin Geiger, Joseph Koesters, and David Wilkes May 1990 14 p
(AD-A223034; WRDC-TR-90-1079) Avail: NTIS HC A03/MF A01 CSCL 17/4

The design, development of effective and affordable electronic warfare systems has become a difficult challenge which requires full exploitation of the most advanced technology. Recent history has demonstrated that cost, effectiveness and reliability factors have almost driven on-board self-protection electronic countermeasure (EC) systems to the edge of operational viability. The future must include aggressive and innovative use of new technology to produce penetration aids that are operationally useful and supportable. In the mean time, threat density and sophistication make the basic problem of finding, identifying, and countering all types of threat signals very difficult. The operational choices, as a result, have expanded to include smart jamming, support jamming in several different forms (stand-off, UAV), expendables (chaff, decoys) and a greater dependence on threat awareness and avoidance. These choices make it imperative to exploit technology to its fullest and in turn they provide an opportunity whereby technologies can be shown to impact the real capability needed operationally. As a result, trends of evolving technologies and visions of what they can mean for the future of electronic warfare are shaping present-day electronic warfare research. GRA

N90-26247# Axiomatix, Los Angeles, CA.
DYNAMIC JAMMING OF NETWORKS Final Report, 15 Apr. 1987 - 15 Apr. 1990
Andreas Polydoros, Gaylord K. Huth, and Unjeng Cheng 31 Mar. 1990 12 p
(Contract DAAL03-87-C-0007)
(AD-A223044; R9003-4; ARO-24649.10-EL-S) Avail: NTIS HC A03/MF A01 CSCL 17/4

The problem addressed in this report is the intelligent, topology-selective jamming of spread-spectrum networks. The key

goal has been to develop analytical and simulation tools which quantify the effect of jamming strategies upon the network operation, both at the link-access and the end-to-end layer. The purpose of these tools (called herein the AJ network analyzer) is to help study the tradeoffs between the jammers' strategies and choices, versus the corresponding choices of the communicators (users). An important feature of the analyzer is the modular incorporation of any jammer/user interaction at the physical (waveform) level within the analyzer framework, so that a variety of modulation/coding/spreading/jamming formats could be studied with regard to their impact upon the higher-layer performance measures. GRA

N90-26248# Axiomatix, Los Angeles, CA.
A NOVEL COMMUNICATION NETWORK SIMULATOR Interim Report
Unjeng Cheng 31 Mar. 1990 7 p
(Contract DAAL03-87-C-0007)
(AD-A223045; R9003-3; ARO-24649.9-EL-S) Avail: NTIS HC A02/MF A01 CSCL 25/2

This report presents the theoretical background of the Network Simulator, which is used for investigating the performance of communication networks under various jamming threats. To demonstrate the operation of a communication network under various jamming scenarios, we provide two spread-spectrum models: direct-sequence and frequency-hoping. The use of the spread-spectrum physical layer is to provide adequate anti-jamming capability. A salient feature of the Network Simulator is its capability to simulate the nonstationary jamming strategy. This is important because analytical models of nonstationary jamming do not exist. GRA

33 ELECTRONICS AND ELECTRICAL ENGINEERING

Includes test equipment and maintainability; components, e.g., tunnel diodes and transistors; microminiaturization; and integrated circuitry.

For related information see also *60 Computer Operations and Hardware* and *76 Solid-State Physics.*

N90-26249# Department of the Army, Washington, DC.
ACTIVE LAG ANGLE DEVICE Patent Application
Troy L. Hester, inventor (to Army) 2 Apr. 1990 7 p
(AD-D014538; US-Patent-Appl-SN-502968) Avail: NTIS HC A02/MF A01 CSCL 13/8

An active lag angular device is provided in which an electric torque motor is mounted and has a rotary shaft that is connected to a reference surface structure for rotating the reference surface structure about an axis of rotation that coincides with the axis of the rotator of the motor. The reference surface structure has pulleys mounted thereon so that an optical fiber can approach the active lag angle device at a guide pulley along an axis that coincides with the axis of the rotator shaft of the motor and be turned by the pulleys and directed along a substantially constant position relative to the reference surface structure. GRA

N90-26250*# National Aeronautics and Space Administration. Lewis Research Center, Cleveland, OH.
DESIGN OF AN OPTICALLY CONTROLLED Ka-BAND GaAs MMIC PHASED-ARRAY ANTENNA
Richard R. Kunath, Paul C. Claspy, Mark A. Richard (Case Western Reserve Univ., Cleveland, OH.), and Kul B. Bhasin 1990 9 p Presented at the Optoelectronics and Laser Applications in Science and Engineering, Los Angeles, CA, 14-19 Jan. 1990; sponsored by Society of Photo-Optical Instrumentation Engineers
(NASA-TM-103147; E-5500; NAS 1.15:103147) Avail: NTIS HC A02/MF A01 CSCL 09A

Phased array antennas long were investigated to support the agile, multibeam radiating apertures with rapid reconfigurability needs of radar and communications. With the development of the Monolithic Microwave Integrated Circuit (MMIC), phased array antennas having the stated characteristics are becoming realizable. However, at K-band frequencies (20 to 40 GHz) and higher, the problem of controlling the MMICs using conventional techniques either severely limits the array size or becomes insurmountable due to the close spacing of the radiating elements necessary to achieve the desired antenna performance. Investigations were made that indicate using fiber optics as a transmission line for control information for the MMICs provides a potential solution. By adding an optical interface circuit to pre-existing MMIC designs, it is possible to take advantage of the small size, lightweight, mechanical flexibility and RFI/EMI resistant characteristics of fiber optics to distribute MMIC control signals. The architecture, circuit development, testing and integration of optically controlled K-band MMIC phased array antennas are described. Author

N90-26251# Sandia National Labs., Albuquerque, NM.
THE DEVELOPMENT AND CHARACTERIZATION OF ION EXCHANGE MEMBRANES FOR SELECTED ELECTROCHEMICAL POWER SOURCES
C. Arnold, Jr. and R. A. Assink 1990 3 p Presented at the ICOM 1990: International Congress on Membranes and Membrane Processes, Chicago, IL, 20-24 Aug. 1990
(Contract DE-AC04-76DP-00789)
(DE90-009741; SAND-90-1139C; CONF-900892-1) Avail: NTIS HC A01/MF A01

The work is reviewed on the development and characterization of ion exchange membranes in an effort to improve the efficiency of three flowing electrolyte batteries. The batteries are: (1) NASA's iron chromium redox battery; (2) Lockheed's zinc ferricyanide battery; and (3) Johnson Control's zinc bromine battery. These batteries were developed for solar photovoltaic, utility load leveling, and electric vehicle applications, respectively. DOE

N90-26252# Ames Lab., IA.
SELECTIVE ELECTROCATALYSIS OF ANODIC OXYGEN-TRANSFER REACTIONS AT CHEMICALLY MODIFIED, THIN-FILM LEAD DIOXIDE ELECTRODES Ph.D. Thesis - Iowa State Univ. of Science and Technology
Hsiangpin Chang Jan. 1990 60 p
(Contract W-7405-eng-82)
(DE90-011747; IS-T-1437) Avail: NTIS HC A04/MF A01

The strategy to modify PbO2 electrodes for electrocatalysis of oxygen-transfer (O-t) reactions is to incorporate spatially separated catalytic sites into the PbO2 surface. The rate of OH radical formation is promoted at these sites, as is the rate of the O-t reaction, for the latter was demonstrated to be proportional to the former. Chemically modified PbO2 is electrodeposited by addition of Bi(3+), As(III), or Cl(-) to the Pb(2+) plating bath. The electrochemical stability and catalytic activity of the Bi-doped PbO2 (Bi-PbO2) increase with increased Bi/Pb atomic ratio in the mixed oxide which were determined with x ray photoelectron spectroscopy. Microcracked, ultra-thin films of Bi-PbO2 were found at Au, Pt, GC, and Ti electrodes after consecutive deposition and stripping of the thick oxide films. The surface of pure PbO2 can be modified by Bi(3+), As(V), and Cl(-) by electroadsorption. The adsorption method to modify PbO2 is fast and efficient for screening new catalysts. An O-t mediation mechanism was proposed for the electrocatalysis observed at the chemically modified PbO2. DOE

N90-26253# Technical Research Centre of Finland, Espoo. Metals Lab.
PVDF CONTACT PROBES
Jorma Pitkaenen Jun. 1989 29 p Sponsored by Nordisk Industrifond
(VTT-RR-623; ISBN-951-38-3492-1; ISSN-0358-5077; ETN-90-96988) Copyright Avail: NTIS HC A03/MF A01

Three types of contact probes are discussed. A focussing angle beam probe, a normal incidence probe and an acoustic emission probe are investigated. Characteristics of PVDF foils for probe design are dealt with. A probe design program is used to calculate two types of probes in order to determine the properties and behavior of the PVDF foils. Calculated and measured pulses and

frequency spectra are compared. The results agree well with the theoretical estimates. Deviations from the theoretical calculations and measurements are discussed. ESA

N90-26254*# Cornell Univ., Ithaca, NY. Dept. of Computer Science.
MTP: AN ATOMIC MULTICAST TRANSPORT PROTOCOL
Alan O. Freier and Keith Marzullo (Apple Computer, Cupertino, CA.) 30 Jul. 1990 27 p
(Contract NAG2-593; N00140-87-C-8904)
(NASA-CR-186716; NAS 1.26:186716; TR-90-1141) Avail: NTIS HC A03/MF A01 CSCL 09C

Multicast transport protocol (MTP); a reliable transport protocol that utilizes the multicast strategy of applicable lower layer network architectures is described. In addition to transporting data reliably and efficiently, MTP provides the client synchronization necessary for agreement on the receipt of data and the joining of the group of communicants. Author

N90-26255# Central Research Inst. of Electric Power Industry, Tokyo (Japan). Energy and Environment Lab.
STORAGE BATTERY OPERATION TECHNIQUE OF PHOTOVOLTAIC SYSTEM TO PREVENT THE IMBALANCE OF STATE OF CHARGE
Hirotake Kobayashi, Kiyoshi Takigawa, and Yukihiro Takeda 1990 37 p In JAPANESE; ENGLISH summary
(DE90-503032; CRIE-T-88057) Avail: NTIS (US Sales Only) HC A03/MF A01

For the large scale storage battery system of a MW class photovoltaic system, simulation analyses were conducted to prevent the imbalance of state of charge. Effects of the charge and discharge I-V characteristics dispersion of individual storage battery on the dispersion of state of charge were elucidated through these analyses. Furthermore, a proper operation method to prevent the imbalance of state of charge was investigated. In the internal resistance and the electromotive voltage which determines the charge and discharge I-V characteristics, when the dispersion is found in the electromotive voltage in particular, the dispersion of state of charge gets larger. The electromotive voltage of storage battery depends on the specific gravity of electrolyte. Consequently, in order to prevent the imbalance of state of charge, it is important to control the specific gravity. For operating the system effectively preventing the imbalance of state of charge, the specific gravity should be controlled within (+ or -) 0.3 percent of approximate mean value. DOE

N90-26256# Technische Univ., Eindhoven (Netherlands). Electromechanics and Power Electronics.
A MODEL OF THE SYNCHRONOUS MACHINE WITH RECTIFIER, ESPECIALLY FOR CONTROL PURPOSES
M. J. Hoeijmakers and J. M. Vleeshouwers Mar. 1989 116 p In DUTCH; ENGLISH summary
(EUT-89-E-215; ISBN-90-6144-215-X; ISSN-0167-9708; ETN-90-97199) Avail: NTIS HC A06/MF A01

A steady state model and a dynamic model of a synchronous machine with rectifier were derived, starting with the derivation of separate models of the synchronous machine and the rectifier. The dynamic model is a global, rather simple model in which very fast phenomena such as the ripple on the direct current, are neglected. An easy method for the estimation of the quadrature axis machine parameters was developed. A similar method for the direct axis parameters is not yet ready: it appears to be impossible, using the well known three winding model, to estimate parameters which satisfy both the transfer function from armature voltage to armature current and the transfer function from armature voltage to excitation current. A comparison between measured and simulated results shows that the (dynamic) model meets the requirements, except for the phenomena in the excitation winding. ESA

N90-26257# Technische Univ., Eindhoven (Netherlands). Electrical Energy Systems Group.
L-SWITCH: A PC PROGRAM FOR COMPUTING TRANSIENT VOLTAGES AND CURRENTS DURING SWITCHING OFF THREE-PHASE INDUCTANCES
V. K. I. Kalasek and W. M. C. VandenHeuvel Jun. 1989 85 p
(EUT-89-E-221; ISBN-90-6144-221-4; ISSN-0167-9708; ETN-90-97205) Avail: NTIS HC A05/MF A01

The FORTRAN 77 personal computer program L-SWITCH for studying transient voltages and currents during switching off three phase inductive circuits without reignitions, is described. When small inductive currents are interrupted by high voltage circuit breakers current chopping generally occurs and induces overvoltages. Different kinds of coupling between the phases (inductive, capacitive, combined or none) can be introduced for inductances with directly grounded neutral, inductively grounded neutral, and for inductances without grounded neutral. Full listing of the program is included and examples of program outputs are listed. Some graphical outputs are given. ESA

N90-26258# Technische Univ., Eindhoven (Netherlands). Electromechanics and Power Electronics.
A POSSIBILITY TO INCORPORATE SATURATION IN THE SIMPLE, GLOBAL MODEL OF A SYNCHRONOUS MACHINE WITH RECTIFIER
M. J. Hoeijmakers Sep. 1989 62 p
(EUT-89-E-225; ISBN-90-6144-225-7; ISSN-0167-9708; ETN-90-97208) Avail: NTIS HC A04/MF A01

In the global, rather simple model of the synchronous machine with rectifier previously developed, saturation phenomena were not taken into account. A possible way of extending the machine model with saturation is described. Starting with the derivation of the separate models of the synchronous machine and the rectifier, a steady state model and a dynamic model are derived. The dynamic model is a global model, in which very fast phenomena, such as the ripple on the direct current, are neglected. A FORTRAN77 subroutine for the computation of the synchronous machine with rectifier, and an ASCL program for the simulation of a wind-energy conversion system with a synchronous machine of 375 kVA, are given. ESA

N90-26259# Technische Univ., Eindhoven (Netherlands). Faculty of Electrical Engineering.
EXPERIMENTS ON INITIAL BEHAVIOUR OF CORONA GENERATED WITH ELECTRICAL PULSES SUPERIMPOSED ON DC BIAS
R. P. Dahiya, E. M. vanVeldhuizen, W. R. Rutgers, and L. H. T. Rietjens Oct. 1989 69 p Sponsored by Keuring van Electrotechnische Materialen N.V., Arnhem, Netherlands
(EUT-89-E-226; ISBN-90-6144-226-5; ISSN-0167-9708; ETN-90-97209) Avail: NTIS HC A04/MF A01

The pulsed positive corona discharges in air at atmospheric pressure were investigated to delineate the initial behavior of corona discharges generated by fast electrical pulses. The initial development of a pulsed negative corona in a cylindrical configuration was experimentally investigated by analyzing the optical signal emitted from it. Detailed observations are given. The measurement of the time dependence of the optical emission is concluded to be a good way of determining the behavior of pulsed corona discharges under different conditions. It shows clearly the different regimes in which the discharge operates for different parameters such as the DC bias, the peak voltage and rise time of the electric pulse. This can be of great help in working out the optimum parameters for practical applications. ESA

N90-26260# Technische Univ., Eindhoven (Netherlands).
ON TRAVELLING-WAVE-BASED PROTECTION OF HIGH-VOLTAGE NETWORKS Ph.D. Thesis
Mathias Henricus Joh Bollen 1989 140 p
(ISBN-90-9002955-9; ETN-90-97214) Avail: NTIS HC A07/MF A01

An investigation into whether fast protection based on traveling wave principles is possible is presented. The development of

network models for the study of traveling-wave-based protection is performed. The testing of the proposed algorithms for traveling-wave-based protection is presented. Two new algorithms that do not need a communication link were developed. The first one is especially suited for double-circuit lines. The second one is especially suited for switch-on-to-fault detection. Proposals for the design and use of future relays are given. Suggestions for implementation in a relay are given for the three traveling-wave-based algorithms used in the protective scheme. ESA

N90-26261# Institut National Polytechnique, Grenoble (France). Techniques de l'Informatique, des Mathematiques, de la Microelectronique et de la Microscopie Quanti

CONTRIBUTION TO CMOS INTEGRATED CIRCUIT TESTS: STUDY OF THE STUCK-ON AND STUCK-OPEN FAULT TESTS Ph.D. Thesis [CONTRIBUTION AU TEST DES CIRCUITS INTEGRES CMOS: ETUDE DU TEST DES PANNES STUCK-ON ET STUCK-OPEN]

Francois Darlay 1989 169 p In FRENCH; ENGLISH summary Sponsored by EEC

(ETN-90-97256) Avail: NTIS HC A08/MF A01

The detection of transistor level faults, for CMOS technology is addressed. Stuck-on and stuck-open faults are considered. A stuck-on fault converts a logic circuit into a sequential one. The test of different kinds of logical networks is studied. Fan-Out Free (FOF), Non-Reconvergent Fan-Out (NRFO), and Reconvergent Fan-Out (RFO) networks are distinguished. The study of stuck-open faults in FOF and NRFO networks is concluded by the definition of test-sequences allowing the detection of all single and multiple stuck-open faults. For RFO networks, the test sequence invalidation phenomenon may appear and must be considered. A design for testability solution is proposed. The case of muiltiple stuck-on/stuck-open faults is treated. It is shown that the previously defined test sequences also detect these faults. The application of all the obtained results to the definition of a built-in test generator is presented. The comparison of the resultant generator with the existing ones shows a decrease of the number of test vectors. ESA

N90-26262# Technische Univ., Berlin (Germany, F.R.). Fachbereich Elektrotechnik.

SIMULATION OF THE ELECTRICAL AND THERMAL BEHAVIOR OF GAPLESS METAL OXIDE SURGE ARRESTERS UNDER AC-OPERATION CONDITION Ph.D. Thesis [SIMULATION DES ELEKTRISCHEN UND THERMISCHEN VERHALTENS VON FUNKENSTRECKENLOSEN METALLOAXID-ABLEITERN BEI BETRIEB AN WECHSELSPANNUNG]

Volker Hinrischen 1990 203 p In GERMAN; ENGLISH summary Sponsored by DFG

(ETN-90-97309) Avail: NTIS HC A10/MF A02

The simulation process presented is suitable for arresters used in outdoor applications made of a unilinear radially symmetrical column. Both the electrical and thermal behavior of the arrester are modeled by electrical ladder networks. Dynamic thermal behavior, axial distribution of voltage, electrical power and temperature dissipation along the arrester column are taken into account in the simulation process. The computer simulation is verified by cooling and heating tests of different arrester arrangements with a continuous operating voltage of about 150 kV and a rated voltage of 200 kV. Good agreement between calculations and experimental results is shown. ESA

N90-26263# California Univ., Irvine. Dept. of Electrical and Computer Engineering.

DOD-UNIVERSITY RESEARCH INSTRUMENTATION PROGRAM, FY 1986/FY 1987 Final Report, 15 Jul. 1986 - 30 Dec. 1989

Chen S. Tsai 9 Apr. 1990 7 p

(Grant AF-AFOSR-0210-86; AF Proj. 2917)

(AD-A222578; AFOSR-90-0565TR) Avail: NTIS HC A02/MF A01 CSCL 20/2

The objective of this DOD/AFOSR - University Research Instrumentation Program was to purchase and install a scanning electron microscope (SEM) system that is essential for examination and characterization of the detailed dimensions and structures of the integrated optic devices and modules that have been fabricated and explored. The SEM system acquired consists of the following major components: Model SR-50/A basic SEM system by Applied Beam, E-beam blanker unit, Model 5000-2 energy dispersive x ray (EDX) system, Laserwriter, Closed loop water cooling system for the diffusion pump of the SEM basic system. GRA

N90-26264# IBM Watson Research Center, Yorktown Heights, NY.

ROLE OF SURFACE PASSIVATION IN THE INTEGRATED PROCESSING OF MOS STRUCTURES

M. Offenberg, M. Lichr, S. R. Kasi, and G. W. Rubloff 1990 2 p

(AD-A222630) Avail: NTIS HC A01/MF A01 CSCL 09/1

In order to achieve low defect densities and process simplification, future ULSI manufacturing is expected to incorporate multichamber integrated vacuum processing equipment. This raises opportunities for new levels of contamination control, including microscopic reactive impurities as well as particles, but also introduces new questions about how to successfully integrate process steps such as preoxidation cleaning with thermal oxidation. In this paper we describe electrical properties of simple metal oxide semiconductors (MOS) capacitors prepared in a multichamber integrated ultrahigh vacuum (UHV) processing system with in situ analysis capabilities. This system has allowed us to integrate the surface preclean steps with the thermal oxidation process without air exposure between the two. In situ surface analysis has permitted characterization of the precleaned surface, particularly the concentration of oxide and carbon present after different precleaning treatments. GRA

N90-26265# Puerto Rico Univ., Rio Piedras. Dept. of Physics.

STRUCTURED ELECTRODE INTERFACES

L. Blum 1989 14 p Submitted for publication Sponsored in part by NSF

(Contract N00014-81-C-0776)

(AD-A222763; TR-39-ONR) Avail: NTIS HC A03/MF A01 CSCL 09/1

A general discussion of the structure of the charged interface when the surface is not smooth is presented. In particular, the effect of a structured electrode is presented. The electrochemical interface offers a particularly big challenge to the scientist: because it is such an important system, a lot of work has been done on it, and yet because of the intrinsic technical difficulties associated with non-extra high-vacuum surface physics, very little direct structural evidence is available for the active electrode. Optical spectroscopy-techniques such as Surface Enhanced Raman effects (SERS), Surface Infrared Spectroscopy (SIRS), and more recently, Second Harmonic Generation (SHG) are fine examples of diagnostics for structural changes (changes in bonding arrangements), but do not provide unequivocal structural information. The shifts and intensities of the spectral lives depend on local field as well as local structure. GRA

N90-26266# Naval Postgraduate School, Monterey, CA.

ON THE DESIGN AND ANALYSIS OF MULTIPLE-STORAGE ELEMENTS M.S. Thesis

David A. York Dec. 1989 108 p

(AD-A223095) Avail: NTIS HC A06/MF A01 CSCL 09/1

The primary contribution of this thesis is the development of a data storage latch that accepts, stores and provides four-valued logic signals. The latch is implemented in Complementary Metal Oxide Silicon and all logic levels are encoded as voltage. The latch storage state is determined by thresholding operations on its input, and the output is a logically restored replica of that (multiple-valued) input. Detailed analysis of an existing current-mode CMOS design is also presented in this study. A comparison between these devices reveals that the voltage-mode data latch provides less stable intermediate logic states, but

consumes significantly less static power. In addition, the voltage-mode CMOS design can be implemented with the same number of devices that are required for two binary D flip-flops. GRA

N90-26267# Air Force Academy, CO.
EVALUATION OF ROOM-TEMPERATURE CHLOROALUMINATE MOLTEN SALTS AS ELECTROLYTES FOR HIGH ENERGY DENSITY BATTERIES Final Report, Jun. 1988 - Apr. 1990
R. L. Vaughn Apr. 1990 33 p
(AD-A223097; FJSRL-TR-90-0001) Avail: NTIS HC A03/MF A01 CSCL 07/2

This report reviews past battery studies using room-temperature chloroaluminate electrolytes, pointing out problems experienced. The report then summarizes attempts to circumvent these problems. A cell is described that uses a sodium anode, a copper (II) chloride cathode, and room-temperature chloroaluminate electrolyte buffered to the neutral composition. Cells give an open circuit voltage greater than 2.75 volts and discharge near 1 milliAmperes per centimeters squared at voltages greater than 2 volts for more than 20 hours. Cell failure is attributed to the formation of a nonconductive coating on the sodium electrode. Suggestions for future studies are presented. While the room-temperature chloroaluminates appear suitable for high-voltage, low-current batteries, their physical properties may limit their potential for high energy density batteries. GRA

N90-26222*# Jet Propulsion Lab., California Inst. of Tech., Pasadena. Communications Systems Research Section.
INHOMOGENEOUS ELECTRIC FIELD EFFECTS IN A LINEAR RF QUADRUPLE TRAP
R. K. Melborne *In its* The Telecommunications and Data Acquisition Report 15 May 1990 p 51-60 (For primary document see N90-26217 20-32)
Avail: NTIS HC A10/MF A02 CSCL 09C

34 FLUID MECHANICS AND HEAT TRANSFER

Includes boundary layers; hydrodynamics; fluidics; mass transfer; and ablation cooling.

For related information see also *02 Aerodynamics* and *77 Thermodynamics and Statistical Physics.*

N90-26268# Wichita State Univ., KS. Inst. for Aviation Research.
NUMERICAL ANALYSIS OF THREE-DIMENSIONAL PARTICLE-LADEN FLOW EQUATIONS PhD. Thesis
Hoa V. Cao Feb. 1990 180 p
(IAR-90-2) Avail: NTIS HC A09/MF A01

A general numerical method for solving the full 3-D dusty gas viscous flow equations was developed. The dusty gas equations are numerically integrated forward in time by using the time-dependent MacCormack explicit predictor-corrector scheme. The numerical method was validated by computing the pure gas flowfield around a sphere at supersonic flow conditions and comparing these with existing experimental data and other numerical method solutions. Very good agreement is obtained. Two-phase flow results were calculated for a sphere for various combinations of freestream Mach numbers of 1.5 and 3, freestream loading ratios of 0.2 and 0.5, and particle radius of 1, 2, and 5 microns. In addition, flow solutions for a 3-D blunt body at angles of attack of 0, 5, and 10 degrees were also computed with a freestream Mach number of 1.5, a freestream loading ratios of 0.5 and a particle radius of 2 microns. Based on the present results, the following trends were identified: (1) the shock standoff distance is found to decrease and the stagnation properties are found to increase with increasing freestream loading ration and with decreasing particle radius; (2) the gas phase flowfield properties are only slightly different from that of a pure gas flowfield for a flow with a particle radius of 5 microns; and (3) the differences between pure gas and gas-particle flow results decrease with increasing freestream Mach number. Author

N90-26269*# Texas Univ., Austin. Dept. of Mechanical Engineering.
AN INVESTIGATION INTO THE NUMERICAL PREDICTION OF BOUNDARY LAYER TRANSITION USING THE K.Y. CHIEN TURBULENCE MODEL Final Report
Craig A. Stephens and Michael E. Crawford Jun. 1990 192 p
(Grant NAG3-864)
(NASA-CR-185252; NAS 1.26:185252; Rept-89-3) Avail: NTIS HC A09/MF A01 CSCL 20D

Assessments were made of the simulation capabilities of transition models developed at the University of Minnesota, as applied to the Launder-Sharma and Lam-Bremhorst two-equation turbulence models, and at The University of Texas at Austin, as applied to the K. Y. Chien two-equation turbulence model. A major shortcoming in the use of the basic K. Y. Chien turbulence model for low-Reynolds number flows was identified. The problem with the Chien model involved premature start of natural transition and a damped response as the simulation moved to fully turbulent flow at the end of transition. This is in contrast to the other two-equation turbulence models at comparable freestream turbulence conditions. The damping of the transition response of the Chien turbulence model leads to an inaccurate estimate of the start and end of transition for freestream turbulence levels greater than 1.0 percent and to difficulty in calculating proper model constants for the transition model. Author

N90-26270*# Institute for Computer Applications in Science and Engineering, Hampton, VA.
A CRITICAL EVALUATION OF TWO-EQUATION MODELS FOR NEAR WALL TURBULENCE Final Report
Charles G. Speziale, Ridha Abid, and E. Clay Anderson (National Aeronautics and Space Administration. Langley Research Center, Hampton, VA.) Jun. 1990 29 p Submitted for publication
(Contract NAS1-18605)
(NASA-CR-182068; ICASE-90-46; NAS 1.26:182068) Avail: NTIS HC A03/MF A01 CSCL 20D

A variety of two-equation turbulence models,including several versions of the K-epsilon model as well as the K-omega model, are analyzed critically for near wall turbulent flows from a theoretical and computational standpoint. It is shown that the K-epsilon model has two major problems associated with it: the lack of natural boundary conditions for the dissipation rate and the appearance of higher-order correlations in the balance of terms for the dissipation rate at the wall. In so far as the former problem is concerned, either physically inconsistent boundary conditions have been used or the boundary conditions for the dissipation rate have been tied to higher-order derivatives of the turbulent kinetic energy which leads to numerical stiffness. The K-omega model can alleviate these problems since the asymptotic behavior of omega is known in more detail and since its near wall balance involves only exact viscous terms. However, the modeled form of the omega equation that is used in the literature is incomplete-an exact viscous term is missing which causes the model to behave in an asymptotically inconsistent manner. By including this viscous term and by introducing new wall damping functions with improved asymptotic behavior, a new K-tau model (where tau is identical with 1/omega is turbulent time scale) is developed. It is demonstrated that this new model is computationally robust and yields improved predictions for turbulent boundary layers. Author

N90-26271*# Colorado State Univ., Fort Collins.
MEASUREMENT OF TERMS AND PARAMETERS IN TURBULENT MODELS Final Report
Virgil A. Sandborn Jun. 1989 134 p
(Contract NAS8-36354)
(NASA-CR-183993; NAS 1.26:183993) Avail: NTIS HC A07/MF A01 CSCL 20D

Experimental measurements of the mean and turbulent velocity field in a water flow, turn-around-duct is documented. The small

radius of curvature duct experiments were made over a range of Reynolds numbers (based on a duct height of 10 cm) from 70,000 to 500,000. For this particular channel, the flow is dominated by the inertia forces. Use of the local bulk velocity to non-dimensionalize the local velocity was found to limit Reynolds number effects to the regions very close to the wall. Only secondary effects on the flow field were observed when the inlet or exit boundary conditions were altered. The flow over the central two-thirds of the channel was two-dimensional. Mean tangetial and radial velocities, streamlines, pressure distributions, surface shear stress; tangential, radial and lateral turbulent velocities and the Reynolds turbulent shear values are tabulated in other reports. It is evident from the experimental study that a complex numerical modeling technique must be developed to predict the flow in the turn-around-duct. The model must be able to predict relaminarization along the inner-convex-wall. It must also allow for the major increase in turbulence produced by the outer-concave-wall. Author

N90-26272*# Sverdrup Technology, Inc., Brook Park, OH.
TRANSIENT CHARACTERISTICS OF A GROOVED WATER HEAT PIPE WITH VARIABLE HEAT LOAD Final Report
Jong Hoon Jang Jul. 1990 8 p Proposed for presentation at the 1990 Winter Annual Meeting of ASME, Dallas, TX, 25-30 Nov. 1990
(Contracts NAS3-24105; NAS3-25266)
(NASA-CR-185280; E-5668; NAS 1.26:185280) Avail: NTIS HC A02/MF A01 CSCL 20D

The transient characteristics of a grooved water heat pipe were studied by using variable heat load. First, the effects of the property variations of the working fluid with temperature were investigated by operating the water heat pipe at several different temperatures. The experimental results show that, even for the same heat input profile and heat pipe configuration, the heat pipe transports more heat at higher temperature within the tested temperature range. Adequate liquid return to the evaporator due to decreasing viscosity of the working fluid permits continuous vaporization of water without dry-out. Second, rewetting of the evaporator was studied after the evaporator had experienced dry-out. To rewet the evaporator, the elevation of the condenser end was the most effective way. Without elevating the condenser end, rewetting is not straight-forward even with power turned off unless the heat pipe is kept at isothermal condition for sufficiently long time. Author

N90-26273*# National Aeronautics and Space Administration. Lewis Research Center, Cleveland, OH.
LOW-GRAVITY FLUID PHYSICS: A PROGRAM OVERVIEW
Aug. 1990 39 p
(NASA-TM-103215; E-5626; NAS 1.15:103215) Avail: NTIS HC A03/MF A01 CSCL 20D

An overview is presented of the microgravity fluid physics program at Lewis Research Center. One of the main reasons for conducting low gravity research in fluid physics is to study phenomena such as surface tension, interfacial contact angles, and diffusion independent of such gravitationally induced effects as buoyant convection. Fluid physics is at the heart of many space-based technologies including power systems, thermal control systems, and life support systems. Fundamental understanding of fluid physics is a key ingredient to successful space systems design. In addition to describing ground-based and space-based low-gravity facilities, selected experiments are presented which highlight Lewis work in fluid physics. These experiments can be categorized into five theme areas which summarize the work being conducted at Lewis for OSSA: (1) isothermal/iso-solutal capillary phenomena; (2) capillary phenomena with thermal/solutal gradients; (3) thermal-solutal convection; (4) first- and second-order phase transitions in a static fluid; and (5) multiphase flow. Author

N90-26274*# National Aeronautics and Space Administration. Ames Research Center, Moffett Field, CA.
NATURAL MELTING WITHIN A SPHERICAL SHELL
Parviz A. Bahrami Jun. 1990 23 p
(NASA-TM-102822; A-90153; NAS 1.15:102822) Avail: NTIS HC A03/MF A01 CSCL 20D

Fundamental heat transfer experiments were performed on the melting of a phase change medium in a spherical shell. Free expansion of the medium into a void space within the sphere was permitted. A step function temperature jump on the outer shell wall was imposed and the timewise evolution of the melting process and the position of the solid-liquid interface was photographically recorded. Numerical integration of the interface position data yielded information about the melted mass and the energy of melting. It was found that the rate of melting and the heat transfer were significantly affected by the movement of the solid medium to the base of the sphere due to gravity. The energy transfer associated with melting was substantially higher than that predicted by the conduction model. Furthermore, the radio of the measured values of sensible energy in the liquid melt to the energy of melting were nearly proportional to the Stefan number. The experimental results are in agreement with a theory set forth in an earlier paper. Author

N90-26275*# National Aeronautics and Space Administration. Lewis Research Center, Cleveland, OH.
COMPUTATIONAL EXPERIENCE WITH A THREE-DIMENSIONAL ROTARY ENGINE COMBUSTION MODEL
M. S. Raju (Sverdrup Technology, Inc., Brook Park, OH.) and E. A. Willis Apr. 1990 24 p Presented at the Joint Symposium on General Aviation Systems, Ocean City, NJ, 11-12 Apr. 1990; sponsored in part by AIAA and FAA
(Contract NAS3-25266)
(NASA-TM-103104; E-5249; NAS 1.15:103104) Avail: NTIS HC A03/MF A01 CSCL 20D

A new computer code was developed to analyze the chemically reactive flow and spray combustion processes occurring inside a stratified-charge rotary engine. Mathematical and numerical details of the new code were recently described by the present authors. The results are presented of limited, initial computational trials as a first step in a long-term assessment/validation process. The engine configuration studied was chosen to approximate existing rotary engine flow visualization and hot firing test rigs. Typical results include: (1) pressure and temperature histories, (2) torque generated by the nonuniform pressure distribution within the chamber, (3) energy release rates, and (4) various flow-related phenomena. These are discussed and compared with other predictions reported in the literature. The adequacy or need for improvement in the spray/combustion models and the need for incorporating an appropriate turbulence model are also discussed. Author

N90-26276*# National Aeronautics and Space Administration. Lewis Research Center, Cleveland, OH.
GALERKIN FINITE DIFFERENCE LAPLACIAN OPERATORS ON ISOLATED UNSTRUCTURED TRIANGULAR MESHES BY LINEAR COMBINATIONS
Kenneth J. Baumeister 1990 10 p Proposed for presentation at the 1990 Winter Annual Meeting of the ASME, Dallas, TX, 25-30 Nov. 1990
(NASA-TM-103209; E-5617; NAS 1.15:103209) Avail: NTIS HC A02/MF A01 CSCL 20D

The Galerkin weighted residual technique using linear triangular weight functions is employed to develop finite difference formulae in Cartesian coordinates for the Laplacian operator on isolated unstructured triangular grids. The weighted residual coefficients associated with the weak formulation of the Laplacian operator along with linear combinations of the residual equations are used to develop the algorithm. The algorithm was tested for a wide variety of unstructured meshes and found to give satisfactory results. Author

N90-26277# Naval Postgraduate School, Monterey, CA.
CODE ENHANCEMENTS AND VALIDATION OF GASP
Robert W. Walters, P. Cinnella, and D. C. Slack Mar. 1990

17 p Presented at the 8th National Aero-Space Plane Symposium, Monterey, CA, 26-30 Mar. 1990
(NPS-Paper-44) Avail: NTIS HC A03/MF A01

Enhancements to GASP and the validation test cases that were investigated to date are described. GASP is a computational fluid dynamics computer code that solves the integral form of the governing equations, which includes the full Reynolds-averaged Navier-Stokes (NS) equations, the Thin Layer NS equations, the Parabolized NS equations, and the Euler equations. GASP contains a generalized chemistry model and both equilibrium and non-equilibrium thermodynamics models for simulating a wide range of conditions. GASP is highly vectorized and contains a variety of time integration schemes for both steady-state and time-accurate calculations. Additional capabilities including boundary condition options, chemistry models incorporated, and memory management techniques are reviewed in outline format. Author

N90-26278*# National Aeronautics and Space Administration. Lewis Research Center, Cleveland, OH.
INITIAL EXPERIMENTATION ON THE NONVENTED FILL OF A 0.14m3 (5 FT. 3) DEWAR WITH NITROGEN AND HYDROGEN
David J. Chato, Matthew E. Moran, and Ted W. Nyland Jun. 1990 20 p Presented at the 5th Joint Thermophysics and Heat Transfer Conference, Seattle, WA, 18-20 Jun. 1990; sponsored in part by AIAA and ASME
(NASA-TM-103155; E-5517; NAS 1.15:103155; AIAA-90-1681) Avail: NTIS HC A03/MF A01 CSCL 20D

A series of nonvented fills were performed on a 0.14 cu m (5 cu ft) stainless steel dewar. Fills were conducted with a 120 deg cone angle spray nozzle over a range of inflow and initial wall temperatures with both liquid nitrogen and liquid hydrogen. Fill levels in excess of 85 percent liquid were achieved for four out of four nitrogen and two out of five hydrogen tests. Previously developed analytical models were compared to the test results and shown to have general trend agreement. Author

N90-26279*# National Aeronautics and Space Administration. Lewis Research Center, Cleveland, OH.
TWO-DIMENSIONAL MODEL OF A SPACE STATION FREEDOM THERMAL ENERGY STORAGE CANISTER
Thomas W. Kerslake and Mounir B. Ibrahim (Cleveland State Univ., OH.) Aug. 1990 11 p Presented at the 25th Intersociety Energy Conversion Engineering Conference, Reno, NV, 12-17 Aug. 1990; sponsored in part by AIChE, SAE, ACS, AIAA, ASME, and IEEE
(NASA-TM-103124; E-5474; NAS 1.15:103124) Avail: NTIS HC A03/MF A01 CSCL 20D

The Solar Dynamic Power Module being developed for Space Station Freedom uses a eutectic mixture of LiF-CaF2 phase change salt contained in toroidal canisters for thermal energy storage. Results are presented from heat transfer analyses of the phase change salt containment canister. A 2-D, axisymmetric finite difference computer program which models the canister walls, salt, void, and heat engine working fluid coolant was developed. Analyses included effects of conduction in canister walls and solid salt, conduction and free convection in liquid salt, conduction and radiation across salt vapor filled void regions and forced convection in the heat engine working fluid. Void shape, location, growth or shrinkage (due to density difference between the solid and liquid salt phases) were prescribed based on engineering judgement. The salt phase change process was modeled using the enthalpy method. Discussion of results focuses on the role of free-convection in the liquid salt on canister heat transfer performance. This role is shown to be important for interpreting the relationship between ground based canister performance (in l-g) and expected on-orbit performance (in micro-g). Attention is also focused on the influence of void heat transfer on canister wall temperature distributions. The large thermal resistance of void regions is shown to accentuate canister hot spots and temperature gradients. Author

N90-26280# Advisory Group for Aerospace Research and Development, Neuilly-Sur-Seine (France). Fluid Dynamics Panel.
REPORT OF THE FLUID DYNAMICS PANEL WORKING GROUP 10 ON CALCULATION OF 3D SEPARATE TURBULENT FLOWS IN BOUNDARY LAYER LIMIT
May 1990 145 p
(AGARD-AR-255; ISBN-92-835-0560-3) Copyright Avail: NTIS HC A07/MF A01; Non-NATO Nationals requests available only from AGARD/Scientific Publications Executive

The results of a study conducted by Working Group 10 of the AGARD Fluid Dynamics Panel to investigate the limits of boundary layer methods, both the integral and field type formulations, for calculating three-dimensional turbulent separated flow are presented. Test cases used to assess the boundary layer calculations included the DFLVR prolate spheroid at angle of attack and the NASA-Ames Wing C. Comparisons between boundary layer calculations and experimental data are presented for these test cases along with observation, conclusions, and recommendations. Author

N90-26281*# Old Dominion Univ., Norfolk, VA. Dept. of Mechanical Engineering and Mechanics.
ANALYSIS AND MITIGATION OF NUMERICAL DISSIPATION IN INVISCID AND VISCID COMPUTATION OF VORTEX-DOMINATED FLOWS Final Report, Feb. - Nov. 1988
Osama A. Kandil Aug. 1990 55 p
(Grant NAG1-846)
(NASA-CR-186887; NAS 1.26:186887) Avail: NTIS HC A04/MF A01 CSCL 20D

The conservative unsteady Euler equations for the flow relative motion in the moving frame of reference are used to solve for the steady and unsteady flows around sharp-edged delta wings. The resulting equations are solved by using an implicit approximately-factored finite volume scheme. Implicit second-order and explicit second- and fourth-order dissipations are added to the scheme. The boundary conditions are explicitly satisfied. The grid is generated by locally using a modified Joukowski transformation in cross flow planes at the grid chord stations. The computational applications cover a steady flow around a delta wing whose results serve as the initial conditions for the unsteady flow around a pitching delta wing about a large angle of attack. The steady results are compared with the experimental data and the periodic solution is achieved within the third cycle of oscillation. Author

N90-26282*# National Aeronautics and Space Administration. Lewis Research Center, Cleveland, OH.
CALCULATION OF 3D TURBULENT JETS IN CROSSFLOW WITH A MULTIGRID METHOD AND A SECOND-MOMENT CLOSURE MODEL
A. O. Demuren 1990 18 p Proposed for presentation at the International Symposium on Engineering Turbulence Modelling and Measurements, Dubrovnik, Yugoslavia, 24-28 Sep. 1990; sponsored by Assembly of World Conferences on Experimental Heat Transfer, Fluid Mechanics, and Ther
(NASA Order C-99066-G)
(NASA-TM-103159; ICOMP-90-15; E-5527; NAS 1.15:103159) Avail: NTIS HC A03/MF A01 CSCL 20D

A multigrid method is presented for calculating turbulent jets in crossflow. Fairly rapid convergence is obtained with the k-epsilon turbulence model, but computations with a full Reynolds stress turbulence model (RSM) are not yet very efficient. Grid dependency tests show that there are slight differences between results obtained on the two finest grid levels. Computations using the RSM are significantly different from those with k-epsilon model and compare better to experimental data. Some work is still required to improve the efficiency of the computations with the RSM. Author

N90-26283# Stuttgart Univ. (Germany, F.R.). Inst. fuer Raumfahrtsysteme.

A FULLY IMPLICIT ADI METHOD FOR QUASI THREE-DIMENSIONAL FLOWS THROUGH STRAIGHT BLADE ROWS Ph.D. Thesis [EIN VOLLIMPLIZITES ADI-VERFAHREN FUER QUASI-DREIDIMENSIONALE TURBULENTE STROEMUNGEN DURCH GERADE SCHAUFELREIHEN]

Ottmar Schaefer 1988 87 p In GERMAN

(ETN-90-96965) Avail: NTIS HC A05/MF A01

The stability and accuracy of an implicit method for the calculation of plane cascade flows were improved. It is shown that the stability of an implicit solving method can be maintained by the introduction of complete boundary conditions. The accuracy can be essentially improved by appropriate grids, a finite volume discretization, and a special treatment of singular points. Several examples are given. The maximum possible time step depends on the grid, and is limited by the factorization error of the ADI (Alternating Direction Implicit) method. The convergence rate of the method seems to depend on the smallest grid distance.

ESA

N90-26284# Loughborough Univ. of Technology (England). Dept. of Mathematical Sciences.

FRONTOGENESIS IN GRAVITY CURRENTS: AN EXAMPLE WITH NO KNOWN APPLICATIONS IN OCEANOGRAPHY

A. Kay Aug. 1989 21 p

(MATHS-Rept-A-117; ETN-90-97127) Avail: NTIS HC A03/MF A01

The formation of a front depends on the nonuniformity of the initial horizontal density gradient. This frontogenesis and the consequent changes to the flow are studied. The case of an initial quadratic density distribution is theoretically investigated. The solution is found as a power series in time. The steepening of the density gradient occurs at 0 (t to the 2nd power) and the resultant increases in horizontal shear and vertical flow occurring at 0 (t to the 3rd power). Nonlinear partial differential equations and boundary conditions are set up to describe the flow at times beyond that at which the power-series solution is accurate. ESA

N90-26285# National Aerospace Lab., Amsterdam (Netherlands). Informatics Div.

DEVELOPMENT OF A SYSTEM FOR THE NUMERICAL SIMULATION OF EULER FLOWS, WITH RESULTS OF PRELIMINARY 3-D PROPELLER-SLIPSTREAM/EXHAUST-JET CALCULATIONS Progress Report

J. W. Boerstoel 7 Jan. 1988 64 p Sponsored in cooperation with Aeritalia S.p.A., Naples, Italy and Fokker BV

(Contract NIVR-01604N)

(NLR-TR-88008-U; ETN-90-97183) Avail: NTIS HC A04/MF A01

The current status of a computer program system for the numerical simulation of Euler flows is presented. Preliminary test calculation results are shown. They concern the three-dimensional flow around a wing-nacelle-propeller-outlet configuration. The system is constructed to execute four major tasks: block decomposition of the flow domain around given, possibly complex, three-dimensional aerodynamic surfaces; grid generation on the blocked flow domain; Euler-flow simulation on the blocked grid; and graphical visualization of the computed flow on the blocked grid, and postprocessing. The system consists of about 20 codes interfaced by files. Most of the required tasks can be executed. The geometry of complex aerodynamic surfaces in three-dimensional space can be handled. The validation test showed that the system must be improved to increase the speed of the grid generation process. ESA

N90-26286# Technische Univ., Delft (Netherlands).

TRANSIENTS IN TURBULENT CONVECTIVE HEAT TRANSFER TO A FLOW OF SUPERCRITICAL HELIUM Ph.D. Thesis

Rob vanderLinden 1990 264 p Sponsored by Netherlands Technology Foundation

(ETN-90-97217) Avail: NTIS HC A12/MF A02

The features of a turbulent pipe flow with heat transfer from the wall under transient conditions are investigated. A two-dimensional flow model is developed with which the velocity profile and the fluid temperature in the tube can be described. Stationary heat transfer to a fully developed flow can also be described with a surface renewal model. This model is extended to be able to describe the transient heat transfer phenomena in case of an arbitrary varying wall temperature. Both models are validated using transient heat transfer measurements in a supercritical helium flow of Bloem. With the two-dimensional model the hydrodynamics of the transient flow can be investigated; for the velocity profile, the instantaneous velocity change is shown to be constant over the cross section of the tube. The two-dimensional model is shown to be a good tool for predicting both the hydrodynamics in and the heat transfer to a turbulent flow under transient conditions. An application of the model is computed.

ESA

N90-26287# Institut Franco-Allemand de Recherches, Saint-Louis (France).

ANALYSIS OF TURBULENT DENSITY FLUCTUATIONS BY MEANS OF SPONTANEOUS RAMAN DIFFUSION [ANALYSE DES FLUCTUATIONS TURBULENTES DE LA MASSE VOLUMIQUE AU MOYEN DE LA DIFFUSION RAMAN SPONTANEE]

L. Bobin and G. Brom 13 Mar. 1989 26 p In FRENCH

(Contract DRET-87-068)

(ISL-R-103/89; ETN-90-97023) Avail: NTIS HC A03/MF A01

The possibility of using the spontaneous Raman diffusion technique to measure mean local density in turbulent flow is addressed. Lasers required for the measurement of turbulent density fluctuations would need to be at least 100 times as powerful as those currently available. The frequency spectrum of turbulent density fluctuations are determined in the mixing region of a small open jet. The technique used involves the correlation of photons, which provides a self-correlation of the density. The average density thus derived, the quadratic average of the fluctuation, and the spectral power density are derived. This gives a statistical value for the density turbulence. ESA

N90-26288# Royal Aerospace Establishment, Farnborough (England).

COMPUTATIONAL FLUID DYNAMICS FOR MISSILES

J. Hodges 23 Nov. 1989 21 p Presented at RAeS One-Day Conference on Weapon Aerodynamics, 1 Dec. 1988

(RAE-TM-Aero-2171; BR112836; ETN-90-97064) Copyright Avail: NTIS HC A03/MF A01

A brief nonmathematical introduction to the subject of Computational Fluid Dynamics (CFD) is given. Various approximations to the full flow equations are described and their suitability for modeling the aerodynamics of missiles is discussed. A number of CFD codes available in the United Kingdom which are applicable to missile aerodynamics are considered. Each code is described briefly and comparisons between prediction and measurement are shown. ESA

N90-26289# Technische Univ., Delft (Netherlands). Faculty of Aerospace Engineering.

THE EFFECT OF A THREE-DIMENSIONAL SOURCE ON THE FLOW THROUGH A CHANNEL WITH SQUARE CROSS SECTION [HET EFFECT VAN EEN DRIE-DIMENSIONALE BRON OP STROMING DOOR EEN KANAAL MET VIERKANTE DWARSDOORSNEDE]

E. Dobbinga Jun. 1987 82 p In DUTCH

(LR-512; ETN-90-97159) Avail: NTIS HC A05/MF A01

The perturbation of the flow through a channel (wind tunnel) due to a suspension rod for the model or measuring instrument was investigated. The rod is relatively thin, and just behind the model, but the rod carrier is thicker. For the flow calculation this carrier was replaced by a semibody which is induced in a parallel flow by a concentrated three-dimensional flow. The calculation was performed for the case where the semibody is placed in a measuring location with closed walls and square cross section, as well as for the case where the source is placed in an infinitely

wide wind jet. The results show that the flow perturbation by the rod carrier in a measuring location with closed walls is in many cases substantially smaller than in the case of a wide jet. ESA

N90-26290# National Aerospace Lab., Amsterdam (Netherlands). Informatics Div.
INFORMATICS ASPECTS OF LARGE FLOW CALCULATIONS ON THE SX-2 SUPERCOMPUTER
A. Kassies 1 Jun. 1988 18 p In DUTCH; ENGLISH summary Presented at the NLR-WGS Symposium on Rekenen OP DE SX-2, 3 Jun. 1988 Sponsored by Netherlands Agency for Aerospace Engineering
(NLR-MP-88037-U; ETN-90-97187) Avail: NTIS HC A03/MF A01

The three-dimensional multiblock Euler code for arbitrary configurations, developed with a view to computer aided flow calculations for aircraft design, is described from an informatics point of view. A typical three-dimensional Euler calculations on a computational grid with 10 to the 6th power points takes about 10 to the 12th power floating point operations. The SX-2 supercomputer can complete this calculations in two hours, faster than other supercomputers. Furthermore the SX-2 has a very good FORTRAN compiler, but the operating system imposes that each file be allocated beforehand. The large extended memory allows three-dimensional Euler calculations on still finer grids as well as three-dimensional Navier-Stokes calculations. ESA

N90-26291# Alfa Romeo S.p.A., Naples (Italy).
COMPUTATIONAL FLUID DYNAMICS 3-D ANALYSIS FOR ADVANCED TRANSONIC TURBINE DESIGN
S. Colantuoni, A. Colella, and G. Santoriello 1989 28 p Presented at 15th European Rotorcraft Forum, Amsterdam, Netherlands, 12-15 Sep. 1989
(ETN-90-97282) Avail: NTIS HC A03/MF A01

An overview of the most significant applications of the computational fluid dynamics three-dimensional inviscid method to the analysis of an existing transonic turbine stage is presented. The comparison between numerical results and the first experimental detailed measurements are discussed. The flowfield in the exit plane, obtained by a laser anemometry system on a cold air turbine rig, is analyzed. ESA

N90-26292*# National Aeronautics and Space Administration. Pasadena Office, CA.
FLUID-LOOP REACTION SYSTEM Patent Application
T. C. Iskenderian, inventor (to NASA), B. J. Lurie, inventor (to NASA), and J. A. Schier, inventor (to NASA) (Jet Propulsion Lab., California Inst. of Tech., Pasadena.) 31 Jan. 1990 26 p
(Contract NAS7-918)
(NASA-Case-NPO-17204-1-CU; NAS 1.71:NPO-17204-1-CU; US-Patent-Appl-SN-473242) Avail: NTIS HC A03/MF A01 CSCL 20D

An improved fluid actuating system for imparting motion to a body such as a spacecraft is disclosed. The fluid actuating system consists of a fluid mass that may be controllably accelerated through at least one fluid path whereby an opposite acceleration is experienced by the spacecraft. For full control of the spacecraft's orientation, the system would include a plurality of fluid paths. The fluid paths may be circular or irregular, and the fluid paths may be located on the interior or exterior of the spacecraft. NASA

N90-26293# Ballistic Research Labs., Aberdeen Proving Ground, MD.
EFFECT OF INITIAL CONDITIONS ON THE DEVELOPMENT OF TWO-PHASE JETS Final Report, Jan. - Dec. 1989
Csaba K. Zoltani and Ali F. Bicen Apr. 1990 26 p
(DA Proj. 1L1-61102-AH-43)
(AD-A222621; BRL-TR-3100) Avail: NTIS HC A03/MF A01 CSCL 20/4

The results of an experimental investigation into the behavior of an unconfined, steady, fully turbulent, two-phase jet of diameter of 12.7 mm at the exit, with an exit flow velocity of 50 m/s and containing particles with a mass density of loading of 1.5 percent is described. The second phase consisted of glass beads 80 microns in diameter. Velocity profiles in a plane parallel to the exit of the jet at several downstream stations, as well as the rms values, turbulent intensity and velocity cross correlations were measured for both phases. The radial rms velocities of the particles, although similar to those of the fluid, were found to be surprisingly higher than for a jet of 25.4 mm in diameter with a lower exit velocity. Measurements of the particle velocities were extremely sensitive to changes in the upstream boundary conditions. GRA

N90-26294# Iowa Univ., Iowa City. Dept. of Mechanical Engineering.
THE FINITE ANALYTIC METHOD AND ITS APPLICATIONS. VOLUME 1: LAMINAR AND TURBULENT FLOWS PAST TWO-DIMENSIONAL AND AXISYMMETRIC BODIES Final Report
Ching-Jen Chen and Seok Ki Choi Mar. 1990 367 p
(Contract N00167-86-K-0019)
(AD-A222787; IIHR-334-I-Vol-1) Avail: NTIS HC A16/MF A02 CSCL 20/4

A numerical study of laminar and turbulent flows past two-dimensional bodies and axisymmetric bodies is presented. Numerical methods are developed to solve Navier-Stokes equations for two-dimensional and axisymmetric flows in the arbitrary geometries. The complex physical geometry is resolved by use of numerically generated, body-fitted coordinates. The governing equations are written in the transformed domain using the orthogonal velocity components as dependent variables for momentum equations. The governing equations are discretized using both the finite analytic method and the finite volume method. Both one velocity staggered grid method and two velocities staggered method are employed for grid arrangements. The velocity and pressure coupling techniques in these grid arrangements are presented. The solution procedure of the SIMPLER numerical algorithm is used with a parabolic marching technique and a global pressure calculation method. For turbulent flow calculations, both the k-epsilon turbulence model and the two-layer turbulence model are used. GRA

N90-26295# Naval Postgraduate School, Monterey, CA.
EFFECTS OF 2 Hz IMPOSED BULK FLOW UNSTEADINESS ON LAMINAR-TURBULENT TRANSITION IN A STRAIGHT CHANNEL M.S. Thesis
Francis J. Greco Dec. 1989 134 p
(AD-A223028) Avail: NTIS HC A07/MF A01 CSCL 20/4

Laminar/turbulent transition is studied in a straight channel with 2 Hz imposed bulk flow unsteadiness for Reynolds numbers of 1100 to 3800 and Strouhal numbers of 0.121 to 0.035. Channel aspect ratio is 40 to 1 with 1.27 cm height, 50.8 cm width and 4.27 m length. Observations, videos, and photographs of smoke patterns show different subcritical transition events including Tollmien-Schlichting waves, vortex-array type motion evidenced by smoke swirls, ribbon-like patterns, turbulent spots, and fully turbulent flow. Fluctuating intensity magnitudes relative to velocities from imposed unsteadiness are determined from phase-averaged velocity traces. With 2 Hz unsteadiness, transition events begin to occur at lower Reynolds numbers and extend over a wider range of Reynolds numbers compared to flows with no imposed unsteadiness. GRA

35 INSTRUMENTATION AND PHOTOGRAPHY

Includes remote sensors; measuring instruments and gages; detectors; cameras and photographic supplies; and holography.

For aerial photography see *43 Earth Resources and Remote Sensing.* For related information see also *06 Aircraft Instrumentation,* and *19 Spacecraft Instrumentation.*

N90-26296*# National Aeronautics and Space Administration. Langley Research Center, Hampton, VA.
VIDEO CAMERA SYSTEM FOR LOCATING BULLET HOLES IN TARGETS AT A BALLISTICS TUNNEL
A. W. Burner, D. R. Rummler, and W. K. Goad Washington Aug. 1990 18 p
(NASA-TM-4197; L-16772; NAS 1.15:4197) Avail: NTIS HC A03/MF A01 CSCL 14E

A system consisting of a single charge coupled device (CCD) video camera, computer controlled video digitizer, and software to automate the measurement was developed to measure the location of bullet holes in targets at the International Shooters Development Fund (ISDF)/NASA Ballistics Tunnel. The camera/digitizer system is a crucial component of a highly instrumented indoor 50 meter rifle range which is being constructed to support development of wind resistant, ultra match ammunition. The system was designed to take data rapidly (10 sec between shoots) and automatically with little operator intervention. The system description, measurement concept, and procedure are presented along with laboratory tests of repeatability and bias error. The long term (1 hour) repeatability of the system was found to be 4 microns (one standard deviation) at the target and the bias error was found to be less than 50 microns. An analysis of potential errors and a technique for calibration of the system are presented. Author

N90-26297# Department of the Army, Washington, DC.
MULTICOLOR INFRARED PHOTODETECTOR Patent Application
Kwong-Kit Choi, inventor (to Army) 2 Apr. 1990 21 p
(AD-D014511; US-Patent-Appl-SN-503015) Avail: NTIS HC A03/MF A01 CSCL 17/5

This patent application discloses a multicolor infrared detection device comprising a number of doped quantum well structural units. Each unit consists of a thick well and a thin well separated by a thin barrier. This agreement produces strong coupling. Infrared radiation incident on the device gives rise to intersubband absorption. For each transition of photosignal results which allows the detection of a plurality of incident frequencies. GRA

N90-26298# General Accounting Office, Washington, DC. National Security and International Affairs Div.
TECHNOLOGY DEVELOPMENT: FUTURE USE OF NASA'S LARGE FORMAT CAMERA IS UNCERTAIN
Charles F. Rey, Ilene H. Fliegel, and Karl A. Rohner Jun. 1990 30 p
(GAO/NSIAD-90-142; B-238709) Avail: NTIS HC A03/MF A01; also available from GAO, Gaithersburg, MD HC first five copies free, additional copies $2.00

The Large Format Camera, developed as a project to verify an engineering concept or design, has been flown only once, in 1984, on the shuttle Challenger. Since this flight, the camera has been in storage. NASA had expected that, following the camera's successful demonstration, other government agencies or private companies with special interests in photographic applications would absorb the costs for further flights using the Large Format Camera. But, because shuttle transportation costs for the Large Format Camera were estimated to be approximately $20 million (in 1987 dollars) per flight and the market for selling Large Format Camera products was limited, NASA was not successful in interesting other agencies or private companies in paying the costs. Using the camera on the space station does not appear to be a realistic alternative. Using the camera aboard NASA's Earth Resources Research (ER-2) aircraft may be feasible. Until the final disposition of the camera is decided, NASA has taken actions to protect it from environmental deterioration. The Government Accounting Office (GAO) recommends that the NASA Administrator should consider, first, using the camera on an aircraft such as the ER-2. NASA plans to solicit the private sector for expressions of interest in such use of the camera, at no cost to the government, and will be guided by the private sector response. Second, GAO recommends that if aircraft use is determined to be infeasible, NASA should consider transferring the camera to a museum, such as the National Air and Space Museum. J.P.S.

N90-26299*# National Aeronautics and Space Administration. Lewis Research Center, Cleveland, OH.
OPTICAL CHARACTERIZATION OF CLOUDS OF FINE LIQUID-NITROGEN PARTICLES
Robert D. Ingebo 1990 7 p Presented at the 21st Annual Meeting of the Fine Particle Society, San Diego, CA, 21-25 Aug. 1990
(NASA-TM-103208; E-5616; NAS 1.15:103208) Avail: NTIS HC A02/MF A01 CSCL 14B

Characteristic drop size, D sub 32, of clouds of fine liquid nitrogen particles was measured with a scattered light scanning instrument developed at NASA-Lewis. Calibration of the instrument was accomplished with suspensions of monosized polystyrene spheres and the scattered light scanner was then used to investigate the mechanism of liquid nitrogen jet disintegration in high velocity gas flow. The Sauter mean diameter, D sub 32, was found to vary inversely with nitrogen gas mass-flux raised to the 1.33 power. Values of D sub 32 varied from 5 to 25 microns and the mass-flux exponent 1.33 agrees well with theory for liquid jet breakup in high velocity gas flow. Loss of fine particles due to the high vaporization rate of liquid nitrogen was avoided by sampling the spray 1.3 cm downstream of the nozzle orifice. The presence of high velocity and thermal gradients in the gas phase also made sampling of the particles quite difficult. As a result, it was necessary to correct the measurements for background noise produced by both highly turbulent gas flow and thermally induced density gradients in the gas phase. Author

N90-26300# Lawrence Livermore National Lab., CA.
MULTIPLE TARGET TRACKING IN A WIDE-FIELD-OF-VIEW CAMERA SYSTEM
Hye-Sook Park, Timothy S. Axelrod, Nicholas J. Colella, Michael E. Colvin, and Arno G. Ledebuhr May 1990 8 p Presented at the Technical Symposia on Optical Engineering and Photonics in Aerospace Sensing, Orlando, FL, 16-20 Apr. 1990
(Contract W-7405-eng-48)
(DE90-013488; UCRL-101921; CONF-900451-4) Avail: NTIS HC A02/MF A01

A real-time-multiple-target-tracking system is being developed using a wide-field-of-view (WFOV) camera. The high resolution WFOV camera was conceived as part of the Strategic Defense Initiative Research at Lawrence Livermore National Laboratory. The camera system consists of a lens made of concentric solid blocks of index matching glasses, CCDs arrayed on the focal plane, and a custom VLSI image processor to extract the targets. This paper will briefly review the existing prototype system, the on-going effort to cover the full field of view using digital CCD cameras, the production of custom VLSI chips developed to extract centroids in real time, and the implementation of transputers to run the tracking algorithms. DOE

N90-26301# Rolls-Royce Ltd., Derby (England). Dept. of Vibration.
A NUMERICAL SIMULATION OF THE QUASI-HETERODYNE TECHNIQUE FOR DOUBLE-PULSED HOLOGRAPHIC VIBRATION MEASUREMENTS
V. B. McKee and R. J. Parker 25 Apr. 1989 13 p Presented at the SIRA Stress and Vibration Conference, London, England, 14 Mar. 1989 Submitted for publication
(PNR90622; VDM00109; ETN-90-97137) Copyright Avail: NTIS HC A03/MF A01

A portion of the work being carried out on the quasi-heterodyne

or fringe-shifting technique as applied to double-pulsed holographic vibration measurements is reported. The conventional result of double-pulsed vibration holograms is a set of fringes representing contours of equal displacement. The fringes can yield a full field measurement of the object's displaced shape in sufficient detail for theoretical model correlation. The quasi-heterodyne technique enables the fringes to be converted to numeric displacement data over the whole of the visible surface of an object. ESA

N90-26302# Rolls-Royce Ltd., Derby (England). Advanced Research Lab.
PRACTICAL DEVELOPMENTS IN HOLOGRAPHIC INTERFEROMETRY
R. J. Parker 10 May 1989 31 p Presented at the Royal Aeronautical Society Conference on Flow Visualization Using Laser Techniques, Coventry, England, 10 May 1989 Sponsored in part by Ministry of Defence Procurement Executive, London, England
(PNR90669; ETN-90-97153) Copyright Avail: NTIS HC A03/MF A01

Holography, as a very powerful tool for studying compressible flows is studied. It is a non-intrusive technique capable of both qualitative and quantitative assessment. A number of applications to both 2-D and 3-D flow fields are described including: real time flow visualization, flow in wind tunnels, rotating transonic flows, and fringe interpretation. ESA

N90-26303# Rolls-Royce Ltd., Derby (England). Advanced Research Lab.
HOLOGRAPHY AND HOLOGRAPHIC INTERFEROMETRY
R. J. Parker 27 Feb. 1989 33 p Presented at the Laser Workshop Course on Lasers and Optics in Engineering Meteorology, Colchester, England, 27 Feb. - 3 Mar. 1989 Sponsored in part by Ministry of Defence Procurement Executive, London, England
(PNR90670; ETN-90-97154) Copyright Avail: NTIS HC A03/MF A01

Applications of holography developed over the last twenty years are reviewed. These cover all the major fields within holographic interferometry: flow visualization, nondestructive testing, vibration analysis and holographic contouring. Of equal interest to the techniques themselves are the problems encountered and overcome in applying these techniques in a demanding, at times hostile, industrial environment away from the laboratory. The extensive use of high power pulsed lasers has greatly facilitated this move and allowed holography to be used routinely in normal component-test areas. ESA

N90-26304*# National Aeronautics and Space Administration. Marshall Space Flight Center, Huntsville, AL.
ROTATING-UNBALANCED-MASS DEVICES AND METHODS FOR SCANNING BALLOON-BORNE-EXPERIMENTS, FREE-FLYING SPACECRAFT, AND SPACE SHUTTLE/SPACE STATION ATTACHED EXPERIMENTS Patent Application
Michael E. Polites, inventor (to NASA) 23 May 1990 40 p
(NASA-Case-MFS-28425-1; NAS 1.71:MFS-28425-1; US-Patent-Appl-SN-527462) Avail: NTIS HC A03/MF A01 CSCL 14B

A method and apparatus for scanning balloon-borne experiments, free-flying spacecraft, or gimballed experiments mounted on a space shuttle or space station, makes use of one or more rotating unbalanced mass devices for selectively generating circular, line, or raster scan patterns for the experiment line of sight. An auxiliary control system may also be used in combination with the rotating unbalanced mass device, for target acquisition, keeping the scan centered on the target, or for producing complementary motion for raster scanning. The rotating unbalanced mass makes use of a mass associated with a drive shaft, such mass having a center of gravity which is displaced from the drive shaft rotation axis. The drive shaft is driven with a substantially constant angular velocity, thereby resulting in relatively low power requirements since no acceleration or deceleration of the mass is generally involved during steady state operations. The resulting centrifugal force of the rotating unbalanced mass is used to generate desired reaction forces on the experiment or spacecraft to create a desired scan pattern for the experiment line of sight. NASA

N90-26224*# Jet Propulsion Lab., California Inst. of Tech., Pasadena. Guidance and Control Section.
APPLICATION OF INERTIAL INSTRUMENTS FOR DSN ANTENNA POINTING AND TRACKING
D. B. Eldred, N. M. Nerheim, and K. G. Holmes *In its* The Telecommunications and Data Acquisition Report 15 May 1990 p 73-98 (For primary document see N90-26217 20-32)
Avail: NTIS HC A10/MF A02 CSCL 14B

N90-26746*# Jet Propulsion Lab., California Inst. of Tech., Pasadena.
HIGH RESOLUTION SPECTROSCOPY IN THE MICROWAVE AND FAR INFRARED
Herbert M. Pickett *In* NASA, Goddard Space Flight Center, First International Conference on Laboratory Research for Planetary Atmospheres May 1990 p 27-36 (For primary document see N90-26744 20-91)
Avail: NTIS HC A21/MF A03 CSCL 14B

36 LASERS AND MASERS

Includes parametric amplifiers.
For related information see also *76 Solid-State Physics.*

N90-26305 Department of the Navy, Washington, DC.
APPARATUS FOR THE EFFICIENT WAVELENGTH CONVERSION OF LASER RADIATION Patent
Myung K. Chun, inventor (to Navy), Lew Goldberg, inventor (to Navy), and Joseph F. Weller, inventor (to Navy) 6 Mar. 1990 16 p Filed 26 Jun. 1989 Supersedes N90-17125 (28 - 9, p 1228), AD-D014314
(AD-D014506; US-Patent-4,907,238; US-Patent-Appl-SN-370965; US-Patent-Class-372-32) Avail: US Patent and Trademark Office CSCL 09/3

An apparatus for generating coherent radiation at a desired frequency is disclosed. In a preferred embodiment the apparatus comprises: an injection-locked semiconductor diode structure having a large active area for emitting a diffraction-limited beam at a preselected frequency; optics for focusing the diffraction-limited beam into a focused beam; a nonlinear crystal responsive to the focused beam for producing a beam of laser power which includes an output beam at a desired harmonic of the preselected frequency; and a device for passing the output beam in a given direction. In a modification of the preferred embodiment, the output of the injection-locked semiconductor diode structure is mixed with an emission from a laser source in the nonlinear crystal to produce a desired sum or difference frequency. GRA

N90-26306*# Stanford Univ., CA. Dept. of Applied Physics.
SOLID-STATE LASERS FOR COHERENT COMMUNICATION AND REMOTE SENSING Semiannual Progress Report, 1 Oct. 1989 - 31 Mar. 1990
Robert L. Byer Jun. 1990 54 p
(Grant NAGw-1760)
(NASA-CR-186634; NAS 1.26:186634) Avail: NTIS HC A04/MF A01 CSCL 09C

Laser development, high efficiency, high power second harmonic generation, operation of optical parametric oscillators for wavelength diversity and tunability, and studies in coherent communications are reviewed. Author

N90-26307# Science Research Lab., Inc., Somerville, MA.
NEW DISCHARGE PUMPING METHOD FOR CO2 LASERS Report, 1 Feb. - 30 Nov. 1989
Jonah Jacob 31 Jan. 1990 68 p
(Contract DAAH01-88-C-0138; ARPA Order 6259)
(AD-A220898) Avail: NTIS HC A04/MF A01 CSCL 09/3

A pulsed CO2 laser system has been designed, fabricated, and successfully tested. Laser pulses have been generated with

measured output energy of 600 mJ, pulse length 40 microsecond, and conversion efficiency of 14 percent in a 3:2:1 (HeN2:CO2) gas mixture. The laser operates at a total gas pressure between 5 and 40 Torr, and utilizes a COLD-I all-solid-state CO2 laser driver. Typical current, voltage, and laser output traces are presented and compared to numerically simulated curves, showing reasonable agreement. The theoretical model of CO2 laser discharges has been extended and utilized to analyze the steady state solutions and stability criteria for three regimes of operation: the stiff voltage case, the stiff current case, and the finite external impedance case. Numerical solutions are presented for the temporal evolution of the electron (plasma) density, the metastable density, and the electric field under various conditions. The theory of RF discharge stabilization has been extended to two spatial dimensions, and numerical results are presented for the stiff current and the stiff voltage cases. In a repetitively pulsed CO2 laser, the lasing gas must be cooled between pulses to preserve efficiency. Conduction cooling has been examined as an advanced alternative to the traditional flow loop approach. This concept minimizes the weight of the laser head. A thermal analysis of a pulsed CO2 laser head with conduction cooling is presented. GRA

N90-26308*# Old Dominion Univ., Norfolk, VA. Dept. of Physics.
THEORETICAL STUDIES OF SOLAR PUMPED LASERS Final Report, period ending 31 Aug. 1990
Wynford L. Harries May 1990 198 p
(Grant NsG-1568)
(NASA-CR-186712; NAS 1.26:186712; ODU-TR-PTR-90-2) Avail: NTIS HC A09/MF A02 CSCL 20E

One concept for collecting solar energy is to use large solar collectors and then use lasers as energy converters whose output beams act as transmission lines to deliver the energy to a destination. The efficiency of the process would be improved if the conversion could be done directly using solar pumped lasers, and the possibility of making such lasers is studied. There are many applications for such lasers, and these are examined. By including the applications first, the requirements for the lasers will be more evident. They are especially applicable to the Space program, and include cases where no other methods of delivering power seem possible. Using the lasers for conveying information and surveillance is also discussed. Many difficulties confront the designer of an efficient system for power conversion. These involve the nature of the solar spectrum, the method of absorbing the energy, the transfer of power into laser beams, and finally, the far field patterns of the beams. The requirements of the lasers are discussed. Specific laser configurations are discussed. The thrust is into gas laser systems, because for space applications, the laser could be large, and also the medium would be uniform and not subject to thermal stresses. Dye and solid lasers are treated briefly. For gas lasers, a chart of the various possibilities is shown, and the various families of gas lasers divided according to the mechanisms of absorbing solar radiation and of lasing. Several specific models are analyzed and evaluated. Overall conclusions for the program are summarized, and the performances of the lasers related to the requirements of various applications.
Author

N90-26309*# National Aeronautics and Space Administration. Langley Research Center, Hampton, VA.
THE EFFECTS OF PRETREATMENT CONDITIONS ON A Pt/SnO2 CATALYST FOR THE OXIDATION OF CO IN CO2 LASERS
David R. Schryer, John D. VanNorman, Kenneth G. Brown, and Jacqueline Schryer (Old Dominion Univ., Norfolk, VA.) 1989 23 p Submitted for publication
(NASA-TM-103487; NAS 1.15:103487) Avail: NTIS HC A03/MF A01 CSCL 20E

CO oxidation catalysts with high activity at 25 to 100 C are important for long life, closed cycle operation of pulsed CO2 lasers. A reductive pretreatment with either CO or H2 was shown to significantly enhance the activity of a commercially available platinum on tin (IV) oxide (Pt/SnO2) catalyst relative to an oxidative or inert pretreatment of no pretreatment. Pretreatment at temperatures of 175 C and above causes an initial dip in the observed CO2 yield before the steady state yield is attained. This dip was found to be caused by dehydration of the catalyst during pretreatment and is readily eliminated by humidifying the catalyst or the reaction gas mixture. It is hypothesized that the effect of humidification is to increase the concentration of OH groups on the catalyst surface which play a role in the reaction mechanism.
Author

N90-26310# Los Alamos National Lab., NM.
CHARACTERIZATION OF A HIGH-INTENSITY, SUBPICOSECOND XeCl LASER SYSTEM
Antoinette J. Taylor, Timothy R. Gosnell, Jeff P. Roberts, Dave C. MacPherson, and Charles R. Tallman 1990 12 p Presented at the Ultrafast Phenomena, Monterey, CA, 14-17 May 1990
(Contract W-7405-eng-36)
(DE90-011970; LA-UR-90-1692; CONF-9005210-2) Avail: NTIS HC A03/MF A01

Recent advances in ultrafast lasers and large aperture optical amplifiers have spurred the development of terawatt-class laser systems capable of delivering focal-spot intensities in excess of 10(exp 19) W/sq cm. At these extremely high intensities, the optical field strength is more than twenty times larger than the Bohr electric field, e/a(sub o)(sup 2), permitting for the first time investigations of the optical properties of matter in a previously unexplored intensity regime. A terawatt-class laser system based on the amplification of subpicosecond pulses in XeCl discharge amplifiers is described. Although several terawatt laser systems have been previously reported, complete characterization of the performance of these devices has not been made: Only for a few of these systems has the final output pulsewidth been determined, while measurements of the focal-spot diameter obtained upon focusing of the fully amplified beam have not been reported at all. DOE

N90-26311# Sandia National Labs., Albuquerque, NM.
LASER TECHNIQUES FOR STUDYING CHEMICAL VAPOR DEPOSITION
Pauline Ho, William G. Breiland, and Michael E. Coltrin 1990 3 p Presented at the Meeting on Optical Spectroscopic Instrumentation and Techniques for the 1990s: Applications in Astronomy, Chemistry and Physics, Las Cruces, NM, 4-6 Jun. 1990
(Contract DE-AC04-76DP-00789)
(DE90-012921; SAND-89-2860C; CONF-900656-2) Avail: NTIS HC A01/MF A01

Chemical vapor deposition (CVD) is widely used to produce thin films for microelectronics, protective coatings and other materials processing applications. Despite the large number of applications, however, little is known about the fundamental chemistry and physics of most CVD processes. CVD recipes have generally been determined empirically, but as process requirements become more stringent, a more basic understanding will be needed to improve reactor design and speed process optimization. In situ measurements of the reacting gas are important steps toward gaining such an understanding, both from the standpoint of characterizing the reactor and testing models of a CVD process. Our work, a coordinated program of experimental and theoretical research in the fundamental mechanisms of CVD, illustrates the application of laser techniques to the understanding of a CVD system. A number of laser based techniques were used to probe CVD systems and the measurements were compared with predictions from computer models, primarily for the silane CVD system. The silane CVD model solves the 2-D, steady- tate boundary layer equations of fluid flow coupled to 26 elementary chemical reactions describing the thermal decomposition of silane and the subsequent reactions of intermediate species that result in the deposition of a silicon film. DOE

N90-26312# Connecticut Coll., New London.
A COMPACT, HIGH-POWERED FAR-INFRARED (FIR) LASER Final Technical Report, 30 Sep. 1987 - 31 Jan. 1990

Thomas E. Wilson 21 Apr. 1990 17 p
(Contract DE-AC03-87SF-17128)
(DE90-009996; DOE/SF-17128/T2) Avail: NTIS HC A03/MF A01

A compact CO2-(13)CH3F laser system where the FIR laser cavity is inserted in a pump, three-monitor CO2 laser cavity, with optically-switched semiconductor cavity-dumping, will be designed and tested. The 1.207 mm cavity-dumped oscillator is expected to be characterized by predominantly single longitudinal mode, narrow linewidth operation and to produce peak power of order 100 kW in pulses of order 10 ns duration. The 1.2 mm wavelength lies in an atmospheric transmission window (1 dB/km at sea level), which opens up the possibility of millimeter wave space of ground based radar and communications systems. The laser can also be used as a FIR spectroscopic source to investigate dynamic properties of elementary excitations of the solid state. DOE

N90-26313# Lawrence Livermore National Lab., CA.
OASIS, LLNL VERSION: SOFTWARE MAINTENANCE MANUAL
J. M. Auerbach Mar. 1990 11 p
(Contract W-7405-eng-48)
(DE90-013522; UCRL-ID-103139) Avail: NTIS HC A03/MF A01

The OASIS laser beam propagation code has been used extensively to support design and analysis in the Free Electron Laser Master Oscillator Program, the Medium Power Solid State Laser Program, and the Active Optical Countermeasures Program. The version of OASIS currently used at the Lawrence Livermore National Laboratory (LLNL) is significantly enhanced compared to the initial version supplied by the Air Force Weapons Laboratory. This software maintenance manual presents the details of the LLNL version of OASIS so it can be modified as necessary by new personnel. The manual presents in great detail the content and organization of the OASIS software. DOE

N90-26314# Lawrence Livermore National Lab., CA.
DAMAGE MEASUREMENTS ON OPTICAL MATERIALS FOR USE IN HIGH-PEAK-POWER LASERS
F. Rainer, R. M. Brusasco, J. H. Campbell, F. P. DeMarco, R. P. Gonzales, M. R. Kozlowski, F. P. Milanovich, A. J. Morgan, M. S. Scrivener, and M. C. Staggs et al 2 May 1990 11 p Presented at the 21st Annual Symposium on Optical Materials for High Power Lasers, Boulder, CO, 1-3 Nov. 1989
(Contract W-7405-eng-48)
(DE90-013489; UCRL-102205; CONF-891163-2) Avail: NTIS HC A03/MF A01

Recently, efforts were expanded to develop state-of-the-art optical components for use in large scale, high peak power, solid state lasers. Laser induced damage to many of these components sets critical constraints on construction costs and limits the peak powers attainable in current and proposed devices. Increasing the damage threshold whenever possible by improving materials fabrication technology is therefore the ultimate goal. The research has resulted in an extensive database of laser damage measurements. Summaries are presented of these measurements with particular emphasis on those taken at 1064 nm and 355 nm. DOE

N90-26315# Lawrence Livermore National Lab., CA.
LASER DAMAGE DATABASE AT 1064 nm
F. Rainer, R. P. Gonzales, and A. J. Morgan Mar. 1990 18 p Presented at the 21st Annual Symposium on Optical Materials for High Power Lasers, Boulder, CO, Nov. 1989
(Contract W-7405-eng-48)
(DE90-013490; UCRL-101767; CONF-891163-3) Avail: NTIS HC A03/MF A01

In conjunction with the diversification of laser damage testing capabilities, a database was expanded of threshold measurements and parameter variations at 1064 nm. This includes all tests at low pulse repetition frequencies (PRF) ranging from single shots to 120 Hz. These tests were conducted on the Reptile laser facility since 1987 and the Variable Pulse Laser (VPL) facility since 1988. Pulse durations ranged from 1 to 16 ns. DOE

N90-26316# Old Dominion Univ., Norfolk, VA. Dept. of Physics.
SDIO/IST ULTRASHORT WAVELENGTH LASER: NOVEL EXPERIMENTAL SCHEMES FOR OBSERVING THE MOESSBAUER EFFECT IN LONG-LIVED NUCLEAR LEVELS AND NUCLEAR COHERENT STATES Final Technical Report, for period ending 26 May 1990
Gilbert R. Hoy May 1990 31 p
(Contract N00014-87-K-2015)
(AD-A222607; PTR-90-4) Avail: NTIS HC A03/MF A01 CSCL 20/8

Our results indicate that the Mossbauer Effect is occurring for the 88-KeV transition of Silver 109 in silver single crystals. Furthermore, the effect appears to be an order of magnitude smaller in the horizontal geometry than in the vertical geometry. Using our model calculations, the size of the M.E. in the vertical geometry is consistent with a line broadening factor of only about 5. This would appear to be an unphysical result. These results suggest that gravitational sweeping is playing a significant role in producing an observable M.E. Very soon we will make further model calculations incorporating the gravitational sweeping mechanism in order to evaluate its significance. In addition, we are presently performing further experiments using a thicker silver single-crystal sample which should shed light on this question. The search for the M.E. in ultra-narrow gamma-ray transitions (lifetimes on the order of seconds) is difficult. One of the methods used is based on the increased self-absorption of gamma-rays emitted in a particular direction as the temperature of the sample is lowered. This increase in absorption at low temperature is an indication of the occurrence of the M.E. There are substantial difficulties, outlined above, associated with this technique because changes in the gamma-ray counting rates as a function of temperature are associated with a number of experimental factors other than the occurrence of the M.E. GRA

N90-26317# Ballistic Research Labs., Aberdeen Proving Ground, MD.
EXCIMER LASER FRAGMENTATION STUDIES OF SELECTED OXIMES: NASCENT OH INTERNAL ENERGY DISTRIBUTIONS AND THE SEARCH OF H2CN FLUORESCENCE
Rosario C. Sausa, William R. Anderson, Andrzej W. Miziolek, and Paul J. Dagdigian (Johns Hopkins Univ., Baltimore, MD.) May 1990 32 p Submitted for publication
(DA Proj. 1L1-61102-AH-43)
(AD-A222622; BRL-TR-3094) Avail: NTIS HC A03/MF A01 CSCL 09/3

Excimer laser excitation (193 nm) of formaldoxime (H2 CN-OH) or the methylated homologs, R2R2CH-OH where R1, R2 = H or CH3, results in dissociation. The upper limit for the quantum yield of fluorescence of the R1R2CN is estimated to be between 1 to 10 percent depending on the precursor used. The OH companion radical was probed by laser induced fluorescence (LIF) utilizing the A-X (2-1) and (1,0) bands near 34700 cm-1, and the nascent rotational, vibrational, and ground electronic state spin-orbit distributions determined. No laser induced fluorescence of the R1R2CN radical could be observed upon irradiation in the regions where the radicals are known to absorb, 280 to 295 nm. From the nascent OH product distributions, we calculate that only 2.5 Kcal/mole of the excess energy appears as OH product internal energy, thus leaving about 80 Kcal/mole to be divided between the R1R2CN fragment and translation. We, therefore, conclude that it is highly likely that the upper states of these radicals probed in the 280 to 295 nm region are predissociative. GRA

N90-26318# Rochester Univ., NY. Dept. of Physics and Astronomy.
DURIP: INSTRUMENTATION FOR LASER SWITCHED POWER LINAC Final Report, 1 Dec. 1988 - 30 Nov. 1989
A. C. Melissinos and W. Donaldson 28 Mar. 1990 13 p
(Grant AF-AFOSR-0131-89)
(AD-A222629; AFOSR-90-0582TR) Avail: NTIS HC A03/MF A01 CSCL 09/3

A 6 cm radius, single stage, electron accelerator that uses a

photoconductive switch to couple an electromagnetic pulse into a radial transmission line is being developed. The switch consists of a ring GaAs which is closed with a ring of a laser light from a Phosphate glass regenerative amplifier. We are investigating the acceleration picosecond electron bunches in fields on the order of several MeV/m. GRA

N90-26319# Massachusetts Inst. of Tech., Cambridge. Lincoln Lab.
LASER RADAR ANGULAR TRACKING
Alan L. Kachelmyer 1990 21 p Repr. from Laser Radar 5, v. 1222, 1990 p 24-42
(Contract F19628-90-C-0002)
(AD-A222741; ESD-TR-90-051) Avail: NTIS HC A03/MF A01 CSCL 17/9

This paper deals with the theory of monopulse angle tracking with a laser radar employing heterodyne detection. The detector is assumed to be of the quadrant type. The target's angular location is inferred from the location of its diffraction pattern in the detector plane. A generalized gain characteristic for the detector can be used to relate the strength of the matched filter outputs, which correspond to the spatial regions (halves) of the detector surface, to the corresponding angular location of the target. The maximum likelihood angle estimator is derived for a speckle target. The performance of an approximation to the maximum likelihood angle estimator is evaluated for the both speckle and glint targets. The angle estimator performance is also evaluated in the presence of atmospheric turbulence and beam jitter. GRA

37 MECHANICAL ENGINEERING

Includes auxiliary systems (nonpower); machine elements and processes; and mechanical equipment.

N90-26320*# Rockwell International Corp., Canoga Park, CA. Rocketdyne Div.
REUSABLE ROCKET ENGINE TURBOPUMP HEALTH MONITORING SYSTEM, PART 3 Final Report
John G. Perry 14 Mar. 1989 42 p
(Contract NAS3-25279)
(NASA-CR-182294; NAS 1.26:182294; RI/RD89-171-Pt-3) Avail: NTIS HC A03/MF A01 CSCL 13I

Degradation mechanisms and sensor identification/selection resulted in a list of degradation modes and a list of sensors that are utilized in the diagnosis of these degradation modes. The sensor list is divided into primary and secondary indicators of the corresponding degradation modes. The signal conditioning requirements are discussed, describing the methods of producing the Space Shuttle Main Engine (SSME) post-hot-fire test data to be utilized by the Health Monitoring System. Development of the diagnostic logic and algorithms is also presented. The knowledge engineering approach, as utilized, includes the knowledge acquisition effort, characterization of the expert's problem solving strategy, conceptually defining the form of the applicable knowledge base, and rule base, and identifying an appropriate inferencing mechanism for the problem domain. The resulting logic flow graphs detail the diagnosis/prognosis procedure as followed by the experts. The nature and content of required support data and databases is also presented. The distinction between deep and shallow types of knowledge is identified. Computer coding of the Health Monitoring System is shown to follow the logical inferencing of the logic flow graphs/algorithms. Author

N90-26321*# Georgia Inst. of Tech., Atlanta. School of Mechanical Engineering.
MICRO CORING APPARATUS Advanced Design Program
David Collins, Marshall Brooks, Paul Chen, Paul Dwelle, and Ben Fischer Mar. 1989 56 p
(Grant NGT-21-002-800)
(NASA-CR-183072; NAS 1.26:183072; ME-4182) Avail: NTIS HC A04/MF A01 CSCL 13I

A micro-coring apparatus for lunar exploration applications, that is compatible with the other components of the Walking Mobile Platform, was designed. The primary purpose of core sampling is to gain an understanding of the geological composition and properties of the prescribed environment. This procedure has been used extensively for Earth studies and in limited applications during lunar explorations. The corer is described and analyzed for effectiveness. Author

N90-26322*# Georgia Inst. of Tech., Atlanta. School of Mechanical Engineering.
LUNAR DEEP DRILL APPARATUS Advanced Design Program
Jill Harvey, ed. Jun. 1989 464 p
(Grant NGT-21-002-080)
(NASA-CR-182756; NAS 1.26:182756; ME-4182) Avail: NTIS HC A20/MF A03 CSCL 13I

A self contained, mobile drilling and coring system was designed to operate on the Lunar surface and be controlled remotely from earth. The system uses SKITTER (Spatial Kinematic Inertial Translatory Tripod Extremity Robot) as its foundation and produces Lunar core samples two meters long and fifty millimeters in diameter. The drill bit used for this is composed of 30 per carat diamonds in a sintered tungsten carbide matrix. To drill up to 50 m depths, the bit assembly will be attached to a drill string made from 2 m rods which will be carried in racks on SKITTER. Rotary power for drilling will be supplied by a Curvo-Synchronous motor. SKITTER is to support this system through a hexagonal shaped structure which will contain the drill motor and the power supply. A micro-coring drill will be used to remove a preliminary sample 5 mm in diameter and 20 mm long from the side of the core. This whole system is to be controlled from earth. This is carried out by a continuously monitoring PLC onboard the drill rig. A touch screen control console allows the operator on earth to monitor the progress of the operation and intervene if necessary. Author

N90-26323*# Georgia Inst. of Tech., Atlanta. School of Mechanical Engineering.
PROOF OF PRINCIPLE MODEL FOR A LUNAR DUMPTRUCK Advanced Design Program
Jill Ann Harvey Jun. 1989 19 p
(Grant NGT-22-002-080)
(NASA-CR-182557; NAS 1.26:182557; ME-8501) Avail: NTIS HC A03/MF A01 CSCL 13I

A proof-of-principle model of a two wheeled lunar dump truck was designed to display at the 1989 Summer Conference. The dump truck consists of a cylindrical bucket suspended between two wheels with the center of gravity of the bucket lower than the axis of the wheels. This gives the truck great stability in rough terrain. One motor on each wheel controls the movement of the truck and limits the moving parts to only two. The design of the mechanical drive, the electrical system, and the control systems are examined. Conclusion and recommendations are given. Author

N90-26324*# Thiokol Corp., Brigham City, UT. Space Operations.
QM-8 FINAL PERFORMANCE EVALUATION REPORT: SEALS, VOLUME 4
L. V. Nelsen Jun. 1989 206 p
(Contract NAS8-30490)
(NASA-CR-183958; NAS 1.26:183958; TWR-17591-Vol-4; WBS-HQ302-10-10; DR-5-3) Avail: NTIS HC A10/MF A02 CSCL 13I

The Space Shuttle Redesigned Solid Rocket Motor (RSRM) static test of Qualification Motor-8 (QM-8) was conducted. The QM-8 test article was the fifth full-scale, full-duration test, and the third qualification motor to incorporate the redesigned case field joint and nozzle-to-case joint. This was the second static test conducted in the T-97 test facility, which is equipped with actuators for inducing external side loads to a 360 degree external tank (ET) attach ring during test motor operation, and permits heating/cooling of an entire motor. The QM-8 motor was cooled to a temperature which ensured that the maximum propellant mean

bulk temperature (PMBT) of 40 F was achieved at firing. All test results are not included, but rather, the performance of the metal case, field joints, and nozzle-to-case joint is addressed. The involvement is studied of the Structural Applications and Structural Design Groups with the QM-8 test which includes: assembly procedures of the field and nozzle-to-case joints, joint leak check results, structural test results, and post-test inspection evaluations.
Author

N90-26325*# Thiokol Corp., Brigham City, UT. Space Operations.
FLIGHT SET 360L001 (STS-26) IGNITER, POST FLIGHT Final Report
Elgie J. Hale 5 Apr. 1990 39 p
(Contract NAS8-30490)
(NASA-CR-183957; NAS 1.26:183957; TWR-17272-Vol-6; WBS-4B102-10-03; ECS-1012; DR-5-3-Type-2) Avail: NTIS HC A03/MF A01 CSCL 13I

Space Transportation System (STS-26) was launched from KSC pad 39B. Two of the Redesigned Solid Rocket Motors (RSRM) were part of the launch system and are designated RSRM-1A and RSRM-1B. Each of these motors were initiated by an 1U75164 igniter. The post flight condition of the igniters and associated components is documented. The overall performance of the igniter components was excellent. No damage or heat affected areas were noted. The sealing elements of the igniter functioned as expected with no evidence of erosion or blowby. The thermal protection system protected all areas adequately. No excessive erosion was noted. Corrosion was found in the special bolt holes in the igniter chamber. The corrosion will not affect refurbishment of the chamber. Beginning with flight 5 grease has been added to the chamber holes to prevent this erosion. Author

N90-26326# Massachusetts Inst. of Tech., Cambridge. Artificial Intelligence Lab.
TWILIGHT ZONES AND CORNERSTONES: A GNAT ROBOT DOUBLE FEATURE
Anita M. Flynn, Rodney A. Brooks, and Lee S. Taurow Jul. 1989 39 p
(Contracts N00014-86-K-0685; N00014-85-K-0124)
(AD-A220026; AI-M-1126) Avail: NTIS HC A03/MF A01 CSCL 12/9

We want to build tiny gnat-sized robots, a millimeter or two in diameter. They will be cheap, disposable, totally self-contained autonomous agents able to do useful things in the world. This paper consists of two parts. The first describes why we want to build them. The second is a technical outline of how to go about it. Gnat robots are going to change the world. GRA

N90-26327# Wichita State Univ., KS. National Inst. for Aviation Research.
DESIGN AND CONSTRUCTION OF A WALL-CLIMBING ROBOT M.S. Thesis
Sami M. Maari Jun. 1990 75 p
(NIAR-90-20) Avail: NTIS HC A04/MF A01

A Wall-Climbing Robot was designed. The robot uses compressed air to achieve a safe attachment to vertical, curved surfaces. The robot performs certain tasks including inspection of the aircraft fuselage in very hard to reach areas by the human workers, riveting and deriveting, painting the aircraft. It has the capability of climbing on the walls of tall buildings while carrying heavy weights compared to its weight. The design was successfully completed, then the robot was manufactured, assembled, and tested. The result proved its validity by demonstrating the actual robot moving on different types of surfaces. The robot as a hardware seems to be very reliable in performing the tasks designed for it under heavy payload conditions. Special consideration of the ease of maintainability was taken by the designer. Author

N90-26328*# Georgia Inst. of Tech., Atlanta. School of Mechanical Engineering.
CONTROL STRATEGY FOR COOPERATING DISPARATE MANIPULATORS
Jae Young Lew [1989] 22 p
(Grant NAG1-623)
(NASA-CR-186809; NAS 1.26:186809) Avail: NTIS HC A03/MF A01 CSCL 13I

To manipulate large payloads typical of space construction, the concept of a small arm mounted on the end of a large arm is introduced. The main purposes of such a configuration are to increase the structural stiffness of the robot by bracing against or locking to a stationary frame, and to maintain a firm position constraint between the robot's base and workpieces by grasping them. Possible topologies for a combination of disparate large and small arms are discussed, and kinematics, dynamics, controls, and coordination of the two arms, especially when they brace at the tip of the small arm, are developed. The feasibility and improvement in performance are verified, not only with analytical work and simulation results but also with experiments on the existing arrangement Robotic Arm Large and Flexible and Small Articulated Manipulator. Author

N90-26329*# Georgia Inst. of Tech., Atlanta. School of Mechanical Engineering.
AN INVERSE DYNAMIC METHOD YIELDING FLEXIBLE MANIPULATOR STATE TRAJECTORIES
Dong-Soo Kwon and Wayne J. Book 1990 8 p
(Grant NAG1-623)
(NASA-CR-186807; NAS 1.26:186807) Avail: NTIS HC A02/MF A01 CSCL 13I

An inverse dynamic equation for a flexible manipulator is derived in a state form. By dividing the inverse system into the causal part and the anticausal part, torque is calculated in the time domain for a certain end point trajectory, as well as trajectories of all state variables. The open loop control of the inverse dynamic method shows an excellent result in simulation. For practical applications, a control strategy adapting feedback tracking control to the inverse dynamic feedforward control is illustrated, and its good experimental result is presented. Author

N90-26330*# Old Dominion Univ., Norfolk, VA. Advanced Design Program.
DESIGN OF AN AUTONOMOUS LUNAR CONSTRUCTION UTILITY VEHICLE
Robert L. Ash, Mason Chew, and Iain Dixon, ed. 1990 168 p
(Grant NGT-21-002-800)
(NASA-CR-186832; NAS 1.26:186832) Avail: NTIS HC A08/MF A01 CSCL 13I

In order to prepare a site for a manned lunar base, an autonomously operated construction vehicle is necessary. A Lunar Construction Utility Vehicle (LCUV), which utilizes interchangeable construction implements, was designed conceptually. Some elements of the machine were studied in greater detail. Design of an elastic loop track system has advanced to the testing stage. A standard coupling device was designed to insure a proper connection between the different construction tools and the LCUV. Autonomous control of the track drive motors was simulated successfully through the use of a joystick and computer interface. A study of hydrogen-oxygen fuel cells has produced estimates of reactant and product size requirements and identified multi-layer insulation techniques. Research on a 100 kW heat rejection system has determined that it is necessary to house a radiator panel on a utility trailer. The impact of a 720 hr use cycle has produced a very large logistical support lien which requires further study.
Author

N90-26331*# Maryland Univ., College Park.
UNIVERSITY OF MARYLAND WALKING ROBOT: A DESIGN PROJECT FOR UNDERGRADUATE STUDENTS
Bob Olsen, Jim Bielec, Dave Hartsig, Mani Oliva, Phil Grotheer, Morad Hekmat, David Russell, Hossein Tavakoli, Gary Young, and Tom Nave et al 1990 130 p
(Grant NGT-21-002-800)
(NASA-CR-186839; NAS 1.26:186839) Avail: NTIS HC A07/MF A01 CSCL 13I

The design and construction required that the walking robot

machine be capable of completing a number of tasks including walking in a straight line, turning to change direction, and maneuvering over an obstable such as a set of stairs. The machine consists of two sets of four telescoping legs that alternately support the entire structure. A gear-box and crank-arm assembly is connected to the leg sets to provide the power required for the translational motion of the machine. By retracting all eight legs, the robot comes to rest on a central Bigfoot support. Turning is accomplished by rotating the machine about this support. The machine can be controlled by using either a user operated remote tether or the on-board computer for the execution of control commands. Absolute encoders are attached to all motors (leg, main drive, and Bigfoot) to provide the control computer with information regarding the status of the motors (up-down motion, forward or reverse rotation). Long and short range infrared sensors provide the computer with feedback information regarding the machine's relative position to a series of stripes and reflectors. These infrared sensors simulate how the robot might sense and gain information about the environment of Mars. Author

N90-26332*# Florida State Univ., Tallahassee. Dept. of Mechanical Engineering.

LUNAR ARTICULATED REMOTE TRANSPORTATION SYSTEM Annual Report

Geoffrey Beech, Gerald Conley, Claudine Diaz, Timothy DiMella, Pete Dodson, Jeff Hykin, Byron Richards, Kroy Richardson, Christie Shetzer, and Melissa VanDyke Jun. 1990 164 p

(Grant NGT-21-002-800)

(NASA-CR-186817-Vol-1; NAS 1.26:186817-Vol-1) Avail: NTIS HC A08/MF A01 CSCL 13I

A first generation lunar transportation vehicle was designed for use on the surface of the Moon between the years 2010 and 2020. Attention is focussed on specific design details on all components of the Lunar Articulated Remote Transportation System (Lunar ARTS). The Lunar ARTS will be a three cart, six-wheeled articulated vehicle. It's purpose will be for the transportation of astronauts and/or materials for excavation purposes at a short distance from the base (37.5 kilometers). The power system includes fuel cells for both the primary system and the back-up system. The vehicle has the option of being operated in a manned or unmanned mode. The unmanned mode includes stereo imaging with signal processing for navigation. For manned missions the display console is a digital readout displayed on the inside of the asronaut's helmet. A microprocessor is also on board the vehicle. Other components of the vehicle include: a double wishbone/flexible hemispherical wheel suspension; chassis; a steering system; motors; seat restraints, heat rejection systems; solar flare protection; dust protection; and meteoroid protection. A one-quarter scale dynamic model was built to study the dynamic behavior of the vehicle. The dynamic model closely captures the mechanical and electrical details of the total design. Author

N90-26333*# Florida State Univ., Tallahassee. Dept. of Mechanical Engineering.

DESIGN OF A LUNAR TRANSPORTATION SYSTEM, VOLUME 2 Annual Report

Jun. 1990 191 p

(Grant NGT-21-002-800)

(NASA-CR-186833-Vol-2; NAS 1.26:186833-Vol-2) Avail: NTIS HC A09/MF A01 CSCL 13I

The Spring 1990 Introduction to Design class was asked to conceptually design second generation lunar vehicles and equipment as a semester design project. A brief summary of four of the final projects, is presented. The designs were to facilitate the transportation of personnel and materials. The eight topics to choose from included flying vehicles, ground based vehicles, robotic arms, and life support systems. A lunar flying vehicle that uses clean propellants for propulsion is examined. A design that will not contribute to the considerable amount of caustic pollution already present in the sparse lunar atmosphere is addressed by way of ballistic flight techniques. A second generation redesign of the current Extra Vehicular Activity (EVA) suit to increase operating time, safety, and efficiency is also addressed. A separate life support system is also designed to be permanently attached to the lunar rover. The two systems would interact through the use of an umbilical cord connection. A ground based vehicle which will travel for greater distances than a 37.5 kilometer radius from a base on the lunar surface was designed. The vehicle is pressurized due to the fact that existing lunar rovers are limited by the EVA suits currently in use. A robotic arm for use at lunar bases or on roving vehicles on the lunar surface was designed. The arm was originally designed as a specimen gathering device, but it can be used for a wide range of tasks through the use of various attachments. Author

N90-26334*# Army Aviation Systems Command, Cleveland, OH.

EFFICIENCY STUDY COMPARING TWO HELICOPTER PLANETARY REDUCTION STAGES

Timothy L. Krantz and Robert F. Handschuh Jul. 1990 11 p Presented at the 26th Joint Propulsion Conference, Orlando, FL, 16-18 Jul. 1990; sponsored in part by AIAA, SAE, ASME, and ASEE

(DA Proj. 1L1-62211-A-47-A)

(NASA-TM-103106; E-5405; NAS 1.15:103106; AVSCOM-TM-90-C-005) Avail: NTIS HC A03/MF A01 CSCL 13I

A study was conducted to compare the efficiency of two helicopter transmission planetary reduction stages. Experimental measurements and analytical predictions were made. The analysis predicted and experiments verified that one planetary stage was a more efficient design due to the type of planet bearing used in the stage. The effects of torque, speed, lubricant type, and lubricant temperature on planetary efficiency are discussed. Author

N90-26335# National Aerospace Lab., Tokyo (Japan). Aeroengine Div.

RESEARCH AND DEVELOPMENT OF ADVANCED GAS TURBINE

May 1989 74 p In JAPANESE; ENGLISH summary

(DE90-503377; NAL-TR-1023) Avail: NTIS (US Sales Only) HC A04/MF A01

The purposes of this research and development are as follows: to establish the technologies for a gas turbine with high efficiency and low emissions through the research and development of appropriate technology and heightening a turbine inlet temperature; to investigate the comprehensive energy supply systems such as district cooling and heating, a combined-cycle power generation system using the newly developed gas turbine; thus, to improve an overall thermal efficiency drastically. As a first stage of the study, a pilot plant of the high efficiency gas turbine was completed in order to realize the combined-cycle power plant with the overall thermal efficiency of 55 percent which is a final target, then demonstration operation of the plant was conducted. A waste heat boiler and a steam turbine which were integrated into the plant were simulated by a computer, and estimate calculations were carried out using a calculated value from the gas turbine by on-line. In the next stage, high temperature and high pressure components such as a turbine and a combustor were designed and were fabricated by way of trial, then efficiency, durability and reliability of the components were verified through a high temperature and high speed turbine test equipment. DOE

N90-26336# New Energy Development Organization, Tokyo (Japan).

SURVEY OF APPLICABILITY OF ELECTRIC VEHICLES (EVS) IN SPECIFIC REGIONS SUCH AS RESORTS

Mar. 1989 70 p In JAPANESE; ENGLISH summary

(DE90-503592; NEDO-P-8819) Avail: NTIS (US Sales Only) HC A04/MF A01

Electric vehicles (EVs) are expected to be widely used in anticipation of their merits for environmental protection, and reduction of oil consumption. Unfortunately, they are not yet popular because of their inferiority of performance and cost compared to conventional vehicles. On the other hand environmental destruction in some resort areas due to traffic jams and exhaust gases

becomes an issue. The actual condition of EV introduction in these areas are examined. The EV applicability for selected areas are investigated by conducting case studies from social, technical, and economic viewpoints. Author

N90-26337# Loughborough Univ. of Technology (England). Dept. of Mathematical Sciences.
ON CONTROLLER CHOICE FOR ROBUST SLIDING MODE PERFORMANCE
S. K. Spurgeon Nov. 1989 27 p
(MATHS-Rept-A-107; ETN-90-97123) Avail: NTIS HC A03/MF A01

The robustness properties of sliding behavior are considered. The choice of nonlinear control structure is studied. The performance of two classes of variable structure controllers in the presence of unmatched uncertainty is discussed. Criteria for suitable choice of nonlinear control structure are presented and the concept of a performance sliding mode introduced. A numerical example is given illustrating the phenomenon described. ESA

N90-26338*# National Aeronautics and Space Administration. Lewis Research Center, Cleveland, OH.
A HIGH-SPEED PHOTOGRAPHY STUDY OF CAVITATION IN A DYNAMICALLY LOADED JOURNAL BEARING
D. C. Sun (State Univ. of New York, Binghamton.) and D. E. Brewe 1990 27 p Presented at the Joint Tribology Conference, Toronto, Ontario, 7-10 Oct. 1990; sponsored by ASME and STLE
(DA Proj. 1L1-61102-AH-45)
(NASA-TM-103178; E-5547; NAS 1.15:103178; AVSCOM-TR-90-C-013) Avail: NTIS HC A03/MF A01 CSCL 13I

The earlier study made by Jacobson and Hamrock on the cavitation of liquid lubricant films in a dynamically loaded journal bearing was repeated with a quartz sleeve, which was more rigid than the Polymethylmethacrylate (PMMA) sleeve used previously. Various improvements of the test rig were made concomitantly so that the experimental errors could be better controlled and assessed. The updated speed photography experiment and its results are described. Author

N90-26339*# National Aeronautics and Space Administration. Pasadena Office, CA.
DIRECT DRIVE ROBOTIC HAND Patent Application
Szakaly, inventor (to NASA) (Jet Propulsion Lab., California Inst. of Tech., Pasadena.) 28 Jun. 1990 22 p
(Contract NAS7-918)
(NASA-Case-NPO-17917-1-CU; NAS 1.71:NPO-17917-1-CU; US-Patent-Appl-SN-545015) Avail: NTIS HC A03/MF A01 CSCL 13I

An end effector system uses a frameless motor driving a lead screw with oppositely threaded ends to control engagement of the grippers. Grip force sensor frames are configured from rectangular, tubular boxes and act as four bar linkages to maintain gripping faces in parallel during deformation. Semiconductor strain gages are mounted as strain gage bridges on the deforming faces of the frames. Additional sensor inputs are available from a force torque sensor frame which acts as a pair of concentric rigid bodies interconnected by four beams. Each beam carries a pair of strain gage bridges so that three orthogonal axes of data may be collected. Local electronics converts serial data from an optical connection to a host processor into phase locked parallel data used to control and monitor the hand motor and gages. A state machine is used in lieu of a local processor for higher speed and greater robustness. High voltage, narrow width strain gage excitation pulses are applied simultaneously to all gages to improve the signal to noise ratio and data integrity. Parallel sample and hold circuits simultaneously sample the gages before the information is applied to analog to digital converters. D/A converters are used to remove offsets under host processor control which may result from hand orientation and/or gripping in order to maximize the sensitivity of the analog sensor data which may be transmitted within the data constraints of the hand electronics subsystem. NASA

N90-26340*# National Aeronautics and Space Administration. Lyndon B. Johnson Space Center, Houston, TX.
POWER SAW Patent Application
Jimmy D. Bradley, inventor (to NASA) 28 Feb. 1990 16 p
(NASA-Case-MSC-21469-1; NAS 1.71:MSC-21469-1; US-Patent-Appl-SN-486458) Avail: NTIS HC A03/MF A01 CSCL 13I

A power saw is disclosed for space or robotic operations with jaw members for clamping to a work piece by an operation of a lever arm. The saw assembly is slidably mounted on the jaw assembly and fed into the work piece by a hand operated feed screw. The saw assembly includes a motor and gear belt. A current sensing circuit provides a current signal which actuates colored lights to visually depict the load on the saw blade during the cutting operations. NASA

N90-26341*# National Aeronautics and Space Administration. Lyndon B. Johnson Space Center, Houston, TX.
ALIGNMENT POSITIONING MECHANISM Patent Application
Peter M. Fantasia, inventor (to NASA) 26 Jan. 1990 17 p
(NASA-Case-MSC-21502-1; NAS 1.71:MSC-21502-1; US-Patent-Appl-SN-470663) Avail: NTIS HC A03/MF A01 CSCL 13I

An alignment positioning mechanism for correcting and compensating for misalignment of structures to be coupled is disclosed. The mechanism comprises a power screw with a base portion and a threaded shank portion. A mounting fixture is provided for rigidly coupling base portion to the mounting interface of a supporting structure with the axis of the screw perpendicular thereto. A traveling ball nut threaded on the power screw is formed with an external annular arcuate surface configured in the form of a spherical segment and enclosed by a ball nut housing with a conforming arcuate surface for permitting gimballed motion thereon. The ball nut housing is provided with a mounting surface which is positionable in cooperable engagement with the mounting interface of a primary structure to be coupled to the supporting structure. Cooperative means are provided on the ball nut and ball nut housing, respectively, for positioning the ball nut and ball nut housing in relative gimballed position within a predetermined range of relative angular relationship whereby severe structural stresses due to unequal loadings and undesirable bending moments on the mechanism are avoided. NASA

N90-26342*# National Aeronautics and Space Administration. Lyndon B. Johnson Space Center, Houston, TX.
BIDIRECTIONAL DRIVE AND BRAKE MECHANISM Patent Application
Scott A. Swan, inventor (to NASA) 23 May 1990 19 p
(NASA-Case-MSC-21540-1; NAS 1.71:MSC-21540-1; US-Patent-Appl-SN-527508) Avail: NTIS HC A03/MF A01 CSCL 13I

A space transport vehicle is disclosed as including a body which is arranged to be movably mounted on an elongated guide member disposed in outer space and driven therealong. A drive wheel is mounted on a drive shaft and arranged to be positioned in rolling engagement with the elongated guide carrying the vehicle. A brake member is arranged on the drive shaft for movement into and out of engagement with an adjacent surface of the drive wheel. An actuator is mounted on the body to be manually moved back and forth between spaced positions in an arc of movement. A ratchet-and-pawl mechanism is arranged to operate upon movements of the actuator in one direction between first and second positions for coupling the actuator to the drive wheel to incrementally rotate the wheel in one rotational direction and to operate upon movements of the actuator in the opposite direction for uncoupling the actuator from the wheel. The brake member is threadedly coupled to the drive shaft in order that the brake member will be operated only when the actuator is moved on beyond its first and second positions for shifting the brake member along the drive shaft and into frictional engagement with the adjacent surface on the drive wheel. NASA

N90-26343# Naval Postgraduate School, Monterey, CA. Dept. of Computer Science.
GUIDANCE AND CONTROL SYSTEM FOR AN AUTONOMOUS UNDERWATER VEHICLE M.S. Thesis
Michael John Cloutier Jun. 1990 161 p
(AD-A222709; AD-E501236) Avail: NTIS HC A08/MF A01 CSCL 17/7

The Naval Postgraduate School (NPS) is currently involved in a long-term project to investigate and develop real-time control software, artificial intelligence, computer architecture and control systems theory as they pertain to U.S. Navy autonomous vehicle programs. In support of this goal, the NPS is currently designing and fabricating a testbed autonomous underwater vehicle. This work describes the design, development, and testing of a Guidance Subsystem for this testbed vehicle which uses portions of cubic spirals as the desired path to follow between waypoints. In addition, data translation firmware and real-time software for the control surfaces and main motors is designed, implemented and tested. The process of selecting and implementing an appropriate computer architecture in support of these goals is also discussed and detailed, along with the choice of associated computer hardware and real-time operating system software. GRA

N90-26228*# Jet Propulsion Lab., California Inst. of Tech., Pasadena. Communications Systems Research Section.
INITIAL RESULTS ON FAULT DIAGNOSIS OF DSN ANTENNA CONTROL ASSEMBLIES USING PATTERN RECOGNITION TECHNIQUES
P. Smyth and J. Mellstrom *In its* The Telecommunications and Data Acquisition Report 15 May 1990 p 136-151 (For primary document see N90-26217 20-32)
Avail: NTIS HC A10/MF A02 CSCL 13I

38 QUALITY ASSURANCE AND RELIABILITY

Includes product sampling procedures and techniques; and quality control.

N90-26344*# Cornell Univ., Ithaca, NY. Dept. of Computer Science.
MAKING REAL-TIME REACTIVE SYSTEMS RELIABLE
Keith Marzullo and Mark Wood 30 Mar. 1990 7 p
(Contract NAG2-593; N00140-87-C-8904)
(NASA-CR-186642; NAS 1.26:186642) Avail: NTIS HC A02/MF A01 CSCL 14D

A reactive system is characterized by a control program that interacts with an environment (or controlled program). The control program monitors the environment and reacts to significant events by sending commands to the environment. This structure is quite general. Not only are most embedded real time systems reactive systems, but so are monitoring and debugging systems and distributed application management systems. Since reactive systems are usually long running and may control physical equipment, fault tolerance is vital. The research tries to understand the principal issues of fault tolerance in real time reactive systems and to build tools that allow a programmer to design reliable, real time reactive systems. In order to make real time reactive systems reliable, several issues must be addressed: (1) How can a control program be built to tolerate failures of sensors and actuators. To achieve this, a methodology was developed for transforming a control program that references physical value into one that tolerates sensors that can fail and can return inaccurate values; (2) How can the real time reactive system be built to tolerate failures of the control program. Towards this goal, whether the techniques presented can be extended to real time reactive systems is investigated; and (3) How can the environment be specified in a way that is useful for writing a control program. Towards this goal, whether a system with real time constraints can be expressed as an equivalent system without such constraints is also investigated. Author

N90-26345# Wichita State Univ., KS. Inst. for Aviation Research.
NEURAL NETWORKS FOR DETECTING DEFECTS IN AIRCRAFT STRUCTURES
Behnam Bahr and Tarabishy M. Nabeel Apr. 1990 14 p
(IAR-90-4) Avail: NTIS HC A03/MF A01

There are various nondestructive testing (NDT) inspection methods, such as vision, eddy current, and ultrasonic used for crack or corrosion detection of the skin or the structures of aircraft around rivets and fasteners. These methods require a skilled technician to identify the existence of the cracks. Despite the training that a technician goes through, human error is identified to be one of the major contributing factors to problems in the determination of the safety of aircraft. There has been some effort to develop expert systems that can be used by technicians. However, there is currently no expert system developed that can learn and improve its capability as it encounters new situations. The neural network and its possibility for aiding the technician in detecting defects is reviewed. Author

N90-26346# Wichita State Univ., KS. National Inst. for Aviation Research.
ROBOTIC-AIDED SYSTEM FOR INSPECTION OF AGING AIRCRAFT
Behnam Bahr and Sami Maari May 1990 13 p
(NIAR-90-9) Avail: NTIS HC A03/MF A01

There have been numerous catastrophic failures of in service aircraft due to cracks, corrosion, and human errors. Unfortunately, experts involved with this problem frequently reach different conclusions about the cause of the failure. But, in general they all agree that the reduction of human error is needed in inspection and maintenance of the aircraft; particularly aging aircraft which have been in service more than 15 to 19 years. Therefore, the objective of this work is to illustrate how a robotic system can be used for inspection aircraft. A new mobile robot concept for inspection of aircraft is presented. This approach will be especially useful for areas that are on the aircraft fuselage and not within easy reach. The robot can be programmed to follow a specified path while inspecting the structure. Vision and other inspection systems will be used to record the surface condition of the aircraft. The results of inspection regardless of technique (vision, eddy current, etc.), can be transmitted to the technician or an expert system for detection of cracks with/without human involvement. By using several robots simultaneously, the inspection time can be reduced with more consistent results. Author

N90-26347# Idaho National Engineering Lab., Idaho Falls.
FIELD EXPERIENCE IN USING LASER ACOUSTIC SENSING FOR INSPECTION
J. G. Rodriguez, D. M. Tow, and B. A. Barna 1989 5 p
Presented at the 16th Annual Review of Progress in Quantitative Nondestructive Evaluation, Brunswick, GA, 23-28 Jul. 1989
(Contract DE-AC07-76ID-01570)
(DE90-012954; EGG-M-89196; CONF-890770-12) Avail: NTIS HC A01/MF A01

Research being performed to develop a viable noncontacting nondestructive evaluation (NDE) technique for measuring the extent of bonding has led to the development of a laser sensor field system. The noncontacting laser sensor has been used to collect data from diffuse surfaces, such as the Thermal Protection System (TPS) tile on the space shuttle orbiter. The bonded material is gently excited with an acoustic signal, and the displacement is detected and related to the degree of bond. Controlled experiments in the laboratory have provided useful information on the dynamic response of TPS tiles. It has been shown that several candidate signatures are common to all the pedigree tiles. This degree of consistency in the tile-SIP (strain isolation pad) dynamic response proves that an unbond can be detected for a known tile and established the basis for extending the analysis capability to arbitrary tiles for which there is not historical data. The field tests of the noncontacting laser acoustic sensor system, conducted at Kennedy Space Center (KSC), investigated the vibrational environment of the Orbiter Processing Facility (OPF) and its effect

on the measurement and analysis techniques being developed. The data collected showed that for orbiter locations, such as the body flap and elevon, the data analysis scheme, and/or the sensor, will require modification to accommodate the ambient motion. Several methods have been identified for accomplishing this and a solution is seen as readily achievable. It was established that the tile response was similar to that observed in the laboratory. Of the most importance, however, is that the field environment will not affect the physics of the dynamic response that is related to bond condition. All of this information is fundamental to any future design and development of a prototype system. DOE

N90-26348# Rolls-Royce Ltd., Derby (England).
NDT IN AEROSPACE: THE NEXT DECADE (1990'S)
R. G. Taylor 16 Aug. 1989 7 p Presented at the British Inst. Meeting, Minneapolis, MN, 16 Aug. 1989
(PNR90628; ETN-90-97139) Copyright Avail: NTIS HC A02/MF A01

Significant changes taking place in the aerospace industry, particularly in the area of aeroengine manufacture, which will have a considerable impact on the future role of nondestructive testing (NDT), are explained. The role of integrated inspection is discussed. Emphasis is on the manufacturing community rather than in-service NDT. The main changes are product life and reliability, materials development, and manufacturing strategy. ESA

N90-26349# Rolls-Royce Ltd., Derby (England).
THE ROLE OF NDI IN THE CERTIFICATION OF TURBINE ENGINE COMPONENTS
R. G. Taylor, Sharon I. Vukelich, and Thomas D. Cooper (Wright Research Development Center, Wright-Patterson AFB, OH.) 3 Oct. 1989 6 p Presented at the AGARD Specialists Meeting, 3-5 Oct. 1989
(PNR90629; ETN-90-97140) Copyright Avail: NTIS HC A02/MF A01

The historical reasons for the different approaches developed by the United Kingdom and U.S. in the use of NDI (non-destructive inspection) for the certification and lifting of aircraft gas turbine engine components are discussed. The current status of these activities, and future developments which may have the effect of minimizing the differences which exist, are reviewed. ESA

N90-26350# National Aerospace Lab., Amsterdam (Netherlands). Structures and Materials Div.
CHARACTERIZATION OF INSPECTION PERFORMANCE
J. H. Heida 7 Nov. 1988 10 p Presented at the 12th World Conference on Non-Destructive Testing, Amsterdam, Netherlands, 23-28 Apr. 1989
(NLR-MP-88068-U; ETN-90-97193) Avail: NTIS HC A02/MF A01

For a characterization of inspection performance it is necessary to consider both the Probability Of Detection (POD) of defects in flawed specimens and the Probability Of Recognition (POR) of unflawed specimens. Different aspects of this characterization are discussed. The magnetic inspection results of a test specimen population consisting of about 200 identical aircraft landing gear components are used. It is concluded that for a quantitative characterization of the inspection performance, minimum values for both the POD and POR must be established. A way to visualize the inspection performance is a diagram in which both POD and POR are presented. ESA

N90-26351# Technische Univ., Delft (Netherlands).
NONDESTRUCTIVE ONE- AND TWO-DIMENSIONAL DOPING PROFILING BY INVERSE METHODS Ph.D. Thesis
Gerardus Johannes L. Ouwerling 1989 198 p
(ETN-90-97264) Avail: NTIS HC A09/MF A01

Two related numerical methods for the interpretation of electrical measurement data are proposed and applied. They were derived by regarding the determination of the doping profile as an inverse problem; analogies with inverse problems from geophysics and biophysics are found. Both numerical methods rely on the minimization of a least squares error sum of the difference between the measured and simulated electrical characteristics of the device. The first method uses a parametrized model of the doping profile. The second method comprises the iterative solution of a dedicated linear least squares system, that is derived from the internal state of the device. Both methods were successfully applied to real and simulated measurement data from 1-D and 2-D devices. ESA

N90-26352# Grenoble-1 Univ. (France). Techniques de l'informatique, des mathematiques, de la microelectronique et de la Microscopie Quanti
STATISTICAL ANALYSIS OF A SOFTWARE RELIABILITY MODEL [ANALYSE STATISTIQUE D'UN MODELE DE FIABILITE DES LOGICIELS]
Olivier Gaudoni and Jean-Louis Soler Jun. 1989 25 p In FRENCH
(IMAG-RR-781-M; ETN-90-97223) Avail: NTIS HC A03/MF A01

In most of the software reliability studies, the validity of the statistical methods applied is not investigated. An approach is presented in which the quality of the parameter estimators is studied. An accurate analysis of the distribution function is performed. Optimal estimators, obtained by means of the root mean square method, are proposed. A new method for testing the reliability increase is presented. This test is shown to be as suitable as the Laplace test. The test adequacy and validity concerning the model predictions are studied. ESA

N90-26353# Grenoble-1 Univ. (France). Techniques de l'Informatique, des Mathematiques, de la Microelectronique et de la Microscopie Quanti
A BAYESIAN PROPORTIONAL MODEL FOR SOFTWARE RELIABILITY [UN MODELE PROPORTIONNEL BAYESIEN EN FIABILITE DES LOGICIELS]
Olivier Gaudoin, Christian Lavergne, and Jean-Louis Soler Dec. 1989 19 p In FRENCH
(IMAG-RR-795-M; ETN-90-97229) Avail: NTIS HC A03/MF A01

A new model on software reliability, called the Lognormal proportional model is presented. It is based on the Bayesian proportional model (or Moranda geometric model). The hypothesis defining the model came from practical considerations. The parameters' meaning is interpreted as a function of the quality of the corrections performed. By transforming the model into a linear one, with variance components, these parameters are estimated. The asymptotic properties of the estimators are established. A statistical test to compare the models is obtained. ESA

39 STRUCTURAL MECHANICS

Includes structural element design and weight analysis; fatigue; and thermal stress.

For applications see *05 Aircraft Design, Testing and Performance* and *18 Spacecraft Design, Testing and Performance.*

N90-26354*# Georgia Inst. of Tech., Atlanta. School of Aerospace Engineering.
MODELING OF COMPOSITE BEAMS AND PLATES FOR STATIC AND DYNAMIC ANALYSIS Interim Semiannual Report, 17 Jan. - 16 Jul. 1990
Dewey H. Hodges, Ali R. Atilgan, and Bok Woo Lee 1990 30 p Sponsored in part by Army Aerostructures Directorate, Hampton, VA
(Grant NAG1-1094)
(NASA-CR-186459; NAS 1.26:186459) Avail: NTIS HC A03/MF A01 CSCL 20K

A rigorous theory and corresponding computational algorithms was developed for a variety of problems regarding the analysis of composite beams and plates. The modeling approach is intended to be applicable to both static and dynamic analysis of generally anisotropic, nonhomogeneous beams and plates. Development of

a theory for analysis of the local deformation of plates was the major focus. Some work was performed on global deformation of beams. Because of the strong parallel between beams and plates, the two were treated together as thin bodies, especially in cases where it will clarify the meaning of certain terminology and the motivation behind certain mathematical operations. Author

N90-26355*# General Electric Co., Cincinnati, OH. Aircraft Engine Business Group.
ELEVATED TEMPERATURE CRACK GROWTH Final Report
K. S. Kim, R. H. Vanstone, S. N. Malik, and J. H. Laflen Nov. 1988 293 p
(Contract NAS3-23940)
(NASA-CR-182247; NAS 1.26:182247; R89AEB-325) Avail: NTIS HC A13/MF A02 CSCL 20K

A study was performed to examine the applicability of path-independent (P-I) integrals to crack growth problems in hot section components of gas turbine aircraft engines. Alloy 718 was used and the experimental parameters included combined temperature and strain cycling, thermal gradients, elastic-plastic strain levels, and mean strains. A literature review was conducted of proposed P-I integrals, and those capable of analyzing hot section component problems were selected and programmed into the postprocessor of a finite element code. Detailed elastic-plastic finite element analyses were conducted to simulate crack growth and crack closure of the test specimen, and to evaluate the P-I integrals. It was shown that the selected P-I integrals are very effective for predicting crack growth for isothermal conditions. Author

N90-26356# Wichita State Univ., KS. National Inst. for Aviation Research.
A COMPARISON OF THE POST-BUCKLING BEHAVIOR OF METALLIC AND COMPOSITE PLATES WITH CENTRALLY LOCATED CUTOUTS M.S. Thesis
Massud Rouhi May 1990 188 p
(NIAR-90-14) Avail: NTIS HC A09/MF A01

An experimental investigation of the post-buckling characteristics of aluminum, graphite-epoxy, and graphite/PEEK square flat panels with centrally located circular holes is presented. The stability, post-buckling, ultimate strength, and energy absorption behavior of 0.08 inch thick aluminum panels were compared to that of composite plates. A post-buckling test fixture was designed and developed to examine compressive buckling, post-buckling, and failure mechanisms of the panels. Experimental results indicate that both the metallic and composite panels have significant post-buckling strengths and load carrying capabilities well beyond their initial buckling load with similar mode shapes of the buckling and post-buckling deformations. However, the presence of a circular cutout reduces the post-buckling strength of the plate but could actually increase the critical buckling load. The results of an analytical study of this structural response, using the nonlinear capability of the MSC/NASTRAN finite element computer code, were compared with the experimental measurements. Agreement between experimental results and finite element analyses was good. The energy absorption capability of panels was found to be a function of the plate thickness and the diameter of the centrally located hole. Author

N90-26357# Wichita State Univ., KS. Inst. for Aviation Research.
ANALYSIS OF STRAIN RELAXATION IN Au/Ni MULTILAYERS BY X RAY DIFFRACTION
J. Chaudhuri, V. Gondhalekar, S. Shah, and A. F. Jankowski (Lawrence Livermore National Lab., CA.) Nov. 1989 8 p
(Grant NSF DMR-86-05564)
(IAR-89-25) Avail: NTIS HC A02/MF A01

The strain distributions within individual layers in an Au/Ni multilayer system were obtained by an interactive fitting of the experimental x ray diffraction pattern with a kinematic model. The depth profile of strain in the modulation direction was obtained for these metallic multilayers with repeat periodicities ranging from 1.19 nm to 4.26 nm. It was found that the role of interfacial coherency and strengthening is of great importance in understanding the origin of the supermodulus effect in metallic multilayers. Author

N90-26358*# Rockwell International Corp., Canoga Park, CA.
THE STRUCTURAL DYNAMICS ANALYSIS OF THE MAIN INJECTOR LOX INLET TEE AND ITS REDESIGN
E. Romano 1989 26 p Presented at the ASME Computer in Engineering Conference, Anaheim, CA, 1 Jul. 1989
(Contract NAS8-40000)
(NASA-CR-186764; NAS 1.26:186764) Avail: NTIS HC A03/MF A01 CSCL 20K

A ground test of a specially instrumented Space Shuttle Main Engine (SSME) revealed excessively high strains in the high pressure Liquid Oxygen (LOX) inlet line which carries LOX to the Main Injector. The inlet tee acts as a manifold which utilizes two splitter vanes to direct the flow of LOX into the main injector. When the high strains were discovered, it was thought that these splitter vanes, coupled with high energy flow was the source. This resulted not only in high strains in the LOX inlet tee, but excessive vibration at a frequency of 4000 Hz located at the gimbal bearing, and at the main injector. This was later to be known as The 4kHz Phenomenon. The dynamic analysis which was used to predict the response due to the 4kHz phenomenon and the analysis used to aid in the design modification required to the hardware to reduce or eliminate the phenomenon is examined. Author

N90-26359*# National Aeronautics and Space Administration. Lewis Research Center, Cleveland, OH.
DESIGN OF CERAMIC COMPONENTS WITH THE NASA/CARES COMPUTER PROGRAM
Noel N. Nemeth, Jane M. Manderscheid, and John P. Gyekenyesi Apr. 1990 14 p Submitted for publication Original contains color illustrations
(NASA-TM-102369; E-5038; NAS 1.15:102369) Avail: NTIS HC A03/MF A01; 2 functional color pages CSCL 20K

The ceramics analysis and reliability evaluation of structures (CARES) computer program is described. The primary function of the code is to calculate the fast-fracture reliability or failure probability of macro-scopically isotropic ceramic components. These components may be subjected to complex thermomechanical loadings, such as those found in heat engine applications. CARES uses results from MSC/NASTRAN or ANSYS finite-element analysis programs to evaluate how inherent surface and/or volume type flaws component reliability. CARES utilizes the Batdorf model and the two-parameter Weibull cumulative distribution function to describe the effects of multiaxial stress states on material strength. The principle of independent action (PIA) and the Weibull normal stress averaging models are also included. Weibull material strength parameters, the Batdorf crack density coefficient, and other related statistical quantities are estimated from four-point bend bar or uniform uniaxial tensile specimen fracture strength data. Parameter estimation can be performed for a single or multiple failure modes by using a least-squares analysis or a maximum likelihood method. Kolmogorov-Smirnov and Anderson-Darling goodness-to-fit-tests, 90 percent confidence intervals on the Weibull parameters, and Kanofsky-Srinivasan 90 percent confidence band values are also provided. Examples are provided to illustrate the various features of CARES. Author

N90-26360# Oak Ridge National Lab., TN. Metals and Ceramics Div.
INFLUENCE OF THERMAL CONDITIONING MEDIA ON CHARPY SPECIMEN TEST TEMPERATURE
Randy K. Nanstad, Ronald L. Swain, and Reynold G. Berggren 1989 16 p Presented at the Symposium on Charpy Impact Test: Factors and Variables, Orlando, FL, 8-9 Nov. 1989
(Contract DE-AC05-84OR-21400)
(DE90-012784; CONF-8911193-2) Avail: NTIS HC A03/MF A01

The Charpy V-notch (CVN) impact test is used extensively for determining the toughness of structural materials. Research

programs in many technologies concerned with structural integrity perform such testing to obtain Charpy energy vs. temperature curves. American Society for Testing and Materials Method E 23 includes rather strict requirements regarding determination and control of specimen test temperature. It specifies minimum soaking times dependent on the use of liquids or gases as the medium for thermally conditioning the specimen. The method also requires that impact of the specimen occur within 5 s removal from the conditioning medium. It does not, however, provide guidance regarding choice of conditioning media. This investigation was primarily conducted to investigate the changes in specimen temperature which occur when water is used for thermal conditioning. A standard CVN impact specimen of low-alloy steel was instrumented with surface-mounted and embedded thermocouples. Dependent on the media used, the specimen was heated or cooled to selected temperatures in the range -100 to 100 C using cold nitrogen gas, heated air, acetone and dry ice, methanol and dry ice, heated oil, or heated water. After temperature stabilization, the specimen was removed from the conditioning medium while the temperatures were recorded four times per second from all thermocouples using a data acquisition system and a computer. The results show that evaporative cooling causes significant changes in the specimen temperatures when water is used for conditioning. Conditioning in the other media did not result in such significant changes. The results demonstrate that, even within the guidelines of E 23, significant test temperature changes can occur which may substantially affect the Charpy impact test results if water is used for temperature conditioning.
DOE

N90-26361*# National Aeronautics and Space Administration. Langley Research Center, Hampton, VA.
STRUCTURAL MECHANICS DIVISION RESEARCH AND TECHNOLOGY PLANS FOR FY 1990 AND ACCOMPLISHMENTS FOR FY 1989
Kay S. Bales Apr. 1990 99 p
(NASA-TM-102654; NAS 1.15:102654) Avail: NTIS HC A05/MF A01 CSCL 20K

The Objectives, FY 1990 Plans, Approach, and FY 1990 Milestones for the Structural Mechanics Division's research programs are presented. FY 1989 Accomplishments are presented where applicable. This information is useful in program coordination with other governmental organizations in areas of mutual interest.
Author

N90-26362*# National Aeronautics and Space Administration. Langley Research Center, Hampton, VA.
INTERGRATION OF SYSTEM IDENTIFICATION AND ROBUST CONTROLLER DESIGNS FOR FLEXIBLE STRUCTURES IN SPACE
Jer-Nan Juang and Jiann-Shiun Lew (Old Dominion Univ., Norfolk, VA.) Jul. 1990 17 p
(NASA-TM-102695; NAS 1.15:102695) Avail: NTIS HC A03/MF A01 CSCL 20K

An approach is developed using experimental data to identify a reduced-order model and its model error for a robust controller design. There are three steps involved in the approach. First, an approximately balanced model is identified using the Eigensystem Realization Algorithm, which is an identification algorithm. Second, the model error is calculated and described in frequency domain in terms of the H(infinity) norm. Third, a pole placement technique in combination with a H(infinity) control method is applied to design a controller for the considered system. A set experimental data from an existing setup, namely the Mini-Mast system, is used to illustrate and verify the approach.
Author

N90-26363*# National Aeronautics and Space Administration. Langley Research Center, Hampton, VA.
SCALING EFFECTS IN THE STATIC AND DYNAMIC RESPONSE OF GRAPHITE-EPOXY BEAM-COLUMNS Ph.D. Thesis - Virginia Polytechnic Inst. and State Univ.
Karen E. Jackson Jul. 1990 279 p
(NASA-TM-102697; NAS 1.15:102697; AVSCOM-TR-90-B-006) Avail: NTIS HC A13/MF A02 CSCL 20K

Scale model technology represents one method of investigating the behavior of advanced, weight-efficient composite structures under a variety of loading conditions. It is necessary, however, to understand the limitations involved in testing scale model structures before the technique can be fully utilized. These limitations, or scaling effects, are characterized. in the large deflection response and failure of composite beams. Scale model beams were loaded with an eccentric axial compressive load designed to produce large bending deflections and global failure. A dimensional analysis was performed on the composite beam-column loading configuration to determine a model law governing the system response. An experimental program was developed to validate the model law under both static and dynamic loading conditions. Laminate stacking sequences including unidirectional, angle ply, cross ply, and quasi-isotropic were tested to examine a diversity of composite response and failure modes. The model beams were loaded under scaled test conditions until catastrophic failure. A large deflection beam solution was developed to compare with the static experimental results and to analyze beam failure. Also, the finite element code DYCAST (DYnamic Crash Analysis of STructure) was used to model both the static and impulsive beam response. Static test results indicate that the unidirectional and cross ply beam responses scale as predicted by the model law, even under severe deformations. In general, failure modes were consistent between scale models within a laminate family; however, a significant scale effect was observed in strength. The scale effect in strength which was evident in the static tests was also observed in the dynamic tests. Scaling of load and strain time histories between the scale model beams and the prototypes was excellent for the unidirectional beams, but inconsistent results were obtained for the angle ply, cross ply, and quasi-isotropic beams. Results show that valuable information can be obtained from testing on scale model composite structures, especially in the linear elastic response region. However, due to scaling effects in the strength behavior of composite laminates, caution must be used in extrapolating data taken from a scale model test when that test involves failure of the structure.
Author

N90-26364*# National Aeronautics and Space Administration. Lewis Research Center, Cleveland, OH.
APPLICATION OF SYMBOLIC COMPUTATIONS TO THE CONSTITUTIVE MODELING OF STRUCTURAL MATERIALS
Steven M. Arnold, H. Q. Tan, and X. Dong (Akron Univ., OH.) 1990 17 p Proposed for presentation at the 1990 Winter Annual Meeting of ASME, Dallas, TX, 25-30 Nov. 1990
(Grant NAG3-872)
(NASA-TM-103225; E-5641; NAS 1.15:103225) Avail: NTIS HC A03/MF A01 CSCL 20K

In applications involving elevated temperatures, the derivation of mathematical expressions (constitutive equations) describing the material behavior can be quite time consuming, involved and error-prone. Therefore intelligent application of symbolic systems to faciliate this tedious process can be of significant benefit. Presented here is a problem oriented, self contained symbolic expert system, named SDICE, which is capable of efficiently deriving potential based constitutive models in analytical form. This package, running under DOE MACSYMA, has the following features: (1) potential differentiation (chain rule), (2) tensor computations (utilizing index notation) including both algebraic and calculus; (3) efficient solution of sparse systems of equations; (4) automatic expression substitution and simplification; (5) back substitution of invariant and tensorial relations; (6) the ability to form the Jacobian and Hessian matrix; and (7) a relational data base. Limited aspects of invariant theory were also incorporated into SDICE due to the utilization of potentials as a starting point and the desire for these potentials to be frame invariant (objective). The uniqueness of SDICE resides in its ability to manipulate expressions in a general yet pre-defined order and simplify expressions so as to limit expression growth. Results are displayed, when applicable, utilizing index notation. SDICE was designed to aid and complement the human constitutive model developer. A

number of examples are utilized to illustrate the various features contained within SDICE. It is expected that this symbolic package can and will provide a significant incentive to the development of new constitutive theories. Author

N90-26365# Central Research Inst. of Electric Power Industry, Tokyo (Japan). Energy and Environment Lab.
DEVELOPMENT OF CREEP-FATIGUE DAMAGE DETECTION METHOD OF ROTOR STEEL BY ULTRASONIC WAVE MEASUREMENT
Masaaki Matsubara, Akihito Nitta, Shinsuke Sakai, and Hiroyuki Okamura May 1989 60 p In JAPANESE; ENGLISH summary (DE90-503792; CRIE-T-88078) Avail: NTIS (US Sales Only) HC A04/MF A01

Nondestruction test for steam turbine rotor steel was studied in reference to the evaluation study for remainder in life of the aged thermal power generation equipment. According to the existing research, Fourier transform spectrum analysis can be done, and ultrasonic parameter can be accurately evaluated. And attenuation constant is considered to be effective to detect creep-fatigue damage. The accurate measurement for ultrasonic parameter can be realized by this method which was adopted in the study, as the position of probe is precisely controlled by personal computer. Damage distribution and crack initiation can be detected by this method more accurately than the conventional hardness method. Though the detection of local damage is important problem, application of envelope method and spectral method were considered to be effective among attenuation constant evaluation method. About the creep-fatigue damage detection method of rotor steel by ultrasonic wave, effectiveness of this method could be verified by specimen experiment by means of adjustment and establishment of basic technology. DOE

N90-26366# Technische Univ., Berlin (Germany, F.R.). Inst. fuer Luft- und Raumfahrt.
PLATE RODS AND LEAF SPRINGS WITH HYBRID STRUCTURE: CROSS SECTION OPTIMIZATION FOLLOWING DIFFERENT TARGET CRITERIA [PLATTENSTAEBE UND BLATTFEDERN IN HYBRIDBAUWEISE QUERSCHNITT-OPTIMIERTUNG NACH VERSCHIENEN ZIELKRITERIEN]
Reinhard Faass 1989 76 p In GERMAN
(ILR-Mitt-227(1989); ETN-90-97003) Avail: NTIS HC A05/MF A01

The design optimization of plate rods and leaf springs was investigated. The layer thickness of the hybrid (different materials) plate tools was optimized taking into account different design criteria for leaf springs and the elasticity characteristics of the fiber composites which depend on the tensile and compression loading. The advantages of some optimized hybrid cross sections as compared to homogeneous cross sections are discussed. The results of the calculations are confirmed by bend tests on plate rods. ESA

N90-26367# Rolls-Royce Ltd., Derby (England).
FATIGUE LIFE ASSESSMENT USING A SHORT CRACK GROWTH MODEL
J. R. Yates (Sheffield Univ., England) and L. Grabowski 1 Jun. 1990 9 p Presented at Fatigue 1990, Hawaii, Jun. 1990
(PNR90663; ETN-90-97149) Copyright Avail: NTIS HC A02/MF A01

A two stage model was developed to describe the fatigue crack growth of short and long cracks. The model was validated using data obtained from fatigue crack growth studies on Waspaloy. Lifetimes predicted using the model are in good agreement with those observed in experimental work. ESA

N90-26368# Technische Univ., Delft (Netherlands). Faculty of Aerospace Engineering.
THE BLUNT NOTCH BEHAVIOUR OF METAL LAMINATES: ARALL AND GLARE
C. A. J. R. Vermeeren Jan. 1990 63 p
(LR-617; ETN-90-97180) Avail: NTIS HC A04/MF A01

The use of stress concentration factor to describe blunt notch properties of ARALL is evaluated. The blunt notch theory for aluminum alloys is discussed. Results for ARALL laminates are discussed and a test series is proposed. The stress concentration factor value is based on the size and geometry of the notch. For aluminum almost no size effect is found. The size effect for ARALL laminates is investigated by using different specimen widths with the same stress concentration factor value. The failure mechanism for ARALL laminates is different for different fibers. GLARE showed static delamination for certain specimens with high fiber volume percentage. The delamination can level off the stress distribution in the prepreg layer and thus give higher blunt notch strength. ESA

N90-26369# Technische Univ., Delft (Netherlands). Faculty of Aerospace Engineering.
INVESTIGATION OF CRACK-CLOSURE PREDICTION MODELS FOR FATIGUE IN ALUMINIUM ALLOY SHEET UNDER FLIGHT-SIMULATION LOADING
Utama Herawan Padmadinata Mar. 1990 361 p Sponsored by Agency for the Assessment and Application of Technology, Jakarta, Indonesia
(LR-619; ETN-90-97181) Avail: NTIS HC A16/MF A02

The need for crack growth prediction methods for use in the aircraft industry is addressed. Relevant aspects of fatigue macrocrack growth are covered. Characteristics of simulation load histories, restricted to load spectra for aircraft wings, are discussed. The crack closure methods, PREFFAS, ONERA, and CORPUS are considered and results of flight simulation fatigue tests were collected to check the reliability of the models. The analysis of the three models showed that the effect of severe downwards loads is a weak point for all three models. The accuracy obtained with the CORPUS model appeared to be quite acceptable for practical applications. Points for further study revealed by the investigation are summarized. ESA

N90-26370# National Aerospace Lab., Amsterdam (Netherlands). Structures and Materials Div.
STATIC AND FATIGUE STRENGTH OF AN ADHESIVE BONDED CFRP BUTT-STRAP JOINT: THE EFFECTS OF STACKING SEQUENCE AND TEMPERATURE
W. vanderHoeven 28 Feb. 1988 67 p
(Contract NIVR-01408N)
(NLR-TR-88036-U; ETN-90-97184) Avail: NTIS HC A04/MF A01

The effect of temperature and the effect of the orientation of plies directly adjacent to the adhesive layer on the mechanical properties of an adhesive bonded composite joint CFRP (Carbon Fiber Reinforced Plastics) are studied. Static and constant amplitude fatigue tests were performed on bonded double butt-strap joints at 70 C, room temperature and -50 C. Two joint configurations were tested which only varied in the stacking sequence of the bonded adhesive. Analytical and numerical solution techniques were used to calculate the stress distributions in the configurations tested. The results indicated that temperature had a pronounced effect on the mechanical properties of the joint. The static strength increases with decreasing test temperature. Both an increase to 70 C and a decrease to 50 C had a detrimental effect on the fatigue resistance. The largest reductions occurred at 50 C. The stacking sequence in the straps had hardly any effect on the static strength of the joint. Some effect was observed on the fatigue resistance when tested at room temperature. The highest fatigue lives were found for specimens having straps with 0 degrees outer plies. ESA

N90-26371# Costruzioni Aeronautiche Giovanni Agusta S.p.A., Cascina Costa (Italy). Div. Elicotteri.
RESIDUAL STRESSES MEASUREMENTS BY MEANS OF X RAY DIFFRACTION ON ELECTRON BEAM WELDED JOINTS AND LASER HARDENED SURFACES
G. P. Mor (Centro Informazioni Studi Esperienze, Milan, Italy) and R. Pezzoni Jun. 1989 8 p
(ETN-90-97269) Avail: NTIS HC A02/MF A01

X ray diffraction techniques are applied to the evaluation of residual stresses induced by two metallurgical processes: electron beam welding (EBW) and laser surface hardening (LSH) on low alloy steel of aeronautical interest. This technique is shown to be capable of measuring great stress gradients and microstructural strains which can be correlated to the microhardness. In particular, residual stresses distribution is measured with high resolution on AISI 4140 steel surfaces subjected to laser hardening consisting of two successive and partially overlapping tracks on AISI 9310 subjected to EBW. ESA

N90-26372*# State Univ. of New York, Buffalo. Dept. of Mechanical and Aerospace Engineering.
RELIABILITY ANALYSIS OF CONTINUOUS FIBER COMPOSITE LAMINATES Final Report
David J. Thomas and Robert C. Wetherhold Jul. 1990 31 p
(Grant NAG3-862)
(NASA-CR-185265; NAS 1.26:185265) Avail: NTIS HC A03/MF A01 CSCL 20K

A composite lamina may be viewed as a homogeneous solid whose directional strengths are random variables. Calculation of the lamina reliability under a multi-axial stress state can be approached by either assuming that the strengths act separately (modal or independent action), or that they interact through a quadratic interaction criterion. The independent action reliability may be calculated in closed form, while interactive criteria require simulations; there is currently insufficient data to make a final determination of preference between them. Using independent action for illustration purposes, the lamina reliability may be plotted in either stress space or in a non-dimensional representation. For the typical laminated plate structure, the individual lamina reliabilities may be combined in order to produce formal upper and lower bounds of reliability for the laminate, similar in nature to the bounds on properties produced from variational elastic methods. These bounds are illustrated for a (0/plus or minus 15)sub s Graphite/Epoxy (GR/EP) laminate. And addition, simple physically plausible phenomenological rules are proposed for redistribution of load after a lamina has failed. These rules are illustrated by application to (0/plus or minus 15)sub s and (90/plus or minus 45/0)sub s GR/EP laminates and results are compared with respect to the proposed bounds. Author

N90-26373*# National Aeronautics and Space Administration. Lewis Research Center, Cleveland, OH.
STRUCTURAL DYNAMICS BRANCH RESEARCH AND ACCOMPLISHMENTS Report, FY 1989
Jul. 1990 51 p
(NASA-TM-102488; E-5279; NAS 1.15:102488) Avail: NTIS HC A04/MF A01 CSCL 20K

Summaries are presented of fiscal year 1989 research highlights from the Structural Dynamics Branch at NASA Lewis Research Center. Highlights from the branch's major work areas include aeroelasticity, vibration control, dynamic systems, and computation structural methods. A listing of the fiscal year 1989 branch publications is given. Author

N90-26374# Applied Research Lab., State College, PA.
AN EXPERIMENTAL SYSTEM FOR MEASURING THE WAVENUMBER-FREQUENCY RESPONSE OF TIMOSHENKO BEAMS
K. Grosh, W. J. Hughes, and C. B. Burroughs Jun. 1990 312 p
(Contract N00039-88-C-0051)
(AD-A222569; TR-90-007) Avail: NTIS HC A14/MF A02 CSCL 20/11

The wavenumber-frequency response of Timoshenko beams to multiple point drives is studied. An experimental system to excite a free-free Timoshenko beam and measure the resulting velocity is developed. Piezoelectric shakers/force gate units are designed and built to excite the beam and measure the applied forces. Experiments varying the number of shakers used and the wavenumber to which the drive voltage sent to the shakers used and the wavenumber to which the drive voltage sent to the shakers is steered are performed. The wavenumber-frequency dependence of the force and velocity are measured and compared to theoretical predictions. These comparisons show excellent agreement between the measured and theoretical results. A theoretical investigation into the effect of the velocity measurement array is performed. Also, the finite beam admittance is examined. The piezoelectric shakers are modeled using equivalent circuits, which successfully predict the force output and the force gage sensitivity. The experiments show that the wavenumber content of the discrete shakers could be steered to the wavenumbers chosen over a wide frequency range (the frequency range of measurement was 2 to 12 kHz). The finite beam admittance is shown to approach the infinite beam admittance in regions where the wavenumber content of the forcing function are high. GRA

42 GEOSCIENCES (GENERAL)

No abstracts in this category.

43 EARTH RESOURCES AND REMOTE SENSING

Includes remote sensing of earth resources by aircraft and spacecraft; photogrammetry; and aerial photography.

For instrumentation see *35 Instrumentation and Photography.*

N90-26375*# Purdue Univ., West Lafayette, IN. School of Electrical Engineering.
HIRIS PERFORMANCE STUDY
John P. Kerekes and David A. Landgrebe Apr. 1989 40 p
(Grants NAGw-925; NSF ECS-85-07405)
(NASA-CR-186649; NAS 1.26:186649; TR-EE-89-23) Avail: NTIS HC A03/MF A01 CSCL 05B

The remote sensing system simulation is used to study a proposed sensor concept. An overview of the instrument and its parameters is presented, along with the model of the instrument as implemented in the simulation. Signal-to-noise levels of the instrument under a variety of system configurations are presented and discussed. Classification performance under these varying configurations is also shown, along with relationships between signal-to-noise ratios, feature selection, and classification performance. Author

N90-26376*# Purdue Univ., West Lafayette, IN. School of Electrical Engineering.
MODELING, SIMULATION, AND ANALYSIS OF OPTICAL REMOTE SENSING SYSTEMS
John Paul Kerekes and David A. Landgrebe Aug. 1989 201 p
(Grants NAGw-925; NSF ECS-85-07405)
(NASA-CR-186648; NAS 1.26:186648; TR-EE-89-49) Avail: NTIS HC A10/MF A02 CSCL 05B

Remote Sensing of the Earth's resources from space-based sensors has evolved in the past 20 years from a scientific experiment to a commonly used technological tool. The scientific applications and engineering aspects of remote sensing systems have been studied extensively. However, most of these studies have been aimed at understanding individual aspects of the remote sensing process while relatively few have studied their interrelations. A motivation for studying these interrelationships has arisen with the advent of highly sophisticated configurable sensors as part of the Earth Observing System (EOS) proposed by NASA for the 1990's. Two approaches to investigating remote sensing systems are developed. In one approach, detailed models of the scene, the sensor, and the processing aspects of the system are implemented in a discrete simulation. This approach is useful in

creating simulated images with desired characteristics for use in sensor or processing algorithm development. A less complete, but computationally simpler method based on a parametric model of the system is also developed. In this analytical model the various informational classes are parameterized by their spectral mean vector and covariance matrix. These class statistics are modified by models for the atmosphere, the sensor, and processing algorithms and an estimate made of the resulting classification accuracy among the informational classes. Application of these models is made to the study of the proposed High Resolution Imaging Spectrometer (HRIS). The interrelationships among observational conditions, sensor effects, and processing choices are investigated with several interesting results. Author

N90-26377*# Vermont Univ., Burlington. Remote Sensing Applications Program.

[PRACTICAL APPLICATIONS OF REMOTE SENSING TECHNOLOGY] Final Report, 1 Jun. 1978 - 31 May 1987

Roy A. Whitmore, Jr. 1 Aug. 1990 57 p

(Grant NsG-7453)

(NASA-CR-186810; NAS 1.26:186810) Avail: NTIS HC A04/MF A01 CSCL 08B

Land managers increasingly are becoming dependent upon remote sensing and automated analysis techniques for information gathering and synthesis. Remote sensing and geographic information system (GIS) techniques provide quick and economical information gathering for large areas. The outputs of remote sensing classification and analysis are most effective when combined with a total natural resources data base within the capabilities of a computerized GIS. Some examples are presented of the successes, as well as the problems, in integrating remote sensing and geographic information systems. The need to exploit remotely sensed data and the potential that geographic information systems offer for managing and analyzing such data continues to grow. New microcomputers with vastly enlarged memory, multi-fold increases in operating speed and storage capacity that was previously available only on mainframe computers are a reality. Improved raster GIS software systems have been developed for these high performance microcomputers. Vector GIS systems previously reserved for mini and mainframe systems are available to operate on these enhanced microcomputers. One of the more exciting areas that is beginning to emerge is the integration of both raster and vector formats on a single computer screen. This technology will allow satellite imagery or digital aerial photography to be presented as a background to a vector display. Author

N90-26378*# Nebraska Univ., Lincoln. Dept. of Agricultural Meteorology.

MEASURING AND MODELING NEAR-SURFACE REFLECTED AND EMITTED RADIATION FLUXES AT THE FIFE SITE Final Report, 15 Apr. 1987 - 31 May 1990

Blaine L. Blad, Elizabeth A. Walter-Shea, Patrick J. Starks, Roel C. Vining, Cynthia J. Hays, and Mark A. Mesarch Jun. 1990 163 p

(Grant NAG5-894)

(NASA-CR-180953; NAS 1.26:180953; Ag-Met-PR-90-1) Avail: NTIS HC A08/MF A01 CSCL 02F

Information is presented pertaining to the measurement and estimation of reflected and emitted components of the radiation balance. Information is included about reflectance and transmittance of solar radiation from and through the leaves of some grass and forb prairie species, bidirectional reflectance from a prairie canopy is discussed and measured and estimated fluxes are described of incoming and outgoing longwave and shortwave radiation. Results of the study showed only very small differences in reflectances and transmittances for the adaxial and abaxial surfaces of grass species in the visible and infrared wavebands, but some differences in the infrared wavebands were noted for the forbs. Reflectance from the prairie canopy changed as a function of solar and view zenith angles in the solar principal plane with definite asymmetry about nadir. The surface temperature of prairie canopies was found to vary by as much as 5 C depending on view zenith and azimuth position and on the solar azimuth. Aerodynamic temperature calculated from measured sensible heat fluxes ranged from 0 to 3 C higher than nadir-viewed temperatures. Models were developed to estimate incoming and reflected shortwave radiation from data collected with a Barnes Modular Multiband Radiometer. Several algorithms for estimating incoming longwave radiation were evaluated and compared to actual measures of that parameter. Net radiation was calculated using the estimated components of the shortwave radiation streams, determined from the algorithms developed, and from the longwave radiation streams provided by the Brunt, modified Deacon, and the Stefan-Boltzmann models. Estimates of net radiation were compared to measured values and found to be within the measurement error of the net radiometers used in the study. Author

N90-26379# Instituto de Pesquisas Espaciais, Sao Jose dos Campos (Brazil).

PATTERN CLASSIFICATION OF TEXTURA BY MOMENT AND DISTANCE AUTOCORRELATION FUNCTION [CLASSIFICACAO DE AMOSTRAS DE TEXTURA POR MOMENTOS E DISTANCIA DA FUNCAO DE AUTOCORRELACAO]

Silvia Shizueli, Luciano VieiraDutra, and Nelson D. AvilaMascarenhas Oct. 1989 8 p In PORTUGESE Presented at the 4th Latin American Symposium on Remote Sensing, Bariloche, Argentina, 20-24 Nov. 1989

(INPE-4976-PRE/1541) Avail: NTIS HC A02/MF A01

Two methods are developed for classification of textures based on the coefficient function of image autocorrelation (FAC). The first method utilizes a distance between 2 autocorrelation functions, which is defined as the quadratic difference integral between 2 FAC's. The second method utilizes a transformed distance log of FAC force. In both cases an unknown texture is classified as being of the same texture class whose distance is minor. The results are presented using images presented in the scientific writings of Brodatz (1956). Transl. by B. G.

N90-26380# Instituto de Pesquisas Espaciais, Sao Jose dos Campos (Brazil).

HIERARCHICAL STRUCTURE OF POLYGONAL DATA FOR SPATIAL ANALYSIS AND REPRESENTATION OF CARTOGRAPHICAL DATA [ESTRUTURA HIERARQUICA DE DADOS POLIGONAIS PARA ANALISE ESPACIAL E REPRESENTACAO DE DOCUMENTOS CARTOGRAFICOS]

Joao ArgemirodeCarvalhoPaiva and Guaraci Jose Erthal Oct. 1989 9 p In PORTUGESE Presented at the 4th Latin American Symposium on Remote Sensing, Bariloche, Argentina, 20-24 Nov. 1989

(INPE-4986-PRE/1548) Avail: NTIS HC A02/MF A01

Methodologies are shown which were developed and utilized within the Geographic Information System (GIS) of INPE, by generating a polygonal data structure, which permits the best representation between thematic bodies, and a rapid and efficient recovery, analysis, and selection of bodies when plotting data. The two basic bodies, lines and polygons, are described as stored forms and generated topology, which are utilized for the analysis and visual representation of polygonal data. Transl. by B. G.

N90-26381# Instituto de Pesquisas Espaciais, Sao Jose dos Campos (Brazil).

CLASSIFICATION REGIONS IN REMOTE SENSING IMAGERY UTILIZING SPATIAL CHARACTERISTICS [CLASSIFICACAO DE REGIOES EM IMAGENS DE SENSORIAMENTO REMOTO UTILIZANDO ATRIBUTOS ESPACIAIS]

Sueli PissarraCastellari and Luciano VieiraDutra Oct. 1989 8 p In PORTUGESE Presented at the 4th Latin American Symposium on Remote Sensors, Bariloche, Argentina, 20-24 Nov., 1989

(INPE-4913-PRE/1514) Avail: NTIS HC A02/MF A01

The performance of two pattern classifiers which utilize spatial conjuncture characteristics with spectral characteristics are studied. The spatial characteristics were obtained with the use of a variation operator (Dutra and Mascarenhas, 1984) on original channel texture. The result of this operator is filtered by a bandpass filter with a 3 x 3 core for reducing the influence of noise and the

resultant channel, as well as the original, are utilized with characteristics for pattern classifiers. The results of these pattern classifiers are evaluated and compared with the results of pattern classification for the majority of point classes of the pattern classifiers in a point by point scheme. Transl. by B. G.

N90-26382*# Massachusetts Inst. of Tech., Cambridge. Center for Electromagnetic Theory and Applications.
REMOTE SENSING OF EARTH TERRAIN Semiannual Progress Report, 1 Jan. - 30 Jun. 1990
Jin Au Kong and Herng-Aung Yueh 30 Jun. 1990 20 p
(Grant NAGw-1617)
(NASA-CR-186888; NAS 1.26:186888) Avail: NTIS HC A03/MF A01 CSCL 08B

The layered random medium model is used to investigate the fully polarimetric scattering of electromagnetic waves from vegetation. The vegetation canopy is modeled as an anisotropic random medium containing nonspherical scatterers with preferred alignment. The underlying medium is considered as a homogeneous half space. The scattering effect of the vegetation canopy are characterized by 3-D correlation functions with variances and correlation lengths respectively corresponding to the fluctuation strengths and the physical geometries of the scatterers. The strong fluctuation theory is used to calculate the anisotropic effective permittivity tensor of the random medium and the distorted Born approximation is then applied to obtain the covariance matrix which describes the fully polarimetric scattering properties of the vegetation field. This model accounts for all the interaction processes between the boundaries and the scatterers and includes all the coherent effects due to wave propagation in different directions such as the constructive and destructive interferences. For a vegetation canopy with low attenuation, the boundary between the vegetation and the underlying medium can give rise to significant coherent effects. Author

N90-26383# Grenoble-1 Univ. (France). Lab. d'Informatique Fondamentale et d'Intelligence Artificielle.
SURFACE RECONSTRUCTION BASED ON CRITICAL CONTOURS IN A MULTI-IMAGE CONTEXT [RECONSTRUCTION DE SURFACES A PARTIR DES CONTOURS CRITIQUES, DANS UN CONTEXTE MULTI-IMAGES]
Emmanuel Arbogast and Roger Mohr 14 Jun. 1989 19 p In FRENCH; ENGLISH summary
(RR-784-I-IMAG-94-LIFIA; ETN-90-97236) Avail: NTIS HC A03/MF A01

It is shown that the observation of occluding contours combined with camera movement allows reconstruction of the observed surface. The results are demonstrated under very light constraints, generalizing previous results. The technique is shown to be applicable to any movement of the camera, under perspective projection with surfaces observed in parts or even with lines of discontinuity. One of the advantages of the technique is in obtaining natural parallelization. The algorithm used allows for simple segmentation into parallel processes with pipeline intercommunication. ESA

N90-26384*# National Aeronautics and Space Administration. Pasadena Office, CA.
IMPROVING THE GEOMETRIC FIDELITY OF IMAGING SYSTEMS EMPLOYING SENSOR ARRAYS Patent Application
Kenneth L. Jones, inventor (to NASA) (Jet Propulsion Lab., California Inst. of Tech., Pasadena.) 28 Jun. 1990 19 p
(Contract NAS7-918)
(NASA-Case-NPO-17970-1-CU; NAS 1.71:NPO-17970-1-CU; US-Patent-Appl-SN-545014) Avail: NTIS HC A03/MF A01 CSCL 14B

A sensor assembly to be carried on an aircraft or spacecraft which will travel along an arbitrary flight path, for providing an image of terrain over which the craft travels, is disclosed. The assembly includes a main linear sensor array and a plurality of auxiliary sensor arrays oriented parallel to, and at respectively different distances from, the main array. By comparing the image signals produced by the main sensor array with those produced by each auxiliary array, information relating to variations in velocity of the craft carrying the assembly can be obtained. The signals from each auxiliary array will provide information relating to a respectively different frequency range. NASA

N90-26385# Forschungsinstitut fuer Informationsverarbeitung, Ettlingen (Germany, F.R.).
AUTOMATIC LINE NETWORK EXTRACTION FROM AERIAL IMAGERY OF URBAN AREAS THROUGH KNOWLEDGE BASED IMAGE ANALYSIS Final Technical Report, Nov. 1986 - Aug. 1989
H. Fueger, K. Jurkiewicz, H. Kazmierczak, B. Nicolin, and W. Ott Aug. 1989 161 p
(Contract DAJA45-86-C-0049; DA Proj. 1L1-61102-BH-57)
(AD-A222675; FIM-209; R/D-5679-EN-01; ETL-0568) Avail: NTIS HC A08/MF A01 CSCL 08/5

Different methods for automatic detection of line objects applied to aerial images to extract streets from urban scenes are investigated. First, test results achieved from two existing methods of low level iconic image processing by stream following (line tracking) and structured parallel operations (image filtering, feature extraction) are given. Second, a medium level iconic image processing method developed for edge and area segmentation is described and results from image segmentation are presented symbolically. Then two preliminary approaches of high level symbolic processing by knowledge based blackboard oriented structure analysis are tested. One is originating with preprocessing by low level edge filtering, the other by medium level area segmentation. First results from the image understanding method for street network extraction are presented. GRA

44 ENERGY PRODUCTION AND CONVERSION

Includes specific energy conversion systems, e.g., fuel cells; global sources of energy; geophysical conversion; and windpower.

For related information see also *07 Aircraft Propulsion and Power, 20 Spacecraft Propulsion and Power,* and *28 Propellants and Fuels.*

N90-26386# Sandia National Labs., Albuquerque, NM.
SILICON CONCENTRATOR SOLAR CELL DEVELOPMENT
Martin A. Green, Zhao Jianhua, Wang Aihua, and A. W. Blakers (New South Wales Univ., Kensington, Australia) May 1990 53 p
(Contract DE-AC04-76DP-00789)
(DE90-011782; SAND-89-7043) Avail: NTIS HC A04/MF A01

This project involved the development and supply of 550 silicon concentrator solar cells for use in prototype point-focus concentrator modules. The cells were to have a designed illumination area of 12.5 by 12.5 mm and to be designed for use with prismatic covers at a geometric concentration ratio of 200X. The target efficiency of 24 percent was comfortably exceeded, with efficiencies as high as 25.2 percent reached in the designed concentration ratio range. A combined lens/cell efficiency of 24.4 percent was measured at Sandia using a cell supplied during this project and a point focus Fresnel lens. Subsequently, a peak module efficiency of 20.3 percent was achieved at Sandia using 12 cells and lenses. This is believed to be the first photovoltaic module to surpass the 20 percent efficiency milestone. DOE

N90-26387# Sandia National Labs., Albuquerque, NM.
DENDRITIC WEB SILICON PHOTOVOLTAIC CELL RESEARCH
J. A. Easoz, R. Rosey, R. B. Campbell, R. Rupnik, R. P. Sprecace, P. A. Piotrowski, J. P. McHugh, and R. G. Seidensticker (Westinghouse Electric Corp., Pittsburgh, PA.) May 1990 32 p
(Contract DE-AC04-76DP-00789)
(DE90-011786; SAND-89-7044) Avail: NTIS HC A03/MF A01

The evaluation is summarized of a checkpoint demonstration of the throughout capability of the silicon dendritic web growth

process. The demonstrated throughput of about 20,000 sq.cm/furnace/week was less than desired for a commercial production facility, however the results clearly indicated that the desired 35,000 sq.cm/furnace/week would be reached with continuous melt replenishment during growth. Improvements in seeding and increase in crystal length would increase the throughput even more. Solar cells subsequently fabricated on the material grown during the demonstration had average efficiency levels (14 percent) equivalent to cells fabricated on web produced prior to the demonstration run. Finally, a business analysis based on the present results gave estimated photovoltaic module costs in agreement with potential commercial viability. DOE

N90-26388# Helsinki Univ. of Technology, Espoo (Finland).
THE USE OF HYDROGEN IN ENERGY ECONOMY OF FINLAND
Vesa Arpiainen (Technical Research Centre of Finland, Espoo.) Sep. 1989 96 p In FINNISH; ENGLISH summary
(DE90-796180; NEMO-13) Avail: NTIS (US Sales Only) HC A05/MF A01

In this preliminary survey the possibilities of using hydrogen in energy supply are examined. The survey is based on domestic and international literature. DOE

N90-26389# Sandia National Labs., Albuquerque, NM.
APPLICATION OF InAlAs/GaAs SUPERLATTICE ALLOYS TO GaAs SOLAR CELLS
T. J. Drummond, J. Gee, F. L. Terry, and R. Weng (Michigan Univ., Ann Arbor.) 1990 6 p Presented at the 21st IEEE Photovoltaic Specialists Conference, Kissimmee, FL, 21-25 May 1990
(Contract DE-AC04-76DP-00789)
(DE90-013070; SAND-90-1560C; CONF-900542-13) Avail: NTIS HC A02/MF A01

AlGaAs/GaAs solar cells are typically characterized as having relatively high interface recombination velocities at the heteroface. This work examines some of the factors influencing the design of solar cell window layers and considers the effect of substituting InAlAs/GaAs superlattice alloys and InAlAs bulk alloys in place of AlGaAs. Potential advantages are reduced surface recombination at the heterojunction, reduced thermionic emission into the window layer, thinner window layers and reduced absorption in the window layer. DOE

N90-26390# Idaho National Engineering Lab., Idaho Falls. Fusion Safety Program.
PARAMETRIC DESIGN STUDIES OF TOROIDAL MAGNETIC ENERGY STORAGE UNITS
J. Stephen Herring 1990 7 p Presented at the 25th Intersociety Energy Conversion Engineering Conference, Reno, NV, 12-17 Aug. 1990 Submitted for publication
(Contract DE-AC07-76ID-01570)
(DE90-013086; EGG-M-89521; CONF-900801-15) Avail: NTIS HC A02/MF A01

Superconducting magnetic energy storage (SMES) units have a number of advantages as storage devices. Electrical current is the input, output and stored medium, allowing for completely solid-state energy conversion. The magnets themselves have no moving parts. The round trip efficiency is higher than those for batteries, compressed air or pumped hydro. Output power can be very high, allowing complete discharge of the unit within a few seconds. Finally, the unit can be designed for a very large number of cycles, limited basically by fatigue in the structural components. A small systems code was written to produce and evaluate self-consistent designs for toroidal superconducting energy storage units. The units can use either low temperature or high temperature superconductors. The coils have D shape where the conductor and its stabilizer/structure is loaded only in tension and the centering forces are borne by a bucking cylinder. The coils are convectively cooled from a cryogenic reservoir in the bore of the coils. The coils are suspended in a cylindrical metal shell which protects the magnet during rail, automotive or shipboard use. It is important to note that the storage unit does not rely on its surroundings for structural support, other than normal gravity and inertial loads. Designs are presented for toroidal energy storage units produced by the systems code. A wide range of several parameters have been considered, resulting in units storing from 1 MJ to 72 GJ. Maximum fields range from 5 T to 20 T. The masses and volumes of the coils, bucking cylinder, coolant, insulation and outer shell are calculated. For unattended use, the allowable operating time using only the boiloff of the cryogenic fluid for refrigeration is calculated. For larger units, the coils were divided into modules suitable for normal truck or rail transport. DOE

N90-26391*# Washington Univ., Seattle. Dept. of Aeronautics and Astronautics.
MEGAWATT SOLAR POWER SYSTEMS FOR LUNAR SURFACE OPERATIONS Final Report
Brian Adams, Sam Alhadeff, Shawn Beard, David Carlile, David Cook, Craig Douglas, Don Garcia, David Gillespie, Raymond Golingo, and Drew Gonzalez et al 21 Jun. 1990 228 p
(Grant NGT-21-002-800)
(NASA-CR-186509; NAS 1.26:186509; AA-420; AA-421) Avail: NTIS HC A11/MF A02 CSCL 10B

Lunar surface operations require habitation, transportation, life support, scientific, and manufacturing systems, all of which require some form of power. As an alternative to nuclear power, the development of a modular one megawatt solar power system is studied, examining both photovoltaic and dynamic cycle conversion methods, along with energy storage, heat rejection, and power backup subsystems. For photovoltaic power conversion, two systems are examined. First, a substantial increase in photovoltaic conversion efficiency is realized with the use of new GaAs/GaSb tandem photovoltaic cells, offering an impressive overall array efficiency of 23.5 percent. Since these new cells are still in the experimental phase of development, a currently available GaAs cell providing 18 percent efficiency is examined as an alternate to the experimental cells. Both Brayton and Stirling cycles, powered by linear parabolic solar concentrators, are examined for dynamic cycle power conversion. The Brayton cycle is studied in depth since it is already well developed and can provide high power levels fairly efficiently in a compact, low mass system. The dynamic conversion system requires large scale waste heat rejection capability. To provide this heat rejection, a comparison is made between a heat pipe/radiative fin system using advanced composites, and a potentially less massive liquid droplet radiator system. To supply power through the lunar night, both a low temperature alkaline fuel cell system and an experimental high temperature monolithic solid-oxide fuel cell system are considered. The reactants for the fuel cells are stored cryogenically in order to avoid the high tankage mass required by conventional gaseous storage. In addition, it is proposed that the propellant tanks from a spent, prototype lunar excursion vehicle be used for this purpose, therefore resulting in a significant overall reduction in effective storage system mass. Author

N90-26392# Midwest Research Inst., Golden, CO.
INTERIM QUALIFICATION TESTS AND PROCEDURES FOR TERRESTRIAL PHOTOVOLTAIC THIN-FILM FLAT-PLATE MODULES
R. DeBlasio, L. Mrig, and D. Waddington Jan. 1990 25 p
(Contract DE-AC02-83CH-10093)
(DE90-000354; SERI/TR-213-3624) Avail: NTIS HC A03/MF A01

This document provides recommended procedures and specifications for qualification tests that are structured to evaluate terrestrial thin-film flat-plate photovoltaic nonconcentrating modules intended for power generation applications. The qualification tests provided in this document are designed to evaluate flat-plate thin-film photovoltaic (PV) module design performance and susceptibility to known failure mechanisms. Emphasis is placed on testing and evaluating module performance characteristics and design features that will affect possible degradation of module performance and physical properties resulting from solar exposure, environmental weathering, mechanical loading, corrosion, and

module shadowing. Because of limited thin-film module field operation experience and the evolutionary nature of new thin-film module material technologies and designs, these tests should not be considered definitive or complete, nor do they provide a basis to predict 30-year field life. Current understanding of failure and degradation mechanisms and the relationship between accelerated tests and field reliability is not sufficient to allow accurate estimation of life-expectancy, nor are the cycling tests given in this document considered to be equivalent to a full 30-year field exposure. However, the test and evaluation procedures given in this document provide a common approach for conducting qualification tests. Acceptable results from these tests should provide reasonable assurance that the modules that pass these tests will perform reliably in the field but for an unspecified period of time. DOE

N90-26393# Morgantown Technology Center, WV. Office of Fossil Energy.

HEAT ENGINES Technology Status Report

N. F. Rekos, Jr., ed. and E. L. Parsons, Jr., ed. Sep. 1989 38 p

(DE90-000485; DOE/METC-90-0267) Avail: NTIS HC A03/MF A01

For the past decade, the Department of Energy (DOE) has sponsored projects to develop diesel and gas turbine engines capable of operating on low-cost, coal-based fuels. Much of the current work addresses the use of coal-water fuel (CWF) in diesel and turbines, although there is some work with dry coal feed and other coal fuels. Both the diesel and gas turbine portions of the program include proof-of-concept and support projects. Specific highlights of the program include: engine tests and economic analyses have shown that CWF can replace 70 percent of the diesel oil used in the duty cycle of a typical main-line locomotive; A. D. Little and Cooper-Bessemer completed a system and economic study of coal-fueled diesel engines for modular power and industrial cogeneration markets. The coal-fueled diesel was found to be competitive at fuel oil prices of $5.50 per million British thermal units (MBtu); Over 200 hours of testing have been completed using CWF in full-scale, single-cylinder diesel engines. Combustion efficiencies have exceeded 99 percent; Both CWF and dry coal fuel forms can be burned in short residence time in-line combustors and in off-base combustors with a combustion efficiency of over 99 percent; Rich/lean combustion systems employed by the three major DOE contractors have demonstrated low NO(sub x) emissions levels; Contractors have also achieved promising results for controlling sulfur oxide (SO(sub x)) emissions using calcium-based sorbents; Slagging combustors have achieved between 65 and 95 percent slag capture, which will limit particulate loading on pre-turbine cleanup devices. For many of the gas turbine and diesel applications emission standards do not exist. Our goal is to develop coal-fueled diesels and gas turbines that not only meet all applicable emission standards that do exist, but also are capable of meeting possible future standards. DOE

N90-26394# Deutsche Forschungsanstalt fuer Luft- und Raumfahrt, Stuttgart (Germany, F.R.). Gruppe Solarenergiewandlung.

QUALIFICATION OF CONCENTRATING MIRROR SYSTEMS WITH THE HERMES MEASUREMENT SYSTEM AND THE HELIOS SIMULATION PROGRAM

Juergen Kleih Aug. 1989 53 p In GERMAN; ENGLISH summary

(DLR-FB-89-51; ISSN-0171-1342; ETN-90-97005) Avail: NTIS HC A04/MF A01; DLR, VB-PL-DO, Postfach 40 60 58, 5000 Cologne, Fed. Republic of Germany, 22.50 Deutsche marks

An overview of direct and indirect methods of measuring highly concentrated solar radiation is presented. The methods are used to qualify solar power plants (parabolic dishes up to tower systems). The HERMES measuring system is described. HERMES is used to examine two membrane concentrators, 17 and 7.5 m in diameter. Maximum measured values of radiant flux density are greater than 2 mw/sq m for the 17 m mirror and greater than 9 mw/sq m for the 7.5 mirror, normalized to a direct insolation of 800 w/sq m. The HELIOS computer code is used as a checking tool for the measurements. Acceptable agreement between the measurements and calculated values is found. ESA

N90-26395# Research Inst. of National Defence, Stockholm (Sweden). Dept. of Weapon Systems, Effects, and Protection.

A SEARCH ROUTINE FOR OPTIMIZATION IN A WIND POWER SYSTEM WITH VARIABLE SPEED

Bertil Landkvist and Eskil Ulen Jan. 1990 17 p In SWEDISH; ENGLISH summary

(FOA-C-20779-2.1; ISSN-0347-3694; ETN-90-97098) Avail: NTIS HC A03/MF A01

Windpowered machines with variable speed should normally go with optimal velocity ratio. A practical experience with a search routine is described, which automatically gives the gain in the necessary feedback loop. If the wind increases or decreases, the engine seeks another optimum. A velocity distribution diagram, before the system reaches a steady state, is presented. Important parameters (independent variables) were tested. ESA

N90-26396*# National Aeronautics and Space Administration. Lewis Research Center, Cleveland, OH.

MODELING AND OPTIMIZATION OF A REGENERATIVE FUEL CELL SYSTEM USING THE ASPEN PROCESS SIMULATOR

Thomas M. Maloney (Sverdrup Technology, Inc., Brook Park, OH.) and Harold F. Leibecki 1990 7 p Presented at the 25th Intersociety Energy Conversion Engineering Conference, Reno, NV, 12-17 Aug. 1990; cosponsored by AIChE, ANS, SAE, ACS, AIAA, ASME, and IEEE

(NASA-TM-103210; E-5618; NAS 1.15:103210) Avail: NTIS HC A02/MF A01 CSCL 10C

The Hydrogen-Oxygen Regenerative Fuel Cell System was identified as a key component for energy storage in support of future lunar missions. Since the H2-O2 regenerative electrochemical conversion technology has not yet been tested in space applications, it is necessary to implement predictive techniques to develop initial feasible system designs. The ASPEN simulation software furnishes a constructive medium for analyzing and for optimizing such systems. A rudimentary regenerative fuel cell system design was examined using the ASPEN simulator and this modular approach allows for easy addition of supplementary ancillary components and easy integration with life support systems. The modules included in the preliminary analyses may serve as the fundamental structure for more complicated energy storage systems. Author

N90-26397*# National Aeronautics and Space Administration. Lewis Research Center, Cleveland, OH.

NASA AEROSPACE FLIGHT BATTERY SYSTEMS PROGRAM

Michelle A. Manzo and Patricia M. ODonnell 1990 7 p Presented at the 25th Intersociety Energy Conversion Engineering Conference, Reno, NV, 12-17 Aug. 1990; cosponsored by AIChE, ANS, SAE, ACS, AIAA, ASME, and IEEE

(NASA-TM-103237; E-5656; NAS 1.15:103237) Avail: NTIS HC A02/MF A01 CSCL 10C

The major objective of the NASA Aerospace Flight Battery Systems Program is to provide NASA with the policy and posture to increase and ensure the safety, performance and reliability of batteries for space power systems. The program plan has been modified in the past year to reflect changes in the agency's approach to battery related problems that are affecting flight programs. Primary attention in the Battery Program is being devoted to the development of an advanced nickel-cadmium cell design and the qualification of vendors to produce cells for flight programs. As part of a unified Battery Program, the development of a nickel-hydrogen standard and primary cell issues are also being pursued to provide high performance NASA Standards and space qualified state-of-the-art primary cells. The resolution of issues is being addressed with the full participation of the aerospace battery community. Author

45 ENVIRONMENT POLLUTION

Includes atmospheric, noise, thermal, and water pollution.

N90-26398# Office of Technology Assessment, Washington, DC.
CATCHING OUR BREATH: NEXT STEPS FOR REDUCING URBAN OZONE
Jul. 1989 249 p
(PB90-130451; OTA-O-412) Avail: NTIS HC A11/MF A02; SOD HC $10.00 as 052-003-01158-1 CSCL 13B

A third attempt is made to craft an ozone control program which raises several controversial issues: How great a threat ozone poses to human health, agricultural production, and environmental welfare; What technical measures to take against this hard to control pollutant; and How to encourage development of new controls. Some areas of discussion are: Ozone and the Clean Air Act; Health effects of ozone; Effect of ozone on crops and forests; Lowering ozone; Effects of controlling volatile organic compounds and nitrogen oxides; Controlling emissions of volatile organic compounds; and New opportunities for controlling ozone. Author

N90-26399*# National Aeronautics and Space Administration. Langley Research Center, Hampton, VA.
MEASUREMENTS OF TROPOSPHERIC NITRIC ACID OVER THE WESTERN UNITED STATES AND NORTHEASTERN PACIFIC OCEAN
P. J. LeBel, B. J. Huebert, H. I. Schiff, S. A. Vay, S. E. VanBramer, and D. R. Hastie (York Univ., Ontario) 1990 25 p Submitted for publication
(NASA-TM-103470; NAS 1.15:103470) Avail: NTIS HC A03/MF A01 CSCL 13B

Over 240 measurements of nitric acid (HNO3) were made in the free troposphere as well as in the boundary layer. Marine HNO3 measurement results were strikingly similar to results from GAMETAG and other past atmospheric field experiments. The marine boundary layer HNO3 average, 62 parts-per-trillion by volume (pptv), was 1/3 lower than the marine free tropospheric average, 108 pptv, suggesting that the boundary layer is a sink for tropospheric nitric acid, probably by dry deposition. Nitric acid measurements on a nighttime continental flight gave a free tropospheric average of 218 pptv, substantially greater than the daytime continental free tropospheric 5-flight average of 61 pptv. However, the nighttime results may be influenced by highly convective conditions that existed from thunderstorms in the vicinity during that night flight. The continental boundary layer HNO3 average of 767 pptv is an order of magnitude greater than the free tropospheric average, indicating that the boundary layer is a source of free tropospheric HNO3. The distribution of continental boundary layer HNO3 data, from averages of 123 over rural Nevada and Utah to 1057 pptv in the polluted San Joaquin Valley of California suggest a close tie between boundary layer HNO3 and anthropogenic activity. Author

N90-26400*# National Aeronautics and Space Administration. Langley Research Center, Hampton, VA.
MEASUREMENTS OF CH4, N2O, CO, H2O AND O3 IN THE MIDDLE ATMOSPHERE BY THE ATMOS EXPERIMENT ON SPACELAB 3
M. R. Gunson, C. B. Farmer, R. H. Norton, R. Zander, C. P. Rinsland, J. H. Shaw, and Bo-Cai Gao (Ohio State Univ., Columbus.) 1989 68 p Submitted for publication
(NASA-TM-103476; NAS 1.15:103476) Avail: NTIS HC A04/MF A01 CSCL 13B

The volume mixing ratios of five minor gases (CH4, N2O, CO, H2O, and O3) were retrieved through the middle atmosphere from the analysis of 0.01/cm resolution infrared solar occultation spectra recorded near 28 N and 48 S latitudes with the ATMOS (Atmospheric Trace Molecule Spectroscopy) instrument, flown on board Spacelab 3. The results, which constitute the first simultaneous observations of continuous profiles through the middle atmosphere for these gases, are in general agreement with reported measurements from ground, balloon and satellite-based instruments for the same seasons. In detail, the vertical profiles of these gases show the effects of the upper and middle atmospheric transport patterns dominant during the season of these observations. The profiles inferred at different longitudes around 28 N suggest a near-uniform zonal distribution of these gases. Although based on fewer observations, the sunrise occultation measurements point to a larger variability in the vertical distribution of these gases at 48 S. Author

N90-26401*# National Aeronautics and Space Administration. Langley Research Center, Hampton, VA.
THE GLOBAL CONSEQUENCES OF INCREASING TROPOSPHERIC OZONE CONCENTRATIONS
Jack Fishman Feb. 1989 20 p Submitted for publication
(NASA-TM-103477; NAS 1.15:103477) Avail: NTIS HC A03/MF A01 CSCL 13B

Recent analyses of long term records of tropospheric ozone measurements in the Northern Hemisphere suggest that it is increasing at a rate of 1 to 2 percent per year. Because of this, it is argued that the amount of atmospheric warming due to increasing tropospheric ozone is comparable to, or possibly even greater than, the amount of warming due to the increase of carbon dioxide. Unlike all other climatically important trace gases, ozone is toxic, and increases in its concentration will result in serious environmental damage, as well as impairment of human health. Author

N90-26402*# National Aeronautics and Space Administration. Langley Research Center, Hampton, VA.
NEW OBSERVATIONS OF STRATOSPHERIC N2O5
C. P. Rinsland, G. C. Toon, C. B. Farmer, R. H. Norton, and J. S. Namkung (ST Systems Corp., Hampton, VA.) 1989 39 p Submitted for publication
(Contract NAS1-18460)
(NASA-TM-103478; NAS 1.15:103478) Avail: NTIS HC A03/MF A01 CSCL 13B

The unequivocal detection of N2O5 in the stratosphere was reported by Toon et al. based on measurements of the absorption by the N2O5 bands at 1246 and 1720/cm in solar occulation spectra recorded at sunrise near 47 S latitude by the Atmospheric Trace Molecule Spectroscopy (ATMOS) experiment during the Spacelab 3 (SL3) shuttle mission. Additional measurements and analysis of stratospheric N2O5 derived from the ATMOS/SL3 spectra are reported. The primary results are the detection and measurement of N2O5 absorption at sunset in the lower stratosphere, the inversion of a precise (approximately 10 percent) N2O5 sunrise vertical distribution between 25.5 and 37.5 km altitude, and the identification and measurement of absorption by the N2O5 743/cm band at sunrise. Assuming 4.32 x 10(sup -17) and 4.36 x 10(sup -17)/cm/molecule/sq cm respectively for the integrated intensities of the 1246 and 743/cm bands at stratospheric temperatures, retrieved volume mixing ratios in parts per billion by volume (ppbv) at sunrise (47 S latitude) are 1.32 + or - 0.34 at 37.5 km, 1.53 + or - 0.35 at 35.5 km, 1.63 + or - 0.36 at 33.5 km, 1.60 + or - 0.34 at 31.5 km, 1.43 + or - 0.30 at 29.5 km, 1.15 + or - 0.24 at 27.5 km, and 0.73 + or - 0.15 at 25.5 km. Retrieved VMRs in ppbv at sunset (30 N latitude) are 0.13 + or - 0.05 at 29.5 km, 0.14 + or - 0.05 at 27.5 km, and 0.10 + or - 0.04 at 25.5 km. Quoted error limits (1 sigma) include the error in the assumed band intensities (approximately 20 percent). Within the error limits of the measurements, the inferred mixing ratios at sunrise agree with diurnal photochemical model predictions obtained by two groups using current photochemical data. The measured mixing ratios at sunset are lower than the model predictions with differences of about a factor of 2 at 25 km altitude. Author

N90-26403# Stockholm Univ. (Sweden). Dept. of Meteorology.
NORDIC SYMPOSIUM ON ATMOSPHERIC CHEMISTRY
Howard B. Ross, ed. Mar. 1990 121 p Symposium held in Stockholm, Sweden, 6-8 Dec. 1989
(CM-78; ISSN-0280-445X; ETN-90-97038) Avail: NTIS HC A06/MF A01

The papers given at the Nordic symposium on atmospheric chemistry are presented. Deposition on the Baltic sea, the study of long range transport and deposition of pollutants, and an atmospheric chemistry trajectory model are discussed. Global tropospheric sulfur simulations, the relative importance of greenhouse gases, and vertical ozone probing are described. The transfer of mercury between the atmosphere and lake or soil surfaces and measurement of turpenes in coniferous forests are described. The formation and kinetics of N2O and the photodissociation of N2O in the stratosphere and mesosphere are discussed. The partitioning of H2SO4 in clouds is described. For individual titles, see N90-26404 through N90-26430.

N90-26404# Finnish Meteorological Office, Helsinki. Air Quality Dept.
DEPOSITION TO THE BALTIC SEA
Sylvain M. Joffre *In* Stockholm Univ., Nordic Symposium on Atmospheric Chemistry Mar. 1990 4 p Sponsored in part by Nordic Council of Ministers (For primary document see N90-26403 20-45)
Avail: NTIS HC A06/MF A01

The total deposition of sulfur (SO2, SO4) and nitrogen (NO2, NH3, NO3 and NH4) in the Baltic sea area is studied. The values presented are based on an atmospheric model and on a scarce number of actual measurements. Both model and observational results give a total annual deposition of 1.1 to 1.4 g(S)/sq m for sulfur compounds. For nitrogen compounds a discrepancy appears between the two types of estimates. Total nitrogen deposition is estimated at 0.6 to 1.3 g(N)/sq m. Wet deposition represents 60 percent of total sulfur deposition and 80 percent of total nitrogen deposition. The large scatter of these estimates indicates significant variability in the processes. An analytical rather than a bulk approach is called for. ESA

N90-26405# Norwegian Meteorological Inst., Blindern.
VERIFICATION AND IMPROVEMENT OF THE EMEP MODEL FOR LONG-RANGE TRANSPORT AND DEPOSITION OF POLLUTANTS
Hilde Sandnes *In* Stockholm, Univ., Nordic Symposium on Atmospheric Chemistry Mar. 1990 3 p (For primary document see N90-26403 20-45)
Avail: NTIS HC A06/MF A01

The chemical and meteorological activities of European Monitoring and Evaluation Program (EMEP) are described. EMEP is a cooperative program for monitoring and evaluating the long range transmission of air pollutants in Europe. Over the period of 1980 to 1986 a decrease of 16.4 percent was seen in European sulfur emission. Model experiments carried out to estimate the concentration changes due to emission regulations and the meteorological factors are described. The ability of the model to predict the concentrations observed is tested. A NOX model run between 1985 and 1988 is described. The model is shown to predict concentrations reasonably well at stations in central Europe. At stations near the coast, the model tends to underpredict the concentration level. ESA

N90-26406# Finnish Meteorological Office, Helsinki. Air Quality Dept.
AN EULERIAN TRANSPORT MODEL FOR NO(SUB x)-COMPOUNDS
Marke Hongisto *In* Stockholm Univ., Nordic Symposium on Atmospheric Chemistry Mar. 1990 4 p (For primary document see N90-26403 20-45)
Avail: NTIS HC A06/MF A01

A 3-D, time dependent Eulerian grid model for transport, transformation, and removal of NOX compounds is described. Comparisons of two 100 hour case simulations for first five days of January and June 1985 are discussed. The simulation results are presented as test runs to illustrate the capability and nature of the model. Changes in some numerical algorithms make it such that the model is not directly applicable in its present form. The definition of the height at which emissions mix is identified as one of the difficulties in setting up such a model. ESA

N90-26407# Finnish Meteorological Office, Helsinki. Air Quality Dept.
THE LONG-TERM VARIATION OF LEAD-210 IN RELATION TO PARTICLE-BOUND SULPHUR IN SURFACE AIR IN FINLAND
Anni Reissell *In* Stockholm Univ., Nordic Symposium on Atmospheric Chemistry Mar. 1990 3 p Sponsored in part by Nessling Foundation and Wiipurilainen Osakunta (For primary document see N90-26403 20-45)
Avail: NTIS HC A06/MF A01

The use of natural and artificial radioactive elements as tracers in environmental studies is described. The concentrations and ratios of daughter nuclides of natural radioactive series, as well as cosmogenic and fission products, are applied to determining the lifetime of aerosol particles. The origins of air masses and exchanges between different layers of the atmosphere are studied using such radioactive tracers. The concentrations of 210-Pb in air filter samples collected weekly in urban and rural locations are used. It is concluded that increasing concentrations of CO2 will add to normal meteorological fluctuations. The change in the frequency of atmospheric circulation patterns is predicted to have an effect on the dispersion and deposition patterns of pollution derived components. ESA

N90-26408# Institutet foer Vatten-Och Luftvaardsforskning, Goeteborg (Sweden).
FURTHER DEVELOPMENT AND APPLICATION OF AN ATMOSPHERIC CHEMISTRY TRAJECTORY MODEL
Karin Calander *In* Stockholm Univ., Nordic Symposium on Atmospheric Chemistry Mar. 1990 5 p (For primary document see N90-26403 20-45)
Avail: NTIS HC A06/MF A01

A Swedish version of the Harwell atmospheric chemistry trajectory model is described. The model describes different chemical and physical processes influencing the concentrations of 180 species in an air parcel moving with the wind. The meteorological description is simplified. The model can therefore treat the chemical processes very thoroughly. The chemical and photochemical transformations of about 180 species in over 300 reactions can be followed. The calculations are based on the chemical transformations occurring in gas phase. Forty different hydrocarbons and their entire reaction lapse are described. The model can be adapted to treat the breakdown lapse of ninety different hydrocarbons. ESA

N90-26409# Stockholm Univ. (Sweden). Div. of Geochemistry and Petrology.
NATURAL AND ANTHROPOGENIC COMPOUNDS IN BULK PRECIPITATION AT BLIDOE (ARCHIPELAGO OF STOCKHOLM, SWEDEN)
Kurt Bostroem, Birgitta Bostroem, and Per Andersson *In its* Nordic Symposium on Atmospheric Chemistry Mar. 1990 4 p (For primary document see N90-26403 20-45)
Avail: NTIS HC A06/MF A01

Biological processes which cause chemical variations in the atmosphere are studied. Several elements are used in tracing rain water provenance to avoid underdetermined systems. Na, Ca, K, Mg, Sr, P, S, Si, Al, Ti, Fe, Mn, Zn, and Ba are quickly determined by means of atomic emission spectroscopy with an inductively coupled plasma for excitation. Rain water collected at Blidoe from 1984 to 1987 is studied. An acid washed all plastic sampler consisting of a funnel on top of a 2 liter bottle is used for collecting the rain water samples. The data does not take rock volatilization nor forest fires into consideration as sources of metals in the atmosphere. ESA

N90-26410# Stockholm Univ. (Sweden). Dept. of Meteorology.
SOME RESULTS FROM THE PRECIPITATION CHEMISTRY MEASUREMENT PROGRAMME IN SWEDEN
Lennart Granat *In its* Nordic Symposium on Atmospheric Chemistry Mar. 1990 3 p (For primary document see N90-26403 20-45)
Avail: NTIS HC A06/MF A01

Trends in wet deposition over Sweden are highlighted with

data from the Swedish air and precipitation network. The data is a source of information about chemical processes in the atmosphere and can be used for atmospheric model validation. The representativeness of estimated concentration/deposition data is estimated. Steps taken to make such estimates possible are described. These include placing wet-only collectors in parallel with bulk collectors at several sites. The equipment used is compared with a number of other devices for rain chemistry measurements. ESA

N90-26411# Copenhagen Univ. (Denmark). Dept. of Glaciology.
ICE CORE STUDIES AND THE PAST ATMOSPHERIC ENVIRONMENT OF POLAR REGIONS
Jorgen Peder Steffensen *In* Stockholm Univ., Nordic Symposium on Atmospheric Chemistry Mar. 1990 4 p (For primary document see N90-26403 20-45)
Avail: NTIS HC A06/MF A01

Ice sheets and glaciers in areas where no melting takes place are used to study past atmospheric environments. Bubbles of air trapped in the glacier ice are used to study CO2 and CH4 concentrations in the atmosphere during the last ice age. Changes in the chemical composition of the snow or ice are studied as reflecting changes in the atmospheric environment. The concentrations of Cl, NO3 and SO4 are measured by means of ion chromatography. The bulk dust concentration is measured by a laser light scattering technique. No anthropogenic effect on the content of Cl and dust is observed in central Greenland ice core samples. ESA

N90-26412# Copenhagen Univ. (Denmark). Inst. of Geophysics.
THE RENLAND ICE CORE (GREENLAND): A SOURCE FOR CLIMATIC STUDIES OVER 100,000 YEARS
Margareta Hansson, Henrik Clausen, and Sigfus Johnsen (Iceland Univ., Reykjavik.) *In* Stockholm Univ., Nordic Symposium on Atmospheric Chemistry Mar. 1990 3 p (For primary document see N90-26403 20-45)
Avail: NTIS HC A06/MF A01

The isotopic composition of H2O and the amount of precipitation for specific years are measured using ice core samples. A careful selection of drilling site and a knowledge of the effects linked with ice flow conditions are identified as being essential in accurately interpreting atmospheric changes from ice core. Drilling of a deep ice core in Greenland during 1988 is described. The core is drilled on the dome of an ice cap built up of precipitation always deposited at a constant altitude at this particular coastal location. The sampling site has remained unchanged thus ensuring good core analysis accuracy. ESA

N90-26413# Stockholm Univ. (Sweden). Dept. of Meteorology.
RESULTS FROM GLOBAL TROPOSPHERIC SULPHUR SIMULATIONS
Joakim Langner, Henning Rodhe, and Ulf Hansson *In its* Nordic Symposium on Atmospheric Chemistry Mar. 1990 4 p (For primary document see N90-26403 20-45)
Avail: NTIS HC A06/MF A01

The oxidation of gaseous sulfur compounds to form sulfate aerosols is studied. The process is thought to be a major source of Cloud Condensation Nuclei (CCN). Changes in the concentration of CCN are studied in terms of their potential climatic effect. Global 3-D model simulations of the atmospheric stage of the sulfur cycle are presented. Estimates of natural and anthropogenic emissions are used in developing these models. The models are in good agreement (within 15 percent) for individual grid squares where good observations are available (Europe and north eastern U.S.). ESA

N90-26414# Stockholm Univ. (Sweden). Dept. of Meteorology.
A COMPARISON OF THE CONTRIBUTION OF VARIOUS GASES TO THE GREENHOUSE EFFECT
Henning Rodhe *In its* Nordic Symposium on Atmospheric Chemistry Mar. 1990 4 p (For primary document see N90-26403 20-45)
Avail: NTIS HC A06/MF A01

The accumulated greenhouse effect of a given emission of various gases is compared to that of an emission of CO2. The secondary contributions of methane, forming ozone, and carbon dioxide during photochemical breakdown are taken into consideration. For every emitted mole of CH4, the formation of one mole of O3 and one mole of CO2 is predicted. CO2 emissions due to burning a variety of different fuels, coal, oil or natural gas are estimated. Spillage of natural gas, which consists primarily of CH4, can reduce its benefits as far as the greenhouse effect is concerned. The decrease in CO2 emissions is counteracted by the spilled CH4. Spillage of natural gas can however be held to 7 percent or less, which makes switching from oil to natural gas a viable solution. A break even value for natural gas spillage is calculated at 5 to 10 percent when comparing oil and natural gas combustion. ESA

N90-26415# Institutet foer Vatten-Och Luftvaardsforskning, Goeteborg (Sweden).
RESULTS FROM THE IVL TOR STATION AT ROERVIK, SWEDEN. A CONTRIBUTION TO THE EURATRAC SUBPROJECT TOR
Anne Lindskog *In* Stockholm Univ., Nordic Symposium on Atmospheric Chemistry Mar. 1990 5 p Sponsored by Swedish Environmental Protection Agency (For primary document see N90-26403 20-45)
Avail: NTIS HC A06/MF A01

The Tropospheric Ozone Research (TOR) subproject of EUROTRAC is described. EUROTRAC is a joint European environmental project studying the impact of human activities on the troposphere over Europe. Results of measurements of ozone, nonmethane hydrocarbons, C2 to C5, Peroxy acetyl nitrate, H2O2 and standard meteorology at the Rorvik station during 1989 are presented. The techniques used in these measurements are described. Variations in the levels of individual hydrocarbons during two episodes in June and August are analyzed in detail. ESA

N90-26416# Lund Inst. of Tech. (Sweden). Dept. of Physics.
VERTICAL OZONE PROBING WITH LIDAR
H. Edner, P. Ragnarson, S. Svanberg, and Eva Wallinder *In* Stockholm Univ., Nordic Symposium on Atmospheric Chemistry Mar. 1990 4 p (For primary document see N90-26403 20-45)
Avail: NTIS HC A06/MF A01

Lidar as a tool for use in measuring air pollution is discussed. The techniques involved in analyzing the backscattered light for the pulsed laser lidar beam are described. The Tropospheric Environmental Studies by Laser Sounding (TESLAS) project is described. The use of lidar in measuring tropospheric ozone is discussed. An ozone lidar system constructed within the TESLAS project is described. The system is to be used for monitoring ozone up to 5 to 8 km. A more powerful stratospheric system which could be mounted in a movable container is described. ESA

N90-26417# Stockholm Univ. (Sweden). Dept. of Meteorology.
PHYTOPLANKTON AND ITS CONTRIBUTION TO THE ATMOSPHERIC SULFUR BUDGET OF NORTHERN EUROPE
Caroline Leck *In its* Nordic Symposium on Atmospheric Chemistry Mar. 1990 4 p (For primary document see N90-26403 20-45)
Avail: NTIS HC A06/MF A01

An attempt is made to characterize the magnitude and variability of marine sulfur emission in the northern European area. Measurement of biogenically produced reduced sulfur compounds in the surface waters of the Baltic and North seas over the course of July 1988 are described. It is concluded that on an annual basis, biogenic sulfur emissions from the Baltic Sea, the Kattegat/Skagerrak and the North Sea are negligible compared to anthropogenic emissions in northern Europe. During Summer months however, the biogenic sulfur emissions can be as high as 20 to 70 percent of anthropogenic emissions. ESA

N90-26418# Lund Univ. (Sweden). Dept. of Nuclear Physics.
CHARACTERIZATION OF BIOGENIC AEROSOL PARTICLES FROM THE AMAZON BASIN DURING DRY AND WET SEASON
Paulo Artaxo *In* Stockholm Univ., Nordic Symposium on Atmospheric Chemistry Mar. 1990 4 p (For primary document see N90-26403 20-45)
Avail: NTIS HC A06/MF A01

The characteristics of gases and aerosol particles in the atmosphere of the Amazon basin are studied. The Amazon Boundary Layer Experiment (ABLE) which is part of the Global Tropospheric Experiment (GTE) is described. The aerosol sampling and analysis techniques used are described. Results of sampling and analysis surveys to date are presented. It is concluded that, considering the vast area of tropical rain forests and the aerosol concentrations recorded, biogenic particles are important in the global aerosol budget, and in the global biogeochemical cycles of various elements. Continuing deforestation of the Amazon basin is predicted to alter the amount of cloud condensation nuclei with possible effects in global weather and climate. ESA

N90-26419# Chambre Regionale de Commerce et de l'Industrie de Lorraine, Nancy (France). Dept. of Inorganic Chemistry.
THE TRANSFER OF MERCURY BETWEEN THE ATMOSPHERE AND LAKE OR SOIL SURFACES
Zifan F. Xiao, John Munthe, W. H. Schroeder, and Oliver Lindqvist *In* Stockholm Univ., Nordic Symposium on Atmospheric Chemistry Mar. 1990 4 p (For primary document see N90-26403 20-45)
Avail: NTIS HC A06/MF A01

A flux chamber technique for the measurement of volatile mercury species is described. It is used to measure the direction and magnitude of the flux of mercury over lake and soil surfaces. Measurements carried out over four obligotrophic lakes with different mercury concentrations in their fish as well as different humic contents are described. The measuring apparatus is outlined and described. The measurements are concluded to be reasonably reliable. Significant diurnal and large seasonal variations in surface emission fluxes of vapor phase mercury are found in the waters from the four Swedish forest lakes. ESA

N90-26420# Chambre Regionale de Commerce et de l'Industrie de Lorraine, Nancy (France). Dept. of Inorganic Chemistry.
THE AQUEOUS ATMOSPHERIC CHEMISTRY OF MERCURY
John Munthe and Oliver Lindqvist *In* Stockholm Univ., Nordic Symposium on Atmospheric Chemistry Mar. 1990 4 p (For primary document see N90-26403 20-45)
Avail: NTIS HC A06/MF A01

The mobility of mercury in the atmosphere is studied. Its mobility is dependent on the chemical form in which it is present. The predominant vapor species can be transported over long distances due to its volatility. Oxidation experiments on mercury are described. Photochemically induced reduction of divalent mercury is studied. Results of these experiments indicate that monovalent mercury, if formed in cloud or rain water, will be rapidly oxidized by ozone or radicals. Experimental results confirm the presence of a very fast reaction between elemental mercury and ozone. ESA

N90-26421# Kuopio Univ. (Finland). Dept. of Environmental Sciences.
MEASUREMENTS OF MONOTERPENES IN A CONIFEROUS FOREST
Juuti Soile, Raunemaa Taisto, and Ruuskanen Juhani *In* Stockholm Univ., Nordic Symposium on Atmospheric Chemistry Mar. 1990 4 p (For primary document see N90-26403 20-45)
Avail: NTIS HC A06/MF A01

Monoterpenes emitted by coniferous forests are studied. They can be oxidized in the air and combined with nitrogen oxides, participate in photochemical reactions. The monoterpene levels in a young pine forest during Summer months are studied. Measurements performed in a dense forest of young pines (Pinus sylvestris) in central Finland are described. The greater monoterpene concentrations are recorded during June and August. Monoterpene levels vary diurnally reaching a maxima during the nights. During the daytime, monoterpenes are consumed by chemical reactions and dispersed by atmospheric turbulence. ESA

N90-26422# Stockholm Univ. (Sweden). Dept. of Meteorology.
TERPENE CONCENTRATIONS AND EMISSIONS IN A SCOTS PINE FOREST
Robert Janson *In its* Nordic Symposium on Atmospheric Chemistry Mar. 1990 3 p (For primary document see N90-26403 20-45)
Avail: NTIS HC A06/MF A01

Measurement of five monoterpenes (alpha-pinene, 3-carene, limonene, beta-pinene, and camphene) made in a forest of Scotsch pine (Pinus sylvestris) in Sweden is described. The stand is 125 years old with a density of 390 trees per hectare. The techniques used for collecting air samples are described. Vertical profiles are obtained using a 50 m tower. Emissions are found to consist primarily of alpha-pinene and 3-carene. Total terpene emissions ranging from 15 to 800 ug/hr per sq m of leaf area are observed. Minimum emissions are observed at night, reaching a maximum during the day between 12 and 2 pm. ESA

N90-26423# Stockholm Univ. (Sweden). Dept. of Meteorology.
THE DIURNAL OZONE CYCLE IN A CONIFEROUS FOREST: THE IMPORTANCE OF METEOROLOGY AND CHEMISTRY
Abstract Only
Christer Johansson, Jiang-Fen Zheng (Georgia Inst. of Tech., Atlanta.), and Henning Rodhe *In its* Nordic Symposium on Atmospheric Chemistry Mar. 1990 1 p Previously announced in IAA as A90-23795 (For primary document see N90-26403 20-45)
Avail: NTIS HC A06/MF A01

A 1-D model of turbulent diffusion and chemistry in the boundary layer is applied to the analysis of diurnal variations in O3 concentrations in a Swedish coniferous forest. Meteorological observations concerning wind speed, temperature, relative humidity and global radiation are used to describe diurnal variations in mixing and dry deposition. It is concluded that large diurnal variation in the concentration of terpenes is expected. High terpene concentrations near the surface at night may become an important sink for O3. During stable night conditions the loss of O3 through reactions with terpenes is predicted to be about as important as dry deposition. The impact of terpenes on the O3 concentration during the day depends on the NOX level. ESA

N90-26424# Oslo Univ. (Norway). Inst. of Geophysics.
STRATOSPHERIC CHEMISTRY
Frode Stordal *In* Stockholm Univ., Nordic Symposium on Atmospheric Chemistry Mar. 1990 4 p (For primary document see N90-26403 20-45)
Avail: NTIS HC A06/MF A01

The effects of solar ultraviolet radiation on the chemistry of the stratosphere are discussed. The active chemistry of the stratosphere is due in part to the mixing of free radicals and atoms dissociated by UV radiation. The role played by ozone in the stratosphere is discussed. The role played by radicals in the oxygen, hydrogen, nitrogen, chlorine and bromine families in the gas phase loss chemistry of ozone is described. Their photochemical lifetime at different levels in the stratosphere is discussed. Heterogeneous reactions taking place on the surfaces of particles are described. By such reactions, inactive HCl is converted to compounds that destroy ozone (ClO). The large ozone reductions which occur in the lower stratosphere in the spring season in Antartica are the result of such reactions taking place on polar stratospheric clouds. ESA

N90-26425# Goeteborg Univ. (Sweden). Dept. of Inorganic Chemistry.
FORMATION KINETICS OF N2O IN THE ATMOSPHERE
Susanne Boerjesson, Ingvar Waengberg, and Evert Ljungstroem *In* Stockholm, Nordic Symposium on Atmospheric Chemistry Mar. 1990 3 p (For primary document see N90-26403 20-45)
Avail: NTIS HC A06/MF A01

The sources of increase of N2O concentration in the troposphere are discussed. The dangers involved in a continuing increase in concentration of the gas both in its effects on global temperature and the UV radiation climate are described. As N2O absorbs infrared radiation at a wavelength which is relatively free of other atmospheric absorption, a small change in concentration may have large effects on the equilibrium temperature of the Earth. Experiments carried out to test how much N2O is produced in fossil fuel combustion are described. ESA

N90-26426# Goeteborg Univ. (Sweden). Dept. of Physical Chemistry.
PHOTODISSOCIATION OF NO2: INFLUENCE OF PHOTOLYSIS WAVELENGTH AND TEMPERATURE DEPENDENCE ON PRODUCT FORMATION
Per-Anders Elofson and Evert Ljungstroem *In* Stockholm Univ., Nordic Symposium on Atmospheric Chemistry Mar. 1990 4 p (For primary document see N90-26403 20-45)
Avail: NTIS HC A06/MF A01

A Monte Carlo simulation model is used to study the photodissociation of NO2 molecules at wavelengths between 360 and 415 nm. It is assumed in the model that there is no electronic surface barrier to decomposition after the photolysis photon has been absorbed. The conservation of total angular momentum leads to a dynamical barrier which must be surmounted by the photolysis fragments en route to free products. Previous models have not taken this effect into account. The model can give information not only on energy consumption, but on product states and energy yields. It can give information about possible specific energy release which may be important in determining the rates of subsequent reactions. ESA

N90-26427# Stockholm Univ. (Sweden). Dept. of Meteorology.
PHOTODISSOCIATION OF O2 IN THE STRATOSPHERE AND MESOSPHERE: A GENERAL PARAMETRIZATION OF THE SCHUMMAN-RUNGE BANDS
Donal P. Murtagh *In its* Nordic Symposium on Atmospheric Chemistry Mar. 1990 2 p (For primary document see N90-26403 20-45)
Avail: NTIS HC A06/MF A01

Absorption cross sections are recomputed and effective photodissociation rates for solar radiation penetration in the atmosphere are calculated. Corrections to previously published values are presented. The ratio of photodissociation rates obtained for Summer and Winter conditions at 65 deg north with a solar zenith angle of 75 deg is presented to point out the discrepancies in the values published previously. A parameterization technique is presented designed to take care of all the effects in a simple way. For each of the seventeen standard spectral regions the effective photodissociation cross section at a given place in the atmosphere is related to the O2 column density along the absorption path and to the local temperature. ESA

N90-26428# Stockholm Univ. (Sweden). Dept. of Meteorology.
THE COLLECTION AND ANALYSIS OF ATMOSPHERIC PEROXIDES
Claes deServes *In its* Nordic Symposium on Atmospheric Chemistry Mar. 1990 2 p (For primary document see N90-26403 20-45)
Avail: NTIS HC A06/MF A01

The ambient levels and diurnal variations in atmospheric peroxide concentrations are studied. An instrument used for the measurement of peroxides in ambient air using Flow Injection Analysis (FIA) is described. The detection of peroxides is based on an enzymatic coupling of p-hydroxyphenyl acetic acid to form a fluorescent dimer. The fluorescence reaction is sensitive to H2O2 and organic peroxides. To differentiate H2O2 from the organics, an MnO2 reactor is used. Another method is to selectively remove H2O2 with catalase. A comparison between the two methods yields vastly different results. ESA

N90-26429# Stockholm Univ. (Sweden). Dept. of Meteorology.
DESTRUCTION OF PEROXY RADICAL BY Cu ION CATALYSED REACTIONS ON ATMOSPHERIC PARTICLES
Howard B. Ross and Kevin J. Noone *In* Stockholm Univ., Nordic Symposium on Atmospheric Chemistry Mar. 1990 3 p (For primary document see N90-26403 20-45)
Avail: NTIS HC A06/MF A01

A Cu mediated reaction leading to the production of H2O2 is studied. The reaction is studied in the laboratory using aerosols doped with various amounts of Cu ions. To determine if Cu mediated reactions are important to H2O chemistry in the ambient atmosphere, Cu molalities are calculated from measured Cu aerosols concentrations, mass and number size distribution data from a site in central Sweden. Calculations carried out on the basis of these collected data are presented. The results indicate that reactions between peroxy radicals and aerosols may be significant source of hydrogen peroxide in the atmosphere. ESA

N90-26430# Stockholm Univ. (Sweden). Dept. of Inorganic Chemistry.
HETEROGENEOUS TRANSFORMATION OF PEROXYACETYLNITRATE
Ingvar Waengberg, Sarka Langrova, and Evert Ljungstroem *In* Stockholm, Univ., Nordic Symposium on Atmospheric Chemistry Mar. 1990 4 p (For primary document see N90-26403 20-45)
Avail: NTIS HC A06/MF A01

Peroxyacetylnitrate (PAN), a semistable product formed when volatile hydrocarbons undergo photochemical oxidation in the presence of nitrogen oxides, is described. PAN is a potent eye irritant and a phytotoxic substance. It serves as a reservoir for nitrogen oxides. The thermal and photochemical decomposition reactions leading to possible rerelease of the nitrogen as NO2 are discussed. The results of tests on the various chemical reactions involved in the decomposition are presented. These results indicate that the decomposition of PAN into peroxyacetyl radicals and NO2 is not effected by heterogeneous reactions. ESA

46 GEOPHYSICS

Includes aeronomy; upper and lower atmosphere studies; ionospheric and magnetospheric physics; and geomagnetism.

For space radiation see *93 Space Radiation*.

N90-26431# Lanchester Polytechnic, Coventry (England). Dept. of Geography.
THE 5TH INTERNATIONAL SYMPOSIUM ON PALAEOLIMNOLOGY Abstract Only
Sep. 1989 123 p Symposium held in Cumbria, England, Sep. 1989
(Contract DAJA45-89-M-0085)
(AD-A219244; R/D-6176-EN-02) Avail: NTIS HC A06/MF A01 CSCL 08/7

Abstracts of papers given at this symposium are presented. Some representative titles are: Recent lake acidification (reversible studies using lake sediments); Variations of diatom stratigraphy in varved lake sediments; 241-Am dating of lake sediments; DISCO, a diatom database for paleolimnological research; Sedimentation pattern in a deep clear water lake in s.w. Sweden; Deposition of radionuclides upon an upland drainage basin in mid-Wales; Taphonomy of diatom assemblages in lake sediments; and Chernobyl Cs-134 and Cs-137 in Swedish varved lake sediment. E.R.

N90-26432*# National Aeronautics and Space Administration. Langley Research Center, Hampton, VA.
ANNUAL AND INTERANNUAL VARIATIONS OF EARTH-EMITTED RADIATION BASED ON A 10-YEAR DATA SET
T. Dale Bess, G. Louis Smith, Thomas P. Charlock, and Fred G. Rose (Planning Research Corp., Hampton, VA.) Jan. 1989

44 p Submitted for publication
(NASA-TM-103465; NAS 1.15:103465) Avail: NTIS HC A03/MF A01 CSCL 04A

The method of empirical orthogonal functions (EOF) was applied to a 10-year data set of outgoing longwave radiation. Spherical harmonic functions are used as a basis set for producing equal area map results. The following findings are noted. The first EOF accounts for 66 percent of the variance. After that, each EOF accounts for only a small variance, forming a slowly converging series. The first two EOF's describe mainly the annual cycle. The third EOF is primarily the semiannual cycle although many other EOF's also contain significant semiannual parts. These results reaffirm those based on a shorter data set. In addition, a much stronger spring/fall mode was found in the central equatorial Pacific Ocean for the second EOF than was found earlier. This difference is attributed to the use of broadband radiometer data which were available for the present study. The earlier study used data from a window channel instrument which is not as sensitive to water vapor variations. The fourth EOF describes much of the 1976 to 1977 and 1982 to 1983 ENSO phenomena. There is typically a gap in the spectrum between a semiannual peak and the annual cycle for all but the first EOF. A semiannual OLR dipole straddles the Asian-Australian monsoon track. Author

N90-26433*# National Aeronautics and Space Administration. Langley Research Center, Hampton, VA.
EARTH RADIATION BUDGET EXPERIMENT (ERBE) VALIDATION
Bruce R. Barkstrom, Edwin F. Harrison, G. Louis Smith, Richard N. Green, James F. Kibler, and Robert D. Cess (State Univ. of New York, Stony Brook.) 1990 59 p Submitted for publication
(NASA-TM-103481; NAS 1.15:103481) Avail: NTIS HC A04/MF A01 CSCL 04A

During the past 4 years, data from the Earth Radiation Budget Experiment (ERBE) have been undergoing detailed examination. There is no direct source of groundtruth for the radiation budget. Thus, this validation effort has had to rely heavily upon intercomparisons between different types of measurements. The ERBE SCIENCE Team chose 10 measures of agreement as validation criteria. Late in August 1988, the Team agreed that the data met these conditions. As a result, the final, monthly averaged data products are being archived. These products, their validation, and some results for January 1986 are described. Information is provided on obtaining the data from the archive. Author

N90-26434# Los Alamos National Lab., NM.
IMPORTANT EXPERIMENTS TO TEST FOR LONGER-RANGED NEW GRAVITATIONAL FORCES
Michael Martin Nieto and T. Goldman 1990 14 p Presented at the 25th IUPAP International Conference on High Energy Physics, Singapore, 2-8 Aug. 1990
(Contract W-7405-eng-36)
(DE90-012102; LA-UR-90-1866; CONF-900822-3) Avail: NTIS HC A03/MF A01

Four experiments are discussed, three of which are underway, and find them to be of critical importance in testing for longer range, static, non-Newtonian gravity. DOE

N90-26435*# Georgia Inst. of Tech., Atlanta. School of Earth and Atmospheric Sciences.
THE NASA/MSFC GLOBAL REFERENCE ATMOSPHERIC MODEL, 1990 VERSION (GRAM-90) Final Report
C. G. Justus, F. N. Alyea, and D. M. Cunnold Jul. 1990 103 p Sponsored in part by Georgia Univ.
(Grant NAG8-078)
(NASA-CR-186717; NAS 1.26:186717) Avail: NTIS HC A06/MF A01 CSCL 04A

A new (1990) version of the Global Reference Atmospheric Model (GRAM-90) is presented and discussed. GRAM-90 incorporates extensive new data, mostly collected under the Middle Atmosphere Program (MAP), to produce a completely revised middle atmosphere model (20 to 120 km). Because of earlier data sparseness in this altitude region, previous version of GRAM relied on a six-month displacement of Northern Hemisphere data to represent the Southern Hemisphere. GRAM-90 alleviates this shortcoming by utilizing actual data from the Southern Hemisphere for each month. The GRAM-90 program is described with extensive documentation on the program operation and usage. Sample results are presented, in the form of height-latitude and latitude-longitude plots. Comparisons are made between the empirically-based GRAM-based GRAM-90 model and results from a first principles stratospheric circulation model (SCM) in the 20 to 80 km height region. Specific areas of improvement of GRAM-90 over the earlier GRAM model results are also noted. Author

N90-26436*# Utah State Univ., Logan.
MICROSPACECRAFT AND EARTH OBSERVATION: ELECTRICAL FIELD (ELF) MEASUREMENT PROJECT
Tanya Olsen, Scot Elkington, Scott Parker, Grover Smith, Andrew Shumway, Craig Christensen, Mehrdad Parsa, Layne Larsen, Ranae Martinez, and George Powell et al 1990 189 p
(Grant NGT-21-002-800)
(NASA-CR-186821; NAS 1.26:186821) Avail: NTIS HC A09/MF A01 CSCL 04A

The Utah State University space system design project for 1989 to 1990 focuses on the design of a global electrical field sensing system to be deployed in a constellation of microspacecraft. The design includes the selection of the sensor and the design of the spacecraft, the sensor support subsystems, the launch vehicle interface structure, on board data storage and communications subsystems, and associated ground receiving stations. Optimization of satellite orbits and spacecraft attitude are critical to the overall mapping of the electrical field and, thus, are also included in the project. The spacecraft design incorporates a deployable sensor array (5 m booms) into a spinning oblate platform. Data is taken every 0.1 seconds by the electrical field sensors and stored on-board. An omni-directional antenna communicates with a ground station twice per day to down link the stored data. Wrap-around solar cells cover the exterior of the spacecraft to generate power. Nine Pegasus launches may be used to deploy fifty such satellites to orbits with inclinations greater than 45 deg. Piggyback deployment from other launch vehicles such as the DELTA 2 is also examined. Author

N90-26437*# Lunar and Planetary Inst., Houston, TX.
PROCEEDINGS OF A WORKSHOP ON LUNAR VOLCANIC GLASSES: SCIENTIFIC AND RESOURCE POTENTIAL
John W. Delano, ed. and Grant H. Heiken, ed. 3 Aug. 1990 77 p Workshop held in Houston, TX, 10-11 Oct. 1989
(Contract NASw-4066)
(NASA-CR-186631; NAS 1.26:186631; LPI-TR-90-02) Avail: NTIS HC A05/MF A01 CSCL 08K

This workshop on lunar mare volcanism was the first since 1975 to deal with the major scientific advances that have occurred in this general subject, and the first ever to deal specifically with volcanic glasses. Lunar volcanic glasses are increasingly being recognized as the best geochemical and petrologic probes into the lunar mantle. Lunar volcanic glasses, of which 25 compositional varieties are presently known, appear to represent primary magmas that were produced by partial melting of differentiated mantle source regions at depths of perhaps 400 to 500 km. These high-magnesian picritic magmas were erupted onto the lunar surface in fire fountains associated with the release of indigenous lunar volatiles. The cosmic significance of this volatile component, in an otherwise depleted Moon, remains a lingering puzzle. The resource potential, if any, of the surface-correlated volatile sublimates on the volcanic glass spherules had not been systematically addressed prior to this workshop. Author

N90-26438# Los Alamos National Lab., NM.
A STUDY OF POSITRONS FROM SOVIET NUCLEAR POWERED SATELLITES AS TRACERS FOR MAGNETOSPHERIC RESEARCH
E. W. Hones, Jr. (Mission Research Corp., Los Alamos, NM.) 1990 14 p Presented at the 28th COSPAR Plenary Conference,

The Hague, Netherlands, 25 Jun. - 6 Jul. 1990
(Contract W-7405-eng-36)
(DE90-013157; LA-UR-90-2132; CONF-9006220-2) Avail: NTIS HC A03/MF A01

Two Soviet satellites carrying nuclear reactors operated in circular 790 km orbits (65 deg inclination) in 1987 and 1988. Positrons generated in the satellites' surfaces by the intense reactor gamma radiation escaped and were trapped for periods of minutes to hours in the geomagnetic field. These positrons have been observed on many occasions by gamma ray sensors on the SMM satellite (in 500 km orbit) which identify the positrons by the 511 keV gamma rays created when they annihilate in the satellite surface. The SMM detector provides a time resolution of 64 milliseconds. It has recorded positron rise-times of less than 0.5 second (corresponding to about 1 positron gyroradius) on many occasions as it encounters the low-L edge of positrons injected by the Soviet satellites as far as half-way around the earth. The potential was studied of these sharply defined positron shells as magnetospheric tracers and as a means for examining particle diffusion and loss processes. DOE

N90-26439# Los Alamos National Lab., NM.
ON THE NATURE OF THE PLASMA SHEET BOUNDARY LAYER
E. W. Hones, Jr. (Mission Research Corp., Los Alamos, NM.) 1990 19 p Presented at the 28th COSPAR Plenary Conference, The Hague, Netherlands, 25 Jun. - 6 Jul. 1990
(Contract W-7405-eng-36)
(DE90-013158; LA-UR-90-2131; CONF-9006220-1) Avail: NTIS HC A03/MF A01

The regions of the plasma sheet adjacent to the north and south lobes of the magnetotail have been described by many experimenters as locations of beams of energetic ions and fast-moving plasma directed primarily earthward and tailward along magnetic field lines. Measurements taken as satellites passed through one or the other of these boundary layers have frequently revealed near-earth mirroring of ions and a vertical segregation of velocities of both earthward-moving and mirroring ions with the fastest ions being found nearest the lobe-plasma sheet interface. These are features expected for particles from a distant tail source (bar E) (times) (bar B) drifting in a dawn-to-dusk electric field and are consistent with the source being a magnetic reconnection region. The plasma sheet boundary layers are thus understood as separatrix layers, bounded at their lobeward surfaces by the separatrices from the distant neutral line. The observations that support this interpretation are reviewed. DOE

N90-26440# Technische Univ., Delft (Netherlands). Dept. of Physics.
QUANTUM BALLISTIC AND ADIABATIC ELECTRON TRANSPORT, STUDIED WITH QUANTUM POINT CONTACTS Ph.D. Thesis
Bart Jan vanWees 1989 132 p Sponsored by Stichting voor Fundamenteel Onderzoek der Materie, Netherlands
(ETN-90-97262) Avail: NTIS HC A07/MF A01

An experimental and theoretical study of quantum ballistic transport in Quantum Point Contacts (QPCs), defined in the 2-D electron gas of a high mobility GaAs/Al0.33Ga0.67As heterojunction is presented. In zero magnetic field the conductance of QPC shows the formation of quantized plateaux. The experimental results are explained with a model. Deviations from ideal quantization are discussed. The experimental results are compared with model calculations. Energy averaging of the conductance is studied, both as a function of temperature and voltage across the device. The application of a magnetic field leads to the magnetic depopulation of the one-dimensional sub-bands in the QPC. The zero field quantization and the high magnetic field quantization are shown to be two extremes of a more general quantization phenomenon. The transition from Ohmic to adiabatic transport in the same dual QPC device is studied. In agreement with the theoretical expectation, the resistance of the device is equal to the sum of the resistances of the individual QPCs in the absence of a magnetic field. In high magnetic fields, the resistance is determined by QPC with the largest resistance. ESA

N90-26441# Purdue Univ., West Lafayette, IN. Dept. of Chemistry.
IONIC ATMOSPHERE EFFECTS ON THE ENERGETICS OF THERMAL AND OPTICAL ELECTRON-EXCHANGE REACTIONS: APPLICATION TO FERROCENIUM-FERROCENE SELF EXCHANGE
A. M. Kuznetsov, D. K. Phelps, and M. J. Weaver 1 May 1990 28 p
(Contract N00014-89-J-1452)
(AD-A222605; TR-95) Avail: NTIS HC A03/MF A01 CSCL 04/1

A treatment of ionic-atmosphere effects upon symmetrical electron-transfer reactions resulting from added electrolyte is outlined. Relationships are derived on the basis of the extended Debye-Huckel model for the increase in the activation free energy, associated with reorganization of the ionic atmosphere for homogeneous-phase reactions involving a pair of spherical reactants with varying internuclear distance R. Similar relationships apply to the energetics of symmetrical optical electron transfer, since the increase in the optical transition energy, should equal the corresponding ionic atmosphere reorganization energy, under the anticipated linear response conditions. GRA

N90-26442# Massachusetts Inst. of Tech., Cambridge. Dept. of Chemistry.
FORMATION AND DEACTIVATION OF VIBRATIONALLY EXCITED ATMOSPHERIC MOLECULES Final Report, 1 Jul. 1986 - 31 Mar. 1990
J. Steinfeld, C. Fell, M. Phillips, J. Klaassen, and C. Van Zoeren 20 Mar. 1990 111 p
(Contract F19628-86-C-0139; AF Proj. 2310)
(AD-A222660; GL-TR-90-0057) Avail: NTIS HC A06/MF A01 CSCL 20/3

Research on the following topics is summarized: (1) quenching of N(2D) atoms by atomic oxygen; (2) reactions of N(2P) atoms; (3) detection of N(4S) atoms by resonantly enhanced multiphoton ionization; (4) a kinetic model for partially saturated, resonantly enhanced multiphoton ionization of diatomic molecules; and (5) stimulated-emission pumping of nitric oxide. GRA

47 METEOROLOGY AND CLIMATOLOGY

Includes weather forecasting and modification.

N90-26443# National Oceanographic Data Center, Washington, DC.
MARINERS WEATHER LOG, VOLUME 33, NUMBER 2, SPRING 1989 Quarterly Report
Richard M. DeAngelis, ed. 1989 77 p
(PB90-146838) Avail: NTIS HC A05/MF A01 CSCL 04B

This quarterly journal presents notes and articles of interest to meteorologists and other interested in weather in general. Topics include: Looking for icebergs; North Atlantic tropical cyclones; The Chicago seiches; Whale oil and wicks; Beyond the rainbow; Sea photography; Radio officers tips; Marine observation program; and Hurrican alley. E.R.

N90-26444# National Oceanographic Data Center, Washington, DC.
MARINERS WEATHER LOG, VOLUME 33, NUMBER 3, SUMMER 1989 Quarterly Report
Richard M. DeAngelis, ed. 1989 77 p
(PB90-146846) Avail: NTIS HC A05/MF A01 CSCL 04B

This quarterly journal presents articles of interest to meteorologists, etc. Some titles of interest are: Sentinels on watch; Persistent marine debris; Eastern North Pacific hurricanes; Whale oil and wicks; Beyond the rainbow; Sea photography; The mailbag; and Marine observation program. E.R.

N90-26445# National Oceanographic Data Center, Washington, DC.
MARINERS WEATHER LOG, VOLUME 33, NUMBER 4, FALL 1989 Quarterly Report
Richard M. DeAngelis, ed. 1989 81 p
(PB90-146853) Avail: NTIS HC A05/MF A01 CSCL 04B

This journal presents articles and news of interest to the weather watcher. Some topics of interest are: China Sea rescue; Sentinels on watch; Whale oil and wicks; Beyond the rainbow; The mailbag; Radio officer tips; Sea photography; Editor's desk; Marine observation program; and Hurrican alley. E.R.

N90-26446*# National Aeronautics and Space Administration. Langley Research Center, Hampton, VA.
THE 27-28 OCTOBER 1986 FIRE IFO CIRRUS CASE STUDY: COMPARISON OF RADIATIVE TRANSFER THEORY WITH OBSERVATIONS BY SATELLITE AND AIRCRAFT
Bruce A. Wielicki, J. T. Suttles, Andrew J. Heymsfield, Ronald M. Welch, James D. Spinhirne, Man-Li C. Wu, David OC. Starr, Lindsay Parker, and Robert F. Arduini (Planning Research Corp., Hampton, VA.) Mar. 1989 61 p Submitted for publication Prepared in cooperation with NASA, Goddard Space Flight Center
(NASA-TM-103468; NAS 1.15:103468) Avail: NTIS HC A04/MF A01 CSCL 04B

Observations of cirrus and altocumulus clouds during the First International Satellite Cloud Climatology Project Regional Experiment (FIRE) are compared to theoretical models of cloud radiative properties. Three tests are performed. First, LANDSAT radiances are used to compare the relationship between nadir reflectance ot 0.83 micron and beam emittance at 11.5 microns with that predicted for model calculations using spherical and nonspherical phase functions. Good agreement is found between observations and theory when water droplets dominate. Poor agreement is found when ice particles dominate, especially using scattering phase functions for spherical particles. Even when compared to a laboratory measured ice particle phase function, the observations show increased side scattered radiation relative to the theoretical calculations. Second, the anisotropy of conservatively scattered radiation is examined using simultaneous multiple angle views of the cirrus from LANDSAT and ER-2 aircraft radiometers. Observed anisotropy gives good agreement with theoretical calculations using the laboratory measured ice particle phase function and poor agreement with a spherical particle phase function. Third, Landsat radiances at 0.83, 1.65, and 2.21 microns are used to infer particle phase and particle size. For water droplets, good agreement is found with King Air FSSP particle probe measurements in the cloud. For ice particles, the LANDSAT radiance observations predict an effective radius of 60 microns versus aircraft observations of about 200 microns. It is suggested that this descrepancy may be explained by uncertainty in the imaginary index of ice and by inadequate measurements of small ice particles by microphysical probes. Author

N90-26447*# National Aeronautics and Space Administration. Langley Research Center, Hampton, VA.
THE 27-28 OCTOBER 1986 FIRE IFO CIRRUS CASE STUDY: CIRRUS PARAMETER RELATIONSHIPS DERIVED FROM SATELLITE AND LIDAR DATA
Patrick Minnis, David F. Young, Kenneth Sassen, Joseph M. Alvarez, and Christian J. Grund (Wisconsin Univ., Madison.) Mar. 1989 89 p Submitted for publication
(Contracts NAG1-882; N00014-87-K-0436; DAAG29-84-K-0069)
(NASA-TM-103469; NAS 1.15:103469) Avail: NTIS HC A05/MF A01 CSCL 04B

Cirrus cloud radiative and physical characteristics are determined using a combination of ground-based, aircraft, and satellite measurements taken as part of the First ISCCP Regional Experiment (FIRE) Cirrus Intensive Field Observations (IFO) during October and November 1986. Lidar backscatter data are used to define cloud base, center, and top heights and the corresponding temperatures. Coincident GOES 4 km visible (0.65 microns) and 8 km infrared window (11.5 microns) radiances are analyzed to determine cloud emittances and reflectances. Infrared optical depth is computed from the emittance results. Visible optical depth is derived from reflectance using a theoretical ice crystal scattering model and an empirical bidirectional reflectance mode. No clouds with visible optical depths greater than 5 or infrared optical depths less than 0.1 were used in the analysis. Average cloud thickness ranged from 0.5 km to 8 km for the 71 scenes. An average visible scattering efficiency of 2.1 was found for this data set. The results reveal a significant dependence of scattering efficiency on cloud temperature. Author

N90-26448*# Clemson Univ., SC. Radar Systems Lab.
ANALYSIS AND IMPROVED DESIGN CONSIDERATIONS FOR AIRBORNE PULSE DOPPLER RADAR SIGNAL PROCESSING IN THE DETECTION OF HAZARDOUS WINDSHEAR
Jonggil Lee 11 May 1990 142 p
(Grant NAG1-928)
(NASA-CR-186792; NAS 1.26:186792; TR-051190-357OP; TR-12)
Avail: NTIS HC A07/MF A01 CSCL 04B

High resolution windspeed profile measurements are needed to provide reliable detection of hazardous low altitude windshear with an airborne pulse Doppler radar. The system phase noise in a Doppler weather radar may degrade the spectrum moment estimation quality and the clutter cancellation capability which are important in windshear detection. Also the bias due to weather return Doppler spectrum skewness may cause large errors in pulse pair spectral parameter estimates. These effects are analyzed for the improvement of an airborne Doppler weather radar signal processing design. A method is presented for the direct measurement of windspeed gradient using low pulse repetition frequency (PRF) radar. This spatial gradient is essential in obtaining the windshear hazard index. As an alternative, the modified Prony method is suggested as a spectrum mode estimator for both the clutter and weather signal. Estimation of Doppler spectrum modes may provide the desired windshear hazard information without the need of any preliminary processing requirement such as clutter filtering. The results obtained by processing a NASA simulation model output support consideration of mode identification as one component of a windshear detection algorithm. Author

N90-26449*# South Dakota School of Mines and Technology, Rapid City. Inst. of Atmospheric Sciences.
ESTIMATION OF CONVECTIVE RAIN VOLUMES UTILIZING THE ARE-TIME-INTEGRAL TECHNIQUE
L. Ronald Johnson and Paul L. Smith 1990 4 p
(Grant NAG5-386)
(NASA-CR-186814; NAS 1.26:186814) Avail: NTIS HC A01/MF A01 CSCL 04B

Interest in the possibility of developing useful estimates of convective rainfall with Area-Time Integral (ATI) methods is increasing. The basis of the ATI technique is the observed strong correlation between rainfall volumes and ATI values. This means that rainfall can be estimated by just determining the ATI values, if previous knowledge of the relationship to rain volume is available to calibrate the technique. Examples are provided of the application of the ATI approach to gage, radar, and satellite measurements. For radar data, the degree of transferability in time and among geographical areas is examined. Recent results on transferability of the satellite ATI calculations are presented. Author

N90-26450# Cologne Univ. (Germany, F.R.). Inst. fuer Geophysik und Meteorologie.
AIRCRAFT MEASUREMENTS OF THE TURBULENCE STRUCTURE IN CIRRUS CLOUDS Ph.D. Thesis [FLUGZEUGMESSUNGEN DER TURBULENZSTRUKTUR IN CIRRUSWOLKEN]
Markus Quante 1989 150 p In GERMAN; ENGLISH summary
(ISSN-0069-5882; ETN-90-96969) Avail: NTIS HC A07/MF A01

Data on turbulence in cirrus clouds, derived during two flight missions in the framework of the International Cirrus Experiment, were analyzed. The examined cirrus clouds ranged between altitudes of 7 to 11 km at temperatures between -30 and -56 C.

Both cloud fields were characterized by a significant vertical wind shear and a stably stratified flow. The turbulence shows typical signs of a thermally stable shear flow characterized by the coexistence of waves and quasi 2-D, horizontal motions with intermittent, weak turbulence. Vertical motions are dominated by the stable stratification. Turbulence mainly occurs on scales below 500 m, suggesting a small scale organization of the clouds in accordance with published model calculations and results from other in situ observations. Besides local convection, shear-induced Kelvin-Helmholtz instabilities may be considered as a possible source of the intermittent turbulence. ESA

48 OCEANOGRAPHY

Includes biological, dynamic, and physical oceanography; and marine resources.

For related information see also *43 Earth Resources and Remote Sensing.*

N90-26451*# Princeton Univ., NJ. Program in Statistics and Operations Research.

SPATIAL CROSS-CORRELATION OF ANTARCTIC SEA ICE AND SEABED TOPOGRAPHY

Richard D. DeVeaux and Michael J. Phelan 1990 46 p (Grant NAGw-1763)

(NASA-CR-186815; NAS 1.26:186815) Avail: NTIS HC A03/MF A01 CSCL 08C

A time series of derived sea ice concentrations as observed about Antarctica by the Nimbus-7 Scanning Multichannel Microwave Radiometer (SMMR) satellite in 1983 is considered. The degree of spatial cross correlation between these data and seabed topography is quantified. The approach is to implement a statistical image processing filter designed to extract local patterns of spatial cross correlation over the entire sea ice field as it undergoes daily changes. Throughout the sea ice, it was found that large scale variations in sea ice concentration correlate systematically with variations in the topography of the seabed. Generally speaking, high concentrations of sea ice occur over deep ocean, whereas areas of encavement, early dissipation and polynya formation develop over topographic features of high elevation. The latter was studied in detail with respect to the features Maud Rise, Astrid Ridge and the continental shelf in the Cosmonaut and Ross Seas. In each case, it is shown that an encavement in sea ice, a polynya, or both develops in the vicinity of the feature in question. As these results are quantified in terms of spatial cross correlation, a potential role is inferred for seabed topography in such fluctuations in the sea ice about Antarctica. Author

51 LIFE SCIENCES (GENERAL)

N90-26452*# National Aeronautics and Space Administration. Ames Research Center, Moffett Field, CA.

THE US EXPERIMENTS FLOWN ON THE SOVIET BIOSATELLITE COSMOS 1887 Final Reports

James P. Connolly, ed., Richard E. Grindeland, ed., and Rodney W. Ballard, ed. Feb. 1990 501 p

(NASA-TM-102254; A-90013; NAS 1.15:102254) Avail: NTIS HC A22/MF A03 CSCL 06C

Cosmos 1887, a biosatellite containing biological and radiation experiments from the Soviet Union, the United States and seven other countries, was launched on September 29, 1987. One Rhesus monkey's feeder stopped working two days into the flight and a decision was made to terminate the mission after 12 1/2 days. The biosatellite returned to Earth on October 12, 1987. A system malfunction, during the reentry procedure, caused the Cosmos 1887 spacecraft to land approximately 1800 miles beyond the intended landing site and delayed the start of the postflight procedures by approximately 44 hours. Further information on the conditions at landing and postflight activities is included in the Mission Operations portion of this document. U.S. and U.S.S.R. specialists jointly conducted 26 experiments on this mission, including the postflight transfer of data, hardware and biosamples to the U.S. For individual titles, see N90-26453 through N90-26478.

N90-26453*# Medical Coll. of Wisconsin, Milwaukee. Dept. of Anatomy and Cellular Biology.

EFFECTS OF MICROGRAVITY ON RAT MUSCLE

D. A. Riley *In* NASA, Ames Research Center, The US Experiments Flown on the Soviet Biosatellite Cosmos 1887 Feb. 1990 p 45-49 (For primary document see N90-26452 20-51)

Avail: NTIS HC A22/MF A03 CSCL 06C

It is well known that humans exposed to long term spaceflight experience undesirable progressive muscle weakness and increased fatigability. This problem has prompted the implementation of inflight exercise programs because most investigators believe that the major cause of diminished muscle performance is a combination of disuse and decreased workload. Inflight exercise has improved muscle health, but deficits have persisted, indicating that either the regimens utilized were suboptimal or there existed additional debilitating factors which were not remedied by exercise. Clarification of this question requires an improved understanding of the cellular and molecular basis of spaceflight-induced muscle deterioration. To this end, multiple investigations have been performed on the muscles from rats orbited 5 to 22 days in Cosmos biosatellites and Spacelab-3 (2,4,5,8,10 to 14,16,18,19,21 to 23,25,27,28). The eight Cosmos 1887 investigations examined the structural and biochemical changes in skeletal and cardiac muscles of rats exposed to microgravity for 12.5 days and returned to terrestrial gravity 2.3 days before tissues were collected. Even though interpretation of these results was complicated by the combination of inflight and postflight induced alterations, the consensus is that there is marked heterogeneity in both degree and type of responses from the whole muscle level down to the molecular level. Collectively, the muscle investigations of Cosmos 1887 clearly illustrate the wide diversity of muscle tissue responses to spaceflight. Judging from the summary report of this mission, heterogeneity of responses is not unique to muscle tissue. Elucidating the mechanism underlying this heterogeneity holds the key to explaining adaptation of the organism to prolonged spaceflight. Author

N90-26454*# Columbia Univ., New York, NY. School of Oral and Dental Surgery.

EFFECTS OF MICROGRAVITY ON RAT BONE, CARTLAGE AND CONNECTIVE TISSUES

S. Doty *In* NASA, Ames Research Center, The US Experiments Flown on the Soviet Biosatellite Cosmos 1887 Feb. 1990 p 51-56 (For primary document see N90-26452 20-51)

Avail: NTIS HC A22/MF A03 CSCL 06C

The response to hypogravity by the skeletal system was originally thought to be the result of a reduction in weight bearing. Thus a reduced rate of new bone formation in the weight-bearing bones was accepted, when found, as an obvious result of hypogravity. However, data on non-weight-bearing tissues have begun to show that other physiological changes can be expected to occur to animals during spaceflight. This overview of the Cosmos 1887 data discusses these results as they pertain to individual bones or tissues because the response seems to depend on the architecture and metabolism of each tissue under study. Various effects were seen in different tissues from the rats flown on Cosmos 1887. The femur showed a reduced bone mineral content but only in the central region of the diaphysis. This same region in the tibia showed changes in the vascularity of bone as well as some osteocytic cell death. The humerus demonstrated reduced morphometric characteristics plus a decrease in mechanical stiffness. Bone mineral crystals did not mature normally as a result of flight, suggesting a defect in the matrix mineralization process. Note that these changes relate directly to the matrix portion of the bone or some function of bone which slowly responds to changes in the environment. However, most cellular functions of bone are rapid responders. The stimulation of osteoblast precursor

cells, the osteoblast function in collagen synthesis, a change in the proliferation rate of cells in the epiphyseal growth plate, the synthesis and secretion of osteocalcin, and the movement of water into or out of tissues, are all processes which respond to environmental change. These rapidly responding events produced results from Cosmos 1887 which were frequently quite different from previous space flight data. Author

N90-26455*# National Aeronautics and Space Administration. Ames Research Center, Moffett Field, CA.

EXPERIMENT K-6-01. DISTRIBUTION AND BIOCHEMISTRY OF MINERAL AND MATRIX IN THE FEMURS OF RATS

S. Arnaud, G. Mechanic, P. Buckendahl, T. Bromage, A. Boyde, J. Elliott, E. Katz, and G Durnova (Institute of Biomedical Problems, Moscow, USSR) *In its* The US Experiments Flown on the Soviet Biosatellite Cosmos 1887 Feb. 1990 p 63-84 (For primary document see N90-26452 20-51)

Avail: NTIS HC A22/MF A03 CSCL 06C

Previous analyses of the composition of mineral and matrix in the bone of young rats following space flight has revealed deficits in calcium, phosphorus, and osteocalcin, a non-collagenous protein, without an associated decrease in collagen. To characterize the location and nature of this mineralization defect in a weight bearing long bone, the femur, researchers attempted to relate the spatial distribution of mineral in situ in the proximal, central and distal thirds of the femoral diaphysis to the biochemical composition of bone from the same area. Biochemical analyses revealed lower concentrations of calcium, phosphorus and osteocalcin but not collagen only in the central third of the diaphysis of the flight animals (F) compared to synchronous controls (S). Collagen concentration was reduced only in the proximal third of the diaphysis, where all 3 crosslinks, expressed as nM/mol collagen were higher in F than S. A new technique, x ray microtomography, with a resolution of 26 microns, was used to obtain semi-quantitative data on mineral distribution in reconstructed sections of wet whole bone. To improve the resolution of the mineral density distribution, images of the surfaces of cut sections were analyzed by backscattered electrons in a scanning electron microscope (BSE). There was good agreement between the results of the two stereochemical techniques which revealed distinct patterns of mineralization in transverse and longitudinal directions of the diaphysis. The novel methodology developed for this flight experiment shows considerable promise in elucidating the biochemical nature of what appear to be regional alterations in the mineralization of long bones of animals exposed to spaceflight. Author

N90-26456*# National Aeronautics and Space Administration. Ames Research Center, Moffett Field, CA.

EXPERIMENT K-6-02. BIOMEDICAL, BIOCHEMICAL AND MORPHOLOGICAL ALTERATIONS OF MUSCLE AND DENSE, FIBROUS CONNECTIVE TISSUES DURING 14 DAYS OF SPACEFLIGHT

A. Vailas, R. Zernicke, R. Grindeland, and A. Kaplanski (Institute of Biomedical Problems, Moscow, USSR) *In its* The US Experiments Flown on the Soviet Biosatellite Cosmos 1887 Feb. 1990 p 85-112 (For primary document see N90-26452 20-51)

Avail: NTIS HC A22/MF A03 CSCL 06C

Findings on the connective tissue response to short-term space flight (12 days) are discussed. Specifically, data regarding the biochemical, biomechanical and morphological characteristics of selected connective tissues (humerus, vertebral body, tendon and skeletal muscle) of growing rats is given. Results are given concerning the humerus cortical bone, the vertebral bone, nutritional effects on bone biomechanical properties, and soft tense fiber connective tissue response. Author

N90-26457*# National Aeronautics and Space Administration. Ames Research Center, Moffett Field, CA.

EXPERIMENT K-6-03. GRAVITY AND SKELETAL GROWTH, PART 1. PART 2: MORPHOLOGY AND HISTOCHEMISTRY OF BONE CELLS AND VASCULATURE OF THE TIBIA; PART 3: NUCLEAR VOLUME ANALYSIS OF OSTEOBLAST HISTOGENESIS IN PERIODONTAL LIGAMENT CELLS; PART 4: INTERVERTEBRAL DISC SWELLING PRESSURE ASSOCIATED WITH MICROGRAVITY

E. Holton, A. Hargens, M. Gonsalves, D. Berretta, S. Doty, W. Roberts, L. Garetto, A. Kaplansky, G. Durnova, and S. Gott (California Univ., San Diego.) et al *In its* The US Experiments Flown on the Soviet Biosatellite Cosmos 1887 Feb. 1990 p 113-149 (For primary document see N90-26452 20-51)

Avail: NTIS HC A22/MF A03 CSCL 06C

Bone area, bone electrophysiology, bone vascularity, osteoblast morphology, and osteoblast histogenesis were studied in rats associated with Cosmos 1887. The results suggest that the synchronous animals were the only group with a significantly larger bone area than the basal group, that the bone electrical potential was more negative in flight than in the synchronous rats, that the endosteal osteoblasts from flight rats had greater numbers of transitional Golgi vesicles but no difference in the large Golgi saccules or the alkaline phosphatase activity, that the perioteal vasculature in the shaft of flight rats often showed very dense intraluminal deposits with adjacent degenerating osteocytes as well as lipid accumulations within the lumen of the vessels and sometimes degeneration of the vascular wall (this change was not present in the metaphyseal region of flight animals), and that the progenitor cells decreased in flight rats while the preosteoblasts increased compared to controls. Many of the results suggest that the animals were beginning to recover from the effects of spaceflight during the two day interval between landing and euthanasia; flight effects, such as the vascular changes, did not appear to recover. Author

N90-26458*# California Univ., San Francisco. Dept. of Radiology.

EXPERIMENT K-6-04. TRACE ELEMENT BALANCE IN RATS DURING SPACEFLIGHT

C. E. Cann, P. Patterson-Buckendahl, G. Durnova, and A. Kaplansky (Institute of Biomedical Problems, Moscow, USSR) *In* NASA, Ames Research Center, The US Experiments Flown on the Soviet Biosatellite Cosmos 1887 Feb. 1990 p 151-155 (For primary document see N90-26452 20-51)

Avail: NTIS HC A22/MF A03 CSCL 06C

Exposure to microgravity causes alterations in the skeletal and mineral homeostatic systems. Little is known about the effects of flight in an older skeleton; limited data suggest that bone resorption is increased after 5 days but no data are available about other metabolic effects. The response of a more slowly-growing skeleton to microgravity may be different than that of a younger animal, similar to the different responses seen in adolescents and adult humans to immobilization. This experiment was designed to investigate changes occurring in skeletal and mineral homeostatis in these older rats flown for two weeks in space. We may expect that the two portions of the rat vertebra, the vertebral body and the posterior elements, will show different responses to spaceflight. The results of the analyses from this study confirm major differences between portions of the vertebra. The posterior bone is more highly mineralized, evidenced by increased concentration (per unit weight of bone) of calcium (5 percent), phosphorus (6 percent) and osteocalcin (37 percent), similar to the differences seen between proximal and mid humerus in previous studies. The major increase in osteocalcin content indicates the presence of mature, low-turnover bone. The difference between flight and control animals were minimal in these older, slower-growing rats. Mass of whole vertebrae increased 6.2 percent in synchronous rats compared to less than 2 percent in flight rats over the 16 days when compared to basal controls, suggesting a decreased rate of bone growth in flight. Compared to young rats in which vertebral mass increased over 40 percent in 10 days in

controls and 20 percent in flight rats, this may be a clear indication that even in the older skeleton bone growth will slow in microgravity. Author

N90-26459*# Texas Univ., Galveston. Dept. of Surgery.
EXPERIMENT K-6-05. THE MATURATON OF BONE AND DENTIN MATRICES IN RATS FLOWN ON COSMOS 1887
D. Simmons, M. Grynpas, G. Rosenberg, and G. Durnova (Institute of Biomedical Problems, Moscow, USSR) *In* NASA, Ames Research Center, The US Experiments Flown on the Soviet Biosatellite Cosmos 1887 Feb. 1990 p 157-168 (For primary document see N90-26452 20-51)
Avail: NTIS HC A22/MF A03 CSCL 06C

The chemistry, hydroxyapatite crystal size, and maturation of the bone and dentin is characterized in rats exposed to microgravity for 12.5d in a Soviet Biosatellite (Cosmos-1887). Calvarial and vertebral bone ash was subnormal, but contained a normal percent composition of Ca, P, and Mg. These tissues varied from the norm by having lower Ca/P and higher Ca/Mg ratios than any of their age-matched controls (Vivarium and Synchronous Groups). Gradient density analyses (calvaria) indicated a strong shift to the lower sp.gr. fractions which was commensurate with impaired rates of matrix-mineral maturation. X-ray diffraction data were confirmatory. Bone hydroxyapatite crystal growth in Flight rats was preferentially altered in a way to reduce the dimension of their C-axis. Flight rat dentin was normal with respect to age-matched control Ca, P, Mg, and Zn concentrations and their Ca/P and Ca/Mg ratios. These observations affirm the concept that microgravity adversely affects the maturation of newly formed matrix and mineral moieties in bone. Author

N90-26460*# Texas Univ. Health Science Center, Houston.
EXPERIMENT K-6-06. MORPHOMETRIC AND EM ANALYSES OF TIBIAL EPIPHYSEAL PLATES FROM COSMOS 1887 RATS
P. J. Duke, D. Montufar-Solis, and G. Durnova (Institute of Biomedical Problems, Moscow, USSR) *In* NASA, Ames Research Center, The US Experiments Flown on the Soviet Biosatellite Cosmos 1887 Feb. 1990 p 169-182 (For primary document see N90-26452 20-51)
Avail: NTIS HC A22/MF A03 CSCL 06C

Light and electron microscopy studies were carried out on decalcified tibial epiphyseal plates of rats flown aboard Cosmos 1887 (12.5d flight plus 53.5h recovery). Analysis of variance showed that the proliferative zone of flight animals was significantly higher than that of synchronous controls, while the hypertrophic/calcification zone was significantly reduced. Flight animals had more cells than synchronous controls in the proliferative zone, and less in the hypertrophic/calcification region. The total number of cells, however, was significantly higher in flight animals. No differences were found for perimeter or shape factor of growth plates, but area was significantly lower in flight animals in comparison to synchronous controls. Collagen fibrils in flight animals were shorter and wider than in synchronous controls. The time required for a cell to cycle through the growth plate is 2 to 3 days, so most of the cells and matrix present were formed after the animals had returned to 1 g, and probably represent stages of recovery from microgravity exposure, which in itself is an interesting question. Author

N90-26461*# California Univ., Los Angeles. Dept. of Kinesiology.
EXPERIMENT K-6-07. METABOLIC AND MORPHOLOGIC PROPERTIES OF MUSCLE FIBERS AFTER SPACEFLIGHT
R. Edgerton, B. Miu, Thomas P. Martin, R. Roy, J. Marini, J. J. Leger, V. Oganov, and E. Ilyina-Kakueva (Institute of Biomedical Problems, Moscow, USSR) *In* NASA, Ames Research Center, The US Experiments Flown on the Soviet Biosatellite Cosmos 1887 Feb. 1990 p 183-205 (For primary document see N90-26452 20-51)
Avail: NTIS HC A22/MF A03 CSCL 06C

The present study demonstrates that the general capability of skeletal muscle to maintain its proteins decreases rapidly in response to space flight. The present findings suggest further that the magnitude of enzymatic and cell volumes changes in response to space flight depend on several factors including the muscle and its fiber type composition. It appears that in order to associate physiological relevance to the observed enzymatic changes, cell volume should be considered also. Although it remains unclear as to the stimulus, or lack of stimulus, that triggers the rapid changes in muscle proteins in response to space flight, ground-based models of muscle atrophy suggest that the reduction in mechanical loading of muscle may be more important than the total amount of activation over a 24-hr period. Author

N90-26462*# Louisville Univ., KY. Dept. of Physiology and Biophysics.
EXPERIMENT K-6-08. BIOCHEMICAL AND HISTOCHEMICAL OBSERVATIONS OF VASTUS MEDIALIS
X. J. Musacchia, J. M. Steffen, R. D. Fell, and V. S. Oganov (Institute of Biomedical Problems, Moscow, USSR) *In* NASA, Ames Research Center, The US Experiments Flown on the Soviet Biosatellite Cosmos 1887 Feb. 1990 p 207-214 (For primary document see N90-26452 20-51)
Avail: NTIS HC A22/MF A03 CSCL 06C

Muscles of the hindlimb in the rat have been used to demonstrate the effects of unloading in weightlessness and in animal models used to mimic weightlessness. The vastus medialis (VM) is discussed here. Samples were obtained from rats exposed to weightlessness for 12 days in Cosmos 1887 (Experiment K-6-08, coordinated by Dr. V.S. Oganov). The principal objective of this study was to ascertain if the vastus medialis responded to 12 days of microgravity exposure. The loss in muscle mass is greatest, -43 percent, when comparing F vs B, and least, -13 percent, when comparing F vs. V. Taken at face value these differences may be misleading. Due to the variability of the muscle weight in the basal group, these muscle mass losses may be exaggerated. In terms of percent water, there were no differences between the flight and the control groups. In spite of the limited sample, researchers conclude that muscle mass changes in the VM are not significant. Although some of the morphological parameters suggest a small degree of atrophy in the vastus medialis, the biochemical analyses (protein, RNA and DNA) suggest that these may be minimal and functionally nonsignificant. The relatively similar CS and LDH activities of VM from F and various control groups, as well as the lack of difference in LPL activity between F and S rats, suggests that there is little or no effect on the oxidative or glycolytic function of this muscle. Since the VM is chiefly a mixed fast twitch muscle, these metabolic indices of energy production are relatively unchanged. The results of VM studies are in agreement with previous observations of another type II fast twitch muscle, the EDL, from SL-3 rats which did not respond markedly to weightlessness and whole body suspension. Author

N90-26463*# Medical Coll. of Wisconsin, Milwaukee. Dept. of Anatomy and Cellular Biology.
EXPERIMENT K-6-09. MORPHOLOGICAL AND BIOCHEMICAL INVESTIGATION OF MICROGRAVITY-INDUCED NERVE AND MUSCLE BREAKDOWN. PART 1: INVESTIGATION OF NERVE AND MUSCLE BREAKDOWN DURING SPACEFLIGHT; PART 2: BIOCHEMICAL ANALYSIS OF EDL AND PLT MUSCLES
D. A. Riley, S. Ellis, J. Bain, F. Sedlak, G. Slocum, and V. Oganov (Institute of Biomedical Problems, Moscow, USSR) *In* NASA, Ames Research Center, The US Experiments Flown on the Soviet Biosatellite Cosmos 1887 Feb. 1990 p 215-261 (For primary document see N90-26452 20-51)
Avail: NTIS HC A22/MF A03 CSCL 06C

The present findings on rat hindlimb muscles suggest that skeletal muscle weakness induced by prolonged spaceflight can result from a combination of muscle fiber atrophy, muscle fiber segmental necrosis, degeneration of motor nerve terminals and destruction of microcirculatory vessels. Damage was confined to the red adductor longus (AL) and soleus muscles. The midbelly region of the AL muscle had more segmental necrosis and edema than the ends. Macrophages and neutrophils were the major mononucleated cells infiltrating and phagocytosing the cellular debris. Toluidine blue-positive mast cells were significantly

decreased in Flight AL muscles compared to controls; this indicated that degranulation of mast cells contributed to tissue edema. Increased ubiquitination of disrupted myofibrils may have promoted myofilament degradation. Overall, mitochondria content and SDH activity were normal, except for a decrease in the subsarcolemmal region. The myofibrillar ATPase activity shifted toward the fast type in the Flight AL muscles. Some of the pathological changes may have occurred or been exacerbated during the 2 day postflight period of readaptation to terrestrial gravity. While simple atrophy should be reversible by exercise, restoration of pathological changes depends upon complex processes of regeneration by stem cells. Initial signs of muscle and nerve fiber regeneration were detected. Even though regeneration proceeds on Earth, the space environment may inhibit repair and cause progressive irreversible deterioration during long term missions. Muscles obtained from Flight rats sacrificed immediately (within a few hours) after landing are needed to distinguish inflight changes from postflight readaptation. Author

N90-26464*# California Univ., Irvine. Dept. of Physiology and Biophysics.

EXPERIMENT K-6-10. EFFECTS OF ZERO GRAVITY ON MYOFIBRIL PROTEIN CONTENT AND ISOMYOSIN DISTRIBUTION IN RODENT SKELETAL MUSCLE

K. Baldwin, R. Herrick, and V. Oganov (Institute of Biomedical Problems, Moscow, USSR) *In* NASA, Ames Research Center, The US Experiments Flown on the Soviet Biosatellite Cosmos 1887 Feb. 1990 p 263-273 (For primary document see N90-26452 20-51)

Avail: NTIS HC A22/MF A03 CSCL 06C

The purpose of this experiment was to investigate the effects of 12 days of zero gravity (0G) exposure (Cosmos 1887 Biosputnik) on the enzymatic properties, protein content, and isomyosin distribution of the myofibril fraction of the slow-twitch vastus intermedius (VI) and the fast-twitch vastus lateralis (VL) muscles of adult male rats. Measurements were obtained on three experimental groups (n=5 each group) designated as flight-group (FG), vivarium-control (VC), and synchronous-control (SC). Body weight of the FG was significantly lower than the two control groups (p less than 0.05). Compared to the two control groups, VI weight was lower by 23 percent (p less than 0.10); whereas no such reduction was observed for the VL muscle. Myofibril yields (mg protein/g of muscle) in the VI were 35 percent lower in the FG compared to the controls (p less than 0.05); whereas, no such pattern was apparent for the VL muscle. When myofibril yields were expressed on a muscle basis (mg/g x muscle weight), the loss of myofibril protein was more exaggerated and suggests that myofibril protein degradation is an early event in the muscle atrophy response to 0G. Analysis of myosin isoforms indicated that slow-myosin was the primary isoform lost in the calculated degradation of total myosin. No evidence of loss of the fast isomyosins was apparent for either muscle following space flight. Myofibril ATPase activity of the VI was increased in the FG compared to controls, which is consistent with the observation of preferential slow-myosin degradation. These data suggest that muscles containing a high percent of slow-twitch fibers undergo greater degrees of myofibril protein degradation than do muscles containing predominantly fast-twitch fibers in response to a relatively short period of 0G exposure, and the primary target appears to be the slow-myosin molecule. Author

N90-26465*# Texas Univ. Health Science Center, Houston. Dept. of Physiology and Cell Biology.

EXPERIMENT K-6-11. ACTIN mRNA AND CYTOCHROME c mRNA CONCENTRATIONS IN THE TRICEPTS BRACHIA MUSCLE OF RATS

F. W. Booth, P. R. Morrison, D. B. Thomason, and V. S. Oganov (Institute of Biomedical Problems, Moscow, USSR) *In* NASA, Ames Research Center, The US Experiments Flown on the Soviet Biosatellite Cosmos 1887 Feb. 1990 p 275-278 (For primary document see N90-26452 20-51)

(Grant NAG2-239)

Avail: NTIS HC A22/MF A03 CSCL 06C

It is well known that some skeletal muscles atrophy as a result of weightlessness (Steffen and Musacchia 1986) and as a result of hindlimb suspension (Tischler et al., 1985, Thomason et al., 1987). Because the content of protein is determined by the rates of protein synthesis and degradation, a decrease in protein synthesis rate, or an increase in the protein degradation, or changes in both could produce the atrophy. Indeed, an increased protein degradation (Tischler et al., 1985) and a decreased protein synthesis (Thomason et al., 1988) have been observed in skeletal muscles of suspended hindlimbs of rats. Any decrease in protein synthesis rate could be caused by decreases in mRNA concentrations. Such decreases in the concentration and content of alpha-actin mRNA and cytochrome c mRNA have been noted in skeletal muscles of hindlimb suspended rats (Babij and Booth, 1988). From these findings researchers hypothesized that alpha-actin mRNA and cytochrome c mRNA would decrease in the triceps brachia muscle of Cosmos 1887 rats. Author

N90-26466*# National Aeronautics and Space Administration. Ames Research Center, Moffett Field, CA.

EXPERIMENT K-6-12. MORPHOMETRIC STUDIES OF ATRIAL OR GRANULES AND HEPATOCYTES. PART 1: MORPHOMETRIC STUDY OF THE LIVER; PART 2: THE ATRIAL GRANULAR ACCUMULATIONS

L. M. Kraft, L. C. Keil, and I. A. Popova (Institute of Biomedical Problems, Moscow, USSR) *In its* The US Experiments Flown on the Soviet Biosatellite Cosmos 1887 Feb. 1990 p 279-296 (For primary document see N90-26452 20-51)

Avail: NTIS HC A22/MF A03 CSCL 06C

The livers of flight, F, rats from the Cosmos 1887 mission were markedly paler and heavier than those of the synchronous, S, and vivarium, V, controls. In the F group, microscopic study revealed extensive hepatocytic intracytoplasmic vacuolization which was moderate in the S and minimal in the V groups. The vacuoles were not sudanophilic and therefore were regarded as glycogenic in origin. To obtain objective data concerning the extent of the vacuolization, livers were examined by computer assisted morphometry. Measurements of profile area and perimeter of the hepatocyte nuclei and vacuoles were evaluated according to stereological principles. Results indicated that the volume density of the nuclei was less in the F group than in the S(p equal less than 0.0002) and V(p equal less than 0.001) groups. Mean volume of individual nuclei did not differ. Volume density of the vacuoles was greater in the F than in the V group (p equal less than 0.02) while their mean diameter was less (p equal less than 0.05). To ascertain the relationship between increase in liver weight of the flight animals and the results of this study, an assumption was made that the specific gravity of the vacuolar contents was similar to the other extranuclear components of the hepatocyte. On that basis, calculations showed that the elevated vacuolar volume density in the flight group did not cause the increased liver weight in those animals, but that the non-nuclear, non-vacuolar parenchymal compartment did contribute significantly. Factors that may have played a causal role in liver weight and vacuolar compartment increases are discussed. Author

N90-26467*# National Aeronautics and Space Administration. Ames Research Center, Moffett Field, CA.

EXPERIMENT K-6-13. MORPHOLOGICAL AND BIOCHEMICAL EXAMINATION OF HEART TISSUE. PART 1: EFFECTS OF MICROGRAVITY ON THE MYOCARDIAL FINE STRUCTURE OF RATS FLOWN ON COSMOS 1887. ULTRASTRUCTURE STUDIES. PART 2: CELLULAR DISTRIBUTION OF CYCLIC AMPDEPENDENT PROTEIN KINASE REGULATORY SUBUNITS IN HEART MUSCLE OF RATS FLOWN ON COSMOS 1887

D. E. Philpott, K. Kato, J. Stevenson, Jaime Miquel, M. I. Mednieks, W. Sapp, I. A. Popova, and L. V. Serova (Institute of Biomedical Problems, Moscow, USSR) *In its* The US Experiments Flown on the Soviet Biosatellite Cosmos 1887 Feb. 1990 p 297-329 (For primary document see N90-26452 20-51)

Avail: NTIS HC A22/MF A03 CSCL 06C

The left ventricle of hearts from rats flown on the Cosmos 1887 biosatellite for 12.5 days was compared to the same tissue

of synchronous and vivarium control animals maintained in a ground based laboratory. The volume density of the mitochondria in the myocardium of the space-flown animals was statistically less (p equal less than 0.01) than that of the synchronous or vivarium control rats. Exposure to microgravity resulted in a certain degree of myocardial degeneration manifested in mitochondrial changes and accumulation of myeloid bodies. Generalized myofibrillar edema was also observed. Author

N90-26468*# Emory Univ., Atlanta, GA. Dept. of Biochemistry.
EXPERIMENT K-6-14. HEPATIC FUNCTION IN RATS AFTER SPACEFLIGHT
A. Merrill, Jr., M. Hoel, E. Wang, D. Jones, J. Hargrove, R. Mullins, and I. Popova (Institute of Biomedical Problems, Moscow, USSR) *In* NASA, Ames Research Center, The US Experiments Flown on the Soviet Biosatellite Cosmos 1887 Feb. 1990 p 331-343 (For primary document see N90-26452 20-51)
Avail: NTIS HC A22/MF A03 CSCL 06C

To determine the possible biochemical consequences of prolonged weightlessness on liver function, tissue samples from rats that had flown aboard Cosmos 1887 were analyzed for hepatic protein, glycogen and lipids as well as the activities of a number of key enzymes involved in metabolism of these compounds and xenobiotics. Among the parameters measured, the major differences were elevations in the hepatic glycogen content and HMG-CoA reductase activities of the rats flown on Cosmos 1887, and a decrease in the amount of microsomal cytochrome P sub 450 and the activity of aniline hydroxylase, a cytochrome P sub 450-dependent enzyme. Decreases in these two indices of the microsomal mixed-function oxidase system indicated that spaceflight may compromise the ability of liver to metabolize drugs and toxins. The higher HMG-CoA reductase correlated with elevated levels of serum cholestrol. Other changes included somewhat higher blood glucose, creatinine, SGOT, and much greater alkaline phosphatase and BUN. These results generally support the earlier observation of changes in these parameters (Merrill et al., Am. J. Physiol. 252:R22-R226, 1987). The importance of these alterations in liver function is not known; however, they have the potential to complicate long-term spaceflight. Author

N90-26469*# National Aeronautics and Space Administration. Ames Research Center, Moffett Field, CA.
EXPERIMENT K-6-16. MORPHOLOGICAL EXAMINATION OF RAT TESTES. THE EFFECT OF COSMOS 1887 FLIGHT ON SPERMATOGONIAL POPULATION AND TESTOSTERONE LEVEL IN RAT TESTES
D. E. Philpott, K. Kato, J. Stevenson, M. Vasques, W. Sapp, C. Williams, I. A. Popova, and L. V. Serova (Institute of Biomedical Problems, Moscow, USSR) *In its* The US Experiments Flown on the Soviet Biosatellite Cosmos 1887 Feb. 1990 p 345-358 (For primary document see N90-26452 20-51)
Avail: NTIS HC A22/MF A03 CSCL 06C

Testes from rats flown on Cosmos 1887 for twelve and a half days were compared to basal control, synchronous control and vivarium maintained rats. When the mean weights of flight testes, normalized for weight/100 gms, were compared to the vivarium controls they were 6.7 percent lighter. Although the flight testes were lighter than the synchronous, the difference is not significant. Counts of spermatogonial cells from 5 animals in each group revealed a 4 percent decrease in flight compared to vivarium controls. In both cases the t-Test significance was less than 0.02. The serum testosterone levels of all animals (flight, synchronous and vivarium) were significantly below the basal controls. Author

N90-26470*# Colorado State Univ., Fort Collins. Coll. of Veterinary Medicine and Biomedical Sciences.
EXPERIMENT K-6-17. STRUCTURAL CHANGES AND CELL TURNOVER IN THE RATS SMALL INTESTINE INDUCED BY SPACEFLIGHT
R. W. Phillips, H. R. Sawyer, and K. V. Smirnov (Institute of Biomedical Problems, Moscow, USSR) *In* NASA, Ames Research Center, The US Experiments Flown on the Soviet Biosatellite Cosmos 1887 Feb. 1990 p 359-363 (For primary document see N90-26452 20-51)
Avail: NTIS HC A22/MF A03 CSCL 06C

The purpose of this project was to test the hypothesis that the generalized, whole body decrease in synthetic activity associated with microgravity conditions of space flight as evidenced by negative nitrogen balance and muscle atrophy (Nicogossian and Parker, 1982; Oganov, 1981), as well as inhibited lymphocyte proliferation (Bechler and Cogoli, 1986), would be evident in cells characterized by a rapid rate of turnover. As a model, researchers chose to study the turnover of mucosal cells lining the jejunum of the small intestine, since these cells are among the most rapidly proliferating in the body. Under normal conditions, epithelial cells that line the small intestine are continually produced in the crypts of Lieberkuhn. These cells migrate out of the crypts onto intestinal villi, are progressively pushed up the villus as new crypt cells are formed, and ultimately reach the tip of villi where they are then descquamated. In rats, the entire process, from initial proliferation in crypts to desquamation, takes approximately 2 days (Cairnie et al., 1965; Lipkin, 1973). In this study, researchers determined the mitotic index for mucosal cells lining the proximal, middle, and distal regions of the jejunum in rats from three treatment groups (synchronous control, vivarium control and flight), and measured the depth of the crypts of Lieberkuhn and the length of villi present in each of the three jejunal regions sampled. Author

N90-26471*# National Aeronautics and Space Administration. Ames Research Center, Moffett Field, CA.
EXPERIMENT K-6-18. STUDY OF MUSCARINIC AND GABA (BENZODIAZEPINE) RECEPTORS IN THE SENSORY-MOTOR CORTEX, HIPPCAMPUS AND SPINAL CODE
N. Daunton, F. DAmelio, and I. Krasnov (Institute of Biomedical Problems, Moscow, USSR) *In its* The US Experiments Flown on the Soviet Biosatellite Cosmos 1887 Feb. 1990 p 365-370 (For primary document see N90-26452 20-51)
Avail: NTIS HC A22/MF A03 CSCL 06C

Frontal lobe samples of rat brains flown aboard Cosmos 1887 were processed for the study of muscarinic (cholinergic) and GABA (benzodiazepine) receptors and for immunocytochemical localization of the neurotransmitter gamma-aminobutyric acid (GABA) and glial fibrillary acidic protein (GFAP). Although radioactive labeling of both muscarinic cholinergic and GABA (benzodiazepine) receptors proved to be successful with the techniques employed, distinct receptor localization of individual laminae of the frontal neocortex was not possible since the sampling of the area was different in the various groups of animals. In spite of efforts made for proper orientation and regional identification of laminae, it was found that a densitometric (quantitation of autoradiograms) analysis of the tissue did not contribute to the final interpretation of the effects of weightlessness on these receptors. As to the immunocytochemical studies the use of both markers, GFAP and GABA antiserum, confirmed the suitability of the techniques for use in frozen material. However, similar problems to those encountered in the receptor studies prevented an adequate interpretation of the effects of micro-G exposure on the localization and distribution of GABA and GFAP. This study did, however, confirm the feasibility of investigating neurotransmitters and their receptors in future space flight experiments. Author

N90-26472*# San Jose State Univ., CA. Dept. of Biological Sciences.
EXPERIMENT K-6-19. PINEAL PHYSIOLOGY IN MICROGRAVITY: RELATION TO RAT GONADAL FUNCTION
D. Holley, M. R. I. Soliman, F. Kaddis, C. Markley, and I. Krasnov (Institute of Biomedical Problems, Moscow, USSR) *In* NASA, Ames Research Center, The US Experiments Flown on the Soviet Biosatellite Cosmos 1887 Feb. 1990 p 371-385 (For primary document see N90-26452 20-51)
Avail: NTIS HC A22/MF A03 CSCL 06C

One of the most interesting concomitants to spaceflight and exposure to microgravity has been the disturbing alteration in calcium metabolism and resulting skeletal effects. It was recognized

as early as 1685 (cited in Kitay and Altschule, 1954) that the pineal of humans calcified with age. However, little can be found in the literature relating calcification and pineal function. Given the link between exposure to microgravity and perturbation of calcium metabolism and the fact that the pineal is apparently one of the only soft tissues to calcify, researchers examined pineal calcium content following the spaceflight. Researchers concluded that the spaceflight resulted in a stress response as indicated by adrenal hypertrophy, that gonadal function was compromised, and that the pineal may be linked as part of the mechanism of the responses noted. Author

N90-26473*# National Aeronautics and Space Administration. Ames Research Center, Moffett Field, CA.

EXPERIMENT K-6-20. THE EFFECT OF SPACEFLIGHT ON PITUITARY OXYTOCIN AND VASOPRESSIN CONTENT OF RATS

L. Keil, J. Evans, R. Grindeland, and I. Krasnov (Institute of Biomedical Problems, Moscow, USSR) *In its* The US Experiments Flown on the Soviet Biosatellite Cosmos 1887 Feb. 1990 p 387-392 (For primary document see N90-26452 20-51)

Avail: NTIS HC A22/MF A03 CSCL 06C

Pituitary levels of oxytocin (OT) and vasopressin (AVP) were measured in rats exposed to 12.5 days of spaceflight (FLT) as well as ground-based controls, one group synchronously maintained in flight-type cages with similar feeding schedules (SYN), and one group in vivarium cages (VIV). Flight rats had significantly less (p less than 0.05) pituitary OT and AVP(1.10 plus or minus 0.04 and 1.69 plus or minus 0.07 micron g, n=5) than either the SYN(1.60 plus or minus 0.08 and 2.11 plus or minus 0.04 micron g, n=5) or VIV (1.54 plus or minus 0.03 and 2.10 plus or minus 0.09 micron g, n=5) control groups, respectively. Because the FLT group mean body weight was significantly less (p less than 0.05) than either control group, the pituitary hormone content was also calculated on the basis of posterior pituitary protein content. When calculated in this manner, pituitary OT in the FLT rats (5.09 plus or minus 0.15 micron g/mg protein) was significantly less (p less than 0.05) than SYN(7.66 plus or minus 0.39 micron g/mg protein) or VIV controls (8.11 plus or minus 0.64 micron g/mg protein). Pituitary AVP was also less in the FLT animals (7.80 plus or minus 0.13 micron g/mg protein) compared to either SYN(9.84 plus or minus 0.51, p less than 0.05) or VIV controls (11.01 plus or minus 0.76, p less than 0.05). The reduced levels of pituitary OT and AVP may have resulted from increased hormone secretion resulting from the combined effects of water deprivation and the stress of the novel microgravity environment. Author

N90-26474*# Washington Univ., Saint Louis, MO.

EXPERIMENT K-6-21. EFFECT OF MICROGRAVITY ON 1) METABOLIC ENZYMES OF TYPE 1 AND TYPE 2 MUSCLE FIBERS AND ON 2) METABOLIC ENZYMES, NEUTRANSMITTER AMINO ACIDS, AND NEUROTRANSMITTER ASSOCIATED ENZYMES IN MOTOR AND SOMATOSENSORY CEREBRAL CORTEX. PART 1: METABOLIC ENZYMES OF INDIVIDUAL MUSCLE FIBERS; PART 2: METABOLIC ENZYMES OF HIPPOCAMPUS AND SPINAL CORD

O. Lowry, D. McDougal, Jr., Patti M. Nemeth, M.-Y. Chi Maggie, M. Pusateri, J. Carter, J. Manchester, Beverly Norris, and I. Krasnov (Institute of Biomedical Problems, Moscow, USSR) *In* NASA, Ames Research Center, The US Experiments Flown on the Soviet Biosatellite Cosmos 1887 Feb. 1990 p 393-418 (For primary document see N90-26452 20-51)

Avail: NTIS HC A22/MF A03 CSCL 06C

The individual fibers of any individual muscle vary greatly in enzyme composition, a fact which is obscured when enzyme levels of a whole muscle are measured. The purpose of this study was therefore to assess the changes due to weightless on the enzyme patterns composed by the individual fibers within the flight muscles. In spite of the limitation in numbers of muscles examined, it is apparent that: (1) that the size of individual fibers (i.e., their dry weight) was reduced about a third, (2) that this loss in dry mass was accompanied by changes in the eight enzymes studied, and (3) that these changes were different for the two muscles, and different for the two enzyme groups. In the soleus muscle the absolute amounts of the three enzymes of oxidative metabolism decreased about in proportion to the dry weight loss, so that their concentration in the atrophic fibers was almost unchanged. In contrast, there was little loss among the four enzymes of glycogenolysis - glycolysis so that their concentrations were substantially increased in the atrophic fibers. In the TA muscle, these seven enzymes were affected in just the opposite direction. There appeared to be no absolute loss among the oxidative enzymes, whereas the glycogenolytic enzymes were reduced by nearly half, so that the concentrations of the first metabolic group were increased within the atrophic fibers and the concentrations of the second group were only marginally decreased. The behavior of hexokinase was exceptional in that it did not decrease in absolute terms in either type of muscle and probably increased as much as 50 percent in soleus. Thus, their was a large increase in concentration of this enzyme in the atrophied fibers of both muscles. Another clear-cut finding was the large increase in the range of activities of the glycolytic enzymes among individual fibers of TA muscles. This was due to the emergence of TA fibers with activities for enzymes of this group extending down to levels as low as those found in control soleus muscles. It would be interesting to know if this represents a transition stage, and whether with prolonged weightlessness most of the fibers would be transformed into a low glycogenolytic type. Author

N90-26475*# National Aeronautics and Space Administration. Ames Research Center, Moffett Field, CA.

EXPERIMENT K-6-22. GROWTH HORMONE REGULATION, SYNTHESIS AND SECRETION IN MICROGRAVITY. PART 1: SOMATOTROPH PHYSIOLOGY. PART 2: IMMUNOHISTOCHEMICAL ANALYSIS OF HYPOTHALAMIC HORMONES. PART 3: PLASMA ANALYSIS

R. Grindeland, W. Vale, W. Hymer, P. Sawchenko, M. Vasques, I. Krasnov, A. Kaplanski, and I. Victorov (Brain Research Inst., Moscow, USSR) *In its* The US Experiments Flown on the Soviet Biosatellite Cosmos 1887 Feb. 1990 p 419-470 (For primary document see N90-26452 20-51)

Avail: NTIS HC A22/MF A03 CSCL 06C

The objectives of the 1887 mission were: (1) to determine if the results of the SL-3 pituitary gland experiment (1) were repeatable; and (2) to determine what effect a longer mission would have on the rat pituitary gland growth hormone (GH) system. In the 1887 experiment two issues were considered especially important. First, it was recognized that cells prepared from individual rat pituitary glands should be considered separately so that the data from the 5 glands could be analyzed in a statistically meaningful way. Second, results of the SL-3 flight involving the hollow fiber implant and HPLC GH-variant experiments suggested that the biological activity of the hormone had been negatively affected by flight. The results of the 1887 experiment documented the wisdom of addressing both issues in the protocol. Thus, the reduction in secretory capacity of flight cells during subsequent extended cell culture on Earth was documented statistically, and thereby established the validity of the SL-3 result. The results of both flight experiments thus support the contention that there is a secretory lesion in pituitary GH cells of flight animals. The primary objective of both missions was a clear definition of the effect of spaceflight on the GH cell system. There can no longer be any reasonable doubt that this system is affected in microgravity. One explanation for the reason(s) underlying the better known effects of spaceflight on organisms, viz. changes in bone, muscle and immune systems may very well rest with such changes in bGH. In spite of the fact that rats in the Cosmos 1887 flight were on Earth for two days after flight, the data show that the GH system had still not recovered from the effects of flight. Many questions remain. One of the more important concerns the GRF responsiveness of somatotrophs after flight. This will be tested in an upcoming experiment. Author

N90-26476*# National Aeronautics and Space Administration. Ames Research Center, Moffett Field, CA.
EXPERIMENT K-6-23. EFFECT OF SPACEFLIGHT ON LEVELS AND FUNCTION OF IMMUNE CELLS
A. D. Mandel, G. Sonnenfeld, W. Berry, G. Taylor, S. R. Wellhausen, I. Konstantinova, A. Lesnyak, and B. Fuchs (Institute of Human Morphology, Moscow, USSR) *In its* The US Experiments Flown on the Soviet Biosatellite Cosmos 1887 Feb. 1990 p 471-480 (For primary document see N90-26452 20-51)
Avail: NTIS HC A22/MF A03 CSCL 06C

Two different immunology experiments were performed on samples received from rats flown on Cosmos 1887. In the first experiment, rat bone marrow cells were examined in Moscow for their response to colony stimulating factor-M. In the second experiment, rat spleen and bone marrow cells were stained in Moscow with a variety of antibodies directed against cell surface antigenic markers. These cells were preserved and shipped to the United States where they were subjected to analysis on a flow cytometer. The results of the studies indicate that bone marrow cells from flown rats showed a decreased response to colony stimulating factor than did bone marrow cells from control rats. There was a higher percentage of spleen cells from flown rats staining positively for pan-T-cell, suppressor-T-cell and innate interleukin-2 receptor antigens than from control animals. In addition, a higher percentage of cells that appeared to be part of the myelogenous population of bone marrow cells from flown rats stained positively for surface immunoglobulin than did equivalent cells from control rats. Author

N90-26477*# San Francisco Univ., CA. Physics Research Lab.
EXPERIMENT K-6-24, K-6-25, K-6-26. RADIATION DOSIMETRY AND SPECTROMETRY
E. V. Benton, A. Frank, E. R. Benton, V. Dudkin, and A. Marennyi (Institute of Biomedical Problems, Moscow, USSR) *In* NASA, Ames Research Center, The US Experiments Flown on the Soviet Biosatellite Cosmos 1887 Feb. 1990 p 483-511 (For primary document see N90-26452 20-51)
(Contract NCC2-521; NAG9-235)
Avail: NTIS HC A22/MF A03 CSCL 06C

Radiation experiments flown by the University of San Francisco on the Cosmos 1887 spacecraft were designed to measure the depth dependence of both total dose and heavy particle flux, dose and dose equivalent, down to very thin shielding. Three experiments were flown and were located both inside and outside the Cosmos 1887 spacecraft. Tissue absorbed dose rates of 264 to 0.028 rad d(-1) under shielding of 0.013 to 3.4 g/sq cm of (7)LiF were found outside the spacecraft and 0.025 rad d(-1) inside. Heavy particle fluxes of 3.43 to 1.03 x 10 to the minus 3rd power cm -2 sub s -1 sub sr -1 under shielding of 0.195 to 1.33 g/sq cm plastic were found outside the spacecraft and 4.25 times 10 to the minus 4th power cm -2 sub s -1 sub sr -1 inside (LET infinity H2O greater than or equal to 4 keV/micron m). The corresponding heavy particle dose equivalent rates outside the spacecraft were 30.8 to 19.8 mrem d(-1) and 11.4 mrem d(-1) inside. The large dose and particle fluxes found at small shielding thicknesses emphasize the importance of these and future measurements at low shielding, for predicting radiation effects on space materials and experiments where shielding is minimal and on astronauts during EVA. The Cosmos 1887 mission contained a variety of international radiobiological investigations to which the measurements apply. The high inclination orbit (62 degrees) of this mission provided a radiation environment which is seldom available to U.S. investigators. The radiation measurements will be compared with those of other research groups and also with those performed on the Shuttle, and will be used to refine computer models employed to calculate radiation exposures on other spacecraft, including the Space Station. Author

N90-26478*# San Francisco Univ., CA. Dept. of Radiology.
EXPERIMENT K-6-27. ANALYSIS OF RADIOGRAPHS AND BIOSAMPLES FROM PRIMATE STUDIES
C. Cann, A. Rakhmanov, and V. Karolkov (Institute of Biomedical Problems, Moscow, USSR) *In* NASA, Ames Research Center, The US Experiments Flown on the Soviet Biosatellite Cosmos 1887 Feb. 1990 p 513-519 (For primary document see N90-26452 20-51)
Avail: NTIS HC A22/MF A03 CSCL 06C

Serial high-contrast radiographs were obtained of both arms and the right leg of two flight and four control monkeys for the period L-60 to S+16. Longitudinal growth of the tibia, radius and ulna was linear over this period in the control monkeys. In the flight monkey for whom the feeder malfunctioned, there were significant decreases in growth of the long bones. There were also hypermineralized growth arrest lines produced in the distal radial and ulnar metaphyses following resumption of growth. In the other flight monkey, there was a suggestion of decreased long bone growth during flight and immediate postflight periods, but this recovered by the end of the postflight control experiment. There was also an increase in intracortical resorption, indicative of skeletal activation. No major changes in cortical thickness or other parameters were noted, but modification of the techniques to obtain very high quality radiographs in further studies should allow subtle changes in these processes to be quantified. Author

N90-26479*# Florida Univ., Gainesville. Dept. of Aerospace Engineering, Mechanics and Engineering Science.
IMPLEMENTATION OF SENSOR AND CONTROL DESIGNS FOR BIOREGENERATIVE SYSTEMS Final Report
Pedro R. Rodriguez, ed. May 1990 118 p
(Contract NASw-4435)
(NASA-CR-186655; NAS 1.26:186655) Avail: NTIS HC A06/MF A01 CSCL 06B

The goal of the Spring 1990 EGM 4001 Design class was to design, fabricate, and test sensors and control systems for a closed loop life support system (CLLSS). The designs investigated were to contribute to the development of NASA's Controlled Ecological Life Support System (CELSS) at Kennedy Space Center (KSC). Designs included a seed moisture content sensor, a porous medium wetness sensor, a plant health sensor, and a neural network control system. The seed group focused on the design and implementation of a sensor that could detect the moisture content of a seed batch. The porous medium wetness group concentrated on the development of a sensor to monitor the amount of nutrient solution within a porous plate incorporating either infrared reflectance or thermal conductance properties. The plant health group examined the possibility of remotely monitoring the health of the plants within the Biomass Production Chamber (BPC) using infrared reflectance properties. Finally, the neural network group concentrated on the ability to use parallel processing in order to control a robot arm and analyze the data from the health sensor to detect regions of a plant. Author

N90-26480*# National Aeronautics and Space Administration. John F. Kennedy Space Center, Cocoa Beach, FL.
PROXIMATE COMPOSITION OF SEED AND BIOMASS FROM SOYBEAN PLANTS GROWN AT DIFFERENT CARBON MONOXIDE (CO2) CONCENTRATIONS
R. M. Wheeler, C. L. Mackowiak (Bionetics Corp., Cocoa Beach, FL.), and J. C. Sager May 1990 30 p
(Contract NAS10-11624)
(NASA-TM-103496; NAS 1.15:103496) Avail: NTIS HC A03/MF A01 CSCL 06B

Soybean plants were grown for 90 days at 500, 1000, 2000, and 5000 ubar (ppm) carbon dioxide (CO2) and compared for proximate nutritional value. For both cultivars (MC and PX), seed protein levels were highest at 1000 (39.3 and 41.9 percent for MC and PX) and lowest at 2000 (34.7 and 38.9 percent for MC and PX). Seed fat (oil) levels were highest at 2000 (21.2 and 20.9 percent for MC and PX) and lowest at 5000 (13.6 and 16.6 percent for MC and PX). Seed carbohydrate levels were highest at 500 (31.5 and 28.4 percent for MC and PX) and lowest at 2000 (20.9 and 20.8 percent for MC and PX). When adjusted for total seed yield per unit growing area, the highest production of protein and carbohydrate occurred with MC at 1000, while equally high amounts of fat were produced with MC at 1000 and 2000. Seed set and

pod development at 2000 were delayed in comparison to other CO2 treatments; thus the proportionately high fat and low protein at 2000 may have been a result of the delay in plant maturity rather than CO2 concentration. Stem crude fiber and carbohydrate levels for both cultivars increased with increased CO2. Leaf protein and crude fiber levels also tended to rise with increased CO2 but leaf carbohydrate levels decreased as CO2 was increased. The results suggest that CO2 effects on total seed yield out-weighed any potential advantages to changes in seed composition.
Author

N90-26481# Wisconsin Univ., Madison. Dept. of Botany.
GAS EXCHANGE CHARACTERISTICS AS INDICATORS OF THE BASIC LIMITING FACTORS IN PHOTOSYNTHESIS Cumulative Report, 1987 - May 1989
Thomas D. Sharkey 1989 8 p
(Contract DE-FG02-87ER-13785)
(DE90-012399; DOE/ER-13785/3) Avail: NTIS HC A02/MF A01

Photosynthesis provides essentially all of the primary productivity on Earth. The rate of photosynthesis varies widely between and even within species. The basic processes are similar in most C3 plant species and so the differences in the rate of photosynthesis must be governed by feedback mechanisms regulating the rate of photosynthesis to meet the needs of the plant. Understanding these feedback mechanisms may allow us to modify them to adapt photosynthesis to the needs of humans. Researchers have concentrated on one feedback mechanism. This feedback mechanism comes into play when the capacity for starch and sucrose synthesis cannot keep pace with the chloroplast's ability to produce triose phosphate. Researchers have demonstrated that this type of feedback can occur under natural conditions and that both electron transport and Rubsico (RuBP) carboxylase are reduced in activity during this feedback. It is demonstrated that the reduced activity of RuBP carboxylase is caused by reduced carbamylation. These studies have led researcher to speculate that the role of RuBP carboxylase decarbamylation (deactivation) is to regulate the pool of free phosphate inside the chloroplast stroma. In these and other ways this research has contributed to our understanding of how the rate of photosynthesis is established in plants and how that rate might be modified in the future.
DOE

N90-26482# Illinois Univ., Urbana.
PHOTOSYNTHESIS IN INTACT PLANTS Progress Report
1990 36 p
(Contract DE-FG02-86ER-13594)
(DE90-013699; DOE/ER-13594/3) Avail: NTIS HC A03/MF A01

Progress in the two years since the last renewal application has been excellent. The approach of basing the field work on a sound foundation of laboratory studies has enabled is to use methods which provide unambiguous assays of well characterized reactions. Excellent progress was made in several laboratory studies which will have direct applications in future field work, and have introduced to the laboratory a range of molecular genetics techniques which will allows the exploration of new options in the attempt to understand function at the level of molecular structure.
DOE

N90-26483# University of Southern California, Los Angeles. Dept. of Chemistry.
COMPUTER SIMULATION OF CHEMICAL REACTIONS IN SYNTHETIC MODEL COMPOUNDS AND GENETICALLY ENGINEERED ACTIVE SITES Final Report, 1 Jul. 1989 - 30 Jun. 1990
Arieh Warshel 23 May 1990 6 p
(Contract N00014-87-K-0507)
(AD-A222611) Avail: NTIS HC A02/MF A01 CSCL 06/1

The main objective of this project is to advance our understanding of the principles of biological recognition and specificity by using computer simulation approaches. Such approaches are expected to be essential for detailed elucidation of the origin of the enormous power of biological catalysts and to help in exploiting the resulting insight in designing a new generation of highly specific molecular systems. Our computer simulation models have progressed to the level where we can reproduce the effect of genetic modifications of enzymes on its catalytic power in a semiquantitative way. We are also able to estimate in a reasonable way the overall catalytic effect of some enzymes. In three years of this contract we have tried to exploit the fast accumulation of experimental information about genetically modified enzymes in developing clearer design principles.
GRA

52 AEROSPACE MEDICINE

Includes physiological factors; biological effects of radiation; and effects of weightlessness on man and animals.

N90-26484# Air Force Human Resources Lab., Williams AFB, AZ. Operations Training Div.
EYE TRACKING DEVICE FOR THE MEASUREMENT OF FLIGHT PERFORMANCE IN SIMULATORS Final Technical Report, Oct. 1987 - Apr. 1989
Kevin W. Dixon, Victoria A. Rojas, Gretchen M. Krueger, and Luke Simcik Brooks AFB, TX AFSC Mar. 1990 13 p
(AD-A220075; AFHRL-TP-89-18) Avail: NTIS HC A03/MF A01 CSCL 06/16

The use of an eye position monitor as a research tool for evaluating the field-of-view (FOV) requirements for simulator visual systems is discussed. Traditional evaluation methods rely on the use of pilot opinion and/or objective pilot performance measures. Neither provides a direct index of the pilot's visual behavior under alternative FOV conditions. Without a direct measure, interpretation of data is often problematic. The use of an eye position monitor provides a useful adjunct to these traditional methods. Described here are the system architecture, initial implementation, advantages and limitations, and future application.
GRA

N90-26485*# National Aeronautics and Space Administration. John F. Kennedy Space Center, Cocoa Beach, FL.
HEMODYNAMIC AND ADH RESPONSES TO CENTRAL BLOOD VOLUME SHIFTS IN CARDIAC-DENERVATED HUMANS
V. A. Convertino, C. A. Thompson, B. A. Benjamin, L. C. Keil, W. M. Savin, E. P. Gordon, W. L. Haskell, J. S. Schroeder, and H. Sandler (National Aeronautics and Space Administration. Ames Research Center, Moffett Field, CA.) 1990 29 p
(Contract NAS10-10285)
(NASA-TM-103471; NAS 1.15:103471) Avail: NTIS HC A03/MF A01 CSCL 06P

Hemodynamic responses and antidiuretic hormone (ADH) were measured during body position changes designed to induce blood volume shifts in ten cardiac transplant recipients to assess the contribution of cardiac and vascular volume receptors in the control of ADH secretion. Each subject underwent 15 min of a control period in the seated posture, then assumed a lying posture for 30 min at 6 deg head down tilt (HDT) followed by 20 min of seated recovery. Venous blood samples and cardiac dimensions (echocardiography) were taken at 0 and 15 min before HDT, 5, 15, and 30 min of HDT, and 5, 15, and 30 min of seated recovery. Blood samples were analyzed for hematocrit, plasma osmolality, plasma renin activity (PRA), and ADH. Resting plasma volume (PV) was measured by Evans blue dye and percent changes in PV during posture changes were calculated from changes in hematocrit. Heart rate (HR) and blood pressure (BP) were recorded every 2 min. Results indicate that cardiac volume receptors are not the only mechanism for the control of ADH release during acute blood volume shifts in man.
Author

N90-26486# Tel-Aviv Univ. (Israel).
ADJUSTMENT AND VALIDATION OF THE MATHEMATICAL PREDICTION MODEL FOR SWEAT RATE, HEART RATE, AND BODY TEMPERATURE UNDER OUTDOOR CONDITIONS Final Report, 7 Oct. 1985 - 7 Oct. 1987

Y. Shapiro, D. Moran, and Y. Epstein Aug. 1989 53 p
(Contract DAMD17-85-G-5044; DA Proj. 3E1-62777-A-879)
(AD-A222599) Avail: NTIS HC A04/MF A01 CSCL 06/1

The Military Ergonomics Division at USARIEM has developed, based on their indoor laboratory studies, individual predictive equations for rectal temperature (Tre) and sweat loss (msw). These primary physiological inputs serve in a comprehensive model that predicts the expected physical work/rest cycle, the maximum single physical work time, and the associated water requirements. These predictive equations were studied in order to validate, and if necessary to adjust, and model for use under outdoor conditions with special reference to soldiers wearing CB protective garments. GRA

N90-26487# Navy Experimental Diving Unit, Panama City, FL.
ARCTIC COLD WEATHER MEDICINE AND ACCIDENTAL HYPOTHERMIA Final Report
John A. Sterba Mar. 1990 31 p
(AD-A223090; NEDU-2-90) Avail: NTIS HC A03/MF A01 CSCL 06/5

Arctic ice camp diving operations require routine and emergency medical care to be provided by a U.S. Navy Corpsman trained as a Diving Medical Technician (DMT). This report will discuss common medical illnesses and injuries that occur in the Artic. It is based on a review of medical and operational literature and a recent deployment to the Artic. Topics discussed in this report include: cold acclimatization, recommendations for staying warm, conducting sick call and common medical problems such as dehydration, skin conditions, upper respiratory conditions, cold injuries including nonfreezing cold injury and frostbite, eye conditions, infectious diseases, psychological stresses, and common accidents and injuries encountered in the Artic. Due to much controversy in the medical and lay literature, the field treatment of hypothermia is discussed separately, reviewing both medical research and current treatment guidelines. GRA

53 BEHAVIORAL SCIENCES

Includes psychological factors; individual and group behavior; crew training and evaluation; and psychiatric research.

N90-26488*# Old Dominion Univ., Norfolk, VA. Dept. of Electrical and Computer Engineering.
INVESTIGATION OF AUTOMATED TASK LEARNING, DECOMPOSITION AND SCHEDULING Final Report, period ending 28 Feb. 1990
David L. Livingston, Gursel Serpen, and Chandrashekar L. Masti Jul. 1990 88 p
(Grant NAG1-962)
(NASA-CR-186791; NAS 1.26:186791) Avail: NTIS HC A05/MF A01 CSCL 05I

The details and results of research conducted in the application of neural networks to task planning and decomposition are presented. Task planning and decomposition are operations that humans perform in a reasonably efficient manner. Without the use of good heuristics and usually much human interaction, automatic planners and decomposers generally do not perform well due to the intractable nature of the problems under consideration. The human-like performance of neural networks has shown promise for generating acceptable solutions to intractable problems such as planning and decomposition. This was the primary reasoning behind attempting the study. The basis for the work is the use of state machines to model tasks. State machine models provide a useful means for examining the structure of tasks since many formal techniques have been developed for their analysis and synthesis. It is the approach to integrate the strong algebraic foundations of state machines with the heretofore trial-and-error approach to neural network synthesis. Author

N90-26489# Universal Energy Systems, Inc., Dayton, OH.
THE RETRIEVAL OF INFORMATION FROM SECONDARY MEMORY: A REVIEW AND NEW FINDINGS Final Report, Sep. 1987 - Mar. 1988
David L. Strayer and Arthur F. Kramer Dec. 1989 195 p
(Contract F33615-84-D-0505; AF Proj. 2313)
(AD-A222760; AAMRL-TR-88-041) Avail: NTIS HC A09/MF A01 CSCL 05/8

Memory search was compared when the memorized items were either in primary or secondary memory. Distractor tasks were used to require secondary memory storage during a memory retrieval task. The additive effects of memory load and delay support the interpretation of separate retrieval and memory search processes. In a second experiment, event related potentials were used to examine the hypothesis that the increase in reaction time from primary to secondary memory was due to the insertion of a retrieval process prior to memory comparison. P300 latency data suggest that stimulus evaluation and response related processing are both affected by delay. GRA

54 MAN/SYSTEM TECHNOLOGY AND LIFE SUPPORT

Includes human engineering; biotechnology; and space suits and protective clothing.

For related information see also *16 Space Transportation.*

N90-26490*# Florida Univ., Gainesville. Dept. of Aerospace Engineering, Mechanics and Engineering Science.
DESIGN OF SENSORS FOR CONTROL OF CLOSED LOOP LIFE SUPPORT SYSTEMS Final Report
Jul. 1990 7 p
(Contract NASw-4435)
(NASA-CR-186656; NAS 1.26:186656) Avail: NTIS HC A02/MF A01 CSCL 06K

A brief summary is presented of a Engineering Design sequence, a cooperation between NASA-Kennedy and the University of Florida on the Controlled Environmental Life Support System (CELSS) program. Part of the class was devoted to learning general principles and techniques of design. The next portion of the class was devoted to learning to design, actually fabricating and testing small components and subsystems of a CELSS. E.R.

N90-26491 Department of the Navy, Washington, DC.
HELMET-MOUNTED HEAD RESTRAINT Patent
Michael H. Patterson, inventor (to Navy) 20 Mar. 1990 4 p
Filed 3 Nov. 1988 Supersedes N90-16394 (28 - 8, p 1105), AD-D014233
(AD-D014536; US-Patent-4,909,459; US-Patent-Appl-SN-266955)
Avail: US Patent and Trademark Office CSCL 05/8

This patent discloses a head restraint for the occupant of a vehicle seat. It restrains the forward and downward movement of the occupant's head when subjected to large deceleration forces. The restraint includes a strap assembly which encircles the back of the occupant's head and releasably connects to his helmet adjacent to each of his ears at two locations. A retaining strap is slidably connected by a loop to the strap assembly and extends behind the head to a retracting means fixed in the seat. The retracting means pulls the head back against the seat when the deceleration forces exceed a predetermined level, as during flight maneuvers. During normal flight conditions, the occupant is able to move his head freely from side to side as the strap assembly slides through the loop. GRA

N90-26492*# Georgia Inst. of Tech., Atlanta. Center for Man-Machine Systems Research.
PILOT INTERACTION WITH AUTOMATED AIRBORNE DECISION MAKING SYSTEMS Final Report
John M. Hammer 1990 57 p
(Grant NAG2-123)

(NASA-CR-186730; NAS 1.26:186730) Avail: NTIS HC A04/MF A01 CSCL 05H

Ways in which computers can aid the decision making of an human operator of an aerospace system are investigated. The approach taken is to aid rather than replace the human operator, because operational experience has shown that humans can enhance the effectiveness of systems. As systems become more automated, the role of the operator has shifted to that of a manager and problem solver. This shift has created the research area of how to aid the human in this role. Published research in four areas is described. A discussion is presented of the DC-8 flight simulator at Georgia Tech. Author

N90-26493# Wichita State Univ., KS. Inst. for Aviation Research.

CHOOSING A PILOT SUBJECTIVE WORKLOAD SCALE TO FIT FLIGHT OPERATIONAL REQUIREMENTS

Randall M. Chambers and Kevin J. Kilmer Oct. 1989 26 p (IAR-89-21) Avail: NTIS HC A03/MF A01

The assessment of pilot and aircrew workload is vital to the success of flight operations. It is also important in the design of cockpit instrumentation, display and control subsystems, and flight tests, whether it be civilian or military. Currently, there are three different types of subjective assessment scales available for pilot subjective workload evaluations: (1) the Modified Cooper-Harper Scale; (2) the NASA TLX Scale; and (3) the Subjective Workload Assessment Technique (SWAT). Engineering design information and human factors data concerning the advantages and disadvantages of each scale is provided. Also, recommendations and constraints regarding the pilot's use of these scales in design, test, and operations are provided. Author

N90-26494# Wichita State Univ., KS. National Inst. for Aviation Research.

BIODYNAMIC SIMULATIONS OF AN AIRCRAFT PILOT/PASSENGER IN VARIOUS CRASH ENVIRONMENTS

Hamid Lankarani, Deren Ma, and Gayle Ermer May 1990 26 p (NIAR-90-6) Avail: NTIS HC A03/MF A01

A simple multiple-segment model of the human body is developed in order to examine its dynamic response under the action of external forcing conditions. The system is modeled as a collection of rigid elements interconnected by an array of kinematic joints constraining the relative motion of the elements. These elements include upper body combined with head and neck, lower legs, and thighs. Nonlinear rotational springs are incorporated at the joints accounting for the anatomical characteristics and limits. The constructed model is used to simulate the post-crash behavior of an aircraft pilot or passenger during surges such as frontal/side collisions and crashes in the vertical plane. A mathematical representation of the seat and interaction of the passenger with the seat cushion and back is developed. Restraints representing the seatbelts are also introduced in the model in a few different configurations. The complete model is then subjected to various pulse accelerations or decelerations in different directions. To perform a dynamic analysis a 3-D code is developed that generates and numerically solves the governing differential equations of motion in a systematic fashion. This feature of generality allows future additions to the present simple model or construction of more advanced models in a convenient way. This computerized model and the results of the simulations provide a base for predicting the motion behavior of the human body parts during crashes, understanding the effects of various types of seats and seatbelts on passenger safety, and design of mechanisms for crash protection and cockpit/cabin interior elements. Author

N90-26495# Wichita State Univ., KS. National Inst. for Aviation Research.

HUMAN PERFORMANCE IN COCKPIT-RELATED SYSTEMS

Randall M. Chambers and Mihriban Cihangirli May 1990 18 p (NIAR-90-7) Avail: NTIS HC A03/MF A01

A complex cognitive assessment battery of computerized cognitive performance tests was installed in the cockpit of a flight simulator, and cognitive performance capabilities of thirty volunteer subjects were measured on nine cognitive tests. Research on the effects of cockpit-related conditions on cognitive performance indicated that performance capabilities were affected by the process of attending to and reading selected instruments in the cockpit. Aircraft noise of 90 dBA significantly increased subjective mental workload without altering cognitive performance significantly. Although there were many individual differences among the thirty volunteer test subjects, mean cognitive performance for the fifteen males was not significantly different from the mean cognitive performance of the fifteen females. Author

N90-26496# Wichita State Univ., KS. National Inst. for Aviation Research.

HUMAN FACTORS: THE HUMAN INTERFACE WITH AIRCRAFT INTERIORS

Randall Chambers, Jeffrey Fernandez, Srikanth Nandigam, and Vankatesh Palaniswamy Jun. 1990 29 p (NIAR-90-18) Avail: NTIS HC A03/MF A01

The pilot, crew, and passengers interface with the aircraft's interior, its operational performance, its protective features and crash worthiness, its utilization during linear and angular accelerations and decelerations, and its management during crisis of a severe stress of impact and fire. Human factors considerations enter into the measurement and evaluation of crashworthiness performance, especially in the design criteria for seats, seat belts, shoulder harness, air bags, floors, and wall structures. Human factors considerations and design criteria also enter into the measurement and evaluation of performance, especially in crisis management and control, and performance of flight crew and passengers during fire, escape, depressurization, and other emergency situations. The human interface for protection in Gx accelerations and decelerations, and in Gy and Gz, have important design criteria for seats, back angle, shoulder straps and seat belts, dynamic and static supports, for head, neck, and torso. Body size and position for adults and for children require special considerations within acceleration fields produced within varying transportation systems. Subjective judgments of ride quality, comfort, and well-being are important in the human use of restraints and other interior protective components. Similarily, physiological indices and specific body distortions during deceleration, impact and burn provide important design criteria. Human use of controls and displays during emergency preparations and escape add specific design criteria and requirements for aircraft interior development. Author

N90-26497*# Pennsylvania Univ., Philadelphia. Dept. of Computer and Information Science.

ASSEMBLY VIA DISASSEMBLY: A CASE IN MACHINE PERCEPTUAL DEVELOPMENT

Ruzena K. Bajcsy and Constantine J. Tsikos Jan. 1989 12 p Sponsored in part by DEC Corp., IBM Corp. and LORD Corp. (Contracts NAG5-1045; F49620-85-K-0018; DAA29-84-K-0061; DAA29-84-9-0027; N00014-85-K-0807; NSF MCS-82-19196; NSF IRI-84-10413; NSF INT-85-14199; NSF DMC-85-17315; NATO-0224/85) (NASA-CR-186867; NAS 1.26:186867; MS-CIS-89-04; Grasp-Lab-173) Avail: NTIS HC A03/MF A01 CSCL 05H

First results in the effort of learning about representations of objects is presented. The questions attempted to be answered are: What is innate and what must be derived from the environment. The problem is casted in the framework of disassembly of an object into two parts. Author

N90-26498*# Pennsylvania Univ., Philadelphia. Dept. of Computer and Information Science.

GRASPING WITH MECHANICAL INTELLIGENCE M.S. Thesis

Nathan Thatcher Ulrich Dec. 1988 79 p (Contract NAG5-1045; N00140-85-K-0807; NSF MEA-81-19884; NSF DCR-84-10771; NSF INT-85-14199; NSF DMC-85-17315; NSF DCR-82-19196) (NASA-CR-186864; NAS 1.26:186864; MS-CIS-89-51; Grasp-Lab-190) Avail: NTIS HC A05/MF A01 CSCL 05H

Many robotic hands have been designed and a number have been built. Because of the difficulty of controlling and using complex hands, which usually have nine or more degrees of freedom, the simple one- or two-degree-of-freedom gripper is still the most common robotic end effector. A new category of device is presented: a medium-complexity end effector. With three to five degrees of freedom, such a tool is much easier to control and use, as well as more economical, compact and lightweight than complex hands. In order to increase the versatility, it was necessary to identify grasping primitives and to implement them in the mechanism. In addition, power and enveloping grasps are stressed over fingertip and precision grasps. The design is based upon analysis of object apprehension types, requisite characteristics for active sensing, and a determination of necessary environmental interactions. Contained are the general concepts necessary to the design of a medium-complexity end effector, an analysis of typical performance, and a computer simulation of a grasp planning algorithm specific to this type of mechanism. Finally, some details concerning the UPenn Hand-a tool designed for the research laboratory-are presented. Author

N90-26499*# Wisconsin Univ., Milwaukee. Space Architecture Design Group.

GENESIS LUNAR OUTPOST CRITERIA AND DESIGN

Timothy Hansmann, ed. & comp., Gary T. Moore, ed. & comp., Dino J. Baschiera, Joe Paul Fieber, and Janis Huebner Moths 11 Jun. 1990 119 p

(Contract NASw-4435)

(NASA-CR-186831; NAS 1.26:186831; R90-1; ISBN-0-938744-69-0) Avail: NTIS HC A06/MF A01 CSCL 05H

This design study--the third in the space architecture series--focused on the requirements of an early stage lunar outpost. The driving assumptions of the scenario was that the base would serve as a research facility and technology testbed for future Mars missions, a habitat supporting 12 persons for durations of up to 20 months, and would sustain the following five experimental facilities: Lunar surface mining and production analysis facility, construction technology and materials testbed, closed environmental life support system (CELSS) test facility, lunar farside observatory, and human factors and environment-behavior research facility. Based upon the criteria set forth in a previous programming document, three preliminary lunar base designs were developed. Each of the three schemes studied a different construction method and configuration. The designs were then evaluated in terms of environmental response, human habitability, transportability, constructability, construction dependability and resilience, and their suitability in carrying out the desired scientific research. The positive points of each scheme were then further developed by the entire project team, resulting in one integrated lunar outpost design. Author

N90-26500*# Kansas State Univ., Manhattan. Dept. of Mechanical Engineering.

AUTOMATION OF CLOSED ENVIRONMENTS IN SPACE FOR HUMAN COMFORT AND SAFETY Report, 1989-1990

1990 121 p

(Grant NGT-21-002-800)

(NASA-CR-186834; NAS 1.26:186834) Avail: NTIS HC A06/MF A01 CSCL 05H

The results are presented of the first year of a three year project on the automation of the Environmental Control and Life Support System (ECLSS) of the Space Station Freedom (SSF). The results are applicable to other future space mission. The work was done by the Kansas State University NASA/USRA interdisciplinary student design team. The six ECLSS subsystems and how they interact are discussed. Proposed control schemes and their rationale are discussed for the Atmosphere Revitalization (AR) subsystem. Finally, a description of the mathematical models for many components of the ECLSS control system is given. Author

N90-26501*# Idaho Univ., Moscow. Dept. of Mechanical Engineering.

GREENHOUSE DESIGN FOR A MARTIAN COLONY: STRUCTURAL, SOLAR COLLECTION AND LIGHT DISTRIBUTION SYSTEMS

[1990] 93 p

(Grant NGT-21-002-800)

(NASA-CR-186818; NAS 1.26:186818) Avail: NTIS HC A05/MF A01 CSCL 05H

The inflatable structure serves as an ideal greenhouse while being feasible to transport and easy to assemble on Mars. Locating the structure underground protects it from the extreme environmental variations on the surface. The proposed lighting system provides all the necessary light for photosynthesis with little external power demand. These considerations make the proposed greenhouse design a viable means of providing an ongoing food supply for a Martian colony. Author

N90-26502# Norwegian Defence Research Establishment, Kjeller.

HUMAN PERFORMANCE MODELS

Oivind Skare 7 Feb. 1990 229 p In NORWEGIAN; ENGLISH summary

(FFI-90/7002; ISSN-0802-2437; ETN-90-97035) Avail: NTIS HC A11/MF A02

An overview of human performance models is given. The models are classified after Rasmussen's framework for characterizing various categories of behavior and after basic tasks which an operator is assumed to perform. The overview is concentrated on quantitative models and dynamic man machine systems. It is used on a command and weapon control system. Each activity in a weapon engagement is decomposed to a set of basic tasks. An experiment performed with chosen subjects is described. Different aspects with respect to how these subjects combine information are examined. ESA

N90-26503*# Maryland Univ., College Park. Inst. for Physical Science and Technology.

DEVELOPMENT OF EYE-SAFE LIDAR FOR AEROSOL MEASUREMENTS Final Report, 1988-1989

Upendra N. Singh and Thomas D. Wilderson Aug. 1990 8 p

(Grant NAG5-1114)

(NASA-CR-186905; NAS 1.26:186905; BN-1114) Avail: NTIS HC A02/MF A01 CSCL 06Q

Research is summarized on the development of an eye safe Raman conversion system to carry out lidar measurements of aerosol and clouds from an airborne platform. Radiation is produced at the first Stokes wavelength of 1.54 micron in the eye safe infrared, when methane is used as the Raman-active medium, the pump source being a Nd:YAG laser at 1.064 micron. Results are presented for an experimental study of the dependence of the 1.54 micron first Stokes radiation on the focusing geometry, methane gas pressure, and pump energy. The specific new technique developed for optimizing the first Stokes generation involves retroreflecting the backward-generated first Stokes light back into the Raman cell as a seed Stokes beam which is then amplified in the temporal tail of the pump beam. Almost 20 percent conversion to 1.54 micron is obtained. Complete, assembled hardware for the Raman conversion system was delivered to the Goddard Space Flight Center for a successful GLOBE flight (1989) to measure aerosol backscatter around the Pacific basin. Author

N90-26504# Syracuse Univ., NY. Dept. of Chemical Engineering and Materials Science.

DEVELOPMENT OF MEMBRANE PROCESS FOR CARBON DIOXIDE SEPARATION FROM DIVING ATMOSPHERE

S. A. Stern and K. A. Lokhandnala May 1990 84 p

(AD-A222606; NCSC-CR-20C-1-90) Avail: NTIS HC A05/MF A01 CSCL 13/10

Computer simulations show that membrane separation processes can be used effectively to remove Carbon dioxide 2 from exhaled air in an underwater breathing apparatus. Membrane separation processes are based on the selective permeation of

the components of a gas mixture through nonporous polymer membranes. A permeator module provided with membranes in the form of asymmetric or composite hollow fibers is best suited for CO2 removal from exhaled air. The operation of such a permeator, designed to reduce the CO2 concentration in exhaled air from about 4 to 1 mole-percent, was simulated in order to determine its optimum dimensions and membrane are requirement. The exhaled air will flow in such a permeator in an axial direction inside the hollow fibers, while the external surface of the fibers will be in contact with sea water. The fraction of the exhaled air permeating through the hollow fibers (the permeate) will be enriched in CO2, which will be dissipated in the sea water. GRA

N90-26505# Krug International, San Antonio, TX. Technology Services Div.
AIRCREW LIFE SUPPORT SYSTEMS ENHANCEMENT Final Report, 1 Aug. 1985 - 30 Apr. 1989
Robert W. Krutz, Jr., Thomas E. Nesthus, William R. Scott, James T. Webb, Cherie J. Noles, Janet F. Wiegman, Rosalind A. Chavez, and Bijan Eshaghian Feb. 1990 108 p
(Contract F33615-85-C-4503; AF Proj. 7930)
(AD-A222626; USAFSAM-TR-89-26) Avail: NTIS HC A06/MF A01 CSCL 06/5

This final report is a summary of the contract objectives and accomplishments; it includes a complete bibliography of reports generated for the Crew Technology Division. The scientific, engineering, and technical team from KRUG International provided support in accordance with task assignments developed from the statement of work as summarized in each of the 11 areas discussed in this report. Each summary is followed by a review of the accomplishments with reference, where appropriate, to the appendix which lists publications documenting the work completed. GRA

N90-26506# Naval Postgraduate School, Monterey, CA.
MOTION SICKNESS, VISUAL DISPLAYS, AND ARMORED VEHICLE DESIGN Contractor Report, Oct. 1988 - Sep. 1989
Apr. 1990 129 p Proceedings of a Conference on Wraparound Visual Displays, Waltham, MA 14-15 Jan. 1988
(AD-A222678; BRL-CR-629) Avail: NTIS HC A07/MF A01 CSCL 06/10

The report analyzes the operational requirements of low-profile armored vehicles and the underlying causes of motion sickness symptoms arising from conflicting visual vestibular cues. The report identifies some of the probable determinants of motion sickness symptoms and recommends profitable directions for further research on this topic. GRA

N90-26507# Illinois Univ., Urbana-Champaign.
PSYCHOPHYSIOLOGICAL ASSESSMENT OF PILOT WORKLOAD IN AN APPLIED SETTING M.S. Thesis
John Steven Bell 1990 139 p Sponsored by AFIT, Wright-Patterson AFB, OH
(AD-A222707; AD-E501236; AFIT/CI/CIA-90-026) Avail: NTIS HC A07/MF A01 CSCL 05/8

One of the greatest problems facing researchers, design teams, and practitioners of engineering psychology is to determine that the product of their labors, whether a new type of computer interface or a new concept cockpit in a next generation aircraft, places demands upon the operator that are consistent with the known limits of human performance capacities. It is one thing to have a machine that performs a task with great efficiency. It is quite another to place a human operator at the controls of this machine and obtain ideal performance efficiency levels. Engineers are most concerned that the machine they have constructed is functionally capable of performing the operations it was designed for and sustaining its function within some specified lifetime. The machine's functional parameters are easily tested and relatively well understood. GRA

N90-26508# North Carolina Univ., Chapel Hill. Dept. of Computer Science.
A REAL-TIME OPTICAL 3D TRACKER FOR HEAD-MOUNTED DISPLAY SYSTEMS
Jih-fang Wang, Vernon Chi, and Henry Fuchs Mar. 1990 11 p
(Contract N00014-86-K-0680; NIH-RR-02170)
(AD-A222747) Avail: NTIS HC A03/MF A01 CSCL 17/11

A new optical system for real-time, three-dimensional position tracking is described. This system adopts and inside-out tracking paradigm. The working environment is a room where the ceiling is lined with a regular pattern of infrared LEDs flashing under the systems's control. Three cameras are mounted on a helmet which the user wears. Each camera uses a lateral effect photodiode as the recording surface. The 2-D positions of the LED images inside the field of view of the cameras are detected and reported in real time. The measured 2-D image positions and the known 3-D positions of the LEDs are used to compute the position and orientation of the camera assembly in space. We have designed an iterative algorithm to estimate the 3-D position of the camera assembly in space. The algorithms is a generalized version of the Church's method, and allows for multiple cameras with nonconvergent nodal points. Several equations are formulated to predict the system's error analytically. The requirements of accuracy, speed, adequate working volume, light weight and small size of the tracker are also addressed. GRA

55 SPACE BIOLOGY

Includes exobiology; planetary biology; and extraterrestrial life.

No abstracts in this category.

59 MATHEMATICAL AND COMPUTER SCIENCES (GENERAL)

N90-26509*# Institute for Computer Applications in Science and Engineering, Hampton, VA.
RUN-TIME PARALLELIZATION AND SCHEDULING OF LOOPS Final Report
Joel H. Saltz, Ravi Mirchandaney, and Kay Crowley (Yale Univ., New Haven, CT.) May 1990 25 p Revised Submitted for publication
(Contracts NAS1-18605; N00014-86-K-0310; NSF ASC-88-19374)
(NASA-CR-182039; NAS 1.26:182039; ICASE-90-34; ICASE-88-70-Rev) Avail: NTIS HC A03/MF A01 CSCL 12A

Run time methods are studied to automatically parallelize and schedule iterations of a do loop in certain cases, where compile-time information is inadequate. The methods presented involve execution time preprocessing of the loop. At compile-time, these methods set up the framework for performing a loop dependency analysis. At run time, wave fronts of concurrently executable loop iterations are identified. Using this wavefront information, loop iterations are reordered for increased parallelism. Symbolic transformation rules are used to produce: inspector procedures that perform execution time preprocessing and executors or transformed versions of source code loop structures. These transformed loop structures carry out the calculations planned in the inspector procedures. Performance results are presented from experiments conducted on the Encore Multimax. These results illustrate that run time reordering of loop indices can have a significant impact on performance. Furthermore, the overheads associated with this type of reordering are amortized when the loop is executed several times with the same dependency structure. Author

N90-26510*# Institute for Computer Applications in Science and Engineering, Hampton, VA.
[RESEARCH CONDUCTED AT THE INSTITUTE FOR COMPUTER APPLICATIONS IN SCIENCE AND ENGINEERING IN APPLIED MATHEMATICS, NUMERICAL ANALYSIS, AND COMPUTER SCIENCE] Final Report, 1 Oct. 1989 - 31 Mar. 1990
Jun. 1990 58 p
(Contract NAS1-18605)
(NASA-CR-182057; NAS 1.26:182057) Avail: NTIS HC A04/MF A01 CSCL 12A

Research conducted at the Institute for Computer Applications in Science and Engineering in applied mathematics, numerical analysis, and computer science is summarized. Author

N90-26511*# National Aeronautics and Space Administration. Langley Research Center, Hampton, VA.
KNOWLEDGE-BASED SYSTEM FOR FLIGHT INFORMATION MANAGEMENT Thesis
Wendell R. Ricks Jun. 1990 90 p
(NASA-TM-102685; NAS 1.15:102685) Avail: NTIS HC A05/MF A01 CSCL 09B

The use of knowledge-based system (KBS) architectures to manage information on the primary flight display (PFD) of commercial aircraft is described. The PFD information management strategy used tailored the information on the PFD to the tasks the pilot performed. The KBS design and implementation of the task-tailored PFD information management application is described. The knowledge acquisition and subsequent system design of a flight-phase-detection KBS is also described. The flight-phase output of this KBS was used as input to the task-tailored PFD information management KBS. The implementation and integration of this KBS with existing aircraft systems and the other KBS is described. The flight tests are examined of both KBS's, collectively called the Task-Tailored Flight Information Manager (TTFIM), which verified their implementation and integration, and validated the software engineering advantages of the KBS approach in an operational environment. Author

60 COMPUTER OPERATIONS AND HARDWARE

Includes hardware for computer graphics, firmware, and data processing.

For components see *33 Electronics and Electrical Engineering.*

N90-26512*# Toledo Univ., OH. Dept. of Computer Science.
COMPUTER ARCHITECTURE EVALUATION FOR STRUCTURAL DYNAMICS COMPUTATIONS: PROJECT SUMMARY Final Technical Report, 10 Feb. 1986 - 7 Aug. 1989
Hilda M. Standley 1989 10 p
(Grant NAG3-699)
(NASA-CR-186137; NAS 1.26:186137) Avail: NTIS HC A02/MF A01 CSCL 09B

The intent of the proposed effort is the examination of the impact of the elements of parallel architectures on the performance realized in a parallel computation. To this end, three major projects are developed: a language for the expression of high level parallelism, a statistical technique for the synthesis of multicomputer interconnection networks based upon performance prediction, and a queueing model for the analysis of shared memory hierarchies. Author

N90-26513*# Michigan Univ., Ann Arbor. Dept. of Electrical Engineering and Computer Science.
ADAPTIVE FAULT-TOLERANT ROUTING IN HYPERCUBE MULTICOMPUTERS
Ming-Syan Chen and Kang G. Shin (IBM Watson Research Center, Yorktown Heights, NY.) 1990 39 p Submitted for publication
(Contracts NAG1-296; N00014-85-K-0122; N00014-85-K-0531)
(NASA-CR-186781; NAS 1.26:186781) Avail: NTIS HC A03/MF A01 CSCL 09B

A connected hypercube with faulty links and/or nodes is called an injured hypercube. To enable any non-faulty node to communicate with any other non-faulty node in an injured hypercube, the information on component failures has to be made available to non-faulty nodes so as to route messages around the faulty components. A distributed adaptive fault tolerant routing scheme is proposed for an injured hypercube in which each node is required to know only the condition of its own links. Despite its simplicity, this scheme is shown to be capable of routing messages successfully in an injured hypercube as long as the number of faulty components is less than n. Moreover, it is proved that this scheme routes messages via shortest paths with a rather high probabiltiy and the expected length of a resulting path is very close to that of a shortest path. Since the assumption that the number of faulty components is less than n in an n-dimensional hypercube might limit the usefulness of the above scheme, a routing scheme is introduced based on depth-first search which works in the presence of an arbitrary number of faulty components. Due to the insufficient information on faulty components, the paths chosen by the above scheme may not always be the shortest. To guarantee that all messages be routed via shortest paths, it is proposed that every mode be equipped with more information than that on its own links. The effects of this additional information on routing efficiency are analyzed, and the additional information to be kept at each node for the shortest path routing is determined. Several examples and remarks are also given to illustrate the results. Author

N90-26514# Stanford Linear Accelerator Center, CA.
APPLICATIONS FOR THE SCALABLE COHERENT INTERFACE
David B. Gustavson Apr. 1990 14 p Presented at the Computing in High Energy Physics, Santa Fe, NM, 9-13 Apr. 1990
(Contract DE-AC03-76SF-00515)
(DE90-011795; SU-SLAC-Pub-5244; CONF-9004190-7) Avail: NTIS HC A03/MF A01

IEEE P1596, the Scalable Coherent Interface (formerly known as SuperBus) is based on experience gained while developing Fastbus (ANSI/IEEE 960-1986, IEC 935), Futurebus (IEEE P896.x) and other modern high performance buses. SCI goals include a minimum bandwidth of 1 GByte/sec per processor in multiprocessor systems with thousands of processors; efficient support of a coherent distributed-cache image of distributed shared memory; support for bridges which interface to existing or future buses; and support for inexpensive small rings as well as for general switched interconnections like Banyan, Omega, or crossbar networks. The status of the work in progress is reported and some applications in data acquisition and physics are suggested. DOE

N90-26515*# California Polytechnic State Univ., San Luis Obispo. Dept. of Aeronautical Engineering.
A COMPUTER MODULE USED TO CALCULATE THE HORIZONTAL CONTROL SURFACE SIZE OF A CONCEPTUAL AIRCRAFT DESIGN
Doral R. Sandlin and Stephen Mark Swanson Aug. 1990 122 p
(Contract NCC2-236)
(NASA-CR-186872; NAS 1.26:186872) Avail: NTIS HC A06/MF A01 CSCL 09B

The creation of a computer module used to calculate the size of the horizontal control surfaces of a conceptual aircraft design is discussed. The control surface size is determined by first calculating the size needed to rotate the aircraft during takeoff, and, second, by determining if the calculated size is large enough to maintain stability of the aircraft throughout any specified mission. The tail size needed to rotate during takeoff is calculated from a summation of forces about the main landing gear of the aircraft. The stability of the aircraft is determined from a summation of forces about the center of gravity during different phases of the aircraft's flight. Included in the horizontal control surface analysis are: downwash effects on an aft tail, upwash effects on a forward

canard, and effects due to flight in close proximity to the ground. Comparisons of production aircraft with numerical models show good accuracy for control surface sizing. A modified canard design verified the accuracy of the module for canard configurations. Added to this stability and control module is a subroutine that determines one of the three design variables, for a stable vectored thrust aircraft. These include forward thrust nozzle position, aft thrust nozzle angle, and forward thrust split. Author

N90-26516# Technische Univ., Eindhoven (Netherlands). Digital Systems Group.

THE BIT FULL-DECOMPOSITION OF SEQUENTIAL MACHINES

L. Jozwiak May 1989 26 p

(EUT-89-E-223; ISBN-90-6144-223-0; ISSN-0167-9708; ETN-90-97207) Avail: NTIS HC A03/MF A01

The decomposition theory of sequential machines aims to find answers to the following important practical problem: how to decompose a complex sequential machine into a number of simpler partial machines in order to: simplify the design, implementation and verification process; make it possible to process the separate partial machines and to implement the machine with existing building blocks or inside of a limited silicon area. The classification of full-decompositions is provided and the theoretical foundations of bit full-decomposition is described. Definitions of a bit partition and bit partition pairs are introduced and their usefulness to bit full-decompositions is shown. It is proved that the bit full-decomposition can be treated as a special case of the symbol full-decomposition; therefore, no new decomposition theory is needed for this case, but the symbol full-decomposition theory together with the theorems introduced here constitute the theory of bit full-decomposition. A comparison is made between the symbol and the bit full-decompositions and some practical conclusions and remarks are presented. An example illustrating the possibility and the practical usefulness of bit full-decomposition is given. ESA

N90-26517# Institut National Polytechnique, Grenoble (France). Lab. Conception de Systemes Integres.

CONCEPTION OF A RECONFIGURABLE MICROPROCESSOR Ph.D. Thesis [CONCEPTION D'UN MICROPROCESSEUR CONFIGURABLE]

Mohammed Soueidan 1989 251 p In FRENCH; ENGLISH summary

(ETN-90-97248) Avail: NTIS HC A12/MF A02

The design and realization of a reconfigurable microprocessor which tolerates manufacturing defects is presented. This microprocessor was designed to be the core of a microcontroller dedicated to high safety automatic applications. Redundant elements able to replace defective ones are integrated on the wafer. Particular attention is given to the arithmetic and logic units, for which the evaluation criteria are the complexity, the performance, the testability and reconfigurability. Data compaction circuits based on polynomial division integrated in this microprocessor are studied. A second prototype of the HYETI microprocessor was manufactured with the HCMOS3 1.2 microns technology. ESA

N90-26518*# National Aeronautics and Space Administration. Pasadena Office, CA.

SELF-CHECKING ON-LINE TESTABLE STATIC RAM Patent Application

S. Chau, inventor (to NASA) and D. Rennels, inventor (to NASA) (Jet Propulsion Lab., California Inst. of Tech., Pasadena.) 26 Jun. 1990 26 p

(Contract NAS7-918)

(NASA-Case-NPO-17939-1-CU; NAS 1.71:NPO-17939-1-CU; US-Patent-Appl-SN-543915) Avail: NTIS HC A03/MF A01 CSCL 09B

This is a fault-tolerant random access memory for use in fault-tolerant computers. It comprises a plurality of memory chips each comprising a plurality of on-line testable and correctable memory cells disposed in rows and columns for holding individually addressable binary bits and provision for error detection incorporated into each memory cell for outputting an error signal whenever a transient error occurs therein. In one embodiment, each of the memory cells comprises a pair of static memory sub-cells for simultaneously receiving and holding a common binary data bit written to the memory cell and the error detection provision comprises comparator logic for continuously sensing and comparing the contents of the memory sub-cells to one another and for outputting the error signal whenever the contents do not match. In another embodiment, each of the memory cells comprises a static memory sub-cell and a dynamic memory sub-cell for simultaneously receiving and holding a common binary data bit written to the memory cell and the error detection provision comprises comparator logic for continuously sensing and comparing the contents of the static memory sub-cell to the dynamic memory sub-cell and for outputting the error signal whenever the contents do not match. Capability for correction of errors is also included. NASA

N90-26519*# National Aeronautics and Space Administration. Pasadena Office, CA.

HIGH SPEED MAGNETO-RESISTIVE RANDOM ACCESS MEMORY Patent Application

Wu, inventor (to NASA), Stadler, inventor (to NASA), and Katti, inventor (to NASA) (Jet Propulsion Lab., California Inst. of Tech., Pasadena.) 28 Jun. 1990 25 p

(Contract NAS7-918)

(NASA-Case-NPO-17954-1-CU; NAS 1.71:NPO-17954-1-CU; US-Patent-Appl-SN-545019) Avail: NTIS HC A03/MF A01 CSCL 09B

A high speed read MRAM memory element is configured from a sandwich of magnetizable, ferromagnetic film surrounding a magneto-resistive film which may be ferromagnetic or not. One outer ferromagnetic film has a higher coercive force than the other and therefore remains magnetized in one sense while the other may be switched in sense by a switching magnetic field. The magneto-resistive film is therefore sensitive to the amplitude of the resultant field between the outer ferromagnetic films and may be constructed of a high resistivity, high magneto-resistive material capable of higher sensing currents. This permits higher read voltages and therefore faster read operations. Alternate embodiments with perpendicular anisotropy, and in-plane anisotropy are shown, including an embodiment which uses high permeability guides to direct the closing flux path through the magneto-resistive material. High density, high speed, radiation hard, memory matrices may be constructed from these memory elements. NASA

N90-26520# Massachusetts Inst. of Tech., Cambridge. Lab. for Computer Science.

ATOMIC SNAPSHOTS OF SHARED MEMORY

Yehuda Afek, Hagit Attiya, Danny Dolev, Eli Gafni, Michael Merritt, and Nir Shavit (Hebrew Univ., Jerusalem, Israel) May 1990 26 p

(Contracts N00014-83-K-0125; N00014-85-K-0168; N00014-89-J-1988; NSF CCR-86-11442)

(AD-A222765; MIT/LCS/TM-429) Avail: NTIS HC A03/MF A01 CSCL 12/6

An atomic snapshot memory is a shared data structure allowing concurrent processes to store information in a collection of shared registers, all of which may be read in a single atomic scan operation. This paper presents three wait-free implementations of atomic snapshot memory. Two constructions implement wait-free single-writer atomic snapshot memory from wait-free atomic single-writer, n-reader registers. A third construction implements a wait-free n-writer atomic snapshot memory from n-writer, n-reader registers. The first implementation uses unbounded (integer) fields in these registers, while the other implementations use only bounded registers. GRA

61 COMPUTER PROGRAMMING AND SOFTWARE

Includes computer programs, routines, alogorithms, and specific applications, e.g., CAD/CAM.

N90-26521 New South Wales Univ., Kensington (Australia). School of Chemical Engineering and Industrial Chemistry.
COMPUTER ANALYSIS OF CHROMATOGRAPHIC DATA Ph.D. Thesis Abstract Only
Ross James Smith Jan. 1989 3 p
Avail: Issuing Activity

An investigation of several methods for the presentation of qualitative retention data in chromatography showed that the retention index system of Kovats was the superior method, especially when interlaboratory comparisons were required. This system was investigated as to its reproducibility and accuracy not only in calculating Kovats indices, but also in the estimation of the column dead time, an intermediate parameter which is of great importance when fundamental data such as Henry's Law constants, and adsorption isotherms are being estimated. A number of mathematical methods for the calculation of Kovats indices using n-alkane standards were evaluated. It was shown that a previously unreported problem in several methods concerned their poor performance under certain conditions which made them unsuitable for such calculations. The analysis of the equation for calculating Kovats' indices led to the discovery of a problem with the equation. Of the two possible solutions, it was shown that the addition of a e(sup c) to the parameter which previously had been reported as the column dead volume was required to achieve accurate mathematical dead volumes. A comparison of the use of n-alkanes and the use of the noble gases for the estimation of dead volume, showed that the careful use of n-alkanes and the addition of the e(sup c) gave accurate results to within the experimental error. This analysis also emphasised the need to carefully choose the n-alkane standards. For the columns investigated, the use of methane to n-pentane proved to consistently produce the best results. An investigation of the effect of temperature showed that the trend varied greatly between columns. Author

N90-26522*# Research Inst. for Advanced Computer Science, Moffett Field, CA.
CAPACITY FOR PATTERNS AND SEQUENCES IN KANERVA'S SDM AS COMPARED TO OTHER ASSOCIATIVE MEMORY MODELS
James D. Keeler (Stanford Univ., CA.) Dec. 1987 12 p Sponsored in part by DARPA
(Contract NCC2-408)
(NASA-CR-180701; NAS 1.26:180701; RIACS-TR-87.29) Avail: NTIS HC A03/MF A01 CSCL 09B

The information capacity of Kanerva's Sparse Distributed Memory (SDM) and Hopfield-type neural networks is investigated. Under the approximations used, it is shown that the total information stored in these systems is proportional to the number connections in the network. The proportionality constant is the same for the SDM and Hopfield-type models independent of the particular model, or the order of the model. The approximations are checked numerically. This same analysis can be used to show that the SDM can store sequences of spatiotemporal patterns, and the addition of time-delayed connections allows the retrieval of context dependent temporal patterns. A minor modification of the SDM can be used to store correlated patterns. Author

N90-26523# National Aeronautical Lab., Bangalore (India). Systems Engineering Div.
COMPUTER AIDED HANDLING QUALITIES EVALUATION IN FREQUENCY DOMAIN
Shyam Chetty and U. N. Usha May 1989 25 p
(NAL-TM-SE-8902) Avail: NTIS HC A03/MF A01

The computer aided evaluation of frequency domain handling qualities (HQ) criteria for modern aircraft was made. To evaluate the pilot-in-the-loop criterion (Neal-Smith, Relax Static Stability or other related criteria) a vector optimisation technique was employed. This technique enables the user to directly obtain the required results (including graphical output) in a systematic manner without any trial and error. The interactive software package is flexible as it allows the designer to specify his requirements and handling qualities bounds by suitably selecting the performance index vector elements. This feature is important as the HQ specifications for modern aircraft are yet to be well defined and are strongly dependent on the configuration/task. Author

N90-26524*# National Aeronautics and Space Administration. Ames Research Center, Moffett Field, CA.
ISIS AND META PROJECTS Progress Report
Kenneth Birman, Robert Cooper, and Keith Marzullo 22 Feb. 1990 13 p Presented at the Workshop on Mission Critical Operating Systems, Washington, DC, Nov. 1989
(Contract NAG2-593; N00140-87-C-8904; ARPA Order 6037)
(NASA-CR-186645; NAS 1.26:186645) Avail: NTIS HC A03/MF A01 CSCL 09B

ISIS and META are two distributed systems projects at Cornell University. The ISIS project, has developed a new methodology, virtual synchrony, for writing robust distributed software. This approach is directly supported by the ISIS Toolkit, a programming system that is distributed to over 300 academic and industrial sites. Several interesting applications that exploit the strengths of ISIS, including an NFS-compatible replicated file system, are being developed. The META project, is about distributed control in a soft real time environment incorporating feedback. This domain encompasses examples as diverse as monitoring inventory and consumption on a factory floor and performing load-balancing on a distributed computing system. One of the first uses of META is for distributed application management: the tasks of configuring a distributed program, dynamically adapting to failures, and monitoring its performance. Recent progress and current plans are presented. This approach to distributed computing, a philosophy that is believed to significantly distinguish the work from that of others in the field, is explained. Author

N90-26525*# MCR Technology, Inc., Goleta, CA.
AN EXPERT SYSTEM BASED SOFTWARE SIZING TOOL, PHASE 2 Final Report
David Friedlander 1990 340 p
(Contract NAS7-1033)
(NASA-CR-186706; NAS 1.26:186706) Avail: NTIS HC A15/MF A02 CSCL 09B

A software tool was developed for predicting the size of a future computer program at an early stage in its development. The system is intended to enable a user who is not expert in Software Engineering to estimate software size in lines of source code with an accuracy similar to that of an expert, based on the program's functional specifications. The project was planned as a knowledge based system with a field prototype as the goal of Phase 2 and a commercial system planned for Phase 3. The researchers used techniques from Artificial Intelligence and knowledge from human experts and existing software from NASA's COSMIC database. They devised a classification scheme for the software specifications, and a small set of generic software components that represent complexity and apply to large classes of programs. The specifications are converted to generic components by a set of rules and the generic components are input to a nonlinear sizing function which makes the final prediction. The system developed for this project predicted code sizes from the database with a bias factor of 1.06 and a fluctuation factor of 1.77, an accuracy similar to that of human experts but without their significant optimistic bias. Author

N90-26526*# Maryland Univ., College Park. Dept. of Computer Science.
AUTOPLAN: A SELF-PROCESSING NETWORK MODEL FOR AN EXTENDED BLOCKS WORLD PLANNING ENVIRONMENT Final Technical Report
C. Lynne DAutrechy, James A. Reggia, and Frank McFadden Jun. 1990 49 p

(Grants NAG1-885; NSF IRI-84-51430)
(NASA-CR-186733; NAS 1.26:186733; UMIACS-TR-90-78; CS-TR-2483) Avail: NTIS HC A03/MF A01 CSCL 09B

Self-processing network models (neural/connectionist models, marker passing/message passing networks, etc.) are currently undergoing intense investigation for a variety of information processing applications. These models are potentially very powerful in that they support a large amount of explicit parallel processing, and they cleanly integrate high level and low level information processing. However they are currently limited by a lack of understanding of how to apply them effectively in many application areas. The formulation of self-processing network methods for dynamic, reactive planning is studied. The long-term goal is to formulate robust, computationally effective information processing methods for the distributed control of semiautonomous exploration systems, e.g., the Mars Rover. The current research effort is focusing on hierarchical plan generation, execution and revision through local operations in an extended blocks world environment. This scenario involves many challenging features that would be encountered in a real planning and control environment: multiple simultaneous goals, parallel as well as sequential action execution, action sequencing determined not only by goals and their interactions but also by limited resources (e.g., three tasks, two acting agents), need to interpret unanticipated events and react appropriately through replanning, etc. Author

N90-26527*# Research Triangle Inst., Research Triangle Park, NC.

SOFTWARE REQUIREMENTS: GUIDANCE AND CONTROL SOFTWARE DEVELOPMENT SPECIFICATION

B. Edward Withers, Don C. Rich, Douglas S. Lowman, and R. C. Buckland Jun. 1990 115 p
(Contract NAS1-17964)
(NASA-CR-182058; NAS 1.26:182058) Avail: NTIS HC A06/MF A01 CSCL 09B

The software requirements for an implementation of Guidance and Control Software (GCS) are specified. The purpose of the GCS is to provide guidance and engine control to a planetary landing vehicle during its terminal descent onto a planetary surface and to communicate sensory information about that vehicle and its descent to some receiving device. The specification was developed using the structured analysis for real time system specification methodology by Hatley and Pirbhai and was based on a simulation program used to study the probability of success of the 1976 Viking Lander missions to Mars. Three versions of GCS are being generated for use in software error studies. Author

N90-26528*# Notre Dame Univ., IN. Dept. of Electrical Engineering.

A HYBRID M-ALGORITHM/SEQUENTIAL DECODER FOR CONVOLUTIONAL AND TRELLIS CODES

Fu-Quan Wang and Daniel J. Costello, Jr. 29 Jun. 1990 5 p
(Grants NAG5-557; NSF NCR-89-03429)
(NASA-CR-186863; NAS 1.26:186863) Avail: NTIS HC A01/MF A01 CSCL 09B

The Viterbi Algorithm (VA) is optimum in the sense of being maximum likelihood for decoding codes with a trellis structure. However, since the VA is in fact an exhaustive search of the code trellis, the complexity of the VA grows exponentially with the constraint length upsilon. This limits its application to codes with small values of upsilon and relatively modest coding gains. The M-Algorithm (MA) is a limited search scheme which carries forward M paths in the trellis, all of the same length. All successors of the M paths are extended at the next trellis depth, and all but the best M of these are dropped. Since a limited search convolutional decoder will flounder indefinitely if one of the paths in storage is not the correct one, the data are usually transmitted in blocks. It has been shown that the performance of the MA approaches the VA at high signal to noise ratios (SNR's) with an M which is far less than the 2 sup upsilon states in the full trellis. Thus the MA can be used with larger values of upsilon, making larger coding gains possible at high SNR's. However, it still requires a relatively large fixed computational effort to achieve good performance. Author

N90-26529# Oak Ridge National Lab., TN. Computing and Telecommunications Div.

AUTOMATED SENSITIVITY ANALYSIS WITH THE GRADIENT ENHANCED SOFTWARE SYSTEM (GRESS)

J. E. Horwedel May 1990 37 p
(Contract DE-AC05-84OR-21400; DOE Proj. 3410-6926)
(DE90-011291; ORNL/M-1121) Avail: NTIS HC A03/MF A01

GRESS automates the implementation of the well-known adjoint method for performing a comprehensive sensitivity analysis of existing FORTRAN 77 computer models. The GRESS ADjoint matrix GENerator (ADGEN) option is used to calculate first derivatives and sensitivities of selected model results with respect to all input data. A small problem used to exercise most of the major program options for a GRESS/ADGEN application is provided. A description of the input and output from each processing step as well as the method for controlling the application is presented. The report is designed to aid users of the GRESS ADGEN option. DOE

N90-26530# Sandia National Labs., Livermore, CA. Applied Mechanics Dept.

ANTIPASTO: AN INTERACTIVE MESH GENERATOR AND PREPROCESSOR FOR TWO-DIMENSIONAL ANALYSIS PROGRAMS

Paul E. Nielan, Kenneth J. Perano, and William E. Mason May 1990 214 p Sponsored in part by the BRL
(Contract DE-AC04-76DR-00789)
(DE90-011755; SAND-90-8203) Avail: NTIS HC A10/MF A02

ANTIPASTO is an interactive 2-D preprocessor based on innovative user interface concepts, newly developed geometric modeling and mesh generation algorithms, and device-independent graphics. It allows the analyst to generate, with greatly reduced effort, a complete input file for many finite element programs including the DOE programs PASTA2D, TACO2D, GNATSII, NIKE2D, and DYNA2D. ANTIPASTO uses composite parametric cubics to store all lines and curves necessary to construct a mesh. Closed curves are supported because they allow more natural problem descriptions. The HPM algorithm developed at the University of California at Davis allows element meshes to be generated within arbitrarily complex regions with curved sides. ANTIPASTO currently supports the meshing of regions with one, two, three, four, five and six sides. Through the use of powerful grouping commands, elements, nodes, and boundary nodes can be identified and combined into named groups. The group names are available for use in specifying material properties, initial conditions, and boundary conditions such as constraints, loads, and slidelines. Groups can be specified in geometric terms. For example, all the elements within an arbitrary closed curve can be added to a group. This concept of geometric problem specification has several important implications. First, the analyst need not ever be concerned with node or element numbers. The model is completely described in terms of its geometry. Second, the mesh can be modified without the need to modify any other part of the model description. Finally, global mesh modification commands (such as a command to refine the entire mesh) can also be used without affecting any other part of the model description. ANTIPASTO presently runs on VAX computers under VMS and on CRAY computers under UNICOS. Versions for SUN and Macintosh workstations are being developed. DOE

N90-26531# Sandia National Labs., Albuquerque, NM. Applied Mechanics Div.

SUPES VERSION 2.1: A SOFTWARE UTILITIES PACKAGE FOR THE ENGINEERING SCIENCES

John R. Red-Horse, William C. Mills-Curran, and Dennis P. Flanagan (Hibbitt, Karlsson and Sorensen, Inc., Providence, RI.) May 1990 80 p
(Contract DE-AC04-76DP-00789)
(DE90-011763; SAND-90-0247) Avail: NTIS HC A05/MF A01

The Software Utilities Package for the Engineering Sciences (SUPES) is a collection of subprograms which perform frequently used non-numerical services for the engineering applications programmer. The three functional categories of SUPES are: (1) input command parsing; (2) dynamic memory management; and (3) system dependent utilities. The subprograms in categories one and two are written in standard FORTRAN-77, while the subprograms in category three are written to provide a standardized FORTRAN interface to several system dependent features. DOE

N90-26532# Stanford Linear Accelerator Center, CA.
OBJECT ORIENTED PROGRAMMING
Paul F. Kunz Apr. 1990 12 p Presented at the Computing in High Energy Physics, Santa Fe, NM, 9-13 Apr. 1990
(Contract DE-AC03-76SF-00515)
(DE90-011797; SU-SLAC-Pub-5241; CONF-9004190-8) Avail: NTIS HC A03/MF A01

This paper is an introduction to object oriented programming techniques. It tries to explain the concepts by using analogies with traditional programming. The object oriented approach is not inherently difficult, but most programmers find a relatively high threshold in learning it. Thus, this paper will attempt to convey the concepts with examples rather than explain the formal theory. DOE

N90-26533*# Institute for Computer Applications in Science and Engineering, Hampton, VA.
THE USE OF LANCZO'S METHOD TO SOLVE THE LARGE GENERALIZED SYMMETRIC EIGENVALUE PROBLEM IN PARALLEL Final Report
Mark T. Jones and Merrell L. Patrick (Duke Univ., Durham, NC.) Jul. 1990 29 p
(Contract NAS1-18605; NAG1-466; AF-AFOSR-0117-88)
(NASA-CR-182072; ICASE-90-48; NAS 1.26:182072) Avail: NTIS HC A03/MF A01 CSCL 09B

The generalized eigenvalue problem, K chi = lambda M sub chi, is of significant practical importance, especially in structural engineering where it arises as the vibration and buckling problems. New software, LANZ, based on Lanczo's method was developed for solving these problems and runs on SUN 3, SUN 4, Convex C-220, Cray 2, and Cray Y-MP systems. Preliminary results of using the Force to obtain a multiprocessor implementation of LANZ on MIMD parallel/vector systems are reported. A parallel execution time model of LANZ is defined and used to predict the performance of LANZ as well as examine hypothetical modifications to LANZ. The results of using dynamic shifting to improve parallelism are presented. Finally, the results of assigning a group of processors to separate shifts and finding all the desired eigenvalues using LANZ in parallel are reported. Author

N90-26534*# Purdue Univ., West Lafayette, IN. Dept. of Computer Science.
GRAPHICS APPLICATIONS UTILIZING PARALLEL PROCESSING Final Report, 1 Feb. 1989 - 30 Jun. 1990
John R. Rice 23 Jul. 1990 77 p
(Grant NAG1-789)
(NASA-CR-186719; NAS 1.26:186719) Avail: NTIS HC A05/MF A01 CSCL 09B

The results are presented of research conducted to develop a parallel graphic application algorithm to depict the numerical solution of the 1-D wave equation, the vibrating string. The research was conducted on a Flexible Flex/32 multiprocessor and a Sequent Balance 21000 multiprocessor. The wave equation is implemented using the finite difference method. The synchronization issues that arose from the parallel implementation and the strategies used to alleviate the effects of the synchronization overhead are discussed. Author

N90-26535*# Cornell Univ., Ithaca, NY. Dept. of Computer Science.
TOOLS FOR DISTRIBUTED APPLICATION MANAGEMENT
Keith Marzullo, Robert Cooper, Mark Wood, and Kenneth Birman Jun. 1990 32 p
(Grant NAG2-593)
(NASA-CR-186627; NAS 1.26:186627; TR-90-1136) Avail: NTIS HC A03/MF A01 CSCL 09B

Distributed application management consists of monitoring and controlling an application as it executes in a distributed environment. It encompasses such activities as configuration, initialization, performance monitoring, resource scheduling, and failure response. The Meta system is described: a collection of tools for constructing distributed application management software. Meta provides the mechanism, while the programmer specifies the policy for application management. The policy is manifested as a control program which is a soft real-time reactive program. The underlying application is instrumented with a variety of built-in and user-defined sensors and actuators. These define the interface between the control program and the application. The control program also has access to a database describing the structure of the application and the characteristics of its environment. Some of the more difficult problems for application management occur when pre-existing, nondistributed programs are integrated into a distributed application for which they may not have been intended. Meta allows management functions to be retrofitted to such programs with a minimum of effort. Author

N90-26536*# Northwestern Univ., Evanston, IL. Dept. of Civil Engineering.
PARALLEL PROCESSORS AND NONLINEAR STRUCTURAL DYNAMICS ALGORITHMS AND SOFTWARE Final Technical Report, 1 Mar. 1986 - 31 May 1990
Ted Belytschko 1990 152 p
(Grant NAG1-650)
(NASA-CR-186755; NAS 1.26:186755) Avail: NTIS HC A08/MF A01 CSCL 09B

Techniques are discussed for the implementation and improvement of vectorization and concurrency in nonlinear explicit structural finite element codes. In explicit integration methods, the computation of the element internal force vector consumes the bulk of the computer time. The program can be efficiently vectorized by subdividing the elements into blocks and executing all computations in vector mode. The structuring of elements into blocks also provides a convenient way to implement concurrency by creating tasks which can be assigned to available processors for evaluation. The techniques were implemented in a 3-D nonlinear program with one-point quadrature shell elements. Concurrency and vectorization were first implemented in a single time step version of the program. Techniques were developed to minimize processor idle time and to select the optimal vector length. A comparison of run times between the program executed in scalar, serial mode and the fully vectorized code executed concurrently using eight processors shows speed-ups of over 25. Conjugate gradient methods for solving nonlinear algebraic equations are also readily adapted to a parallel environment. A new technique for improving convergence properties of conjugate gradients in nonlinear problems is developed in conjunction with other techniques such as diagonal scaling. A significant reduction in the number of iterations required for convergence is shown for a statically loaded rigid bar suspended by three equally spaced springs. Author

N90-26537# Allied-Signal Aerospace Co., Kansas City, MO.
INTEGRATING EXPERT SYSTEMS WITH SOLID MODELING THROUGH INTERPROCESS COMMUNICATIONS AND THE APPLICATIONS INTERFACE SPECIFICATION
Keith E. Hummel and Michael L. Wolf Mar. 1990 13 p Presented at the ASME International Conference on Computers in Engineering, Boston, MA, 5-9 Aug. 1990
(Contract DE-AC04-76DP-00613)
(DE90-012996; KCP-613-4278; CONF-900837-4) Avail: NTIS HC A03/MF A01

Arguably the most elusive problems to automate in engineering are those that require a large degree of spatial reasoning. One of the most significant reasons for this has been the lack of appropriate software tools with which to perform research and development. The optimal software environment should integrate

the symbolic reasoning capabilities of an expert system with the analytic reasoning capabilities of a solid modeling system. This paper describes such an environment, developed using interprocess communications and a standarized solid modeling interface language. This integration has resulted in a seamless coupling that provides an expert system with dynamic access to the full power of a solid modeling system. The details of the interprocess communications protocol, the solid modeling interface language, and the data dependency tracking technique are discussed. DOE

N90-26538# Lawrence Livermore National Lab., CA.
COMPUTER ANIMATION IN MATHEMATICS, SCIENCE, AND ART
Nelson L. Max 1989 12 p Presented at the Conference on Computers in Mathematics, Palo Alto, CA, Sep. 1989 Submitted for publication Sponsored in part by Fujitsu Ltd., Japan
(Contract W-7405-eng-48; NSF GY-7699; NSF HES-70-3128; NSF SED-75-15112)
(DE90-013051; UCRL-JC-104010; CONF-8909342-1) Avail: NTIS HC A03/MF A01

At the conference whose proceedings make up this volume, my presentation consisted of a collection of excerpts from computer animated films. Since I showed only my own films, a description of my personal experiences in computer animation seems appropriate for this paper, with indications of the films shown at the conference, and where they can be obtained. DOE

N90-26539# Los Alamos National Lab., NM.
AN ANGULAR WEIGHTING APPROACH FOR CALCULATING GRADIENTS AND DIVERGENCES
Ronald C. Kirkpatrick 1990 9 p Presented at the Free Lagrange Conference, Jackson Lake, WY, 3-7 Jun. 1990 Submitted for publication
(Contract W-7405-eng-36)
(DE90-013164; LA-UR-90-2061; CONF-9006195-2) Avail: NTIS HC A02/MF A01

There are several desirable properties for a free Lagrange algorithm: a Lagrangian nature, reciprocity, minimization of numerical noise, numerical efficiency, and the ability to extend the algorithms to 3-D. In addition, some integral hydro formulations allow the mass points to drift among the other points because the divergences and gradients do not depend explicitly on the position of a mass point between two other mass points. Therefore, another desirable property is a restoring force that keeps the mesh regular. An algorithm based on the angles subtended by the Voronoi polygon sides satisfies all the above criteria, except the fourth; this is because of the necessity of using trigonometric functions. Nevertheless, this loss of efficiency may be compensated by the avoidance of reconnection noise. DOE

N90-26540# Brown Univ., Providence, RI. Dept. of Physics.
LEVEL-2 SYSTEM: PROGRAMMERS-USERS MANUAL
J. S. Hoftun 15 Jun. 1990 31 p
(Contract DE-AC02-76ER-03130)
(DE90-013324; DOE/ER-03130/51; COO-3130TC-51) Avail: NTIS HC A03/MF A01

This manual describes the design and implementation of particular parts of the system for running high level filter code in the Level-2 farm of MicroVAX computers. The various chapters detail the interfaces to this system both from the point of programming TOOLs for inclusion in the filter-code and from the point of writing VMS programs to perform control and/or monitoring of this system. A lot of detailed descriptions about how this system works are omitted. It is separated into several chapters, each of which may have been released before as separate notes. The information in this manual supersedes ALL such previous notes. DOE

N90-26541# Norwegian Defence Research Establishment, Kjeller.
DOCUMENTATION OF PROGRAM TANKPLOT
Rune Stadsnes and Jan Troim 28 Dec. 1989 87 p In ENGLISH and NORWEGIAN
(FFI-89/7019; ISSN-0802-2437; ETN-90-97032) Avail: NTIS HC A05/MF A01

The program, intended for analysis of data from the wake experiment in the plasma tank, is presented. The program reads the raw-data from files on VAX. The data is sorted, calibrated and made ready for plotting. The user can choose among different graphical displays: contour plots, three-dimensional plots and just plotting of curves. ESA

N90-26542# Centre de Recherches Scientifiques et Techniques de l'Industrie des Fabrications Metalliques, Brussels (Belgium). Afd. Machinebouw.
CAD/CAM REINFORCES THE COMPETITIVE EDGE OF EUROPEAN MOULDMAKERS
Pieter Kesteloot, Jean-Pierre Kruth (Katholieke Univ. te Leuven, Belgium), and K. U. Leuven Dec. 1989 15 p Sponsored by Commission of the European Communities
(CRIF-MC-88; ETN-90-97087) Copyright Avail: NTIS HC A03/MF A01

A Computer Aided Design (CAD)/Computer Aided Manufacturing (CAM) program, developed for European mouldmakers is described. The geometry input, mould design, and manufacture and quality control aspects are discussed. The aim of the project is elaborating complementary software tools to be integrated with existing CAD/CAM systems. Concerning the acquisition of product geometry, data communication by means of CAD neutral format files on magnetic tape or digitizing clay or wooden models is analyzed. Application examples on the turbine and shoe industries are given. ESA

N90-26543# Loughborough Univ. of Technology (England). Dept. of Mathematical Sciences.
EFFICIENT GENERALIZED CONJUGATE GRADIENT ALGORITHMS. PART 2: IMPLEMENTATION
Y. F. Hu and C. Storey Sep. 1989 18 p
(MATHS-Rept-A-118-Pt-2; ETN-90-97128) Avail: NTIS HC A03/MF A01

A new, generalized, conjugate gradient algorithm is proposed and its convergence investigated. The algorithm is compared numerically with other modified conjugate gradient methods and with limited memory quasi-Newton methods. Six different implementations of a conjugate method and the storage requirements are shown. The conjugate gradient appears to be efficient in terms of iteration numbers and has modest storage requirements. ESA

N90-26544# Rolls-Royce Ltd., Derby (England).
MATERIAL SELECTION AND DESIGN: AN EXPERT SYSTEM APPROACH
R. J. Bamkin and B. J. Piearcey 21 Jun. 1989 12 p Presented at the Open Meeting on Material Selection and Design, Birmingham, England, 7 Jun. 1989
(PNR90611; MEG0931; ETN-90-97133) Copyright Avail: NTIS HC A03/MF A01

Material selection as part of a larger design process is discussed. The results of an expert system developed to demonstrate the technology are presented. The material selection tasks are summarized graphically, which demonstrates that there is no particular time in the designs development when selection happens. The desire for automation of material selection is discussed. The demonstrator and model are detailed. Features to be considered are summarized. The problem of insuring that the information necessary for considering multidisciplinary problems is generally available to a routine system program is discussed. ESA

N90-26545# Technische Univ., Eindhoven (Netherlands). Automatic System Design Group.
LASER: A LAYOUT SENSITIVITY EXPLORER. REPORT AND USER'S MANUAL
Jose PinedadeGyvez Mar. 1989 60 p

(EUT-89-E-216; ISBN-90-6144-216-8; ISSN-0167-9708;
ETN-90-97200) Avail: NTIS HC A04/MF A01

As the IC (Integrated Circuit) pattern resolutions tend to become smaller the layout geometry plays a more important role in IC yield. The probability that a chip will fail is directly related to the way that the IC artwork is laid out. By examining the possible places where catastrophic defects may occur, potential faults can be prevented and thus the reliability of the design can be estimated. Realistic yield simulation tools must consider the specific layout. A system capable of interactively finding the critical areas for shorts and breaks, the sensitivity, and the yield of the IC artwork, for any range of defect sizes is presented. The implementation is based on a simple scanline algorithm and performs only one layout extraction for any span of defect sizes. ESA

N90-26546# Technische Univ., Eindhoven (Netherlands). Information Theory Group.

CONVERSES FOR WRITE-UNIDIRECTIONAL MEMORIES

Frans M. J. Willems May 1989 18 p
(EUT-89-E-220; ISBN-90-6144-220-6; ISSN-0167-9708;
ETN-90-97204) Avail: NTIS HC A03/MF A01

The transformation of a write-unidirectional memory channel into a channel that behaves identical in even and odd cycles is shown. For this derived channel it is proved that the average-error capacity cannot exceed log sub 2 ((1 + square root of 5)/2) = 0.69424... For the average-error capacity of the derived channel in the situation where both encoder and the decoder are uninformed, an even better upper bound (0.54588..) is found. In this case however it is assumed that in all cycles the same code is used. ESA

N90-26547# Technische Univ., Eindhoven (Netherlands). Faculty of Electrical Engineering.

THE FULL-DECOMPOSITION OF SEQUENTIAL MACHINES WITH THE SEPARATE REALIZATION OF THE NEXT-STATE AND OUTPUT FUNCTIONS

L. Jozwiak Mar. 1989 21 p
(EUT-89-E-222; ISBN-90-6144-222-2; ISSN-0167-9708;
ETN-90-97206) Avail: NTIS HC A03/MF A01

The decomposition theory of sequential machines aims to find answers to the following important practical problem: how to decompose a complex sequential machine into a number of simpler partial machines in order to: simplify the design, implementation and verification process; make it possible to process the separate partial machines and to implement the machine with existing building blocks or inside of a limited silicon area. Decomposition of the states, as well as the inputs and outputs of sequential machines is considered. A special full-decomposition strategy is investigated: the full-decomposition of sequential machines with the separate realization of the next-state and output functions. This strategy has several advantages compared to the case where a sequential machine is considered as a unit. The results of theoretical investigations are presented. The notions and theorems provided have straightforward practical interpretations and can be directly used in order to develop programs computing different sorts of decompositions for sequential machines. ESA

N90-26548# Royal Signals and Radar Establishment, Malvern (England).

THE RATIONALE AND SPECIFICATION OF THE ELLA GRAPHICS SYSTEMS

C. S. Wood, N. E. Peeling, and J. I. Thomson Nov. 1989 105 p
(RSRE-89017; BR112677; ETN-90-97060) Copyright Avail: NTIS HC A06/MF A01

The ELLA graphical language includes graphical representations of most of the high level abstractions in text ELLA, in particular high level data-types and behavioral constructs. The graphical editor allows a designer to draw a circuit using these abstractions, which is then compiled into the ELLA system. Graphical and text declarations can be used in exactly equivalent ways in the extended ELLA system specified. The graphical input system thus gives the designer the freedom to use ELLA graphics or text where each is most appropriate, without losing the high level design capabilities when he prefers to use graphics. ESA

N90-26549# Grenoble-1 Univ. (France). Equipe de Geometrie Algorithmique.

A PARALLEL ALGORITHM FOR SURFACE PLANE INTERSECTION

A. Kaufmann Nov. 1989 49 p
(IMAG-RR-794-M; ETN-90-97228) Avail: NTIS HC A03/MF A01

The problem of intersection between a surface and a plane, well-known in sequential programming, is studied for parallel computers. A parallel algorithm for computers with distributed memory is proposed. A ring network and a hypercube network are used. The interest of this algorithm is shown by several examples implemented on a hypercube FPS T40 (32 processors). ESA

N90-26550# Grenoble-1 Univ. (France). Lab. ARTEMIS.

FORMAL VERIFICATION OF THE JANUS ON-LINE MULTIPLIER

Salem Ashraf Jul. 1989 36 p
(IMAG-RR-785-I; ETN-90-97234) Avail: NTIS HC A03/MF A01

The formal proof of the on-line redundant multiplier JANUS is presented. The multiplier using the hardware description language VHLD is described. The VHLD description is translated to a functional programming language OBJ. OBJ is used to construct the temporal equations of the multiplier outputs. The time variable is eliminated and the equations are transformed into LISP functions. The Baugh-Wooley two's complement multiplier is used as specification. The equivalence between this specification and the multiplier output is proved using the tautology checker TACHE. ESA

N90-26551# Grenoble-1 Univ. (France). Lab. d'Informatique Fondamentale et d'Intelligence Artificielle.

SEGMENTATION BEFORE AND AFTER RECONSTRUCTION OF 3-D SURFACES IN DEPTH IMAGERY [SEGMENTATION AVANT/APRES RECONSTRUCTION DE SURFACES 3-D DANS DES IMAGES DE PROFONDEUR]

Jean-Paul Schmidt and Yves Demazeau Oct. 1989 43 p In FRENCH; ENGLISH summary
(RR-788-I-IMAG-97-LIFIA; ETN-90-97237) Avail: NTIS HC A03/MF A01

A survey of various segmentation methods used in obtaining a range image (or depth map) of three-dimensional objects is presented. Two main approaches are used in segmentation techniques. The first consists of reconstructing objects, usually by simple surface approximations, then inferring an implicit segmentation at the location of the intersection between reconstructed surfaces. The second technique begins with a segmentation of the image using differential geometry characteristics (especially Gaussian and mean curvatures). The patches thus obtained are then characterized (qualitatively or quantitatively) in order to perform the reconstruction. The different methods are evaluated and compared. ESA

N90-26552# Grenoble-1 Univ. (France). Techniques de l'Informatique, des Mathematiques, de la Microelectronique et de la Microscopie Quanti

STUDY OF A CLASS OF NON CONVEX OPTIMIZATION ALGORITHMS: IMPLEMENTATION AND APPLICATIONS Ph.D. Thesis [ETUDE D'UNE CLASSE D'ALGORITHMES D'OPTIMISATION NON CONVEXE IMPLEMENTATION ET APPLICATIONS]

Jamal Chaarani 1989 100 p In FRENCH
(ETN-90-97241) Avail: NTIS HC A05/MF A01

Existing algorithms are modified. Variations of the algorithms are developed for practical application to the fuel-pool problem presented by the French petroleum company ELF. A comparative study of the methods used is presented. The Tuy cup method, the branch bound method and an exterior approximation method

are compared. The characteristics of optimal solutions are compared. These characteristics are used in developing new algorithms. ESA

N90-26553# Grenoble-1 Univ. (France). Techniques de l'Informatique, des Mathematiques, de la Microelectronique et de la Microscopie Quanti

ADAPTIVE AND COMPARATIVE STUDIES OF OPTIMIZATION ALGORITHMS: IMPLEMENTATIONS AND APPLICATIONS Ph.D. Thesis [ETUDES ADAPTATIVES ET COMPARATIVES DE CERTAINS ALGORITHMES EN OPTIMISATION. IMPLEMENTATIONS EFFECTIVES ET APPLICATIONS]

Adnan Yassine 1989 256 p In FRENCH; ENGLISH summary
(ETN-90-97243) Avail: NTIS HC A12/MF A02

Comparative and adaptive optimization algorithms are studied. Their implementation and application to solving various problems in applied mathematics is presented. The algorithms studied include an algorithm for finding solutions to general linear programming problems. Lemke's pivoting method, the conditional conjugate method and the inverse partial method to solve convex quadratic programs are studied. Outer approximation methods, cutting plane methods and trust region methods for non-convex optimization are discussed. ESA

N90-26554# Institut National Polytechnique, Grenoble (France). Techniques de l'Informatique, des Mathematiques, de la Microelectronique et de la Microscopie Quanti

CONTRIBUTION TO THE DEFINITION AND APPLICATION OF NAUTILE (A NEW ENVIRONMENT FOR THE CONCEPTION AND ASSEMBLING OF INTEGRATED CIRCUITS) Ph.D. Thesis [CONTRIBUTION A LA DEFINITION ET A LA MISE EN OEUVRE DE NAUTILE (UN NOUVEL ENVIRONNEMEMENT POUR LA CONCEPTION ET L'ASSEMBLAGE DES CIRCUITS INTEGRES]

Armand Hornik 1989 148 p In FRENCH
(ETN-90-97251) Avail: NTIS HC A07/MF A01

A new system for the construction of integrated circuits is discussed. The investigation is a contribution to the New Automatic and Technology Independent Layout Environment (NAUTILE) project. From the analysis of the existing systems, a new one is defined. The proposed system must perform the conception of VLSI (Very Large Scale Integration) circuits in such a way that they can be easily coupled to the existing circuits, they are independent of the technology and generate different configurations for a circuit. The prototype of the NAUTILE system is described. ESA

N90-26555# Laboratoire d'Automatique et d'Analyse des Systemes, Toulouse (France). Equipe Outils et Logiciels pour la Communication.

FORMAL VERIFICATION OF DISTRIBUTED COMPUTING SYSTEMS: LOGIC CHARACTERIZATION OF BEHAVIOUR EQUIVALENCE Ph.D. Thesis

Francois Vernadat 1989 149 p In FRENCH; ENGLISH summary
(LAAS-89386; ETN-90-97258) Avail: NTIS HC A07/MF A01

The verification of distributed computing system specifications aims to check system executions relative to the required properties. These properties concern logic propositions about system states and events performed by the system. Two approaches are compared, and combined: one is based on observational equivalence, the other is based on temporal logic. The main method consists of doriving an explanatory model from a description of the global behavior and a particular property. A least model is associated with a specific question, by preserving analysis capacity. An equivalence relation is proposed which preserves logic properties. This approach was developed within a software environment for communication protocol analysis. ESA

N90-26556# Carnegie-Mellon Univ., Pittsburgh, PA. Robotics Inst.

INNOVATIVE DESIGN SYSTEMS: WHERE ARE WE, AND WHERE DO WE GO FROM HERE

D. Navinchandra 12 Jan. 1990 48 p
(AD-A222586; AD-E951478; CMU-RI-TR-90-01) Avail: NTIS HC A03/MF A01 CSCL 12/5

The state of the art in systems that innovate are reviewed. The review concentrates more on the techniques used in these systems rather than what the system actually did. Some of the important issues are reviewed for DA systems that work in domains requiring non-routine and innovative approaches to problem solving. This part covers issues such as analogy and metaphor, exploration and discovery and creativity. Before talking about tools and techniques, innovative designs are characterized. Earlier definitions of innovative design have tended to finess over details. For example, innovative design has been defined as any design that is: new or different or elegant or uses new ideas or is an improvement over its peers. Such a definition is correct, but it does not tell us how to measure newness. How new is something. A little more light is shed on the problem of trying to distinguish between innovative and routine design. No definition will ever be complete or accurate, but something is better than nothing. The real purpose of trying to define innovative design is to try and identify the characteristics of innovative design. With a list of such characteristics, research efforts can be better focused. If DA systems that emulate some of the characteristics of innovative design can be built, then, such systems can be said to have some form of innovative behavior. GRA

N90-26557# Naval Postgraduate School, Monterey, CA. Dept. of Operations Research.

UEDIT: A FULL-SCALE, SCROLLABLE APL2 SPREADSHEET INPUT/OUTPUT EDITOR

Peter A. Lewis and Uwe H. Steinfeld Apr. 1990 35 p Prepared for ONR, Arlington, VA
(AD-A222712; AD-E501236; NPS55-90-08) Avail: NTIS HC A03/MF A01 CSCL 12/5

A full-screen, scrollable spreadsheet-like editor written in the APL2 language is described for inputting, examining and outputting data. Mixed numeric and character arrays can be read into or read out to formatted DOS files (ASCII) or comma delimited DOS files. Alternatively a bulk mode input facility allows for rapid direct data entry, or data can be examined and edited cell-by-cell in the usual way. Columns, rows or blocks of data can be highlighted in a chosen color, shadowed, moved or copied. In addition APL functions entered on the command line can use the blocks as input or output. A facility for coding missing values is also provided. Major-to-minor (lexicographic) sorts can be performed on selected columns, and conditional or unconditional frequency tabulations and cross-tabulations of selected columns can be performed. Output is obtained as a new spreadsheet, or equivalently, as an APL2 matrix. In particular, two-way cross-tabulations of multiple columns are laid out in the spreadsheet like draftsman plots to facilitate investigation and explanation of multivariate categorical data. No numerical coding of the data is needed. GRA

N90-26558*# Illinois Univ., Urbana. Coordinated Science Lab.

SINGLE-PASS MEMORY SYSTEM EVALUATION FOR MULTIPROGRAMMING WORKLOADS

Thomas M. Conte and Wen-mei W. Hwu May 1990 25 p Sponsored in part by NCR, Liberty, SC
(Contract NAG1-613; N00014-88-K-0656; NSF MIP-88-09478)
(NASA-CR-186553; NAS 1.26:186553; AD-A222808;
UILU-ENG-90-2214; CSG-122) Avail: NTIS HC A03/MF A01 CSCL 09/2

Modern memory systems are composed of levels of cache memories, a virtual memory system, and a backing store. Varying more than a few design parameters and measuring the performance of such systems has traditionally be constrained by the high cost of simulation. Models of cache performance recently introduced reduce the cost simulation but at the expense of accuracy of performance prediction. Stack-based methods predict performance accurately using one pass over the trace for all cache sizes, but these techniques have been limited to fully-associative organizations. This paper presents a stack-based method of evaluating the performance of cache memories using a

recurrence/conflict model for the miss ratio. Unlike previous work, the performance of realistic cache designs, such as direct-mapped caches, are predicted by the method. The method also includes a new approach to the problem of the effects of multiprogramming. This new technique separates the characteristics of the individual program from that of the workload. The recurrence/conflict method is shown to be practical, general, and powerful by comparing its performance to that of a popular traditional cache simulator. The authors expect that the availability of such a tool will have a large impact on future architectural studies of memory systems. GRA

N90-26559# Rome Air Development Center, Griffiss AFB, NY.
ATN DESIGN TOOL Report, for Jun. - Jul. 1989
Sharon M. Walter and Scott B. Gregory Mar. 1990 59 p
(AF Proj. 5581)
(AD-A223030; RADC-TR-90-49) Avail: NTIS HC A04/MF A01 CSCL 05/2

An Augmented Transition Network (ATN) is one of the most widely used formalisms for parsing Natural Language sentences. This report describes the ATN Design Tool, a tool that allows a user to graphically design ATN grammars and graphically demonstrate their use for parsing sentences. Online assistance for every aspect of creating a grammar and lexicon, including provisions for saving them to files, is available within the Tool. GRA

N90-26560# California Univ., Berkeley. Div. of Computer Science.
LANGUAGE SUPPORT FOR PARALLEL COMPUTATION Final Report, Sep. 1988 - Sep. 1989
C. V. Ramamoorthy Apr. 1990 212 p
(Contract F30602-88-D-0027)
(AD-A223072; RADC-TR-90-47) Avail: NTIS HC A10/MF A01 CSCL 12/5

This final technical report summarizes the research accomplished under the Expert Science and Engineering (ES and E) program by the University of California at Berkeley through Syracuse University. The research effort, entitled Parallel Extensions for Object Oriented Programming, examined communication aspects leading to language support for parallel computation. The work undertaken in this effort has extended concurrent programming languages in their communication primitives. Although many abstraction mechanisms have been used in programming languages, including control abstraction mechanisms (such as procedures) and data abstraction mechanisms (such as data types), communication abstraction mechanisms have been found to be the most useful for parallel/concurrent programming paradigms. Work accomplished in this effort has extended those mechanisms, concentrating on inter-process communication. A formal model for concurrent systems, called the Synchronous Token-based Communicating State (STOCS) model, has been used to model and analyze concurrent systems. Since present concurrent languages do not support any form of analysis of the communication structure of programs, two new constructs based on STOCS formalism have been developed to support high level specification handshake and unit. A fair and efficient algorithm for execution of multi-process shared events is also presented. GRA

62 COMPUTER SYSTEMS

Includes computer networks and special application computer systems.

N90-26561 New South Wales Univ., Kensington (Australia). School of Electrical Engineering and Computer Science.
PANDA: A DISTRIBUTED MULTIPROCESSOR OPERATING SYSTEM Ph.D. Thesis Abstract Only
Peter Chubb 1989 2 p
Avail: Issuing Activity

PANDA is a design for a distributed multiprocessor and an operating system. PANDA is designed to allow easy expansion of both hardware and software. As such, the PANDA kernel provides only message passing and memory and process management. The other features needed for the system (device drivers, secondary storage management, etc.) are provided as replaceable user tasks. PANDA's design and implementation, both hardware and software are presented. PANDA uses multiple 68010 processors sharing memory on a VME bus, each such node potentially connected to others via a high speed network. The machine is completely homogeneous: there are no differences between processors that are detectable by programs running on the machine. A single two-processor node has been constructed. Each processor contains memory management circuits designed to allow processors to share page table safely. PANDA presents a programmers' model similar to the hardware model: a job is divided into multiple tasks, each having its own address space. Peripheral devices such as disc drives are represented within PANDA by tasks. The design is such that PANDA should provide a useful testbed for file systems and device drivers, as these can be installed without recompiling PANDA itself, and without rebooting the machine. Author

N90-26562# Argonne National Lab., IL. Mathematics and Computer Science Div.
PARALLEL PROGRAMMING WITH ALGORITHMIC SKELETONS
Ian Foster and Rick Stevens 1990 19 p Presented at the International Conference on Parallel Processing, St. Charles, 13-17 Aug. 1990
(Contract W-31-109-eng-38)
(DE90-010536; CONF-900874-2) Avail: NTIS HC A03/MF A01

An approach to parallel program development is described based on the use of algorithmic skeletons: templates for parallel algorithms, into which users slot application-specific routines to construct parallel programs. Key features of the proposal are the use of a high-level notation to express concurrent algorithms and the use of automated source-to-source transformations to implement skeletons. These features support the construction of new skeletons from old by both modification and composition. This in turn encourages an exploratory programming style, in which programmers experiment to develop good parallel implementations of applications. The use of a high-level notation encourages the user to view libraries of skeletons as archives expertise that can be consulted, modified, and extended when developing parallel programs. The application of the approach using examples is illustrated. DOE

N90-26563*# Old Dominion Univ., Norfolk, VA. Dept. of Electrical and Computer Engineering.
ATAMM MULTICOMPUTER OPERATING SYSTEM FUNCTIONAL SPECIFICATION Progress Report, Feb. - Aug. 1990
R. Mielke, J. Stoughton, S. Som, R. Obando, M. Malekpour, and B. Mandala Aug. 1990 73 p
(Contract NCC1-136)
(NASA-CR-186845; NAS 1.26:186845) Avail: NTIS HC A04/MF A01 CSCL 09B

The Algorithm To Architecture Mapping Model (ATAMM) is a marked graph model which describes the implementation of a decomposed algorithm on a data flow computer architecture. AMOS, the ATAMM Multicomputer Operating System, is an operating system which implements the ATAMM rules. A first generation version of AMOS has been developed for the Advanced Development Module (ADM), a four processor architecture based on the Westinghouse VHSIC 1750A instruction set processor. A second generation version of AMOS is being developed for the Generic VHSIC Spaceborne Computer (GVSC), a spaceborne four processor breadboard which also is based on the VHSIC 1750A instruction set architecture. The ATAMM model is defined and illustrated by example. Time performance of algorithms executed according to the ATAMM rules is considered. Strategies are described for generating operating conditions for predictable performance based on the number of available computing resources. The ADM implementation of AMOS is presented. Finally,

enhancements planned for the GVSC implementation of AMOS are described. The AMOS functional features as modified to include the enhancements are to be implemented in the GVSC breadboard system. Author

N90-26564*# National Aeronautics and Space Administration. Hugh L. Dryden Flight Research Facility, Edwards, CA.
AN AUTOMATED CALIBRATION LABORATORY FOR FLIGHT RESEARCH INSTRUMENTATION: REQUIREMENTS AND A PROPOSED DESIGN APPROACH
Nora ONeill-Rood and Richard D. Glover May 1990 16 p Presented at the 36th ISA International Instrumentation Symposium, Denver, CO, 7-10 May 1990
(NASA-TM-101719; H-1594; NAS 1.15:101719) Avail: NTIS HC A03/MF A01 CSCL 09B

NASA's Dryden Flight Research Facility (Ames-Dryden), operates a diverse fleet of research aircraft which are heavily instrumented to provide both real time data for in-flight monitoring and recorded data for postflight analysis. Ames-Dryden's existing automated calibration (AUTOCAL) laboratory is a computerized facility which tests aircraft sensors to certify accuracy for anticipated harsh flight environments. Recently, a major AUTOCAL lab upgrade was initiated; the goal of this modernization is to enhance productivity and improve configuration management for both software and test data. The new system will have multiple testing stations employing distributed processing linked by a local area network to a centralized database. The baseline requirements for the new AUTOCAL lab and the design approach being taken for its mechanization are described. Author

N90-26565# Oak Ridge Gaseous Diffusion Plant, TN.
PACIFIC MISSILE TEST CENTER INFORMATION RESOURCES MANAGEMENT ORGANIZATION (CODE 0300): THE ORACLE CLIENT-SERVER AND DISTRIBUTED PROCESSING ARCHITECTURE
A. L. Beckwith and J. T. Phillips 10 Jun. 1990 21 p Sponsored in part by Pacific Missile Test Center, Point Muju, CA
(Contract DE-AC05-84OT-21400)
(DE90-013271; K/DSRD-419) Avail: NTIS HC A03/MF A01

Computing architectures using distributed processing and distributed databases are increasingly becoming considered acceptable solutions for advanced data processing systems. This is occurring even though there is still considerable professional debate as to what truly distributed computing actually is and despite the relative lack of advanced relational database management software (RDBMS) capable of meeting database and system integrity requirements for developing reliable integrated systems. The functionally is investigated of ORACLE data base management software that is performing distributed processing between a MicroVAX/VMS minicomputer and three MS-DOS-based microcomputers. The ORACLE database resides on the MicroVAX and is accessed from the microcomputers with ORACLE SQL*NET, DECnet, and ORACLE PC TOOL PACKS. Data gathered during the study reveals that there is a demonstrable decrease in CPU demand on the MicroVAX, due to distributed processing, when the ORACLE PC Tools are used to access the database as opposed to database access from dumb terminals. Also discovered were several hardware/software constraints that must be considered in implementing various software modules. The results of the study indicate that this distributed data processing architecture is becoming sufficiently mature, reliable, and should be considered for developing applications that reduce processing on central hosts. DOE

N90-26566# Technische Univ., Eindhoven (Netherlands). Group Digital Systems.
MINAS: AN ALGORITHM FOR SYSTEMATIC STATE ASSIGNMENT OF SEQUENTIAL MACHINES: COMPUTATIONAL ASPECTS AND RESULTS
J. L. Duarte Apr. 1989 123 p
(EUT-89-E-217; ISBN-90-6144-217-6; ISSN-0167-9708; ETN-90-97201) Avail: NTIS HC A06/MF A01

One of the central problems in the physical realization of sequential machines is the selection of binary codes to represent the internal states of the machine. The method of maximal adjacencies can be viewed as an approach to the state assignment problem. Research concentrating on simple, practical strategies to implement that method is presented. A fully described program in PASCAL was included and serves a twofold purpose: it exposes concrete practical solutions, which encourages the reader to try other strategies on his (her) own; it was conceived from a general standpoint that allows checking of the correctness of different theoretic concepts emerging from the method of maximal adjacencies. A set of industrial sequential machines was chosen to test the program. Results from other existing methods are reported. ESA

N90-26567# Technische Univ., Eindhoven (Netherlands). Design Automation Section.
FROM NETWORK TO ARTWORK: AUTOMATIC SCHEMATIC DIAGRAM GENERATION
G. J. P. Koster and L. Stok Apr. 1989 86 p
(EUT-89-E-219; ISBN-90-6144-219-2; ISSN-0167-9708; ETN-90-97203) Avail: NTIS HC A05/MF A01

During the automatic generation of complex very large scale integration circuits from a high level description it is necessary to provide some graphical feedback to the designer. This can be done by drawing a schematic diagram of a temporarily constructed network. To overcome the time consuming manual drawing of such diagrams, an automatic schematic diagram generator is developed. The generator is composed out of a placement and a routing part. For both parts user oriented algorithms based on some guidelines traditionally followed in manual drawing of schematic diagrams are constructed. The algorithms are implemented and results are shown. ESA

N90-26568# Technische Univ., Delft (Netherlands).
EFFICIENT NETWORK TOPOLOGIES FOR EXTENSIBLE MASSIVELY PARALLEL COMPUTERS Ph.D. Thesis
Ferdinand Peper 1989 261 p
(ETN-90-97220) Avail: NTIS HC A12/MF A02

Extensible massively parallel computers consist of many processors, which can be extended with additional processors without changing their underlying structure. Such computers are suited for computation intensive applications. Their computation capacity can be tailored to the requirements of a user without the need to adapt software. The mechanism that provides for communication between processors is studied. A method to construct statical communication networks for extensible parallel computers is described. A fundamental problem of communication mechanisms is considered. An infinite class of extensible networks, which are based on the Cartesian graph product is constructed. A particular aspect of these networks is considered, the so-called local connectivities between the nodes. The infinite graphs which are at the base of these networks are described and several properties of the infinite graphs are deduced. ESA

N90-26569# Technische Univ., Eindhoven (Netherlands). Digital Systems Group.
DESIGN OF A UNIVERSAL PROTOCOL SYSTEM ARCHITECTURE: SPECIFICATION OF FUNCTIONS AND SERVICES Final Report
M. R. M. Winter Dec. 1989 102 p
(EUT-89-E-230; ISBN-90-6144-230-3; ISSN-0167-9708; ETN-90-97210) Avail: NTIS HC A06/MF A01

A framework of a protocol subsystem architecture using a maximum of parallelism is described. As many protocols show a great similarity concerning establishment, maintenance and release, a start is made to model a universal protocol subsystem. In addition to an informal description of the processes within the universal protocol subsystem, a formal description is given of most of these processes. Parallelism was used where reasonable to perform a rate of data communication as high as possible. Multiple concurrent connections can be served in parallel. Transmission and reception of data can be performed in parallel. Processes can also operate in parallel if protocol data units are pipelined through the subsystem

in analog to pipelining within the communication system. In analog to multitasking on one CPU (Central Processing Unit), multiple connections can be served by one communication entity quasi-parallel. A global overview of the several processes and their mutual communications is given. Additional requirements on management of these processes and on memory are described. ESA

N90-26570# Grenoble-1 Univ. (France). Lab. ARTEMIS.
PARALLELIZATION OF AN ANNEALING SIMULATION APPLIED TO IMPROVING TETRAHEDRIC GRIDS [UNE PARALLELISATION DU RECUIT SIMULE APPLIQUE A L'AMELIORATION DES MAILLAGES TETRAEDIQUES]
C. Lacote, J. Mailfert, and J. P. Uhry Dec. 1989 42 p In FRENCH
(IMAG-RR-796-M; ETN-90-97235) Avail: NTIS HC A03/MF A01

A distributed algorithm of the simulated annealing method is presented. It is used to improve the meshes in tetrahedrons of a domain D in finite element calculus. Various parallelization techniques of simulated annealing are examined. Self-adaptable parallelization established between different processors is discussed. It is based on a division of the domain with moving frontiers. Improvements obtained on meshes of real domains are shown. The program is run on a T40 hypercube with 32 processors. ESA

N90-26571# Grenoble-1 Univ. (France). Lab. d'Informatique Fondamentale et d'Intelligence Artificielle.
PRINCIPLES OF FP2: TERM ALGEBRAS FOR SPECIFICATION OF PARALLEL MACHINES
Ph. Schnoebelen and Ph. Jorrand Oct. 1989 49 p Submitted for publication Sponsored in part by EEC and CNRS
(RR-789-I-IMAG-98-LIFIA; ETN-90-97238) Avail: NTIS HC A03/MF A01

The principles of FP2 (functional parallel programming) are presented. A language where systems of parallel processes are described by means of a form of terms rewrite rules is included. A specific feature of FP2 is that compound programs can be flattened into elementary presentations in a semantically correct way. Techniques from the field of term rewriting can be used to compute with these elementary presentations and to prove properties of programs expressed in the CTL temporal logic. ESA

N90-26572# Grenoble-1 Univ. (France). Groupe Calcul Parallele.
IMPLEMENTATION OF ALGORITHMS USED IN CALCULATING THE TENSOR PRODUCT OF MATRICES ON A DISTRIBUTED MEMORY MACHINE [IMPLEMENTATION D'ALGORITHMES DE CALCUL DU PRODUIT TENSORIEL DES MATRICES SUR UNE MACHINE A MEMOIRE DISTRIBUEE]
Abderezak Touzene and Brigitte Plateau Sep. 1989 25 p In FRENCH; ENGLISH summary
(IMAG-RR-786-I; ETN-90-97239) Avail: NTIS HC A03/MF A01

Parallel systems modeling and queuing network models lead to a huge state space. State space generation is handled by a decomposition technique using tensor algebra operators. Parallel algorithms based on this method, using a multiprocessor with distributed memories are described. The interprocessor communication is based on message passing. Two communication topologies are studied: hypercube broadcast and torus pipeline. The speed of carrying out the calculations by linear and parallel processing is compared. A speed-up factor of almost 16 is obtained in parallel procession, a figure close to the ideal value. ESA

N90-26573# Institut National Polytechnique, Grenoble (France). Techniques de l'Informatique, des Mathematiques, de la Microelectronique et de la Microscopie Quanti
PARALLEL ALGORITHM FOR DISTRIBUTED MEMORY COMPUTERS (APPLICATIONS TO MATRICIAL ALGORITHMS) Ph.D. Thesis [ALGORITHMIQUE PARALLELE POUR LES MACHINES A MEMOIRE DISTRIBUEE (APPLICATION AUX ALGORITHMES MATRICIELS)]
Bernard Tourancheau 1989 167 p In FRENCH
(ETN-90-97252) Avail: NTIS HC A08/MF A01

From basic algorithms, different complexity results are presented for calculation and communication in distributed memory computers. The network topologies examined are the linear array, ring, grid, hypercube and the whole network. A systolic array is described for Jordan diagonalization. Studies relating to acceleration and data allocation are carried out. Experiments with Jordan and Gauss algorithms are performed on the hypercube FPS T20 (16 processors). ESA

N90-26574# Institut National Polytechnique, Grenoble (France). Techniques de l'Informatique, des Mathematiques, de la Microelectronique et de la Microscopie Quanti
MULTILAYERED NEURAL NETWORKS: LEARNING ALGORITHMS, IMPLEMENTATION ON HYPERCUBE MACHINES, APPLICATIONS Ph.D. Thesis [RESEAUX MULTICOUCHES DE NEURONES ARTIFICIELS: ALGORITHMES D'APPRENTISSAGE, IMPLANTATIONS SUR HYPERCUBE APPLICATIONS]
Shengrui Wang 1989 252 p In FRENCH; ENGLISH summary
(ETN-90-97255) Avail: NTIS HC A12/MF A02

Topics concerning layered neural networks such as implementation on a hypercube machine, applications to the memory modeling and to word recognition, the study of the dynamic behavior of such networks and the improvement of the learning algorithm, are presented. The implementation of layered neural networks on parallel distributed memory machines presents two key problems which are multi-accumulation and all-to-all broadcasting. Algorithms to solve these problems on rings and on hypercubes of processors are proposed. The algorithms on the hypercube are asymptotically optimal. The experimental results obtained on the machine FPS T40 confirm the efficiency of the algorithms. An attempt to use the connectionist model as a new paradigm for modelizing cognitive phenomena is performed. The study of the networks behavior helps to clarify several properties of the function resulted from learning and allow explanation of the conception of the network architecture for the application. The adaptation of the trust-region method resulted in a new learning algorithm which is more efficient and more robust than the gradient back propagation. ESA

N90-26575# Institut National Polytechnique, Grenoble (France). Lab. de Genie Informatique.
MASSIVELY PARALLEL ARCHITECTURE: INTEGRATED CELL NETWORK FOR IMAGE RECONSTRUCTION Ph.D. Thesis [ARCHITECTURE MASSIVEMENT PARALLELE: UN RESEAU DE CELLULES INTEGRE POUR LA RECONSTRUCTION D'IMAGES]
Didier Lattard 1989 289 p In FRENCH; ENGLISH summary
(ETN-90-97257) Avail: NTIS HC A13/MF A02

A highly parallel architecture based on a regular network of cells which have the characteristics to be completely asynchronous is proposed. The cells are able to communicate between themselves using a message routing mechanism. Each cell includes a processing part which realizes the necessary functions of the application, and a routing party which ensures messages transportation. The architecture was validated by developing a machine dedicated to image reconstruction. Each cell deals with a sub-image, and the cellular array is used to realize back-projection and projection processings. The different cell parameters are defined according to temporal constraints. The interface of such an architecture was studied in a host environment. An integrated circuit including one cell was designed. ESA

N90-26576# Naval Ocean Systems Center, San Diego, CA.
SUPERCONCURRENT PROCESSING: A DYNAMIC APPROACH TO HETEROGENEOUS PARALLELISM Final Report
R. F. Freund Mar. 1990 19 p
(AD-A222798; NOSC/TD-1781) Avail: NTIS HC A03/MF A01 CSCL 12/6

There is a growing concensus among supercomputer scientists that super-speed computers of the future will be parallel processors, since the traditional vector processors are only able to pipeline out one or a few results per cycle. Parallel processors and the parallel machines were in such an experimental state that it still made sense to look to vector processing for practical supercomputing. Both of those conditions are changed today, providing computational scientists with the occasion to begin to realize the full power of parallel processing. As we start to do this, however, we realize that while vector processors are basically all very similar to each other, parallel architectures present a wide variety of types. It seems quite unlikely that one of these types will be ideal for a wide range of problems. For that reason, a number of computational scientists are looking at distributed heterogeneous processing as a potential solution. Superconcurrency is one approach to this form of computing.
GRA

63 CYBERNETICS

Includes feedback and control theory, artificial intelligence, robotics and expert systems.

For related information see also *54 Man/System Technology and Life Support.*

N90-26577*# Martin Marietta Space Systems, Inc., Denver, CO. Astronautics Group.
SPACE STATION DEFINITIONS, DESIGN, AND DEVELOPMENT. TASK 5: MULTIPLE ARM TELEROBOT COORDINATION AND CONTROL: MANIPULATOR DESIGN METHODOLOGY Final Report
R. M. Stoughton Jul. 1990 109 p
(Contract NAS1-18230)
(NASA-CR-182043; NAS 1.26:182043; MCR-88-612) Avail: NTIS HC A06/MF A01 CSCL 09B

A proposed methodology applicable to the design of manipulator systems is described. The current design process is especially weak in the preliminary design phase, since there is no accepted measure to be used in trading off different options available for the various subsystems. The design process described uses Cartesian End-Effector Impedance as a measure of performance for the system. Having this measure of performance, it is shown how it may be used to determine the trade-offs necessary to the preliminary design phase. The design process involves three main parts: (1) determination of desired system performance in terms of End-Effector Impedance; (2) trade-off design options to achieve this desired performance; and (3) verification of system performance through laboratory testing. The design process is developed using numerous examples and experiments to demonstrate the feasability of this approach to manipulator design.
Author

N90-26578*# Catholic Univ. of America, Washington, DC. School of Engineering and Architecture.
POSITION CONTROL OF REDUNDANT MANIPULATORS USING AN ADAPTIVE ERROR-BASED CONTROL SCHEME
Charles C. Nguyen and Zhen-Lei Zhou Jul. 1990 13 p
(Grant NAG5-1124)
(NASA-CR-186812; NAS 1.26:186812) Avail: NTIS HC A03/MF A01 CSCL 09B

A Cartesian-space control scheme is developed to control the motion of kinematically redundant manipulators with 7 degrees of freedom (DOF). The control scheme consists mainly of proportional derivative (PD) controllers whose gains are adjusted by an adaptation law driven by the errors between the desired and actual trajectories. The adaptation law is derived using the concept of model reference adaptive control (MRAC) and Lyapunov direct method under the assumption that the manipulator performs non-compliant and slowly-varying motions. The developed control scheme is computationally efficient because its implementation does not require the computation of the manipulator dynamics. Computer simulation performed to evaluate the control scheme performance is presented and discussed.
Author

N90-26579# Royal Signals and Radar Establishment, Malvern (England).
A SUM RULE SATISFIED BY OPTIMIZED FEED-FORWARD LAYERED NETWORKS
D. S. Broomhead, D. Lowe, and A. R. Webb 24 Jan. 1989 9 p
(RSRE-Memo-4341; BR112835; ETN-90-97057) Copyright Avail: NTIS HC A02/MF A01

The following observation is addressed: take a feed-forward layered network (such as a multilayer perceptron or a radial basis function network) which is to operate as a pattern classifier. The network may have several hidden layers, as many nodes as required and any desired nonlinearities on the hidden units. The transfer functions of the output nodes should be linear. If the network is trained (using any appropriate problem) to minimize the sum squared error over all outputs and patterns such that the output weights have minimum norm, then the output values of the trained network for any subsequent input pattern will sum to a constant.
ESA

N90-26580# Royal Signals and Radar Establishment, Malvern (England).
ON NETWORKS, OPTIMIZED FEATURE EXTRACTION, AND THE BAYES DECISION
D. Lowe and A. R. Webb 5 Dec. 1989 25 p
(RSRE-Memo-4342; BR112706; ETN-90-97058) Copyright Avail: NTIS HC A03/MF A01

The problem of multi-class pattern classification using adaptive layered networks is addressed. Networks performing generalized linear discriminant analysis in which a particular parametric form is assumed for the nonlinear functions are reviewed. Training the network consists of a least-square approach that combines a generalized inverse computation to solve for the final layer weights, together with a nonlinear optimization scheme to solve for parameters of the nonlinearities. Such an approach performs feature extraction and classification simultaneously, in which the feature extraction is (optimally) matched to the classification scheme. A general analytic form for the feature extraction criterion is derived and interpreted for specific forms of target coding and error weighting. A particular aspect of the approach is to exhibit how a priori information regarding nonuniform class membership, uneven distribution between train and test sets and misclassification costs may be exploited in a regularized manner in the training phase of networks.
ESA

N90-26581*# Cellulose Conversion Enterprises, Berkeley, CA. Robotics/Electronic Photography.
BEAM RIDER FOR AN ARTICULATED ROBOT MANIPULATOR (ARM) ACCURATE POSITIONING OF LONG FLEXIBLE MANIPULATORS Final Report
M. J. Malachowski Apr. 1990 180 p
(Contract NAS3-25917)
(NASA-CR-185151; NAS 1.26:185151) Avail: NTIS HC A09/MF A01 CSCL 09B

Laser beam positioning and beam rider modules were incorporated into the long hollow flexible segment of an articulated robot manipulator (ARM). Using a single laser beam, the system determined the position of the distal ARM endtip, with millimetric precision, in six degrees of freedom, at distances of up to 10 meters. Preliminary designs, using space rated technology for the critical systems, of a two segmented physical ARM, with a single and a dual degree of freedom articulation, were developed, prototyped, and tested. To control the positioning of the physical ARM, an indirect adaptive controller, which used the mismatch between the position of the laser beam under static and dynamic conditions, was devised. To predict the behavior of the system

and test the concept, a computer simulation model was constructed. A hierarchical artificially intelligent real time ADA operating system program structure was created. The software was designed for implementation on a dedicated VME bus based Intel 80386 administered parallel processing multi-tasking computer system. Author

N90-26582*# Virginia Polytechnic Inst. and State Univ., Blacksburg. Dept. of Computer Science.
A REAL-TIME ROBOT ARM COLLISION DETECTION SYSTEM
Clifford A. Shaffer and Gregory M. Herb 11 Jun. 1990 36 p
(Grant NAG5-1183)
(NASA-CR-185878; NAS 1.26:185878; TR-90-28) Avail: NTIS HC A03/MF A01 CSCL 09B

A data structure and update algorithm are presented for a prototype real time collision detection safety system for a multi-robot environment. The data structure is a variant of the octree, which serves as a spatial index. An octree recursively decomposes 3-D space into eight equal cubic octants until each octant meets some decomposition criteria. The octree stores cylspheres (cylinders with spheres on each end) and rectangular solids as primitives (other primitives can easily be added as required). These primitives make up the two seven degrees-of-freedom robot arms and environment modeled by the system. Octree nodes containing more than a predetermined number N of primitives are decomposed. This rule keeps the octree small, as the entire environment for the application can be modeled using a few dozen primitives. As robot arms move, the octree is updated to reflect their changed positions. During most update cycles, any given primitive does not change which octree nodes it is in. Thus, modification to the octree is rarely required. Incidents in which one robot arm comes too close to another arm or an object are reported. Cycle time for interpreting current joint angles, updating the octree, and detecting/reporting imminent collisions averages 30 milliseconds on an Intel 80386 processor running at 20 MHz. Author

N90-26583# Loughborough Univ. of Technology (England). Dept. of Mathematical Sciences.
ON OUTPUT DEADBEAT CONTROL OF DISCRETE-TIME MULTIVARIABLE SYSTEMS
S. K. Spurgeon and A. C. Pugh Nov. 1989 11 p
(MATHS-Rept-A-122; ETN-90-97131) Avail: NTIS HC A03/MF A01

A direct method to compute output deadbeat controls for linear multivariable systems are discussed. Stable numerical methods are applied. The conventional optimal control problem is used with no cost on the controls. A state weighting matrix ensures cancellation of all stable transmission zeros. An extension to the algorithm showing advantages when dealing with the case of a system with multiple stable transmission zeros is presented. Some misprints in the numerical example used to illustrate the algorithm are corrected. The corrected example then turns out to justify the necessity of the proposed extension. ESA

N90-26584# Technische Univ., Eindhoven (Netherlands). Measurement and Control Group.
H-INFINITY CONTROL: AN EXPLORATORY STUDY M.S. Thesis
A. J. J. vandenBoom Aug. 1988 175 p
(EUT-88-E-211; ISBN-90-6144-211-7; ISSN-0167-9708;
ETN-90-97195) Avail: NTIS HC A08/MF A01

A theory to find the optimal controller, in which mathematical tools are needed such as coprime factorization, spectral factorization and optimal Hankel approximation, is presented which results in a design procedure. The implementation via algorithms, using state-space description, is discussed. One problem in the proposed design procedure is the appearance of jw-axis zeros or poles and strictly proper plants. Two techniques to calculate an approximant for the H sub infinity-optimal controller are described. A case study is presented: three different controllers for a laboratory process (ball-balancing system), i.e., minimizing the signal tracking error, maximizing the robustness and minimizing the mixed sensitivity (a combination of both). The different steps in the design procedure are shown and the properties of each controller are interpreted and compared. ESA

N90-26585# Technische Univ., Eindhoven (Netherlands). Measurement and Control Group.
ON THE ROBUST STABILITY OF MIMO LINEAR FEEDBACK SYSTEMS
Yu-Cai Zhu Dec. 1988 28 p
(EUT-88-E-212; ISBN-90-6144-212-5; ISSN-0167-9708;
ETN-90-97196) Avail: NTIS HC A03/MF A01

The stability of feedback systems where process models are subject to errors is studied. The Multi-Input Multi-Output (MIMO) process is given by a transfer matrix as its nominal model, and by an upper bound matrix as a structured description of the model uncertainty (modeling errors). Robust stability analysis are studied, and several robust stability criteria are compared. Based on the analysis, a procedure for maximizing the robust stability of the feedback system is proposed. The weighting functions selection for the sensitivity minimization are highlighted. ESA

N90-26586# Technische Univ., Eindhoven (Netherlands). Measurement and Control Group.
A NEW SCHEME FOR IDENTIFICATION AND CONTROL
Yu-Cai Zhu, M. H. Driessen, A. A. H. Damen, and P. Eykhoff Dec. 1988 35 p
(EUT-88-E-213; ISBN-90-6144-213-3; ISSN-0167-9708;
ETN-90-97197) Avail: NTIS HC A03/MF A01

The scheme can overcome such difficulties as: the process in open loop is unstable or nearly unstable; the process has some nonlinearity and some time variation. In these cases open loop identification with linear and time-invariant model sets may be very difficult. So the idea is: first use a primary controller for stabilizing the loop, then identify this closed loop system; finally design a controller in the second loop in order to optimize the system. It is shown that by this method a better model will be obtained during the identification procedure, and the two-loop system will maintain the optimality under a condition that is easy to check. For validating the idea, a case study is given. ESA

N90-26587# Institut National Polytechnique, Grenoble (France). Lab. d'Informatique Fondamentale et d'Intelligence Artificielle.
MULTI-SENSORY PERCEPTION OF A GEOMETRICAL STRUCTURE OF A SCENE Ph.D. Thesis [PERCEPTION MULTISENSORIELLE DE LA STRUCTURE GEOMETRIQUE D'UNE SCENE]
Fano Ramparany 1989 155 p In FRENCH; ENGLISH summary Sponsored in part by EEC and Projet National ORASIS
(ETN-90-97245) Avail: NTIS HC A08/MF A01

In order to perform and control tasks, a robot needs precise and complete information about its environment. This requirement is satisfied using a set of multiple independant sensors. A technique that exploits the redundancy and complementarity of information from multiple sensors, to build and maintain a boundary based description of the environment, is presented. Geometric information expressed as an estimate and its uncertainty is considered. This technique was applied to the realization of a vision system that produces a three-dimensional wire frame description of a static environment from a sequence of images taken with a camera mounted on a robot arm. ESA

N90-26588# Institut National Polytechnique, Grenoble (France).
VERIFICATION-CORRECTION OF A PROGRAM FOR INCLUDING UNCERTAINTIES IN THE ROBOT AUTOMATIC PROGRAMMING Ph.D. Thesis [VERIFICATION-CORRECTION DE PROGRAMME POUR LA PRISE EN COMPTE DES INCERTITUDES EN PROGRAMMATION AUTOMATIQUE DES ROBOTS]
Pierre Puget 1989 166 p In FRENCH
(ETN-90-97246) Avail: NTIS HC A08/MF A01

An approach called verification-correction of a program is presented. It ensures the validity and correction of a robot

manipulation program. The program is obtained by planning the input operations, the transport and assembly of the objects. Geometric uncertainties are not considered. The verification step consists of subsequent handling of the initial manipulation uncertainties and ensuring that the constraints are satisfied. If this is not the case, the constraints are sent back for calculation of new minimal conditions. The constraints are used for correcting the program by adding instructions which diminish the uncertainties. The verification-correction program is based in the description of the robot's action. ESA

N90-26589# Institut National Polytechnique, Grenoble (France).
APPLICATION OF ARTIFICIAL INTELLIGENCE TO THE ARCHITECTURAL SYNTHESIS OF VLSI INTEGRATED CIRCUITS Ph.D. Thesis [UNE APPLICATION DE L'INTELLIGENCE ARTIFICIELLE A LA SYNTHESE ARCHITECTURALE DES CIRCUITS INTEGRES VLSI]
Alain Blaise Fonkoua 1989 220 p In FRENCH; ENGLISH summary
(ETN-90-97253) Avail: NTIS HC A10/MF A02

The use of Artificial Intelligence (AI) methods for the automatic synthesis of integrated circuit architectures is investigated. The architectural synthesis problem is introduced. An analysis of the encountered difficulties justifies the use of artificial intelligence methods to automate this task. A critical description of a few expert system generators is given. These concepts are cast in an expert system building tool called ODSE, conceived and programmed in Ada. The knowledge representation formalism, the inference mechanisms, and the implementation are described. The use of ODSE to realize a tool for Architectural Synthesis Aid (ASA) is shown. The methods used by ASA are shown and their expression using ODSE formalism given. The ASA approach is compared to others used in similar tools. Results for a test case using ASA to synthesize a numeric 9th order LEAPFROG filter are given. ESA

N90-26590# Naval Postgraduate School, Monterey, CA.
VARIANCE REDUCTION FOR QUANTILE ESTIMATES IN SIMULATIONS VIA NONLINEAR CONTROLS
Peter A. Lewis and Richard L. Ressler Apr. 1990 35 p
(AD-A222653; NPS55-90-09) Avail: NTIS HC A03/MF A01 CSCL 12/3

Linear controls are a well known simple technique for achieving variance reduction in computer simulation. Unfortunately the effectiveness of a linear control depends upon the correlation between the statistic of interest and the control, which is often low. Since statistics often have a nonlinear relationship with the potential control variables, nonlinear controls offer a means for improvement over linear controls. This paper focuses on the use of nonlinear controls for reducing the variance of quantile estimates in simulation. It is shown that one can substantially reduce the analytic effort required to develop a nonlinear control from a quantile estimator by using a strictly monotone transformation to create the nonlinear control. It is also shown that as one increases the sample size for the quantile estimator, the asymptotic multivariate normal distribution of the quantile of interest and the control reduces the effectiveness of the nonlinear control to that of the linear control. However, the data has to be sectioned to obtained an estimate of the variance of the controlled quantile estimate. Graphical methods are suggested for selecting the section size that maximizes the effectiveness of the nonlinear control. GRA

N90-26591# Carnegie-Mellon Univ., Pittsburgh, PA. Robotics Inst.
COLOR IMAGE PROCESSING FOR NAVIGATION: TWO ROAD TRACKERS
D. Aubert and C. Thorpe Apr. 1990 24 p
(Contract DACA76-89-C-0014)
(AD-A222667; CMU-RI-TR-90-09) Avail: NTIS HC A03/MF A01 CSCL 12/9

To build on autonomous vehicle capable of road following, it is necessary to compute the position and the orientation of the vehicle relative to the road. One way of doing so is to acquire images from a camera on the vehicle and extract some road features from these images. Knowing the geometric transformation between the camera and the ground plane, it is easy to compute the position and the orientation of the vehicle relative to these road features. A system is built to track structured roads, roads that have lane markings, shoulders, and other structures. For these roads, the easiest visual features to track are white lines and the yellow lines. Robust extractors are needed to deal with a variety of roads, light and weather conditions. In the case of the white stripe, we use our knowledge about its shape to extract it. We create a mask with a shape similar to the current white stripe and convolve a search area in the image with it. The maximum correlation gives us the location of the stripe. A large mask is used to reduce the signal/noise ratio, and to be robust in the cases of light and weather variations. Taking into account the current running total during the convolution phases reduces the computational time drastically and so gets a fast operator to track the white stripe. In the case of the yellow stripes, the color is a strong characteristic of this kind of stripe, and the hue is only slightly affected by lighting and weather variations. GRA

N90-26592# Case Western Reserve Univ., Cleveland, OH. Dept. of Computer Engineering.
NEURAL NETWORKS FOR REAL-TIME SENSORY DATA PROCESSING AND SENSORIMOTOR CONTROL
Randall D. Beer 14 Jun. 1990 7 p
(Contract N00014-90-J-1545)
(AD-A223096) Avail: NTIS HC A02/MF A01 CSCL 12/9

One of the critical problems that we faced in modeling the neural control of escape turns in the cockroach was a quantitative analysis of the leg movements that generate the turn. Because the turn is very rapid, often spanning no more than 20 msec, conventional motion analysis techniques could not be employed. For that reason, we acquired an NAC high speed video and computer motion analysis system. With these tools, we have not attained a very good description of the movements that occur at each joint of each leg during turns in response to wind from four different angles relative to the animals body. Figure 1 is a typical stick figure generated by the computer system showing four successive frames at 5 msec intervals. The pairs of legs shown are, from front to back, legs in the prothoracic (T1), mesothoracic (T2), and metathoracic segments. In all legs the coxa, femur, and tibia segments are shown. These segments make two critical joint angles: the coxal-femur (C-F) joint and the femoro-tibial (F-T) joint. GRA

64 NUMERICAL ANALYSIS

Includes iteration, difference equations, and numerical approximation.

N90-26593 New South Wales Univ., Kensington (Australia). School of Mathematics.
PERTURBATION METHODS IN THE THEORY OF WAVES AND BIFURCATION PHENOMENA Ph.D. Thesis Abstract Only
James Patrick Denier Feb. 1989 2 p
Avail: Issuing Activity

The effect of the replacement of the standard bifurcation parameter with a slowly varying bifurcation parameter upon the approach to the bifurcated solutions is considered. Three distinct cases are analyzed: the standard transcritical, the Hopf and the saddle-node bifurcation. Canonical equations are obtained which govern the transition of the system through the bifurcation point. The general solution of these equations are examined. The interaction of normal modes of oppositely signed energy in a Hamiltonian system due to a linear resonance is considered. Two cases are considered, depending on the multiplicity of the normal modes at the point of resonance. A canonical equation which describes the behavior of the system in a region about the point of resonance is derived and solutions of this equation are described. The interaction of waves of opposite signed energy in a three

layer fluid is also studied. A comprehensive examination of the concept of wave energy is given, using both a Eulerian and Generalized Lagrangian mean formulation. It is shown that the total wave energy is ambiguous in the context of negative energy waves. This is remedied by showing that the Lagrangian concept of wave action is more useful in studying the interaction of waves in a three-lyer fluid. A study was made of the interaction of modes of oppositely signed energy in a Hamiltonian system due to the slow passage through resonance of the underlying system. The so called semi-simple case and the nonsemi-simple case are studied, classified according to the multiplicity of the normal modes at the point of resonance. Canonical equations governing the transition of these systems through the point of resonance are derived and possible forms of solution are described. Author

N90-26594 New South Wales Univ., Kensington (Australia). School of Education.

MATHEMATICAL PROBLEM-SOLVING TRANSFER: THE EFFECTS OF COGNITIVE LOAD AND ATTENTION A SCHEMA ACQUISITION AND RULE AUTOMATION Ph.D. Thesis Abstract Only

Graham Andrew Cooper 1988 3 p

Avail: Issuing Activity

Experiments using algebra transformation and algebra word problems were carried out to investigate the consequences of cognitive load and attention on schema acquisition and rule automation. The effects of schema acquisition and rule automation on learning and transfer were also examined. It was hypothesized that schema acquisition would precede rule automation and have a strong effect on problems similar to initial acquisition problems. It was further hypothesized that rule automation would have its primary effect on transfer and that the use of worked examples could facilitate performance on both similar and transfer problems. These hypotheses were based on previous work suggesting that conventional problem-solving through means-ends analysis imposes a heavy cognitive load and misdirects attention. Interspersing a large number of worked examples among conventional problems may reduce the use of means-ends analysis. Experiments 1 and 2 used algebra transformation problems. Subjects who received a heavy emphasis on worked examples were better able to solve both similar and transfer problems than were those subjects trained using conventional problems. Experiments 2 also demonstrated that extended acquisition periods increased performance. Further support was obtained from verbal protocols recorded in Experiment 3. Experiment 4 used algebra word problems. Transfer was again demonstrated using a combination of worked examples and extended acquisition periods. Experiments 5 and 6 used a secondary task paradigm to investigate directly the relations between cognitive load and attention on learning. Several conclusions follow. Firstly, schema and rule automation may facilitate problem-solving on different categories of problems. Secondly, schema acquisition occurs before rule automation, and finally, the use of worked examples facilitates the development of both schemas and rule automation due to reduced cognitive load and redirection of attention. Author

N90-26595*# Institute for Computer Applications in Science and Engineering, Hampton, VA.

ON CENTRAL-DIFFERENCE AND UPWIND SCHEMES Final Report

R. C. Swanson (National Aeronautics and Space Administration. Langley Research Center, Hampton, VA.) and Eli Turkel Jun. 1990 43 p Prepared in cooperation with Tel-Aviv Univ. (Israel) Submitted for publication

(Contract NAS1-18605)

(NASA-CR-182061; ICASE-90-44; NAS 1.26:182061) Avail: NTIS HC A03/MF A01 CSCL 12A

A class of numerical dissipation models for central-difference schemes constructed with second- and fourth-difference terms is considered. The notion of matrix dissipation associated with upwind schemes is used to establish improved shock capturing capability for these models. In addition, conditions are given that guarantee that such dissipation models produce a Total Variation Diminishing (TVD) scheme. Appropriate switches for this type of model to ensure satisfaction of the TVD property are presented. Significant improvements in the accuracy of a central-difference scheme are demonstrated by computing both inviscid and viscous transonic airfoil flows. Author

N90-26596# Reynolds Electrical and Engineering Co., Inc., Las Vegas, NV.

ESTIMATING THE PARAMETERS OF A SPORADICALLY OBSERVED QUEUE

Lawrence E. Barker, Daniel B. Ramey, and Miyong Song (Central Intelligence Agency, Washington, DC.) 1990 4 p Presented at the American Statistical Society, Anaheim, CA, 20-24 Aug. 1990

(Contract DE-AC08-89NV-1063)

(DE90-012903; CONF-9008101-2) Avail: NTIS HC A01/MF A01

Let X(t) be the number of customers in a queue at time t. Assume the queue is either M/M/1 or M/M/(infinity). Suppose the number is counted of customers x(sub i) at x t(sub 0) less than t(sub 1) less than (hor ellipsis) less than t(sub n), where t(sub i)'s do not depend on the number of customers in the queue. Write u(sub i) = t(sub i) - t(sub i-1). Let lambda/mu. Lambda and mu are estimated, by maximizing the likelihood function. The likelihood function is presented and then the maximization problem is discussed. DOE

N90-26597# Los Alamos National Lab., NM. Center for Nonlinear Studies.

ON TRAVELING WAVE SOLUTIONS OF A SET OF COUPLED BOUSSINESQ-LIKE EQUATIONS

V. Muto, P. S. Lomdahl, and P. L. Christiansen (Technical Univ. of Denmark, Lyngby.) Jun. 1990 16 p Presented at the 10th Annual Conference on Nonlinear Science: the Next Decade, Los Alamos, NM, 21-25 May 1990 Submitted for publication

(Contract W-7405-eng-36)

(DE90-013182; LA-UR-90-1960; CONF-9005237-1) Avail: NTIS HC A03/MF A01

A set of coupled partial differential equations of Boussinesq type are derived in the continuum limit from the equations of motion of Toda lattice with a transversal degree of freedom. Here the numerical stability of a hybrid traveling wave solution of such system (with longitudinal and transversal components) is investigated. DOE

N90-26598# Universitaet der Bundeswehr, Hamburg (Germany, F.R.). Fachbereich Maschinenbau.

NUMERICAL TREATMENT OF SHELL CROSSING SINGULARITIES IN THE SPHERICALLLY SYMMETRIC GRAVITATIONAL COLLAPSE Ph.D. Thesis [NUMERISCHE BERHANDLUNG VON SHELL CROSSING SINGULARITAETEN BEIM KUGELSYMMETRISCHEN GRAVITATIONSKOLLAPS]

Andreas Titze 1989 60 p In GERMAN

(ETN-90-96967) Avail: NTIS HC A04/MF A01

A numerical method for the solution of hyperbolic partial quasilinear differential equation systems with two variables was developed, implemented and tested, as a basis for the numerical treatment of the general relativistic spherically symmetric gravitational collapse of an ideal liquid. It is shown that in the relativistic case no initial data exists which with an unlimited equation of state can lead to a singularity. This situation is shown to be very similar to the Newton analogon. Classical calculations without gravitational effects show that the effect of gravitation on the local hydrodynamics is very small. Hence, singularities occurring in the relativistic case can be classified as hydrodynamics singularities whose existence is independent of the general relativistic treatment of the problem. ESA

N90-26599# Loughborough Univ. of Technology (England). Dept. of Mathematical Sciences.

G2-CONTINUITY IN HOMOGENEOUS CO-ORDINATES

J. V. Ball and M. C. Harrison Dec. 1988 14 p

(MATHS-Rept-A-110; ETN-90-97124) Avail: NTIS HC A03/MF A01

The G sub 2 continuity conditions in homogeneous coodinates are investigated. The conditions at the joints of composite rational curves are are studied. The homogeneous coordinates are introduced through rational cubic parametric curve segments. Symmetric and non-symmetric form equations are provided. Blending functions ensuring that an easy rational curve joins with G sub 2 continuity are determined. ESA

N90-26600# Loughborough Univ. of Technology (England). Dept. of Mathematical Sciences.

THE SYSTEM MATRIX CHARACTERISATION OF INPUT-OUTPUT EQUIVALENCE

A. C. Pugh, G. Hayton, and A. B. Walker (Hull Univ., England) Jun. 1989 11 p

(MATHS-Rept-A-112; ETN-90-97125) Avail: NTIS HC A03/MF A01

The notion of input-output equivalence is defined. Its complete characterization as a matrix transformation of the relevant system matrices is presented. The results show that the obtained system matrix relation is necessary and sufficient for the invariance of the function matrix. An example is given where it is possible to pick a transformation of extended strict system equivalence out of the entire set of input-output equivalence transformations connecting a system matrix with its normalized form. ESA

N90-26601# Loughborough Univ. of Technology (England). Dept. of Mathematical Sciences.

RATIONAL CUBICS WITH G2-CONTINUITY

J. Ball and M. C. Harrisson Jun. 1989 24 p

(MATHS-Rept-A-113; ETN-90-97126) Avail: NTIS HC A03/MF A01

A rational G sub 2 spline is defined in terms of a set of joint parameters. The curve form is shown to process symmetry with respect to curve direction. Both rational B-splines and rational Beta-splines are shown to be special cases of it. The relaxation continuity conditions from C sub 2 to G sub 2 continuity generates extra freedom in generating rational cubic curves. ESA

N90-26602# Technische Univ., Eindhoven (Netherlands). Dept. of Mathematics and Computer Science.

LARGE SETS OF BLOCK DESIGNS Ph.D. Thesis

Qingde Kang 1989 96 p

(ETN-90-97212) Avail: NTIS HC A05/MF A01

Several G-designs are investigated. Given a collection G of directed graphs, a G-design (X,B) is a set X with a family B of directed graphs, each isomorphic to some member of G. The cases where G consists of trees or paths or cycles, and in most cases where G consists entirely of small graphs, the spectrum was determined completely. Reduction of the existence problem for the six values of v to the construction of two relatively small structures is demonstrated. As a generalization of the directed three cycle case, the directed k-cycle is considered. The Mendelsohn, transitive and Steiner triple systems are examined. ESA

N90-26603# Grenoble-1 Univ. (France). Techniques de l'Informatique, des Mathematiques, de la Microelectronique et de la Microscopie Quanti

PREDISSIMILARITIES, PREFILTERS, AND ULTRAMETRICS ON AN ARBITRARY SET

Bernard VanCustem and Frank Critley (Warwick Univ., Coventry, England) Sep. 1989 32 p Sponsored by Royal Society, London, England; Ministere de l'Education Nationale, Paris, France; and British Council

(IMAG-RR-970-M; ETN-90-97224) Avail: NTIS HC A03/MF A01

The topological idea of a prefilter on an arbitrary set and applications are presented. The prefilters on S are shown to be in natural bijection with the predissimilarities on S. The range of a prefilter comprises the closed balls centred on elements of S and defined by the corresponding predissimilarity. This bijection permits the ultrametrics on S to be characterized within the predissimilarities on S. In the case where S is a finite set, there are two classical bijections involving the ultrametrics on S, one in terms of dendrograms on S, the other in terms of indexed hierarchies on S. Examples show that these bijections do not hold for general S. The generalized dendograms on S and the indexed regular generalized hierarchies on S are defined. These two new bijections reduce to the classical ones when S is finite. ESA

N90-26604# Grenoble-1 Univ. (France). Techniques de l'Informatique, des Mathematiques, de la Microelectronique et de la Microscopie Quanti

STRONG CONSISTENCY OF THE LEAST SQUARES ESTIMATOR FOR A NON-ERGODIC THRESHOLD AUTOREGRESSIVE MODEL

Dinh Tuan Pham, Ki Si Chan, and Howell Tong (Kent Univ., Canterbury, England) Oct. 1989 13 p Presented at the Edinburgh International Workshop on Nonlinear Time Series, Edinburgh, Scotland, Jul. 1989; sponsored by Science Research Council, England

(IMAG-RR-791-M; ETN-90-97225) Avail: NTIS HC A03/MF A01

The least squares estimator of a non-ergodic first order self-exciting threshold autoregressive model is investigated. The thresold of the model is assumed to be known and equal to zero. The conditions for which the model is stationary and geometrically ergodic are given. The case in which ergodicity does not hold is discussed. ESA

N90-26605# Grenoble-1 Univ. (France). Techniques de l'Informatique, des Mathematiques, de la Microelectronique et de la Microscopie Quanti

ASYMPTOTIC LAW OF THE ORTHOGONAL EMPIRICAL FUNCTIONS AND APPLICATIONS, PART 2 [LOI ASYMPTOTIQUE DES FONCTIONS ORTHOGONALES EMPIRIQUES ET APPLICATIONS, 2]

Rene Blacher Oct. 1989 67 p In FRENCH; ENGLISH summary

(IMAG-RR-792-M-Pt-2; ETN-90-97226) Avail: NTIS HC A04/MF A01

A study of orthogonal empirical functions is carried out. The proof of their asymptotic distributions is presented. The Hilbertian test of independence is built with estimation of parameters. The Chi-squared test of independence with estimation of parameters is considered. The asymptotic distributions of conditional empirical probability, of conditional empirical density, of dependence empirical density, and of the squares estimators in the linear regression are investigated. ESA

N90-26606# Grenoble-1 Univ. (France). Techniques de l'Informatique, des Mathematiques, de la Microelectronique et de la Microscopie Quanti

ASYMPTOTIC OPTIMALITY OF THE FAST RANDOMIZED VERSIONS OF GCV AND C(SUB L) IN RIDGE REGRESSION AND REGULARIZATION

Didier A. Girard Oct. 1989 14 p

(IMAG-RR-793-M; ETN-90-97227) Avail: NTIS HC A03/MF A01

Ridge regression is a technique to estimate the coefficients of a linear model. The method of regularization is a similar approach used to solve underdetermined linear equations with discrete noisy data. The choice of the smoothing (or regularization) parameter h is studied. Generalized Cross Validation (GVC) and Mallows' C(sub L) are methods for estimating a value for h, from the data. The purpose of the study is to show that the convergence results also hold for new methods. ESA

N90-26607# Grenoble-1 Univ. (France). Techniques de l'Informatique, des Mathematiques, de la Microelectronique et de la Microscopie Quanti

SEARCH OF PRIMITIVE POLYNOMIALS OVER FINITE FIELDS

Marc Rybowicz Dec. 1989 21 p

(IMAG-RR-797-M; ETN-90-97230) Avail: NTIS HC A03/MF A01

A conjectural deterministic algorithm for computing primitive elements of extensions of GF(2) and some experimental results are given. Both module reductions of polynomials with integer coefficients and a method by Varshamov and Gamkrelidze which allows building of a primitive polynomial from a polynomial of lower order are used. The proof of the polynomial regular behavior leading to a deterministic algorithm is considered. ESA

N90-26608# Grenoble-1 Univ. (France). Techniques de l'Informatique, des Mathematiques, de la Microelectronique et de la Microscopie Quanti

CALCULATION OF THE ALGEBRAIC CURVES PARAMETERIZATION: HAMBURGER-NOETHER EXPANSIONS [CALCUL DE PARAMETERISATION DE COURBES ALGEBRIQUES: LES DEVELOPPEMENTS DEHAMBURGER-NOETHER]

Marc Ribowicz Dec. 1989 96 p IN FRENCH; ENGLISH summary

(IMAG-RR-798-M; ETN-90-97231) Avail: NTIS HC A05/MF A01

A tool for the study of singularities of algebraic plane curves, the so-called Hamburger-Noether expansions, are described. These expansions provide the same information about a singular point as the Puiseux expansions do over a field of characteristic zero. An algorithm for computing these expansions extending the one given by Campillo for an irreducible algebroid curve are presented. Some results from singularity theory are reviewed. ESA

N90-26609# Grenoble-1 Univ. (France).

COMBINATORIAL PROBLEMS USING A HYPERCUBE AND HAMMING GRAPHS Ph.D. Thesis [QUELQUES PROBLEMES COMBINATOIRES SUR L'HYPERCUBE ET LES GRAPHES DE HAMMING]

Michel Mollard 1989 163 p In ENGLISH and FRENCH

(ETN-90-97240) Avail: NTIS HC A08/MF A01

Hamming graphs and associated graph types are discussed. Hypercube summits with particular properties are studied. The common properties of graph theory: absorbants, Hamiltonian cycles, etc, are discussed. A generalized formula summarizing the guiding concepts of graceful trees is presented. Several conjectures in the area of graceful trees are resolved. Several papers in the area of elegant valuations, colorations and other graceful mathematical problems are presented. ESA

N90-26610# Institut National Polytechnique, Grenoble (France). Lab. d'Informatique Fondamentale et d'Intelligence Artificielle.

UNIFICATION AND DISUNIFICATION: THEORY AND APPLICATIONS Ph.D. Thesis [UNIFICATION ET DESUNIFICATION. THEORIE ET APPLICATIONS]

Hubert Comon 1989 240 p In FRENCH; ENGLISH summary

(ETN-90-97247) Avail: NTIS HC A11/MF A02

An equational formula is a first order formula whose only predicate symbol is equality. Transformation rules for such formulas are proposed and their correctness in various models are studied. Some controls on these rules are investigated. Termination and completeness results with respect to solved forms are derived. Several definitions of a solved form are considered. A complete axiomatization of finite trees over a finite alphabet are proposed. The termination results are given for minimal control. Disunification algorithms can be derived by strengthening the control. The results are extended to rational trees. Some applications are investigated. The study of correctness in algebraic specifications is carried out. It is shown how it is possible to compute a grammar for the language of irreducible ground instances of a term. An algorithm for cleaning such grammars is proposed. In particular, this shows that emptiness (and thus so-called inductive reducibility) is decided in this way. ESA

N90-26611# Institut National Polytechnique, Grenoble (France). Lab. ARTEMIS.

GENERATION AND IMPROVEMENT OF MESHES FOR FINITE ELEMENTS METHODS IN TWO AND THREE DIMENSIONS Ph.D. Thesis

Jean-Yves Talon 1989 146 p In FRENCH; ENGLISH summary

(ETN-90-97249) Avail: NTIS HC A07/MF A01

The generations and improvement of meshes in simplex for the finite elements method is discussed. It is shown that it is possible to triangulate any planar domain (even with holes), defined by an external countour and a set of internal points for its discretization. An algorithm to compute triangular meshes is presented. It is proved that the calculation for converting the diagonals into a convex quadrilateral enables any feasible topology to be attained. The tridimensional case is examined. Several properties of tetrahedrization are given. Several heuristics of topological improvement of tetrahedral meshes are described. Their practical efficiency with some industrial examples taken from fluid mechanics are compared. ESA

N90-26612# Institut National Polytechnique, Grenoble (France). Techniques de l'Informatique, des Mathematiques, de la Microelectronique et de la Microscopie Quanti

CONTRIBUTION TO THE STUDY OF DIFFERENTIAL EQUATIONS AND TO THE DIFFERENCES IN THE COMPLEX FIELD Ph.D. Thesis [CONTRIBUTION A L'ETUDE DES EQUATIONS DIFFERENTIELLES ET AUX DIFFERENCES DANS LE CHAMP COMPLEXE]

My Abdelfattah Barkatou 1989 201 p In FRENCH

(ETN-90-97250) Avail: NTIS HC A10/MF A02

The formal solution of linear differential equations in the complex field is given. Software for solving second order equations in the neighborhood of all singular points is developed. It is shown that the Newton algorithm can be modified for simplifying the calculations. The equations showing linear differences in the complex field are studied. An algorithm which allows asymptotic solutions for a linear recurrent equation with polynomial coefficients is proposed. Systems of factorial series coefficients are also studied. ESA

N90-26613# Technische Hochschule, Darmstadt (Germany, F.R.). Fachbereich Mathematik.

CARTESIAN CLOSED CATEGORIES OF DOMAINS Ph.D. Thesis

Achim Jung 1988 107 p

(ETN-90-97284) Avail: NTIS HC A06/MF A01

The description of the input domain in the framework of a computer program for numerical calculation is investigated. The basic results of the theory of directed complete partial orders are summarized. The Smith's result is discussed and a proof is given. Several algebric domains, with well-behaved function space are divided into L-domains and bifinite domains. The general algebric directed-complete partial orders and continuous functions are discussed. ESA

N90-26614*# National Aeronautics and Space Administration. Lewis Research Center, Cleveland, OH.

PARALLEL/DISTRIBUTED DIRECT METHOD FOR SOLVING LINEAR SYSTEMS

Avi Lin (Temple Univ., Philadelphia, PA.) Jul. 1990 18 p

(NASA Order C-99066-G)

(NASA-TM-103229; ICOMP-90-18; E-5645; NAS 1.15:103229)

Avail: NTIS HC A03/MF A01 CSCL 12A

A new family of parallel schemes for directly solving linear systems is presented and analyzed. It is shown that these schemes exhibit a near optimal performance and enjoy several important features: (1) For large enough linear systems, the design of the appropriate paralleled algorithm is insensitive to the number of processors as its performance grows monotonically with them; (2) It is especially good for large matrices, with dimensions large relative to the number of processors in the system; (3) It can be used in both distributed parallel computing environments and tightly

coupled parallel computing systems; and (4) This set of algorithms can be mapped onto any parallel architecture without any major programming difficulties or algorithmical changes. Author

N90-26615*# National Aeronautics and Space Administration. Lewis Research Center, Cleveland, OH.
ASYMPTOTIC ANALYSIS OF DISSIPATIVE WAVES WITH APPLICATIONS TO THEIR NUMERICAL SIMULATION
Thomas Hagstrom (State Univ. of New York, Stony Brook.) Aug. 1990 15 p
(Grant NASA Order C-99066-G; NSF DMS-89-05314)
(NASA-TM-103231; ICOMP-90-19; E-5647; NAS 1.15:103231)
Avail: NTIS HC A03/MF A01 CSCL 12A

Various problems involving the interplay of asymptotics and numerics in the analysis of wave propagation in dissipative systems are studied. A general approach to the asymptotic analysis of linear, dissipative waves is developed. It was applied to the derivation of asymptotic boundary conditions for numerical solutions on unbounded domains. Applications include the Navier-Stokes equations. Multidimensional traveling wave solutions to reaction-diffusion equations are also considered. A preliminary numerical investigation of a thermo-diffusive model of flame propagation in a channel with heat loss at the walls is presented. Author

N90-26616*# National Aeronautics and Space Administration. Lewis Research Center, Cleveland, OH.
EFFICIENT IMPLEMENTATION OF MINIMAL POLYNOMIAL AND REDUCED RANK EXTRAPOLATION METHODS
Avram Sidi (Israel Inst. of Tech., Haifa.) Aug. 1990 43 p
(NASA Order C-99066-G)
(NASA-TM-103240; ICOMP-90-20; E-5658; NAS 1.15:103240)
Avail: NTIS HC A03/MF A01 CSCL 12A

The minimal polynomial extrapolation (MPE) and reduced rank extrapolation (RRE) are two effective techniques that have been used in accelerating the convergence of vector sequences, such as those that are obtained from iterative solution of linear and nonlinear systems of equation. Their definitions involve some linear least squares problems, and this causes difficulties in their numerical implementation. Timewise efficient and numerically stable implementations for MPE and RRE are developed. A computer program written in FORTRAN 77 is also appended and applied to some model problems. Author

N90-26617# Naval Ocean Systems Center, San Diego, CA.
CANONICAL EIGENVALUES. PART 1: GENERAL THEORY
Technical Report, Mar. 1986 - Jul. 1989
Melvin A. Pedersen, David F. Gordon, and Fell Hosmer Feb. 1990 20 p
(AD-A222812; NOSC/TR-1332-Pt-1) Avail: NTIS HC A03/MF A01 CSCL 12/2

A formulation of the eigenvalue problem, here referred to as the canonical eigenvalue method or canonical eigenvalue theory, was developed to facilitate analysis of mode coupling effects in double ducts in underwater acoustics. This canonical eigenvalue method can also be used if eigenvalue curves as a function of some variable parameter, such as frequency, are required to analyze some acoustic phenomenon. Also, if one or more eigenvalues are required at many values of such a parameter, as for instance in broadband simulations, the canonical eigenvalue method is a useful eigenvalue computation technique. This report is one of a series of reports that explain the canonical eigenvalue method and demonstrate its application to various acoustic ducts, including some double ducts. The chief objective of this report is to present the general theory of canonical eigenvalues. In the approach taken here, the eigenvalue equation is couched in purely mathematical terms, involving two-dimensionless variables and a set of dimensionless parameters related to the sound-speed profile. The physical quantities of interest, such as frequency and phase and group velocity, are generated after the eigenvalues have been determined. This approach has a number of advantages over customary approaches. GRA

N90-26618# Illinois State Univ., Normal. Dept. of Mathematics.
APPLIED MATHEMATICAL MODULES FOR USE IN A LINEAR ALGEBRA SERVICE COURSE Thesis
Shirley Jo Zander May 1990 281 p Sponsored by AFIT, Wright-Patterson AFB, OH
(AD-A222814; AFIT/CI/CIA-90-012D) Avail: NTIS HC A13/MF A02 CSCL 12/1

The purpose of this study was to develop several applications which could be used to supplement an undergraduate course in linear algebra for non-mathematics majors. These applications were drawn from the fields of biology, graph theory, and physics. The biology application examined how a system of linear equations could be used to determine the concentration of substances dissolved in a colored liquid. In the graph theory application, linear algebra was applied to analyze properties of spanning trees and to illustrate how they would be employed to solve transportation problems. The third application showed how linear algebra is used to solve systems of second order linear differential equations, which could be used to model small vibrations in molecules. Each application was designed so that and instructor of linear algebra could use it either as an independent study project or as an integrated part of the course. These three applications are arranged by degree of difficulty and sequenced as they would be introduced in a linear algebra course. On the whole, the students participating in the testing of these applications felt that exposure to examples such as these during their Mathematics 175 course would have increased their understanding and enjoyment of linear algebra. This finding supports the overall goal of this study. GRA

65 STATISTICS AND PROBABILITY

Includes data sampling and smoothing; Monte Carlo method; and stochastic processes.

N90-26619*# Army Avionics Research and Development Activity, Fort Eustis, VA.
CLOSED-FORM SOLUTION OF DECOMPOSABLE STOCHASTIC MODELS
Jon A. Sjogren 1990 41 p
(NASA-TM-103466; NAS 1.15:103466) Avail: NTIS HC A03/MF A01 CSCL 12A

Markov and semi-Markov processes are increasingly being used in the modeling of complex reconfigurable systems (fault tolerant computers). The estimation of the reliability (or some measure of performance) of the system reduces to solving the process for its state probabilities. Such a model may exhibit numerous states and complicated transition distributions, contributing to an expensive and numerically delicate solution procedure. Thus, when a system exhibits a decomposition property, either structurally (autonomous subsystems), or behaviorally (component failure versus reconfiguration), it is desirable to exploit this decomposition in the reliability calculation. In interesting cases there can be failure states which arise from non-failure states of the subsystems. Equations are presented which allow the computation of failure probabilities of the total (combined) model without requiring a complete solution of the combined model. This material is presented within the context of closed-form functional representation of probabilities as utilized in the Symbolic Hierarchical Automated Reliability and Performance Evaluator (SHARPE) tool. The techniques adopted enable one to compute such probability functions for a much wider class of systems at a reduced computational cost. Several examples show how the method is used, especially in enhancing the versatility of the SHARPE tool. Author

N90-26620# Grenoble-1 Univ. (France). Techniques de l'Informatique, des Mathematiques, de la Microelectronique et de la Microscopie Quanti

A STUDY OF THE ASYMPTOTIC PROPERTIES OF LEAST SQUARE ESTIMATORS FOR MULTIPLE PHASE REGRESSION PROBLEMS Ph.D. Thesis [ETUDE DES PROPRIETES ASYMPTOTIQUES DES ESTIMATEURS DES MOINDRES CARRES POUR DES PROBLEMES DE REGRESSION A PHASES MULTIPLES]

Samira Benzekri 1989 266 p In FRENCH
(ETN-90-97244) Avail: NTIS HC A12/MF A02

A classic static problem of regression analysis is studied. The shear problem studied involves detection and estimation of the other parameters involved in the model. A decision procedure for helping to choose between two approximate nonlinear regression models is developed. The procedure is applied to a specific case in which one of the two approximate models is a combination of functions displaying shear behavior. Multiple phase modeling is used to test the model. ESA

N90-26621# North Carolina Univ., Chapel Hill. Dept. of Statistics.

DICHOTOMIES FOR CERTAIN PRODUCT MEASURES AND STABLE PROCESSES

Mauro S. DEF Marques and Stamatis Cambanis Mar. 1990 33 p
(Contract F49620-85-C-0144; AF Proj. 2304)
(AD-A222568; AFOSR-90-0648TR) Avail: NTIS HC A03/MF A01 CSCL 12/3

Necessary and sufficient conditions for equivalence or singularity of certain product measures are given and applied to the problem of distinguishing a sequence of random vectors from affine transformations of itself. In particular sequences of independent stable random variables are considered and the singularity of sequences with different indexes of stability is proved. Using these results the dichotomy, two processes are either equivalent or singular, is established for certain classes of stable processes, such as independently scattered measures and harmonizable processes. Also sufficient conditions for singularity and necessary conditions for absolute continuity are given for p sub th order processes. GRA

N90-26622# Rice Univ., Houston, TX. Dept. of Computer Science.

CAUSAL DISTRIBUTED BREAKPOINTS

Jerry Fowler and Willy Zwaenepoel Feb. 1990 12 p Submitted for publication
(Contract N00014-88-K-0140; NSF CCR-87-16914; NSF CDA-86-19893)
(AD-A222613; RICE-COMP-TR90-107) Avail: NTIS HC A03/MF A01 CSCL 12/5

A causal distributed breakpoint is initiated by a sequential breakpoint in one process of a distributed computation, and restores each process in the computation to the earliest state that reflects all events that happened before the breakpoint. A causal distributed breakpoint is the natural extension for distributed programs of the conventional notion of a breakpoint in a sequential program. An algorithm for finding the causal distributed breakpoint given a sequential breakpoint in one of the processes, is presented. Approximately consistent checkpoint sets are used for efficiently restoring each process to its state in a causal distributed breakpoint. Causal distributed breakpoints assume deterministic processes that communicate solely by messages. The dependencies that arise from communication between processes are logged. Dependency logging and approximately consistent checkpoint sets have been implemented on a network of SUN workstations running the V-System. Overhead on the message passing primitive varies between 1 and 14 percent for dependency logging. Execution time overhead for a 200 x 200 Gaussian elimination is less than 4 percent, and generates a dependency log of 288 kilobytes. GRA

N90-26623# Naval Postgraduate School, Monterey, CA. Dept. of Operations Research.

NONLINEAR MODELING OF TIME SERIES USING MULTIVARIATE ADAPTIVE REGRESSION SPLINES (MARS)

Peter A. Lewis and James G. Stevens Apr. 1990 38 p Prepared for ONR, Arlington, VA
(AD-A222710; AD-E501236; NPS55-90-10) Avail: NTIS HC A03/MF A01 CSCL 12/3

MARS is a new methodology, due to Friedman, for nonlinear regression modeling. MARS can be conceptualized as a generalization of recursive partitioning that uses spline fitting in lieu of other simple functions. Given a set of predictor variables, MARS fits a model in a form of an expansion of product spline basis functions of predictors chosen during a forward and backward recursive partitioning strategy. MARS produces continuous models for discrete data that can have multiple partitions and multilinear terms. Predictor variable contributions and interactions in a MARS model may be analyzed using an ANOVA style decomposition. By letting the predictor variables in MARS be lagged values of a time series, one obtains a new method for nonlinear autoregressive threshold modeling of time series. A significant feature of this extension of MARS is its ability to produce models with limit cycles when modeling time series data that exhibit periodic behavior. In a physical context, limit cycles represent a stationary state of sustained oscillations, a satisfying behavior for any model of a time series with periodic behavior. Analysis of the Wolf sunspot numbers with MARS appears to give an improvement over existing nonlinear Threshold and Bilinear models. GRA

N90-26624# Naval Postgraduate School, Monterey, CA. Dept. of Operations Research.

REVERSED RESIDUALS IN AUTOREGRESSIVE TIME SERIES ANALYSIS

Peter A. Lewis and A. J. Lawrance Apr. 1990 16 p Prepared for ONR, Arlington, VA
(AD-A222711; AD-E501236; NPS55-90-11) Avail: NTIS HC A03/MF A01 CSCL 12/3

Both linear and nonlinear time series can have directional features, features which indicate that the series do not maintain identical statistical properties when the direction on the time scale is reversed. The main purpose of the present paper is to develop the analysis of these features and to indicate and illustrate how they can be used for the investigation and modelling of linear or nonlinear autoregressive statistical models. In particular, the aim of the paper is to introduce the idea of reversed residuals and to develop some of their properties. Particular pairs of reversed and ordinary residuals are shown to produce partial autocorrelation coefficients: quadratic types of partial autocorrelation coefficients are introduced to assess dependence associated with nonlinear models which nevertheless have linear autoregressive (Yule-Walker) correlation structures. GRA

N90-26625# Maryland Univ., College Park. Dept. of Computer Science.

EVALUATION OF A DECOMPOSITION APPROACH FOR REAL-TIME SCHEDULING USING A STOCHASTIC MODEL

Xiaoping Yuan and Ashok K. Agrawala 30 Apr. 1990 18 p
(Contract DASG60-87-C-0066)
(AD-A222726; UMIACS-TR-90-58; CS-TR-2462) Avail: NTIS HC A03/MF A01 CSCL 12/5

In this paper, a stochastic model is developed to evaluate the decomposition scheduling approach. Since the scheduling complexity of the approach directly depends on the number of tasks in every subset, we calculate the probability of the event that there are n tasks in a subset, for any n, and then the expected number of tasks in a subset. The results indicate that the decomposition scheduling technique not only assures the generation of a feasible schedule if one exists, but also is computationally efficient. GRA

66 SYSTEMS ANALYSIS

Includes mathematical modeling; network analysis; and operations research.

N90-26626# Lawrence Livermore National Lab., CA.
ASATS VS BRILLIANT PEBBLES
Roger D. Speed Mar. 1990 35 p
(Contract W-7405-eng-48)
(DE90-010348; UCRL-ID-103669) Avail: NTIS HC A03/MF A01

The cost exchange ratio is examined of Brilliant Pebbles satellites when attacked by small, ground-based, non-nuclear ASATs. If the satellites have no defenses, the exchange ratio is likely to be at least 40:1 in favor of the attacker in a general war or 4:1 in his favor in a war of attrition. The use of maneuver, decoys, and space-based defensive rockets to defeat that ASAT threat were examined, but none of these approaches appears to be clearly economically advantageous. DOE

N90-26627# Los Alamos National Lab., NM. Accelerator Technology Div.
THERMAL MANAGEMENT OF AN ACCELERATOR SYSTEM IN SPACE
Don W. Reid 1990 14 p Presented at the Prospector 1: Key Issues in Space Technology, Park City, UT, 20-22 Mar. 1990
(Contract W-7405-eng-36)
(DE90-013153; LA-UR-90-2159; CONF-9003178-1) Avail: NTIS HC A03/MF A01

For the past several years the Accelerator Technology Division at Los Alamos National Laboratory has been working under Strategic Defense Initiative sponsorship to develop a Neutral Particle Beam (NPB) weapon system. A weapon grade NPB system generates 10s of MWs of waste energy which must be dissipated in some fashion. There are only three ways that heat may be dissipated in space. The first is to expel a hot gas or liquid from the spacecraft. The second method is to directly radiate the generated heat to deep space. The third method is to dissipate the heat in some type of thermal mass storage. The objective of this workshop is to try to determine the best way to dissipate MWs in space. DOE

67 THEORETICAL MATHEMATICS

Includes topology and number theory.

No abstracts in this category.

70 PHYSICS (GENERAL)

For precision time and time interval (PTTI) see *35 Instrumentation and Photography;* for geophysics, astrophysics or solar physics see *46 Geophysics, 90 Astrophysics,* or *92 Solar Physics.*

N90-26628 New South Wales Univ., Kensington (Australia). School of Mechanical and Industrial Engineering.
MOBILITY STUDIES IN MULTILOOP SPATIAL LINKAGES Ph.D. Thesis Abstract Only
Min Hu Jun. 1988 3 p
Avail: Issuing Activity

Problems associated with the generation of new mobile solutions for multiloop networks are studied, especially Kempe's linkages and their derivatives, both in the plane and in space. Chapter 1 gives a brief review of the research activities carried out prior to this thesis in the area of mobility analysis of over constrained linkages, and an outline of the projects involved in the present work. Chapter 2 is concerned with the kinematic and kinetic analysis of a single loop 5-bar over constrained linkage. A complete analysis of a special Goldberg's 5-bar linkage was carried out, and the input-output relationships are obtained by using link-coordinate transformation matrices. The possibility of its application in a mixing machine is also discussed. In chapter 3 various attempts are made to search for mobile spatial counterparts of Kempe's linkages, and a line-symmetric spatial analogue of Kempe's point-symmetric linkage was discovered. A new algebraic method, called the equal ratio method, is introduced in Chapter 4. This technique is used to solve the link-vector loop equations for individual loops in a network, and can quickly reduce the sizes of the equations and the number of variables. Chapter 5 is a re-analysis of Kempe's linkages. It aims to help interested readers to a better understanding of this group of linkages. Chapter 6 comprises a search for the mobile solutions of a new category of multi-loop over constrained networks, which originates from special cases of Kempe's linkages but is seen to be an independent category. Chapter 7 sets out the principal conclusions, and offers some suggestions for future study. Author

N90-26629# Scripps Institution of Oceanography, La Jolla, CA.
ABSOLUTE MEASUREMENTS OF GRAVITY Final Report, 25 Apr. 1986 - 24 Jul. 1989
Mark A. Zumberge and Glenn S. Sasagawa Jul. 1989 21 p
(Contract F19628-86-K-0020)
(AD-A222731; GL-TR-90-0045) Avail: NTIS HC A03/MF A01 CSCL 08/5

The Institute of Geophysics and Planetary Physics (IGPP) has completed a two-phase three-year program of absolute gravity research and development. The development phase included modifications to an existing absolute gravity meter. Our goal was to incorporate state-of-the-art technology and portability while maintaining meter accuracy. The research phase included both field testing of the modified meter and the establishment of new absolute gravity sites. In particular, we were able to survey absolutely a series of closely spaced sites along existing calibration lines. GRA

N90-26630# Puerto Rico Univ., Rio Piedras. Dept. of Physics.
EXACT RESULTS FOR THE STRUCTURED LIQUID-SOLID INTERFACE
L. Blum and D. A. Huckaby (Texas Christian Univ., Fort Worth.) 30 Apr. 1990 12 p Submitted for publication Sponsored in part by Welch, (Robert A.) Foundation
(Contract N00014-81-C-0776)
(AD-A222762; TR-40-ONR) Avail: NTIS HC A03/MF A01 CSCL 07/4

The theoretical discussion of smooth surfaces is considerably simpler than that of a realistic surface, in which the solid, usually a metal, has a well defined crystal structure. The reason is that in the case of a smooth surface the problem is one-dimensional, rather than three-dimensional. The analysis of a realistic metal surface potential in contact with an ionic solution is extremely difficult, and requires the use of very large computers. A simple model of a structured interface is discussed which predicts surface phase behavior, for the adsorbed layers, and which is mathematically tractable. In fact, if the correlation functions of the smooth surface model are known to all orders, then properties and correlation functions of our model can be computed exactly, at least in principle. GRA

N90-26631# Colorado Univ., Boulder. Dept. of Electrical Engineering.
RESONANT COUPLING THROUGH A SLOT TO A LOADED CYLINDRICAL CAVITY: EXPERIMENTAL RESULTS Final Technical Report
John D. Norgard and Ronald M. Sega Mar. 1990 84 p
(Contract F30602-81-C-0205)
(AD-A223000; RADC-TR-89-382) Avail: NTIS HC A05/MF A01 CSCL 20/3

The effect of cavity geometry on the energy coupled through a slot aperture is investigated through the use of planar mappings of the internal cavity field. A copper cylinder, closed at both ends,

is constructed with copper mesh sections incorporated at the ends of the cylinder and in the cylinder wall opposite a thin slot aperture placed in the wall. The frequencies used for testing are 2 to 4 GHz. Internal field mapping is accomplished by placing thin carbon-loaded sheets in the plane of interest and recording the digitized temperature distribution using an infrared scanning system. The sheets are calibrated such that the temperature data is transformed to current densities or electric field strengths. Using several positions for the detection material, a three-dimensional field profile is obtained. The onset of the internal cavity resonance is studied as it is related to the energy coupled through small apertures. GRA

71 ACOUSTICS

Includes sound generation, transmission and attenuation. For noise pollution see *45 Environmental Pollution*.

N90-26632*# Florida Atlantic Univ., Boca Raton. Center for Acoustics and Vibration.
POWER FLOW ANALYSIS OF TWO COUPLED PLATES WITH ARBITRARY CHARACTERISTICS Semiannual Report No. 4
J. M. Cuschieri Jun. 1990 46 p
(Grant NAG1-685)
(NASA-CR-182033; NAS 1.26:182033) Avail: NTIS HC
A03/MF A01 CSCL 20A

In the last progress report (Feb. 1988) some results were presented for a parametric analysis on the vibrational power flow between two coupled plate structures using the mobility power flow approach. The results reported then were for changes in the structural parameters of the two plates, but with the two plates identical in their structural characteristics. Herein, limitation is removed. The vibrational power input and output are evaluated for different values of the structural damping loss factor for the source and receiver plates. In performing this parametric analysis, the source plate characteristics are kept constant. The purpose of this parametric analysis is to determine the most critical parameters that influence the flow of vibrational power from the source plate to the receiver plate. In the case of the structural damping parametric analysis, the influence of changes in the source plate damping is also investigated. The results obtained from the mobility power flow approach are compared to results obtained using a statistical energy analysis (SEA) approach. The significance of the power flow results are discussed together with a discussion and a comparison between the SEA results and the mobility power flow results. Furthermore, the benefits derived from using the mobility power flow approach are examined. Author

N90-26633*# General Electric Co., Cincinnati, OH. Advanced Technology Operations.
HIGH SPEED TURBOPROP AEROACOUSTIC STUDY (COUNTERROTATION). VOLUME 1: MODEL DEVELOPMENT Final Report
C. E. Whitfield, R. Mani, and P. R. Gliebe Jul. 1990 121 p
(Contract NAS3-23721)
(NASA-CR-185241; NAS 1.26:185241) Avail: NTIS HC
A06/MF A01 CSCL 20A

The isolated counterrotating high speed turboprop noise prediction program was compared with model data taken in the GE Aircraft Engines Cell 41 anechoic facility, the Boeing Transonic Wind Tunnel, and in NASA-Lewis' 8x6 and 9x15 wind tunnels. The predictions show good agreement with measured data under both low and high speed simulated flight conditions. The installation effect model developed for single rotation, high speed turboprops was extended to include counterotation. The additional effect of mounting a pylon upstream of the forward rotor was included in the flow field modeling. A nontraditional mechanism concerning the acoustic radiation from a propeller at angle of attach was investigated. Predictions made using this approach show results that are in much closer agreement with measurement over a range of operating conditions than those obtained via traditional fluctuating force methods. The isolated rotors and installation effects models were combines into a single prediction program, results of which were compared with data taken during the flight test of the B727/UDF engine demonstrator aircraft. Satisfactory comparisons between prediction and measured data for the demonstrator airplane, together with the identification of a nontraditional radiation mechanism for propellers at angle of attack are achieved. Author

N90-26634*# Duke Univ., Durham, NC. School of Engineering.
ASYMPTOTIC MODAL ANALYSIS AND STATISTICAL ENERGY ANALYSIS Progress Report, 15 Oct. 1989 - 14 Apr. 1990
Earl H. Dowell and Linda F. Peretti 1990 22 p Presented at the 118th Acoustical Society of America Meeting, Saint Louis, MO, 27 Nov. - 1 Dec. 1989
(Grant NAG1-709)
(NASA-CR-186732; NAS 1.26:186732) Avail: NTIS HC
A03/MF A01 CSCL 20A

The sound field of a structural-acoustic enclosure was subject to experimental analysis and theoretical description in order to develop an efficient and accurate method for predicting sound pressure levels in enclosures such as aircraft fuselages. Asymptotic Modal Analysis (AMA) is the method under investigation. AMA is derived from classical modal analysis (CMA) by considering the asymptotic limit of the sound pressure level as the number of acoustic and/or structural modes approaches infinity. Using AMA, results identical to those of Statistical Energy Analysis (SEA) were obtained for the spatially-averaged sound pressure levels in the interior. AMA is systematically derived from CMA and therefore the degree of generality of the end result can be adjusted through the choice of appropriate simplifying assumptions. For example, AMA can be used to obtain local sound pressure levels at particular points inside the enclosure, or to include the effects of varying the size and/or location of the sound source. AMA theoretical results were compared with CMA theory and also with experiment for the case where the structural-acoustic enclosure is a rectangular cavity with part of one wall flexible and vibrating, while the rest of the cavity is rigid. Author

N90-26635*# National Aeronautics and Space Administration. Lewis Research Center, Cleveland, OH.
AEROACOUSTICS OF ADVANCED PROPELLERS
John F. Groeneweg 1990 21 p Presented at the 17th Congress of the International Council of Aeronautical Sciences, Stockholm, Sweden, 9-14 Sep. 1990; sponsored by AIAA
(NASA-TM-103137; E-5446; NAS 1.15:103137) Avail: NTIS HC
A03/MF A01 CSCL 20A

The aeroacoustics of advanced, high speed propellers (propfans) are reviewed from the perspective of NASA research conducted in support of the Advanced Turboprop Program. Aerodynamic and acoustic components of prediction methods for near and far field noise are summarized for both single and counterrotation propellers in uninstalled and configurations. Experimental results from tests at both takeoff/approach and cruise conditions are reviewed with emphasis on: (1) single and counterrotation model tests in the NASA Lewis 9 by 15 (low speed) and 8 by 6 (high speed) wind tunnels, and (2) full scale flight tests of a 9 ft (2.74 m) diameter single rotation wing mounted tractor and a 11.7 ft (3.57 m) diameter counterrotation aft mounted pusher propeller. Comparisons of model data projected to flight with full scale flight data show good agreement validating the scale model wind tunnel approach. Likewise, comparisons of measured and predicted noise level show excellent agreement for both single and counterrotation propellers. Progress in describing angle of attack and installation effects is also summarized. Finally, the aeroacoustic issues associated with ducted propellers (very high bypass fans) are discussed. Author

N90-26636# Aeronautical Research Inst. of Sweden, Stockholm. Dept. of Aerodynamics.
A PRELIMINARY STUDY OF THE MASKING OF WIND TURBINE NOISE BY AMBIENT SOUND
L. Ekstroem and S Ljunggren (Ingemansson Anatrol A.B., Askim, Sweden) Jan. 1990 12 p Presented at EWEC 1989, Glasgow,

Scotland
(Contract STEV-506-266-3)
(FFA-TN-1990-01; ETN-90-97093) Avail: NTIS HC A03/MF A01

An assessment of the masking effect on the noise from wind turbines by ambient sound is presented. The periodic modulation of the wind turbine noise is studied and gaps in the wind sound are analyzed. Introductory studies of two new topics are carried out: long time covariation of the wind speeds at high and low height above the ground; and covariation of turbine and background sound for three hypothetical turbine concepts. ESA

N90-26637# Rolls-Royce Ltd., Derby (England).
BRINGING AIRCRAFT NOISE TESTING DOWN TO EARTH
M. J. T. Smith 21 Apr. 1989 20 p Presented at the 1989 European Propulsion Forum on Modern Techniques and Development of Engine Component Testing: Bringing Aircraft Noise Testing Down to Earth, Bath, England, 19-21 Apr. 1989
(PNR90642; ETN-90-97146) Copyright Avail: NTIS HC A03/MF A01

Specifications and a description of the noise test facility at Hucknall (United Kingdom) are presented. The facility was constructed to allow a 35 KN (80,000 lb) thrust class engine to be tested and the structure capable of development to take 50 KN. The acoustic data collection system is described and its benefits outlined. Considerations to the local environment are outlined and the construction, experience and status are discussed. The concept of test bed rotatability improved the window of test opportunity three to fourfold and the use of digital techniques allows a full engine test of about 10 stabilized power conditions to be completed within one hour. Analysis is subsequently carried out overnight and real time data is available on line at the time of test. ESA

N90-26638# Technische Univ., Delft (Netherlands). Dept. of Electrical Engineering.
SURFACE ACOUSTIC WAVE FILTERS IN ZnO-SiO2-Si LAYERED STRUCTURES: DESIGN, TECHNOLOGY, AND MONOLITHIC INTEGRATION WITH ELECTRONIC CIRCUITRY Ph.D. Thesis
Jacobus Hendrik Visser 1989 140 p
(Contract STW-DEL-44/47-0592)
(ETN-90-97218) Avail: NTIS HC A07/MF A01

The design and technology of Surface Acoustic Wave (SAW) filters in ZnO SiO2 Si layered structures is investigated. SAW propagation and transduction properties with respect to dispersion, higher order Rayleigh-wave modes and fabrication tolerances in the piezoelectric layer thickness are studied. The conditions for SAW amplification by the interaction of the acoustic wave with the drifting charge carriers in the silicon substrate are examined. The monolithic integration of these SAW filters with electronic circuitry in one single chip and the fabrication of interdigital patterns with electrode widths down to 200 nm are realized. Experimental results of SAW delay lines, SAW transversal filters and SAW resonator filters are given. Application of silicon integrated SAW filters in an FM upconversion radio receiver is discussed. ESA

N90-26639# Georgia Inst. of Tech., Atlanta.
APPLICATION AND EXTENSION OF AN ANALYTICAL MODEL OF THE CONFINED ACOUSTIC BEAM GENERATED BY A TRANSDUCER Final Report
Jerry H. Ginsberg 1990 404 p
(Contract N00014-85-K-0872)
(AD-A222994) Avail: NTIS HC A18/MF A03 CSCL 17/1

The primary goal of this project was to develop an overall description of transducer radiation in which finite amplitude effects, diffraction, and spherical spreading are treated consistently, without limitation to a specific spatial domain or a specific type of input to the projector. Initially, the mathematical tools for this work were those used to develop the nonlinear King integral for nonlinear effects arising in the sound beam generated by a harmonic input. These techniques combined singular perturbation theory and asymptotic analysis of the behavior in specific domains. The general approach uses King integral in linear theory, which is a Fourier-Bessel integral transform, to develop the second order source terms that generate nonlinearities in the response. There are two kinds of nonlinear effects that arise at the second order. Some produce terms that remain bounded as the signal propagates. (One such effect is associated with the fact that the input from the transducer originates from a moving boundary, rather than the much simpler description, $z = 0$.) The smallness of the acoustic Mach number leads to the conclusion that these fixed magnitude effects cannot account for measured levels of distortion. The other group of nonlinear effects arise from resonance-like phenomena. These terms lead to distortion that grows with increasing distance. Shocks ultimately form this effect, unless dissipation is adequate to overcome the nonlinear distortion process. GRA

72 ATOMIC AND MOLECULAR PHYSICS

Includes atomic structure, electron properties, and molecular spectra.

N90-26640*# National Aeronautics and Space Administration. Langley Research Center, Hampton, VA.
A CLOSED FORM SOLUTION TO HZE PROPAGATION
John W. Wilson, L. W. Townsend, S. L. Lamkin, and B. D. Ganapol (Arizona Univ., Tucson.) 1989 21 p Submitted for publication
(NASA-TM-103482; NAS 1.15:103482) Avail: NTIS HC A03/MF A01 CSCL 20H

An analytic solution for high energy heavy ion transport assuming straightahead and velocity conserving interactions with constant nuclear cross reactions is given in terms of a Green's function. The series solution for the Green's function is rapidly convergent for most practical applications. The Green's function technique can be applied with equal success to laboratory beams as well as to galactic cosmic rays allowing laboratory validation of the resultant space shielding code. Author

N90-26641# California Inst. of Tech., Pasadena. Dept. of Chemistry.
IMAGING AND SPECTROSCOPY OF SMALL MOLECULES BY SCANNING TUNNELING MICROSCOPY Annual Report, for 1 Jun. 1989 - 31 May 1990
John D. Baldeschwieler 25 May 1990 21 p
(Contract N00014-88-K-0214)
(AD-A222572) Avail: NTIS HC A03/MF A01 CSCL 20/6

Ultra-high vacuum (UHV)-scanning tunneling microscopy was used to image for the first time an individual double helix of deoxyribonucleic acid with atomic resolution. DNA was deposited onto a highly oriented pyrolitic graphite (HOPG) surface without chemical modification and imaged with an STM to reveal structure down to the atomic-scale. The images represent the hightest magnification of a single molecule of DNA by any technique to date. The goal was to explore the effects of surface defects on the electronic structure of semiconductors. GRA

N90-26642# Florida Univ., Gainesville. Quantum Theory Project.
MOLECULAR INTERACTIONS AND PROPERTIES WITH MANY-BODY METHODS Final Report, 1 Nov. 1987 - 31 Oct. 1989
Rodney J. Bartlett 17 Apr. 1990 21 p
(Grant AF-AFOSR-0041-88; AF Proj. 2301)
(AD-A222631; AFOSR-90-0583TR) Avail: NTIS HC A03/MF A01 CSCL 20/5

During the course of this research, coupled cluster/many-body perturbation theory (CC/MBPT) theories have been established as being among the most accurate available, and very efficient and generally applicable computer codes have been developed to perform CC/MBPT calculations. These methods have been employed for the first time in large scale ab initio calculations of potential energy surfaces. Two of the papers produced in this research have been identified by authorities as being among the

most influential papers in the 50-year history of computational quantum chemistry, and four have been identified by Current Contents as qualifying as science citation classics. GRA

N90-26643# North Carolina Univ., Chapel Hill. Dept. of Chemistry.
ISOTHERMAL COMPRESSIBILITY OF SPC/E WATER Interim Report
K. Motakabbir and M. Berkowitz Apr. 1990 22 p Revised Submitted for publication
(Contract N00014-89-J-1169)
(AD-A222723; Rept-2) Avail: NTIS HC A03/MF A01 CSCL 20/4

Molecular dynamics computer simulations on rigid SPC/E water molecules were performed. The goal of the simulations is to study the behavior of isothermal compressibility, which was calculated in the simulations at T=298, 273 and 248 K. The calculated isothermal compressibilities at these temperatures display a trend contrary to the experimental observations. The hydrogen bonded network in water was also investigated. No correlation between the temperature dependence of isothermal compressibility and the number of hydrogen bonded pentagons was observed. GRA

N90-26223*# Jet Propulsion Lab., California Inst. of Tech., Pasadena. Communications Systems Research Section.
A STUDY OF THE INFLUENCE OF Hg(6(3)P2) POPULATION IN A LOW-PRESSURE DISCHARGE ON MERCURY ION EMISSION AT 194.2 nm
L. Maleki, B. J. Blasenheim, and G. R. Janik *In its* The Telecommunications and Data Acquisition Report 15 May 1990 p 61-72 (For primary document see N90-26217 20-32)
Avail: NTIS HC A10/MF A02 CSCL 20H

N90-26760*# National Inst. of Standards and Technology, Gaithersburg, MD. Chemical Kinetics Div.
NEW ELECTRONIC STATES OF NH AND ND OBSERVED BY RESONANCE ENHANCED MULTIPHOTON IONIZATION SPECTROSCOPY
Russell D. Johnson, III and Jeffrey W. Hudgens *In* NASA, Goddard Space Flight Center, First International Conference on Laboratory Research for Planetary Atmospheres May 1990 p 164-167 (For primary document see N90-26744 20-91)
Avail: NTIS HC A21/MF A03 CSCL 20H

N90-26767*# Pittsburgh Univ., PA. Dept. of Physics and Astronomy.
DISSOCIATIVE RECOMBINATION OF MOLECULAR IONS WITH ELECTRONS
Rainer Johnsen *In* NASA, Goddard Space Flight Center, First International Conference on Laboratory Research for Planetary Atmospheres May 1990 p 232-236 (For primary document see N90-26744 20-91)
(Grants NAGw-1764; NGL-39-0110137)
Avail: NTIS HC A21/MF A03 CSCL 20H

N90-26771*# Colorado Univ., Boulder. Dept. of Chemistry and Biochemistry.
UV AND VUV SPECTROSCOPY AND PHOTOCHEMISTRY OF SMALL MOLECULES IN A SUPERSONIC JET
E. Ruehl (Freie Univ., Berlin, Germany, F.R.) and V. Vaida *In* NASA, Goddard Space Flight Center, First International Conference on Laboratory Research for Planetary Atmospheres May 1990 p 255-259 Sponsored in part by NSF; Petroleum Research Fund; and Deutsche Forschungsgemeinschaft (For primary document see N90-26744 20-91)
Avail: NTIS HC A21/MF A03 CSCL 20H

N90-26779*# Jet Propulsion Lab., California Inst. of Tech., Pasadena.
ELECTRON-IMPACT SPECTROSCOPY
S. Trajmar *In* NASA, Goddard Space Flight Center, First International Conference on Laboratory Research for Planetary Atmospheres May 1990 p 386-398 (For primary document see N90-26744 20-91)
Avail: NTIS HC A21/MF A03 CSCL 20H

N90-26780*# Georgia Univ., Athens. Dept. of Chemistry.
OPTICAL SIGNATURES OF MOLECULAR PARTICLES VIA MASS-SELECTED CLUSTER SPECTROSCOPY
Michael A. Duncan *In* NASA, Goddard Space Flight Center, First International Conference on Laboratory Research for Planetary Atmospheres May 1990 p 399-404 (For primary document see N90-26744 20-91)
Avail: NTIS HC A21/MF A03 CSCL 20H

N90-26783*# California Univ., Los Angeles. Space Sciences Center.
PHOTON SPUTTERING OF H2O ICES: A PRELIMINARY REPORT
C. Y. Robert Wu and D. L. Judge *In* NASA, Goddard Space Flight Center, First International Conference on Laboratory Research for Planetary Atmospheres May 1990 p 414-419 (For primary document see N90-26744 20-91)
Avail: NTIS HC A21/MF A03 CSCL 20H

73 NUCLEAR AND HIGH-ENERGY PHYSICS

Includes elementary and nuclear particles; and reactor theory.

For space radiation see *93 Space Radiation.*

N90-26644# Continuous Electron Beam Accelerator Facility, Newport New, VA.
A BEAUTY FACTORY USING AN SRF LINAC AND A STORAGE RING
J. J. Bisognano, J. R. Boyce, D. Douglas, S. Heifets, J. Kewisch, G. Krafft, and R. Rossmanith 23 Jun. 1989 5 p
(Contract DE-AC05-84ER-40150)
(CEBAF-PR-89-017) Avail: NTIS HC A01/MF A01; also available from CEBAF Library, 12000 Jefferson Ave., Newport News, VA 23606

A brief review is presented of accelerator facilities proposed for measuring CP violation in the B-meson system. In light of this comparison requirements are discussed for a B-factory using an e(+) storage ring beam colliding with a superconducting RF linac e(-) beam to produce a luminosity of 10(exp 34)/sq cm/sec. Author

N90-26645# Boeing Aerospace Co., Kent, WA.
MULTIMEGAWATT SPACE NUCLEAR POWER SUPPLY, PHASE 1. VOLUME 2: PHASE 2 PLAN D180-30619-6 Final Report
17 Feb. 1989 115 p
(Contract DE-AC07-88ID-12754)
(DE90-012431; DOE/ID-12754/T1-Vol-2) Avail: NTIS HC A06/MF A01

The Phase 2 program objectives are to: (1) demonstrate concept feasibility, (2) develop a preliminary design, and (3) complete Phase 3 engineering development and ground test plans. The approach to accomplish these objectives is to prove technical feasibility of our baseline design early in the program while maintaining flexibility to easily respond to changing requirements and advances in technology. This approach recognizes that technology is advancing rapidly while the operational phase MSNPS is 15 to 20 years in the future. This plan further recognizes that the weapons platform and Advanced Launch System (ALS) are in very early program definition stages; consequently, their requirements, interfaces, and technological basis will evolve. The phase 2 plan is outlined along with task scheduling of the various program aspects. DOE

N90-26646# Boeing Aerospace Co., Kent, WA.
MULTIMEGAWATT SPACE NUCLEAR POWER SUPPLY, PHASE 1. VOLUME 3: ANNOTATED OUTLINE OF PRELIMINARY SAFETY ASSESSMENT D180-30619-7 Final Report
17 Feb. 1989 28 p
(Contract DE-AC07-88ID-12754)
(DE90-012432; DOE/ID-12754/T2-Vol-3) Avail: NTIS HC A03/MF A01

The preliminary safety assessment report analyzes the potential radiological risk of the integrated MSNPS with the launch vehicle including interface with the weapon system. Most emphasis will be placed the prime power concept design. Safety problems can occur any time during the entire life cycle of the system including contingency phases. The preliminary safety assessment report is to be delivered at the end of phase 2. This assessment will be the basis of the safety requirements which will be applied to the design of the MSNPS as it develops in subsequent phases. The assessment also focuses design activities on specific high-risk scenarios and missions that may impact safety. DOE

N90-26647# Boeing Aerospace Co., Kent, WA.
MULTIMEGAWATT SPACE NUCLEAR POWER SUPPLY, PHASE 1. SUPPLEMENT: D180-30619-8 Final Report
17 Feb. 1989 162 p
(Contract DE-AC07-88ID-12754)
(DE90-012433; DOE/ID-12754/T3-Suppl) Avail: NTIS HC A08/MF A01

This Specification establishes the performance, design, development, and test requirements for the Boeing Multimegawatt Space Nuclear Power System (MSNPS). The Boeing Multimegawatt Space Power System is part of the DOE/SDIO Multimegawatt Space Nuclear Power Program. The purpose of this program is to provide a space-based nuclear power system to meet the needs of SDIO missions. The Boeing MSNPS is a category 1 concept which is capable of delivering 10's of MW(e) for 100's of seconds with effluent permitted. A design goal is for the system to have growth or downscale capability for other power system concepts. The growth objective is to meet the category 3 capability of 100's of MW(e) for 100's of seconds, also with effluent permitted. The purpose of this preliminary document is to guide the conceptual design effort throughout the Phase 1 study effort. This document will be updated throughout the study. It will thus result in a record of the development of the design effort. DOE

N90-26648# Brown Univ., Providence, RI. Dept. of Physics.
A RESEARCH PROGRAM IN THEORETICAL HIGH ENERGY PHYSICS Progress Report
David Feldman, Herbert M. Fried, Antal Jevicki, Kyungsik Kang, and Chung-I. Tan 30 Jun. 1990 24 p
(Contract DE-AC02-76ER-03130)
(DE90-013322; DOE/ER-03130/453; BROWN-HET-758) Avail: NTIS HC A03/MF A01

Research this past year was carried out in the fields of cosmic strings and galaxy formation, inflationary models of the universe, topological defects and phase transitions, group contractions and chiral fermions, low frequency approximations in (QCD), loop bremsstrahlung of e(+)e(-) and mu(+)mu(-)) pairs in heavy ion collisions, approximations to solutions of non-linear differential equations, the use of continued functions as solution to vortex problems, string theory and large-N matrix models, topological expansions in QCD, 1-D string theory and its infrared divergences, strings in less than one dimension, hadron-hadron interactions and the possible existence of the odderon, electroweak interactions and possible new physics in the TeV range, axions, quark flavor mixings and neutrino oscillations, large-N matrix models and their relation to string theories and 2-D quantized gravity, and the statistical mechanics of strings at high temperatures. DOE

74 OPTICS

Includes light phenomena; and optical devices.
For lasers see *36 Lasers and Masers.*

N90-26649*# Massachusetts Univ., Amherst. Dept. of Electrical and Computer Engineering.
HIGH SPEED ALL OPTICAL NETWORKS Annual Report, 1 May 1989 - 30 Apr. 1990
Imrich Chlamtac and Aura Ganz 1990 132 p
(Grant NAG2-578)
(NASA-CR-185311; NAS 1.26:185311) Avail: NTIS HC A07/MF A01 CSCL 20F

An inherent problem of conventional point-to-point wide area network (WAN) architectures is that they cannot translate optical transmission bandwidth into comparable user available throughput due to the limiting electronic processing speed of the switching nodes. The first solution to wavelength division multiplexing (WDM) based WAN networks that overcomes this limitation is presented. The proposed Lightnet architecture takes into account the idiosyncrasies of WDM switching/transmission leading to an efficient and pragmatic solution. The Lightnet architecture trades the ample WDM bandwidth for a reduction in the number of processing stages and a simplification of each switching stage, leading to drastically increased effective network throughputs. The principle of the Lightnet architecture is the construction and use of virtual topology networks, embedded in the original network in the wavelength domain. For this construction Lightnets utilize the new concept of lightpaths which constitute the links of the virtual topology. Lightpaths are all-optical, multihop, paths in the network that allow data to be switched through intermediate nodes using high throughput passive optical switches. The use of the virtual topologies and the associated switching design introduce a number of new ideas, which are discussed in detail. Author

N90-26650 Toronto Univ. (Ontario). Inst. for Aerospace Studies.
AN EMBEDDED FIBRE OPTIC SENSOR FOR IMPACT DAMAGE DETECTION IN COMPOSITE MATERIALS
Neil David William Glossop Sep. 1989 218 p Sponsored in part by deHavilland Aircraft Co. of Canada; Ontario Univ. Research Incentive Fund; Ontario Laser and Lightwave Research Centre; and Ontario Centre for Materials Research
(Grant STR-0012487)
(UTIAS-332; ISSN-0082-5255) Copyright Avail: Issuing Activity

A structurally embedded fiber optic damage detection sensor for composite materials is described. The system is designed specifically for the detection of barely visible damage resulting from low velocity impacts in Kevlar-epoxy laminates. By monitoring the light transmission properties of optical fiber embedded in the composite, it was shown that the integrity of the material can be accurately determined. The effect of several parameters on the sensitivity of the system was investigated, including the effect of the optical fiber orientation and depth of embedding within the composite. A novel surface was also developed for the optical fibers to ensure they will fracture at the requisite damage level. The influence of the optical fiber sensors on the tensile and compressive material properties and on the impact resistance of the laminate was also studied. Extensive experimental results from impact tests are reported and a numerical model of the impact event is presented which is able to predict and model the damage mechanism and sensor system. A new and powerful method of nondestructive evaluation for translucent composite materials based on image enhanced backlighting is also described. Author

N90-26651*# National Aeronautics and Space Administration. Langley Research Center, Hampton, VA.
OPTICAL TRANSMISSION THROUGH A POLARIZATION PRESERVING SINGLE MODE OPTICAL FIBER AT TWO Ar(+) LASER WAVELENGTHS
Ken K. Tedjojuwono and William W. Hunter, Jr. 1989 19 p Submitted for publication
(NASA-TM-103475; NAS 1.15:103475) Avail: NTIS HC A03/MF A01 CSCL 20F

The transmission characteristics of two Ar(+) laser wavelengths through a twenty meter Panda type Polarization Preserving Single Mode Optical Fiber (PPSMOF) were measured. The measurements were done with both single and multi-longitudinal mode radiation. In the single longitudinal mode case, a degrading Stimulated Brillouin Scattering (SBS) is observed as a backward scattering loss. By choosing an optimum coupling system and manipulating the input polarization, the threshold of the SBS onset can be raised and the transmission efficiency can be increased. Author

N90-26652*# Chicago Univ., IL. Dept. of Electrical Engineering and Computer Science.
THEORY OF BIAXIAL GRADED-INDEX OPTICAL FIBER M.S. Thesis
Stephen F. Kawalko 1990 107 p Sponsored in part by the Pacific Missile Test Center
(Grant NAG2-544)
(NASA-CR-186882; NAS 1.26:186882) Avail: NTIS HC A06/MF A01 CSCL 20F

A biaxial graded-index fiber with a homogeneous cladding is studied. Two methods, wave equation and matrix differential equation, of formulating the problem and their respective solutions are discussed. For the wave equation formulation of the problem it is shown that for the case of a diagonal permittivity tensor the longitudinal electric and magnetic fields satisfy a pair of coupled second-order differential equations. Also, a generalized dispersion relation is derived in terms of the solutions for the longitudinal electric and magnetic fields. For the case of a step-index fiber, either isotropic or uniaxial, these differential equations can be solved exactly in terms of Bessel functions. For the cases of an istropic graded-index and a uniaxial graded-index fiber, a solution using the Wentzel, Krammers and Brillouin (WKB) approximation technique is shown. Results for some particular permittivity profiles are presented. Also the WKB solutions is compared with the vector solution found by Kurtz and Streifer. For the matrix formulation it is shown that the tangential components of the electric and magnetic fields satisfy a system of four first-order differential equations which can be conveniently written in matrix form. For the special case of meridional modes, the system of equations splits into two systems of two equations. A general iterative technique, asymptotic partitioning of systems of equations, for solving systems of differential equations is presented. As a simple example, Bessel's differential equation is written in matrix form and is solved using this asymptotic technique. Low order solutions for particular examples of a biaxial and uniaxial graded-index fiber are presented. Finally numerical results obtained using the asymptotic technique are presented for particular examples of isotropic and uniaxial step-index fibers and isotropic, uniaxial and biaxial graded-index fibers. Author

N90-26653# Societe Bertin et Cie, Plaisir (France). Optics and Optoelectronics Div.
A DUAL-WAVELENGTH PASSIVE HOMODYNE DETECTION UNIT FOR FIBER-COUPLED WHITE-LIGHT INTERFEROMETERS
M. Lequime, C. Lecot, H. Giovannini, and S. Huard (Ecole Nationale Superieure du Petrole et des Monteurs, Marseille, France) 1990 15 p Presented at Fiber Optic Sensors 4, The Hague, Netherlands, 14 Mar. 1990
(ETN-90-97036) Avail: NTIS HC A03/MF A01

Graphics are presented representing steps in the achievement of an industrial emission/detection unit Accord. Industrial application areas and specific requirements for the transduction are listed. A general description with encoding and multiplexing graphics system characteristics is given. Performances and application examples are provided graphically. Conclusions on these are listed commercial availability specified. ESA

N90-26654# Rolls-Royce Ltd., Derby (England). Advanced Research Lab.
COHERENT OPTICAL TECHNIQUES FOR INDUSTRIAL INSPECTION
R. J. Parker 22 Jun. 1989 19 p Presented at the SIRA Course on Automatic On-Line Industrial Inspection, Chislehurst, England, 22-23 Jun. 1989
(PNR90605; ETN-90-97132) Copyright Avail: NTIS HC A03/MF A01

Two coherent optical techniques capable of providing full-field data for inspection purposes are considered. The techniques are holographic interferometry and Electronic Laser Speckle Interferometry (ESPI). Developments in technology which allowed them to be considered as practical techniques for industrial inspection are reviewed. Further foreseeable improvements which would allow them to be applied on line in a fully automated way are indicated. ESA

N90-26655# Technische Univ., Delft (Netherlands). Faculty of Aerospace Engineering.
REFRACTIVE ERROR ANALYSIS IN THE INTERFEROMETRIC MEASUREMENT OF 2-D DENSITY FIELDS CONTAINING STRONG GRADIENTS
T. A. W. M. Lanen Jan. 1990 44 p
(LR-616; ETN-90-97179) Avail: NTIS HC A03/MF A01

To demonstrate the effects of light deflection in nonhomogeneous media, two test media are investigated that allow an analytic determination of their interferograms: a medium with a linear density distribution and a medium with an exponential density distribution. These test media show that focusing the interferogram into the plane at two thirds of the field width (measured in the direction of light propagation) will minimize the error present in the interferogram due to light deflection. To allow the investigation of the effects of light deflection in an arbitrary inhomogeneous medium on the interferogram, a numeric scheme is given to compute the ray trajectories when traversing the medium. With this scheme the effects of light deflection in several characteristic density distributions are demonstrated. Focusing the interferogram into the plane at two thirds of the field width appears to be preferable. If, despite choosing the plane of focus at two thirds of the field width, the effects of light deflection on the interferogram are still too serious, a correction procedure can be carried out. The distortion of the interferogram due to the three-dimensionality of the density field and due to the misalignment of the beam traversing the density field is discussed. ESA

N90-26656# Technische Univ., Delft (Netherlands). Lab. of Electrical Materials.
OPTICAL PROPERTIES AND TRANSPORT PROPERTIES OF HYDROGENATED AMORPHOUS SILICON Ph.D. Thesis
Johan vandenHeuvel 1989 143 p Sponsored by Netherlands Organization for Scientific Research
(ETN-90-97215) Avail: NTIS HC A07/MF A01

Hydrogenated amorphous silicon (a-Si:H) is a relatively new semiconductor. The optical properties and transport properties of a-Si:H are studied. These properties are closely related to the performance of a-Si:H solar cells. The optical properties are studied and a description of the fabrication of the layers and devices of a-Si:H is given. The Space Charge Limited Current (SCLC) method is investigated. It is shown that high electric fields do not disturb the SCLC measurements. This result is a confirmation of the theoretical models for the gap states of a-Si:H. The density of gap states obtained by the SCLC method show a large temperature dependence. The density of gap states of a-Si:H is supposed to be independent of the temperature. It is shown that the temperature dependence is caused by the tail states near the conduction band edge, and not by a change in the density of gap states. ESA

N90-26657# School of Aerospace Medicine, Brooks AFB, TX.
COMPUTER MODELING WAVE PROPAGATION WITH A VARIATION OF THE HELMHOLTZ-KIRCHHOFF RELATION Interim Report, Jan. - Nov. 1989
Paul G. Rudolf, Jeffrey J. Tollett, and Rebecca R. McGowan (Trinity Univ., San Antonio, TX.) 1 Mar. 1990 8 p Repr. from Applied Optics, v. 29, no. 7, 1 Mar. 1990
(AF Proj. 7757)
(AD-A222746; USAFSAM-JA-89-62) Avail: NTIS HC A02/MF A01 CSCL 20/6

A computational technique is presented by which complex diffraction effects associated with scalar waves may be easily modeled. The approach uses a variation of the Kirchhoff equation, derived from basic principles. The modification involves the choice of a Green's function which represents a continuous distribution of inward propagating point sources on the bounding surface, as opposed to the single point source at the observation point in the standard derivation. The resultant equation is easily modeled numerically. The diffracting screen need not be flat and the aperture shape is unrestricted. The technique works well in the near-or far-field. A wide variety of incident wavefronts are modeled; there can be any amplitude variation, any wave-shape, and the wave may impinge from any direction. Restrictions on the method are that the wave may be monochromatic, scalar, and that the medium through which the wave propagates be homogeneous. The output of the calculation is a simulated diffraction pattern, plotted as an intensity distribution. Comparison is made to analytic calculations in the Fraunhofer (far-field) case and to experimental results in the Fresnel (near-field) regime. Kirchhoff boundary conditions are used in all cases. Examples are also worked for light propagating at extreme angles to the optical axis and for a severely asymmetric aperture. Finally the radiation field produced by an extended, contorted source is modeled. GRA

N90-26226*# Jet Propulsion Lab., California Inst. of Tech., Pasadena. Communications Systems Research Section.
A TWO-TELESCOPE RECEIVER DESIGN FOR DEEP SPACE OPTICAL COMMUNICATIONS
K. Shaik *In its* The Telecommunications and Data Acquisition Report 15 May 1990 p 114-120 (For primary document see N90-26217 20-32)
Avail: NTIS HC A10/MF A02 CSCL 20F

N90-26227*# Jet Propulsion Lab., California Inst. of Tech., Pasadena. Tracking Systems and Applications Section.
PRELIMINARY ERROR BUDGET FOR AN OPTICAL RANGING SYSTEM: RANGE, RANGE RATE, AND DIFFERENCED RANGE OBSERVABLES
W. M. Folkner and M. H. Finger *In its* The Telecommunications and Data Acquisition Report 15 May 1990 p 121-135 (For primary document see N90-26217 20-32)
Avail: NTIS HC A10/MF A02 CSCL 20F

75 PLASMA PHYSICS

Includes magnetohydrodynamics and plasma fusion.
For ionospheric plasmas see *46 Geophysics*. For space plasmas see *90 Astrophysics*.

N90-26658# Old Dominion Univ., Norfolk, VA.
APPLICATION OF THE RESULTS OF CARBON PELLET MODELING TO THE PROBLEM OF PLASMA PENETRATION
L. L. Vahala, A. G. ElCashlan, G. A. Gerdin, and P. B. Parks (General Atomic Co., San Diego, CA.) 1990 11 p Presented at the 9th Topical Conference on High-Temperature Plasma Diagnostics, Hyannis, MA, 7-10 May 1990
(Contract DE-FG05-88ER-53278)
(DE90-012713; CONF-900557-10) Avail: NTIS HC A03/MF A01

The assumptions of the evaporation model for low-Z pellets interacting with magnetic fusion plasmas developed by P. B. Parks are tested. These assumptions are that the vapor density profile in the region adjacent to the pellet surface, falls off with radial distance as r(-)(alpha), where 5 less than alpha less than 6, and that the ionization time for the transition between charge states tau (sub zi), is much less than a flow time for the vapor in this same region tau (sub f) (i.e., for r less than approx 3 sonic radii). The first assumption is tested by solving a two-parameter eigenvalue problem for the evaporation cloud in the region interior to the sonic radius; the results are found to be consistent with the low-Z evaporation model. The second assumption, that tau (sub zi) (much less than) tau (sub f), is tested at the sonic radius using the results from atomic physics and the low-Z evaporation model. It is found that indeed tau (sub zi) (much less than) tau (sub f) for plasmas with parameters close to thermonuclear conditions (e.g., TFTR and CIT), but not for those of smaller Tokamaks such as TEXT. The results of pellet penetration calculations for the conditions of the TEXT carbon-pellet injection experiments are presented which show better agreement with experiment if the shielding fraction is calculated at each step of the pellet-penetration calculation, the effect of ionization is ignored, and if the effect of possible uncertainties in the background plasma parameters is included. DOE

N90-26659# Los Alamos National Lab., NM.
CONFINEMENT OF NONNEUTRAL PLASMA IN UNCONVENTIONAL GEOMETRIES
Leaf Turner 1990 6 p Presented at the 4th International Workshop on Slow-Positron Beam Technologies for Solids and Surfaces, London, Ontario, 3-6 Jul. 1990
(Contract W-7405-eng-36)
(DE90-013048; LA-UR-90-2178; CONF-900798-1) Avail: NTIS HC A02/MF A01

Interest in efficient storage of cold, nonneutral plasma has been motivated by the elegant studies on cryogenic nonneutral electron plasmas at UCSD and by the remarkable results obtained from the laser-cooled ion plasmas at the NIST, Boulder, Colorado. Also motivating the study is the perceived need to develop the most expedient means of storing antimatter, whether it be antiprotons for gravitational studies or positrons for a variety of physics experiments and diagnostic purposes. One of the most explored technologies of confining nonneutral plasmas is the Penning trap. The maximum number density of cold nonneutral plasma that can be stored in such a trap is B(sup 2)/2(mu)(sub 0)mc(sup 2), in which B(sup 2)/2(mu)(sub 0) is the (homogeneous) magnetic energy density and mc(sup 2) is the rest energy of the stored charges. A synopsis is presented of the results of the theoretical exploration of the effect on this hydrostatic limit, the so-called Brillouin limit, of altering the geometry of the confining vacuum magnetic field while maintaining the field's azimuthal symmetry. In particular, equilibrium confinement is analyzed by, first, a poloidal magnetic field, B(sub 4)(r,z)(cflx r) + B(sub z)(r,z)(cflx z), and second, a toroidal magnetic field, along with the concomitant electrostatic fields. DOE

N90-26660# General Atomic Co., San Diego, CA.
THE EFFECTS OF CARBONIZATION ON THE CONFINEMENT PROPERTIES OF THE DIII-D H-MODE
D. P. Schissel, J. C. DeBoo, J. R. Ferron, G. L. Jackson, K. H. Burrell, R. J. Groebner, A. G. Kellman, S. Lippmann, T. W. Petrie, and E. J. Strait et al Jun. 1990 4 p Presented at the 17th European Conference on Controlled Fusion and Plasma Heating, Amsterdam, Netherlands, 25-29 Jun. 1990 Submitted for publication
(Contract DE-AC03-89ER-51114)
(DE90-013297; GA-A-20085; CONF-900602-14) Avail: NTIS HC A02/MF A01

Understanding and increasing the energy confinement time (tau (sub E) is identical with W(sub T)/P(sub T)) remains a primary goal a fusion research. A primary technique utilized to increase tau (sub E) within a given machine is to operate at a higher plasma current. Although Z(sub eef) in DIII-D is generally less than or = 2, high radiated power (P(sub rad)/P(sub T) greater than or = 0.6)) and metal accumulation have been observed during high current (I(sub p) greater than or = 2 MA)) beam heated D(exp 0) yields D(+) H-mode discharges. Reduction of metallic impurity influx has been obtained on numerous tokamaks with the introduction of a thin carbon film. The successful carbonization of the DIII-D vacuum vessel which allowed for routine high current operation is reported and the confinement properties of carbonized discharges are examined. DOE

N90-26661# Sandia National Labs., Albuquerque, NM.
SOFT x RAY RESIST CHARACTERIZATION: STUDIES WITH A LASER PLASMA x RAY SOURCE

Glenn D. Kubiak, Duane A. Outka (Sandia National Labs., Livermore, CA.), and John M. Zeigler 1990 9 p Presented at the Symposium on Microlithography, San Jose, CA, 4-9 Mar. 1990
(Contract DE-AC04-76DP-00789)
(DE90-013493; SAND-90-1534C; CONF-900312-1) Avail: NTIS HC A02/MF A01

Little work has been performed to characterize the exposure sensitivity, contrast, and tone of candidate resists for photon energies between 100 to 300 eV, the range in which projection soft x ray lithography will be developed. The characterization is reported of near edge x ray absorption fine structure (NEXAFS) spectra, exposure sensitivity, contrast, and post-exposure processing of selected polysilane resists at photon energies close to the Si L(sub 2,3) absorption edge (100 eV). Absorption resonance features were found in the NEXAFS spectra which was assign to excitation into Si--Si and Si--C (sigma)* orbitals. Using monochromatized XUV exposures on the Si--Si (sigma)* resonance at 105 eV, followed by solvent dissolution development, the exposure sensitivity curves were measured of these resists. Sensitivities were found in the range of 600 to 3000 mJ/sq cm and contrasts in the range from 0.5 to 1.4, depending on the polysilane side chain. Exposure sensitivity measurements were made at 92 eV, below the edge. Sensitivity decreases slightly compared to 105 eV exposures and the saturation depth and contrast both increase, as expected. It was also found that exposing resist films to oxygen after XUV exposure, but before development increases the sensitivity markedly. DOE

N90-26662# Royal Aerospace Establishment, Farnborough (England).
SENSITIVITY ANALYSIS WITH A SIMPLE CHARGING CODE
A. J. Sims and G. L. Wrenn 4 Jan. 1990 25 p Presented at Spacecraft Charging Technology Conference, Monterey, CA, 31 Oct. - 3 Nov. 1989
(RAE-TM-Space-374; BR113095; ETN-90-97065) Copyright Avail: NTIS HC A03/MF A01

An overview of the EQUIPOT code, developed to compute the equilibrium potential of a surface in a given plasma environment, is presented. A sensitivity analysis is performed on the properties of a shaded kapton patch on a spherical, conducting, sunlit spacecraft subject to an ambient plasma environment which will produce large, negative potentials. Two main results are obtained: firstly, identification of the important role played by the high incident energy part of the secondary electron yield curve and secondly the ability of a low density, cold plasma component to limit negative charging. ESA

76 SOLID-STATE PHYSICS

Includes superconductivity.

For related information, see also *33 Electronics and Electrical Engineering* and *36 Lasers and Masers.*

N90-26663*# Stanford Univ., CA. Center for Materials Research.
PROTEIN CRYSTAL GROWTH IN LOW GRAVITY Annual Technical Report, 27 Apr. 1989 - 26 Apr. 1990
Robert S. Feigelson Jun. 1990 40 p
(Grant NAG8-774)
(NASA-CR-186243; NAS 1.26:186243; SU-CMR-90-5) Avail: NTIS HC A03/MF A01 CSCL 20L

The effect of low gravity on the growth of protein crystals and those parameters which will affect growth and crystal quality was studied. The proper design of the flight hardware and experimental protocols are highly dependent on understanding the factors which influence the nucleation and growth of crystals of biological macromolecules. Thus, those factors are investigated and the body of knowledge which has been built up for small molecule crystallization. These data also provide a basis of comparison for the results obtained from low-g experiments. The flows around growing crystals are detailed. The preliminary study of the growth of isocitrate lyase, the crystal morphologies found and the preliminary x ray results are discussed. The design of two apparatus for protein crystal growth by temperature control are presented along with preliminary results. Author

N90-26664*# Akron Univ., OH. Dept. of Mechanical Engineering.
TEMPERATURE AND MELT SOLID INTERFACE CONTROL DURING CRYSTAL GROWTH Final Technical Report, 1 May - 14 Nov. 1989
Celal Batur Jul. 1990 47 p
(Contract NCC3-109)
(NASA-CR-186731; NAS 1.26:186731) Avail: NTIS HC A03/MF A01 CSCL 20L

Findings on the adaptive control of a transparent Bridgman crystal growth furnace are summarized. The task of the process controller is to establish a user specified axial temperature profile by controlling the temperatures in eight heating zones. The furnace controller is built around a computer. Adaptive PID (Proportional Integral Derivative) and Pole Placement control algorithms are applied. The need for adaptive controller stems from the fact that the zone dynamics changes with respect to time. The controller was tested extensively on the Lead Bromide crystal growth. Several different temperature profiles and ampoule's translational rates are tried. The feasibility of solid liquid interface quantification by image processing was determined. The interface is observed by a color video camera and the image data file is processed to determine if the interface is flat, convex or concave. Author

N90-26665# Los Alamos National Lab., NM. Neuromagnetometry Lab.
EXPERIMENTS ON SUPERCONDUCTOR IMAGING SURFACE MAGNETOMETRY
W. C. Overton, Jr., D. B. vanHulsteyn, and E. R. Flynn 1990 3 p Presented at the 19th International Conference on Low Temperature Physics, Brighton, England, 16-22 Aug. 1990
(Contract W-7405-eng-36)
(DE90-008925; LA-UR-90-964; CONF-900806-3) Avail: NTIS HC A01/MF A01

The recent development of a new concept in magnetometry has led to experiments to evaluate the performance of such systems. The superconductor imaging surface magnetometer employs superconducting plates and shells to deflect magnetic noise and to image nearby dipole sources while the SQUID pick-up coils are located in areas where the noise has been greatly reduced. The experiments reported confirm the principles of imaging magnetometry for detecting nearby dipole sources. DOE

N90-26666# Oak Ridge National Lab., TN. Solid State Div.
LARGE, ORIENTATION-DEPENDENT ENHANCEMENTS OF CRITICAL CURRENTS IN Y1Ba2Cu3O(7-x) EPITAXIAL THIN FILMS: EVIDENCE FOR INTRINSIC FLUX PINNING
D. K. Christen, C. E. Klabunde, R. Feenstra, D. H. Lowndes, D. Norton, J. D. Budai, H. R. Kerchner, L. A. Boatner, J. R. Thompson, and J. Narayan (North Carolina State Univ., Raleigh.) et al 1990 3 p Presented at the 19th International Conference on Low Temperature Physics, Brighton, England, 16-22 Aug. 1990 Submitted for publication
(Contract DE-AC05-84OR-21400)
(DE90-009424; CONF-900806-5) Avail: NTIS HC A01/MF A01

The basal plane transport critical current density J sub c of YBCO epitaxial thin films is strongly anisotropic, leading to large enhancements of J sub c when H is precisely parallel to the copper-oxygen planes. Experimental evidence shows that the enhancement is a bulk phenomenon, and the orientation dependence is compared with a model of intrinsic flux pinning by the layered crystal structure. DOE

N90-26667# Argonne National Lab., IL. Materials and Components Technology Div.
MATERIALS RESEARCH ISSUES IN SUPERCONDUCTING LEVITATION AND SUSPENSION AS APPLIED TO MAGNETIC BEARINGS

Francis C. Moon (Cornell Univ., Ithaca, NY.) and John R. Hull 1990 7 p Presented at the 25th Intersociety Energy Conversion Engineering Conference, Reno, NV, 12-17 Aug. 1990
(Contract W-31-109-eng-38)
(DE90-011147; CONF-900801-9) Avail: NTIS HC A02/MF A01

Current research issues associated with the improvement of high temperature superconductor materials for magnetic bearing applications are discussed. Major parameters of interest include magnetic pressure, magnetic stiffness, and damping. The understanding of and improvement in magnetic flux pinning within individual grains are seen as key to large improvements in the major parameters. The necessary material properties and routes to achieving those properties differ for those applications that require minimization of rotational losses versus those that require large magnetic pressures. Increased attention to characterization of the superconducting materials in terms of the bearing performance properties is desired, and chemical stability and mechanical strength of superconducting grains within a support matrix are recognized as vital success of commercial applications. DOE

N90-26668# Oak Ridge National Lab., TN. Metals and Ceramics Div.
DIFFUSION-ACCOMMODATED GRAIN BOUNDARY SLIDING IN A POLYCRYSTAL
P. M. Hazzledine and J. H. Schneibel 1990 6 p Presented at the Spring Meeting of the Materials Research Society, San Francisco, CA, 16-21 Apr. 1990
(Contract DE-AC05-84OR-21400)
(DE90-012727; CONF-900466-60) Avail: NTIS HC A02/MF A01

A 2-D model for diffusional creep (Coble creep) and diffusion-accommodated grain boundary sliding in polycrystals was developed. The results obtained for small symmetrical clusters of grains reproduce Spingarn and Nix's work. For clusters of irregularly shaped grains the material deposition and removal rates, the fluxes along the grain boundaries, the grain boundary tractions as well as the grain boundary sliding rates are irregular and can all be calculated. DOE

N90-26669# Sandia National Labs., Albuquerque, NM.
MOLECULAR DYNAMICS SIMULATIONS OF GRAIN-BOUNDARY DIFFUSION FOR VARYING TILT ANGLE GEOMETRIES
Steven J. Plimpton 1990 6 p Presented at the Spring Meeting of the Materials Research Society, San Francisco, CA, 16-21 Apr. 1990 Sponsored in part by Semiconductor Research Corp.
(Contract DE-AC04-76DP-00789)
(DE90-012919; SAND-89-2857C; CONF-900466-65) Avail: NTIS HC A02/MF A01

The effect of structure and geometry on grain boundary self-diffusion is investigated. Using static structures found by relaxation techniques (conjugate gradients) as starting points for a molecular dynamic simulation of a bicrystal model, diffusion coefficients and activation energies are calculated for (100) fcc Al and bcc (alpha)-Fe tilt boundaries. These quantities are derived by monitoring the mean squared displacement of atom in the grain boundary region as the simulation progresses and the temperature of the simulated solid is changed. The angular, directional, and structural dependence of the simulated diffusion are discussed and compared to experimental measures and theoretical predictions. The implementation of the molecular dynamics algorithm on a parallel supercomputer is also briefly discussed to illustrate the performance benefits these computers make possible. DOE

N90-26670# Idaho National Engineering Lab., Idaho Falls.
NDE (NONDESTRUCTIVE EVALUATION) OF CRITICAL CURRENTS IN HIGH T(SUB c) SUPERCONDUCTORS
K. L. Telschow and T. K. OBrien 1990 6 p Presented at the 8th Symposium on Energy Engineering Sciences, Argonne, IL, 9-11 May 1990
(Contract DE-AC07-76ID-01570)
(DE90-012953; EGG-M-90175; CONF-9005183-2) Avail: NTIS HC A02/MF A01

The use of an electromagnetic probe as a nondestructive evaluation tool for determining critical current dissipation in high (Tc) superconducting materials is described. The probe inductively generates a current in the superconductor that adds to the externally produced transport current. Dissipation is detected in the probe response whenever the net current in the material exceeds the critical value at the location of the probe. Results are presented for a simultaneous measurement of critical current dissipation with the contact 4-point probe DC method and the noncontacting inductive method described. Interpretation of the probe response is given in terms of the homogeneous isotropic London model. DOE

N90-26671# Oak Ridge National Lab., TN. Metals and Ceramics Div.
CRYSTAL GROWTH AND DEFORMATION BEHAVIOR OF TiAl ALUMINIDES
B. F. Oliver, B. Y. Huang, and W. C. Oliver Apr. 1990 32 p
(Contract DE-AC05-84OR-21400)
(DE90-012972; ORNL/TM-11159) Avail: NTIS HC A03/MF A01

The development is studied of single phase TiAl based alloys. The work has three segments: processing, mechanical testing, and alloying characteristics. The processing consists of developing a technique for growing large, high purity single crystals. Some of these crystals have been tested to determine their hardness and compression strength. The microstructures of the compressed specimens is discussed. Finally, two important preliminary findings of the alloy development program concerning additions of gallium and manganese is discussed. DOE

N90-26672# Sao Paulo Univ. (Brazil). Inst. de Fisica.
CHARACTERIZATION OF NbTi MULTIFILAMENTARY SUPERCONDUCTING WIRES M.S. Thesis [CARACTERIZACAO DE FIOS SUPERCONDUTORES MULTIFILAMENTARES DE NBTI]
Geni Vellego 1988 66 p In PORTUGUESE; ENGLISH summary
(DE90-626245; INIS-BR-1979) Avail: NTIS (US Sales Only) HC A04/MF A01

Pirelli is developing superconducting multifilamentary NbTi wires, with current carrying capacities of up to 500 A, for use in magnetic resonance imaging (MRI) systems and in small research magnets. Pirelli and IFUSP have developed a system for assessing wire performance, whose quality is comparable to the equivalent systems at the Brookhaven National Laboratory (BNL) and at the National Bureau of Standards (NBS). In particular, a high sensitivity is required for critical current measurements, so that the modern criteria for definition of critical current can be used. These involve conductor resistivities of the order of 10(exp -12) ohm-cm. The methods of measurements of critical current in applied magnetic fields, of residual resistance ratio and of copper to superconductor ratio are described. The results of the first tests performed in Pirelli wires and in wires of other manufacturers are described. These include tests on a NBS standard quality as results obtained at BNL or NBS on the same wires. So this system can be very useful throughout the Pirelli program. DOE

N90-26673# Iowa State Univ. of Science and Technology, Ames. Dept. of Chemistry.
HIGH TEMPERATURE x RAY DIFFRACTION AND LANDAU THEORY INVESTIGATIONS OF ORDER-DISORDER TRANSITION IN DEFECT NaCl-TYPE SOLIDS Ph.D. Thesis
Sung Jin Kim Jan. 1990 108 p
(Contract W-7405-eng-82)
(DE90-011807; IS-T-1478) Avail: NTIS HC A06/MF A01

The nature of the order-disorder transitions in a series of NaCl-type materials was investigated using high temperature powder x ray diffraction. The Landau theory of symmetry and phase transitions was applied to interpret the continuous thermal

symmetry breaking transitions, and all possible thermal symmetry breaking transition starting from the rock salt type structure were determined. Known examples together with those which were observed are reported. The diffraction data were analyzed by modified Rietveld-type full profile refinement. DOE

N90-26674# Oak Ridge National Lab., TN.
THE EFFECT OF CRYSTAL ORIENTATION ON DAMAGE ACCUMULATION IN CHROMIUM-IMPLANTED Al2O3
M. E. OHern, L. J. Romana, C. J. McHargue, C. W. White, and J. C. McCallum 1990 20 p Presented at the 15th Symposium on Effects of Radiation on Materials, Nashville, TN, 17-21 Jun. 1990
(Contract DE-AC05-84OR-21400)
(DE90-012294; CONF-900623-11) Avail: NTIS HC A03/MF A01

Chromium-implantation of single crystal aluminium oxide (Al2O3) was shown to be anisotropic with respect to damage accumulation. Ultra-low load indentation and Rutherford Backscattering Spectroscopy (RBS) were used to demonstrate the dependence of radiation damage on fluence and crystal orientation. Single crystal Al2O3 specimens of c-axis (/0001/ normal to the surface) and a-axis (/1120/ normal to the surface) orientations were ion-implanted simultaneously and found to possess different near-surface mechanical properties. Subsequent RBS-ion channeling examination indicated different amounts of disorder in both the aluminum and oxygen sublattices for the two orientations. These results imply a higher amorphization threshold in terms of implantation fluence for the a-axis oriented samples. DOE

N90-26675# Argonne National Lab., IL. Chemistry Div.
STUDIES ON ION SCATTERING AND SPUTTERING PROCESSES RELEVANT TO ION BEAM SPUTTER DEPOSITION OF MULTICOMPONENT THIN FILMS
O. Auciello, M. S. Ameen, A. R. Krauss, A. I. Kingon (North Carolina State Univ., Raleigh.), and M. A. Ray 1989 5 p Presented at the Materials Research Society Fall Meeting, Boston, MA, 27 Nov. - 2 Dec. 1989 Submitted for publication
(Contracts W-31-109-eng-38; DE-FG05-88ER-45359; N00014-88-K-0525; N00014-88-K-0526; NSF DMR-88-07367)
(DE90-010071; CONF-891119-123) Avail: NTIS HC A01/MF A01

Results from computer simulation and experiments on ion scattering and sputtering processes in ion beam sputter deposition of high Tc superconducting and ferroelectric thin films are presented. It is demonstrated that scattering of neutralized ions from the targets can result in undesirable erosion of, and inert gas incorporation in, the growing films, depending on the ion/target atom mass ratio and ion beam angle of incidence/target/substrate geometry. The studies indicate that sputtering Kr(+) or Xe(+) ions is preferable to the most commonly used Ar(+) ions, since the undesirable phenomena mentioned above are minimized for the first two ions. These results are used to determine optimum sputter deposition geometry and ion beam parameters for growing multicomponent oxide thin films by ion beam sputter-deposition. DOE

N90-26676# Argonne National Lab., IL. Materials Science Div.
CRITICAL CURRENT DENSITY, FLUX CREEP, AND MICROSTRUCTURE IN A Bi-Sr-Ca-Cu-O SYSTEM
Donglu Shi, M. S. Boley, J. G. Chen, Ming Xu, M. M. Fang, U. Welp, K. Vandervoort, and J. M. Hong 1989 4 p Presented at the Materials Research Society Fall Meeting, Boston, MA, 27 Nov. - 2 Dec. 1989
(Contract W-31-109-eng-38)
(DE90-010457; CONF-891119-125) Avail: NTIS HC A01/MF A01

Magnetization hysteresis and zero-field-cooled magnetic relaxation was measured for liquid quenched Bi-Sr-Ca-Cu-O samples at various temperatures. It was found that there is a close correlation between the magnetic behavior and the microstructures of the samples. The magnetization hysteresis greatly increases in the samples with a large amount of crystal defects such as precipitates and stacking faults in the matrix of the material. It was also found that the flux creep is enhanced as a result of these microstructural changes. DOE

N90-26677# Technische Univ., Delft (Netherlands). Vakgroep Optica.
VACUUM DEPOSITION BY PULSED LASER RADIATION: PLASMA COMPOSITION, DEPOSITION TECHNIQUES, AND THIN FILM PROPERTIES Ph.D. Thesis
Shi Liang 1989 120 p Sponsored by Ministerie van Economische Zaken, s'Gravenhage, Netherlands
(ETN-90-97263) Avail: NTIS HC A06/MF A01

Thin films for optical purposes are investigated. Pulsed laser induced evaporation and sputtering for thin film deposition techniques are applied. The evaporation behavior of SiO2, Al2O3 and TiO2 films and their mechanical and optical properties are described. The effects produced by the absorption of pulsed laser radiation on a solid target surface are discussed. The instrumentation for the study of the kinetic energy distribution and mass composition of positive ions produced by pulsed laser evaporation of solid materials is presented. The results obtained by the pulsed laser induced sputtering deposition are discussed. ESA

N90-26678# Deutsche Forschungsanstalt fuer Luft- und Raumfahrt, Cologne (Germany, F.R.). Inst. fuer Raumsimulation.
UNDERCOOLING AND SOLIDIFICATION
Dieter M. Herlach and Rainer Willnecker Nov. 1989 39 p Submitted for publication
(DLR-FB-90-020; ISSN-0171-1342; ETN-90-97013) Avail: NTIS HC A03/MF A01

Experimental techniques used to achieve deep undercooling at slow cooling rates are reviewed. The basic ideas behind nucleation theory are presented. Theoretical concepts are discussed with special attention given to homogeneous versus heterogeneous nucleation. Experimental work on rapid solidification in undercooled liquids is reviewed. The theoretical progress in this field is presented with emphasis on the steady state aspects of dendritic growth. The consequences of unconstrained solidification are evaluated with respect to the formation of metastable microstructures. The central position of undercooling experiments among various rapid solidification techniques is emphasized. ESA

N90-26679# Institut Franco-Allemand de Recherches, Saint-Louis (France).
THE STUDY OF VF2/VF3 PIEZOELECTRIC COPOLYMETERES SUBMITTED TO SHOCKS [ETUDE DU COMPORTEMENT SOUS CHOC DE COPOLYMERES VF2/VF3 PIEZOELECTRIQUES]
F. Bauer and R. A. Graham 12 Apr. 1989 16 p In FRENCH Presented at 3rd Symposium on Hautes Pressions Dynamiques, La Grande Motte, France, 5-9 Jun. 1989
(ISL-CO-210/9; ETN-90-97022) Avail: NTIS HC A03/MF A01

The electric response of VF2/VF3 receptors 55 microns thick submitted to a polarization in the region of 8 microC per sq cm is studied. The receptors are submitted to calibrated shock waves varying between 0.2 and 30 Gpa. Liberated electric charge profiles by copolymer gages over time are presented. The piezoelectric response is shown to be a direction function of pressure up to 30 Gpa. The sensitivity of piezoelectric copolymers seems superior to that of standard polyvinylidine-fluoride receptors. New uses for ferroelectric polymers are predicted. ESA

N90-26680# Grenoble-1 Univ. (France). Techniques de l'Informatique, des Mathematiques, de la Microelectronique et de la Microscopie Quanti
MATHEMATICAL SIMULATION OF HEAT EXCHANGES AND THERMOELASTIC CONSTRAINTS IN CZOCHRALSKI CRYSTAL GROWTH Ph.D. Thesis [SIMULATION NUMERIQUE DES ECHANGES THERMIQUES ET DES CONTRAINTES THERMOELASTIQUES DANS UN TIRAGE CZOCHRALSKI]

Christian Perret 25 Oct. 1989 163 p In FRENCH
(ETN-90-97242) Avail: NTIS HC A08/MF A01

The Czochralski method of monocrystal formation by drawing out a section of a melt is described. Mathematical simulation of the heat exchanges occurring during such a Czochralski procedure is presented. The thermoelastic constraints within the crystal are discussed. The data from this thermal and numeric study is analyzed by means of CRISTAL software based on finite element methods so as to make it accessible to physicists and other users. The equations and algorithms used in the analysis are presented in detail. ESA

N90-26681# Laboratoire d'Automatique et d'Analyse des Systemes, Toulouse (France). Groupe Composants et Circuits a Effet de Champ.

RAPID THERMAL PROCESSING: A STUDY OF THE SILICON OXIDATION AND OF THE IMPLANTED BORON ACTIVATION Ph.D. Thesis

Francois Marou 1990 137 p In FRENCH; ENGLISH summary
(LAAS-90051; ETN-90-97259) Avail: NTIS HC A07/MF A01

The potentialities shown by the rapid thermal processing in the domain of implanted boron diffusion in silicon and the growth of thin oxide layers are examined. The characteristics of a rapid thermal furnace are shown to agree with the specification chart of clean-rooms of the future: they should be automatic, robotic, and ensure an ultra-clean environment to the wafers. The problems concerning the temperature measurement and the homogeneity control are shown. Solutions based on the use of susceptors or on wafer-loading with thermal screening are proposed. Two applications are presented: the annealing of implanted boron and the rapid oxidation of silicon. The first one confirms the attendance of an enhanced diffusion phenomenon in the initial phase of the annealing, due to the defects of implantation. The second one shows the analysis of the first atomic layers of oxide versus the oxidation kinetics. The influence of the pre-oxidation cleaning and of the post-oxidation annealing on the quality of the obtained oxide is established. The study of the boron diffusion under rapid oxidation confirms that it is enhanced for it is correlated to the growth rate of SiO2. ESA

N90-26682*# National Aeronautics and Space Administration. Lewis Research Center, Cleveland, OH.

ELLIPSOMETRIC STUDY OF YBa2Cu3O(7-x) LASER ABLATED AND CO-EVAPORATED FILMS

S. A. Alterovitz, R. E. Sieg, J. D. Warner, M. A. Stan (Kent State Univ., OH.), and S. Vitta 1990 8 p Presented at the International Conference on Electronic Materials 1990, Newark, NJ, 17-19 Sep. 1990; sponsored by Materials Research Society
(NASA-TM-103223; E-5637; NAS 1.15:103223) Avail: NTIS HC A02/MF A01 CSCL 20L

High temperature superconducting films of YBa2Cu3O(7-x) (YBCO were grown on SrTiO3, LaA1O3, and YSZ substrates using two techniques: excimer laser ablation with in situ annealing and co-evaporation of Y, Cu, and BaF2 with ex-situ annealing. Film thicknesses were typically 5000 A, with predominant c-axis alignment perpendicular to the substrate. Critical temperatures up to Tc(R=O)=90 K were achieved by both techniques. Ellipsometric measurements were taken in the range 1.6 to 4.3 eV using a variable angle spectroscopic ellipsometer. The complex dielectric function of the laser ablated films was reproducible from run to run, and was found to be within 10 percent of that previously reported for (001) oriented single crystals. A dielectric overlayer was observed in these films, with an index of refraction of approximately 1.55 and nearly zero absorption. For the laser ablated films the optical properties were essentially independent of substrate material. The magnitude of the dielectric function obtained for the co-evaported films was much lower than the value reported for single crystals, and was sample dependent. Author

N90-26683*# National Aeronautics and Space Administration. Lewis Research Center, Cleveland, OH.

DIELECTRIC FUNCTION OF InGaAs IN THE VISIBLE

S. A. Alterovitz, R. E. Sieg, H. D. Yao, P. G. Snyder, J. A. Woollam, J. Pamulapati, P. K. Bhattacharya, and P. A. Sekula-Moise (Spire Corp., Bedford, MA.) 1990 8 p Presented at the 2nd International Conference on Electronic Materials, Newark, NJ, 17-19 Sep. 1990; sponsored by Materials Research Society
(Grants NAG3-988; NAS3-25867)
(NASA-TM-103246; E-5672; NAS 1.15:103246) Avail: NTIS HC A02/MF A01 CSCL 20L

Measurements are reported of the dielectric function of thermodynamically stable In(x)Ga(1-x)As in the composition range 0.3 equal to or less than X = to or less than 0.7. The optically thick samples of InGaAs were made by molecular beam epitaxy (MBE) in the range 0.4 = to or less than X = to or less than 0.7 and by metal-organic chemical vapor deposition (MOCVD) for X = 0.3. The MBE made samples, usually 1 micron thick, were grown on semi-insulating InP and included a strain release structure. The MOCVD sample was grown on GaAs and was 2 microns thick. The dielectric functions were measured by variable angle spectroscopic ellipsometry in the range 1.55 to 4.4 eV. The data was analyzed assuming an optically thick InGaAs material with an oxide layer on top. The thickness of this layer was estimated by comparing the results for the InP lattice matched material, i.e., X = 0.53, with results published in the literature. The top oxide layer mathematically for X = 0.3 and X = 0.53 was removed to get the dielectric function of the bare InGaAs. In addition, the dielectric function of GaAs in vacuum, after a protective arsenic layer was removed. The dielectric functions for X = 0, 0.3, and 0.53 together with the X = 1 result from the literature to evaluate an algorithm for calculating the dielectric function of InGaAs for an arbitrary value of X(0 = to or less than X = to or less than 1) were used. Results of the dielectric function calculated using the algorithm were compared with experimental data. Author

N90-26684*# National Aeronautics and Space Administration. Pasadena Office, CA.

PASSIVATION OF HIGH TEMPERATURE SUPERCONDUCTORS Patent Application

Richard P. Vasquez, inventor (to NASA) (Jet Propulsion Lab., California Inst. of Tech., Pasadena.) 28 Jun. 1990 25 p
(Contract NAS7-918)
(NASA-Case-NPO-17949-1-CU; NAS 1.71:NPO-17949-1-CU; US-Patent-Appl-SN-545016) Avail: NTIS HC A03/MF A01 CSCL 20L

The surfaces of high temperature superconductors such as YBa(2)Cu(3)O(7-x) are passivated by reacting the native Y, Ba and Cu metal ions with an anion such as sulfate or oxalate to form a surface film that is impervious to water and has a solubility in water of no more than 10(exp -3) M. The passivating treatment is preferably conducted by immersing the surface in dilute aqueous acid solution since more soluble species dissolve into the solution. The treatment does not degrade the superconducting properties of the bulk material. NASA

N90-26685*# National Aeronautics and Space Administration. Pasadena Office, CA.

MBE GROWTH TECHNOLOGY FOR HIGH QUALITY STRAINED III-V LAYERS Patent Application

Frank J. Grunthaner, inventor (to NASA), John K. Liu, inventor (to NASA), and Bruce R. Hancock, inventor (to NASA) (Jet Propulsion Lab., California Inst. of Tech., Pasadena.) 30 Mar. 1990 12 p
(Contract NAS7-918)
(NASA-Case-NPO-17723-1-CU; NAS 1.71:NPO-17723-1-CU; US-Patent-Appl-SN-506137) Avail: NTIS HC A03/MF A01 CSCL 20L

The III-V films are grown on large automatically perfect terraces of III-V substrates which have a different lattice constant, with temperature and Group III and V arrival rates chosen to give a Group III element stable surface. The growth is pulsed to inhibit Group III metal accumulation of low temperature, and to permit the film to relax to equilibrium. The method of the invention: (1) minimizes starting step density on sample surface; (2) deposits InAs and GaAs using an interrupted growth mode (0.25 to 2 monolayers at a time); (3) maintains the instantaneous surface

stoichiometry during growth (As-stable for GaAs, In-stable for InAs); and (4) uses time-resolved RHEED to achieve aspects (1) through (3). NASA

N90-26686# Polytechnic Inst. of New York, Brooklyn. Dept. of Physics.
FULL VECTOR WAVE CALCULATION OF PHOTONIC BAND STRUCTURES IN FACE-CENTERED CUBIC DIELECTRIC MEDIA
K. M. Leung and Y. F. Liu 1990 14 p
(Contract N00014-89-J-0050)
(AD-A222616) Avail: NTIS HC A03/MF A01 CSCL 20/12

The photonic band structure of a face-centered cubic lattice of spheres in a uniform host medium is calculated. The plane wave method is used to solve the exact Maxwell's equations without the use of the scalar approximation. Detailed comparisons with the available experimental results are made. GRA

N90-26687# North Carolina Univ., Chapel Hill. Dept. of Chemistry.
STRUCTURE AND DYNAMICS OF WATER AT THE PT (111) INTERFACE: MOLECULAR DYNAMICS STUDY
K. Raghavan, K. Foster, K. Motakabbir, and M. Berkowitz 18 May 1990 38 p Submitted for publication
(Contract N00014-89-J-1169)
(AD-A222628; TR-3) Avail: NTIS HC A03/MF A01 CSCL 20/2

An analytical form of the interaction potential between rigid water-rigid metal surface, which takes into account the surface symmetry and its corrugation is developed. Using this potential the structure and dynamics of water at Pt (111) interface is investigated. At 300 K the adjacent to the metal surface water layer displays solid-like properties. The next two layers of water display ordering similar to ice-I. Beyond these three layers the structure and dynamics of water is bulk like. GRA

N90-26688# Massachusetts Inst. of Tech., Cambridge. Dept. of Chemistry.
STIBATHIOLANES: SYNTHESIS, SOLID STATE STRUCTURE, AND SOLUTION BEHAVIOR Technical Report No. 4
Richard A. Fisher, Ralph B. Nielsen, William M. Davis, and Stephen L. Buchwald 6 Jun. 1990 29 p Submitted for publication
Sponsored in part by the American Chemical Society
(Contracts N00014-88-K-0307; DE-FG05-86ER-75292)
(AD-A223255; TR-4) Avail: NTIS HC A03/MF A01 CSCL 09/1

Interest in organometallic compounds of the main group metals has recently grown tremendously, due in part to the wide variety of applications of these compounds in the materials sciences. Despite this new activity, the synthetic strategies for main group organometallics have remained relatively undeveloped. The majority of syntheses of these compounds involve classical metathesis reactions between a main group halide and an organometallic compound such as an organolithium or Grignard reagent and are limited by a lack of selectivity and by the availability of suitable organometallic precursors. The latter limitation is severe for main group metallacycles because of the paucity of suitable 1, n(n=3,4,5)-dianionic reagents or their equivalents, which are most often used for the synthesis of this class of molecules. GRA

77 THERMODYNAMICS AND STATISTICAL PHYSICS

Includes quantum mechanics; theoretical physics; and Bose and Fermi statistics.

For related information see also *25 Inorganic and Physical Chemistry* and *34 Fluid Mechanics and Heat Transfer.*

N90-26689*# Illinois Univ., Urbana-Champaign. Dept. of Computer Science.
QUALITATIVE AND QUANTITATIVE REASONING ABOUT THERMODYNAMICS
Gordon Skorstad and Ken Forbus 6 Nov. 1989 13 p Presented at the Tenth Annual Conference of the Cognitive Science Society, Aug. 1989
(Grant NAG9-137)
(NASA-CR-186788; NAS 1.26:186788; UIUCDCS-R-89-1554; UILU-ENG-89-1773) Avail: NTIS HC A03/MF A01 CSCL 20M

One goal of qualitative physics is to capture the tacit knowledge of engineers and scientists. It is shown how Qualitative Process theory can be used to express concepts of engineering thermodynamics. In particular, it is shown how to integrate qualitative and quantitative knowledge to solve textbook problems involving thermodynamic cycles, such as gas turbine plants and steam power plants. These ideas were implemented in a program called SCHISM. Its analysis of a sample textbook problem is described and plans for future work are discussed. Author

N90-26690# Los Alamos National Lab., NM.
A LATTICE GAS MODEL FOR THERMOHYDRODYNAMICS
Shiyi Chen, Hudong Chen, Gary D. Doolen, Semion Gutman, and Minxu Lee 3 May 1990 32 p Presented at the Dynamics of Concentrated Systems Conference, Los Alamos, NM, 13-15 Jun. 1989 Submitted for publication
(Contract W-7405-eng-36)
(DE90-011964; LA-UR-90-1589; CONF-8906332-1) Avail: NTIS HC A03/MF A01

The FHP lattice gas model is extended to include a temperature variable in order to study thermohydrodynamics. The compressible Navier-Stokes equations are derived using a Chapman-Enskog expansion. Heat conduction and convention problems are investigated, including Benard convention. It is shown that the usual FHP rescaling procedure can be avoided by controlling the temperature. DOE

N90-26691# Loughborough Univ. of Technology (England). Dept. of Mathematical Sciences.
A NEW CLASS OF EXACT SOLUTIONS OF THE VACUUM QUADRATIC POINCARE GAUGE FIELD THEORY
P. Singh and J. B. Griffiths Sep. 1989 10 p Sponsored by Science Research Council, England
(MATHS-Rept-A-119; ETN-90-97129) Avail: NTIS HC A02/MF A01

A class of algebraically special exact solutions of the vacuum quadratic Poincare gauge field theory is presented. The solutions are of type 3 and type N. They have a nonexpanding, shear-free and twist-free geodesic repeated principal null congruence. The metric is of Kundt's class. The torsion components are solutions of certain differential equations. The solutions obtained using a generalized spin coefficient formalism are shown. ESA

N90-26692# Loughborough Univ. of Technology (England). Dept. of Mathematical Sciences.
ON TRIVECTOR TORSION IN VACUUM QUADRATIC POINCARE GAUGE FIELD THEORY
P. Singh Nov. 1989 6 p Sponsored by Science Research Council, England
(MATHS-Rept-A-121; ETN-90-97130) Avail: NTIS HC A02/MF A01

The vacuum field equations of the Quadratic Poincare Gauge Field Theory (QPGFT) are solved for the case when the torsion is trivector. The contorsion tensor for this case is given. It is shown that there are no solutions of vacuum QPGFT, when S to the power of mu is non-null. When S to the power of mu is null, it is proved that any solution of vacuum QPGFT, whose V(sub 4) part is also a solution of Einstein's vacuum field equations with a cosmological constant, is necessarily of algebraic type N. This solution has an expansion-free, shear-free and twist-free geodesic repeated principal null congruence. ESA

80 SOCIAL SCIENCES (GENERAL)

Includes educational matters.

N90-26693*# National Aeronautics and Space Administration. Lewis Research Center, Cleveland, OH.
LAUNCHING A DREAM: A TEACHERS GUIDE TO A SIMULATED SPACE SHUTTLE MISSION
1989 105 p
(NASA-TM-89715; NAS 1.15:89715) Avail: NTIS HC A06/MF A01 CSCL 05I

Two simulated shuttle missions cosponsored by the NASA Lewis Research Center and Cleveland, Ohio, area schools are highlighted in this manual for teachers. A simulated space shuttle mission is an opportunity for students of all ages to plan, train for, and conduct a shuttle mission. Some students are selected to be astronauts, flight planners, and flight controllers. Other students build and test the experiments that the astronauts will conduct. Some set up mission control, while others design the mission patch. Students also serve as security officers or carry out public relations activities. For the simulated shuttle mission, school buses or recreation vehicles are converted to represent shuttle orbiters. All aspects of a shuttle mission are included. During preflight activities the shuttle is prepared, and experiments and a flight plan are made ready for launch day. The flight itself includes lifting off, conducting experiments on orbit, and rendezvousing with the crew from the sister school. After landing back at the home school, the student astronauts are debriefed and hold press conferences. The astronauts celebrate their successful missions with their fellow students at school and with the community at an evening postflight recognition program. To date, approximately 6,000 students have been involved in simulated shuttle missions with the Lewis Research Center. A list of participating schools, along with the names of their space shuttles, is included. Educations outcomes and other positive effects for the students are described. J.P.S.

N90-26694# Wichita State Univ., KS. National Inst. for Aviation Research.
A MEASUREMENT OF THE EFFECTIVENESS OF THE AIRWAY SCIENCE PROGRAM TO MEET FEDERAL AVIATION ADMINISTRATION WORK FORCE NEEDS
Brent D. Bowen May 1990 28 p
(NIAR-90-5) Avail: NTIS HC A03/MF A01

A potential means is proposed to enhance air traffic control safety through increased human performance capabilities of the nation's Air Traffic Controller Work Force. The FAA initiated the Airway Science Program to facilitate the development of collegiate education programs as a means of meeting future FAA manpower needs, primarily in the area of air traffic control. The FAA realized that it must update the skill level of its work force to adapt to an increasingly technical and automated environment. Research data gathered through this study should allow the FAA to better understand the potential of the Airway Science Program to enhance air traffic safety. This program allows the availability of a means of pre-hire training through a baccalaureate degree program which stresses technical and managerial capabilities. This will provide an air traffic control work force with the increased human performance capabilities which are required to staff the increasingly difficult systems of the rapidly developing National Airspace System. Author

81 ADMINISTRATION AND MANAGEMENT

Includes management planning and research.

N90-26695# Rolls-Royce Ltd., Derby (England).
MAKING IT HAPPEN: PROJECT MANAGEMENT
Geoff Collis 21 Jun. 1989 9 p Presented at the Lucas Seminar, Shirley, England, 21 Jun. 1989
(PNR90618; ETN-90-97134) Copyright Avail: NTIS HC A02/MF A01

Objectives and organization of program management specific to the Rolls-Royce company are outlined. The concept as a master program is described. Central program management interfaces, culture and style are depicted. The program culture is based on the functions managing and achieving their commitments on time. A small central team works with the customer and across all internal functions on a by exception basis to ensure that master program and engine delivery contracts are achieved on time. ESA

N90-26696# Rolls-Royce Ltd., Derby (England). Systems and Computing Research.
THE VALUE OF REAL EXPERIENCE
Stewart B. L. Wilson 10 Oct. 1989 19 p Presented at the Computers in Manufacturing Conference 1989, 10 Oct. 1989
(PNR90619; ETN-90-97136) Copyright Avail: NTIS HC A03/MF A01

An interpretation of Computer Integrated Management (CIM) is presented. Techniques of computer engineering and control systems engineering, embodying principles of topdown understanding and planning of the business processes and their shared data needs, and bottom up implementation of simplified procedures within the integration plan, were adopted. The need to understand the real overall business needs of the enterprise, and the understanding and integration of shared data as the vital technical element are proposed approaches to CIM. ESA

N90-26697# Massachusetts Inst. of Tech., Cambridge. Lab. for Information and Decision Systems.
EFFECT OF ORGANIZATIONAL STRUCTURE ON PERFORMANCE OF DECISION MAKING TEAMS Ph.D. Thesis
Victoria Y. Jin May 1990 218 p
(Contracts N00014-85-K-0782; N00014-84-K-0519)
(AD-A223160; LIDS-TH-1976) Avail: NTIS HC A10/MF A02 CSCL 05/1

Distributed decision making (DDM) organizations consist of human decision makers (DMs) and equipment, structured so as to accomplish a set of given tasks. A multi-person, model-driven experiment has been designed to investigate the effect of organization structure on performance. The experiment has been designed on the basis of an existing mathematical model of interacting DMs and organizational structures. In the experiment, a distributed decision making environment was created. Two organizational structures were used in the investigation: a parallel organization and a hierarchical organization. The experimental results show that the variation in performance is less between different teams than between individual DMs within a team. Therefore, organizational performance is more predictable than individual performance. Interaction among DMs in an organization compensates for differences in individual performance characteristics. The main controlled variable in the experiment was the available time to perform a task. Decrease in available time introduced time pressure. The experimental results confirm a hypothesis which predicts that with decreasing available time, a significant degradation of performance occurs first in the organization which has the highest minimum required workload. These results are consistent with the findings from the theoretical model. GRA

82 DOCUMENTATION AND INFORMATION SCIENCE

Includes information management; information storage and retrieval technology; technical writing; graphic arts; and micrography.

For computer documentation see *61 Computer Programming and Software.*

N90-26698*# Massachusetts Inst. of Tech., Cambridge. Lab. for Computer Science.

ANALYSIS OF RANDOM DROP FOR GATEWAY CONGESTION CONTROL M.S. Thesis

Emam Salaheddin Hashem Nov. 1989 109 p Original contains color illustrations

(Grant NAG2-582)

(NASA-CR-186736; NAS 1.26:186736; MIT/LCS/TR-465) Avail: NTIS HC A06/MF A01; 23 functional color pages CSCL 05B

Lately, the growing demand on the Internet has prompted the need for more effective congestion control policies. Currently No Gateway Policy is used to relieve and signal congestion, which leads to unfair service to the individual users and a degradation of overall network performance. Network simulation was used to illustrate the character of Internet congestion and its causes. A newly proposed gateway congestion control policy, called Random Drop, was considered as a promising solution to the pressing problem. Random Drop relieves resource congestion upon buffer overflow by choosing a random packet from the service queue to be dropped. The random choice should result in a drop distribution proportional to the bandwidth distribution among all contending TCP connections, thus applying the necessary fairness. Nonetheless, the simulation experiments demonstrate several shortcomings with this policy. Because Random Drop is a congestion control policy, which is not applied until congestion has already occurred, it usually results in a high drop rate that hurts too many connections including well-behaved ones. Even though the number of packets dropped is different from one connection to another depending on the buffer utilization upon overflow, the TCP recovery overhead is high enough to neutralize these differences, causing unfair congestion penalties. Besides, the drop distribution itself is an inaccurate representation of the average bandwidth distribution, missing much important information about the bandwidth utilization between buffer overflow events. A modification of Random Drop to do congestion avoidance by applying the policy early was also proposed. Early Random Drop has the advantage of avoiding the high drop rate of buffer overflow. The early application of the policy removes the pressure of congestion relief and allows more accurate signaling of congestion. To be used effectively, algorithms for the dynamic adjustment of the parameters of Early Random Drop to suite the current network load must still be developed. Author

N90-26699# Oak Ridge National Lab., TN.

INTERNATIONAL STANDARDS FOR TEXT PREPARATION AND INTERCHANGE

James David Mason 1 Jun. 1990 35 p

(Contract DE-AC05-84OR-21400)

(DE90-011868; ORNL/FTR-3618) Avail: NTIS HC A03/MF A01

As DOE seeks to move towards electronic production, management, and dissemination of scientific and technical information, it has for several years been involved in the development of international standards for text preparation and interchange. In support of this effort, the traveler serves as Convenor of ISO/IEC JTC1/SC18/WG8; during this trip he convened the spring meeting of WG8 in Bath. After the WG8 meeting, the traveler represented WG8 at the annual meeting of its parent committee, ISO/IEC JTCI/SC18 at the Association Francaise de Normalisation in Paris. Because ISO TC46 (Documentation) was meeting at the same time as SC18 and the traveler is SC18's liaison to TC46, he was able to attend several sessions of that committee as well. DOE

N90-26700* National Aeronautics and Space Administration, Washington, DC.

NASA PATENT ABSTRACTS BIBLIOGRAPHY: A CONTINUING BIBLIOGRAPHY. SECTION 2: INDEXES (SUPPLEMENT 37)

Jan. 1989 507 p

(NASA-SP-7039(37)-Sect-2; NAS 1.21:7039(37)-Sect-2) Avail: NTIS HC A22; NTIS standing order as PB90-911100, $32.00 domestic, $64.00 foreign CSCL 05B

A subject index is provided for over 4600 patents and patent applications for the period May 1969 through June 1990. Additional indexes list personal authors, corporate authors, contract numbers, NASA case numbers, U.S. patent class numbers, U.S. patent numbers, and NASA accession numbers. Author

N90-26701*# Jet Propulsion Lab., California Inst. of Tech., Pasadena.

THE BROWSE FILE OF NASA/JPL QUICK-LOOK RADAR IMAGES FROM THE LOCH LINNHE 1989 EXPERIMENT

Walter E. Brown, Jr., ed. 15 Nov. 1989 143 p

(Contract NAS7-918)

(NASA-CR-186855; NAS 1.26:186855; JPL-Publ-89-44) Avail: NTIS HC A07/MF A01 CSCL 05B

The Jet Propulsion Laboratory (JPL) Aircraft Synthetic Aperture Radar (AIRSAR) was deployed to Scotland to obtain radar imagery of ship wakes generated in Loch Linnhe. These observations were part of a joint US and UK experiment to study the internal waves generated by ships under partially controlled conditions. The AIRSAR was mounted on the NASA-Ames DC-8 aircraft. The data acquisition sequence consisted of 8 flights, each about 6 hours in duration, wherein 24 observations of the instrumented site were made on each flight. This Browse File provides the experimenters with a reference of the real time imagery (approximately 100 images) obtained on the 38-deg track. These radar images are copies of those obtained at the time of observation and show the general geometry of the ship wake features. To speed up processing during this flight, the images were all processed around zero Doppler, and thus azimuth ambiguities often occur when the drift angel (yaw) exceeded a few degrees. However, even with the various shortcomings, it is believed that the experimenter will find the Browse File useful in establishing a basis for further investigations. Author

N90-26702# Argonne National Lab., IL.

A METHODOLOGY FOR BENCHMARKING DISTRIBUTED DATABASE MANAGEMENT SYSTEMS

Cyril U. Orji 1990 24 p Presented at the 16th International Conference on Very Large Databases, Brisbane, Australia, 13-16 Aug. 1990 Sponsored in part by Veterans Benefits Administration

(Contract W-31-109-eng-38)

(DE90-007801; CONF-900875-1) Avail: NTIS HC A03/MF A01

A methodology for benchmarking distributed database management systems is proposed. A distributed environment is characterized in terms of the communication costs incurred in data movement between sites, the number of nodes that participate in processing a query and the data distribution scheme used in the network. These are used as a basis for identifying eight query types that capture the query performance characteristics in the network. Finally, an experimental outline is sketched to illustrate the steps in validating the methodology. DOE

N90-26703# Cornell Univ., Ithaca, NY. Dept. of Computer Science.

KNOWLEDGE AND INHIBITION IN ASYNCHRONOUS DISTRIBUTED SYSTEMS Ph.D. Thesis

Kimberly Elaine Taylor Jul. 1990 85 p

(TR-90-1139) Copyright Avail: NTIS HC A05/MF A01 CSCL 05B

In an asynchronous distributed system, processes communicate only via message passing along channels with unbounded transmission time. Relative process speeds are arbitrary and processes do not have access to a common clock. For such systems, a useful means of providing temporal structure is the

causality relation. Causality imposes a partial order on the events of an execution based on the necessity of certain events preceding other events. Causality can be used to give a sensible definition of a distributed global state in an asynchronous system, known as a consistent cut. A new knowledge-theoretic logic is described, with formal semantic definitions, for reasoning about causality and consistent cuts. The logic includes concurrent common knowledge, a new form of distributed agreement, which has an analogous role to that of common knowledge in synchronous systems. It is shown to be a necessary and sufficient condition for performing concurrent actions in asynchronous systems, and has a role in many distributed applications such as check- pointing, deadlock detection, and broadcasting. Concurrent common knowledge is also shown to be attainable by class of protocols termed distinguishable-consistent-cut protocols, or DCCPs. Four simple and efficient DCCPs and trade-offs between them are examined. These trade-offs involve message complexities, necessity of FIFO channels, and the degrees to which events of the underlying system are suspended during execution of the protocols. Such suspensions are called inhibition and multiple forms of inhibition that are used in distributed protocols are defined. The DCCPs are classified according to their inhibitory characteristics, and new results which demonstrate close relationships between inhibition and the existence of DCCPs are proven. Author

N90-26704# General Accounting Office, Washington, DC. Information Management and Technology Div.
SPACE OPERATIONS: NASA IS NOT PROPERLY SAFEGUARDING VALUABLE DATA FROM PAST MISSIONS
Stephen A. Schwartz, Ronald W. Beers, Mirko J. Dolak, David T. Schwartz, and Darlene D. Rush Mar. 1990 78 p
(GAO/IMTEC-90-1; B-237585) Avail: NTIS HC A05/MF A01; also available from GAO, Gaithersburg, MD HC first five copies free, additional copies $2.00

NASA is responsible for space exploration and the management, archiving, and dissemination of space science data. Since 1958, the agency has spent about $24 billion on its space science program and successfully launched over 260 scientific missions. Data from these mission have expanded our understanding of the earth, its solar system, and the universe. Through these past missions NASA has acquired a massive volume of data stored on an estimated 1 million reels of magnetic tape for immediate and long-term scientific use. The nation's long-term ability to monitor changes in the earth's environment, such as the depletion of ozone and the destruction of tropical rain forests, may depend on data from early missions. Future missions are expected to produce additional volumes of data unparalleled in NASA's history, and will likely require the use of advanced data storage technologies. Many of the data from NASA missions are irreplaceable. Government agencies are required to follow specific regulations in the management, maintenance and storage of magnetic tapes to ensure the long-term preservation of data, the prompt disposal of unneeded tapes, and the efficient management of storage resources. The National Archives and Records Administration (NARA) and the General Services Administration (GSA) are responsible for periodic reviews of NASA's data management and archival activities. The General Accounting Office (GAO) has identified a number of problem areas, some of which are being addressed by NASA. However, without the allocation of adequate resources to improve the tape storage and archival facilities, the continuing deterioration of the magnetic tapes may result in the permanent loss of irreplaceable space science data. NASA also needs to continue to improve its space science data management, to effectively and efficiently handle the massive volumes of data expected from its future missions. J.P.S.

N90-26705*# Jet Propulsion Lab., California Inst. of Tech., Pasadena.
CREATING A VAPEPS DATABASE: A VAPEPS TUTORIAL
Final Report
George Graves 15 Jan. 1989 110 p Sponsored in part by AF
(Contract NAS7-918)
(NASA-CR-186629; JPL-Publ-89-15; NAS 1.26:186629) Avail: NTIS HC A06/MF A01 CSCL 05B

A procedural method is outlined for creating a Vibroacoustic Payload Environment Prediction System (VAPEPS) Database. The method of presentation employs flowcharts of sequential VAPEPS Commands used to create a VAPEPS Database. The commands are accompanied by explanatory text to the right of the command in order to minimize the need for repetitive reference to the VAPEPS user's manual. The method is demonstrated by examples of varying complexity. It is assumed that the reader has acquired a basic knowledge of the VAPEPS software program. Author

N90-26706# Department of Energy, Oak Ridge, TN.
ENERGY DATA BASE: SUBJECT CATEGORIES AND SCOPE
1990 60 p
(DE90-009212; ETDE/PUB-1) Avail: NTIS HC A04/MF A01

The purpose of this publication is twofold: to support organizations or individuals who select informational materials for inclusion in the ETDE (Energy Technology Data Exchange) and for use as an aid in database searching. Subject categories and corresponding codes are established to define the scope of, or degree of interest in, energy information to be selected by those who enter machine-readable bibliographic records into the Energy Data Base. For persons conducting online searching or creating selective dissemination of information (SDI) subsets, this publication facilitates the selection of energy topics. These scope notes and category definitions also apply to online energy databases identified as ENERGY on STN International (Federal Republic of Germany) and as DOE ENERGY offered by Dialog Information Services (USA). DOE

N90-26707# Pacific Northwest Lab., Richland, WA.
VISTA (VERTICAL INTEGRATION OF SCIENCE, TECHNOLOGY, AND APPLICATIONS) USER INTERFACE SOFTWARE STUDY
G. Chin Apr. 1990 23 p
(Contract DE-AC06-76RL-01830)
(DE90-010003; PNL-7247) Avail: NTIS HC A03/MF A01

The Vertical Integration of Science, Technology, and Applications (VISTA) project is an initiative to employ modern information and communications technology for rapid and effective application of basic research results by end users. Developed by the Pacific Northwest Laboratory, VISTA's purpose is to develop and deploy information systems (software or software/hardware products) to broad segments of various markets. Inherent in these products would be mechanisms for accessing PNL-resident information about the problem. A goal of VISTA is to incorporate existing, commercially available user interface technology into the VISTA UIMS. Commercial systems are generally more complete, reliable, and cost-effective than software developed in-house. The objective of this report is to examine the current state of commercial user interface software and discuss the implications of selections thereof. This report begins by describing the functionality of the user interface as it applies to users and application developers. Next, a reference model is presented defining the various operational software layers of a graphical user interface. The main body follows which examines current user interface technology by sampling a number of commercial systems. Both the window system and user interface toolkit markets are surveyed. A summary of the current technology concludes this report. DOE

N90-26708# Central Research Inst. of Electric Power Industry, Chiba (Japan).
CONSTRUCTION OF GEOLOGICAL AND GEOTECHNICAL INFORMATION DATABASE
Haruhiko Kuno and Kenzo Kiho May 1989 35 p In JAPANESE; ENGLISH summary
(DE90-503417; CRIE-U-88072) Avail: NTIS (US Sales Only) HC A03/MF A01

A database named GEOID (Geological and Geotechnical Information Database) was developed to effectively utilize practical results surveyed and researched in the past. This GEOID is

composed of five database groups, that is, database of CRIEPI reports; rock and rockmass properties; Japanese Atlas including coastlines, river flowpath, and drainage area; landslide distribution data concerning areas designated to prevent landslide; and geological map of representative geological area distributing in Japan: and the retrieval system. Features are to be the specialized data for power source development and structural maintenance, etc. and to be able to utilize 26 retrieval keywords. The information retrieval can be done by character inputting and by designating a range on Japanese Atlas and informations for properties are processed statistically. This system was developed by utilizing practical experiences on geological surveys and researches and by studying each item from inputting to utilizing conditions. The management, operation and utilization are limited to CRIEPI and each electric power corporation to offer and utilize these informations and are not opened to other organizations. DOE

N90-26709# Rolls-Royce Ltd., Derby (England).
PROTOTYPING AN IN-HOUSE BUSINESS INTELLIGENCE DATABASE
Richard J. Self 23 Mar. 1990 10 p Presented at the Library Association Industrial Group, Portsmouth, England, 23-25 Mar. 1990
(PNR90665; ETN-90-97151) Copyright Avail: NTIS HC A02/MF A01

Some of the key issues of business intelligence operations and their impact on the definition of a business intelligence system are reviewed. The impact of the current, rapid developments in computing technology on the choices available for developing a system is considered. A short overview of the prototyping approach to system development is given. The current Rolls-Royce approach to developing an in-house prototype system is summarized. ESA

N90-26710*# National Aeronautics and Space Administration. Langley Research Center, Hampton, VA.
GRAMMAR, PUNCTUATION, AND CAPITALIZATION: A HANDBOOK FOR TECHNICAL WRITERS AND EDITORS
Mary K. McCaskill Washington 1990 112 p
(NASA-SP-7084; L-16617; NAS 1.21:7084) Avail: NTIS HC A06/MF A01 CSCL 05B

Writing problems are addressed which are often encountered in technical documents and preferences are indicated (Langley's) when authorities do not agree. It is directed toward professional writers, editors, and proofreaders. Those whose profession lies in other areas (for example, research or management), but who have occasion to write or review others' writing will also find this information useful. A functional attitude toward grammar and punctuation is presented. Chapter 1 on grammar presents grammatical problems related to each part of speech. Chapter 2 on sentence structure concerns syntax, that is, effective arrangement of words, with emphasis on methods of revision to improve writing effectiveness. Chapter 3 addresses punctuation marks, presenting their function, situations when they are required or incorrect, and situations when they are appropriate but optional. Chapter 4 presents capitalization, which is mostly a matter of editorial style and preference rather than a matter of generally accepted rules. An index and glossary are included. Author

83 ECONOMICS AND COST ANALYSIS

Includes cost effectiveness studies.

N90-26231*# Jet Propulsion Lab., California Inst. of Tech., Pasadena. Software Product Assurance Section.
LONG-RANGE PLANNING COST MODEL FOR SUPPORT OF FUTURE SPACE MISSIONS BY THE DEEP SPACE NETWORK
J. S. Sherif, D. S. Remer (Harvey Mudd Coll., Claremont, CA.), and H. R. Buchanan *In its* The Telecommunications and Data Acquisition Report 15 May 1990 p 179-190 (For primary document see N90-26217 20-32)
Avail: NTIS HC A10/MF A02 CSCL 05C

84 LAW, POLITICAL SCIENCE AND SPACE POLICY

Includes NASA appropriation hearings; aviation law; space law and policy; international law; international cooperation; and patent policy.

N90-26711# European Space Agency, Paris (France).
MANNED SPACE STATIONS: LEGAL ISSUES
T. Duc Guyenne, ed. Jan. 1990 216 p In ENGLISH and FRENCH International colloquium held in Paris, France, 7-8 Nov. 1989; sponsored by CNES
(ESA-SP-305; ISBN-92-9092-062-9; ISSN-0379-6566; ETN-90-96979) Copyright Avail: NTIS HC A10/MF A02; also available from EPD, ESTEC, Noordwijk, Netherlands, 40 Dutch guilders

The technical characteristics and functions of different space stations are reviewed. The legal aspects of the U.S./International Space Station are reviewed. Damage responsability in the case of space stations is discussed. The legal aspects of international cooperation on the MIR Space Station are reviewed. The partnership concept and international management are reviewed. Astronaut legal status and rights are discussed. Crossborder movements of personnel, goods, or technologies, are discussed. Intellectual property rights and U.S. patent law as applied to Space Stations is reviewed. The legal protection of inventions or innovations is discussed. For individual titles, see N90-26712 through N90-26727.

N90-26712# European Space Agency, Paris (France).
TECHNICAL CHARACTERISTICS AND FUNCTIONS OF DIFFERENT TYPES OF SPACE STATIONS [LES CARACTERISTIQUES TECHNIQUES ET LES FONCTIONS DES DIVERS TYPES DE STATIONS SPATIALES] **c18**
J.-J. Dordain *In its* Manned Space Station: Legal Aspects Jan. 1990 p 19-2 In FRENCH (For primary document see N90-26711 20-84)
Copyright Avail: NTIS HC A10/MF A02; also available from EPD, ESTEC, Noordwijk, Netherlands, 40 Dutch guilders

Skylab, MIR, and the International Space Station Freedom are described. The Columbus program involved in the Freedom Space Station is given particular attention. Reduced gravity effects, operational characteristics, and access by different categories of users are described. Possible uses of space stations are described. Physiological aspects of reduced gravity are discussed especially as concerns circulation. An operations scenario for the use of a space station is reviewed. The complexities involved in combining a huge number of participants and users are described. ESA

N90-26713# Mississippi Univ., University. Law Center.
THE US/INTERNATIONAL SPACE STATION: LEGAL ASPECTS OF SPACE OBJECTS AND JURISDICTION AND CONTROL
S. Gorove *In* ESA, Manned Space Stations: Legal Aspects Jan. 1990 p 27-33 (For primary document see N90-26711 20-84)
Copyright Avail: NTIS HC A10/MF A02; also available from EPD, ESTEC, Noordwijk, Netherlands, 40 Dutch guilders

The intergovernmental agreement to establish and operate an international joint venture in the development of increasing outer space utilization is discussed. Various legal aspects of the agreement are analyzed. Jurisdiction and control aspects are discussed. Provisions added to the Outer Space Treaty are described. General, as well as, criminal jurisdiction is discussed. Issues of registration, liability, and property rights concerning non-Earth materials launched from a celestial body into outer space are discussed. ESA

N90-26714# Societe Francaise de Droit Aerien et Spatial, Blere.
DAMAGE RESPONSIBILITY AND LIABILITY IN SPACE STATIONS [LA RESPONSABILITE POUR DOMMAGES DANS LE CAS DES STATIONS SPATIALES] **c18**
M. Bourely *In* ESA, Manned Space Stations: Legal Aspects

Jan. 1990 p 35-42 In FRENCH (For primary document see N90-26711 20-84)
Copyright Avail: NTIS HC A10/MF A02; also available from EPD, ESTEC, Noordwijk, Netherlands, 40 Dutch guilders

The legal system developed to handle damage responsibility problems in the framework of the International Space Station program is described. An assessment of the system is made to assess its capability of handling all possible situations that may arise in space station liability. Details of the intergovernmental agreement drawn up on 29 Sep. 1988 are presented. The areas not covered in this agreement are listed and discussed. The agreement is concluded to be satisfactory on the whole, but still incomplete. Urgency in addressing these incomplete points is stressed. ESA

N90-26715# Academy of Sciences (USSR), Moscow. Inst. of Space Law.
MIR: A SOVIET SPACE STATION. SOME LEGAL ASPECTS OF INTERNATIONAL COOPERATION
V. S. Vereshchetin *In* ESA, Manned Space Stations: Legal Aspects Jan. 1990 p 51-54 (For primary document see N90-26711 20-84)
Copyright Avail: NTIS HC A10/MF A02; also available from EPD, ESTEC, Noordwijk, Netherlands, 40 Dutch guilders

The history of the MIR Space Station is reviewed. Various operational aspects and characteristics of the Space Sation are described. The legal regime for foreign or joint experiments in the Space Station are reviewed. Examples of agreements between the USSR and Austria are presented to illustrate the type of intergovernmental cooperation possible. The need for development of a special agreement on manned space flights to supplement provisions within universal international space law is stressed. ESA

N90-26716# Bundesministerium fuer Forschung und Technologie, Bonn (Germany, F.R.).
THE INTERNATIONAL SPACE STATION: THE LEGAL FRAMEWORK
Reinhard Loosch *In* ESA, Manned Space Stations: Legal Aspects Jan. 1990 p 55 -58 (For primary document see N90-26711 20-84)
Copyright Avail: NTIS HC A10/MF A02; also available from EPD, ESTEC, Noordwijk, Netherlands, 40 Dutch guilders

The history of the international Space Station negotiations is summarized. The overall setup of the Space Station agreements is presented. The hierarchy among them and in relation to other international instruments is outlined. Key features in the agreements are given special attention. The issue of peaceful purposes versus national security is given particular attention. The European position in the framework of the agreements is discussed. Letters between the German Ministry for Research and Technology and the U.S. Department of State regarding signing of the final agreements are presented. ESA

N90-26717# European Space Agency, Paris (France). Legal Service.
THE PARTNERSHIP CONCEPT AND INTERNATIONAL MANAGEMENT
K. J. Madders *In its* Manned Space Stations: Legal Aspects Jan. 1990 p 59-61 (For primary document see N90-26711 20-84)
Copyright Avail: NTIS HC A10/MF A02; also available from EPD, ESTEC, Noordwijk, Netherlands, 40 Dutch guilders

Donations of authority and reservations of autonomy in international partnerships is discussed. The practical deployment of concessions in relation to management is shown to reveal that cooperation is not a one way street. The factor of complementarity is identified as critical to the understanding of a genuine partnership. The use of the space agreements drawn up in Sep. 1988 as a reference point in undertaking future large scale cooperative projects is discussed. Its possible application to better environmental management on Earth is suggested. ESA

N90-26718# Paris Univ. (France). Inst. de Droit Compare.
THE INTERNATIONAL SPACE STATION: CONDITIONS OF ACCESS AND USE [LA STATION INTERNATIONALE: CONDITIONS D'ACCES ET D'UTILISATION]
S. Courteix *In its* Manned Space Stations: Legal Aspects Jan. 1990 p 63-77 In FRENCH (For primary document see N90-26711 20-84)
Copyright Avail: NTIS HC A10/MF A02; also available from EPD, ESTEC, Noordwijk, Netherlands, 40 Dutch guilders

Aspects of the Intergovernmental Agreement (IGA) on space are discussed. The effect of specific aspects of the agreements on the agreements drawn up in relation to the International Space Station development are described. The concept of Freedom to develop, explore, and use extra-atmospheric space is examined more closely. The access of various partners to the Space Station is discussed. The space and utilities available to each partner aboard the Space Station is described in detail. The respective positions of each of the partners involved in the Space Station project are described in depth. ESA

N90-26719# International Inst. of Space Law, Eh Baarn (Netherlands).
HUMAN WORK IN SPACE: THE ASTRONAUT'S LEGAL STATUS. INTRODUCTION
I. H. Ph. Diedericks-Verschoor *In* ESA, Manned Space Stations: Legal Aspects Jan. 1990 p 85-86 In FRENCH (For primary document see N90-26711 20-84)
Copyright Avail: NTIS HC A10/MF A02; also available from EPD, ESTEC, Noordwijk, Netherlands, 40 Dutch guilders

The legal status of astronauts is discussed. Differences in the legal status of astronauts working in national versus international space stations are investigated. Movement of goods, personnel, or ideas across borders is discussed from a legal point of view. The issue of whether the laws governing human interaction on Earth are applicable to the conditions within a space station is addressed. Risks to astronauts in a space environment are assessed. ESA

N90-26720# Szczecin Univ., Lodz (Poland). Faculty of Law and Administration.
THE MANNED NATIONAL SPACE STATION: INTERNATIONAL LEGAL CONSIDERATIONS [LA STATION SPATIALE NATIONALE HABITEE: ASPECTS JURIDIQUES INTERNATIONAUX]
A. Gorbiel *In* ESA, Manned Space Stations: Legal Aspects Jan. 1990 p 87-88 In FRENCH (For primary document see N90-26711 20-84)
Copyright Avail: NTIS HC A10/MF A02; also available from EPD, ESTEC, Noordwijk, Netherlands, 40 Dutch guilders

The lack of legislation capable of handling the legal problems which can arise with relation to a manned space station is criticized. Suggestions for a framework to be used in setting up such legislation are presented. The issue of international versus national missions is addressed in a legal context. The definition of what constitutes a manned space station is discussed. The opinions of various authorities in space law are quoted on this subject. The need to better organize the subcommittee of the United Nations concerned with drawing up space law legislation, is stressed. ESA

N90-26721# Bundesministerium fuer Forschung und Technologie, Bonn (Germany, F.R.).
THE ASTRONAUTS' LEGAL STATUS: THE INTERNATIONAL SPACE STATION
J. Reifarth *In* ESA, Manned Space Stations: Legal Aspects Jan. 1990 p 89-92 (For primary document see N90-26711 20-84)
Copyright Avail: NTIS HC A10/MF A02; also available from EPD, ESTEC, Noordwijk, Netherlands, 40 Dutch guilders

Aspects of astronaut legal status as derived from the Intergovernmental Space Station Agreement (IGA) are discussed. The personal status of the astronauts is defined. Patent law considerations pertaining to the work or discoveries carried out by

an astronaut are discussed. Liability considerations are discussed. Questions of criminal jurisdiction are addressed. It is concluded that the legal status of an astronaut will essentially be similar to his or her national status as regards public, private, patent, and usually also criminal law. ESA

N90-26722# Ministere des Affaires Exterieures du Canada, Ottawa (Ontario).
CROSSBORDER MOVEMENTS: GOODS, PERSONNEL AND TECHNOLOGIES [LES MOUVEMENTS TRANSFRONTIERES: BIENS, PERSONNES ET TECHNOLOGIES]
P. Dubois *In* ESA, Manned Space Station: Legal Aspects Jan. 1990 p 93-100 In FRENCH (For primary document see N90-26711 20-84)
Copyright Avail: NTIS HC A10/MF A02; also available from EPD, ESTEC, Noordwijk, Netherlands, 40 Dutch guilders

Aspects of the special import and export agreements made between the four main partners in the International Space Station programs are described. The legal framework of exchanges between the four partner countries is outlined. Property rights and transit status are discussed. Mutual renunciation to recourse in matters of shared responsibility and issue of authorizations and rights are addressed. The areas of competence of each of the four partner countries are identified. The legal role of the mission commander is given particular attention. ESA

N90-26723# Gantt (J. B.), Washington, DC.
SPACE STATION INTELLECTUAL PROPERTY RIGHTS AND US PATENT LAW
J. B. Gantt *In* ESA, Manned Space Stations: Legal Aspects Jan. 1990 p 107-114 (For primary document see N90-26711 20-84)
Copyright Avail: NTIS HC A10/MF A02; also available from EPD, ESTEC, Noordwijk, Netherlands, 40 Dutch guilders

The principles governing intellectual property rights associated with Space Station activity are investigated. The article 21 of the Intergovernmental Space Station Agreement (IGA) is given particular attention. The separate provisions required to apportion jurisdiction among the European partner states within ESA are discussed. The status of U.S. as it relates to inventions in outer space is examined and the provisions of pending legislation in implementation of the IGA and clarification of U.S. law are analyzed. ESA

N90-26724# Roussel-Uclaf, Paris (France). Direction de l'Innovation et de la Prospective.
SPACE MANUFACTURE: PROTECTION AND VALUATION OF INNOVATIONS FROM A USERS POINT OF VIEW [LES FABRICATIONS DANS L'ESPACE: PROTECTION ET VALOORISATION DES INNOVATIONS LE POINT DE VUE D'UN UTILISATEUR]
J. P. Raynaud and V. Vache *In* ESA, Manned Space Stations: Legal Aspects Jan. 1990 p 115-116 In FRENCH (For primary document see N90-26711 20-84)
Copyright Avail: NTIS HC A10/MF A02; also available from EPD, ESTEC, Noordwijk, Netherlands, 40 Dutch guilders

Various technological and economic aspects of space manufacturing and space commercialization are addressed. Research carried out in reduced gravity manufacturing are described. Difficulties in promoting more research in space while protecting the secrecy of the test results carried out by industrial investors are discussed. The need for legislation protecting the patent rights of discoveries made in space is called for. Possible developments in the field of biotechnology due to spaceborne experiments are described. The Space Bio Separation (SBS) program is used as an example of the kind of legal problems facing industrial development in space. ESA

N90-26725# Max-Planck-Inst. for Foreign and International Patent, Copyright and Competition Law, Munich (Germany, F.R.).
PRODUCTION ACTIVITIES IN SPACE: THE PROBLEMS OF PROTECTION
D. Stauder *In* ESA, Manned Space Stations: Legal Aspects Jan. 1990 p 117-121 (For primary document see N90-26711 20-84)
Copyright Avail: NTIS HC A10/MF A02; also available from EPD, ESTEC, Noordwijk, Netherlands, 40 Dutch guilders

The issue of patent law in its role of protecting technical innovations or inventions made on space stations, objects, labs, or modules is addressed. The legal problems within patent law in protecting knowledge and inventions are described. The difficulties caused by the application of different national patent systems in the very confined area of a space station are discussed. The notions of unlawful misappropriation of knowledge are defined. Contracts of confidentiality are described. Contracts of co-inventorship are discussed. Territoriality and infringing acts are considered. ESA

N90-26726# Aerospatiale, Les Mureaux (France). Service Juridique.
POSSIBLE SOLUTIONS [LES SOLUTIONS POSSIBLES]
M. F. Murphy *In* ESA, Manned Space Stations: Legal Aspects Jan. 1990 p 123-126 In FRENCH (For primary document see N90-26711 20-84)
Copyright Avail: NTIS HC A10/MF A02; also available from EPD, ESTEC, Noordwijk, Netherlands, 40 Dutch guilders

The fact that national patent laws are applied to inventions made on a space vehicle under the legal control of a certain country is criticized. Difficulties which arise due to this practice are addressed. A series of solutions are proposed to resolve these problems. One solution is to maintain the status quo for inventions made on Earth. The second is to protect the inventions made in space by patent legislation by the organization which initiated the experiments leading to the inventions. An international code is proposed which would deliver special patent rights recognized by all countries and organizations. ESA

N90-26727# Groupe de Travail sur le Droit de l'Espace, Paris (France).
SPACE LAW PUT TO THE TEST BY THE INTERNATIONAL SPACE STATION [LE DROIT DE L'ESPACE A L'EPREUVE DE LA STATION SPATIALE]
C. A. Colliard *In its* Manned Space Stations: Legal Aspects Jan. 1990 p 133-136 In FRENCH (For primary document see N90-26711 20-84)
Copyright Avail: NTIS HC A10/MF A02; also available from EPD, ESTEC, Noordwijk, Netherlands, 40 Dutch guilders

The relationship between the Intergovernmental Space Station Agreement (IGA) and the principles of space law drawn up in the 1967 treaty on satellite agreements is investigated. It is concluded that the two agreements have a great deal in common and that in fact the text of IGA is often taken directly from that of the previous agreement. Certain vague areas in the IGA are identified. The most important of these are the principle of politico in space activities and the definition of pacific or exclusively pacific operation of spacecraft. ESA

85 URBAN TECHNOLOGY AND TRANSPORTATION

Includes applications of space technology to urban problems; technology transfer; technology assessment; and surface and mass transportation.

For related information see also *03 Air Transportation and Safety, 16 Space Transportation,* and *44 Energy Production and Conversion.*

N90-26728*# Garrett Turbine Engine Co., Phoenix, AZ.
ADVANCED TURBINE TECHNOLOGY APPLICATIONS PROJECT (ATTAP) Annual Report, 1989
Feb. 1990 215 p
(Contract DEN3-335)
(NASA-CR-185240; DOE/NASA/0335-2; NAS 1.26:185240; GARRETT-31-8071(2)) Avail: NTIS HC A10/MF A02 CSCL 21E

This report is the second in a series of Annual Technical Summary Reports for the Advanced Turbine Technology Applications Project (ATTAP). Plans and progress are covered for ceramics development for commercial automotive applications over the period January 1 through December 31, 1989. Project effort conducted under this contract is part of the DOE Gas Turbine Highway Vehicle System program. This program is directed to provide the U.S. automotive industry the high-risk, long-range technology necessary to produce gas turbine engines for automobiles with reduced fuel consumption, reduced environmental impact, and a decreased reliance on scarce materials and resources. The program is oriented toward developing the high-risk technology of ceramic structural component design and fabrication, such that industry can carry this technology forward to production in the 1990s. The ATTAP test bed engine, carried over from the previous AGT101 project, is being used for verification testing of the durability of next generation ceramic components, and their suitability for service at Reference Powertrain Design conditions. The technical effort conducted by GAPD and the ATTAP subcontractors over the second year of the project is reported. Topics covered include ceramic processing definition and refinement, design improvements to the ATTAP test bed engine and test rigs and the methodology development of ceramic impact and fracture mechanisms. Appendices include reports by ATTAP subcontractors in the development of silicon nitride and silicon carbide families of materials and processes. Author

N90-26729*# National Aeronautics and Space Administration. Lewis Research Center, Cleveland, OH.

PRELIMINARY DESIGNS FOR 25 kWe ADVANCED STIRLING CONVERSION SYSTEMS FOR DISH ELECTRIC APPLICATIONS Final Report

Richard K. Shaltens and Jeffrey G. Schreiber 1990 19 p Presented at the 25th Intersociety Conversion Engineering Conference, Reno, NV, 12-17 Aug. 1990; sponsored by AIChE, ANS, SAE, ACS, AIAA, ASME, and IEEE Prepared for DOE, Washington, DC

(Contract DE-AT04-85AL-33408)

(NASA-TM-103188; DOE/NASA/33408-4; E-5573; NAS 1.15:103188) Avail: NTIS HC A03/MF A01 CSCL 10A

Under the Department of Energy's (DOE) Solar Thermal Technology Program, Sandia National Laboratories is evaluating heat engines for terrestrial Solar Distributed Heat Receivers. The Stirling engine has been identified by Sandia as one of the most promising engines for terrestrial applications. The Stirling engine also has the potential to meet DOE's performance and cost goals. The NASA Lewis Research Center is conducting Stirling engine technology development activities directed toward a dynamic power source for space applications. Space power systems requirements include high reliability, very long life, low vibration and high efficiency. The free-piston Stirling engine has the potential for future high power space conversion systems, either nuclear or solar powered. Although both applications appear to be quite different, their requirements complement each other. Preliminary designs feature a free-piston Stirling engine, a liquid metal heat transport system, and a means to provide nominally 25 kW electric power to a utility grid while meeting DOE's performance and long term cost goals. The Cummins design incorporates a linear alternator to provide the electrical output, while the STC design generates electrical power indirectly through a hydraulic pump/motor coupled to an induction generator. Both designs for the ASCS's will use technology which can reasonably be expected to be available in the early 1990's Author

88 SPACE SCIENCES (GENERAL)

No abstracts in this category.

89 ASTRONOMY

Includes radio, gamma-ray, and infrared astronomy, and astrometry.

N90-26730*# National Aeronautics and Space Administration, Washington, DC.

REPORTS OF PLANETARY ASTRONOMY, 1990

Jul. 1990 152 p

(NASA-TM-4205; NAS 1.15:4205) Avail: NTIS HC A08/MF A01 CSCL 03A

Summaries of reports written by principal investigators funded through the Planetary Astronomy Program of NASA's Solar System Exploration Division, Office of Space Science and Applications are compiled. The summaries are designed to provide information about scientific research projects conducted in the Planetary Astronomy Program in 1989 through 1990 and to facilitate communication and coordination among concerned scientists and interested persons in universities, government, and industry. Highlights of recent accomplishments in planetary astronomy are included. Author

N90-26731*# California Inst. of Tech., Pasadena.

SUBMILLIMETER AND MILLIMETER OBSERVATIONS OF SOLAR SYSTEM OBJECTS Final Technical Report, 1986 - 1989

Duane O. Muhleman 7 Jul. 1990 13 p

(Grant NGL-05-002-114)

(NASA-CR-186636; NAS 1.26:186636) Avail: NTIS HC A03/MF A01 CSCL 03A

Microwave spectroscopy of solar system objects was supported. It necessarily involves millimeter and submillimeter wavelengths where rotational transitions reside. The existing national facilities are at OVRO, the 12-meter at Kitt Peak, UC array at Hat Creek, the Caltech CSO on Mauna Kea, and the 14-meter at the Univ. of Massachusetts, near Amherst. The group used all of these instruments in the last year except the Univ. of Massachusetts 14-meter. This wavelength range (0.3 to 3 mm) is about to enjoy an explosion of interest as submillimeter receivers become better and easier to use. This region of the spectrum is rich in transitions of molecules that exist in the planetary atmospheres which can be studied for temperature-pressure profiles, wind tracers, and atmospheric chemistry. The list of solar system objects that have been recently addressed with these techniques include: (1) Venus: CO studies of T-P profiles, winds, and photochemistry; SO2 detections; Continuum mapping remains to be done at 1 mm; (2) Earth H2O, CO, NO, NO2, O(18)O, etc. as a test bed for other atmospheres; (3) Mars: H2O, CO, O(18)O studies of T-P profiles, winds (fall of 1990), and photochemistry; (4) Saturn: Same as Jupiter plus submillimeter and millimeter mapping of the ring system; (5) Uranus and Neptune: Continuum thermal mapping; and (6) Titan: CO, HCN, and HC3NT-P information and photochemistry. Recent results are given. Author

N90-26732# Los Alamos National Lab., NM.

ASTRONOMY AT ULTRA-HIGH ENERGIES: RESULTS FROM THE CYGNUS EXPERIMENT

D. E. Alexandreas, R. C. Allen, S. D. Biller, G. M. Dion, X.-Q. Lu, P. R. Vishwanath, G. B. Yodh, D. Berley, C. Y. Chang, and Todd J. Haines (Maryland Univ., College Park.) et al 1990 9 p Presented at the 15th General Meeting of the Division of Particles and Fields of the American Physical Society, Houston, TX, 3-6 Jan. 1990; sponsored by Maryland Univ., College Park, MD

(Contract W-7405-eng-36)

(DE90-011979; LA-UR-90-1634; CONF-900135-8) Avail: NTIS HC A02/MF A01

The CYGNUS experiment is composed of an air-shower array and muon detectors, located in Los Alamos, NM, and operating at energies above 50 TeV. Recent results include a search for emission from Cygnus X-3 during the radio outbursts of June and July 1989, preliminary results from a search for diffuse emission from the galactic plane, and preliminary results from a search for emission from possible Northern Hemisphere point sources, both known and unknown. DOE

N90-26733# University of Southern California, Marina del Rey. Information Sciences Inst.
RHETORICAL STRUCTURE THEORY AND TEXT ANALYSIS
William C. Mann, Christian M. I. M. Matthiessen, and Sandra A. Thompson Nov. 1989 67 p
(Contracts F49620-87-C-0005; FQ8671-84-01007; MDA903-87-C-0641; NSF IST-84-08726)
(AD-A222655; ISI/RR-89-242) Avail: NTIS HC A04/MF A01 CSCL 05/7

Recent research on text generation has shown that there is a need for stronger linguistic theories that tell in detail how texts communicate. The prevailing theories are very difficult to compare, and it is also very difficult to see how they might be combined into stronger theories. To make comparison and combination a bit more approachable, we have created a book which is designed to encourage comparison. A dozen different authors or teams, all experienced in discourse research, are given exactly the same text to analyze. The text is an appeal for money by a lobbying organization in Washington, DC. It informs, stimulates and manipulates the reader in a fascinating way. The joint analysis is far more insightful than any one team's analysis alone. This paper is our contribution to the book. Rhetorical Structure Theory (RST), the focus of this paper, is a way to account for the functional potential of text, its capacity to achieve the purposes of speakers and produce effects in hearers. It also shows a way to distinguish coherent texts from incoherent ones, and identifies consequences of text structure. GRA

90 ASTROPHYSICS

Includes cosmology; celestial mechanics; space plasmas; and interstellar and interplanetary gases and dust.
For related information see also *75 Plasma Physics*.

N90-26734*# Princeton Univ., NJ.
COMMENT ON HIGH RESOLUTION SIMULATIONS OF COSMIC STRINGS. 1: NETWORK EVOLOUTION
Neil Turok and Andreas Albrecht (Fermi National Accelerator Lab., Batavia, IL.) Mar. 1990 7 p Sponsored in part by DOE and the Alfred Sloan Foundation
(Grants NAGw-1340; NSF PHY-80-19754)
(NASA-CR-186606; NAS 1.26:186606; FERMILAB-Pub-90/53-A) Avail: NTIS HC A02/MF A01 CSCL 03B

Comments are made on recent claims (Albrecht and Turok, 1989) regarding simulations of cosmic string evolution. Specially, it was claimed that results were dominated by a numerical artifact which rounds out kinks on a scale of the order of the correlation length on the network. This claim was based on an approximate analysis of an interpolation equation which is solved herein. The typical rounding scale is actually less than one fifth of the correlation length, and comparable with other numerical cutoffs. Results confirm previous estimates of numerical uncertainties, and show that the approximations poorly represent the real solutions to the interpolation equation. Author

N90-26735*# Fermi National Accelerator Lab., Batavia, IL.
BARYOGENESIS IN EXTENDED INFLATION. 2: BARYOGENESIS VIA PRIMORDIAL BLACK HOLES
John D. Barrow, Edmund J. Copeland, Edward W. Kolb, and Andrew R. Liddle (Sussex Univ., Brighton, England) Jul. 1990 32 p
(Grant NAGw-1340)
(NASA-CR-182843; NAS 1.26:182843; FERMILAB-Pub-90/98-A-2; Sussex-AST-90/7-1-2) Avail: NTIS HC A03/MF A01 CSCL 03B

Baryogenesis at the end of extended inflation is studied. Extended inflation is brought to an end by the collisions of bubble walls surrounding regions of true vacuum, a process which produces particles well out of thermal equilibrium. The possibility that the wall collisions may provide a significant density of primordial black holes is considered and their possible role in generating a baryon asymmetry is examined. Author

N90-26736# Centro Brasileiro de Pesquisas Fisicas, Rio de Janeiro.
NONSTANDARD BIG BANG MODELS
M. O. Calvao and J. A. S. Lima (Universidade Federal do Rio Grande do Norte, Natal, Brazil) 1989 15 p Submitted for publication Sponsored in part by CNPq and CAPES
(DE90-625593; CBPF-NF-027/89) Avail: NTIS (US Sales Only) HC A03/MF A01

The usual FRW hot big-bang cosmologies were generalized by considering the equation of state rho = Anm + gamma-1 (sup -1)p, where m is the rest mass of the fluid particles and A is a dimensionless constant. Explicit analytic solutions are given for the flat case (epsilon=O). For large cosmological times these extended models behave as the standard Einstein-de Sitter universes regardless of the values of A and gamma. Unlike the usual FRW flat case the deceleration parameter q is a time dependent function and its present value, q(approx equal) 1, obtained from the luminosity distance versus redshift relation, may be fitted by taking, for instance, A=1 and gamma = 5/3 (monatomic relativistic gas with much greater than k(sub B)T). In all cases the universe cools obeying the same temperature law of the FRW (Friedman Robertson Walker) models and it is shown that the age of the universe is only slightly modified. DOE

N90-26737*# Yerkes Observatory, Williams Bay, WI.
THE INTERSTELLAR D1 LINE AT HIGH RESOLUTION
L. M. Hobbs and D. E. Welty 1990 17 p Submitted for publication
(Grant NAGw-1475)
(NASA-CR-184915; NAS 1.26:184915) Avail: NTIS HC A03/MF A01 CSCL 03B

Observations at a resolving power or a velocity resolution are reported of the interstellar D(sub 1) line of Na I in the spectra of gamma Cas, delta Ori, epsilon Ori, pi Sco, delta Cyg, and alpha Cyg. An echelle grating was used in a double-pass configuration with a CCD detector in the coude spectrograph of the 2.7 m reflector at McDonald Observatory. At least 42 kinematically distinct clouds are detected along the light paths to the five more distant stars, in addition to a single cloud seen toward delta Cyg. The absorption lines arising in 13 of the clouds are sufficiently narrow and unblended to reveal clearly resolved hyperfine structure components split by 1.05 km/s. An additional 13 clouds apparently show comparably narrow, but more strongly blended, lines. For each individual cloud, upper limits T(sub max) and (v sub t)(sub max) on the temperature and the turbulent velocity, respectively, are derived by fitting the observed lines with theoretical absorption profiles. Author

N90-26738*# Lunar and Planetary Inst., Houston, TX.
PRESS ABSTRACTS OF THE 21ST LUNAR AND PLANETARY SCIENCE CONFERENCE
Mar. 1990 64 p Conference held in Houston, TX, 12-16 Mar. 1990 Prepared in cooperation with Universities Space Research Association, Houston, TX
(Contract NASw-4066)
(NASA-CR-186874; NAS 1.26:186874; LIP-740) Avail: NTIS HC A04/MF A01 CSCL 03B

The Program Committee for the Twenty-fisrt Lunar and Planetary Science Conference has chosen these contributions as having the greatest potential interest for the general public. The papers in this collection were written for general presentation, avoiding jargon and unnecessarily complex terms. More technical abstracts will be found in Lunar and Planetary Science XXI. Representative titles are: Ancient Ocean-Land-Atmosphere Interactions on Mars: Global Model and Geological Evidence; Oxygen Isotopic Compositions of Ordinary Chondrites and Their Chondrules; Exposure Ages and Collisional History of L-Chondrite Parent Bodies; Models of Solar-Powered Geysers on Triton; and Search for Life: A Science Rationale for a Permanent Base on Mars. Author

N90-26739*# Lunar and Planetary Inst., Houston, TX.
PROCEEDINGS OF A WORKSHOP ON ANTARCTIC METEORITE STRANDING SURFACES
W. A. Cassidy, ed. and I. M. Whillans, ed. 3 Aug. 1990 110 p Workshop held at Pittsburgh, PA, 13-15 Jul. 1988 Sponsored in part by NSF
(Contract NASw-4066)
(NASA-CR-186575; LPI-TR-90-03; NAS 1.26:186575) Avail: NTIS HC A06/MF A01 CSCL 03B

The discovery of large numbers of meteorites on the Antarctic Ice Sheet is one of the most exciting developments in polar science in recent years. The meteorites are found on areas of ice called stranding surfaces. Because of the sudden availability of hundreds, and then thousands, of new meteorite specimens at these sites, the significance of the discovery of meteorite stranding surfaces in Antarctica had an immediate and profound impact on planetary science, but there is also in this discovery an enormous, largely unrealized potential to glaciology for records of climatic and ice sheet changes. The glaciological interest derives from the antiquity of the ice in meteorite stranding surfaces. This exposed ice covers a range of ages, probably between zero and more than 500,000 years. The Workshop on Antarctic Meteorite Stranding Surfaces was convened to explore this potential and to devise a course of action that could be recommended to granting agencies. The workshop recognized three prime functions of meteorite stranding surfaces. They provide: (1) A proxy record of climatic change (i.e., a long record of climatic change is probably preserved in the exposed ice stratigraphy); (2) A proxy record of ice volume change; and (3) A source of unique nonterrestrial material. Author

N90-26740*# Lunar and Planetary Inst., Houston, TX.
PROCEEDINGS OF A WORKSHOP ON DIFFERENCES BETWEEN ANTARCTIC AND NON-ANTARCTIC METEORITES
Christian Koeberl, ed. and William A. Cassidy, ed. 1989 107 p Workshop held in Vienna, Austria, 27-28 Jul. 1989 Sponsored in part by Vienna Univ.
(Contract NASw-4066)
(NASA-CR-184918; NAS 1.26:184918; LPI-TR-90-01) Avail: NTIS HC A06/MF A01 CSCL 03B

The known facts, together with new research results are reviewed, in order to examine apparent differences between the Antarctic and non-Antarctic populations. In view of the statistically significant number of Antarctic meteorites, and the existence of rare or previously unknown types of meteorites among the Antarctic meteorite collection, the question was really not so much whether there are differences, but to define which ones are significant and what their origin is. Two main causes for the possible differences have been suggested previously, namely differences in the meteorite parent populations and secondary effects (e.g., weathering). The workshop was structured to contain sessions on chemical, isotopic, petrological, and mineralogical studies of meteorites from the two collections; terrestrial age determinations; discussions on mass frequency distributions; relative abundances of meteorite types; and terrestrial meteorite flux rates and their possible changes with time. Author

N90-26741*# National Aeronautics and Space Administration. Marshall Space Flight Center, Huntsville, AL.
THE CHARGED PARTICLE RADIATION ENVIRONMENT FOR AXAF
Marshall Joy Jul. 1990 16 p
(NASA-TM-100405; NAS 1.15:100405) Avail: NTIS HC A03/MF A01 CSCL 03B

The Advanced X Ray Astrophysics Facility (AXAF) will be subjected to several sources of charged particle radiation during its 15-year orbital lifetime: geomagnetically-trapped electrons and protons, galactic cosmic ray particles, and solar flare events. These radiation levels are presented for the AXAF orbit for use in the design of the observatory's science instruments. Author

N90-26742# Brown Univ., Providence, RI. Dept. of Physics.
A RESEARCH PROGRAM IN PHYSICS OF THE EARLY UNIVERSE Progress Report
Robert H. Brandenberger 30 Jun. 1990 7 p
(Contract DE-AC02-76ER-03130)
(DE90-013319; DOE/ER-03130/454) Avail: NTIS HC A02/MF A01

Since June 1989 most of the research has been devoted to early Universe cosmology. The four focal points have been: Galaxy and large scale structure formation with cosmic strings. Quantum field theoretical effects near cosmic strings and their observational signatures. Dynamics of inflationary Universe models. Quantum particle production and formation of topological defects during phase transitions. DOE

N90-26232*# Jet Propulsion Lab., California Inst. of Tech., Pasadena. Telecommunications Science and Engineering Div.
RINGS OF EARTH DETECTED BY ORBITAL DEBRIS RADAR
R. Goldstein and L. Randolph *In its* The Telecommunications and Data Acquisition Report 15 May 1990 p 191-195 (For primary document see N90-26217 20-32)
Avail: NTIS HC A10/MF A02 CSCL 03B

N90-26772*# California Univ., Davis. Dept. of Chemistry.
LABORATORY STUDIES OF PHOTODISSOCIATION PROCESSES RELEVANT TO THE FORMATION OF COMETARY RADICALS
R. S. Urdahl, Y. Bao, and W. M. Jackson *In* NASA, Goddard Space Flight Center, First International Conference on Laboratory Research for Planetary Atmospheres May 1990 p 260-264 (For primary document see N90-26744 20-91)
(Grant NAGw-903)
Avail: NTIS HC A21/MF A03 CSCL 03B

N90-26781*# National Aeronautics and Space Administration. Goddard Space Flight Center, Greenbelt, MD.
STUDY OF THE POLYOXYMETHYLENE AND ITS SPUTTERED FRAGMENTS: IMPLICATIONS FOR COMETS
Marla H. Moore (Maryland Univ., College Park.) and Toshihiko Tanabe *In its* First International Conference on Laboratory Research for Planetary Atmospheres May 1990 p 405-410 (For primary document see N90-26744 20-91)
Avail: NTIS HC A21/MF A03 CSCL 03B

91 LUNAR AND PLANETARY EXPLORATION

Includes planetology; and manned and unmanned flights.

For spacecraft design or space stations see *18 Spacecraft Design, Testing and Performance.*

N90-26743*# National Aeronautics and Space Administration, Washington, DC.
DIRECTORY OF RESEARCH PROJECTS: PLANETARY GEOLOGY AND GEOPHYSICS PROGRAM
Henry Holt, ed. Jul. 1990 171 p
(NASA-TM-4211; NAS 1.15:4211) Avail: NTIS HC A08/MF A01 CSCL 03B

Information about currently funded scientific research within the Planetary Geology and Geophysics Program is provided, including the proposal summary sheet from each proposal funded under the program during fiscal year 1990. Information about the research project, including title, principal investigator, institution, summary of research objectives, past accomplishments, and proposed new investigations is also provided. Author

N90-26744*# National Aeronautics and Space Administration. Goddard Space Flight Center, Greenbelt, MD.
FIRST INTERNATIONAL CONFERENCE ON LABORATORY RESEARCH FOR PLANETARY ATMOSPHERES
Kenneth Fox, ed., John E. Allen, Jr., ed., Louis J. Stief, ed., and Diana T. Quillen, ed. (Bowie State Univ., MD.) May 1990 481 p Conference held in Bowie, MD, 25-27 Oct. 1989
(NASA-CP-3077; Rept-90B00106; NAS 1.55:3077) Avail: NTIS HC A21/MF A03 CSCL 03B

Proceedings of the First International Conference on Laboratory Research for Planetary Atmospheres are presented. The covered areas of research include: photon spectroscopy, chemical kinetics, thermodynamics, and charged particle interactions. This report contains the 12 invited papers, 27 contributed poster papers, and 5 plenary review papers presented at the conference. A list of attendees and a reprint of the Report of the Subgroup on Strategies for Planetary Atmospheres Exploration (SPASE) are provided in two appendices. For individual titles, see N90-26745 through N90-26783.

N90-26745*# Georgia Inst. of Tech., Atlanta. School of Electrical Engineering.

LABORATORY MEASUREMENTS OF MICROWAVE AND MILLIMETER-WAVE PROPERTIES OF PLANETARY CONSTITUENTS

Paul G. Steffes *In* NASA, Goddard Space Flight Center, First International Conference on Laboratory Research for Planetary Atmospheres May 1990 p 5-26 Previously announced as N90-10815 (For primary document see N90-26744 20-91)
(Grant NAGw-533)
Avail: NTIS HC A21/MF A03 CSCL 03B

Accurate data on microwave and millimeter-wave properties of potential planetary atmospheric constituents is critical for the proper interpretation of radio occultation measurements, and of radio astronomical observations of both continuum and spectral line emissions. Such data is also needed to correct for atmospheric effects on radar studies of surface reflectivity. Since the refractive and absorptive properties of atmospheric constituents often vary drastically from theoretically predicted profiles, especially under the extreme conditions characteristic of the planetary atmosphere, laboratory measurements under simulated planetary conditions are required. The instrumentation and techniques used for laboratory measurement of the refractivity and absorptivity of atmospheric constituents at wavelengths longward of 1 mm, under simulated planetary conditions (temperature, pressure, and broadening gases) are reviewed. Techniques for measuring both gases and condensates are considered. Also reviewed are the relative accuracies of the various techniques. Laboratory measurements are reviewed which have already been made, and additional measurements which are needed for interpretation of data from Venus and the outer planets, are highlighted. Author

N90-26746*# Jet Propulsion Lab., California Inst. of Tech., Pasadena.

HIGH RESOLUTION SPECTROSCOPY IN THE MICROWAVE AND FAR INFRARED **c35**

Herbert M. Pickett *In* NASA, Goddard Space Flight Center, First International Conference on Laboratory Research for Planetary Atmospheres May 1990 p 27-36 (For primary document see N90-26744 20-91)
Avail: NTIS HC A21/MF A03 CSCL 14B

High resolution rotational spectroscopy has long been central to remote sensing techniques in atmospheric sciences and astronomy. As such, laboratory measurements must supply the required data to make direct interpretation of data for instruments which sense atmospheres using rotational spectra. Spectral measurements in the microwave and far infrared regions are also very powerful tools when combined with infrared measurements for characterizing the rotational structure of vibrational spectra. In the past decade new techniques were developed which have pushed high resolution spectroscopy into the wavelength region between 25 micrometers and 2 mm. Techniques to be described include: (1) harmonic generation of microwave sources, (2) infrared laser difference frequency generation, (3) laser sideband generation, and (4) ultrahigh resolution interferometers. Author

N90-26747*# National Aeronautics and Space Administration. Goddard Space Flight Center, Greenbelt, MD.

HIGH RESOLUTION INFRARED SPECTROSCOPY OF PLANETARY MOLECULES USING DIODE LASERS AND FOURIER TRANSFORM SPECTROMETERS

Donald E. Jennings *In its* First International Conference on Laboratory Research for Planetary Atmospheres May 1990 p 37-53 (For primary document see N90-26744 20-91)
Avail: NTIS HC A21/MF A03 CSCL 03B

Modern observations of infrared molecular lines in planets are performed at spectral resolutions which are as high as those available in the laboratory. Analysis of such data requires laboratory measurements at the highest possible resolution, which also yield accurate line positions and intensities. For planetary purposes the spectrometer must be coupled to sample cells which can be reduced in temperature and varied in pressure. An approach which produces the full range of required molecular line parameters uses a combination of tunable diode lasers and Fourier transform spectrometers (FTS). The FTS provides board spectral coverage and good calibration accuracy, while the diode laser can be used to study those regions which are not resolved by the FTS. Author

N90-26748*# Tennessee Univ., Knoxville. Dept. of Physics and Astronomy.

LABORATORY STUDIES, ANALYSIS, AND INTERPRETATION OF THE SPECTRA OF HYDROCARBONS PRESENT IN PLANETARY ATMOSPHERES INCLUDING CYANOACETYLENE, ACETYLENE, PROPANE, AND ETHANE

William E. Blass, Stephen J. Daunt, Antoni V. Peters (Concordia Univ., Montreal, Quebec), and Mark C. Weber *In* NASA, Goddard Space Flight Center, First International Conference on Laboratory Research for Planetary Atmospheres May 1990 p 54-63 (For primary document see N90-26744 20-91)
Avail: NTIS HC A21/MF A03 CSCL 03B

Combining broadband Fourier transform spectrometers (FTS) from the McMath facility at NSO and from NRC in Ottawa and narrow band TDL data from the laboratories with computational physics techniques has produced a broad range of results for the study of planetary atmospheres. Motivation for the effort flows from the Voyager/IRIS observations and the needs of Voyager analysis for laboratory results. In addition, anticipation of the Cassini mission adds incentive to pursue studies of observed and potentially observable constituents of planetary atmospheres. Current studies include cyanoacetylene, acetylene, propane, and ethane. Particular attention is devoted to cyanoacetylen (H3CN) which is observed in the atmosphere of Titan. The results of a high resolution infrared laboratory study of the line positions of the 663, 449, and 22.5/cm fundamental bands are presented. Line position, reproducible to better than 5 MHz for the first two bands, are available for infrared astrophysical searches. Intensity and broadening studies are in progress. Acetylene is a nearly ubiquitous atmospheric constituent of the outer planets and Titan due to the nature of methane photochemistry. Results of ambient temperature absolute intensity measurements are presented for the fundamental and two two-quantum hotband in the 730/cm region. Low temperature hotband intensity and linewidth measurements are planned. Author

N90-26749*# National Inst. of Standards and Technology, Gaithersburg, MD. Molecular Spectroscopy Div.

INFRARED SPECTRA OF VAN DE WAALS COMPLEXES OF IMPORTANCE IN PLANETARY ATMOSPHERES

G. T. Fraser, A. S. Pine, and W. J. Lafferty *In* NASA, Goddard Space Flight Center, First International Conference on Laboratory Research for Planetary Atmospheres May 1990 p 64-68 (For primary document see N90-26744 20-91)
Avail: NTIS HC A21/MF A03 CSCL 03B

It has been suggested that (CO2)2 and Ar-CO2 are important constituents of the planetary atmospheres of Venus and Mars. Recent results on the laboratory spectroscopy of CO2 containing van der Waals complexes which may be of use in the modeling of the spectra of planetary atmospheres are presented. Sub-Doppler infrared spectra were obtained for (CO2)2, (CO2)3, and rare-gas-CO2 complexes in the vicinity of the CO2 Fermi diad at 2.7 micrometers using a color-center-laser optothermal spectrometer. From the spectroscopic constants the geometries of the complexes have been determined and van der Waals vibrational frequencies have been estimated. The equilibrium

configurations are C2h, C3h, and C2v, for (CO2)2, (CO2)3, and the rare-gas-CO2 complexes, respectively. Most of the homogeneous linewidths for the revibrational transitions range from 0.5 to 22 MHz, indicating that predissociation is as much as four orders of magnitude faster than radiative processes for vibrational relaxation in these complexes. Author

N90-26750*# Stanford Univ., CA. Center for Radar Astronomy.
LABORATORY MEASUREMENTS AND MODELING OF MICROWAVE ABSORPTION BY AMMONIA IN GAS MIXTURES APPLICABLE TO GIANT PLANET ATMOSPHERES
T. R. Spilker *In* NASA, Goddard Space Flight Center, First International Conference on Laboratory Research for Planetary Atmospheres May 1990 p 69-73 (For primary document see N90-26744 20-91)
Avail: NTIS HC A21/MF A03 CSCL 03B

Accurate knowledge of the microwave absorption behavior of ammonia is critical to the correct interpretation of radio astronomical and radio occultation data from the giant planets. New cavity resonator techniques developed at the Stanford Center for Radar Astronomy have allowed accurate laboratory measurements of the microwave absorptivity and refractivity spectra of gas mixtures containing trace amounts of ammonia. A parameterized version of the modified Ben-Reuven formalism of Berge and Bulkis was optimized to fit the new data. The new formalism produced by this method predicts ammonia absorptivity much more accurately than previous formalism over a significant range of conditions. B.G.

N90-26751*# National Aeronautics and Space Administration. Ames Research Center, Moffett Field, CA.
RECENT HIGH RESOLUTION LABORATORY DETERMINATIONS OF LINE BROADENING AND INTENSITY PARAMETERS: PH3, CH3D, AND CO2
C. B. Suarez, C. Chackerian, Jr., F. P. J. Valero, and G. Tarrago (Paris Univ., Orsay, France) *In* NASA, Goddard Space Flight Center, First International Conference on Laboratory Research for Planetary Atmospheres May 1990 p 74-77 (For primary document see N90-26744 20-91)
Avail: NTIS HC A21/MF A03 CSCL 03B

Recent unpublished laboratory work on rovibrational line strengths and broadening coefficients which is of interest in the study of planetary atmospheres was reviewed. The molecules discussed are PH3, CH3D and CO2. Author

N90-26752*# National Inst. of Standards and Technology, Gaithersburg, MD. Molecular Spectroscopy Div.
MICROWAVE SPECTRA OF VAN DER WAALS COMPLEXES OF IMPORTANCE IN PLANETARY ATMOSPHERES
R. D. Suenram and F. J. Lovas *In* NASA, Goddard Space Flight Center, First International Conference on Laboratory Research for Planetary Atmospheres May 1990 p 78-84 (For primary document see N90-26744 20-91)
Avail: NTIS HC A21/MF A03 CSCL 03B

The Fourier-transform Fabry-Perot pulsed-molecular-beam microwave spectrometer at NIST was used to study the microwave spectra of a number of molecular dimers and trimers that may be present in planetary atmospheres. The weak van der Waals bonds associated with these species usually give rise to rotational-tunneling splittings in the microwave spectra. The microwave spectrum of the water dimer species was used to illustrate the complications that can arise in the study of the rotational spectra of these loosely bound species. In addition to the water dimer species, the microwave spectra of the following hydrogen-bonded and van der Waals complexes were studied: (CO2)2-H2O, CO2-(H2O)2, CO2-H2S, N2-H2O, CO-H2O, SO2-H2O, and O3-H2O. Author

N90-26753*# State Univ. of New York, Stony Brook. Inst. for Atmospheric Sciences.
INFRARED LINE PARAMETERS AT LOW TEMPERATURES RELEVANT TO PLANETARY ATMOSPHERES
Prasad Varanasi *In* NASA, Goddard Space Flight Center, First International Conference on Laboratory Research for Planetary Atmospheres May 1990 p 85-89 (For primary document see N90-26744 20-91)
(Grant NGR-33-015-139)
Avail: NTIS HC A21/MF A03 CSCL 03B

Employing the techniques that were described in several publications for measuring infrared lineshifts, linewidths and line intensities with a tunable diode laser, these parameters were measures for lines in the important infrared bands of several molecules of interest to the planetary astronomer at low temperatures that are relevant to planetary atmospheres using He, Ne, Ar, H2, N2, O2, and air as the perturbers. In addition to obtaining the many original data on the temperature dependence of the intensities and linewidths, it was also the first measurement of the same for the collision-induced lineshift of an infrared line and it showed that it was markedly different from that of the corresponding collision-broadened linewidth. Author

N90-26754*# California Univ., Los Angeles. Space Sciences Center.
ABSOLUTE VACUUM ULTRAVIOLET PHOTOABSORPTION CROSS SECTION STUDIES OF ATOMIC AND MOLECULAR SPECIES: TECHNIQUES AND OBSERVATIONAL DATA
D. L. Judge and C. Y. R. Wu *In* NASA, Goddard Space Flight Center, First International Conference on Laboratory Research for Planetary Atmospheres May 1990 p 93-113 Sponsored in part by NSF (For primary document see N90-26744 20-91)
(Grant NGR-05-018-180)
Avail: NTIS HC A21/MF A03 CSCL 03B

Absorption of a high energy photon (greater than 6 eV) by an isolated molecule results in the formation of highly excited quasi-discrete or continuum states which evolve through a wide range of direct and indirect photochemical processes. These are: photoionization and autoionization, photodissociation and predissociation, and fluorescence. The ultimate goal is to understand the dynamics of the excitation and decay processes and to quantitatively measure the absolute partial cross sections for all processes which occur in photoabsorption. Typical experimental techniques and the status of observational results of particular interest to solar system observations are presented. Author

N90-26755*# Massachusetts Inst. of Tech., Cambridge. Dept. of Chemistry.
DETERMINATION OF MOLECULAR SPECTROSCOPIC PARAMETERS AND ENERGY-TRANSFER RATES BY DOUBLE-RESONANCE SPECTROSCOPY
J. I. Steinfeld, B. Foy, J. Hetzler, C. Flannery, J. Klaassen, Y. Mizugai (Sophia Univ., Tokyo, Japan), and S. Coy *In* NASA, Goddard Space Flight Center, First International Conference on Laboratory Research for Planetary Atmospheres May 1990 p 114-128 Sponsored in part by NSF and AFOSR (For primary document see N90-26744 20-91)
(Grant NAGw-1667)
Avail: NTIS HC A21/MF A03 CSCL 03B

The spectroscopy of small to medium-size polyatomic molecules can be extremely complex, especially in higher-lying overtone and combination vibrational levels. The high density of levels also complicates the understanding of inelastic collision processes, which is required to model energy transfer and collision broadening of spectral lines. Both of these problems can be addressed by double-resonance spectroscopy, i.e., time-resolved pump-probe measurements using microwave, infrared, near-infrared, and visible-wavelength sources. Information on excited-state spectroscopy, transition moments, inelastic energy transfer rates and propensity rules, and pressure-broadening parameters may be obtained from such experiments. Examples are given for several species of importance in planetary atmospheres, including ozone, silane, ethane, and ammonia. Author

N90-26756*# National Inst. of Standards and Technology, Boulder, CO. Joint Inst. for Laboratory Astrophysics.

NOVEL LASER GAIN AND TIME-RESOLVED FTIR STUDIES OF PHOTOCHEMISTRY

Stephen R. Leone *In* NASA, Goddard Space Flight Center, First International Conference on Laboratory Research for Planetary Atmospheres May 1990 p 129-140 Prepared in cooperation with Colorado Univ., Boulder Sponsored in part by DOE; NSF; and AFWL (For primary document see N90-26744 20-91)
Avail: NTIS HC A21/MF A03 CSCL 03B

Several techniques are discussed which can be used to explore laboratory photochemical processes and kinetics relevant to planetary atmospheres; these include time-resolved laser gain-versus-absorption spectroscopy and time-resolved Fourier transform infrared (FTIR) emission studies. The laser gain-versus-absorption method employed tunable diode and F-center lasers to determine the yields of excited photofragments and their kinetics. The time-resolved FTIR technique synchronizes the sweep of a commercial FTIR with a pulsed source of light to obtain emission spectra of novel transient species in the infrared. These methods are presently being employed to investigate molecular photodissociation, the yields of excited states of fragments, their subsequent reaction kinetics, Doppler velocity distributions, and velocity-changing collisions of translationally fast atoms. Such techniques may be employed in future investigations of planetary atmospheres, for example to study polycyclic aromatic hydrocarbons related to cometary emissions, to analyze acetylene decomposition products and reactions, and to determine spectral features in the near infrared and infrared wavelength regions for planetary molecules and clusters. Author

N90-26757*# Institute for Space and Terrestrial Science, York (Ontario). Space Astrophysics Lab.

HIGH RESOLUTION, LOW TEMPERATURE PHOTOABSORPTION CROSS-SECTION OF C2H2 WITH APPLICATION TO SATURN'S ATMOSPHERE

John Caldwell, C. Y. R. Wu, T. J. Xia, D. L. Judge (University of Southern California, Los Angeles.), and R. Wagener *In* NASA, Goddard Space Flight Center, First International Conference on Laboratory Research for Planetary Atmospheres May 1990 p 142-146 (For primary document see N90-26744 20-91)
Avail: NTIS HC A21/MF A03 CSCL 03B

New laboratory observations of the VUV absorption cross-section of C2H2, obtained under physical conditions approximating stratospheres of the giant planets, were combined with IUE observations of the albedo of Saturn, for which improved data reduction techniques have been used, to produce new models for that atmosphere. When the effects of C2H2 absorption are accounted for, additional absorption by other molecules is required. The best-fitting model also includes absorption by PH3, H2O, C2H6 and CH4. A small residual disagreement near 1600 A suggests that an additional trace species may be required to complete the model. Author

N90-26758*# National Aeronautics and Space Administration. Ames Research Center, Moffett Field, CA.

GAUSSIAN QUADRATURE EXPONENTIAL SUM MODELING OF NEAR INFRARED METHANE LABORATORY SPECTRA OBTAINED AT TEMPERATURES FROM 106 TO 297 K

Lawrence P. Giver, D. C. Benner, M. G. Tomasko, U. Fink, and D. Kerola (Arizona Univ., Tucson.) *In* NASA, Goddard Space Flight Center, First International Conference on Laboratory Research for Planetary Atmospheres May 1990 p 147-156 (For primary document see N90-26744 20-91)
Avail: NTIS HC A21/MF A03 CSCL 03B

Transmission measurements made on near-infrared laboratory methane spectra have previously been fit using a Malkmus band model. The laboratory spectra were obtained in three groups at temperatures averaging 112, 188, and 295 K; band model fitting was done separately for each temperature group. These band model parameters cannot be used directly in scattering atmosphere model computations, so an exponential sum model is being developed which includes pressure and temperature fitting parameters. The goal is to obtain model parameters by least square fits at 10/cm intervals from 3800 to 9100/cm. These results will be useful in the interpretation of current planetary spectra and also NIMS spectra of Jupiter anticipated from the Galileo mission. Author

N90-26759*# National Aeronautics and Space Administration. Goddard Space Flight Center, Greenbelt, MD.

MEASUREMENTS OF THE METHANE RELAXATION TIMES FOR APPLICATION TO THE INFRARED EMISSION MODELS OF THE UPPER ATMOSPHERES OF OUTER PLANETS AND TITAN

Rangasayi N. Halthore, John J. Caldwell, John E. Allen, Jr., Jim A. Burt, Kuanghua Yang, and Paul Delaney (York Univ., Downsview, Ontario) *In its* First International Conference on Laboratory Research for Planetary Atmospheres May 1990 p 157-163 Sponsored in part by Institute for Space and Terrestrial Science, York, Ontario (For primary document see N90-26744 20-91)
Avail: NTIS HC A21/MF A03 CSCL 03B

The 7.8 micrometer emission from the nu(sub 4) band of methane (CH4) is a regularly observed feature in the stratosphere of all the giant planets and Titan. On Jupiter, enhancements in this emission are associated with the infrared hot spots in the auroral zone. Attempts to model this phenomenon in particular, and to understand the role of methane in general, have been hampered in part by a lack of adequate laboratory measurements of the collisional relaxation times for the nu(sub 3) and nu(sub 4) levels over the appropriate temperature range. To provide this needed data, a series of laboratory experiments were initiated. In the experimental arrangement the nu(sub3) band of methane is pumped at 3.3 micrometers using a pulsed infrared source (Nd:YAG/dye laser system equipped with a wave-length extender). The radiative lifetime of the nu(sub 3) level (approximately 37 ms) is much shorter than the nu(sub 4) lifetime (approximately 390 ms); however, a rapid V-V energy transfer rate ensures that the nu(sub 4) level is substantially populated. The photoacoustic technique is used to acquire relaxation rate information. The experiments are performed using a low-temperature, low-pressure cell. Experimental apparatus and technique are described. In addition some of the experimental difficulties associated with making these measurements are discussed and some preliminary results are presented. Author

N90-26760*# National Inst. of Standards and Technology, Gaithersburg, MD. Chemical Kinetics Div.

NEW ELECTRONIC STATES OF NH AND ND OBSERVED BY RESONANCE ENHANCED MULTIPHOTON IONIZATION SPECTROSCOPY c72

Russell D. Johnson, III and Jeffrey W. Hudgens *In* NASA, Goddard Space Flight Center, First International Conference on Laboratory Research for Planetary Atmospheres May 1990 p 164-167 (For primary document see N90-26744 20-91)
Avail: NTIS HC A21/MF A03 CSCL 20H

Resonance Enhanced MultiPhoton Ionization (REMPI) spectra of NH and ND, which reveal four new electronic states are presented. Transitions from NH a 1 delta to 3s and 3p Rydberg states in both NH and ND have been observed and rotationally analyzed. The transitions were observed in the wavelength range of 258 to 288 nm. The state assignments are: e 1 pi (3s sigma) at 82857/cm, f 1 pi (3p sigma) at 86378/cm, g 1 delta (3p pi) at 88141/cm and h 1 sigma (3p pi) at 89151/cm. Author

N90-26761*# National Aeronautics and Space Administration. Goddard Space Flight Center, Greenbelt, MD.

INTRACAVITY DYE-LASER ABSORPTION SPECTROSCOPY (IDLAS) FOR APPLICATION TO PLANETARY MOLECULES

Todd M. Lang (Maryland Univ., College Park.) and John E. Allen, Jr. *In its* First International Conference on Laboratory Research for Planetary Atmospheres May 1990 p 168-172 (For primary document see N90-26744 20-91)
Avail: NTIS HC A21/MF A03 CSCL 03B

Time-resolved, quasi-continuous wave, intracavity dye-laser absorption spectroscopy is applied to the investigation of absolute

absorption coefficients for vibrational-rotational overtone bands of water at visible wavelengths. Emphasis is placed on critical factors affecting detection sensitivity and data analysis. Typical generation-time dependent absorption spectra are given. Author

N90-26762*# Missouri Univ., Saint Louis. Dept. of Chemistry.
METHANE OVERTONE ABSORPTION BY INTRACAVITY LASER SPECTROSCOPY
James J. OBrien *In* NASA, Goddard Space Flight Center, First International Conference on Laboratory Research for Planetary Atmospheres May 1990 p 173-177 (For primary document see N90-26744 20-91)
Avail: NTIS HC A21/MF A03 CSCL 03B

Interpretation of planetary methane (CH4) visible-near IR spectra, used to develop models of planetary atmospheres, has been hampered by a lack of suitable laboratory spectroscopic data. The particular CH4 spectral bands are due to intrinsically weak, high overtone-combination transitions too complex for classical spectroscopic analysis. The traditional multipass cell approach to measuring spectra of weakly absorbing species is insufficiently sensitive to yield reliable results for some of the weakest CH4 absorption features and is difficult to apply at the temperatures of the planetary environments. A time modulated form of intracavity laser spectroscopy (ILS), has been shown to provide effective absorption pathlengths of 100 to 200 km with sample cells less than 1 m long. The optical physics governing this technique and the experimental parameters important for obtaining reliable, quantitative results are now well understood. Quantitative data for CH4 absorption obtained by ILS have been reported recently. Illustrative ILS data for CH4 absorption in the 619.7 nm and 681.9 nm bands are presented. New ILS facilities at UM-St. Louis will be used to measure CH4 absorption in the 700 to 1000 nm region under conditions appropriate to the planetary atmospheres. Author

N90-26763*# California Inst. of Tech., Pasadena. Geological and Planetary Sciences Div.
CHEMICAL KINETICS AND MODELING OF PLANETARY ATMOSPHERES
Yuk L. Yung *In* NASA, Goddard Space Flight Center, First International Conference on Laboratory Research for Planetary Atmospheres May 1990 p 181-209 (For primary document see N90-26744 20-91)
(Grant NAGw-1509)
Avail: NTIS HC A21/MF A03 CSCL 03B

A unified overview is presented for chemical kinetics and chemical modeling in planetary atmospheres. The recent major advances in the understanding of the chemistry of the terrestrial atmosphere make the study of planets more interesting and relevant. A deeper understanding suggests that the important chemical cycles have a universal character that connects the different planets and ultimately link together the origin and evolution of the solar system. The completeness (or incompleteness) of the data base for chemical kinetics in planetary atmospheres will always be judged by comparison with that for the terrestrial atmosphere. In the latter case, the chemistry of H, O, N, and Cl species is well understood. S chemistry is poorly understood. In the atmospheres of Jovian planets and Titan, the C-H chemistry of simple species (containing 2 or less C atoms) is fairly well understood. The chemistry of higher hydrocarbons and the C-N, P-N chemistry is much less understood. In the atmosphere of Venus, the dominant chemistry is that of chlorine and sulfur, and very little is known about C1-S coupled chemistry. A new frontier for chemical kinetics both in the Earth and planetary atmospheres is the study of heterogeneous reactions. The formation of the ozone hole on Earth, the ubiquitous photochemical haze on Venus and in the Jovian planets and Titan all testify to the importance of heterogeneous reactions. It remains a challenge to connect the gas phase chemistry to the production of aerosols. Author

N90-26764*# Catholic Univ. of America, Washington, DC. Dept. of Chemistry.
KINETICS AND THERMOCHEMISTRY OF POLYATOMIC FREE RADICALS: NEW RESULTS AND NEW UNDERSTANDINGS **c25**
David Gutman and Irene R. Slagle *In* NASA, Goddard Space Flight Center, First International Conference on Laboratory Research for Planetary Atmospheres May 1990 p 210-220 Sponsored in part by DOE and NSF (For primary document see N90-26744 20-91)
Avail: NTIS HC A21/MF A03 CSCL 07D

An experimental facility for the study of the chemical kinetics of polyatomic free radicals is described which consists of a heatable tubular reactor coupled to a photoionization mass spectrometer. Its use in different kinds of chemical kinetic studies is also discussed. Examples presented include studies of the C2H3 + O2, C2H3 + HC1, CH3 + O, and CH3 + CH3 reactions. The heat of formation of C2H3 was obtained from the results of the study of the C2H3 + HC1 reaction. Author

N90-26765*# Howard Univ., Washington, DC. Dept. of Chemistry.
THE HEAT OF FORMATION OF CN RADICALS AND RADIATIVE LIFETIMES OF THE A 1 SIGMA - STATE OF C2N2 **c25**
Samuel A. Barts, Karen V. Pinnex, and Joshua B. Halpern *In* NASA, Goddard Space Flight Center, First International Conference on Laboratory Research for Planetary Atmospheres May 1990 p 221-226 Sponsored in part by DOE; Danforth Foundation; and Department of Education (For primary document see N90-26744 20-91)
(Grant NAG5-785)
Avail: NTIS HC A21/MF A03 CSCL 07D

Radiative lifetimes have been measured for the stable vibrational levels of the A 1 sigma - electronic state of C2N2. They range from 1.3 microsec for the 4(sub 0)(sup 1) level to 0.66 microsec for the 1(sub 0)(sup 1) 4(sub 0)(sup 1) level and in general decrease with increasing vibrational excitation. Self-quenching rate constants range from gas kinetic to ten times that. Foreign gas quenching rates are slower. Observation of emission from the 1(sub 0)(sup 1) 4(sub 0)(sup 1) level sets a lower limit for the heat of formation of CN of 439.11 kJ/mol. Author

N90-26766*# National Inst. of Standards and Technology, Gaithersburg, MD. Chemical Kinetics Div.
A LABORATORY INVESTIGATION OF THE PRODUCTION AND PROPERTIES OF MOLECULAR AND RADICAL SPECIES PERTINENT TO PLANETARY ATMOSPHERES
Askar Fahr, John Herron, and Allan H. Laufer (Department of Energy, Washington, DC.) *In* NASA, Goddard Space Flight Center, First International Conference on Laboratory Research for Planetary Atmospheres May 1990 p 227-231 (For primary document see N90-26744 20-91)
Avail: NTIS HC A21/MF A03 CSCL 03B

Vinylidene (H2C=C) is shown to be the largest photodecomposition channel in the direct photolysis of both C2H2 and C2H4. The chemistry of H2C=C as it relates to planetary atmospheres is discussed. The vinyl radical (C2H3), important in the acetylene chemistry cycle, has been directly observed spectroscopically and the kinetics of several key reactions of this species measured. Author

N90-26767*# Pittsburgh Univ., PA. Dept. of Physics and Astronomy.
DISSOCIATIVE RECOMBINATION OF MOLECULAR IONS WITH ELECTRONS **c72**
Rainer Johnsen *In* NASA, Goddard Space Flight Center, First International Conference on Laboratory Research for Planetary Atmospheres May 1990 p 232-236 (For primary document see N90-26744 20-91)
(Grants NAGw-1764; NGL-39-0110137)
Avail: NTIS HC A21/MF A03 CSCL 20H

An overview is presented for the present state of the art of

laboratory measurements of the dissociative recombination of molecular ions with electrons. Most work has focussed on obtaining rates and their temperature dependence, as these are of primary interest for model calculations of ionospheres. A comparison of data obtained using the microwave afterglow method, the flowing afterglow technique, and the merged beam technique shows that generally the agreement is quite good, but there are some serious discrepancies, especially in the case of H(3+) recombination, that need to be resolved. Results of some earlier experimental work need to be reexamined in the light of more recent developments. Such cases are pointed out and a compilation of rate coefficients that have withstood scrutiny is presented. Recent advances in experimental methods, such as the use of laser-in-duced fluorescence, make it possible to identify some neutral products of dissociative recombination. What has been done so far and what results one might expect from future work are briefly reviewed. Author

N90-26768*# National Aeronautics and Space Administration. Goddard Space Flight Center, Greenbelt, MD.

RATE CONSTANT FOR REACTION OF ATOMIC HYDROGEN WITH GERMANE

David F. Nava, Walter A. Payne, George Marston, and Louis J. Stief *In its* First International Conference on Laboratory Research for Planetary Atmospheres May 1990 p 237-243 (For primary document see N90-26744 20-91)

Avail: NTIS HC A21/MF A03 CSCL 03B

Due to the interest in the chemistry of germane in the atmospheres of Jupiter and Saturn, and because previously reported kinetic reaction rate studies at 298 K gave results differing by a factor of 200, laboratory measurements were performed to determine the reaction rate constant for H + GeH4. Results of the study at 298 K, obtained via the direct technique of flash photolysis-resonance fluorescence, yield the reaction rate constant, k = (4.08 + or - 0.22) x 10(exp -12) cu cm/s. Author

N90-26769*# National Aeronautics and Space Administration. Goddard Space Flight Center, Greenbelt, MD.

ROLE OF THE METHYLENE AMIDOGEN (H2CN) RADICAL IN THE ATMOSPHERES OF TITAN AND JUPITER

F. L. Nesbitt, G. Marston, and L. J. Stief *In its* First International Conference on Laboratory Research for Planetary Atmospheres May 1990 p 244-248 (For primary document see N90-26744 20-91)

Avail: NTIS HC A21/MF A03 CSCL 03B

The methylene amidogen (H2CN) radical can be shown to be an important intermediate in models for the formation of HCN (via N + CH3) and the recombination of H to H2 (via H + HCN) on Titan as well as in models for the formation of HCN (via NH2 + C2H3) in the atmosphere of Jupiter. Experiments in our laboratory in a discharge flow system with mass spectrometric detection of both reactants and products have established that the major product channel (90 percent for the reaction N + CH3 is that leading to H2CN + H. The same result was obtained for N + CD3 yields D2CN + D. The rate constant for the reaction D + D2CN yields DCN + D2 was measured for the first time and k(298 K) greater than 7 x 10(exp -11) cu cm/s was found. The same result was obtained for the H atom reaction. This is the final step in the reaction sequence leading to HCN on both Titan and Jupiter and to formation of H2 from H on Titan. The first measurement of the ionization potentials for H2CN and D2CN was also made. From electron impact studies I.P. = (9.6 + or - 1.0) eV was obtained for both radicals. An upperlimit of I.P. less than 11.6 eV came from observations of the H2CN radical by photoionization mass spectrometry using an Ar resonance lamp (106.7 nm). Further photoionization experiments are planned using synchrotron radiation plus monochromator as a tunable vacuum UV light source. Author

N90-26770*# National Aeronautics and Space Administration. Goddard Space Flight Center, Greenbelt, MD.

LABORATORY MEASUREMENTS AND METHANE PHOTOCHEMISTRY MODELING

P. N. Romani (Science Systems and Applications, Inc., Seabrook, MD.) *In its* First International Conference on Laboratory Research for Planetary Atmospheres May 1990 p 249-254 (For primary document see N90-26744 20-91)

(Contract NAS5-30134)

Avail: NTIS HC A21/MF A03 CSCL 03B

Methane is photolyzed by the solar UV in the stratosphere of Saturn. Subsequent photochemistry leads to the production of acetylene (C2H2) and diacetylene (C4H2). These species are produced where it is relatively warm (T is greater than or equal to 140 K), but the tropopause temperature of Saturn (approximately 80 K) is low enough that these two species may freeze out to their respective ices. Numerical models which include both photochemistry and condensation loss make predictions about the mixing ratios of these species and haze production rates. These models are dependent upon knowing reaction pathways and their associated kinetic reaction rate constants and vapor pressures. How uncertainties in the chemistry and improvements in the vapor pressures affect model predictions for Saturn are discussed. Author

N90-26771*# Colorado Univ., Boulder. Dept. of Chemistry and Biochemistry.

UV AND VUV SPECTROSCOPY AND PHOTOCHEMISTRY OF SMALL MOLECULES IN A SUPERSONIC JET **c72**

E. Ruehl (Freie Univ., Berlin, Germany, F.R.) and V. Vaida *In* NASA, Goddard Space Flight Center, First International Conference on Laboratory Research for Planetary Atmospheres May 1990 p 255-259 Sponsored in part by NSF; Petroleum Research Fund; and Deutsche Forschungsgemeinschaft (For primary document see N90-26744 20-91)

Avail: NTIS HC A21/MF A03 CSCL 20H

UV and VUV absorption and emission spectroscopy is used to probe jet cooled molecules, free radicals, and clusters in the gas phase. Due to efficient cooling inhomogeneous effects on spectral line widths are eliminated. Therefore from these spectra, both structural and dynamical information is obtained. The photoproducts of these reactions are probed by resonance enhanced multiphoton ionization. Author

N90-26772*# California Univ., Davis. Dept. of Chemistry.

LABORATORY STUDIES OF PHOTODISSOCIATION PROCESSES RELEVANT TO THE FORMATION OF COMETARY RADICALS **c90**

R. S. Urdahl, Y. Bao, and W. M. Jackson *In* NASA, Goddard Space Flight Center, First International Conference on Laboratory Research for Planetary Atmospheres May 1990 p 260-264 (For primary document see N90-26744 20-91)

(Grant NAGw-903)

Avail: NTIS HC A21/MF A03 CSCL 03B

The strength of the C2(d 3 Pi g yields a 3 Pi u) Swan band emission in the spectra of cometary comae identifies this species as a prominent constituent of the coma gas. It was previously suggested that the formation of cometary C2 proceeds via the secondary photolysis of the C2H radical. The detection of C2H in the interstellar medium and the recent analysis of the radial variation in C2(delta V=O) surface brightness of Comet Halley support the postulate that C2 is a third-generation molecule. Measurement of the C2 and C2H translational energy distributions produced from the multiphoton dissociation (MPD) of acetylene at 193 nm are identified . Time-resolved FTIR emission studies of the nascent C2H radical formed in the C2H2 yields C2H + H reaction verify that this species is produced both vibrationally and electronically excited. A survey of the internal energy distributions of the C2 fragments produced from the MPD of acetylene using a high intensity ArF laser is currently in progress in the laboratory. Recent experiments have focused on the measurement of rotational energy distribution for the C2(A 1 Pi u, a 3 Pi u) fragments. The C2(a 3 Pi u) detection capability is currently being improved by performing this experiment in a molecular beam, thus allowing for discrimination between initial emission and laser-induced fluorescence (LIF). Although the experiments performed to date provide considerable evidence in support of C2H yields C2 + H reaction, there is an

important distinction to be made when comparing the laboratory conditions to those typically found in comets. The C2H radicals generated in the laboratory experiments are formed vibrationally and/or electronically excited. Any rotationally/vibrationally excited C2H present in cometary comae will quickly undergo radiative relaxation in the infrared to their lowest rotational and vibrational state. Experiments are currently under way to confirm the cometary formation of C2 via the VUV dissociation of cold C2H. Author

N90-26773*# Max-Planck-Inst. fuer Chemie, Mainz (Germany, F.R.).

THE APPLICATIONS OF CHEMICAL THERMODYNAMICS AND CHEMICAL KINETICS TO PLANETARY ATMOSPHERES RESEARCH

Bruce Fegley, Jr. *In* NASA, Goddard Space Flight Center, First International Conference on Laboratory Research for planetary Atmospheres May 1990 p 267-302 (For primary document see N90-26744 20-91)

Avail: NTIS HC A21/MF A03 CSCL 03B

A review of the applications of chemical thermodynamics and chemical kinetics to planetary atmospheres research during the past four decades is presented with an emphasis on chemical equilibrium models and thermochemical kinetics. Several current problems in planetary atmospheres research such as the origin of the atmospheres of the terrestrial planets, atmosphere-surface interactions on Venus and Mars, deep mixing in the atmospheres of the gas giant planets, and the origin of the atmospheres of outer planet satellites all require laboratory data on the kinetics of thermochemical reactions for their solution. Author

N90-26774*# Cornell Univ., Ithaca, NY. Lab. for Planetary Studies.

LIQUID-VAPOR EQUILIBRIUM OF MULTICOMPONENT CRYOGENIC SYSTEMS **c25**

W. Reid Thompson, Jorge C. G. Calado (Instituto Superior Tecnico, Lisbon, Portugal), and John A. Zollweg *In* NASA, Goddard Space Flight Center, First International Conference on Laboratory Research for Planetary Atmospheres May 1990 p 303-326 (For primary document see N90-26744 20-91)

(Grant NAGw-1444)

Avail: NTIS HC A21/MF A03 CSCL 07D

Liquid-vapor and solid-vapor equilibria at low to moderate pressures and low temperatures are important in many solar system environments, including the surface and clouds of Titan, the clouds of Uranus and Neptune, and the surfaces of Mars and Triton. The familiar cases of ideal behavior are limiting cases of a general thermodynamic representation for the vapor pressure of each component in a homogeneous multicomponent system. The fundamental connections of laboratory measurements to thermodynamic models are through the Gibbs-Duhem relation and the Gibbs-Helmholtz relation. Using laboratory measurements of the total pressure, temperature, and compositions of the liquid and vapor phases at equilibrium, the values of these parameters can be determined. The resulting model for vapor-liquid equilibrium can then conveniently and accurately be used to calculate pressures, compositions, condensation altitudes, and their dependencies on changing climatic conditions. A specific system being investigated is CH4-C2H6-N2, at conditions relevant to Titan's surface and atmosphere. Discussed are: the modeling of existing data on CH4-N2, with applications to the composition of Titan's condensate clouds; some new measurements on the CH4-C2H6 binary, using a high-precision static/volumetric system, and on the C2H6-N2 binary, using the volumetric system and a sensitive cryogenic flow calorimeter; and describe a new cryogenic phase-equilibrium vessel with which we are beginning a detailed, systematic study of the three constituent binaries and the ternary CH4-C2H6-N2 system at temperatures ranging from 80 to 105 K and pressures from 0.1 to 7 bar. Author

N90-26775*# National Aeronautics and Space Administration. Ames Research Center, Moffett Field, CA.

OPTICAL CONSTANTS OF SOLID METHANE **c25**

Bishun N. Khare, W. R. Thompson, C. Sagan, E. T. Arakawa, C. Bruel, J. P. Judish, R. K. Khanna (Maryland Univ., College Park.), and J. B. Pollack *In* NASA, Goddard Space Flight Center, First International Conference on Laboratory Research for Planetary Atmospheres May 1990 p 327-339 (For primary document see N90-26744 20-91)

(Contract NGR-33-010-220; NGR-33-010-082; NAGw-637; DE-AC05-84OR-21400)

Avail: NTIS HC A21/MF A03 CSCL 07D

Methane is the most abundant simple organic molecule in the outer solar system bodies. In addition to being a gaseous constituent of the atmospheres of the Jovian planets and Titan, it is present in the solid form as a constituent of icy surfaces such as those of Triton and Pluto, and as cloud condensate in the atmospheres of Titan, Uranus, and Neptune. It is expected in the liquid form as a constituent of the ocean of Titan. Cometary ices also contain solid methane. The optical constants for both solid and liquid phases of CH4 for a wide temperature range are needed for radiative transfer calculations, for studies of reflection from surfaces, and for modeling of emission in the far infrared and microwave regions. The astronomically important visual to near infrared measurements of solid methane optical constants are conspicuously absent from the literature. Preliminary results are presented on the optical constants of solid methane for the 0.4 to 2.6 micrometer region. Deposition onto a substrate at 10 K produces glassy (semi-amorphous) material. Annealing this material at approximately 33 K for approximately 1 hour results in a crystalline material as seen by sharper, more structured bands and negligible background extinction due to scattering. The constant k is reported for both the amorphous and the crystalline (annealed) states. Typical values (at absorption maxima) are in the .001 to .0001 range. Below lambda = 1.1 micrometers the bands are too weak to be detected by transmission through the films less than or equal to 215 micrometers in thickness, employed in the studies to date. Using previously measured values of the real part of the refractive index, n, of liquid methane at 110 K, n is computed for solid methane using the Lorentz-Lorenz relationship. Work is in progress to extend the measurements of optical constants n and k for liquid and solid to both shorter and longer wavelengths, eventually providing a complete optical constants database for condensed CH4. Author

N90-26776*# Cornell Univ., Ithaca, NY. Lab. for Planetary Studies.

OPTICAL CONSTRAINTS OF KEROGEN FROM 0.15 TO 40 MICRONS: COMPARISON WITH METEORITIC ORGANICS **c25**

Bishun N. Khare, W. R. Thompson, C. Sagan, E. T. Arakawa, C. Meisse, and I. Gilmour (Chicago Univ., IL.) *In* NASA, Goddard Space Flight Center, First International Conference on Laboratory Research for Planetary Atmospheres May 1990 p 340-356 Sponsored in part by Norris (Kenneth T. and Eileen L.) Foundation (For primary document see N90-26744 20-91)

(Contract NAG9-52; NGR-33-010-101; DE-AC05-84OR-21400; NSF EAR-86-09218)

Avail: NTIS HC A21/MF A03 CSCL 07D

Kerogens are dark, complex organic materials produced on the Earth primarily by geologic processing of biologic materials, but kerogens have chemical and spectral similarities to some classes of highly processed extraterrestrial organic materials. Kerogen-like solids were proposed as constitutents of the very dark reddish surfaces of some asteroids and are also spectrally similar to some carbonaceous organic residues and the lapetus dark material. Kerogen can thus serve as a useful laboratory analog to very dark, spectrally red extraterrestrial materials; its optical constants can be used to investigate the effects of particle size, void space and mixing of bright and dark components in models of scattering by dark asteroidal, cometary, and satellite surfaces. Measurements of the optical constants of both Type 2 kerogen and of macromolecular organic residue from the Murchison carbonaceous chondrite via transmission and reflection measurements on thin films are reported. The real part of the refractive index, n, is determined by variable incidence-angle reflectance to be 1.60 + or - 0.05 from 0.4 to 2.0 micrometers

wavelength. Work extending the measurement of n to longer wavelengths is in progress. The imaginary part of the refractive index, k, shows substantial structure from 0.15 to 40 micrometers. The values are accurate to + or - 20 percent in the UV and IR regions and to + or - 30 percent in the visible. The k values of organic residues were also measured from the Murchison meteorite. Comparison of the kerogen and Murchison data reveals that between 0.15 and 40 microns, Murchison has a similar structure but no bands as sharp as in kerogen, and that the k values for Murchison are significantly higher than those of kerogen. Author

N90-26777*# National Aeronautics and Space Administration. Goddard Space Flight Center, Greenbelt, MD.
VAPOR PRESSURES OF ACETYLENE AT LOW TEMPERATURES **c25**
C. M. Masterson, John E. Allen, Jr., G. F. Kraus, and R. K. Khanna (Maryland Univ., College Park.) *In its* First International Conference on Laboratory Research for Planetary Atmospheres May 1990 p 357-362 (For primary document see N90-26744 20-91)
Avail: NTIS HC A21/MF A03 CSCL 07D

The atmospheres of many of the outer planets and their satellites contain a large number of hydrocarbon species. In particular, acetylene (C2H2) has been identified at Jupiter, Saturn and its satellite Titan, Uranus and Neptune. In the lower atmospheres of these planets, where colder temperatures prevail, the condensation and/or freezing of acetylene is probable. In order to obtain accurate models of the acetylene in these atmospheres, it is necessary to have a complete understanding of its vapor pressures at low temperatures. Vapor pressures at low temperatures for acetylene are being determined. The vapor pressures are measured with two different techniques in order to cover a wide range of temperatures and pressures. In the first, the acetylene is placed in a sample tube which is immersed in a low temperature solvent/liquid nitrogen slush bath whose temperature is measured with a thermocouple. The vapor pressure is then measured directly with a capacitance manometer. For lower pressures, a second technique which was called the thin-film infrared method (TFIR) was developed. It involves measuring the disappearance rate of a thin film of acetylene at a particular temperature. The spectra are then analyzed using previously determined extinction coefficient values, to determine the disappearance rate R (where R = delta n/delta t, the number of molecules that disappear per unit time). This can be related to the vapor pressure directly. This technique facilitates measurement of the lower temperatures and pressures. Both techniques have been calibrated using CO2, and have shown good agreement with the existing literature data. Author

N90-26778*# Virginia Univ., Charlottesville. Dept. of Nuclear Engineering and Engineering Physics.
LABORATORY STUDIES OF THE INTERACTION OF IONS WITH CONDENSED GASES: PLANETARY APPLICATIONS
J. W. Boring and R. E. Johnson *In* NASA, Goddard Space Flight Center, First International Conference on Laboratory Research for Planetary Atmospheres May 1990 p 365-385 (For primary document see N90-26744 20-91)
Avail: NTIS HC A21/MF A03 CSCL 03B

The work described is concerned with laboratory studies of the processes that produce the ejection of molecules from the surfaces of condensed gas solids, the change in the chemistry of the surface materials, and the relationship of these results to processes occurring in the solar system. Included is a discussion of the experimental techniques employed in making these laboratory measurements. Author

N90-26779*# Jet Propulsion Lab., California Inst. of Tech., Pasadena.
ELECTRON-IMPACT SPECTROSCOPY **c72**
S. Trajmar *In* NASA, Goddard Space Flight Center, First International Conference on Laboratory Research for Planetary Atmospheres May 1990 p 386-398 (For primary document see N90-26744 20-91)
Avail: NTIS HC A21/MF A03 CSCL 20H

The methods of electron impact spectroscopy and cross section measurements are discussed and compared to optical spectroscopy. A brief summary of the status of this field and the available data is given. Author

N90-26780*# Georgia Univ., Athens. Dept. of Chemistry.
OPTICAL SIGNATURES OF MOLECULAR PARTICLES VIA MASS-SELECTED CLUSTER SPECTROSCOPY **c72**
Michael A. Duncan *In* NASA, Goddard Space Flight Center, First International Conference on Laboratory Research for Planetary Atmospheres May 1990 p 399-404 (For primary document see N90-26744 20-91)
Avail: NTIS HC A21/MF A03 CSCL 20H

A new molecular beam apparatus was developed to study optical absorption in cold (less than 100 K) atomic clusters and complexes produced by their condensation with simple molecular gases. In this instrument, ionized clusters produced in a laser vaporization nozzle source are mass selected and studied with photodissociation spectroscopy at visible and ultraviolet wavelengths. This new approach can be applied to synthesize and characterize numerous particulates and weakly bound complexes expected in planetary atmospheres and in comets. Author

N90-26781*# National Aeronautics and Space Administration. Goddard Space Flight Center, Greenbelt, MD.
STUDY OF THE POLYOXYMETHYLENE AND ITS SPUTTERED FRAGMENTS: IMPLICATIONS FOR COMETS **c90**
Marla H. Moore (Maryland Univ., College Park.) and Toshihiko Tanabe *In its* First International Conference on Laboratory Research for Planetary Atmospheres May 1990 p 405-410 (For primary document see N90-26744 20-91)
Avail: NTIS HC A21/MF A03 CSCL 03B

Laboratory mass spectra of sputtered polyoxymethylene (POM) reveals a fragmentation pattern consistent with observed peaks in the PICCA experiment on board the Giotto spacecraft. Both commercially available POM and radiation synthesized POM have been used in the studies. Synthesized POM was identified using infrared absorption spectra after proton irradiation of H2CO ice on silicate grains at 20 K. Laboratory results suggest that similar type sputtering is a possible mechanism for removing species from comet grains. Author

N90-26782*# Erlangen-Nuremberg Univ. (Germany, F.R.).
PROTON IRRADIATION OF SIMPLE GAS MIXTURES: INFLUENCE OF IRRADIATION PARAMETERS
Norbert J. Sack, R. Schuster, and A. Hofmann *In* NASA, Goddard Space Flight Center, First International Conference on Laboratory Research for Planetary Atmospheres May 1990 p 411-413 (For primary document see N90-26744 20-91)
Avail: NTIS HC A21/MF A03 CSCL 03B

In order to get information about the influence of irradiation parameters on radiolysis processes of astrophysical interest, methane gas targets were irradiated with 6.5 MeV protons at a pressure of 1 bar and room temperature. Yields of higher hydrocarbons like ethane or propane were found by analysis of irradiated gas samples using gas chromatography. The handling of the proton beam was of great experimental importance for determining the irradiation parameters. In a series of experiments current density of the proton beam and total absorbed energy were shown to have a large influence on the yields of produced hydrocarbons. Mechanistic interpretations of the results are given and conclusions are drawn with regard to the chemistry and the simulation of various astrophysical systems. Author

N90-26783*# California Univ., Los Angeles. Space Sciences Center.
PHOTON SPUTTERING OF H2O ICES: A PRELIMINARY REPORT **c72**
C. Y. Robert Wu and D. L. Judge *In* NASA, Goddard Space Flight Center, First International Conference on Laboratory

Research for Planetary Atmospheres May 1990 p 414-419
(For primary document see N90-26744 20-91)
Avail: NTIS HC A21/MF A03 CSCL 20H

A preliminary measurement of the total yields of ejected ions and electrons from H2O ices has been carried out using the He I 584 A resonance line as the incident photon beam. The H2O ices were prepared at 77 K in an ultrahigh vacuum system. The total yield of the ejected ion species and electrons was determined to be 8.8x10(exp -5) and 4.2x10(exp -4), respectively. Author

N90-26784*# Arizona Univ., Tucson. Lunar and Planetary Lab.
INVESTIGATION OF THE SATURN DUST ENVIRONMENT FROM THE ANALYSIS OF ENERGETIC CHARGED PARTICLE MEASUREMENTS Final Technical Report, Jan. - Dec. 1989
L. L. Hood 1989 33 p
(Grant NAG2-576)
(NASA-CR-186727; NAS 1.26:186727) Avail: NTIS HC A03/MF A01 CSCL 03B

In order to assist the Cassini project in evaluating risks of collisions with particulate matter in the rotational equatorial plane, available Pioneer 11 and Voyager energetic charged particle data were reinvestigated to constrain the column mass density of absorbing material within several radial ranges. Within the orbit of Mimas, CRAND proton phase space densities maximize near 2.67 R sub s and exhibit secondary maximum at 2.43 R sub s. From the condition that sources must exceed losses near these maxima and using available theoretical models for CRAND proton production rates, upper bounds on the column mass density at these two radial locations are calculated. Detailed fits of radial diffusion models to the observed flux maxima yield somewhat more restrictive upper limits. The upper limits compare to a lower limit on the column mass density, estimated from previous model calculations by Van Allen. Aside from continuous rings, longitudinally limited, low optical depth clouds of particulates may exist in orbit with several of the inner satellites including Mimas and Enceladus. A brief review of Voyager energetic particle microsignatures that suggest the presence of material co-orbiting with these two satellites is presented. Finally, Pioneer 11 and Voyager measurements of low energy electron fluxes exhibit minima near the location of the tenuous E Ring centered on approx. 4 R sub s. Pioneer 11 pitch angle distributions appear to support the possibility that direct absorption by Ring E particulates produced the observed flux decreases. Author

92 SOLAR PHYSICS

Includes solar activity, solar flares, solar radiation and sunspots.

For related information see *93 Space Radiation.*

N90-26785*# National Aeronautics and Space Administration. Marshall Space Flight Center, Huntsville, AL.
NONPOTENTIAL MAGNETIC FIELDS AT SITES OF GAMMA RAY FLARES
M. J. Hagyard, P. Venkatakrishnan, and J. B. Smith, Jr. (Alabama A & M Univ., Huntsville.) [1988] 18 p Submitted for publication Sponsored in part by AFGL
(NASA-TM-103493; NAS 1.15:103493) Avail: NTIS HC A03/MF A01 CSCL 03B

The relation between the degree of nonpotentiality of photospheric magnetic fields and the occurrence of gamma ray flares is examined. The parameter delta phi (magnetic shear) and the strength of the magnetic field intensity are used as measures of the degree of nonpotentiality, where delta phi is defined as the angular difference between the observed direction of the transverse component of the photospheric field and the direction of the potential field prescribed by the distribution of measured photospheric flux. An analysis of the great flare of April 24 to 25, 1984 is presented as an example of this technique to quantify the nonpotential characteristics of the pre-flare magnetic field. For this flare, which produced a large gamma ray event, strong shear and high field strengths prevailed over an extended length of the magnetic neutral line where the flare occurred. Moreover, the flare began near the area of strongest measured shear (89 to 90 deg). Four other flaring regions were analyzed; one of these produced a moderate gamma ray event while the other three did not produce detectable gamma rays. For all four regions the flares were located in the area where the field was not nonpotential, regardless of the class of flare. The fields of the gamma ray flares were compared with those associated with the flares without gamma rays, and little distinction was found in the degree of magnetic shear. The major difference is seen in the extent of the sheared field: for gamma ray events, the field is sheared over a longer length of the neutral line. Author

93 SPACE RADIATION

Includes cosmic radiation; and inner and outer earth's radiation belts.

For biological effects of radiation see *52 Aerospace Medicine.* For theory see *73 Nuclear and High-Energy Physics.*

N90-26786# Lawrence Livermore National Lab., CA. Inst. for Geophysics and Planetary Physics.
RADIO LOUD FAR-INFRARED GALAXIES
Arjun Dey, Joseph C. Shields (California Univ., Berkeley.), and Wil J. M. VanBreugel Mar. 1990 7 p Submitted for publication
(Contract W-7405-eng-48)
(DE90-012993; UCRL-JC-103406) Avail: NTIS HC A02/MF A01

The first results are presented of a multiwavelength study of IRAS galaxies with excess radio emission. The sample was selected by cross correlating the IRAS Faint Source Survey. and the Point Source Catalogue with the Texas radio survey. Recent optical (imaging and spectroscopic) and radio (VLA) observations are discussed. These observations will be used to investigate possible connections between radio galaxy activity, star formation and galaxy interactions. DOE

N90-26787# Lawrence Livermore National Lab., CA.
A SITE FOR THE ASTROPHYSICAL GAMMA RAY PROCESS
W. Michael Howard, Bradley S. Meyer, and Stanford E. Woosley (California Univ., Santa Cruz.) Apr. 1990 8 p Presented at the International Symposium on Nuclear Astrophysics: Nuclei in the Cosmos, Vienna, Austria, 18-22 Jun. 1990
(Contract W-7405-eng-48)
(DE90-013473; UCRL-JC-104223; CONF-9006212-1) Avail: NTIS HC A02/MF A01

The origin of the proton-rich isotopes of the heavy elements in nature has been studied for over thirty years. Specifically, the p-isotopes are those stable nuclear isotopes with mass number 74 (approx. less than) A that lie on the proton-rich side of the valley of beta-stability and are bypassed by the neutron capture chains that are thought responsible for producing the bulk of the heavy elements. A leading model for the origin of the p-isotopes involves transmuting heavy elements into lighter p-isotopes via a series of nuclear photodisintegrations involving (gamma,n), (gamma,p) and (gamma, alpha) reactions. Such a model, called the gamma-process, is quite successful in reproducing the bulk of the rare p-isotopes if one assumes a solar-system distribution of heavy elements, temperatures in the range 2.0 (approx. less than) T(sub 9) (approx. less than) 3.0 and a hydrodynamical expansion timescale of order 1 sec. Such thermodynamic conditions occur quite naturally when the neon-oxygen layers of massive stars (M greater than 10M(sub 0)) undergo type II supernovae explosions. However, a major failure of this model is that the solar-system abundance pattern of some light p-isotopes is not well reproduced due to a lack of sufficient seeds with A greater than 96. Enhancing the heavy elements with prior s-processing during core helium burning is insufficient because the peak of such a s-process distribution is only near A = 80. Proton captures play no role in the gamma-process because in the neon-oxygen rich layer the proton mass density is too low to induce captures on the relevant

timescales. However, neutron captures may slightly modify the distribution. It is proposed that the requisite thermodynamic conditions may also occur in Type Ia supernovae, when carbon-oxygen white dwarfs explode by deflagration. DOE

99 GENERAL

N90-26788# Advisory Group for Aerospace Research and Development, Neuilly-Sur-Seine (France).
AGARD HIGHLIGHTS 90/1
Mar. 1990 57 p
Copyright Avail: NTIS HC A04/MF A01; Non-NATO Nationals requests available only from AGARD/Scientific Publications Executive

Progress made in AGARD programs is reported. Topics addressed include: the Turkish defense industry; Turkish aviation and the aeronautical industry; structures and materials in the 90s; the collaborative role of AGARD in recent advances in rotorcraft system identification; and new defense research document policy. B.G.

N90-26789*# National Aeronautics and Space Administration. Lewis Research Center, Cleveland, OH.
THE LESSONS OF VARSOVIAN'S RECONNAISSANCE
D. J. Bents Jun. 1990 27 p Presented at the Case for Mars 4, Boulder, CO, 4-8 Jun. 1990; sponsored in part by JPL, NASA Ames Research Center, NASA Johnson Space Center, NASA Marshall Space Flight Center, American Astronautical Society, LANL, and Planetary Society
(NASA-TM-103207; E-5615; NAS 1.15:103207) Avail: NTIS HC A03/MF A01 CSCL 05D

The role played by advanced technology is illustrated with respect to the anticipated era of discovery and exploration (in space): how bold new exploration initiatives may or may not be enabled. Enabling technology makes the mission feasible. To be truly enabling, however, the technology must not only render the proposed mission technically feasible, but also make it viable economically; that is, low enough in cost (relative to the economy supporting it) that urgent national need is not required for justification, low enough that risks can be programmatically tolerated. An allegorical parallel is drawn to the Roman Empire of the second century AD, shown to have possessed by that time the necessary knowledge, motivation, means, and technical capability of mounting, through the use of innovative mission planning, an initiative similar to Columbus' voyage. They failed to do so; not because they lacked the vision, but because their technology was not advanced enough to make it an acceptable proposition economically. Speculation, based on the historical perspective, is made on the outcome of contemporary plans for future exploration showing how they will be subjected to the same historical forces, within limits imposed by the state of technology development, that shaped the timing of that previous era of discovery and exploration. Author

Typical Subject Index Listing

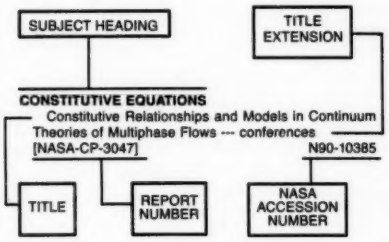

The subject heading is a key to the subject content of the document. Titles, report numbers, and accession numbers of pertinent documents are provided under each subject heading. When the title is insufficiently descriptive of the document content, a title extension has been added, separated from the title by three hyphens. The report number helps to indicate the type of document cited (e.g., NASA report, NASA translation, NASA contractor report). The NASA accession number is the number by which the document abstracts are arranged in this journal and by which the document is sold or requested. The titles, with title extensions if present, are arranged under each subject heading in ascending accession number order. The subject headings have been selected from the latest revision of the *NASA Thesaurus* (NASA SP-7064).

A

ABLATION
Ellipsometric study of YBa2Cu3O(7-x) laser ablated and co-evaporated films
[NASA-TM-103223] N90-26682

ABRASION
Aeolian removal of dust from radiator surfaces on Mars
[NASA-TM-103205] N90-26068

ABRASIVES
Erosion mechanisms in composite materials and ripple formation mechanism in erosion
[IAR-89-4-PT-2] N90-26079

ABSORPTION CROSS SECTIONS
Photodissociation of O2 in the stratosphere and mesosphere: A general parametrization of the Schumman-Runge Bands N90-26427
Absolute vacuum ultraviolet photoabsorption cross section studies of atomic and molecular species: Techniques and observational data N90-26754
High resolution, low temperature photoabsorption cross-section of C2H2 with application to Saturn's atmosphere N90-26757

ABSORPTION SPECTRA
Soft x ray resist characterization: Studies with a laser plasma x ray source
[DE90-013493] N90-26661

ABSORPTION SPECTROSCOPY
Temperature and OH concentrations in a solid propellant flame using absorption techniques
[AD-A222591] N90-26100
Intracavity Dye-Laser Absorption Spectroscopy (IDLAS) for application to planetary molecules N90-26761
Methane overtone absorption by intracavity laser spectroscopy N90-26762

ABSORPTIVITY
Laboratory measurements of microwave and millimeter-wave properties of planetary constituents N90-26745
Laboratory measurements and modeling of microwave absorption by ammonia in gas mixtures applicable to giant planet atmospheres N90-26750

ABSTRACTS
Proceedings of the Second Symposium on GPS Applications in space, volume 1
[AD-A219978] N90-25962
Proceedings of the Second Symposium on GPS Applications in Space, volume 2
[AD-A219979] N90-25963
Press abstracts of the 21st Lunar and Planetary Science Conference
[NASA-CR-186874] N90-26738

ACCELERATION (PHYSICS)
Vibration test procedures for orbiter sidewall-mounted payloads, phase 2
[AD-A220774] N90-26038
Viking data analysis
[AD-A222609] N90-26062
DURIP: Instrumentation for laser switched power LINAC
[AD-A222629] N90-26318
Absolute measurements of gravity
[AD-A222731] N90-26629

ACCESS CONTROL
Multiple-access techniques for communication over dispersive radio channels N90-26196
Packet radio network concepts for the Norwegian field army N90-26206

ACCIDENTS
Arctic cold weather medicine and accidental hypothermia
[AD-A223090] N90-26487

ACCURACY
NASA project status reports: Congressional requirements can be met, but reliability must be ensured
[GAO/NSIAD-90-40] N90-26169
Earth Radiation Budget Experiment (ERBE) validation
[NASA-TM-103481] N90-26433

ACETYL COMPOUNDS
Heterogeneous transformation of peroxyacetylnitrate N90-26430

ACETYLENE
Laboratory studies, analysis, and interpretation of the spectra of hydrocarbons present in planetary atmospheres including cyanoacetylene, acetylene, propane, and ethane N90-26748
High resolution, low temperature photoabsorption cross-section of C2H2 with application to Saturn's atmosphere N90-26757
Laboratory studies of photodissociation processes relevant to the formation of cometary radicals N90-26772
Vapor pressures of acetylene at low temperatures N90-26777

ACOUSTIC ATTENUATION
A preliminary study of the masking of wind turbine noise by ambient sound
[FFA-TN-1990-01] N90-26636

ACOUSTIC DUCTS
Canonical eigenvalues. Part 1: General theory
[AD-A222812] N90-26617

ACOUSTIC EMISSION
Study on failure modes of boron fiber reinforced aluminum composite materials by AE method, part 2
[DE90-505522] N90-26086
Application and extension of an analytical model of the confined acoustic beam generated by a transducer
[AD-A222994] N90-26639

ACOUSTIC PROPERTIES
Aerodynamic loads and blade vortex interaction noise prediction
[ISL-PU-310/89] N90-25942
Asymptotic modal analysis and statistical energy analysis
[NASA-CR-186732] N90-26634

ACOUSTICS
Creating a VAPEPS database: A VAPEPS tutorial
[NASA-CR-186629] N90-26705

ACOUSTO-OPTICS
Acousto-optic signature analysis for inspection of the orbiter thermal protection tile bonds
[DE90-013089] N90-26043

ACRYLATES
Mass spectrometry of poly(methyl methacrylate)s of low molecular weight N90-26091

ACTIVATION (BIOLOGY)
Dynamical solvent effects on electron-transfer processes: Recent progress and perspectives
[AD-A222603] N90-26101

ACTIVE CONTROL
Design and implementation of robust decentralized control laws for the ACES structure at Marshall Space Flight Center
[NASA-CR-4310] N90-26046

ACTUATORS
Simulated dynamic response of a servovalve controlled hydraulic actuator
[NASA-TM-101644] N90-26167
Fluid-loop reaction system
[NASA-CASE-NPO-17204-1-CU] N90-26292

ADA (PROGRAMMING LANGUAGE)
Application of artificial intelligence to the architectural synthesis of VLSI integrated circuits
[ETN-90-97253] N90-26589

ADAPTATION
Nonlinear modeling of time series using Multivariate Adaptive Regression Splines (MARS)
[AD-A222710] N90-26623

ADAPTIVE CONTROL
Beam rider for an Articulated Robot Manipulator (ARM) accurate positioning of long flexible manipulators
[NASA-CR-185151] N90-26581
Temperature and melt solid interface control during crystal growth
[NASA-CR-186731] N90-26664

ADDITION RESINS
Condensation polyimides
[NASA-TM-103487] N90-26129

ADENOSINE TRIPHOSPHATE
Experiment K-6-10. Effects of zero gravity on myofibril protein content and isomyosin distribution in rodent skeletal muscle N90-26464

ADHESION TESTS
Resistivity, adhesive strength, and residual stress measurements of thin film metallizations on single crystal quartz
[DE90-011902] N90-26135
Renewed aging control of adhesion of inhibitor on the gas generator charges for RB 24
[FOA-C-20780-2.1] N90-26153

ADHESIVE BONDING
Static and fatigue strength of an adhesive bonded CFRP butt-strap joint: The effects of stacking sequence and temperature
[NLR-TR-88036-U] N90-26370

ADHESIVES
Molecular structure of interphases between DGEBA/BTDA adhesives and silver substances using surface-enhanced Raman scattering
[AD-A222750] N90-26157

ADJOINTS
Automated sensitivity analysis with the Gradient Enhanced Software System (GRESS)
[DE90-011291] N90-26529

ADSORPTION
The application of HREELS to model catalysts: CO and C2H4 adsorption on Pt/Al2O3
[AD-A222744] N90-26103
Exact results for the structured liquid-solid interface
[AD-A222762] N90-26630

ADVANCED LAUNCH SYSTEM (STS)
Trajectory optimization for an asymmetric launch vehicle
[NASA-CR-185630] N90-26033
Multimegawatt space nuclear power supply, phase 1. Volume 2: Phase 2 plan D180-30619-6
[DE90-012431] N90-26645

AERIAL PHOTOGRAPHY
Automatic line network extraction from aerial imagery of urban areas through knowledge based image analysis
[AD-A222675] N90-26385
AEROACOUSTICS
Aeroacoustics of advanced propellers
[NASA-TM-103137] N90-26635
AEROASSIST
Guidance and control strategies for aerospace vehicles
[NASA-CR-186878] N90-26013
Project SPARC: Space-based aeroassisted reusable craft
[NASA-CR-186816] N90-26051
AEROBRAKING
Guidance and control strategies for aerospace vehicles
[NASA-CR-186878] N90-26013
The effect of interplanetary trajectory options on a manned Mars aerobrake configuration
[NASA-TP-3019] N90-26036
Project SPARC: Space-based aeroassisted reusable craft
[NASA-CR-186816] N90-26051
The aerobraking space transfer vehicle
[NASA-CR-186819] N90-26053
AERODYNAMIC BRAKES
Preliminary subsystem designs for the Assured Crew Return Vehicle (ACRV), volume 1
[NASA-CR-186677-VOL-1] N90-26039
AERODYNAMIC CHARACTERISTICS
Prediction methodologies for nonlinear aerodynamic characteristics of control surfaces
[NIAR-90-17] N90-25937
Effect of tail size reductions on longitudinal aerodynamic characteristics of a three surface F-15 model with nonaxisymmetric nozzles
[NASA-TP-3036] N90-25938
Identification of aerodynamic models for maneuvering aircraft
[NASA-CR-186630] N90-25943
Technical evaluation report on the Fluid Dynamics Panel Symposium on Computational Methods for Aerodynamic Design (Inverse) and Optimization
[AGARD-AR-267] N90-25947
Computation of viscous aerodynamic characteristics of 2-D airfoils for helicopter applications
[NLR-MP-88052-U] N90-25951
The role of computational fluids dynamics in missile aerodynamics
[NLR-MP-88072-U] N90-25952
Effect of vortex generators on the aerodynamic wing characteristics and body of revolution
[AD-A222813] N90-25955
Transatmospheric vehicle research
[NASA-CR-186705] N90-25970
AERODYNAMIC CONFIGURATIONS
AM-X high incidence trials, development and results
[ETN-90-97277] N90-26016
AERODYNAMIC DRAG
Application of laminar flow control to supersonic transport configurations
[NASA-CR-181917] N90-25944
AERODYNAMIC HEATING
A brief review of some mechanisms causing boundary layer transition at high speeds
[NASA-TM-102834] N90-25945
Space plane model for visual measurement of aerodynamic heating
[DE90-505514] N90-25949
A computational study of the effectiveness of coating materials for KE projectile fins subjected to the combined effects of inbore and aerodynamic heating
[AD-A222595] N90-26155
AERODYNAMIC INTERFERENCE
A contribution to the improvement of the accuracy in the parameter identification of nonlinear processes, by example of the aircraft motion
[ETN-90-96961] N90-25974
AERODYNAMIC LOADS
Aerodynamic loads and blade vortex interaction noise prediction
[ISL-PU-310/89] N90-25942
Identification of aerodynamic models for maneuvering aircraft
[NASA-CR-186630] N90-25943
Formation of design envelope criterion in terms of deterministic spectral procedure
[RAE-TM-SS-9] N90-25953
An in-flight interaction of the X-29A canard and flight control system
[NASA-TM-101718] N90-25973
AERODYNAMIC NOISE
A preliminary study of the masking of wind turbine noise by ambient sound
[FFA-TN-1990-01] N90-26636
AERODYNAMICS
An unsteady lifting surface method for single rotation propellers
[NASA-CR-4302] N90-25940
Identification of aerodynamic models for maneuvering aircraft
[NASA-CR-186630] N90-25943
Computational fluid dynamics for missiles
[RAE-TM-AERO-2171] N90-26288
AEROELASTICITY
Structural dynamics branch research and accomplishments
[NASA-TM-102488] N90-26373
AERONAUTICAL ENGINEERING
Combustion in the gas turbine. Part 1: Combustor types and design
[CIT/SME/VKI/RS/1] N90-25986
AEROSOLS
Atmospheric correction of thematic mapping measurements about seabeds of the German Bay
[GKSS-89/E/47] N90-26029
Characterization of biogenic aerosol particles from the Amazon Basin during dry and wet season N90-26418
Development of eye-safe lidar for aerosol measurements
[NASA-CR-186905] N90-26503
AEROSPACE ENGINEERING
Materials and structures for 2000 and beyond: An attempted forecast by the DLR Materials and Structures Department
[ESA-TT-1154-REV] N90-26173
NASA Patent Abstracts Bibliography: A continuing bibliography. Section 2: Indexes (supplement 37)
[NASA-SP-7039(37)-SECT-2] N90-26700
AEROSPACE ENVIRONMENTS
Comparison of currents predicted by NASCAP/LEO model simulations with elementary Langmuir-type bare probe models for an insulated cable containing a single pinhole
[NASA-TM-102486] N90-26054
Experiment K-6-09. Morphological and biochemical investigation of microgravity-induced nerve and muscle breakdown. Part 1: Investigation of nerve and muscle breakdown during spaceflight; Part 2: Biochemical analysis of EDL and PLT muscles N90-26463
Automation of closed environments in space for human comfort and safety
[NASA-CR-186834] N90-26500
AEROSPACE INDUSTRY
Winged cargo return vehicle. Volume 1: Conceptual design
[NASA-CR-186823] N90-26050
AEROSPACE PLANES
Space plane model for visual measurement of aerodynamic heating
[DE90-505514] N90-25949
Background, current status, and prognosis of the ongoing slush hydrogen technology development program for the NASP
[NASA-TM-103220] N90-26055
Prediction of the ullage gas thermal stratification in a NASP vehicle propellant tank experimental simulation using FLOW-3D
[NASA-TM-103217] N90-26160
AEROSPACE SYSTEMS
Low-gravity fluid physics: A program overview
[NASA-TM-103215] N90-26273
Bidirectional drive and brake mechanism
[NASA-CASE-MSC-21540-1] N90-26342
NASA aerospace flight battery systems program
[NASA-TM-103237] N90-26397
Pilot interaction with automated airborne decision making systems
[NASA-CR-186730] N90-26492
Preliminary designs for 25 kWe advanced Stirling conversion systems for dish electric applications
[NASA-TM-103188] N90-26729
AEROSPACE VEHICLES
PDWAP: A preliminary design and weights analysis program for aerospace vehicles
[AD-A222614] N90-25979
Guidance and control strategies for aerospace vehicles
[NASA-CR-186878] N90-26013
AEROTHERMOCHEMISTRY
Results from the IVL TOR Station at Roervik, Sweden. A contribution to the EURATRAC subproject TOR N90-26415
AEROTHERMODYNAMICS
Experimental aerothermodynamic research of hypersonic aircraft
[NASA-CR-186903] N90-25954
Structural Mechanics Division research and technology plans for FY 1990 and accomplishments for FY 1989
[NASA-TM-102654] N90-26361
AGING (MATERIALS)
Second Annual International Conference on Aging Aircraft
[AD-A222715] N90-25961
Effect of casting procedures and diesel engine environment on the behavior of aluminum titanate
[AD-A223079] N90-26126
Renewed aging control of adhesion of inhibitor on the gas generator charges for RB 24
[FOA-C-20780-2.1] N90-26153
AGREEMENTS
The International Space Station: The legal framework N90-26716
The partnership concept and international management N90-26717
The International Space Station: Conditions of access and use N90-26718
The manned national space station: International legal considerations N90-26720
Crossborder movements: Goods, personnel and technologies N90-26722
Space law put to the test by the International Space Station N90-26727
AIR BAG RESTRAINT DEVICES
Human factors: The human interface with aircraft interiors
[NIAR-90-18] N90-26496
AIR LAND INTERACTIONS
The applications of chemical thermodynamics and chemical kinetics to planetary atmospheres research N90-26773
AIR POLLUTION
Catching our breath: Next steps for reducing urban ozone
[PB90-130451] N90-26398
Measurements of tropospheric nitric acid over the Western United States and Northeastern Pacific Ocean
[NASA-TM-103470] N90-26399
Results from global tropospheric sulphur simulations N90-26413
AIR QUALITY
Pollutants: Production and methods of reduction
[CIT/SME/VKI/RS/6] N90-25990
AIR SAMPLING
Terpene concentrations and emissions in a Scots pine forest N90-26422
AIR TRAFFIC CONTROL
Aviation safety: Serious problems continue to trouble the air traffic control work force. Report to congressional requesters
[GAO/RCED-89-112] N90-25959
The disturbance processes on the data links of the mode-S air traffic control system
[ETN-90-96960] N90-25965
Mobile satellite communications for civil aviation
[NLR-MP-88068-U] N90-26238
A measurement of the effectiveness of the Airway Science Program to meet Federal Aviation Administration work force needs
[NIAR-90-5] N90-26694
AIR TRAFFIC CONTROLLERS (PERSONNEL)
Aviation safety: Conditions within the air traffic control work force. Fact sheet for congressional requesters
[GAO/RCED-89-113FS] N90-25958
Aviation safety: Serious problems continue to trouble the air traffic control work force. Report to congressional requesters
[GAO/RCED-89-112] N90-25959
A measurement of the effectiveness of the Airway Science Program to meet Federal Aviation Administration work force needs
[NIAR-90-5] N90-26694
AIR WATER INTERACTIONS
Measurements of tropospheric nitric acid over the Western United States and Northeastern Pacific Ocean
[NASA-TM-103470] N90-26399
Mariners Weather Log, volume 33, number 2, Spring 1989
[PB90-146838] N90-26443
Mariners Weather Log, volume 33, number 3, Summer 1989
[PB90-146846] N90-26444
Mariners Weather Log, volume 33, number 4, Fall 1989
[PB90-146853] N90-26445
AIRBORNE EQUIPMENT
Analysis and improved design considerations for airborne pulse Doppler radar signal processing in the detection of hazardous windshear
[NASA-CR-186792] N90-26448
Aircraft measurements of the turbulence structure in cirrus clouds
[ISSN-0069-5882] N90-26450

AIRCRAFT ACCIDENTS
Computational crash dynamics. Project 1.2: Computational crash dynamics analysis
[IAR-89-19] N90-25956
AIRCRAFT COMPARTMENTS
Human factors: The human interface with aircraft interiors
[NIAR-90-18] N90-26496
AIRCRAFT CONFIGURATIONS
Feasibility study for a microwave-powered ozone sniffer aircraft, volume 2
[NASA-CR-186676] N90-25967
AIRCRAFT CONSTRUCTION MATERIALS
Towards 2000: The composite engine
[PNR90646] N90-26000
The impact and requirements of new materials on aeroengines
[PNR90671] N90-26003
Metal matrix composites and powder processing for aero-engine applications
[PNR90617] N90-26087
Materials and structures for 2000 and beyond: An attempted forecast by the DLR Materials and Structures Department
[ESA-TT-1154-REV] N90-26173
Material selection and design: An expert system approach
[PNR90611] N90-26544
AGARD highlights 90/1 N90-26788
AIRCRAFT CONTROL
An investigation of the use of singular perturbation methods and modal control theory in the derivation or aircraft control schemes
[MATHS-REPT-A-106] N90-26014
AIRCRAFT DESIGN
Prediction methodologies for nonlinear aerodynamic characteristics of control surfaces
[NIAR-90-17] N90-25937
Technical evaluation report on the Fluid Dynamics Panel Symposium on Computational Methods for Aerodynamic Design (Inverse) and Optimization
[AGARD-AR-267] N90-25947
Formation of design envelope criterion in terms of deterministic spectral procedure
[RAE-TM-SS-9] N90-25953
Feasibility study for a microwave-powered ozone sniffer aircraft, volume 2
[NASA-CR-186676] N90-25967
Global Sentry: NASA/USRA high altitude reconnaissance aircraft design, volume 2
[NASA-CR-186820-VOL-2] N90-25971
A contribution to the economic, optimal dimensioning, and shaping of aircraft structures using a design model
[ETN-90-96966] N90-25976
Towards 2000: The composite engine
[PNR90646] N90-26000
Prediction of rotating disc flow and heat transfer in gas turbine engines
[PNR90650] N90-26001
A computer module used to calculate the horizontal control surface size of a conceptual aircraft design
[NASA-CR-186872] N90-26515
AIRCRAFT ENGINES
Stage 2 re-engining: The only way to achieve a real stage 3 aircraft
[PNR90636] N90-25977
Towards 2000: The composite engine
[PNR90646] N90-26000
Prediction of rotating disc flow and heat transfer in gas turbine engines
[PNR90650] N90-26001
Prediction and measurement of rotor blade/stator vane dynamic characteristics of a modern aero-engine axial compressor
[PNR90667] N90-26002
The impact and requirements of new materials on aeroengines
[PNR90671] N90-26003
Aircraft exhaust emissions: An engine manufacturer's perspective
[PNR90675] N90-26004
Handbook of uncertainty methodology for engine testing at Pyestock (England)
[RAE-TM-P-1179] N90-26007
Metal matrix composites and powder processing for aero-engine applications
[PNR90617] N90-26087
NDT in aerospace: The next decade (1990's)
[PNR90628] N90-26348
Elevated temperature crack growth
[NASA-CR-182247] N90-26355
Bringing aircraft noise testing down to Earth
[PNR90642] N90-26637
AIRCRAFT FUELS
Study of high-speed civil transports. Summary
[NASA-CR-4236] N90-25966
AIRCRAFT HAZARDS
A NASA/university/industry consortium for research on aircraft ice protection
[IAR-89-18] N90-25969
AIRCRAFT INSTRUMENTS
Qualitative evaluation of a conformal velocity vector display for use at high angles-of-attack in fighter aircraft
[NASA-TM-102629] N90-25981
AIRCRAFT MAINTENANCE
Second Annual International Conference on Aging Aircraft
[AD-A222715] N90-25961
Robotic-aided system for inspection of aging aircraft
[NIAR-90-9] N90-26346
AIRCRAFT MODELS
Prediction methodologies for nonlinear aerodynamic characteristics of control surfaces
[NIAR-90-17] N90-25937
Wind tunnel study of wake downwash behind A 6 percent scale model B1-B aircraft
[DE90-011783] N90-25941
AIRCRAFT NOISE
High speed turboprop aeroacoustic study (counterrotation). Volume 1: Model development
[NASA-CR-185241] N90-26633
Bringing aircraft noise testing down to Earth
[PNR90642] N90-26637
AIRCRAFT PERFORMANCE
Handbook of uncertainty methodology for engine testing at Pyestock (England)
[RAE-TM-P-1179] N90-26007
AIRCRAFT PILOTS
Biodynamic simulations of an aircraft pilot/passenger in various crash environments
[NIAR-90-6] N90-26494
AIRCRAFT RELIABILITY
Second Annual International Conference on Aging Aircraft
[AD-A222715] N90-25961
AIRCRAFT SAFETY
Aviation safety: Conditions within the air traffic control work force. Fact sheet for congressional requesters
[GAO/RCED-89-113FS] N90-25958
Aviation safety: Serious problems continue to trouble the air traffic control work force. Report to congressional requesters
[GAO/RCED-89-112] N90-25959
AIRCRAFT SPIN
AM-X high incidence trials, development and results
[ETN-90-97277] N90-26016
AIRCRAFT STRUCTURES
Computational crash dynamics. Project 1.2: Computational crash dynamics analysis
[IAR-89-19] N90-25956
A contribution to the economic, optimal dimensioning, and shaping of aircraft structures using a design model
[ETN-90-96966] N90-25976
Mechanical paint removal techniques for aircraft structures
[NIAR-90-12] N90-26166
Materials and structures for 2000 and beyond: An attempted forecast by the DLR Materials and Structures Department
[ESA-TT-1154-REV] N90-26173
Neural networks for detecting defects in aircraft structures
[IAR-90-4] N90-26345
AIRCRAFT WAKES
Wind tunnel study of wake downwash behind A 6 percent scale model B1-B aircraft
[DE90-011783] N90-25941
AIRFOILS
Computation of viscous aerodynamic characteristics of 2-D airfoils for helicopter applications
[NLR-MP-88052-U] N90-25951
On central-difference and upwind schemes
[NASA-CR-182061] N90-26595
AIRLINE OPERATIONS
Stage 2 re-engining: The only way to achieve a real stage 3 aircraft
[PNR90636] N90-25977
ALGEBRA
Application of symbolic computations to the constitutive modeling of structural materials
[NASA-TM-103225] N90-26384
Principles of FP2: Term algebras for specification of parallel machines
[RR-789-I-IMAG-98-LIFIA] N90-26571
Mathematical problem-solving transfer: The effects of cognitive load and attention a schema acquisition and rule automation N90-26594
Unification and disunification: Theory and applications
[ETN-90-97247] N90-26610
Applied mathematical modules for use in a linear algebra service course
[AD-A222814] N90-26618
ALGORITHMS
Supersonic combustor modeling N90-25992
Guidance and targeting for the strategic target system
[DE90-005239] N90-26031
The origin of poorly conditioned susceptibility matrix within inverse CVM algorithm in the case of Pd(sub 3)V: A comparison to the case of Ni(sub 3)V
[DE90-012464] N90-26110
Application of inertial instruments for DSN antenna pointing and tracking N90-26224
Implementation of an algorithm for travelling-wave-based directional detection
[EUT-89-E-214] N90-26239
Modeling, simulation, and analysis of optical remote sensing systems
[NASA-CR-186648] N90-26376
A hybrid M-algorithm/sequential decoder for convolutional and trellis codes
[NASA-CR-186863] N90-26528
Automated sensitivity analysis with the Gradient Enhanced Software System (GRESS)
[DE90-011291] N90-26529
ANTIPASTO: An interactive mesh generator and preprocessor for two-dimensional analysis programs
[DE90-011755] N90-26530
Parallel processors and nonlinear structural dynamics algorithms and software
[NASA-CR-186755] N90-26536
An angular weighting approach for calculating gradients and divergences
[DE90-013164] N90-26539
Efficient generalized conjugate gradient algorithms. Part 2: Implementation
[MATHS-REPT-A-118-PT-2] N90-26543
A parallel algorithm for surface plane intersection
[IMAG-RR-794-M] N90-26549
Study of a class of non convex optimization algorithms: Implementation and applications
[ETN-90-97241] N90-26552
Adaptive and comparative studies of optimization algorithms: Implementations and applications
[ETN-90-97243] N90-26553
Parallel programming with algorithmic skeletons
[DE90-010536] N90-26562
MINAS: An algorithm for systematic state assignment of sequential machines: Computational aspects and results
[EUT-89-E-217] N90-26566
From network to artwork: Automatic schematic diagram generation
[EUT-89-E-219] N90-26567
Implementation of algorithms used in calculating the tensor product of matrices on a distributed memory machine
[IMAG-RR-786-I] N90-26572
Parallel algorithm for distributed memory computers (applications to matricial algorithms)
[ETN-90-97252] N90-26573
Multilayered neural networks: Learning algorithms, implementation on hypercube machines, applications
[ETN-90-97255] N90-26574
On output deadbeat control of discrete-time multivariable systems
[MATHS-REPT-A-122] N90-26583
Search of primitive polynomials over finite fields
[IMAG-RR-797-M] N90-26607
Unification and disunification: Theory and applications
[ETN-90-97247] N90-26610
Contribution to the study of differential equations and to the differences in the complex field
[ETN-90-97250] N90-26612
Parallel/distributed direct method for solving linear systems
[NASA-TM-103229] N90-26614
Causal distributed breakpoints
[AD-A222613] N90-26622
ALIGNMENT
Alignment positioning mechanism
[NASA-CASE-MSC-21502-1] N90-26341
ALTERNATING DIRECTION IMPLICIT METHODS
A fully implicit ADI method for quasi three-dimensional flows through straight blade rows
[ETN-90-96965] N90-26283
ALUMINATES
Evaluation of room-temperature chloroaluminate molten salts as electrolytes for high energy density batteries
[AD-A223097] N90-26267
ALUMINIDES
Crystal growth and deformation behavior of TiAl aluminides
[DE90-012972] N90-26671
ALUMINUM
Effect of casting procedures and diesel engine environment on the behavior of aluminum titanate
[AD-A223079] N90-26126

ALUMINUM ALLOYS
Erosion mechanisms in composite materials and ripple formation mechanism in erosion
[IAR-89-4-PT-2] N90-26079
The influence of microstructure on the tensile behavior of an aluminum metal matrix composite
[NASA-TM-102694] N90-26082
Investigation of thermo-mechanical effects in silicon carbide Whisker/Al alloy composites
[AD-A222635] N90-26089
A study of the fatigue behavior in scratched samples of Al-Li alloy (2090-T3)
[IAR-89-24] N90-26107
Compendium of material test results on HY-130 and Ti-3Al2V metals in support of United States navy programs
[DE90-011754] N90-26112
Damping capacity of aluminum 6061-indium alloys
[AD-A222602] N90-26124
Fracture toughness and failure mechanisms in commercial 2091 Al-Li sheet at cryogenic temperatures
[AD-A222603] N90-26125
Mechanical paint removal techniques for aircraft structures
[NIAR-90-12] N90-26166
The blunt notch behaviour of metal laminates: ARALL and GLARE
[LR-617] N90-26368
Investigation of crack-closure prediction models for fatigue in aluminium alloy sheet under flight-simulation loading
[LR-619] N90-26369
Crystal growth and deformation behavior of TiAl aluminides
[DE90-012972] N90-26671
ALUMINUM GALLIUM ARSENIDES
Apparatus for the efficient wavelength conversion of laser radiation
[AD-D014506] N90-26305
Application of InAlAs/GaAs superlattice alloys to GaAs solar cells
[DE90-013070] N90-26389
ALUMINUM NITRIDES
Polymeric aluminasilazane precursors for aluminosilicon nitride
[AD-A222755] N90-26158
ALUMINUM OXIDES
The application of HREELS to model catalysts: CO and C2H4 adsorption on Pt/Al2O3
[AD-A222744] N90-26103
The effect of crystal orientation on damage accumulation in chromium-implanted Al2O3
[DE90-012294] N90-26674
AMAZON REGION (SOUTH AMERICA)
Characterization of biogenic aerosol particles from the Amazon Basin during dry and wet season N90-26418
AMBIENCE
A preliminary study of the masking of wind turbine noise by ambient sound
[FFA-TN-1990-01] N90-26636
AMMONIA
Laboratory measurements and modeling of microwave absorption by ammonia in gas mixtures applicable to giant planet atmospheres N90-26750
AMMONIUM PERCHLORATES
RSRM-9 (360L009): Ballistics mass properties
[NASA-CR-183944] N90-26064
AMMUNITION
Video camera system for locating bullet holes in targets at a ballistics tunnel
[NASA-TM-4197] N90-26296
AMORPHOUS MATERIALS
Wear mechanisms of amorphous carbon and zirconia coatings on rigid disk magnetic recording media
[DE90-011053] N90-26133
AMORPHOUS SILICON
Optical properties and transport properties of hydrogenated amorphous silicon
[ETN-90-97215] N90-26656
AMPLIFIERS
DURIP: Instrumentation for laser switched power LINAC
[AD-A222629] N90-26318
AMPLITUDE DISTRIBUTION ANALYSIS
In-band amplitude dispersion on a microwave link N90-26189
AMPLITUDES
Application and extension of an analytical model of the confined acoustic beam generated by a transducer
[AD-A222994] N90-26639
ANALYSIS (MATHEMATICS)
Dynamic jamming of networks
[AD-A223044] N90-26247
Applied mathematical modules for use in a linear algebra service course
[AD-A222814] N90-26618
A closed form solution to HZE propagation
[NASA-TM-103482] N90-26640
ANALYZERS
Dynamic jamming of networks
[AD-A223044] N90-26247
ANGLE OF ATTACK
Qualitative evaluation of a conformal velocity vector display for use at high angles-of-attack in fighter aircraft
[NASA-TM-102629] N90-25981
AM-X high incidence trials, development and results
[ETN-90-97277] N90-26016
ANGLES (GEOMETRY)
Laser radar angular tracking
[AD-A222741] N90-26319
ANHYDRIDES
Molecular structure of interphases between DGEBA/BTDA adhesives and silver substances using surface-enhanced Raman scattering
[AD-A222750] N90-26157
ANISOTROPIC PLATES
Modeling of composite beams and plates for static and dynamic analysis
[NASA-CR-186459] N90-26354
ANISOTROPY
Theory of circular dielectric waveguide with anisotropic sheet cover
[NASA-CR-186883] N90-26235
High speed magneto-resistive random access memory
[NASA-CASE-NPO-17954-1-CU] N90-26519
ANNEALING
Parallelization of an annealing simulation applied to improving tetrahedric grids
[IMAG-RR-796-M] N90-26570
Rapid thermal processing: A study of the silicon oxidation and of the implanted boron activation
[LAAS-90051] N90-26681
Ellipsometric study of YBa2Cu3O(7-x) laser ablated and co-evaporated films
[NASA-TM-103223] N90-26682
ANNUAL VARIATIONS
In-band amplitude dispersion on a microwave link N90-26189
Annual and interannual variations of Earth-emitted radiation based on a 10-year data set
[NASA-TM-103465] N90-26432
ANNULAR FLOW
Decay of secondary flow and the associated loss variation downstream of an annual turbine stator cascade
[DE90-505520] N90-25984
ANTARCTIC REGIONS
Spatial cross-correlation of Antarctic Sea ice and seabed topography
[NASA-CR-186815] N90-26451
Proceedings of a Workshop on Antarctic Meteorite Stranding Surfaces
[NASA-CR-186575] N90-26739
Proceedings of a workshop on Differences Between Antarctic and Non-Antarctic Meteorites
[NASA-CR-184918] N90-26740
ANTENNA ARRAYS
Feasibility study of a synthesis procedure for array feeds to improve radiation performance of large distorted reflector antennas
[NASA-CR-186641] N90-26213
Design of an optically controlled Ka-band GaAs MMIC phased-array antenna
[NASA-TM-103147] N90-26250
ANTENNA DESIGN
Antennas for portable VHF-FM receivers
[BBC-RD-1990/1] N90-26211
Design and performance analysis of the DSS-13 beam waveguide antenna N90-26225
DSS 15, 45, and 65 34-meter high efficiency antenna radio frequency performance enhancement by tilt added to the subreflector during elevation angle changes N90-26229
ANTENNA FEEDS
Design and performance analysis of the DSS-13 beam waveguide antenna N90-26225
ANTENNA RADIATION PATTERNS
Feasibility study of a synthesis procedure for array feeds to improve radiation performance of large distorted reflector antennas
[NASA-CR-186641] N90-26213
Scattering from coated structures and antenna pattern control using impedance surfaces, part A/B
[NASA-CR-186871] N90-26233
ANTENNAS
Structures for remotely deployable precision antennas
[NASA-CR-182065] N90-26061
Antennas for portable VHF-FM receivers
[BBC-RD-1990/1] N90-26211
ANTIBODIES
Experiment K-6-23. Effect of spaceflight on levels and function of immune cells N90-26476
ANTIGENS
Experiment K-6-23. Effect of spaceflight on levels and function of immune cells N90-26476
ANTIMATTER
Confinement of nonneutral plasma in unconventional geometries
[DE90-013048] N90-26659
ANTIREFLECTION COATINGS
Damage measurements on optical materials for use in high-peak-power lasers
[DE90-013489] N90-26314
Laser damage database at 1064 nm
[DE90-013490] N90-26315
APOGEES
Hard start problem of the apogee engine for the ETS-6
[DE90-505525] N90-26072
APPLICATIONS PROGRAMS (COMPUTERS)
Computer aided handling qualities evaluation in frequency domain
[NAL-TM-SE-8902] N90-26523
Tools for distributed application management
[NASA-CR-186627] N90-26535
APPROXIMATION
Computational fluid dynamics for missiles
[RAE-TM-AERO-2171] N90-26288
H-infinity control: An exploratory study
[EUT-88-E-211] N90-26584
Comment on high resolution simulations of cosmic strings. 1: Network evoloution
[NASA-CR-186606] N90-26734
AQUEOUS SOLUTIONS
Passivation of high temperature superconductors
[NASA-CASE-NPO-17949-1-CU] N90-26684
ARC JET ENGINES
Preliminary plume characteristics of an arcjet thruster
[NASA-TM-103241] N90-26071
ARCHITECTURE (COMPUTERS)
Technical evaluation report on the Guidance and Control Panel 49th Symposium on Fault Tolerant Design Concepts for Highly Integrated Flight Critical Guidance and Control Systems
[AGARD-AR-281] N90-26012
OASIS, LLNL version: Software maintenance manual
[DE90-013522] N90-26313
Guidance and control system for an autonomous underwater vehicle
[AD-A222709] N90-26343
Computer architecture evaluation for structural dynamics computations: Project summary
[NASA-CR-186137] N90-26512
Applications for the scalable coherent interface
[DE90-011795] N90-26514
ANTIPASTO: An interactive mesh generator and preprocessor for two-dimensional analysis programs
[DE90-011755] N90-26530
SUPES version 2.1: A Software Utilities Package for the Engineering Sciences
[DE90-011763] N90-26531
Level-2 system: Programmers-users manual
[DE90-013324] N90-26540
Single-pass memory system evaluation for multiprogramming workloads
[NASA-CR-186553] N90-26558
Language support for parallel computation
[AD-A223072] N90-26560
Parallel programming with algorithmic skeletons
[DE90-010536] N90-26562
ATAMM multicomputer operating system functional specification
[NASA-CR-186845] N90-26563
Pacific missile test center information resources management organization (code 0300): The ORACLE client-server and distributed processing architecture
[DE90-013271] N90-26565
Design of a universal protocol system architecture: Specification of functions and services
[EUT-89-E-230] N90-26569
Massively parallel architecture: Integrated cell network for image reconstruction
[ETN-90-97257] N90-26575
Superconcurrent processing: A dynamic approach to heterogeneous parallelism
[AD-A222798] N90-26576
Application of artificial intelligence to the architectural synthesis of VLSI integrated circuits
[ETN-90-97253] N90-26589
High speed all optical networks
[NASA-CR-185311] N90-26649
A methodology for benchmarking distributed database management systems
[DE90-007801] N90-26702
ARCTIC REGIONS
Arctic cold weather medicine and accidental hypothermia
[AD-A223090] N90-26487

ARMOR
Motion sickness, visual displays, and armored vehicle design
[AD-A222678] N90-26506
ARRAYS
A novel multireceiver communications system configuration based on optimal estimation theory
[NASA-CR-186847] N90-26216
ARTIFICIAL INTELLIGENCE
Twilight zones and cornerstones: A gnat robot double feature
[AD-A220026] N90-26326
Guidance and control system for an autonomous underwater vehicle
[AD-A222709] N90-26343
Automatic line network extraction from aerial imagery of urban areas through knowledge based image analysis
[AD-A222675] N90-26385
Grasping with mechanical intelligence
[NASA-CR-186864] N90-26496
ATN design tool
[AD-A223030] N90-26559
Multilayered neural networks: Learning algorithms, implementation on hypercube machines, applications
[ETN-90-97255] N90-26574
A sum rule satisfied by optimized feed-forward layered networks
[RSRE-MEMO-4341] N90-26579
On networks, optimized feature extraction, and the Bayes decision
[RSRE-MEMO-4342] N90-26580
Application of artificial intelligence to the architectural synthesis of VLSI integrated circuits
[ETN-90-97253] N90-26589
Rhetorical structure theory and text analysis
[AD-A222655] N90-26733
ASSEMBLING
Assembly via disassembly: A case in machine perceptual development
[NASA-CR-186867] N90-26497
ASTEROIDS
Optical constraints of kerogen from 0.15 to 40 microns: Comparison with meteoritic organics N90-26776
ASTRONAUTS
Project Exodus
[NASA-CR-186836] N90-26026
Rings of Earth detected by orbital debris radar N90-26232
Human work in space: The astronaut's legal status. Introduction N90-26719
The astronauts' legal status: The International Space Station N90-26721
ASTRONOMICAL MODELS
Nonstandard big bang models
[DE90-625593] N90-26736
Photon sputtering of H2O ices: A preliminary report N90-26783
ASTRONOMY
Reports of planetary astronomy, 1990
[NASA-TM-4205] N90-26730
Astronomy at ultra-high energies: Results from the CYGNUS experiment
[DE90-011979] N90-26732
ASTROPHYSICS
Laboratory studies of photodissociation processes relevant to the formation of cometary radicals N90-26772
Proton irradiation of simple gas mixtures: Influence of irradiation parameters N90-26782
ASYMMETRY
Trajectory optimization for an asymmetric launch vehicle
[NASA-CR-185630] N90-26033
Baryogenesis in extended inflation. 2: Baryogenesis via primordial black holes
[NASA-CR-182843] N90-26735
ASYMPTOTIC METHODS
A critical evaluation of two-equation models for near wall turbulence
[NASA-CR-182068] N90-26270
Variance reduction for quantile estimates in simulations via nonlinear controls
[AD-A222653] N90-26590
Asymptotic optimality of the fast randomized versions of GCV and C(sub L) in ridge regression and regularization
[IMAG-RR-793-M] N90-26606
A study of the asymptotic properties of least square estimators for multiple phase regression problems
[ETN-90-97244] N90-26620
ASYMPTOTIC PROPERTIES
Asymptotic law of the orthogonal empirical functions and applications, part 2
[IMAG-RR-792-M-PT-2] N90-26605
A study of the asymptotic properties of least square estimators for multiple phase regression problems
[ETN-90-97244] N90-26620
ASYMPTOTIC SERIES
Contribution to the study of differential equations and to the differences in the complex field
[ETN-90-97250] N90-26612
Asymptotic analysis of dissipative waves with applications to their numerical simulation
[NASA-TM-103231] N90-26615
Asymptotic modal analysis and statistical energy analysis
[NASA-CR-186732] N90-26634
Application and extension of an analytical model of the confined acoustic beam generated by a transducer
[AD-A222994] N90-26639
ATMOSPHERIC BOUNDARY LAYER
Measurements of tropospheric nitric acid over the Western United States and Northeastern Pacific Ocean
[NASA-TM-103470] N90-26399
ATMOSPHERIC CHEMISTRY
Digital filtering of plume emission spectra
[NASA-TM-103135] N90-26070
Nordic Symposium on Atmospheric Chemistry
[CM-78] N90-26403
Further development and application of an atmospheric chemistry trajectory model N90-26408
Natural and anthropogenic compounds in bulk precipitation at Blidoe (archipelago of Stockholm, Sweden) N90-26409
Some results from the precipitation chemistry measurement programme in Sweden N90-26410
Ice core studies and the past atmospheric environment of polar regions N90-26411
The Renland ice core (Greenland): A source for climatic studies over 100,000 years N90-26412
Results from global tropospheric sulphur simulations N90-26413
The aqueous atmospheric chemistry of mercury N90-26420
Terpene concentrations and emissions in a Scots pine forest N90-26422
The diurnal ozone cycle in a coniferous forest: The importance of meteorology and chemistry N90-26423
Stratospheric chemistry N90-26424
Photodissociation of NO2: Influence of photolysis wavelength and temperature dependence on product formation N90-26426
The collection and analysis of atmospheric peroxides N90-26428
Destruction of peroxy radical by Cu ion catalysed reactions on atmospheric particles N90-26429
Heterogeneous transformation of peroxyacetylnitrate N90-26430
Formation and deactivation of vibrationally excited atmospheric molecules
[AD-A222660] N90-26442
Submillimeter and millimeter observations of solar system objects
[NASA-CR-186836] N90-26731
Absolute vacuum ultraviolet photoabsorption cross section studies of atomic and molecular species: Techniques and observational data N90-26754
Novel laser gain and time-resolved FTIR studies of photochemistry N90-26756
Kinetics and thermochemistry of polyatomic free radicals: New results and new understandings N90-26764
A laboratory investigation of the production and properties of molecular and radical species pertinent to planetary atmospheres N90-26766
The applications of chemical thermodynamics and chemical kinetics to planetary atmospheres research N90-26773
ATMOSPHERIC CIRCULATION
Measurements of CH4, N2O, CO, H2O and O3 in the middle atmosphere by the ATMOS experiment on Spacelab 3
[NASA-TM-103476] N90-26400
The long-term variation of lead-210 in relation to particle-bound sulphur in surface air in Finland N90-26407
Further development and application of an atmospheric chemistry trajectory model N90-26408
ATMOSPHERIC COMPOSITION
Measurements of CH4, N2O, CO, H2O and O3 in the middle atmosphere by the ATMOS experiment on Spacelab 3
[NASA-TM-103476] N90-26400
The global consequences of increasing tropospheric ozone concentrations
[NASA-TM-103477] N90-26401
Nordic Symposium on Atmospheric Chemistry
[CM-78] N90-26403
Further development and application of an atmospheric chemistry trajectory model N90-26408
The Renland ice core (Greenland): A source for climatic studies over 100,000 years N90-26412
The diurnal ozone cycle in a coniferous forest: The importance of meteorology and chemistry N90-26423
Formation kinetics of N2O in the atmosphere N90-26425
Laboratory measurements of microwave and millimeter-wave properties of planetary constituents N90-26745
Laboratory studies, analysis, and interpretation of the spectra of hydrocarbons present in planetary atmospheres including cyanoacetylene, acetylene, propane, and ethane N90-26748
Infrared spectra of van de Waals complexes of importance in planetary atmospheres N90-26749
ATMOSPHERIC CORRECTION
Atmospheric correction of thematic mapping measurements about seabeds of the German Bay
[GKSS-89/E/47] N90-26029
ATMOSPHERIC EFFECTS
Ionic atmosphere effects on the energetics of thermal and optical electron-exchange reactions: Application to ferrocenium-ferrocene self exchange
[AD-A222605] N90-26441
ATMOSPHERIC ENTRY SIMULATION
The effect of interplanetary trajectory options on a manned Mars aerobrake configuration
[NASA-TP-3019] N90-26036
ATMOSPHERIC MODELS
Verification and improvement of the EMEP model for long-range transport and deposition of pollutants N90-26405
An Eulerian transport model for NO(sub x)-compounds N90-26406
Some results from the precipitation chemistry measurement programme in Sweden N90-26410
Results from global tropospheric sulphur simulations N90-26413
The NASA/MSFC Global Reference Atmospheric Model, 1990 version (GRAM-90)
[NASA-CR-186717] N90-26435
Infrared line parameters at low temperatures relevant to planetary atmospheres N90-26753
Gaussian quadrature exponential sum modeling of near infrared methane laboratory spectra obtained at temperatures from 106 to 297 K N90-26758
Measurements of the methane relaxation times for application to the infrared emission models of the upper atmospheres of outer planets and Titan N90-26759
Chemical kinetics and modeling of planetary atmospheres N90-26763
Liquid-vapor equilibrium of multicomponent cryogenic systems N90-26774
ATMOSPHERIC TEMPERATURE
Photodissociation of NO2: Influence of photolysis wavelength and temperature dependence on product formation N90-26426
ATMOSPHERIC TURBULENCE
Aircraft measurements of the turbulence structure in cirrus clouds
[ISSN-0069-5882] N90-26450
ATOMIC STRUCTURE
One-dimensional sigma-conjugated polysilylenes: Science and technology
[DE90-012902] N90-26146
Soft x ray resist characterization: Studies with a laser plasma x ray source
[DE90-013493] N90-26661
New electronic states of NH and ND observed by resonance enhanced multiphoton ionization spectroscopy N90-26760
Laboratory studies of the interaction of ions with condensed gases: Planetary applications N90-26778
ATOMS
Absolute vacuum ultraviolet photoabsorption cross section studies of atomic and molecular species: Techniques and observational data N90-26754
Rate constant for reaction of atomic hydrogen with germane N90-26768
ATROPHY
Experiment K-6-07. Metabolic and morphologic properties of muscle fibers after spaceflight N90-26461
Experiment K-6-08. Biochemical and histochemical observations of vastus medialis N90-26462
Experiment K-6-09. Morphological and biochemical investigation of microgravity-induced nerve and muscle breakdown. Part 1: Investigation of nerve and muscle breakdown during spaceflight; Part 2: Biochemical analysis of EDL and PLT muscles N90-26463
Experiment K-6-10. Effects of zero gravity on myofibril protein content and isomyosin distribution in rodent skeletal muscle N90-26464
Experiment K-6-11. Actin mRNA and cytochrome c mRNA concentrations in the tricepts brachia muscle of rats N90-26465

Experiment K-6-21. Effect of microgravity on 1) metabolic enzymes of type 1 and type 2 muscle fibers and on 2) metabolic enzymes, neutransmitter amino acids, and neurotransmitter associated enzymes in motor and somatosensory cerebral cortex. Part 1: Metabolic enzymes of individual muscle fibers; part 2: metabolic enzymes of hippocampus and spinal cord N90-26474

ATTACK AIRCRAFT

AM-X high incidence trials, development and results [ETN-90-97277] N90-26016

ATTENTION

Mathematical problem-solving transfer: The effects of cognitive load and attention a schema acquisition and rule automation N90-26594

ATTENUATION

Software set-up for data processing of depolarization due to rain and ice crystals in the Olympus project [EUT-89-E-218] N90-26240

Interaction of electromagnetic signals with particulate clouds [AD-A222804] N90-26244

ATTENUATION COEFFICIENTS

Vapor pressures of acetylene at low temperatures N90-26777

ATTITUDE (INCLINATION)

Molecular dynamics simulations of grain-boundary diffusion for varying tilt angle geometries [DE90-012919] N90-26669

ATTITUDE CONTROL

Fluid-loop reaction system [NASA-CASE-NPO-17204-1-CU] N90-26292

AURORAS

Viking data analysis [AD-A222609] N90-26062

AUSTENITE

The effect of manganese on the onset of the stage 2 reaction in an austempered ductile iron matrix [DE90-011804] N90-26119

AUTOCORRELATION

Pattern classification of textura by moment and distance autocorrelation function [INPE-4976-PRE/1541] N90-26379

Reversed residuals in autoregressive time series analysis [AD-A222711] N90-26624

AUTOMATA THEORY

The bit full-decomposition of sequential machines [EUT-89-E-223] N90-26516

The full-decomposition of sequential machines with the separate realization of the next-state and output functions [EUT-89-E-222] N90-26547

AUTOMATIC CONTROL

Guidance and control system for an autonomous underwater vehicle [AD-A222709] N90-26343

Pilot interaction with automated airborne decision making systems [NASA-CR-186730] N90-26492

Verification-correction of a program for including uncertainties in the robot automatic programming [ETN-90-97246] N90-26588

AUTOMATIC FREQUENCY CONTROL

Tracking performance of a combined Costas/AFC-loop under noisy Rayleigh/Rician channel conditions with additive Gaussian noise jamming [ETN-90-96964] N90-26237

AUTOMATIC PILOTS

Robustness evaluation of H2 and H(infinity) control theory as applied to a transport aircraft [AD-A222795] N90-26018

AUTONOMOUS NAVIGATION

Color image processing for navigation: Two road trackers [AD-A222667] N90-26591

AUTONOMY

Autonomous space processor for orbital debris [NASA-CR-186691] N90-26044

AUTOREGRESSIVE PROCESSES

Strong consistency of the least squares estimator for a non-ergodic threshold autoregressive model [IMAG-RR-791-M] N90-26604

AUXILIARY POWER SOURCES

Advanced Turbine Technology Applications Project (ATTAP) [NASA-CR-185240] N90-26728

AVIONICS

Space Transportation Avionics Technology Symposium. Volume 1: Executive summary [NASA-CP-3081] N90-25980

Biconic cargo return vehicle with an advanced recovery system. Volume 1: Conceptual design [NASA-CR-186520] N90-26052

Equipment feasibility study: Very high frequency communication equipment (136-137 megahertz) [DOT/FAA/CT-TN89/72] N90-26210

AXIAL LOADS

Evaluation of fracture strength properties of silicon carbide ceramics under cyclic/static axial loading at ultra-high temperature [DE90-503402] N90-26147

AXIAL STRESS

High temperature multiaxiale creep testing of Nimonic 115 [RAE-TM-P-1182] N90-26122

AXISYMMETRIC BODIES

The finite analytic method and its applications. Volume 1: Laminar and turbulent flows past two-dimensional and axisymmetric bodies [AD-A222787] N90-26294

AXISYMMETRIC FLOW

Prediction of two-dimensional time-dependent gasdynamic flows for hypersonic studies [UTIAS-335] N90-25935

B

B-1 AIRCRAFT

Wind tunnel study of wake downwash behind A 6 percent scale model B1-B aircraft [DE90-011783] N90-25941

BACKSCATTERING

The 27-28 October 1986 FIRE IFO cirrus case study: Cirrus parameter relationships derived from satellite and lidar data [NASA-TM-103469] N90-26447

Development of eye-safe lidar for aerosol measurements [NASA-CR-186905] N90-26503

BALLISTICS

RSRM-9 (360L009): Ballistics mass properties [NASA-CR-183944] N90-26064

Flight motor set 360L007 (STS-33R) [NASA-CR-183979] N90-26067

Video camera system for locating bullet holes in targets at a ballistics tunnel [NASA-TM-4197] N90-26296

BALLOON-BORNE INSTRUMENTS

Rotating-unbalanced-mass devices and methods for scanning balloon-borne-experiments, free-flying spacecraft, and space shuttle/space station attached experiments [NASA-CASE-MFS-28425-1] N90-26304

BALTIC SEA

Deposition to the Baltic Sea N90-26404

Phytoplankton and its contribution to the atmospheric sulfur budget of northern Europe N90-26417

BAND STRUCTURE OF SOLIDS

Full vector wave calculation of photonic band structures in face-centered cubic dielectric media [AD-A222616] N90-26686

BANDPASS FILTERS

Classification regions in remote sensing imagery utilizing spatial characteristics [INPE-4913-PRE/1514] N90-26381

BARIUM OXIDES

Large, orientation-dependent enhancements of critical currents in Y1Ba2Cu3O(7-x) epitaxial thin films: Evidence for intrinsic flux pinning [DE90-009424] N90-26666

Ellipsometric study of YBa2Cu3O(7-x) laser ablated and co-evaporated films [NASA-TM-103223] N90-26682

BARYONS

Baryogenesis in extended inflation. 2: Baryogenesis via primordial black holes [NASA-CR-182843] N90-26735

BATTERY CHARGERS

Survey of applicability of electric vehicles (EVs) in specific regions such as resorts [DE90-503592] N90-26336

BAYES THEOREM

A Bayesian proportional model for software reliability [IMAG-RR-795-M] N90-26353

On networks, optimized feature extraction, and the Bayes decision [RSRE-MEMO-4342] N90-26580

BAYS (STRUCTURAL UNITS)

Vibration test procedures for orbiter sidewall-mounted payloads, phase 2 [AD-A220774] N90-26038

BCH CODES

A versatile integrated block codes encoder-decoder N90-26197

BEAM WAVEGUIDES

Design and performance analysis of the DSS-13 beam waveguide antenna N90-26225

BEAMS (RADIATION)

Structures for remotely deployable precision antennas [NASA-CR-182065] N90-26061

Application and extension of an analytical model of the confined acoustic beam generated by a transducer [AD-A222994] N90-26639

BEAMS (SUPPORTS)

Damage states in laminated composite three-point bend specimens: An experimental-analytical correlation study [NASA-TM-101800] N90-26083

Modeling of composite beams and plates for static and dynamic analysis [NASA-CR-186459] N90-26354

BEARING (DIRECTION)

Implementation of an algorithm for travelling-wave-based directional detection [EUT-89-E-214] N90-26239

BENDING

Buckling and postbuckling behavior of square compression-loaded graphite-epoxy plates with circular cutouts [NASA-TP-3007] N90-26077

Damage states in laminated composite three-point bend specimens: An experimental-analytical correlation study [NASA-TM-101800] N90-26083

BESSEL FUNCTIONS

Application and extension of an analytical model of the confined acoustic beam generated by a transducer [AD-A222994] N90-26639

Theory of biaxial graded-index optical fiber [NASA-CR-186882] N90-26652

BIBLIOGRAPHIES

Supersonic wind tunnel nozzles: A selected, annotated bibliography to aid in the development of quiet wind tunnel technology [NASA-CR-4294] N90-26019

Technology for large space systems: A bibliography with indexes (supplement 22) [NASA-SP-7046(22)] N90-26056

Aircrew life support systems enhancement [AD-A222626] N90-26505

NASA Patent Abstracts Bibliography: A continuing bibliography. Section 2: Indexes (supplement 37) [NASA-SP-7039(37)-SECT-2] N90-26700

BIDIRECTIONAL REFLECTANCE

Measuring and modeling near-surface reflected and emitted radiation fluxes at the FIFE site [NASA-CR-180953] N90-26378

BIG BANG COSMOLOGY

Nonstandard big bang models [DE90-625593] N90-26736

BINARY CODES

Converses for write-unidirectional memories [EUT-89-E-220] N90-26546

BINDERS (MATERIALS)

Understanding silica binders [PNR90625] N90-26150

BIOCHEMISTRY

Experiment K-6-08. Biochemical and histochemical observations of vastus medialis N90-26462

Experiment K-6-09. Morphological and biochemical investigation of microgravity-induced nerve and muscle breakdown. Part 1: Investigation of nerve and muscle breakdown during spaceflight; Part 2: Biochemical analysis of EDL and PLT muscles N90-26463

Experiment K-6-13. Morphological and biochemical examination of heart tissue. Part 1: Effects of microgravity on the myocardial fine structure of rats flown on Cosmos 1887. Ultrastructure studies. Part 2: Cellular distribution of cyclic ampdependent protein kinase regulatory subunits in heart muscle of rats flown on Cosmos 1887 N90-26467

Experiment K-6-14. Hepatic function in rats after spaceflight N90-26468

Photosynthesis in intact plants [DE90-013699] N90-26482

Computer simulation of chemical reactions in synthetic model compounds and genetically engineered active sites [AD-A222611] N90-26483

BIODYNAMICS

Experiment K-6-02. Biomedical, biochemical and morphological alterations of muscle and dense, fibrous connective tissues during 14 days of spaceflight N90-26456

Biodynamic simulations of an aircraft pilot/passenger in various crash environments [NIAR-90-6] N90-26494

BIOGEOCHEMISTRY

Nordic Symposium on Atmospheric Chemistry [CM-78] N90-26403

BIOLOGICAL EFFECTS

Natural and anthropogenic compounds in bulk precipitation at Blidoe (archipelago of Stockholm, Sweden) N90-26409

Experiment K-6-16. Morphological examination of rat testes. The effect of Cosmos 1887 flight on spermatogonial population and testosterone level in rat testes N90-26469

BIOLOGICAL EVOLUTION
Press abstracts of the 21st Lunar and Planetary Science Conference
[NASA-CR-186874] N90-26738
BIOMASS
Proximate composition of seed and biomass from soybean plants grown at different carbon monoxide (CO2) concentrations
[NASA-TM-103496] N90-26480
BIOSYNTHESIS
Gas exchange characteristics as indicators of the basic limiting factors in photosynthesis
[DE90-012399] N90-26481
BIT ERROR RATE
A versatile integrated block codes encoder-decoder N90-26197
Converses for write-unidirectional memories
[EUT-89-E-220] N90-26546
BIT SYNCHRONIZATION
Propagation Effects and Circuit Performance of Modern Military Radio Systems with Particular Emphasis on Those Employing Bandspreading
[AGARD-CP-442] N90-26178
New synchronisation techniques applicable to multi-tone transmission systems N90-26199
Synchronization of frequency shift transmission and the effect of oversampling N90-26200
New approaches for rapid synchronisation frequency hoppers N90-26201
BLACK HOLES (ASTRONOMY)
Baryogenesis in extended inflation. 2: Baryogenesis via primordial black holes
[NASA-CR-182843] N90-26735
BLADE-VORTEX INTERACTION
Aerodynamic loads and blade vortex interaction noise prediction
[ISL-PU-310/89] N90-25942
BLOCK DIAGRAMS
Large sets of block designs
[ETN-90-97212] N90-26602
BLOOD PRESSURE
Hemodynamic and ADH responses to central blood volume shifts in cardiac-denervated humans
[NASA-TM-103471] N90-26485
BLOOD VOLUME
Hemodynamic and ADH responses to central blood volume shifts in cardiac-denervated humans
[NASA-TM-103471] N90-26485
BLUNT BODIES
Numerical analysis of three-dimensional particle-laden flow equations
[IAR-90-2] N90-26268
BODIES OF REVOLUTION
Effect of vortex generators on the aerodynamic wing characteristics and body of revolution
[AD-A222813] N90-25955
BODY TEMPERATURE
Adjustment and validation of the mathematical prediction model for sweat rate, heart rate, and body temperature under outdoor conditions
[AD-A222599] N90-26486
BONDING
Acousto-optic signature analysis for inspection of the orbiter thermal protection tile bonds
[DE90-013089] N90-26043
Field experience in using laser acoustic sensing for inspection
[DE90-012954] N90-26347
Microwave spectra of van der Waals complexes of importance in planetary atmospheres N90-26752
BONE DEMINERALIZATION
Experiment K-6-04. Trace element balance in rats during spaceflight N90-26458
BONE MARROW
The interaction of polymeric materials with ceramic surfaces with special reference to the behaviour of bioceramics N90-26127
Experiment K-6-23. Effect of spaceflight on levels and function of immune cells N90-26476
BONE MINERAL CONTENT
Effects of microgravity on rat bone, cartilage and connective tissues N90-26454
Experiment K-6-01. Distribution and biochemistry of mineral and matrix in the femurs of rats N90-26455
Experiment K-6-04. Trace element balance in rats during spaceflight N90-26458
Experiment K-6-05. The maturaton of bone and dentin matrices in rats flown on Cosmos 1887 N90-26459
Experiment K-6-27. Analysis of radiographs and biosamples from primate studies N90-26478
BONES
The interaction of polymeric materials with ceramic surfaces with special reference to the behaviour of bioceramics N90-26127
Effects of microgravity on rat bone, cartilage and connective tissues N90-26454
Experiment K-6-02. Biomedical, biochemical and morphological alterations of muscle and dense, fibrous connective tissues during 14 days of spaceflight N90-26456
Experiment K-6-03. Gravity and skeletal growth, part 1. Part 2: Morphology and histochemistry of bone cells and vasculature of the tibia; Part 3: Nuclear volume analysis of osteoblast histogenesis in periodontal ligament cells; Part 4: Intervertebral disc swelling pressure associated with microgravity N90-26457
Experiment K-6-04. Trace element balance in rats during spaceflight N90-26458
Experiment K-6-05. The maturaton of bone and dentin matrices in rats flown on Cosmos 1887 N90-26459
Experiment K-6-06. Morphometric and EM analyses of tibial epiphyseal plates from Cosmos 1887 rats N90-26460
BOOSTER ROCKET ENGINES
PDWAP: A preliminary design and weights analysis program for aerospace vehicles
[AD-A222614] N90-25979
BORON
Effect of boron on intergranular hot cracking in Ni-Cr-Fe superalloys containing niobium
[NASA-CR-186714] N90-26115
Rapid thermal processing: A study of the silicon oxidation and of the implanted boron activation
[LAAS-90051] N90-26681
BORON ALLOYS
Formation of Titanium-boron surface alloys by excimer laser mixing
[DE90-013172] N90-26118
BORON FIBERS
Study on failure modes of boron fiber reinforced aluminum composite materials by AE method, part 2
[DE90-505522] N90-26086
BOUNDARIES
A critical evaluation of two-equation models for near wall turbulence
[NASA-CR-182068] N90-26270
BOUNDARY LAYER CONTROL
Application of laminar flow control to supersonic transport configurations
[NASA-CR-181917] N90-25944
BOUNDARY LAYER SEPARATION
Report of the Fluid Dynamics Panel Working Group 10 on calculation of 3D separate turbulent flows in boundary layer limit
[AGARD-AR-255] N90-26280
BOUNDARY LAYER STABILITY
Effects of forebody geometry on subsonic boundary-layer stability
[NASA-CR-4314] N90-25939
Application of laminar flow control to supersonic transport configurations
[NASA-CR-181917] N90-25944
BOUNDARY LAYER TRANSITION
A brief review of some mechanisms causing boundary layer transition at high speeds
[NASA-TM-102834] N90-25945
An investigation into the numerical prediction of boundary layer transition using the K.Y. Chien turbulence model
[NASA-CR-185252] N90-26269
Effects of 2 Hz imposed bulk flow unsteadiness on laminar-turbulent transition in a straight channel
[AD-A223028] N90-26295
BOUNDARY LAYERS
A brief review of some mechanisms causing boundary layer transition at high speeds
[NASA-TM-102834] N90-25945
BOUSSINESQ APPROXIMATION
On traveling wave solutions of a set of coupled Boussinesq-like equations
[DE90-013182] N90-26597
BRAIN
Experiment K-6-18. Study of muscarinic and gaba (benzodiazepine) receptors in the sensory-motor cortex, hippcampus and spinal code N90-26471
BRAKES (FOR ARRESTING MOTION)
Bidirectional drive and brake mechanism
[NASA-CASE-MSC-21540-1] N90-26342
BRAKING
Preliminary subsystem designs for the Assured Crew Return Vehicle (ACRV), volume 1
[NASA-CR-186677-VOL-1] N90-26039
BRANCHING (MATHEMATICS)
Perturbation methods in the theory of waves and bifurcation phenomena N90-26593
BRAYTON CYCLE
Megawatt solar power systems for lunar surface operations
[NASA-CR-186509] N90-26391
BRIDGMAN METHOD
Temperature and melt solid interface control during crystal growth
[NASA-CR-186731] N90-26664
BRILLOUIN EFFECT
NMR and optical studies of piezoelectric polymers
[DE90-012459] N90-26137
BRITTLENESS
Evaluation of fracture strength properties of silicon carbide ceramics under cyclic/static axial loading at ultra-high temperature
[DE90-503402] N90-26147
Development of ceramic hybrid combustor: Design and combustion test results
[DE90-503442] N90-26149
BROADBAND
Progress and remaining issues in the development of a wideband HF channel model and simulation N90-26182
Broadband analysis of ground wave propagation at a50 to 400 MHz N90-26185
Estimation of the impulse response of a broadband mobile radio channel in suburbia at 910 MHz N90-26187
Wideband characterization of forest propagation channels N90-26188
An experimental medium speed wideband modem N90-26194
BROADCASTING
Texstar: The all-Texas educational satellite system
[NASA-CR-186654] N90-26045
Experimentation of a transmission system data processing by meteor bursts N90-26207
BROKEN SYMMETRY
High temperature x ray diffraction and Landau theory investigations of order-disorder transition in defect NaCl-type solids
[DE90-011807] N90-26673
BUBBLES
Bubble, Drop and Particle Unit (BDPU): A multi-user microgravity facility
[IAF-89-431] N90-26164
BUCKLING
Buckling and postbuckling behavior of square compression-loaded graphite-epoxy plates with circular cutouts
[NASA-TP-3007] N90-26077
A comparison of the post-buckling behavior of metallic and composite plates with centrally located cutouts
[NIAR-90-14] N90-26356
The use of Lanczo's method to solve the large generalized symmetric Eigenvalue problem in parallel
[NASA-CR-182072] N90-26533
BURNING RATE
RSRM-9 (360L009): Ballistics mass properties
[NASA-CR-183944] N90-26064
BUS CONDUCTORS
Applications for the scalable coherent interface
[DE90-011795] N90-26514
BUTT JOINTS
Static and fatigue strength of an adhesive bonded CFRP butt-strap joint: The effects of stacking sequence and temperature
[NLR-TR-88036-U] N90-26370

C

CALCIFICATION
Experiment K-6-19. Pineal physiology in microgravity: Relation to rat gonadal function N90-26472
CALCIUM
Experiment K-6-01. Distribution and biochemistry of mineral and matrix in the femurs of rats N90-26455
Experiment K-6-19. Pineal physiology in microgravity: Relation to rat gonadal function N90-26472
CALCIUM METABOLISM
Experiment K-6-19. Pineal physiology in microgravity: Relation to rat gonadal function N90-26472
CALCULUS
Application of symbolic computations to the constitutive modeling of structural materials
[NASA-TM-103225] N90-26364
CALIBRATING
Electric field strength meters for the HF, VHF, and UHF bands
[BBC-RD-1990/3] N90-26212
Video camera system for locating bullet holes in targets at a ballistics tunnel
[NASA-TM-4197] N90-26296
Optical characterization of clouds of fine liquid-nitrogen particles
[NASA-TM-103208] N90-26299

An automated calibration laboratory for flight research instrumentation: Requirements and a proposed design approach
[NASA-TM-101719] N90-26564
Absolute measurements of gravity
[AD-A222731] N90-26629

CAMERAS
Technology development: Future use of NASA's large format camera is uncertain
[GAO/NSIAD-90-142] N90-26298
Multiple target tracking in a wide-field-of-view camera system
[DE90-013488] N90-26300
Color image processing for navigation: Two road trackers
[AD-A222667] N90-26591

CANARD CONFIGURATIONS
Effect of tail size reductions on longitudinal aerodynamic characteristics of a three surface F-15 model with nonaxisymmetric nozzles
[NASA-TP-3036] N90-25938
An in-flight interaction of the X-29A canard and flight control system
[NASA-TM-101718] N90-25973
A computer module used to calculate the horizontal control surface size of a conceptual aircraft design
[NASA-CR-186872] N90-26515

CANOPIES (VEGETATION)
Measuring and modeling near-surface reflected and emitted radiation fluxes at the FIFE site
[NASA-CR-180953] N90-26378
Remote sensing of Earth terrain
[NASA-CR-186888] N90-26382

CANS
Two-dimensional model of a Space Station Freedom thermal energy storage canister
[NASA-TM-103124] N90-26279

CAPACITORS
Role of surface passivation in the integrated processing of MOS structures
[AD-A222630] N90-26264

CARBON
Wear mechanisms of amorphous carbon and zirconia coatings on rigid disk magnetic recording media
[DE90-011053] N90-26133
Application of the results of carbon pellet modeling to the problem of plasma penetration
[DE90-012713] N90-26658

CARBON DIOXIDE
Aircraft exhaust emissions: An engine manufacturer's perspective
[PNR90675] N90-26004
Gas exchange characteristics as indicators of the basic limiting factors in photosynthesis
[DE90-012399] N90-26481
Development of membrane process for carbon dioxide separation from diving atmosphere
[AD-A222606] N90-26504
Recent high resolution laboratory determinations of line broadening and intensity parameters: PH3, CH3D, and CO2 N90-26751

CARBON DIOXIDE CONCENTRATION
Proximate composition of seed and biomass from soybean plants grown at different carbon monoxide (CO2) concentrations
[NASA-TM-103496] N90-26480

CARBON DIOXIDE LASERS
New discharge pumping method for CO2 lasers
[AD-A220898] N90-26307
The effects of pretreatment conditions on a Pt/SnO2 catalyst for the oxidation of CO in CO2 lasers
[NASA-TM-103487] N90-26309
A compact, high-powered Far-Infrared (FIR) laser
[DE90-009996] N90-26312

CARBON FIBER REINFORCED PLASTICS
Static and fatigue strength of an adhesive bonded CFRP butt-strap joint: The effects of stacking sequence and temperature
[NLR-TR-88036-U] N90-26370

CARBON MONOXIDE
Mars in situ propellants: Carbon monoxide and oxygen ignition experiments
[NASA-TM-103202] N90-26065
The application of HREELS to model catalysts: CO and C2H4 adsorption on Pt/Al2O3
[AD-A222744] N90-26103
Proximate composition of seed and biomass from soybean plants grown at different carbon monoxide (CO2) concentrations
[NASA-TM-103496] N90-26480

CARBON-CARBON COMPOSITES
Carbon-carbon composites: Emerging materials for hypersonic flight
[NASA-TM-103472] N90-26080

CARBONIZATION
The effects of carbonization on the confinement properties of the DIII-D H-mode
[DE90-013297] N90-26660

CARDIOVASCULAR SYSTEM
Hemodynamic and ADH responses to central blood volume shifts in cardiac-denervated humans
[NASA-TM-103471] N90-26485

CARGO
Biconic cargo return vehicle with an advanced recovery system. Volume 1: Conceptual design
[NASA-CR-186520] N90-26052

CARGO SPACECRAFT
Project Exodus
[NASA-CR-186836] N90-26026
Winged cargo return vehicle. Volume 1: Conceptual design
[NASA-CR-186823] N90-26050

CARTESIAN COORDINATES
Galerkin finite difference Laplacian operators on isolated unstructured triangular meshes by linear combinations
[NASA-TM-103209] N90-26276
Space station definitions, design, and development. Task 5: Multiple arm telerobot coordination and control: Manipulator design methodology
[NASA-CR-182043] N90-26577
Cartesian closed categories of domains
[ETN-90-97284] N90-26613

CASCADE FLOW
Decay of secondary flow and the associated loss variation downstream of an annual turbine stator cascade
[DE90-505520] N90-25984
A fully implicit ADI method for quasi three-dimensional flows through straight blade rows
[ETN-90-96965] N90-26283

CASSEGRAIN OPTICS
DSS 15, 45, and 65 34-meter high efficiency antenna radio frequency performance enhancement by tilt added to the subreflector during elevation angle changes N90-26229

CASSINI MISSION
Investigation of the Saturn dust environment from the analysis of energetic charged particle measurements
[NASA-CR-186727] N90-26784

CASTING
Effect of casting procedures and diesel engine environment on the behavior of aluminum titanate
[AD-A223079] N90-26126

CATALYSIS
Electrochemical, in situ Raman spectroscopic, and conductivity studies of polypyrrole incorporating large size anions: Conducting nature of reduced form
[AD-A222739] N90-26102
The application of HREELS to model catalysts: CO and C2H4 adsorption on Pt/Al2O3
[AD-A222744] N90-26103
The catalytic synthesis of inorganic polymers for high temperature applications and as ceramic precursors
[AD-A222620] N90-26156

CATALYSTS
The effects of pretreatment conditions on a Pt/SnO2 catalyst for the oxidation of CO in CO2 lasers
[NASA-TM-103487] N90-26309
Destruction of peroxy radical by Cu ion catalysed reactions on atmospheric particles N90-26429
Computer simulation of chemical reactions in synthetic model compounds and genetically engineered active sites
[AD-A222611] N90-26483

CATALYTIC ACTIVITY
Destruction of peroxy radical by Cu ion catalysed reactions on atmospheric particles N90-26429

CAVITATION FLOW
Microstructural dependence of the cavitation damage function in FCC materials
[DE90-012898] N90-26113
A high-speed photography study of cavitation in a dynamically loaded journal bearing
[NASA-TM-103178] N90-26338

CAVITY RESONATORS
Resonant coupling through a slot to a loaded cylindrical cavity: Experimental results
[AD-A223000] N90-26631

CELL ANODES
Evaluation of room-temperature chloroaluminate molten salts as electrolytes for high energy density batteries
[AD-A223097] N90-26267

CELL CATHODES
Evaluation of room-temperature chloroaluminate molten salts as electrolytes for high energy density batteries
[AD-A223097] N90-26267

CELLS (BIOLOGY)
Experiment K-6-06. Morphometric and EM analyses of tibial epiphyseal plates from Cosmos 1887 rats N90-26460
Experiment K-6-17. Structural changes and cell turnover in the rats small intestine induced by spaceflight N90-26470
Experiment K-6-22. Growth hormone regulation, synthesis and secretion in microgravity. Part 1: Somatotroph physiology. Part 2: Immunohistochemical analysis of hypothalamic hormones. Part 3: Plasma analysis N90-26475
Experiment K-6-23. Effect of spaceflight on levels and function of immune cells N90-26476

CENTIMETER WAVES
Validity domain of the scalar Kirchhoff and Rayleigh-Sommerfeld diffraction theories in the near field of small phase objects: Comparison between calculation models and microwave measure
[ETN-90-96963] N90-26236

CENTRAL PROCESSING UNITS
Practical applications of remote sensing technology
[NASA-CR-186810] N90-26377

CENTRIFUGAL FORCE
Structural analysis and optimization of a propfan blade using a finite element method
[DLR-FB-90-01] N90-26006
Rotating-unbalanced-mass devices and methods for scanning balloon-borne-experiments, free-flying spacecraft, and space shuttle/space station attached experiments
[NASA-CASE-MFS-28425-1] N90-26304

CERAMIC COATINGS
A computational study of the effectiveness of coating materials for KE projectile fins subjected to the combined effects of inbore and aerodynamic heating
[AD-A222595] N90-26155

CERAMIC FIBERS
The effect of interfacial characteristics on the mechanical performance of ceramic-ceramic composites
[AD-A223031] N90-26090

CERAMIC MATRIX COMPOSITES
The application of engineering ceramics in gas turbines
[PNR90676] N90-26005
Extension of a noninteractive reliability model for ceramic matrix composites
[NASA-CR-185267] N90-26142

CERAMICS
Towards 2000: The composite engine
[PNR90646] N90-26000
Vitreous joining of SiC fiber reinforced SiC composites
[DE90-012951] N90-26081
The effect of interfacial characteristics on the mechanical performance of ceramic-ceramic composites
[AD-A223031] N90-26090
The interaction of polymeric materials with ceramic surfaces with special reference to the behaviour of bioceramics N90-26127
Determination of the stress distributions in a ceramic: Tensile specimen using numerical techniques
[NASA-TM-101914] N90-26132
Tensile strength measurement techniques for structural ceramics
[DE90-012193] N90-26136
Real-time monitoring of ceramic sintering with laser ultrasonics
[DE90-012960] N90-26140
Laser ultrasonic measurements on ceramic materials with rough surfaces
[DE90-012961] N90-26141
Extension of a noninteractive reliability model for ceramic matrix composites
[NASA-CR-185267] N90-26142
Evaluation of fracture strength properties of silicon carbide ceramics under cyclic/static axial loading at ultra-high temperature
[DE90-503402] N90-26147
Development of ceramic fiber type combustor: Improvement of combustor and combustion test results
[DE90-503441] N90-26148
Development of ceramic hybrid combustor: Design and combustion test results
[DE90-503442] N90-26149
The catalytic synthesis of inorganic polymers for high temperature applications and as ceramic precursors
[AD-A222620] N90-26156
Design of ceramic components with the NASA/CARES computer program
[NASA-TM-102369] N90-26359
Advanced Turbine Technology Applications Project (ATTAP)
[NASA-CR-185240] N90-26728

CERIUM COMPOUNDS
Searching for heavy fermion materials in Ce intermetallic compounds
[DE90-011809] N90-26116

CERTIFICATION
Probabilistic approach to the certification for fatigue durability of composite structures
[DE90-505521] N90-26085
Electric field strength meters for the HF, VHF, and UHF bands
[BBC-RD-1990/3] N90-26212
The role of NDI in the certification of turbine engine components
[PNR90629] N90-26349
CHANNEL CAPACITY
Continuous on-line link error rate detector
[AD-D014510] N90-26209
CHANNEL FLOW
Measurement of terms and parameters in turbulent models
[NASA-CR-183993] N90-26271
The effect of a three-dimensional source on the flow through a channel with square cross section
[LR-512] N90-26289
Effects of 2 Hz imposed bulk flow unsteadiness on laminar-turbulent transition in a straight channel
[AD-A223028] N90-26295
CHANNEL NOISE
Tracking performance of a combined Costas/AFC-loop under noisy Rayleigh/Rician channel conditions with additive Gaussian noise jamming
[ETN-90-96964] N90-26237
CHANNELS (DATA TRANSMISSION)
A digital Meteor-Burst Communication (MBC) propagation path simulator N90-26190
Channel selection and control procedures in an automatic HF system N90-26193
CHARACTERIZATION
Characterization of inspection performance
[NLR-MP-88068-U] N90-26350
The system matrix characterisation of input-output equivalence
[MATHS-REPT-A-112] N90-26600
CHARGE COUPLED DEVICES
Multiple target tracking in a wide-field-of-view camera system
[DE90-013488] N90-26300
CHARGE EFFICIENCY
Storage battery operation technique of photovoltaic system to prevent the imbalance of state of charge
[DE90-503032] N90-26255
CHARGED PARTICLES
First International Conference on Laboratory Research for Planetary Atmospheres
[NASA-CP-3077] N90-26744
Investigation of the Saturn dust environment from the analysis of energetic charged particle measurements
[NASA-CR-186727] N90-26784
CHARPY IMPACT TEST
Influence of thermal conditioning media on Charpy specimen test temperature
[DE90-012784] N90-26360
CHEMICAL ANALYSIS
Oxidation and sulfidation of Type 310S stainless steel at elevated temperatures
[DE90-010149] N90-26109
Short-range structure of fluorine-modified phosphate glass
[DE90-013494] N90-26145
Electromagnetic inverse scattering of buried objects
[ETN-90-97216] N90-26242
Nordic Symposium on Atmospheric Chemistry
[CM-78] N90-26403
Deposition to the Baltic Sea N90-26404
Natural and anthropogenic compounds in bulk precipitation at Blidoe (archipelago of Stockholm, Sweden) N90-26409
Measurements of monoterpenes in a coniferous forest N90-26421
Terpene concentrations and emissions in a Scots pine forest N90-26422
The collection and analysis of atmospheric peroxides N90-26428
Experiment K-6-09. Morphological and biochemical investigation of microgravity-induced nerve and muscle breakdown. Part 1: Investigation of nerve and muscle breakdown during spaceflight; Part 2: Biochemical analysis of EDL and PLT muscles N90-26463
CHEMICAL BONDS
Short-range structure of fluorine-modified phosphate glass
[DE90-013494] N90-26145
One-dimensional sigma-conjugated polysilylenes: Science and technology
[DE90-012902] N90-26146
CHEMICAL COMPOSITION
Chemical structure and kinetics at liquid/solid interfaces
[AD-A222766] N90-26105
Verification and improvement of the EMEP model for long-range transport and deposition of pollutants N90-26405
Optical constraints of kerogen from 0.15 to 40 microns: Comparison with meteoritic organics N90-26776
Laboratory studies of the interaction of ions with condensed gases: Planetary applications N90-26778
CHEMICAL EFFECTS
The chemical effects of the Martian environment on power system component materials: A theoretical approach
[NASA-TM-103203] N90-26074
CHEMICAL ENGINEERING
Development of microencapsulation techniques
[AD-A223032] N90-26159
CHEMICAL EVOLUTION
Proton irradiation of simple gas mixtures: Influence of irradiation parameters N90-26782
CHEMICAL PROPULSION
Project LOCOST: Laser or Chemical Hybrid Orbital Space Transport
[NASA-CR-186822] N90-26042
CHEMICAL REACTIONS
Supersonic combustor modeling N90-25992
Critical evaluation of Jet-A spray combustion using propane chemical kinetics in gas turbine combustion simulated by KIVA-2
[NASA-TM-103173] N90-26170
Computer simulation of chemical reactions in synthetic model compounds and genetically engineered active sites
[AD-A222611] N90-26483
Stibathiolanes: Synthesis, solid state structure, and solution behavior
[AD-A223255] N90-26688
CHIPS (ELECTRONICS)
Multiple target tracking in a wide-field-of-view camera system
[DE90-013488] N90-26300
LASER: A Layout Sensitivity Explorer. Report and user's manual
[EUT-89-E-216] N90-26545
CHIRP SIGNALS
An experimental medium speed wideband modem N90-26194
CHLORIDES
Evaluation of room-temperature chloroaluminate molten salts as electrolytes for high energy density batteries
[AD-A223097] N90-26267
CHLOROPLASTS
Gas exchange characteristics as indicators of the basic limiting factors in photosynthesis
[DE90-012399] N90-26481
CHONDRITES
Press abstracts of the 21st Lunar and Planetary Science Conference
[NASA-CR-186874] N90-26738
CHROMATOGRAPHY
Computer analysis of chromatographic data N90-26521
CHROMIUM ALLOYS
A resistance strain gage with repeatable and cancellable apparent strain for use to 800 C
[NASA-CR-185256] N90-26063
CIRCUIT DIAGRAMS
LASER: A Layout Sensitivity Explorer. Report and user's manual
[EUT-89-E-216] N90-26545
CIRCUIT PROTECTION
Simulation of the electrical and thermal behavior of gapless metal oxide surge arresters under AC-operation condition
[ETN-90-97309] N90-26262
CIRCULAR WAVEGUIDES
Theory of circular dielectric waveguide with anisotropic sheet cover
[NASA-CR-186883] N90-26235
CIRRUS CLOUDS
The 27-28 October 1986 FIRE IFO Cirrus case study: Comparison of radiative transfer theory with observations by satellite and aircraft
[NASA-TM-103468] N90-26446
The 27-28 October 1986 FIRE IFO cirrus case study: Cirrus parameter relationships derived from satellite and lidar data
[NASA-TM-103469] N90-26447
Aircraft measurements of the turbulence structure in cirrus clouds
[ISSN-0069-5882] N90-26450
CITIES
Automatic line network extraction from aerial imagery of urban areas through knowledge based image analysis
[AD-A222675] N90-26385
CIVIL AVIATION
Study of high-speed civil transports. Summary
[NASA-CR-4236] N90-25966
Mobile satellite communications for civil aviation
[NLR-MP-88066-U] N90-26238
CLAMPS
Power saw
[NASA-CASE-MSC-21469-1] N90-26340
CLASSIFICATIONS
Initial results on fault diagnosis of DSN antenna control assemblies using pattern recognition techniques N90-26228
Pattern classification of textura by moment and distance autocorrelation function
[INPE-4976-PRE/1541] N90-26379
Classification regions in remote sensing imagery utilizing spatial characteristics
[INPE-4913-PRE/1514] N90-26381
A sum rule satisfied by optimized feed-forward layered networks
[RSRE-MEMO-4341] N90-26579
On networks, optimized feature extraction, and the Bayes decision
[RSRE-MEMO-4342] N90-26580
CLEANING
Role of surface passivation in the integrated processing of MOS structures
[AD-A222630] N90-26264
CLEAVAGE
Hydrogen induced fracture characteristics of single crystal nickel-based superalloys
[NASA-CR-183992] N90-26108
CLIMATE
Annual and interannual variations of Earth-emitted radiation based on a 10-year data set
[NASA-TM-103485] N90-26432
CLIMATOLOGY
The 27-28 October 1986 FIRE IFO Cirrus case study: Comparison of radiative transfer theory with observations by satellite and aircraft
[NASA-TM-103468] N90-26446
Liquid-vapor equilibrium of multicomponent cryogenic systems N90-26774
CLOSED ECOLOGICAL SYSTEMS
Implementation of sensor and control designs for bioregenerative systems
[NASA-CR-186655] N90-26479
Design of sensors for control of closed loop life support systems
[NASA-CR-186656] N90-26490
Genesis lunar outpost criteria and design
[NASA-CR-186831] N90-26499
Automation of closed environments in space for human comfort and safety
[NASA-CR-186834] N90-26500
CLOSURE LAW
Calculation of 3D turbulent jets in crossflow with a multigrid method and a second-moment closure model
[NASA-TM-103159] N90-26282
CLOUDS
Interaction of electromagnetic signals with particulate clouds
[AD-A222804] N90-26244
Optical characterization of clouds of fine liquid-nitrogen particles
[NASA-TM-103208] N90-26299
CLOUDS (METEOROLOGY)
The aqueous atmospheric chemistry of mercury N90-26420
CLUSTER ANALYSIS
Predissimilarities, prefilters, and ultrametrics on an arbitrary set
[IMAG-RR-970-M] N90-26603
CLUTTER
The variably trimmed mean CFAR detector for nonhomogeneous background
[AD-A222801] N90-26243
CMOS
Contribution to CMOS integrated circuit tests: Study of the stuck-on and stuck-open fault tests
[ETN-90-97256] N90-26261
On the design and analysis of multiple-storage elements
[AD-A223095] N90-26266
COAL
Heat engines
[DE90-000485] N90-26393
COATINGS
A resistance strain gage with repeatable and cancellable apparent strain for use to 800 C
[NASA-CR-185256] N90-26063
Mechanical properties of silica coatings
[DE90-012721] N90-26138
Mechanical properties of coatings and interfaces
[DE90-012726] N90-26139
Scattering from coated structures and antenna pattern control using impedance surfaces, part A/B
[NASA-CR-186871] N90-26233

COCKPIT SIMULATORS
Human performance in cockpit-related systems
[NIAR-90-7] N90-26495
COCKPITS
Choosing a pilot subjective workload scale to fit flight operational requirements
[IAR-89-21] N90-26493
Human performance in cockpit-related systems
[NIAR-90-7] N90-26495
Psychophysiological assessment of pilot workload in an applied setting
[AD-A222707] N90-26507
COCKROACHES
Neural networks for real-time sensory data processing and sensorimotor control
[AD-A223096] N90-26592
CODE DIVISION MULTIPLE ACCESS
Multiple-access techniques for communication over dispersive radio channels N90-26196
CODING
A versatile integrated block codes encoder-decoder N90-26197
Direct-sequence spread spectrum system
[AD-A223021] N90-26245
A hybrid M-algorithm/sequential decoder for convolutional and trellis codes
[NASA-CR-186863] N90-26528
Converses for write-unidirectional memories
[EUT-89-E-220] N90-26546
UEDIT: A full-scale, scrollable APL2 spreadsheet input/output editor
[AD-A222712] N90-26557
COEFFICIENTS
Search of primitive polynomials over finite fields
[IMAG-RR-797-M] N90-26607
COGNITION
Mathematical problem-solving transfer: The effects of cognitive load and attention a schema acquisition and rule automation N90-26594
Qualitative and quantitative reasoning about thermodynamics
[NASA-CR-186788] N90-26689
COHERENT RADIATION
Apparatus for the efficient wavelength conversion of laser radiation
[AD-D014506] N90-26305
COLD ACCLIMATIZATION
Arctic cold weather medicine and accidental hypothermia
[AD-A223090] N90-26487
COLD WEATHER
Arctic cold weather medicine and accidental hypothermia
[AD-A223090] N90-26487
COLLAGENS
Experiment K-6-01. Distribution and biochemistry of mineral and matrix in the femurs of rats N90-26455
COLLISION AVOIDANCE
A real-time robot arm collision detection system
[NASA-CR-185878] N90-26582
COLLISION PARAMETERS
A real-time robot arm collision detection system
[NASA-CR-185878] N90-26582
COLLISIONS
Baryogenesis in extended inflation. 2: Baryogenesis via primordial black holes
[NASA-CR-182843] N90-26735
COLOR
Multicolor infrared photodetector
[AD-D014511] N90-26297
COLUMBUS SPACE STATION
Technical characteristics and functions of different types of space stations N90-26712
The US/International Space Station: Legal aspects of space objects and jurisdiction and control N90-26713
Damage responsibility and liability in space stations N90-26714
The International Space Station: The legal framework N90-26716
Crossborder movements: Goods, personnel and technologies N90-26722
Space Station intellectual property rights and US patent law N90-26723
Space law put to the test by the International Space Station N90-26727
COMBINATORIAL ANALYSIS
Combinatorial problems using a hypercube and Hamming graphs
[ETN-90-97240] N90-26609
COMBUSTIBLE FLOW
Subsonic combustor flow modeling: State of the art of CFD techniques for reacting and combusting flow N90-25991
COMBUSTION
Combustion instrumentation N90-25996
Flight motor set 360L007 (STS-33R)
[NASA-CR-183979] N90-26067
Supersonic reacting internal flow fields
[NASA-TM-103480] N90-26094
Carbon deposition model for oxygen-hydrocarbon combustion. Task 6: Data analysis and formulation of an empirical model
[NASA-CR-183986] N90-26095
Critical evaluation of Jet-A spray combustion using propane chemical kinetics in gas turbine combustion simulated by KIVA-2
[NASA-TM-103173] N90-26170
COMBUSTION CHAMBERS
Measurement of velocity and temperature profiles at the exit plane of a tubular gas turbine combustor
[DE90-505519] N90-25983
Combustion in the gas turbine. Part 1: Combustor types and design
[CIT/SME/VKI/RS/1] N90-25986
Combustion in the gas turbine. Part 2: Preliminary design and performance
[CIT/SME/VKI/RS/3] N90-25987
Aircraft exhaust emissions: An engine manufacturer's perspective
[PNR90675] N90-26004
Hard start problem of the apogee engine for the ETS-6
[DE90-505525] N90-26072
Development of ceramic fiber type combustor: Improvement of combustor and combustion test results
[DE90-503441] N90-26148
Development of ceramic hybrid combustor: Design and combustion test results
[DE90-503442] N90-26149
COMBUSTION CHEMISTRY
Gas Turbine Combustion, volume 1
[VKI-LS-1990-02-VOL-1] N90-25985
Turbulent combustion modeling for turbo-jet combustion chambers N90-25993
Chemistry of combustion processes N90-25994
Critical evaluation of Jet-A spray combustion using propane chemical kinetics in gas turbine combustion simulated by KIVA-2
[NASA-TM-103173] N90-26170
COMBUSTION EFFICIENCY
Gas Turbine Combustion, volume 1
[VKI-LS-1990-02-VOL-1] N90-25985
Pollutants: Production and methods of reduction
[CIT/SME/VKI/RS/6] N90-25990
Subsonic combustor flow modeling: State of the art of CFD techniques for reacting and combusting flow N90-25991
Supersonic combustor modeling N90-25992
Turbulent combustion modeling for turbo-jet combustion chambers N90-25993
Subsonic combustor testing N90-25997
Supersonic combustor testing N90-25998
Heat engines
[DE90-000485] N90-26393
COMBUSTION PHYSICS
Mars in situ propellants: Carbon monoxide and oxygen ignition experiments
[NASA-TM-103202] N90-26065
New findings and instrumentation from the NASA Lewis microgravity facilities
[NASA-TM-103189] N90-26163
Critical evaluation of Jet-A spray combustion using propane chemical kinetics in gas turbine combustion simulated by KIVA-2
[NASA-TM-103173] N90-26170
Computational experience with a three-dimensional rotary engine combustion model
[NASA-TM-103104] N90-26275
COMBUSTION PRODUCTS
Formation kinetics of N2O in the atmosphere N90-26425
COMBUSTION STABILITY
Gas Turbine Combustion, volume 1
[VKI-LS-1990-02-VOL-1] N90-25985
Combustion in the gas turbine. Part 3: Fuel injection, ignition and stability
[CIT/SME/VKI/RS/4] N90-25988
Liquid fueled ramjet combustion instability: Acoustical and vortical interactions with burning sprays
[AD-A222752] N90-26104
COMETARY ATMOSPHERES
Laboratory studies of photodissociation processes relevant to the formation of cometary radicals N90-26772
COMETS
Laboratory studies of photodissociation processes relevant to the formation of cometary radicals N90-26772
Optical constraints of kerogen from 0.15 to 40 microns: Comparison with meteoritic organics N90-26776
Study of the polyoxymethylene and its sputtered fragments: Implications for comets N90-26781
Photon sputtering of H2O ices: A preliminary report N90-26783
COMFORT
Human factors: The human interface with aircraft interiors
[NIAR-90-18] N90-26496
COMMERCIAL AIRCRAFT
Study of high-speed civil transports. Summary
[NASA-CR-4236] N90-25966
Knowledge-based system for flight information management
[NASA-TM-102685] N90-26511
COMMUNICATION
Solid-state lasers for coherent communication and remote sensing
[NASA-CR-186634] N90-26306
COMMUNICATION NETWORKS
A new technique in the global reliability of cyclic communications network
[NASA-TM-103479] N90-26214
A novel communication network simulator
[AD-A223045] N90-26248
COMPETITION
Space shuttle: Follow-up evaluation of NASA's solid rocket motor procurement. Report to the Chairman, Committee on Government Operations, House of Representatives
[GAO/NSIAD-89-89] N90-26066
COMPLEX SYSTEMS
Applications of different design methodologies in navigation systems and development at JPL N90-26221
Closed-form solution of decomposable stochastic models
[NASA-TM-103466] N90-26619
COMPONENT RELIABILITY
Design of ceramic components with the NASA/CARES computer program
[NASA-TM-102369] N90-26359
Closed-form solution of decomposable stochastic models
[NASA-TM-103466] N90-26619
COMPOSITE MATERIALS
Computational crash dynamics. Project 1.2: Computational crash dynamics analysis
[IAR-89-19] N90-25956
The impact and requirements of new materials on aeroengines
[PNR90671] N90-26003
Erosion mechanisms in composite materials and ripple formation mechanism in erosion
[IAR-89-4-PT-2] N90-26079
Composite materials with improved properties in compression: Synthesis of 3-methylene-1,1-Dichlorosilacyclobutane and 1,1-dichlorosilacyclopent-3-ene
[AD-A222615] N90-26088
The effect of interfacial characteristics on the mechanical performance of ceramic-ceramic composites
[AD-A223031] N90-26090
Development of ceramic fiber type combustor: Improvement of combustor and combustion test results
[DE90-503441] N90-26148
COMPOSITE PROPELLANTS
RSRM-9 (360L009): Ballistics mass properties
[NASA-CR-183944] N90-26064
Hard start problem of the apogee engine for the ETS-6
[DE90-505525] N90-26072
COMPOSITE STRUCTURES
Damage states in laminated composite three-point bend specimens: An experimental-analytical correlation study
[NASA-TM-101800] N90-26083
Probabilistic approach to the certification for fatigue durability of composite structures
[DE90-505521] N90-26085
Modeling of composite beams and plates for static and dynamic analysis
[NASA-CR-186459] N90-26354
Scaling effects in the static and dynamic response of graphite-epoxy beam-columns
[NASA-TM-102697] N90-26363
COMPRESSIBILITY
A comparison of the post-buckling behavior of metallic and composite plates with centrally located cutouts
[NIAR-90-14] N90-26356
Isothermal compressibility of SPC/E water
[AD-A222723] N90-26643
COMPRESSIBLE FLOW
Practical developments in holographic interferometry
[PNR90669] N90-26302

COMPRESSION LOADS
Buckling and postbuckling behavior of square compression-loaded graphite-epoxy plates with circular cutouts
[NASA-TP-3007] N90-26077
COMPRESSIVE STRENGTH
The interaction of polymeric materials with ceramic surfaces with special reference to the behaviour of bioceramics N90-26127
Resistivity, adhesive strength, and residual stress measurements of thin film metallizations on single crystal quartz
[DE90-011902] N90-26135
COMPRESSOR ROTORS
Prediction and measurement of rotor blade/stator vane dynamic characteristics of a modern aero-engine axial compressor
[PNR90667] N90-26002
COMPRESSORS
Performance evaluation of LE-7 high pressure pumps
[DE90-505523] N90-26034
COMPUTATION
Computational crash dynamics. Project 1.2: Computational crash dynamics analysis
[IAR-89-19] N90-25956
Superconcurrent processing: A dynamic approach to heterogeneous parallelism
[AD-A222798] N90-26576
Causal distributed breakpoints
[AD-A222613] N90-26622
Molecular interactions and properties with many-body methods
[AD-A222631] N90-26642
Full vector wave calculation of photonic band structures in face-centered cubic dielectric media
[AD-A222616] N90-26686
COMPUTATIONAL FLUID DYNAMICS
Technical evaluation report on the Fluid Dynamics Panel Symposium on Computational Methods for Aerodynamic Design (Inverse) and Optimization
[AGARD-AR-267] N90-25947
Computation of viscous aerodynamic characteristics of 2-D airfoils for helicopter applications
[NLR-MP-88052-U] N90-25951
The role of computational fluids dynamics in missile aerodynamics
[NLR-MP-88072-U] N90-25952
Turbine blade heat transfer coefficient evaluation by modified version of STAN5. Comparison with experimental data
[ETN-90-97283] N90-26008
Liquid fueled ramjet combustion instability: Acoustical and vortical interactions with burning sprays
[AD-A222752] N90-26104
A computational study of the effectiveness of coating materials for KE projectile fins subjected to the combined effects of inbore and aerodynamic heating
[AD-A222595] N90-26155
Computational experience with a three-dimensional rotary engine combustion model
[NASA-TM-103104] N90-26275
Code enhancements and validation of GASP
[NPS-PAPER-44] N90-26277
Report of the Fluid Dynamics Panel Working Group 10 on calculation of 3D separate turbulent flows in boundary layer limit
[AGARD-AR-255] N90-26280
A fully implicit ADI method for quasi three-dimensional flows through straight blade rows
[ETN-90-96965] N90-26283
Development of a system for the numerical simulation of Euler flows, with results of preliminary 3-D propeller-slipstream/exhaust-jet calculations
[NLR-TR-88008-U] N90-26285
Computational fluid dynamics for missiles
[RAE-TM-AERO-2171] N90-26288
Informatics aspects of large flow calculations on the SX-2 supercomputer
[NLR-MP-88037-U] N90-26290
Computational fluid dynamics 3-D analysis for advanced transonic turbine design
[ETN-90-97282] N90-26291
COMPUTATIONAL GRIDS
Euler analysis comparison with LDV data for an advanced counter-rotation propfan at cruise
[NASA-TM-103249] N90-25946
Galerkin finite difference Laplacian operators on isolated unstructured triangular meshes by linear combinations
[NASA-TM-103209] N90-26276
Calculation of 3D turbulent jets in crossflow with a multigrid method and a second-moment closure model
[NASA-TM-103159] N90-26282
Informatics aspects of large flow calculations on the SX-2 supercomputer
[NLR-MP-88037-U] N90-26290
The finite analytic method and its applications. Volume 1: Laminar and turbulent flows past two-dimensional and axisymmetric bodies
[AD-A222787] N90-26294
An angular weighting approach for calculating gradients and divergences
[DE90-013164] N90-26539
Parallelization of an annealing simulation applied to improving tetrahedric grids
[IMAG-RR-796-M] N90-26570
Generation and improvement of meshes for finite elements methods in two and three dimensions
[ETN-90-97249] N90-26611
COMPUTER AIDED DESIGN
Feasibility study for a microwave-powered ozone sniffer aircraft, volume 2
[NASA-CR-186676] N90-25967
Supersonic combustor modeling N90-25992
Extension of a noninteractive reliability model for ceramic matrix composites
[NASA-CR-185267] N90-26142
Modeling and optimization of a regenerative fuel cell system using the ASPEN process simulator
[NASA-TM-103210] N90-26396
A computer module used to calculate the horizontal control surface size of a conceptual aircraft design
[NASA-CR-186872] N90-26515
CAD/CAM reinforces the competitive edge of European mouldmakers
[CRIF-MC-88] N90-26542
Material selection and design: An expert system approach
[PNR90611] N90-26544
Contribution to the definition and application of NAUTILE (A new environment for the conception and assembling of integrated circuits)
[ETN-90-97251] N90-26554
ATN design tool
[AD-A223030] N90-26559
Application of artificial intelligence to the architectural synthesis of VLSI integrated circuits
[ETN-90-97253] N90-26589
COMPUTER AIDED MANUFACTURING
Integrating expert systems with solid modeling through interprocess communications and the applications interface specification
[DE90-012996] N90-26537
CAD/CAM reinforces the competitive edge of European mouldmakers
[CRIF-MC-88] N90-26542
Contribution to the definition and application of NAUTILE (A new environment for the conception and assembling of integrated circuits)
[ETN-90-97251] N90-26554
From network to artwork: Automatic schematic diagram generation
[EUT-89-E-219] N90-26567
COMPUTER ANIMATION
Autonomous space processor for orbital debris
[NASA-CR-186691] N90-26044
Computer animation in mathematics, science, and art
[DE90-013051] N90-26538
From network to artwork: Automatic schematic diagram generation
[EUT-89-E-219] N90-26567
COMPUTER GRAPHICS
Feasibility study for a microwave-powered ozone sniffer aircraft, volume 2
[NASA-CR-186676] N90-25967
Computer simulation of gear tooth manufacturing processes
[NASA-CR-185200] N90-26171
OASIS, LLNL version: Software maintenance manual
[DE90-013522] N90-26313
Graphics applications utilizing parallel processing
[NASA-CR-186719] N90-26534
Computer animation in mathematics, science, and art
[DE90-013051] N90-26538
The rationale and specification of the ELLA graphics systems
[RSRE-89017] N90-26548
UEDIT: A full-scale, scrollable APL2 spreadsheet input/output editor
[AD-A222712] N90-26557
ATN design tool
[AD-A223030] N90-26559
COMPUTER NETWORKS
Computer architecture evaluation for structural dynamics computations: Project summary
[NASA-CR-186137] N90-26512
Applications for the scalable coherent interface
[DE90-011795] N90-26514
Integrating expert systems with solid modeling through interprocess communications and the applications interface specification
[DE90-012996] N90-26537
Language support for parallel computation
[AD-A223072] N90-26560
Pacific missile test center information resources management organization (code 0300): The ORACLE client-server and distributed processing architecture
[DE90-013271] N90-26565
High speed all optical networks
[NASA-CR-185311] N90-26649
Analysis of random drop for gateway congestion control
[NASA-CR-186736] N90-26698
COMPUTER PROGRAMMING
Applications of different design methodologies in navigation systems and development at JPL N90-26221
Software set-up for data processing of depolarization due to rain and ice crystals in the Olympus project
[EUT-89-E-218] N90-26240
ISIS and META projects
[NASA-CR-186645] N90-26524
An expert system based software sizing tool, phase 2
[NASA-CR-186706] N90-26525
Software requirements: Guidance and control software development specification
[NASA-CR-182058] N90-26527
ANTIPASTO: An interactive mesh generator and preprocessor for two-dimensional analysis programs
[DE90-011755] N90-26530
SUPES version 2.1: A Software Utilities Package for the Engineering Sciences
[DE90-011763] N90-26531
Object oriented programming
[DE90-011797] N90-26532
Innovative design systems: Where are we, and where do we go from here
[AD-A222586] N90-26556
From network to artwork: Automatic schematic diagram generation
[EUT-89-E-219] N90-26567
Design of a universal protocol system architecture: Specification of functions and services
[EUT-89-E-230] N90-26569
Verification-correction of a program for including uncertainties in the robot automatic programming
[ETN-90-97246] N90-26588
COMPUTER PROGRAMS
Turbine blade heat transfer coefficient evaluation by modified version of STAN5. Comparison with experimental data
[ETN-90-97283] N90-26008
Prediction of the ullage gas thermal stratification in a NASP vehicle propellant tank experimental simulation using FLOW-3D
[NASA-TM-103217] N90-26160
Integrated support structure
[NASA-CR-186835] N90-26162
Critical evaluation of Jet-A spray combustion using propane chemical kinetics in gas turbine combustion simulated by KIVA-2
[NASA-TM-103173] N90-26170
L-SWITCH: A PC program for computing transient voltages and currents during switching off three-phase inductances
[EUT-89-E-221] N90-26257
A possibility to incorporate saturation in the simple, global model of a synchronous machine with rectifier
[EUT-89-E-225] N90-26258
Code enhancements and validation of GASP
[NPS-PAPER-44] N90-26277
Informatics aspects of large flow calculations on the SX-2 supercomputer
[NLR-MP-88037-U] N90-26290
Design of ceramic components with the NASA/CARES computer program
[NASA-TM-102369] N90-26359
Qualification of concentrating mirror systems with the HERMES measurement system and the HELIOS simulation program
[DLR-FB-89-51] N90-26394
A computer module used to calculate the horizontal control surface size of a conceptual aircraft design
[NASA-CR-186872] N90-26515
An expert system based software sizing tool, phase 2
[NASA-CR-186706] N90-26525
Software requirements: Guidance and control software development specification
[NASA-CR-182058] N90-26527
A hybrid M-algorithm/sequential decoder for convolutional and trellis codes
[NASA-CR-186863] N90-26528
Automated sensitivity analysis with the Gradient Enhanced Software System (GRESS)
[DE90-011291] N90-26529
Level-2 system: Programmers-users manual
[DE90-013324] N90-26540

Documentation of program Tankplot
[FFI-89/7019] N90-26541
CAD/CAM reinforces the competitive edge of European mouldmakers
[CRIF-MC-88] N90-26542
LASER: A Layout Sensitivity Explorer. Report and user's manual
[EUT-89-E-216] N90-26545
Pacific missile test center information resources management organization (code 0300): The ORACLE client-server and distributed processing architecture
[DE90-013271] N90-26565
MINAS: An algorithm for systematic state assignment of sequential machines: Computational aspects and results
[EUT-89-E-217] N90-26566
From network to artwork: Automatic schematic diagram generation
[EUT-89-E-219] N90-26567
Contribution to the study of differential equations and to the differences in the complex field
[ETN-90-97250] N90-26612
Cartesian closed categories of domains
[ETN-90-97284] N90-26613
Efficient implementation of minimal polynomial and reduced rank extrapolation methods
[NASA-TM-103240] N90-26616
Sensitivity analysis with a simple charging code
[RAE-TM-SPACE-374] N90-26662

COMPUTER STORAGE DEVICES
High speed magneto-resistive random access memory
[NASA-CASE-NPO-17954-1-CU] N90-26519
Atomic snapshots of shared memory
[AD-A222765] N90-26520
Single-pass memory system evaluation for multiprogramming workloads
[NASA-CR-186553] N90-26558

COMPUTER SYSTEMS DESIGN
Prototyping an in-house business intelligence database
[PNR90665] N90-26709

COMPUTER SYSTEMS PERFORMANCE
SUPES version 2.1: A Software Utilities Package for the Engineering Sciences
[DE90-011763] N90-26531
Closed-form solution of decomposable stochastic models
[NASA-TM-103466] N90-26619

COMPUTER SYSTEMS PROGRAMS
Tools for distributed application management
[NASA-CR-186627] N90-26535

COMPUTER TECHNIQUES
Research conducted at the Institute for Computer Applications in Science and Engineering in applied mathematics, numerical analysis, and computer science
[NASA-CR-182057] N90-26510
Computer analysis of chromatographic data N90-26521
Computer aided handling qualities evaluation in frequency domain
[NAL-TM-SE-8902] N90-26523
Exact results for the structured liquid-solid interface
[AD-A222762] N90-26630

COMPUTER VISION
Feasibility study for a microwave-powered ozone sniffer aircraft, volume 2
[NASA-CR-186676] N90-25967

COMPUTERIZED SIMULATION
Two-dimensional Euler and Navier-Stokes Time accurate simulations of fan rotor flows
[NASA-TM-102402] N90-25948
Performance of a supercharged direct-injection stratified-charge rotary combustion engine
[NASA-TM-103105] N90-25982
Model following control system design: Preliminary ATTAS in-flight simulation test results
[PD-FC-9003] N90-26010
An investigation of the use of singular perturbation methods and modal control theory in the derivation of aircraft control schemes
[MATHS-REPT-A-106] N90-26014
Guidance and targeting for the strategic target system
[DE90-005239] N90-26031
Modelling of the processing of incompatible polymer blends
[ETN-90-97211] N90-26152
Simulated dynamic response of a servovalve controlled hydraulic actuator
[NASA-TM-101644] N90-26167
Computer simulation of gear tooth manufacturing processes
[NASA-CR-185200] N90-26171
Initial results on fault diagnosis of DSN antenna control assemblies using pattern recognition techniques N90-26228
Simulation of the electrical and thermal behavior of gapless metal oxide surge arresters under AC-operation condition
[ETN-90-97309] N90-26262
Modeling, simulation, and analysis of optical remote sensing systems
[NASA-CR-186648] N90-26376
Qualification of concentrating mirror systems with the HERMES measurement system and the HELIOS simulation program
[DLR-FB-89-51] N90-26394
Modeling and optimization of a regenerative fuel cell system using the ASPEN process simulator
[NASA-TM-103210] N90-26396
Computer simulation of chemical reactions in synthetic model compounds and genetically engineered active sites
[AD-A222611] N90-26483
Object oriented programming
[DE90-011797] N90-26532
Parallelization of an annealing simulation applied to improving tetrahedric grids
[IMAG-RR-796-M] N90-26570
Position control of redundant manipulators using an adaptive error-based control scheme
[NASA-CR-186612] N90-26578
Beam rider for an Articulated Robot Manipulator (ARM) accurate positioning of long flexible manipulators
[NASA-CR-185151] N90-26581
Variance reduction for quantile estimates in simulations via nonlinear controls
[AD-A222653] N90-26590
Isothermal compressibility of SPC/E water
[AD-A222723] N90-26643
Computer modeling wave propagation with a variation of the Helmholtz-Kirchhoff relation
[AD-A222746] N90-26657
Sensitivity analysis with a simple charging code
[RAE-TM-SPACE-374] N90-26662
Molecular dynamics simulations of grain-boundary diffusion for varying tilt angle geometries
[DE90-012919] N90-26669
Structure and dynamics of water at the Pt(111) interface: Molecular dynamics study
[AD-A222628] N90-26687

COMPUTERS
Self-checking on-line testable static RAM
[NASA-CASE-NPO-17939-1-CU] N90-26518
ISIS and META projects
[NASA-CR-186645] N90-26524
Closed-form solution of decomposable stochastic models
[NASA-TM-103466] N90-26619

CONCENTRATORS
Silicon concentrator solar cell development
[DE90-011782] N90-26386

CONCURRENT PROCESSING
Parallel processors and nonlinear structural dynamics algorithms and software
[NASA-CR-186755] N90-26536
Knowledge and inhibition in asynchronous distributed systems
[TR-90-1139] N90-26703

CONDENSATES
Laboratory measurements of microwave and millimeter-wave properties of planetary constituents N90-26745
Optical constants of solid methane N90-26775

CONDENSATION NUCLEI
Results from global tropospheric sulphur simulations N90-26413
Characterization of biogenic aerosol particles from the Amazon Basin during dry and wet season N90-26418

CONDUCTIVE HEAT TRANSFER
New discharge pumping method for CO2 lasers
[AD-A220898] N90-26307

CONFERENCES
Second Annual International Conference on Aging Aircraft
[AD-A222715] N90-25961
Proceedings of the Second Symposium on GPS Applications in space, volume 1
[AD-A219978] N90-25962
Proceedings of the Second Symposium on GPS Applications in Space, volume 2
[AD-A219979] N90-25963
Space Transportation Avionics Technology Symposium. Volume 1: Executive summary
[NASA-CP-3081] N90-25980
Technical evaluation report on the Guidance and Control Panel 49th Symposium on Fault Tolerant Design Concepts for Highly Integrated Flight Critical Guidance and Control Systems
[AGARD-AR-281] N90-26012
Proceedings of the LDEF Materials Data Analysis Workshop
[NASA-CP-10046] N90-26075
The 5th International symposium on palaeolimnology
[AD-A219244] N90-26431
Proceedings of a workshop on Lunar Volcanic Glasses: Scientific and Resource Potential
[NASA-CR-186631] N90-26437
Motion sickness, visual displays, and armored vehicle design
[AD-A222678] N90-26506
Press abstracts of the 21st Lunar and Planetary Science Conference
[NASA-CR-186874] N90-26738
Proceedings of a Workshop on Antarctic Meteorite Stranding Surfaces
[NASA-CR-186575] N90-26739
Proceedings of a workshop on Differences Between Antarctic and Non-Antarctic Meteorites
[NASA-CR-184918] N90-26740
First International Conference on Laboratory Research for Planetary Atmospheres
[NASA-CP-3077] N90-26744

CONGESTION
Analysis of random drop for gateway congestion control
[NASA-CR-186736] N90-26698

CONGRESSIONAL REPORTS
Aviation safety: Conditions within the air traffic control work force. Fact sheet for congressional requesters
[GAO/RCED-89-113FS] N90-25958
Aviation safety: Serious problems continue to trouble the air traffic control work force. Report to congressional requesters
[GAO/RCED-89-112] N90-25959
Space exploration: Cost, schedule, and performance of NASA's Mars Observer Mission. Fact sheet for the Chairman, Subcommittee on Science, Technology, and Space, Committee on Commerce, Science, and Transportation, US Senate
[GAO/NSIAD-88-137FS] N90-26021
Space exploration: Cost, schedule, and performance of NASA's Magellan Mission to Venus. Fact sheet for the Chairman, Subcommittee on Science, Technology, and Space, Committee on Commerce, Science, and Transportation, US Senate
[GAO/NSIAD-88-130FS] N90-26022
Space exploration: Cost, schedule, and performance of NASA's Ulysses Mission to the Sun. Fact sheet for the Chairman, Subcommittee on Science, Technology, and Space, Committee on Commerce, Science, and Transportation, US Senate
[GAO/NSIAD-88-129FS] N90-26023
Space program: Space debris a potential threat to Space Station and shuttle
[GAO/IMTEC-90-18] N90-26024
Space exploration: Cost, schedule, and performance of NASA's Galileo Mission to Jupiter. Fact sheet for the Chairman, Subcommittee on Science, Technology, and Space, Committee on Commerce, Science, and Transportation, US Senate
[GAO/NSIAD-88-138FS] N90-26025
Space transportation: NASA has no firm need for increasingly costly orbital maneuvering vehicle
[GAO/NSIAD-90-192] N90-26041
Space shuttle: Follow-up evaluation of NASA's solid rocket motor procurement. Report to the Chairman, Committee on Government Operations, House of Representatives
[GAO/NSIAD-89-89] N90-26066
NASA project status reports: Congressional requirements can be met, but reliability must be ensured
[GAO/NSIAD-90-40] N90-26169
Space operations: NASA's communications support for Earth orbiting spacecraft. Report to Chairman, Subcommittee on Space Science and Applications, Committee on Science, Space and Technology, House of Representatives
[GAO/IMTEC-89-41] N90-26215
Technology development: Future use of NASA's large format camera is uncertain
[GAO/NSIAD-90-142] N90-26298
Space operations: NASA is not properly safeguarding valuable data from past missions
[GAO/IMTEC-90-1] N90-26704

CONIFERS
Measurements of monoterpenes in a coniferous forest N90-26421
Terpene concentrations and emissions in a Scots pine forest N90-26422
The diurnal ozone cycle in a coniferous forest: The importance of meteorology and chemistry N90-26423

CONJUGATE GRADIENT METHOD
Trajectory optimization for an asymmetric launch vehicle
[NASA-CR-185630] N90-26033

Efficient generalized conjugate gradient algorithms. Part 2: Implementation
[MATHS-REPT-A-118-PT-2] N90-26543

CONNECTIVE TISSUE
Effects of microgravity on rat bone, cartilage and connective tissues N90-26454
Experiment K-6-02. Biomedical, biochemical and morphological alterations of muscle and dense, fibrous connective tissues during 14 days of spaceflight N90-26456

CONSOLES
Lunar deep drill apparatus
[NASA-CR-182756] N90-26322

CONSTANTS
Rate constant for reaction of atomic hydrogen with germane N90-26768
Role of the methylene amidogen (H2CN) radical in the atmospheres of Titan and Jupiter N90-26769
Optical constants of solid methane N90-26775

CONSTITUTIVE EQUATIONS
Application of symbolic computations to the constitutive modeling of structural materials
[NASA-TM-103225] N90-26364

CONSTRAINTS
Human factors: The human interface with aircraft interiors
[NIAR-90-18] N90-26496

CONSTRUCTION
Design and performance analysis of the DSS-13 beam waveguide antenna N90-26225
Design of an autonomous Lunar construction utility vehicle
[NASA-CR-186832] N90-26330

CONTAMINANTS
An overview of the joint FAA/NASA aircraft/ground runway friction program
[NASA-TM-103486] N90-25957

CONTAMINATION
Role of surface passivation in the integrated processing of MOS structures
[AD-A222630] N90-26264

CONTINENTAL SHELVES
Spatial cross-correlation of Antarctic Sea ice and seabed topography
[NASA-CR-186815] N90-26451

CONTINUITY (MATHEMATICS)
G2-continuity in homogeneous co-ordinates
[MATHS-REPT-A-110] N90-26599
Rational cubics with G2-continuity
[MATHS-REPT-A-113] N90-26601

CONTOUR SENSORS
Surface reconstruction based on critical contours in a multi-image context
[RR-784-I-IMAG-94-LIFIA] N90-26383

CONTRACTS
Production activities in space: The problems of protection N90-26725

CONTROL EQUIPMENT
Making real-time reactive systems reliable
[NASA-CR-186642] N90-26344

CONTROL SIMULATION
Robustness evaluation of H2 and H(infinity) control theory as applied to a transport aircraft
[AD-A222795] N90-26018
Variance reduction for quantile estimates in simulations via nonlinear controls
[AD-A222653] N90-26590

CONTROL STABILITY
H-infinity control: An exploratory study
[EUT-88-E-211] N90-26584

CONTROL SURFACES
Research at NASA's NFAC wind tunnels
[NASA-TM-102827] N90-25933
Prediction methodologies for nonlinear aerodynamic characteristics of control surfaces
[NIAR-90-17] N90-25937
A computer module used to calculate the horizontal control surface size of a conceptual aircraft design
[NASA-CR-186872] N90-26515

CONTROL SYSTEMS DESIGN
Synthesis of individual rotor blade control system for gust alleviation
[NASA-TM-101886] N90-25972
Hot gas ingestion characteristics and flow visualization of a vectored thrust STOVL concept
[NASA-TM-103212] N90-26009
Model following control system design: Preliminary ATTAS in-flight simulation test results
[PD-FC-9003] N90-26010
H-infinity based integrated flight-propulsion control design for a STOVL aircraft in transition flight
[NASA-TM-103198] N90-26011
An investigation of the use of singular perturbation methods and modal control theory in the derivation or aircraft control schemes
[MATHS-REPT-A-106] N90-26014
Design and implementation of robust decentralized control laws for the ACES structure at Marshall Space Flight Center
[NASA-CR-4310] N90-26046
Packet radio network concepts for the Norwegian field army N90-26206
A model of the synchronous machine with rectifier, especially for control purposes
[EUT-89-E-215] N90-26256
On controller choice for robust sliding mode performance
[MATHS-REPT-A-107] N90-26337

CONTROL THEORY
An investigation of the use of singular perturbation methods and modal control theory in the derivation or aircraft control schemes
[MATHS-REPT-A-106] N90-26014
Low-speed wind tunnel investigation of the static stability and control characteristics of an advanced turboprop configuration with the propellers placed over the tail
[NASA-CR-186900] N90-26017
Robustness evaluation of H2 and H(infinity) control theory as applied to a transport aircraft
[AD-A222795] N90-26018
Design and implementation of robust decentralized control laws for the ACES structure at Marshall Space Flight Center
[NASA-CR-4310] N90-26046
Manufacturing control: A basis for analysis
[PNR90639] N90-26174
Inference and control mechanisms in NEXT 2.0
[NLR-MP-88062-U] N90-26175
Control strategy for cooperating disparate manipulators
[NASA-CR-186809] N90-26328
Guidance and control system for an autonomous underwater vehicle
[AD-A222709] N90-26343
Assembly via disassembly: A case in machine perceptual development
[NASA-CR-186867] N90-26497
Research conducted at the Institute for Computer Applications in Science and Engineering in applied mathematics, numerical analysis, and computer science
[NASA-CR-182057] N90-26510
On the robust stability of MIMO linear feedback systems
[EUT-88-E-212] N90-26585

CONTROLLABILITY
Orbiter utilization as an ACRV
[NASA-TM-102700] N90-26032
Computer aided handling qualities evaluation in frequency domain
[NAL-TM-SE-8902] N90-26523

CONTROLLERS
H-infinity based integrated flight-propulsion control design for a STOVL aircraft in transition flight
[NASA-TM-103198] N90-26011
Literature concerning control and display technology applicable to the Orbital Maneuvering Vehicle (OMV)
[NASA-CR-186790] N90-26048
Intergration of system identification and robust controller designs for flexible structures in space
[NASA-TM-102695] N90-26362
Position control of redundant manipulators using an adaptive error-based control scheme
[NASA-CR-186812] N90-26578
A new scheme for identification and control
[EUT-88-E-213] N90-26586
Temperature and melt solid interface control during crystal growth
[NASA-CR-186731] N90-26664

CONVECTION
Estimation of convective rain volumes utilizing the are-time-integral technique
[NASA-CR-186814] N90-26449
A lattice gas model for thermohydrodynamics
[DE90-011964] N90-26690

CONVECTIVE HEAT TRANSFER
Transients in turbulent convective heat transfer to a flow of supercritical helium
[ETN-90-97217] N90-26286

CONVERGENCE
Efficient generalized conjugate gradient algorithms. Part 2: Implementation
[MATHS-REPT-A-118-PT-2] N90-26543

COOLING
The application of engineering ceramics in gas turbines
[PNR90676] N90-26005
Time temperature relations during rubber forming continuous fiber reinforced thermoplastics
[LR-620] N90-26151

COOLING SYSTEMS
Combustor cooling aspects
[CIT/SME/VKI/RS/5] N90-25989

COORDINATES
G2-continuity in homogeneous co-ordinates
[MATHS-REPT-A-110] N90-26599
Rational cubics with G2-continuity
[MATHS-REPT-A-113] N90-26601

COPOLYMERS
NMR and optical studies of piezoelectric polymers
[DE90-012459] N90-26137
The catalytic synthesis of inorganic polymers for high temperature applications and as ceramic precursors
[AD-A222620] N90-26156

COPPER
Destruction of peroxy radical by Cu ion catalysed reactions on atmospheric particles N90-26429

COPPER OXIDES
Large, orientation-dependent enhancements of critical currents in Y1Ba2Cu3O(7-x) epitaxial thin films: Evidence for intrinsic flux pinning
[DE90-009424] N90-26666
NDE (Nondestructive evaluation) of critical currents in high T(sub c) superconductors
[DE90-012953] N90-26670
Ellipsometric study of YBa2Cu3O(7-x) laser ablated and co-evaporated films
[NASA-TM-103223] N90-26682

CORE SAMPLING
Micro coring apparatus
[NASA-CR-183072] N90-26321
Lunar deep drill apparatus
[NASA-CR-182756] N90-26322
Ice core studies and the past atmospheric environment of polar regions N90-26411
The Renland ice core (Greenland): A source for climatic studies over 100,000 years N90-26412

CORES
Micro coring apparatus
[NASA-CR-183072] N90-26321
Lunar deep drill apparatus
[NASA-CR-182756] N90-26322

CORRECTION
Feasibility study of a synthesis procedure for array feeds to improve radiation performance of large distorted reflector antennas
[NASA-CR-186641] N90-26213
Alignment positioning mechanism
[NASA-CASE-MSC-21502-1] N90-26341

CORROSION
Flight set 360L001 (STS-26) igniter, post flight
[NASA-CR-183957] N90-26325

COSMOLOGY
A research program in theoretical high energy physics
[DE90-013322] N90-26648
Comment on high resolution simulations of cosmic strings. 1: Network evolution
[NASA-CR-186606] N90-26734
A research program in physics of the early universe
[DE90-013319] N90-26742

COSMOS SATELLITES
The US Experiments Flown on the Soviet Biosatellite Cosmos 1887
[NASA-TM-102254] N90-26452

COST ANALYSIS
Long-range planning cost model for support of future space missions by the deep space network N90-26231

COST EFFECTIVENESS
The aerobraking space transfer vehicle
[NASA-CR-186819] N90-26053

COST ESTIMATES
Space exploration: Cost, schedule, and performance of NASA's Mars Observer Mission. Fact sheet for the Chairman, Subcommittee on Science, Technology, and Space, Committee on Commerce, Science, and Transportation, US Senate
[GAO/NSIAD-88-137FS] N90-26021
Space exploration: Cost, schedule, and performance of NASA's Magellan Mission to Venus. Fact sheet for the Chairman, Subcommittee on Science, Technology, and Space, Committee on Commerce, Science, and Transportation, US Senate
[GAO/NSIAD-88-130FS] N90-26022
Space exploration: Cost, schedule, and performance of NASA's Galileo Mission to Jupiter. Fact sheet for the Chairman, Subcommittee on Science, Technology, and Space, Committee on Commerce, Science, and Transportation, US Senate
[GAO/NSIAD-88-138FS] N90-26025
Space transportation: NASA has no firm need for increasingly costly orbital maneuvering vehicle
[GAO/NSIAD-90-192] N90-26041
Long-range planning cost model for support of future space missions by the deep space network N90-26231

COST REDUCTION
Minimization of the cost of information transfer in HF spread spectrum transmission N90-26198

COSTS
Space exploration: Cost, schedule, and performance of NASA's Magellan Mission to Venus. Fact sheet for the Chairman, Subcommittee on Science, Technology, and Space, Committee on Commerce, Science, and Transportation, US Senate
[GAO/NSIAD-88-130FS] N90-26022
Space exploration: Cost, schedule, and performance of NASA's Ulysses Mission to the Sun. Fact sheet for the Chairman, Subcommittee on Science, Technology, and Space, Committee on Commerce, Science, and Transportation, US Senate
[GAO/NSIAD-88-129FS] N90-26023
Preliminary designs for 25 kWe advanced Stirling conversion systems for dish electric applications
[NASA-TM-103188] N90-26729
COUNTER ROTATION
Euler analysis comparison with LDV data for an advanced counter-rotation propfan at cruise
[NASA-TM-103249] N90-25946
High speed turboprop aeroacoustic study (counterrotation). Volume 1: Model development
[NASA-CR-185241] N90-26633
COUPLING
Resonant coupling through a slot to a loaded cylindrical cavity: Experimental results
[AD-A223000] N90-26631
CRACK CLOSURE
Small crack growth and its influence in near alpha-titanium alloys
[RAE-TM-P-1171] N90-26121
Elevated temperature crack growth
[NASA-CR-182247] N90-26355
Investigation of crack-closure prediction models for fatigue in aluminium alloy sheet under flight-simulation loading
[LR-619] N90-26369
CRACK INITIATION
Damage states in laminated composite three-point bend specimens: An experimental-analytical correlation study
[NASA-TM-101800] N90-26083
Microstructural design for fatigue crack growth resistance in Ni-base alloy
[PNR90632] N90-26120
Small crack growth and its influence in near alpha-titanium alloys
[RAE-TM-P-1171] N90-26121
CRACK PROPAGATION
Microstructural design for fatigue crack growth resistance in Ni-base alloy
[PNR90632] N90-26120
Small crack growth and its influence in near alpha-titanium alloys
[RAE-TM-P-1171] N90-26121
Elevated temperature crack growth
[NASA-CR-182247] N90-26355
Fatigue life assessment using a short crack growth model
[PNR90663] N90-26367
CRACKING (FRACTURING)
Effect of boron on intergranular hot cracking in Ni-Cr-Fe superalloys containing niobium
[NASA-CR-186714] N90-26115
CRACKS
Development of creep-fatigue damage detection method of rotor steel by ultrasonic wave measurement
[DE90-503792] N90-26365
CRASHES
Computational crash dynamics. Project 1.2: Computational crash dynamics analysis
[IAR-89-19] N90-25956
Biodynamic simulations of an aircraft pilot/passenger in various crash environments
[NIAR-90-6] N90-26494
CRASHWORTHINESS
Computational crash dynamics. Project 1.2: Computational crash dynamics analysis
[IAR-89-19] N90-25956
Human factors: The human interface with aircraft interiors
[NIAR-90-18] N90-26496
CREEP PROPERTIES
Microstructural dependence of the cavitation damage function in FCC materials
[DE90-012898] N90-26113
Development of creep-fatigue damage detection method of rotor steel by ultrasonic wave measurement
[DE90-503792] N90-26365
Diffusion-accommodated grain boundary sliding in a polycrystal
[DE90-012727] N90-26668
Critical current density, flux creep, and microstructure in a Bi-Sr-Ca-Cu-O system
[DE90-010457] N90-26676
CREEP STRENGTH
Application of high performance metals in gas turbine engines
[PNR90640] N90-25999
CREEP TESTS
High temperature multiaxiale creep testing of Nimonic 115
[RAE-TM-P-1182] N90-26122
CRIME
The astronauts' legal status: The International Space Station N90-26721
CRITERIA
Statistical treatment of slow strain rate data for assessment of hydrogen embrittlement in low alloy high strength steel
[ARL-MAT-R-122] N90-26106
CROSS CORRELATION
Spatial cross-correlation of Antarctic Sea ice and seabed topography
[NASA-CR-186815] N90-26451
CROSS FLOW
Calculation of 3D turbulent jets in crossflow with a multigrid method and a second-moment closure model
[NASA-TM-103159] N90-26282
CROSS SECTIONS
The effect of a three-dimensional source on the flow through a channel with square cross section
[LR-512] N90-26289
CRYOGENIC COOLING
Multicomponent gas sorption Joule-Thomson refrigerator
[NASA-CASE-NPO-17569-1-CU] N90-26176
CRYOGENIC EQUIPMENT
Initial experimentation on the nonvented fill of a 0.14m3 (5 ft. 3) dewar with nitrogen and hydrogen
[NASA-TM-103155] N90-26278
CRYOGENIC TEMPERATURE
Fracture toughness and failure mechanisms in commercial 2091 Al-Li sheet at cryogenic temperatures
[AD-A222603] N90-26125
CRYOGENICS
Debris/ice/TPS assessment and photographic analysis for shuttle mission STS-31R
[NASA-TM-102790] N90-26040
Liquid-vapor equilibrium of multicomponent cryogenic systems N90-26774
CRYSTAL DEFECTS
Twin boundaries, interfaces and modulated structures in martensites
[DE90-012899] N90-26111
Crystal growth and deformation behavior of TiAl aluminides
[DE90-012972] N90-26671
High temperature x ray diffraction and Landau theory investigations of order-disorder transition in defect NaCl-type solids
[DE90-011807] N90-26673
Critical current density, flux creep, and microstructure in a Bi-Sr-Ca-Cu-O system
[DE90-010457] N90-26676
CRYSTAL GROWTH
Hydrogen induced fracture characteristics of single crystal nickel-based superalloys
[NASA-CR-183992] N90-26108
Dendritic web silicon photovoltaic cell research
[DE90-011786] N90-26387
Temperature and melt solid interface control during crystal growth
[NASA-CR-186731] N90-26664
Crystal growth and deformation behavior of TiAl aluminides
[DE90-012972] N90-26671
MBE growth technology for high quality strained III-V layers
[NASA-CASE-NPO-17723-1-CU] N90-26685
CRYSTAL LATTICES
The origin of poorly conditioned susceptibility matrix within inverse CVM algorithm in the case of Pd(sub 3)V: A comparison to the case of Ni(sub 3)V
[DE90-012464] N90-26110
MBE growth technology for high quality strained III-V layers
[NASA-CASE-NPO-17723-1-CU] N90-26685
CRYSTAL OPTICS
Apparatus for the efficient wavelength conversion of laser radiation
[AD-D014506] N90-26305
CRYSTAL STRUCTURE
Formation of cubic LI2 phases from Al3Ti and Al3Zr by transition metal substitutions for Al
[DE90-012288] N90-26117
Exact results for the structured liquid-solid interface
[AD-A222762] N90-26630
Large, orientation-dependent enhancements of critical currents in Y1Ba2Cu3O(7-x) epitaxial thin films: Evidence for intrinsic flux pinning
[DE90-009424] N90-26666
Molecular dynamics simulations of grain-boundary diffusion for varying tilt angle geometries
[DE90-012919] N90-26669
Optical constants of solid methane N90-26775
CRYSTAL SURFACES
Structure and dynamics of water at the Pt (111) interface: Molecular dynamics study
[AD-A222628] N90-26687
CRYSTALLIZATION
Protein crystal growth in low gravity
[NASA-CR-186243] N90-26663
Mathematical simulation of heat exchanges and thermoelastic constraints in Czochralski crystal growth
[ETN-90-97242] N90-26680
CRYSTALLOGRAPHY
The effect of crystal orientation on damage accumulation in chromium-implanted Al2O3
[DE90-012294] N90-26674
CRYSTALS
Protein crystal growth in low gravity
[NASA-CR-186243] N90-26663
CUBIC LATTICES
Molecular dynamics simulations of grain-boundary diffusion for varying tilt angle geometries
[DE90-012919] N90-26669
CURING
Characterization of a thermally imidized soluble polyimide film
[NASA-TM-103484] N90-26131
Evolution of structure and viscoelasticity in diethanolamine-cured epoxy
[DE90-011256] N90-26134
CURRENT DENSITY
Critical current density, flux creep, and microstructure in a Bi-Sr-Ca-Cu-O system
[DE90-010457] N90-26676
CURVES (GEOMETRY)
Calculation of the algebraic curves parameterization: Hamburger-Noether expansions
[IMAG-RR-798-M] N90-26608
CUTTING
Power saw
[NASA-CASE-MSC-21469-1] N90-26340
CYANO COMPOUNDS
The heat of formation of CN radicals and radiative lifetimes of the A 1 Sigma - state of C2N2 N90-26765
CYANOACETYLENE
Laboratory studies, analysis, and interpretation of the spectra of hydrocarbons present in planetary atmospheres including cyanoacetylene, acetylene, propane, and ethane N90-26748
CYCLOBUTANE
Composite materials with improved properties in compression: Synthesis of 3-methylene-1,1-Dichlorosilacyclobutane and 1,1-dichlorosilacyclopent-3-ene
[AD-A222615] N90-26088
CYCLONES
Mariners Weather Log, volume 33, number 2, Spring 1989
[PB90-146838] N90-26443
CYGNUS CONSTELLATION
The interstellar D1 line at high resolution
[NASA-CR-184915] N90-26737
CYTOCHROMES
Experiment K-6-11. Actin mRNA and cytochrome c mRNA concentrations in the tricepts brachia muscle of rats N90-26465
CZOCHRALSKI METHOD
Mathematical simulation of heat exchanges and thermoelastic constraints in Czochralski crystal growth
[ETN-90-97242] N90-26680

D

DAMAGE
Vibration test procedures for orbiter sidewall-mounted payloads, phase 1
[AD-A220773] N90-26037
Vibration test procedures for orbiter sidewall-mounted payloads, phase 2
[AD-A220774] N90-26038
Damage states in laminated composite three-point bend specimens: An experimental-analytical correlation study
[NASA-TM-101800] N90-26083
Microstructural dependence of the cavitation damage function in FCC materials
[DE90-012898] N90-26113
Mechanical paint removal techniques for aircraft structures
[NIAR-90-12] N90-26166

Flight set 360L001 (STS-26) igniter, post flight
[NASA-CR-183957] N90-26325
Development of creep-fatigue damage detection method of rotor steel by ultrasonic wave measurement
[DE90-503792] N90-26365

DAMPING
Damping capacity of aluminum 6061-indium alloys
[AD-A222802] N90-26124
A critical evaluation of two-equation models for near wall turbulence
[NASA-CR-182068] N90-26270

DATA ACQUISITION
The Telecommunications and Data Acquisition Report
[NASA-CR-186852] N90-26217
The browse file of NASA/JPL quick-look radar images from the Loch Linnhe 1989 experiment
[NASA-CR-186855] N90-26701

DATA BASE MANAGEMENT SYSTEMS
The EISI (Elemental and Interplanar Spacing Index) index: A search/match tool for electron diffraction phase analysis
[DE90-010832] N90-26097
Compendium of material test results on HY-130 and Ti-3Al2V metals in support of United States navy programs
[DE90-011754] N90-26112
Damage measurements on optical materials for use in high-peak-power lasers
[DE90-013489] N90-26314
Laser damage database at 1064 nm
[DE90-013490] N90-26315
Pacific missile test center information resources management organization (code 0300): The ORACLE client-server and distributed processing architecture
[DE90-013271] N90-26565
International standards for text preparation and interchange
[DE90-011868] N90-26699
A methodology for benchmarking distributed database management systems
[DE90-007801] N90-26702
Construction of geological and geotechnical information database
[DE90-503417] N90-26708
Prototyping an in-house business intelligence database
[PNR90665] N90-26709

DATA BASES
Proceedings of the LDEF Materials Data Analysis Workshop
[NASA-CP-10046] N90-26075
Compendium of material test results on HY-130 and Ti-3Al2V metals in support of United States navy programs
[DE90-011754] N90-26112
Reusable rocket engine turbopump health monitoring system, part 3
[NASA-CR-182294] N90-26320
Application of symbolic computations to the constitutive modeling of structural materials
[NASA-TM-103225] N90-26364
An automated calibration laboratory for flight research instrumentation: Requirements and a proposed design approach
[NASA-TM-101719] N90-26564
Creating a VAPEPS database: A VAPEPS tutorial
[NASA-CR-186629] N90-26705
Energy data base: Subject categories and scope
[DE90-009212] N90-26706
Construction of geological and geotechnical information database
[DE90-503417] N90-26708
Chemical kinetics and modeling of planetary atmospheres N90-26763

DATA INTEGRATION
The value of real experience
[PNR90619] N90-26696

DATA LINKS
The disturbance processes on the data links of the mode-S air traffic control system
[ETN-90-96960] N90-25965
Experimental analysis of the HF linkage N90-26181
Experimental study of a digital mobile radio spread spectrum in an urban site N90-26205
Continuous on-line link error rate detector
[AD-D014510] N90-26209
Space operations: NASA's communications support for Earth orbiting spacecraft. Report to Chairman, Subcommittee on Space Science and Applications, Committee on Science, Space and Technology, House of Representatives
[GAO/IMTEC-89-41] N90-26215

DATA MANAGEMENT
Space operations: NASA is not properly safeguarding valuable data from past missions
[GAO/IMTEC-90-1] N90-26704
VISTA (Vertical Integration of Science, Technology, and Applications) user interface software study
[DE90-010003] N90-26707

DATA PROCESSING
Software set-up for data processing of depolarization due to rain and ice crystals in the Olympus project
[EUT-89-E-218] N90-26240
Documentation of program Tankplot
[FFI-89/7019] N90-26541
UEDIT: A full-scale, scrollable APL2 spreadsheet input/output editor
[AD-A222712] N90-26557
Neural networks for real-time sensory data processing and sensorimotor control
[AD-A223096] N90-26592

DATA REDUCTION
Prediction methodologies for nonlinear aerodynamic characteristics of control surfaces
[NIAR-90-17] N90-25937

DATA STORAGE
On the design and analysis of multiple-storage elements
[AD-A223095] N90-26266
Space operations: NASA is not properly safeguarding valuable data from past missions
[GAO/IMTEC-90-1] N90-26704

DATA STRUCTURES
Atomic snapshots of shared memory
[AD-A222765] N90-26520

DATA SYSTEMS
A global common-user system for the provision of HF propagation data N90-26180

DATA TRANSMISSION
The disturbance processes on the data links of the mode-S air traffic control system
[ETN-90-96960] N90-25965
Experimental analysis of the HF linkage N90-26181
Channel selection and control procedures in an automatic HF system N90-26193
Experimentation of a transmission system data processing by meteor bursts N90-26207
System factors to be considered in assessing propagation effects on modern digital satellite communications systems N90-26208
Microspacecraft and Earth observation: Electrical field (ELF) measurement project
[NASA-CR-186821] N90-26436
Applications for the scalable coherent interface
[DE90-011795] N90-26514
Design of a universal protocol system architecture: Specification of functions and services
[EUT-89-E-230] N90-26569
A methodology for benchmarking distributed database management systems
[DE90-007801] N90-26702

DEBRIS
Debris/ice/TPS assessment and photographic analysis for shuttle mission STS-31R
[NASA-TM-102790] N90-26040

DECISION MAKING
NASA project status reports: Congressional requirements can be met, but reliability must be ensured
[GAO/NSIAD-90-40] N90-26169
Survey of applicability of electric vehicles (EVs) in specific regions such as resorts
[DE90-503592] N90-26336
Pilot interaction with automated airborne decision making systems
[NASA-CR-186730] N90-26492
A study of the asymptotic properties of least square estimators for multiple phase regression problems
[ETN-90-97244] N90-26620
Effect of organizational structure on performance of decision making teams
[AD-A223160] N90-26697
The lessons of Varsovian's reconnaissance
[NASA-TM-103207] N90-26789

DECODERS
A hybrid M-algorithm/sequential decoder for convolutional and trellis codes
[NASA-CR-186863] N90-26528

DECODING
A hybrid M-algorithm/sequential decoder for convolutional and trellis codes
[NASA-CR-186863] N90-26528

DECOMPOSITION
The bit full-decomposition of sequential machines
[EUT-89-E-223] N90-26516
The full-decomposition of sequential machines with the separate realization of the next-state and output functions
[EUT-89-E-222] N90-26547
Closed-form solution of decomposable stochastic models
[NASA-TM-103466] N90-26619

DECOMPRESSION SICKNESS
Aircrew life support systems enhancement
[AD-A222626] N90-26505

DEEP SPACE NETWORK
A novel multireceiver communications system configuration based on optimal estimation theory
[NASA-CR-186847] N90-26216
The Telecommunications and Data Acquisition Report
[NASA-CR-186852] N90-26217
Goldstone intracomplex connected element interferometry N90-26218
Information content of a single pass of phase-delay data from a short baseline connected element interferometer N90-26220
Applications of different design methodologies in navigation systems and development at JPL N90-26221
Application of inertial instruments for DSN antenna pointing and tracking N90-26224
Design and performance analysis of the DSS-13 beam waveguide antenna N90-26225
Initial results on fault diagnosis of DSN antenna control assemblies using pattern recognition techniques N90-26228
Long-range planning cost model for support of future space missions by the deep space network N90-26231

DEFECTS
Comparison of currents predicted by NASCAP/LEO model simulations with elementary Langmuir-type bare probe models for an insulated cable containing a single pinhole
[NASA-TM-102486] N90-26054
Neural networks for detecting defects in aircraft structures
[IAR-90-4] N90-26345

DEFENSE INDUSTRY
AGARD highlights 90/1 N90-26788

DEFLECTION
Refractive error analysis in the interferometric measurement of 2-D density fields containing strong gradients
[LR-616] N90-26655

DEFORESTATION
Characterization of biogenic aerosol particles from the Amazon Basin during dry and wet season N90-26418

DEFORMATION
Structural analysis and optimization of a propfan blade using a finite element method
[DLR-FB-90-01] N90-26006
Crystal growth and deformation behavior of TiAl aluminides
[DE90-012972] N90-26671

DEGENERATION
Experiment K-6-09. Morphological and biochemical investigation of microgravity-induced nerve and muscle breakdown. Part 1: Investigation of nerve and muscle breakdown during spaceflight; Part 2: Biochemical analysis of EDL and PLT muscles N90-26463

DEGRADATION
Aeolian removal of dust from radiator surfaces on Mars
[NASA-TM-103205] N90-26068
The chemical effects of the Martian environment on power system component materials: A theoretical approach
[NASA-TM-103203] N90-26074
Quantitative confirmation of diffusion-limited oxidation theories
[DE90-012997] N90-26143
Reusable rocket engine turbopump health monitoring system, part 3
[NASA-CR-182294] N90-26320
Space operations: NASA is not properly safeguarding valuable data from past missions
[GAO/IMTEC-90-1] N90-26704

DEHYDRATION
The effects of pretreatment conditions on a Pt/SnO2 catalyst for the oxidation of CO in CO2 lasers
[NASA-TM-103487] N90-26309

DEICERS
A NASA/university/industry consortium for research on aircraft ice protection
[IAR-89-18] N90-25969

DELAMINATING
Strain energy release rate analysis of delamination in a tapered laminate subjected to tension load
[NASA-TM-102592] N90-26076

DELAY
Space exploration: Cost, schedule, and performance of NASA's Galileo Mission to Jupiter. Fact sheet for the Chairman, Subcommittee on Science, Technology, and Space, Committee on Commerce, Science, and Transportation, US Senate
[GAO/NSIAD-88-138FS] N90-26025
Active lag angle device
[AD-D014538] N90-26249

DELTA WINGS
Experimental study on vortex and shock wave development on a 65 deg delta wing
[NLR-MP-88033-U] N90-25950
DEMODULATION
New approaches for rapid synchronisation frequency hoppers N90-26201
QPSK loop lock detection in the advanced receiver N90-26230
DENDRITIC CRYSTALS
Dendritic web silicon photovoltaic cell research
[DE90-011786] N90-26387
DENSIFICATION
Densification studies of refractory materials using Hot Isostatic Pressing (HIP) and tantalum containment
[DE90-013481] N90-26114
DENSITY (MASS/VOLUME)
Analysis of turbulent density fluctuations by means of spontaneous Raman diffusion
[ISL-R-103/89] N90-26287
Experiment K-6-12. Morphometric studies of atrial or granules and hepatocytes. Part 1: Morphometric study of the liver; Part 2: The atrial granular accumulations N90-26466
DEOXYRIBONUCLEIC ACID
Imaging and spectroscopy of small molecules by scanning tunneling microscopy
[AD-A222572] N90-26641
DEPLOYMENT
Structures for remotely deployable precision antennas
[NASA-CR-182065] N90-26061
DEPOLARIZATION
Software set-up for data processing of depolarization due to rain and ice crystals in the Olympus project
[EUT-89-E-218] N90-26240
DEPOSITION
Carbon deposition model for oxygen-hydrocarbon combustion. Task 6: Data analysis and formulation of an empirical model
[NASA-CR-183986] N90-26095
Measurements of tropospheric nitric acid over the Western United States and Northeastern Pacific Ocean
[NASA-TM-103470] N90-26399
DESIGN ANALYSIS
Prediction methodologies for nonlinear aerodynamic characteristics of control surfaces
[NIAR-90-17] N90-25937
PDWAP: A preliminary design and weights analysis program for aerospace vehicles
[AD-A222614] N90-25979
Structural analysis and optimization of a propfan blade using a finite element method
[DLR-FB-90-01] N90-26006
Background, current status, and prognosis of the ongoing slush hydrogen technology development program for the NASP
[NASA-TM-103220] N90-26055
Computational fluid dynamics 3-D analysis for advanced transonic turbine design
[ETN-90-97282] N90-26291
Design of an autonomous Lunar construction utility vehicle
[NASA-CR-186832] N90-26330
The structural dynamics analysis of the main injector LOX inlet tee and its redesign
[NASA-CR-186764] N90-26358
Parametric design studies of toroidal magnetic energy storage units
[DE90-013086] N90-26390
Design of sensors for control of closed loop life support systems
[NASA-CR-186656] N90-26490
A computer module used to calculate the horizontal control surface size of a conceptual aircraft design
[NASA-CR-186872] N90-26515
Conception of a reconfigurable microprocessor
[ETN-90-97248] N90-26517
Space station definitions, design, and development. Task 5: Multiple arm telerobot coordination and control: Manipulator design methodology
[NASA-CR-182043] N90-26577
Surface acoustic wave filters in ZnO-SiO2-Si layered structures: Design, technology, and monolithic integration with electronic circuitry
[ETN-90-97218] N90-26638
DESORPTION
Mass spectrometry of poly(methyl methacrylate)s of low molecular weight N90-26091
Multicomponent gas sorption Joule-Thomson refrigerator
[NASA-CASE-NPO-17569-1-CU] N90-26176
DESULFURIZING
Regenerative Cu La zeolite supported desulfurizing sorbents
[NASA-CASE-NPO-17480-1-CU] N90-26098
DETECTION
The variably trimmed mean CFAR detector for nonhomogeneous background
[AD-A222801] N90-26243
Laser radar angular tracking
[AD-A222741] N90-26319
Neural networks for detecting defects in aircraft structures
[IAR-90-4] N90-26345
Field experience in using laser acoustic sensing for inspection
[DE90-012954] N90-26347
A study of positrons from Soviet nuclear powered satellites as tracers for magnetospheric research
[DE90-013157] N90-26438
Analysis and improved design considerations for airborne pulse Doppler radar signal processing in the detection of hazardous windshear
[NASA-CR-186792] N90-26448
A real-time robot arm collision detection system
[NASA-CR-185878] N90-26582
Resonant coupling through a slot to a loaded cylindrical cavity: Experimental results
[AD-A223000] N90-26631
DETERIORATION
Space operations: NASA is not properly safeguarding valuable data from past missions
[GAO/IMTEC-90-1] N90-26704
DIATOMIC MOLECULES
Rotational and translational effects in collisions of electronically excited diatomic hydrides
[NASA-CR-186770] N90-26093
DICHOTOMIES
Dichotomies for certain product measures and stable processes
[AD-A222568] N90-26521
DIELECTRIC PROPERTIES
The study of VF2/VF3 piezoelectric copolymeteres submitted to shocks
[ISL-CO-210/9] N90-26679
Ellipsometric study of YBa2Cu3O(7-x) laser ablated and co-evaporated films
[NASA-TM-103223] N90-26682
Dielectric function of InGaAs in the visible
[NASA-TM-103246] N90-26683
DIELECTRICS
Chemical structure and kinetics at liquid/solid interfaces
[AD-A222766] N90-26105
Theory of circular dielectric waveguide with anisotropic sheet cover
[NASA-CR-186883] N90-26235
DIENES
Quantitative confirmation of diffusion-limited oxidation theories
[DE90-012997] N90-26143
DIESEL ENGINES
Effect of casting procedures and diesel engine environment on the behavior of aluminum titanate
[AD-A223079] N90-26126
Heat engines
[DE90-000485] N90-26393
DIESEL FUELS
Regenerative Cu La zeolite supported desulfurizing sorbents
[NASA-CASE-NPO-17480-1-CU] N90-26098
Heat engines
[DE90-000485] N90-26393
DIFFERENTIAL EQUATIONS
Code enhancements and validation of GASP
[NPS-PAPER-44] N90-26277
Contribution to the study of differential equations and to the differences in the complex field
[ETN-90-97250] N90-26612
Theory of biaxial graded-index optical fiber
[NASA-CR-186882] N90-26652
DIFFRACTION
Scattering from coated structures and antenna pattern control using impedance surfaces, part A/B
[NASA-CR-186871] N90-26233
DIFFRACTION PATTERNS
A numerical simulation of the quasi-heterodyne technique for double-pulsed holographic vibration measurements
[PNR90622] N90-26301
Analysis of strain relaxation in Au/Ni multilayers by x ray diffraction
[IAR-89-25] N90-26357
Computer modeling wave propagation with a variation of the Helmholtz-Kirchhoff relation
[AD-A222746] N90-26657
DIFFUSION
Quantitative confirmation of diffusion-limited oxidation theories
[DE90-012997] N90-26143
DIFFUSION LENGTH
Estimation of minority carrier diffusion lengths in InP/GaAs solar cells
[NASA-TM-103213] N90-26069
DIGITAL FILTERS
Digital filtering of plume emission spectra
[NASA-TM-103135] N90-26070
DIGITAL SYSTEMS
Radio channel measurement and modelling for future mobile radio systems N90-26184
System factors to be considered in assessing propagation effects on modern digital satellite communications systems N90-26208
DIMENSIONAL ANALYSIS
A contribution to the economic, optimal dimensioning, and shaping of aircraft structures using a design model
[ETN-90-96966] N90-25976
Scaling effects in the static and dynamic response of graphite-epoxy beam-columns
[NASA-TM-102697] N90-26363
DIOXIDES
Selective electrocatalysis of anodic oxygen-transfer reactions at chemically modified, thin-film lead dioxide electrodes
[DE90-011747] N90-26252
DIRECT CURRENT
Experiments on initial behaviour of corona generated with electrical pulses superimposed on DC bias
[EUT-89-E-226] N90-26259
DIRECTION FINDING
Man-made noise in a military environment N90-26191
Implementation of an algorithm for travelling-wave-based directional detection
[EUT-89-E-214] N90-26239
DISCRETE FUNCTIONS
On output deadbeat control of discrete-time multivariable systems
[MATHS-REPT-A-122] N90-26583
DISPLAY DEVICES
Qualitative evaluation of a conformal velocity vector display for use at high angles-of-attack in fighter aircraft
[NASA-TM-102629] N90-25981
Literature concerning control and display technology applicable to the Orbital Maneuvering Vehicle (OMV)
[NASA-CR-186790] N90-26048
Choosing a pilot subjective workload scale to fit flight operational requirements
[IAR-89-21] N90-26493
Motion sickness, visual displays, and armored vehicle design
[AD-A222678] N90-26506
Knowledge-based system for flight information management
[NASA-TM-102685] N90-26511
DISSIPATION
Analysis and mitigation of numerical dissipation in inviscid and viscid computation of vortex-dominated flows
[NASA-CR-186887] N90-26281
On central-difference and upwind schemes
[NASA-CR-182061] N90-26595
Asymptotic analysis of dissipative waves with applications to their numerical simulation
[NASA-TM-103231] N90-26615
DISSOCIATION
Excimer laser fragmentation studies of selected oximes: Nascent OH internal energy distributions and the search of H2CN fluorescence
[AD-A222622] N90-26317
Dissociative recombination of molecular ions with electrons N90-26767
DISTORTION
Remote sensing of Earth terrain
[NASA-CR-186888] N90-26382
DISTRIBUTED PARAMETER SYSTEMS
ISIS and META projects
[NASA-CR-186645] N90-26524
Autoplan: A self-processing network model for an extended blocks world planning environment
[NASA-CR-186733] N90-26526
DISTRIBUTED PROCESSING
ISIS and META projects
[NASA-CR-186645] N90-26524
Autoplan: A self-processing network model for an extended blocks world planning environment
[NASA-CR-186733] N90-26526
Tools for distributed application management
[NASA-CR-186627] N90-26535
Formal verification of distributed computing systems: Logic characterization of behaviour equivalence
[LAAS-89386] N90-26555
An automated calibration laboratory for flight research instrumentation: Requirements and a proposed design approach
[NASA-TM-101719] N90-26564

Pacific missile test center information resources management organization (code 0300): The ORACLE client-server and distributed processing architecture
[DE90-013271] N90-26565
Parallel algorithm for distributed memory computers (applications to matricial algorithms)
[ETN-90-97252] N90-26573
Superconcurrent processing: A dynamic approach to heterogeneous parallelism
[AD-A222798] N90-26576
Parallel/distributed direct method for solving linear systems
[NASA-TM-103229] N90-26614
Causal distributed breakpoints
[AD-A222613] N90-26622
A methodology for benchmarking distributed database management systems
[DE90-007801] N90-26702
Knowledge and inhibition in asynchronous distributed systems
[TR-90-1139] N90-26703

DIURNAL VARIATIONS
New observations of stratospheric N2O5
[NASA-TM-103478] N90-26402
The collection and analysis of atmospheric peroxides N90-26428

DIVING (UNDERWATER)
Arctic cold weather medicine and accidental hypothermia
[AD-A223090] N90-26487
Development of membrane process for carbon dioxide separation from diving atmosphere
[AD-A222606] N90-26504

DOCUMENTATION
Documentation of program Tankplot
[FFI-89/7019] N90-26541

DOMAINS
Cartesian closed categories of domains
[ETN-90-97284] N90-26613

DOPED CRYSTALS
Nondestructive one- and two-dimensional doping profiling by inverse methods
[ETN-90-97264] N90-26351

DOSIMETERS
Experiment K-6-24, K-6-25, K-6-26. Radiation dosimetry and spectrometry N90-26477

DOUBLE BASE PROPELLANTS
Renewed aging control of adhesion of inhibitor on the gas generator charges for RB 24
[FOA-C-20780-2.1] N90-26153

DOWNLINKING
Microspacecraft and Earth observation: Electrical field (ELF) measurement project
[NASA-CR-186821] N90-26436

DOWNWASH
Wind tunnel study of wake downwash behind A 6 percent scale model B1-B aircraft
[DE90-011783] N90-25941

DRILLING
Lunar deep drill apparatus
[NASA-CR-182756] N90-26322

DROP SIZE
Optical characterization of clouds of fine liquid-nitrogen particles
[NASA-TM-103208] N90-26299

DROP TRANSFER
Bubble, Drop and Particle Unit (BDPU): A multi-user microgravity facility
[IAF-89-431] N90-26164

DROPS (LIQUIDS)
Liquid fueled ramjet combustion instability: Acoustical and vortical interactions with burning sprays
[AD-A222752] N90-26104
Bubble, Drop and Particle Unit (BDPU): A multi-user microgravity facility
[IAF-89-431] N90-26164
The 27-28 October 1986 FIRE IFO Cirrus case study: Comparison of radiative transfer theory with observations by satellite and aircraft
[NASA-TM-103468] N90-26446

DUCTILITY
Formation of cubic LI2 phases from Al3Ti and Al3Zr by transition metal substitutions for Al
[DE90-012288] N90-26117
The effect of manganese on the onset of the stage 2 reaction in an austempered ductile iron matrix
[DE90-011804] N90-26119

DUCTS
Measurement of terms and parameters in turbulent models
[NASA-CR-183993] N90-26271

DURABILITY
Probabilistic approach to the certification for fatigue durability of composite structures
[DE90-505521] N90-26085
Advanced Turbine Technology Applications Project (ATTAP)
[NASA-CR-185240] N90-26728

DUST
Aeolian removal of dust from radiator surfaces on Mars
[NASA-TM-103205] N90-26068
Investigation of the Saturn dust environment from the analysis of energetic charged particle measurements
[NASA-CR-186727] N90-26784

DYE LASERS
Theoretical studies of solar pumped lasers
[NASA-CR-186712] N90-26308
Characterization of a high-intensity, subpicosecond XeCl laser system
[DE90-011970] N90-26310
Intracavity Dye-Laser Absorption Spectroscopy (IDLAS) for application to planetary molecules N90-26761

DYNAMIC CHARACTERISTICS
Chemical structure and kinetics at liquid/solid interfaces
[AD-A222766] N90-26105

DYNAMIC CONTROL
An inverse dynamic method yielding flexible manipulator state trajectories
[NASA-CR-186807] N90-26329
On controller choice for robust sliding mode performance
[MATHS-REPT-A-107] N90-26337

DYNAMIC LOADS
Scaling effects in the static and dynamic response of graphite-epoxy beam-columns
[NASA-TM-102697] N90-26363

DYNAMIC MODELS
Research at NASA's NFAC wind tunnels
[NASA-TM-102827] N90-25933
Formation of design envelope criterion in terms of deterministic spectral procedure
[RAE-TM-SS-9] N90-25953
A reduced-dynamic technique for precise orbit determination N90-26219
A model of the synchronous machine with rectifier, especially for control purposes
[EUT-89-E-215] N90-26256

DYNAMIC RESPONSE
Computational crash dynamics. Project 1.2: Computational crash dynamics analysis
[IAR-89-19] N90-25956
An in-flight interaction of the X-29A canard and flight control system
[NASA-TM-101718] N90-25973
An investigation of the use of singular perturbation methods and modal control theory in the derivation or aircraft control schemes
[MATHS-REPT-A-106] N90-26014
Simulated dynamic response of a servovalve controlled hydraulic actuator
[NASA-TM-101644] N90-26167
The structural dynamics analysis of the main injector LOX inlet tee and its redesign
[NASA-CR-186764] N90-26358
Scaling effects in the static and dynamic response of graphite-epoxy beam-columns
[NASA-TM-102697] N90-26363
Structural dynamics branch research and accomplishments
[NASA-TM-102488] N90-26373
Biodynamic simulations of an aircraft pilot/passenger in various crash environments
[NIAR-90-6] N90-26494

DYNAMIC STRUCTURAL ANALYSIS
An in-flight interaction of the X-29A canard and flight control system
[NASA-TM-101718] N90-25973
Modeling of composite beams and plates for static and dynamic analysis
[NASA-CR-186459] N90-26354
The structural dynamics analysis of the main injector LOX inlet tee and its redesign
[NASA-CR-186764] N90-26358
Structural dynamics branch research and accomplishments
[NASA-TM-102488] N90-26373
Parallel processors and nonlinear structural dynamics algorithms and software
[NASA-CR-186755] N90-26536
Power flow analysis of two coupled plates with arbitrary characteristics
[NASA-CR-182033] N90-26632

DYNAMICAL SYSTEMS
A contribution to the improvement of the accuracy in the parameter identification of nonlinear processes, by example of the aircraft motion
[ETN-90-96961] N90-25974
A new scheme for identification and control
[EUT-88-E-213] N90-26586

E

EARTH ATMOSPHERE
Ice core studies and the past atmospheric environment of polar regions N90-26411

EARTH AXIS
Application of inertial instruments for DSN antenna pointing and tracking N90-26224

EARTH IONOSPHERE
Viking data analysis
[AD-A222609] N90-26062

EARTH MAGNETOSPHERE
Viking data analysis
[AD-A222609] N90-26062
A study of positrons from Soviet nuclear powered satellites as tracers for magnetospheric research
[DE90-013157] N90-26438

EARTH OBSERVATIONS (FROM SPACE)
Microspacecraft and Earth observation: Electrical field (ELF) measurement project
[NASA-CR-186821] N90-26436

EARTH OBSERVING SYSTEM (EOS)
Modeling, simulation, and analysis of optical remote sensing systems
[NASA-CR-186648] N90-26376

EARTH ORBITS
Space operations: NASA's communications support for Earth orbiting spacecraft. Report to Chairman, Subcommittee on Space Science and Applications, Committee on Science, Space and Technology, House of Representatives
[GAO/IMTEC-89-41] N90-26215

EARTH RADIATION BUDGET EXPERIMENT
Earth Radiation Budget Experiment (ERBE) validation
[NASA-TM-103481] N90-26433

ECONOMIC ANALYSIS
A contribution to the economic, optimal dimensioning, and shaping of aircraft structures using a design model
[ETN-90-96966] N90-25976
ASATs vs Brilliant Pebbles
[DE90-010348] N90-26626

ECONOMICS
Study of high-speed civil transports. Summary
[NASA-CR-4236] N90-25966
Survey of applicability of electric vehicles (EVs) in specific regions such as resorts
[DE90-503592] N90-26336

EDEMA
Experiment K-6-09. Morphological and biochemical investigation of microgravity-induced nerve and muscle breakdown. Part 1: Investigation of nerve and muscle breakdown during spaceflight; Part 2: Biochemical analysis of EDL and PLT muscles N90-26463

EDITING ROUTINES (COMPUTERS)
UEDIT: A full-scale, scrollable APL2 spreadsheet input/output editor
[AD-A222712] N90-26557

EDUCATION
Texstar: The all-Texas educational satellite system
[NASA-CR-186654] N90-26045
Applied mathematical modules for use in a linear algebra service course
[AD-A222814] N90-26618
A measurement of the effectiveness of the Airway Science Program to meet Federal Aviation Administration work force needs
[NIAR-90-5] N90-26694

EIGENVALUES
The use of Lanczo's method to solve the large generalized symmetric Eigenvalue problem in parallel
[NASA-CR-182072] N90-26533
Canonical eigenvalues. Part 1: General theory
[AD-A222812] N90-26617

EJECTION
Laboratory studies of the interaction of ions with condensed gases: Planetary applications N90-26778

ELASTIC WAVES
Real-time monitoring of ceramic sintering with laser ultrasonics
[DE90-012960] N90-26140
Laser ultrasonic measurements on ceramic materials with rough surfaces
[DE90-012961] N90-26141

ELECTRIC BATTERIES
Electrochemical, in situ Raman spectroscopic, and conductivity studies of polypyrrole incorporating large size anions: Conducting nature of reduced form
[AD-A222739] N90-26102
The development and characterization of ion exchange membranes for selected electrochemical power sources
[DE90-009741] N90-26251
Evaluation of room-temperature chloroaluminate molten salts as electrolytes for high energy density batteries
[AD-A223097] N90-26267

ELECTRIC CORONA
Experiments on initial behaviour of corona generated with electrical pulses superimposed on DC bias
[EUT-89-E-226] N90-26259
ELECTRIC CURRENT
Parametric design studies of toroidal magnetic energy storage units
[DE90-013066] N90-26390
ELECTRIC DISCHARGES
Storage battery operation technique of photovoltaic system to prevent the imbalance of state of charge
[DE90-503032] N90-26255
ELECTRIC FIELD STRENGTH
Electric field strength meters for the HF, VHF, and UHF bands
[BBC-RD-1990/3] N90-26212
Resonant coupling through a slot to a loaded cylindrical cavity: Experimental results
[AD-A223000] N90-26631
ELECTRIC FIELDS
Inhomogeneous electric field effects in a linear RF quadruple trap N90-26222
Microspacecraft and Earth observation: Electrical field (ELF) measurement project
[NASA-CR-186821] N90-26436
Confinement of nonneutral plasma in unconventional geometries
[DE90-013048] N90-26659
ELECTRIC MOTOR VEHICLES
Survey of applicability of electric vehicles (EVs) in specific regions such as resorts
[DE90-503582] N90-26336
ELECTRIC POTENTIAL
Comparison of currents predicted by NASCAP/LEO model simulations with elementary Langmuir-type bare probe models for an insulated cable containing a single pinhole
[NASA-TM-102486] N90-26054
A possibility to incorporate saturation in the simple, global model of a synchronous machine with rectifier
[EUT-89-E-225] N90-26258
High speed magneto-resistive random access memory
[NASA-CASE-NPO-17954-1-CU] N90-26519
ELECTRIC POWER SUPPLIES
The development and characterization of ion exchange membranes for selected electrochemical power sources
[DE90-009741] N90-26251
ELECTRIC PULSES
Experiments on initial behaviour of corona generated with electrical pulses superimposed on DC bias
[EUT-89-E-226] N90-26259
ELECTRICAL FAULTS
Implementation of an algorithm for travelling-wave-based directional detection
[EUT-89-E-214] N90-26239
LASER: A Layout Sensitivity Explorer. Report and user's manual
[EUT-89-E-216] N90-26545
ELECTRICAL IMPEDANCE
An experimental system for measuring the wavenumber-frequency response of Timoshenko beams
[AD-A222569] N90-26374
ELECTRICAL MEASUREMENT
Nondestructive one- and two-dimensional doping profiling by inverse methods
[ETN-90-97264] N90-26351
ELECTRICAL RESISTANCE
Quantum ballistic and adiabatic electron transport, studied with quantum point contacts
[ETN-90-97262] N90-26440
ELECTRICAL RESISTIVITY
Searching for heavy fermion materials in Ce intermetallic compounds
[DE90-011809] N90-26116
Resistivity, adhesive strength, and residual stress measurements of thin film metallizations on single crystal quartz
[DE90-011902] N90-26135
The development and characterization of ion exchange membranes for selected electrochemical power sources
[DE90-009741] N90-26251
High speed magneto-resistive random access memory
[NASA-CASE-NPO-17954-1-CU] N90-26519
Experiments on superconductor imaging surface magnetometry
[DE90-008925] N90-26665
ELECTROACOUSTIC TRANSDUCERS
Application and extension of an analytical model of the confined acoustic beam generated by a transducer
[AD-A222994] N90-26839
ELECTROCATALYSTS
Selective electrocatalysis of anodic oxygen-transfer reactions at chemically modified, thin-film lead dioxide electrodes
[DE90-011747] N90-26252
ELECTROCHEMISTRY
Electrochemical, in situ Raman spectroscopic, and conductivity studies of polypyrrole incorporating large size anions: Conducting nature of reduced form
[AD-A222739] N90-26102
The development and characterization of ion exchange membranes for selected electrochemical power sources
[DE90-009741] N90-26251
Structured electrode interfaces
[AD-A222763] N90-26265
ELECTRODES
Electrode carrying wire for GTAW welding
[NASA-CASE-MFS-29491-1] N90-26168
Selective electrocatalysis of anodic oxygen-transfer reactions at chemically modified, thin-film lead dioxide electrodes
[DE90-011747] N90-26252
Structured electrode interfaces
[AD-A222763] N90-26265
ELECTROLYTES
Storage battery operation technique of photovoltaic system to prevent the imbalance of state of charge
[DE90-503032] N90-26255
Ionic atmosphere effects on the energetics of thermal and optical electron-exchange reactions: Application to ferrocenium-ferrocene self exchange
[AD-A222605] N90-26441
ELECTROLYTIC CELLS
Evaluation of room-temperature chloroaluminate molten salts as electrolytes for high energy density batteries
[AD-A223097] N90-26267
ELECTROMAGNETIC ABSORPTION
Laboratory measurements and modeling of microwave absorption by ammonia in gas mixtures applicable to giant planet atmospheres N90-26750
Optical signatures of molecular particles via mass-selected cluster spectroscopy N90-26780
ELECTROMAGNETIC COMPATIBILITY
Resonant coupling through a slot to a loaded cylindrical cavity: Experimental results
[AD-A223000] N90-26631
ELECTROMAGNETIC INTERACTIONS
Interaction of electromagnetic signals with particulate clouds
[AD-A222804] N90-26244
ELECTROMAGNETIC INTERFERENCE
The disturbance processes on the data links of the mode-S air traffic control system
[ETN-90-96960] N90-25965
Minimization of the cost of information transfer in HF spread spectrum transmission N90-26198
ELECTROMAGNETIC MEASUREMENT
NDE (Nondestructive evaluation) of critical currents in high T(sub c) superconductors
[DE90-012953] N90-26670
ELECTROMAGNETIC RADIATION
Transmission, reflection, and radiation at junction planes of different open waveguides
[ISBN-90-9002864-1] N90-26241
Remote sensing of Earth terrain
[NASA-CR-186888] N90-26382
Resonant coupling through a slot to a loaded cylindrical cavity: Experimental results
[AD-A223000] N90-26631
ELECTROMAGNETIC SCATTERING
Electromagnetic inverse scattering of buried objects
[ETN-90-97216] N90-26242
ELECTROMAGNETIC WAVE TRANSMISSION
Transmission, reflection, and radiation at junction planes of different open waveguides
[ISBN-90-9002864-1] N90-26241
ELECTROMECHANICAL DEVICES
A possibility to incorporate saturation in the simple, global model of a synchronous machine with rectifier
[EUT-89-E-225] N90-26258
ELECTRON ACCELERATORS
DURIP: Instrumentation for laser switched power LINAC
[AD-A222629] N90-26318
ELECTRON DIFFRACTION
The EISI (Elemental and Interplanar Spacing Index) index: A search/match tool for electron diffraction phase analysis
[DE90-010832] N90-26097
ELECTRON DIFFUSION
Estimation of minority carrier diffusion lengths in InP/GaAs solar cells
[NASA-TM-103213] N90-26069
ELECTRON GAS
Quantum ballistic and adiabatic electron transport, studied with quantum point contacts
[ETN-90-97262] N90-26440
ELECTRON IMPACT
Electron-impact spectroscopy N90-26779
ELECTRON MICROSCOPES
DoD-University research instrumentation program, FY 1986/FY 1987
[AD-A222578] N90-26263
ELECTRON MICROSCOPY
The application of HREELS to model catalysts: CO and C2H4 adsorption on Pt/Al2O3
[AD-A222744] N90-26103
Structures and mechanical properties of near-beta titanium alloys TiV10Fe2Al3 and TiV10Cu3Al3
[ONERA-NT-1989-3] N90-26123
Experiment K-6-06. Morphometric and EM analyses of tibial epiphyseal plates from Cosmos 1887 rats N90-26460
ELECTRON PUMPING
New discharge pumping method for CO2 lasers
[AD-A220898] N90-26307
ELECTRON SCATTERING
Electron-impact spectroscopy N90-26779
ELECTRON SPECTROSCOPY
The application of HREELS to model catalysts: CO and C2H4 adsorption on Pt/Al2O3
[AD-A222744] N90-26103
ELECTRON TRANSFER
Dynamical solvent effects on electron-transfer processes: Recent progress and perspectives
[AD-A222603] N90-26101
Ionic atmosphere effects on the energetics of thermal and optical electron-exchange reactions: Application to ferrocenium-ferrocene self exchange
[AD-A222605] N90-26441
ELECTRONIC COUNTERMEASURES
HF spread spectrum, an audit of the power requirements and LPI vulnerability N90-26203
ELECTRONIC EQUIPMENT TESTS
PVDF contact probes
[VTT-RR-623] N90-26253
ELECTRONIC WARFARE
Electronic warfare technology: Trends and visions
[AD-A223034] N90-26246
ELECTRONS
The charged particle radiation environment for AXAF
[NASA-TM-100405] N90-26741
Dissociative recombination of molecular ions with electrons N90-26767
ELLIPSOMETERS
Ellipsometric study of YBa2Cu3O(7-x) laser ablated and co-evaporated films
[NASA-TM-103223] N90-26682
EMBEDDING
An embedded fibre optic sensor for impact damage detection in composite materials
[UTIAS-332] N90-26650
EMERGENCIES
Orbiter utilization as an ACRV
[NASA-TM-102700] N90-26032
Preliminary subsystem designs for the Assured Crew Return Vehicle (ACRV), volume 1
[NASA-CR-186677-VOL-1] N90-26039
Space operations: NASA's communications support for Earth orbiting spacecraft. Report to Chairman, Subcommittee on Space Science and Applications, Committee on Science, Space and Technology, House of Representatives
[GAO/IMTEC-89-41] N90-26215
Human factors: The human interface with aircraft interiors
[NIAR-90-18] N90-26496
EMERGENCY BREATHING TECHNIQUES
Arctic cold weather medicine and accidental hypothermia
[AD-A223090] N90-26487
EMISSION
Astronomy at ultra-high energies: Results from the CYGNUS experiment
[DE90-011979] N90-26732
EMISSION SPECTRA
Digital filtering of plume emission spectra
[NASA-TM-103135] N90-26070
EMITTANCE
Measuring and modeling near-surface reflected and emitted radiation fluxes at the FIFE site
[NASA-CR-180953] N90-26378
ENCAPSULATING
Development of microencapsulation techniques
[AD-A223032] N90-26159
END EFFECTORS
Direct drive robotic hand
[NASA-CASE-NPO-17917-1-CU] N90-26339
Grasping with mechanical intelligence
[NASA-CR-186864] N90-26498
Space station definitions, design, and development. Task 5: Multiple arm telerobot coordination and control: Manipulator design methodology
[NASA-CR-182043] N90-26577

ENERGETIC PARTICLES
Investigation of the Saturn dust environment from the analysis of energetic charged particle measurements [NASA-CR-186727] N90-26784
ENERGY BUDGETS
Measuring and modeling near-surface reflected and emitted radiation fluxes at the FIFE site [NASA-CR-180953] N90-26378
ENERGY CONVERSION
Analysis of a Mars-stationary orbiting microwave power transmission system [NASA-TM-101344] N90-26172
ENERGY CONVERSION EFFICIENCY
Silicon concentrator solar cell development [DE90-011782] N90-26386
Megawatt solar power systems for lunar surface operations [NASA-CR-186509] N90-26391
ENERGY DISSIPATION
The application of HREELS to model catalysts: CO and C2H4 adsorption on Pt/Al2O3 [AD-A222744] N90-26103
ENERGY DISTRIBUTION
Excimer laser fragmentation studies of selected oximes: Nascent OH internal energy distributions and the search of H2CN fluorescence [AD-A222622] N90-26317
Vacuum deposition by pulsed laser radiation: Plasma composition, deposition techniques, and thin film properties [ETN-90-97263] N90-26677
ENERGY LEVELS
New electronic states of NH and ND observed by resonance enhanced multiphoton ionization spectroscopy N90-26760
ENERGY STORAGE
The use of hydrogen in energy economy of Finland [DE90-796180] N90-26388
ENERGY TECHNOLOGY
The use of hydrogen in energy economy of Finland [DE90-796180] N90-26388
Energy data base: Subject categories and scope [DE90-009212] N90-26706
ENERGY TRANSFER
Rotational and translational effects in collisions of electronically excited diatomic hydrides [NASA-CR-186770] N90-26093
Theoretical studies of solar pumped lasers [NASA-CR-186712] N90-26308
A closed form solution to HZE propagation [NASA-TM-103482] N90-26640
Determination of molecular spectroscopic parameters and energy-transfer rates by double-resonance spectroscopy N90-26755
Measurements of the methane relaxation times for application to the infrared emission models of the upper atmospheres of outer planets and Titan N90-26759
ENGINE CONTROL
Software requirements: Guidance and control software development specification [NASA-CR-182058] N90-26527
ENGINE DESIGN
Transatmospheric vehicle research [NASA-CR-186705] N90-25970
Combustion in the gas turbine. Part 1: Combustor types and design [CIT/SME/VKI/RS/1] N90-25986
Combustion in the gas turbine. Part 2: Preliminary design and performance [CIT/SME/VKI/RS/3] N90-25987
Combustion in the gas turbine. Part 3: Fuel injection, ignition and stability [CIT/SME/VKI/RS/4] N90-25988
Combustor cooling aspects [CIT/SME/VKI/RS/5] N90-25989
Supersonic combustor testing N90-25998
Prediction and measurement of rotor blade/stator vane dynamic characteristics of a modern aero-engine axial compressor [PNR90667] N90-26002
The impact and requirements of new materials on aeroengines [PNR90671] N90-26003
Research and development of advanced gas turbine [DE90-503377] N90-26335
Preliminary designs for 25 kWe advanced Stirling conversion systems for dish electric applications [NASA-TM-103188] N90-26729
ENGINE INLETS
Research and development of advanced gas turbine [DE90-503377] N90-26335
ENGINE MONITORING INSTRUMENTS
Reusable rocket engine turbopump health monitoring system, part 3 [NASA-CR-182294] N90-26320
ENGINE NOISE
Stage 2 re-engining: The only way to achieve a real stage 3 aircraft [PNR90636] N90-25977
ENGINE PARTS
Combustion in the gas turbine. Part 2: Preliminary design and performance [CIT/SME/VKI/RS/3] N90-25987
The application of engineering ceramics in gas turbines [PNR90676] N90-26005
The role of NDI in the certification of turbine engine components [PNR90629] N90-26349
ENGINE TESTS
Gas Turbine Combustion, volume 2 [VKI-LS-1990-02-VOL-2] N90-25995
Combustion instrumentation N90-25996
Subsonic combustor testing N90-25997
Supersonic combustor testing N90-25998
Handbook of uncertainty methodology for engine testing at Pyestock (England) [RAE-TM-P-1179] N90-26007
QM-8 final performance evaluation report: SEALS, volume 4 [NASA-CR-183958] N90-26324
Bringing aircraft noise testing down to Earth [PNR90642] N90-26637
Advanced Turbine Technology Applications Project (ATTAP) [NASA-CR-185240] N90-26728
ENVIRONMENT EFFECTS
Proceedings of the LDEF Materials Data Analysis Workshop [NASA-CP-10046] N90-26075
Characterization of biogenic aerosol particles from the Amazon Basin during dry and wet season N90-26418
ENVIRONMENT MODELS
An Eulerian transport model for NO(sub x)-compounds N90-26406
ENVIRONMENT POLLUTION
Survey of applicability of electric vehicles (EVs) in specific regions such as resorts [DE90-503592] N90-26336
ENVIRONMENTAL CONTROL
Fluid Phase Separation (FPS) experiment for flight on a space shuttle Get Away Special (GAS) canister [NASA-CR-186830] N90-26161
Automation of closed environments in space for human comfort and safety [NASA-CR-186834] N90-26500
ENVIRONMENTAL MONITORING
Vertical ozone probing with lidar N90-26416
ENVIRONMENTAL SURVEYS
The transfer of mercury between the atmosphere and lake or soil surfaces N90-26419
ENVIRONMENTAL TESTS
The chemical effects of the Martian environment on power system component materials: A theoretical approach [NASA-TM-103203] N90-26074
Effect of casting procedures and diesel engine environment on the behavior of aluminum titanate [AD-A223079] N90-26126
Soil experiment [NASA-CR-184927] N90-26165
ENZYME ACTIVITY
Experiment K-6-10. Effects of zero gravity on myofibril protein content and isomyosin distribution in rodent skeletal muscle N90-26464
Experiment K-6-14. Hepatic function in rats after spaceflight N90-26468
ENZYMES
Experiment K-6-21. Effect of microgravity on 1) metabolic enzymes of type 1 and type 2 muscle fibers and on 2) metabolic enzymes, neutransmitter amino acids, and neurotransmitter associated enzymes in motor and somatosensory cerebral cortex. Part 1: Metabolic enzymes of individual muscle fibers; part 2: metabolic enzymes of hippocampus and spinal cord N90-26474
Computer simulation of chemical reactions in synthetic model compounds and genetically engineered active sites [AD-A222611] N90-26483
EPITAXY
Large, orientation-dependent enhancements of critical currents in Y1Ba2Cu3O(7-x) epitaxial thin films: Evidence for intrinsic flux pinning [DE90-009424] N90-26666
EPOXY MATRIX COMPOSITES
Strain energy release rate analysis of delamination in a tapered laminate subjected to tension load [NASA-TM-102592] N90-26076
Erosion mechanisms in composite materials and ripple formation mechanism in erosion [IAR-89-4-PT-1] N90-26078
EPOXY RESINS
Evolution of structure and viscoelasticity in diethanolamine-cured epoxy [DE90-011256] N90-26134
EQUATIONS OF MOTION
Identification of aerodynamic models for maneuvering aircraft [NASA-CR-186630] N90-25943
EQUATIONS OF STATE
Nonstandard big bang models [DE90-625593] N90-26736
EQUATORIAL ORBITS
Space operations: NASA's communications support for Earth orbiting spacecraft. Report to Chairman, Subcommittee on Space Science and Applications, Committee on Science, Space and Technology, House of Representatives [GAO/IMTEC-89-41] N90-26215
EQUIPOTENTIALS
Sensitivity analysis with a simple charging code [RAE-TM-SPACE-374] N90-26662
EQUIVALENT CIRCUITS
An experimental system for measuring the wavenumber-frequency response of Timoshenko beams [AD-A222569] N90-26374
ERGODIC PROCESS
Strong consistency of the least squares estimator for a non-ergodic threshold autoregressive model [IMAG-RR-791-M] N90-26604
EROSION
Erosion mechanisms in composite materials and ripple formation mechanism in erosion [IAR-89-4-PT-1] N90-26078
Erosion mechanisms in composite materials and ripple formation mechanism in erosion [IAR-89-4-PT-2] N90-26079
Flight set 360L001 (STS-26) igniter, post flight [NASA-CR-183957] N90-26325
ERROR ANALYSIS
Handbook of uncertainty methodology for engine testing at Pyestock (England) [RAE-TM-P-1179] N90-26007
Continuous on-line link error rate detector [AD-D014510] N90-26209
Information content of a single pass of phase-delay data from a short baseline connected element interferometer N90-26220
Initial results on fault diagnosis of DSN antenna control assemblies using pattern recognition techniques N90-26228
Video camera system for locating bullet holes in targets at a ballistics tunnel [NASA-TM-4197] N90-26296
Self-checking on-line testable static RAM [NASA-CASE-NPO-17939-1-CU] N90-26518
Refractive error analysis in the interferometric measurement of 2-D density fields containing strong gradients [LR-616] N90-26655
ERROR CORRECTING CODES
A versatile integrated block codes encoder-decoder N90-26197
New synchronisation techniques applicable to multi-tone transmission systems N90-26199
Verification-correction of a program for including uncertainties in the robot automatic programming [ETN-90-97246] N90-26588
ERROR SIGNALS
Self-checking on-line testable static RAM [NASA-CASE-NPO-17939-1-CU] N90-26518
ERRORS
Feasibility study of a synthesis procedure for array feeds to improve radiation performance of large distorted reflector antennas [NASA-CR-186641] N90-26213
Preliminary error budget for an optical ranging system: Range, range rate, and differenced range observables N90-26227
ESCAPE SYSTEMS
Orbiter utilization as an ACRV [NASA-TM-102700] N90-26032
ESTIMATES
Estimation of convective rain volumes utilizing the are-time-integral technique [NASA-CR-186814] N90-26449
Variance reduction for quantile estimates in simulations via nonlinear controls [AD-A222653] N90-26590
ESTIMATING
A novel multireceiver communications system configuration based on optimal estimation theory [NASA-CR-186847] N90-26216
Estimation of convective rain volumes utilizing the are-time-integral technique [NASA-CR-186814] N90-26449

ETHANE
Laboratory studies, analysis, and interpretation of the spectra of hydrocarbons present in planetary atmospheres including cyanoacetylene, acetylene, propane, and ethane N90-26748
ETHYLENE
The application of HREELS to model catalysts: CO and C2H4 adsorption on Pt/Al2O3
[AD-A222744] N90-26103
Quantitative confirmation of diffusion-limited oxidation theories
[DE90-012997] N90-26143
EULER EQUATIONS OF MOTION
The role of computational fluids dynamics in missile aerodynamics
[NLR-MP-88072-U] N90-25952
Analysis and mitigation of numerical dissipation in inviscid and viscid computation of vortex-dominated flows
[NASA-CR-186887] N90-26281
Development of a system for the numerical simulation of Euler flows, with results of preliminary 3-D propeller-slipstream/exhaust-jet calculations
[NLR-TR-88006-U] N90-26285
An Eulerian transport model for NO(sub x)-compounds N90-26406
EUROPEAN SPACE PROGRAMS
Space exploration: Cost, schedule, and performance of NASA's Ulysses Mission to the Sun. Fact sheet for the Chairman, Subcommittee on Science, Technology, and Space, Committee on Commerce, Science, and Transportation, US Senate
[GAO/NSIAD-88-129FS] N90-26023
EUTECTICS
Two-dimensional model of a Space Station Freedom thermal energy storage canister
[NASA-TM-103124] N90-26279
EVAPORATION
Ellipsometric study of YBa2Cu3O(7-x) laser ablated and co-evaporated films
[NASA-TM-103223] N90-26682
EXCIMER LASERS
Formation of Titanium-boron surface alloys by excimer laser mixing
[DE90-013172] N90-26118
Excimer laser fragmentation studies of selected oximes: Nascent OH internal energy distributions and the search of H2CN fluorescence
[AD-A222622] N90-26317
EXCITATION
Rotational and translational effects in collisions of electronically excited diatomic hydrides
[NASA-CR-186770] N90-26093
A study of the influence of Hg(6(3)P2) population in a low-pressure discharge on mercury ion emission at 194.2 nm N90-26223
Excimer laser fragmentation studies of selected oximes: Nascent OH internal energy distributions and the search of H2CN fluorescence
[AD-A222622] N90-26317
Formation and deactivation of vibrationally excited atmospheric molecules
[AD-A222660] N90-26442
EXHAUST EMISSION
Pollutants: Production and methods of reduction
[CIT/SME/VKI/RS/6] N90-25990
Aircraft exhaust emissions: An engine manufacturer's perspective
[PNR90675] N90-26004
EXHAUST GASES
Digital filtering of plume emission spectra
[NASA-TM-103135] N90-26070
EXHAUST NOZZLES
Hot gas ingestion characteristics and flow visualization of a vectored thrust STOVL concept
[NASA-TM-103212] N90-26009
EXOBIOLOGY
The US Experiments Flown on the Soviet Biosatellite Cosmos 1887
[NASA-TM-102254] N90-26452
EXPENDABLE STAGES (SPACECRAFT)
IRIS system and future application to expandable launchers
[IAF-89-212] N90-26035
EXPERIENCE
The value of real experience
[PNR90619] N90-26696
EXPERIMENT DESIGN
Integrated support structure
[NASA-CR-186835] N90-26162
Launching a dream: A teachers guide to a simulated space shuttle mission
[NASA-TM-89715] N90-26693
EXPERT SYSTEMS
Inference and control mechanisms in NEXT 2.0
[NLR-MP-88062-U] N90-26175
Reusable rocket engine turbopump health monitoring system, part 3
[NASA-CR-182294] N90-26320
Neural networks for detecting defects in aircraft structures
[IAR-90-4] N90-26345
Robotic-aided system for inspection of aging aircraft
[NIAR-90-9] N90-26346
Application of symbolic computations to the constitutive modeling of structural materials
[NASA-TM-103225] N90-26364
Knowledge-based system for flight information management
[NASA-TM-102685] N90-26511
An expert system based software sizing tool, phase 2
[NASA-CR-186706] N90-26525
Integrating expert systems with solid modeling through interprocess communications and the applications interface specification
[DE90-012896] N90-26537
Material selection and design: An expert system approach
[PNR90611] N90-26544
Prototyping an in-house business intelligence database
[PNR90665] N90-26709
EXTERNAL TANKS
Debris/ice/TPS assessment and photographic analysis for shuttle mission STS-31R
[NASA-TM-102790] N90-26040
QM-8 final performance evaluation report: SEALS, volume 4
[NASA-CR-183958] N90-26324
EXTRACTION
Automatic line network extraction from aerial imagery of urban areas through knowledge based image analysis
[AD-A222675] N90-26385
EXTRAPOLATION
Efficient implementation of minimal polynomial and reduced rank extrapolation methods
[NASA-TM-103240] N90-26616
EXTRAVEHICULAR ACTIVITY
Design of a lunar transportation system, volume 2
[NASA-CR-186833-VOL-2] N90-26333
EXTREMELY HIGH FREQUENCIES
Design and performance analysis of the DSS-13 beam waveguide antenna N90-26225
EXTREMELY LOW FREQUENCIES
Microspacecraft and Earth observation: Electrical field (ELF) measurement project
[NASA-CR-186821] N90-26436
EYE MOVEMENTS
Eye tracking device for the measurement of flight performance in simulators
[AD-A220075] N90-26484

F

F-15 AIRCRAFT
Effect of tail size reductions on longitudinal aerodynamic characteristics of a three surface F-15 model with nonaxisymmetric nozzles
[NASA-TP-3036] N90-25938
FABRICATION
A resistance strain gage with repeatable and cancellable apparent strain for use to 800 C
[NASA-CR-185256] N90-26063
Carbon-carbon composites: Emerging materials for hypersonic flight
[NASA-TM-103472] N90-26080
Advanced Turbine Technology Applications Project (ATTAP)
[NASA-CR-185240] N90-26728
FACE CENTERED CUBIC LATTICES
Full vector wave calculation of photonic band structures in face-centered cubic dielectric media
[AD-A222616] N90-26686
FACTORIZATION
H-infinity control: An exploratory study
[EUT-88-E-211] N90-26584
FAILURE
Evaluation of room-temperature chloroaluminate molten salts as electrolytes for high energy density batteries
[AD-A223097] N90-26267
FAILURE ANALYSIS
Study on failure modes of boron fiber reinforced aluminum composite materials by AE method, part 2
[DE90-505522] N90-26086
A comparison of the post-buckling behavior of metallic and composite plates with centrally located cutouts
[NIAR-90-14] N90-26356
Design of ceramic components with the NASA/CARES computer program
[NASA-TM-102369] N90-26359
Scaling effects in the static and dynamic response of graphite-epoxy beam-columns
[NASA-TM-102697] N90-26363
FAILURE MODES
Study on failure modes of boron fiber reinforced aluminum composite materials by AE method, part 2
[DE90-505522] N90-26086
Extension of a noninteractive reliability model for ceramic matrix composites
[NASA-CR-185267] N90-26142
FALSE ALARMS
The variably trimmed mean CFAR detector for nonhomogeneous background
[AD-A222801] N90-26243
FAR INFRARED RADIATION
A compact, high-powered Far-Infrared (FIR) laser
[DE90-009996] N90-26312
High resolution spectroscopy in the microwave and far infrared N90-26746
FAR ULTRAVIOLET RADIATION
Absolute vacuum ultraviolet photoabsorption cross section studies of atomic and molecular species: Techniques and observational data N90-26754
FARM CROPS
Catching our breath: Next steps for reducing urban ozone
[PB90-130451] N90-26398
FASTENERS
Neural networks for detecting defects in aircraft structures
[IAR-90-4] N90-26345
FATIGUE (MATERIALS)
Probabilistic approach to the certification for fatigue durability of composite structures
[DE90-505521] N90-26085
Small crack growth and its influence in near alpha-titanium alloys
[RAE-TM-P-1171] N90-26121
Development of creep-fatigue damage detection method of rotor steel by ultrasonic wave measurement
[DE90-503792] N90-26365
Fatigue life assessment using a short crack growth model
[PNR90663] N90-26367
FATIGUE LIFE
A study of the fatigue behavior in scratched samples of Al-Li alloy (2090-T3)
[IAR-89-24] N90-26107
Microstructural design for fatigue crack growth resistance in Ni-base alloy
[PNR90632] N90-26120
FATIGUE TESTS
A study of the fatigue behavior in scratched samples of Al-Li alloy (2090-T3)
[IAR-89-24] N90-26107
Investigation of crack-closure prediction models for fatigue in aluminium alloy sheet under flight-simulation loading
[LR-619] N90-26369
Static and fatigue strength of an adhesive bonded CFRP butt-strap joint: The effects of stacking sequence and temperature
[NLR-TR-88036-U] N90-26370
FAULT TOLERANCE
Technical evaluation report on the Guidance and Control Panel 49th Symposium on Fault Tolerant Design Concepts for Highly Integrated Flight Critical Guidance and Control Systems
[AGARD-AR-281] N90-26012
Making real-time reactive systems reliable
[NASA-CR-186642] N90-26344
Adaptive fault-tolerant routing in hypercube multicomputers
[NASA-CR-186781] N90-26513
Self-checking on-line testable static RAM
[NASA-CASE-NPO-17939-1-CU] N90-26518
Closed-form solution of decomposable stochastic models
[NASA-TM-103466] N90-26619
FEASIBILITY ANALYSIS
Dendritic web silicon photovoltaic cell research
[DE90-011786] N90-26387
FEEDBACK CONTROL
Synthesis of individual rotor blade control system for gust alleviation
[NASA-TM-101886] N90-25972
Robustness evaluation of H2 and H(infinity) control theory as applied to a transport aircraft
[AD-A222795] N90-26018
ISIS and META projects
[NASA-CR-186645] N90-26524
On the robust stability of MIMO linear feedback systems
[EUT-88-E-212] N90-26585

FEMALES
Human performance in cockpit-related systems
[NIAR-90-7] N90-26495
FEMUR
Experiment K-6-01. Distribution and biochemistry of mineral and matrix in the femurs of rats N90-26455
FERMIONS
Searching for heavy fermion materials in Ce intermetallic compounds
[DE90-011809] N90-26116
FERROCENES
Ionic atmosphere effects on the energetics of thermal and optical electron-exchange reactions: Application to ferrocenium-ferrocene self exchange
[AD-A222605] N90-26441
FERROELECTRICITY
The study of VF2/VF3 piezoelectric copolymeteres submitted to shocks
[ISL-CO-210/9] N90-26679
FERROMAGNETIC FILMS
High speed magneto-resistive random access memory
[NASA-CASE-NPO-17954-1-CU] N90-26519
FIBER COMPOSITES
Vitreous joining of SiC fiber reinforced SiC composites
[DE90-012951] N90-26081
The influence of microstructure on the tensile behavior of an aluminum metal matrix composite
[NASA-TM-102694] N90-26082
Study on failure modes of boron fiber reinforced aluminum composite materials by AE method, part 2
[DE90-505522] N90-26086
Plate rods and leaf springs with hybrid structure: Cross section optimization following different target criteria
[ILR-MITT-227(1989)] N90-26366
Reliability analysis of continuous fiber composite laminates
[NASA-CR-185265] N90-26372
An embedded fibre optic sensor for impact damage detection in composite materials
[UTIAS-332] N90-26650
FIBER OPTICS
Design of an optically controlled Ka-band GaAs MMIC phased-array antenna
[NASA-TM-103147] N90-26250
An embedded fibre optic sensor for impact damage detection in composite materials
[UTIAS-332] N90-26650
FIBER ORIENTATION
Damage states in laminated composite three-point bend specimens: An experimental-analytical correlation study
[NASA-TM-101800] N90-26083
FIBERS
Towards 2000: The composite engine
[PNR90646] N90-26000
Development of ceramic hybrid combustor: Design and combustion test results
[DE90-503442] N90-26149
FIELD STRENGTH
Characterization of a high-intensity, subpicosecond XeCl laser system
[DE90-011970] N90-26310
FIELD THEORY (ALGEBRA)
Search of primitive polynomials over finite fields
[IMAG-RR-797-M] N90-26607
FIELD THEORY (PHYSICS)
A new class of exact solutions of the vacuum quadratic Poincare gauge field theory
[MATHS-REPT-A-119] N90-26691
On trivector torsion in vacuum quadratic Poincare gauge field theory
[MATHS-REPT-A-121] N90-26692
FIGHTER AIRCRAFT
Qualitative evaluation of a conformal velocity vector display for use at high angles-of-attack in fighter aircraft
[NASA-TM-102629] N90-25981
FILM THICKNESS
Ellipsometric study of YBa2Cu3O(7-x) laser ablated and co-evaporated films
[NASA-TM-103223] N90-26682
FINITE DIFFERENCE THEORY
Trajectory optimization for an asymmetric launch vehicle
[NASA-CR-185630] N90-26033
Galerkin finite difference Laplacian operators on isolated unstructured triangular meshes by linear combinations
[NASA-TM-103209] N90-26276
Two-dimensional model of a Space Station Freedom thermal energy storage canister
[NASA-TM-103124] N90-26279
FINITE ELEMENT METHOD
Computational crash dynamics. Project 1.2: Computational crash dynamics analysis
[IAR-89-19] N90-25956
Structural analysis and optimization of a propfan blade using a finite element method
[DLR-FB-90-01] N90-26006
Strain energy release rate analysis of delamination in a tapered laminate subjected to tension load
[NASA-TM-102582] N90-26076
Determination of the stress distributions in a ceramic: Tensile specimen using numerical techniques
[NASA-TM-101914] N90-26132
Computer simulation of gear tooth manufacturing processes
[NASA-CR-185200] N90-26171
A comparison of the post-buckling behavior of metallic and composite plates with centrally located cutouts
[NIAR-90-14] N90-26356
Design of ceramic components with the NASA/CARES computer program
[NASA-TM-102369] N90-26359
ANTIPASTO: An interactive mesh generator and preprocessor for two-dimensional analysis programs
[DE90-011755] N90-26530
Parallel processors and nonlinear structural dynamics algorithms and software
[NASA-CR-186755] N90-26536
Generation and improvement of meshes for finite elements methods in two and three dimensions
[ETN-90-97249] N90-26611
FINITE VOLUME METHOD
The finite analytic method and its applications. Volume 1: Laminar and turbulent flows past two-dimensional and axisymmetric bodies
[AD-A222787] N90-26294
FINS
A computational study of the effectiveness of coating materials for KE projectile fins subjected to the combined effects of inbore and aerodynamic heating
[AD-A222595] N90-26155
FIRE EXTINGUISHERS
Testing of flame screens and flame arresters as Devices designed to Prevent the Passage of Flame (DPPF) into tanks containing flammable atmospheres according to an IMO standard
[AD-A222566] N90-26177
FIRE PREVENTION
Testing of flame screens and flame arresters as Devices designed to Prevent the Passage of Flame (DPPF) into tanks containing flammable atmospheres according to an IMO standard
[AD-A222566] N90-26177
FIRST AID
Arctic cold weather medicine and accidental hypothermia
[AD-A223090] N90-26487
FISSIONABLE MATERIALS
Multimegawatt space nuclear power supply, phase 1. Supplement: D180-30619-8
[DE90-012433] N90-26647
FLAME DEFLECTORS
Testing of flame screens and flame arresters as Devices designed to Prevent the Passage of Flame (DPPF) into tanks containing flammable atmospheres according to an IMO standard
[AD-A222566] N90-26177
FLAME PROPAGATION
Chemistry of combustion processes N90-25994
Testing of flame screens and flame arresters as Devices designed to Prevent the Passage of Flame (DPPF) into tanks containing flammable atmospheres according to an IMO standard
[AD-A222566] N90-26177
Asymptotic analysis of dissipative waves with applications to their numerical simulation
[NASA-TM-103231] N90-26615
FLAME SPECTROSCOPY
Temperature and OH concentrations in a solid propellant flame using absorption techniques
[AD-A222591] N90-26100
FLAMES
Asymptotic analysis of dissipative waves with applications to their numerical simulation
[NASA-TM-103231] N90-26615
FLAMMABILITY
Testing of flame screens and flame arresters as Devices designed to Prevent the Passage of Flame (DPPF) into tanks containing flammable atmospheres according to an IMO standard
[AD-A222566] N90-26177
FLAPPING
Synthesis of individual rotor blade control system for gust alleviation
[NASA-TM-101886] N90-25972
FLEXIBLE BODIES
Design and implementation of robust decentralized control laws for the ACES structure at Marshall Space Flight Center
[NASA-CR-4310] N90-26046
Intergration of system identification and robust controller designs for flexible structures in space
[NASA-TM-102695] N90-26362
FLIGHT CHARACTERISTICS
H-infinity based integrated flight-propulsion control design for a STOVL aircraft in transition flight
[NASA-TM-103198] N90-26011
Orbiter utilization as an ACRV
[NASA-TM-102700] N90-26032
Eye tracking device for the measurement of flight performance in simulators
[AD-A220075] N90-26484
FLIGHT CONTROL
Identification of aerodynamic models for maneuvering aircraft
[NASA-CR-186630] N90-25943
An in-flight interaction of the X-29A canard and flight control system
[NASA-TM-101718] N90-25973
Technical evaluation report on the Guidance and Control Panel 49th Symposium on Fault Tolerant Design Concepts for Highly Integrated Flight Critical Guidance and Control Systems
[AGARD-AR-281] N90-26012
Guidance and control strategies for aerospace vehicles
[NASA-CR-186878] N90-26013
Robustness evaluation of H2 and H(infinity) control theory as applied to a transport aircraft
[AD-A222795] N90-26018
Software requirements: Guidance and control software development specification
[NASA-CR-182058] N90-26527
FLIGHT CREWS
An analysis of requirements for a P-3 windshear training program
[AD-A222577] N90-25960
Choosing a pilot subjective workload scale to fit flight operational requirements
[IAR-89-21] N90-26493
Human factors: The human interface with aircraft interiors
[NIAR-90-18] N90-26496
Aircrew life support systems enhancement
[AD-A222626] N90-26505
FLIGHT ENVELOPES
Identification of aerodynamic models for maneuvering aircraft
[NASA-CR-186630] N90-25943
FLIGHT INSTRUMENTS
Flight motor set 360L007 (STS-33R)
[NASA-CR-183979] N90-26067
FLIGHT MECHANICS
The applicability of simple helicopter models for flight mechanics studies
[ETN-90-96962] N90-25975
FLIGHT OPERATIONS
An overview of the joint FAA/NASA aircraft/ground runway friction program
[NASA-TM-103486] N90-25957
Choosing a pilot subjective workload scale to fit flight operational requirements
[IAR-89-21] N90-26493
FLIGHT PATHS
Transatmospheric vehicle research
[NASA-CR-186705] N90-25970
Improving the geometric fidelity of imaging systems employing sensor arrays
[NASA-CASE-NPO-17970-1-CU] N90-26384
FLIGHT PLANS
Enroute flight planning: The design of cooperative planning systems
[NASA-CR-186797] N90-25964
FLIGHT SAFETY
An overview of the joint FAA/NASA aircraft/ground runway friction program
[NASA-TM-103486] N90-25957
Aviation safety: Serious problems continue to trouble the air traffic control work force. Report to congressional requesters
[GAO/RCED-89-112] N90-25959
FLIGHT SIMULATION
Model following control system design: Preliminary ATTAS in-flight simulation test results
[PD-FC-9003] N90-26010
Investigation of crack-closure prediction models for fatigue in aluminium alloy sheet under flight-simulation loading
[LR-619] N90-26369
Launching a dream: A teachers guide to a simulated space shuttle mission
[NASA-TM-89715] N90-26693
FLIGHT SIMULATORS
Eye tracking device for the measurement of flight performance in simulators
[AD-A220075] N90-26484
Pilot interaction with automated airborne decision making systems
[NASA-CR-186730] N90-26492

Human performance in cockpit-related systems
[NIAR-90-7] N90-26495

FLIGHT TESTS
Research at NASA's NFAC wind tunnels
[NASA-TM-102827] N90-25933
Flight testing of a natural laminar flow airfoil using gliders
[PD-CF-9005] N90-25936
Model following control system design: Preliminary ATTAS in-flight simulation test results
[PD-FC-9003] N90-26010
Aeroacoustics of advanced propellers
[NASA-TM-103137] N90-26635

FLIGHT TRAINING
An analysis of requirements for a P-3 windshear training program
[AD-A222577] N90-25960

FLOW CHARACTERISTICS
Analysis of turbulent density fluctuations by means of spontaneous Raman diffusion
[ISL-R-103/89] N90-26287

FLOW DISTRIBUTION
Identification of aerodynamic models for maneuvering aircraft
[NASA-CR-186630] N90-25943
Euler analysis comparison with LDV data for an advanced counter-rotation propfan at cruise
[NASA-TM-103249] N90-25946
Two-dimensional Euler and Navier-Stokes Time accurate simulations of fan rotor flows
[NASA-TM-102402] N90-25948
Effect of vortex generators on the aerodynamic wing characteristics and body of revolution
[AD-A222613] N90-25955
Hot gas ingestion characteristics and flow visualization of a vectored thrust STOVL concept
[NASA-TM-103212] N90-26009
Supersonic reacting internal flow fields
[NASA-TM-103480] N90-26094
Numerical analysis of three-dimensional particle-laden flow equations
[IAR-90-2] N90-26268
Measurement of terms and parameters in turbulent models
[NASA-CR-183993] N90-26271
Frontogenesis in gravity currents: An example with no known applications in oceanography
[MATHS-REPT-A-117] N90-26284
Computational fluid dynamics 3-D analysis for advanced transonic turbine design
[ETN-90-97262] N90-26291
Practical developments in holographic interferometry
[PNR90669] N90-26302
Laser techniques for studying chemical vapor deposition
[DE90-012921] N90-26311
Aircraft measurements of the turbulence structure in cirrus clouds
[ISSN-0069-5882] N90-26450
High speed turboprop aeroacoustic study (counterrotation). Volume 1: Model development
[NASA-CR-185241] N90-26633

FLOW EQUATIONS
Numerical analysis of three-dimensional particle-laden flow equations
[IAR-90-2] N90-26268
Computational fluid dynamics for missiles
[RAE-TM-AERO-2171] N90-26288
The finite analytic method and its applications. Volume 1: Laminar and turbulent flows past two-dimensional and axisymmetric bodies
[AD-A222787] N90-26294

FLOW GEOMETRY
Effects of forebody geometry on subsonic boundary-layer stability
[NASA-CR-4314] N90-25939
The finite analytic method and its applications. Volume 1: Laminar and turbulent flows past two-dimensional and axisymmetric bodies
[AD-A222787] N90-26294

FLOW STABILITY
New discharge pumping method for CO2 lasers
[AD-A220898] N90-26307

FLOW VELOCITY
Effect of initial conditions on the development of two-phase jets
[AD-A222621] N90-26293

FLOW VISUALIZATION
Space plane model for visual measurement of aerodynamic heating
[DE90-505514] N90-25949
Hot gas ingestion characteristics and flow visualization of a vectored thrust STOVL concept
[NASA-TM-103212] N90-26009
Informatics aspects of large flow calculations on the SX-2 supercomputer
[NLR-MP-88037-U] N90-26290
Practical developments in holographic interferometry
[PNR90669] N90-26302
Holography and holographic interferometry
[PNR90670] N90-26303

FLUID DYNAMICS
Transatmospheric vehicle research
[NASA-CR-186705] N90-25970
Carbon deposition model for oxygen-hydrocarbon combustion. Task 6: Data analysis and formulation of an empirical model
[NASA-CR-183986] N90-26095
New findings and instrumentation from the NASA Lewis microgravity facilities
[NASA-TM-103189] N90-26163
Bubble, Drop and Particle Unit (BDPU): A multi-user microgravity facility
[IAF-89-431] N90-26164
Low-gravity fluid physics: A program overview
[NASA-TM-103215] N90-26273

FLUID FILMS
A high-speed photography study of cavitation in a dynamically loaded journal bearing
[NASA-TM-103178] N90-26338

FLUID FLOW
Prediction of the ullage gas thermal stratification in a NASP vehicle propellant tank experimental simulation using FLOW-3D
[NASA-TM-103217] N90-26160
Computational experience with a three-dimensional rotary engine combustion model
[NASA-TM-103104] N90-26275

FLUID JETS
UV and VUV spectroscopy and photochemistry of small molecules in a supersonic jet N90-26771

FLUID MECHANICS
Fluid Phase Separation (FPS) experiment for flight on a space shuttle Get Away Special (GAS) canister
[NASA-CR-186830] N90-26161
Isothermal compressibility of SPC/E water
[AD-A222723] N90-26643

FLUIDS
Fluid-loop reaction system
[NASA-CASE-NPO-17204-1-CU] N90-26292

FLUORESCENCE
Chemical structure and kinetics at liquid/solid interfaces
[AD-A222766] N90-26105
Dissociative recombination of molecular ions with electrons N90-26767

FLUORINE
Short-range structure of fluorine-modified phosphate glass
[DE90-013494] N90-26145

FLUX PINNING
Materials research issues in superconducting levitation and suspension as applied to magnetic bearings
[DE90-011147] N90-26667

FLY BY WIRE CONTROL
Model following control system design: Preliminary ATTAS in-flight simulation test results
[PD-FC-9003] N90-26010

FOREBODIES
Effects of forebody geometry on subsonic boundary-layer stability
[NASA-CR-4314] N90-25939

FORECASTING
Study of high-speed civil transports. Summary
[NASA-CR-4236] N90-25966

FORESTS
Wideband characterization of forest propagation channels N90-26188
Catching our breath: Next steps for reducing urban ozone
[PB90-130451] N90-26398
Measurements of monoterpenes in a coniferous forest N90-26421
Terpene concentrations and emissions in a Scots pine forest N90-26422

FORMALDEHYDE
Study of the polyoxymethylene and its sputtered fragments: Implications for comets N90-26781

FORMALISM
Formal verification of distributed computing systems: Logic characterization of behaviour equivalence
[LAAS-89386] N90-26555

FORMAT
UEDIT: A full-scale, scrollable APL2 spreadsheet input/output editor
[AD-A222712] N90-26557

FORMING TECHNIQUES
CAD/CAM reinforces the competitive edge of European mouldmakers
[CRIF-MC-88] N90-26542

FOSSIL FUELS
Formation kinetics of N2O in the atmosphere N90-26425

FOURIER TRANSFORMATION
Formation of design envelope criterion in terms of deterministic spectral procedure
[RAE-TM-SS-9] N90-25953
Application and extension of an analytical model of the confined acoustic beam generated by a transducer
[AD-A222994] N90-26639
High resolution infrared spectroscopy of planetary molecules using diode lasers and Fourier transform spectrometers N90-26747
Novel laser gain and time-resolved FTIR studies of photochemistry N90-26756

FRACTALS
Fractal structure and fractal time in silica sol-gels
[DE90-013197] N90-26144

FRACTURE MECHANICS
Hydrogen induced fracture characteristics of single crystal nickel-based superalloys
[NASA-CR-183992] N90-26108
Fracture toughness and failure mechanisms in commercial 2091 Al-Li sheet at cryogenic temperatures
[AD-A222803] N90-26125
Evaluation of fracture strength properties of silicon carbide ceramics under cyclic/static axial loading at ultra-high temperature
[DE90-503402] N90-26147
Fatigue life assessment using a short crack growth model
[PNR90663] N90-26367

FRACTURE STRENGTH
The effect of manganese on the onset of the stage 2 reaction in an austempered ductile iron matrix
[DE90-011804] N90-26119
Microstructural design for fatigue crack growth resistance in Ni-base alloy
[PNR90632] N90-26120
Fracture toughness and failure mechanisms in commercial 2091 Al-Li sheet at cryogenic temperatures
[AD-A222803] N90-26125
Fracture toughness of polyimide films
[NASA-TM-103473] N90-26130
Influence of thermal conditioning media on Charpy specimen test temperature
[DE90-012784] N90-26360
Static and fatigue strength of an adhesive bonded CFRP butt-strap joint: The effects of stacking sequence and temperature
[NLR-TR-88036-U] N90-26370

FRACTURING
Hydrogen induced fracture characteristics of single crystal nickel-based superalloys
[NASA-CR-183992] N90-26108

FRAGMENTATION
Excimer laser fragmentation studies of selected oximes: Nascent OH internal energy distributions and the search of H2CN fluorescence
[AD-A222622] N90-26317
Study of the polyoxymethylene and its sputtered fragments: Implications for comets N90-26781

FRAGMENTS
Study of the polyoxymethylene and its sputtered fragments: Implications for comets N90-26781

FREE ELECTRON LASERS
OASIS, LLNL version: Software maintenance manual
[DE90-013522] N90-26313

FREE RADICALS
Kinetics and thermochemistry of polyatomic free radicals: New results and new understandings N90-26764
UV and VUV spectroscopy and photochemistry of small molecules in a supersonic jet N90-26771

FREE VIBRATION
An experimental system for measuring the wavenumber-frequency response of Timoshenko beams
[AD-A222569] N90-26374

FREQUENCY ANALYZERS
Channel selection and control procedures in an automatic HF system N90-26193
PVDF contact probes
[VTT-RR-623] N90-26253

FREQUENCY HOPPING
New synchronisation techniques applicable to multi-tone transmission systems N90-26199
New approaches for rapid synchronisation frequency hoppers N90-26201

FREQUENCY MEASUREMENT
Electric field strength meters for the HF, VHF, and UHF bands
[BBC-RD-1990/3] N90-26212

FREQUENCY MODULATION
CORA: A direct sequence spread spectrum radio for voice and data N90-26195

Direct-sequence spread spectrum system
[AD-A223021] N90-26245

FREQUENCY RANGES
Equipment feasibility study: Very high frequency communication equipment (136-137 megahertz)
[DOT/FAA/CT-TN89/72] N90-26210
Improving the geometric fidelity of imaging systems employing sensor arrays
[NASA-CASE-NPO-17970-1-CU] N90-26384

FREQUENCY SHIFT
Synchronization of frequency shift transmission and the effect of oversampling N90-26200

FREQUENCY SHIFT KEYING
New synchronisation techniques applicable to multi-tone transmission systems N90-26199
Combined effects of fast and selective fading on performance of PSK and MSK with coherent detection N90-26204

FREQUENCY STANDARDS
Information content of a single pass of phase-delay data from a short baseline connected element interferometer N90-26220

FREQUENCY SYNCHRONIZATION
Optimal synchronization of spread spectrum sequenced by nontransferable switching operators N90-26183

FRESNEL LENSES
Silicon concentrator solar cell development
[DE90-011782] N90-26386

FRICTION
An overview of the joint FAA/NASA aircraft/ground runway friction program
[NASA-TM-103486] N90-25957

FRICTION DRAG
A brief review of some mechanisms causing boundary layer transition at high speeds
[NASA-TM-102834] N90-25945

FRICTION FACTOR
Bidirectional drive and brake mechanism
[NASA-CASE-MSC-21540-1] N90-26342

FRONTS
Frontogenesis in gravity currents: An example with no known applications in oceanography
[MATHS-REPT-A-117] N90-26284

FROSTBITE
Arctic cold weather medicine and accidental hypothermia
[AD-A223090] N90-26487

FUEL CAPSULES
Application of the results of carbon pellet modeling to the problem of plasma penetration
[DE90-012713] N90-26658

FUEL CELLS
Megawatt solar power systems for lunar surface operations
[NASA-CR-186509] N90-26391

FUEL COMBUSTION
Performance of a supercharged direct-injection stratified-charge rotary combustion engine
[NASA-TM-103105] N90-25982
Liquid fueled ramjet combustion instability: Acoustical and vortical interactions with burning sprays
[AD-A222752] N90-26104
A comparison of the contribution of various gases to the greenhouse effect N90-26414

FUEL CONSUMPTION
Methods and apparatus for providing real-time control of a gaseous propellant rocket propulsion system
[NASA-CASE-MSC-21542-1] N90-26073
Advanced Turbine Technology Applications Project (ATTAP)
[NASA-CR-185240] N90-26728

FUEL INJECTION
Combustion in the gas turbine. Part 3: Fuel injection, ignition and stability
[CIT/SME/VKI/RS/4] N90-25988

FUEL OILS
A comparison of the contribution of various gases to the greenhouse effect N90-26414

FUEL TESTS
Subsonic combustor testing N90-25997

FUNCTIONAL DESIGN SPECIFICATIONS
Contribution to the definition and application of NAUTILE (A new environment for the conception and assembling of integrated circuits)
[ETN-90-97251] N90-26554
ATAMM multicomputer operating system functional specification
[NASA-CR-186845] N90-26563

FUNCTIONS (MATHEMATICS)
Cartesian closed categories of domains
[ETN-90-97284] N90-26613

FURNACES
Temperature and melt solid interface control during crystal growth
[NASA-CR-186731] N90-26664

FUSELAGES
Design and construction of a wall-climbing robot
[NIAR-90-20] N90-26327
Asymptotic modal analysis and statistical energy analysis
[NASA-CR-186732] N90-26634

G

GALACTIC COSMIC RAYS
A closed form solution to HZE propagation
[NASA-TM-103482] N90-26640
The charged particle radiation environment for AXAF
[NASA-TM-100405] N90-26741

GALACTIC EVOLUTION
A research program in theoretical high energy physics
[DE90-013322] N90-26648
A research program in physics of the early universe
[DE90-013319] N90-26742
Radio loud far-infrared galaxies
[DE90-012993] N90-26786

GALAXIES
Astronomy at ultra-high energies: Results from the CYGNUS experiment
[DE90-011979] N90-26732

GALERKIN METHOD
Galerkin finite difference Laplacian operators on isolated unstructured triangular meshes by linear combinations
[NASA-TM-103209] N90-26276

GALILEO PROJECT
Space exploration: Cost, schedule, and performance of NASA's Galileo Mission to Jupiter. Fact sheet for the Chairman, Subcommittee on Science, Technology, and Space, Committee on Commerce, Science, and Transportation, US Senate
[GAO/NSIAD-88-138FS] N90-26025

GALLIUM ARSENIDES
DURIP: Instrumentation for laser switched power LINAC
[AD-A222629] N90-26318
Dielectric function of InGaAs in the visible
[NASA-TM-103246] N90-26683
MBE growth technology for high quality strained III-V layers
[NASA-CASE-NPO-17723-1-CU] N90-26685

GAMMA RAYS
Nonpotential magnetic fields at sites of gamma ray flares
[NASA-TM-103493] N90-26785

GAS CHROMATOGRAPHY
Proton irradiation of simple gas mixtures: Influence of irradiation parameters N90-26782

GAS COMPOSITION
The global consequences of increasing tropospheric ozone concentrations
[NASA-TM-103477] N90-26401
Results from the IVL TOR Station at Roervik, Sweden. A contribution to the EURATRAC subproject TOR N90-26415

GAS COOLING
New discharge pumping method for CO2 lasers
[AD-A220898] N90-26307

GAS DYNAMICS
Prediction of two-dimensional time-dependent gasdynamic flows for hypersonic studies
[UTIAS-335] N90-25935

GAS EXCHANGE
Gas exchange characteristics as indicators of the basic limiting factors in photosynthesis
[DE90-012399] N90-26481

GAS EXPANSION
Multicomponent gas sorption Joule-Thomson refrigerator
[NASA-CASE-NPO-17569-1-CU] N90-26176

GAS FLOW
Prediction of two-dimensional time-dependent gasdynamic flows for hypersonic studies
[UTIAS-335] N90-25935
Combustion in the gas turbine. Part 2: Preliminary design and performance
[CIT/SME/VKI/RS/3] N90-25987
Numerical analysis of three-dimensional particle-laden flow equations
[IAR-90-2] N90-26268
Optical characterization of clouds of fine liquid-nitrogen particles
[NASA-TM-103208] N90-26299

GAS GENERATORS
Carbon deposition model for oxygen-hydrocarbon combustion. Task 6: Data analysis and formulation of an empirical model
[NASA-CR-183986] N90-26095
Renewed aging control of adhesion of inhibitor on the gas generator charges for RB 24
[FOA-C-20780-2.1] N90-26153

GAS GIANT PLANETS
Preliminary error budget for an optical ranging system: Range, range rate, and differenced range observables N90-26227
Measurements of the methane relaxation times for application to the infrared emission models of the upper atmospheres of outer planets and Titan N90-26759
Chemical kinetics and modeling of planetary atmospheres N90-26763
Kinetics and thermochemistry of polyatomic free radicals: New results and new understandings N90-26764
Vapor pressures of acetylene at low temperatures N90-26777

GAS MIXTURES
Multicomponent gas sorption Joule-Thomson refrigerator
[NASA-CASE-NPO-17569-1-CU] N90-26176
Testing of flame screens and flame arresters as Devices designed to Prevent the Passage of Flame (DPPF) into tanks containing flammable atmospheres according to an IMO standard
[AD-A222566] N90-26177
Laboratory measurements and modeling of microwave absorption by ammonia in gas mixtures applicable to giant planet atmospheres N90-26750
Proton irradiation of simple gas mixtures: Influence of irradiation parameters N90-26782

GAS TUNGSTEN ARC WELDING
Electrode carrying wire for GTAW welding
[NASA-CASE-MFS-29491-1] N90-26168

GAS TURBINE ENGINES
Gas Turbine Combustion, volume 1
[VKI-LS-1990-02-VOL-1] N90-25985
Combustion in the gas turbine. Part 1: Combustor types and design
[CIT/SME/VKI/RS/1] N90-25986
Combustion in the gas turbine. Part 2: Preliminary design and performance
[CIT/SME/VKI/RS/3] N90-25987
Combustion in the gas turbine. Part 3: Fuel injection, ignition and stability
[CIT/SME/VKI/RS/4] N90-25988
Combustor cooling aspects
[CIT/SME/VKI/RS/5] N90-25989
Pollutants: Production and methods of reduction
[CIT/SME/VKI/RS/6] N90-25990
Subsonic combustor flow modeling: State of the art of CFD techniques for reacting and combusting flow N90-25991
Chemistry of combustion processes N90-25994
Gas Turbine Combustion, volume 2
[VKI-LS-1990-02-VOL-2] N90-25995
Towards 2000: The composite engine
[PNR90646] N90-26000
Prediction of rotating disc flow and heat transfer in gas turbine engines
[PNR90650] N90-26001
Aircraft exhaust emissions: An engine manufacturer's perspective
[PNR90675] N90-26004
The application of engineering ceramics in gas turbines
[PNR90676] N90-26005
Elevated temperature crack growth
[NASA-CR-182247] N90-26355
Advanced Turbine Technology Applications Project (ATTAP)
[NASA-CR-185240] N90-26728

GAS TURBINES
Measurement of velocity and temperature profiles at the exit plane of a tubular gas turbine combustor
[DE90-505519] N90-25983
Critical evaluation of Jet-A spray combustion using propane chemical kinetics in gas turbine combustion simulated by KIVA-2
[NASA-TM-103173] N90-26170
Research and development of advanced gas turbine
[DE90-503377] N90-26335

GASES
A lattice gas model for thermohydrodynamics
[DE90-011964] N90-26690
Laboratory studies of the interaction of ions with condensed gases: Planetary applications N90-26778

GEAR TEETH
Computer simulation of gear tooth manufacturing processes
[NASA-CR-185200] N90-26171

GEARS
Computer simulation of gear tooth manufacturing processes
[NASA-CR-185200] N90-26171

GELS
Fractal structure and fractal time in silica sol-gels
[DE90-013197] N90-26144

GENETICS
Photosynthesis in intact plants
[DE90-013699] N90-26482
Computer simulation of chemical reactions in synthetic model compounds and genetically engineered active sites
[AD-A222611] N90-26483
GEOCHEMISTRY
Proceedings of a workshop on Lunar Volcanic Glasses: Scientific and Resource Potential
[NASA-CR-186631] N90-26437
GEOCHRONOLOGY
The 5th International symposium on palaeolimnology
[AD-A219244] N90-26431
GEOGRAPHIC INFORMATION SYSTEMS
Practical applications of remote sensing technology
[NASA-CR-186810] N90-26377
Hierarchical structure of polygonal data for spatial analysis and representation of cartographical data
[INPE-4966-PRE/1548] N90-26380
GEOLOGICAL SURVEYS
Construction of geological and geotechnical information database
[DE90-503417] N90-26708
GEOLOGY
Micro coring apparatus
[NASA-CR-183072] N90-26321
Press abstracts of the 21st Lunar and Planetary Science Conference
[NASA-CR-186874] N90-26738
GEOMAGNETIC TAIL
On the nature of the plasma sheet boundary layer
[DE90-013158] N90-26439
GEOMETRY
Improving the geometric fidelity of imaging systems employing sensor arrays
[NASA-CASE-NPO-17970-1-CU] N90-26384
GEOPHYSICS
Directory of research projects: Planetary geology and geophysics program
[NASA-TM-4211] N90-26743
GEOSTROPHIC WIND
The NASA/MSFC Global Reference Atmospheric Model, 1990 version (GRAM-90)
[NASA-CR-186717] N90-26435
GEOSYNCHRONOUS ORBITS
Texstar: The all-Texas educational satellite system
[NASA-CR-186654] N90-26045
Project SPARC: Space-based aeroassisted reusable craft
[NASA-CR-186816] N90-26051
GEOTECHNICAL ENGINEERING
Construction of geological and geotechnical information database
[DE90-503417] N90-26708
GERMANIUM
Rate constant for reaction of atomic hydrogen with germane N90-26768
GET AWAY SPECIALS (STS)
Integrated support structure
[NASA-CR-186835] N90-26162
GIBBS-HELMHOLTZ EQUATIONS
Liquid-vapor equilibrium of multicomponent cryogenic systems N90-26774
GLACIERS
Ice core studies and the past atmospheric environment of polar regions N90-26411
GLACIOLOGY
Ice core studies and the past atmospheric environment of polar regions N90-26411
The Renland ice core (Greenland): A source for climatic studies over 100,000 years N90-26412
Proceedings of a Workshop on Antarctic Meteorite Stranding Surfaces
[NASA-CR-186575] N90-26739
GLASS
Vitreous joining of SiC fiber reinforced SiC composites
[DE90-012951] N90-26081
Short-range structure of fluorine-modified phosphate glass
[DE90-013494] N90-26145
Proceedings of a workshop on Lunar Volcanic Glasses: Scientific and Resource Potential
[NASA-CR-186631] N90-26437
GLASS FIBER REINFORCED PLASTICS
Strain energy release rate analysis of delamination in a tapered laminate subjected to tension load
[NASA-TM-102592] N90-26076
Erosion mechanisms in composite materials and ripple formation mechanism in erosion
[IAR-89-4-PT-1] N90-26078
GLASS TRANSITION TEMPERATURE
Vitreous joining of SiC fiber reinforced SiC composites
[DE90-012951] N90-26081
GLIDERS
Flight testing of a natural laminar flow airfoil using gliders
[PD-CF-9005] N90-25936
GLINT
Laser radar angular tracking
[AD-A222741] N90-26319
GLOBAL POSITIONING SYSTEM
Proceedings of the Second Symposium on GPS Applications in space, volume 1
[AD-A219978] N90-25962
Proceedings of the Second Symposium on GPS Applications in Space, volume 2
[AD-A219979] N90-25963
A reduced-dynamic technique for precise orbit determination N90-26219
GOALS
Making it happen: Project management
[PNR90618] N90-26695
GOES 4
The 27-28 October 1986 FIRE IFO cirrus case study: Cirrus parameter relationships derived from satellite and lidar data
[NASA-TM-103469] N90-26447
GOLD
Analysis of strain relaxation in Au/Ni multilayers by x ray diffraction
[IAR-89-25] N90-26357
GOVERNMENT PROCUREMENT
Space transportation: NASA has no firm need for increasingly costly orbital maneuvering vehicle
[GAO/NSIAD-90-192] N90-26041
Space shuttle: Follow-up evaluation of NASA's solid rocket motor procurement. Report to the Chairman, Committee on Government Operations, House of Representatives
[GAO/NSIAD-89-89] N90-26066
GRADIENTS
Automated sensitivity analysis with the Gradient Enhanced Software System (GRESS)
[DE90-011291] N90-26529
GRAIN BOUNDARIES
Microstructural dependence of the cavitation damage function in FCC materials
[DE90-012898] N90-26113
Densification studies of refractory materials using Hot Isostatic Pressing (HIP) and tantalum containment
[DE90-013481] N90-26114
Diffusion-accommodated grain boundary sliding in a polycrystal
[DE90-012727] N90-26668
Molecular dynamics simulations of grain-boundary diffusion for varying tilt angle geometries
[DE90-012919] N90-26669
GRAMMARS
ATN design tool
[AD-A223030] N90-26559
Grammar, punctuation, and capitalization: A handbook for technical writers and editors
[NASA-SP-7084] N90-26710
GRAPH THEORY
Combinatorial problems using a hypercube and Hamming graphs
[ETN-90-97240] N90-26609
GRAPHITE-EPOXY COMPOSITES
Buckling and postbuckling behavior of square compression-loaded graphite-epoxy plates with circular cutouts
[NASA-TP-3007] N90-26077
A comparison of the post-buckling behavior of metallic and composite plates with centrally located cutouts
[NIAR-90-14] N90-26356
Scaling effects in the static and dynamic response of graphite-epoxy beam-columns
[NASA-TM-102697] N90-26363
Reliability analysis of continuous fiber composite laminates
[NASA-CR-185265] N90-26372
GRAPHS (CHARTS)
Large sets of block designs
[ETN-90-97212] N90-26602
GRASSES
Measuring and modeling near-surface reflected and emitted radiation fluxes at the FIFE site
[NASA-CR-180953] N90-26378
GRAVIMETERS
Absolute measurements of gravity
[AD-A222731] N90-26629
GRAVIMETRY
Absolute measurements of gravity
[AD-A222731] N90-26629
GRAVITATION
Application of inertial instruments for DSN antenna pointing and tracking N90-26224
Absolute measurements of gravity
[AD-A222731] N90-26629
GRAVITATIONAL COLLAPSE
Numerical treatment of shell crossing singularities in the spherically symmetric gravitational collapse
[ETN-90-96967] N90-26598
GRAVITATIONAL EFFECTS
New findings and instrumentation from the NASA Lewis microgravity facilities
[NASA-TM-103189] N90-26163
Soil experiment
[NASA-CR-184927] N90-26165
Natural melting within a spherical shell
[NASA-TM-102622] N90-26274
The US Experiments Flown on the Soviet Biosatellite Cosmos 1887
[NASA-TM-102254] N90-26452
Effects of microgravity on rat muscle N90-26453
Experiment K-6-01. Distribution and biochemistry of mineral and matrix in the femurs of rats N90-26455
Experiment K-6-03. Gravity and skeletal growth, part 1. Part 2: Morphology and histochemistry of bone cells and vasculature of the tibia; Part 3: Nuclear volume analysis of osteoblast histogenesis in periodontal ligament cells; Part 4: Intervertebral disc swelling pressure associated with microgravity N90-26457
Experiment K-6-04. Trace element balance in rats during spaceflight N90-26458
Experiment K-6-05. The maturaton of bone and dentin matrices in rats flown on Cosmos 1887 N90-26459
Experiment K-6-06. Morphometric and EM analyses of tibial epiphyseal plates from Cosmos 1887 rats N90-26460
Experiment K-6-08. Biochemical and histochemical observations of vastus medialis N90-26462
Experiment K-6-10. Effects of zero gravity on myofibril protein content and isomyosin distribution in rodent skeletal muscle N90-26464
Experiment K-6-21. Effect of microgravity on 1) metabolic enzymes of type 1 and type 2 muscle fibers and on 2) metabolic enzymes, neutransmitter amino acids, and neurotransmitter associated enzymes in motor and somatosensory cerebral cortex. Part 1: Metabolic enzymes of individual muscle fibers; part 2: metabolic enzymes of hippocampus and spinal cord N90-26474
Experiment K-6-22. Growth hormone regulation, synthesis and secretion in microgravity. Part 1: Somatotroph physiology. Part 2: Immunohistochemical analysis of hypothalamic hormones. Part 3: Plasma analysis N90-26475
Refractive error analysis in the interferometric measurement of 2-D density fields containing strong gradients
[LR-616] N90-26655
GRAVITATIONAL FIELDS
Important experiments to test for longer-ranged new gravitational forces
[DE90-012102] N90-26434
GRAVITATIONAL PHYSIOLOGY
The US Experiments Flown on the Soviet Biosatellite Cosmos 1887
[NASA-TM-102254] N90-26452
Effects of microgravity on rat bone, cartilage and connective tissues N90-26454
Experiment K-6-01. Distribution and biochemistry of mineral and matrix in the femurs of rats N90-26455
Experiment K-6-02. Biomedical, biochemical and morphological alterations of muscle and dense, fibrous connective tissues during 14 days of spaceflight N90-26456
Experiment K-6-03. Gravity and skeletal growth, part 1. Part 2: Morphology and histochemistry of bone cells and vasculature of the tibia; Part 3: Nuclear volume analysis of osteoblast histogenesis in periodontal ligament cells; Part 4: Intervertebral disc swelling pressure associated with microgravity N90-26457
Experiment K-6-04. Trace element balance in rats during spaceflight N90-26458
Experiment K-6-05. The maturaton of bone and dentin matrices in rats flown on Cosmos 1887 N90-26459
Experiment K-6-06. Morphometric and EM analyses of tibial epiphyseal plates from Cosmos 1887 rats N90-26460
Experiment K-6-08. Biochemical and histochemical observations of vastus medialis N90-26462
Experiment K-6-09. Morphological and biochemical investigation of microgravity-induced nerve and muscle breakdown. Part 1: Investigation of nerve and muscle breakdown during spaceflight; Part 2: Biochemical analysis of EDL and PLT muscles N90-26463
Experiment K-6-12. Morphometric studies of atrial or granules and hepatocytes. Part 1: Morphometric study of the liver; Part 2: The atrial granular accumulations N90-26466

Experiment K-6-13. Morphological and biochemical examination of heart tissue. Part 1: Effects of microgravity on the myocardial fine structure of rats flown on Cosmos 1887. Ultrastructure studies. Part 2: Cellular distribution of cyclic ampdependent protein kinase regulatory subunits in heart muscle of rats flown on Cosmos 1887
N90-26467

Experiment K-6-14. Hepatic function in rats after spaceflight
N90-26468

Experiment K-6-21. Effect of microgravity on 1) metabolic enzymes of type 1 and type 2 muscle fibers and on 2) metabolic enzymes, neutransmitter amino acids, and neurotransmitter associated enzymes in motor and somatosensory cerebral cortex. Part 1: Metabolic enzymes of individual muscle fibers; part 2: metabolic enzymes of hippocampus and spinal cord
N90-26474

Experiment K-6-22. Growth hormone regulation, synthesis and secretion in microgravity. Part 1: Somatotroph physiology. Part 2: Immunohistochemical analysis of hypothalamic hormones. Part 3: Plasma analysis
N90-26475

GRAVITATIONAL WAVES

Frontogenesis in gravity currents: An example with no known applications in oceanography
[MATHS-REPT-A-117]
N90-26284

GREEN'S FUNCTIONS

A closed form solution to HZE propagation
[NASA-TM-103482]
N90-26640

Computer modeling wave propagation with a variation of the Helmholtz-Kirchhoff relation
[AD-A222746]
N90-26657

GREENHOUSE EFFECT

Nordic Symposium on Atmospheric Chemistry
[CM-78]
N90-26403

A comparison of the contribution of various gases to the greenhouse effect
N90-26414

GREENHOUSES

Greenhouse design for a Martian colony: Structural, solar collection and light distribution systems
[NASA-CR-186818]
N90-26501

GRID GENERATION (MATHEMATICS)

ANTIPASTO: An interactive mesh generator and preprocessor for two-dimensional analysis programs
[DE90-011755]
N90-26530

Generation and improvement of meshes for finite elements methods in two and three dimensions
[ETN-90-97249]
N90-26611

GROUND HANDLING

An overview of the joint FAA/NASA aircraft/ground runway friction program
[NASA-TM-103486]
N90-25957

GROUND STATIONS

Space operations: NASA's communications support for Earth orbiting spacecraft. Report to Chairman, Subcommittee on Space Science and Applications, Committee on Science, Space and Technology, House of Representatives
[GAO/IMTEC-89-41]
N90-26215

Goldstone intracomplex connected element interferometry
N90-26218

Microspacecraft and Earth observation: Electrical field (ELF) measurement project
[NASA-CR-186821]
N90-26436

Bringing aircraft noise testing down to Earth
[PNR90642]
N90-26637

GROUND WAVE PROPAGATION

Broadband analysis of ground wave propagation at a50 to 400 MHz
N90-26185

GROUND WIND

Aeolian removal of dust from radiator surfaces on Mars
[NASA-TM-103205]
N90-26068

GROWTH

Experiment K-6-06. Morphometric and EM analyses of tibial epiphyseal plates from Cosmos 1887 rats
N90-26460

Experiment K-6-22. Growth hormone regulation, synthesis and secretion in microgravity. Part 1: Somatotroph physiology. Part 2: Immunohistochemical analysis of hypothalamic hormones. Part 3: Plasma analysis
N90-26475

Experiment K-6-27. Analysis of radiographs and biosamples from primate studies
N90-26478

GUIDANCE (MOTION)

Guidance and control system for an autonomous underwater vehicle
[AD-A222709]
N90-26343

GUST ALLEVIATORS

Synthesis of individual rotor blade control system for gust alleviation
[NASA-TM-101886]
N90-25972

H

HABITABILITY

Genesis lunar outpost criteria and design
[NASA-CR-186831]
N90-26499

HABITATS

Terrapin technologies manned Mars mission proposal
[NASA-CR-186838]
N90-26027

Genesis lunar outpost criteria and design
[NASA-CR-186831]
N90-26499

HALIDES

Stibathiolanes: Synthesis, solid state structure, and solution behavior
[AD-A223255]
N90-26688

HAMILTONIAN FUNCTIONS

Perturbation methods in the theory of waves and bifurcation phenomena
N90-26593

HANDBOOKS

Wright Research and Development Center test facilities handbook
[AD-A222582]
N90-26020

Grammar, punctuation, and capitalization: A handbook for technical writers and editors
[NASA-SP-7084]
N90-26710

HANKEL FUNCTIONS

H-infinity control: An exploratory study
[EUT-88-E-211]
N90-26584

HARDNESS

Mechanical properties of silica coatings
[DE90-012721]
N90-26138

The effect of crystal orientation on damage accumulation in chromium-implanted Al2O3
[DE90-012294]
N90-26674

HARMONIC FUNCTIONS

Annual and interannual variations of Earth-emitted radiation based on a 10-year data set
[NASA-TM-103465]
N90-26432

HARMONIC GENERATORS

Apparatus for the efficient wavelength conversion of laser radiation
[AD-D014506]
N90-26305

HARMONIC MOTION

Application and extension of an analytical model of the confined acoustic beam generated by a transducer
[AD-A222994]
N90-26639

HARNESSES

Human factors: The human interface with aircraft interiors
[NIAR-90-18]
N90-26496

HAZARDS

Space program: Space debris a potential threat to Space Station and shuttle
[GAO/IMTEC-90-18]
N90-26024

Space shuttle: Follow-up evaluation of NASA's solid rocket motor procurement. Report to the Chairman, Committee on Government Operations, House of Representatives
[GAO/NSIAD-89-89]
N90-26066

Rings of Earth detected by orbital debris radar
N90-26232

Analysis and improved design considerations for airborne pulse Doppler radar signal processing in the detection of hazardous windshear
[NASA-CR-186792]
N90-26448

HEAD DOWN TILT

Hemodynamic and ADH responses to central blood volume shifts in cardiac-denervated humans
[NASA-TM-103471]
N90-26485

HEAD MOVEMENT

Helmet-mounted head restraint
[AD-D014536]
N90-26491

HEALTH

The global consequences of increasing tropospheric ozone concentrations
[NASA-TM-103477]
N90-26401

HEART

Experiment K-6-13. Morphological and biochemical examination of heart tissue. Part 1: Effects of microgravity on the myocardial fine structure of rats flown on Cosmos 1887. Ultrastructure studies. Part 2: Cellular distribution of cyclic ampdependent protein kinase regulatory subunits in heart muscle of rats flown on Cosmos 1887
N90-26467

HEART RATE

Hemodynamic and ADH responses to central blood volume shifts in cardiac-denervated humans
[NASA-TM-103471]
N90-26485

Adjustment and validation of the mathematical prediction model for sweat rate, heart rate, and body temperature under outdoor conditions
[AD-A222599]
N90-26486

HEAT EXCHANGERS

Two-dimensional model of a Space Station Freedom thermal energy storage canister
[NASA-TM-103124]
N90-26279

HEAT FLUX

Measuring and modeling near-surface reflected and emitted radiation fluxes at the FIFE site
[NASA-CR-180953]
N90-26378

HEAT OF FORMATION

The heat of formation of CN radicals and radiative lifetimes of the A 1 Sigma - state of C2N2
N90-26765

HEAT PIPES

Transient characteristics of a grooved water heat pipe with variable heat load
[NASA-CR-185280]
N90-26272

HEAT RADIATORS

Aeolian removal of dust from radiator surfaces on Mars
[NASA-TM-103205]
N90-26068

HEAT RESISTANT ALLOYS

Hydrogen induced fracture characteristics of single crystal nickel-based superalloys
[NASA-CR-183992]
N90-26108

HEAT SHIELDING

Carbon-carbon composites: Emerging materials for hypersonic flight
[NASA-TM-103472]
N90-26080

HEAT STORAGE

Two-dimensional model of a Space Station Freedom thermal energy storage canister
[NASA-TM-103124]
N90-26279

HEAT TRANSFER

Performance of a supercharged direct-injection stratified-charge rotary combustion engine
[NASA-TM-103105]
N90-25982

Combustor cooling aspects
[CIT/SME/VKI/RS/5]
N90-25989

Prediction of rotating disc flow and heat transfer in gas turbine engines
[PNR90650]
N90-26001

Prediction of the ullage gas thermal stratification in a NASP vehicle propellant tank experimental simulation using FLOW-3D
[NASA-TM-103217]
N90-26160

Transient characteristics of a grooved water heat pipe with variable heat load
[NASA-CR-185280]
N90-26272

Natural melting within a spherical shell
[NASA-TM-102822]
N90-26274

Two-dimensional model of a Space Station Freedom thermal energy storage canister
[NASA-TM-103124]
N90-26279

Structural Mechanics Division research and technology plans for FY 1990 and accomplishments for FY 1989
[NASA-TM-102654]
N90-26361

Thermal management of an accelerator system in space
[DE90-013153]
N90-26627

Mathematical simulation of heat exchanges and thermoelastic constraints in Czochralski crystal growth
[ETN-90-97242]
N90-26680

A lattice gas model for thermohydrodynamics
[DE90-011964]
N90-26690

Preliminary designs for 25 kWe advanced Stirling conversion systems for dish electric applications
[NASA-TM-103188]
N90-26729

HEAT TRANSFER COEFFICIENTS

Turbine blade heat transfer coefficient evaluation by modified version of STAN5. Comparison with experimental data
[ETN-90-97283]
N90-26008

HEAT TREATMENT

Rapid thermal processing: A study of the silicon oxidation and of the implanted boron activation
[LAAS-90051]
N90-26681

HEAVY IONS

Heavy ion tests on programmable VLSI
[ETN-90-97254]
N90-26057

A closed form solution to HZE propagation
[NASA-TM-103482]
N90-26640

HEIGHT

The 27-28 October 1986 FIRE IFO cirrus case study: Cirrus parameter relationships derived from satellite and lidar data
[NASA-TM-103469]
N90-26447

HELICOPTER DESIGN

Research at NASA's NFAC wind tunnels
[NASA-TM-102827]
N90-25933

HELICOPTER PERFORMANCE

Agusta methodology for pitch link loads prediction in preliminary design phase
[ETN-90-97270]
N90-25978

HELICOPTER PROPELLER DRIVE

Efficiency study comparing two helicopter planetary reduction stages
[NASA-TM-103106]
N90-26334

HELICOPTER TAIL ROTORS

The applicability of simple helicopter models for flight mechanics studies
[ETN-90-96962]
N90-25975

HELICOPTERS
Computation of viscous aerodynamic characteristics of 2-D airfoils for helicopter applications
[NLR-MP-88052-U] N90-25951
HELIOSPHERE
Space exploration: Cost, schedule, and performance of NASA's Ulysses Mission to the Sun. Fact sheet for the Chairman, Subcommittee on Science, Technology, and Space, Committee on Commerce, Science, and Transportation, US Senate
[GAO/NSIAD-88-129FS] N90-26023
HELIUM
Transients in turbulent convective heat transfer to a flow of supercritical helium
[ETN-90-97217] N90-26286
HELMET MOUNTED DISPLAYS
Helmet-mounted head restraint
[AD-D014536] N90-26491
A real-time optical 3D tracker for head-mounted display systems
[AD-A222747] N90-26508
HEMODYNAMIC RESPONSES
Hemodynamic and ADH responses to central blood volume shifts in cardiac-denervated humans
[NASA-TM-103471] N90-26485
HESSIAN MATRICES
Application of symbolic computations to the constitutive modeling of structural materials
[NASA-TM-103225] N90-26364
HETERODYNING
Laser radar angular tracking
[AD-A222741] N90-26319
HETEROJUNCTIONS
Application of InAlAs/GaAs superlattice alloys to GaAs solar cells
[DE90-013070] N90-26389
HEURISTIC METHODS
Applications of different design methodologies in navigation systems and development at JPL N90-26221
Investigation of automated task learning, decomposition and scheduling
[NASA-CR-186791] N90-26488
HIERARCHIES
Hierarchical structure of polygonal data for spatial analysis and representation of cartographical data
[INPE-4986-PRE/1548] N90-26380
Effect of organizational structure on performance of decision making teams
[AD-A223160] N90-26697
HIGH ALTITUDE
Global Sentry: NASA/USRA high altitude reconnaissance aircraft design, volume 2
[NASA-CR-186820-VOL-2] N90-25971
HIGH ENERGY INTERACTIONS
Important experiments to test for longer-ranged new gravitational forces
[DE90-012102] N90-26434
A research program in theoretical high energy physics
[DE90-013322] N90-26648
HIGH FREQUENCIES
Progress and remaining issues in the development of a wideband HF channel model and simulation N90-26182
Channel selection and control procedures in an automatic HF system N90-26193
An experimental medium speed wideband modem N90-26194
Synchronization of frequency shift transmission and the effect of oversampling N90-26200
Equipment feasibility study: Very high frequency communication equipment (136-137 megahertz)
[DOT/FAA/CT-TN89/72] N90-26210
Software set-up for data processing of depolarization due to rain and ice crystals in the Olympus project
[EUT-89-E-218] N90-26240
HIGH LEVEL LANGUAGES
Language support for parallel computation
[AD-A223072] N90-26560
HIGH PRESSURE
Performance evaluation of LE-7 high pressure pumps
[DE90-505523] N90-26034
HIGH RESOLUTION
The application of HREELS to model catalysts: CO and C2H4 adsorption on Pt/Al2O3
[AD-A222744] N90-26103
HIRIS performance study
[NASA-CR-186649] N90-26375
The interstellar D1 line at high resolution
[NASA-CR-184915] N90-26737
High resolution spectroscopy in the microwave and far infrared N90-26746
High resolution infrared spectroscopy of planetary molecules using diode lasers and Fourier transform spectrometers N90-26747
Recent high resolution laboratory determinations of line broadening and intensity parameters: PH3, CH3D, and CO2 N90-26751
High resolution, low temperature photoabsorption cross-section of C2H2 with application to Saturn's atmosphere N90-26757
HIGH SPEED
Study of high-speed civil transports. Summary
[NASA-CR-4236] N90-25966
High speed magneto-resistive random access memory
[NASA-CASE-NPO-17954-1-CU] N90-26519
HIGH SPEED PHOTOGRAPHY
Debris/ice/TPS assessment and photographic analysis for shuttle mission STS-31R
[NASA-TM-102790] N90-26040
A high-speed photography study of cavitation in a dynamically loaded journal bearing
[NASA-TM-103178] N90-26338
HIGH STRENGTH STEELS
Statistical treatment of slow strain rate data for assessment of hydrogen embrittlement in low alloy high strength steel
[ARL-MAT-R-122] N90-26106
HIGH TEMPERATURE
Carbon-carbon composites: Emerging materials for hypersonic flight
[NASA-TM-103472] N90-26080
Extension of a noninteractive reliability model for ceramic matrix composites
[NASA-CR-185267] N90-26142
Elevated temperature crack growth
[NASA-CR-182247] N90-26355
Application of symbolic computations to the constitutive modeling of structural materials
[NASA-TM-103225] N90-26364
HIGH TEMPERATURE GASES
Hot gas ingestion characteristics and flow visualization of a vectored thrust STOVL concept
[NASA-TM-103212] N90-26009
HIGH TEMPERATURE SUPERCONDUCTORS
Pressure dependence of thermoelectric power of high T(sub c) 123 compound
[PD-MT-9001] N90-26092
Materials research issues in superconducting levitation and suspension as applied to magnetic bearings
[DE90-011147] N90-26667
NDE (Nondestructive evaluation) of critical currents in high T(sub c) superconductors
[DE90-012953] N90-26670
Studies on ion scattering and sputtering processes relevant to ion beam sputter deposition of multicomponent thin films
[DE90-010071] N90-26675
Critical current density, flux creep, and microstructure in a Bi-Sr-Ca-Cu-O system
[DE90-010457] N90-26676
Passivation of high temperature superconductors
[NASA-CASE-NPO-17949-1-CU] N90-26684
HIGH TEMPERATURE TESTS
High temperature multiaxiale creep testing of Nimonic 115
[RAE-TM-P-1182] N90-26122
HIGH VOLTAGES
On travelling-wave-based protection of high-voltage networks
[ISBN-90-9002955-9] N90-26260
Direct drive robotic hand
[NASA-CASE-NPO-17917-1-CU] N90-26339
HILBERT TRANSFORMATION
Asymptotic law of the orthogonal empirical functions and applications, part 2
[IMAG-RR-792-M-PT-2] N90-26505
HISTOCHEMICAL ANALYSIS
Experiment K-6-03. Gravity and skeletal growth, part 1. Part 2: Morphology and histochemistry of bone cells and vasculature of the tibia; Part 3: Nuclear volume analysis of osteoblast histogenesis in periodontal ligament cells; Part 4: Intervertebral disc swelling pressure associated with microgravity N90-26457
Experiment K-6-08. Biochemical and histochemical observations of vastus medialis N90-26462
HISTORIES
The lessons of Varsovian's reconnaissance
[NASA-TM-103207] N90-26789
HOLES (MECHANICS)
A comparison of the post-buckling behavior of metallic and composite plates with centrally located cutouts
[NIAR-90-14] N90-26356
HOLOGRAMMETRY
A numerical simulation of the quasi-heterodyne technique for double-pulsed holographic vibration measurements
[PNR90622] N90-26301
HOLOGRAPHIC INTERFEROMETRY
Practical developments in holographic interferometry
[PNR90669] N90-26302
Holography and holographic interferometry
[PNR90670] N90-26303
Coherent optical techniques for industrial inspection
[PNR90605] N90-26654
HOLOGRAPHY
A numerical simulation of the quasi-heterodyne technique for double-pulsed holographic vibration measurements
[PNR90622] N90-26301
Holography and holographic interferometry
[PNR90670] N90-26303
HOMODYNE RECEPTION
A dual-wavelength passive homodyne detection unit for fiber-coupled white-light interferometers
[ETN-90-97036] N90-26653
HOMOGENEITY
G2-continuity in homogeneous co-ordinates
[MATHS-REPT-A-110] N90-26599
HONEYCOMB STRUCTURES
Development of ceramic fiber type combustor: Improvement of combustor and combustion test results
[DE90-503441] N90-26148
HORMONES
Experiment K-6-20. The effect of spaceflight on pituitary oxytocin and vasopressin content of rats N90-26473
HORN ANTENNAS
Scattering from coated structures and antenna pattern control using impedance surfaces, part A/B
[NASA-CR-186871] N90-26233
HOT ISOSTATIC PRESSING
Densification studies of refractory materials using Hot Isostatic Pressing (HIP) and tantalum containment
[DE90-013481] N90-26114
HUMAN BEHAVIOR
Human performance models
[FFI-90/7002] N90-26502
HUMAN BEINGS
Effect of organizational structure on performance of decision making teams
[AD-A223160] N90-26697
HUMAN BODY
Biodynamic simulations of an aircraft pilot/passenger in various crash environments
[NIAR-90-6] N90-26494
HUMAN FACTORS ENGINEERING
Literature concerning control and display technology applicable to the Orbital Maneuvering Vehicle (OMV)
[NASA-CR-186790] N90-26048
Pilot interaction with automated airborne decision making systems
[NASA-CR-186730] N90-26492
Choosing a pilot subjective workload scale to fit flight operational requirements
[IAR-89-21] N90-26493
Human factors: The human interface with aircraft interiors
[NIAR-90-18] N90-26496
Motion sickness, visual displays, and armored vehicle design
[AD-A222678] N90-26506
HUMAN PERFORMANCE
Neural networks for detecting defects in aircraft structures
[IAR-90-4] N90-26345
Robotic-aided system for inspection of aging aircraft
[NIAR-90-9] N90-26346
Human performance models
[FFI-90/7002] N90-26502
Effect of organizational structure on performance of decision making teams
[AD-A223160] N90-26697
HURRICANES
Mariners Weather Log, volume 33, number 3, Summer 1989
[PB90-146846] N90-26444
HYBRID PROPULSION
Project LOCOST: Laser or Chemical Hybrid Orbital Space Transport
[NASA-CR-186822] N90-26042
HYBRID STRUCTURES
Plate rods and leaf springs with hybrid structure: Cross section optimization following different target criteria
[ILR-MITT-227(1989)] N90-26366
HYDRAULIC EQUIPMENT
Simulated dynamic response of a servovalve controlled hydraulic actuator
[NASA-TM-101644] N90-26167
HYDRIDES
Rotational and translational effects in collisions of electronically excited diatomic hydrides
[NASA-CR-186770] N90-26093
HYDROCARBON FUELS
Regenerative Cu La zeolite supported desulfurizing sorbents
[NASA-CASE-NPO-17480-1-CU] N90-26098

HYDROCARBONS
Carbon deposition model for oxygen-hydrocarbon combustion. Task 6: Data analysis and formulation of an empirical model
[NASA-CR-183986] N90-26095
Results from the IVL TOR Station at Roervik, Sweden. A contribution to the EURATRAC subproject TOR
N90-26415
HYDROCYANIC ACID
Role of the methylene amidogen (H2CN) radical in the atmospheres of Titan and Jupiter N90-26769
HYDRODYNAMICS
A lattice gas model for thermohydrodynamics
[DE90-011964] N90-26690
HYDROGEN
Mars in situ propellants: Carbon monoxide and oxygen ignition experiments
[NASA-TM-103202] N90-26065
Hydrogen induced fracture characteristics of single crystal nickel-based superalloys
[NASA-CR-183992] N90-26108
Isothermal compressibility of SPC/E water
[AD-A222723] N90-26643
Rate constant for reaction of atomic hydrogen with germane N90-26768
HYDROGEN COMPOUNDS
Optical properties and transport properties of hydrogenated amorphous silicon
[ETN-90-97215] N90-26656
HYDROGEN EMBRITTLEMENT
Statistical treatment of slow strain rate data for assessment of hydrogen embrittlement in low alloy high strength steel
[ARL-MAT-R-122] N90-26106
HYDROGEN ENGINES
Gas Turbine Combustion, volume 2
[VKI-LS-1990-02-VOL-2] N90-25995
Supersonic combustor testing N90-25998
HYDROGEN FUELS
The use of hydrogen in energy economy of Finland
[DE90-796180] N90-26388
HYDROGEN OXYGEN ENGINES
Performance evaluation of LE-7 high pressure pumps
[DE90-505523] N90-26034
HYDROGEN PEROXIDE
Destruction of peroxy radical by Cu ion catalysed reactions on atmospheric particles N90-26429
HYDROGENATION
Mass spectrometry of poly(methyl methacrylate)s of low molecular weight N90-26091
HYDROSTATIC PRESSURE
Pressure dependence of thermoelectric power of high T(sub c) 123 compound
[PD-MT-9001] N90-26092
HYDROXYL EMISSION
Temperature and OH concentrations in a solid propellant flame using absorption techniques
[AD-A222591] N90-26100
HYPERCUBE MULTIPROCESSORS
Adaptive fault-tolerant routing in hypercube multicomputers
[NASA-CR-186781] N90-26513
A parallel algorithm for surface plane intersection
[IMAG-RR-794-M] N90-26549
Parallelization of an annealing simulation applied to improving tetrahedric grids
[IMAG-RR-796-M] N90-26570
Implementation of algorithms used in calculating the tensor product of matrices on a distributed memory machine
[IMAG-RR-786-I] N90-26572
Multilayered neural networks: Learning algorithms, implementation on hypercube machines, applications
[ETN-90-97255] N90-26574
HYPERFINE STRUCTURE
The interstellar D1 line at high resolution
[NASA-CR-184915] N90-26737
HYPERSONIC AIRCRAFT
Experimental aerothermodynamic research of hypersonic aircraft
[NASA-CR-186903] N90-25954
Maneuvering by means of lateral jets
[ISL-CO-255/88] N90-26015
HYPERSONIC FLIGHT
Transatmospheric vehicle research
[NASA-CR-186705] N90-25970
Carbon-carbon composites: Emerging materials for hypersonic flight
[NASA-TM-103472] N90-26080
HYPERSONIC FLOW
Prediction of two-dimensional time-dependent gasdynamic flows for hypersonic studies
[UTIAS-335] N90-25935
HYPERSONIC INLETS
Prediction of two-dimensional time-dependent gasdynamic flows for hypersonic studies
[UTIAS-335] N90-25935
HYPERSONIC VEHICLES
Transatmospheric vehicle research
[NASA-CR-186705] N90-25970
PDWAP: A preliminary design and weights analysis program for aerospace vehicles
[AD-A222614] N90-25979
Supersonic reacting internal flow fields
[NASA-TM-103480] N90-26094
HYPERSONICS
Prediction of two-dimensional time-dependent gasdynamic flows for hypersonic studies
[UTIAS-335] N90-25935
HYPERVELOCITY IMPACT
Space program: Space debris a potential threat to Space Station and shuttle
[GAO/IMTEC-90-18] N90-26024
HYPOTHERMIA
Arctic cold weather medicine and accidental hypothermia
[AD-A223090] N90-26487
HYPOTHESES
The retrieval of information from secondary memory: A review and new findings
[AD-A222760] N90-26489
HYSTERESIS
Critical current density, flux creep, and microstructure in a Bi-Sr-Ca-Cu-O system
[DE90-010457] N90-26676

I

IAPETUS
Optical constraints of kerogen from 0.15 to 40 microns: Comparison with meteoritic organics N90-26776
ICE
The 27-28 October 1986 FIRE IFO Cirrus case study: Comparison of radiative transfer theory with observations by satellite and aircraft
[NASA-TM-103468] N90-26446
Proceedings of a Workshop on Antarctic Meteorite Stranding Surfaces
[NASA-CR-186575] N90-26739
Photon sputtering of H2O ices: A preliminary report
N90-26783
ICE FORMATION
A NASA/university/industry consortium for research on aircraft ice protection
[IAR-89-18] N90-25969
ICEBERGS
Mariners Weather Log, volume 33, number 2, Spring 1989
[PB90-146838] N90-26443
IGNITERS
Flight set 360L001 (STS-26) igniter, post flight
[NASA-CR-183957] N90-26325
IGNITION
RSRM-9 (360L009): Ballistics mass properties
[NASA-CR-183944] N90-26064
Mars in situ propellants: Carbon monoxide and oxygen ignition experiments
[NASA-TM-103202] N90-26065
Flight motor set 360L007 (STS-33R)
[NASA-CR-183979] N90-26067
Critical evaluation of Jet-A spray combustion using propane chemical kinetics in gas turbine combustion simulated by KIVA-2
[NASA-TM-103173] N90-26170
IGNITION SYSTEMS
Combustion in the gas turbine. Part 3: Fuel injection, ignition and stability
[CIT/SME/VKI/RS/4] N90-25988
ILLUMINATING
Greenhouse design for a Martian colony: Structural, solar collection and light distribution systems
[NASA-CR-186818] N90-26501
IMAGE ANALYSIS
Automatic line network extraction from aerial imagery of urban areas through knowledge based image analysis
[AD-A222675] N90-26385
IMAGE ENHANCEMENT
DSS 15, 45, and 65 34-meter high efficiency antenna radio frequency performance enhancement by tilt added to the subreflector during elevation angle changes
N90-26229
IMAGE FILTERS
Automatic line network extraction from aerial imagery of urban areas through knowledge based image analysis
[AD-A222675] N90-26385
Spatial cross-correlation of Antarctic Sea ice and seabed topography
[NASA-CR-186815] N90-26451
IMAGE PROCESSING
Multiple target tracking in a wide-field-of-view camera system
[DE90-013488] N90-26300
Pattern classification of textura by moment and distance autocorrelation function
[INPE-4976-PRE/1541] N90-26379
Classification regions in remote sensing imagery utilizing spatial characteristics
[INPE-4913-PRE/1514] N90-26381
Automatic line network extraction from aerial imagery of urban areas through knowledge based image analysis
[AD-A222675] N90-26385
Segmentation before and after reconstruction of 3-D surfaces in depth imagery
[RR-788-I-IMAG-97-LIFIA] N90-26551
Color image processing for navigation: Two road trackers
[AD-A222667] N90-26591
IMAGE RECONSTRUCTION
Surface reconstruction based on critical contours in a multi-image context
[RR-784-I-IMAG-94-LIFIA] N90-26383
Segmentation before and after reconstruction of 3-D surfaces in depth imagery
[RR-788-I-IMAG-97-LIFIA] N90-26551
Massively parallel architecture: Integrated cell network for image reconstruction
[ETN-90-97257] N90-26575
IMAGERY
Surface reconstruction based on critical contours in a multi-image context
[RR-784-I-IMAG-94-LIFIA] N90-26383
IMAGING SPECTROMETERS
Modeling, simulation, and analysis of optical remote sensing systems
[NASA-CR-186648] N90-26376
IMAGING TECHNIQUES
Improving the geometric fidelity of imaging systems employing sensor arrays
[NASA-CASE-NPO-17970-1-CU] N90-26384
Segmentation before and after reconstruction of 3-D surfaces in depth imagery
[RR-788-I-IMAG-97-LIFIA] N90-26551
Experiments on superconductor imaging surface magnetometry
[DE90-008925] N90-26665
IMMUNOLOGY
Experiment K-6-23. Effect of spaceflight on levels and function of immune cells N90-26476
IMPACT DAMAGE
Space program: Space debris a potential threat to Space Station and shuttle
[GAO/IMTEC-90-18] N90-26024
An embedded fibre optic sensor for impact damage detection in composite materials
[UTIAS-332] N90-26650
IMPACT PREDICTION
Space program: Space debris a potential threat to Space Station and shuttle
[GAO/IMTEC-90-18] N90-26024
IMPACT TESTS
An embedded fibre optic sensor for impact damage detection in composite materials
[UTIAS-332] N90-26650
IMPEDANCE
Scattering from coated structures and antenna pattern control using impedance surfaces, part A/B
[NASA-CR-186871] N90-26233
IMPLANTATION
The interaction of polymeric materials with ceramic surfaces with special reference to the behaviour of bioceramics N90-26127
IMPULSES
Estimation of the impulse response of a broadband mobile radio channel in suburbia at 910 MHz
N90-26187
IMPURITIES
Role of surface passivation in the integrated processing of MOS structures
[AD-A222630] N90-26264
IN-FLIGHT MONITORING
An automated calibration laboratory for flight research instrumentation: Requirements and a proposed design approach
[NASA-TM-101719] N90-26564
INDEXES (DOCUMENTATION)
The EISI (Elemental and Interplanar Spacing Index) index: A search/match tool for electron diffraction phase analysis
[DE90-010832] N90-26097
INDIUM ALLOYS
Damping capacity of aluminum 6061-indium alloys
[AD-A222802] N90-26124

INDIUM ARSENIDES
Application of InAlAs/GaAs superlattice alloys to GaAs isolar cells
[DE90-013070] N90-26389
INDIUM COMPOUNDS
Dielectric function of InGaAs in the visible
[NASA-TM-103246] N90-26683
INDUCTANCE
L-SWITCH: A PC program for computing transient voltages and currents during switching off three-phase inductances
[EUT-89-E-221] N90-26257
INDUSTRIAL MANAGEMENT
Making it happen: Project management
[PNR90618] N90-26695
INDUSTRIAL SAFETY
Space shuttle: Follow-up evaluation of NASA's solid rocket motor procurement. Report to the Chairman, Committee on Government Operations, House of Representatives
[GAO/NSIAD-89-89] N90-26066
INELASTIC COLLISIONS
Determination of molecular spectroscopic parameters and energy-transfer rates by double-resonance spectroscopy N90-26755
INERTIAL GUIDANCE
Guidance and targeting for the strategic target system
[DE90-005239] N90-26031
INFERENCE
Inference and control mechanisms in NEXT 2.0
[NLR-MP-88062-U] N90-26175
INFORMATION
Information content of a single pass of phase-delay data from a short baseline connected element interferometer N90-26220
Capacity for patterns and sequences in Kanerva's SDM as compared to other associative memory models
[NASA-CR-180701] N90-26522
INFORMATION DISSEMINATION
NASA project status reports: Congressional requirements can be met, but reliability must be ensured
[GAO/NSIAD-90-40] N90-26169
MTP: An atomic multicast transport protocol
[NASA-CR-186716] N90-26254
International standards for text preparation and interchange
[DE90-011868] N90-26699
INFORMATION MANAGEMENT
Knowledge-based system for flight information management
[NASA-TM-102685] N90-26511
International standards for text preparation and interchange
[DE90-011868] N90-26699
INFORMATION RETRIEVAL
The EISI (Elemental and Interplanar Spacing Index) index: A search/match tool for electron diffraction phase analysis
[DE90-010832] N90-26097
The retrieval of information from secondary memory: A review and new findings
[AD-A222760] N90-26489
Energy data base: Subject categories and scope
[DE90-009212] N90-26706
INFORMATION SYSTEMS
Energy data base: Subject categories and scope
[DE90-009212] N90-26706
VISTA (Vertical Integration of Science, Technology, and Applications) user interface software study
[DE90-010003] N90-26707
INFORMATION TRANSFER
Minimization of the cost of information transfer in HF spread spectrum transmission N90-26198
INFRARED ASTRONOMY
Recent high resolution laboratory determinations of line broadening and intensity parameters: PH3, CH3D, and CO2 N90-26751
INFRARED DETECTORS
Multicolor infrared photodetector
[AD-D014511] N90-26297
INFRARED LASERS
A compact, high-powered Far-Infrared (FIR) laser
[DE90-009996] N90-26312
INFRARED RADIATION
The 27-28 October 1986 FIRE IFO cirrus case study: Cirrus parameter relationships derived from satellite and lidar data
[NASA-TM-103469] N90-26447
Implementation of sensor and control designs for bioregenerative systems
[NASA-CR-186655] N90-26479
Development of eye-safe lidar for aerosol measurements
[NASA-CR-186905] N90-26503
Infrared line parameters at low temperatures relevant to planetary atmospheres N90-26753
INFRARED SCANNERS
Debris/ice/TPS assessment and photographic analysis for shuttle mission STS-31R
[NASA-TM-102790] N90-26040
Resonant coupling through a slot to a loaded cylindrical cavity: Experimental results
[AD-A223000] N90-26631
INFRARED SPECTRA
Measurements of CH4, N2O, CO, H2O and O3 in the middle atmosphere by the ATMOS experiment on Spacelab 3
[NASA-TM-103476] N90-26400
Infrared spectra of van de Waals complexes of importance in planetary atmospheres N90-26749
Novel laser gain and time-resolved FTIR studies of photochemistry N90-26756
Gaussian quadrature exponential sum modeling of near infrared methane laboratory spectra obtained at temperatures from 106 to 297 K N90-26758
Measurements of the methane relaxation times for application to the infrared emission models of the upper atmospheres of outer planets and Titan N90-26759
INFRARED SPECTROMETERS
HIRIS performance study
[NASA-CR-186649] N90-26375
INFRARED SPECTROSCOPY
High resolution infrared spectroscopy of planetary molecules using diode lasers and Fourier transform spectrometers N90-26747
INJECTION LASERS
Apparatus for the efficient wavelength conversion of laser radiation
[AD-D014506] N90-26305
INJECTORS
Subsonic combustor testing N90-25997
The structural dynamics analysis of the main injector LOX inlet tee and its redesign
[NASA-CR-186764] N90-26358
INLET TEMPERATURE
Research and development of advanced gas turbine
[DE90-503377] N90-26335
INPUT/OUTPUT ROUTINES
A search routine for optimization in a wind power system with variable speed
[FOA-C-20779-2.1] N90-26395
UEDIT: A full-scale, scrollable APL2 spreadsheet input/output editor
[AD-A222712] N90-26557
The system matrix characterisation of input-output equivalence
[MATHS-REPT-A-112] N90-26600
INSPECTION
Debris/ice/TPS assessment and photographic analysis for shuttle mission STS-31R
[NASA-TM-102790] N90-26040
Acousto-optic signature analysis for inspection of the orbiter thermal protection tile bonds
[DE90-013089] N90-26043
Design and construction of a wall-climbing robot
[NIAR-90-20] N90-26327
Neural networks for detecting defects in aircraft structures
[IAR-90-4] N90-26345
Robotic-aided system for inspection of aging aircraft
[NIAR-90-9] N90-26346
Field experience in using laser acoustic sensing for inspection
[DE90-012954] N90-26347
NDT in aerospace: The next decade (1990's)
[PNR90628] N90-26348
The role of NDI in the certification of turbine engine components
[PNR90629] N90-26349
Characterization of inspection performance
[NLR-MP-88068-U] N90-26350
Coherent optical techniques for industrial inspection
[PNR90605] N90-26654
INSULATION
Comparison of currents predicted by NASCAP/LEO model simulations with elementary Langmuir-type bare probe models for an insulated cable containing a single pinhole
[NASA-TM-102486] N90-26054
Flight motor set 360L007 (STS-33R)
[NASA-CR-183979] N90-26067
INSURANCE (CONTRACTS)
Damage responsibility and liability in space stations N90-26714
INTAKE SYSTEMS
The structural dynamics analysis of the main injector LOX inlet tee and its redesign
[NASA-CR-186764] N90-26358
INTEGRAL EQUATIONS
Estimation of convective rain volumes utilizing the are-time-integral technique
[NASA-CR-186814] N90-26449
INTEGRALS
Elevated temperature crack growth
[NASA-CR-182247] N90-26355
INTEGRATED CIRCUITS
Design of an optically controlled Ka-band GaAs MMIC phased-array antenna
[NASA-TM-103147] N90-26250
LASER: A Layout Sensitivity Explorer. Report and user's manual
[EUT-89-E-216] N90-26545
Massively parallel architecture: Integrated cell network for image reconstruction
[ETN-90-97257] N90-26575
INTERFACES
The effect of interfacial characteristics on the mechanical performance of ceramic-ceramic composites
[AD-A223031] N90-26090
Structured electrode interfaces
[AD-A222763] N90-26265
INTERFEROMETERS
Information content of a single pass of phase-delay data from a short baseline connected element interferometer N90-26220
Absolute measurements of gravity
[AD-A222731] N90-26629
A dual-wavelength passive homodyne detection unit for fiber-coupled white-light interferometers
[ETN-90-97036] N90-26653
INTERFEROMETRY
Goldstone intracomplex connected element interferometry N90-26218
Refractive error analysis in the interferometric measurement of 2-D density fields containing strong gradients
[LR-616] N90-26655
INTERMETALLICS
Searching for heavy fermion materials in Ce intermetallic compounds
[DE90-011809] N90-26116
INTERNAL COMBUSTION ENGINES
Critical evaluation of Jet-A spray combustion using propane chemical kinetics in gas turbine combustion simulated by KIVA-2
[NASA-TM-103173] N90-26170
INTERNAL WAVES
The browse file of NASA/JPL quick-look radar images from the Loch Linnhe 1989 experiment
[NASA-CR-186855] N90-26701
INTERNATIONAL COOPERATION
Space exploration: Cost, schedule, and performance of NASA's Ulysses Mission to the Sun. Fact sheet for the Chairman, Subcommittee on Science, Technology, and Space, Committee on Commerce, Science, and Transportation, US Senate
[GAO/NSIAD-88-129FS] N90-26023
Manned Space Stations: Legal Issues
[ESA-SP-305] N90-26711
The US/International Space Station: Legal aspects of space objects and jurisdiction and control N90-26713
MIR: A Soviet Space Station. Some legal aspects of international cooperation N90-26715
The International Space Station: The legal framework N90-26716
The partnership concept and international management N90-26717
The International Space Station: Conditions of access and use N90-26718
Human work in space: The astronaut's legal status. Introduction N90-26719
The manned national space station: International legal considerations N90-26720
The astronauts' legal status: The International Space Station N90-26721
Crossborder movements: Goods, personnel and technologies N90-26722
Space Station intellectual property rights and US patent law N90-26723
Possible solutions N90-26726
Space law put to the test by the International Space Station N90-26727
INTERPLANETARY NAVIGATION
The effect of interplanetary trajectory options on a manned Mars aerobrake configuration
[NASA-TP-3019] N90-26036
INTERPLANETARY TRAJECTORIES
The effect of interplanetary trajectory options on a manned Mars aerobrake configuration
[NASA-TP-3019] N90-26036
INTERPOLATION
Comment on high resolution simulations of cosmic strings. 1: Network evoloution
[NASA-CR-186606] N90-26734
INTERPROCESSOR COMMUNICATION
Applications for the scalable coherent interface
[DE90-011795] N90-26514

Integrating expert systems with solid modeling through interprocess communications and the applications interface specification
[DE90-012996] N90-26537
A parallel algorithm for surface plane intersection
[IMAG-RR-794-M] N90-26549
Implementation of algorithms used in calculating the tensor product of matrices on a distributed memory machine
[IMAG-RR-786-I] N90-26572

INTERROGATION
A parallel algorithm for surface plane intersection
[IMAG-RR-794-M] N90-26549

INTERSTELLAR MATTER
The interstellar D1 line at high resolution
[NASA-CR-184915] N90-26737

INTESTINES
Experiment K-6-17. Structural changes and cell turnover in the rats small intestine induced by spaceflight N90-26470

INVENTIONS
Production activities in space: The problems of protection N90-26725
Possible solutions N90-26726

INVISCID FLOW
Analysis and mitigation of numerical dissipation in inviscid and viscid computation of vortex-dominated flows
[NASA-CR-186887] N90-26281
Computational fluid dynamics 3-D analysis for advanced transonic turbine design
[ETN-90-97282] N90-26291

ION BEAMS
A closed form solution to HZE propagation
[NASA-TM-103482] N90-26640
Studies on ion scattering and sputtering processes relevant to ion beam sputter deposition of multicomponent thin films
[DE90-010071] N90-26675

ION DISTRIBUTION
Nondestructive one- and two-dimensional doping profiling by inverse methods
[ETN-90-97264] N90-26351

ION EMISSION
A study of the influence of Hg(6(3)P2) population in a low-pressure discharge on mercury ion emission at 194.2 nm N90-26223

ION EXCHANGE MEMBRANE ELECTROLYTES
The development and characterization of ion exchange membranes for selected electrochemical power sources
[DE90-009741] N90-26251

ION IMPLANTATION
The effect of crystal orientation on damage accumulation in chromium-implanted Al2O3
[DE90-012294] N90-26674
Rapid thermal processing: A study of the silicon oxidation and of the implanted boron activation
[LAAS-90051] N90-26681

ION RECOMBINATION
Dissociative recombination of molecular ions with electrons N90-26767

ION SCATTERING
Studies on ion scattering and sputtering processes relevant to ion beam sputter deposition of multicomponent thin films
[DE90-010071] N90-26675

IONIC COLLISIONS
A research program in physics of the early universe
[DE90-013319] N90-26742

IONIC REACTIONS
Ionic atmosphere effects on the energetics of thermal and optical electron-exchange reactions: Application to ferrocenium-ferrocene self exchange
[AD-A222605] N90-26441

IONIZATION
New electronic states of NH and ND observed by resonance enhanced multiphoton ionization spectroscopy N90-26760
UV and VUV spectroscopy and photochemistry of small molecules in a supersonic jet N90-26771

IONOSPHERIC DISTURBANCES
Experimental analysis of the HF linkage N90-26181
System factors to be considered in assessing propagation effects on modern digital satellite communications systems N90-26208

IONOSPHERIC PROPAGATION
Effects of ionospheric modification on system performance N90-26202

IONS
Laboratory studies of the interaction of ions with condensed gases: Planetary applications N90-26778

IRIS SATELLITES
IRIS system and future application to expandable launchers
[IAF-89-212] N90-26035

IRON ALLOYS
The effect of manganese on the onset of the stage 2 reaction in an austempered ductile iron matrix
[DE90-011804] N90-26119

IRRADIATION
A study of the influence of Hg(6(3)P2) population in a low-pressure discharge on mercury ion emission at 194.2 nm N90-26223
Excimer laser fragmentation studies of selected oximes: Nascent OH internal energy distributions and the search of H2CN fluorescence
[AD-A222622] N90-26317

ISOTOPIC LABELING
The Renland ice core (Greenland): A source for climatic studies over 100,000 years N90-26412

ISOTROPY
Theory of biaxial graded-index optical fiber
[NASA-CR-186882] N90-26652

ITERATION
Run-time parallelization and scheduling of loops
[NASA-CR-182039] N90-26509

ITERATIVE SOLUTION
Efficient implementation of minimal polynomial and reduced rank extrapolation methods
[NASA-TM-103240] N90-26616

J

JAMMING
Tracking performance of a combined Costas/AFC-loop under noisy Rayleigh/Rician channel conditions with additive Gaussian noise jamming
[ETN-90-96964] N90-26237
Electronic warfare technology: Trends and visions
[AD-A223034] N90-26246
Dynamic jamming of networks
[AD-A223044] N90-26247
A novel communication network simulator
[AD-A223045] N90-26248

JET CONTROL
Maneuvering by means of lateral jets
[ISL-CO-255/88] N90-26015

JOINTS (JUNCTIONS)
Vitreous joining of SiC fiber reinforced SiC composites
[DE90-012951] N90-26081

JOULE-THOMSON EFFECT
Multicomponent gas sorption Joule-Thomson refrigerator
[NASA-CASE-NPO-17569-1-CU] N90-26176

JOURNAL BEARINGS
A high-speed photography study of cavitation in a dynamically loaded journal bearing
[NASA-TM-103178] N90-26338

JUPITER (PLANET)
NASA/USRA university advanced design program at the University of Illinois for the 1989-1990 academic year
[NASA-CR-186829] N90-26049

JUPITER ATMOSPHERE
Space exploration: Cost, schedule, and performance of NASA's Galileo Mission to Jupiter. Fact sheet for the Chairman, Subcommittee on Science, Technology, and Space, Committee on Commerce, Science, and Transportation, US Senate
[GAO/NSIAD-88-138FS] N90-26025
Rate constant for reaction of atomic hydrogen with germane N90-26768
Role of the methylene amidogen (H2CN) radical in the atmospheres of Titan and Jupiter N90-26769

JUPITER PROBES
Space exploration: Cost, schedule, and performance of NASA's Galileo Mission to Jupiter. Fact sheet for the Chairman, Subcommittee on Science, Technology, and Space, Committee on Commerce, Science, and Transportation, US Senate
[GAO/NSIAD-88-138FS] N90-26025

JUPITER SATELLITES
Space exploration: Cost, schedule, and performance of NASA's Galileo Mission to Jupiter. Fact sheet for the Chairman, Subcommittee on Science, Technology, and Space, Committee on Commerce, Science, and Transportation, US Senate
[GAO/NSIAD-88-138FS] N90-26025
Laboratory studies of the interaction of ions with condensed gases: Planetary applications N90-26778

K

K-EPSILON TURBULENCE MODEL
A critical evaluation of two-equation models for near wall turbulence
[NASA-CR-182068] N90-26270
Calculation of 3D turbulent jets in crossflow with a multigrid method and a second-moment closure model
[NASA-TM-103159] N90-26282

KARMAN-BODEWADT FLOW
Prediction of rotating disc flow and heat transfer in gas turbine engines
[PNR90650] N90-26001

KEPLER LAWS
Forbidden tangential orbit transfers between intersecting Keplerian orbits
[NASA-TP-3031] N90-26028

KEROGEN
Optical constraints of kerogen from 0.15 to 40 microns: Comparison with meteoritic organics N90-26776

KINEMATICS
Control strategy for cooperating disparate manipulators
[NASA-CR-186809] N90-26328
Analysis of strain relaxation in Au/Ni multilayers by x ray diffraction
[IAR-89-25] N90-26357
Biodynamic simulations of an aircraft pilot/passenger in various crash environments
[NIAR-90-6] N90-26494
Position control of redundant manipulators using an adaptive error-based control scheme
[NASA-CR-186812] N90-26578
Mobility studies in multiloop spatial linkages N90-26628

KINETIC ENERGY
A computational study of the effectiveness of coating materials for KE projectile fins subjected to the combined effects of inbore and aerodynamic heating
[AD-A222595] N90-26155

KINETICS
Formation and deactivation of vibrationally excited atmospheric molecules
[AD-A222660] N90-26442
Novel laser gain and time-resolved FTIR studies of photochemistry N90-26756

KIRCHHOFF LAW OF RADIATION
Computer modeling wave propagation with a variation of the Helmholtz-Kirchhoff relation
[AD-A222746] N90-26657

KNOWLEDGE BASES (ARTIFICIAL INTELLIGENCE)
Knowledge-based system for flight information management
[NASA-TM-102685] N90-26511

KNOWLEDGE REPRESENTATION
Knowledge and inhibition in asynchronous distributed systems
[TR-90-1139] N90-26703

L

LABORATORIES
An automated calibration laboratory for flight research instrumentation: Requirements and a proposed design approach
[NASA-TM-101719] N90-26564

LAGRANGE COORDINATES
An angular weighting approach for calculating gradients and divergences
[DE90-013164] N90-26539

LAKES
The transfer of mercury between the atmosphere and lake or soil surfaces N90-26419
The 5th International symposium on palaeolimnology
[AD-A219244] N90-26431

LAMINAR BOUNDARY LAYER
Interactive calculation procedures for mixed compression inlets
[NASA-CR-186581] N90-25934
Effects of forebody geometry on subsonic boundary-layer stability
[NASA-CR-4314] N90-25939
Application of laminar flow control to supersonic transport configurations
[NASA-CR-181917] N90-25944

LAMINAR FLOW
Chemistry of combustion processes N90-25994
The finite analytic method and its applications. Volume 1: Laminar and turbulent flows past two-dimensional and axisymmetric bodies
[AD-A222787] N90-26294
Effects of 2 Hz imposed bulk flow unsteadiness on laminar-turbulent transition in a straight channel
[AD-A223028] N90-26295

LAMINAR FLOW AIRFOILS
Flight testing of a natural laminar flow airfoil using gliders
[PD-CF-9005] N90-25936

LAMINAR HEAT TRANSFER
Turbine blade heat transfer coefficient evaluation by modified version of STAN5. Comparison with experimental data
[ETN-90-97283] N90-26008

LAMINATES
Strain energy release rate analysis of delamination in a tapered laminate subjected to tension load
[NASA-TM-102582] N90-26076
Damage states in laminated composite three-point bend specimens: An experimental-analytical correlation study
[NASA-TM-101800] N90-26083
Fracture toughness and failure mechanisms in commercial 2091 Al-Li sheet at cryogenic temperatures
[AD-A222803] N90-26125
The blunt notch behaviour of metal laminates: ARALL and GLARE
[LR-617] N90-26368
Reliability analysis of continuous fiber composite laminates
[NASA-CR-185265] N90-26372
LAND USE
Practical applications of remote sensing technology
[NASA-CR-186810] N90-26377
LANDAU FACTOR
High temperature x ray diffraction and Landau theory investigations of order-disorder transition in defect NaCl-type solids
[DE90-011807] N90-26673
LANDING AIDS
Preliminary subsystem designs for the Assured Crew Return Vehicle (ACRV), volume 1
[NASA-CR-186677-VOL-1] N90-26039
LANDSAT SATELLITES
The 27-28 October 1986 FIRE IFO Cirrus case study: Comparison of radiative transfer theory with observations by satellite and aircraft
[NASA-TM-103468] N90-26446
LANDSAT 5
Atmospheric correction of thematic mapping measurements about seabeds of the German Bay
[GKSS-89/E/47] N90-26029
LAPLACE TRANSFORMATION
Galerkin finite difference Laplacian operators on isolated unstructured triangular meshes by linear combinations
[NASA-TM-103209] N90-26276
LARGE SCALE INTEGRATION
Multiple target tracking in a wide-field-of-view camera system
[DE90-013488] N90-26300
LARGE SPACE STRUCTURES
Design and implementation of robust decentralized control laws for the ACES structure at Marshall Space Flight Center
[NASA-CR-4310] N90-26046
Technology for large space systems: A bibliography with indexes (supplement 22)
[NASA-SP-7046(22)] N90-26056
Structures for remotely deployable precision antennas
[NASA-CR-182065] N90-26061
Feasibility study of a synthesis procedure for array feeds to improve radiation performance of large distorted reflector antennas
[NASA-CR-186641] N90-26213
Intergration of system identification and robust controller designs for flexible structures in space
[NASA-TM-102695] N90-26362
LASER ANEMOMETERS
Effect of initial conditions on the development of two-phase jets
[AD-A222621] N90-26293
LASER APPLICATIONS
Laser ultrasonic measurements on ceramic materials with rough surfaces
[DE90-012961] N90-26141
Laser techniques for studying chemical vapor deposition
[DE90-012921] N90-26311
Field experience in using laser acoustic sensing for inspection
[DE90-012954] N90-26347
Ellipsometric study of YBa2Cu3O(7-x) laser ablated and co-evaporated films
[NASA-TM-103223] N90-26682
LASER BEAMS
Apparatus for the efficient wavelength conversion of laser radiation
[AD-D014506] N90-26305
Theoretical studies of solar pumped lasers
[NASA-CR-186712] N90-26308
DURIP: Instrumentation for laser switched power LINAC
[AD-A222629] N90-26318
Beam rider for an Articulated Robot Manipulator (ARM) accurate positioning of long flexible manipulators
[NASA-CR-185151] N90-26581
LASER DAMAGE
Damage measurements on optical materials for use in high-peak-power lasers
[DE90-013489] N90-26314
Laser damage database at 1064 nm
[DE90-013490] N90-26315
LASER DOPPLER VELOCIMETERS
Euler analysis comparison with LDV data for an advanced counter-rotation propfan at cruise
[NASA-TM-103249] N90-25946
Combustion instrumentation N90-25996
LASER INDUCED FLUORESCENCE
Excimer laser fragmentation studies of selected oximes: Nascent OH internal energy distributions and the search of H2CN fluorescence
[AD-A222622] N90-26317
LASER INTERFEROMETRY
Coherent optical techniques for industrial inspection
[PNR90605] N90-26654
LASER MATERIALS
Theoretical studies of solar pumped lasers
[NASA-CR-186712] N90-26308
LASER OUTPUTS
A study of the influence of Hg(6(3)P2) population in a low-pressure discharge on mercury ion emission at 194.2 nm N90-26223
DURIP: Instrumentation for laser switched power LINAC
[AD-A222629] N90-26318
Novel laser gain and time-resolved FTIR studies of photochemistry N90-26756
LASER PLASMAS
Soft x ray resist characterization: Studies with a laser plasma x ray source
[DE90-013493] N90-26661
LASER POWER BEAMING
Characterization of a high-intensity, subpicosecond XeCl laser system
[DE90-011970] N90-26310
LASER PROPULSION
Project LOCOST: Laser or Chemical Hybrid Orbital Space Transport
[NASA-CR-186822] N90-26042
LASER SPECTROSCOPY
A study of the influence of Hg(6(3)P2) population in a low-pressure discharge on mercury ion emission at 194.2 nm N90-26223
Novel laser gain and time-resolved FTIR studies of photochemistry N90-26756
Methane overtone absorption by intracavity laser spectroscopy N90-26762
LASERS
SDIO/IST ultrashort wavelength laser: Novel experimental schemes for observing the Moessbauer effect in long-lived nuclear levels and nuclear coherent states
[AD-A222607] N90-26316
Field experience in using laser acoustic sensing for inspection
[DE90-012954] N90-26347
Development of eye-safe lidar for aerosol measurements
[NASA-CR-186905] N90-26503
LASING
Theoretical studies of solar pumped lasers
[NASA-CR-186712] N90-26308
A compact, high-powered Far-Infrared (FIR) laser
[DE90-009996] N90-26312
LATERAL CONTROL
Maneuvering by means of lateral jets
[ISL-CO-255/88] N90-26015
LAUNCH DATES
Space exploration: Cost, schedule, and performance of NASA's Galileo Mission to Jupiter. Fact sheet for the Chairman, Subcommittee on Science, Technology, and Space, Committee on Commerce, Science, and Transportation, US Senate
[GAO/NSIAD-88-138FS] N90-26025
LAUNCH VEHICLES
PDWAP: A preliminary design and weights analysis program for aerospace vehicles
[AD-A222614] N90-25979
Guidance and targeting for the strategic target system
[DE90-005239] N90-26031
Trajectory optimization for an asymmetric launch vehicle
[NASA-CR-185630] N90-26033
IRIS system and future application to expandable launchers
[IAF-89-212] N90-26035
LAUNCH WINDOWS
Space exploration: Cost, schedule, and performance of NASA's Galileo Mission to Jupiter. Fact sheet for the Chairman, Subcommittee on Science, Technology, and Space, Committee on Commerce, Science, and Transportation, US Senate
[GAO/NSIAD-88-138FS] N90-26025
LAUNCHING
Flight motor set 360L007 (STS-33R)
[NASA-CR-183979] N90-26067
LAUNCHING PADS
Soil stabilization mat for lunar launch/landing site
[NASA-CR-186690] N90-26128
LAUNCHING SITES
Soil stabilization mat for lunar launch/landing site
[NASA-CR-186690] N90-26128
LEAD ISOTOPES
The long-term variation of lead-210 in relation to particle-bound sulphur in surface air in Finland N90-26407
LEAD OXIDES
Selective electrocatalysis of anodic oxygen-transfer reactions at chemically modified, thin-film lead dioxide electrodes
[DE90-011747] N90-26252
LEADING EDGES
Experimental study on vortex and shock wave development on a 65 deg delta wing
[NLR-MP-88033-U] N90-25950
LEARNING
Mathematical problem-solving transfer: The effects of cognitive load and attention a schema acquisition and rule automation N90-26594
LEAST SQUARES METHOD
Variance reduction for quantile estimates in simulations via nonlinear controls
[AD-A222653] N90-26590
Strong consistency of the least squares estimator for a non-ergodic threshold autoregressive model
[IMAG-RR-791-M] N90-26604
A study of the asymptotic properties of least square estimators for multiple phase regression problems
[ETN-90-97244] N90-26620
Gaussian quadrature exponential sum modeling of near infrared methane laboratory spectra obtained at temperatures from 106 to 297 K N90-26758
LECTURES
Texstar: The all-Texas educational satellite system
[NASA-CR-186654] N90-26045
LEG (ANATOMY)
Neural networks for real-time sensory data processing and sensorimotor control
[AD-A223096] N90-26592
LEGAL LIABILITY
Damage responsibility and liability in space stations N90-26714
The astronauts' legal status: The International Space Station N90-26721
LESIONS
Experiment K-6-22. Growth hormone regulation, synthesis and secretion in microgravity. Part 1: Somatotroph physiology. Part 2: Immunohistochemical analysis of hypothalamic hormones. Part 3: Plasma analysis N90-26475
LEVITATION
Materials research issues in superconducting levitation and suspension as applied to magnetic bearings
[DE90-011147] N90-26667
LIFE (DURABILITY)
Proceedings of the LDEF Materials Data Analysis Workshop
[NASA-CP-10046] N90-26075
NDT in aerospace: The next decade (1990's)
[PNR90628] N90-26348
Fatigue life assessment using a short crack growth model
[PNR90663] N90-26367
Multimegawatt space nuclear power supply, phase 1. Volume 3: Annotated outline of preliminary safety assessment D180-30619-7
[DE90-012432] N90-26646
LIFE SUPPORT SYSTEMS
Fluid Phase Separation (FPS) experiment for flight on a space shuttle Get Away Special (GAS) canister
[NASA-CR-186830] N90-26161
Automation of closed environments in space for human comfort and safety
[NASA-CR-186834] N90-26500
Development of membrane process for carbon dioxide separation from diving atmosphere
[AD-A222606] N90-26504
Aircrew life support systems enhancement
[AD-A222626] N90-26505
LIGAMENTS
Experiment K-6-03. Gravity and skeletal growth, part 1. Part 2: Morphology and histochemistry of bone cells and vasculature of the tibia; Part 3: Nuclear volume analysis of osteoblast histogenesis in periodontal ligament cells; Part 4: Intervertebral disc swelling pressure associated with microgravity N90-26457
LIGHT CURVE
The interstellar D1 line at high resolution
[NASA-CR-184915] N90-26737

LIGHT EMISSION
Experiments on initial behaviour of corona generated with electrical pulses superimposed on DC bias
[EUT-89-E-226] N90-26259
LIGHT SCATTERING
Interaction of electromagnetic signals with particulate clouds
[AD-A222804] N90-26244
Optical characterization of clouds of fine liquid-nitrogen particles
[NASA-TM-103208] N90-26299
LIGHT TRANSMISSION
An embedded fibre optic sensor for impact damage detection in composite materials
[UTIAS-332] N90-26650
Optical transmission through a polarization preserving single mode optical fiber at two Ar(+) laser wavelengths
[NASA-TM-103475] N90-26651
LIMNOLOGY
The 5th International symposium on palaeolimnology
[AD-A219244] N90-26431
LINE SPECTRA
Infrared line parameters at low temperatures relevant to planetary atmospheres N90-26753
LINEAR ACCELERATORS
DURIP: Instrumentation for laser switched power LINAC
[AD-A222629] N90-26318
A beauty factory using an SRF linac and a storage ring
[CEBAF-PR-89-017] N90-26644
LINEAR EQUATIONS
Asymptotic optimality of the fast randomized versions of GCV and C(sub L) in ridge regression and regularization
[IMAG-RR-793-M] N90-26606
Contribution to the study of differential equations and to the differences in the complex field
[ETN-90-97250] N90-26612
Efficient implementation of minimal polynomial and reduced rank extrapolation methods
[NASA-TM-103240] N90-26616
Applied mathematical modules for use in a linear algebra service course
[AD-A222814] N90-26618
LINEAR PROGRAMMING
Adaptive and comparative studies of optimization algorithms: Implementations and applications
[ETN-90-97243] N90-26553
LINEAR SYSTEMS
Inhomogeneous electric field effects in a linear RF quadruple trap N90-26222
On output deadbeat control of discrete-time multivariable systems
[MATHS-REPT-A-122] N90-26583
On the robust stability of MIMO linear feedback systems
[EUT-88-E-212] N90-26585
Parallel/distributed direct method for solving linear systems
[NASA-TM-103229] N90-26614
LINEAR TRANSFORMATIONS
A Bayesian proportional model for software reliability
[IMAG-RR-795-M] N90-26353
Asymptotic law of the orthogonal empirical functions and applications, part 2
[IMAG-RR-792-M-PT-2] N90-26605
LINES (GEOMETRY)
Hierarchical structure of polygonal data for spatial analysis and representation of cartographical data
[INPE-4986-PRE/1548] N90-26380
LINGUISTICS
Rhetorical structure theory and text analysis
[AD-A222655] N90-26733
LININGS
Experiment K-6-17. Structural changes and cell turnover in the rats small intestine induced by spaceflight N90-26470
LINKAGES
Mobility studies in multiloop spatial linkages N90-26628
LIQUEFIED GASES
Performance evaluation of LE-7 high pressure pumps
[DE90-505523] N90-26034
LIQUID CRYSTALS
NMR and optical studies of piezoelectric polymers
[DE90-012459] N90-26137
LIQUID FUELS
Liquid fueled ramjet combustion instability: Acoustical and vortical interactions with burning sprays
[AD-A222752] N90-26104
LIQUID HYDROGEN
Initial experimentation on the nonvented fill of a 0.14m3 (5 ft. 3) dewar with nitrogen and hydrogen
[NASA-TM-103155] N90-26278
LIQUID NITROGEN
Initial experimentation on the nonvented fill of a 0.14m3 (5 ft. 3) dewar with nitrogen and hydrogen
[NASA-TM-103155] N90-26278
Optical characterization of clouds of fine liquid-nitrogen particles
[NASA-TM-103208] N90-26299
LIQUID OXYGEN
The structural dynamics analysis of the main injector LOX inlet tee and its redesign
[NASA-CR-186764] N90-26358
LIQUID PHASES
Fluid Phase Separation (FPS) experiment for flight on a space shuttle Get Away Special (GAS) canister
[NASA-CR-186830] N90-26161
Two-dimensional model of a Space Station Freedom thermal energy storage canister
[NASA-TM-103124] N90-26279
Optical constants of solid methane N90-26775
LIQUID ROCKET PROPELLANTS
Methods and apparatus for providing real-time control of a gaseous propellant rocket propulsion system
[NASA-CASE-MSC-21542-1] N90-26073
LIQUID SURFACES
Chemical structure and kinetics at liquid/solid interfaces
[AD-A222766] N90-26105
Exact results for the structured liquid-solid interface
[AD-A222762] N90-26630
LIQUID-SOLID INTERFACES
Chemical structure and kinetics at liquid/solid interfaces
[AD-A222766] N90-26105
Exact results for the structured liquid-solid interface
[AD-A222762] N90-26630
LIQUID-VAPOR EQUILIBRIUM
Liquid-vapor equilibrium of multicomponent cryogenic systems N90-26774
LITHIUM ALLOYS
A study of the fatigue behavior in scratched samples of Al-Li alloy (2090-T3)
[IAR-89-24] N90-26107
Fracture toughness and failure mechanisms in commercial 2091 Al-Li sheet at cryogenic temperatures
[AD-A222803] N90-26125
LIVER
Experiment K-6-12. Morphometric studies of atrial or granules and hepatocytes. Part 1: Morphometric study of the liver; Part 2: The atrial granular accumulations N90-26466
Experiment K-6-14. Hepatic function in rats after spaceflight N90-26468
LOADS (FORCES)
An unsteady lifting surface method for single rotation propellers
[NASA-CR-4302] N90-25940
Strain energy release rate analysis of delamination in a tapered laminate subjected to tension load
[NASA-TM-102592] N90-26076
QM-8 final performance evaluation report: SEALS, volume 4
[NASA-CR-183958] N90-26324
Power saw
[NASA-CASE-MSC-21469-1] N90-26340
Experiment K-6-07. Metabolic and morphologic properties of muscle fibers after spaceflight N90-26481
LOCAL AREA NETWORKS
An automated calibration laboratory for flight research instrumentation: Requirements and a proposed design approach
[NASA-TM-101719] N90-26564
Efficient network topologies for extensible massively parallel computers
[ETN-90-97220] N90-26568
LOCOMOTIVES
Heat engines
[DE90-000485] N90-26393
LOGARITHMS
Converses for write-unidirectional memories
[EUT-89-E-220] N90-26546
LOGIC CIRCUITS
Implementation of an algorithm for travelling-wave-based directional detection
[EUT-89-E-214] N90-26239
On the design and analysis of multiple-storage elements
[AD-A223095] N90-26266
Conception of a reconfigurable microprocessor
[ETN-90-97248] N90-26517
Formal verification of the JANUS on-line multiplier
[IMAG-RR-785-I] N90-26550
LOGIC DESIGN
The bit full-decomposition of sequential machines
[EUT-89-E-223] N90-26516
The full-decomposition of sequential machines with the separate realization of the next-state and output functions
[EUT-89-E-222] N90-26547
MINAS: An algorithm for systematic state assignment of sequential machines: Computational aspects and results
[EUT-89-E-217] N90-26566
LOGIC PROGRAMMING
MINAS: An algorithm for systematic state assignment of sequential machines: Computational aspects and results
[EUT-89-E-217] N90-26566
LOGISTICS
Planning for Space Station Freedom laboratory payload integration
[NASA-CR-186751] N90-26047
LOGISTICS MANAGEMENT
Manufacturing control: A basis for analysis
[PNR90639] N90-26174
LONG DURATION EXPOSURE FACILITY
Proceedings of the LDEF Materials Data Analysis Workshop
[NASA-CP-10046] N90-26075
LONG DURATION SPACE FLIGHT
Effects of microgravity on rat muscle N90-26453
LOOPS
A new scheme for identification and control
[EUT-88-E-213] N90-26586
Mobility studies in multiloop spatial linkages N90-26628
LOSSES
Decay of secondary flow and the associated loss variation downstream of an annual turbine stator cascade
[DE90-505520] N90-25984
LOW MOLECULAR WEIGHTS
Mass spectrometry of poly(methyl methacrylate)s of low molecular weight N90-26091
LOW PRESSURE
A study of the influence of Hg(6(3)P2) population in a low-pressure discharge on mercury ion emission at 194.2 nm N90-26223
LOW REYNOLDS NUMBER
The Screem-J4D: A proposal in response to a low Reynolds number station keeping mission
[NASA-CR-186664] N90-25968
LOW SPEED STABILITY
Low-speed wind tunnel investigation of the static stability and control characteristics of an advanced turboprop configuration with the propellers placed over the tail
[NASA-CR-186900] N90-26017
LOW TEMPERATURE
Infrared line parameters at low temperatures relevant to planetary atmospheres N90-26753
High resolution, low temperature photoabsorption cross-section of C2H2 with application to Saturn's atmosphere N90-26757
Vapor pressures of acetylene at low temperatures N90-26777
LUBRICANTS
A high-speed photography study of cavitation in a dynamically loaded journal bearing
[NASA-TM-103178] N90-26338
LUNAR ATMOSPHERE
Design of a lunar transportation system, volume 2
[NASA-CR-186833-VOL-2] N90-26333
LUNAR BASES
Figure of merit studies of beam power concepts for advanced space exploration
[NASA-CR-186720] N90-26234
Design of an autonomous Lunar construction utility vehicle
[NASA-CR-186832] N90-26330
Design of a lunar transportation system, volume 2
[NASA-CR-186833-VOL-2] N90-26333
Genesis lunar outpost criteria and design
[NASA-CR-186831] N90-26499
LUNAR ENVIRONMENT
Soil experiment
[NASA-CR-184927] N90-26165
LUNAR EXPLORATION
Micro coring apparatus
[NASA-CR-183072] N90-26321
LUNAR FLYING VEHICLES
Design of a lunar transportation system, volume 2
[NASA-CR-186833-VOL-2] N90-26333
LUNAR LANDING SITES
Soil stabilization mat for lunar launch/landing site
[NASA-CR-186690] N90-26128
LUNAR LAUNCH
Soil stabilization mat for lunar launch/landing site
[NASA-CR-186690] N90-26128

LUNAR MANTLE
Proceedings of a workshop on Lunar Volcanic Glasses: Scientific and Resource Potential
[NASA-CR-186631] N90-26437
LUNAR MARIA
Proceedings of a workshop on Lunar Volcanic Glasses: Scientific and Resource Potential
[NASA-CR-186631] N90-26437
LUNAR OBSERVATORIES
Genesis lunar outpost criteria and design
[NASA-CR-186631] N90-26499
LUNAR ROVING VEHICLES
Micro coring apparatus
[NASA-CR-183072] N90-26321
Design of a lunar transportation system, volume 2
[NASA-CR-186833-VOL-2] N90-26333
LUNAR SOIL
Soil stabilization mat for lunar launch/landing site
[NASA-CR-186690] N90-26128
Soil experiment
[NASA-CR-184927] N90-26165
LUNAR SURFACE
Lunar deep drill apparatus
[NASA-CR-182756] N90-26322
Lunar articulated remote transportation system
[NASA-CR-186817-VOL-1] N90-26332
Design of a lunar transportation system, volume 2
[NASA-CR-186833-VOL-2] N90-26333
Megawatt solar power systems for lunar surface operations
[NASA-CR-186509] N90-26391
Proceedings of a workshop on Lunar Volcanic Glasses: Scientific and Resource Potential
[NASA-CR-186631] N90-26437
Genesis lunar outpost criteria and design
[NASA-CR-186631] N90-26499
LUNAR SURFACE VEHICLES
Proof of principle model for a lunar dumptruck
[NASA-CR-182557] N90-26323
Design of an autonomous Lunar construction utility vehicle
[NASA-CR-186832] N90-26330

M

MACHINE LEARNING
Multilayered neural networks: Learning algorithms, implementation on hypercube machines, applications
[ETN-90-97255] N90-26574
MACHINING
Integrating expert systems with solid modeling through interprocess communications and the applications interface specification
[DE90-012996] N90-26537
MAGELLAN PROJECT (NASA)
Space exploration: Cost, schedule, and performance of NASA's Magellan Mission to Venus. Fact sheet for the Chairman, Subcommittee on Science, Technology, and Space, Committee on Commerce, Science, and Transportation, US Senate
[GAO/NSIAD-88-130FS] N90-26022
MAGMA
Proceedings of a workshop on Lunar Volcanic Glasses: Scientific and Resource Potential
[NASA-CR-186631] N90-26437
MAGNETIC BEARINGS
Materials research issues in superconducting levitation and suspension as applied to magnetic bearings
[DE90-011147] N90-26667
MAGNETIC DIPOLES
Experiments on superconductor imaging surface magnetometry
[DE90-008925] N90-26665
MAGNETIC DISKS
Wear mechanisms of amorphous carbon and zirconia coatings on rigid disk magnetic recording media
[DE90-011053] N90-26133
MAGNETIC ENERGY STORAGE
Parametric design studies of toroidal magnetic energy storage units
[DE90-013086] N90-26390
MAGNETIC FIELD RECONNECTION
On the nature of the plasma sheet boundary layer
[DE90-013158] N90-26439
MAGNETIC FIELDS
Space exploration: Cost, schedule, and performance of NASA's Galileo Mission to Jupiter. Fact sheet for the Chairman, Subcommittee on Science, Technology, and Space, Committee on Commerce, Science, and Transportation, US Senate
[GAO/NSIAD-88-138FS] N90-26025
Confinement of nonneutral plasma in unconventional geometries
[DE90-013048] N90-26659
Characterization of NbTi multifilamentary superconducting wires
[DE90-626245] N90-26672
MAGNETIC FLUX
Materials research issues in superconducting levitation and suspension as applied to magnetic bearings
[DE90-011147] N90-26667
MAGNETIC MEASUREMENT
Experiments on superconductor imaging surface magnetometry
[DE90-008925] N90-26665
MAGNETIC PERMEABILITY
Searching for heavy fermion materials in Ce intermetallic compounds
[DE90-011809] N90-26116
MAGNETIC RECORDING
Wear mechanisms of amorphous carbon and zirconia coatings on rigid disk magnetic recording media
[DE90-011053] N90-26133
MAGNETIC STORAGE
Space operations: NASA is not properly safeguarding valuable data from past missions
[GAO/IMTEC-90-1] N90-26704
MAGNETIC SUSPENSION
Materials research issues in superconducting levitation and suspension as applied to magnetic bearings
[DE90-011147] N90-26667
MAGNETIC TAPES
Space operations: NASA is not properly safeguarding valuable data from past missions
[GAO/IMTEC-90-1] N90-26704
MAGNETO-OPTICS
Polymeric aluminasilazane precursors for aluminosilicon nitride
[AD-A222755] N90-26158
MAGNETOMETERS
Experiments on superconductor imaging surface magnetometry
[DE90-008925] N90-26665
MAINTAINABILITY
Design and construction of a wall-climbing robot
[NIAR-90-20] N90-26327
MAINTENANCE
OASIS, LLNL version: Software maintenance manual
[DE90-013522] N90-26313
MALES
Human performance in cockpit-related systems
[NIAR-90-7] N90-26495
MAN ENVIRONMENT INTERACTIONS
Measurements of tropospheric nitric acid over the Western United States and Northeastern Pacific Ocean
[NASA-TM-103470] N90-26399
MAN MACHINE SYSTEMS
Qualitative evaluation of a conformal velocity vector display for use at high angles-of-attack in fighter aircraft
[NASA-TM-102629] N90-25981
Human performance models
[FFI-90/7002] N90-26502
Psychophysiological assessment of pilot workload in an applied setting
[AD-A222707] N90-26507
MAN-COMPUTER INTERFACE
VISTA (Vertical Integration of Science, Technology, and Applications) user interface software study
[DE90-010003] N90-26707
MANAGEMENT INFORMATION SYSTEMS
NASA project status reports: Congressional requirements can be met, but reliability must be ensured
[GAO/NSIAD-90-40] N90-26169
The value of real experience
[PNR90619] N90-26696
Prototyping an in-house business intelligence database
[PNR90665] N90-26709
MANAGEMENT METHODS
The value of real experience
[PNR90619] N90-26696
MANAGEMENT PLANNING
Making it happen: Project management
[PNR90618] N90-26695
The value of real experience
[PNR90619] N90-26696
MANAGEMENT SYSTEMS
Making real-time reactive systems reliable
[NASA-CR-186642] N90-26344
MANEUVERABILITY
Identification of aerodynamic models for maneuvering aircraft
[NASA-CR-186630] N90-25943
MANEUVERS
Identification of aerodynamic models for maneuvering aircraft
[NASA-CR-186630] N90-25943
Maneuvering by means of lateral jets
[ISL-CO-255/88] N90-26015
MANGANESE
The effect of manganese on the onset of the stage 2 reaction in an austempered ductile iron matrix
[DE90-011804] N90-26119
MANIPULATORS
Control strategy for cooperating disparate manipulators
[NASA-CR-186809] N90-26328
An inverse dynamic method yielding flexible manipulator state trajectories
[NASA-CR-186807] N90-26329
Space station definitions, design, and development. Task 5: Multiple arm telerobot coordination and control: Manipulator design methodology
[NASA-CR-182043] N90-26577
Position control of redundant manipulators using an adaptive error-based control scheme
[NASA-CR-186812] N90-26578
Beam rider for an Articulated Robot Manipulator (ARM) accurate positioning of long flexible manipulators
[NASA-CR-185151] N90-26581
MANNED MARS MISSIONS
Project Exodus
[NASA-CR-186836] N90-26026
Terrapin technologies manned Mars mission proposal
[NASA-CR-186838] N90-26027
The effect of interplanetary trajectory options on a manned Mars aerobrake configuration
[NASA-TP-3019] N90-26036
Possible applications of tethered systems to Mars exploration missions
[IAF-89-489] N90-26060
MANNED SPACECRAFT
The astronauts' legal status: The International Space Station N90-26721
MANPOWER
A measurement of the effectiveness of the Airway Science Program to meet Federal Aviation Administration work force needs
[NIAR-90-5] N90-26694
MANUALS
Launching a dream: A teachers guide to a simulated space shuttle mission
[NASA-TM-89715] N90-26693
MANUFACTURING
Towards 2000: The composite engine
[PNR90646] N90-26000
Influence of the manufacturing conditions on the microstructure and mechanical properties of the silicon nitride
[ISAL-90-0008] N90-26154
Computer simulation of gear tooth manufacturing processes
[NASA-CR-185200] N90-26171
Manufacturing control: A basis for analysis
[PNR90639] N90-26174
NDT in aerospace: The next decade (1990's)
[PNR90628] N90-26348
Conception of a reconfigurable microprocessor
[ETN-90-97248] N90-26517
MANY BODY PROBLEM
Molecular interactions and properties with many-body methods
[AD-A222631] N90-26642
MAPPING
Automatic line network extraction from aerial imagery of urban areas through knowledge based image analysis
[AD-A222675] N90-26385
Converses for write-unidirectional memories
[EUT-89-E-220] N90-26546
MARINE ENVIRONMENTS
Mariners Weather Log, volume 33, number 2, Spring 1989
[PB90-146838] N90-26443
Mariners Weather Log, volume 33, number 3, Summer 1989
[PB90-146846] N90-26444
Mariners Weather Log, volume 33, number 4, Fall 1989
[PB90-146853] N90-26445
MARKERS
Experiment K-6-18. Study of muscarinic and gaba (benzodiazepine) receptors in the sensory-motor cortex, hippcampus and spinal code N90-26471
MARS (PLANET)
Greenhouse design for a Martian colony: Structural, solar collection and light distribution systems
[NASA-CR-186818] N90-26501
Press abstracts of the 21st Lunar and Planetary Science Conference
[NASA-CR-186874] N90-26738

MARS ATMOSPHERE
Space exploration: Cost, schedule, and performance of NASA's Mars Observer Mission. Fact sheet for the Chairman, Subcommittee on Science, Technology, and Space, Committee on Commerce, Science, and Transportation, US Senate
[GAO/NSIAD-88-137FS] N90-26021
Mars in situ propellants: Carbon monoxide and oxygen ignition experiments
[NASA-TM-103202] N90-26065
The chemical effects of the Martian environment on power system component materials: A theoretical approach
[NASA-TM-103203] N90-26074
Infrared spectra of van de Waals complexes of importance in planetary atmospheres N90-26749

MARS ENVIRONMENT
Space exploration: Cost, schedule, and performance of NASA's Mars Observer Mission. Fact sheet for the Chairman, Subcommittee on Science, Technology, and Space, Committee on Commerce, Science, and Transportation, US Senate
[GAO/NSIAD-88-137FS] N90-26021

MARS OBSERVER
Space exploration: Cost, schedule, and performance of NASA's Mars Observer Mission. Fact sheet for the Chairman, Subcommittee on Science, Technology, and Space, Committee on Commerce, Science, and Transportation, US Senate
[GAO/NSIAD-88-137FS] N90-26021

MARS SURFACE
Space exploration: Cost, schedule, and performance of NASA's Mars Observer Mission. Fact sheet for the Chairman, Subcommittee on Science, Technology, and Space, Committee on Commerce, Science, and Transportation, US Senate
[GAO/NSIAD-88-137FS] N90-26021
Terrapin technologies manned Mars mission proposal
[NASA-CR-186838] N90-26027
Aeolian removal of dust from radiator surfaces on Mars
[NASA-TM-103205] N90-26068
The chemical effects of the Martian environment on power system component materials: A theoretical approach
[NASA-TM-103203] N90-26074
Analysis of a Mars-stationary orbiting microwave power transmission system
[NASA-TM-101344] N90-26172
University of Maryland walking robot: A design project for undergraduate students
[NASA-CR-186839] N90-26331
Autoplan: A self-processing network model for an extended blocks world planning environment
[NASA-CR-186733] N90-26526
Press abstracts of the 21st Lunar and Planetary Science Conference
[NASA-CR-186874] N90-26738

MARTENSITE
Twin boundaries, interfaces and modulated structures in martensites
[DE90-012899] N90-26111

MASS SPECTRA
Study of the polyoxymethylene and its sputtered fragments: Implications for comets N90-26781

MASS SPECTROSCOPY
Mass spectrometry of poly(methyl methacrylate)s of low molecular weight N90-26091

MASS TRANSFER
Photon sputtering of H2O ices: A preliminary report N90-26783

MASSIVELY PARALLEL PROCESSORS
Efficient network topologies for extensible massively parallel computers
[ETN-90-97220] N90-26568
Massively parallel architecture: Integrated cell network for image reconstruction
[ETN-90-97257] N90-26575

MATCHED FILTERS
Laser radar angular tracking
[AD-A222741] N90-26319

MATHEMATICAL LOGIC
Formal verification of distributed computing systems: Logic characterization of behaviour equivalence
[LAAS-89386] N90-26555

MATHEMATICAL MODELS
Aerodynamic loads and blade vortex interaction noise prediction
[ISL-PU-310/89] N90-25942
The applicability of simple helicopter models for flight mechanics studies
[ETN-90-96962] N90-25975
Agusta methodology for pitch link loads prediction in preliminary design phase
[ETN-90-97270] N90-25978
Performance of a supercharged direct-injection stratified-charge rotary combustion engine
[NASA-TM-103105] N90-25982
Subsonic combustor flow modeling: State of the art of CFD techniques for reacting and combusting flow N90-25991
Turbulent combustion modeling for turbo-jet combustion chambers N90-25993
Background, current status, and prognosis of the ongoing slush hydrogen technology development program for the NASP
[NASA-TM-103220] N90-26055
The origin of poorly conditioned susceptibility matrix within inverse CVM algorithm in the case of Pd(sub 3)V: A comparison to the case of Ni(sub 3)V
[DE90-012464] N90-26110
Extension of a noninteractive reliability model for ceramic matrix composites
[NASA-CR-185267] N90-26142
Modelling of the processing of incompatible polymer blends
[ETN-90-97211] N90-26152
Simulated dynamic response of a servovalve controlled hydraulic actuator
[NASA-TM-101644] N90-26167
Optimal synchronization of spread spectrum sequenced by nontransferable switching operators N90-26183
Radio channel measurement and modelling for future mobile radio systems N90-26184
Long-range planning cost model for support of future space missions by the deep space network N90-26231
Validity domain of the scalar Kirchhoff and Rayleigh-Sommerfeld diffraction theories in the near field of small phase objects: Comparison between calculation models and microwave measure
[ETN-90-96963] N90-26236
A model of the synchronous machine with rectifier, especially for control purposes
[EUT-89-E-215] N90-26256
A possibility to incorporate saturation in the simple, global model of a synchronous machine with rectifier
[EUT-89-E-225] N90-26258
An investigation into the numerical prediction of boundary layer transition using the K.Y. Chien turbulence model
[NASA-CR-185252] N90-26269
A numerical simulation of the quasi-heterodyne technique for double-pulsed holographic vibration measurements
[PNR90622] N90-26301
An inverse dynamic method yielding flexible manipulator state trajectories
[NASA-CR-186807] N90-26329
Application of symbolic computations to the constitutive modeling of structural materials
[NASA-TM-103225] N90-26364
Fatigue life assessment using a short crack growth model
[PNR90663] N90-26367
Investigation of crack-closure prediction models for fatigue in aluminium alloy sheet under flight-simulation loading
[LR-619] N90-26369
Modeling, simulation, and analysis of optical remote sensing systems
[NASA-CR-186648] N90-26376
Measuring and modeling near-surface reflected and emitted radiation fluxes at the FIFE site
[NASA-CR-180953] N90-26378
Nordic Symposium on Atmospheric Chemistry
[CM-78] N90-26403
Adjustment and validation of the mathematical prediction model for sweat rate, heart rate, and body temperature under outdoor conditions
[AD-A222599] N90-26486
Human performance models
[FFI-90/7002] N90-26502
A computer module used to calculate the horizontal control surface size of a conceptual aircraft design
[NASA-CR-186872] N90-26515
H-infinity control: An exploratory study
[EUT-88-E-211] N90-26584
On central-difference and upwind schemes
[NASA-CR-182061] N90-26595
Combinatorial problems using a hypercube and Hamming graphs
[ETN-90-97240] N90-26609
Nonlinear modeling of time series using Multivariate Adaptive Regression Splines (MARS)
[AD-A222710] N90-26623
Reversed residuals in autoregressive time series analysis
[AD-A222711] N90-26624
Evaluation of a decomposition approach for real-time scheduling using a Stochastic model
[AD-A222726] N90-26625
Application and extension of an analytical model of the confined acoustic beam generated by a transducer
[AD-A222994] N90-26639
An embedded fibre optic sensor for impact damage detection in composite materials
[UTIAS-332] N90-26650
Dielectric function of InGaAs in the visible
[NASA-TM-103246] N90-26683
A lattice gas model for thermohydrodynamics
[DE90-011964] N90-26690
Laboratory studies, analysis, and interpretation of the spectra of hydrocarbons present in planetary atmospheres including cyanoacetylene, acetylene, propane, and ethane N90-26748
Laboratory measurements and modeling of microwave absorption by ammonia in gas mixtures applicable to giant planet atmospheres N90-26750
Laboratory measurements and methane photochemistry modeling N90-26770
Investigation of the Saturn dust environment from the analysis of energetic charged particle measurements
[NASA-CR-186727] N90-26784

MATHEMATICS
Computer animation in mathematics, science, and art
[DE90-013051] N90-26538

MATRICES (CIRCUITS)
High speed magneto-resistive random access memory
[NASA-CASE-NPO-17954-1-CU] N90-26519

MATRICES (MATHEMATICS)
On output deadbeat control of discrete-time multivariable systems
[MATHS-REPT-A-122] N90-26583
The system matrix characterisation of input-output equivalence
[MATHS-REPT-A-112] N90-26600
Rational cubics with G2-continuity
[MATHS-REPT-A-113] N90-26601
Large sets of block designs
[ETN-90-97212] N90-26602
Mobility studies in multiloop spatial linkages N90-26628

MATRIX MATERIALS
The effect of interfacial characteristics on the mechanical performance of ceramic-ceramic composites
[AD-A223031] N90-26090

MAXIMA
MINAS: An algorithm for systematic state assignment of sequential machines: Computational aspects and results
[EUT-89-E-217] N90-26566

MAXIMUM LIKELIHOOD ESTIMATES
A hybrid M-algorithm/sequential decoder for convolutional and trellis codes
[NASA-CR-186863] N90-26528
Estimating the parameters of a sporadically observed queue
[DE90-012903] N90-26596

MEASURING INSTRUMENTS
Electric field strength meters for the HF, VHF, and UHF bands
[BBC-RD-1990/3] N90-26212
Qualification of concentrating mirror systems with the HERMES measurement system and the HELIOS simulation program
[DLR-FB-89-51] N90-26394

MECHANICAL DEVICES
Alignment positioning mechanism
[NASA-CASE-MSC-21502-1] N90-26341

MECHANICAL PROPERTIES
Probabilistic approach to the certification for fatigue durability of composite structures
[DE90-505521] N90-26085
The effect of interfacial characteristics on the mechanical performance of ceramic-ceramic composites
[AD-A223031] N90-26090
Structures and mechanical properties of near-beta titanium alloys TiV10Fe2Al3 and TiV10Cu3Al3
[ONERA-NT-1989-3] N90-26123
Mechanical properties of coatings and interfaces
[DE90-012726] N90-26139
Extension of a noninteractive reliability model for ceramic matrix composites
[NASA-CR-185267] N90-26142
Influence of the manufacturing conditions on the microstructure and mechanical properties of the silicon nitride
[ISAL-90-0008] N90-26154
Soil experiment
[NASA-CR-184927] N90-26165
Design of ceramic components with the NASA/CARES computer program
[NASA-TM-102369] N90-26359

MECHANIZATION
Technical evaluation report on the Guidance and Control Panel 49th Symposium on Fault Tolerant Design Concepts for Highly Integrated Flight Critical Guidance and Control Systems
[AGARD-AR-281] N90-26012
MEDICAL PERSONNEL
Arctic cold weather medicine and accidental hypothermia
[AD-A223090] N90-26487
MEDICAL SERVICES
Arctic cold weather medicine and accidental hypothermia
[AD-A223090] N90-26487
MELTING
Natural melting within a spherical shell
[NASA-TM-102822] N90-26274
MELTS (CRYSTAL GROWTH)
Mathematical simulation of heat exchanges and thermoelastic constraints in Czochralski crystal growth
[ETN-90-97242] N90-26680
MEMBRANES
Development of membrane process for carbon dioxide separation from diving atmosphere
[AD-A222606] N90-26504
MEMORY
The retrieval of information from secondary memory: A review and new findings
[AD-A222760] N90-26489
MEMORY (COMPUTERS)
Computer architecture evaluation for structural dynamics computations: Project summary
[NASA-CR-186137] N90-26512
Atomic snapshots of shared memory
[AD-A222765] N90-26520
Capacity for patterns and sequences in Kanerva's SDM as compared to other associative memory models
[NASA-CR-180701] N90-26522
Converses for write-unidirectional memories
[EUT-89-E-220] N90-26546
Single-pass memory system evaluation for multiprogramming workloads
[NASA-CR-186553] N90-26558
PANDA: A distributed multiprocessor operating system N90-26561
MENTAL PERFORMANCE
Human performance in cockpit-related systems
[NIAR-90-7] N90-26495
MERCURY (METAL)
A study of the influence of Hg(6(3)P2) population in a low-pressure discharge on mercury ion emission at 194.2 nm N90-26223
The transfer of mercury between the atmosphere and lake or soil surfaces N90-26419
The aqueous atmospheric chemistry of mercury N90-26420
MESONS
A beauty factory using an SRF linac and a storage ring
[CEBAF-PR-89-017] N90-26644
MESOSPHERE
Photodissociation of O2 in the stratosphere and mesosphere: A general parametrization of the Schumman-Runge Bands N90-26427
MESSAGE PROCESSING
CORA: A direct sequence spread spectrum radio for voice and data N90-26195
Synchronization of frequency shift transmission and the effect of oversampling N90-26200
New approaches for rapid synchronisation frequency hoppers N90-26201
MTP: An atomic multicast transport protocol
[NASA-CR-186716] N90-26254
Knowledge and inhibition in asynchronous distributed systems
[TR-90-1139] N90-26703
MESSAGES
PANDA: A distributed multiprocessor operating system N90-26561
METABOLISM
Experiment K-6-07. Metabolic and morphologic properties of muscle fibers after spaceflight N90-26461
Experiment K-6-08. Biochemical and histochemical observations of vastus medialis N90-26462
Experiment K-6-21. Effect of microgravity on 1) metabolic enzymes of type 1 and type 2 muscle fibers and on 2) metabolic enzymes, neutransmitter amino acids, and neurotransmitter associated enzymes in motor and somatosensory cerebral cortex. Part 1: Metabolic enzymes of individual muscle fibers; part 2: metabolic enzymes of hippocampus and spinal cord N90-26474
METAL FATIGUE
A study of the fatigue behavior in scratched samples of Al-Li alloy (2090-T3)
[IAR-89-24] N90-26107
METAL FOILS
Analysis of strain relaxation in Au/Ni multilayers by x ray diffraction
[IAR-89-25] N90-26357
METAL IONS
A study of the influence of Hg(6(3)P2) population in a low-pressure discharge on mercury ion emission at 194.2 nm N90-26223
METAL MATRIX COMPOSITES
Towards 2000: The composite engine
[PNR90646] N90-26000
The influence of microstructure on the tensile behavior of an aluminum metal matrix composite
[NASA-TM-102694] N90-26082
Metal matrix composites and powder processing for aero-engine applications
[PNR90617] N90-26087
Investigation of thermo-mechanical effects in silicon carbide Whisker/Al alloy composites
[AD-A222635] N90-26089
METAL OXIDE SEMICONDUCTORS
Role of surface passivation in the integrated processing of MOS structures
[AD-A222630] N90-26264
METAL PLATES
Buckling and postbuckling behavior of square compression-loaded graphite-epoxy plates with circular cutouts
[NASA-TP-3007] N90-26077
A comparison of the post-buckling behavior of metallic and composite plates with centrally located cutouts
[NIAR-90-14] N90-26356
METAL SHEETS
Fracture toughness and failure mechanisms in commercial 2091 Al-Li sheet at cryogenic temperatures
[AD-A222803] N90-26125
METAL SURFACES
Erosion mechanisms in composite materials and ripple formation mechanism in erosion
[IAR-89-4-PT-2] N90-26079
Exact results for the structured liquid-solid interface
[AD-A222762] N90-26630
Structure and dynamics of water at the Pt(111) interface: Molecular dynamics study
[AD-A222628] N90-26687
METALLIZING
Resistivity, adhesive strength, and residual stress measurements of thin film metallizations on single crystal quartz
[DE90-011902] N90-26135
METALLOGRAPHY
Damping capacity of aluminum 6061-indium alloys
[AD-A222802] N90-26124
METASTABLE STATE
A study of the influence of Hg(6(3)P2) population in a low-pressure discharge on mercury ion emission at 194.2 nm N90-26223
METEOR TRAILS
Experimentation of a transmission system data processing by meteor bursts N90-26207
METEORITES
Proceedings of a Workshop on Antarctic Meteorite Stranding Surfaces
[NASA-CR-186575] N90-26739
Proceedings of a workshop on Differences Between Antarctic and Non-Antarctic Meteorites
[NASA-CR-184918] N90-26740
METEORITIC COMPOSITION
Press abstracts of the 21st Lunar and Planetary Science Conference
[NASA-CR-186874] N90-26738
METEOROID CONCENTRATION
Proceedings of a workshop on Differences Between Antarctic and Non-Antarctic Meteorites
[NASA-CR-184918] N90-26740
METEOROID SHOWERS
A digital Meteor-Burst Communication (MBC) propagation path simulator N90-26190
METEOROLOGICAL RADAR
Analysis and improved design considerations for airborne pulse Doppler radar signal processing in the detection of hazardous windshear
[NASA-CR-186792] N90-26448
METEOROLOGICAL SERVICES
Some results from the precipitation chemistry measurement programme in Sweden N90-26410
METHANE
Measurements of CH4, N2O, CO, H2O and O3 in the middle atmosphere by the ATMOS experiment on Spacelab 3
[NASA-TM-103476] N90-26400
Laboratory studies, analysis, and interpretation of the spectra of hydrocarbons present in planetary atmospheres including cyanoacetylene, acetylene, propane, and ethane N90-26748
Gaussian quadrature exponential sum modeling of near infrared methane laboratory spectra obtained at temperatures from 106 to 297 K N90-26758
Measurements of the methane relaxation times for application to the infrared emission models of the upper atmospheres of outer planets and Titan N90-26759
Methane overtone absorption by intracavity laser spectroscopy N90-26762
Laboratory measurements and methane photochemistry modeling N90-26770
Optical constants of solid methane N90-26775
METHYL COMPOUNDS
Mass spectrometry of poly(methyl methacrylate)s of low molecular weight N90-26091
METHYLENE
Dynamics of micellar oligomeric and monomeric sodium 10-undecenoate
[AD-A222570] N90-26099
Role of the methylene amidogen (H2CN) radical in the atmospheres of Titan and Jupiter N90-26769
METRIC SPACE
Predissimilarities, prefilters, and ultrametrics on an arbitrary set
[IMAG-RR-970-M] N90-26603
MICROCOMPUTERS
Practical applications of remote sensing technology
[NASA-CR-186810] N90-26377
MICROCRACKS
A study of the fatigue behavior in scratched samples of Al-Li alloy (2090-T3)
[IAR-89-24] N90-26107
Effect of boron on intergranular hot cracking in Ni-Cr-Fe superalloys containing niobium
[NASA-CR-186714] N90-26115
Small crack growth and its influence in near alpha-titanium alloys
[RAE-TM-P-1171] N90-26121
MICROELECTRONICS
Multiple target tracking in a wide-field-of-view camera system
[DE90-013488] N90-26300
MICROPROCESSORS
Conception of a reconfigurable microprocessor
[ETN-90-97248] N90-26517
Level-2 system: Programmers-users manual
[DE90-013324] N90-26540
MICROSTRUCTURE
Application of high performance metals in gas turbine engines
[PNR90640] N90-25999
The influence of microstructure on the tensile behavior of an aluminum metal matrix composite
[NASA-TM-102694] N90-26082
Investigation of thermo-mechanical effects in silicon carbide Whisker/Al alloy composites
[AD-A222635] N90-26089
Hydrogen induced fracture characteristics of single crystal nickel-based superalloys
[NASA-CR-183992] N90-26108
Microstructural dependence of the cavitation damage function in FCC materials
[DE90-012898] N90-26113
Microstructural design for fatigue crack growth resistance in Ni-base alloy
[PNR90632] N90-26120
Structures and mechanical properties of near-beta titanium alloys TiV10Fe2Al3 and TiV10Cu3Al3
[ONERA-NT-1989-3] N90-26123
Influence of the manufacturing conditions on the microstructure and mechanical properties of the silicon nitride
[ISAL-90-0008] N90-26154
DoD-University research instrumentation program, FY 1986/FY 1987
[AD-A222578] N90-26263
Critical current density, flux creep, and microstructure in a Bi-Sr-Ca-Cu-O system
[DE90-010457] N90-26676
MICROWAVE ANTENNAS
Design of an optically controlled Ka-band GaAs MMIC phased-array antenna
[NASA-TM-103147] N90-26250
MICROWAVE ATTENUATION
Laboratory measurements and modeling of microwave absorption by ammonia in gas mixtures applicable to giant planet atmospheres N90-26750
MICROWAVE POWER BEAMING
Analysis of a Mars-stationary orbiting microwave power transmission system
[NASA-TM-101344] N90-26172
MICROWAVE RADIOMETERS
Spatial cross-correlation of Antarctic Sea ice and seabed topography
[NASA-CR-186815] N90-26451

MICROWAVE SPECTRA
Laboratory measurements and modeling of microwave absorption by ammonia in gas mixtures applicable to giant planet atmospheres N90-26750
Microwave spectra of van der Waals complexes of importance in planetary atmospheres N90-26752
MICROWAVES
In-band amplitude dispersion on a microwave link N90-26189
Laboratory measurements of microwave and millimeter-wave properties of planetary constituents N90-26745
High resolution spectroscopy in the microwave and far infrared N90-26746
MIDDLE ATMOSPHERE
Measurements of CH4, N2O, CO, H2O and O3 in the middle atmosphere by the ATMOS experiment on Spacelab 3
[NASA-TM-103476] N90-26400
The NASA/MSFC Global Reference Atmospheric Model, 1990 version (GRAM-90)
[NASA-CR-186717] N90-26435
MILITARY OPERATIONS
ASATs vs Brilliant Pebbles
[DE90-010348] N90-26626
MILLIMETER WAVES
Figure of merit studies of beam power concepts for advanced space exploration
[NASA-CR-186720] N90-26234
Submillimeter and millimeter observations of solar system objects
[NASA-CR-186636] N90-26731
Laboratory measurements of microwave and millimeter-wave properties of planetary constituents N90-26745
MIMD (COMPUTERS)
The use of Lanczo's method to solve the large generalized symmetric Eigenvalue problem in parallel
[NASA-CR-182072] N90-26533
MINERALOGY
Proceedings of a workshop on Differences Between Antarctic and Non-Antarctic Meteorites
[NASA-CR-184918] N90-26740
MINERALS
Experiment K-6-01. Distribution and biochemistry of mineral and matrix in the femurs of rats N90-26455
MINIATURIZATION
Twilight zones and cornerstones: A gnat robot double feature
[AD-A220026] N90-26326
MINORITY CARRIERS
Estimation of minority carrier diffusion lengths in InP/GaAs solar cells
[NASA-TM-103213] N90-26069
MIR SPACE STATION
Technical characteristics and functions of different types of space stations N90-26712
MIR: A Soviet Space Station. Some legal aspects of international cooperation N90-26715
MIRRORS
Qualification of concentrating mirror systems with the HERMES measurement system and the HELIOS simulation program
[DLR-FB-89-51] N90-26394
MISALIGNMENT
Alignment positioning mechanism
[NASA-CASE-MSC-21502-1] N90-26341
MISSILE CONFIGURATIONS
The role of computational fluids dynamics in missile aerodynamics
[NLR-MP-88072-U] N90-25952
MISSILE SYSTEMS
Computational fluid dynamics for missiles
[RAE-TM-AERO-2171] N90-26288
MISSION PLANNING
Space exploration: Cost, schedule, and performance of NASA's Mars Observer Mission. Fact sheet for the Chairman, Subcommittee on Science, Technology, and Space, Committee on Commerce, Science, and Transportation, US Senate
[GAO/NSIAD-88-137FS] N90-26021
Terrapin technologies manned Mars mission proposal
[NASA-CR-186838] N90-26027
Biconic cargo return vehicle with an advanced recovery system. Volume 1: Conceptual design
[NASA-CR-186520] N90-26052
Applications of different design methodologies in navigation systems and development at JPL N90-26221
Launching a dream: A teachers guide to a simulated space shuttle mission
[NASA-TM-89715] N90-26693
The lessons of Varsovian's reconnaissance
[NASA-TM-103207] N90-26789
MITOSIS
Experiment K-6-17. Structural changes and cell turnover in the rats small intestine induced by spaceflight N90-26470
MIXING
Formation of Titanium-boron surface alloys by excimer laser mixing
[DE90-013172] N90-26118
MIXING LAYERS (FLUIDS)
Supersonic combustor modeling N90-25992
MIXTURES
Heat engines
[DE90-000485] N90-26393
MOBILE COMMUNICATION SYSTEMS
Broadband analysis of ground wave propagation at a50 to 400 MHz N90-26185
Measurement and simulation of widespread mobile radio channel characteristics N90-26186
Packet radio network concepts for the Norwegian field army N90-26206
Mobile satellite communications for civil aviation
[NLR-MP-88066-U] N90-26238
MOBILITY
Mobility studies in multiloop spatial linkages N90-26628
MODEL REFERENCE ADAPTIVE CONTROL
Position control of redundant manipulators using an adaptive error-based control scheme
[NASA-CR-186812] N90-26578
MODELS
Space plane model for visual measurement of aerodynamic heating
[DE90-505514] N90-25949
H-infinity based integrated flight-propulsion control design for a STOVL aircraft in transition flight
[NASA-TM-103198] N90-26011
MODEMS
An experimental medium speed wideband modem N90-26194
MOISTURE CONTENT
Implementation of sensor and control designs for bioregenerative systems
[NASA-CR-186655] N90-26479
MOLDS
Understanding silica binders
[PNR90625] N90-26150
CAD/CAM reinforces the competitive edge of European mouldmakers
[CRIF-MC-88] N90-26542
MOLECULAR ABSORPTION
Chemical structure and kinetics at liquid/solid interfaces
[AD-A222766] N90-26105
MOLECULAR BEAM EPITAXY
Dielectric function of InGaAs in the visible
[NASA-TM-103246] N90-26683
MBE growth technology for high quality strained III-V layers
[NASA-CASE-NPO-17723-1-CU] N90-26685
MOLECULAR BIOLOGY
Photosynthesis in intact plants
[DE90-013699] N90-26482
MOLECULAR COLLISIONS
Rotational and translational effects in collisions of electronically excited diatomic hydrides
[NASA-CR-186770] N90-26093
MOLECULAR GASES
Digital filtering of plume emission spectra
[NASA-TM-103135] N90-26070
Absolute vacuum ultraviolet photoabsorption cross section studies of atomic and molecular species: Techniques and observational data N90-26754
A laboratory investigation of the production and properties of molecular and radical species pertinent to planetary atmospheres N90-26766
Optical signatures of molecular particles via mass-selected cluster spectroscopy N90-26780
MOLECULAR INTERACTIONS
Molecular interactions and properties with many-body methods
[AD-A222631] N90-26642
MOLECULAR IONS
Dissociative recombination of molecular ions with electrons N90-26767
MOLECULAR RELAXATION
Dynamics of micellar oligomeric and monomeric sodium 10-undecenoate
[AD-A222570] N90-26099
Infrared spectra of van de Waals complexes of importance in planetary atmospheres N90-26749
Measurements of the methane relaxation times for application to the infrared emission models of the upper atmospheres of outer planets and Titan N90-26759
MOLECULAR SPECTROSCOPY
Imaging and spectroscopy of small molecules by scanning tunneling microscopy
[AD-A222572] N90-26641
Determination of molecular spectroscopic parameters and energy-transfer rates by double-resonance spectroscopy N90-26755
New electronic states of NH and ND observed by resonance enhanced multiphoton ionization spectroscopy N90-26760
MOLECULAR STRUCTURE
Chemical structure and kinetics at liquid/solid interfaces
[AD-A222766] N90-26105
Molecular structure of interphases between DGEBA/BTDA adhesives and silver substances using surface-enhanced Raman scattering
[AD-A222750] N90-26157
Photosynthesis in intact plants
[DE90-013699] N90-26482
Computer simulation of chemical reactions in synthetic model compounds and genetically engineered active sites
[AD-A222611] N90-26483
Isothermal compressibility of SPC/E water
[AD-A222723] N90-26643
MOLECULAR WEIGHT
Evolution of structure and viscoelasticity in diethanolamine-cured epoxy
[DE90-011256] N90-26134
MOLECULES
Isothermal compressibility of SPC/E water
[AD-A222723] N90-26643
Stibathiolanes: Synthesis, solid state structure, and solution behavior
[AD-A223255] N90-26688
High resolution infrared spectroscopy of planetary molecules using diode lasers and Fourier transform spectrometers N90-26747
Recent high resolution laboratory determinations of line broadening and intensity parameters: PH3, CH3D, and CO2 N90-26751
Infrared line parameters at low temperatures relevant to planetary atmospheres N90-26753
Intracavity Dye-Laser Absorption Spectroscopy (IDLAS) for application to planetary molecules N90-26761
UV and VUV spectroscopy and photochemistry of small molecules in a supersonic jet N90-26771
MOLTEN SALT ELECTROLYTES
Evaluation of room-temperature chloroaluminate molten salts as electrolytes for high energy density batteries
[AD-A223097] N90-26267
MOMENTUM TRANSFER
Fluid-loop reaction system
[NASA-CASE-NPO-17204-1-CU] N90-26292
MONITORS
Lunar deep drill apparatus
[NASA-CR-182756] N90-26322
Eye tracking device for the measurement of flight performance in simulators
[AD-A220075] N90-26484
MONKEYS
Experiment K-6-27. Analysis of radiographs and biosamples from primate studies N90-26478
MONOMERS
Dynamics of micellar oligomeric and monomeric sodium 10-undecenoate
[AD-A222570] N90-26099
Condensation polyimides
[NASA-TM-103467] N90-26129
Quantitative confirmation of diffusion-limited oxidation theories
[DE90-012997] N90-26143
MOON
Proceedings of a workshop on Lunar Volcanic Glasses: Scientific and Resource Potential
[NASA-CR-186631] N90-26437
MORALE
Aviation safety: Conditions within the air traffic control work force. Fact sheet for congressional requesters
[GAO/RCED-89-113FS] N90-25958
MORPHOLOGY
Erosion mechanisms in composite materials and ripple formation mechanism in erosion
[IAR-89-4-PT-1] N90-26078
Experiment K-6-02. Biomedical, biochemical and morphological alterations of muscle and dense, fibrous connective tissues during 14 days of spaceflight N90-26456
Experiment K-6-03. Gravity and skeletal growth, part 1. Part 2: Morphology and histochemistry of bone cells and vasculature of the tibia; Part 3: Nuclear volume analysis of osteoblast histogenesis in periodontal ligament cells; Part 4: Intervertebral disc swelling pressure associated with microgravity N90-26457

Experiment K-6-06. Morphometric and EM analyses of tibial epiphyseal plates from Cosmos 1887 rats N90-26460
Experiment K-6-08. Biochemical and histochemical observations of vastus medialis N90-26462
Experiment K-6-09. Morphological and biochemical investigation of microgravity-induced nerve and muscle breakdown. Part 1: Investigation of nerve and muscle breakdown during spaceflight; Part 2: Biochemical analysis of EDL and PLT muscles N90-26463
Experiment K-6-12. Morphometric studies of atrial or granules and hepatocytes. Part 1: Morphometric study of the liver; Part 2: The atrial granular accumulations N90-26466
Experiment K-6-13. Morphological and biochemical examination of heart tissue. Part 1: Effects of microgravity on the myocardial fine structure of rats flown on Cosmos 1887. Ultrastructure studies. Part 2: Cellular distribution of cyclic ampdependent protein kinase regulatory subunits in heart muscle of rats flown on Cosmos 1887 N90-26467
Experiment K-6-16. Morphological examination of rat testes. The effect of Cosmos 1887 flight on spermatogonial population and testosterone level in rat testes N90-26469

MOSSBAUER EFFECT
SDIO/IST ultrashort wavelength laser: Novel experimental schemes for observing the Moessbauer effect in long-lived nuclear levels and nuclear coherent states [AD-A222607] N90-26316

MOTION PICTURES
Computer animation in mathematics, science, and art [DE90-013051] N90-26538

MOTION SICKNESS
Motion sickness, visual displays, and armored vehicle design [AD-A222678] N90-26506

MOUNTING
Vibration test procedures for orbiter sidewall-mounted payloads, phase 1 [AD-A220773] N90-26037
Alignment positioning mechanism [NASA-CASE-MSC-21502-1] N90-26341

MULTIPATH TRANSMISSION
A global common-user system for the provision of HF propagation data N90-26180
Experimental study of a digital mobile radio spread spectrum in an urban site N90-26205

MULTIPHASE FLOW
Low-gravity fluid physics: A program overview [NASA-TM-103215] N90-26273

MULTIPLEXING
Design of a universal protocol system architecture: Specification of functions and services [EUT-89-E-230] N90-26569

MULTIPLIERS
Formal verification of the JANUS on-line multiplier [IMAG-RR-785-I] N90-26550

MULTIPROCESSING (COMPUTERS)
Computer architecture evaluation for structural dynamics computations: Project summary [NASA-CR-186137] N90-26512
Adaptive fault-tolerant routing in hypercube multicomputers [NASA-CR-186781] N90-26513
Applications for the scalable coherent interface [DE90-011795] N90-26514
The use of Lanczo's method to solve the large generalized symmetric Eigenvalue problem in parallel [NASA-CR-182072] N90-26533
Graphics applications utilizing parallel processing [NASA-CR-186719] N90-26534
Language support for parallel computation [AD-A223072] N90-26560
PANDA: A distributed multiprocessor operating system N90-26561
ATAMM multicomputer operating system functional specification [NASA-CR-186845] N90-26563

MULTIPROGRAMMING
Single-pass memory system evaluation for multiprogramming workloads [NASA-CR-186553] N90-26558

MULTIVARIATE STATISTICAL ANALYSIS
Variance reduction for quantile estimates in simulations via nonlinear controls [AD-A222653] N90-26590

MUONS
Astronomy at ultra-high energies: Results from the CYGNUS experiment [DE90-011979] N90-26732

MURCHISON METEORITE
Optical constraints of kerogen from 0.15 to 40 microns: Comparison with meteoritic organics N90-26776

MUSCLES
Effects of microgravity on rat muscle N90-26453
Experiment K-6-02. Biomedical, biochemical and morphological alterations of muscle and dense, fibrous connective tissues during 14 days of spaceflight N90-26456
Experiment K-6-04. Trace element balance in rats during spaceflight N90-26458
Experiment K-6-07. Metabolic and morphologic properties of muscle fibers after spaceflight N90-26461
Experiment K-6-08. Biochemical and histochemical observations of vastus medialis N90-26462
Experiment K-6-09. Morphological and biochemical investigation of microgravity-induced nerve and muscle breakdown. Part 1: Investigation of nerve and muscle breakdown during spaceflight; Part 2: Biochemical analysis of EDL and PLT muscles N90-26463
Experiment K-6-10. Effects of zero gravity on myofibril protein content and isomyosin distribution in rodent skeletal muscle N90-26464
Experiment K-6-11. Actin mRNA and cytochrome c mRNA concentrations in the triceps brachia muscle of rats N90-26465
Experiment K-6-21. Effect of microgravity on 1) metabolic enzymes of type 1 and type 2 muscle fibers and on 2) metabolic enzymes, neutransmitter amino acids, and neurotransmitter associated enzymes in motor and somatosensory cerebral cortex. Part 1: Metabolic enzymes of individual muscle fibers; part 2: metabolic enzymes of hippocampus and spinal cord N90-26474

MUSCULAR FUNCTION
Effects of microgravity on rat muscle N90-26453
Experiment K-6-07. Metabolic and morphologic properties of muscle fibers after spaceflight N90-26461

MUSCULOSKELETAL SYSTEM
Experiment K-6-07. Metabolic and morphologic properties of muscle fibers after spaceflight N90-26461

MUSEUMS
Technology development: Future use of NASA's large format camera is uncertain [GAO/NSIAD-90-142] N90-26298

N

NACELLES
Interactive calculation procedures for mixed compression inlets [NASA-CR-186581] N90-25934

NARROWBAND
A narrowband tactical communication system for the VHF and UHF mobile radio bands N90-26192
New synchronisation techniques applicable to multi-tone transmission systems N90-26199

NASA PROGRAMS
Winged cargo return vehicle. Volume 1: Conceptual design [NASA-CR-186823] N90-26050
Design of sensors for control of closed loop life support systems [NASA-CR-186656] N90-26490
NASA Patent Abstracts Bibliography: A continuing bibliography. Section 2: Indexes (supplement 37) [NASA-SP-7039(37)-SECT-2] N90-26700

NASA SPACE PROGRAMS
Proceedings of the Second Symposium on GPS Applications in space, volume 1 [AD-A219978] N90-25962

NASTRAN
A comparison of the post-buckling behavior of metallic and composite plates with centrally located cutouts [NIAR-90-14] N90-26356
Design of ceramic components with the NASA/CARES computer program [NASA-TM-102369] N90-26359

NATIONAL AEROSPACE PLANE PROGRAM
Background, current status, and prognosis of the ongoing slush hydrogen technology development program for the NASP [NASA-TM-103220] N90-26055
Carbon-carbon composites: Emerging materials for hypersonic flight [NASA-TM-103472] N90-26080
Prediction of the ullage gas thermal stratification in a NASP vehicle propellant tank experimental simulation using FLOW-3D [NASA-TM-103217] N90-26160

NATIONAL AIRSPACE SYSTEM
A measurement of the effectiveness of the Airway Science Program to meet Federal Aviation Administration work force needs [NIAR-90-5] N90-26694

NATURAL GAS
A comparison of the contribution of various gases to the greenhouse effect N90-26414

NAVIER-STOKES EQUATION
Two-dimensional Euler and Navier-Stokes Time accurate simulations of fan rotor flows [NASA-TM-102402] N90-25948
Code enhancements and validation of GASP [NPS-PAPER-44] N90-26277
The finite analytic method and its applications. Volume 1: Laminar and turbulent flows past two-dimensional and axisymmetric bodies [AD-A222787] N90-26294

NAVIGATION
The Telecommunications and Data Acquisition Report [NASA-CR-186852] N90-26217
Goldstone intracomplex connected element interferometry N90-26218

NAVIGATION SATELLITES
Proceedings of the Second Symposium on GPS Applications in Space, volume 2 [AD-A219979] N90-25963

NEAR FIELDS
Validity domain of the scalar Kirchhoff and Rayleigh-Sommerfeld diffraction theories in the near field of small phase objects: Comparison between calculation models and microwave measure [ETN-90-96963] N90-26236

NEODYMIUM LASERS
Real-time monitoring of ceramic sintering with laser ultrasonics [DE90-012960] N90-26140

NEPTUNE (PLANET)
Liquid-vapor equilibrium of multicomponent cryogenic systems N90-26774

NERVES
Experiment K-6-09. Morphological and biochemical investigation of microgravity-induced nerve and muscle breakdown. Part 1: Investigation of nerve and muscle breakdown during spaceflight; Part 2: Biochemical analysis of EDL and PLT muscles N90-26463

NETWORK ANALYSIS
Packet radio network concepts for the Norwegian field army N90-26206
On travelling-wave-based protection of high-voltage networks [ISBN-90-9002955-9] N90-26260
Automatic line network extraction from aerial imagery of urban areas through knowledge based image analysis [AD-A222675] N90-26385
Parallel algorithm for distributed memory computers (applications to matricial algorithms) [ETN-90-97252] N90-26573
High speed all optical networks [NASA-CR-185311] N90-26649

NETWORK CONTROL
Analysis of random drop for gateway congestion control [NASA-CR-186736] N90-26698

NETWORK SYNTHESIS
Investigation of automated task learning, decomposition and scheduling [NASA-CR-186791] N90-26488

NEURAL NETS
Neural networks for detecting defects in aircraft structures [IAR-90-4] N90-26345
Investigation of automated task learning, decomposition and scheduling [NASA-CR-186791] N90-26488
Assembly via disassembly: A case in machine perceptual development [NASA-CR-186867] N90-26497
Capacity for patterns and sequences in Kanerva's SDM as compared to other associative memory models [NASA-CR-180701] N90-26522
Multilayered neural networks: Learning algorithms, implementation on hypercube machines, applications [ETN-90-97255] N90-26574
Neural networks for real-time sensory data processing and sensorimotor control [AD-A223096] N90-26592

NEUROTRANSMITTERS
Experiment K-6-18. Study of muscarinic and gaba (benzodiazepine) receptors in the sensory-motor cortex, hippcampus and spinal code N90-26471

NEUTRON DIFFRACTION
Texture of materials by time-of-flight neutron diffraction [DE90-008968] N90-26096

NEUTRON SCATTERING
NMR and optical studies of piezoelectric polymers [DE90-012459] N90-26137

NEWTON METHODS
Efficient generalized conjugate gradient algorithms. Part 2: Implementation [MATHS-REPT-A-118-PT-2] N90-26543

NICKEL
Analysis of strain relaxation in Au/Ni multilayers by x ray diffraction
[IAR-89-25] N90-26357
NICKEL ALLOYS
Microstructural design for fatigue crack growth resistance in Ni-base alloy
[PNR90632] N90-26120
High temperature multiaxiale creep testing of Nimonic 115
[RAE-TM-P-1182] N90-26122
NICKEL CADMIUM BATTERIES
NASA aerospace flight battery systems program
[NASA-TM-103237] N90-26397
NICKEL HYDROGEN BATTERIES
NASA aerospace flight battery systems program
[NASA-TM-103237] N90-26397
NIMBUS 7 SATELLITE
Spatial cross-correlation of Antarctic Sea ice and seabed topography
[NASA-CR-186815] N90-26451
NIOBIUM
Characterization of NbTi multifilamentary superconducting wires
[DE90-626245] N90-26672
NIOBIUM ALLOYS
Effect of boron on intergranular hot cracking in Ni-Cr-Fe superalloys containing niobium
[NASA-CR-186714] N90-26115
NITRAMINE PROPELLANTS
Temperature and OH concentrations in a solid propellant flame using absorption techniques
[AD-A222591] N90-26100
NITRATES
Heterogeneous transformation of peroxyacetylnitrate N90-26430
NITRIC ACID
Measurements of tropospheric nitric acid over the Western United States and Northeastern Pacific Ocean
[NASA-TM-103470] N90-26399
NITROGEN ATOMS
Formation and deactivation of vibrationally excited atmospheric molecules
[AD-A222660] N90-26442
NITROGEN COMPOUNDS
Deposition to the Baltic Sea N90-26404
NITROGEN DIOXIDE
Photodissociation of NO2: Influence of photolysis wavelength and temperature dependence on product formation N90-26426
NITROGEN OXIDES
Aircraft exhaust emissions: An engine manufacturer's perspective
[PNR90675] N90-26004
Catching our breath: Next steps for reducing urban ozone
[PB90-130451] N90-26398
Measurements of CH4, N2O, CO, H2O and O3 in the middle atmosphere by the ATMOS experiment on Spacelab 3
[NASA-TM-103476] N90-26400
New observations of stratospheric N2O5
[NASA-TM-103478] N90-26402
Verification and improvement of the EMEP model for long-range transport and deposition of pollutants N90-26405
An Eulerian transport model for NO(sub x)-compounds N90-26406
Formation and deactivation of vibrationally excited atmospheric molecules
[AD-A222660] N90-26442
NITROUS OXIDES
Formation kinetics of N2O in the atmosphere N90-26425
NOISE INTENSITY
Aeroacoustics of advanced propellers
[NASA-TM-103137] N90-26635
NOISE MEASUREMENT
Man-made noise in a military environment N90-26191
Bringing aircraft noise testing down to Earth
[PNR90642] N90-26637
NOISE PREDICTION
High speed turboprop aeroacoustic study (counterrotation). Volume 1: Model development
[NASA-CR-185241] N90-26633
NOISE PREDICTION (AIRCRAFT)
Aerodynamic loads and blade vortex interaction noise prediction
[ISL-PU-310/89] N90-25942
Aeroacoustics of advanced propellers
[NASA-TM-103137] N90-26635
NOISE REDUCTION
Stage 2 re-engining: The only way to achieve a real stage 3 aircraft
[PNR90636] N90-25977
Low-speed wind tunnel investigation of the static stability and control characteristics of an advanced turboprop configuration with the propellers placed over the tail
[NASA-CR-186900] N90-26017
Man-made noise in a military environment N90-26191
Classification regions in remote sensing imagery utilizing spatial characteristics
[INPE-4913-PRE/1514] N90-26381
A preliminary study of the masking of wind turbine noise by ambient sound
[FFA-TN-1990-01] N90-26636
NOMOGRAPHS
Debris/ice/TPS assessment and photographic analysis for shuttle mission STS-31R
[NASA-TM-102790] N90-26040
NONAQUEOUS ELECTROLYTES
Electrochemical, in situ Raman spectroscopic, and conductivity studies of polypyrrole incorporating large size anions: Conducting nature of reduced form
[AD-A222739] N90-26102
NONDESTRUCTIVE TESTS
Acousto-optic signature analysis for inspection of the orbiter thermal protection tile bonds
[DE90-013089] N90-26043
Holography and holographic interferometry
[PNR90670] N90-26303
Neural networks for detecting defects in aircraft structures
[IAR-90-4] N90-26345
Field experience in using laser acoustic sensing for inspection
[DE90-012954] N90-26347
NDT in aerospace: The next decade (1990's)
[PNR90628] N90-26348
The role of NDI in the certification of turbine engine components
[PNR90629] N90-26349
Characterization of inspection performance
[NLR-MP-88068-U] N90-26350
Nondestructive one- and two-dimensional doping profiling by inverse methods
[ETN-90-97264] N90-26351
Development of creep-fatigue damage detection method of rotor steel by ultrasonic wave measurement
[DE90-503792] N90-26365
An embedded fibre optic sensor for impact damage detection in composite materials
[UTIAS-332] N90-26650
NDE (Nondestructive evaluation) of critical currents in high T(sub c) superconductors
[DE90-012953] N90-26670
NONLINEAR EQUATIONS
Parallel processors and nonlinear structural dynamics algorithms and software
[NASA-CR-186755] N90-26536
Efficient implementation of minimal polynomial and reduced rank extrapolation methods
[NASA-TM-103240] N90-26616
NONLINEAR SYSTEMS
A contribution to the improvement of the accuracy in the parameter identification of nonlinear processes, by example of the aircraft motion
[ETN-90-96961] N90-25974
Variance reduction for quantile estimates in simulations via nonlinear controls
[AD-A222653] N90-26590
NONLINEARITY
Prediction methodologies for nonlinear aerodynamic characteristics of control surfaces
[NIAR-90-17] N90-25937
Nonlinear modeling of time series using Multivariate Adaptive Regression Splines (MARS)
[AD-A222710] N90-26623
NORTH ATLANTIC TREATY ORGANIZATION (NATO)
AGARD highlights 90/1 N90-26788
NORTH SEA
Phytoplankton and its contribution to the atmospheric sulfur budget of northern Europe N90-26417
NOTCH STRENGTH
The blunt notch behaviour of metal laminates: ARALL and GLARE
[LR-617] N90-26368
NOTCH TESTS
Fracture toughness of polyimide films
[NASA-TM-103473] N90-26130
NOZZLE FLOW
Effect of tail size reductions on longitudinal aerodynamic characteristics of a three surface F-15 model with nonaxisymmetric nozzles
[NASA-TP-3036] N90-25938
Hot gas ingestion characteristics and flow visualization of a vectored thrust STOVL concept
[NASA-TM-103212] N90-26009
NOZZLE GEOMETRY
Effect of tail size reductions on longitudinal aerodynamic characteristics of a three surface F-15 model with nonaxisymmetric nozzles
[NASA-TP-3036] N90-25938
NUCLEAR ELECTRIC PROPULSION
Project Exodus
[NASA-CR-186836] N90-26026
NUCLEAR FUELS
Multimegawatt space nuclear power supply, phase 1. Volume 3: Annotated outline of preliminary safety assessment D180-30619-7
[DE90-012432] N90-26646
Multimegawatt space nuclear power supply, phase 1. Supplement: D180-30619-8
[DE90-012433] N90-26647
NUCLEAR FUSION
Application of the results of carbon pellet modeling to the problem of plasma penetration
[DE90-012713] N90-26658
NUCLEAR MAGNETIC RESONANCE
Dynamics of micellar oligomeric and monomeric sodium 10-undecenoate
[AD-A222570] N90-26099
NUCLEAR REACTIONS
A closed form solution to HZE propagation
[NASA-TM-103482] N90-26640
NUCLEAR REACTORS
The chemical effects of the Martian environment on power system component materials: A theoretical approach
[NASA-TM-103203] N90-26074
Analysis of a Mars-stationary orbiting microwave power transmission system
[NASA-TM-101344] N90-26172
NUCLEAR WEAPONS
ASATs vs Brilliant Pebbles
[DE90-010348] N90-26626
NUCLEATION
Undercooling and solidification
[DLR-FB-90-020] N90-26678
NUMERICAL ANALYSIS
Research conducted at the Institute for Computer Applications in Science and Engineering in applied mathematics, numerical analysis, and computer science
[NASA-CR-182057] N90-26510
Computer analysis of chromatographic data N90-26521
Numerical treatment of shell crossing singularities in the spherically symmetric gravitational collapse
[ETN-90-96967] N90-26598
Asymptotic analysis of dissipative waves with applications to their numerical simulation
[NASA-TM-103231] N90-26615
NUMERICAL FLOW VISUALIZATION
Development of a system for the numerical simulation of Euler flows, with results of preliminary 3-D propeller-slipstream/exhaust-jet calculations
[NLR-TR-88008-U] N90-26285
NUMERICAL INTEGRATION
Natural melting within a spherical shell
[NASA-TM-102822] N90-26274
NUMERICAL STABILITY
Dichotomies for certain product measures and stable processes
[AD-A222568] N90-26621
NUTRITION
Proximate composition of seed and biomass from soybean plants grown at different carbon monoxide (CO2) concentrations
[NASA-TM-103496] N90-26480

O

OBJECT PROGRAMS
Object oriented programming
[DE90-011797] N90-26532
OBLIQUE SHOCK WAVES
Interactive calculation procedures for mixed compression inlets
[NASA-CR-186581] N90-25934
OCEAN BOTTOM
Atmospheric correction of thematic mapping measurements about seabeds of the German Bay
[GKSS-89/E/47] N90-26029
OCEAN DYNAMICS
Mariners Weather Log, volume 33, number 2, Spring 1989
[PB90-146838] N90-26443
Mariners Weather Log, volume 33, number 3, Summer 1989
[PB90-146846] N90-26444

OCEANOGRAPHY
Frontogenesis in gravity currents: An example with no known applications in oceanography
[MATHS-REPT-A-117] N90-26284
OLIGOMERS
Dynamics of micellar oligomeric and monomeric sodium 10-undecenoate
[AD-A222570] N90-26099
ON-LINE SYSTEMS
Continuous on-line link error rate detector
[AD-D014510] N90-26209
Self-checking on-line testable static RAM
[NASA-CASE-NPO-17939-1-CU] N90-26518
Formal verification of the JANUS on-line multiplier
[IMAG-RR-785-I] N90-26550
ONBOARD EQUIPMENT
Space operations: NASA's communications support for Earth orbiting spacecraft. Report to Chairman, Subcommittee on Space Science and Applications, Committee on Science, Space and Technology, House of Representatives
[GAO/IMTEC-89-41] N90-26215
OPENINGS
Buckling and postbuckling behavior of square compression-loaded graphite-epoxy plates with circular cutouts
[NASA-TP-3007] N90-26077
OPERATING SYSTEMS (COMPUTERS)
Tools for distributed application management
[NASA-CR-186627] N90-26535
PANDA: A distributed multiprocessor operating system N90-26561
ATAMM multicomputer operating system functional specification
[NASA-CR-186845] N90-26563
OPERATIONS RESEARCH
Launching a dream: A teachers guide to a simulated space shuttle mission
[NASA-TM-89715] N90-26693
OPERATOR PERFORMANCE
Aviation safety: Serious problems continue to trouble the air traffic control work force. Report to congressional requesters
[GAO/RCED-89-112] N90-25959
OPERATORS (MATHEMATICS)
Galerkin finite difference Laplacian operators on isolated unstructured triangular meshes by linear combinations
[NASA-TM-103209] N90-26276
OPTICAL COMMUNICATION
A two-telescope receiver design for deep space optical communications N90-26226
High speed all optical networks
[NASA-CR-185311] N90-26649
OPTICAL FIBERS
Active lag angle device
[AD-D014538] N90-26249
An embedded fibre optic sensor for impact damage detection in composite materials
[UTIAS-332] N90-26650
Optical transmission through a polarization preserving single mode optical fiber at two Ar(+) laser wavelengths
[NASA-TM-103475] N90-26651
Theory of biaxial graded-index optical fiber
[NASA-CR-186882] N90-26652
A dual-wavelength passive homodyne detection unit for fiber-coupled white-light interferometers
[ETN-90-97036] N90-26653
OPTICAL HETERODYNING
A numerical simulation of the quasi-heterodyne technique for double-pulsed holographic vibration measurements
[PNR90622] N90-26301
OPTICAL MEASUREMENT
Preliminary error budget for an optical ranging system: Range, range rate, and differenced range observables N90-26227
OPTICAL PROPERTIES
Optical properties and transport properties of hydrogenated amorphous silicon
[ETN-90-97215] N90-26656
Ellipsometric study of YBa2Cu3O(7-x) laser ablated and co-evaporated films
[NASA-TM-103223] N90-26682
OPTICAL RADAR
Laser radar angular tracking
[AD-A222741] N90-26319
Vertical ozone probing with lidar N90-26416
The 27-28 October 1986 FIRE IFO cirrus case study: Cirrus parameter relationships derived from satellite and lidar data
[NASA-TM-103469] N90-26447
Development of eye-safe lidar for aerosol measurements
[NASA-CR-186905] N90-26503
OPTICAL TRACKING
Color image processing for navigation: Two road trackers
[AD-A222667] N90-26591
OPTIMAL CONTROL
Model following control system design: Preliminary ATTAS in-flight simulation test results
[PD-FC-9003] N90-26010
OPTIMIZATION
A contribution to the economic, optimal dimensioning, and shaping of aircraft structures using a design model
[ETN-90-96966] N90-25976
Plate rods and leaf springs with hybrid structure: Cross section optimization following different target criteria
[ILR-MITT-227(1989)] N90-26366
A search routine for optimization in a wind power system with variable speed
[FOA-C-20779-2.1] N90-26395
Modeling and optimization of a regenerative fuel cell system using the ASPEN process simulator
[NASA-TM-103210] N90-26396
Microspacecraft and Earth observation: Electrical field (ELF) measurement project
[NASA-CR-186821] N90-26436
Study of a class of non convex optimization algorithms: Implementation and applications
[ETN-90-97241] N90-26552
Adaptive and comparative studies of optimization algorithms: Implementations and applications
[ETN-90-97243] N90-26553
A sum rule satisfied by optimized feed-forward layered networks
[RSRE-MEMO-4341] N90-26579
On networks, optimized feature extraction, and the Bayes decision
[RSRE-MEMO-4342] N90-26580
ORBIT CALCULATION
Proceedings of the Second Symposium on GPS Applications in Space, volume 2
[AD-A219979] N90-25963
A reduced-dynamic technique for precise orbit determination N90-26219
Applications of different design methodologies in navigation systems and development at JPL N90-26221
ORBIT TRANSFER VEHICLES
Project LOCOST: Laser or Chemical Hybrid Orbital Space Transport
[NASA-CR-186822] N90-26042
Project SPARC: Space-based aeroassisted reusable craft
[NASA-CR-186816] N90-26051
ORBITAL ASSEMBLY
Control strategy for cooperating disparate manipulators
[NASA-CR-186809] N90-26328
ORBITAL MANEUVERING VEHICLES
Space transportation: NASA has no firm need for increasingly costly orbital maneuvering vehicle
[GAO/NSIAD-90-192] N90-26041
Literature concerning control and display technology applicable to the Orbital Maneuvering Vehicle (OMV)
[NASA-CR-186790] N90-26048
Biconic cargo return vehicle with an advanced recovery system. Volume 1: Conceptual design
[NASA-CR-186520] N90-26052
ORBITAL MECHANICS
The aerobraking space transfer vehicle
[NASA-CR-186819] N90-26053
A reduced-dynamic technique for precise orbit determination N90-26219
ORBITAL VELOCITY
Rings of Earth detected by orbital debris radar N90-26232
ORDER-DISORDER TRANSFORMATIONS
The origin of poorly conditioned susceptibility matrix within inverse CVM algorithm in the case of Pd(sub 3)V: A comparison to the case of Ni(sub 3)V
[DE90-012464] N90-26110
High temperature x ray diffraction and Landau theory investigations of order-disorder transition in defect NaCl-type solids
[DE90-011807] N90-26673
ORGANIC MATERIALS
Optical constraints of kerogen from 0.15 to 40 microns: Comparison with meteoritic organics N90-26776
ORGANIC SILICON COMPOUNDS
Polymeric aluminasilazane precursors for aluminosilicon nitride
[AD-A222755] N90-26158
ORGANIZATIONS
Effect of organizational structure on performance of decision making teams
[AD-A223160] N90-26697
ORGANOMETALLIC POLYMERS
Polymeric aluminasilazane precursors for aluminosilicon nitride
[AD-A222755] N90-26158
Stibathiolanes: Synthesis, solid state structure, and solution behavior
[AD-A223255] N90-26688
ORTHOGONAL FUNCTIONS
Annual and interannual variations of Earth-emitted radiation based on a 10-year data set
[NASA-TM-103465] N90-26432
Asymptotic law of the orthogonal empirical functions and applications, part 2
[IMAG-RR-792-M-PT-2] N90-26605
ORTHOTROPIC PLATES
Buckling and postbuckling behavior of square compression-loaded graphite-epoxy plates with circular cutouts
[NASA-TP-3007] N90-26077
OUTER SPACE TREATY
Manned Space Stations: Legal Issues
[ESA-SP-305] N90-26711
The US/International Space Station: Legal aspects of space objects and jurisdiction and control N90-26713
Damage responsibility and liability in space stations N90-26714
MIR: A Soviet Space Station. Some legal aspects of international cooperation N90-26715
The partnership concept and international management N90-26717
The International Space Station: Conditions of access and use N90-26718
OXIDATION
A resistance strain gage with repeatable and cancellable apparent strain for use to 800 C
[NASA-CR-185256] N90-26063
Carbon-carbon composites: Emerging materials for hypersonic flight
[NASA-TM-103472] N90-26080
Oxidation and sulfidation of Type 310S stainless steel at elevated temperatures
[DE90-010149] N90-26109
Quantitative confirmation of diffusion-limited oxidation theories
[DE90-012997] N90-26143
Role of surface passivation in the integrated processing of MOS structures
[AD-A222630] N90-26264
The effects of pretreatment conditions on a Pt/SnO2 catalyst for the oxidation of CO in CO2 lasers
[NASA-TM-103487] N90-26309
Rapid thermal processing: A study of the silicon oxidation and of the implanted boron activation
[LAAS-90051] N90-26681
OXIDATION-REDUCTION REACTIONS
Electrochemical, in situ Raman spectroscopic, and conductivity studies of polypyrrole incorporating large size anions: Conducting nature of reduced form
[AD-A222739] N90-26102
OXIDE FILMS
Selective electrocatalysis of anodic oxygen-transfer reactions at chemically modified, thin-film lead dioxide electrodes
[DE90-011747] N90-26252
Studies on ion scattering and sputtering processes relevant to ion beam sputter deposition of multicomponent thin films
[DE90-010071] N90-26675
OXYGEN
Mars in situ propellants: Carbon monoxide and oxygen ignition experiments
[NASA-TM-103202] N90-26065
Photodissociation of O2 in the stratosphere and mesosphere: A general parametrization of the Schumman-Runge Bands N90-26427
OZONE
Catching our breath: Next steps for reducing urban ozone
[PB90-130451] N90-26398
Measurements of CH4, N2O, CO, H2O and O3 in the middle atmosphere by the ATMOS experiment on Spacelab 3
[NASA-TM-103476] N90-26400
The global consequences of increasing tropospheric ozone concentrations
[NASA-TM-103477] N90-26401
The diurnal ozone cycle in a coniferous forest: The importance of meteorology and chemistry N90-26423
OZONE DEPLETION
Results from the IVL TOR Station at Roervik, Sweden. A contribution to the EURATRAC subproject TOR N90-26415
Vertical ozone probing with lidar N90-26416
Stratospheric chemistry N90-26424
OZONOMETRY
Vertical ozone probing with lidar N90-26416

The diurnal ozone cycle in a coniferous forest: The importance of meteorology and chemistry N90-26423

P

PACIFIC OCEAN
Measurements of tropospheric nitric acid over the Western United States and Northeastern Pacific Ocean [NASA-TM-103470] N90-26399
PACKET SWITCHING
An overview of Canadian radio propagation/communications technologies research N90-26179
Optimal synchronization of spread spectrum sequenced by nontransferable switching operators N90-26183
PACKETS (COMMUNICATION)
Analysis of random drop for gateway congestion control [NASA-CR-186736] N90-26698
PAINTS
Statistical treatment of slow strain rate data for assessment of hydrogen embrittlement in low alloy high strength steel [ARL-MAT-R-122] N90-26106
Mechanical paint removal techniques for aircraft structures [NIAR-90-12] N90-26166
PALEONTOLOGY
The 5th International symposium on palaeolimnology [AD-A219244] N90-26431
PANEL METHOD (FLUID DYNAMICS)
An unsteady lifting surface method for single rotation propellers [NASA-CR-4302] N90-25940
PARABOLIC REFLECTORS
Feasibility study of a synthesis procedure for array feeds to improve radiation performance of large distorted reflector antennas [NASA-CR-186641] N90-26213
PARACHUTE DESCENT
Wind tunnel study of wake downwash behind A 6 percent scale model B1-B aircraft [DE90-011783] N90-25941
PARALLEL COMPUTERS
Principles of FP2: Term algebras for specification of parallel machines [RR-789-I-IMAG-98-LIFIA] N90-26571
Parallel algorithm for distributed memory computers (applications to matricial algorithms) [ETN-90-97252] N90-26573
PARALLEL PLATES
Modeling of composite beams and plates for static and dynamic analysis [NASA-CR-186459] N90-26354
PARALLEL PROCESSING (COMPUTERS)
Run-time parallelization and scheduling of loops [NASA-CR-182039] N90-26509
Research conducted at the Institute for Computer Applications in Science and Engineering in applied mathematics, numerical analysis, and computer science [NASA-CR-182057] N90-26510
Autoplan: A self-processing network model for an extended blocks world planning environment [NASA-CR-186733] N90-26526
Graphics applications utilizing parallel processing [NASA-CR-186719] N90-26534
Parallel processors and nonlinear structural dynamics algorithms and software [NASA-CR-186755] N90-26536
A parallel algorithm for surface plane intersection [IMAG-RR-794-M] N90-26549
Efficient network topologies for extensible massively parallel computers [ETN-90-97220] N90-26568
Design of a universal protocol system architecture: Specification of functions and services [EUT-89-E-230] N90-26569
Parallelization of an annealing simulation applied to improving tetrahedric grids [IMAG-RR-796-M] N90-26570
Principles of FP2: Term algebras for specification of parallel machines [RR-789-I-IMAG-98-LIFIA] N90-26571
Implementation of algorithms used in calculating the tensor product of matrices on a distributed memory machine [IMAG-RR-786-I] N90-26572
Parallel algorithm for distributed memory computers (applications to matricial algorithms) [ETN-90-97252] N90-26573
Parallel/distributed direct method for solving linear systems [NASA-TM-103229] N90-26614
PARALLEL PROGRAMMING
Language support for parallel computation [AD-A223072] N90-26560
Parallel programming with algorithmic skeletons [DE90-010536] N90-26562
Efficient network topologies for extensible massively parallel computers [ETN-90-97220] N90-26568
PARAMETER IDENTIFICATION
A contribution to the improvement of the accuracy in the parameter identification of nonlinear processes, by example of the aircraft motion [ETN-90-96961] N90-25974
A model of the synchronous machine with rectifier, especially for control purposes [EUT-89-E-215] N90-26256
Research conducted at the Institute for Computer Applications in Science and Engineering in applied mathematics, numerical analysis, and computer science [NASA-CR-182057] N90-26510
A new scheme for identification and control [EUT-88-E-213] N90-26586
PARAMETERIZATION
Calculation of the algebraic curves parameterization: Hamburger-Noether expansions [IMAG-RR-798-M] N90-26608
PARAMETRIC AMPLIFIERS
Solid-state lasers for coherent communication and remote sensing [NASA-CR-186634] N90-26306
PARSING ALGORITHMS
ATN design tool [AD-A223030] N90-26559
PARTICLE ACCELERATORS
Thermal management of an accelerator system in space [DE90-013153] N90-26627
PARTICLE BEAMS
Thermal management of an accelerator system in space [DE90-013153] N90-26627
PARTICLE COLLISIONS
Electron-impact spectroscopy N90-26779
Investigation of the Saturn dust environment from the analysis of energetic charged particle measurements [NASA-CR-186727] N90-26784
PARTICLE DIFFUSION
A study of positrons from Soviet nuclear powered satellites as tracers for magnetospheric research [DE90-013157] N90-26438
Diffusion-accommodated grain boundary sliding in a polycrystal [DE90-012727] N90-26668
PARTICLE INTERACTIONS
First International Conference on Laboratory Research for Planetary Atmospheres [NASA-CP-3077] N90-26744
PARTICLE MOTION
Bubble, Drop and Particle Unit (BDPU): A multi-user microgravity facility [IAF-89-431] N90-26164
PARTICLE PRODUCTION
A research program in physics of the early universe [DE90-013319] N90-26742
PARTICLE SIZE DISTRIBUTION
Combustion instrumentation N90-25996
Texture of materials by time-of-flight neutron diffraction [DE90-008968] N90-26096
PARTICLE TRAJECTORIES
Rings of Earth detected by orbital debris radar N90-26232
PARTICULATES
Interaction of electromagnetic signals with particulate clouds [AD-A222804] N90-26244
Optical signatures of molecular particles via mass-selected cluster spectroscopy N90-26780
PASSENGERS
Biodynamic simulations of an aircraft pilot/passenger in various crash environments [NIAR-90-6] N90-26494
Human factors: The human interface with aircraft interiors [NIAR-90-18] N90-26496
PASSIVITY
Passivation of high temperature superconductors [NASA-CASE-NPO-17949-1-CU] N90-26684
PATENT APPLICATIONS
Active lag angle device [AD-D014538] N90-26249
Multicolor infrared photodetector [AD-D014511] N90-26297
Rotating-unbalanced-mass devices and methods for scanning balloon-borne-experiments, free-flying spacecraft, and space shuttle/space station attached experiments [NASA-CASE-MFS-28425-1] N90-26304
Power saw [NASA-CASE-MSC-21469-1] N90-26340
Alignment positioning mechanism [NASA-CASE-MSC-21502-1] N90-26341
MBE growth technology for high quality strained III-V layers [NASA-CASE-NPO-17723-1-CU] N90-26685
PATENT POLICY
NASA Patent Abstracts Bibliography: A continuing bibliography. Section 2: Indexes (supplement 37) [NASA-SP-7039(37)-SECT-2] N90-26700
Manned Space Stations: Legal Issues [ESA-SP-305] N90-26711
The astronauts' legal status: The International Space Station N90-26721
Space Station intellectual property rights and US patent law N90-26723
Space manufacture: Protection and valuation of innovations from a users point of view N90-26724
Production activities in space: The problems of protection N90-26725
Possible solutions N90-26726
PATENTS
Possible solutions N90-26726
PATTERN RECOGNITION
Initial results on fault diagnosis of DSN antenna control assemblies using pattern recognition techniques N90-26228
Pattern classification of textura by moment and distance autocorrelation function [INPE-4976-PRE/1541] N90-26379
A sum rule satisfied by optimized feed-forward layered networks [RSRE-MEMO-4341] N90-26579
On networks, optimized feature extraction, and the Bayes decision [RSRE-MEMO-4342] N90-26580
PAYLOAD CONTROL
IRIS system and future application to expandable launchers [IAF-89-212] N90-26035
PAYLOAD INTEGRATION
Planning for Space Station Freedom laboratory payload integration [NASA-CR-186751] N90-26047
Integrated support structure [NASA-CR-186835] N90-26162
PAYLOADS
Rotating-unbalanced-mass devices and methods for scanning balloon-borne-experiments, free-flying spacecraft, and space shuttle/space station attached experiments [NASA-CASE-MFS-28425-1] N90-26304
PELLETS
Application of the results of carbon pellet modeling to the problem of plasma penetration [DE90-012713] N90-26658
PERFORMANCE PREDICTION
Enroute flight planning: The design of cooperative planning systems [NASA-CR-186797] N90-25964
Performance of a supercharged direct-injection stratified-charge rotary combustion engine [NASA-TM-103105] N90-25982
Handbook of uncertainty methodology for engine testing at Pyestock (England) [RAE-TM-P-1179] N90-26007
On controller choice for robust sliding mode performance [MATHS-REPT-A-107] N90-26337
Statistical analysis of a software reliability model [IMAG-RR-781-M] N90-26352
Modeling and optimization of a regenerative fuel cell system using the ASPEN process simulator [NASA-TM-103210] N90-26396
PERFORMANCE TESTS
Performance evaluation of LE-7 high pressure pumps [DE90-505523] N90-26034
Heavy ion tests on programmable VLSI [ETN-90-97254] N90-26057
Development of ceramic hybrid combustor: Design and combustion test results [DE90-503442] N90-26149
Design and performance analysis of the DSS-13 beam waveguide antenna N90-26225
Contribution to CMOS integrated circuit tests: Study of the stuck-on and stuck-open fault tests [ETN-90-97256] N90-26261
QM-8 final performance evaluation report: SEALS, volume 4 [NASA-CR-183958] N90-26324

Interim qualification tests and procedures for terrestrial photovoltaic thin-film flat-plate modules
[DE90-000354] N90-26392
The retrieval of information from secondary memory: A review and new findings
[AD-A222760] N90-26489
Advanced Turbine Technology Applications Project (ATTAP)
[NASA-CR-185240] N90-26728

PERMEABILITY
Quantitative confirmation of diffusion-limited oxidation theories
[DE90-012997] N90-26143
Development of membrane process for carbon dioxide separation from diving atmosphere
[AD-A222606] N90-26504

PEROXIDES
The collection and analysis of atmospheric peroxides N90-26428
Heterogeneous transformation of peroxyacetylnitrate N90-26430

PERSONAL COMPUTERS
L-SWITCH: A PC program for computing transient voltages and currents during switching off three-phase inductances
[EUT-89-E-221] N90-26257

PERTURBATION
The effect of a three-dimensional source on the flow through a channel with square cross section
[LR-512] N90-26289

PERTURBATION THEORY
An investigation of the use of singular perturbation methods and modal control theory in the derivation or aircraft control schemes
[MATHS-REPT-A-106] N90-26014
Chemical structure and kinetics at liquid/solid interfaces
[AD-A222766] N90-26105
Perturbation methods in the theory of waves and bifurcation phenomena N90-26593
Application and extension of an analytical model of the confined acoustic beam generated by a transducer
[AD-A222994] N90-26639

PHASE DIAGRAMS
The origin of poorly conditioned susceptibility matrix within inverse CVM algorithm in the case of Pd(sub 3)V: A comparison to the case of Ni(sub 3)V
[DE90-012464] N90-26110

PHASE ERROR
Combined effects of fast and selective fading on performance of PSK and MSK with coherent detection N90-26204

PHASE LOCKED SYSTEMS
New approaches for rapid synchronisation frequency hoppers N90-26201
Direct drive robotic hand
[NASA-CASE-NPO-17917-1-CU] N90-26339

PHASE SHIFT KEYING
Combined effects of fast and selective fading on performance of PSK and MSK with coherent detection N90-26204
QPSK loop lock detection in the advanced receiver N90-26230

PHASE TRANSFORMATIONS
Dynamical solvent effects on electron-transfer processes: Recent progress and perspectives
[AD-A222603] N90-26101
Twin boundaries, interfaces and modulated structures in martensites
[DE90-012899] N90-26111
Fractal structure and fractal time in silica sol-gels
[DE90-013197] N90-26144
Low-gravity fluid physics: A program overview
[NASA-TM-103215] N90-26273
Natural melting within a spherical shell
[NASA-TM-102822] N90-26274

PHASED ARRAYS
Design of an optically controlled Ka-band GaAs MMIC phased-array antenna
[NASA-TM-103147] N90-26250

PHOSPHATES
Short-range structure of fluorine-modified phosphate glass
[DE90-013494] N90-26145

PHOTOABSORPTION
Absolute vacuum ultraviolet photoabsorption cross section studies of atomic and molecular species: Techniques and observational data N90-26754
High resolution, low temperature photoabsorption cross-section of C2H2 with application to Saturn's atmosphere N90-26757

PHOTOCHEMICAL REACTIONS
New observations of stratospheric N2O5
[NASA-TM-103478] N90-26402
A comparison of the contribution of various gases to the greenhouse effect N90-26414
Measurements of monoterpenes in a coniferous forest N90-26421
Stratospheric chemistry N90-26424
Heterogeneous transformation of peroxyacetylnitrate N90-26430
Soft x ray resist characterization: Studies with a laser plasma x ray source
[DE90-013493] N90-26661
Laboratory studies, analysis, and interpretation of the spectra of hydrocarbons present in planetary atmospheres including cyanoacetylene, acetylene, propane, and ethane N90-26748
Absolute vacuum ultraviolet photoabsorption cross section studies of atomic and molecular species: Techniques and observational data N90-26754
Novel laser gain and time-resolved FTIR studies of photochemistry N90-26756
Chemical kinetics and modeling of planetary atmospheres N90-26763
Laboratory measurements and methane photochemistry modeling N90-26770
UV and VUV spectroscopy and photochemistry of small molecules in a supersonic jet N90-26771
Laboratory studies of photodissociation processes relevant to the formation of cometary radicals N90-26772

PHOTODISSOCIATION
Photodissociation of O2 in the stratosphere and mesosphere: A general parametrization of the Schumman-Runge Bands N90-26427
Absolute vacuum ultraviolet photoabsorption cross section studies of atomic and molecular species: Techniques and observational data N90-26754
Laboratory studies of photodissociation processes relevant to the formation of cometary radicals N90-26772
Optical signatures of molecular particles via mass-selected cluster spectroscopy N90-26780

PHOTOGRAPHS
Debris/ice/TPS assessment and photographic analysis for shuttle mission STS-31R
[NASA-TM-102790] N90-26040

PHOTOIONIZATION
Formation and deactivation of vibrationally excited atmospheric molecules
[AD-A222660] N90-26442
Role of the methylene amidogen (H2CN) radical in the atmospheres of Titan and Jupiter N90-26769

PHOTOLYSIS
Photodissociation of NO2: Influence of photolysis wavelength and temperature dependence on product formation N90-26426
Rate constant for reaction of atomic hydrogen with germane N90-26768

PHOTOMETERS
Multicolor infrared photodetector
[AD-D014511] N90-26297

PHOTONS
Astronomy at ultra-high energies: Results from the CYGNUS experiment
[DE90-011979] N90-26732
First International Conference on Laboratory Research for Planetary Atmospheres
[NASA-CP-3077] N90-26744
Photon sputtering of H2O ices: A preliminary report N90-26783

PHOTONUCLEAR REACTIONS
A site for the astrophysical gamma ray process
[DE90-013473] N90-26787

PHOTOSPHERE
Nonpotential magnetic fields at sites of gamma ray flares
[NASA-TM-103493] N90-26785

PHOTOSYNTHESIS
Gas exchange characteristics as indicators of the basic limiting factors in photosynthesis
[DE90-012399] N90-26481
Photosynthesis in intact plants
[DE90-013699] N90-26482
Greenhouse design for a Martian colony: Structural, solar collection and light distribution systems
[NASA-CR-186818] N90-26501

PHOTOVOLTAIC CELLS
Interim qualification tests and procedures for terrestrial photovoltaic thin-film flat-plate modules
[DE90-000354] N90-26392

PHOTOVOLTAIC CONVERSION
The chemical effects of the Martian environment on power system component materials: A theoretical approach
[NASA-TM-103203] N90-26074
Storage battery operation technique of photovoltaic system to prevent the imbalance of state of charge
[DE90-503032] N90-26255
Megawatt solar power systems for lunar surface operations
[NASA-CR-186509] N90-26391

PHYSICAL EXERCISE
Effects of microgravity on rat muscle N90-26453
Experiment K-6-09. Morphological and biochemical investigation of microgravity-induced nerve and muscle breakdown. Part 1: Investigation of nerve and muscle breakdown during spaceflight; Part 2: Biochemical analysis of EDL and PLT muscles N90-26463

PHYSIOLOGICAL EFFECTS
Damage measurements on optical materials for use in high-peak-power lasers
[DE90-013489] N90-26314
Laser damage database at 1064 nm
[DE90-013490] N90-26315

PHYSIOLOGICAL RESPONSES
The retrieval of information from secondary memory: A review and new findings
[AD-A222760] N90-26489

PHYSIOLOGY
Effects of microgravity on rat bone, cartilage and connective tissues N90-26454

PHYTOPLANKTON
Phytoplankton and its contribution to the atmospheric sulfur budget of northern Europe N90-26417

PIEZOELECTRIC GAGES
The study of VF2/VF3 piezoelectric copolymeteres submitted to shocks
[ISL-CO-210/9] N90-26679

PIEZOELECTRICITY
NMR and optical studies of piezoelectric polymers
[DE90-012459] N90-26137
The study of VF2/VF3 piezoelectric copolymeteres submitted to shocks
[ISL-CO-210/9] N90-26679

PILOT PERFORMANCE
Eye tracking device for the measurement of flight performance in simulators
[AD-A220075] N90-26484
Pilot interaction with automated airborne decision making systems
[NASA-CR-186730] N90-26492
Psychophysiological assessment of pilot workload in an applied setting
[AD-A222707] N90-26507

PINEAL GLAND
Experiment K-6-19. Pineal physiology in microgravity: Relation to rat gonadal function N90-26472

PINHOLES
Comparison of currents predicted by NASCAP/LEO model simulations with elementary Langmuir-type bare probe models for an insulated cable containing a single pinhole
[NASA-TM-102486] N90-26054

PIPELINING (COMPUTERS)
Design of a universal protocol system architecture: Specification of functions and services
[EUT-89-E-230] N90-26569

PITUITARY GLAND
Experiment K-6-20. The effect of spaceflight on pituitary oxytocin and vasopressin content of rats N90-26473
Experiment K-6-22. Growth hormone regulation, synthesis and secretion in microgravity. Part 1: Somatotroph physiology. Part 2: Immunohistochemical analysis of hypothalamic hormones. Part 3: Plasma analysis N90-26475

PITUITARY HORMONES
Experiment K-6-22. Growth hormone regulation, synthesis and secretion in microgravity. Part 1: Somatotroph physiology. Part 2: Immunohistochemical analysis of hypothalamic hormones. Part 3: Plasma analysis N90-26475

PLANAR STRUCTURES
Forbidden tangential orbit transfers between intersecting Keplerian orbits
[NASA-TP-3031] N90-26028

PLANETARY ATMOSPHERES
Submillimeter and millimeter observations of solar system objects
[NASA-CR-186836] N90-26731
First International Conference on Laboratory Research for Planetary Atmospheres
[NASA-CP-3077] N90-26744
Laboratory measurements of microwave and millimeter-wave properties of planetary constituents N90-26745
Laboratory studies, analysis, and interpretation of the spectra of hydrocarbons present in planetary atmospheres including cyanoacetylene, acetylene, propane, and ethane N90-26748
Infrared spectra of van de Waals complexes of importance in planetary atmospheres N90-26749
Recent high resolution laboratory determinations of line broadening and intensity parameters: PH3, CH3D, and CO2 N90-26751

Microwave spectra of van der Waals complexes of importance in planetary atmospheres N90-26752
Infrared line parameters at low temperatures relevant to planetary atmospheres N90-26753
Determination of molecular spectroscopic parameters and energy-transfer rates by double-resonance spectroscopy N90-26755
Novel laser gain and time-resolved FTIR studies of photochemistry N90-26756
High resolution, low temperature photoabsorption cross-section of C2H2 with application to Saturn's atmosphere N90-26757
Measurements of the methane relaxation times for application to the infrared emission models of the upper atmospheres of outer planets and Titan N90-26759
Intracavity Dye-Laser Absorption Spectroscopy (IDLAS) for application to planetary molecules N90-26761
Methane overtone absorption by intracavity laser spectroscopy N90-26762
Chemical kinetics and modeling of planetary atmospheres N90-26763
A laboratory investigation of the production and properties of molecular and radical species pertinent to planetary atmospheres N90-26766
The applications of chemical thermodynamics and chemical kinetics to planetary atmospheres research N90-26773
Optical constants of solid methane N90-26775
Optical signatures of molecular particles via mass-selected cluster spectroscopy N90-26780
Proton irradiation of simple gas mixtures: Influence of irradiation parameters N90-26782

PLANETARY BASES
Figure of merit studies of beam power concepts for advanced space exploration
[NASA-CR-186720] N90-26234
Press abstracts of the 21st Lunar and Planetary Science Conference
[NASA-CR-186874] N90-26738

PLANETARY COMPOSITION
High resolution infrared spectroscopy of planetary molecules using diode lasers and Fourier transform spectrometers N90-26747

PLANETARY EVOLUTION
Reports of planetary astronomy, 1990
[NASA-TM-4205] N90-26730

PLANETARY GEOLOGY
Directory of research projects: Planetary geology and geophysics program
[NASA-TM-4211] N90-26743

PLANETARY ORBITS
Reports of planetary astronomy, 1990
[NASA-TM-4205] N90-26730

PLANETARY SURFACES
Analysis of a Mars-stationary orbiting microwave power transmission system
[NASA-TM-101344] N90-26172

PLANETARY WAVES
Annual and interannual variations of Earth-emitted radiation based on a 10-year data set
[NASA-TM-103465] N90-26432

PLANNING
Enroute flight planning: The design of cooperative planning systems
[NASA-CR-186797] N90-25964
Structural Mechanics Division research and technology plans for FY 1990 and accomplishments for FY 1989
[NASA-TM-102654] N90-26361
Investigation of automated task learning, decomposition and scheduling
[NASA-CR-186791] N90-26488
Autoplan: A self-processing network model for an extended blocks world planning environment
[NASA-CR-186733] N90-26526

PLASMA COMPOSITION
Vacuum deposition by pulsed laser radiation: Plasma composition, deposition techniques, and thin film properties
[ETN-90-97263] N90-26677

PLASMA CONTROL
Confinement of nonneutral plasma in unconventional geometries
[DE90-013048] N90-26659
The effects of carbonization on the confinement properties of the DIII-D H-mode
[DE90-013297] N90-26660

PLASMA CURRENTS
Effects of ionospheric modification on system performance N90-26202
Application of the results of carbon pellet modeling to the problem of plasma penetration
[DE90-012713] N90-26658
The effects of carbonization on the confinement properties of the DIII-D H-mode
[DE90-013297] N90-26660

PLASMA DIAGNOSTICS
The effects of carbonization on the confinement properties of the DIII-D H-mode
[DE90-013297] N90-26660

PLASMA HEATING
Effects of ionospheric modification on system performance N90-26202
The effects of carbonization on the confinement properties of the DIII-D H-mode
[DE90-013297] N90-26660

PLASMA LAYERS
On the nature of the plasma sheet boundary layer
[DE90-013158] N90-26439

PLASMA PHYSICS
Sensitivity analysis with a simple charging code
[RAE-TM-SPACE-374] N90-26662

PLASMA SHEATHS
Comparison of currents predicted by NASCAP/LEO model simulations with elementary Langmuir-type bare probe models for an insulated cable containing a single pinhole
[NASA-TM-102486] N90-26054

PLASMA-ELECTROMAGNETIC INTERACTION
Effects of ionospheric modification on system performance N90-26202

PLASMAS (PHYSICS)
Sensitivity analysis with a simple charging code
[RAE-TM-SPACE-374] N90-26662

PLASTICS
PVDF contact probes
[VTT-RR-623] N90-26253

PLATES (STRUCTURAL MEMBERS)
Reliability analysis of continuous fiber composite laminates
[NASA-CR-185265] N90-26372

PLATINUM
A resistance strain gage with repeatable and cancellable apparent strain for use to 800 C
[NASA-CR-185256] N90-26063
The application of HREELS to model catalysts: CO and C2H4 adsorption on Pt/Al2O3
[AD-A222744] N90-26103

PLOTTING
Documentation of program Tankplot
[FFI-89/7019] N90-26541

PLUMES
Digital filtering of plume emission spectra
[NASA-TM-103135] N90-26070
Preliminary plume characteristics of an arcjet thruster
[NASA-TM-103241] N90-26071

POINCARE PROBLEM
A new class of exact solutions of the vacuum quadratic Poincare gauge field theory
[MATHS-REPT-A-119] N90-26691
On trivector torsion in vacuum quadratic Poincare gauge field theory
[MATHS-REPT-A-121] N90-26692

POINTING CONTROL SYSTEMS
Application of inertial instruments for DSN antenna pointing and tracking N90-26224

POISSON EQUATION
Nondestructive one- and two-dimensional doping profiling by inverse methods
[ETN-90-97264] N90-26351

POLARIZATION CHARACTERISTICS
Remote sensing of Earth terrain
[NASA-CR-186888] N90-26382

POLICIES
Tools for distributed application management
[NASA-CR-186627] N90-26535
AGARD highlights 90/1 N90-26788

POLLUTION
Pollutants: Production and methods of reduction
[CIT/SME/VKI/RS/6] N90-25990

POLLUTION CONTROL
Catching our breath: Next steps for reducing urban ozone
[PB90-130451] N90-26398

POLLUTION TRANSPORT
Nordic Symposium on Atmospheric Chemistry
[CM-78] N90-26403
Deposition to the Baltic Sea N90-26404
Verification and improvement of the EMEP model for long-range transport and deposition of pollutants N90-26405
An Eulerian transport model for NO(sub x)-compounds N90-26406
The long-term variation of lead-210 in relation to particle-bound sulphur in surface air in Finland N90-26407
Further development and application of an atmospheric chemistry trajectory model N90-26408
The transfer of mercury between the atmosphere and lake or soil surfaces N90-26419
The aqueous atmospheric chemistry of mercury N90-26420

POLYATOMIC MOLECULES
Determination of molecular spectroscopic parameters and energy-transfer rates by double-resonance spectroscopy N90-26755
Kinetics and thermochemistry of polyatomic free radicals: New results and new understandings N90-26764

POLYBUTADIENE
RSRM-9 (360L009): Ballistics mass properties
[NASA-CR-183944] N90-26064

POLYCRYSTALS
Diffusion-accommodated grain boundary sliding in a polycrystal
[DE90-012727] N90-26668

POLYGONS
Hierarchical structure of polygonal data for spatial analysis and representation of cartographical data
[INPE-4986-PRE/1548] N90-26380

POLYIMIDE RESINS
Condensation polyimides
[NASA-TM-103467] N90-26129

POLYIMIDES
Condensation polyimides
[NASA-TM-103467] N90-26129
Fracture toughness of polyimide films
[NASA-TM-103473] N90-26130
Characterization of a thermally imidized soluble polyimide film
[NASA-TM-103484] N90-26131

POLYMER BLENDS
Modelling of the processing of incompatible polymer blends
[ETN-90-97211] N90-26152

POLYMER CHEMISTRY
Quantitative confirmation of diffusion-limited oxidation theories
[DE90-012997] N90-26143
Fractal structure and fractal time in silica sol-gels
[DE90-013197] N90-26144
One-dimensional sigma-conjugated polysilylenes: Science and technology
[DE90-012902] N90-26146
Development of microencapsulation techniques
[AD-A223032] N90-26159

POLYMER PHYSICS
Modelling of the processing of incompatible polymer blends
[ETN-90-97211] N90-26152

POLYMERIC FILMS
Characterization of a thermally imidized soluble polyimide film
[NASA-TM-103484] N90-26131
Development of membrane process for carbon dioxide separation from diving atmosphere
[AD-A222606] N90-26504

POLYMERIZATION
Condensation polyimides
[NASA-TM-103467] N90-26129
Characterization of a thermally imidized soluble polyimide film
[NASA-TM-103484] N90-26131

POLYNOMIALS
Search of primitive polynomials over finite fields
[IMAG-RR-797-M] N90-26607
Calculation of the algebraic curves parameterization: Hamburger-Noether expansions
[IMAG-RR-798-M] N90-26608
Efficient implementation of minimal polynomial and reduced rank extrapolation methods
[NASA-TM-103240] N90-26616

POPULATIONS
A study of the influence of Hg(6(3)P2) population in a low-pressure discharge on mercury ion emission at 194.2 nm N90-26223
Proceedings of a workshop on Differences Between Antarctic and Non-Antarctic Meteorites
[NASA-CR-184918] N90-26740

POROSITY
Regenerative Cu La zeolite supported desulfurizing sorbents
[NASA-CASE-NPO-17480-1-CU] N90-26098
The interaction of polymeric materials with ceramic surfaces with special reference to the behaviour of bioceramics N90-26127

PORPHYRINS
Electrochemical, in situ Raman spectroscopic, and conductivity studies of polypyrrole incorporating large size anions: Conducting nature of reduced form
[AD-A222739] N90-26102

POSITION (LOCATION)
Qualitative evaluation of a conformal velocity vector display for use at high angles-of-attack in fighter aircraft
[NASA-TM-102629] N90-25981
A reduced-dynamic technique for precise orbit determination N90-26219

Electromagnetic inverse scattering of buried objects
[ETN-90-97216] N90-26242
Video camera system for locating bullet holes in targets at a ballistics tunnel
[NASA-TM-4197] N90-26296
Position control of redundant manipulators using an adaptive error-based control scheme
[NASA-CR-186812] N90-26578

POSITION ERRORS
Continuous on-line link error rate detector
[AD-D014510] N90-26209

POSITION SENSING
Assembly via disassembly: A case in machine perceptual development
[NASA-CR-186867] N90-26497

POSITIONING
Alignment positioning mechanism
[NASA-CASE-MSC-21502-1] N90-26341
Eye tracking device for the measurement of flight performance in simulators
[AD-A220075] N90-26484
Beam rider for an Articulated Robot Manipulator (ARM) accurate positioning of long flexible manipulators
[NASA-CR-185151] N90-26581

POSITRONS
A study of positrons from Soviet nuclear powered satellites as tracers for magnetospheric research
[DE90-013157] N90-26438

POSTFLIGHT ANALYSIS
An automated calibration laboratory for flight research instrumentation: Requirements and a proposed design approach
[NASA-TM-101719] N90-26564

POTENTIAL FIELDS
Nonpotential magnetic fields at sites of gamma ray flares
[NASA-TM-103493] N90-26785

POWDER (PARTICLES)
Synthesis of high purity sinterable silicon carbide powder
[DE90-012029] N90-26084
The EISI (Elemental and Interplanar Spacing Index) index: A search/match tool for electron diffraction phase analysis
[DE90-010832] N90-26097

POWDER METALLURGY
The influence of microstructure on the tensile behavior of an aluminum metal matrix composite
[NASA-TM-102694] N90-26082
Metal matrix composites and powder processing for aero-engine applications
[PNR90617] N90-26087

POWER BEAMING
Figure of merit studies of beam power concepts for advanced space exploration
[NASA-CR-186720] N90-26234

POWER SPECTRA
Formation of design envelope criterion in terms of deterministic spectral procedure
[RAE-TM-SS-9] N90-25953

PRECIPITATION (METEOROLOGY)
Some results from the precipitation chemistry measurement programme in Sweden N90-26410
The aqueous atmospheric chemistry of mercury N90-26420

PREDICTION ANALYSIS TECHNIQUES
Efficiency study comparing two helicopter planetary reduction stages
[NASA-TM-103106] N90-26334
Investigation of crack-closure prediction models for fatigue in aluminium alloy sheet under flight-simulation loading
[LR-619] N90-26369
Modeling and optimization of a regenerative fuel cell system using the ASPEN process simulator
[NASA-TM-103210] N90-26396
Aeroacoustics of advanced propellers
[NASA-TM-103137] N90-26635

PREDICTIONS
An investigation into the numerical prediction of boundary layer transition using the K.Y. Chien turbulence model
[NASA-CR-185252] N90-26269
Elevated temperature crack growth
[NASA-CR-182247] N90-26355
An expert system based software sizing tool, phase 2
[NASA-CR-186706] N90-26525
Laboratory measurements and methane photochemistry modeling N90-26770

PREDICTOR-CORRECTOR METHODS
Numerical analysis of three-dimensional particle-laden flow equations
[IAR-90-2] N90-26268

PREMIXING
Turbulent combustion modeling for turbo-jet combustion chambers N90-25993

PREPROCESSING
Run-time parallelization and scheduling of loops
[NASA-CR-182039] N90-26509

PRESSURE BROADENING
Determination of molecular spectroscopic parameters and energy-transfer rates by double-resonance spectroscopy N90-26755

PRESSURE DEPENDENCE
Pressure dependence of thermoelectric power of high T(sub c) 123 compound
[PD-MT-9001] N90-26092

PRESSURE DISTRIBUTION
Aerodynamic loads and blade vortex interaction noise prediction
[ISL-PU-310/89] N90-25942
Application of laminar flow control to supersonic transport configurations
[NASA-CR-181917] N90-25944

PRESSURE SUITS
Aircrew life support systems enhancement
[AD-A222626] N90-26505

PRESSURIZED CABINS
Long cycle pressurized logistics module: An Italian contribution to the Space Station Freedom logistics scenario
[IAF-89-083] N90-26058

PRETREATMENT
The effects of pretreatment conditions on a Pt/SnO2 catalyst for the oxidation of CO in CO2 lasers
[NASA-TM-103487] N90-26309

PRIMARY BATTERIES
NASA aerospace flight battery systems program
[NASA-TM-103237] N90-26397

PROBABILITY DISTRIBUTION FUNCTIONS
Evaluation of a decomposition approach for real-time scheduling using a Stochastic model
[AD-A222726] N90-26525

PROBABILITY THEORY
Statistical treatment of slow strain rate data for assessment of hydrogen embrittlement in low alloy high strength steel
[ARL-MAT-R-122] N90-26106
A new technique in the global reliability of cyclic communications network
[NASA-TM-103479] N90-26214
The variably trimmed mean CFAR detector for nonhomogeneous background
[AD-A222801] N90-26243
Design of ceramic components with the NASA/CARES computer program
[NASA-TM-102369] N90-26359
Software requirements: Guidance and control software development specification
[NASA-CR-182058] N90-26527
Closed-form solution of decomposable stochastic models
[NASA-TM-103466] N90-26619

PROBLEM SOLVING
Enroute flight planning: The design of cooperative planning systems
[NASA-CR-186797] N90-25964
Informatics aspects of large flow calculations on the SX-2 supercomputer
[NLR-MP-88037-U] N90-26290
Reusable rocket engine turbopump health monitoring system, part 3
[NASA-CR-182294] N90-26320
Pilot interaction with automated airborne decision making systems
[NASA-CR-186730] N90-26492
Innovative design systems: Where are we, and where do we go from here
[AD-A222586] N90-26556
Mathematical problem-solving transfer: The effects of cognitive load and attention a schema acquisition and rule automation N90-26594
Unification and disunification: Theory and applications
[ETN-90-97247] N90-26610
Efficient implementation of minimal polynomial and reduced rank extrapolation methods
[NASA-TM-103240] N90-26616
Qualitative and quantitative reasoning about thermodynamics
[NASA-CR-186788] N90-26689
A new class of exact solutions of the vacuum quadratic Poincare gauge field theory
[MATHS-REPT-A-119] N90-26691
On trivector torsion in vacuum quadratic Poincare gauge field theory
[MATHS-REPT-A-121] N90-26692

PROCESS CONTROL (INDUSTRY)
Integrating expert systems with solid modeling through interprocess communications and the applications interface specification
[DE90-012996] N90-26537
On the robust stability of MIMO linear feedback systems
[EUT-88-E-212] N90-26585
A new scheme for identification and control
[EUT-88-E-213] N90-26586

PROGRAM VERIFICATION (COMPUTERS)
Making real-time reactive systems reliable
[NASA-CR-186642] N90-26344
Verification-correction of a program for including uncertainties in the robot automatic programming
[ETN-90-97246] N90-26588

PROGRAMMING LANGUAGES
Object oriented programming
[DE90-011797] N90-26532
Principles of FP2: Term algebras for specification of parallel machines
[RR-789-I-IMAG-98-LIFIA] N90-26571

PROJECT MANAGEMENT
The Telecommunications and Data Acquisition Report
[NASA-CR-186852] N90-26217
Making it happen: Project management
[PNR90618] N90-26695

PROJECT PLANNING
Background, current status, and prognosis of the ongoing slush hydrogen technology development program for the NASP
[NASA-TM-103220] N90-26055

PROJECTILES
A computational study of the effectiveness of coating materials for KE projectile fins subjected to the combined effects of inbore and aerodynamic heating
[AD-A222595] N90-26155

PROP-FAN TECHNOLOGY
Euler analysis comparison with LDV data for an advanced counter-rotation propfan at cruise
[NASA-TM-103249] N90-25946
Structural analysis and optimization of a propfan blade using a finite element method
[DLR-FB-90-01] N90-26006
Aeroacoustics of advanced propellers
[NASA-TM-103137] N90-26635

PROPANE
Critical evaluation of Jet-A spray combustion using propane chemical kinetics in gas turbine combustion simulated by KIVA-2
[NASA-TM-103173] N90-26170
Laboratory studies, analysis, and interpretation of the spectra of hydrocarbons present in planetary atmospheres including cyanoacetylene, acetylene, propane, and ethane N90-26748

PROPELLANT COMBUSTION
Mars in situ propellants: Carbon monoxide and oxygen ignition experiments
[NASA-TM-103202] N90-26065
Temperature and OH concentrations in a solid propellant flame using absorption techniques
[AD-A222591] N90-26100

PROPELLANT GRAINS
RSRM-9 (360L009): Ballistics mass properties
[NASA-CR-183944] N90-26064

PROPELLANT TANKS
Prediction of the ullage gas thermal stratification in a NASP vehicle propellant tank experimental simulation using FLOW-3D
[NASA-TM-103217] N90-26160

PROPELLANT TRANSFER
Initial experimentation on the nonvented fill of a 0.14m3 (5 ft. 3) dewar with nitrogen and hydrogen
[NASA-TM-103155] N90-26278

PROPELLANTS
Mars in situ propellants: Carbon monoxide and oxygen ignition experiments
[NASA-TM-103202] N90-26065

PROPELLER BLADES
Agusta methodology for pitch link loads prediction in preliminary design phase
[ETN-90-97270] N90-25978
Low-speed wind tunnel investigation of the static stability and control characteristics of an advanced turboprop configuration with the propellers placed over the tail
[NASA-CR-186900] N90-26017

PROPELLER FANS
Euler analysis comparison with LDV data for an advanced counter-rotation propfan at cruise
[NASA-TM-103249] N90-25946
Aeroacoustics of advanced propellers
[NASA-TM-103137] N90-26635

PROPELLER SLIPSTREAMS
Development of a system for the numerical simulation of Euler flows, with results of preliminary 3-D propeller-slipstream/exhaust-jet calculations
[NLR-TR-88008-U] N90-26285

PROPELLERS
An unsteady lifting surface method for single rotation propellers
[NASA-CR-4302] N90-25940

Aeroacoustics of advanced propellers
[NASA-TM-103137] N90-26635
PROPULSION
H-infinity based integrated flight-propulsion control design for a STOVL aircraft in transition flight
[NASA-TM-103198] N90-26011
RSRM-9 (360L009): Ballistics mass properties
[NASA-CR-183944] N90-26064
Supersonic reacting internal flow fields
[NASA-TM-103480] N90-26094
PROPULSION SYSTEM PERFORMANCE
The Screem-J4D: A proposal in response to a low Reynolds number station keeping mission
[NASA-CR-186664] N90-25968
The effect of interplanetary trajectory options on a manned Mars aerobrake configuration
[NASA-TP-3019] N90-26036
Supersonic reacting internal flow fields
[NASA-TM-103480] N90-26094
PROPYLENE
Quantitative confirmation of diffusion-limited oxidation theories
[DE90-012997] N90-26143
PROSTHETIC DEVICES
The interaction of polymeric materials with ceramic surfaces with special reference to the behaviour of bioceramics N90-26127
PROTECTION
Carbon-carbon composites: Emerging materials for hypersonic flight
[NASA-TM-103472] N90-26080
On travelling-wave-based protection of high-voltage networks
[ISBN-90-9002955-9] N90-26260
PROTEIN CRYSTAL GROWTH
Protein crystal growth in low gravity
[NASA-CR-186243] N90-26663
PROTEIN SYNTHESIS
Experiment K-6-11. Actin mRNA and cytochrome c mRNA concentrations in the tricepts brachia muscle of rats N90-26465
PROTEINS
Experiment K-6-10. Effects of zero gravity on myofibril protein content and isomyosin distribution in rodent skeletal muscle N90-26464
Experiment K-6-11. Actin mRNA and cytochrome c mRNA concentrations in the tricepts brachia muscle of rats N90-26465
Experiment K-6-14. Hepatic function in rats after spaceflight N90-26468
Experiment K-6-20. The effect of spaceflight on pituitary oxytocin and vasopressin content of rats N90-26473
Proximate composition of seed and biomass from soybean plants grown at different carbon monoxide (CO2) concentrations
[NASA-TM-103496] N90-26480
PROTOCOL (COMPUTERS)
Extension of a noninteractive reliability model for ceramic matrix composites
[NASA-CR-185267] N90-26142
A versatile integrated block codes encoder-decoder N90-26197
MTP: An atomic multicast transport protocol
[NASA-CR-186716] N90-26254
Formal verification of distributed computing systems: Logic characterization of behaviour equivalence
[LAAS-89386] N90-26555
Design of a universal protocol system architecture: Specification of functions and services
[EUT-89-E-230] N90-26569
Analysis of random drop for gateway congestion control
[NASA-CR-186736] N90-26698
Knowledge and inhibition in asynchronous distributed systems
[TR-90-1139] N90-26703
PROTON IRRADIATION
Proton irradiation of simple gas mixtures: Influence of irradiation parameters N90-26782
PROTONS
The charged particle radiation environment for AXAF
[NASA-TM-100405] N90-26741
Investigation of the Saturn dust environment from the analysis of energetic charged particle measurements
[NASA-CR-186727] N90-26784
A site for the astrophysical gamma ray process
[DE90-013473] N90-26787
PROVING
Earth Radiation Budget Experiment (ERBE) validation
[NASA-TM-103481] N90-26433
Formal verification of the JANUS on-line multiplier
[IMAG-RR-785-I] N90-26550
Formal verification of distributed computing systems: Logic characterization of behaviour equivalence
[LAAS-89386] N90-26555
PSYCHOLOGICAL TESTS
Human performance in cockpit-related systems
[NIAR-90-7] N90-26495
PSYCHOPHYSIOLOGY
Psychophysiological assessment of pilot workload in an applied setting
[AD-A222707] N90-26507
PULSE AMPLITUDE
In-band amplitude dispersion on a microwave link N90-26189
PULSE COMMUNICATION
A digital Meteor-Burst Communication (MBC) propagation path simulator N90-26190
PULSE DOPPLER RADAR
Analysis and improved design considerations for airborne pulse Doppler radar signal processing in the detection of hazardous windshear
[NASA-CR-186792] N90-26448
PULSED LASERS
A numerical simulation of the quasi-heterodyne technique for double-pulsed holographic vibration measurements
[PNR90622] N90-26301
Holography and holographic interferometry
[PNR90670] N90-26303
New discharge pumping method for CO2 lasers
[AD-A220898] N90-26307
Vacuum deposition by pulsed laser radiation: Plasma composition, deposition techniques, and thin film properties
[ETN-90-97263] N90-26677
PUMPS
Performance evaluation of LE-7 high pressure pumps
[DE90-505523] N90-26034
PURITY
Synthesis of high purity sinterable silicon carbide powder
[DE90-012029] N90-26084
PYROLYTIC MATERIALS
Polymeric aluminasilazane precursors for aluminosilicon nitride
[AD-A222755] N90-26158
PYRROLES
Electrochemical, in situ Raman spectroscopic, and conductivity studies of polypyrrole incorporating large size anions: Conducting nature of reduced form
[AD-A222739] N90-26102

Q

QUADRATURES
QPSK loop lock detection in the advanced receiver N90-26230
Gaussian quadrature exponential sum modeling of near infrared methane laboratory spectra obtained at temperatures from 106 to 297 K N90-26758
QUADRUPOLES
Inhomogeneous electric field effects in a linear RF quadruple trap N90-26222
QUALIFICATIONS
QM-8 final performance evaluation report: SEALS, volume 4
[NASA-CR-183958] N90-26324
Qualification of concentrating mirror systems with the HERMES measurement system and the HELIOS simulation program
[DLR-FB-89-51] N90-26394
QUALITY CONTROL
Space shuttle: Follow-up evaluation of NASA's solid rocket motor procurement. Report to the Chairman, Committee on Government Operations, House of Representatives
[GAO/NSIAD-89-89] N90-26066
Characterization of inspection performance
[NLR-MP-88068-U] N90-26350
Dendritic web silicon photovoltaic cell research
[DE90-011786] N90-26387
QUANTILES
Variance reduction for quantile estimates in simulations via nonlinear controls
[AD-A222653] N90-26590
QUANTITATIVE ANALYSIS
Neural networks for real-time sensory data processing and sensorimotor control
[AD-A223096] N90-26592
Qualitative and quantitative reasoning about thermodynamics
[NASA-CR-186788] N90-26689
QUANTUM CHEMISTRY
Molecular interactions and properties with many-body methods
[AD-A222631] N90-26642
QUANTUM ELECTRODYNAMICS
Quantum ballistic and adiabatic electron transport, studied with quantum point contacts
[ETN-90-97262] N90-26440
QUANTUM ELECTRONICS
Quantum ballistic and adiabatic electron transport, studied with quantum point contacts
[ETN-90-97262] N90-26440
QUANTUM MECHANICS
Important experiments to test for longer-ranged new gravitational forces
[DE90-012102] N90-26434
A research program in theoretical high energy physics
[DE90-013322] N90-26648
QUANTUM THEORY
Excimer laser fragmentation studies of selected oximes: Nascent OH internal energy distributions and the search of H2CN fluorescence
[AD-A222622] N90-26317
QUANTUM WELLS
Multicolor infrared photodetector
[AD-D014511] N90-26297
QUARTZ
Resistivity, adhesive strength, and residual stress measurements of thin film metallizations on single crystal quartz
[DE90-011902] N90-26135
QUENCHING (ATOMIC PHYSICS)
Rotational and translational effects in collisions of electronically excited diatomic hydrides
[NASA-CR-186770] N90-26093
QUENCHING (COOLING)
Undercooling and solidification
[DLR-FB-90-020] N90-26678
QUEUEING THEORY
Computer architecture evaluation for structural dynamics computations: Project summary
[NASA-CR-186137] N90-26512
Estimating the parameters of a sporadically observed queue
[DE90-012903] N90-26596

R

RADAR
The variably trimmed mean CFAR detector for nonhomogeneous background
[AD-A222801] N90-26243
RADAR ASTRONOMY
Laboratory measurements and modeling of microwave absorption by ammonia in gas mixtures applicable to giant planet atmospheres N90-26750
RADAR CORNER REFLECTORS
Scattering from coated structures and antenna pattern control using impedance surfaces, part A/B
[NASA-CR-186871] N90-26233
RADAR IMAGERY
The browse file of NASA/JPL quick-look radar images from the Loch Linnhe 1989 experiment
[NASA-CR-186855] N90-26701
RADAR MEASUREMENT
Estimation of convective rain volumes utilizing the are-time-integral technique
[NASA-CR-186814] N90-26449
Development of eye-safe lidar for aerosol measurements
[NASA-CR-186905] N90-26503
RADAR TRACKING
Laser radar angular tracking
[AD-A222741] N90-26319
RADAR TRANSMISSION
Software set-up for data processing of depolarization due to rain and ice crystals in the Olympus project
[EUT-89-E-218] N90-26240
RADIANCE
The 27-28 October 1986 FIRE IFO Cirrus case study: Comparison of radiative transfer theory with observations by satellite and aircraft
[NASA-TM-103468] N90-26440
RADIANT FLUX DENSITY
Qualification of concentrating mirror systems with the HERMES measurement system and the HELIOS simulation program
[DLR-FB-89-51] N90-26394
Computer modeling wave propagation with a variation of the Helmholtz-Kirchhoff relation
[AD-A222746] N90-26657
RADIATION DAMAGE
The effect of crystal orientation on damage accumulation in chromium-implanted Al2O3
[DE90-012294] N90-26674
RADIATION DISTRIBUTION
Application and extension of an analytical model of the confined acoustic beam generated by a transducer
[AD-A222994] N90-26639

RADIATION DOSAGE
The US Experiments Flown on the Soviet Biosatellite Cosmos 1887
[NASA-TM-102254] N90-26452
Experiment K-6-24, K-6-25, K-6-26. Radiation dosimetry and spectrometry N90-26477
RADIATION EFFECTS
Experiment K-6-16. Morphological examination of rat testes. The effect of Cosmos 1887 flight on spermatogonial population and testosterone level in rat testes N90-26469
Experiment K-6-24, K-6-25, K-6-26. Radiation dosimetry and spectrometry N90-26477
The charged particle radiation environment for AXAF
[NASA-TM-100405] N90-26741
RADIATION SHIELDING
Experiment K-6-24, K-6-25, K-6-26. Radiation dosimetry and spectrometry N90-26477
RADIATION SOURCES
High resolution spectroscopy in the microwave and far infrared N90-26746
RADIATIVE LIFETIME
Measurements of the methane relaxation times for application to the infrared emission models of the upper atmospheres of outer planets and Titan N90-26759
The heat of formation of CN radicals and radiative lifetimes of the A 1 Sigma - state of C2N2 N90-26765
RADIATIVE TRANSFER
The 27-28 October 1986 FIRE IFO Cirrus case study: Comparison of radiative transfer theory with observations by satellite and aircraft
[NASA-TM-103466] N90-26446
RADICALS
The heat of formation of CN radicals and radiative lifetimes of the A 1 Sigma - state of C2N2 N90-26765
A laboratory investigation of the production and properties of molecular and radical species pertinent to planetary atmospheres N90-26766
Role of the methylene amidogen (H2CN) radical in the atmospheres of Titan and Jupiter N90-26769
Laboratory studies of photodissociation processes relevant to the formation of cometary radicals N90-26772
RADIO COMMUNICATION
Propagation Effects and Circuit Performance of Modern Military Radio Systems with Particular Emphasis on Those Employing Bandspreading
[AGARD-CP-442] N90-26178
An overview of Canadian radio propagation/communications technologies research N90-26179
Progress and remaining issues in the development of a wideband HF channel model and simulation N90-26182
Broadband analysis of ground wave propagation at a50 to 400 MHz N90-26185
CORA: A direct sequence spread spectrum radio for voice and data N90-26195
Experimentation of a transmission system data processing by meteor bursts N90-26207
Continuous on-line link error rate detector
[AD-D014510] N90-26209
RADIO EQUIPMENT
A novel communication network simulator
[AD-A223045] N90-26248
RADIO FILTERS
Surface acoustic wave filters in ZnO-SiO2-Si layered structures: Design, technology, and monolithic integration with electronic circuitry
[ETN-90-97218] N90-26638
RADIO FREQUENCIES
Analysis of a Mars-stationary orbiting microwave power transmission system
[NASA-TM-101344] N90-26172
Radio channel measurement and modelling for future mobile radio systems N90-26184
Measurement and simulation of widespread mobile radio channel characteristics N90-26186
Estimation of the impulse response of a broadband mobile radio channel in suburbia at 910 MHz N90-26187
A narrowband tactical communication system for the VHF and UHF mobile radio bands N90-26192
Multiple-access techniques for communication over dispersive radio channels N90-26196
Experimental study of a digital mobile radio spread spectrum in an urban site N90-26205
Inhomogeneous electric field effects in a linear RF quadruple trap N90-26222
DSS 15, 45, and 65 34-meter high efficiency antenna radio frequency performance enhancement by tilt added to the subreflector during elevation angle changes N90-26229
RADIO FREQUENCY INTERFERENCE
Propagation Effects and Circuit Performance of Modern Military Radio Systems with Particular Emphasis on Those Employing Bandspreading
[AGARD-CP-442] N90-26178
A global common-user system for the provision of HF propagation data N90-26180
Experimental analysis of the HF linkage N90-26181
Progress and remaining issues in the development of a wideband HF channel model and simulation N90-26182
RADIO GALAXIES
Radio loud far-infrared galaxies
[DE90-012993] N90-26786
RADIO OCCULTATION
Laboratory measurements of microwave and millimeter-wave properties of planetary constituents N90-26745
Laboratory measurements and modeling of microwave absorption by ammonia in gas mixtures applicable to giant planet atmospheres N90-26750
RADIO RECEIVERS
A global common-user system for the provision of HF propagation data N90-26180
RADIO SPECTRA
Experimental study of a digital mobile radio spread spectrum in an urban site N90-26205
RADIO TRANSMISSION
An overview of Canadian radio propagation/communications technologies research N90-26179
Optimal synchronization of spread spectrum sequenced by nontransferable switching operators N90-26183
Radio channel measurement and modelling for future mobile radio systems N90-26184
Measurement and simulation of widespread mobile radio channel characteristics N90-26186
Wideband characterization of forest propagation channels N90-26188
Man-made noise in a military environment N90-26191
Multiple-access techniques for communication over dispersive radio channels N90-26196
Minimization of the cost of information transfer in HF spread spectrum transmission N90-26198
New synchronisation techniques applicable to multi-tone transmission systems N90-26199
Effects of ionospheric modification on system performance N90-26202
Combined effects of fast and selective fading on performance of PSK and MSK with coherent detection N90-26204
Packet radio network concepts for the Norwegian field army N90-26206
RADIO TRANSMITTERS
A global common-user system for the provision of HF propagation data N90-26180
Preliminary error budget for an optical ranging system: Range, range rate, and differenced range observables N90-26227
RADIO WAVES
Astronomy at ultra-high energies: Results from the CYGNUS experiment
[DE90-011979] N90-26732
RADIOACTIVE DECAY
The long-term variation of lead-210 in relation to particle-bound sulphur in surface air in Finland N90-26407
RADIOACTIVE ISOTOPES
The long-term variation of lead-210 in relation to particle-bound sulphur in surface air in Finland N90-26407
RADIOBIOLOGY
Experiment K-6-24, K-6-25, K-6-26. Radiation dosimetry and spectrometry N90-26477
RADIOGRAPHY
Experiment K-6-27. Analysis of radiographs and biosamples from primate studies N90-26478
Soft x ray resist characterization: Studies with a laser plasma x ray source
[DE90-013493] N90-26661
RADIOMETERS
Annual and interannual variations of Earth-emitted radiation based on a 10-year data set
[NASA-TM-103465] N90-26432
RADIOMETRIC CORRECTION
Atmospheric correction of thematic mapping measurements about seabeds of the German Bay
[GKSS-89/E/47] N90-26029
RAIN
Natural and anthropogenic compounds in bulk precipitation at Blidoe (archipelago of Stockholm, Sweden) N90-26409
Estimation of convective rain volumes utilizing the are-time-integral technique
[NASA-CR-186814] N90-26449
RAMAN LASERS
Analysis of turbulent density fluctuations by means of spontaneous Raman diffusion
[ISL-R-103/89] N90-26287
Laser techniques for studying chemical vapor deposition
[DE90-012921] N90-26311
RAMAN SPECTRA
Molecular structure of interphases between DGEBA/BTDA adhesives and silver substances using surface-enhanced Raman scattering
[AD-A222750] N90-26157
Analysis of turbulent density fluctuations by means of spontaneous Raman diffusion
[ISL-R-103/89] N90-26287
Development of eye-safe lidar for aerosol measurements
[NASA-CR-186905] N90-26503
RAMAN SPECTROSCOPY
Electrochemical, in situ Raman spectroscopic, and conductivity studies of polypyrrole incorporating large size anions: Conducting nature of reduced form
[AD-A222739] N90-26102
Short-range structure of fluorine-modified phosphate glass
[DE90-013494] N90-26145
RAMJET ENGINES
Gas Turbine Combustion, volume 1
[VKI-LS-1990-02-VOL-1] N90-25985
Liquid fueled ramjet combustion instability: Acoustical and vortical interactions with burning sprays
[AD-A222752] N90-26104
RANDOM ACCESS MEMORY
Self-checking on-line testable static RAM
[NASA-CASE-NPO-17939-1-CU] N90-26518
High speed magneto-resistive random access memory
[NASA-CASE-NPO-17954-1-CU] N90-26519
RANDOM NOISE
Multiple-access techniques for communication over dispersive radio channels N90-26196
RANDOM VARIABLES
Dichotomies for certain product measures and stable processes
[AD-A222568] N90-26621
RANGE AND RANGE RATE TRACKING
Preliminary error budget for an optical ranging system: Range, range rate, and differenced range observables N90-26227
RANGEFINDING
Preliminary error budget for an optical ranging system: Range, range rate, and differenced range observables N90-26227
RASTER SCANNING
Rotating-unbalanced-mass devices and methods for scanning balloon-borne-experiments, free-flying spacecraft, and space shuttle/space station attached experiments
[NASA-CASE-MFS-28425-1] N90-26304
RATS
Effects of microgravity on rat muscle N90-26453
Effects of microgravity on rat bone, cartilage and connective tissues N90-26454
Experiment K-6-01. Distribution and biochemistry of mineral and matrix in the femurs of rats N90-26455
Experiment K-6-03. Gravity and skeletal growth, part 1. Part 2: Morphology and histochemistry of bone cells and vasculature of the tibia; Part 3: Nuclear volume analysis of osteoblast histogenesis in periodontal ligament cells; Part 4: Intervertebral disc swelling pressure associated with microgravity N90-26457
Experiment K-6-04. Trace element balance in rats during spaceflight N90-26458
Experiment K-6-05. The maturaton of bone and dentin matrices in rats flown on Cosmos 1887 N90-26459
Experiment K-6-06. Morphometric and EM analyses of tibial epiphyseal plates from Cosmos 1887 rats N90-26460
Experiment K-6-08. Biochemical and histochemical observations of vastus medialis N90-26462
Experiment K-6-09. Morphological and biochemical investigation of microgravity-induced nerve and muscle breakdown. Part 1: Investigation of nerve and muscle breakdown during spaceflight; Part 2: Biochemical analysis of EDL and PLT muscles N90-26463
Experiment K-6-10. Effects of zero gravity on myofibril protein content and isomyosin distribution in rodent skeletal muscle N90-26464
Experiment K-6-11. Actin mRNA and cytochrome c mRNA concentrations in the tricepts brachia muscle of rats N90-26465
Experiment K-6-12. Morphometric studies of atrial or granules and hepatocytes. Part 1: Morphometric study of the liver; Part 2: The atrial granular accumulations N90-26466

Experiment K-6-13. Morphological and biochemical examination of heart tissue. Part 1: Effects of microgravity on the myocardial fine structure of rats flown on Cosmos 1887. Ultrastructure studies. Part 2: Cellular distribution of cyclic ampdependent protein kinase regulatory subunits in heart muscle of rats flown on Cosmos 1887 N90-26467

Experiment K-6-14. Hepatic function in rats after spaceflight N90-26468

Experiment K-6-16. Morphological examination of rat testes. The effect of Cosmos 1887 flight on spermatogonial population and testosterone level in rat testes N90-26469

Experiment K-6-17. Structural changes and cell turnover in the rats small intestine induced by spaceflight N90-26470

Experiment K-6-18. Study of muscarinic and gaba (benzodiazepine) receptors in the sensory-motor cortex, hippcampus and spinal code N90-26471

Experiment K-6-19. Pineal physiology in microgravity: Relation to rat gonadal function N90-26472

Experiment K-6-20. The effect of spaceflight on pituitary oxytocin and vasopressin content of rats N90-26473

Experiment K-6-22. Growth hormone regulation, synthesis and secretion in microgravity. Part 1: Somatotroph physiology. Part 2: Immunohistochemical analysis of hypothalamic hormones. Part 3: Plasma analysis N90-26475

Experiment K-6-23. Effect of spaceflight on levels and function of immune cells N90-26476

REACTION KINETICS

Synthesis of high purity sinterable silicon carbide powder
[DE90-012029] N90-26084

Carbon deposition model for oxygen-hydrocarbon combustion. Task 6: Data analysis and formulation of an empirical model
[NASA-CR-183986] N90-26095

Liquid fueled ramjet combustion instability: Acoustical and vortical interactions with burning sprays
[AD-A222752] N90-26104

Chemical structure and kinetics at liquid/solid interfaces
[AD-A222766] N90-26105

Critical evaluation of Jet-A spray combustion using propane chemical kinetics in gas turbine combustion simulated by KIVA-2
[NASA-TM-103173] N90-26170

Formation kinetics of N2O in the atmosphere N90-26425

First International Conference on Laboratory Research for Planetary Atmospheres
[NASA-CP-3077] N90-26744

Novel laser gain and time-resolved FTIR studies of photochemistry N90-26756

Chemical kinetics and modeling of planetary atmospheres N90-26763

Kinetics and thermochemistry of polyatomic free radicals: New results and new understandings N90-26764

The heat of formation of CN radicals and radiative lifetimes of the A 1 Sigma - state of C2N2 N90-26765

A laboratory investigation of the production and properties of molecular and radical species pertinent to planetary atmospheres N90-26766

Rate constant for reaction of atomic hydrogen with germane N90-26768

Role of the methylene amidogen (H2CN) radical in the atmospheres of Titan and Jupiter N90-26769

Laboratory measurements and methane photochemistry modeling N90-26770

The applications of chemical thermodynamics and chemical kinetics to planetary atmospheres research N90-26773

REACTION TIME

The retrieval of information from secondary memory: A review and new findings
[AD-A222760] N90-26489

REACTIVITY

Making real-time reactive systems reliable
[NASA-CR-186642] N90-26344

REACTOR MATERIALS

Multimegawatt space nuclear power supply, phase 1. Supplement: D180-30619-8
[DE90-012433] N90-26647

REACTOR SAFETY

Multimegawatt space nuclear power supply, phase 1. Volume 2: Phase 2 plan D180-30619-6
[DE90-012431] N90-26645

Multimegawatt space nuclear power supply, phase 1. Volume 3: Annotated outline of preliminary safety assessment D180-30619-7
[DE90-012432] N90-26646

REACTOR TECHNOLOGY

Multimegawatt space nuclear power supply, phase 1. Volume 3: Annotated outline of preliminary safety assessment D180-30619-7
[DE90-012432] N90-26646

REAL TIME OPERATION

Methods and apparatus for providing real-time control of a gaseous propellant rocket propulsion system
[NASA-CASE-MSC-21542-1] N90-26073

Real-time monitoring of ceramic sintering with laser ultrasonics
[DE90-012960] N90-26140

Guidance and control system for an autonomous underwater vehicle
[AD-A222709] N90-26343

Making real-time reactive systems reliable
[NASA-CR-186642] N90-26344

A real-time optical 3D tracker for head-mounted display systems
[AD-A222747] N90-26508

ISIS and META projects
[NASA-CR-186645] N90-26524

Software requirements: Guidance and control software development specification
[NASA-CR-182058] N90-26527

Tools for distributed application management
[NASA-CR-186627] N90-26535

A real-time robot arm collision detection system
[NASA-CR-185878] N90-26582

Neural networks for real-time sensory data processing and sensorimotor control
[AD-A223096] N90-26592

The browse file of NASA/JPL quick-look radar images from the Loch Linnhe 1989 experiment
[NASA-CR-186855] N90-26701

RECEIVERS

Antennas for portable VHF-FM receivers
[BBC-RD-1990/1] N90-26211

A novel multireceiver communications system configuration based on optimal estimation theory
[NASA-CR-186847] N90-26216

A two-telescope receiver design for deep space optical communications N90-26226

QPSK loop lock detection in the advanced receiver N90-26230

RECEPTION DIVERSITY

In-band amplitude dispersion on a microwave link N90-26189

RECIPROCITY THEOREM

Electromagnetic inverse scattering of buried objects
[ETN-90-97216] N90-26242

RECOMBINATION REACTIONS

Application of InAlAs/GaAs superlattice alloys to GaAs solar cells
[DE90-013070] N90-26389

RECONNAISSANCE AIRCRAFT

Global Sentry: NASA/USRA high altitude reconnaissance aircraft design, volume 2
[NASA-CR-186820-VOL-2] N90-25971

RECORDS MANAGEMENT

Space operations: NASA is not properly safeguarding valuable data from past missions
[GAO/IMTEC-90-1] N90-26704

RECTENNAS

Analysis of a Mars-stationary orbiting microwave power transmission system
[NASA-TM-101344] N90-26172

RECTIFIERS

A model of the synchronous machine with rectifier, especially for control purposes
[EUT-89-E-215] N90-26256

A possibility to incorporate saturation in the simple, global model of a synchronous machine with rectifier
[EUT-89-E-225] N90-26258

RECURSIVE FUNCTIONS

Large sets of block designs
[ETN-90-97212] N90-26602

REDUCED GRAVITY

Fluid Phase Separation (FPS) experiment for flight on a space shuttle Get Away Special (GAS) canister
[NASA-CR-186830] N90-26161

New findings and instrumentation from the NASA Lewis microgravity facilities
[NASA-TM-103189] N90-26163

Bubble, Drop and Particle Unit (BDPU): A multi-user microgravity facility
[IAF-89-431] N90-26164

Low-gravity fluid physics: A program overview
[NASA-TM-103215] N90-26273

The US Experiments Flown on the Soviet Biosatellite Cosmos 1887
[NASA-TM-102254] N90-26452

Effects of microgravity on rat muscle N90-26453

Effects of microgravity on rat bone, cartilage and connective tissues N90-26454

Experiment K-6-03. Gravity and skeletal growth, part 1. Part 2: Morphology and histochemistry of bone cells and vasculature of the tibia; Part 3: Nuclear volume analysis of osteoblast histogenesis in periodontal ligament cells; Part 4: Intervertebral disc swelling pressure associated with microgravity N90-26457

Experiment K-6-04. Trace element balance in rats during spaceflight N90-26458

Experiment K-6-05. The maturaton of bone and dentin matrices in rats flown on Cosmos 1887 N90-26459

Experiment K-6-06. Morphometric and EM analyses of tibial epiphyseal plates from Cosmos 1887 rats N90-26460

Experiment K-6-08. Biochemical and histochemical observations of vastus medialis N90-26462

Experiment K-6-12. Morphometric studies of atrial or granules and hepatocytes. Part 1: Morphometric study of the liver; Part 2: The atrial granular accumulations N90-26466

Experiment K-6-13. Morphological and biochemical examination of heart tissue. Part 1: Effects of microgravity on the myocardial fine structure of rats flown on Cosmos 1887. Ultrastructure studies. Part 2: Cellular distribution of cyclic ampdependent protein kinase regulatory subunits in heart muscle of rats flown on Cosmos 1887 N90-26467

Experiment K-6-17. Structural changes and cell turnover in the rats small intestine induced by spaceflight N90-26470

Experiment K-6-19. Pineal physiology in microgravity: Relation to rat gonadal function N90-26472

Experiment K-6-20. The effect of spaceflight on pituitary oxytocin and vasopressin content of rats N90-26473

Experiment K-6-21. Effect of microgravity on 1) metabolic enzymes of type 1 and type 2 muscle fibers and on 2) metabolic enzymes, neutransmitter amino acids, and neurotransmitter associated enzymes in motor and somatosensory cerebral cortex. Part 1: Metabolic enzymes of individual muscle fibers; part 2: metabolic enzymes of hippocampus and spinal cord N90-26474

Experiment K-6-22. Growth hormone regulation, synthesis and secretion in microgravity. Part 1: Somatotroph physiology. Part 2: Immunohistochemical analysis of hypothalamic hormones. Part 3: Plasma analysis N90-26475

Protein crystal growth in low gravity
[NASA-CR-186243] N90-26663

REDUNDANCY ENCODING

Channel selection and control procedures in an automatic HF system N90-26193

Conception of a reconfigurable microprocessor
[ETN-90-97248] N90-26517

Multi-sensory perception of a geometrical structure of a scene
[ETN-90-97245] N90-26587

REENTRY VEHICLES

Preliminary subsystem designs for the Assured Crew Return Vehicle (ACRV), volume 1
[NASA-CR-186677-VOL-1] N90-26039

REFLECTANCE

Estimation of the impulse response of a broadband mobile radio channel in suburbia at 910 MHz N90-26187

The 27-28 October 1986 FIRE IFO Cirrus case study: Comparison of radiative transfer theory with observations by satellite and aircraft
[NASA-TM-103468] N90-26446

The 27-28 October 1986 FIRE IFO cirrus case study: Cirrus parameter relationships derived from satellite and lidar data
[NASA-TM-103469] N90-26447

Implementation of sensor and control designs for bioregenerative systems
[NASA-CR-186655] N90-26479

REFLECTOR ANTENNAS

Feasibility study of a synthesis procedure for array feeds to improve radiation performance of large distorted reflector antennas
[NASA-CR-186641] N90-26213

REFLECTORS

Structures for remotely deployable precision antennas
[NASA-CR-182065] N90-26061

REFRACTION

Refractive error analysis in the interferometric measurement of 2-D density fields containing strong gradients
[LR-616] N90-26655

REFRACTIVITY

Laboratory measurements of microwave and millimeter-wave properties of planetary constituents N90-26745

REFRACTORY MATERIALS

Metal matrix composites and powder processing for aero-engine applications
[PNR90617] N90-26087

Densification studies of refractory materials using Hot Isostatic Pressing (HIP) and tantalum containment
[DE90-013481] N90-26114
Development of ceramic hybrid combustor: Design and combustion test results
[DE90-503442] N90-26149

REFRIGERATORS
Multicomponent gas sorption Joule-Thomson refrigerator
[NASA-CASE-NPO-17569-1-CU] N90-26178

REGENERATION (ENGINEERING)
Regenerative Cu La zeolite supported desulfurizing sorbents
[NASA-CASE-NPO-17480-1-CU] N90-26098

REGENERATION (PHYSIOLOGY)
Implementation of sensor and control designs for bioregenerative systems
[NASA-CR-186655] N90-26479

REGENERATIVE FUEL CELLS
The chemical effects of the Martian environment on power system component materials: A theoretical approach
[NASA-TM-103203] N90-26074
Modeling and optimization of a regenerative fuel cell system using the ASPEN process simulator
[NASA-TM-103210] N90-26396

REGISTERS (COMPUTERS)
Atomic snapshots of shared memory
[AD-A222755] N90-26520

REGRESSION ANALYSIS
Variance reduction for quantile estimates in simulations via nonlinear controls
[AD-A222653] N90-26590
Asymptotic optimality of the fast randomized versions of GCV and C(sub L) in ridge regression and regularization
[IMAG-RR-793-M] N90-26606
A study of the asymptotic properties of least square estimators for multiple phase regression problems
[ETN-90-97244] N90-26620
Nonlinear modeling of time series using Multivariate Adaptive Regression Splines (MARS)
[AD-A222710] N90-26623

REGRESSION COEFFICIENTS
Reversed residuals in autoregressive time series analysis
[AD-A222711] N90-26624

REINFORCING FIBERS
Development of ceramic fiber type combustor: Improvement of combustor and combustion test results
[DE90-503441] N90-26148
Time temperature relations during rubber forming continuous fiber reinforced thermoplastics
[LR-620] N90-26151

RELAXATION TIME
Dynamics of micellar oligomeric and monomeric sodium 10-undecenoate
[AD-A222570] N90-26099

RELIABILITY
NASA project status reports: Congressional requirements can be met, but reliability must be ensured
[GAO/NSIAD-90-40] N90-26169
A new technique in the global reliability of cyclic communications network
[NASA-TM-103479] N90-26214
Electronic warfare technology: Trends and visions
[AD-A223034] N90-26246
Statistical analysis of a software reliability model
[IMAG-RR-781-M] N90-26352
A Bayesian proportional model for software reliability
[IMAG-RR-795-M] N90-26353
Interim qualification tests and procedures for terrestrial photovoltaic thin-film flat-plate modules
[DE90-000354] N90-26392
Preliminary designs for 25 kWe advanced Stirling conversion systems for dish electric applications
[NASA-TM-103188] N90-26729

RELIABILITY ANALYSIS
Extension of a noninteractive reliability model for ceramic matrix composites
[NASA-CR-185267] N90-26142
Reliability analysis of continuous fiber composite laminates
[NASA-CR-185265] N90-26372

RELIABILITY ENGINEERING
NDT in aerospace: The next decade (1990's)
[PNR90628] N90-26348
LASER: A Layout Sensitivity Explorer. Report and user's manual
[EUT-89-E-216] N90-26545

REMOTE CONTROL
Lunar articulated remote transportation system
[NASA-CR-186817-VOL-1] N90-26332

REMOTE SENSING
The Telecommunications and Data Acquisition Report
[NASA-CR-186852] N90-26217
Solid-state lasers for coherent communication and remote sensing
[NASA-CR-186634] N90-26306
HIRIS performance study
[NASA-CR-186649] N90-26375
Practical applications of remote sensing technology
[NASA-CR-186810] N90-26377
Classification regions in remote sensing imagery utilizing spatial characteristics
[INPE-4913-PRE/1514] N90-26381
Remote sensing of Earth terrain
[NASA-CR-186888] N90-26382

REMOTELY PILOTED VEHICLES
The Screem-J4D: A proposal in response to a low Reynolds number station keeping mission
[NASA-CR-186664] N90-25968
Literature concerning control and display technology applicable to the Orbital Maneuvering Vehicle (OMV)
[NASA-CR-186790] N90-26048

REMOVAL
Autonomous space processor for orbital debris
[NASA-CR-186691] N90-26044
Mechanical paint removal techniques for aircraft structures
[NIAR-90-12] N90-26166
Assembly via disassembly: A case in machine perceptual development
[NASA-CR-186867] N90-26497

REPORTS
NASA project status reports: Congressional requirements can be met, but reliability must be ensured
[GAO/NSIAD-90-40] N90-26169

REQUIREMENTS
A real-time optical 3D tracker for head-mounted display systems
[AD-A222747] N90-26508

RESCUE OPERATIONS
Mariners Weather Log, volume 33, number 4, Fall 1989
[PB90-146853] N90-26445

RESEARCH AIRCRAFT
Experimental aerothermodynamic research of hypersonic aircraft
[NASA-CR-186903] N90-25954
Technology development: Future use of NASA's large format camera is uncertain
[GAO/NSIAD-90-142] N90-26298
An automated calibration laboratory for flight research instrumentation: Requirements and a proposed design approach
[NASA-TM-101719] N90-26564

RESEARCH AND DEVELOPMENT
Research at NASA's NFAC wind tunnels
[NASA-TM-102827] N90-25933
Wright Research and Development Center test facilities handbook
[AD-A222582] N90-26020

RESEARCH FACILITIES
New findings and instrumentation from the NASA Lewis microgravity facilities
[NASA-TM-103189] N90-26163
Structural Mechanics Division research and technology plans for FY 1990 and accomplishments for FY 1989
[NASA-TM-102654] N90-26361
Structural dynamics branch research and accomplishments
[NASA-TM-102488] N90-26373
Genesis lunar outpost criteria and design
[NASA-CR-186831] N90-26499

RESIDUAL STRESS
Resistivity, adhesive strength, and residual stress measurements of thin film metallizations on single crystal quartz
[DE90-011902] N90-26135
Residual stresses measurements by means of x ray diffraction on electron beam welded joints and laser hardened surfaces
[ETN-90-97269] N90-26371

RESONANCE
New electronic states of NH and ND observed by resonance enhanced multiphoton ionization spectroscopy N90-26760
UV and VUV spectroscopy and photochemistry of small molecules in a supersonic jet N90-26771

RESONANCE FLUORESCENCE
Rate constant for reaction of atomic hydrogen with germane N90-26768

RESONANCE TESTING
Vibration test procedures for orbiter sidewall-mounted payloads, phase 2
[AD-A220774] N90-26038

RESONANT FREQUENCIES
Vibration test procedures for orbiter sidewall-mounted payloads, phase 1
[AD-A220773] N90-26037

RESONANT VIBRATION
Vibration test procedures for orbiter sidewall-mounted payloads, phase 2
[AD-A220774] N90-26038

RETURN TO EARTH SPACE FLIGHT
Winged cargo return vehicle. Volume 1: Conceptual design
[NASA-CR-186823] N90-26050

REUSABLE HEAT SHIELDING
Acousto-optic signature analysis for inspection of the orbiter thermal protection tile bonds
[DE90-013089] N90-26043

RHEOELECTRICAL SIMULATION
Simulation of the electrical and thermal behavior of gapless metal oxide surge arresters under AC-operation condition
[ETN-90-97309] N90-26262

RIDING QUALITY
Human factors: The human interface with aircraft interiors
[NIAR-90-18] N90-26496

RIGID STRUCTURES
Direct drive robotic hand
[NASA-CASE-NPO-17917-1-CU] N90-26339

RIPPLES
Erosion mechanisms in composite materials and ripple formation mechanism in erosion
[IAR-89-4-PT-1] N90-26078
Erosion mechanisms in composite materials and ripple formation mechanism in erosion
[IAR-89-4-PT-2] N90-26079

RISK
Space program: Space debris a potential threat to Space Station and shuttle
[GAO/IMTEC-90-18] N90-26024

RIVETS
Neural networks for detecting defects in aircraft structures
[IAR-90-4] N90-26345

ROADS
Color image processing for navigation: Two road trackers
[AD-A222667] N90-26591

ROBOT ARMS
Control strategy for cooperating disparate manipulators
[NASA-CR-186809] N90-26328
Design of a lunar transportation system, volume 2
[NASA-CR-186833-VOL-2] N90-26333
Direct drive robotic hand
[NASA-CASE-NPO-17917-1-CU] N90-26339
Grasping with mechanical intelligence
[NASA-CR-186864] N90-26498
Beam rider for an Articulated Robot Manipulator (ARM) accurate positioning of long flexible manipulators
[NASA-CR-185151] N90-26581
A real-time robot arm collision detection system
[NASA-CR-185878] N90-26582
Multi-sensory perception of a geometrical structure of a scene
[ETN-90-97245] N90-26587

ROBOT DYNAMICS
An inverse dynamic method yielding flexible manipulator state trajectories
[NASA-CR-186807] N90-26329
Assembly via disassembly: A case in machine perceptual development
[NASA-CR-186867] N90-26497

ROBOT SENSORS
Multi-sensory perception of a geometrical structure of a scene
[ETN-90-97245] N90-26587

ROBOTICS
Lunar deep drill apparatus
[NASA-CR-182756] N90-26322
Twilight zones and cornerstones: A gnat robot double feature
[AD-A220026] N90-26326
Power saw
[NASA-CASE-MSC-21469-1] N90-26340
Robotic-aided system for inspection of aging aircraft
[NIAR-90-9] N90-26346
Grasping with mechanical intelligence
[NASA-CR-186864] N90-26498
Neural networks for real-time sensory data processing and sensorimotor control
[AD-A223096] N90-26592

ROBOTS
Twilight zones and cornerstones: A gnat robot double feature
[AD-A220026] N90-26326
Design and construction of a wall-climbing robot
[NIAR-90-20] N90-26327
Control strategy for cooperating disparate manipulators
[NASA-CR-186809] N90-26328

University of Maryland walking robot: A design project for undergraduate students
[NASA-CR-186839] N90-26331
Robotic-aided system for inspection of aging aircraft
[NIAR-90-9] N90-26346
Space station definitions, design, and development. Task 5: Multiple arm telerobot coordination and control: Manipulator design methodology
[NASA-CR-182043] N90-26577
Verification-correction of a program for including uncertainties in the robot automatic programming
[ETN-90-97246] N90-26588

ROBUSTNESS (MATHEMATICS)
Robustness evaluation of H2 and H(infinity) control theory as applied to a transport aircraft
[AD-A222795] N90-26018
On controller choice for robust sliding mode performance
[MATHS-REPT-A-107] N90-26337
Direct drive robotic hand
[NASA-CASE-NPO-17917-1-CU] N90-26339
Intergration of system identification and robust controller designs for flexible structures in space
[NASA-TM-102695] N90-26362
On the robust stability of MIMO linear feedback systems
[EUT-88-E-212] N90-26585

ROCKET ENGINES
Hard start problem of the apogee engine for the ETS-6
[DE90-505525] N90-26072
QM-8 final performance evaluation report: SEALS, volume 4
[NASA-CR-183958] N90-26324

ROCKET OXIDIZERS
Hard start problem of the apogee engine for the ETS-6
[DE90-505525] N90-26072

RODENTS
Experiment K-6-10. Effects of zero gravity on myofibril protein content and isomyosin distribution in rodent skeletal muscle N90-26464

RODS
Plate rods and leaf springs with hybrid structure: Cross section optimization following different target criteria
[ILR-MITT-227(1989)] N90-26366

ROTARY ENGINES
Performance of a supercharged direct-injection stratified-charge rotary combustion engine
[NASA-TM-103105] N90-25982
Computational experience with a three-dimensional rotary engine combustion model
[NASA-TM-103104] N90-26275

ROTARY WING AIRCRAFT
AGARD highlights 90/1 N90-26788

ROTATING SHAFTS
Active lag angle device
[AD-D014538] N90-26249

ROTATION
An unsteady lifting surface method for single rotation propellers
[NASA-CR-4302] N90-25940
Rotating-unbalanced-mass devices and methods for scanning balloon-borne-experiments, free-flying spacecraft, and space shuttle/space station attached experiments
[NASA-CASE-MFS-28425-1] N90-26304

ROTATIONAL SPECTRA
High resolution spectroscopy in the microwave and far infrared N90-26746
Microwave spectra of van der Waals complexes of importance in planetary atmospheres N90-26752

ROTOR BLADES
Synthesis of individual rotor blade control system for gust alleviation
[NASA-TM-101886] N90-25972

ROTOR DYNAMICS
The applicability of simple helicopter models for flight mechanics studies
[ETN-90-96962] N90-25975

ROTORS
An unsteady lifting surface method for single rotation propellers
[NASA-CR-4302] N90-25940
Two-dimensional Euler and Navier-Stokes Time accurate simulations of fan rotor flows
[NASA-TM-102402] N90-25948
Development of creep-fatigue damage detection method of rotor steel by ultrasonic wave measurement
[DE90-503792] N90-26365

ROUTES
Adaptive fault-tolerant routing in hypercube multicomputers
[NASA-CR-186781] N90-26513

ROVING VEHICLES
University of Maryland walking robot: A design project for undergraduate students
[NASA-CR-186839] N90-26331
Autoplan: A self-processing network model for an extended blocks world planning environment
[NASA-CR-186733] N90-26526

RUBBER
Quantitative confirmation of diffusion-limited oxidation theories
[DE90-012997] N90-26143

RUN TIME (COMPUTERS)
Run-time parallelization and scheduling of loops
[NASA-CR-182039] N90-26509

RUNGE-KUTTA METHOD
Two-dimensional Euler and Navier-Stokes Time accurate simulations of fan rotor flows
[NASA-TM-102402] N90-25948

RUNWAYS
An overview of the joint FAA/NASA aircraft/ground runway friction program
[NASA-TM-103486] N90-25957

S

S GLASS
Erosion mechanisms in composite materials and ripple formation mechanism in erosion
[IAR-89-4-PT-1] N90-26078

S MATRIX THEORY
Predissimilarities, prefilters, and ultrametrics on an arbitrary set
[IMAG-RR-970-M] N90-26603

SAFETY DEVICES
Helmet-mounted head restraint
[AD-D014536] N90-26491

SAFETY FACTORS
Aviation safety: Conditions within the air traffic control work force. Fact sheet for congressional requesters
[GAO/RCED-89-113FS] N90-25958
Multimegawatt space nuclear power supply, phase 1. Volume 3: Annotated outline of preliminary safety assessment D180-30619-7
[DE90-012432] N90-26646

SAMPLING
Optical characterization of clouds of fine liquid-nitrogen particles
[NASA-TM-103208] N90-26299

SATELLITE COMMUNICATION
Texstar: The all-Texas educational satellite system
[NASA-CR-186654] N90-26045
System factors to be considered in assessing propagation effects on modern digital satellite communications systems N90-26208
Mobile satellite communications for civil aviation
[NLR-MP-88066-U] N90-26238
Software set-up for data processing of depolarization due to rain and ice crystals in the Olympus project
[EUT-89-E-218] N90-26240

SATELLITE CONTROL
Fluid-loop reaction system
[NASA-CASE-NPO-17204-1-CU] N90-26292

SATELLITE DESIGN
Perspective features of the tethered systems for space applications
[ETN-90-97279] N90-26059

SATELLITE GROUND SUPPORT
Space operations: NASA's communications support for Earth orbiting spacecraft. Report to Chairman, Subcommittee on Space Science and Applications, Committee on Science, Space and Technology, House of Representatives
[GAO/IMTEC-89-41] N90-26215

SATELLITE IMAGERY
Practical applications of remote sensing technology
[NASA-CR-186810] N90-26377

SATELLITE OBSERVATION
The 27-28 October 1986 FIRE IFO cirrus case study: Cirrus parameter relationships derived from satellite and lidar data
[NASA-TM-103469] N90-26447
Estimation of convective rain volumes utilizing the are-time-integral technique
[NASA-CR-186814] N90-26449
Laboratory studies, analysis, and interpretation of the spectra of hydrocarbons present in planetary atmospheres including cyanoacetylene, acetylene, propane, and ethane N90-26748

SATELLITE SURFACES
Optical constraints of kerogen from 0.15 to 40 microns: Comparison with meteoritic organics N90-26776

SATELLITE TRACKING
A reduced-dynamic technique for precise orbit determination N90-26219
Tracking performance of a combined Costas/AFC-loop under noisy Rayleigh/Rician channel conditions with additive Gaussian noise jamming
[ETN-90-96964] N90-26237

SATURN (PLANET)
High resolution, low temperature photoabsorption cross-section of C2H2 with application to Saturn's atmosphere N90-26757

SATURN ATMOSPHERE
Investigation of the Saturn dust environment from the analysis of energetic charged particle measurements
[NASA-CR-186727] N90-26784

SATURN SATELLITES
Laboratory studies of the interaction of ions with condensed gases: Planetary applications N90-26778

SCALE EFFECT
Scaling effects in the static and dynamic response of graphite-epoxy beam-columns
[NASA-TM-102697] N90-26363

SCALE MODELS
Wind tunnel study of wake downwash behind A 6 percent scale model B1-B aircraft
[DE90-011783] N90-25941
Measurement of velocity and temperature profiles at the exit plane of a tubular gas turbine combustor
[DE90-505519] N90-25983
Scaling effects in the static and dynamic response of graphite-epoxy beam-columns
[NASA-TM-102697] N90-26363

SCANNERS
DoD-University research instrumentation program, FY 1986/FY 1987
[AD-A222578] N90-26263
Optical characterization of clouds of fine liquid-nitrogen particles
[NASA-TM-103208] N90-26299

SCANNING TUNNELING MICROSCOPY
Imaging and spectroscopy of small molecules by scanning tunneling microscopy
[AD-A222572] N90-26641

SCATTERING
Scattering from coated structures and antenna pattern control using impedance surfaces, part A/B
[NASA-CR-186871] N90-26233
The 27-28 October 1986 FIRE IFO cirrus case study: Cirrus parameter relationships derived from satellite and lidar data
[NASA-TM-103469] N90-26447

SCATTERING COEFFICIENTS
Scattering from coated structures and antenna pattern control using impedance surfaces, part A/B
[NASA-CR-186871] N90-26233

SCATTERING CROSS SECTIONS
Electron-impact spectroscopy N90-26779

SCATTERING FUNCTIONS
The 27-28 October 1986 FIRE IFO Cirrus case study: Comparison of radiative transfer theory with observations by satellite and aircraft
[NASA-TM-103468] N90-26448

SCENE ANALYSIS
Multi-sensory perception of a geometrical structure of a scene
[ETN-90-97245] N90-26587

SCHEDULES
Space exploration: Cost, schedule, and performance of NASA's Mars Observer Mission. Fact sheet for the Chairman, Subcommittee on Science, Technology, and Space, Committee on Commerce, Science, and Transportation, US Senate
[GAO/NSIAD-88-137FS] N90-26021
Space exploration: Cost, schedule, and performance of NASA's Magellan Mission to Venus. Fact sheet for the Chairman, Subcommittee on Science, Technology, and Space, Committee on Commerce, Science, and Transportation, US Senate
[GAO/NSIAD-88-130FS] N90-26022
Space exploration: Cost, schedule, and performance of NASA's Ulysses Mission to the Sun. Fact sheet for the Chairman, Subcommittee on Science, Technology, and Space, Committee on Commerce, Science, and Transportation, US Senate
[GAO/NSIAD-88-129FS] N90-26023

SCHEDULING
Investigation of automated task learning, decomposition and scheduling
[NASA-CR-186791] N90-26488
Run-time parallelization and scheduling of loops
[NASA-CR-182039] N90-26509
Evaluation of a decomposition approach for real-time scheduling using a Stochastic model
[AD-A222726] N90-26625

SCHOOLS
Launching a dream: A teachers guide to a simulated space shuttle mission
[NASA-TM-89715] N90-26693

SCHWARTZ INEQUALITY
Formation of design envelope criterion in terms of deterministic spectral procedure
[RAE-TM-SS-9] N90-25953
SCIENTISTS
Qualitative and quantitative reasoning about thermodynamics
[NASA-CR-186788] N90-26689
SCINTILLATION COUNTERS
Astronomy at ultra-high energies: Results from the CYGNUS experiment
[DE90-011979] N90-26732
SEA ICE
Spatial cross-correlation of Antarctic Sea ice and seabed topography
[NASA-CR-186815] N90-26451
SEALING
Flight set 360L001 (STS-26) igniter, post flight
[NASA-CR-183957] N90-26325
SEARCH PROFILES
The EISI (Elemental and Interplanar Spacing Index) index: A search/match tool for electron diffraction phase analysis
[DE90-010832] N90-26097
SEASONS
Measurements of CH4, N2O, CO, H2O and O3 in the middle atmosphere by the ATMOS experiment on Spacelab 3
[NASA-TM-103476] N90-26400
SEAT BELTS
Biodynamic simulations of an aircraft pilot/passenger in various crash environments
[NIAR-90-6] N90-26494
Human factors: The human interface with aircraft interiors
[NIAR-90-18] N90-26496
SEATS
Biodynamic simulations of an aircraft pilot/passenger in various crash environments
[NIAR-90-6] N90-26494
Human factors: The human interface with aircraft interiors
[NIAR-90-18] N90-26496
SECONDARY FLOW
Decay of secondary flow and the associated loss variation downstream of an annual turbine stator cascade
[DE90-505520] N90-25984
Measurement of terms and parameters in turbulent models
[NASA-CR-183993] N90-26271
SECRETIONS
Experiment K-6-20. The effect of spaceflight on pituitary oxytocin and vasopressin content of rats N90-26473
Experiment K-6-22. Growth hormone regulation, synthesis and secretion in microgravity. Part 1: Somatotroph physiology. Part 2: Immunohistochemical analysis of hypothalamic hormones. Part 3: Plasma analysis N90-26475
SECURITY
Space operations: NASA is not properly safeguarding valuable data from past missions
[GAO/IMTEC-90-1] N90-26704
SEDIMENTS
The 5th International symposium on palaeolimnology
[AD-A219244] N90-26431
SEEDS
Implementation of sensor and control designs for bioregenerative systems
[NASA-CR-186655] N90-26479
Proximate composition of seed and biomass from soybean plants grown at different carbon monoxide (CO2) concentrations
[NASA-TM-103496] N90-26480
SELECTION
Material selection and design: An expert system approach
[PNR90611] N90-26544
SELECTIVE DISSEMINATION OF INFORMATION
Energy data base: Subject categories and scope
[DE90-009212] N90-26706
SELECTIVE FADING
An experimental medium speed wideband modem N90-26194
Combined effects of fast and selective fading on performance of PSK and MSK with coherent detection N90-26204
SELF DIFFUSION (SOLID STATE)
Molecular dynamics simulations of grain-boundary diffusion for varying tilt angle geometries
[DE90-012919] N90-26669
SELF ORGANIZING SYSTEMS
A sum rule satisfied by optimized feed-forward layered networks
[RSRE-MEMO-4341] N90-26579
On networks, optimized feature extraction, and the Bayes decision
[RSRE-MEMO-4342] N90-26580
SELF TESTS
Self-checking on-line testable static RAM
[NASA-CASE-NPO-17939-1-CU] N90-26518
SEMICONDUCTOR LASERS
Apparatus for the efficient wavelength conversion of laser radiation
[AD-D014506] N90-26305
A compact, high-powered Far-Infrared (FIR) laser
[DE90-009996] N90-26312
High resolution infrared spectroscopy of planetary molecules using diode lasers and Fourier transform spectrometers N90-26747
SENSITIVITY
Sensitivity analysis with a simple charging code
[RAE-TM-SPACE-374] N90-26662
SENSORIMOTOR PERFORMANCE
Experiment K-6-18. Study of muscarinic and gaba (benzodiazepine) receptors in the sensory-motor cortex, hippcampus and spinal code N90-26471
SENSORY PERCEPTION
Multi-sensory perception of a geometrical structure of a scene
[ETN-90-97245] N90-26587
Neural networks for real-time sensory data processing and sensorimotor control
[AD-A223096] N90-26592
SEPARATED FLOW
Identification of aerodynamic models for maneuvering aircraft
[NASA-CR-186630] N90-25943
Report of the Fluid Dynamics Panel Working Group 10 on calculation of 3D separate turbulent flows in boundary layer limit
[AGARD-AR-255] N90-26280
SEPARATION
Fluid Phase Separation (FPS) experiment for flight on a space shuttle Get Away Special (GAS) canister
[NASA-CR-186830] N90-26161
SEQUENCING
Optimal synchronization of spread spectrum sequenced by nontransferable switching operators N90-26183
Direct-sequence spread spectrum system
[AD-A223021] N90-26245
MTP: An atomic multicast transport protocol
[NASA-CR-186716] N90-26254
Causal distributed breakpoints
[AD-A222613] N90-26622
SEQUENTIAL COMPUTERS
The bit full-decomposition of sequential machines
[EUT-89-E-223] N90-26516
The full-decomposition of sequential machines with the separate realization of the next-state and output functions
[EUT-89-E-222] N90-26547
MINAS: An algorithm for systematic state assignment of sequential machines: Computational aspects and results
[EUT-89-E-217] N90-26566
SERIES (MATHEMATICS)
Strong consistency of the least squares estimator for a non-ergodic threshold autoregressive model
[IMAG-RR-791-M] N90-26604
Reversed residuals in autoregressive time series analysis
[AD-A222711] N90-26624
SERIES EXPANSION
Calculation of the algebraic curves parameterization: Hamburger-Noether expansions
[IMAG-RR-798-M] N90-26608
SERVOMECHANISMS
Simulated dynamic response of a servovalve controlled hydraulic actuator
[NASA-TM-101644] N90-26167
SHAFTS (MACHINE ELEMENTS)
Bidirectional drive and brake mechanism
[NASA-CASE-MSC-21540-1] N90-26342
SHAPES
A contribution to the economic, optimal dimensioning, and shaping of aircraft structures using a design model
[ETN-90-96966] N90-25976
Feasibility study of a synthesis procedure for array feeds to improve radiation performance of large distorted reflector antennas
[NASA-CR-186641] N90-26213
SHELLS (STRUCTURAL FORMS)
Understanding silica binders
[PNR90625] N90-26150
SHIELDING
Development of ceramic hybrid combustor: Design and combustion test results
[DE90-503442] N90-26149
Electrode carrying wire for GTAW welding
[NASA-CASE-MFS-29491-1] N90-26168
Rings of Earth detected by orbital debris radar N90-26232
A closed form solution to HZE propagation
[NASA-TM-103482] N90-26640
SHIPS
The browse file of NASA/JPL quick-look radar images from the Loch Linnhe 1989 experiment
[NASA-CR-186855] N90-26701
SHOCK WAVE INTERACTION
Interactive calculation procedures for mixed compression inlets
[NASA-CR-186581] N90-25934
SHOCK WAVES
Experimental study on vortex and shock wave development on a 65 deg delta wing
[NLR-MP-88033-U] N90-25950
The study of VF2/VF3 piezoelectric copolymeteres submitted to shocks
[ISL-CO-210/9] N90-26679
SHRINKAGE
Mechanical properties of silica coatings
[DE90-012721] N90-26138
SIDEWINDER MISSILES
Renewed aging control of adhesion of inhibitor on the gas generator charges for RB 24
[FOA-C-20780-2.1] N90-26153
SIGNAL DETECTION
A two-telescope receiver design for deep space optical communications N90-26226
Interaction of electromagnetic signals with particulate clouds
[AD-A222804] N90-26244
SIGNAL DETECTORS
Interaction of electromagnetic signals with particulate clouds
[AD-A222804] N90-26244
SIGNAL DISTORTION
Radio channel measurement and modelling for future mobile radio systems N90-26184
SIGNAL FADING
An overview of Canadian radio propagation/communications technologies research N90-26179
A global common-user system for the provision of HF propagation data N90-26180
Measurement and simulation of widespread mobile radio channel characteristics N90-26186
In-band amplitude dispersion on a microwave link N90-26189
Tracking performance of a combined Costas/AFC-loop under noisy Rayleigh/Rician channel conditions with additive Gaussian noise jamming
[ETN-90-96964] N90-26237
SIGNAL PROCESSING
The disturbance processes on the data links of the mode-S air traffic control system
[ETN-90-96960] N90-25965
A two-telescope receiver design for deep space optical communications N90-26226
QPSK loop lock detection in the advanced receiver N90-26230
Analysis and improved design considerations for airborne pulse Doppler radar signal processing in the detection of hazardous windshear
[NASA-CR-186792] N90-26448
Assembly via disassembly: A case in machine perceptual development
[NASA-CR-186867] N90-26497
SIGNAL RECEPTION
Experimental study of a digital mobile radio spread spectrum in an urban site N90-26205
SIGNAL TO NOISE RATIOS
Direct drive robotic hand
[NASA-CASE-NPO-17917-1-CU] N90-26339
HIRIS performance study
[NASA-CR-186649] N90-26375
SIGNATURE ANALYSIS
Acousto-optic signature analysis for inspection of the orbiter thermal protection tile bonds
[DE90-013089] N90-26043
Optical signatures of molecular particles via mass-selected cluster spectroscopy N90-26780
SILANES
One-dimensional sigma-conjugated polysilylenes: Science and technology
[DE90-012902] N90-26146
Laser techniques for studying chemical vapor deposition
[DE90-012921] N90-26311
SILICON
Composite materials with improved properties in compression: Synthesis of 3-methylene-1,1-Dichlorosilacyclobutane and 1,1-dichlorosilacyclopent-3-ene
[AD-A222615] N90-26088

The catalytic synthesis of inorganic polymers for high temperature applications and as ceramic precursors
[AD-A222620] N90-26156
Rapid thermal processing: A study of the silicon oxidation and of the implanted boron activation
[LAAS-90051] N90-26681

SILICON ALLOYS
Erosion mechanisms in composite materials and ripple formation mechanism in erosion
[IAR-89-4-PT-2] N90-26079

SILICON CARBIDES
Vitreous joining of SiC fiber reinforced SiC composites
[DE90-012951] N90-26081
Synthesis of high purity sinterable silicon carbide powder
[DE90-012029] N90-26084
Investigation of thermo-mechanical effects in silicon carbide Whisker/Al alloy composites
[AD-A222635] N90-26089
Evaluation of fracture strength properties of silicon carbide ceramics under cyclic/static axial loading at ultra-high temperature
[DE90-503402] N90-26147

SILICON DIOXIDE
Mechanical properties of silica coatings
[DE90-012721] N90-26138
Fractal structure and fractal time in silica sol-gels
[DE90-013197] N90-26144
Understanding silica binders
[PNR90625] N90-26150
Surface acoustic wave filters in ZnO-SiO2-Si layered structures: Design, technology, and monolithic integration with electronic circuitry
[ETN-90-97218] N90-26638

SILICON NITRIDES
The interaction of polymeric materials with ceramic surfaces with special reference to the behaviour of bioceramics N90-26127
Tensile strength measurement techniques for structural ceramics
[DE90-012193] N90-26136
Influence of the manufacturing conditions on the microstructure and mechanical properties of the silicon nitride
[ISAL-90-0008] N90-26154
Polymeric aluminasilazane precursors for aluminosilicon nitride
[AD-A222755] N90-26158

SILICON OXIDES
Mechanical properties of coatings and interfaces
[DE90-012726] N90-26139

SILICON POLYMERS
One-dimensional sigma-conjugated polysilylenes: Science and technology
[DE90-012902] N90-26146
Polymeric aluminasilazane precursors for aluminosilicon nitride
[AD-A222755] N90-26158

SILVER
Molecular structure of interphases between DGEBA/BTDA adhesives and silver substances using surface-enhanced Raman scattering
[AD-A222750] N90-26157
SDIO/IST ultrashort wavelength laser: Novel experimental schemes for observing the Moessbauer effect in long-lived nuclear levels and nuclear coherent states
[AD-A222607] N90-26316

SIMULATION
Formation of design envelope criterion in terms of deterministic spectral procedure
[RAE-TM-SS-9] N90-25953
Qualitative evaluation of a conformal velocity vector display for use at high angles-of-attack in fighter aircraft
[NASA-TM-102629] N90-25981
Comparison of currents predicted by NASCAP/LEO model simulations with elementary Langmuir-type bare probe models for an insulated cable containing a single pinhole
[NASA-TM-102486] N90-26054
An inverse dynamic method yielding flexible manipulator state trajectories
[NASA-CR-186807] N90-26329
Biodynamic simulations of an aircraft pilot/passenger in various crash environments
[NIAR-90-6] N90-26494
Canonical eigenvalues. Part 1: General theory
[AD-A222812] N90-26617
Analysis of random drop for gateway congestion control
[NASA-CR-186736] N90-26698

SIMULATORS
A digital Meteor-Burst Communication (MBC) propagation path simulator N90-26190
A novel communication network simulator
[AD-A223045] N90-26248
Single-pass memory system evaluation for multiprogramming workloads
[NASA-CR-186553] N90-26558

SIMULTANEOUS EQUATIONS
A possibility to incorporate saturation in the simple, global model of a synchronous machine with rectifier
[EUT-89-E-225] N90-26258

SINGLE CRYSTALS
Hydrogen induced fracture characteristics of single crystal nickel-based superalloys
[NASA-CR-183992] N90-26108
Resistivity, adhesive strength, and residual stress measurements of thin film metallizations on single crystal quartz
[DE90-011902] N90-26135
SDIO/IST ultrashort wavelength laser: Novel experimental schemes for observing the Moessbauer effect in long-lived nuclear levels and nuclear coherent states
[AD-A222607] N90-26316
Crystal growth and deformation behavior of TiAl aluminides
[DE90-012972] N90-26671

SINGULARITY (MATHEMATICS)
Numerical treatment of shell crossing singularities in the spherically symmetric gravitational collapse
[ETN-90-96967] N90-26598
Calculation of the algebraic curves parameterization: Hamburger-Noether expansions
[IMAG-RR-798-M] N90-26608
Contribution to the study of differential equations and to the differences in the complex field
[ETN-90-97250] N90-26612
Dichotomies for certain product measures and stable processes
[AD-A222568] N90-26621

SINTERING
Synthesis of high purity sinterable silicon carbide powder
[DE90-012029] N90-26084
Real-time monitoring of ceramic sintering with laser ultrasonics
[DE90-012960] N90-26140

SIZE (DIMENSIONS)
PDWAP: A preliminary design and weights analysis program for aerospace vehicles
[AD-A222614] N90-25979

SKIN FRICTION
A brief review of some mechanisms causing boundary layer transition at high speeds
[NASA-TM-102834] N90-25945

SKYLAB 1
Technical characteristics and functions of different types of space stations N90-26712

SLIDING
On controller choice for robust sliding mode performance
[MATHS-REPT-A-107] N90-26337

SLIPSTREAMS
Prediction of two-dimensional time-dependent gasdynamic flows for hypersonic studies
[UTIAS-335] N90-25935

SLOTS
Resonant coupling through a slot to a loaded cylindrical cavity: Experimental results
[AD-A223000] N90-26631

SLURRIES
Subsonic combustor testing N90-25997
Understanding silica binders
[PNR90625] N90-26150

SLUSH HYDROGEN
Background, current status, and prognosis of the ongoing slush hydrogen technology development program for the NASP
[NASA-TM-103220] N90-26055

SOFTWARE ENGINEERING
Technical evaluation report on the Guidance and Control Panel 49th Symposium on Fault Tolerant Design Concepts for Highly Integrated Flight Critical Guidance and Control Systems
[AGARD-AR-281] N90-26012
Statistical analysis of a software reliability model
[IMAG-RR-781-M] N90-26352
A Bayesian proportional model for software reliability
[IMAG-RR-795-M] N90-26353
Practical applications of remote sensing technology
[NASA-CR-186810] N90-26377
An expert system based software sizing tool, phase 2
[NASA-CR-186706] N90-26525
Parallel processors and nonlinear structural dynamics algorithms and software
[NASA-CR-186755] N90-26536
Documentation of program Tankplot
[FFI-89/7019] N90-26541
Study of a class of non convex optimization algorithms: implementation and applications
[ETN-90-97241] N90-26552
VISTA (Vertical Integration of Science, Technology, and Applications) user interface software study
[DE90-010003] N90-26707

SOFTWARE TOOLS
Inference and control mechanisms in NEXT 2.0
[NLR-MP-88062-U] N90-26175
ISIS and META projects
[NASA-CR-186645] N90-26524
An expert system based software sizing tool, phase 2
[NASA-CR-186706] N90-26525
SUPES version 2.1: A Software Utilities Package for the Engineering Sciences
[DE90-011763] N90-26531
CAD/CAM reinforces the competitive edge of European mouldmakers
[CRIF-MC-88] N90-26542
ATN design tool
[AD-A223030] N90-26559

SOIL SCIENCE
Soil experiment
[NASA-CR-184927] N90-26165

SOLAR ACTIVITY EFFECTS
Space exploration: Cost, schedule, and performance of NASA's Ulysses Mission to the Sun. Fact sheet for the Chairman, Subcommittee on Science, Technology, and Space, Committee on Commerce, Science, and Transportation, US Senate
[GAO/NSIAD-88-129FS] N90-26023

SOLAR ARRAYS
The chemical effects of the Martian environment on power system component materials: A theoretical approach
[NASA-TM-103203] N90-26074
Analysis of a Mars-stationary orbiting microwave power transmission system
[NASA-TM-101344] N90-26172

SOLAR CELLS
Estimation of minority carrier diffusion lengths in InP/GaAs solar cells
[NASA-TM-103213] N90-26069
Silicon concentrator solar cell development
[DE90-011782] N90-26386
Dendritic web silicon photovoltaic cell research
[DE90-011786] N90-26387
Application of InAlAs/GaAs superlattice alloys to GaAs solar cells
[DE90-013070] N90-26389
Megawatt solar power systems for lunar surface operations
[NASA-CR-186509] N90-26391

SOLAR COLLECTORS
Megawatt solar power systems for lunar surface operations
[NASA-CR-186509] N90-26391
Preliminary designs for 25 kWe advanced Stirling conversion systems for dish electric applications
[NASA-TM-103188] N90-26729

SOLAR ENERGY
The use of hydrogen in energy economy of Finland
[DE90-796180] N90-26388

SOLAR FLARES
The charged particle radiation environment for AXAF
[NASA-TM-100405] N90-26741
Nonpotential magnetic fields at sites of gamma ray flares
[NASA-TM-103493] N90-26785

SOLAR GENERATORS
Qualification of concentrating mirror systems with the HERMES measurement system and the HELIOS simulation program
[DLR-FB-89-51] N90-26394

SOLAR MAGNETIC FIELD
Nonpotential magnetic fields at sites of gamma ray flares
[NASA-TM-103493] N90-26785

SOLAR RADIATION
Photodissociation of O2 in the stratosphere and mesosphere: A general parametrization of the Schumman-Runge Bands N90-26427

SOLAR REFLECTORS
Qualification of concentrating mirror systems with the HERMES measurement system and the HELIOS simulation program
[DLR-FB-89-51] N90-26394

SOLAR SYSTEM
The Telecommunications and Data Acquisition Report
[NASA-CR-186852] N90-26217
Preliminary error budget for an optical ranging system: Range, range rate, and differenced range observables N90-26227
Reports of planetary astronomy, 1990
[NASA-TM-4205] N90-26730

Submillimeter and millimeter observations of solar system objects
[NASA-CR-186636] N90-26731
Absolute vacuum ultraviolet photoabsorption cross section studies of atomic and molecular species: Techniques and observational data N90-26754

SOLAR-PUMPED LASERS
Theoretical studies of solar pumped lasers
[NASA-CR-186712] N90-26308

SOLID CRYOGENS
Optical constants of solid methane N90-26775

SOLID PHASES
Optical constants of solid methane N90-26775
Laboratory studies of the interaction of ions with condensed gases: Planetary applications N90-26778

SOLID PROPELLANT ROCKET ENGINES
Space shuttle: Follow-up evaluation of NASA's solid rocket motor procurement. Report to the Chairman, Committee on Government Operations, House of Representatives
[GAO/NSIAD-89-89] N90-26066
Flight motor set 360L007 (STS-33R)
[NASA-CR-183979] N90-26067
Flight set 360L001 (STS-26) igniter, post flight
[NASA-CR-183957] N90-26325

SOLID STATE
A compact, high-powered Far-Infrared (FIR) laser
[DE90-009996] N90-26312
Stibathiolanes: Synthesis, solid state structure, and solution behavior
[AD-A223255] N90-26688

SOLID STATE LASERS
Solid-state lasers for coherent communication and remote sensing
[NASA-CR-186634] N90-26306
OASIS, LLNL version: Software maintenance manual
[DE90-013522] N90-26313
Damage measurements on optical materials for use in high-peak-power lasers
[DE90-013489] N90-26314

SOLID SURFACES
Chemical structure and kinetics at liquid/solid interfaces
[AD-A222766] N90-26105

SOLID-SOLID INTERFACES
Quantum ballistic and adiabatic electron transport, studied with quantum point contacts
[ETN-90-97262] N90-26440

SOLIDIFICATION
Effect of boron on intergranular hot cracking in Ni-Cr-Fe superalloys containing niobium
[NASA-CR-186714] N90-26115
Formation of Titanium-boron surface alloys by excimer laser mixing
[DE90-013172] N90-26118
Undercooling and solidification
[DLR-FB-90-020] N90-26678

SOLIDIFIED GASES
Optical constants of solid methane N90-26775

SOLUBILITY
Passivation of high temperature superconductors
[NASA-CASE-NPO-17949-1-CU] N90-26684

SOLUTIONS
Characterization of a thermally imidized soluble polyimide film
[NASA-TM-103484] N90-26131

SOLVENTS
Dynamical solvent effects on electron-transfer processes: Recent progress and perspectives
[AD-A222603] N90-26101

SONDES
PVDF contact probes
[VTT-RR-623] N90-26253

SOOT
Combustor cooling aspects
[CIT/SME/VKI/RS/5] N90-25989
Carbon deposition model for oxygen-hydrocarbon combustion. Task 6: Data analysis and formulation of an empirical model
[NASA-CR-183986] N90-26095

SORBENTS
Regenerative Cu La zeolite supported desulfurizing sorbents
[NASA-CASE-NPO-17480-1-CU] N90-26098
Multicomponent gas sorption Joule-Thomson refrigerator
[NASA-CASE-NPO-17569-1-CU] N90-26176

SORPTION
Multicomponent gas sorption Joule-Thomson refrigerator
[NASA-CASE-NPO-17569-1-CU] N90-26176

SOUND FIELDS
Asymptotic modal analysis and statistical energy analysis
[NASA-CR-186732] N90-26634

SOUND WAVES
A preliminary study of the masking of wind turbine noise by ambient sound
[FFA-TN-1990-01] N90-26636
Surface acoustic wave filters in ZnO-SiO2-Si layered structures: Design, technology, and monolithic integration with electronic circuitry
[ETN-90-97218] N90-26638

SOYBEANS
Proximate composition of seed and biomass from soybean plants grown at different carbon monoxide (CO2) concentrations
[NASA-TM-103496] N90-26480

SPACE COLONIES
Greenhouse design for a Martian colony: Structural, solar collection and light distribution systems
[NASA-CR-186818] N90-26501

SPACE COMMERCIALIZATION
Space manufacture: Protection and valuation of innovations from a users point of view N90-26724

SPACE DEBRIS
Space program: Space debris a potential threat to Space Station and shuttle
[GAO/IMTEC-90-18] N90-26024
Autonomous space processor for orbital debris
[NASA-CR-186691] N90-26044
Rings of Earth detected by orbital debris radar N90-26232

SPACE EXPLORATION
Space exploration: Cost, schedule, and performance of NASA's Mars Observer Mission. Fact sheet for the Chairman, Subcommittee on Science, Technology, and Space, Committee on Commerce, Science, and Transportation, US Senate
[GAO/NSIAD-88-137FS] N90-26021
Space exploration: Cost, schedule, and performance of NASA's Magellan Mission to Venus. Fact sheet for the Chairman, Subcommittee on Science, Technology, and Space, Committee on Commerce, Science, and Transportation, US Senate
[GAO/NSIAD-88-130FS] N90-26022
Space exploration: Cost, schedule, and performance of NASA's Ulysses Mission to the Sun. Fact sheet for the Chairman, Subcommittee on Science, Technology, and Space, Committee on Commerce, Science, and Transportation, US Senate
[GAO/NSIAD-88-129FS] N90-26023
Space exploration: Cost, schedule, and performance of NASA's Galileo Mission to Jupiter. Fact sheet for the Chairman, Subcommittee on Science, Technology, and Space, Committee on Commerce, Science, and Transportation, US Senate
[GAO/NSIAD-88-138FS] N90-26025
Possible applications of tethered systems to Mars exploration missions
[IAF-89-489] N90-26060
Reports of planetary astronomy, 1990
[NASA-TM-4205] N90-26730
Directory of research projects: Planetary geology and geophysics program
[NASA-TM-4211] N90-26743
The lessons of Varsovian's reconnaissance
[NASA-TM-103207] N90-26789

SPACE FLIGHT
Effects of microgravity on rat bone, cartilage and connective tissues N90-26454
Experiment K-6-02. Biomedical, biochemical and morphological alterations of muscle and dense, fibrous connective tissues during 14 days of spaceflight N90-26456
Experiment K-6-03. Gravity and skeletal growth, part 1. Part 2: Morphology and histochemistry of bone cells and vasculature of the tibia; Part 3: Nuclear volume analysis of osteoblast histogenesis in periodontal ligament cells; Part 4: Intervertebral disc swelling pressure associated with microgravity N90-26457
Experiment K-6-04. Trace element balance in rats during spaceflight N90-26458
Experiment K-6-05. The maturation of bone and dentin matrices in rats flown on Cosmos 1887 N90-26459
Experiment K-6-06. Morphometric and EM analyses of tibial epiphyseal plates from Cosmos 1887 rats N90-26460
Experiment K-6-07. Metabolic and morphologic properties of muscle fibers after spaceflight N90-26461
Experiment K-6-09. Morphological and biochemical investigation of microgravity-induced nerve and muscle breakdown. Part 1: Investigation of nerve and muscle breakdown during spaceflight; Part 2: Biochemical analysis of EDL and PLT muscles N90-26463
Experiment K-6-12. Morphometric studies of atrial or granules and hepatocytes. Part 1: Morphometric study of the liver; Part 2: The atrial granular accumulations N90-26466
Experiment K-6-14. Hepatic function in rats after spaceflight N90-26468
Experiment K-6-17. Structural changes and cell turnover in the rats small intestine induced by spaceflight N90-26470
Experiment K-6-19. Pineal physiology in microgravity: Relation to rat gonadal function N90-26472
Experiment K-6-20. The effect of spaceflight on pituitary oxytocin and vasopressin content of rats N90-26473
Experiment K-6-23. Effect of spaceflight on levels and function of immune cells N90-26476
Experiment K-6-27. Analysis of radiographs and biosamples from primate studies N90-26478

SPACE LABORATORIES
Planning for Space Station Freedom laboratory payload integration
[NASA-CR-186751] N90-26047

SPACE LAW
Manned Space Stations: Legal Issues
[ESA-SP-305] N90-26711
The US/International Space Station: Legal aspects of space objects and jurisdiction and control N90-26713
Damage responsibility and liability in space stations N90-26714
MIR: A Soviet Space Station. Some legal aspects of international cooperation N90-26715
The International Space Station: The legal framework N90-26716
The partnership concept and international management N90-26717
The International Space Station: Conditions of access and use N90-26718
Human work in space: The astronaut's legal status. Introduction N90-26719
The manned national space station: International legal considerations N90-26720
The astronauts' legal status: The International Space Station N90-26721
Crossborder movements: Goods, personnel and technologies N90-26722
Space Station intellectual property rights and US patent law N90-26723
Space manufacture: Protection and valuation of innovations from a users point of view N90-26724
Space law put to the test by the International Space Station N90-26727

SPACE LOGISTICS
Long cycle pressurized logistics module: An Italian contribution to the Space Station Freedom logistics scenario
[IAF-89-083] N90-26058

SPACE MANUFACTURING
Space manufacture: Protection and valuation of innovations from a users point of view N90-26724

SPACE MISSIONS
Proceedings of the Second Symposium on GPS Applications in space, volume 1
[AD-A219978] N90-25962
Proceedings of the Second Symposium on GPS Applications in Space, volume 2
[AD-A219979] N90-25963
Space exploration: Cost, schedule, and performance of NASA's Mars Observer Mission. Fact sheet for the Chairman, Subcommittee on Science, Technology, and Space, Committee on Commerce, Science, and Transportation, US Senate
[GAO/NSIAD-88-137FS] N90-26021
Preliminary subsystem designs for the Assured Crew Return Vehicle (ACRV), volume 1
[NASA-CR-186677-VOL-1] N90-26039
Project LOCOST: Laser or Chemical Hybrid Orbital Space Transport
[NASA-CR-186822] N90-26042
Long-range planning cost model for support of future space missions by the deep space network N90-26231
New observations of stratospheric N2O5
[NASA-TM-103478] N90-26402

SPACE NAVIGATION
Proceedings of the Second Symposium on GPS Applications in space, volume 1
[AD-A219978] N90-25962
Applications of different design methodologies in navigation systems and development at JPL N90-26221

SPACE PERCEPTION
Segmentation before and after reconstruction of 3-D surfaces in depth imagery
[RR-788-I-IMAG-97-LIFIA] N90-26551

SPACE POWER REACTORS
Multimegawatt space nuclear power supply, phase 1. Volume 2: Phase 2 plan D180-30619-6
[DE90-012431] N90-26645
Multimegawatt space nuclear power supply, phase 1. Volume 3: Annotated outline of preliminary safety assessment D180-30619-7
[DE90-012432] N90-26646

Multimegawatt space nuclear power supply, phase 1. Supplement: D180-30619-8
[DE90-012433] N90-26647

SPACE PROBES
NASA/USRA university advanced design program at the University of Illinois for the 1989-1990 academic year
[NASA-CR-186829] N90-26049

SPACE PROCESSING
Fluid Phase Separation (FPS) experiment for flight on a space shuttle Get Away Special (GAS) canister
[NASA-CR-186830] N90-26161

SPACE PROGRAMS
Theoretical studies of solar pumped lasers
[NASA-CR-186712] N90-26308

SPACE SHUTTLE BOOSTERS
QM-8 final performance evaluation report: SEALS, volume 4
[NASA-CR-183958] N90-26324

SPACE SHUTTLE MAIN ENGINE
Digital filtering of plume emission spectra
[NASA-TM-103135] N90-26070
Reusable rocket engine turbopump health monitoring system, part 3
[NASA-CR-182294] N90-26320
The structural dynamics analysis of the main injector LOX inlet tee and its redesign
[NASA-CR-186764] N90-26358

SPACE SHUTTLE MISSIONS
Launching a dream: A teachers guide to a simulated space shuttle mission
[NASA-TM-89715] N90-26693

SPACE SHUTTLE ORBITERS
Orbiter utilization as an ACRV
[NASA-TM-102700] N90-26032
Vibration test procedures for orbiter sidewall-mounted payloads, phase 1
[AD-A220773] N90-26037

SPACE SHUTTLE PAYLOADS
Vibration test procedures for orbiter sidewall-mounted payloads, phase 1
[AD-A220773] N90-26037
Vibration test procedures for orbiter sidewall-mounted payloads, phase 2
[AD-A220774] N90-26038
Technology development: Future use of NASA's large format camera is uncertain
[GAO/NSIAD-90-142] N90-26298

SPACE SHUTTLES
Research at NASA's NFAC wind tunnels
[NASA-TM-102827] N90-25933
Debris/ice/TPS assessment and photographic analysis for shuttle mission STS-31R
[NASA-TM-102790] N90-26040
Acousto-optic signature analysis for inspection of the orbiter thermal protection tile bonds
[DE90-013089] N90-26043
Winged cargo return vehicle. Volume 1: Conceptual design
[NASA-CR-186823] N90-26050
The aerobraking space transfer vehicle
[NASA-CR-186819] N90-26053
Flight motor set 360L007 (STS-33R)
[NASA-CR-183979] N90-26067
Field experience in using laser acoustic sensing for inspection
[DE90-012954] N90-26347

SPACE STATION STRUCTURES
Perspective features of the tethered systems for space applications
[ETN-90-97279] N90-26059

SPACE STATIONS
Project Exodus
[NASA-CR-186836] N90-26026
National space test centers, Lewis research center facilities
[NASA-TM-103187] N90-26030
Orbiter utilization as an ACRV
[NASA-TM-102700] N90-26032
Preliminary subsystem designs for the Assured Crew Return Vehicle (ACRV), volume 1
[NASA-CR-186677-VOL-1] N90-26039
Project LOCOST: Laser or Chemical Hybrid Orbital Space Transport
[NASA-CR-186822] N90-26042
Planning for Space Station Freedom laboratory payload integration
[NASA-CR-186751] N90-26047
Winged cargo return vehicle. Volume 1: Conceptual design
[NASA-CR-186823] N90-26050
Biconic cargo return vehicle with an advanced recovery system. Volume 1: Conceptual design
[NASA-CR-186520] N90-26052
Technology for large space systems: A bibliography with indexes (supplement 22)
[NASA-SP-7046(22)] N90-26056
Long cycle pressurized logistics module: An Italian contribution to the Space Station Freedom logistics scenario
[IAF-89-083] N90-26058
Two-dimensional model of a Space Station Freedom thermal energy storage canister
[NASA-TM-103124] N90-26279
Rotating-unbalanced-mass devices and methods for scanning balloon-borne-experiments, free-flying spacecraft, and space shuttle/space station attached experiments
[NASA-CASE-MFS-28425-1] N90-26304
Automation of closed environments in space for human comfort and safety
[NASA-CR-186834] N90-26500
Space station definitions, design, and development. Task 5: Multiple arm telerobot coordination and control: Manipulator design methodology
[NASA-CR-182043] N90-26577
Manned Space Stations: Legal Issues
[ESA-SP-305] N90-26711
Technical characteristics and functions of different types of space stations N90-26712
Human work in space: The astronaut's legal status. Introduction N90-26719
The manned national space station: International legal considerations N90-26720

SPACE TRANSPORTATION
Space Transportation Avionics Technology Symposium. Volume 1: Executive summary
[NASA-CP-3081] N90-25980
Space transportation: NASA has no firm need for increasingly costly orbital maneuvering vehicle
[GAO/NSIAD-90-192] N90-26041

SPACE TRANSPORTATION SYSTEM
Flight set 360L001 (STS-26) igniter, post flight
[NASA-CR-183957] N90-26325

SPACE TRANSPORTATION SYSTEM FLIGHTS
Debris/ice/TPS assessment and photographic analysis for shuttle mission STS-31R
[NASA-TM-102790] N90-26040
Flight motor set 360L007 (STS-33R)
[NASA-CR-183979] N90-26067

SPACE TUGS
Space transportation: NASA has no firm need for increasingly costly orbital maneuvering vehicle
[GAO/NSIAD-90-192] N90-26041

SPACE WEAPONS
Guidance and targeting for the strategic target system
[DE90-005239] N90-26031
ASATs vs Brilliant Pebbles
[DE90-010348] N90-26626
Thermal management of an accelerator system in space
[DE90-013153] N90-26627
Multimegawatt space nuclear power supply, phase 1. Volume 2: Phase 2 plan D180-30619-6
[DE90-012431] N90-26645
Multimegawatt space nuclear power supply, phase 1. Volume 3: Annotated outline of preliminary safety assessment D180-30619-7
[DE90-012432] N90-26646
Multimegawatt space nuclear power supply, phase 1. Supplement: D180-30619-8
[DE90-012433] N90-26647

SPACEBORNE EXPERIMENTS
Proceedings of the LDEF Materials Data Analysis Workshop
[NASA-CP-10046] N90-26075
The US Experiments Flown on the Soviet Biosatellite Cosmos 1887
[NASA-TM-102254] N90-26452
Experiment K-6-24, K-6-25, K-6-26. Radiation dosimetry and spectrometry N90-26477
Production activities in space: The problems of protection N90-26725
Possible solutions N90-26726

SPACEBORNE PHOTOGRAPHY
Technology development: Future use of NASA's large format camera is uncertain
[GAO/NSIAD-90-142] N90-26298

SPACECRAFT CHARGING
Comparison of currents predicted by NASCAP/LEO model simulations with elementary Langmuir-type bare probe models for an insulated cable containing a single pinhole
[NASA-TM-102486] N90-26054
Sensitivity analysis with a simple charging code
[RAE-TM-SPACE-374] N90-26662

SPACECRAFT CONFIGURATIONS
Space exploration: Cost, schedule, and performance of NASA's Mars Observer Mission. Fact sheet for the Chairman, Subcommittee on Science, Technology, and Space, Committee on Commerce, Science, and Transportation, US Senate
[GAO/NSIAD-88-137FS] N90-26021

SPACECRAFT CONSTRUCTION MATERIALS
Proceedings of the LDEF Materials Data Analysis Workshop
[NASA-CP-10046] N90-26075
Materials and structures for 2000 and beyond: An attempted forecast by the DLR Materials and Structures Department
[ESA-TT-1154-REV] N90-26173
Experiment K-6-24, K-6-25, K-6-26. Radiation dosimetry and spectrometry N90-26477

SPACECRAFT CONTROL
The Screem-J4D: A proposal in response to a low Reynolds number station keeping mission
[NASA-CR-186664] N90-25968
Guidance and control strategies for aerospace vehicles
[NASA-CR-186878] N90-26013

SPACECRAFT DESIGN
Autonomous space processor for orbital debris
[NASA-CR-186691] N90-26044
NASA/USRA university advanced design program at the University of Illinois for the 1989-1990 academic year
[NASA-CR-186829] N90-26049
The aerobraking space transfer vehicle
[NASA-CR-186819] N90-26053
Long cycle pressurized logistics module: An Italian contribution to the Space Station Freedom logistics scenario
[IAF-89-083] N90-26058
Fluid-loop reaction system
[NASA-CASE-NPO-17204-1-CU] N90-26292
Structural dynamics branch research and accomplishments
[NASA-TM-102488] N90-26373
Microspacecraft and Earth observation: Electrical field (ELF) measurement project
[NASA-CR-186821] N90-26436
Space station definitions, design, and development. Task 5: Multiple arm telerobot coordination and control: Manipulator design methodology
[NASA-CR-182043] N90-26577

SPACECRAFT DOCKING
Biconic cargo return vehicle with an advanced recovery system. Volume 1: Conceptual design
[NASA-CR-186520] N90-26052

SPACECRAFT ELECTRONIC EQUIPMENT
Heavy ion tests on programmable VLSI
[ETN-90-97254] N90-26057

SPACECRAFT INSTRUMENTS
Microspacecraft and Earth observation: Electrical field (ELF) measurement project
[NASA-CR-186821] N90-26436

SPACECRAFT LAUNCHING
Trajectory optimization for an asymmetric launch vehicle
[NASA-CR-185630] N90-26033

SPACECRAFT MODULES
Project SPARC: Space-based aeroassisted reusable craft
[NASA-CR-186816] N90-26051
Long cycle pressurized logistics module: An Italian contribution to the Space Station Freedom logistics scenario
[IAF-89-083] N90-26058

SPACECRAFT ORBITS
Space operations: NASA's communications support for Earth orbiting spacecraft. Report to Chairman, Subcommittee on Space Science and Applications, Committee on Science, Space and Technology, House of Representatives
[GAO/IMTEC-89-41] N90-26215

SPACECRAFT POWER SUPPLIES
The aerobraking space transfer vehicle
[NASA-CR-186819] N90-26053
The chemical effects of the Martian environment on power system component materials: A theoretical approach
[NASA-TM-103203] N90-26074
NASA aerospace flight battery systems program
[NASA-TM-103237] N90-26397
Multimegawatt space nuclear power supply, phase 1. Volume 2: Phase 2 plan D180-30619-6
[DE90-012431] N90-26645
Multimegawatt space nuclear power supply, phase 1. Volume 3: Annotated outline of preliminary safety assessment D180-30619-7
[DE90-012432] N90-26646

SPACECRAFT PROPULSION
National space test centers, Lewis research center facilities
[NASA-TM-103187] N90-26030
NASA/USRA university advanced design program at the University of Illinois for the 1989-1990 academic year
[NASA-CR-186829] N90-26049

SPACECRAFT REENTRY
Guidance and control strategies for aerospace vehicles
[NASA-CR-186878] N90-26013
SPACECRAFT STABILITY
The Screem-J4D: A proposal in response to a low Reynolds number station keeping mission
[NASA-CR-186664] N90-25968
SPACECRAFT STRUCTURES
Design and implementation of robust decentralized control laws for the ACES structure at Marshall Space Flight Center
[NASA-CR-4310] N90-26046
Materials and structures for 2000 and beyond: An attempted forecast by the DLR Materials and Structures Department
[ESA-TT-1154-REV] N90-26173
SPACECRAFT TRACKING
Goldstone intracomplex connected element interferometry N90-26218
SPACELAB
New observations of stratospheric N2O5
[NASA-TM-103478] N90-26402
SPACELAB PAYLOADS
Bubble, Drop and Particle Unit (BDPU): A multi-user microgravity facility
[IAF-89-431] N90-26164
SPACETENNAS
Feasibility study of a synthesis procedure for array feeds to improve radiation performance of large distorted reflector antennas
[NASA-CR-186641] N90-26213
SPECIFIC HEAT
Searching for heavy fermion materials in Ce intermetallic compounds
[DE90-011809] N90-26116
SPECIFICATIONS
Vibration test procedures for orbiter sidewall-mounted payloads, phase 2
[AD-A220774] N90-26038
Software requirements: Guidance and control software development specification
[NASA-CR-182058] N90-26527
The rationale and specification of the ELLA graphics systems
[RSRE-89017] N90-26548
Multimegawatt space nuclear power supply, phase 1. Supplement: D180-30619-8
[DE90-012433] N90-26647
SPECKLE INTERFEROMETRY
Coherent optical techniques for industrial inspection
[PNR90605] N90-26654
SPECTRA
Annual and interannual variations of Earth-emitted radiation based on a 10-year data set
[NASA-TM-103465] N90-26432
SPECTRAL RESOLUTION
The interstellar D1 line at high resolution
[NASA-CR-184915] N90-26737
SPECTRAL SIGNATURES
Optical signatures of molecular particles via mass-selected cluster spectroscopy N90-26780
SPECTROMETERS
Experiment K-6-24, K-6-25, K-6-26. Radiation dosimetry and spectrometry N90-26477
High resolution infrared spectroscopy of planetary molecules using diode lasers and Fourier transform spectrometers N90-26747
SPECTROSCOPIC ANALYSIS
Laboratory measurements of microwave and millimeter-wave properties of planetary constituents N90-26745
SPECTROSCOPY
Preliminary plume characteristics of an arcjet thruster
[NASA-TM-103241] N90-26071
Measurements of CH4, N2O, CO, H2O and O3 in the middle atmosphere by the ATMOS experiment on Spacelab 3
[NASA-TM-103476] N90-26400
First International Conference on Laboratory Research for Planetary Atmospheres
[NASA-CP-3077] N90-26744
High resolution spectroscopy in the microwave and far infrared N90-26746
Electron-impact spectroscopy N90-26779
Optical signatures of molecular particles via mass-selected cluster spectroscopy N90-26780
SPECTRUM ANALYSIS
High resolution spectroscopy in the microwave and far infrared N90-26746
SPEECH BASEBAND COMPRESSION
A narrowband tactical communication system for the VHF and UHF mobile radio bands N90-26192
SPERMATOZOA
Experiment K-6-16. Morphological examination of rat testes. The effect of Cosmos 1887 flight on spermatogonial population and testosterone level in rat testes N90-26469
SPHERES
Full vector wave calculation of photonic band structures in face-centered cubic dielectric media
[AD-A222616] N90-26686
SPHERICAL SHELLS
Natural melting within a spherical shell
[NASA-TM-102822] N90-26274
SPLEEN
Experiment K-6-23. Effect of spaceflight on levels and function of immune cells N90-26476
SPLINE FUNCTIONS
G2-continuity in homogeneous co-ordinates
[MATHS-REPT-A-110] N90-26599
Rational cubics with G2-continuity
[MATHS-REPT-A-113] N90-26601
Asymptotic optimality of the fast randomized versions of GCV and C(sub L) in ridge regression and regularization
[IMAG-RR-793-M] N90-26606
Nonlinear modeling of time series using Multivariate Adaptive Regression Splines (MARS)
[AD-A222710] N90-26623
SPLITTING
Microwave spectra of van der Waals complexes of importance in planetary atmospheres N90-26752
SPRAY CHARACTERISTICS
Subsonic combustor testing N90-25997
SPRAYERS
Liquid fueled ramjet combustion instability: Acoustical and vortical interactions with burning sprays
[AD-A222752] N90-26104
Critical evaluation of Jet-A spray combustion using propane chemical kinetics in gas turbine combustion simulated by KIVA-2
[NASA-TM-103173] N90-26170
SPREAD SPECTRUM TRANSMISSION
Propagation Effects and Circuit Performance of Modern Military Radio Systems with Particular Emphasis on Those Employing Bandspreading
[AGARD-CP-442] N90-26178
An overview of Canadian radio propagation/communications technologies research N90-26179
Optimal synchronization of spread spectrum sequenced by nontransferable switching operators N90-26183
CORA: A direct sequence spread spectrum radio for voice and data N90-26195
Minimization of the cost of information transfer in HF spread spectrum transmission N90-26198
Synchronization of frequency shift transmission and the effect of oversampling N90-26200
HF spread spectrum, an audit of the power requirements and LPI vulnerability N90-26203
Experimental study of a digital mobile radio spread spectrum in an urban site N90-26205
Direct-sequence spread spectrum system
[AD-A223021] N90-26245
Dynamic jamming of networks
[AD-A223044] N90-26247
A novel communication network simulator
[AD-A223045] N90-26248
SPRINGS (ELASTIC)
Plate rods and leaf springs with hybrid structure: Cross section optimization following different target criteria
[ILR-MITT-227(1989)] N90-26366
SPUTTERING
Studies on ion scattering and sputtering processes relevant to ion beam sputter deposition of multicomponent thin films
[DE90-010071] N90-26675
Study of the polyoxymethylene and its sputtered fragments: Implications for comets N90-26781
Photon sputtering of H2O ices: A preliminary report N90-26783
STAINLESS STEELS
Oxidation and sulfidation of Type 310S stainless steel at elevated temperatures
[DE90-010149] N90-26109
STALLING
Computation of viscous aerodynamic characteristics of 2-D airfoils for helicopter applications
[NLR-MP-88052-U] N90-25951
STANDARDIZATION
VISTA (Vertical Integration of Science, Technology, and Applications) user interface software study
[DE90-010003] N90-26707
STANDARDS
NASA project status reports: Congressional requirements can be met, but reliability must be ensured
[GAO/NSIAD-90-40] N90-26169
International standards for text preparation and interchange
[DE90-011868] N90-26699
STAR FORMATION
Radio loud far-infrared galaxies
[DE90-012993] N90-26786
A site for the astrophysical gamma ray process
[DE90-013473] N90-26787
STARS
Astronomy at ultra-high energies: Results from the CYGNUS experiment
[DE90-011979] N90-26732
STATE ESTIMATION
MINAS: An algorithm for systematic state assignment of sequential machines: Computational aspects and results
[EUT-89-E-217] N90-26566
H-infinity control: An exploratory study
[EUT-88-E-211] N90-26584
STATIC LOADS
Agusta methodology for pitch link loads prediction in preliminary design phase
[ETN-90-97270] N90-25978
Evaluation of fracture strength properties of silicon carbide ceramics under cyclic/static axial loading at ultra-high temperature
[DE90-503402] N90-26147
Scaling effects in the static and dynamic response of graphite-epoxy beam-columns
[NASA-TM-102697] N90-26363
STATIC STABILITY
Low-speed wind tunnel investigation of the static stability and control characteristics of an advanced turboprop configuration with the propellers placed over the tail
[NASA-CR-186900] N90-26017
Soil stabilization mat for lunar launch/landing site
[NASA-CR-186690] N90-26128
STATIC TESTS
QM-8 final performance evaluation report: SEALS, volume 4
[NASA-CR-183958] N90-26324
Scaling effects in the static and dynamic response of graphite-epoxy beam-columns
[NASA-TM-102697] N90-26363
STATIONKEEPING
The Screem-J4D: A proposal in response to a low Reynolds number station keeping mission
[NASA-CR-186664] N90-25968
STATISTICAL ANALYSIS
Handbook of uncertainty methodology for engine testing at Pyestock (England)
[RAE-TM-P-1179] N90-26007
Viking data analysis
[AD-A222609] N90-26062
Statistical treatment of slow strain rate data for assessment of hydrogen embrittlement in low alloy high strength steel
[ARL-MAT-R-122] N90-26106
Broadband analysis of ground wave propagation at a50 to 400 MHz N90-26185
Application of inertial instruments for DSN antenna pointing and tracking N90-26224
Statistical analysis of a software reliability model
[IMAG-RR-781-M] N90-26352
A Bayesian proportional model for software reliability
[IMAG-RR-795-M] N90-26353
Analysis and improved design considerations for airborne pulse Doppler radar signal processing in the detection of hazardous windshear
[NASA-CR-186792] N90-26448
Computer architecture evaluation for structural dynamics computations: Project summary
[NASA-CR-186137] N90-26512
Estimating the parameters of a sporadically observed queue
[DE90-012903] N90-26596
Power flow analysis of two coupled plates with arbitrary characteristics
[NASA-CR-182033] N90-26632
Asymptotic modal analysis and statistical energy analysis
[NASA-CR-186732] N90-26634
STATORS
Decay of secondary flow and the associated loss variation downstream of an annual turbine stator cascade
[DE90-505520] N90-25984
Prediction and measurement of rotor blade/stator vane dynamic characteristics of a modern aero-engine axial compressor
[PNR90667] N90-26002
STEADY FLOW
Analysis and mitigation of numerical dissipation in inviscid and viscid computation of vortex-dominated flows
[NASA-CR-186887] N90-26281

STEAM TURBINES
Research and development of advanced gas turbine
[DE90-503377] N90-26335
STEELS
Residual stresses measurements by means of x ray diffraction on electron beam welded joints and laser hardened surfaces
[ETN-90-97269] N90-26371
STEERING
Structures for remotely deployable precision antennas
[NASA-CR-182065] N90-26061
STIRLING CYCLE
Preliminary designs for 25 kWe advanced Stirling conversion systems for dish electric applications
[NASA-TM-103188] N90-26729
STIRLING ENGINES
Preliminary designs for 25 kWe advanced Stirling conversion systems for dish electric applications
[NASA-TM-103188] N90-26729
STOCHASTIC PROCESSES
Closed-form solution of decomposable stochastic models
[NASA-TM-103466] N90-26619
Dichotomies for certain product measures and stable processes
[AD-A222568] N90-26621
Evaluation of a decomposition approach for real-time scheduling using a Stochastic model
[AD-A222726] N90-26625
STOICHIOMETRY
High temperature x ray diffraction and Landau theory investigations of order-disorder transition in defect NaCl-type solids
[DE90-011807] N90-26673
MBE growth technology for high quality strained III-V layers
[NASA-CASE-NPO-17723-1-CU] N90-26685
STORAGE BATTERIES
Storage battery operation technique of photovoltaic system to prevent the imbalance of state of charge
[DE90-503032] N90-26255
STORAGE RINGS (PARTICLE ACCELERATORS)
A beauty factory using an SRF linac and a storage ring
[CEBAF-PR-89-017] N90-26644
STRAIN DISTRIBUTION
Analysis of strain relaxation in Au/Ni multilayers by x ray diffraction
[IAR-89-25] N90-26357
STRAIN ENERGY RELEASE RATE
Strain energy release rate analysis of delamination in a tapered laminate subjected to tension load
[NASA-TM-102592] N90-26076
STRAIN GAGES
A resistance strain gage with repeatable and cancellable apparent strain for use to 800 C
[NASA-CR-185256] N90-26063
STRAIN RATE
Statistical treatment of slow strain rate data for assessment of hydrogen embrittlement in low alloy high strength steel
[ARL-MAT-R-122] N90-26106
STRAPS
Helmet-mounted head restraint
[AD-D014536] N90-26491
STRATOSPHERE
New observations of stratospheric N2O5
[NASA-TM-103478] N90-26402
Stratospheric chemistry N90-26424
Photodissociation of O2 in the stratosphere and mesosphere: A general parametrization of the Schumman-Runge Bands N90-26427
Laboratory measurements and methane photochemistry modeling N90-26770
STRESS ANALYSIS
Strain energy release rate analysis of delamination in a tapered laminate subjected to tension load
[NASA-TM-102592] N90-26076
High temperature multiaxiale creep testing of Nimonic 115
[RAE-TM-P-1182] N90-26122
Determination of the stress distributions in a ceramic: Tensile specimen using numerical techniques
[NASA-TM-101914] N90-26132
Calculation of 3D turbulent jets in crossflow with a multigrid method and a second-moment closure model
[NASA-TM-103159] N90-26282
Design of ceramic components with the NASA/CARES computer program
[NASA-TM-102369] N90-26359
Static and fatigue strength of an adhesive bonded CFRP butt-strap joint: The effects of stacking sequence and temperature
[NLR-TR-88036-U] N90-26370
STRESS CONCENTRATION
The blunt notch behaviour of metal laminates: ARALL and GLARE
[LR-617] N90-26368
STRESS DISTRIBUTION
Damage states in laminated composite three-point bend specimens: An experimental-analytical correlation study
[NASA-TM-101800] N90-26083
Determination of the stress distributions in a ceramic: Tensile specimen using numerical techniques
[NASA-TM-101914] N90-26132
Residual stresses measurements by means of x ray diffraction on electron beam welded joints and laser hardened surfaces
[ETN-90-97269] N90-26371
STRESS INTENSITY FACTORS
The blunt notch behaviour of metal laminates: ARALL and GLARE
[LR-617] N90-26368
STRESS MEASUREMENT
Resistivity, adhesive strength, and residual stress measurements of thin film metallizations on single crystal quartz
[DE90-011902] N90-26135
STRESS RELAXATION
Analysis of strain relaxation in Au/Ni multilayers by x ray diffraction
[IAR-89-25] N90-26357
STRESSES
Determination of the stress distributions in a ceramic: Tensile specimen using numerical techniques
[NASA-TM-101914] N90-26132
STRING THEORY
A research program in theoretical high energy physics
[DE90-013322] N90-26648
Comment on high resolution simulations of cosmic strings. 1: Network evoloution
[NASA-CR-186606] N90-26734
A research program in physics of the early universe
[DE90-013319] N90-26742
STRONGLY COUPLED PLASMAS
Viking data analysis
[AD-A222609] N90-26062
STRUCTURAL ANALYSIS
Structural analysis and optimization of a propfan blade using a finite element method
[DLR-FB-90-01] N90-26006
Biconic cargo return vehicle with an advanced recovery system. Volume 1: Conceptual design
[NASA-CR-186520] N90-26052
Integrated support structure
[NASA-CR-186835] N90-26162
Structured electrode interfaces
[AD-A222763] N90-26265
Design of ceramic components with the NASA/CARES computer program
[NASA-TM-102369] N90-26359
Structural Mechanics Division research and technology plans for FY 1990 and accomplishments for FY 1989
[NASA-TM-102654] N90-26361
Research conducted at the Institute for Computer Applications in Science and Engineering in applied mathematics, numerical analysis, and computer science
[NASA-CR-182057] N90-26510
STRUCTURAL DESIGN
Structures for remotely deployable precision antennas
[NASA-CR-182065] N90-26061
Micro coring apparatus
[NASA-CR-183072] N90-26321
QM-8 final performance evaluation report: SEALS, volume 4
[NASA-CR-183958] N90-26324
Design and construction of a wall-climbing robot
[NIAR-90-20] N90-26327
Advanced Turbine Technology Applications Project (ATTAP)
[NASA-CR-185240] N90-26728
STRUCTURAL ENGINEERING
The application of engineering ceramics in gas turbines
[PNR90676] N90-26005
Technology for large space systems: A bibliography with indexes (supplement 22)
[NASA-SP-7046(22)] N90-26056
The use of Lanczo's method to solve the large generalized symmetric Eigenvalue problem in parallel
[NASA-CR-182072] N90-26533
Construction of geological and geotechnical information database
[DE90-503417] N90-26708
STRUCTURAL FAILURE
Integrated support structure
[NASA-CR-186835] N90-26162
STRUCTURAL VIBRATION
Power flow analysis of two coupled plates with arbitrary characteristics
[NASA-CR-182033] N90-26632
Creating a VAPEPS database: A VAPEPS tutorial
[NASA-CR-186629] N90-26705
STUDENTS
Winged cargo return vehicle. Volume 1: Conceptual design
[NASA-CR-186823] N90-26050
SUBMILLIMETER WAVES
Submillimeter and millimeter observations of solar system objects
[NASA-CR-186636] N90-26731
SUBREFLECTORS
DSS 15, 45, and 65 34-meter high efficiency antenna radio frequency performance enhancement by tilt added to the subreflector during elevation angle changes N90-26229
SUBSONIC FLOW
Effects of forebody geometry on subsonic boundary-layer stability
[NASA-CR-4314] N90-25939
Subsonic combustor flow modeling: State of the art of CFD techniques for reacting and combusting flow N90-25991
SUBSONIC SPEED
Gas Turbine Combustion, volume 2
[VKI-LS-1990-02-VOL-2] N90-25995
SUBSTRATES
Molecular structure of interphases between DGEBA/BTDA adhesives and silver substances using surface-enhanced Raman scattering
[AD-A222750] N90-26157
MBE growth technology for high quality strained III-V layers
[NASA-CASE-NPO-17723-1-CU] N90-26685
SULFIDATION
Oxidation and sulfidation of Type 310S stainless steel at elevated temperatures
[DE90-010149] N90-26109
SULFUR
Phytoplankton and its contribution to the atmospheric sulfur budget of northern Europe N90-26417
SULFUR COMPOUNDS
Results from global tropospheric sulphur simulations N90-26413
Phytoplankton and its contribution to the atmospheric sulfur budget of northern Europe N90-26417
SULFUR DIOXIDES
Deposition to the Baltic Sea N90-26404
Verification and improvement of the EMEP model for long-range transport and deposition of pollutants N90-26405
SUM RULES
A sum rule satisfied by optimized feed-forward layered networks
[RSRE-MEMO-4341] N90-26579
SUN
Space exploration: Cost, schedule, and performance of NASA's Ulysses Mission to the Sun. Fact sheet for the Chairman, Subcommittee on Science, Technology, and Space, Committee on Commerce, Science, and Transportation, US Senate
[GAO/NSIAD-88-129FS] N90-26023
SUPERCOMPUTERS
Informatics aspects of large flow calculations on the SX-2 supercomputer
[NLR-MP-88037-U] N90-26290
Superconcurrent processing: A dynamic approach to heterogeneous parallelism
[AD-A222798] N90-26576
SUPERCONDUCTING FILMS
Studies on ion scattering and sputtering processes relevant to ion beam sputter deposition of multicomponent thin films
[DE90-010071] N90-26675
Ellipsometric study of YBa2Cu3O(7-x) laser ablated and co-evaporated films
[NASA-TM-103223] N90-26682
SUPERCONDUCTING MAGNETS
Parametric design studies of toroidal magnetic energy storage units
[DE90-013086] N90-26390
SUPERCONDUCTIVITY
A beauty factory using an SRF linac and a storage ring
[CEBAF-PR-89-017] N90-26644
Passivation of high temperature superconductors
[NASA-CASE-NPO-17949-1-CU] N90-26684
SUPERCONDUCTORS
Experiments on superconductor imaging surface magnetometry
[DE90-008925] N90-26665

Characterization of NbTi multifilamentary superconducting wires
[DE90-626245] N90-26672
SUPERCOOLING
Undercooling and solidification
[DLR-FB-90-020] N90-26678
SUPERHIGH FREQUENCIES
Design and performance analysis of the DSS-13 beam waveguide antenna N90-26225
SUPERNOVAE
A site for the astrophysical gamma ray process
[DE90-013473] N90-26787
SUPERSONIC AIRCRAFT
Interactive calculation procedures for mixed compression inlets
[NASA-CR-186581] N90-25934
SUPERSONIC COMBUSTION
Supersonic combustor modeling N90-25992
Supersonic reacting internal flow fields
[NASA-TM-103480] N90-26094
SUPERSONIC COMBUSTION RAMJET ENGINES
Transatmospheric vehicle research
[NASA-CR-186705] N90-25970
Supersonic combustor modeling N90-25992
Gas Turbine Combustion, volume 2
[VKI-LS-1990-02-VOL-2] N90-25995
Supersonic reacting internal flow fields
[NASA-TM-103480] N90-26094
SUPERSONIC FLOW
Supersonic reacting internal flow fields
[NASA-TM-103480] N90-26094
UV and VUV spectroscopy and photochemistry of small molecules in a supersonic jet N90-26771
SUPERSONIC NOZZLES
Supersonic wind tunnel nozzles: A selected, annotated bibliography to aid in the development of quiet wind tunnel technology
[NASA-CR-4294] N90-26019
SUPERSONIC TRANSPORTS
Application of laminar flow control to supersonic transport configurations
[NASA-CR-181917] N90-25944
SUPERSONIC WIND TUNNELS
Euler analysis comparison with LDV data for an advanced counter-rotation propfan at cruise
[NASA-TM-103249] N90-25946
Supersonic wind tunnel nozzles: A selected, annotated bibliography to aid in the development of quiet wind tunnel technology
[NASA-CR-4294] N90-26019
SUPPORT SYSTEMS
Terrapin technologies manned Mars mission proposal
[NASA-CR-186838] N90-26027
SURFACE ACOUSTIC WAVE DEVICES
Surface acoustic wave filters in ZnO-SiO2-Si layered structures: Design, technology, and monolithic integration with electronic circuitry
[ETN-90-97218] N90-26638
SURFACE CRACKS
Fracture toughness of polyimide films
[NASA-TM-103473] N90-26130
SURFACE LAYERS
Surface reconstruction based on critical contours in a multi-image context
[RR-784-I-IMAG-94-LIFIA] N90-26383
Exact results for the structured liquid-solid interface
[AD-A222762] N90-26630
Structure and dynamics of water at the Pt (111) interface: Molecular dynamics study
[AD-A222628] N90-26687
SURFACE PROPERTIES
Molecular structure of interphases between DGEBA/BTDA adhesives and silver substances using surface-enhanced Raman scattering
[AD-A222750] N90-26157
Surface reconstruction based on critical contours in a multi-image context
[RR-784-I-IMAG-94-LIFIA] N90-26383
Exact results for the structured liquid-solid interface
[AD-A222762] N90-26630
Laboratory studies of the interaction of ions with condensed gases: Planetary applications N90-26778
SURFACE ROUGHNESS
Laser ultrasonic measurements on ceramic materials with rough surfaces
[DE90-012961] N90-26141
SURFACE TEMPERATURE
Measuring and modeling near-surface reflected and emitted radiation fluxes at the FIFE site
[NASA-CR-180953] N90-26376
SURFACE VEHICLES
Lunar articulated remote transportation system
[NASA-CR-186817-VOL-1] N90-26332
SURFACES
Formation of Titanium-boron surface alloys by excimer laser mixing
[DE90-013172] N90-26118
SURFACTANTS
Dynamics of micellar oligomeric and monomeric sodium 10-undecenoate
[AD-A222570] N90-26099
SURGES
L-SWITCH: A PC program for computing transient voltages and currents during switching off three-phase inductances
[EUT-89-E-221] N90-26257
Simulation of the electrical and thermal behavior of gapless metal oxide surge arresters under AC-operation condition
[ETN-90-97309] N90-26262
SURVEILLANCE RADAR
Vertical ozone probing with lidar N90-26416
SURVEYS
Aviation safety: Conditions within the air traffic control work force. Fact sheet for congressional requesters
[GAO/RCED-89-113FS] N90-25958
Aviation safety: Serious problems continue to trouble the air traffic control work force. Report to congressional requesters
[GAO/RCED-89-112] N90-25959
SURVIVAL
An analysis of requirements for a P-3 windshear training program
[AD-A222577] N90-25960
SWEAT
Adjustment and validation of the mathematical prediction model for sweat rate, heart rate, and body temperature under outdoor conditions
[AD-A222599] N90-26486
SWITCHING
DURIP: Instrumentation for laser switched power LINAC
[AD-A222629] N90-26318
SYMMETRY
Liquid fueled ramjet combustion instability: Acoustical and vortical interactions with burning sprays
[AD-A222752] N90-26104
SYNCHRONISM
Direct-sequence spread spectrum system
[AD-A223021] N90-26245
MTP: An atomic multicast transport protocol
[NASA-CR-186716] N90-26254
A model of the synchronous machine with rectifier, especially for control purposes
[EUT-89-E-215] N90-26256
A possibility to incorporate saturation in the simple, global model of a synchronous machine with rectifier
[EUT-89-E-225] N90-26258
Knowledge and inhibition in asynchronous distributed systems
[TR-90-1139] N90-26703
SYNCHRONOUS PLATFORMS
Texstar: The all-Texas educational satellite system
[NASA-CR-186654] N90-26045
SYNTHESIS (CHEMISTRY)
Synthesis of high purity sinterable silicon carbide powder
[DE90-012029] N90-26084
Composite materials with improved properties in compression: Synthesis of 3-methylene-1,1-Dichiorosilacyclobutane and 1,1-dichlorosilacyclopent-3-ene
[AD-A222615] N90-26088
Condensation polyimides
[NASA-TM-103467] N90-26129
Stibathiolanes: Synthesis, solid state structure, and solution behavior
[AD-A223255] N90-26688
SYNTHETIC APERTURE RADAR
The browse file of NASA/JPL quick-look radar images from the Loch Linnhe 1989 experiment
[NASA-CR-186855] N90-26701
SYSTEM IDENTIFICATION
Intergration of system identification and robust controller designs for flexible structures in space
[NASA-TM-102695] N90-26362
AGARD highlights 90/1 N90-26788
SYSTEMS ANALYSIS
Single-pass memory system evaluation for multiprogramming workloads
[NASA-CR-186553] N90-26558
SYSTEMS ENGINEERING
Enroute flight planning: The design of cooperative planning systems
[NASA-CR-186797] N90-25964
National space test centers, Lewis research center facilities
[NASA-TM-103187] N90-26030
A novel multireceiver communications system configuration based on optimal estimation theory
[NASA-CR-186847] N90-26216
Applications of different design methodologies in navigation systems and development at JPL N90-26221
Low-gravity fluid physics: A program overview
[NASA-TM-103215] N90-26273
Automation of closed environments in space for human comfort and safety
[NASA-CR-186834] N90-26500
Innovative design systems: Where are we, and where do we go from here
[AD-A222586] N90-26556
SYSTEMS INTEGRATION
Technical evaluation report on the Guidance and Control Panel 49th Symposium on Fault Tolerant Design Concepts for Highly Integrated Flight Critical Guidance and Control Systems
[AGARD-AR-281] N90-26012
Intergration of system identification and robust controller designs for flexible structures in space
[NASA-TM-102695] N90-26362
SYSTEMS MANAGEMENT
Making real-time reactive systems reliable
[NASA-CR-186642] N90-26344
SYSTEMS SIMULATION
A new scheme for identification and control
[EUT-88-E-213] N90-26586
SYSTOLIC ARRAYS
Parallel algorithm for distributed memory computers (applications to matricial algorithms)
[ETN-90-97252] N90-26573

T

T SHAPE
The structural dynamics analysis of the main injector LOX inlet tee and its redesign
[NASA-CR-186764] N90-26358
TABULATION PROCESSES
UEDIT: A full-scale, scrollable APL2 spreadsheet input/output editor
[AD-A222712] N90-26557
TAIL ASSEMBLIES
Effect of tail size reductions on longitudinal aerodynamic characteristics of a three surface F-15 model with nonaxisymmetric nozzles
[NASA-TP-3036] N90-25938
TAKEOFF
An overview of the joint FAA/NASA aircraft/ground runway friction program
[NASA-TM-103486] N90-25957
TANKS (COMBAT VEHICLES)
Motion sickness, visual displays, and armored vehicle design
[AD-A222678] N90-26506
TANTALUM
Densification studies of refractory materials using Hot Isostatic Pressing (HIP) and tantalum containment
[DE90-013481] N90-26114
TARGET ACQUISITION
Guidance and targeting for the strategic target system
[DE90-005239] N90-26031
TARGETS
Qualitative evaluation of a conformal velocity vector display for use at high angles-of-attack in fighter aircraft
[NASA-TM-102629] N90-25981
The variably trimmed mean CFAR detector for nonhomogeneous background
[AD-A222801] N90-26243
Multiple target tracking in a wide-field-of-view camera system
[DE90-013488] N90-26300
TASKS
Design and construction of a wall-climbing robot
[NIAR-90-20] N90-26327
Investigation of automated task learning, decomposition and scheduling
[NASA-CR-186791] N90-26488
TDR SATELLITES
Space operations: NASA's communications support for Earth orbiting spacecraft. Report to Chairman, Subcommittee on Space Science and Applications, Committee on Science, Space and Technology, House of Representatives
[GAO/IMTEC-89-41] N90-26215
TEAMS
Effect of organizational structure on performance of decision making teams
[AD-A223160] N90-26697
TECHNICAL WRITING
Grammar, punctuation, and capitalization: A handbook for technical writers and editors
[NASA-SP-7084] N90-26710

TECHNOLOGICAL FORECASTING
Materials and structures for 2000 and beyond: An attempted forecast by the DLR Materials and Structures Department
[ESA-TT-1154-REV] N90-26173
TECHNOLOGY ASSESSMENT
Autonomous space processor for orbital debris
[NASA-CR-186691] N90-26044
Tensile strength measurement techniques for structural ceramics
[DE90-012193] N90-26136
Figure of merit studies of beam power concepts for advanced space exploration
[NASA-CR-186720] N90-26234
Electronic warfare technology: Trends and visions
[AD-A223034] N90-26246
VISTA (Vertical Integration of Science, Technology, and Applications) user interface software study
[DE90-010003] N90-26707
Prototyping an in-house business intelligence database
[PNR90665] N90-26709
The lessons of Varsovian's reconnaissance
[NASA-TM-103207] N90-26789
TECHNOLOGY TRANSFER
International standards for text preparation and interchange
[DE90-011868] N90-26699
TECHNOLOGY UTILIZATION
Materials and structures for 2000 and beyond: An attempted forecast by the DLR Materials and Structures Department
[ESA-TT-1154-REV] N90-26173
Theoretical studies of solar pumped lasers
[NASA-CR-186712] N90-26308
Advanced Turbine Technology Applications Project (ATTAP)
[NASA-CR-185240] N90-26728
Preliminary designs for 25 kWe advanced Stirling conversion systems for dish electric applications
[NASA-TM-103188] N90-26729
TELECOMMUNICATION
A novel multireceiver communications system configuration based on optimal estimation theory
[NASA-CR-186847] N90-26216
The Telecommunications and Data Acquisition Report
[NASA-CR-186852] N90-26217
TELEMETRY
Preliminary error budget for an optical ranging system: Range, range rate, and differenced range observables N90-26227
TELEOPERATORS
Space station definitions, design, and development. Task 5: Multiple arm telerobot coordination and control: Manipulator design methodology
[NASA-CR-182043] N90-26577
TELESCOPES
A two-telescope receiver design for deep space optical communications N90-26226
TEMPER (METALLURGY)
The effect of manganese on the onset of the stage 2 reaction in an austempered ductile iron matrix
[DE90-011804] N90-26119
TEMPERATURE CONTROL
Thermal management of an accelerator system in space
[DE90-013153] N90-26627
TEMPERATURE DEPENDENCE
Photodissociation of NO2: Influence of photolysis wavelength and temperature dependence on product formation N90-26426
Infrared line parameters at low temperatures relevant to planetary atmospheres N90-26753
TEMPERATURE DISTRIBUTION
Temperature and OH concentrations in a solid propellant flame using absorption techniques
[AD-A222591] N90-26100
TEMPERATURE EFFECTS
Extension of a noninteractive reliability model for ceramic matrix composites
[NASA-CR-185267] N90-26142
Fluid Phase Separation (FPS) experiment for flight on a space shuttle Get Away Special (GAS) canister
[NASA-CR-186830] N90-26161
Influence of thermal conditioning media on Charpy specimen test temperature
[DE90-012784] N90-26360
Static and fatigue strength of an adhesive bonded CFRP butt-strap joint: The effects of stacking sequence and temperature
[NLR-TR-88036-U] N90-26370
TEMPERATURE MEASUREMENT
Vapor pressures of acetylene at low temperatures N90-26777
TEMPERATURE PROFILES
Measurement of velocity and temperature profiles at the exit plane of a tubular gas turbine combustor
[DE90-505519] N90-25983
Resonant coupling through a slot to a loaded cylindrical cavity: Experimental results
[AD-A223000] N90-26631
TENSILE PROPERTIES
The influence of microstructure on the tensile behavior of an aluminum metal matrix composite
[NASA-TM-102694] N90-26082
Compendium of material test results on HY-130 and Ti-3Al2V metals in support of United States navy programs
[DE90-011754] N90-26112
Fracture toughness and failure mechanisms in commercial 2091 Al-Li sheet at cryogenic temperatures
[AD-A222803] N90-26125
TENSILE STRENGTH
Application of high performance metals in gas turbine engines
[PNR90640] N90-25999
The effect of manganese on the onset of the stage 2 reaction in an austempered ductile iron matrix
[DE90-011804] N90-26119
The interaction of polymeric materials with ceramic surfaces with special reference to the behaviour of bioceramics N90-26127
Tensile strength measurement techniques for structural ceramics
[DE90-012193] N90-26136
TENSOR ANALYSIS
A new class of exact solutions of the vacuum quadratic Poincare gauge field theory
[MATHS-REPT-A-119] N90-26691
TENSORS
Application of symbolic computations to the constitutive modeling of structural materials
[NASA-TM-103225] N90-26364
Implementation of algorithms used in calculating the tensor product of matrices on a distributed memory machine
[IMAG-RR-786-I] N90-26572
A new class of exact solutions of the vacuum quadratic Poincare gauge field theory
[MATHS-REPT-A-119] N90-26691
On trivector torsion in vacuum quadratic Poincare gauge field theory
[MATHS-REPT-A-121] N90-26692
TERPENES
Measurements of monoterpenes in a coniferous forest N90-26421
Terpene concentrations and emissions in a Scots pine forest N90-26422
TERRAIN
Remote sensing of Earth terrain
[NASA-CR-186888] N90-26382
TERRAIN ANALYSIS
Technical evaluation report on the Guidance and Control Panel 49th Symposium on Fault Tolerant Design Concepts for Highly Integrated Flight Critical Guidance and Control Systems
[AGARD-AR-281] N90-26012
Improving the geometric fidelity of imaging systems employing sensor arrays
[NASA-CASE-NPO-17970-1-CU] N90-26384
TEST CHAMBERS
Research at NASA's NFAC wind tunnels
[NASA-TM-102827] N90-25933
TEST FACILITIES
Wright Research and Development Center test facilities handbook
[AD-A222582] N90-26020
National space test centers, Lewis research center facilities
[NASA-TM-103187] N90-26030
High temperature multiaxiale creep testing of Nimonic 115
[RAE-TM-P-1182] N90-26122
Bringing aircraft noise testing down to Earth
[PNR90642] N90-26637
TEST FIRING
Supersonic combustor testing N90-25998
TEST PATTERN GENERATORS
Contribution to CMOS integrated circuit tests: Study of the stuck-on and stuck-open fault tests
[ETN-90-97256] N90-26261
TESTES
Experiment K-6-16. Morphological examination of rat testes. The effect of Cosmos 1887 flight on spermatogonial population and testosterone level in rat testes N90-26469
TETHERED SATELLITES
Perspective features of the tethered systems for space applications
[ETN-90-97279] N90-26059
Possible applications of tethered systems to Mars exploration missions
[IAF-89-489] N90-26060
TETHERING
Perspective features of the tethered systems for space applications
[ETN-90-97279] N90-26059
Possible applications of tethered systems to Mars exploration missions
[IAF-89-489] N90-26060
TETRAHEDRONS
Parallelization of an annealing simulation applied to improving tetrahedric grids
[IMAG-RR-796-M] N90-26570
TEXAS
Texstar: The all-Texas educational satellite system
[NASA-CR-186654] N90-26045
TEXTBOOKS
Rhetorical structure theory and text analysis
[AD-A222655] N90-26733
TEXTS
The rationale and specification of the ELLA graphics systems
[RSRE-89017] N90-26548
TEXTURES
Texture of materials by time-of-flight neutron diffraction
[DE90-008968] N90-26096
Pattern classification of textura by moment and distance autocorrelation function
[INPE-4976-PRE/1541] N90-26379
Classification regions in remote sensing imagery utilizing spatial characteristics
[INPE-4913-PRE/1514] N90-26381
THEMATIC MAPPING
Atmospheric correction of thematic mapping measurements about seabeds of the German Bay
[GKSS-89/E/47] N90-26029
THERMAL ANALYSIS
Flight motor set 360L007 (STS-33R)
[NASA-CR-183979] N90-26067
New discharge pumping method for CO2 lasers
[AD-A220898] N90-26307
THERMAL INSULATION
Space plane model for visual measurement of aerodynamic heating
[DE90-505514] N90-25949
THERMAL PROTECTION
Acousto-optic signature analysis for inspection of the orbiter thermal protection tile bonds
[DE90-013089] N90-26043
The aerobraking space transfer vehicle
[NASA-CR-186819] N90-26053
A computational study of the effectiveness of coating materials for KE projectile fins subjected to the combined effects of inbore and aerodynamic heating
[AD-A222595] N90-26155
Flight set 360L001 (STS-26) igniter, post flight
[NASA-CR-183957] N90-26325
Field experience in using laser acoustic sensing for inspection
[DE90-012954] N90-26347
THERMAL SIMULATION
Simulation of the electrical and thermal behavior of gapless metal oxide surge arresters under AC-operation condition
[ETN-90-97309] N90-26262
THERMOCHEMISTRY
Kinetics and thermochemistry of polyatomic free radicals: New results and new understandings N90-26764
The applications of chemical thermodynamics and chemical kinetics to planetary atmospheres research N90-26773
THERMODYNAMIC CYCLES
Qualitative and quantitative reasoning about thermodynamics
[NASA-CR-186788] N90-26689
THERMODYNAMIC EFFICIENCY
Research and development of advanced gas turbine
[DE90-503377] N90-26335
THERMODYNAMIC EQUILIBRIUM
Baryogenesis in extended inflation. 2: Baryogenesis via primordial black holes
[NASA-CR-182843] N90-26735
THERMODYNAMIC PROPERTIES
Isothermal compressibility of SPC/E water
[AD-A222723] N90-26643
Mathematical simulation of heat exchanges and thermoelastic constraints in Czochralski crystal growth
[ETN-90-97242] N90-26680
THERMODYNAMICS
Performance of a supercharged direct-injection stratified-charge rotary combustion engine
[NASA-TM-103105] N90-25982

Investigation of thermo-mechanical effects in silicon carbide Whisker/Al alloy composites
[AD-A222635] N90-26089
Code enhancements and validation of GASP
[NPS-PAPER-44] N90-26277
Isothermal compressibility of SPC/E water
[AD-A222723] N90-26643
Qualitative and quantitative reasoning about thermodynamics
[NASA-CR-186788] N90-26689
A lattice gas model for thermohydrodynamics
[DE90-011964] N90-26690
First International Conference on Laboratory Research for Planetary Atmospheres
[NASA-CP-3077] N90-26744
Liquid-vapor equilibrium of multicomponent cryogenic systems N90-26774

THERMOELECTRICITY
Pressure dependence of thermoelectric power of high T(sub c) 123 compound
[PD-MT-9001] N90-26092

THERMOPHYSICAL PROPERTIES
Effect of casting procedures and diesel engine environment on the behavior of aluminum titanate
[AD-A223079] N90-26126
Critical evaluation of Jet-A spray combustion using propane chemical kinetics in gas turbine combustion simulated by KIVA-2
[NASA-TM-103173] N90-26170

THERMOPLASTIC RESINS
Time temperature relations during rubber forming continuous fiber reinforced thermoplastics
[LR-620] N90-26151

THERMOPLASTICITY
Fracture toughness of polyimide films
[NASA-TM-103473] N90-26130

THIN FILMS
Resistivity, adhesive strength, and residual stress measurements of thin film metallizations on single crystal quartz
[DE90-011902] N90-26135
Selective electrocatalysis of anodic oxygen-transfer reactions at chemically modified, thin-film lead dioxide electrodes
[DE90-011747] N90-26252
Interim qualification tests and procedures for terrestrial photovoltaic thin-film flat-plate modules
[DE90-000354] N90-26392
Large, orientation-dependent enhancements of critical currents in Y1Ba2Cu3O(7-x) epitaxial thin films: Evidence for intrinsic flux pinning
[DE90-009424] N90-26666
Studies on ion scattering and sputtering processes relevant to ion beam sputter deposition of multicomponent thin films
[DE90-010071] N90-26675
Vacuum deposition by pulsed laser radiation: Plasma composition, deposition techniques, and thin film properties
[ETN-90-97263] N90-26677

THIN PLATES
Modeling of composite beams and plates for static and dynamic analysis
[NASA-CR-186459] N90-26354

THREE DIMENSIONAL BODIES
Segmentation before and after reconstruction of 3-D surfaces in depth imagery
[RR-788-I-IMAG-97-LIFIA] N90-26551

THREE DIMENSIONAL BOUNDARY LAYER
Report of the Fluid Dynamics Panel Working Group 10 on calculation of 3D separate turbulent flows in boundary layer limit
[AGARD-AR-255] N90-26280

THREE DIMENSIONAL FLOW
Numerical analysis of three-dimensional particle-laden flow equations
[IAR-90-2] N90-26268
A fully implicit ADI method for quasi three-dimensional flows through straight blade rows
[ETN-90-96965] N90-26283
The effect of a three-dimensional source on the flow through a channel with square cross section
[LR-512] N90-26289
Informatics aspects of large flow calculations on the SX-2 supercomputer
[NLR-MP-88037-U] N90-26290

THREE DIMENSIONAL MODELS
Computational experience with a three-dimensional rotary engine combustion model
[NASA-TM-103104] N90-26275

THRUST CONTROL
Guidance and control strategies for aerospace vehicles
[NASA-CR-186878] N90-26013

TIBIA
Experiment K-6-27. Analysis of radiographs and biosamples from primate studies N90-26478

TILES
Acousto-optic signature analysis for inspection of the orbiter thermal protection tile bonds
[DE90-013089] N90-26043
Field experience in using laser acoustic sensing for inspection
[DE90-012954] N90-26347

TIME DEPENDENCE
Prediction of two-dimensional time-dependent gasdynamic flows for hypersonic studies
[UTIAS-335] N90-25935
Experiments on initial behaviour of corona generated with electrical pulses superimposed on DC bias
[EUT-89-E-226] N90-26259

TIME LAG
Model following control system design: Preliminary ATTAS in-flight simulation test results
[PD-FC-9003] N90-26010

TIME OPTIMAL CONTROL
On output deadbeat control of discrete-time multivariable systems
[MATHS-REPT-A-122] N90-26583

TIME SERIES ANALYSIS
Nonlinear modeling of time series using Multivariate Adaptive Regression Splines (MARS)
[AD-A222710] N90-26623
Reversed residuals in autoregressive time series analysis
[AD-A222711] N90-26624

TIME SHARING
Atomic snapshots of shared memory
[AD-A222765] N90-26520

TIME TEMPERATURE PARAMETER
Time temperature relations during rubber forming continuous fiber reinforced thermoplastics
[LR-620] N90-26151

TIMOSHENKO BEAMS
An experimental system for measuring the wavenumber-frequency response of Timoshenko beams
[AD-A222569] N90-26374

TIRES
An overview of the joint FAA/NASA aircraft/ground runway friction program
[NASA-TM-103486] N90-25957

TITAN
Role of the methylene amidogen (H2CN) radical in the atmospheres of Titan and Jupiter N90-26769
Liquid-vapor equilibrium of multicomponent cryogenic systems N90-26774

TITANATES
Effect of casting procedures and diesel engine environment on the behavior of aluminum titanate
[AD-A223079] N90-26126

TITANIUM
Characterization of NbTi multifilamentary superconducting wires
[DE90-626245] N90-26672

TITANIUM ALLOYS
Application of high performance metals in gas turbine engines
[PNR90640] N90-25999
Compendium of material test results on HY-130 and Ti-3Al2V metals in support of United States navy programs
[DE90-011754] N90-26112
Formation of Titanium-boron surface alloys by excimer laser mixing
[DE90-013172] N90-26118
Small crack growth and its influence in near alpha-titanium alloys
[RAE-TM-P-1171] N90-26121
Structures and mechanical properties of near-beta titanium alloys TiV10Fe2Al3 and TiV10Cu3Al3
[ONERA-NT-1989-3] N90-26123
Crystal growth and deformation behavior of TiAl aluminides
[DE90-012972] N90-26671

TOPOGRAPHY
Estimation of the impulse response of a broadband mobile radio channel in suburbia at 910 MHz N90-26187
Spatial cross-correlation of Antarctic Sea ice and seabed topography
[NASA-CR-186815] N90-26451

TOPOLOGY
Hierarchical structure of polygonal data for spatial analysis and representation of cartographical data
[INPE-4986-PRE/1548] N90-26380
Predissimilarities, prefilters, and ultrametrics on an arbitrary set
[IMAG-RR-970-M] N90-26603
Generation and improvement of meshes for finite elements methods in two and three dimensions
[ETN-90-97249] N90-26611

TORCHES
Electrode carrying wire for GTAW welding
[NASA-CASE-MFS-29491-1] N90-26168

TOROIDS
Parametric design studies of toroidal magnetic energy storage units
[DE90-013086] N90-26390
Confinement of nonneutral plasma in unconventional geometries
[DE90-013048] N90-26659

TORQUE
Direct drive robotic hand
[NASA-CASE-NPO-17917-1-CU] N90-26339

TORQUE MOTORS
Active lag angle device
[AD-D014538] N90-26249

TORSION
On trivector torsion in vacuum quadratic Poincare gauge field theory
[MATHS-REPT-A-121] N90-26692

TORSIONAL STRESS
Agusta methodology for pitch link loads prediction in preliminary design phase
[ETN-90-97270] N90-25978

TOUGHNESS
Fracture toughness and failure mechanisms in commercial 2091 Al-Li sheet at cryogenic temperatures
[AD-A222803] N90-26125

TOXICITY
The global consequences of increasing tropospheric ozone concentrations
[NASA-TM-103477] N90-26401

TRACE ELEMENTS
Natural and anthropogenic compounds in bulk precipitation at Blidoe (archipelago of Stockholm, Sweden) N90-26409
Experiment K-6-04. Trace element balance in rats during spaceflight N90-26458

TRACKED VEHICLES
Design of an autonomous Lunar construction utility vehicle
[NASA-CR-186832] N90-26330

TRACKING (POSITION)
Application of inertial instruments for DSN antenna pointing and tracking N90-26224
QPSK loop lock detection in the advanced receiver N90-26230
Multiple target tracking in a wide-field-of-view camera system
[DE90-013488] N90-26300
Eye tracking device for the measurement of flight performance in simulators
[AD-A220075] N90-26484
A real-time optical 3D tracker for head-mounted display systems
[AD-A222747] N90-26508

TRACKING NETWORKS
Automatic line network extraction from aerial imagery of urban areas through knowledge based image analysis
[AD-A222675] N90-26385

TRADEOFFS
Knowledge and inhibition in asynchronous distributed systems
[TR-90-1139] N90-26703

TRAINING ANALYSIS
Aircrew life support systems enhancement
[AD-A222826] N90-26505

TRAINING EVALUATION
An analysis of requirements for a P-3 windshear training program
[AD-A222577] N90-25960

TRAJECTORIES
An inverse dynamic method yielding flexible manipulator state trajectories
[NASA-CR-186807] N90-26329

TRAJECTORY ANALYSIS
Further development and application of an atmospheric chemistry trajectory model N90-26408

TRAJECTORY OPTIMIZATION
Trajectory optimization for an asymmetric launch vehicle
[NASA-CR-185830] N90-26033
The effect of interplanetary trajectory options on a manned Mars aerobrake configuration
[NASA-TP-3019] N90-26036

TRANSATMOSPHERIC VEHICLES
Transatmospheric vehicle research
[NASA-CR-186705] N90-25970

TRANSDUCERS
A dual-wavelength passive homodyne detection unit for fiber-coupled white-light interferometers
[ETN-90-97036] N90-26653

TRANSFER FUNCTIONS
System factors to be considered in assessing propagation effects on modern digital satellite communications systems N90-26208
H-infinity control: An exploratory study [EUT-88-E-211] N90-26584
A new scheme for identification and control [EUT-88-E-213] N90-26586
TRANSFER ORBITS
Guidance and control strategies for aerospace vehicles [NASA-CR-186878] N90-26013
Forbidden tangential orbit transfers between intersecting Keplerian orbits [NASA-TP-3031] N90-26028
IRIS system and future application to expandable launchers [IAF-89-212] N90-26035
Project SPARC: Space-based aeroassisted reusable craft [NASA-CR-186816] N90-26051
TRANSFERRING
The aerobraking space transfer vehicle [NASA-CR-186819] N90-26053
TRANSFORMATIONS (MATHEMATICS)
Mathematical problem-solving transfer: The effects of cognitive load and attention a schema acquisition and rule automation N90-26594
The system matrix characterisation of input-output equivalence [MATHS-REPT-A-112] N90-26600
Unification and disunification: Theory and applications [ETN-90-97247] N90-26610
Mobility studies in multiloop spatial linkages N90-26628
TRANSIENT HEATING
Transients in turbulent convective heat transfer to a flow of supercritical helium [ETN-90-97217] N90-26286
TRANSITION FLIGHT
H-infinity based integrated flight-propulsion control design for a STOVL aircraft in transition flight [NASA-TM-103198] N90-26011
TRANSITION METALS
Formation of cubic LI2 phases from Al3Ti and Al3Zr by transition metal substitutions for Al [DE90-012288] N90-26117
TRANSMISSION EFFICIENCY
Transmission, reflection, and radiation at junction planes of different open waveguides [ISBN-90-9002864-1] N90-26241
Optical transmission through a polarization preserving single mode optical fiber at two Ar(+) laser wavelengths [NASA-TM-103475] N90-26651
TRANSMISSION LINES
Packet radio network concepts for the Norwegian field army N90-26206
DURIP: Instrumentation for laser switched power LINAC [AD-A222629] N90-26318
TRANSMISSION LOSS
Wideband characterization of forest propagation channels N90-26188
TRANSMISSIONS (MACHINE ELEMENTS)
Efficiency study comparing two helicopter planetary reduction stages [NASA-TM-103106] N90-26334
TRANSMITTER RECEIVERS
Equipment feasibility study: Very high frequency communication equipment (136-137 megahertz) [DOT/FAA/CT-TN89/72] N90-26210
TRANSMITTERS
Man-made noise in a military environment N90-26191
TRANSONIC WIND TUNNELS
Effect of tail size reductions on longitudinal aerodynamic characteristics of a three surface F-15 model with nonaxisymmetric nozzles [NASA-TP-3036] N90-25938
TRANSPORT AIRCRAFT
Study of high-speed civil transports. Summary [NASA-CR-4236] N90-25966
Robustness evaluation of H2 and H(infinity) control theory as applied to a transport aircraft [AD-A222795] N90-26018
TRANSPORT PROPERTIES
Optical properties and transport properties of hydrogenated amorphous silicon [ETN-90-97215] N90-26656
TRANSPORT VEHICLES
Bidirectional drive and brake mechanism [NASA-CASE-MSC-21540-1] N90-26342
TRANSPORTATION
Biconic cargo return vehicle with an advanced recovery system. Volume 1: Conceptual design [NASA-CR-186520] N90-26052
Design of a lunar transportation system, volume 2 [NASA-CR-186833-VOL-2] N90-26333
TRAPPED PARTICLES
Inhomogeneous electric field effects in a linear RF quadruple trap N90-26222
A study of the influence of Hg(6(3)P2) population in a low-pressure discharge on mercury ion emission at 194.2 nm N90-26223
TRAPPING
Inhomogeneous electric field effects in a linear RF quadruple trap N90-26222
TRAVELING WAVES
Implementation of an algorithm for travelling-wave-based directional detection [EUT-89-E-214] N90-26239
On travelling-wave-based protection of high-voltage networks [ISBN-90-9002955-9] N90-26260
On traveling wave solutions of a set of coupled Boussinesq-like equations [DE90-013182] N90-26597
TREES (MATHEMATICS)
Large sets of block designs [ETN-90-97212] N90-26602
Combinatorial problems using a hypercube and Hamming graphs [ETN-90-97240] N90-26609
Unification and disunification: Theory and applications [ETN-90-97247] N90-26610
TRENDS
Technical evaluation report on the Guidance and Control Panel 49th Symposium on Fault Tolerant Design Concepts for Highly Integrated Flight Critical Guidance and Control Systems [AGARD-AR-281] N90-26012
TRIANGULATION
Generation and improvement of meshes for finite elements methods in two and three dimensions [ETN-90-97249] N90-26611
TROPOSPHERE
Measurements of tropospheric nitric acid over the Western United States and Northeastern Pacific Ocean [NASA-TM-103470] N90-26399
The global consequences of increasing tropospheric ozone concentrations [NASA-TM-103477] N90-26401
Results from the IVL TOR Station at Roervik, Sweden. A contribution to the EURATRAC subproject TOR N90-26415
Formation kinetics of N2O in the atmosphere N90-26425
TROPOSPHERIC SCATTERING
Measurement and simulation of widespread mobile radio channel characteristics N90-26186
TRUCKS
Proof of principle model for a lunar dumptruck [NASA-CR-182557] N90-26323
TURBINE BLADES
Turbine blade heat transfer coefficient evaluation by modified version of STAN5. Comparison with experimental data [ETN-90-97283] N90-26008
TURBINE ENGINES
The role of NDI in the certification of turbine engine components [PNR90629] N90-26349
TURBINE EXHAUST NOZZLES
Computational fluid dynamics 3-D analysis for advanced transonic turbine design [ETN-90-97282] N90-26291
TURBINE INSTRUMENTS
Combustion instrumentation N90-25996
TURBINE PUMPS
Reusable rocket engine turbopump health monitoring system, part 3 [NASA-CR-182294] N90-26320
TURBINES
Decay of secondary flow and the associated loss variation downstream of an annual turbine stator cascade [DE90-505520] N90-25984
TURBOCOMPRESSORS
Application of high performance metals in gas turbine engines [PNR90640] N90-25999
Prediction and measurement of rotor blade/stator vane dynamic characteristics of a modern aero-engine axial compressor [PNR90667] N90-26002
TURBOJET ENGINES
Turbulent combustion modeling for turbo-jet combustion chambers N90-25993
TURBOPROP AIRCRAFT
High speed turboprop aeroacoustic study (counterrotation). Volume 1: Model development [NASA-CR-185241] N90-26633
TURBULENCE
Formation of design envelope criterion in terms of deterministic spectral procedure [RAE-TM-SS-9] N90-25953
A critical evaluation of two-equation models for near wall turbulence [NASA-CR-182068] N90-26270
Measurement of terms and parameters in turbulent models [NASA-CR-183993] N90-26271
Effect of initial conditions on the development of two-phase jets [AD-A222621] N90-26293
TURBULENCE EFFECTS
Aircraft measurements of the turbulence structure in cirrus clouds [ISSN-0069-5882] N90-26450
TURBULENCE MODELS
An investigation into the numerical prediction of boundary layer transition using the K.Y. Chien turbulence model [NASA-CR-185252] N90-26269
Report of the Fluid Dynamics Panel Working Group 10 on calculation of 3D separate turbulent flows in boundary layer limit [AGARD-AR-255] N90-26280
TURBULENT BOUNDARY LAYER
Interactive calculation procedures for mixed compression inlets [NASA-CR-186581] N90-25934
A critical evaluation of two-equation models for near wall turbulence [NASA-CR-182068] N90-26270
Report of the Fluid Dynamics Panel Working Group 10 on calculation of 3D separate turbulent flows in boundary layer limit [AGARD-AR-255] N90-26280
TURBULENT DIFFUSION
The diurnal ozone cycle in a coniferous forest: The importance of meteorology and chemistry N90-26423
TURBULENT FLOW
Turbulent combustion modeling for turbo-jet combustion chambers N90-25993
Chemistry of combustion processes N90-25994
An investigation into the numerical prediction of boundary layer transition using the K.Y. Chien turbulence model [NASA-CR-185252] N90-26269
Report of the Fluid Dynamics Panel Working Group 10 on calculation of 3D separate turbulent flows in boundary layer limit [AGARD-AR-255] N90-26280
Analysis of turbulent density fluctuations by means of spontaneous Raman diffusion [ISL-R-103/89] N90-26287
The finite analytic method and its applications. Volume 1: Laminar and turbulent flows past two-dimensional and axisymmetric bodies [AD-A222787] N90-26294
Effects of 2 Hz imposed bulk flow unsteadiness on laminar-turbulent transition in a straight channel [AD-A223028] N90-26295
TURBULENT HEAT TRANSFER
Turbine blade heat transfer coefficient evaluation by modified version of STAN5. Comparison with experimental data [ETN-90-97283] N90-26008
Transients in turbulent convective heat transfer to a flow of supercritical helium [ETN-90-97217] N90-26286
TURBULENT JETS
Calculation of 3D turbulent jets in crossflow with a multigrid method and a second-moment closure model [NASA-TM-103159] N90-26282
TVD SCHEMES
Prediction of two-dimensional time-dependent gasdynamic flows for hypersonic studies [UTIAS-335] N90-25935
On central-difference and upwind schemes [NASA-CR-182061] N90-26595
TWO BODY PROBLEM
Forbidden tangential orbit transfers between intersecting Keplerian orbits [NASA-TP-3031] N90-26028
TWO DIMENSIONAL BODIES
The finite analytic method and its applications. Volume 1: Laminar and turbulent flows past two-dimensional and axisymmetric bodies [AD-A222787] N90-26294
TWO PHASE FLOW
Numerical analysis of three-dimensional particle-laden flow equations [IAR-90-2] N90-26268
Effect of initial conditions on the development of two-phase jets [AD-A222621] N90-26293

U

U-2 AIRCRAFT
Technology development: Future use of NASA's large format camera is uncertain
[GAO/NSIAD-90-142] N90-26298

UDIMET ALLOYS
Application of high performance metals in gas turbine engines
[PNR90640] N90-25999

ULLAGE
Prediction of the ullage gas thermal stratification in a NASP vehicle propellant tank experimental simulation using FLOW-3D
[NASA-TM-103217] N90-26160

ULNA
Experiment K-6-27. Analysis of radiographs and biosamples from primate studies N90-26478

ULTRAHIGH FREQUENCIES
Estimation of the impulse response of a broadband mobile radio channel in suburbia at 910 MHz N90-26187
Wideband characterization of forest propagation channels N90-26188
A narrowband tactical communication system for the VHF and UHF mobile radio bands N90-26192
Electric field strength meters for the HF, VHF, and UHF bands
[BBC-RD-1990/3] N90-26212

ULTRAHIGH VACUUM
Imaging and spectroscopy of small molecules by scanning tunneling microscopy
[AD-A222572] N90-26641

ULTRASONIC FLAW DETECTION
Development of creep-fatigue damage detection method of rotor steel by ultrasonic wave measurement
[DE90-503792] N90-26365

ULTRASONIC TESTS
Laser ultrasonic measurements on ceramic materials with rough surfaces
[DE90-012961] N90-26141

ULTRASONIC WAVE TRANSDUCERS
PVDF contact probes
[VTT-RR-623] N90-26253

ULTRASONICS
Real-time monitoring of ceramic sintering with laser ultrasonics
[DE90-012960] N90-26140

ULTRAVIOLET RADIATION
Stratospheric chemistry N90-26424

ULTRAVIOLET SPECTROSCOPY
UV and VUV spectroscopy and photochemistry of small molecules in a supersonic jet N90-26771

ULYSSES MISSION
Space exploration: Cost, schedule, and performance of NASA's Ulysses Mission to the Sun. Fact sheet for the Chairman, Subcommittee on Science, Technology, and Space, Committee on Commerce, Science, and Transportation, US Senate
[GAO/NSIAD-88-129FS] N90-26023

UNDERGROUND STRUCTURES
Greenhouse design for a Martian colony: Structural, solar collection and light distribution systems
[NASA-CR-186818] N90-26501

UNDERWATER ACOUSTICS
Canonical eigenvalues. Part 1: General theory
[AD-A222812] N90-26617

UNDERWATER BREATHING APPARATUS
Development of membrane process for carbon dioxide separation from diving atmosphere
[AD-A222606] N90-26504

UNDERWATER VEHICLES
Guidance and control system for an autonomous underwater vehicle
[AD-A222709] N90-26343

UNITED STATES
Measurements of tropospheric nitric acid over the Western United States and Northeastern Pacific Ocean
[NASA-TM-103470] N90-26399

UNIVERSE
Nonstandard big bang models
[DE90-625593] N90-26736
A research program in physics of the early universe
[DE90-013319] N90-26742

UNIVERSITY PROGRAM
NASA/USRA university advanced design program at the University of Illinois for the 1989-1990 academic year
[NASA-CR-186829] N90-26049

UNMANNED SPACECRAFT
NASA/USRA university advanced design program at the University of Illinois for the 1989-1990 academic year
[NASA-CR-186829] N90-26049
Possible applications of tethered systems to Mars exploration missions
[IAF-89-489] N90-26060

UNSTEADY AERODYNAMICS
Identification of aerodynamic models for maneuvering aircraft
[NASA-CR-186630] N90-25943
Two-dimensional Euler and Navier-Stokes Time accurate simulations of fan rotor flows
[NASA-TM-102402] N90-25948

UNSTEADY FLOW
An unsteady lifting surface method for single rotation propellers
[NASA-CR-4302] N90-25940
Two-dimensional Euler and Navier-Stokes Time accurate simulations of fan rotor flows
[NASA-TM-102402] N90-25948
Analysis and mitigation of numerical dissipation in inviscid and viscid computation of vortex-dominated flows
[NASA-CR-186887] N90-26281
Effects of 2 Hz imposed bulk flow unsteadiness on laminar-turbulent transition in a straight channel
[AD-A223028] N90-26295

UPLINKING
Preliminary error budget for an optical ranging system: Range, range rate, and differenced range observables N90-26227

UPPER ATMOSPHERE
Measurements of the methane relaxation times for application to the infrared emission models of the upper atmospheres of outer planets and Titan N90-26759

URANUS (PLANET)
Liquid-vapor equilibrium of multicomponent cryogenic systems N90-26774

USER MANUALS (COMPUTER PROGRAMS)
PDWAP: A preliminary design and weights analysis program for aerospace vehicles
[AD-A222614] N90-25979
The NASA/MSFC Global Reference Atmospheric Model, 1990 version (GRAM-90)
[NASA-CR-186717] N90-26435
Level-2 system: Programmers-users manual
[DE90-013324] N90-26540
LASER: A Layout Sensitivity Explorer. Report and user's manual
[EUT-89-E-216] N90-26545
Creating a VAPEPS database: A VAPEPS tutorial
[NASA-CR-186629] N90-26705

V

V/STOL AIRCRAFT
Hot gas ingestion characteristics and flow visualization of a vectored thrust STOVL concept
[NASA-TM-103212] N90-26009
H-infinity based integrated flight-propulsion control design for a STOVL aircraft in transition flight
[NASA-TM-103198] N90-26011

VACUUM APPARATUS
Role of surface passivation in the integrated processing of MOS structures
[AD-A222630] N90-26264

VACUUM DEPOSITION
Vacuum deposition by pulsed laser radiation: Plasma composition, deposition techniques, and thin film properties
[ETN-90-97263] N90-26677

VALIDITY
Validity domain of the scalar Kirchhoff and Rayleigh-Sommerfeld diffraction theories in the near field of small phase objects: Comparison between calculation models and microwave measure
[ETN-90-96963] N90-26236

VAN DER WAAL FORCES
Infrared spectra of van de Waals complexes of importance in planetary atmospheres N90-26749
Microwave spectra of van der Waals complexes of importance in planetary atmospheres N90-26752

VANADIUM ALLOYS
Compendium of material test results on HY-130 and Ti-3Al2V metals in support of United States navy programs
[DE90-011754] N90-26112
Formation of Titanium-boron surface alloys by excimer laser mixing
[DE90-013172] N90-26118

VANES
Prediction and measurement of rotor blade/stator vane dynamic characteristics of a modern aero-engine axial compressor
[PNR90667] N90-26002
The structural dynamics analysis of the main injector LOX inlet tee and its redesign
[NASA-CR-186764] N90-26358

VAPOR DEPOSITION
Laser techniques for studying chemical vapor deposition
[DE90-012921] N90-26311
Dielectric function of InGaAs in the visible
[NASA-TM-103246] N90-26683

VAPOR PRESSURE
Vapor pressures of acetylene at low temperatures N90-26777

VARIATIONS
Spatial cross-correlation of Antarctic Sea ice and seabed topography
[NASA-CR-186815] N90-26451

VECTOR ANALYSIS
Superconcurrent processing: A dynamic approach to heterogeneous parallelism
[AD-A222798] N90-26576
Full vector wave calculation of photonic band structures in face-centered cubic dielectric media
[AD-A222616] N90-26686

VELOCITY DISTRIBUTION
Measurement of terms and parameters in turbulent models
[NASA-CR-183993] N90-26271
Effect of initial conditions on the development of two-phase jets
[AD-A222621] N90-26293
A search routine for optimization in a wind power system with variable speed
[FOA-C-20779-2.1] N90-26395
Canonical eigenvalues. Part 1: General theory
[AD-A222812] N90-26617

VELOCITY MEASUREMENT
Measurement of velocity and temperature profiles at the exit plane of a tubular gas turbine combustor
[DE90-505519] N90-25983
An experimental system for measuring the wavenumber-frequency response of Timoshenko beams
[AD-A222569] N90-26374

VENUS (PLANET)
Space exploration: Cost, schedule, and performance of NASA's Magellan Mission to Venus. Fact sheet for the Chairman, Subcommittee on Science, Technology, and Space, Committee on Commerce, Science, and Transportation, US Senate
[GAO/NSIAD-88-130FS] N90-26022

VENUS ATMOSPHERE
Infrared spectra of van de Waals complexes of importance in planetary atmospheres N90-26749
Chemical kinetics and modeling of planetary atmospheres N90-26763

VENUS SURFACE
Space exploration: Cost, schedule, and performance of NASA's Magellan Mission to Venus. Fact sheet for the Chairman, Subcommittee on Science, Technology, and Space, Committee on Commerce, Science, and Transportation, US Senate
[GAO/NSIAD-88-130FS] N90-26022

VERBAL COMMUNICATION
Mathematical problem-solving transfer: The effects of cognitive load and attention a schema acquisition and rule automation N90-26594

VERTICAL DISTRIBUTION
Measurements of CH4, N2O, CO, H2O and O3 in the middle atmosphere by the ATMOS experiment on Spacelab 3
[NASA-TM-103476] N90-26400
Vertical ozone probing with lidar N90-26416
VISTA (Vertical Integration of Science, Technology, and Applications) user interface software study
[DE90-010003] N90-26707

VERY HIGH FREQUENCIES
Man-made noise in a military environment N90-26191
A narrowband tactical communication system for the VHF and UHF mobile radio bands N90-26192
HF spread spectrum, an audit of the power requirements and LPI vulnerability N90-26203
Experimentation of a transmission system data processing by meteor bursts N90-26207
Equipment feasibility study: Very high frequency communication equipment (136-137 megahertz)
[DOT/FAA/CT-TN89/72] N90-26210
Antennas for portable VHF-FM receivers
[BBC-RD-1990/1] N90-26211
Electric field strength meters for the HF, VHF, and UHF bands
[BBC-RD-1990/3] N90-26212

VERY LARGE SCALE INTEGRATION
Heavy ion tests on programmable VLSI
[ETN-90-97254] N90-26057
Contribution to CMOS integrated circuit tests: Study of the stuck-on and stuck-open fault tests
[ETN-90-97256] N90-26261

Contribution to the definition and application of NAUTILE (A new environment for the conception and assembling of integrated circuits)
[ETN-90-97251] N90-26554
Application of artificial intelligence to the architectural synthesis of VLSI integrated circuits
[ETN-90-97253] N90-26589
VERY LONG BASE INTERFEROMETRY
Information content of a single pass of phase-delay data from a short baseline connected element interferometer N90-26220
VIABILITY
Electronic warfare technology: Trends and visions
[AD-A223034] N90-26246
VIBRATION
An unsteady lifting surface method for single rotation propellers
[NASA-CR-4302] N90-25940
Rotational and translational effects in collisions of electronically excited diatomic hydrides
[NASA-CR-186770] N90-26093
The use of Lanczo's method to solve the large generalized symmetric Eigenvalue problem in parallel
[NASA-CR-182072] N90-26533
Asymptotic modal analysis and statistical energy analysis
[NASA-CR-186732] N90-26634
VIBRATION DAMPING
Design and implementation of robust decentralized control laws for the ACES structure at Marshall Space Flight Center
[NASA-CR-4310] N90-26046
Structural dynamics branch research and accomplishments
[NASA-TM-102488] N90-26373
Power flow analysis of two coupled plates with arbitrary characteristics
[NASA-CR-182033] N90-26632
VIBRATION EFFECTS
Power flow analysis of two coupled plates with arbitrary characteristics
[NASA-CR-182033] N90-26632
VIBRATION MEASUREMENT
A numerical simulation of the quasi-heterodyne technique for double-pulsed holographic vibration measurements
[PNR90622] N90-26301
VIBRATION TESTS
Vibration test procedures for orbiter sidewall-mounted payloads, phase 1
[AD-A220773] N90-26037
Vibration test procedures for orbiter sidewall-mounted payloads, phase 2
[AD-A220774] N90-26038
VIBRATIONAL SPECTRA
Formation and deactivation of vibrationally excited atmospheric molecules
[AD-A222660] N90-26442
High resolution spectroscopy in the microwave and far infrared N90-26746
VIBRATIONAL STRESS
Creating a VAPEPS database: A VAPEPS tutorial
[NASA-CR-186629] N90-26705
VIKING LANDER SPACECRAFT
Project Exodus
[NASA-CR-186836] N90-26026
VIKING MARS PROGRAM
The chemical effects of the Martian environment on power system component materials: A theoretical approach
[NASA-TM-103203] N90-26074
VISCOELASTICITY
Evolution of structure and viscoelasticity in diethanolamine-cured epoxy
[DE90-011256] N90-26134
VISCOUS FLOW
Computation of viscous aerodynamic characteristics of 2-D airfoils for helicopter applications
[NLR-MP-88052-U] N90-25951
Numerical analysis of three-dimensional particle-laden flow equations
[IAR-90-2] N90-26268
VISION
Eye tracking device for the measurement of flight performance in simulators
[AD-A220075] N90-26484
VISUAL PERCEPTION
Motion sickness, visual displays, and armored vehicle design
[AD-A222678] N90-26506
VOICE COMMUNICATION
A narrowband tactical communication system for the VHF and UHF mobile radio bands N90-26192
Equipment feasibility study: Very high frequency communication equipment (136-137 megahertz)
[DOT/FAA/CT-TN89/72] N90-26210
VOLCANOES
Proceedings of a workshop on Lunar Volcanic Glasses: Scientific and Resource Potential
[NASA-CR-186631] N90-26437
VOLCANOLOGY
Proceedings of a workshop on Lunar Volcanic Glasses: Scientific and Resource Potential
[NASA-CR-186631] N90-26437
VORTEX GENERATORS
Effect of vortex generators on the aerodynamic wing characteristics and body of revolution
[AD-A222813] N90-25955
VORTICES
Identification of aerodynamic models for maneuvering aircraft
[NASA-CR-186630] N90-25943
Euler analysis comparison with LDV data for an advanced counter-rotation propfan at cruise
[NASA-TM-103249] N90-25946
Experimental study on vortex and shock wave development on a 65 deg delta wing
[NLR-MP-88033-U] N90-25950
Decay of secondary flow and the associated loss variation downstream of an annual turbine stator cascade
[DE90-505520] N90-25984
VULNERABILITY
HF spread spectrum, an audit of the power requirements and LPI vulnerability N90-26203

W

WAKES
The browse file of NASA/JPL quick-look radar images from the Loch Linnhe 1989 experiment
[NASA-CR-186855] N90-26701
WALKING MACHINES
University of Maryland walking robot: A design project for undergraduate students
[NASA-CR-186839] N90-26331
WALL FLOW
A critical evaluation of two-equation models for near wall turbulence
[NASA-CR-182068] N90-26270
WALLS
A critical evaluation of two-equation models for near wall turbulence
[NASA-CR-182068] N90-26270
Measurement of terms and parameters in turbulent models
[NASA-CR-183993] N90-26271
Design and construction of a wall-climbing robot
[NIAR-90-20] N90-26327
Asymptotic analysis of dissipative waves with applications to their numerical simulation
[NASA-TM-103231] N90-26615
Baryogenesis in extended inflation. 2: Baryogenesis via primordial black holes
[NASA-CR-182843] N90-26735
WASPALOY
Fatigue life assessment using a short crack growth model
[PNR90663] N90-26367
WATER
Transient characteristics of a grooved water heat pipe with variable heat load
[NASA-CR-185280] N90-26272
Influence of thermal conditioning media on Charpy specimen test temperature
[DE90-012784] N90-26360
Heat engines
[DE90-000485] N90-26393
Measurements of CH4, N2O, CO, H2O and O3 in the middle atmosphere by the ATMOS experiment on Spacelab 3
[NASA-TM-103476] N90-26400
The 27-28 October 1986 FIRE IFO Cirrus case study: Comparison of radiative transfer theory with observations by satellite and aircraft
[NASA-TM-103468] N90-26446
Isothermal compressibility of SPC/E water
[AD-A222723] N90-26643
Structure and dynamics of water at the Pt(111) interface: Molecular dynamics study
[AD-A222628] N90-26687
Photon sputtering of H2O ices: A preliminary report N90-26783
WATER DEPRIVATION
Experiment K-6-20. The effect of spaceflight on pituitary oxytocin and vasopressin content of rats N90-26473
WATER FLOW
Measurement of terms and parameters in turbulent models
[NASA-CR-183993] N90-26271
WATER LANDING
Preliminary subsystem designs for the Assured Crew Return Vehicle (ACRV), volume 1
[NASA-CR-186677-VOL-1] N90-26039
WATER POLLUTION
The transfer of mercury between the atmosphere and lake or soil surfaces N90-26419
Mariners Weather Log, volume 33, number 3, Summer 1989
[PB90-146846] N90-26444
Mariners Weather Log, volume 33, number 4, Fall 1989
[PB90-146853] N90-26445
WAVE DIFFRACTION
Validity domain of the scalar Kirchhoff and Rayleigh-Sommerfeld diffraction theories in the near field of small phase objects: Comparison between calculation models and microwave measure
[ETN-90-96963] N90-26236
WAVE DISPERSION
Theory of biaxial graded-index optical fiber
[NASA-CR-186882] N90-26652
WAVE EQUATIONS
On traveling wave solutions of a set of coupled Boussinesq-like equations
[DE90-013182] N90-26597
Asymptotic analysis of dissipative waves with applications to their numerical simulation
[NASA-TM-103231] N90-26615
Theory of biaxial graded-index optical fiber
[NASA-CR-186882] N90-26652
WAVE FRONTS
Frontogenesis in gravity currents: An example with no known applications in oceanography
[MATHS-REPT-A-117] N90-26284
WAVE INTERACTION
Perturbation methods in the theory of waves and bifurcation phenomena N90-26593
WAVE PROPAGATION
Laser ultrasonic measurements on ceramic materials with rough surfaces
[DE90-012961] N90-26141
Propagation Effects and Circuit Performance of Modern Military Radio Systems with Particular Emphasis on Those Employing Bandspreading
[AGARD-CP-442] N90-26178
Experimental analysis of the HF linkage N90-26181
Progress and remaining issues in the development of a wideband HF channel model and simulation N90-26182
Wideband characterization of forest propagation channels N90-26188
System factors to be considered in assessing propagation effects on modern digital satellite communications systems N90-26208
Theory of circular dielectric waveguide with anisotropic sheet cover
[NASA-CR-186883] N90-26235
OASIS, LLNL version: Software maintenance manual
[DE90-013522] N90-26313
Remote sensing of Earth terrain
[NASA-CR-186888] N90-26382
Asymptotic analysis of dissipative waves with applications to their numerical simulation
[NASA-TM-103231] N90-26615
Computer modeling wave propagation with a variation of the Helmholtz-Kirchhoff relation
[AD-A222746] N90-26657
WAVE SCATTERING
Broadband analysis of ground wave propagation at a50 to 400 MHz N90-26185
Remote sensing of Earth terrain
[NASA-CR-186888] N90-26382
WAVEGUIDES
Transmission, reflection, and radiation at junction planes of different open waveguides
[ISBN-90-9002864-1] N90-26241
WAVELENGTH DIVISION MULTIPLEXING
High speed all optical networks
[NASA-CR-185311] N90-26649
WAVERIDERS
Project Exodus
[NASA-CR-186836] N90-26026
Terrapin technologies manned Mars mission proposal
[NASA-CR-186838] N90-26027
WEAPON SYSTEMS
Human performance models
[FFI-90/7002] N90-26502
WEAR
Wear mechanisms of amorphous carbon and zirconia coatings on rigid disk magnetic recording media
[DE90-011053] N90-26133
WEATHER
Annual and interannual variations of Earth-emitted radiation based on a 10-year data set
[NASA-TM-103465] N90-26432

Mariners Weather Log, volume 33, number 2, Spring 1989
[PB90-146838] N90-26443
Mariners Weather Log, volume 33, number 3, Summer 1989
[PB90-146846] N90-26444
Mariners Weather Log, volume 33, number 4, Fall 1989
[PB90-146853] N90-26445
Analysis and improved design considerations for airborne pulse Doppler radar signal processing in the detection of hazardous windshear
[NASA-CR-186792] N90-26448

WEATHER STATIONS
Some results from the precipitation chemistry measurement programme in Sweden N90-26410

WEATHERING
Proceedings of a workshop on Differences Between Antarctic and Non-Antarctic Meteorites
[NASA-CR-184918] N90-26740

WEIBULL DENSITY FUNCTIONS
Probabilistic approach to the certification for fatigue durability of composite structures
[DE90-505521] N90-26085

WEIGHT
PDWAP: A preliminary design and weights analysis program for aerospace vehicles
[AD-A222614] N90-25979

WEIGHT REDUCTION
The application of engineering ceramics in gas turbines
[PNR90676] N90-26005

WEIGHTING FUNCTIONS
An angular weighting approach for calculating gradients and divergences
[DE90-013164] N90-26539

WEIGHTLESSNESS
Experiment K-6-08. Biochemical and histochemical observations of vastus medialis N90-26462
Experiment K-6-10. Effects of zero gravity on myofibril protein content and isomyosin distribution in rodent skeletal muscle N90-26464
Experiment K-6-11. Actin mRNA and cytochrome c mRNA concentrations in the triceps brachia muscle of rats N90-26465
Experiment K-6-14. Hepatic function in rats after spaceflight N90-26468
Experiment K-6-18. Study of muscarinic and gaba (benzodiazepine) receptors in the sensory-motor cortex, hippcampus and spinal code N90-26471
Experiment K-6-21. Effect of microgravity on 1) metabolic enzymes of type 1 and type 2 muscle fibers and on 2) metabolic enzymes, neutransmitter amino acids, and neurotransmitter associated enzymes in motor and somatosensory cerebral cortex. Part 1: Metabolic enzymes of individual muscle fibers; part 2: metabolic enzymes of hippocampus and spinal cord N90-26474

WENTZEL-KRAMER-BRILLOUIN METHOD
Theory of biaxial graded-index optical fiber
[NASA-CR-186882] N90-26652

WHEELS
Proof of principle model for a lunar dumptruck
[NASA-CR-182557] N90-26323

WHISKER COMPOSITES
Investigation of thermo-mechanical effects in silicon carbide Whisker/Al alloy composites
[AD-A222635] N90-26089

WIND (METEOROLOGY)
Aeolian removal of dust from radiator surfaces on Mars
[NASA-TM-103205] N90-26068

WIND SHEAR
An analysis of requirements for a P-3 windshear training program
[AD-A222577] N90-25960
The NASA/MSFC Global Reference Atmospheric Model, 1990 version (GRAM-90)
[NASA-CR-186717] N90-26435
Analysis and improved design considerations for airborne pulse Doppler radar signal processing in the detection of hazardous windshear
[NASA-CR-186792] N90-26448

WIND TUNNEL MODELS
Wind tunnel study of wake downwash behind A 6 percent scale model B1-B aircraft
[DE90-011783] N90-25941

WIND TUNNEL TESTS
Wind tunnel study of wake downwash behind A 6 percent scale model B1-B aircraft
[DE90-011783] N90-25941
Experimental aerothermodynamic research of hypersonic aircraft
[NASA-CR-186903] N90-25954
Practical developments in holographic interferometry
[PNR90669] N90-26302

WIND TUNNELS
Research at NASA's NFAC wind tunnels
[NASA-TM-102827] N90-25933
Low-speed wind tunnel investigation of the static stability and control characteristics of an advanced turboprop configuration with the propellers placed over the tail
[NASA-CR-186900] N90-26017
The effect of a three-dimensional source on the flow through a channel with square cross section
[LR-512] N90-26289

WIND TURBINES
A preliminary study of the masking of wind turbine noise by ambient sound
[FFA-TN-1990-01] N90-26636

WIND VELOCITY
Analysis and improved design considerations for airborne pulse Doppler radar signal processing in the detection of hazardous windshear
[NASA-CR-186792] N90-26448

WINDPOWERED GENERATORS
A search routine for optimization in a wind power system with variable speed
[FOA-C-20779-2.1] N90-26395

WING PLANFORMS
Application of laminar flow control to supersonic transport configurations
[NASA-CR-181917] N90-25944

WINGS
Application of laminar flow control to supersonic transport configurations
[NASA-CR-181917] N90-25944
Effect of vortex generators on the aerodynamic wing characteristics and body of revolution
[AD-A222813] N90-25955
Report of the Fluid Dynamics Panel Working Group 10 on calculation of 3D separate turbulent flows in boundary layer limit
[AGARD-AR-255] N90-26280

WIRE
Electrode carrying wire for GTAW welding
[NASA-CASE-MFS-29491-1] N90-26168
Characterization of NbTi multifilamentary superconducting wires
[DE90-626245] N90-26672

WORD PROCESSING
Multilayered neural networks: Learning algorithms, implementation on hypercube machines, applications
[ETN-90-97255] N90-26574

WORK-REST CYCLE
Adjustment and validation of the mathematical prediction model for sweat rate, heart rate, and body temperature under outdoor conditions
[AD-A222599] N90-26486

WORKING FLUIDS
Transient characteristics of a grooved water heat pipe with variable heat load
[NASA-CR-185280] N90-26272
Two-dimensional model of a Space Station Freedom thermal energy storage canister
[NASA-TM-103124] N90-26279

WORKLOADS (PSYCHOPHYSIOLOGY)
Aviation safety: Conditions within the air traffic control work force. Fact sheet for congressional requesters
[GAO/RCED-89-113FS] N90-25958
Effects of microgravity on rat muscle N90-26453
Choosing a pilot subjective workload scale to fit flight operational requirements
[IAR-89-21] N90-26493
Human performance in cockpit-related systems
[NIAR-90-7] N90-26495
Psychophysiological assessment of pilot workload in an applied setting
[AD-A222707] N90-26507

X

X RAY ANALYSIS
Structures and mechanical properties of near-beta titanium alloys TiV10Fe2Al3 and TiV10Cu3Al3
[ONERA-NT-1989-3] N90-26123

X RAY ASTROPHYSICS FACILITY
The charged particle radiation environment for AXAF
[NASA-TM-100405] N90-26741

X RAY DIFFRACTION
Analysis of strain relaxation in Au/Ni multilayers by x ray diffraction
[IAR-89-25] N90-26357
Residual stresses measurements by means of x ray diffraction on electron beam welded joints and laser hardened surfaces
[ETN-90-97269] N90-26371
High temperature x ray diffraction and Landau theory investigations of order-disorder transition in defect NaCl-type solids
[DE90-011807] N90-26673

X RAY SPECTROSCOPY
Short-range structure of fluorine-modified phosphate glass
[DE90-013494] N90-26145

X RAY STRESS MEASUREMENT
Residual stresses measurements by means of x ray diffraction on electron beam welded joints and laser hardened surfaces
[ETN-90-97269] N90-26371

X RAYS
Soft x ray resist characterization: Studies with a laser plasma x ray source
[DE90-013493] N90-26661

X-29 AIRCRAFT
An in-flight interaction of the X-29A canard and flight control system
[NASA-TM-101718] N90-25973

XENON CHLORIDE LASERS
Characterization of a high-intensity, subpicosecond XeCl laser system
[DE90-011970] N90-26310

Y

YIELD POINT
Densification studies of refractory materials using Hot Isostatic Pressing (HIP) and tantalum containment
[DE90-013481] N90-26114

YIELD STRENGTH
Fracture toughness and failure mechanisms in commercial 2091 Al-Li sheet at cryogenic temperatures
[AD-A222803] N90-26125

YTTERBIUM COMPOUNDS
Ellipsometric study of YBa2Cu3O(7-x) laser ablated and co-evaporated films
[NASA-TM-103223] N90-26682

YTTRIUM OXIDES
Large, orientation-dependent enhancements of critical currents in Y1Ba2Cu3O(7-x) epitaxial thin films: Evidence for intrinsic flux pinning
[DE90-009424] N90-26666

Z

ZEOLITES
Regenerative Cu La zeolite supported desulfurizing sorbents
[NASA-CASE-NPO-17480-1-CU] N90-26098

ZINC OXIDES
Surface acoustic wave filters in ZnO-SiO2-Si layered structures: Design, technology, and monolithic integration with electronic circuitry
[ETN-90-97218] N90-26638

ZIRCONIUM OXIDES
Wear mechanisms of amorphous carbon and zirconia coatings on rigid disk magnetic recording media
[DE90-011053] N90-26133

ZONAL FLOW (METEOROLOGY)
The NASA/MSFC Global Reference Atmospheric Model, 1990 version (GRAM-90)
[NASA-CR-186717] N90-26435

Typical Personal Author Index Listing

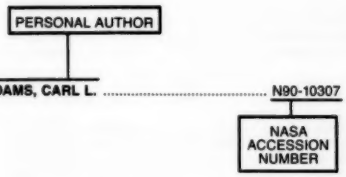

Listings in this index are arranged alphabetically by personal author. The NASA accession number denotes the number by which the citation is identified.

A

ABE, TOSHIO N90-26148
N90-26149
ABID, RIDHA N90-26270
ACORD, AMY L. N90-26128
ADAMS, BRENT L. N90-26113
ADAMS, BRIAN N90-26391
ADELMAN, HENRY G. N90-25970
ADOLF, DOUGLAS N90-26134
AFEK, YEHUDA N90-26520
AGRAWALA, ASHOK K. N90-26625
AIHUA, WANG N90-26386
ALBRECHT, ANDREAS N90-26734
ALEXANDREAS, D. E. N90-26732
ALEXANDRU, MONA-LISA N90-25971
ALHADEFF, SAM N90-26391
ALLEN, JOHN E., JR. N90-26744
N90-26759
N90-26761
N90-26777
ALLEN, R. C. N90-26732
ALTEROVITZ, S. A. N90-26682
N90-26683
ALTMAN, FREDERICK J. N90-26188
ALVAREZ, JOSEPH M. N90-26447
ALYEA, F. N. N90-26435
AMATO, MICHAEL N90-26027
AMBORSKI, ROBERT N90-26161
AMEEN, M. S. N90-26675
AMRO, JOE P. N90-26166
AMUEDO, KURT C. N90-26009
ANDERSON, E. CLAY N90-26270
ANDERSON, R. N90-26097
ANDERSON, WILLIAM R. N90-26317
ANDERSSON, PER N90-26409
ANDREWS, GLEN N90-26053
ARAKAWA, E. T. N90-26775
N90-26776
ARBOGAST, EMMANUEL N90-26383
ARDUINI, ROBERT F. N90-26446
ARGEMIRODECARVALHOPAIVA, JOAO N90-26380
ARNAUD, S. N90-26455
ARNOLD, C., JR. N90-26251
ARNOLD, STEVEN M. N90-26364
ARPIAINEN, VESA N90-26388
ARTAXO, PAULO N90-26418
ASCOUGH, J. C. N90-26007
ASH, ROBERT L. N90-26330
ASHRAF, SALEM N90-26550
ASSINK, R. A. N90-26251
ATILGAN, ALI R. N90-26354
ATTIYA, HAGIT N90-26520
AUBERT, D. N90-26591
AUCIELLO, O. N90-26675
AUERBACH, J. M. N90-26313
AVILAMASCARENHAS, NELSON D. N90-26379
AVILES, JAMES N90-26210
AXELROD, TIMOTHY S. N90-26300

B

BABCOCK, DALE A. N90-26167
BAHR, BEHNAM N90-26345
N90-26346
BAHRAMI, PARVIZ A. N90-26274
BAI, J. J. N90-26187
N90-26205
BAIN, J. N90-26463
BAJCSY, RUZENA K. N90-26497
BALANIS, CONSTANTINE A. N90-26233
BALDESCHWIELER, JOHN D. N90-26159
N90-26641
BALDWIN, K. N90-26464
BALES, KAY S. N90-26361
BALL, J. N90-26601
BALL, J. V. N90-26599
BALLARD, RODNEY W. N90-26452
BALLOUT, YOUSSEF ADEL N90-26078
N90-26079
BAMKIN, R. J. N90-26544
BAO, Y. N90-26772
BARD, STEVEN N90-26176
BARKATOU, MY ABDELFATTAH N90-26612
BARKER, LAWRENCE E. N90-26596
BARKSTROM, BRUCE R. N90-26433
BARNA, B. A. N90-26043
N90-26347
BARRIER, F. N90-26207
BARROW, JOHN D. N90-26735
BARSCH, GERHARD R. N90-26111
BARTLETT, RODNEY J. N90-26642
BARTON, H. A. N90-26002
BARTRAND, TIMOTHY A. N90-25982
BARTS, SAMUEL A. N90-26765
BASCHIERA, DINO J. N90-26499
BASILE, LUCIANO N90-26058
BATHKER, D. N90-26225
BATUR, CELAL N90-26664
BAUER, F. N90-26679
BAUMEISTER, KENNETH J. N90-26276
BEARD, SHAWN N90-26391
BECKWITH, A. L. N90-26565
BEECH, GEOFFREY N90-26332
BEER, RANDALL D. N90-26592
BEERS, RONALD W. N90-26024
N90-26704
BELL, JOHN STEVEN N90-26507
BELROSE, J. S. N90-26179
BELYTSCHKO, TED N90-26536
BENCIC, TIMOTHY J. N90-26009
BENJAMIN, B. A. N90-26485
BENNER, D. C. N90-26758
BENTON, E. R. N90-26477
BENTON, E. V. N90-26477
BENTS, D. J. N90-26789
BENZEKRI, SAMIRA N90-26620
BERG, TORE N90-26206
BERGGREN, REYNOLD G. N90-26360
BERGMANN, HEINRICH N90-26173
BERKOWITZ, M. N90-26643
N90-26687
BERLEY, D. N90-26732
BERRETTA, D. N90-26457
BERRY, W. N90-26476
BERTLES, DANIEL N90-26044
BESS, T. DALE N90-26432
BEVILACQUA, FRANCO N90-26060
BHASIN, KUL B. N90-26250
BHATIA, R. N90-26104
BHATTACHARYA, P. K. N90-26683
BHUSHAN, B. N90-26133
BICEN, ALI F. N90-26293
BIELEC, JIM N90-26331
BILLER, S. D. N90-26732
BIRMAN, KENNETH N90-26524
N90-26535
BIRT, MICHAEL J. N90-26082
BISOGNANO, J. J. N90-26644
BISSET, A. D. N90-26201
BJARKE, LISA J. N90-25973
BLACHER, RENE N90-26605
BLAD, BLAINE L. N90-26378
BLAKERS, A. W. N90-26386
BLASENHEIM, B. J. N90-26223
BLASS, WILLIAM E. N90-26748
BLOUNT, LAURA N90-26161
BLUM, FRANK D. N90-26099
BLUM, L. N90-26265
N90-26630
BOATNER, L. A. N90-26666
BOBIN, L. N90-26287
BOECKER, W. D. N90-26084
BOERIO, F. J. N90-26157
BOERJESSON, SUSANNE N90-26425
BOERSTOEL, J. W. N90-26285
BOLEY, M. S. N90-26676
BOLLEN, M. H. J. N90-26239
BOLLEN, MATHIAS HENRICUS JOHANNES N90-26260
BOOK, WAYNE J. N90-26329
BOOTH, F. W. N90-26465
BORETTI, A. A. N90-25948
BORGHI, R. N90-25993
BORING, J. W. N90-26778
BOSTROEM, BIRGITTA N90-26409
BOSTROEM, KURT N90-26409
BOUCHER, L. N90-26192
BOURELY, M. N90-26714
BOWEN, BRENT D. N90-26694
BOWER, MARK N90-26161
BOWLIN, SAMUEL W. N90-26215
BOYCE, J. R. N90-26644
BOYDE, A. N90-26455
BRADLEY, JIMMY D. N90-26340
BRANDENBERGER, ROBERT H. N90-26742
BRAUN, ROBERT D. N90-26036
BREILAND, WILLIAM G. N90-26311
BREWE, D. E. N90-26338
BRIGHT, MICHELLE M. N90-26011
BRODT, GREGOR N90-26158
BROM, G. N90-26287
BROMAGE, T. N90-26455
BROOKS, MARSHALL N90-26321
BROOKS, RODNEY A. N90-26326
BROOMHEAD, D. S. N90-26579
BROW, R. K. N90-26145
BROWN, KENNETH G. N90-26309
BROWN, SHERMAN D. N90-26090
BROWN, WALTER E., JR. N90-26701
BRUEL, C. N90-26775
BRUNEAU, STEPHEN D. N90-26162
BRUSASCO, R. M. N90-26314
BRYANT, HEATHER N90-26027
BRYANT, RODNEY N90-26026
BRYDON, ALASTAIR N. N90-26194
BUCHANAN, H. R. N90-26231
BUCHWALD, STEPHEN L. N90-26688
BUCKENDAHL, P. N90-26455
BUCKLAND, R. C. N90-26527
BUDAI, J. D. N90-26666
BUETEFISCH, K. A. N90-25950
BUGG, N. N90-26174
BULTITUDE, R. N90-26179
BUNK, WOLFGANG N90-26173
BUONGIORNO, CARLO N90-26059
BURLEY, JAMES R., II N90-25981
BURNER, A. W. N90-26296
BURNS, ROWLAND E. N90-26028
BURRELL, K. H. N90-26660
BURROUGHS, C. B. N90-26374
BURT, JIM A. N90-26759
BUSSOLINO, LUIGI N90-26035
BUTLER, TODD N90-26165
BYER, ROBERT L. N90-26306

C

CALADO, JORGE C. G. N90-26774
CALANDER, KARIN N90-26408
CALDWELL, JOHN N90-26757
CALDWELL, JOHN J. N90-26759
CALVAO, M. O. N90-26736
CAMBANIS, STAMATIS N90-26621
CAMBIER, JEAN-LUC N90-25970
CAMPAGNAC, MARIE-HELENE N90-26123
CAMPBELL, DAVID N90-26044

CAMPBELL, J. H. N90-26314
CAMPBELL, JOHN T. N90-26162
CAMPBELL, R. B. N90-26387
CANDLER, L. W. N90-26122
CANN, C. N90-26478
CANN, C. E. N90-26458
CAO, HOA V. N90-26268
CARATORI, J. N90-26198
CARBONE, D. N90-26008
CARLILE, DAVID N90-26391
CARPENTER, BRIAN N90-26053
CARPENTER, MARK H. N90-25992
CARR, M. J. N90-26097
CARREIRO, L. R. N90-25979
CARSON, GEORGE T., JR. N90-25938
CARTER, J. N90-26474
CASSIDY, W. A. N90-26739
CASSIDY, WILLIAM A. N90-26740
CAVIN, O. BURL N90-26109
CESARE, STEFANO N90-26060
CESS, ROBERT D. N90-26433
CHAARANI, JAMAL N90-26552
CHACKERIAN, C., JR. N90-26751
CHAILLOT, BERNARD N90-26012
CHAMBERS, RANDALL N90-26496
CHAMBERS, RANDALL M. N90-26493
N90-26495
CHAN, A. N90-26180
CHAN, CHAN S. N90-26102
CHAN, KI SI N90-26604
CHANG, A. C. N90-26131
CHANG, C. Y. N90-26732
CHANG, HSIANGPIN N90-26252
CHARLOCK, THOMAS P. N90-26432
CHATO, DAVID J. N90-26278
CHATSWORTH, TOM N90-25971
CHAU, S. N90-26518
CHAUDHURI, J. N90-26357
CHAVEZ, ROSALIND A. N90-26505
CHEN, CHING-JEN N90-26294
CHEN, HUDONG N90-26690
CHEN, J. G. N90-26676
CHEN, MING-SYAN N90-26513
CHEN, PAUL N90-26321
CHEN, PO-SHOU N90-26108
CHEN, SHIYI N90-26690
CHENG, UNJENG N90-26247
N90-26248
CHETTY, SHYAM N90-26010
N90-26523
CHEW, JOHN W. N90-26001
CHEW, MASON N90-26330
CHI, VERNON N90-26508
CHIN, G. N90-26707
CHIN, SUEI N90-25943
CHING, WILLIAM W. L. N90-26127
CHLAMTAC, IMRICH N90-26649
CHOI, KWONG-KIT N90-26297
CHOI, SEOK KI N90-26294
CHRISTEN, D. K. N90-26666
CHRISTENSEN, CRAIG N90-26436
CHRISTIANSEN, P. L. N90-26597
CHRISTMORE, DAN L. N90-25956
CHU, ALPHONSE Y. N90-25972
CHUBB, PETER N90-26561
CHUN, MYUNG K. N90-26305
CHUNG, Y.-W. N90-26133
CIHANGIRLI, MIHRIBAN N90-26495
CINNELLA, P. N90-26277
CITERNE, J. N90-26187
N90-26205
CLARK, D. N90-26179
CLASPY, PAUL C. N90-26250
CLAUSEN, HENRIK N90-26412
CLEARY, JOSEPH W. N90-25954
CLINE, CHARLES N90-26165
CLOUGH, ROGER L. N90-26143
CLOUTIER, MICHAEL JOHN N90-26343
COGBURN, J. W. N90-26126
COHENOUR, MARK W. N90-26128
COLANTUONI, S. N90-26008
N90-26291
COLELLA, A. N90-26291
COLELLA, NICHOLAS J. N90-26300
COLEMAN, JAMES A. N90-26209
COLEMAN, RODNEY N90-26027
COLLIARD, C. A. N90-26727
COLLINS, DAVID N90-26321
COLLINS, EMMANUEL G., JR. N90-26046
COLLIS, GEOFF N90-26695
COLTRIN, MICHAEL E. N90-26311
COLVIN, MICHAEL E. N90-26300
COMON, HUBERT N90-26610
COMPY, CHRIS N90-26027
CONLEY, GERALD N90-26332
CONLEY, W. R. N90-26135
CONNOLLY, JAMES P. N90-26452
CONTE, THOMAS M. N90-26558
CONVERTINO, V. A. N90-26485
COOK, DAVID N90-26391
COON, DENNIS N. N90-26081
COOPER, GRAHAM ANDREW N90-26594
COOPER, ROBERT N90-26524
N90-26535
COOPER, THOMAS D. N90-26349
COPELAND, EDMUND J. N90-26735
CORNETT, KENNETH D. N90-26138
CORNS, STEVE N90-26053
COSTELLO, DANIEL J., JR. N90-26528
COURTEIX, S. N90-26718
COY, S. N90-26755
CRAWFORD, MICHAEL E. N90-26269
CRITLEY, FRANK N90-26603
CROSLEY, DAVID R. N90-26093
CROUSE, PATRICK N90-26027
CROWLEY, KAY N90-26509
CRUNKLETON, JOE N90-26027
CRUZ, JONATHAN N. N90-26032
CUNNOLD, D. M. N90-26435
CURRAN, FRANCIS M. N90-26071
CUSCHIERI, J. M. N90-26632

D

DAGDIGIAN, PAUL J. N90-26317
DAHIYA, R. P. N90-26259
DAMELIO, F. N90-26471
DAMEN, A. A. H. N90-26586
DAMRAUER, R. N90-26088
DANIEL, A. N90-26187
N90-26205
DANIEL, ALAN N90-26161
DARLAY, FRANCOIS N90-26261
DARNELL, M. N90-26180
N90-26196
N90-26199
DAUNT, STEPHEN J. N90-26748
DAUNTON, N. N90-26471
DAUTRECHY, C. LYNNE N90-26526
DAVIS, J. BRADLEY N90-26040
DAVIS, JUDITH R. J. N90-26131
DAVIS, WILLIAM M. N90-26688
DEANGELIS, RICHARD M. N90-26443
N90-26444
N90-26445
DEBLASIO, R. N90-26392
DEBOO, J. C. N90-26660
DEF MARQUES, MAURO S. N90-26621
DEFILIPPI, VANNI N90-26164
DEGNAN, FRANK N90-26169
DELAAT, JOHANNES MARIA N90-26242
DELANEY, PAUL N90-26759
DELANO, JOHN W. N90-26437
DEMARCO, F. P. N90-26314
DEMAZEAU, YVES N90-26551
DEMUREN, A. O. N90-26282
DENBRINKER, C. S. N90-26203
DENIER, JAMES PATRICK N90-26593
DERUITER, HELENA MARIA N90-26241
DESERVES, CLAES N90-26428
DEVEAUX, RICHARD D. N90-26451
DEWITT, R. L. N90-26055
DEY, ARJUN N90-26786
DHILLON, JASKIRAN N90-25971
DIAZ, CLAUDINE N90-26332
DIEDERICKS-VERSCHOOR, I. H. PH. N90-26719
DIEHM, O. N90-26124
DILLON, JENNIFER N90-26026
DIMARTINO, P. N90-26008
DIMELLA, TIMOTHY N90-26332
DION, G. M. N90-26732
DIXON, ALAN N90-26042
DIXON, IAIN N90-26330
DIXON, KEVIN W. N90-26484
DO, HENRY N90-25971
DOBBINGA, E. N90-26289
DODBELE, SIMHA S. N90-25939
DODSON, PETE N90-26332
DOLAK, MIRKO J. N90-26704
DOLEV, DANNY N90-26520
DONALDSON, W. N90-26318
DONG, X. N90-26364
DOOLEN, GARY D. N90-26690
DORDAIN, J.-J. N90-26712
DOTY, S. N90-26454
N90-26457
DOUGLAS, CRAIG N90-26391
DOUGLAS, D. N90-26644
DOWELL, EARL H. N90-26634
DRENDEL, ALBERT S. N90-26064
DRIESSEN, M. H. N90-26586
DRIVER, D. N90-26000
N90-26087
DRUMMOND, J. PHILIP N90-25992
N90-26094
DRUMMOND, T. J. N90-26389
DUARTE, J. L. N90-26586
DUBOIS, P. N90-26722
DUDKIN, V. N90-26477
DUFFY, STEPHEN F. N90-26142
DUGGER, M. T. N90-26133
DUKE, P. J. N90-26460
DUNCAN, MICHAEL A. N90-26780
DURNOVA, G N90-26455
DURNOVA, G. N90-26457
N90-26458
N90-26459
N90-26460
DWELLE, PAUL N90-26321
DYER, GERALD E. N90-26168
DYER, JOHN H. N90-26177

E

EASOZ, J. A. N90-26387
EDENBOROUGH, H. KIPLING N90-25933
EDGERTON, R. N90-26461
EDNER, H. N90-26416
EDWARDS, C. D. N90-26218
EKSTROEM, L. N90-26636
ELCASHLAN, A. G. N90-26658
ELDRED, D. B. N90-26224
ELEMANS, PETRUS HENRICUS MARIA N90-26152
ELKINGTON, SCOT N90-26436
ELLIOTT, J. N90-26455
ELLIS, S. N90-26463
ELOFSON, PER-ANDERS N90-26426
ELSENAAR, A. N90-25950
ELSTON, S. T. N90-26002
ELZEIN, G. N90-26187
N90-26205
EPHRAIM, DANIEL N90-26128
EPSTEIN, Y. N90-26486
ERMER, GAYLE N90-26494
ERTHAL, GUARACI JOSE N90-26380
ESHAGHIAN, BIJAN N90-26505
EVANS, J. N90-26473
EYKHOFF, P. N90-26586

F

FAASS, REINHARD N90-26366
FABES, B. D. N90-26138
N90-26139
FAHR, ASKAR N90-26766
FANG, D. J. N90-26208
FANG, M. M. N90-26676
FANTASIA, PETER M. N90-26341
FARMER, C. B. N90-26400
N90-26402
FEENSTRA, R. N90-26666
FEGLEY, BRUCE, JR. N90-26773
FEIGELSON, ROBERT S. N90-26663
FELDMAN, DAVID N90-26648
FELL, C. N90-26442
FELL, R. D. N90-26462
FERBER, M. K. N90-26132
FERNANDEZ, JEFFREY N90-26496
FERRON, J. R. N90-26660
FERRY, EARL N., JR. N90-26155
FEUERBACHER, BERNDT N90-26173
FIEBER, JOE PAUL N90-26499
FINEL, ALPHONSE N90-26110
FINGER, M. H. N90-26227
FINK, U. N90-26758
FINLEY, HARRY R. N90-26021
N90-26022
N90-26023
N90-26025
N90-26066
FISCHER, BEN N90-26321
FISHER, RICHARD A. N90-26688
FISHMAN, JACK N90-26401
FLANAGAN, DENNIS P. N90-26531
FLANNERY, C. N90-26755
FLEURY, R. N90-26181
FLIEGEL, ILENE H. N90-26298
FLOOD, D. J. N90-26069
FLOOD, JOSEPH D. N90-26009
FLYNN, ANITA M. N90-26326
FLYNN, E. R. N90-26665
FOERSCHING, HANS N90-26173
FOLKNER, W. M. N90-26227
FONKOUA, ALAIN BLAISE N90-26589
FORBUS, KEN N90-26689

FOSTER, IAN N90-26562
FOSTER, K. N90-26687
FOWLER, JERRY N90-26622
FOX, KENNETH N90-26744
FOY, B. N90-26755
FRANK, A. N90-26477
FRASER, G. T. N90-26749
FRASSINELLI, MARK C. N90-25938
FREIER, ALAN O. N90-26254
FREUND, R. F. N90-26576
FRIDLAND, V. YA. N90-25955
FRIED, HERBERT M. N90-26648
FRIEDLANDER, DAVID N90-26525
FUCHS, B. N90-26476
FUCHS, HENRY N90-26508
FUEGER, H. N90-26385
FUJIOKA, TERUTAKA N90-26147

G

GAFNI, ELI N90-26520
GAIER, JAMES R. N90-26068
N90-26074
GALOFARO, JOEL T. N90-26054
GAMBOGI, ROBERT J. N90-26099
GANAPOL, B. D. N90-26640
GANGULY, SUMAN N90-26202
GANTT, J. B. N90-26723
GANZ, AURA N90-26649
GAO, BO-CAI N90-26400
GARCIA, DON N90-26391
GARECHT, DIANE N90-26067
GARETTO, L. N90-26457
GARG, SANJAY N90-26011
GAUDOIN, OLIVIER N90-26353
GAUDONI, OLIVIER N90-26352
GEE, J. N90-26389
GEIGER, KEVIN N90-26246
GERDIN, G. A. N90-26658
GILLEN, KENNETH T. N90-26143
GILLESPIE, DAVID N90-26391
GILMOUR, I. N90-26776
GINSBERG, JERRY H. N90-26639
GIOVANNINI, H. N90-26653
GIRARD, DIDIER A. N90-26606
GIVER, LAWRENCE P. N90-26758
GLIEBE, P. R. N90-26633
GLOSSOP, NEIL DAVID WILLIAM N90-26650
GLOVER, RICHARD D. N90-26564
GNEMMI, P. N90-25942
GOAD, W. K. N90-26296
GOCHOEL, DENNIS N90-26128
GODDARD, K. N90-25977
GOLDBERG, LEW N90-26305
GOLDMAN, T. N90-26434
GOLDSTEIN, R. N90-26232
GOLE, P. N90-26189
GOLEC, C. G. N90-26117
GOLINGO, RAYMOND N90-26391
GONDHALEKAR, V. N90-26357
GONSALVES, M. N90-26457
GONZALES, R. P. N90-26314
N90-26315
GONZALEZ, DREW N90-26391
GORBIEL, A. N90-26720
GORDON, DAVID F. N90-26617
GORDON, E. P. N90-26485
GOROVE, S. N90-26713
GOSNELL, TIMOTHY R. N90-26310
GOTT, GEOFFREY F. N90-26194
GOTT, S. N90-26457
GOTTLIEB, J. J. N90-25935
GOUTELARD, C. N90-26183
N90-26198
GRABOWSKI, L. N90-26120
N90-26367
GRAHAM, R. A. N90-26679
GRANAT, LENNART N90-26410
GRAVES, GEORGE N90-26705
GRECO, FRANCIS J. N90-26295
GREEN, MARTIN A. N90-26386
GREEN, RICHARD N. N90-26433
GREENBERG, PAUL S. N90-26163
GREGORY, SCOTT B. N90-26559
GREWE, GEORGE N90-26026
GRIFFITHS, J. B. N90-26691
GRINDELAND, R. N90-26456
N90-26473
N90-26475
GRINDELAND, RICHARD E. N90-26452
GROEBNER, R. J. N90-26660
GROENEWEG, JOHN F. N90-26635
GROSH, K. N90-26374
GROTH, MARY F. N90-26065
GROTHEER, PHIL N90-26331
GRUENINGER, GERHARD N90-26173
GRUND, CHRISTIAN J. N90-26447
GRUNTHANER, FRANK J. N90-26685
GRYNPAS, M. N90-26459
GUERDAL, ZAFER N90-26083
GUERDENLI, E. N90-26184
GUNSON, M. R. N90-26400
GUSTAVSON, DAVID B. N90-26514
GUTMAN, DAVID N90-26764
GUTMAN, SEMION N90-26690
GUYENNE, T. DUC N90-26711
GYEKENYESI, JOHN P. N90-26359

H

HAERTING, J. N90-25942
HAGEN, KENNETH NORMAN N90-26119
HAGENBERG, T. H. M. N90-26238
HAGOOD, BOB N90-26161
HAGSTROM, THOMAS N90-26615
HAGUE, J. N90-26180
N90-26193
HAGYARD, M. J. N90-26785
HAINES, TODD J. N90-26732
HALE, ELGIE J. N90-26325
HALPERN, JOSHUA B. N90-26765
HALTHORE, RANGASAYI N. N90-26759
HAMMER, JOHN M. N90-26492
HANCOCK, BRUCE R. N90-26685
HANDLEY, JAMES N90-26161
HANDSCHUH, ROBERT F. N90-26334
HANSMANN, TIMOTHY N90-26499
HANSSON, MARGARETA N90-26412
HANSSON, ULF N90-26413
HARDY, M. C. N90-26121
HARDY, T. L. N90-26055
HARDY, TERRY L. N90-26160
HARGENS, A. N90-26457
HARGROVE, J. N90-26468
HARRIES, WYNFORD L. N90-26308
HARRIS, JOEL M. N90-26105
HARRIS, ROBERT N90-26053
HARRISON, EDWIN F. N90-26433
HARRISON, M. C. N90-26599
HARRISSON, M. C. N90-26601
HARTSIG, DAVE N90-26331
HARTUNG, LIN C. N90-26036
HARVEY, JILL N90-26322
HARVEY, JILL ANN N90-26323
HASHEM, EMAM SALAHEDDIN N90-26698
HASKELL, W. L. N90-26485
HASTIE, D. R. N90-26399
HAWKEN, D. F. N90-25935
HAYS, CYNTHIA J. N90-26378
HAYTON, G. N90-26600
HAZZLEDINE, P. M. N90-26668
HECK, MICHAEL L. N90-26032
HEDGEPETH, JOHN M. N90-26061
HEDIGER, DONALD N90-26161
HEIDA, J. H. N90-26350
HEIFETS, S. N90-26644
HEIKEN, GRANT H. N90-26437
HEKMAT, MORAD N90-26331
HELBERG, KENNETH N90-26246
HENNE, PRESTON A. N90-25947
HENSCHEL, F. N90-26010
HENSLEY, D. A. N90-26103
HERB, GREGORY M. N90-26582
HERGENROTHER, P. M. N90-26129
HERLACH, DIETER M. N90-26678
HERRICK, R. N90-26464
HERRING, J. STEPHEN N90-26390
HERRON, JOHN N90-26766
HESTER, TROY L. N90-26249
HETZLER, J. N90-26755
HEYMSFIELD, ANDREW J. N90-26446
HIBEY, JOSEPH L. N90-26013
HIGGINBOTHAM, SCOTT A. N90-26040
HIMES, V. L. N90-26097
HINEDI, S. N90-26230
HINKLEY, J. A. N90-26130
HINRISCHEN, VOLKER N90-26262
HIPOL, P. J. N90-26037
HIRVONEN, JUHA-PEKKA N90-26118
HISAMATSU, TADASHI N90-26148
N90-26149
HO, PAULINE N90-26311
HOBBS, L. M. N90-26737
HODGES, DEWEY H. N90-26354
HODGES, J. N90-26288
HOEIJMAKERS, H. W. M. N90-25952
HOEIJMAKERS, M. J. N90-26256
N90-26258
HOEL, M. N90-26468
HOENIG, CLARENCE N90-26114
HOFFMEYER, J. N90-26182
HOFMANN, A. N90-26782
HOFTUN, J. S. N90-26540
HOLLEY, D. N90-26472
HOLMES, K. G. N90-26224
HOLT, HENRY N90-26743
HOLTON, E. N90-26457
HOMENY, JOSEPH N90-26090
HONARY, B. N90-26196
N90-26199
HONES, E. W., JR. N90-26438
N90-26439
HONG, J. M. N90-26676
HONGISTO, MARKE N90-26406
HOOD, L. L. N90-26784
HOPE, WILBERT WINSTON N90-26091
HORN, WALTER J. N90-25956
HORNIK, ARMAND N90-26554
HORWEDEL, J. E. N90-26529
HOSMER, FELL N90-26617
HOTES, DEBORAH N90-26068
HOUWINK, R. N90-25951
HOWARD, W. MICHAEL N90-26787
HOY, GILBERT R. N90-26316
HU, MIN N90-26628
HU, Y. F. N90-26543
HUANG, B. Y. N90-26671
HUARD, S. N90-26653
HUCKABY, D. A. N90-26630
HUDGENS, JEFFREY W. N90-26760
HUEBERT, B. J. N90-26399
HUGHES, W. J. N90-26374
HUISH, P. W. N90-26184
HULL, JOHN R. N90-26667
HUMMEL, KEITH E. N90-26537
HUNTER, WILLIAM W., JR. N90-26651
HURTADO, EDGAR N90-26027
HUSTON, RONALD L. N90-26171
HUTCHESON, LINTON N90-26165
HUTH, GAYLORD K. N90-26247
HWU, WEN-MEI W. N90-26558
HYKIN, JEFF N90-26332
HYLAND, DAVID C. N90-26046
HYMER, W. N90-26475

I

IBRAHIM, MOUNIR B. N90-26279
ILYINA-KAKUEVA, E. N90-26461
IMBRIALE, W. N90-26225
INGEBO, ROBERT D. N90-26299
ISKENDERIAN, T. C. N90-26292
IVERSON, EIRIK N90-26027
IWAI, LAZUMI N90-26149

J

JACKSON, G. L. N90-26660
JACKSON, KAREN E. N90-26363
JACKSON, W. M. N90-26772
JACOB, JONAH N90-26307
JACOBS, G. A. P. N90-26239
JAIN, LALIT K. N90-26142
JAIN, R. K. N90-26069
JAKUBOWSKI, A. N90-26053
JANG, JONG HOON N90-26272
JANIK, G. R. N90-26223
JANKOWSKI, A. F. N90-26357
JANSON, ROBERT N90-26422
JATA, KUMAR V. N90-26125
JEKELI, CHRISTOPHER N90-25962
N90-25963
JENKINS, M. G. N90-26132
JENKINS, R. W. N90-26179
JENNINGS, DONALD E. N90-26747
JERVIS, THOMAS ROLAND N90-26118
JEVICKI, ANTAL N90-26648
JIANHUA, ZHAO N90-26386
JIMMERSON, LISA N90-26161
JIN, VICTORIA Y. N90-26697
JOFFRE, SYLVAIN M. N90-26404
JOHAL, K. L. N90-26002
JOHANSSON, CHRISTER N90-26423
JOHNS, ALBERT L. N90-26009
JOHNSEN, RAINER N90-26767
JOHNSEN, SIGFUS N90-26412
JOHNSON, L. RONALD N90-26449
JOHNSON, R. E. N90-26778
JOHNSON, RUSSELL D., III N90-26760
JOHNSON, W. STEVEN N90-26082
JOLIVET, J. P. N90-26181
JOLLY, Y. N90-26192
JONES, D. N90-26468
JONES, DENISE R. N90-25981

JONES, J. G. N90-25953
JONES, JACK N90-26176
JONES, KENNETH L. N90-26384
JONES, MARK T. N90-26533
JORRAND, PH. N90-26571
JOY, MARSHALL N90-26741
JOZWIAK, L. N90-26516
N90-26547
JUANG, JER-NAN N90-26362
JUDGE, D. L. N90-26754
N90-26757
N90-26783
JUDISH, J. P. N90-26775
JUHANI, RUUSKANEN N90-26421
JUN, BRIAN N90-26053
JUNG, ACHIM N90-26613
JURKIEWICZ, K. N90-26385
JUSTUS, C. G. N90-26435

K

KACHELMYER, ALAN L. N90-26319
KADDIS, F. N90-26472
KADIRAMANGALAM, MURALI N. N90-26234
KALASEK, V. K. I. N90-26257
KAMIJO, KENJIRO N90-26034
KAMOSA, MIKE N90-26027
KANDIL, OSAMA A. N90-26281
KANG, KYUNGSIK N90-26648
KANG, QINGDE N90-26602
KAPLANSKI, A. N90-26456
N90-26475
KAPLANSKY, A. N90-26457
N90-26458
N90-26478
KAROLKOV, V. N90-26264
KASI, S. R. N90-26243
KASSAM, SALEEM N90-26290
KASSIES, A. N90-26175
KAT, P. J. N90-26040
KATNIK, GREGORY N. N90-26467
KATO, K. N90-26469
N90-26229
KATOW, M. S. N90-26519
KATTI N90-26455
KATZ, E. N90-26549
KAUFMANN, A. N90-26652
KAWALKO, STEPHEN F. N90-26284
KAY, A. N90-26385
KAZMIERCZAK, H. N90-26522
KEELER, JAMES D. N90-25973
KEHOE, MICHAEL W. N90-26473
KEIL, L. N90-26466
KEIL, L. C. N90-26485
N90-26660
KELLMAN, A. G. N90-26169
KEMPER, KAREN L. N90-26120
KENDALL, J. M. N90-25996
KENNEDY, JAN B. N90-26666
KERCHNER, H. R. N90-26375
KEREKES, JOHN P. N90-26376
KEREKES, JOHN PAUL N90-26758
KEROLA, D. N90-26279
KERSLAKE, THOMAS W. N90-26103
KESMODEL, L. L. N90-26542
KESTELOOT, PIETER N90-26644
KEWISCH, J. N90-26775
KHANNA, R. K. N90-26777
KHARE, BISHUN N. N90-26775
N90-26776
KHO, K. S. N90-26191
KIBLER, JAMES F. N90-26433
KIHO, KENZO N90-26708
KILMER, KEVIN J. N90-26493
KIM, K. S. N90-26355
KIM, SUNG JIN N90-26673
KING, K. E. N90-26120
KINGON, A. I. N90-26675
KIRK, G. E. N90-26003
KIRKPATRICK, RONALD C. N90-26539
KISH, JEROME THOMAS N90-26235
KLAASSEN, J. N90-26442
N90-26755
KLABUNDE, C. E. N90-26666
KLEIH, JUERGEN N90-26394
KLEINE, ACHIM N90-26237
KOBAYASHI, HIDEYUKI N90-26072
KOBAYASHI, HIROTAKE N90-26255
KOEBERL, CHRISTIAN N90-26740
KOEPKE, ANDREW N90-26049
KOESTERS, JOSEPH N90-26246
KOLB, EDWARD W. N90-26735
KONG, JIN AU N90-26382
KONSTANTINOVA, I. N90-26476
KORELLIS, JOHN S. N90-26112
KOST, ALICIA N90-26042
KOSTER, G. J. P. N90-26567
KOTLAR, ANTHONY J. N90-26100
KOZLOWSKI, M. R. N90-26314
KRAFFT, G. N90-26644
KRAFT, L. M. N90-26466
KRAFT, LAURI N90-26027
KRAMER, ARTHUR F. N90-26489
KRANTZ, TIMOTHY L. N90-26334
KRASNOV, I. N90-26471
N90-26472
N90-26473
N90-26474
N90-26475
KRAUS, G. F. N90-26777
KRAUSS, A. R. N90-26675
KRUEGER, GRETCHEN M. N90-26484
KRUEGER, O. N90-26029
KRUTH, JEAN-PIERRE N90-26542
KRUTZ, ROBERT W., JR. N90-26505
KUBIAK, GLENN D. N90-26661
KUMAR, R. N90-26216
KUMAR, RENJITH R. N90-26032
KUNATH, RICHARD R. N90-26250
KUNO, HARUHIKO N90-26708
KUNZ, PAUL F. N90-26532
KUSAKA, KAZUO N90-26072
KUZNETSOV, A. M. N90-26441
KWON, DONG-SOO N90-26329

L

LACKEY, KEVIN N90-26188
LACOTE, C. N90-26570
LAFFERTY, W. J. N90-26749
LAFLEN, J. H. N90-26355
LAINE, RICHARD M. N90-26156
LAMKIN, S. L. N90-26640
LAMMERING, ROLF N90-26006
LAMPSHIRE, GREGORY N90-26042
LAN, C. EDWARD N90-25943
LANDGREBE, DAVID A. N90-26375
N90-26376
LANDKVIST, BERTIL N90-26395
LANEN, T. A. W. M. N90-26655
LANG, TODD M. N90-26761
LANGNER, JOAKIM N90-26413
LANGROVA, SARKA N90-26430
LANKARANI, HAMID N90-26494
LAPORTERIE, A. N90-26088
LARSEN, LAYNE N90-26436
LARSEN, ROB N90-26042
LATTARD, DIDIER N90-26575
LAUBER, W. N90-26179
LAUFER, ALLAN H. N90-26766
LAURENT, P. A. N90-26197
LAURIE, EDWARD J. N90-25973
LAVERGNE, CHRISTIAN N90-26353
LAWRANCE, A. J. N90-26624
LAYTON, CHUCK N90-25964
LEBEL, P. J. N90-26399
LECK, CAROLINE N90-26417
LECOT, C. N90-26653
LEDEBUHR, ARNO G. N90-26300
LEE, BOK WOO N90-26354
LEE, BRIAN P. N90-25937
LEE, JONGGIL N90-26448
LEE, KENNETH L. N90-26112
LEE, MINXU N90-26690
LEGER, J. J. N90-26461
LEI, JIH-FEN N90-26063
LEIBECKI, HAROLD F. N90-26396
LEMMON, J. N90-26182
LEONE, STEPHEN R. N90-26756
LEQUIME, M. N90-26653
LEROUX, Y. M. N90-26181
LESNYAK, A. N90-26476
LEUNG, K. M. N90-26686
LEUVEN, K. U. N90-26542
LEVY, ARMAND J. N90-26204
LEW, JAE YOUNG N90-26328
LEW, JIANN-SHIUN N90-26362
LEWIS, PETER A. N90-26557
N90-26590
N90-26623
N90-26624
LI, Y. K. N90-26189
LIANG, SHI N90-26677
LICHR, M. N90-26264
LIDDLE, ANDREW R. N90-26735
LIESE, KARL N90-25975
LIMA, J. A. S. N90-26736
LIN, AVI N90-26614
LIND, ED N90-26210
LINDQVIST, OLIVER N90-26419
N90-26420
LINDSKOG, ANNE N90-26415
LINNE, DIANE L. N90-26065
LIOY, SAVERIO N90-26164
LIPPMANN, S. N90-26660
LIU, JOHN K. N90-26685
LIU, KEFENG N90-26233
LIU, Y. F. N90-26686
LIVINGSTON, DAVID L. N90-26488
LJUNGGREN, S N90-26636
LJUNGSTROEM, EVERT N90-26425
N90-26426
N90-26430
LODGE, J. H. N90-26192
LOKHANDNALA, K. A. N90-26504
LOMDAHL, P. S. N90-26597
LONG, KENWYN J. N90-26172
LOOSCH, REINHARD N90-26716
LORENZ, RUDOLF WERNER N90-26186
LOVAS, F. J. N90-26752
LOWE, D. N90-26579
N90-26580
LOWMAN, DOUGLAS S. N90-26527
LOWNDES, D. H. N90-26666
LOWRY, O. N90-26474
LU, X.-Q. N90-26732
LUKASHUK, S. A. N90-25955
LURIE, B. J. N90-26292

M

MA, DEREN N90-26494
MAAHS, HOWARD G. N90-26080
MAARI, SAMI N90-26346
MAARI, SAMI M. N90-26327
MACHIDA, TAKASHI N90-26149
MACKOWIAK, C. L. N90-26480
MACPHERSON, DAVE C. N90-26310
MADDERS, K. J. N90-26717
MADZSAR, GEORGE C. N90-26070
MAGGIE, M.-Y. CHI N90-26474
MAILAENDER, MARTIN N90-26173
MAILFERT, J. N90-26570
MAKEL, DARBY B. N90-26095
MALACHOWSKI, M. J. N90-26581
MALEKI, L. N90-26223
MALEKPOUR, M. N90-26563
MALIK, S. N. N90-26355
MALONEY, THOMAS M. N90-26396
MANCHESTER, J. N90-26474
MANDALA, B. N90-26563
MANDEL, A. D. N90-26476
MANDERSCHEID, JANE M. N90-26359
MANHEIM, AMY L. N90-26169
MANI, R. N90-26633
MANN, WILLIAM C. N90-26733
MANUEL, G. N90-26088
MANZELLA, DAVID H. N90-26071
MANZO, MICHELLE A. N90-26397
MARCHETTO, B. N90-26016
MARENNYI, A. N90-26477
MARINE, MICKY N90-26044
MARINI, J. N90-26461
MARKLEY, C. N90-26472
MAROU, FRANCOIS N90-26681
MARSTON, G. N90-26769
MARSTON, GEORGE N90-26768
MARTIN, JAMES E. N90-26134
N90-26144
MARTIN, THOMAS P. N90-26461
MARTINEZ, FRANK N90-25971
MARTINEZ, RANAE N90-26436
MARZULLO, KEITH N90-26254
N90-26344
N90-26524
N90-26535
MASON, JAMES DAVID N90-26899
MASON, WILLIAM E. N90-26530
MASTERSON, C. M. N90-26777
MASTI, CHANDRASHEKAR L. N90-26488
MATSUBARA, MASAAKI N90-26147
N90-26365
MATTERN, DUANE L. N90-26011
MATTHIESSEN, CHRISTIAN M. I. M. N90-26733
MAVRIPLIS, DIMITRI N90-26171
MAX, NELSON L. N90-26538
MAZANEK, DANIEL D. N90-26032
MCCALLUM, J. C. N90-26674
MCCASKILL, MARY K. N90-26710
MCCOY, ELAINE N90-25964
MCDOUGAL, D., JR. N90-26474
MCFADDEN, FRANK N90-26526
MCGOWAN, REBECCA R. N90-26657
MCGUIRK, J. J. N90-25991
MCHARGUE, C. J. N90-26674
MCHUGH, J. P. N90-26387

MCKEE, V. B. N90-26301
MCMANIS, G. E., III N90-26101
MCMILLEN, LARRY N90-26210
MCMORROW, JIM N90-26026
MECHANIC, G. N90-26455
MEDNIEKS, M. I. N90-26467
MEHOSKY, B. L. N90-26084
MEISSE, C. N90-26776
MELBORNE, R. K. N90-26222
MELISSINOS, A. C. N90-26318
MELLSTROM, J. N90-26228
MELTON, CRAIG N90-26026
MENARD, J. N90-26181
MENSO, G. N90-26016
MERRILL, A., JR. N90-26468
MERRITT, MICHAEL N90-26520
MESARCH, MARK A. N90-26378
MEYER, BRADLEY S. N90-26787
MEYERS, L. G. N90-26151
MIELKE, R. N90-26563
MIGHELL, A. D. N90-26097
MILANOVICH, F. P. N90-26314
MILEANT, A. N90-26230
MILLER, CHRISTOPHER J. N90-25946
MILLER, GABRIEL N90-26234
MILLS-CURRAN, WILLIAM C. N90-26531
MILLS, D. N90-26150
MIMAKI, TOSHIO N90-26149
MINGS, S. L. N90-26130
MINNIS, PATRICK N90-26447
MIQUEL, JAIME N90-26467
MIRCHANDANEY, RAVI N90-26509
MIU, B. N90-26461
MIYAJIMA, HIROSHI N90-26072
MIYATA, HIROSHI N90-26149
MIZIOLEK, ANDRZEJ W. N90-26317
MIZUGAI, Y. N90-26755
MKHITARYAN, A. M. N90-25955
MOHR, ROGER N90-26383
MOLAVI, K. N90-26104
MOLLARD, MICHEL N90-26609
MONAHAN, BOB N90-26042
MONTUFAR-SOLIS, D. N90-26460
MOON, FRANCIS C. N90-26667
MOORE, GARY T. N90-26499
MOORE, MARLA H. N90-26781
MOR, G. P. N90-26371
MORAN, D. N90-26486
MORAN, MATTHEW E. N90-26278
MORGAN, A. J. N90-26314
N90-26315
MORGAN, GENE E. N90-26168
MORI, NORIYUKI N90-26148
N90-26149
MORRIS, BRIAN G. N90-26073
MORRISON, JAMES N90-26041
MORRISON, P. R. N90-26465
MOTAKABBIR, K. N90-26643
N90-26687
MOTHS, JANIS HUEBNER N90-26499
MRIG, L. N90-26392
MUHLEMAN, DUANE O. N90-26731
MULLINS, R. N90-26468
MUNRO, BRUCE N90-26053
MUNTHE, JOHN N90-26419
N90-26420
MURPHY, M. F. N90-26726
MURTAGH, DONAL P. N90-26427
MUSACCHIA, X. J. N90-26462
MUTO, V. N90-26597
MYERS, ROGER M. N90-26071

N

NABEEL, TARABISHY M. N90-26345
NAGAO, RYUJI N90-26034
NAGEL, A. L. N90-25944
NAIDU, DESINENI S. N90-26013
NAKAKADO, KIMIAKI N90-26149
NAMKUNG, J. S. N90-26402
NANDIGAM, SRIKANTH N90-26496
NANNONI, FABIO N90-25978
NANSTAD, RANDY K. N90-26360
NARAYAN, J. N90-26666
NASTASI, MICHAEL N90-26118
NAUMANN, K. W. N90-26015
NAVA, DAVID F. N90-26768
NAVE, TOM N90-26331
NAVINCHANDRA, D. N90-26556
NEINER, GEORGE H. N90-26009
NELSEN, L. V. N90-26324
NEMETH, MICHAEL P. N90-26077
NEMETH, NOEL N. N90-26359
NEMETH, PATTI M. N90-26474
NERHEIM, N. M. N90-26224
NESBITT, F. L. N90-26769
NESENBERGS, M. N90-26182
NESTHUS, THOMAS E. N90-26505
NGUYEN, CHARLES C. N90-26578
NGUYEN, H. L. N90-26170
NICHOLS, DAVE N90-26044
NICOLIN, B. N90-26385
NIELAN, PAUL E. N90-26530
NIELSEN, RALPH B. N90-26688
NIETO, MICHAEL MARTIN N90-26434
NITTA, AKIHITO N90-26147
N90-26365
NOLES, CHERIE J. N90-26505
NOONE, KEVIN J. N90-26429
NORGARD, JOHN D. N90-26631
NORRIS, BEVERLY N90-26474
NORTON, D. N90-26666
NORTON, R. H. N90-26400
N90-26402
NOURRY, G. N90-26179
NOUSE, HIROYUKI N90-25984
NYLAND, TED W. N90-26278

O

OBANDO, R. N90-26563
OBRIEN, JAMES J. N90-26762
OBRIEN, T. K. N90-26076
N90-26670
ODONNELL, PATRICIA M. N90-26397
OFFENBERG, M. N90-26264
OGANOV, V. N90-26461
N90-26463
N90-26464
OGANOV, V. S. N90-26462
N90-26465
OGATA, TAKASHI N90-26147
OGAWA, AKINORI N90-26086
OHERN, M. E. N90-26674
OKAMURA, HIROYUKI N90-26365
OLAGNON, CHRISTIAN N90-26154
OLIVA, MANI N90-26331
OLIVER, B. F. N90-26671
OLIVER, W. C. N90-26117
N90-26138
N90-26139
N90-26671
OLSEN, BOB N90-26331
OLSEN, TANYA N90-26436
ONEILL-ROOD, NORA N90-26564
ORJI, CYRIL U. N90-26702
OSBORNE, Z. A. N90-26145
OTT, W. N90-26385
OTTO, RALPH N90-26114
OUTKA, DUANE A. N90-26661
OUWERLING, GERARDUS JOHANNES L. N90-26351
OUZTS, PETER J. N90-26011
OVERTON, W. C., JR. N90-26665

P

PADMADINATA, UTAMA HERAWAN N90-26369
PALANISWAMY, VANKATESH N90-26496
PAMULAPATI, J. N90-26683
PANITZ, J. K. G. N90-26135
PARIKH, P. G. N90-25944
PARK, HYE-SOOK N90-26300
PARK, Y. T. N90-26088
PARKER, LINDSAY N90-26446
PARKER, R. J. N90-26301
N90-26302
N90-26303
N90-26654
PARKER, SCOTT N90-26436
PARKS, P. B. N90-26658
PARSA, MEHRDAD N90-26436
PARSONS, E. L., JR. N90-26393
PATRICK, MERRELL L. N90-26533
PATTERSON-BUCKENDAHL, P. N90-26458
PATTERSON, MICHAEL H. N90-26491
PAUDA, JOSE MARIO N90-26244
PAYNE, WALTER A. N90-26768
PEDERSEN, MELVIN A. N90-26617
PEELING, N. E. N90-26548
PEPER, FERDINAND N90-26568
PERANO, KENNETH J. N90-26530
PERETTI, LINDA F. N90-26634
PEREZ-DAVIS, MARLA E. N90-26068
N90-26074
PERRET, CHRISTIAN N90-26680
PERRY, JOHN G. N90-26320
PESCHKE, WILLIAM T. N90-25997
N90-25998
PETERS, ANTONI V. N90-26748
PETERS, ASHISH N90-25971
PETERS, BRUCE N90-26161
PETRICK, S. WALTER N90-26176
PETRIE, T. W. N90-26660
PEZZONI, R. N90-26371
PHAM, DINH TUAN N90-26604
PHELAN, MICHAEL J. N90-26451
PHELPS, D. K. N90-26441
PHILLIPS, COLLEEN M. N90-26024
PHILLIPS, DOUGLAS J. N90-26046
PHILLIPS, J. T. N90-26565
PHILLIPS, M. N90-26442
PHILLIPS, R. W. N90-26470
PHILPOTT, D. E. N90-26467
N90-26469
PICKETT, HERBERT M. N90-26746
PIEARCEY, B. J. N90-26544
PIERSOL, ALLAN G. N90-26037
N90-26038
PINDERA, MAREK-JERZY N90-26083
PINE, A. S. N90-26749
PINEDADEGYVEZ, JOSE N90-26545
PINNEX, KAREN V. N90-26765
PIOTROWSKI, P. A. N90-26387
PISSARRACASTELLARI, SUELI N90-26381
PITKAENEN, JORMA N90-26253
PLATEAU, BRIGITTE N90-26572
PLIMPTON, STEVEN J. N90-26669
PODBOY, GARY G. N90-25946
POE, CLARENCE C. N90-26083
POLITES, MICHAEL E. N90-26304
POLKA, LESLEY A. N90-26233
POLLACK, J. B. N90-26775
POLLOCK, W. J. N90-26106
POLYDOROS, ANDREAS N90-26247
POPOVA, I. N90-26468
POPOVA, I. A. N90-26466
N90-26467
N90-26469
PORTELLI, CLAUDIO N90-26035
PORTER, W. D. N90-26117
POSNER, E. C. N90-26217
POSTANS, P. J. N90-25999
POWELL, GEORGE N90-26436
POWELL, RICHARD W. N90-26036
POWERS, DAVID A. N90-25941
PROSKAWETZ, KARL-OSKAR N90-25974
PROVOST-GRELLIER, ANTOINE N90-26057
PUGET, PIERRE N90-26588
PUGH, A. C. N90-26583
N90-26600
PULLING, ERIC N90-26053
PUSATERI, M. N90-26474

Q

QUANTE, MARKUS N90-26450
QUILLEN, DIANA T. N90-26744
QUINN, J. M. N90-26062

R

RAGHAVAN, K. N90-26687
RAGNARSON, P. N90-26416
RAHN, JEFFREY A. N90-26156
RAINER, F. N90-26314
N90-26315
RAINEY, GERALD N90-26026
RAJU, I. S. N90-26076
RAJU, M. S. N90-26275
RAKHMANOV, A. N90-26478
RAMAMOORTHY, C. V. N90-26560
RAMAMOORTHY, P. N90-25936
RAMASESHA, SHEELA N90-26092
RAMEY, DANIEL B. N90-26596
RAMOHALLI, KUMAR N90-26044
RAMOS, YVETTE N90-26024
RAMPARANY, FANO N90-26587
RANDOLPH, L. N90-26232
RAY, M. A. N90-26675
RAYNAUD, J. P. N90-26724
RED-HORSE, JOHN R. N90-26531
REGGIA, JAMES A. N90-26526
REID, DON W. N90-26627
REIFARTH, J. N90-26721
REISSELL, ANNI N90-26407
REKOS, N. F., JR. N90-26393
REMER, D. S. N90-26231
RENNELS, D. N90-26518
RESHOTKO, ELI N90-25934
RESSLER, RICHARD L. N90-26590
REY, CHARLES N90-26041
REY, CHARLES F. N90-26298
RHODES, GRAHAM SCOTT N90-26017

RIBOWICZ, MARC N90-26606
RICE, JOHN R. N90-26534
RICH, DON C. N90-26527
RICHARD, MARK A. N90-26250
RICHARDS, BYRON N90-26332
RICHARDS, M. C. N90-26064
RICHARDS, ROBERT C. N90-26177
RICHARDSON, JOHN N. N90-26131
RICHARDSON, KROY N90-26332
RICHTER, G. P. N90-26055
RICKS, WENDELL R. N90-26511
RIETJENS, L. H. T. N90-26259
RIGGINS, DAVID W. N90-25992
RILEY, D. A. N90-26453
N90-26463
RINKO, JOHN N90-26026
RINSLAND, C. P. N90-26400
N90-26402
ROBERTS, JEFF P. N90-26310
ROBERTS, JEFFERSON G. N90-26128
ROBERTS, W. N90-26457
ROBINSON, RANDY L. N90-26018
RODHE, HENNING N90-26413
N90-26414
N90-26423
RODRIGUEZ, J. G. N90-26043
N90-26347
RODRIGUEZ, PEDRO R. N90-26479
ROGERS, R. S. C. N90-26084
ROHNER, KARL A. N90-26298
ROJAS, VICTORIA A. N90-26484
ROMANA, L. J. N90-26674
ROMANI, P. N. N90-26770
ROMANO, E. N90-26358
RONCACE, JAMES N90-26065
ROSE, FRED G. N90-26432
ROSENBERG, G. N90-26459
ROSENBERG, SANDERS D. N90-26095
ROSEY, R. N90-26387
ROSKILLY, RONALD R. N90-26030
ROSS, HOWARD B. N90-26403
N90-26429
ROSS, HOWARD D. N90-26163
ROSSMANITH, R. N90-26644
ROTHSCHILD, W. N90-26133
ROUHI, MASSUD N90-26356
ROY, R. N90-26461
RUBLOFF, G. W. N90-26264
RUDOLF, PAUL G. N90-26657
RUEHL, E. N90-26771
RUM, GIOVANNI N90-26035
N90-26058
RUMMLER, D. R. N90-26296
RUPNIK, R. N90-26387
RUSCHAU, JOHN J. N90-26125
RUSH, DARLENE D. N90-26704
RUSSELL, DAVID N90-26331
RUSTAD, JOHN ERIK N90-26206
RUTGERS, W. R. N90-26259
RUTLEDGE, SHARON K. N90-26068
RYBOWICZ, MARC N90-26607

S

SAAD, MOHAMAD N90-26044
SACK, NORBERT J. N90-26782
SAGAN, C. N90-26775
N90-26776
SAGER, J. C. N90-26480
SAKAI, SHINSUKE N90-26365
SALEHUDIN, M. N90-26187
N90-26205
SALEM, J. A. N90-26132
SALPEKAR, S. A. N90-26076
SALTZ, JOEL H. N90-26509
SANDBORN, VIRGIL A. N90-26271
SANDEN, ROLAND N90-26153
SANDLER, H. N90-26485
SANDLIN, DORAL R. N90-26515
SANDNES, HILDE N90-26405
SANTORIELLO, G. N90-26291
SAPP, W. N90-26467
N90-26469
SASAGAWA, GLENN S. N90-26629
SASSEN, KENNETH N90-26447
SATO, MASAHIRO N90-26072
SAUSA, ROSARIO C. N90-26317
SAVIN, W. M. N90-26485
SAWCHENKO, P. N90-26475
SAWYER, H. R. N90-26470
SCHAEFER, OTTMAR N90-26263
SCHAFFAR, M. N90-25942
SCHIER, J. A. N90-26292
SCHIFF, H. I. N90-26399
SCHISSEL, D. P. N90-26660
SCHMIDT, JEAN-PAUL N90-26551
SCHMIDT, V. HUGO N90-26137
SCHMOLZ, PETER N90-25976
SCHNEIBEL, J. H. N90-26117
N90-26668
SCHNEIDER, ALLAN N90-26188
SCHNOEBELEN, PH. N90-26571
SCHREIBER, JEFFREY G. N90-26729
SCHROEDER, J. S. N90-26485
SCHROEDER, W. H. N90-26419
SCHRYER, DAVID R. N90-26309
SCHRYER, JACQUELINE N90-26309
SCHUELLER, R. D. N90-26089
SCHUSTER, R. N90-26782
SCHWARTZ, DAVID T. N90-26704
SCHWARTZ, STEPHEN A. N90-26024
N90-26704
SCOTT, WILLIAM R. N90-26505
SCRIVENER, M. S. N90-26314
SCRUGGS, STEVE N90-26165
SEDLAK, F. N90-26463
SEGA, RONALD M. N90-26631
SEIDENSTICKER, R. G. N90-26387
SEKHON, AMRIT N90-26053
SEKULA-MOISE, P. A. N90-26683
SELF, RICHARD J. N90-26709
SERINKEN, N. M. N90-26179
SEROVA, L. V. N90-26467
N90-26469
SERPEN, GURSEL N90-26488
SEYFERTH, DIETMAR N90-26158
SHAFFER, CLIFFORD A. N90-26582
SHAH, S. N90-26357
SHAIK, K. N90-26226
SHALTENS, RICHARD K. N90-26729
SHAPIRO, Y. N90-26486
SHARKEY, THOMAS D. N90-26481
SHARMA, PRAMOD N90-26098
SHAVIT, NIR N90-26520
SHAW, J. H. N90-26400
SHERIF, J. S. N90-26231
SHETZER, CHRISTIE N90-26332
SHI, DONGLU N90-26676
SHIELDS, JOSEPH C. N90-26786
SHIMODAIRA, KAZUO N90-25983
SHIMOKAWA, TOSHIYUKI N90-26085
SHIN, KANG G. N90-26513
SHIZUEII, SILVIA N90-26379
SHUMWAY, ANDREW N90-26436
SICILA, P. N90-26207
SIDI, AVRAM N90-26616
SIEG, R. E. N90-26682
N90-26683
SIMCIK, LUKE N90-26484
SIMMONS, D. N90-26459
SIMON, R. N90-26088
SIMS, A. J. N90-26662
SINGH, A. K. N90-26092
SINGH, AMAR N. N90-26102
SINGH, DAVID N90-26026
SINGH, P. N90-26691
N90-26692
SINGH, RITI N90-25986
N90-25987
N90-25988
N90-25989
N90-25990
SINGH, UPENDRA N. N90-26503
SIRIGNANO, W. A. N90-26104
SIVIER, KENNETH N90-26049
SJOGREN, JON A. N90-26214
N90-26619
SKARE, OIVIND N90-26502
SKORSTAD, GORDON N90-26689
SKUJINS, MARGARET B. N90-26020
SLACK, D. C. N90-26277
SLAGLE, IRENE R. N90-26764
SLOCUM, G. N90-26463
SLOOFF, J. W. N90-25947
SMIRNOV, K. V. N90-26470
SMITH, G. LOUIS N90-26432
N90-26433
SMITH, GROVER N90-26436
SMITH, J. B., JR. N90-26785
SMITH, M. J. T. N90-25977
N90-26637
SMITH, MIKE N90-26165
SMITH, PAUL L. N90-26449
SMITH, PHILIP J. N90-25964
SMITH, ROSS JAMES N90-26521
SMITH, W. T. N90-26213
SMYTH, P. N90-26228
SNAPE, D. M. N90-26004
SNYDER, P. G. N90-26683
SOFUE, YASUSHI N90-26086
SOICHER, H. N90-26208
SOILE, JUUTI N90-26421
SOLAL, FRANCINE N90-26110
SOLER, JEAN-LOUIS N90-26352
N90-26353
SOLIMAN, M. R. I. N90-26472
SOM, S. N90-26563
SONG, MIYONG N90-26596
SONNENFELD, G. N90-26476
SORAIS, D. N90-26185
N90-26207
SOUEIDAN, MOHAMMED N90-26517
SPARKS, C. J. N90-26117
SPEED, ROGER D. N90-26626
SPEZIALE, CHARLES G. N90-26270
SPILKER, T. R. N90-26750
SPINHIRNE, JAMES D. N90-26446
SPRECACE, R. P. N90-26387
SPURGEON, S. K. N90-26014
N90-26337
N90-26583
STABELLINI, ALESSANDRO N90-25978
STADLER N90-26519
STADSNES, RUNE N90-26541
STAFFORD, R. J. N90-26126
STAGGS, M. C. N90-26314
STAN, M. A. N90-26682
STANDLEY, HILDA M. N90-26512
STARBUCK, J. MICHAEL N90-26083
STARKS, PATRICK J. N90-26378
STARR, DAVID OC. N90-26446
STAUDER, D. N90-26725
STEFFEN, J. M. N90-26462
STEFFENSEN, JORGEN PEDER N90-26411
STEFFES, PAUL G. N90-26745
STEIN, BLAND A. N90-26075
STEINFELD, J. N90-26442
STEINFELD, J. I. N90-26755
STEINFELD, UWE H. N90-26557
STEPHENS, CRAIG A. N90-26269
STEPHENS, JAMES P. N90-26245
STERBA, JOHN A. N90-26487
STERN, S. A. N90-26504
STEVENS, JAMES G. N90-26623
STEVENS, RICK N90-26562
STEVENSON, J. N90-26467
N90-26469
STIEF, L. J. N90-26769
STIEF, LOUIS J. N90-26744
N90-26768
STOK, L. N90-26567
STORDAL, FRODE N90-26424
STOREN, OLE HENRIK N90-26206
STOREY, C. N90-26543
STORM, R. S. N90-26084
STOUGHTON, J. N90-26563
STOUGHTON, R. M. N90-26577
STRAIT, E. J. N90-26660
STRAYER, DAVID L. N90-26489
STRICKLAND, JAMES H. N90-25941
STROCK, THOMAS W. N90-26009
STRUVEN, CHRISTOPHER A. N90-26162
STUREK, FRANK D. N90-26155
STUREK, WALTER B. N90-26155
STUTLER, WILLIAM N90-26114
STUTZMAN, W. L. N90-26213
SUAREZ, C. B. N90-26751
SUENRAM, R. D. N90-26752
SULLIVAN, JEANNE MARIE N90-26033
SUN, D. C. N90-26338
SUN, ZHISHENG N90-26102
SUTTLES, J. T. N90-26446
SVANBERG, S. N90-26416
SWAIN, RONALD L. N90-26360
SWAN, SCOTT A. N90-26342
SWANSON, R. C. N90-26595
SWANSON, STEPHEN MARK N90-26515
SYERS, G. N90-26005
SYLVAIN, M. N90-26189
SZAKALY N90-26339

T

TACHIKAWA, HIROYASU N90-26102
TADANO, MAKOTO N90-26072
TADIOS, EDEN L. N90-25941
TAISTO, RAUNEMAA N90-26421
TAKEDA, YUKIHIRO N90-26255
TAKIGAWA, KIYOSHI N90-26255
TALBOT, PETER D. N90-25972
TALIA, JORGE E. N90-26166
TALLANT, D. R. N90-26145
TALLMAN, CHARLES R. N90-26310
TALON, JEAN-YVES N90-26611
TAMARU, SUGURU N90-25983
TAN, CHUNG-I. N90-26648

TAN, H. Q. N90-26364
TANABE, TOSHIHIKO N90-26781
TANG, JINKE N90-26116
TARRAGO, G. N90-26751
TAUBER, M. E. N90-25945
TAUROW, LEE S. N90-26326
TAVAKOLI, HOSSEIN N90-26331
TAYLOR, ANTOINETTE J. N90-26310
TAYLOR, G. N90-26476
TAYLOR, KIMBERLY ELAINE N90-26703
TAYLOR, R. G. N90-26348
N90-26349
TEDJOJUWONO, KEN K. N90-26651
TELSCHOW, K. L. N90-26140
N90-26141
N90-26670
TENNERY, V. J. N90-26132
N90-26136
TERRY, F. L. N90-26389
THODAY, R. D. C. N90-26211
N90-26212
THOMAS, DAVID J. N90-26372
THOMASON, D. B. N90-26465
THOMPSON, C. A. N90-26485
THOMPSON, J. R. N90-26666
THOMPSON, R. G. N90-26115
THOMPSON, SANDRA A. N90-26733
THOMPSON, W. R. N90-26775
N90-26776
THOMPSON, W. REID N90-26774
THOMSON, J. I. N90-26548
THORNTON, C. L. N90-26219
THORPE, C. N90-26591
THORVALDSEN, T. N90-26195
THURMAN, S. W. N90-26220
N90-26221
TITZE, ANDREAS N90-26598
TOLLETT, JEFFREY J. N90-26657
TOMASKO, M. G. N90-26758
TOMSIK, T. M. N90-26055
TOMSIK, THOMAS M. N90-26160
TONG, HOWELL N90-26604
TONGUZ, INCI OZGUNES N90-26243
TOON, G. C. N90-26402
TORIYAMA, TAKAO N90-25107
TORRE, LARRY P. N90-26047
TOTZECK, MICHAEL N90-26236
TOURANCHEAU, BERNARD N90-26573
TOUZENE, ABDEREZAK N90-26572
TOW, D. M. N90-26043
N90-26347
TOWNSEND, L. W. N90-26640
TRAJMAR, S. N90-26779
TROIM, JAN N90-26541
TROUTMAN, PATRICK A. N90-26032
TRUBENOK, V. D. N90-25955
TSAI, CHEN S. N90-26263
TSAI, W. H. N90-26157
TSIKOS, CONSTANTINE J. N90-26497
TSOU, JIM N90-25971
TURKEL, ELI N90-26595
TURNER, LEAF N90-26659
TUROK, NEIL N90-26734

U

UHRY, J. P. N90-26570
ULEN, ESKIL N90-26395
ULRICH, NATHAN THATCHER N90-26498
URDAHL, R. S. N90-26772
USHA, U. N. N90-26523

V

VACHE, V. N90-26724
VAHALA, L. L. N90-26658
VAIDA, V. N90-26771
VAILAS, A. N90-26456
VALE, W. N90-26475
VALERO, F. P. J. N90-26751
VALLERANI, ERNESTO N90-26058
N90-26059
VAN ZOEREN, C. N90-26442
VANAKEN, D. C. N90-26124
VANBRAMER, S. E. N90-26399
VANBREUGEL, WIL J. M. N90-26786
VANCUSTEM, BERNARD N90-26603
VANDEKAMP, M. M. J. L. N90-26240
VANDENBOOM, A. J. J. N90-26584
VANDENHEUVEL, JOHAN N90-26656
VANDENHEUVEL, W. M. C. N90-26257
VANDERHOEVEN, W. N90-26370
VANDERHOFF, JOHN A. N90-26100
VANDERLINDEN, ROB N90-26286
VANDERVIS, P. A. N90-26191
VANDERVOORT, K. N90-26676
VANDYKE, MELISSA N90-26332
VANEGMOND, J. A. N90-25951
VANGELDER, P. A. N90-25951
VANHULSTEYN, D. B. N90-26665
VANNORMAN, JOHN D. N90-26309
VANSTONE, R. H. N90-26355
VANUFFELEN, J. P. N90-26200
VANVELDHUIZEN, E. M. N90-26259
VANWEES, BART JAN N90-26440
VARANASI, PRASAD N90-26753
VARESIO, FRANCO N90-26035
VASQUES, M. N90-26469
N90-26475
VASQUEZ, RICHARD P. N90-26684
VAUGHN, R. L. N90-26267
VAY, S. A. N90-26399
VELLEGO, GENI N90-26672
VENIER, G. N90-26179
VENKATAKRISHNAN, P. N90-26785
VENKATESWARAN, V. N90-26084
VERESHCHETIN, V. S. N90-26715
VERMEEREN, C. A. J. R. N90-26368
VERNADAT, FRANCOIS N90-26555
VERUTTIPONG, T. N90-26225
VIANCO, P. T. N90-26135
VICTOROV, I. N90-26475
VIEIRADUTRA, LUCIANO N90-26379
N90-26381
VINING, ROEL C. N90-26378
VISHWANATH, P. R. N90-26732
VISSER, JACOBUS HENDRIK N90-26638
VITTA, S. N90-26682
VLEESHOUWERS, J. M. N90-26256
VOECKS, GERALD E. N90-26098
VOGLER, L. N90-26182
VONDREELE, ROBERT B. N90-26096
VUKELICH, SHARON I. N90-26349

W

WADA, KATSUO N90-26149
WADDINGTON, D. N90-26392
WAENGBERG, INGVAR N90-26425
N90-26430
WAGENER, R. N90-26757
WAGNER, CHARLES F., JR. N90-26209
WALKER, A. B. N90-26600
WALLINDER, EVA N90-26416
WALTER-SHEA, ELIZABETH A. N90-26378
WALTER, J. B. N90-26141
WALTER, SHARON M. N90-26559
WALTERS, ROBERT W. N90-26277
WANG, E. N90-26468
WANG, FU-QUAN N90-26528
WANG, JI C. N90-25972
WANG, JIH-FANG N90-26508
WANG, SHENGRUI N90-26574
WARNATZ, J. N90-25994
WARNER, J. D. N90-26682
WARSHEL, ARIEH N90-26483
WATANABE, MITUNORI N90-25949
WATSON, K. N90-26190
WAWNER, F. E., JR. N90-26089
WEAVER, M. J. N90-26101
N90-26441
WEBB, A. R. N90-26579
N90-26580
WEBB, JAMES T. N90-26505
WEBER, MARK C. N90-26748
WELCH, RONALD M. N90-26446
WELLER, JOSEPH F. N90-26305
WELLHAUSEN, S. R. N90-26476
WELP, U. N90-26676
WELTON, WALT N90-26053
WELTY, D. E. N90-26737
WENG, R. N90-26389
WETHERHOLD, ROBERT C. N90-26142
N90-26372
WHALEN, M. V. N90-26055
WHEELER, R. M. N90-26480
WHILLANS, I. M. N90-26739
WHITE, C. W. N90-26674
WHITE, JOHN E. N90-26031
WHITE, KEVIN EUGENE N90-25960
WHITE, PRITCHARD H. N90-26037
N90-26038
WHITE, TONY N90-26246
WHITFIELD, C. E. N90-26633
WHITMORE, ROY A., JR. N90-26377
WIEGMAN, JANET F. N90-26505
WIELICKI, BRUCE A. N90-26446
WILBY, EMMA G. N90-26037
N90-26038
WILBY, JOHN F. N90-26037
N90-26038
WILCOX, ROY C. N90-26108
WILCOXON, JESS N90-26144
WILDERSON, THOMAS D. N90-26503
WILKES, DAVID N90-26246
WILLEMS, FRANS M. J. N90-26546
WILLENBERG, HARVEY J. N90-26047
WILLIAMS, BEN R. N90-26009
WILLIAMS, C. N90-26469
WILLIAMS, MARC H. N90-25940
WILLIAMS, R. J. N90-26002
WILLIS, E. A. N90-26275
WILLIS, EDWARD A. N90-25982
WILLNECKER, RAINER N90-26678
WILSON, JOHN W. N90-26640
WILSON, STEWART B. L. N90-26696
WILSON, THOMAS E. N90-26312
WINGO, DENNIS N90-26161
WINTER, CARL-JOCHEN N90-26173
WINTER, M. R. M. N90-26569
WITHERS, B. EDWARD N90-26527
WOLF, JAMES S. N90-26109
WOLF, MICHAEL L. N90-26537
WOLF, STEPHEN W. D. N90-26019
WOLVERTON, C. D., JR. N90-26177
WONG, C. R. N90-26124
WOOD, C. S. N90-26548
WOOD, MARK N90-26344
N90-26535
WOOLLAM, J. A. N90-26663
WOOSLEY, STANFORD E. N90-26787
WRENN, G. L. N90-26662
WRIGHT, GEOFF N90-26042
WU N90-26519
WU, C. Y. R. N90-26754
N90-26757
WU, C. Y. ROBERT N90-26783
WU, MAN-LI C. N90-26446
WU, S. C. N90-26219

X

XIA, T. J. N90-26757
XIAO, ZIFAN F. N90-26419
XU, MING N90-26676

Y

YAGER, THOMAS J. N90-25957
YAMAMOTO, ATSUMASA N90-25984
YANG, KUANGHUA N90-26759
YAO, H. D. N90-26683
YASSINE, ADNAN N90-26553
YATES, J. R. N90-26367
YEN, TZU-LIANG N90-26026
YING, S.-J. N90-26170
YODH, G. B. N90-26732
YONUSHONIS, T. M. N90-26126
YORK, DAVID A. N90-26266
YOSHIDA, MAKOTO N90-26034
YOUNG, DAVID F. N90-26447
YOUNG, GARY N90-26331
YOUNG, J. T. N90-26157
YOUNG, PHILIP R. N90-26075
N90-26131
YU, YE N90-25971
YUAN, XIAOPING N90-26625
YUEH, HERNG-AUNG N90-26382
YUNCK, T. P. N90-26219
YUNG, YUK L. N90-26763
YURI, ISAO N90-26148
N90-26149

Z

ZAKHIA, NADIM N90-26165
ZANDER, R. N90-26400
ZANDER, SHIRLEY JO N90-26618
ZEIGLER, JOHN M. N90-26146
N90-26661
ZERNICKE, R. N90-26456
ZHANG, ZHI-FAN N90-26156
ZHENG, JIANG-FEN N90-26423
ZHOU, ZHEN-LEI N90-26578
ZHU, YU-CAI N90-26585
N90-26586
ZIEGLER, FRANK N90-25965
ZOCCO, THOMAS G. N90-26118
ZOLLWEG, JOHN A. N90-26774
ZOLTANI, CSABA K. N90-26293
ZUBE, DIETER M. N90-26071
ZUMBERGE, MARK A. N90-26629
ZUMWALT, GLEN W. N90-25969

ZWAENEPOEL, WILLY

ZWAENEPOEL, WILLY N90-28622

CORPORATE SOURCE INDEX

Typical Corporate Source Index Listing

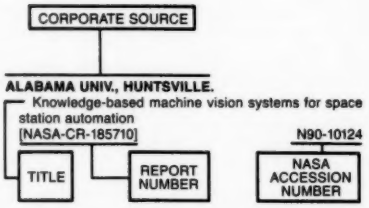

Listings in this index are arranged alphabetically by corporate source. The title of the document provides the user with a brief description of the subject matter. The report number helps to indicate the type of document cited (e.g., NASA report, translation, NASA contractor report). The NASA accession number denotes the number by which the citation is identified. The titles are arranged under each corporate source in ascending accession number order.

A

ACADEMY OF SCIENCES (USSR), MOSCOW.
MIR: A Soviet Space Station. Some legal aspects of international cooperation N90-26715

ADVISORY GROUP FOR AEROSPACE RESEARCH AND DEVELOPMENT, NEUILLY-SUR-SEINE (FRANCE).
Technical evaluation report on the Fluid Dynamics Panel Symposium on Computational Methods for Aerodynamic Design (Inverse) and Optimization
[AGARD-AR-267] N90-25947
Technical evaluation report on the Guidance and Control Panel 49th Symposium on Fault Tolerant Design Concepts for Highly Integrated Flight Critical Guidance and Control Systems
[AGARD-AR-281] N90-26012
Propagation Effects and Circuit Performance of Modern Military Radio Systems with Particular Emphasis on Those Employing Bandspreading
[AGARD-CP-442] N90-26178
Report of the Fluid Dynamics Panel Working Group 10 on calculation of 3D separate turbulent flows in boundary layer limit
[AGARD-AR-255] N90-26280
AGARD highlights 90/1 N90-26788

AERITALIA S.P.A., TURIN (ITALY).
AM-X high incidence trials, development and results
[ETN-90-97277] N90-26016
IRIS system and future application to expandable launchers
[IAF-89-212] N90-26035
Long cycle pressurized logistics module: An Italian contribution to the Space Station Freedom logistics scenario
[IAF-89-083] N90-26058
Perspective features of the tethered systems for space applications
[ETN-90-97279] N90-26059
Possible applications of tethered systems to Mars exploration missions
[IAF-89-489] N90-26060
Bubble, Drop and Particle Unit (BDPU): A multi-user microgravity facility
[IAF-89-431] N90-26164

AEROJET TECHNICAL SYSTEMS CO., SACRAMENTO, CA.
Carbon deposition model for oxygen-hydrocarbon combustion. Task 6: Data analysis and formulation of an empirical model
[NASA-CR-183986] N90-26095

AERONAUTICAL RESEARCH INST. OF SWEDEN, STOCKHOLM.
A preliminary study of the masking of wind turbine noise by ambient sound
[FFA-TN-1990-01] N90-26636

AERONAUTICAL RESEARCH LABS., MELBOURNE (AUSTRALIA).
Statistical treatment of slow strain rate data for assessment of hydrogen embrittlement in low alloy high strength steel
[ARL-MAT-R-122] N90-26106

AEROSPATIALE, LES MUREAUX (FRANCE).
Possible solutions N90-26726

AIR FORCE ACADEMY, CO.
Evaluation of room-temperature chloroaluminate molten salts as electrolytes for high energy density batteries
[AD-A223097] N90-26267

AIR FORCE GEOPHYSICS LAB., HANSCOM AFB, MA.
Proceedings of the Second Symposium on GPS Applications in space, volume 1
[AD-A219978] N90-25962
Proceedings of the Second Symposium on GPS Applications in Space, volume 2
[AD-A219979] N90-25963

AIR FORCE HUMAN RESOURCES LAB., WILLIAMS AFB, AZ.
Eye tracking device for the measurement of flight performance in simulators
[AD-A220075] N90-26484

AIR FORCE INST. OF TECH., WRIGHT-PATTERSON AFB, OH.
Robustness evaluation of H2 and H(infinity) control theory as applied to a transport aircraft
[AD-A222795] N90-26018
Direct-sequence spread spectrum system
[AD-A223021] N90-26245

AIR FORCE SYSTEMS COMMAND, WRIGHT-PATTERSON AFB, OH.
Effect of vortex generators on the aerodynamic wing characteristics and body of revolution
[AD-A222813] N90-25955

AKRON UNIV., OH.
Temperature and melt solid interface control during crystal growth
[NASA-CR-186731] N90-26664

ALABAMA UNIV., BIRMINGHAM.
Effect of boron on intergranular hot cracking in Ni-Cr-Fe superalloys containing niobium
[NASA-CR-186714] N90-26115

ALABAMA UNIV., HUNTSVILLE.
Literature concerning control and display technology applicable to the Orbital Maneuvering Vehicle (OMV)
[NASA-CR-186790] N90-26048
Fluid Phase Separation (FPS) experiment for flight on a space shuttle Get Away Special (GAS) canister
[NASA-CR-186830] N90-26161

ALFA ROMEO S.P.A., NAPLES (ITALY).
Turbine blade heat transfer coefficient evaluation by modified version of STAN5. Comparison with experimental data
[ETN-90-97283] N90-26008
Computational fluid dynamics 3-D analysis for advanced transonic turbine design
[ETN-90-97282] N90-26291

ALLIED-SIGNAL AEROSPACE CO., KANSAS CITY, MO.
Integrating expert systems with solid modeling through interprocess communications and the applications interface specification
[DE90-012996] N90-26537

AMES LAB., IA.
The effect of manganese on the onset of the stage 2 reaction in an austempered ductile iron matrix
[DE90-011804] N90-26119
Selective electrocatalysis of anodic oxygen-transfer reactions at chemically modified, thin-film lead dioxide electrodes
[DE90-011747] N90-26252

APPLIED RESEARCH LAB., STATE COLLEGE, PA.
An experimental system for measuring the wavenumber-frequency response of Timoshenko beams
[AD-A222569] N90-26374

ARGONNE NATIONAL LAB., IL.
Parallel programming with algorithmic skeletons
[DE90-010536] N90-26562
Materials research issues in superconducting levitation and suspension as applied to magnetic bearings
[DE90-011147] N90-26667
Studies on ion scattering and sputtering processes relevant to ion beam sputter deposition of multicomponent thin films
[DE90-010071] N90-26675
Critical current density, flux creep, and microstructure in a Bi-Sr-Ca-Cu-O system
[DE90-010457] N90-26676
A methodology for benchmarking distributed database management systems
[DE90-007801] N90-26702

ARIZONA STATE UNIV., TEMPE.
Scattering from coated structures and antenna pattern control using impedance surfaces, part A/B
[NASA-CR-186871] N90-26233

ARIZONA UNIV., TUCSON.
Autonomous space processor for orbital debris
[NASA-CR-186691] N90-26044
Investigation of the Saturn dust environment from the analysis of energetic charged particle measurements
[NASA-CR-186727] N90-26784

ARMY AVIATION SYSTEMS COMMAND, CLEVELAND, OH.
Efficiency study comparing two helicopter planetary reduction stages
[NASA-TM-103106] N90-26334

ARMY AVIONICS RESEARCH AND DEVELOPMENT ACTIVITY, FORT EUSTIS, VA.
Closed-form solution of decomposable stochastic models
[NASA-TM-103466] N90-26619

ASTRO AEROSPACE CORP., CARPINTERIA, CA.
Structures for remotely deployable precision antennas
[NASA-CR-182065] N90-26061

ASTRON RESEARCH AND ENGINEERING, SANTA MONICA, CA.
Vibration test procedures for orbiter sidewall-mounted payloads, phase 1
[AD-A220773] N90-26037
Vibration test procedures for orbiter sidewall-mounted payloads, phase 2
[AD-A220774] N90-26038

AUBURN UNIV., AL.
Hydrogen induced fracture characteristics of single crystal nickel-based superalloys
[NASA-CR-183992] N90-26108

AXIOMATIX, LOS ANGELES, CA.
Dynamic jamming of networks
[AD-A223044] N90-26247
A novel communication network simulator
[AD-A223045] N90-26248

B

BALLISTIC RESEARCH LABS., ABERDEEN PROVING GROUND, MD.
Temperature and OH concentrations in a solid propellant flame using absorption techniques
[AD-A222591] N90-26100
A computational study of the effectiveness of coating materials for KE projectile fins subjected to the combined effects of inbore and aerodynamic heating
[AD-A222595] N90-26155
Effect of initial conditions on the development of two-phase jets
[AD-A222621] N90-26293
Excimer laser fragmentation studies of selected oximes: Nascent OH internal energy distributions and the search of H2CN fluorescence
[AD-A222622] N90-26317

BOEING AEROSPACE CO., HUNTSVILLE, AL.
Planning for Space Station Freedom laboratory payload integration
[NASA-CR-186751] N90-26047

BOEING AEROSPACE CO., KENT, WA.
Multimegawatt space nuclear power supply, phase 1. Volume 2: Phase 2 plan D180-30619-6
[DE90-012431] N90-26645
Multimegawatt space nuclear power supply, phase 1. Volume 3: Annotated outline of preliminary safety assessment D180-30619-7
[DE90-012432] N90-26646

Multimegawatt space nuclear power supply, phase 1. Supplement: D180-30619-8
[DE90-012433] N90-26647

BOEING COMMERCIAL AIRPLANE CO., SEATTLE, WA.
Application of laminar flow control to supersonic transport configurations
[NASA-CR-181917] N90-25944

BRITISH BROADCASTING CORP., KINGSWOOD (ENGLAND).
Antennas for portable VHF-FM receivers
[BBC-RD-1990/1] N90-26211
Electric field strength meters for the HF, VHF, and UHF bands
[BBC-RD-1990/3] N90-26212

BRITISH TELECOM RESEARCH LABS., IPSWICH (ENGLAND).
Radio channel measurement and modelling for future mobile radio systems N90-26184

BROWN UNIV., PROVIDENCE, RI.
Level-2 system: Programmers-users manual
[DE90-013324] N90-26540
A research program in theoretical high energy physics
[DE90-013322] N90-26648
A research program in physics of the early universe
[DE90-013319] N90-26742

BUNDESMINISTERIUM FUER FORSCHUNG UND TECHNOLOGIE, BONN (GERMANY, F.R.).
The International Space Station: The legal framework N90-26716
The astronauts' legal status: The International Space Station N90-26721

C

CALIFORNIA INST. OF TECH., PASADENA.
Development of microencapsulation techniques
[AD-A223032] N90-26159
Imaging and spectroscopy of small molecules by scanning tunneling microscopy
[AD-A222572] N90-26641
Submillimeter and millimeter observations of solar system objects
[NASA-CR-186636] N90-26731
Chemical kinetics and modeling of planetary atmospheres N90-26763

CALIFORNIA POLYTECHNIC STATE UNIV., SAN LUIS OBISPO.
A computer module used to calculate the horizontal control surface size of a conceptual aircraft design
[NASA-CR-186672] N90-26515

CALIFORNIA STATE POLYTECHNIC UNIV., POMONA.
Global Sentry: NASA/USRA high altitude reconnaissance aircraft design, volume 2
[NASA-CR-186820-VOL-2] N90-25971

CALIFORNIA STATE UNIV., LONG BEACH.
A novel multireceiver communications system configuration based on optimal estimation theory
[NASA-CR-186847] N90-26216

CALIFORNIA UNIV., BERKELEY.
Liquid fueled ramjet combustion instability: Acoustical and vortical interactions with burning sprays
[AD-A222752] N90-26104
Language support for parallel computation
[AD-A223072] N90-26560

CALIFORNIA UNIV., DAVIS.
Laboratory studies of photodissociation processes relevant to the formation of cometary radicals N90-26772

CALIFORNIA UNIV., IRVINE.
DoD-University research instrumentation program, FY 1986/FY 1987
[AD-A222578] N90-26263
Experiment K-6-10. Effects of zero gravity on myofibril protein content and isomyosin distribution in rodent skeletal muscle N90-26464

CALIFORNIA UNIV., LOS ANGELES.
Experiment K-6-07. Metabolic and morphologic properties of muscle fibers after spaceflight N90-26461
Absolute vacuum ultraviolet photoabsorption cross section studies of atomic and molecular species: Techniques and observational data N90-26754
Photon sputtering of H2O ices: A preliminary report N90-26783

CALIFORNIA UNIV., SAN FRANCISCO.
Experiment K-6-04. Trace element balance in rats during spaceflight N90-26458

CARBORUNDUM CO., NIAGARA FALLS, NY.
Synthesis of high purity sinterable silicon carbide powder
[DE90-012029] N90-26084

CARNEGIE-MELLON UNIV., PITTSBURGH, PA.
Innovative design systems: Where are we, and where do we go from here
[AD-A222586] N90-26556
Color image processing for navigation: Two road trackers
[AD-A222667] N90-26591

CASE INST. OF TECH., CLEVELAND, OH.
Interactive calculation procedures for mixed compression inlets
[NASA-CR-186581] N90-25934

CASE WESTERN RESERVE UNIV., CLEVELAND, OH.
Neural networks for real-time sensory data processing and sensorimotor control
[AD-A223096] N90-26592

CATHOLIC UNIV. OF AMERICA, WASHINGTON, DC.
Position control of redundant manipulators using an adaptive error-based control scheme
[NASA-CR-186812] N90-26578
Kinetics and thermochemistry of polyatomic free radicals: New results and new understandings N90-26764

CELLULOSE CONVERSION ENTERPRISES, BERKELEY, CA.
Beam rider for an Articulated Robot Manipulator (ARM) accurate positioning of long flexible manipulators
[NASA-CR-185151] N90-26581

CENTER FOR REMOTE SENSING, MCLEAN, VA.
Effects of ionospheric modification on system performance N90-26202

CENTRAL RESEARCH INST. OF ELECTRIC POWER INDUSTRY, CHIBA (JAPAN).
Construction of geological and geotechnical information database
[DE90-503417] N90-26706

CENTRAL RESEARCH INST. OF ELECTRIC POWER INDUSTRY, TOKYO (JAPAN).
Evaluation of fracture strength properties of silicon carbide ceramics under cyclic/static axial loading at ultra-high temperature
[DE90-502402] N90-26147
Development of ceramic fiber type combustor: Improvement of combustor and combustion test results
[DE90-503441] N90-26148
Development of ceramic hybrid combustor: Design and combustion test results
[DE90-503442] N90-26149
Storage battery operation technique of photovoltaic system to prevent the imbalance of state of charge
[DE90-503032] N90-26255
Development of creep-fatigue damage detection method of rotor steel by ultrasonic wave measurement
[DE90-503792] N90-26365

CENTRE DE RECHERCHES SCIENTIFIQUES ET TECHNIQUES DE L'INDUSTRIE DES FABRICATIONS METALLIQUES, BRUSSELS (BELGIUM).
CAD/CAM reinforces the competitive edge of European mouldmakers
[CRIF-MC-88] N90-26542

CENTRE NATIONAL D'ETUDES DES TELECOMMUNICATIONS, ISSY-LES-MOULINEAUX (FRANCE).
In-band amplitude dispersion on a microwave link N90-26189
Combined effects of fast and selective fading on performance of PSK and MSK with coherent detection N90-26204

CENTRE NATIONAL D'ETUDES DES TELECOMMUNICATIONS, LANNION (FRANCE).
Experimental analysis of the HF linkage N90-26181

CENTRO BRASILEIRO DE PESQUISAS FISICAS, RIO DE JANEIRO.
Nonstandard big bang models
[DE90-625593] N90-26736

CHAMBRE REGIONALE DE COMMERCE ET DE L'INDUSTRIE DE LORRAINE, NANCY (FRANCE).
The transfer of mercury between the atmosphere and lake or soil surfaces N90-26419
The aqueous atmospheric chemistry of mercury N90-26420

CHICAGO UNIV., IL.
Theory of circular dielectric waveguide with anisotropic sheet cover
[NASA-CR-186883] N90-26235
Theory of biaxial graded-index optical fiber
[NASA-CR-186882] N90-26652

CINCINNATI UNIV., OH.
Molecular structure of interphases between DGEBA/BTDA adhesives and silver substances using surface-enhanced Raman scattering
[AD-A222750] N90-26157
Computer simulation of gear tooth manufacturing processes
[NASA-CR-185200] N90-26171

CLEMSON UNIV., SC.
Analysis and improved design considerations for airborne pulse Doppler radar signal processing in the detection of hazardous windshear
[NASA-CR-186792] N90-26448

CLEVELAND STATE UNIV., OH.
Extension of a noninteractive reliability model for ceramic matrix composites
[NASA-CR-185267] N90-26142

COAST GUARD, GROTON, CT.
Testing of flame screens and flame arresters as Devices designed to Prevent the Passage of Flame (DPPF) into tanks containing flammable atmospheres according to an IMO standard
[AD-A222566] N90-26177

COLOGNE UNIV. (GERMANY, F.R.).
Aircraft measurements of the turbulence structure in cirrus clouds
[ISSN-0069-5882] N90-26450

COLORADO STATE UNIV., FORT COLLINS.
Measurement of terms and parameters in turbulent models
[NASA-CR-183993] N90-26271
Experiment K-6-17. Structural changes and cell turnover in the rats small intestine induced by spaceflight N90-26470

COLORADO UNIV., BOULDER.
Resonant coupling through a slot to a loaded cylindrical cavity: Experimental results
[AD-A223000] N90-26631
Novel laser gain and time-resolved FTIR studies of photochemistry N90-26756
UV and VUV spectroscopy and photochemistry of small molecules in a supersonic jet N90-26771

COLUMBIA UNIV., NEW YORK, NY.
Effects of microgravity on rat bone, cartilage and connective tissues N90-26454

COMMUNICATIONS RESEARCH CENTRE, OTTAWA (ONTARIO).
An overview of Canadian radio propagation/communications technologies research N90-26179
A narrowband tactical communication system for the VHF and UHF mobile radio bands N90-26192

CONNECTICUT COLL., NEW LONDON.
A compact, high-powered Far-Infrared (FIR) laser
[DE90-009996] N90-26312

CONTINUOUS ELECTRON BEAM ACCELERATOR FACILITY, NEWPORT NEW, VA.
A beauty factory using an SRF linac and a storage ring
[CEBAF-PR-89-017] N90-26644

COPENHAGEN UNIV. (DENMARK).
Ice core studies and the past atmospheric environment of polar regions N90-26411
The Renland ice core (Greenland): A source for climatic studies over 100,000 years N90-26412

CORNELL UNIV., ITHACA, NY.
MTP: An atomic multicast transport protocol
[NASA-CR-186716] N90-26254
Making real-time reactive systems reliable
[NASA-CR-186642] N90-26344
Tools for distributed application management
[NASA-CR-186627] N90-26535
Knowledge and inhibition in asynchronous distributed systems
[TR-90-1139] N90-26703
Liquid-vapor equilibrium of multicomponent cryogenic systems N90-26774
Optical constraints of kerogen from 0.15 to 40 microns: Comparison with meteoritic organics N90-26776

COSTRUZIONI AERONAUTICHE GIOVANNI AGUSTA S.P.A., CASCINA COSTA (ITALY).
Agusta methodology for pitch link loads prediction in preliminary design phase
[ETN-90-97270] N90-25978
Residual stresses measurements by means of x ray diffraction on electron beam welded joints and laser hardened surfaces
[ETN-90-97269] N90-26371

CRANFIELD INST. OF TECH., BEDFORD (ENGLAND).
Combustion in the gas turbine. Part 1: Combustor types and design
[CIT/SME/VKI/RS/1] N90-25986
Combustion in the gas turbine. Part 2: Preliminary design and performance
[CIT/SME/VKI/RS/3] N90-25987
Combustion in the gas turbine. Part 3: Fuel injection, ignition and stability
[CIT/SME/VKI/RS/4] N90-25988
Combustor cooling aspects
[CIT/SME/VKI/RS/5] N90-25989
Pollutants: Production and methods of reduction
[CIT/SME/VKI/RS/6] N90-25990

CUMMINS ENGINE CO., INC., COLUMBUS, IN.
Effect of casting procedures and diesel engine environment on the behavior of aluminum titanate
[AD-A223079] N90-26126

CYBERCOM CORP., ARLINGTON, VA.
Wideband characterization of forest propagation channels N90-26188

D

DAVID TAYLOR RESEARCH CENTER, BETHESDA, MD.
Damping capacity of aluminum 6061-indium alloys
[AD-A222802] N90-26124

DAYTON UNIV., OH.
Fracture toughness and failure mechanisms in commercial 2091 Al-Li sheet at cryogenic temperatures
[AD-A222803] N90-26125

DEPARTMENT OF ENERGY, OAK RIDGE, TN.
Energy data base: Subject categories and scope
[DE90-009212] N90-26706

DEPARTMENT OF ENERGY, WASHINGTON, DC.
Preliminary designs for 25 kWe advanced Stirling conversion systems for dish electric applications
[NASA-TM-103188] N90-26729

DEPARTMENT OF THE ARMY, WASHINGTON, DC.
Continuous on-line link error rate detector
[AD-D014510] N90-26209

Active lag angle device
[AD-D014538] N90-26249

Multicolor infrared photodetector
[AD-D014511] N90-26297

DEPARTMENT OF THE NAVY, WASHINGTON, DC.
Apparatus for the efficient wavelength conversion of laser radiation
[AD-D014506] N90-26305

Helmet-mounted head restraint
[AD-D014536] N90-26491

DEUTSCHE FORSCHUNGSANSTALT FUER LUFT- UND RAUMFAHRT, COLOGNE (GERMANY, F.R.).
Undercooling and solidification
[DLR-FB-90-020] N90-26678

DEUTSCHE FORSCHUNGSANSTALT FUER LUFT- UND RAUMFAHRT, GOETTINGEN (GERMANY, F.R.).
Structural analysis and optimization of a propfan blade using a finite element method
[DLR-FB-90-01] N90-26006

DEUTSCHE FORSCHUNGSANSTALT FUER LUFT- UND RAUMFAHRT, STUTTGART (GERMANY, F.R.).
Qualification of concentrating mirror systems with the HERMES measurement system and the HELIOS simulation program
[DLR-FB-89-51] N90-26394

DOUGLAS AIRCRAFT CO., INC., LONG BEACH, CA.
Study of high-speed civil transports. Summary
[NASA-CR-4236] N90-25966

DRAPER (CHARLES STARK) LAB., INC., CAMBRIDGE, MA.
Trajectory optimization for an asymmetric launch vehicle
[NASA-CR-185630] N90-26033

DUKE UNIV., DURHAM, NC.
Asymptotic modal analysis and statistical energy analysis
[NASA-CR-186732] N90-26634

E

EDGERTON, GERMESHAUSEN AND GRIER, INC., IDAHO FALLS, ID.
Vitreous joining of SiC fiber reinforced SiC composites
[DE90-012951] N90-26081

ELORET CORP., PALO ALTO, CA.
Experimental aerothermodynamic research of hypersonic aircraft
[NASA-CR-186903] N90-25954

ELORET CORP., SUNNYVALE, CA.
Transatmospheric vehicle research
[NASA-CR-186705] N90-25970

EMORY UNIV., ATLANTA, GA.
Experiment K-6-14. Hepatic function in rats after spaceflight N90-26468

ERLANGEN-NUREMBERG UNIV. (GERMANY, F.R.).
Proton irradiation of simple gas mixtures: Influence of irradiation parameters N90-26782

EUROPEAN SPACE AGENCY, PARIS (FRANCE).
Materials and structures for 2000 and beyond: An attempted forecast by the DLR Materials and Structures Department
[ESA-TT-1154-REV] N90-26173

Manned Space Stations: Legal Issues
[ESA-SP-305] N90-26711

Technical characteristics and functions of different types of space stations N90-26712

The partnership concept and international management N90-26717

F

FEDERAL AVIATION ADMINISTRATION, ATLANTIC CITY, NJ.
Equipment feasibility study: Very high frequency communication equipment (136-137 megahertz)
[DOT/FAA/CT-TN89/72] N90-26210

FERMI NATIONAL ACCELERATOR LAB., BATAVIA, IL.
Baryogenesis in extended inflation. 2: Baryogenesis via primordial black holes
[NASA-CR-182843] N90-26735

FINNISH METEOROLOGICAL OFFICE, HELSINKI.
Deposition to the Baltic Sea N90-26404

An Eulerian transport model for NO(sub x)-compounds N90-26406

The long-term variation of lead-210 in relation to particle-bound sulphur in surface air in Finland N90-26407

FLIGHT SAFETY FOUNDATION, INC., ARLINGTON, VA.
Second Annual International Conference on Aging Aircraft
[AD-A222715] N90-25961

FLORIDA ATLANTIC UNIV., BOCA RATON.
Power flow analysis of two coupled plates with arbitrary characteristics
[NASA-CR-182033] N90-26632

FLORIDA STATE UNIV., TALLAHASSEE.
Lunar articulated remote transportation system
[NASA-CR-186617-VOL-1] N90-26332

Design of a lunar transportation system, volume 2
[NASA-CR-186833-VOL-2] N90-26333

FLORIDA UNIV., GAINESVILLE.
Implementation of sensor and control designs for bioregenerative systems
[NASA-CR-186655] N90-26479

Design of sensors for control of closed loop life support systems
[NASA-CR-186656] N90-26490

Molecular interactions and properties with many-body methods
[AD-A222631] N90-26642

FORSCHUNGSINSTITUT DER DEUTSCHEN BUNDESPOST, DARMSTADT (GERMANY, F.R.).
Measurement and simulation of widespread mobile radio channel characteristics N90-26186

FORSCHUNGSINSTITUT FUER INFORMATIONSVERARBEITUNG, ETTLINGEN (GERMANY, F.R.).
Automatic line network extraction from aerial imagery of urban areas through knowledge based image analysis
[AD-A222675] N90-26385

G

GANTT (J. B.), WASHINGTON, DC.
Space Station intellectual property rights and US patent law N90-26723

GARRETT TURBINE ENGINE CO., PHOENIX, AZ.
Advanced Turbine Technology Applications Project (ATTAP)
[NASA-CR-185240] N90-26728

GENERAL ACCOUNTING OFFICE, WASHINGTON, DC.
Aviation safety: Conditions within the air traffic control work force. Fact sheet for congressional requesters
[GAO/RCED-89-113FS] N90-25958

Aviation safety: Serious problems continue to trouble the air traffic control work force. Report to congressional requesters
[GAO/RCED-89-112] N90-25959

Space exploration: Cost, schedule, and performance of NASA's Mars Observer Mission. Fact sheet for the Chairman, Subcommittee on Science, Technology, and Space, Committee on Commerce, Science, and Transportation, US Senate
[GAO/NSIAD-88-137FS] N90-26021

Space exploration: Cost, schedule, and performance of NASA's Magellan Mission to Venus. Fact sheet for the Chairman, Subcommittee on Science, Technology, and Space, Committee on Commerce, Science, and Transportation, US Senate
[GAO/NSIAD-88-130FS] N90-26022

Space exploration: Cost, schedule, and performance of NASA's Ulysses Mission to the Sun. Fact sheet for the Chairman, Subcommittee on Science, Technology, and Space, Committee on Commerce, Science, and Transportation, US Senate
[GAO/NSIAD-88-129FS] N90-26023

Space program: Space debris a potential threat to Space Station and shuttle
[GAO/IMTEC-90-18] N90-26024

Space exploration: Cost, schedule, and performance of NASA's Galileo Mission to Jupiter. Fact sheet for the Chairman, Subcommittee on Science, Technology, and Space, Committee on Commerce, Science, and Transportation, US Senate
[GAO/NSIAD-88-138FS] N90-26025

Space transportation: NASA has no firm need for increasingly costly orbital maneuvering vehicle
[GAO/NSIAD-90-192] N90-26041

Space shuttle: Follow-up evaluation of NASA's solid rocket motor procurement. Report to the Chairman, Committee on Government Operations, House of Representatives
[GAO/NSIAD-89-89] N90-26066

NASA project status reports: Congressional requirements can be met, but reliability must be ensured
[GAO/NSIAD-90-40] N90-26169

Space operations: NASA's communications support for Earth orbiting spacecraft. Report to Chairman, Subcommittee on Space Science and Applications, Committee on Science, Space and Technology, House of Representatives
[GAO/IMTEC-89-41] N90-26215

Technology development: Future use of NASA's large format camera is uncertain
[GAO/NSIAD-90-142] N90-26298

Space operations: NASA is not properly safeguarding valuable data from past missions
[GAO/IMTEC-90-1] N90-26704

GENERAL ATOMIC CO., SAN DIEGO, CA.
The effects of carbonization on the confinement properties of the DIII-D H-mode
[DE90-013297] N90-26660

GENERAL ELECTRIC CO., CINCINNATI, OH.
Elevated temperature crack growth
[NASA-CR-182247] N90-26355

High speed turboprop aeroacoustic study (counterrotation). Volume 1: Model development
[NASA-CR-185241] N90-26633

GEORGIA INST. OF TECH., ATLANTA.
Soil stabilization mat for lunar launch/landing site
[NASA-CR-186690] N90-26128

Soil experiment
[NASA-CR-184927] N90-26165

Micro coring apparatus
[NASA-CR-183072] N90-26321

Lunar deep drill apparatus
[NASA-CR-182756] N90-26322

Proof of principle model for a lunar dumptruck
[NASA-CR-182557] N90-26323

Control strategy for cooperating disparate manipulators
[NASA-CR-186809] N90-26328

An inverse dynamic method yielding flexible manipulator state trajectories
[NASA-CR-186807] N90-26329

Modeling of composite beams and plates for static and dynamic analysis
[NASA-CR-186459] N90-26354

The NASA/MSFC Global Reference Atmospheric Model, 1990 version (GRAM-90)
[NASA-CR-186717] N90-26435

Pilot interaction with automated airborne decision making systems
[NASA-CR-186730] N90-26492

Application and extension of an analytical model of the confined acoustic beam generated by a transducer
[AD-A222994] N90-26639

Laboratory measurements of microwave and millimeter-wave properties of planetary constituents N90-26745

GEORGIA UNIV., ATHENS.
Optical signatures of molecular particles via mass-selected cluster spectroscopy N90-26780

GKSS-FORSCHUNGSZENTRUM GEESTHACHT (GERMANY, F.R.).
Atmospheric correction of thematic mapping measurements about seabeds of the German Bay
[GKSS-89/E/47] N90-26029

GOETEBORG UNIV. (SWEDEN).
Formation kinetics of N2O in the atmosphere N90-26425

Photodissociation of NO2: Influence of photolysis wavelength and temperature dependence on product formation N90-26426

GRENOBLE-1 UNIV. (FRANCE).
Statistical analysis of a software reliability model
[IMAG-RR-781-M] N90-26352

A Bayesian proportional model for software reliability
[IMAG-RR-795-M] N90-26353

Surface reconstruction based on critical contours in a multi-image context
[RR-784-I-IMAG-94-LIFIA] N90-26383

A parallel algorithm for surface plane intersection
[IMAG-RR-794-M] N90-26549

Formal verification of the JANUS on-line multiplier
[IMAG-RR-785-I] N90-26550
Segmentation before and after reconstruction of 3-D surfaces in depth imagery
[RR-788-I-IMAG-97-LIFIA] N90-26551
Study of a class of non convex optimization algorithms: Implementation and applications
[ETN-90-97241] N90-26552
Adaptive and comparative studies of optimization algorithms: Implementations and applications
[ETN-90-97243] N90-26553
Parallelization of an annealing simulation applied to improving tetrahedric grids
[IMAG-RR-796-M] N90-26570
Principles of FP2: Term algebras for specification of parallel machines
[RR-789-I-IMAG-98-LIFIA] N90-26571
Implementation of algorithms used in calculating the tensor product of matrices on a distributed memory machine
[IMAG-RR-786-I] N90-26572
Predissimilarities, prefilters, and ultrametrics on an arbitrary set
[IMAG-RR-970-M] N90-26603
Strong consistency of the least squares estimator for a non-ergodic threshold autoregressive model
[IMAG-RR-791-M] N90-26604
Asymptotic law of the orthogonal empirical functions and applications, part 2
[IMAG-RR-792-M-PT-2] N90-26605
Asymptotic optimality of the fast randomized versions of GCV and C(sub L) in ridge regression and regularization
[IMAG-RR-793-M] N90-26606
Search of primitive polynomials over finite fields
[IMAG-RR-797-M] N90-26607
Calculation of the algebraic curves parameterization: Hamburger-Noether expansions
[IMAG-RR-798-M] N90-26608
Combinatorial problems using a hypercube and Hamming graphs
[ETN-90-97240] N90-26609
A study of the asymptotic properties of least square estimators for multiple phase regression problems
[ETN-90-97244] N90-26620
Mathematical simulation of heat exchanges and thermoelastic constraints in Czochralski crystal growth
[ETN-90-97242] N90-26680

GROUPE DE TRAVAIL SUR LE DROIT DE L'ESPACE, PARIS (FRANCE).
Space law put to the test by the International Space Station N90-26727

H

HARRIS CORP., MELBOURNE, FL.
Design and implementation of robust decentralized control laws for the ACES structure at Marshall Space Flight Center
[NASA-CR-4310] N90-26046

HELSINKI UNIV. OF TECHNOLOGY, ESPOO (FINLAND).
The use of hydrogen in energy economy of Finland
[DE90-796180] N90-26368

HOWARD UNIV., WASHINGTON, DC.
The heat of formation of CN radicals and radiative lifetimes of the A 1 Sigma - state of C2N2 N90-26765

HULL UNIV. (ENGLAND).
A global common-user system for the provision of HF propagation data N90-26180
A digital Meteor-Burst Communication (MBC) propagation path simulator N90-26190
Channel selection and control procedures in an automatic HF system N90-26193
Multiple-access techniques for communication over dispersive radio channels N90-26196
New synchronisation techniques applicable to multi-tone transmission systems N90-26199

I

IBM WATSON RESEARCH CENTER, YORKTOWN HEIGHTS, NY.
Role of surface passivation in the integrated processing of MOS structures
[AD-A222630] N90-26264

IDAHO NATIONAL ENGINEERING LAB., IDAHO FALLS.
Acousto-optic signature analysis for inspection of the orbiter thermal protection tile bonds
[DE90-013089] N90-26043
Real-time monitoring of ceramic sintering with laser ultrasonics
[DE90-012960] N90-26140
Laser ultrasonic measurements on ceramic materials with rough surfaces
[DE90-012961] N90-26141
Field experience in using laser acoustic sensing for inspection
[DE90-012954] N90-26347
Parametric design studies of toroidal magnetic energy storage units
[DE90-013086] N90-26390
NDE (Nondestructive evaluation) of critical currents in high T(sub c) superconductors
[DE90-012953] N90-26670

IDAHO UNIV., MOSCOW.
Greenhouse design for a Martian colony: Structural, solar collection and light distribution systems
[NASA-CR-186818] N90-26501

ILLINOIS STATE UNIV., NORMAL.
Applied mathematical modules for use in a linear algebra service course
[AD-A222814] N90-26618

ILLINOIS UNIV., CHAMPAIGN.
The retrieval of information from secondary memory: A review and new findings
[AD-A222760] N90-26489

ILLINOIS UNIV., URBANA.
The effect of interfacial characteristics on the mechanical performance of ceramic-ceramic composites
[AD-A223031] N90-26090
Photosynthesis in intact plants
[DE90-013699] N90-26482
Single-pass memory system evaluation for multiprogramming workloads
[NASA-CR-186553] N90-26558

ILLINOIS UNIV., URBANA-CHAMPAIGN.
NASA/USRA university advanced design program at the University of Illinois for the 1989-1990 academic year
[NASA-CR-186829] N90-26049
Psychophysiological assessment of pilot workload in an applied setting
[AD-A222707] N90-26507
Qualitative and quantitative reasoning about thermodynamics
[NASA-CR-186788] N90-26689

IMPERIAL COLL. OF SCIENCE AND TECHNOLOGY, LONDON (ENGLAND).
Subsonic combustor flow modeling: State of the art of CFD techniques for reacting and combusting flow N90-25991

INDIANA UNIV., BLOOMINGTON.
The application of HREELS to model catalysts: CO and C2H4 adsorption on Pt/Al2O3
[AD-A222744] N90-26103

INSTITUT FRANCO-ALLEMAND DE RECHERCHES, SAINT-LOUIS (FRANCE).
Aerodynamic loads and blade vortex interaction noise prediction
[ISL-PU-310/89] N90-25942
Maneuvering by means of lateral jets
[ISL-CO-255/88] N90-26015
Analysis of turbulent density fluctuations by means of spontaneous Raman diffusion
[ISL-R-103/89] N90-26287
The study of VF2/VF3 piezoelectric copolymeteres submitted to shocks
[ISL-CO-210/9] N90-26679

INSTITUT NATIONAL DES SCIENCES APPLIQUEES, LYON (FRANCE).
Influence of the manufacturing conditions on the microstructure and mechanical properties of the silicon nitride
[ISAL-90-0008] N90-26154

INSTITUT NATIONAL DES SCIENCES APPLIQUEES, RENNES (FRANCE).
Estimation of the impulse response of a broadband mobile radio channel in suburbia at 910 MHz N90-26187
Experimental study of a digital mobile radio spread spectrum in an urban site N90-26205

INSTITUT NATIONAL POLYTECHNIQUE, GRENOBLE (FRANCE).
Heavy ion tests on programmable VLSI
[ETN-90-97254] N90-26057
Contribution to CMOS integrated circuit tests: Study of the stuck-on and stuck-open fault tests
[ETN-90-97256] N90-26261
Conception of a reconfigurable microprocessor
[ETN-90-97248] N90-26517
Contribution to the definition and application of NAUTILE (A new environment for the conception and assembling of integrated circuits)
[ETN-90-97251] N90-26554
Parallel algorithm for distributed memory computers (applications to matricial algorithms)
[ETN-90-97252] N90-26573
Multilayered neural networks: Learning algorithms, implementation on hypercube machines, applications
[ETN-90-97255] N90-26574
Massively parallel architecture: Integrated cell network for image reconstruction
[ETN-90-97257] N90-26575
Multi-sensory perception of a geometrical structure of a scene
[ETN-90-97245] N90-26587
Verification-correction of a program for including uncertainties in the robot automatic programming
[ETN-90-97246] N90-26588
Application of artificial intelligence to the architectural synthesis of VLSI integrated circuits
[ETN-90-97253] N90-26589
Unification and disunification: Theory and applications
[ETN-90-97247] N90-26610
Generation and improvement of meshes for finite elements methods in two and three dimensions
[ETN-90-97249] N90-26611
Contribution to the study of differential equations and to the differences in the complex field
[ETN-90-97250] N90-26612

INSTITUTE FOR COMPUTER APPLICATIONS IN SCIENCE AND ENGINEERING, HAMPTON, VA.
A critical evaluation of two-equation models for near wall turbulence
[NASA-CR-182068] N90-26270
Run-time parallelization and scheduling of loops
[NASA-CR-182039] N90-26509
Research conducted at the Institute for Computer Applications in Science and Engineering in applied mathematics, numerical analysis, and computer science
[NASA-CR-182057] N90-26510
The use of Lanczo's method to solve the large generalized symmetric Eigenvalue problem in parallel
[NASA-CR-182072] N90-26533
On central-difference and upwind schemes
[NASA-CR-182061] N90-26595

INSTITUTE FOR SPACE AND TERRESTRIAL SCIENCE, YORK (ONTARIO).
High resolution, low temperature photoabsorption cross-section of C2H2 with application to Saturn's atmosphere N90-26757

INSTITUTE FOR TELECOMMUNICATION SCIENCES, BOULDER, CO.
Progress and remaining issues in the development of a wideband HF channel model and simulation N90-26182

INSTITUTET FOER VATTEN-OCH LUFTVAARDSFORSKNING, GOETEBORG (SWEDEN).
Further development and application of an atmospheric chemistry trajectory model N90-26408
Results from the IVL TOR Station at Roervik, Sweden. A contribution to the EURATRAC subproject TOR N90-26415

INSTITUTO DE PESQUISAS ESPACIAIS, SAO JOSE DOS CAMPOS (BRAZIL).
Pattern classification of textura by moment and distance autocorrelation function
[INPE-4976-PRE/1541] N90-26379
Hierarchical structure of polygonal data for spatial analysis and representation of cartographical data
[INPE-4986-PRE/1548] N90-26380
Classification regions in remote sensing imagery utilizing spatial characteristics
[INPE-4913-PRE/1514] N90-26381

INTERNATIONAL INST. OF SPACE LAW, EH BAARN (NETHERLANDS).
Human work in space: The astronaut's legal status. Introduction N90-26719

IOWA STATE UNIV. OF SCIENCE AND TECHNOLOGY, AMES.
Searching for heavy fermion materials in Ce intermetallic compounds
[DE90-011809] N90-26116
High temperature x ray diffraction and Landau theory investigations of order-disorder transition in defect NaCl-type solids
[DE90-011807] N90-26673

IOWA UNIV., IOWA CITY.
The finite analytic method and its applications. Volume 1: Laminar and turbulent flows past two-dimensional and axisymmetric bodies
[AD-A222787] N90-26294

J

JACKSON STATE UNIV., MS.
Electrochemical, in situ Raman spectroscopic, and conductivity studies of polypyrrole incorporating large size anions: Conducting nature of reduced form
[AD-A222739] N90-26102

JET PROPULSION LAB., CALIFORNIA INST. OF TECH., PASADENA.
Regenerative Cu La zeolite supported desulfurizing sorbents
[NASA-CASE-NPO-17480-1-CU] N90-26098
Multicomponent gas sorption Joule-Thomson refrigerator
[NASA-CASE-NPO-17569-1-CU] N90-26176
A novel multireceiver communications system configuration based on optimal estimation theory
[NASA-CR-186847] N90-26216
The Telecommunications and Data Acquisition Report
[NASA-CR-186852] N90-26217
Goldstone intracomplex connected element interferometry N90-26218
A reduced-dynamic technique for precise orbit determination N90-26219
Information content of a single pass of phase-delay data from a short baseline connected element interferometer N90-26220
Applications of different design methodologies in navigation systems and development at JPL N90-26221
Inhomogeneous electric field effects in a linear RF quadruple trap N90-26222
A study of the influence of Hg(6(3)P2) population in a low-pressure discharge on mercury ion emission at 194.2 nm N90-26223
Application of inertial instruments for DSN antenna pointing and tracking N90-26224
Design and performance analysis of the DSS-13 beam waveguide antenna N90-26225
A two-telescope receiver design for deep space optical communications N90-26226
Preliminary error budget for an optical ranging system: Range, range rate, and differenced range observables N90-26227
Initial results on fault diagnosis of DSN antenna control assemblies using pattern recognition techniques N90-26228
DSS 15, 45, and 65 34-meter high efficiency antenna radio frequency performance enhancement by tilt added to the subreflector during elevation angle changes N90-26229
QPSK loop lock detection in the advanced receiver N90-26230
Long-range planning cost model for support of future space missions by the deep space network N90-26231
Rings of Earth detected by orbital debris radar N90-26232
Fluid-loop reaction system
[NASA-CASE-NPO-17204-1-CU] N90-26292
Direct drive robotic hand
[NASA-CASE-NPO-17917-1-CU] N90-26339
Improving the geometric fidelity of imaging systems employing sensor arrays
[NASA-CASE-NPO-17970-1-CU] N90-26384
Self-checking on-line testable static RAM
[NASA-CASE-NPO-17939-1-CU] N90-26518
High speed magneto-resistive random access memory
[NASA-CASE-NPO-17954-1-CU] N90-26519
Passivation of high temperature superconductors
[NASA-CASE-NPO-17949-1-CU] N90-26684
MBE growth technology for high quality strained III-V layers
[NASA-CASE-NPO-17723-1-CU] N90-26685
The browse file of NASA/JPL quick-look radar images from the Loch Linnhe 1989 experiment
[NASA-CR-186855] N90-26701
Creating a VAPEPS database: A VAPEPS tutorial
[NASA-CR-186629] N90-26705
High resolution spectroscopy in the microwave and far infrared N90-26746
Electron-impact spectroscopy N90-26779

K

KANSAS STATE UNIV., MANHATTAN.
Automation of closed environments in space for human comfort and safety
[NASA-CR-186834] N90-26500
KANSAS UNIV. CENTER FOR RESEARCH, INC., LAWRENCE.
Identification of aerodynamic models for maneuvering aircraft
[NASA-CR-186630] N90-25943
KRUG INTERNATIONAL, SAN ANTONIO, TX.
Aircrew life support systems enhancement
[AD-A222626] N90-26505
KUOPIO UNIV. (FINLAND).
Measurements of monoterpenes in a coniferous forest N90-26421

L

LABORATOIRE D'AUTOMATIQUE ET D'ANALYSE DES SYSTEMES, TOULOUSE (FRANCE).
Formal verification of distributed computing systems: Logic characterization of behaviour equivalence
[LAAS-89386] N90-26555
Rapid thermal processing: A study of the silicon oxidation and of the implanted boron activation
[LAAS-90051] N90-26681
LABORATOIRE D'ETUDE DES TRANSMISSIONS IONOSPHERIQUES, CACHAN (FRANCE).
Optimal synchronization of spread spectrum sequenced by nontransferable switching operators N90-26183
Minimization of the cost of information transfer in HF spread spectrum transmission N90-26198
LANCHESTER POLYTECHNIC, COVENTRY (ENGLAND).
The 5th International symposium on palaeolimnology
[AD-A219244] N90-26431
LAWRENCE LIVERMORE NATIONAL LAB., CA.
The origin of poorly conditioned susceptibility matrix within inverse CVM algorithm in the case of Pd(sub 3)V: A comparison to the case of Ni(sub 3)V
[DE90-012464] N90-26110
Densification studies of refractory materials using Hot Isostatic Pressing (HIP) and tantalum containment
[DE90-013481] N90-26114
Multiple target tracking in a wide-field-of-view camera system
[DE90-013488] N90-26300
OASIS, LLNL version: Software maintenance manual
[DE90-013522] N90-26313
Damage measurements on optical materials for use in high-peak-power lasers
[DE90-013489] N90-26314
Laser damage database at 1064 nm
[DE90-013490] N90-26315
Computer animation in mathematics, science, and art
[DE90-013051] N90-26538
ASATs vs Brilliant Pebbles
[DE90-010348] N90-26626
Radio loud far-infrared galaxies
[DE90-012993] N90-26786
A site for the astrophysical gamma ray process
[DE90-013473] N90-26787
LOCKHEED MISSILES AND SPACE CO., PALO ALTO, CA.
Viking data analysis
[AD-A222609] N90-26062
LONGHORN SATELLITE CO., AUSTIN, TX.
Texstar: The all-Texas educational satellite system
[NASA-CR-186654] N90-26045
LOS ALAMOS NATIONAL LAB., NM.
Texture of materials by time-of-flight neutron diffraction
[DE90-008968] N90-26096
Formation of Titanium-boron surface alloys by excimer laser mixing
[DE90-013172] N90-26118
Characterization of a high-intensity, subpicosecond XeCl laser system
[DE90-011970] N90-26310
Important experiments to test for longer-ranged new gravitational forces
[DE90-012102] N90-26434
A study of positrons from Soviet nuclear powered satellites as tracers for magnetospheric research
[DE90-013157] N90-26438
On the nature of the plasma sheet boundary layer
[DE90-013158] N90-26439
An angular weighting approach for calculating gradients and divergences
[DE90-013164] N90-26539
On traveling wave solutions of a set of coupled Boussinesq-like equations
[DE90-013182] N90-26597
Thermal management of an accelerator system in space
[DE90-013153] N90-26627
Confinement of nonneutral plasma in unconventional geometries
[DE90-013048] N90-26659
Experiments on superconductor imaging surface magnetometry
[DE90-008925] N90-26665
A lattice gas model for thermohydrodynamics
[DE90-011964] N90-26690
Astronomy at ultra-high energies: Results from the CYGNUS experiment
[DE90-011979] N90-26732
LOUGHBOROUGH UNIV. OF TECHNOLOGY (ENGLAND).
An investigation of the use of singular perturbation methods and modal control theory in the derivation or aircraft control schemes
[MATHS-REPT-A-106] N90-26014
Frontogenesis in gravity currents: An example with no known applications in oceanography
[MATHS-REPT-A-117] N90-26284
On controller choice for robust sliding mode performance
[MATHS-REPT-A-107] N90-26337
Efficient generalized conjugate gradient algorithms. Part 2: Implementation
[MATHS-REPT-A-118-PT-2] N90-26543
On output deadbeat control of discrete-time multivariable systems
[MATHS-REPT-A-122] N90-26583
G2-continuity in homogeneous co-ordinates
[MATHS-REPT-A-110] N90-26599
The system matrix characterisation of input-output equivalence
[MATHS-REPT-A-112] N90-26600
Rational cubics with G2-continuity
[MATHS-REPT-A-113] N90-26601
A new class of exact solutions of the vacuum quadratic Poincare gauge field theory
[MATHS-REPT-A-119] N90-26691
On trivector torsion in vacuum quadratic Poincare gauge field theory
[MATHS-REPT-A-121] N90-26692
LOUISVILLE UNIV., KY.
Experiment K-6-08. Biochemical and histochemical observations of vastus medialis N90-26462
LUNAR AND PLANETARY INST., HOUSTON, TX.
Proceedings of a workshop on Lunar Volcanic Glasses: Scientific and Resource Potential
[NASA-CR-186631] N90-26437
Press abstracts of the 21st Lunar and Planetary Science Conference
[NASA-CR-186874] N90-26738
Proceedings of a Workshop on Antarctic Meteorite Stranding Surfaces
[NASA-CR-186575] N90-26739
Proceedings of a workshop on Differences Between Antarctic and Non-Antarctic Meteorites
[NASA-CR-184918] N90-26740
LUND INST. OF TECH. (SWEDEN).
Vertical ozone probing with lidar N90-26416
LUND UNIV. (SWEDEN).
Characterization of biogenic aerosol particles from the Amazon Basin during dry and wet season N90-26418

M

MANCHESTER COLL. OF SCIENCE AND TECHNOLOGY (ENGLAND).
An experimental medium speed wideband modem N90-26194
MARCONI SECURE RADIO SYSTEMS LTD., PORTSMOUTH (ENGLAND).
New approaches for rapid synchronisation frequency hoppers N90-26201
MARTIN MARIETTA SPACE SYSTEMS, INC., DENVER, CO.
Space station definitions, design, and development. Task 5: Multiple arm telerobot coordination and control: Manipulator design methodology
[NASA-CR-182043] N90-26577
MARYLAND UNIV., COLLEGE PARK.
Project Exodus
[NASA-CR-186836] N90-26026
Terrapin technologies manned Mars mission proposal
[NASA-CR-186838] N90-26027
University of Maryland walking robot: A design project for undergraduate students
[NASA-CR-186839] N90-26331
Development of eye-safe lidar for aerosol measurements
[NASA-CR-186905] N90-26503
Autoplan: A self-processing network model for an extended blocks world planning environment
[NASA-CR-186733] N90-26526
Evaluation of a decomposition approach for real-time scheduling using a Stochastic model
[AD-A222726] N90-26625
MASSACHUSETTS INST. OF TECH., CAMBRIDGE.
Polymeric aluminasilazane precursors for aluminosilicon nitride
[AD-A222755] N90-26158
Laser radar angular tracking
[AD-A222741] N90-26319
Twilight zones and cornerstones: A gnat robot double feature
[AD-A220026] N90-26326

Remote sensing of Earth terrain
[NASA-CR-186888] N90-26382
Formation and deactivation of vibrationally excited atmospheric molecules
[AD-A222660] N90-26442
Atomic snapshots of shared memory
[AD-A222765] N90-26520
Stibathiolanes: Synthesis, solid state structure, and solution behavior
[AD-A223255] N90-26688
Effect of organizational structure on performance of decision making teams
[AD-A223160] N90-26697
Analysis of random drop for gateway congestion control
[NASA-CR-186736] N90-26696
Determination of molecular spectroscopic parameters and energy-transfer rates by double-resonance spectroscopy N90-26755

MASSACHUSETTS TECHNOLOGICAL LAB., INC., BETHESDA, MD.
System factors to be considered in assessing propagation effects on modern digital satellite communications systems N90-26208

MASSACHUSETTS UNIV., AMHERST.
High speed all optical networks
[NASA-CR-185311] N90-26649

MAX-PLANCK-INST. FOR FOREIGN AND INTERNATIONAL PATENT, COPYRIGHT AND COMPETITION LAW, MUNICH (GERMANY, F.R.).
Production activities in space: The problems of protection N90-26725

MAX-PLANCK-INST. FUER CHEMIE, MAINZ (GERMANY, F.R.).
The applications of chemical thermodynamics and chemical kinetics to planetary atmospheres research N90-26773

MCAT INST., MOFFETT FIELD, CA.
Supersonic wind tunnel nozzles: A selected, annotated bibliography to aid in the development of quiet wind tunnel technology
[NASA-CR-4294] N90-26019

MCR TECHNOLOGY, INC., GOLETA, CA.
An expert system based software sizing tool, phase 2
[NASA-CR-186706] N90-26525

MEDICAL COLL. OF WISCONSIN, MILWAUKEE.
Effects of microgravity on rat muscle N90-26453
Experiment K-6-09. Morphological and biochemical investigation of microgravity-induced nerve and muscle breakdown. Part 1: Investigation of nerve and muscle breakdown during spaceflight; Part 2: Biochemical analysis of EDL and PLT muscles N90-26463

MICHIGAN UNIV., ANN ARBOR.
Adaptive fault-tolerant routing in hypercube multicomputers
[NASA-CR-186781] N90-26513

MIDWEST RESEARCH INST., GOLDEN, CO.
Interim qualification tests and procedures for terrestrial photovoltaic thin-film flat-plate modules
[DE90-000354] N90-26392

MINISTERE DES AFFAIRES EXTERIEURES DU CANADA, OTTAWA (ONTARIO).
Crossborder movements: Goods, personnel and technologies N90-26722

MINNESOTA UNIV., MINNEAPOLIS.
Winged cargo return vehicle. Volume 1: Conceptual design
[NASA-CR-186823] N90-26050
Biconic cargo return vehicle with an advanced recovery system. Volume 1: Conceptual design
[NASA-CR-186520] N90-26052

MISSISSIPPI UNIV., UNIVERSITY.
The US/International Space Station: Legal aspects of space objects and jurisdiction and control N90-26713

MISSOURI UNIV., ROLLA.
Dynamics of micellar oligomeric and monomeric sodium 10-undecanoate
[AD-A222570] N90-26099

MISSOURI UNIV., SAINT LOUIS.
Methane overtone absorption by intracavity laser spectroscopy N90-26762

MITRE CORP., MCLEAN, VA.
Integrated support structure
[NASA-CR-186835] N90-26162

MONTANA STATE UNIV., BOZEMAN.
NMR and optical studies of piezoelectric polymers
[DE90-012459] N90-26137

MORGANTOWN TECHNOLOGY CENTER, WV.
Heat engines
[DE90-000485] N90-26393

N

NATIONAL AERONAUTICAL LAB., BANGALORE (INDIA).
Flight testing of a natural laminar flow airfoil using gliders
[PD-CF-9005] N90-25936
Model following control system design: Preliminary ATTAS in-flight simulation test results
[PD-FC-9003] N90-26010
Pressure dependence of thermoelectric power of high T(sub c) 123 compound
[PD-MT-9001] N90-26092
Computer aided handling qualities evaluation in frequency domain
[NAL-TM-SE-8902] N90-26523

NATIONAL AERONAUTICS AND SPACE ADMINISTRATION, WASHINGTON, DC.
Space Transportation Avionics Technology Symposium. Volume 1: Executive summary
[NASA-CP-3081] N90-25980
Technology for large space systems: A bibliography with indexes (supplement 22)
[NASA-SP-7046(22)] N90-26056
NASA Patent Abstracts Bibliography: A continuing bibliography. Section 2: Indexes (supplement 37)
[NASA-SP-7039(37)-SECT-2] N90-26700
Reports of planetary astronomy, 1990
[NASA-TM-4205] N90-26730
Directory of research projects: Planetary geology and geophysics program
[NASA-TM-4211] N90-26743

NATIONAL AERONAUTICS AND SPACE ADMINISTRATION. AMES RESEARCH CENTER, MOFFETT FIELD, CA.
Research at NASA's NFAC wind tunnels
[NASA-TM-102827] N90-25933
A brief review of some mechanisms causing boundary layer transition at high speeds
[NASA-TM-102834] N90-25945
Synthesis of individual rotor blade control system for gust alleviation
[NASA-TM-101886] N90-25972
Natural melting within a spherical shell
[NASA-TM-102822] N90-26274
The US Experiments Flown on the Soviet Biosatellite Cosmos 1887
[NASA-TM-102254] N90-26452
Experiment K-6-01. Distribution and biochemistry of mineral and matrix in the femurs of rats N90-26455
Experiment K-6-02. Biomedical, biochemical and morphological alterations of muscle and dense, fibrous connective tissues during 14 days of spaceflight N90-26456
Experiment K-6-03. Gravity and skeletal growth, part 1. Part 2: Morphology and histochemistry of bone cells and vasculature of the tibia; Part 3: Nuclear volume analysis of osteoblast histogenesis in periodontal ligament cells; Part 4: Intervertebral disc swelling pressure associated with microgravity N90-26457
Experiment K-6-12. Morphometric studies of atrial or granules and hepatocytes. Part 1: Morphometric study of the liver; Part 2: The atrial granular accumulations N90-26466
Experiment K-6-13. Morphological and biochemical examination of heart tissue. Part 1: Effects of microgravity on the myocardial fine structure of rats flown on Cosmos 1887. Ultrastructure studies. Part 2: Cellular distribution of cyclic ampdependent protein kinase regulatory subunits in heart muscle of rats flown on Cosmos 1887 N90-26467
Experiment K-6-16. Morphological examination of rat testes. The effect of Cosmos 1887 flight on spermatogonial population and testosterone level in rat testes N90-26469
Experiment K-6-18. Study of muscarinic and gaba (benzodiazepine) receptors in the sensory-motor cortex, hippcampus and spinal code N90-26471
Experiment K-6-20. The effect of spaceflight on pituitary oxytocin and vasopressin content of rats N90-26473
Experiment K-6-22. Growth hormone regulation, synthesis and secretion in microgravity. Part 1: Somatotroph physiology. Part 2: Immunohistochemical analysis of hypothalamic hormones. Part 3: Plasma analysis N90-26475
Experiment K-6-23. Effect of spaceflight on levels and function of immune cells N90-26476
ISIS and META projects
[NASA-CR-186645] N90-26524
Recent high resolution laboratory determinations of line broadening and intensity parameters: PH3, CH3D, and CO2 N90-26751
Gaussian quadrature exponential sum modeling of near infrared methane laboratory spectra obtained at temperatures from 106 to 297 K N90-26758
Optical constants of solid methane N90-26775

NATIONAL AERONAUTICS AND SPACE ADMINISTRATION. GODDARD SPACE FLIGHT CENTER, GREENBELT, MD.
First International Conference on Laboratory Research for Planetary Atmospheres
[NASA-CP-3077] N90-26744
High resolution infrared spectroscopy of planetary molecules using diode lasers and Fourier transform spectrometers N90-26747
Measurements of the methane relaxation times for application to the infrared emission models of the upper atmospheres of outer planets and Titan N90-26759
Intracavity Dye-Laser Absorption Spectroscopy (IDLAS) for application to planetary molecules N90-26761
Rate constant for reaction of atomic hydrogen with germane N90-26768
Role of the methylene amidogen (H2CN) radical in the atmospheres of Titan and Jupiter N90-26769
Laboratory measurements and methane photochemistry modeling N90-26770
Vapor pressures of acetylene at low temperatures N90-26777
Study of the polyoxymethylene and its sputtered fragments: Implications for comets N90-26781

NATIONAL AERONAUTICS AND SPACE ADMINISTRATION. HUGH L. DRYDEN FLIGHT RESEARCH FACILITY, EDWARDS, CA.
An in-flight interaction of the X-29A canard and flight control system
[NASA-TM-101718] N90-25973
An automated calibration laboratory for flight research instrumentation: Requirements and a proposed design approach
[NASA-TM-101719] N90-26564

NATIONAL AERONAUTICS AND SPACE ADMINISTRATION. JOHN F. KENNEDY SPACE CENTER, COCOA BEACH, FL.
Debris/ice/TPS assessment and photographic analysis for shuttle mission STS-31R
[NASA-TM-102790] N90-26040
Proximate composition of seed and biomass from soybean plants grown at different carbon monoxide (CO2) concentrations
[NASA-TM-103496] N90-26480
Hemodynamic and ADH responses to central blood volume shifts in cardiac-denervated humans
[NASA-TM-103471] N90-26485

NATIONAL AERONAUTICS AND SPACE ADMINISTRATION. LYNDON B. JOHNSON SPACE CENTER, HOUSTON, TX.
Methods and apparatus for providing real-time control of a gaseous propellant rocket propulsion system
[NASA-CASE-MSC-21542-1] N90-26073
Power saw
[NASA-CASE-MSC-21469-1] N90-26340
Alignment positioning mechanism
[NASA-CASE-MSC-21502-1] N90-26341
Bidirectional drive and brake mechanism
[NASA-CASE-MSC-21540-1] N90-26342

NATIONAL AERONAUTICS AND SPACE ADMINISTRATION. LANGLEY RESEARCH CENTER, HAMPTON, VA.
Effect of tail size reductions on longitudinal aerodynamic characteristics of a three surface F-15 model with nonaxisymmetric nozzles
[NASA-TP-3036] N90-25938
An overview of the joint FAA/NASA aircraft/ground runway friction program
[NASA-TM-103486] N90-25957
Qualitative evaluation of a conformal velocity vector display for use at high angles-of-attack in fighter aircraft
[NASA-TM-102629] N90-25981
Supersonic combustor modeling N90-25992
Orbiter utilization as an ACRV
[NASA-TM-102700] N90-26032
The effect of interplanetary trajectory options on a manned Mars aerobrake configuration
[NASA-TP-3019] N90-26036
Proceedings of the LDEF Materials Data Analysis Workshop
[NASA-CP-10046] N90-26075
Strain energy release rate analysis of delamination in a tapered laminate subjected to tension load
[NASA-TM-102592] N90-26076
Buckling and postbuckling behavior of square compression-loaded graphite-epoxy plates with circular cutouts
[NASA-TP-3007] N90-26077
Carbon-carbon composites: Emerging materials for hypersonic flight
[NASA-TM-103472] N90-26080
The influence of microstructure on the tensile behavior of an aluminum metal matrix composite
[NASA-TM-102694] N90-26082

Damage states in laminated composite three-point bend specimens: An experimental-analytical correlation study
[NASA-TM-101800] N90-26083
Supersonic reacting internal flow fields
[NASA-TM-103480] N90-26094
Condensation polyimides
[NASA-TM-103467] N90-26129
Fracture toughness of polyimide films
[NASA-TM-103473] N90-26130
Characterization of a thermally imidized soluble polyimide film
[NASA-TM-103484] N90-26131
Simulated dynamic response of a servovalve controlled hydraulic actuator
[NASA-TM-101644] N90-26167
A new technique in the global reliability of cyclic communications network
[NASA-TM-103479] N90-26214
Video camera system for locating bullet holes in targets at a ballistics tunnel
[NASA-TM-4197] N90-26296
The effects of pretreatment conditions on a Pt/SnO2 catalyst for the oxidation of CO in CO2 lasers
[NASA-TM-103487] N90-26309
Structural Mechanics Division research and technology plans for FY 1990 and accomplishments for FY 1989
[NASA-TM-102654] N90-26361
Intergration of system identification and robust controller designs for flexible structures in space
[NASA-TM-102695] N90-26362
Scaling effects in the static and dynamic response of graphite-epoxy beam-columns
[NASA-TM-102697] N90-26363
Measurements of tropospheric nitric acid over the Western United States and Northeastern Pacific Ocean
[NASA-TM-103470] N90-26399
Measurements of CH4, N2O, CO, H2O and O3 in the middle atmosphere by the ATMOS experiment on Spacelab 3
[NASA-TM-103476] N90-26400
The global consequences of increasing tropospheric ozone concentrations
[NASA-TM-103477] N90-26401
New observations of stratospheric N2O5
[NASA-TM-103478] N90-26402
Annual and interannual variations of Earth-emitted radiation based on a 10-year data set
[NASA-TM-103465] N90-26432
Earth Radiation Budget Experiment (ERBE) validation
[NASA-TM-103481] N90-26433
The 27-28 October 1986 FIRE IFO Cirrus case study: Comparison of radiative transfer theory with observations by satellite and aircraft
[NASA-TM-103468] N90-26446
The 27-28 October 1986 FIRE IFO cirrus case study: Cirrus parameter relationships derived from satellite and lidar data
[NASA-TM-103469] N90-26447
Knowledge-based system for flight information management
[NASA-TM-102685] N90-26511
A closed form solution to HZE propagation
[NASA-TM-103482] N90-26640
Optical transmission through a polarization preserving single mode optical fiber at two Ar(+) laser wavelengths
[NASA-TM-103475] N90-26651
Grammar, punctuation, and capitalization: A handbook for technical writers and editors
[NASA-SP-7084] N90-26710

NATIONAL AERONAUTICS AND SPACE ADMINISTRATION. LEWIS RESEARCH CENTER, CLEVELAND, OH.

Euler analysis comparison with LDV data for an advanced counter-rotation propfan at cruise
[NASA-TM-103249] N90-25946
Two-dimensional Euler and Navier-Stokes Time accurate simulations of fan rotor flows
[NASA-TM-102402] N90-25948
Performance of a supercharged direct-injection stratified-charge rotary combustion engine
[NASA-TM-103105] N90-25982
Hot gas ingestion characteristics and flow visualization of a vectored thrust STOVL concept
[NASA-TM-103212] N90-26009
H-infinity based integrated flight-propulsion control design for a STOVL aircraft in transition flight
[NASA-TM-103198] N90-26011
National space test centers, Lewis research center facilities
[NASA-TM-103187] N90-26030
Comparison of currents predicted by NASCAP/LEO model simulations with elementary Langmuir-type bare probe models for an insulated cable containing a single pinhole
[NASA-TM-102486] N90-26054
Background, current status, and prognosis of the ongoing slush hydrogen technology development program for the NASP
[NASA-TM-103220] N90-26055
Mars in situ propellants: Carbon monoxide and oxygen ignition experiments
[NASA-TM-103202] N90-26065
Aeolian removal of dust from radiator surfaces on Mars
[NASA-TM-103205] N90-26068
Estimation of minority carrier diffusion lengths in InP/GaAs solar cells
[NASA-TM-103213] N90-26069
Digital filtering of plume emission spectra
[NASA-TM-103135] N90-26070
Preliminary plume characteristics of an arcjet thruster
[NASA-TM-103241] N90-26071
The chemical effects of the Martian environment on power system component materials: A theoretical approach
[NASA-TM-103203] N90-26074
Determination of the stress distributions in a ceramic: Tensile specimen using numerical techniques
[NASA-TM-101914] N90-26132
Prediction of the ullage gas thermal stratification in a NASP vehicle propellant tank experimental simulation using FLOW-3D
[NASA-TM-103217] N90-26160
New findings and instrumentation from the NASA Lewis microgravity facilities
[NASA-TM-103189] N90-26163
Critical evaluation of Jet-A spray combustion using propane chemical kinetics in gas turbine combustion simulated by KIVA-2
[NASA-TM-103173] N90-26170
Analysis of a Mars-stationary orbiting microwave power transmission system
[NASA-TM-101344] N90-26172
Design of an optically controlled Ka-band GaAs MMIC phased-array antenna
[NASA-TM-103147] N90-26250
Low-gravity fluid physics: A program overview
[NASA-TM-103215] N90-26273
Computational experience with a three-dimensional rotary engine combustion model
[NASA-TM-103104] N90-26275
Galerkin finite difference Laplacian operators on isolated unstructured triangular meshes by linear combinations
[NASA-TM-103209] N90-26276
Initial experimentation on the nonvented fill of a 0.14m3 (5 ft. 3) dewar with nitrogen and hydrogen
[NASA-TM-103155] N90-26278
Two-dimensional model of a Space Station Freedom thermal energy storage canister
[NASA-TM-103124] N90-26279
Calculation of 3D turbulent jets in crossflow with a multigrid method and a second-moment closure model
[NASA-TM-103159] N90-26282
Optical characterization of clouds of fine liquid-nitrogen particles
[NASA-TM-103208] N90-26299
A high-speed photography study of cavitation in a dynamically loaded journal bearing
[NASA-TM-103178] N90-26338
Design of ceramic components with the NASA/CARES computer program
[NASA-TM-102369] N90-26359
Application of symbolic computations to the constitutive modeling of structural materials
[NASA-TM-103225] N90-26364
Structural dynamics branch research and accomplishments
[NASA-TM-102488] N90-26373
Modeling and optimization of a regenerative fuel cell system using the ASPEN process simulator
[NASA-TM-103210] N90-26396
NASA aerospace flight battery systems program
[NASA-TM-103237] N90-26397
Parallel/distributed direct method for solving linear systems
[NASA-TM-103229] N90-26614
Asymptotic analysis of dissipative waves with applications to their numerical simulation
[NASA-TM-103231] N90-26615
Efficient implementation of minimal polynomial and reduced rank extrapolation methods
[NASA-TM-103240] N90-26616
Aeroacoustics of advanced propellers
[NASA-TM-103137] N90-26635
Ellipsometric study of YBa2Cu3O(7-x) laser ablated and co-evaporated films
[NASA-TM-103223] N90-26682
Dielectric function of InGaAs in the visible
[NASA-TM-103246] N90-26683
Launching a dream: A teachers guide to a simulated space shuttle mission
[NASA-TM-89715] N90-26693
Preliminary designs for 25 kWe advanced Stirling conversion systems for dish electric applications
[NASA-TM-103188] N90-26729
The lessons of Varsovian's reconnaissance
[NASA-TM-103207] N90-26789

NATIONAL AERONAUTICS AND SPACE ADMINISTRATION. MARSHALL SPACE FLIGHT CENTER, HUNTSVILLE, AL.

Forbidden tangential orbit transfers between intersecting Keplerian orbits
[NASA-TP-3031] N90-26028
Electrode carrying wire for GTAW welding
[NASA-CASE-MFS-29491-1] N90-26168
Rotating-unbalanced-mass devices and methods for scanning balloon-borne-experiments, free-flying spacecraft, and space shuttle/space station attached experiments
[NASA-CASE-MFS-28425-1] N90-26304
The charged particle radiation environment for AXAF
[NASA-TM-100405] N90-26741
Nonpotential magnetic fields at sites of gamma ray flares
[NASA-TM-103493] N90-26785

NATIONAL AERONAUTICS AND SPACE ADMINISTRATION. PASADENA OFFICE, CA.

Regenerative Cu La zeolite supported desulfurizing sorbents
[NASA-CASE-NPO-17480-1-CU] N90-26098
Multicomponent gas sorption Joule-Thomson refrigerator
[NASA-CASE-NPO-17569-1-CU] N90-26176
Fluid-loop reaction system
[NASA-CASE-NPO-17204-1-CU] N90-26292
Direct drive robotic hand
[NASA-CASE-NPO-17917-1-CU] N90-26339
Improving the geometric fidelity of imaging systems employing sensor arrays
[NASA-CASE-NPO-17970-1-CU] N90-26384
Self-checking on-line testable static RAM
[NASA-CASE-NPO-17939-1-CU] N90-26518
High speed magneto-resistive random access memory
[NASA-CASE-NPO-17954-1-CU] N90-26519
Passivation of high temperature superconductors
[NASA-CASE-NPO-17949-1-CU] N90-26684
MBE growth technology for high quality strained III-V layers
[NASA-CASE-NPO-17723-1-CU] N90-26685

NATIONAL AEROSPACE LAB., AMSTERDAM (NETHERLANDS).

Experimental study on vortex and shock wave development on a 65 deg delta wing
[NLR-MP-88033-U] N90-25950
Computation of viscous aerodynamic characteristics of 2-D airfoils for helicopter applications
[NLR-MP-88052-U] N90-25951
The role of computational fluids dynamics in missile aerodynamics
[NLR-MP-88072-U] N90-25952
Inference and control mechanisms in NEXT 2.0
[NLR-MP-88062-U] N90-26175
Mobile satellite communications for civil aviation
[NLR-MP-88066-U] N90-26238
Development of a system for the numerical simulation of Euler flows, with results of preliminary 3-D propeller-slipstream/exhaust-jet calculations
[NLR-TR-88008-U] N90-26285
Informatics aspects of large flow calculations on the SX-2 supercomputer
[NLR-MP-88037-U] N90-26290
Characterization of inspection performance
[NLR-MP-88068-U] N90-26350
Static and fatigue strength of an adhesive bonded CFRP butt-strap joint: The effects of stacking sequence and temperature
[NLR-TR-88036-U] N90-26370

NATIONAL AEROSPACE LAB., TOKYO (JAPAN).

Space plane model for visual measurement of aerodynamic heating
[DE90-505514] N90-25949
Measurement of velocity and temperature profiles at the exit plane of a tubular gas turbine combustor
[DE90-505519] N90-25983
Decay of secondary flow and the associated loss variation downstream of an annual turbine stator cascade
[DE90-505520] N90-25984
Performance evaluation of LE-7 high pressure pumps
[DE90-505523] N90-26034
Hard start problem of the apogee engine for the ETS-6
[DE90-505525] N90-26072

Probabilistic approach to the certification for fatigue durability of composite structures
[DE90-505521] N90-26085
Study on failure modes of boron fiber reinforced aluminum composite materials by AE method, part 2
[DE90-505522] N90-26086
Research and development of advanced gas turbine
[DE90-503377] N90-26335

NATIONAL INST. OF STANDARDS AND TECHNOLOGY, BOULDER, CO.
Novel laser gain and time-resolved FTIR studies of photochemistry N90-26756

NATIONAL INST. OF STANDARDS AND TECHNOLOGY, GAITHERSBURG, MD.
Infrared spectra of van de Waals complexes of importance in planetary atmospheres N90-26749
Microwave spectra of van der Waals complexes of importance in planetary atmospheres N90-26752
New electronic states of NH and ND observed by resonance enhanced multiphoton ionization spectroscopy N90-26760
A laboratory investigation of the production and properties of molecular and radical species pertinent to planetary atmospheres N90-26766

NATIONAL OCEANOGRAPHIC DATA CENTER, WASHINGTON, DC.
Mariners Weather Log, volume 33, number 2, Spring 1989
[PB90-146836] N90-26443
Mariners Weather Log, volume 33, number 3, Summer 1989
[PB90-146846] N90-26444
Mariners Weather Log, volume 33, number 4, Fall 1989
[PB90-146853] N90-26445

NAVAL OCEAN SYSTEMS CENTER, SAN DIEGO, CA.
Superconcurrent processing: A dynamic approach to heterogeneous parallelism
[AD-A222798] N90-26576
Canonical eigenvalues. Part 1: General theory
[AD-A222812] N90-26617

NAVAL POSTGRADUATE SCHOOL, MONTEREY, CA.
An analysis of requirements for a P-3 windshear training program
[AD-A222577] N90-25960
On the design and analysis of multiple-storage elements
[AD-A223095] N90-26266
Code enhancements and validation of GASP
[NPS-PAPER-44] N90-26277
Effects of 2 Hz imposed bulk flow unsteadiness on laminar-turbulent transition in a straight channel
[AD-A223028] N90-26295
Guidance and control system for an autonomous underwater vehicle
[AD-A222709] N90-26343
Motion sickness, visual displays, and armored vehicle design
[AD-A222678] N90-26506
UEDIT: A full-scale, scrollable APL2 spreadsheet input/output editor
[AD-A222712] N90-26557
Variance reduction for quantile estimates in simulations via nonlinear controls
[AD-A222653] N90-26590
Nonlinear modeling of time series using Multivariate Adaptive Regression Splines (MARS)
[AD-A222710] N90-26623
Reversed residuals in autoregressive time series analysis
[AD-A222711] N90-26624

NAVY EXPERIMENTAL DIVING UNIT, PANAMA CITY, FL.
Arctic cold weather medicine and accidental hypothermia
[AD-A223090] N90-26487

NEBRASKA UNIV., LINCOLN.
Measuring and modeling near-surface reflected and emitted radiation fluxes at the FIFE site
[NASA-CR-180953] N90-26378

NEW ENERGY DEVELOPMENT ORGANIZATION, TOKYO (JAPAN).
Survey of applicability of electric vehicles (EVs) in specific regions such as resorts
[DE90-503592] N90-26336

NEW SOUTH WALES UNIV., KENSINGTON (AUSTRALIA).
Mass spectrometry of poly(methyl methacrylate)s of low molecular weight N90-26091
The interaction of polymeric materials with ceramic surfaces with special reference to the behaviour of bioceramics N90-26127
Computer analysis of chromatographic data N90-26521
PANDA: A distributed multiprocessor operating system N90-26561
Perturbation methods in the theory of waves and bifurcation phenomena N90-26593
Mathematical problem-solving transfer: The effects of cognitive load and attention a schema acquisition and rule automation N90-26594
Mobility studies in multiloop spatial linkages N90-26628

NEW YORK UNIV., NEW YORK.
Figure of merit studies of beam power concepts for advanced space exploration
[NASA-CR-186720] N90-26234

NORTH CAROLINA STATE UNIV., RALEIGH.
Low-speed wind tunnel investigation of the static stability and control characteristics of an advanced turboprop configuration with the propellers placed over the tail
[NASA-CR-186900] N90-26017

NORTH CAROLINA UNIV., CHAPEL HILL.
A real-time optical 3D tracker for head-mounted display systems
[AD-A222747] N90-26508
Dichotomies for certain product measures and stable processes
[AD-A222568] N90-26621
Isothermal compressibility of SPC/E water
[AD-A222723] N90-26643
Structure and dynamics of water at the Pt (111) interface: Molecular dynamics study
[AD-A222628] N90-26687

NORTHWESTERN UNIV., EVANSTON, IL.
Parallel processors and nonlinear structural dynamics algorithms and software
[NASA-CR-186755] N90-26536

NORWEGIAN DEFENCE RESEARCH ESTABLISHMENT, KJELLER.
CORA: A direct sequence spread spectrum radio for voice and data N90-26195
Packet radio network concepts for the Norwegian field army N90-26206
Human performance models
[FFI-90/7002] N90-26502
Documentation of program Tankplot
[FFI-89/7019] N90-26541

NORWEGIAN METEOROLOGICAL INST., BLINDERN.
Verification and improvement of the EMEP model for long-range transport and deposition of pollutants N90-26405

NOTRE DAME UNIV., IN.
The Screem-J4D: A proposal in response to a low Reynolds number station keeping mission
[NASA-CR-186664] N90-25968
A hybrid M-algorithm/sequential decoder for convolutional and trellis codes
[NASA-CR-186863] N90-26528

O

OAK RIDGE GASEOUS DIFFUSION PLANT, TN.
Pacific missile test center information resources management organization (code 0300): The ORACLE client-server and distributed processing architecture
[DE90-013271] N90-26565

OAK RIDGE NATIONAL LAB., TN.
Synthesis of high purity sinterable silicon carbide powder
[DE90-012029] N90-26084
Oxidation and sulfidation of Type 310S stainless steel at elevated temperatures
[DE90-010149] N90-26109
Formation of cubic Ll2 phases from Al3Ti and Al3Zr by transition metal substitutions for Al
[DE90-012288] N90-26117
Tensile strength measurement techniques for structural ceramics
[DE90-012193] N90-26136
Mechanical properties of silica coatings
[DE90-012721] N90-26138
Mechanical properties of coatings and interfaces
[DE90-012726] N90-26139
Influence of thermal conditioning media on Charpy specimen test temperature
[DE90-012784] N90-26360
Automated sensitivity analysis with the Gradient Enhanced Software System (GRESS)
[DE90-011291] N90-26529
Large, orientation-dependent enhancements of critical currents in Y1Ba2Cu3O(7-x) epitaxial thin films: Evidence for intrinsic flux pinning
[DE90-009424] N90-26666
Diffusion-accommodated grain boundary sliding in a polycrystal
[DE90-012727] N90-26668
Crystal growth and deformation behavior of TiAl aluminides
[DE90-012972] N90-26671
The effect of crystal orientation on damage accumulation in chromium-implanted Al2O3
[DE90-012294] N90-26674
International standards for text preparation and interchange
[DE90-011868] N90-26699

OFFICE NATIONAL D'ETUDES ET DE RECHERCHES AEROSPATIALES, PARIS (FRANCE).
Structures and mechanical properties of near-beta titanium alloys TiV10Fe2Al3 and TiV10Cu3Al3
[ONERA-NT-1989-3] N90-26123

OFFICE OF NAVAL RESEARCH, ARLINGTON, VA.
UEDIT: A full-scale, scrollable APL2 spreadsheet input/output editor
[AD-A222712] N90-26557
Nonlinear modeling of time series using Multivariate Adaptive Regression Splines (MARS)
[AD-A222710] N90-26623
Reversed residuals in autoregressive time series analysis
[AD-A222711] N90-26624

OFFICE OF TECHNOLOGY ASSESSMENT, WASHINGTON, DC.
Catching our breath: Next steps for reducing urban ozone
[PB90-130451] N90-26398

OHIO STATE UNIV., COLUMBUS.
Enroute flight planning: The design of cooperative planning systems
[NASA-CR-186797] N90-25964

OLD DOMINION UNIV., NORFOLK, VA.
Guidance and control strategies for aerospace vehicles
[NASA-CR-186878] N90-26013
Analysis and mitigation of numerical dissipation in inviscid and viscid computation of vortex-dominated flows
[NASA-CR-186887] N90-26281
Theoretical studies of solar pumped lasers
[NASA-CR-186712] N90-26308
SDIO/IST ultrashort wavelength laser: Novel experimental schemes for observing the Moessbauer effect in long-lived nuclear levels and nuclear coherent states
[AD-A222607] N90-26316
Design of an autonomous Lunar construction utility vehicle
[NASA-CR-186832] N90-26330
Investigation of automated task learning, decomposition and scheduling
[NASA-CR-186791] N90-26488
ATAMM multicomputer operating system functional specification
[NASA-CR-186845] N90-26563
Application of the results of carbon pellet modeling to the problem of plasma penetration
[DE90-012713] N90-26658

ORGANISATIE VOOR TOEGEPAST NATUURWETENSCHAPPELIJK ONDERZOEK, THE HAGUE (NETHERLANDS).
Man-made noise in a military environment N90-26191

OSLO UNIV. (NORWAY).
Stratospheric chemistry N90-26424

P

PACIFIC NORTHWEST LAB., RICHLAND, WA.
VISTA (Vertical Integration of Science, Technology, and Applications) user interface software study
[DE90-010003] N90-26707

PARIS UNIV. (FRANCE).
The International Space Station: Conditions of access and use N90-26718

PENNSYLVANIA STATE UNIV., UNIVERSITY PARK.
Preliminary subsystem designs for the Assured Crew Return Vehicle (ACRV), volume 1
[NASA-CR-186677-VOL-1] N90-26039
Twin boundaries, interfaces and modulated structures in martensites
[DE90-012899] N90-26111

PENNSYLVANIA UNIV., PHILADELPHIA.
The variably trimmed mean CFAR detector for nonhomogeneous background
[AD-A222801] N90-26243
Assembly via disassembly: A case in machine perceptual development
[NASA-CR-186867] N90-26497
Grasping with mechanical intelligence
[NASA-CR-186864] N90-26498

PITTSBURGH UNIV., PA.
Dissociative recombination of molecular ions with electrons N90-26767

POLYTECHNIC INST. OF NEW YORK, BROOKLYN.
Full vector wave calculation of photonic band structures in face-centered cubic dielectric media
[AD-A222616] N90-26686

PRINCETON UNIV., NJ.
Spatial cross-correlation of Antarctic Sea ice and seabed topography
[NASA-CR-186815] N90-26451
Comment on high resolution simulations of cosmic strings. 1: Network evoloution
[NASA-CR-186606] N90-26734

PUERTO RICO UNIV., RIO PIEDRAS.
Structured electrode interfaces
[AD-A222763] N90-26265
Exact results for the structured liquid-solid interface
[AD-A222762] N90-26630

PURDUE UNIV., WEST LAFAYETTE, IN.
An unsteady lifting surface method for single rotation propellers
[NASA-CR-4302] N90-25940
Dynamical solvent effects on electron-transfer processes: Recent progress and perspectives
[AD-A222603] N90-26101
HIRIS performance study
[NASA-CR-186649] N90-26375
Modeling, simulation, and analysis of optical remote sensing systems
[NASA-CR-186648] N90-26376
Ionic atmosphere effects on the energetics of thermal and optical electron-exchange reactions: Application to ferrocenium-ferrocene self exchange
[AD-A222605] N90-26441
Graphics applications utilizing parallel processing
[NASA-CR-186719] N90-26534

R

REDIFFUSION RADIO SYSTEMS LTD., CRAWLEY (ENGLAND).
HF spread spectrum, an audit of the power requirements and LPI vulnerability N90-26203

RESEARCH INST. FOR ADVANCED COMPUTER SCIENCE, MOFFETT FIELD, CA.
Capacity for patterns and sequences in Kanerva's SDM as compared to other associative memory models
[NASA-CR-180701] N90-26522

RESEARCH INST. OF NATIONAL DEFENCE, STOCKHOLM (SWEDEN).
Renewed aging control of adhesion of inhibitor on the gas generator charges for RB 24
[FOA-C-20780-2.1] N90-26153
A search routine for optimization in a wind power system with variable speed
[FOA-C-20779-2.1] N90-26395

RESEARCH TRIANGLE INST., RESEARCH TRIANGLE PARK, NC.
Software requirements: Guidance and control software development specification
[NASA-CR-182058] N90-26527

REYNOLDS ELECTRICAL AND ENGINEERING CO., INC., LAS VEGAS, NV.
Estimating the parameters of a sporadically observed queue
[DE90-012903] N90-26596

RICE UNIV., HOUSTON, TX.
Causal distributed breakpoints
[AD-A222613] N90-26622

ROCHESTER UNIV., NY.
DURIP: Instrumentation for laser switched power LINAC
[AD-A222629] N90-26318

ROCKWELL INTERNATIONAL CORP., CANOGA PARK, CA.
Reusable rocket engine turbopump health monitoring system, part 3
[NASA-CR-182294] N90-26320
The structural dynamics analysis of the main injector LOX inlet tee and its redesign
[NASA-CR-186764] N90-26358

ROLLS-ROYCE LTD., DERBY (ENGLAND).
Stage 2 re-engining: The only way to achieve a real stage 3 aircraft
[PNR90636] N90-25977
Application of high performance metals in gas turbine engines
[PNR90640] N90-25999
Towards 2000: The composite engine
[PNR90646] N90-26000
Prediction of rotating disc flow and heat transfer in gas turbine engines
[PNR90650] N90-26001
Prediction and measurement of rotor blade/stator vane dynamic characteristics of a modern aero-engine axial compressor
[PNR90667] N90-26002
The impact and requirements of new materials on aeroengines
[PNR90671] N90-26003
Aircraft exhaust emissions: An engine manufacturer's perspective
[PNR90675] N90-26004
The application of engineering ceramics in gas turbines
[PNR90676] N90-26005
Metal matrix composites and powder processing for aero-engine applications
[PNR90617] N90-26087
Microstructural design for fatigue crack growth resistance in Ni-base alloy
[PNR90632] N90-26120
Understanding silica binders
[PNR90625] N90-26150
Manufacturing control: A basis for analysis
[PNR90639] N90-26174
A numerical simulation of the quasi-heterodyne technique for double-pulsed holographic vibration measurements
[PNR90622] N90-26301
Practical developments in holographic interferometry
[PNR90669] N90-26302
Holography and holographic interferometry
[PNR90670] N90-26303
NDT in aerospace: The next decade (1990's)
[PNR90628] N90-26348
The role of NDI in the certification of turbine engine components
[PNR90629] N90-26349
Fatigue life assessment using a short crack growth model
[PNR90663] N90-26367
Material selection and design: An expert system approach
[PNR90611] N90-26544
Bringing aircraft noise testing down to Earth
[PNR90642] N90-26637
Coherent optical techniques for industrial inspection
[PNR90605] N90-26654
Making it happen: Project management
[PNR90618] N90-26695
The value of real experience
[PNR90619] N90-26696
Prototyping an in-house business intelligence database
[PNR90665] N90-26709

ROME AIR DEVELOPMENT CENTER, GRIFFISS AFB, NY.
ATN design tool
[AD-A223030] N90-26559

ROUEN UNIV. (FRANCE).
Turbulent combustion modeling for turbo-jet combustion chambers N90-25993

ROUSSEL-UCLAF, PARIS (FRANCE).
Space manufacture: Protection and valuation of innovations from a users point of view N90-26724

ROYAL AEROSPACE ESTABLISHMENT, FARNBOROUGH (ENGLAND).
Formation of design envelope criterion in terms of deterministic spectral procedure
[RAE-TM-SS-9] N90-25953
Handbook of uncertainty methodology for engine testing at Pyestock (England)
[RAE-TM-P-1179] N90-26007
Small crack growth and its influence in near alpha-titanium alloys
[RAE-TM-P-1171] N90-26121
High temperature multiaxiale creep testing of Nimonic 115
[RAE-TM-P-1182] N90-26122
Computational fluid dynamics for missiles
[RAE-TM-AERO-2171] N90-26288
Sensitivity analysis with a simple charging code
[RAE-TM-SPACE-374] N90-26662

ROYAL SIGNALS AND RADAR ESTABLISHMENT, MALVERN (ENGLAND).
The rationale and specification of the ELLA graphics systems
[RSRE-89017] N90-26548
A sum rule satisfied by optimized feed-forward layered networks
[RSRE-MEMO-4341] N90-26579
On networks, optimized feature extraction, and the Bayes decision
[RSRE-MEMO-4342] N90-26580

S

SAN FRANCISCO UNIV., CA.
Experiment K-6-24, K-6-25, K-6-26. Radiation dosimetry and spectrometry N90-26477
Experiment K-6-27. Analysis of radiographs and biosamples from primate studies N90-26478

SAN JOSE STATE UNIV., CA.
Experiment K-6-19. Pineal physiology in microgravity: Relation to rat gonadal function N90-26472

SANDIA NATIONAL LABS., ALBUQUERQUE, NM.
Wind tunnel study of wake downwash behind A 6 percent scale model B1-B aircraft
[DE90-011783] N90-25941
Guidance and targeting for the strategic target system
[DE90-005239] N90-26031
The EISI (Elemental and Interplanar Spacing Index) index: A search/match tool for electron diffraction phase analysis
[DE90-010832] N90-26097
Wear mechanisms of amorphous carbon and zirconia coatings on rigid disk magnetic recording media
[DE90-011053] N90-26133
Evolution of structure and viscoelasticity in diethanolamine-cured epoxy
[DE90-011256] N90-26134
Resistivity, adhesive strength, and residual stress measurements of thin film metallizations on single crystal quartz
[DE90-011902] N90-26135
Quantitative confirmation of diffusion-limited oxidation theories
[DE90-012997] N90-26143
Fractal structure and fractal time in silica sol-gels
[DE90-013197] N90-26144
Short-range structure of fluorine-modified phosphate glass
[DE90-013494] N90-26145
One-dimensional sigma-conjugated polysilylenes: Science and technology
[DE90-012902] N90-26146
The development and characterization of ion exchange membranes for selected electrochemical power sources
[DE90-009741] N90-26251
Laser techniques for studying chemical vapor deposition
[DE90-012921] N90-26311
Silicon concentrator solar cell development
[DE90-011782] N90-26386
Dendritic web silicon photovoltaic cell research
[DE90-011786] N90-26387
Application of InAlAs/GaAs superlattice alloys to GaAs solar cells
[DE90-013070] N90-26389
SUPES version 2.1: A Software Utilities Package for the Engineering Sciences
[DE90-011763] N90-26531
Soft x ray resist characterization: Studies with a laser plasma x ray source
[DE90-013493] N90-26661
Molecular dynamics simulations of grain-boundary diffusion for varying tilt angle geometries
[DE90-012919] N90-26669

SANDIA NATIONAL LABS., LIVERMORE, CA.
Compendium of material test results on HY-130 and Ti-3Al2V metals in support of United States navy programs
[DE90-011754] N90-26112
ANTIPASTO: An interactive mesh generator and preprocessor for two-dimensional analysis programs
[DE90-011755] N90-26530

SAO PAULO UNIV. (BRAZIL).
Characterization of NbTi multifilamentary superconducting wires
[DE90-626245] N90-26672

SCHOOL OF AEROSPACE MEDICINE, BROOKS AFB, TX.
Computer modeling wave propagation with a variation of the Helmholtz-Kirchhoff relation
[AD-A222746] N90-26657

SCIENCE RESEARCH LAB., INC., SOMERVILLE, MA.
New discharge pumping method for CO2 lasers
[AD-A220898] N90-26307

SCRIPPS INSTITUTION OF OCEANOGRAPHY, LA JOLLA, CA.
Absolute measurements of gravity
[AD-A222731] N90-26629

SOCIETE BERTIN ET CIE, PLAISIR (FRANCE).
A dual-wavelength passive homodyne detection unit for fiber-coupled white-light interferometers
[ETN-90-97036] N90-26653

SOCIETE FRANCAISE DE DROIT AERIEN ET SPATIAL, BLERE.
Damage responsibility and liability in space stations N90-26714

SOUTH DAKOTA SCHOOL OF MINES AND TECHNOLOGY, RAPID CITY.
Estimation of convective rain volumes utilizing the are-time-integral technique
[NASA-CR-186814] N90-26449

SRI INTERNATIONAL CORP., MENLO PARK, CA.
Rotational and translational effects in collisions of electronically excited diatomic hydrides
[NASA-CR-186770] N90-26093
STANFORD LINEAR ACCELERATOR CENTER, CA.
Applications for the scalable coherent interface
[DE90-011795] N90-26514
Object oriented programming
[DE90-011797] N90-26532
STANFORD UNIV., CA.
Solid-state lasers for coherent communication and remote sensing
[NASA-CR-186634] N90-26306
Protein crystal growth in low gravity
[NASA-CR-186243] N90-26663
Laboratory measurements and modeling of microwave absorption by ammonia in gas mixtures applicable to giant planet atmospheres N90-26750
STATE UNIV. OF NEW YORK, BUFFALO.
Reliability analysis of continuous fiber composite laminates
[NASA-CR-185265] N90-26372
STATE UNIV. OF NEW YORK, STONY BROOK.
Infrared line parameters at low temperatures relevant to planetary atmospheres N90-26753
STOCKHOLM UNIV. (SWEDEN).
Nordic Symposium on Atmospheric Chemistry
[CM-78] N90-26403
Natural and anthropogenic compounds in bulk precipitation at Blidoe (archipelago of Stockholm, Sweden) N90-26409
Some results from the precipitation chemistry measurement programme in Sweden N90-26410
Results from global tropospheric sulphur simulations N90-26413
A comparison of the contribution of various gases to the greenhouse effect N90-26414
Phytoplankton and its contribution to the atmospheric sulfur budget of northern Europe N90-26417
Terpene concentrations and emissions in a Scots pine forest N90-26422
The diurnal ozone cycle in a coniferous forest: The importance of meteorology and chemistry N90-26423
Photodissociation of O2 in the stratosphere and mesosphere: A general parametrization of the Schumman-Runge Bands N90-26427
The collection and analysis of atmospheric peroxides N90-26428
Destruction of peroxy radical by Cu ion catalysed reactions on atmospheric particles N90-26429
Heterogeneous transformation of peroxyacetylnitrate N90-26430
STUTTGART UNIV. (GERMANY, F.R.).
A contribution to the economic, optimal dimensioning, and shaping of aircraft structures using a design model
[ETN-90-96966] N90-25976
Chemistry of combustion processes N90-25994
Tracking performance of a combined Costas/AFC-loop under noisy Rayleigh/Rician channel conditions with additive Gaussian noise jamming
[ETN-90-96964] N90-26237
A fully implicit ADI method for quasi three-dimensional flows through straight blade rows
[ETN-90-96965] N90-26283
SVERDRUP TECHNOLOGY, INC., BROOK PARK, OH.
A resistance strain gage with repeatable and cancellable apparent strain for use to 800 C
[NASA-CR-185256] N90-26063
Transient characteristics of a grooved water heat pipe with variable heat load
[NASA-CR-185280] N90-26272
SYRACUSE UNIV., NY.
Development of membrane process for carbon dioxide separation from diving atmosphere
[AD-A222606] N90-26504
SZCZECIN UNIV., LODZ (POLAND).
The manned national space station: International legal considerations N90-26720

T

TECHNICAL RESEARCH CENTRE OF FINLAND, ESPOO.
PVDF contact probes
[VTT-RR-623] N90-26253
TECHNISCHE HOCHSCHULE, DARMSTADT (GERMANY, F.R.).
Cartesian closed categories of domains
[ETN-90-97284] N90-26613
TECHNISCHE UNIV., BERLIN (GERMANY, F.R.).
Validity domain of the scalar Kirchhoff and Rayleigh-Sommerfeld diffraction theories in the near field of small phase objects: Comparison between calculation models and microwave measure
[ETN-90-96963] N90-26236
Simulation of the electrical and thermal behavior of gapless metal oxide surge arresters under AC-operation condition
[ETN-90-97309] N90-26262
Plate rods and leaf springs with hybrid structure: Cross section optimization following different target criteria
[ILR-MITT-227(1989)] N90-26366
TECHNISCHE UNIV., BRUNSWICK (GERMANY, F.R.).
The disturbance processes on the data links of the mode-S air traffic control system
[ETN-90-96960] N90-25965
A contribution to the improvement of the accuracy in the parameter identification of nonlinear processes, by example of the aircraft motion
[ETN-90-96961] N90-25974
The applicability of simple helicopter models for flight mechanics studies
[ETN-90-96962] N90-25975
TECHNISCHE UNIV., DELFT (NETHERLANDS).
Time temperature relations during rubber forming continuous fiber reinforced thermoplastics
[LR-620] N90-26151
Electromagnetic inverse scattering of buried objects
[ETN-90-97216] N90-26242
Transients in turbulent convective heat transfer to a flow of supercritical helium
[ETN-90-97217] N90-26286
The effect of a three-dimensional source on the flow through a channel with square cross section
[LR-512] N90-26289
Nondestructive one- and two-dimensional doping profiling by inverse methods
[ETN-90-97264] N90-26351
The blunt notch behaviour of metal laminates: ARALL and GLARE
[LR-617] N90-26368
Investigation of crack-closure prediction models for fatigue in aluminium alloy sheet under flight-simulation loading
[LR-619] N90-26369
Quantum ballistic and adiabatic electron transport, studied with quantum point contacts
[ETN-90-97262] N90-26440
Efficient network topologies for extensible massively parallel computers
[ETN-90-97220] N90-26568
Surface acoustic wave filters in ZnO-SiO2-Si layered structures: Design, technology, and monolithic integration with electronic circuitry
[ETN-90-97218] N90-26638
Refractive error analysis in the interferometric measurement of 2-D density fields containing strong gradients
[LR-616] N90-26655
Optical properties and transport properties of hydrogenated amorphous silicon
[ETN-90-97215] N90-26656
Vacuum deposition by pulsed laser radiation: Plasma composition, deposition techniques, and thin film properties
[ETN-90-97263] N90-26677
TECHNISCHE UNIV., EINDHOVEN (NETHERLANDS).
Modelling of the processing of incompatible polymer blends
[ETN-90-97211] N90-26152
Implementation of an algorithm for travelling-wave-based directional detection
[EUT-89-E-214] N90-26239
Software set-up for data processing of depolarization due to rain and ice crystals in the Olympus project
[EUT-89-E-218] N90-26240
Transmission, reflection, and radiation at junction planes of different open waveguides
[ISBN-90-9002864-1] N90-26241
A model of the synchronous machine with rectifier, especially for control purposes
[EUT-89-E-215] N90-26256
L-SWITCH: A PC program for computing transient voltages and currents during switching off three-phase inductances
[EUT-89-E-221] N90-26257
A possibility to incorporate saturation in the simple, global model of a synchronous machine with rectifier
[EUT-89-E-225] N90-26258
Experiments on initial behaviour of corona generated with electrical pulses superimposed on DC bias
[EUT-89-E-226] N90-26259
On travelling-wave-based protection of high-voltage networks
[ISBN-90-9002955-9] N90-26260
The bit full-decomposition of sequential machines
[EUT-89-E-223] N90-26516
LASER: A Layout Sensitivity Explorer. Report and user's manual
[EUT-89-E-216] N90-26545
Converses for write-unidirectional memories
[EUT-89-E-220] N90-26546
The full-decomposition of sequential machines with the separate realization of the next-state and output functions
[EUT-89-E-222] N90-26547
MINAS: An algorithm for systematic state assignment of sequential machines: Computational aspects and results
[EUT-89-E-217] N90-26566
From network to artwork: Automatic schematic diagram generation
[EUT-89-E-219] N90-26567
Design of a universal protocol system architecture: Specification of functions and services
[EUT-89-E-230] N90-26569
H-infinity control: An exploratory study
[EUT-88-E-211] N90-26584
On the robust stability of MIMO linear feedback systems
[EUT-88-E-212] N90-26585
A new scheme for identification and control
[EUT-88-E-213] N90-26586
Large sets of block designs
[ETN-90-97212] N90-26602
TEL-AVIV UNIV. (ISRAEL).
Adjustment and validation of the mathematical prediction model for sweat rate, heart rate, and body temperature under outdoor conditions
[AD-A222599] N90-26486
On central-difference and upwind schemes
[NASA-CR-182061] N90-26595
TELECOMMUNICATIONS RADIOELECTRIQUES ET TELEPHONIQUES, LE PLESSIS-ROBINSON (FRANCE).
Synchronization of frequency shift transmission and the effect of oversampling N90-26200
TENNESSEE UNIV., KNOXVILLE.
Laboratory studies, analysis, and interpretation of the spectra of hydrocarbons present in planetary atmospheres including cyanoacetylene, acetylene, propane, and ethane N90-26748
TEXAS UNIV., AUSTIN.
Interaction of electromagnetic signals with particulate clouds
[AD-A222804] N90-26244
An investigation into the numerical prediction of boundary layer transition using the K.Y. Chien turbulence model
[NASA-CR-185252] N90-26269
TEXAS UNIV., GALVESTON.
Experiment K-6-05. The maturaton of bone and dentin matrices in rats flown on Cosmos 1887 N90-26459
TEXAS UNIV. HEALTH SCIENCE CENTER, HOUSTON.
Experiment K-6-06. Morphometric and EM analyses of tibial epiphyseal plates from Cosmos 1887 rats N90-26460
Experiment K-6-11. Actin mRNA and cytochrome c mRNA concentrations in the tricepts brachia muscle of rats N90-26465
THIOKOL CORP., BRIGHAM CITY, UT.
RSRM-9 (360L009): Ballistics mass properties
[NASA-CR-183944] N90-26064
Flight motor set 360L007 (STS-33R)
[NASA-CR-183979] N90-26067
QM-8 final performance evaluation report: SEALS, volume 4
[NASA-CR-183958] N90-26324
Flight set 360L001 (STS-26) igniter, post flight
[NASA-CR-183957] N90-26325
THOMSON-CSF, GENNEVILLIERS (FRANCE).
Broadband analysis of ground wave propagation at a50 to 400 MHz N90-26185
A versatile integrated block codes encoder-decoder N90-26197
Experimentation of a transmission system data processing by meteor bursts N90-26207
TOLEDO UNIV., OH.
Computer architecture evaluation for structural dynamics computations: Project summary
[NASA-CR-186137] N90-26512
TORONTO UNIV. (ONTARIO).
Prediction of two-dimensional time-dependent gasdynamic flows for hypersonic studies
[UTIAS-335] N90-25935
An embedded fibre optic sensor for impact damage detection in composite materials
[UTIAS-332] N90-26650

U

UNITED TECHNOLOGIES RESEARCH CENTER, EAST HARTFORD, CT.
Combustion instrumentation N90-25996
Subsonic combustor testing N90-25997

Supersonic combustor testing N90-25998

UNIVERSAL ENERGY SYSTEMS, INC., DAYTON, OH.
The retrieval of information from secondary memory: A review and new findings
[AD-A222760] N90-26489

UNIVERSITAET DER BUNDESWEHR, HAMBURG (GERMANY, F.R.).
Numerical treatment of shell crossing singularities in the spherically symmetric gravitational collapse
[ETN-90-96967] N90-26598

UNIVERSITIES SPACE RESEARCH ASSOCIATION, HOUSTON, TX.
Press abstracts of the 21st Lunar and Planetary Science Conference
[NASA-CR-186874] N90-26738

UNIVERSITY OF SOUTHERN CALIFORNIA, LOS ANGELES.
Composite materials with improved properties in compression: Synthesis of 3-methylene-1,1-Dichlorosilacyclobutane and 1,1-dichlorosilacyclopent-3-ene
[AD-A222615] N90-26088
Computer simulation of chemical reactions in synthetic model compounds and genetically engineered active sites
[AD-A222611] N90-26483

UNIVERSITY OF SOUTHERN CALIFORNIA, MARINA DEL REY.
Rhetorical structure theory and text analysis
[AD-A222655] N90-26733

UTAH STATE UNIV., LOGAN.
Microspacecraft and Earth observation: Electrical field (ELF) measurement project
[NASA-CR-186821] N90-26436

UTAH UNIV., SALT LAKE CITY.
Chemical structure and kinetics at liquid/solid interfaces
[AD-A222766] N90-26105

V

VERMONT UNIV., BURLINGTON.
Practical applications of remote sensing technology
[NASA-CR-186810] N90-26377

VIGYAN RESEARCH ASSOCIATES, INC., HAMPTON, VA.
Effects of forebody geometry on subsonic boundary-layer stability
[NASA-CR-4314] N90-25939

VIRGINIA POLYTECHNIC INST. AND STATE UNIV., BLACKSBURG.
Project LOCOST: Laser or Chemical Hybrid Orbital Space Transport
[NASA-CR-186822] N90-26042
Project SPARC: Space-based aeroassisted reusable craft
[NASA-CR-186816] N90-26051
The aerobraking space transfer vehicle
[NASA-CR-186819] N90-26053
Feasibility study of a synthesis procedure for array feeds to improve radiation performance of large distorted reflector antennas
[NASA-CR-186641] N90-26213
A real-time robot arm collision detection system
[NASA-CR-185878] N90-26582

VIRGINIA UNIV., CHARLOTTESVILLE.
Investigation of thermo-mechanical effects in silicon carbide Whisker/Al alloy composites
[AD-A222635] N90-26089
Laboratory studies of the interaction of ions with condensed gases: Planetary applications N90-26778

VON KARMAN INST. FOR FLUID DYNAMICS, RHODE-SAINT-GENESE (BELGIUM).
Gas Turbine Combustion, volume 1
[VKI-LS-1990-02-VOL-1] N90-25985
Gas Turbine Combustion, volume 2
[VKI-LS-1990-02-VOL-2] N90-25995

W

WASHINGTON UNIV., SAINT LOUIS, MO.
Experiment K-6-21. Effect of microgravity on 1) metabolic enzymes of type 1 and type 2 muscle fibers and on 2) metabolic enzymes, neutransmitter amino acids, and neurotransmitter associated enzymes in motor and somatosensory cerebral cortex. Part 1: Metabolic enzymes of individual muscle fibers; part 2: metabolic enzymes of hippocampus and spinal cord N90-26474

WASHINGTON UNIV., SEATTLE.
The catalytic synthesis of inorganic polymers for high temperature applications and as ceramic precursors
[AD-A222620] N90-26156
Megawatt solar power systems for lunar surface operations
[NASA-CR-186509] N90-26391

WICHITA STATE UNIV., KS.
Prediction methodologies for nonlinear aerodynamic characteristics of control surfaces
[NIAR-90-17] N90-25937
Computational crash dynamics. Project 1.2: Computational crash dynamics analysis
[IAR-89-19] N90-25956
A NASA/university/industry consortium for research on aircraft ice protection
[IAR-89-18] N90-25969
Erosion mechanisms in composite materials and ripple formation mechanism in erosion
[IAR-89-4-PT-1] N90-26078
Erosion mechanisms in composite materials and ripple formation mechanism in erosion
[IAR-89-4-PT-2] N90-26079
A study of the fatigue behavior in scratched samples of Al-Li alloy (2090-T3)
[IAR-89-24] N90-26107
Mechanical paint removal techniques for aircraft structures
[NIAR-90-12] N90-26166
Numerical analysis of three-dimensional particle-laden flow equations
[IAR-90-2] N90-26268
Design and construction of a wall-climbing robot
[NIAR-90-20] N90-26327
Neural networks for detecting defects in aircraft structures
[IAR-90-4] N90-26345
Robotic-aided system for inspection of aging aircraft
[NIAR-90-9] N90-26346
A comparison of the post-buckling behavior of metallic and composite plates with centrally located cutouts
[NIAR-90-14] N90-26356
Analysis of strain relaxation in Au/Ni multilayers by x ray diffraction
[IAR-89-25] N90-26357
Choosing a pilot subjective workload scale to fit flight operational requirements
[IAR-89-21] N90-26493
Biodynamic simulations of an aircraft pilot/passenger in various crash environments
[NIAR-90-6] N90-26494
Human performance in cockpit-related systems
[NIAR-90-7] N90-26495
Human factors: The human interface with aircraft interiors
[NIAR-90-18] N90-26496
A measurement of the effectiveness of the Airway Science Program to meet Federal Aviation Administration work force needs
[NIAR-90-5] N90-26694

WISCONSIN UNIV., MADISON.
Gas exchange characteristics as indicators of the basic limiting factors in photosynthesis
[DE90-012399] N90-26481

WISCONSIN UNIV., MILWAUKEE.
Genesis lunar outpost criteria and design
[NASA-CR-186831] N90-26499

WORCESTER POLYTECHNIC INST., MA.
Feasibility study for a microwave-powered ozone sniffer aircraft, volume 2
[NASA-CR-186676] N90-25967
Integrated support structure
[NASA-CR-186835] N90-26162

WRIGHT RESEARCH DEVELOPMENT CENTER, WRIGHT-PATTERSON AFB, OH.
PDWAP: A preliminary design and weights analysis program for aerospace vehicles
[AD-A222614] N90-25979
Wright Research and Development Center test facilities handbook
[AD-A222582] N90-26020
Electronic warfare technology: Trends and visions
[AD-A223034] N90-26246

WYOMING UNIV., LARAMIE.
Vitreous joining of SiC fiber reinforced SiC composites
[DE90-012951] N90-26081

Y

YALE UNIV., NEW HAVEN, CT.
Microstructural dependence of the cavitation damage function in FCC materials
[DE90-012898] N90-26113

YERKES OBSERVATORY, WILLIAMS BAY, WI.
The interstellar D1 line at high resolution
[NASA-CR-184915] N90-26737

Typical Contract Number Index Listing

Listings in this index are arranged alphanumerically by contract number. Under each contract number the NASA accession numbers denoting documents that have been produced as a result of research done under that contract are arranged in ascending order. The NASA accession number denotes the number by which the citation is identified.

AF PROJ. 2301 ..... N90-26642
AF PROJ. 2304 ..... N90-26621
AF PROJ. 2309 ..... N90-25962
N90-25963
AF PROJ. 2310 ..... N90-26442
AF PROJ. 2313 ..... N90-26489
AF PROJ. 2418 ..... N90-26125
AF PROJ. 2917 ..... N90-26263
AF PROJ. 3012 ..... N90-25979
AF PROJ. 4143 ..... N90-26062
AF PROJ. 4506 ..... N90-26243
AF PROJ. 5581 ..... N90-26559
AF PROJ. 7757 ..... N90-26657
AF PROJ. 7930 ..... N90-26505
AF-AFOSR-0041-88 ..... N90-26642
AF-AFOSR-0052-87 ..... N90-26243
AF-AFOSR-0117-88 ..... N90-26533
AF-AFOSR-0131-89 ..... N90-26318
AF-AFOSR-0210-86 ..... N90-26263
ARPA ORDER 6037 ..... N90-26524
ARPA ORDER 6259 ..... N90-26307
BM-J034035 ..... N90-26140
BM-J0134035 ..... N90-26141
DA PROJ. 1L1-61102-AH-43 ..... N90-26100
N90-26293
N90-26317
DA PROJ. 1L1-61102-AH-45 ..... N90-26338
DA PROJ. 1L1-61102-BH-57 ..... N90-26385
DA PROJ. 1L1-62105-AH-84 ..... N90-26126
DA PROJ. 1L1-62209-A-47-A N90-26171
DA PROJ. 1L1-62211-A-47-A N90-26334
DA PROJ. 1L1-62618-AH-80 ..... N90-26155
DA PROJ. 3E1-62777-A-879 ..... N90-26486
DAAB07-88-C-A007 ..... N90-26208
DAAG29-84-K-0069 ..... N90-26447
DAAH01-88-C-0138 ..... N90-26307
DAAL03-86-K-0121 ..... N90-26090
DAAL03-87-C-0007 ..... N90-26247
N90-26248
DAAL03-87-G-0003 ..... N90-26107
DAAL03-87-K-0044 ..... N90-26159
DAAL04-87-C-0085 ..... N90-26126
DAA29-84-K-0061 ..... N90-26497
DAA29-84-9-0027 ..... N90-26497
DACA76-89-C-0014 ..... N90-26591
DAJA45-86-C-0049 ..... N90-26385
DAJA45-89-M-0085 ..... N90-26431
DAMD17-85-G-5044 ..... N90-26486
DASG60-87-C-0066 ..... N90-26625
DE-AC02-76ER-03130 ..... N90-26540
N90-26648
N90-26742
DE-AC02-83CH-10093 ..... N90-26392
DE-AC03-76SF-00515 ..... N90-26514
N90-26532
DE-AC03-87SF-17128 ..... N90-26312
DE-AC03-89ER-51114 ..... N90-26660
DE-AC04-76DP-00613 ..... N90-26537
DE-AC04-76DP-00789 ..... N90-25941
N90-26031
N90-26097
N90-26133
N90-26134
N90-26135
N90-26143
N90-26144
N90-26145
N90-26146
N90-26251
N90-26311
N90-26386
N90-26387
N90-26389
N90-26531
N90-26661
N90-26669
DE-AC04-76DR-00789 ..... N90-26112
N90-26530
DE-AC05-76OR-00033 ..... N90-26138
N90-26139
DE-AC05-84ER-40150 ..... N90-26644
DE-AC05-84OR-21000 ..... N90-26138
N90-26139
DE-AC05-84OR-21400 ..... N90-26084
N90-26109
N90-26117
N90-26132
N90-26136
N90-26360
N90-26529
N90-26666
N90-26668
N90-26671
N90-26674
N90-26699
N90-26775
N90-26776
DE-AC05-84OT-21400 ..... N90-26565
DE-AC06-76RL-01830 ..... N90-26707
DE-AC07-76ID-01570 ..... N90-26043
N90-26081
N90-26140
N90-26141
N90-26347
N90-26390
N90-26670
DE-AC07-88ID-12754 ..... N90-26645
N90-26646
N90-26647
DE-AC08-89NV-1063 ..... N90-26596
DE-AT04-85AL-33408 ..... N90-26729
DE-FG02-85ER-45214 ..... N90-26111
DE-FG02-86ER-13594 ..... N90-26482
DE-FG02-87ER-13785 ..... N90-26481
DE-FG02-88ER-45355 ..... N90-26113
DE-FG05-86ER-75292 ..... N90-26688
DE-FG05-88ER-45359 ..... N90-26675
DE-FG05-88ER-53278 ..... N90-26658
DE-FG06-87ER-45292 ..... N90-26137
DEN3-335 ..... N90-26728
DOE PROJ. 3410-6926 ..... N90-26529
DRET-87-068 ..... N90-26287
DTFA03-96-C-00041 ..... N90-25956
FQ8671-84-01007 ..... N90-26733
F04701-87-C-0010 ..... N90-26037
N90-26038
F19628-86-C-0139 ..... N90-26442
F19628-86-K-0020 ..... N90-26629
F19628-90-C-0002 ..... N90-26319
F30602-81-C-0205 ..... N90-26631
F30602-88-D-0027 ..... N90-26243
N90-26560
F33615-84-D-0505 ..... N90-26489
F33615-85-C-4503 ..... N90-26505
F33615-88-C-5437 ..... N90-26125
F49620-85-C-0144 ..... N90-26621
F49620-85-K-0018 ..... N90-26497
F49620-87-C-0005 ..... N90-26733
MDA903-87-C-0641 ..... N90-26733
NAGW-533 ..... N90-26745
NAGW-637 ..... N90-26775
NAGW-903 ..... N90-26772
NAGW-925 ..... N90-26375
N90-26376
NAGW-1340 ..... N90-26734
N90-26735
NAGW-1444 ..... N90-26774
NAGW-1475 ..... N90-26737
NAGW-1509 ..... N90-26763
NAGW-1617 ..... N90-26382
NAGW-1667 ..... N90-26755
NAGW-1760 ..... N90-26306
NAGW-1763 ..... N90-26451
NAGW-1764 ..... N90-26767
NAG1-296 ..... N90-26513
NAG1-343 ..... N90-26083
NAG1-466 ..... N90-26533
NAG1-562 ..... N90-26233
NAG1-613 ..... N90-26558
NAG1-623 ..... N90-26328
N90-26329
NAG1-650 ..... N90-26536
NAG1-685 ..... N90-26632
NAG1-709 ..... N90-26634
NAG1-736 ..... N90-26013
NAG1-789 ..... N90-26534
NAG1-846 ..... N90-26281
NAG1-859 ..... N90-26213
NAG1-882 ..... N90-26447
NAG1-885 ..... N90-26526
NAG1-928 ..... N90-26448
NAG1-962 ..... N90-26488
NAG1-1087 ..... N90-25943
NAG1-1094 ..... N90-26354
NAG2-123 ..... N90-26492
NAG2-239 ..... N90-26485
NAG2-544 ..... N90-26235
N90-26652
NAG2-576 ..... N90-26784
NAG2-578 ..... N90-26649
NAG2-582 ..... N90-26698
NAG2-593 ..... N90-26254
N90-26344
N90-26524
N90-26535
NAG3-140 ..... N90-25934
NAG3-499 ..... N90-25940
NAG3-699 ..... N90-26512
NAG3-862 ..... N90-26142
N90-26372
NAG3-864 ..... N90-26269
NAG3-872 ..... N90-26364
NAG3-988 ..... N90-26683
NAG3-1048 ..... N90-26234
NAG5-386 ..... N90-26449
NAG5-557 ..... N90-26528
NAG5-785 ..... N90-26765
NAG5-894 ..... N90-26378
NAG5-1045 ..... N90-26497
N90-26498
NAG5-1114 ..... N90-26503
NAG5-1124 ..... N90-26578
NAG5-1183 ..... N90-26582
NAG8-078 ..... N90-26435
NAG8-706 ..... N90-26048
NAG8-774 ..... N90-26663
NAG9-52 ..... N90-26776
NAG9-137 ..... N90-26689
NAG9-235 ..... N90-26477
NAL PROJ. FM-8-208 ..... N90-25936
NAL PROJ. MT-0-181 ..... N90-26092
NASA ORDER C-99066-G N90-25948
N90-26282
N90-26614
N90-26615
N90-26616
NASW-4066 ..... N90-26437
N90-26738
N90-26739
N90-26740
NASW-4435 ..... N90-25967
N90-25968
N90-26039
N90-26044
N90-26045
N90-26128
N90-26479

NAS1-15325 ..... N90-25944
NAS1-16956 ..... N90-26093
NAS1-17919 ..... N90-25939
NAS1-17964 ..... N90-26527
NAS1-18000 ..... N90-26131
NAS1-18230 ..... N90-26577
NAS1-18378 ..... N90-25966
NAS1-18460 ..... N90-26402
NAS1-18567 ..... N90-26061
NAS1-18599 ..... N90-26131
NAS1-18605 ..... N90-26270
N90-26509
N90-26510
N90-26533
N90-26595
NAS1-18872 ..... N90-26046
NAS3-23721 ..... N90-26633
NAS3-23940 ..... N90-26355
NAS3-24105 ..... N90-26272
NAS3-25266 ..... N90-26063
N90-26272
N90-26275
NAS3-25279 ..... N90-26320
NAS3-25867 ..... N90-26683
NAS3-25917 ..... N90-26581
NAS5-30134 ..... N90-26770
NAS7-918 ..... N90-26098
N90-26176
N90-26216
N90-26217
N90-26292
N90-26339
N90-26384
N90-26518
N90-26519
N90-26684
N90-26685
N90-26701
N90-26705
NAS7-1033 ..... N90-26525
NAS8-30490 ..... N90-26064
N90-26067
N90-26324
N90-26325
NAS8-34715 ..... N90-26095
NAS8-36354 ..... N90-26271
NAS8-38064 ..... N90-26115
NAS8-38184 ..... N90-26108
NAS8-40000 ..... N90-26358
NAS8-50000 ..... N90-26047
NAS9-18147 ..... N90-26033
NAS10-10285 ..... N90-26485
NAS10-11624 ..... N90-26480
NATO-0224/85 ..... N90-26497
NCC1-123 ..... N90-26017
NCC1-136 ..... N90-26563
NCC2-236 ..... N90-26515
NCC2-267 ..... N90-25972
NCC2-388 ..... N90-25970
NCC2-408 ..... N90-26522
NCC2-416 ..... N90-25954
NCC2-521 ..... N90-26477
NCC2-604 ..... N90-26019
NCC2-615 ..... N90-25964
NCC3-89 ..... N90-26142
NCC3-109 ..... N90-26664
NGL-05-002-114 ..... N90-26731
NGL-39-0110137 ..... N90-26767
NGR-05-018-180 ..... N90-26754
NGR-33-010-082 ..... N90-26775
NGR-33-010-101 ..... N90-26776
NGR-33-010-220 ..... N90-26775
NGR-33-015-139 ..... N90-26753
NGT-21-002-080 ..... N90-26165
N90-26322
NGT-21-002-800 ..... N90-25971
N90-26026
N90-26027
N90-26042
N90-26049
N90-26050
N90-26051
N90-26052
N90-26053
N90-26162
N90-26321
N90-26330
N90-26331
N90-26332
N90-26333
N90-26391
N90-26436
N90-26500
N90-26501
N90-26490
N90-26499
NGT-22-002-080 ..... N90-26323
NGT21-002-800 ..... N90-26161
NIH-RR-02170 ..... N90-26508
NIH-S06-GM-08047 ..... N90-26102
NIVR-01408N N90-26370
NIVR-01604N N90-26285
NSF ASC-88-19374 ..... N90-26509
NSF CCR-86-11442 ..... N90-26520
NSF CCR-87-16914 ..... N90-26622
NSF CDA-86-19893 ..... N90-26622
NSF DCR-82-19196 ..... N90-26498
NSF DCR-84-10771 ..... N90-26498
NSF DMC-85-17315 ..... N90-26497
N90-26498
NSF DMR-86-05564 ..... N90-26357
NSF DMR-88-07367 ..... N90-26675
NSF DMS-89-05314 ..... N90-26615
NSF EAR-86-09218 ..... N90-26776
NSF ECS-85-07405 ..... N90-26375
N90-26376
NSF GY-7699 ..... N90-26538
NSF HES-70-3128 ..... N90-26538
NSF INT-85-14199 ..... N90-26497
N90-26498
NSF IRI-84-10413 ..... N90-26497
NSF IRI-84-51430 ..... N90-26526
NSF IST-84-08726 ..... N90-26733
NSF MCS-82-19196 ..... N90-26497
NSF MEA-81-19884 ..... N90-26498
NSF MIP-88-09478 ..... N90-26558
NSF NCR-89-03429 ..... N90-26526
NSF PHY-90-19754 ..... N00-26734
NSF SED-75-15112 ..... N90-26538
NSG-1588 ..... N90-26308
NSG-3188 ..... N90-26171
NSG-7453 ..... N90-26377
N00014-81-C-0776 ..... N90-26265
N90-26630
N00014-82-K-0322 ..... N90-26158
N00014-83-K-0125 ..... N90-26520
N00014-84-K-0519 ..... N90-26697
N00014-85-K-0122 ..... N90-26513
N00014-85-K-0124 ..... N90-26326
N00014-85-K-0168 ..... N90-26520
N00014-85-K-0179 ..... N90-26089
N00014-85-K-0531 ..... N90-26513
N00014-85-K-0658 ..... N90-26104
N00014-85-K-0782 ..... N90-26697
N00014-85-K-0807 ..... N90-26497
N00014-85-K-0872 ..... N90-26639
N00014-86-C-0159 ..... N90-26062
N00014-86-K-0310 ..... N90-26509
N00014-86-K-0680 ..... N90-26508
N00014-86-K-0685 ..... N90-26326
N00014-87-K-0436 ..... N90-26447
N00014-87-K-0507 ..... N90-26483
N00014-87-K-2015 ..... N90-26316
N00014-88-K-0109 ..... N90-26099
N00014-88-K-0140 ..... N90-26622
N00014-88-K-0214 ..... N90-26641
N00014-88-K-0305 ..... N90-26156
N00014-88-K-0307 ..... N90-26688
N00014-88-K-0525 ..... N90-26675
N00014-88-K-0526 ..... N90-26675
N00014-88-K-0656 ..... N90-26558
N00014-89-J-0050 ..... N90-26686
N00014-89-J-1169 ..... N90-26643
N90-26687
N00014-89-J-1339 ..... N90-26102
N00014-89-J-1412 ..... N90-26105
N00014-89-J-1452 ..... N90-26101
N90-26441
N00014-89-J-1590 ..... N90-26157
N00014-89-J-1775 ..... N90-26103
N00014-89-J-1961 ..... N90-26088
N00014-89-J-1988 ..... N90-26520
N00014-90-J-1545 ..... N90-26592
N00039-88-C-0051 ..... N90-26374
N00140-85-K-0807 ..... N90-26498
N00140-87-C-8904 ..... N90-26254
N90-26344
N90-26524
N00167-86-K-0019 ..... N90-26294
ORNL-86X-00214C N90-26084
RF PROJ. 767591/722399 ..... N90-25964
STEV-506-268-3 ..... N90-26636
STR-0012487 ..... N90-26650
STW-DEL-44/47-0592 ..... N90-26638
W-31-109-ENG-38 ..... N90-26562
N90-26667
N90-26675
N90-26676
N90-26702
W-7405-ENG-36 ..... N90-26096
N90-26118
N90-26310
N90-26434
N90-26438
N90-26439
N90-26539
N90-26597
N90-26627
N90-26659
N90-26665
N90-26690
N90-26732
W-7405-ENG-48 ..... N90-26110
N90-26114
N90-26300
N90-26313
N90-26314
N90-26315
N90-26538
N90-26626
N90-26786
N90-26787
W-7405-ENG-82 ..... N90-26116
N90-26119
N90-26252
N90-26673
176-10-05-70 ..... N90-26401
176-20-03-70 ..... N90-26399
176-30-05-70 ..... N90-26093
199-04-16-11 ..... N90-26640
199-05-12 ..... N90-26452
310-10-60-87-02 ..... N90-26218
310-10-61-84-02 ..... N90-26219
310-10-62-15-00 ..... N90-26222
N90-26223
310-10-63-50-00 ..... N90-26220
N90-26221
310-20-65-67-00 ..... N90-26224
310-20-65-86-08 ..... N90-26225
310-20-67-59-00 ..... N90-26226
310-20-67-89-02 ..... N90-26227
310-30-70-89-02 ..... N90-26228
314-30-41-21-69 ..... N90-26231
314-30-50-58-12 ..... N90-26229
314-40-41-81-11 ..... N90-26230
474-10-52 ..... N90-26279
476-14-06-01 ..... N90-26032
505-43-02 ..... N90-26355
505-44-2C N90-26682
505-45-23-53 ..... N90-25957
505-60-01-02 ..... N90-26094
505-60-11 ..... N90-26274
505-60-41-01 ..... N90-25944
505-60-61 ..... N90-26019
505-61-01-05 ..... N90-26296
505-61-01-06 ..... N90-26651
505-61-41-02 ..... N90-25939
505-61-51 ..... N90-25933
505-62-4D N90-25940
505-62-01 ..... N90-26011
N90-26063
505-62-11 ..... N90-25982
N90-26275
505-62-21 ..... N90-25948
N90-26269
N90-26276
N90-26282
N90-26299
N90-26614
N90-26615
N90-26616
505-62-71 ..... N90-26009
505-62-71-01 ..... N90-25938
505-63-1B N90-26142
N90-26373
505-63-01-05 ..... N90-26076
505-63-01-08 ..... N90-26077
505-63-01-11 ..... N90-26363
505-63-51 ..... N90-26171
N90-26334
505-63-64 ..... N90-26338
505-66-21 ..... N90-26214
N90-26619
505-66-21-01 ..... N90-26527
505-66-71 ..... N90-25981
505-67-21-07 ..... N90-26511
505-80-11-05 ..... N90-26167
505-90-21-01 ..... N90-26270
N90-26509
N90-26510
N90-26533
N90-26595
506-40-61-01 ..... N90-26036
506-41-3K N90-26054
506-41-11 ..... N90-26069
506-41-21 ..... N90-26397
506-42-31 ..... N90-26071
506-42-61 ..... N90-26065

506-43-11 ..... N90-26131
506-43-31-04 ..... N90-26361
506-43-41-02 ..... N90-26061
506-43-71 ..... N90-26080
506-43-71-03 ..... N90-26082
506-44-21 ..... N90-26683
506-45-31 ..... N90-26309
506-48-71-01 ..... N90-26075
510-01-0A N90-26359
510-01-1A N90-26364
510-11-01 ..... N90-26372
533-02-01 ..... N90-26564
533-02-51 ..... N90-25973
535-03-01 ..... N90-25946
N90-26635
535-03-11-03 ..... N90-26632
535-05-01 ..... N90-26633
537-01-11 ..... N90-26170
537-01-31-01 ..... N90-25966
585-01-91-01 ..... N90-26046
590-11-41-01 ..... N90-26577
590-13-21 ..... N90-26272
590-14-61-01 ..... N90-26362
590-21-41 ..... N90-26070
591-14-11 ..... N90-26074
N90-26789
591-14-41 ..... N90-26068
N90-26396
591-23-21 ..... N90-26278
591-42-11 ..... N90-25945
618-21-00-01 ..... N90-26402
618-21-01-00 ..... N90-26400
643-10-01 ..... N90-26172
650-60-20 ..... N90-26250
665-45-30-01 ..... N90-26433
672-22-12-70 ..... N90-26447
674-22-05 ..... N90-26163
674-24-05 ..... N90-26273
677-22-12-70 ..... N90-26446
763-01-21 ..... N90-26055
N90-26160
776-81-63 ..... N90-26729
906-76-40-43-01 ..... N90-26232

REPORT/ACCESSION NUMBER INDEX

Typical Report Number Index Listing

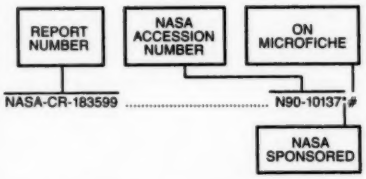

Listings in this index are arranged alphanumerically by report number. The NASA accession number denotes the number by which the citation is identified. An asterisk (*) indicates that the item is a NASA report. A pound sign (#) indicates that the item is available on microfiche.

A-90013 ..... N90-26452* #
A-90153 ..... N90-26274* #
A-90163 ..... N90-26019* #
A-90170 ..... N90-25933* #
A-90186 ..... N90-25945* #

AA-420 ..... N90-26391* #
AA-421 ..... N90-26391* #

AAC-TN-1154 ..... N90-26061* #

AAMRL-TR-88-041 ..... N90-26489 #

AD-A219244 ..... N90-26431 #
AD-A219978 ..... N90-25962 #
AD-A219979 ..... N90-25963 #
AD-A220026 ..... N90-26326 #
AD-A220075 ..... N90-26484 #
AD-A220773 ..... N90-26037 #
AD-A220774 ..... N90-26038 #
AD-A220898 ..... N90-26307 #
AD-A222566 ..... N90-26177 #
AD-A222568 ..... N90-26621 #
AD-A222569 ..... N90-26374 #
AD-A222570 ..... N90-26099 #
AD-A222572 ..... N90-26641 #
AD-A222577 ..... N90-25960 #
AD-A222578 ..... N90-26263 #
AD-A222582 ..... N90-26020 #
AD-A222586 ..... N90-26556 #
AD-A222591 ..... N90-26100 #
AD-A222595 ..... N90-26155 #
AD-A222599 ..... N90-26486 #
AD-A222603 ..... N90-26101 #
AD-A222605 ..... N90-26441 #
AD-A222606 ..... N90-26504 #
AD-A222607 ..... N90-26316 #
AD-A222609 ..... N90-26062 #
AD-A222611 ..... N90-26483 #
AD-A222613 ..... N90-26622 #
AD-A222614 ..... N90-25979 #
AD-A222615 ..... N90-26088 #
AD-A222616 ..... N90-26686 #
AD-A222620 ..... N90-26156 #
AD-A222621 ..... N90-26293 #
AD-A222622 ..... N90-26317 #
AD-A222626 ..... N90-26505 #
AD-A222628 ..... N90-26687 #
AD-A222629 ..... N90-26318 #
AD-A222630 ..... N90-26264 #
AD-A222631 ..... N90-26642 #
AD-A222635 ..... N90-26089 #
AD-A222653 ..... N90-26590 #
AD-A222655 ..... N90-26733 #
AD-A222660 ..... N90-26442 #
AD-A222667 ..... N90-26591 #
AD-A222675 ..... N90-26385 #
AD-A222678 ..... N90-26506 #
AD-A222707 ..... N90-26507 #
AD-A222709 ..... N90-26343 #
AD-A222710 ..... N90-26623 #
AD-A222711 ..... N90-26624 #
AD-A222712 ..... N90-26557 #
AD-A222715 ..... N90-25961 #
AD-A222723 ..... N90-26643 #
AD-A222726 ..... N90-26625 #
AD-A222731 ..... N90-26629 #
AD-A222732 ..... N90-26106 #
AD-A222739 ..... N90-26102 #
AD-A222741 ..... N90-26319 #
AD-A222744 ..... N90-26103 #
AD-A222746 ..... N90-26657 #
AD-A222747 ..... N90-26508 #
AD-A222750 ..... N90-26157 #
AD-A222752 ..... N90-26104 #
AD-A222755 ..... N90-26158 #
AD-A222760 ..... N90-26489 #
AD-A222762 ..... N90-26630 #
AD-A222763 ..... N90-26265 #
AD-A222765 ..... N90-26520 #
AD-A222766 ..... N90-26105 #
AD-A222787 ..... N90-26294 #
AD-A222795 ..... N90-26018 #
AD-A222798 ..... N90-26576 #
AD-A222801 ..... N90-26243 #
AD-A222802 ..... N90-26124 #
AD-A222803 ..... N90-26125 #
AD-A222804 ..... N90-26244 #
AD-A222808 ..... N90-26558* #
AD-A222812 ..... N90-26617 #
AD-A222813 ..... N90-25955 #
AD-A222814 ..... N90-26618 #
AD-A222994 ..... N90-26639 #
AD-A223000 ..... N90-26631 #
AD-A223021 ..... N90-26245 #
AD-A223028 ..... N90-26295 #
AD-A223030 ..... N90-26559 #
AD-A223031 ..... N90-26090 #
AD-A223032 ..... N90-26159 #
AD-A223034 ..... N90-26246 #
AD-A223044 ..... N90-26247 #
AD-A223045 ..... N90-26248 #
AD-A223072 ..... N90-26560 #
AD-A223079 ..... N90-26126 #
AD-A223090 ..... N90-26487 #
AD-A223095 ..... N90-26266 #
AD-A223096 ..... N90-26592 #
AD-A223097 ..... N90-26267 #
AD-A223160 ..... N90-26697 #
AD-A223255 ..... N90-26688 #

AD-D014506 ..... N90-26305
AD-D014510 ..... N90-26209 #
AD-D014511 ..... N90-26297 #
AD-D014536 ..... N90-26491
AD-D014538 ..... N90-26249 #

AD-E501236 ..... N90-26343 #
AD-E501236 ..... N90-26507 #
AD-E501236 ..... N90-26557 #
AD-E501236 ..... N90-26623 #
AD-E501236 ..... N90-26624 #
AD-E951478 ..... N90-26020 #
AD-E951478 ..... N90-26100 #
AD-E951478 ..... N90-26155 #
AD-E951478 ..... N90-26556 #

AFHRL-TP-89-18 ..... N90-26484 #

AFIT/CI/CIA-90-012D ..... N90-26618 #
AFIT/CI/CIA-90-026 ..... N90-26507 #
AFIT/CI/CIA-90-030 ..... N90-26244 #

AFIT/GAE/ENY/89D-30 ..... N90-26018 #

AFIT/GE/ENG/90J-2 ..... N90-26245 #

AFOSR-90-0565TR ..... N90-26263 #
AFOSR-90-0582TR ..... N90-26318 #
AFOSR-90-0583TR ..... N90-26642 #
AFOSR-90-0648TR ..... N90-26621 #

AG-MET-PR-90-1 ..... N90-26378* #

AGARD-AR-255 ..... N90-26280 #
AGARD-AR-267 ..... N90-25947 #
AGARD-AR-281 ..... N90-26012 #

AGARD-CP-442 ..... N90-26178 #

AI-M-1126 ..... N90-26326 #

AIAA-90-0438 ..... N90-25946* #
AIAA-90-1681 ..... N90-26278* #
AIAA-90-1894 ..... N90-26065* #
AIAA-90-1994 ..... N90-26070* #
AIAA-90-2645 ..... N90-26071* #
AIAA-90-3593 ..... N90-26030* #

AR-006-084 ..... N90-26106 #

ARL-MAT-R-122 ..... N90-26106 #

ARO-446 ..... N90-25971* #
ARO-463 ..... N90-25971* #
ARO-23421.12-MS ..... N90-26090 #
ARO-23967.5-CH ..... N90-26159 #
ARO-24649.9-EL-S ..... N90-26248 #
ARO-24649.10-EL-S ..... N90-26247 #

AVSCOM-TM-90-B-003 ..... N90-26076* #
AVSCOM-TM-90-C-003 ..... N90-26171* #
AVSCOM-TM-90-C-005 ..... N90-26334* #

AVSCOM-TR-90-B-006 ..... N90-26363* #
AVSCOM-TR-90-C-013 ..... N90-26338* #

B-222217 ..... N90-25958 #
B-222217 ..... N90-25959 #
B-223785 ..... N90-26066 #
B-230525 ..... N90-26021 #
B-230525 ..... N90-26022 #
B-230525 ..... N90-26023 #
B-230525 ..... N90-26025 #
B-234056 ..... N90-26215 #
B-237585 ..... N90-26704 #
B-237602 ..... N90-26169 #
B-237832 ..... N90-26024 #
B-238709 ..... N90-26298 #
B-239570 ..... N90-26041 #

BBC-RD-1990/1 ..... N90-26211
BBC-RD-1990/3 ..... N90-26212

BN-1114 ..... N90-26503* #

BRL-CR-629 ..... N90-26506 #

BRL-MR-3831 ..... N90-26155 #

BRL-TR-3094 ..... N90-26317 #
BRL-TR-3098 ..... N90-26100 #
BRL-TR-3100 ..... N90-26293 #

BROWN-HET-758 ..... N90-26648 #

BR112079 ..... N90-26121 #
BR112677 ..... N90-26548 #
BR112706 ..... N90-26580 #
BR112835 ..... N90-26579 #
BR112836 ..... N90-26288 #
BR112839 ..... N90-26007 #
BR113062 ..... N90-26122 #
BR113095 ..... N90-26662 #
BR113195 ..... N90-25953 #

CBPF-NF-027/89 ..... N90-26736 #

CCMS-90-06 ..... N90-26083* #

CEBAF-PR-89-017 ..... N90-26644 #

CIT/SME/VKI/RS/1 ..... N90-25986 #
CIT/SME/VKI/RS/3 ..... N90-25987 #
CIT/SME/VKI/RS/4 ..... N90-25988 #
CIT/SME/VKI/RS/5 ..... N90-25989 #
CIT/SME/VKI/RS/6 ..... N90-25990 #

CM-78 ..... N90-26403 #

CMU-RI-TR-90-01 ..... N90-26556 #
CMU-RI-TR-90-09 ..... N90-26591 #

CONF-890770-12 ..... N90-26347 #
CONF-891119-123 ..... N90-26675 #
CONF-891119-125 ..... N90-26676 #
CONF-891163-2 ..... N90-26314 #
CONF-891163-3 ..... N90-26315 #
CONF-900135-8 ..... N90-26732 #
CONF-900312-1 ..... N90-26661 #
CONF-900451-4 ..... N90-26300 #
CONF-900466-58 ..... N90-26110 #
CONF-900466-60 ..... N90-26668 #
CONF-900466-61 ..... N90-26139 #
CONF-900466-62 ..... N90-26138 #
CONF-900466-65 ..... N90-26669 #
CONF-900466-67 ..... N90-26117 #
CONF-900466-68 ..... N90-26144 #
CONF-900542-13 ..... N90-26389 #
CONF-900557-10 ..... N90-26658 #
CONF-900602-14 ..... N90-26660 #
CONF-900623-11 ..... N90-26674 #
CONF-900634-2 ..... N90-26114 #
CONF-900656-2 ..... N90-26311 #
CONF-900736-1 ..... N90-26141 #
CONF-900756-9 ..... N90-26145 #
CONF-900798-1 ..... N90-26659 #
CONF-900801-9 ..... N90-26667 #
CONF-900801-15 ..... N90-26390 #
CONF-900802-3 ..... N90-26143 #
CONF-900806-3 ..... N90-26665 #
CONF-900806-5 ..... N90-26666 #
CONF-900822-3 ..... N90-26434 #
CONF-900837-2 ..... N90-26132* #
CONF-900837-4 ..... N90-26537 #
CONF-900861-1 ..... N90-26031 #
CONF-900870-1 ..... N90-26118 #
CONF-900874-2 ..... N90-26562 #
CONF-900875-1 ..... N90-26702 #
CONF-900877-3 ..... N90-26097 #
CONF-900884-1 ..... N90-26096 #
CONF-900886-1 ..... N90-26109 #
CONF-900892-1 ..... N90-26251 #
CONF-901071-4 ..... N90-26133 #
CONF-8906332-1 ..... N90-26690 #
CONF-8908160-3 ..... N90-26043 #
CONF-8909342-1 ..... N90-26538 #
CONF-8911193-2 ..... N90-26360 #
CONF-9003178-1 ..... N90-26627 #
CONF-9004190-7 ..... N90-26514 #
CONF-9004190-8 ..... N90-26532 #
CONF-9005183-2 ..... N90-26670 #
CONF-9005202-1 ..... N90-26135 #
CONF-9005210-2 ..... N90-26310 #
CONF-9005231-1 ..... N90-26146 #
CONF-9005237-1 ..... N90-26597 #
CONF-9006195-2 ..... N90-26539 #
CONF-9006209-1 ..... N90-26140 #
CONF-9006212-1 ..... N90-26787 #
CONF-9006220-1 ..... N90-26439 #
CONF-9006220-2 ..... N90-26438 #
CONF-9008101-2 ..... N90-26596 #

COO-313OTC-51 ..... N90-26540 #

CRIE-T-88057 ..... N90-26255 #
CRIE-T-88078 ..... N90-26365 #
CRIE-T-88081 ..... N90-26147 #

CRIE-U-88072 ..... N90-26708 #

CRIE-W-88037 ..... N90-26148 #
CRIE-W-88038 ..... N90-26149 #

CRIF-MC-88 ..... N90-26542 #

CS-TR-2462 ..... N90-26625 #
CS-TR-2483 ..... N90-26526* #

CSDL-T-1062 ..... N90-26033* #

CSG-122 ..... N90-26558* #

DE90-000354 ..... N90-26392 #
DE90-000485 ..... N90-26393 #
DE90-005239 ..... N90-26031 #
DE90-007801 ..... N90-26702 #
DE90-008925 ..... N90-26665 #
DE90-008968 ..... N90-26096 #
DE90-009212 ..... N90-26706 #
DE90-009424 ..... N90-26666 #
DE90-009741 ..... N90-26251 #
DE90-009996 ..... N90-26312 #
DE90-010003 ..... N90-26707 #
DE90-010071 ..... N90-26675 #
DE90-010149 ..... N90-26109 #
DE90-010348 ..... N90-26626 #
DE90-010457 ..... N90-26676 #
DE90-010499 ..... N90-26132* #
DE90-010536 ..... N90-26562 #
DE90-010832 ..... N90-26097 #
DE90-011053 ..... N90-26133 #
DE90-011147 ..... N90-26667 #
DE90-011256 ..... N90-26134 #
DE90-011291 ..... N90-26529 #
DE90-011747 ..... N90-26252 #
DE90-011754 ..... N90-26112 #
DE90-011755 ..... N90-26530 #
DE90-011763 ..... N90-26531 #
DE90-011782 ..... N90-26386 #
DE90-011783 ..... N90-25941 #
DE90-011786 ..... N90-26387 #
DE90-011795 ..... N90-26514 #
DE90-011797 ..... N90-26532 #
DE90-011804 ..... N90-26119 #
DE90-011807 ..... N90-26673 #
DE90-011809 ..... N90-26116 #
DE90-011868 ..... N90-26699 #
DE90-011902 ..... N90-26135 #
DE90-011964 ..... N90-26690 #
DE90-011970 ..... N90-26310 #
DE90-011979 ..... N90-26732 #
DE90-012029 ..... N90-26084 #
DE90-012102 ..... N90-26434 #
DE90-012193 ..... N90-26136 #
DE90-012268 ..... N90-26117 #
DE90-012294 ..... N90-26674 #
DE90-012399 ..... N90-26481 #
DE90-012431 ..... N90-26645 #
DE90-012432 ..... N90-26646 #
DE90-012433 ..... N90-26647 #
DE90-012459 ..... N90-26137 #
DE90-012464 ..... N90-26110 #
DE90-012713 ..... N90-26658 #
DE90-012721 ..... N90-26138 #
DE90-012726 ..... N90-26139 #
DE90-012727 ..... N90-26668 #
DE90-012784 ..... N90-26360 #
DE90-012898 ..... N90-26113 #
DE90-012899 ..... N90-26111 #
DE90-012902 ..... N90-26146 #
DE90-012903 ..... N90-26596 #
DE90-012919 ..... N90-26669 #
DE90-012921 ..... N90-26311 #
DE90-012951 ..... N90-26081 #
DE90-012953 ..... N90-26670 #
DE90-012954 ..... N90-26347 #
DE90-012960 ..... N90-26140 #
DE90-012961 ..... N90-26141 #
DE90-012972 ..... N90-26671 #
DE90-012993 ..... N90-26786 #
DE90-012996 ..... N90-26537 #
DE90-012997 ..... N90-26143 #
DE90-013048 ..... N90-26659 #
DE90-013051 ..... N90-26538 #
DE90-013070 ..... N90-26389 #
DE90-013086 ..... N90-26390 #
DE90-013089 ..... N90-26043 #
DE90-013153 ..... N90-26627 #
DE90-013157 ..... N90-26438 #
DE90-013158 ..... N90-26439 #
DE90-013164 ..... N90-26539 #
DE90-013172 ..... N90-26118 #
DE90-013182 ..... N90-26597 #
DE90-013197 ..... N90-26144 #
DE90-013271 ..... N90-26565 #
DE90-013297 ..... N90-26660 #
DE90-013319 ..... N90-26742 #
DE90-013322 ..... N90-26648 #
DE90-013324 ..... N90-26540 #
DE90-013473 ..... N90-26787 #
DE90-013481 ..... N90-26114 #
DE90-013488 ..... N90-26300 #
DE90-013489 ..... N90-26314 #
DE90-013490 ..... N90-26315 #
DE90-013493 ..... N90-26661 #
DE90-013494 ..... N90-26145 #
DE90-013522 ..... N90-26313 #
DE90-013699 ..... N90-26482 #
DE90-503032 ..... N90-26255 #
DE90-503377 ..... N90-26335 #
DE90-503402 ..... N90-26147 #
DE90-503417 ..... N90-26708 #
DE90-503441 ..... N90-26148 #
DE90-503442 ..... N90-26149 #
DE90-503592 ..... N90-26336 #
DE90-503792 ..... N90-26365 #
DE90-505514 ..... N90-25949 #
DE90-505519 ..... N90-25983 #
DE90-505520 ..... N90-25984 #
DE90-505521 ..... N90-26085 #
DE90-505522 ..... N90-26086 #
DE90-505523 ..... N90-26034 #
DE90-505525 ..... N90-26072 #
DE90-625593 ..... N90-26736 #
DE90-626245 ..... N90-26672 #
DE90-786180 ..... N90-26388 #

DFVLR-MITT-89-02-REV ..... N90-26173 #

DLR-FB-89-51 ..... N90-26394 #
DLR-FB-90-01 ..... N90-26006 #
DLR-FB-90-020 ..... N90-26678 #

DOE/ER-03130/51 ..... N90-26540 #
DOE/ER-03130/453 ..... N90-26648 #
DOE/ER-03130/454 ..... N90-26742 #
DOE/ER-13594/3 ..... N90-26482 #
DOE/ER-13785/3 ..... N90-26481 #
DOE/ER-45214/5 ..... N90-26111 #
DOE/ER-45292/11 ..... N90-26137 #
DOE/ER-45355/2 ..... N90-26113 #

DOE/ID-12754/T1-VOL-2 ..... N90-26645 #
DOE/ID-12754/T2-VOL-3 ..... N90-26646 #
DOE/ID-12754/T3-SUPPL ..... N90-26647 #

DOE/METC-90-0267 ..... N90-26393 #

DOE/NASA/0335-2 ..... N90-26728* #
DOE/NASA/33408-4 ..... N90-26729* #

DOE/SF-17128/T2 ..... N90-26312 #

DOT/FAA/CT-TN89/72 ..... N90-26210 #

DOT/FAA/CT-89/35 ..... N90-25961 #

DR-5-3 ..... N90-26324* #
DR-5-3-TYPE-2 ..... N90-26325* #

DTRC/SME-89/111 ..... N90-26124 #

E-4367 ..... N90-26172* #
E-5038 ..... N90-26359* #
E-5095 ..... N90-26054* #
E-5155 ..... N90-25948* #
E-5249 ..... N90-26275* #
E-5279 ..... N90-26373* #
E-5405 ..... N90-26334* #
E-5428 ..... N90-25940* #
E-5430 ..... N90-25982* #
E-5446 ..... N90-26635* #
E-5474 ..... N90-26279* #
E-5478 ..... N90-26070* #
E-5500 ..... N90-26250* #
E-5517 ..... N90-26278* #
E-5527 ..... N90-26282* #
E-5547 ..... N90-26068* #
E-5547 ..... N90-26338* #
E-5551 ..... N90-26170* #
E-5570 ..... N90-26030* #
E-5573 ..... N90-26729* #
E-5575 ..... N90-26163* #
E-5577 ..... N90-26063* #
E-5594 ..... N90-26011* #
E-5607 ..... N90-26065* #
E-5608 ..... N90-26074* #
E-5615 ..... N90-26789* #
E-5616 ..... N90-26299* #
E-5617 ..... N90-26276* #
E-5618 ..... N90-26396* #
E-5621 ..... N90-26142* #
E-5623 ..... N90-26009* #
E-5624 ..... N90-26069* #
E-5626 ..... N90-26273* #
E-5629 ..... N90-26160* #
E-5634 ..... N90-26055* #
E-5637 ..... N90-26682* #
E-5641 ..... N90-26364* #
E-5645 ..... N90-26614* #
E-5647 ..... N90-26615* #
E-5656 ..... N90-26397* #
E-5658 ..... N90-26616* #
E-5659 ..... N90-26071* #
E-5668 ..... N90-26272* #
E-5672 ..... N90-26683* #
E-5676 ..... N90-25946* #

ECS-1012 ..... N90-26325* #

EE-SATCOM-90-2 ..... N90-26213* #

EGG-M-89196 ..... N90-26347 #
EGG-M-89242 ..... N90-26043 #
EGG-M-89513 ..... N90-26140 #

EGG-M-89514 ..... N90-26141 #
EGG-M-89521 ..... N90-26390 #
EGG-M-90175 ..... N90-26670 #

EGG-MS-8933 ..... N90-26081 #

ENAE-412 ..... N90-26026* #
ENAE-412 ..... N90-26027* #

ESA-SP-305 ..... N90-26711 #

ESA-TT-1154-REV ..... N90-26173 #

ESD-TR-90-051 ..... N90-26319 #

ETDE/PUB-1 ..... N90-26706 #

ETL-0568 ..... N90-26385 #

ETN-90-96960 ..... N90-25965 #
ETN-90-96961 ..... N90-25974 #
ETN-90-96962 ..... N90-25975 #
ETN-90-96963 ..... N90-26236 #
ETN-90-96964 ..... N90-26237 #
ETN-90-96965 ..... N90-26283 #
ETN-90-96966 ..... N90-25976 #
ETN-90-96967 ..... N90-26598 #
ETN-90-96969 ..... N90-26450 #
ETN-90-96970 ..... N90-26029 #
ETN-90-96979 ..... N90-26711 #
ETN-90-96988 ..... N90-26253 #
ETN-90-97001 ..... N90-25985 #
ETN-90-97002 ..... N90-25995 #
ETN-90-97003 ..... N90-26366 #
ETN-90-97005 ..... N90-26394 #
ETN-90-97012 ..... N90-26006 #
ETN-90-97013 ..... N90-26678 #
ETN-90-97021 ..... N90-26015 #
ETN-90-97022 ..... N90-26679 #
ETN-90-97023 ..... N90-26287 #
ETN-90-97024 ..... N90-25942 #
ETN-90-97032 ..... N90-26541 #
ETN-90-97035 ..... N90-26502 #
ETN-90-97036 ..... N90-26553 #
ETN-90-97038 ..... N90-26403 #
ETN-90-97057 ..... N90-26579 #
ETN-90-97058 ..... N90-26580 #
ETN-90-97060 ..... N90-26548 #
ETN-90-97064 ..... N90-26288 #
ETN-90-97065 ..... N90-26662 #
ETN-90-97066 ..... N90-25953 #
ETN-90-97067 ..... N90-26121 #
ETN-90-97068 ..... N90-26007 #
ETN-90-97069 ..... N90-26122 #
ETN-90-97087 ..... N90-26542 #
ETN-90-97093 ..... N90-26636 #
ETN-90-97098 ..... N90-26395 #
ETN-90-97099 ..... N90-26153 #
ETN-90-97122 ..... N90-26014 #
ETN-90-97123 ..... N90-26337 #
ETN-90-97124 ..... N90-26599 #
ETN-90-97125 ..... N90-26600 #
ETN-90-97126 ..... N90-26601 #
ETN-90-97127 ..... N90-26284 #
ETN-90-97128 ..... N90-26543 #
ETN-90-97129 ..... N90-26691 #
ETN-90-97130 ..... N90-26692 #
ETN-90-97131 ..... N90-26583 #
ETN-90-97132 ..... N90-26654 #
ETN-90-97133 ..... N90-26544 #
ETN-90-97134 ..... N90-26695 #
ETN-90-97135 ..... N90-26087 #
ETN-90-97136 ..... N90-26696 #
ETN-90-97137 ..... N90-26301 #
ETN-90-97138 ..... N90-26150 #
ETN-90-97139 ..... N90-26348 #
ETN-90-97140 ..... N90-26349 #
ETN-90-97141 ..... N90-26120 #
ETN-90-97143 ..... N90-25977 #
ETN-90-97144 ..... N90-26174 #
ETN-90-97145 ..... N90-25999 #
ETN-90-97146 ..... N90-26637 #
ETN-90-97147 ..... N90-26000 #
ETN-90-97148 ..... N90-26001 #
ETN-90-97149 ..... N90-26367 #
ETN-90-97151 ..... N90-26709 #
ETN-90-97152 ..... N90-26002 #
ETN-90-97153 ..... N90-26302 #
ETN-90-97154 ..... N90-26303 #
ETN-90-97155 ..... N90-26003 #
ETN-90-97156 ..... N90-26004 #
ETN-90-97157 ..... N90-26005 #
ETN-90-97159 ..... N90-26289 #
ETN-90-97179 ..... N90-26655 #
ETN-90-97180 ..... N90-26368 #
ETN-90-97181 ..... N90-26369 #
ETN-90-97182 ..... N90-26151 #
ETN-90-97183 ..... N90-26285 #
ETN-90-97184 ..... N90-26370 #
ETN-90-97186 ..... N90-25960 #
ETN-90-97187 ..... N90-26290 #
ETN-90-97189 ..... N90-25961 #
ETN-90-97191 ..... N90-26175 #
ETN-90-97192 ..... N90-26238 #
ETN-90-97193 ..... N90-26350 #
ETN-90-97194 ..... N90-25962 #
ETN-90-97195 ..... N90-26584 #
ETN-90-97196 ..... N90-26585 #
ETN-90-97197 ..... N90-26586 #
ETN-90-97198 ..... N90-26239 #
ETN-90-97199 ..... N90-26256 #
ETN-90-97200 ..... N90-26545 #
ETN-90-97201 ..... N90-26586 #
ETN-90-97202 ..... N90-26240 #
ETN-90-97203 ..... N90-26587 #
ETN-90-97204 ..... N90-26546 #
ETN-90-97205 ..... N90-26257 #
ETN-90-97206 ..... N90-26547 #
ETN-90-97207 ..... N90-26516 #
ETN-90-97208 ..... N90-26256 #
ETN-90-97209 ..... N90-26259 #
ETN-90-97210 ..... N90-26589 #
ETN-90-97211 ..... N90-26152 #
ETN-90-97212 ..... N90-26602 #
ETN-90-97213 ..... N90-26241 #
ETN-90-97214 ..... N90-26260 #
ETN-90-97215 ..... N90-26656 #
ETN-90-97216 ..... N90-26242 #
ETN-90-97217 ..... N90-26286 #
ETN-90-97218 ..... N90-26638 #
ETN-90-97220 ..... N90-26588 #
ETN-90-97223 ..... N90-26352 #
ETN-90-97224 ..... N90-26603 #
ETN-90-97225 ..... N90-26604 #
ETN-90-97226 ..... N90-26605 #
ETN-90-97227 ..... N90-26606 #
ETN-90-97228 ..... N90-26549 #
ETN-90-97229 ..... N90-26353 #
ETN-90-97230 ..... N90-26607 #
ETN-90-97231 ..... N90-26608 #
ETN-90-97234 ..... N90-26550 #
ETN-90-97235 ..... N90-26570 #
ETN-90-97236 ..... N90-26383 #
ETN-90-97237 ..... N90-26551 #
ETN-90-97238 ..... N90-26571 #
ETN-90-97239 ..... N90-26572 #
ETN-90-97240 ..... N90-26609 #
ETN-90-97241 ..... N90-26552 #
ETN-90-97242 ..... N90-26680 #
ETN-90-97243 ..... N90-26553 #
ETN-90-97244 ..... N90-26620 #
ETN-90-97245 ..... N90-26587 #
ETN-90-97246 ..... N90-26588 #
ETN-90-97247 ..... N90-26610 #
ETN-90-97248 ..... N90-26517 #
ETN-90-97249 ..... N90-26611 #
ETN-90-97250 ..... N90-26612 #
ETN-90-97251 ..... N90-26554 #
ETN-90-97252 ..... N90-26573 #
ETN-90-97253 ..... N90-26589 #
ETN-90-97254 ..... N90-26057 #
ETN-90-97255 ..... N90-26574 #
ETN-90-97256 ..... N90-26281 #
ETN-90-97257 ..... N90-26575 #
ETN-90-97258 ..... N90-26555 #
ETN-90-97259 ..... N90-26681 #
ETN-90-97260 ..... N90-26123 #
ETN-90-97261 ..... N90-26154 #
ETN-90-97262 ..... N90-26440 #
ETN-90-97263 ..... N90-26677 #
ETN-90-97264 ..... N90-26351 #
ETN-90-97269 ..... N90-26371 #
ETN-90-97270 ..... N90-25978 #
ETN-90-97272 ..... N90-26035 #
ETN-90-97277 ..... N90-26016 #
ETN-90-97278 ..... N90-26058 #
ETN-90-97279 ..... N90-26059 #
ETN-90-97280 ..... N90-26060 #
ETN-90-97281 ..... N90-26164 #
ETN-90-97282 ..... N90-26291 #
ETN-90-97283 ..... N90-26008 #
ETN-90-97284 ..... N90-26613 #
ETN-90-97309 ..... N90-26262 #
ETN-90-97357 ..... N90-26173 #

EUT-88-E-211 ..... N90-26584 #
EUT-88-E-212 ..... N90-26585 #
EUT-88-E-213 ..... N90-26586 #
EUT-89-E-214 ..... N90-26239 #
EUT-89-E-215 ..... N90-26256 #
EUT-89-E-216 ..... N90-26545 #
EUT-89-E-217 ..... N90-26586 #
EUT-89-E-218 ..... N90-26240 #
EUT-89-E-219 ..... N90-26587 #
EUT-89-E-220 ..... N90-26546 #
EUT-89-E-221 ..... N90-26257 #
EUT-89-E-222 ..... N90-26547 #
EUT-89-E-223 ..... N90-26516 #
EUT-89-E-225 ..... N90-26256 #
EUT-89-E-226 ..... N90-26259 #
EUT-89-E-230 ..... N90-26589 #

FERMILAB-PUB-90/53-A ..... N90-26734* #
FERMILAB-PUB-90/98-A-2 ..... N90-26735* #

FFA-TN-1990-01 ..... N90-26636 #

FFI-89/7019 ..... N90-26541 #
FFI-90/7002 ..... N90-26502 #

FIM-209 ..... N90-26385 #

FJSRL-TR-90-0001 ..... N90-26267 #

FOA-C-20779-2.1 ..... N90-26395 #
FOA-C-20780-2.1 ..... N90-26153 #

FTD-ID(RS)T-0266-90 ..... N90-25955 #

GA-A-20085 ..... N90-26660 #

GAO/IMTEC-89-41 ..... N90-26215 #
GAO/IMTEC-90-1 ..... N90-26704 #
GAO/IMTEC-90-18 ..... N90-26024 #

GAO/NSIAD-88-129FS ..... N90-26023 #
GAO/NSIAD-88-130FS ..... N90-26022 #
GAO/NSIAD-88-137FS ..... N90-26021 #
GAO/NSIAD-88-138FS ..... N90-26025 #
GAO/NSIAD-89-89 ..... N90-26066 #
GAO/NSIAD-90-40 ..... N90-26169 #
GAO/NSIAD-90-142 ..... N90-26298 #
GAO/NSIAD-90-192 ..... N90-26041 #

GAO/RCED-89-112 ..... N90-25959 #
GAO/RCED-89-113FS ..... N90-25958 #

GARRETT-31-8071(2) ..... N90-26728* #

GKSS-89/E/47 ..... N90-26029 #

GL-ERP-1052-VOL-1 ..... N90-25962 #
GL-ERP-1052-VOL-2 ..... N90-25963 #

GL-TR-90-0032(1)-VOL-1 ..... N90-25962 #
GL-TR-90-0032(2)-VOL-2 ..... N90-25963 #
GL-TR-90-0045 ..... N90-26629 #
GL-TR-90-0057 ..... N90-26442 #

GRASP-LAB-173 ..... N90-26497* #
GRASP-LAB-190 ..... N90-26498* #

H-1590 ..... N90-25973* #
H-1594 ..... N90-26564* #

IAF-89-083 ..... N90-26058 #
IAF-89-212 ..... N90-26035 #
IAF-89-431 ..... N90-26164 #
IAF-89-489 ..... N90-26060 #

IAR-89-4-PT-1 ..... N90-26078 #
IAR-89-4-PT-2 ..... N90-26079 #
IAR-89-18 ..... N90-25969 #
IAR-89-19 ..... N90-25956 #
IAR-89-21 ..... N90-26493 #
IAR-89-24 ..... N90-26107 #
IAR-89-25 ..... N90-26357 #
IAR-90-2 ..... N90-26268 #
IAR-90-4 ..... N90-26345 #

ICASE-88-70-REV ..... N90-26509* #
ICASE-90-34 ..... N90-26509* #
ICASE-90-44 ..... N90-26595* #
ICASE-90-46 ..... N90-26270* #
ICASE-90-48 ..... N90-26533* #

ICOMP-89-29 ..... N90-25948* #
ICOMP-90-15 ..... N90-26282* #
ICOMP-90-18 ..... N90-26614* #
ICOMP-90-19 ..... N90-26615* #
ICOMP-90-20 ..... N90-26616* #

IIHR-334-I-VOL-1 ..... N90-26294 #

ILR-MITT-227(1989) ..... N90-26366 #

IMAG-RR-781-M ..... N90-26352 #
IMAG-RR-785-I ..... N90-26550 #

IMAG-RR-786-I ..... N90-26572 #
IMAG-RR-791-M ..... N90-26604 #
IMAG-RR-792-M-PT-2 ..... N90-26605 #
IMAG-RR-793-M ..... N90-26606 #
IMAG-RR-794-M ..... N90-26549 #
IMAG-RR-795-M ..... N90-26353 #
IMAG-RR-796-M ..... N90-26570 #
IMAG-RR-797-M ..... N90-26607 #
IMAG-RR-798-M ..... N90-26608 #
IMAG-RR-970-M ..... N90-26603 #

INIS-BR-1979 ..... N90-26672 #

INPE-4913-PRE/1514 ..... N90-26381 #
INPE-4976-PRE/1541 ..... N90-26379 #
INPE-4986-PRE/1548 ..... N90-26380 #

INT-PATENT-CLASS-B23K-9/24 ..... N90-26168*

IS-T-1354 ..... N90-26116 #
IS-T-1437 ..... N90-26252 #
IS-T-1476 ..... N90-26119 #
IS-T-1478 ..... N90-26673 #

ISAL-90-0006 ..... N90-26154 #

ISBN-0-938744-69-0 ..... N90-26499* #
ISBN-90-6144-211-7 ..... N90-26584 #
ISBN-90-6144-212-5 ..... N90-26585 #
ISBN-90-6144-213-3 ..... N90-26586 #
ISBN-90-6144-214-1 ..... N90-26239 #
ISBN-90-6144-215-X ..... N90-26256 #
ISBN-90-6144-216-8 ..... N90-26545 #
ISBN-90-6144-217-6 ..... N90-26566 #
ISBN-90-6144-218-4 ..... N90-26240 #
ISBN-90-6144-219-2 ..... N90-26567 #
ISBN-90-6144-220-6 ..... N90-26546 #
ISBN-90-6144-221-4 ..... N90-26257 #
ISBN-90-6144-222-2 ..... N90-26547 #
ISBN-90-6144-223-0 ..... N90-26516 #
ISBN-90-6144-225-7 ..... N90-26258 #
ISBN-90-6144-226-5 ..... N90-26259 #
ISBN-90-6144-230-3 ..... N90-26569 #
ISBN-90-9002864-1 ..... N90-26241 #
ISBN-90-9002955-9 ..... N90-26260 #
ISBN-92-835-0511-5 ..... N90-26178 #
ISBN-92-835-0557-3 ..... N90-25947 #
ISBN-92-835-0559-X ..... N90-26012 #
ISBN-92-835-0560-3 ..... N90-26280 #
ISBN-92-9092-062-9 ..... N90-26711 #
ISBN-951-38-3492-1 ..... N90-26253 #

ISI/RR-89-242 ..... N90-26733 #

ISL-CO-210/9 ..... N90-26679 #
ISL-CO-255/88 ..... N90-26015 #

ISL-PU-310/89 ..... N90-25942 #

ISL-R-103/89 ..... N90-26287 #

ISSN-0171-1342 ..... N90-26394 #

ISSN-0069-5882 ..... N90-26450 #
ISSN-0078-3781 ..... N90-26123 #
ISSN-0082-5255 ..... N90-25935
ISSN-0082-5255 ..... N90-26650
ISSN-0167-9708 ..... N90-26239 #
ISSN-0167-9708 ..... N90-26240 #
ISSN-0167-9708 ..... N90-26256 #
ISSN-0167-9708 ..... N90-26257 #
ISSN-0167-9708 ..... N90-26258 #
ISSN-0167-9708 ..... N90-26259 #
ISSN-0167-9708 ..... N90-26516 #
ISSN-0167-9708 ..... N90-26545 #
ISSN-0167-9708 ..... N90-26546 #
ISSN-0167-9708 ..... N90-26547 #
ISSN-0167-9708 ..... N90-26566 #
ISSN-0167-9708 ..... N90-26567 #
ISSN-0167-9708 ..... N90-26569 #
ISSN-0167-9708 ..... N90-26584 #
ISSN-0167-9708 ..... N90-26585 #
ISSN-0167-9708 ..... N90-26586 #
ISSN-0171-1342 ..... N90-26006 #
ISSN-0171-1342 ..... N90-26678 #
ISSN-0280-445X ..... N90-26403 #
ISSN-0344-9629 ..... N90-26029 #
ISSN-0347-3694 ..... N90-26153 #
ISSN-0347-3694 ..... N90-26395 #
ISSN-0358-5077 ..... N90-26253 #
ISSN-0377-8312 ..... N90-25985 #
ISSN-0377-8312 ..... N90-25995 #
ISSN-0379-6566 ..... N90-26711 #
ISSN-0389-4010 ..... N90-25984 #
ISSN-0389-4010 ..... N90-26034 #
ISSN-0389-4010 ..... N90-26072 #
ISSN-0389-4010 ..... N90-26085 #
ISSN-0389-4010 ..... N90-26086 #
ISSN-0452-2982 ..... N90-25949 #
ISSN-0452-2982 ..... N90-25983 #
ISSN-0802-2437 ..... N90-26502 #
ISSN-0802-2437 ..... N90-26541 #

JPL-PUBL-89-15 ..... N90-26705* #
JPL-PUBL-89-44 ..... N90-26701* #

JPL-TDA-PR-42-101 ..... N90-26217* #

K/DSRD-419 ..... N90-26565 #

KCP-613-4278 ..... N90-26537 #

KFY-FR ..... N90-26095* #

KU-FRL-872-1 ..... N90-25943* #

L-16617 ..... N90-26710* #
L-16661 ..... N90-26036* #
L-16772 ..... N90-26296* #
L-16777 ..... N90-26077* #
L-16800 ..... N90-25938* #

LA-UR-90-964 ..... N90-26665 #
LA-UR-90-1068 ..... N90-26096 #
LA-UR-90-1589 ..... N90-26690 #
LA-UR-90-1634 ..... N90-26732 #
LA-UR-90-1692 ..... N90-26310 #
LA-UR-90-1866 ..... N90-26434 #
LA-UR-90-1960 ..... N90-26597 #
LA-UR-90-2009 ..... N90-26118 #
LA-UR-90-2061 ..... N90-26539 #
LA-UR-90-2131 ..... N90-26439 #
LA-UR-90-2132 ..... N90-26438 #
LA-UR-90-2159 ..... N90-26627 #
LA-UR-90-2178 ..... N90-26659 #

LAAS-89386 ..... N90-26555 #
LAAS-90051 ..... N90-26681 #

LIDS-TH-1976 ..... N90-26697 #

LIP-740 ..... N90-26738* #

LPI-TR-90-01 ..... N90-26740* #
LPI-TR-90-02 ..... N90-26437* #
LPI-TR-90-03 ..... N90-26739* #

LR-512 ..... N90-26289 #
LR-616 ..... N90-26655 #
LR-617 ..... N90-26368 #
LR-619 ..... N90-26369 #
LR-620 ..... N90-26151 #

MATHS-REPT-A-106 ..... N90-26014 #
MATHS-REPT-A-107 ..... N90-26337 #
MATHS-REPT-A-110 ..... N90-26599 #
MATHS-REPT-A-112 ..... N90-26600 #
MATHS-REPT-A-113 ..... N90-26601 #
MATHS-REPT-A-117 ..... N90-26284 #
MATHS-REPT-A-118-PT-2 ..... N90-26543 #
MATHS-REPT-A-119 ..... N90-26691 #
MATHS-REPT-A-121 ..... N90-26692 #
MATHS-REPT-A-122 ..... N90-26583 #

MCR-88-612 ..... N90-26577* #

ME-4182 ..... N90-26128* #
ME-4182 ..... N90-26165* #
ME-4182 ..... N90-26321* #
ME-4182 ..... N90-26322* #
ME-8501 ..... N90-26323* #

MEG0931 ..... N90-26544 #

MIT/LCS/TM-429 ..... N90-26520 #

MIT/LCS/TR-465 ..... N90-26696* #

MP-88-279 ..... N90-26093* #

MS-CIS-89-04 ..... N90-26497* #
MS-CIS-89-51 ..... N90-26498* #

MTL-TR-90-20 ..... N90-26126 #

NAL-TM-SE-8902 ..... N90-26523 #

NAL-TM-608 ..... N90-25949 #
NAL-TM-609 ..... N90-25983 #

NAL-TR-1021T ..... N90-25984 #
NAL-TR-1023 ..... N90-26335 #
NAL-TR-1029T ..... N90-26085 #
NAL-TR-1030-PT-2 ..... N90-26086 #
NAL-TR-1031 ..... N90-26034 #
NAL-TR-1036 ..... N90-26072 #

NAS 1.15:4197 ..... N90-26296* #
NAS 1.15:4205 ..... N90-26730* #
NAS 1.15:4211 ..... N90-26743* #
NAS 1.15:89715 ..... N90-26693* #
NAS 1.15:100405 ..... N90-26741* #
NAS 1.15:101344 ..... N90-26172* #
NAS 1.15:101644 ..... N90-26167* #
NAS 1.15:101718 ..... N90-25973* #
NAS 1.15:101719 ..... N90-26564* #
NAS 1.15:101800 ..... N90-26083* #
NAS 1.15:101886 ..... N90-25972* #
NAS 1.15:101914 ..... N90-26132* #
NAS 1.15:102254 ..... N90-26452* #
NAS 1.15:102369 ..... N90-26359* #
NAS 1.15:102402 ..... N90-25948* #
NAS 1.15:102486 ..... N90-26054* #
NAS 1.15:102488 ..... N90-26373* #
NAS 1.15:102592 ..... N90-26076* #
NAS 1.15:102629 ..... N90-25981* #
NAS 1.15:102654 ..... N90-26361* #
NAS 1.15:102685 ..... N90-26511* #
NAS 1.15:102694 ..... N90-26082* #
NAS 1.15:102695 ..... N90-26362* #
NAS 1.15:102697 ..... N90-26363* #
NAS 1.15:102700 ..... N90-26032* #
NAS 1.15:102790 ..... N90-26040* #
NAS 1.15:102822 ..... N90-26274* #
NAS 1.15:102827 ..... N90-25933* #
NAS 1.15:102834 ..... N90-25945* #
NAS 1.15:103104 ..... N90-26275* #
NAS 1.15:103105 ..... N90-25982* #
NAS 1.15:103106 ..... N90-26334* #
NAS 1.15:103124 ..... N90-26279* #
NAS 1.15:103135 ..... N90-26070* #
NAS 1.15:103137 ..... N90-26635* #
NAS 1.15:103147 ..... N90-26250* #
NAS 1.15:103155 ..... N90-26278* #
NAS 1.15:103159 ..... N90-26282* #
NAS 1.15:103173 ..... N90-26170* #
NAS 1.15:103178 ..... N90-26338* #
NAS 1.15:103187 ..... N90-26030* #
NAS 1.15:103188 ..... N90-26729* #
NAS 1.15:103189 ..... N90-26163* #
NAS 1.15:103198 ..... N90-26011* #
NAS 1.15:103202 ..... N90-26065* #
NAS 1.15:103203 ..... N90-26074* #
NAS 1.15:103205 ..... N90-26068* #
NAS 1.15:103207 ..... N90-26789* #
NAS 1.15:103208 ..... N90-26299* #
NAS 1.15:103209 ..... N90-26276* #
NAS 1.15:103210 ..... N90-26396* #
NAS 1.15:103212 ..... N90-26009* #
NAS 1.15:103213 ..... N90-26069* #
NAS 1.15:103215 ..... N90-26273* #
NAS 1.15:103217 ..... N90-26160* #
NAS 1.15:103220 ..... N90-26055* #
NAS 1.15:103223 ..... N90-26682* #
NAS 1.15:103225 ..... N90-26364* #
NAS 1.15:103229 ..... N90-26614* #
NAS 1.15:103231 ..... N90-26615* #
NAS 1.15:103237 ..... N90-26397* #
NAS 1.15:103240 ..... N90-26616* #
NAS 1.15:103241 ..... N90-26071* #
NAS 1.15:103246 ..... N90-26683* #
NAS 1.15:103249 ..... N90-25946* #
NAS 1.15:103465 ..... N90-26432* #
NAS 1.15:103466 ..... N90-26619* #
NAS 1.15:103467 ..... N90-26129* #
NAS 1.15:103468 ..... N90-26446* #
NAS 1.15:103469 ..... N90-26447* #
NAS 1.15:103470 ..... N90-26399* #
NAS 1.15:103471 ..... N90-26485* #
NAS 1.15:103472 ..... N90-26080* #
NAS 1.15:103473 ..... N90-26130* #
NAS 1.15:103475 ..... N90-26651* #
NAS 1.15:103476 ..... N90-26400* #
NAS 1.15:103477 ..... N90-26401* #
NAS 1.15:103478 ..... N90-26402* #
NAS 1.15:103479 ..... N90-26214* #
NAS 1.15:103480 ..... N90-26094* #
NAS 1.15:103481 ..... N90-26433* #
NAS 1.15:103482 ..... N90-26640* #
NAS 1.15:103484 ..... N90-26131* #
NAS 1.15:103486 ..... N90-25957* #
NAS 1.15:103487 ..... N90-26309* #
NAS 1.15:103493 ..... N90-26785* #
NAS 1.15:103496 ..... N90-26480* #
NAS 1.21:7039(37)-SECT-2 ..... N90-26700*
NAS 1.21:7046(22) N90-26056*
NAS 1.21:7084 ..... N90-26710* #
NAS 1.26:4236 ..... N90-25966* #

NAS 1.26:4294 ..... N90-26019* #
NAS 1.26:4302 ..... N90-25940* #
NAS 1.26:4310 ..... N90-26046* #
NAS 1.26:4314 ..... N90-25939* #
NAS 1.26:180701 ..... N90-26522* #
NAS 1.26:180953 ..... N90-26378* #
NAS 1.26:181917 ..... N90-25944* #
NAS 1.26:182033 ..... N90-26632* #
NAS 1.26:182039 ..... N90-26509* #
NAS 1.26:182043 ..... N90-26577* #
NAS 1.26:182057 ..... N90-26510* #
NAS 1.26:182058 ..... N90-26527* #
NAS 1.26:182061 ..... N90-26595* #
NAS 1.26:182065 ..... N90-26061* #
NAS 1.26:182068 ..... N90-26270* #
NAS 1.26:182072 ..... N90-26533* #
NAS 1.26:182247 ..... N90-26355* #
NAS 1.26:182294 ..... N90-26320* #
NAS 1.26:182557 ..... N90-26323* #
NAS 1.26:182756 ..... N90-26322* #
NAS 1.26:182843 ..... N90-26735* #
NAS 1.26:183072 ..... N90-26321* #
NAS 1.26:183944 ..... N90-26064* #
NAS 1.26:183957 ..... N90-26325* #
NAS 1.26:183958 ..... N90-26324* #
NAS 1.26:183979 ..... N90-26067* #
NAS 1.26:183986 ..... N90-26095* #
NAS 1.26:183992 ..... N90-26108* #
NAS 1.26:183993 ..... N90-26271* #
NAS 1.26:184915 ..... N90-26737* #
NAS 1.26:184918 ..... N90-26740* #
NAS 1.26:184927 ..... N90-26165* #
NAS 1.26:185151 ..... N90-26581* #
NAS 1.26:185200 ..... N90-26171* #
NAS 1.26:185240 ..... N90-26728* #
NAS 1.26:185241 ..... N90-26633* #
NAS 1.26:185252 ..... N90-26269* #
NAS 1.26:185256 ..... N90-26063* #
NAS 1.26:185265 ..... N90-26372* #
NAS 1.26:185267 ..... N90-26142* #
NAS 1.26:185280 ..... N90-26272* #
NAS 1.26:185311 ..... N90-26649* #
NAS 1.26:185630 ..... N90-26033* #
NAS 1.26:185878 ..... N90-26582* #
NAS 1.26:186137 ..... N90-26512* #
NAS 1.26:186243 ..... N90-26663* #
NAS 1.26:186459 ..... N90-26354* #
NAS 1.26:186509 ..... N90-26391* #
NAS 1.26:186520 ..... N90-26052* #
NAS 1.26:186553 ..... N90-26558* #
NAS 1.26:186575 ..... N90-26739* #
NAS 1.26:186581 ..... N90-25934* #
NAS 1.26:186606 ..... N90-26734* #
NAS 1.26:186627 ..... N90-26535* #
NAS 1.26:186629 ..... N90-26705* #
NAS 1.26:186630 ..... N90-25943* #
NAS 1.26:186631 ..... N90-26437* #
NAS 1.26:186634 ..... N90-26306* #
NAS 1.26:186636 ..... N90-26731* #
NAS 1.26:186641 ..... N90-26213* #
NAS 1.26:186642 ..... N90-26344* #
NAS 1.26:186645 ..... N90-26524* #
NAS 1.26:186648 ..... N90-26376* #
NAS 1.26:186649 ..... N90-26375* #
NAS 1.26:186654 ..... N90-26045* #
NAS 1.26:186655 ..... N90-26479* #
NAS 1.26:186656 ..... N90-26490* #
NAS 1.26:186664 ..... N90-25968* #
NAS 1.26:186676 ..... N90-25967* #
NAS 1.26:186677-VOL-1 ..... N90-26039* #
NAS 1.26:186690 ..... N90-26128* #
NAS 1.26:186691 ..... N90-26044* #
NAS 1.26:186705 ..... N90-25970* #
NAS 1.26:186706 ..... N90-26525* #
NAS 1.26:186712 ..... N90-26308* #
NAS 1.26:186714 ..... N90-26115* #
NAS 1.26:186716 ..... N90-26254* #
NAS 1.26:186717 ..... N90-26435* #
NAS 1.26:186719 ..... N90-26534* #
NAS 1.26:186720 ..... N90-26234* #
NAS 1.26:186727 ..... N90-26784* #
NAS 1.26:186730 ..... N90-26492* #
NAS 1.26:186731 ..... N90-26664* #
NAS 1.26:186732 ..... N90-26634* #
NAS 1.26:186733 ..... N90-26526* #
NAS 1.26:186736 ..... N90-26698* #
NAS 1.26:186751 ..... N90-26047* #
NAS 1.26:186755 ..... N90-26536* #
NAS 1.26:186764 ..... N90-26358* #
NAS 1.26:186770 ..... N90-26093* #
NAS 1.26:186781 ..... N90-26513* #
NAS 1.26:186788 ..... N90-26689* #
NAS 1.26:186790 ..... N90-26048* #
NAS 1.26:186791 ..... N90-26488* #
NAS 1.26:186792 ..... N90-26448* #
NAS 1.26:186797 ..... N90-25964* #
NAS 1.26:186807 ..... N90-26329* #
NAS 1.26:186809 ..... N90-26328* #
NAS 1.26:186810 ..... N90-26377* #
NAS 1.26:186812 ..... N90-26578* #
NAS 1.26:186814 ..... N90-26449* #
NAS 1.26:186815 ..... N90-26451* #
NAS 1.26:186816 ..... N90-26051* #
NAS 1.26:186817-VOL-1 ..... N90-26332* #
NAS 1.26:186818 ..... N90-26501* #
NAS 1.26:186819 ..... N90-26053* #
NAS 1.26:186820-VOL-2 ..... N90-25971* #
NAS 1.26:186821 ..... N90-26436* #
NAS 1.26:186822 ..... N90-26042* #
NAS 1.26:186823 ..... N90-26050* #
NAS 1.26:186829 ..... N90-26049* #
NAS 1.26:186830 ..... N90-26161* #
NAS 1.26:186831 ..... N90-26499* #
NAS 1.26:186832 ..... N90-26330* #
NAS 1.26:186833-VOL-2 ..... N90-26333* #
NAS 1.26:186834 ..... N90-26500* #
NAS 1.26:186835 ..... N90-26162* #
NAS 1.26:186836 ..... N90-26026* #
NAS 1.26:186838 ..... N90-26027* #
NAS 1.26:186839 ..... N90-26331* #
NAS 1.26:186845 ..... N90-26563* #
NAS 1.26:186847 ..... N90-26216* #
NAS 1.26:186852 ..... N90-26217* #
NAS 1.26:186855 ..... N90-26701* #
NAS 1.26:186863 ..... N90-26528* #
NAS 1.26:186864 ..... N90-26498* #
NAS 1.26:186867 ..... N90-26497* #
NAS 1.26:186871 ..... N90-26233* #
NAS 1.26:186872 ..... N90-26515* #
NAS 1.26:186874 ..... N90-26738* #
NAS 1.26:186878 ..... N90-26013* #
NAS 1.26:186882 ..... N90-26652* #
NAS 1.26:186883 ..... N90-26235* #
NAS 1.26:186887 ..... N90-26281* #
NAS 1.26:186888 ..... N90-26382* #
NAS 1.26:186900 ..... N90-26017* #
NAS 1.26:186903 ..... N90-25954* #
NAS 1.26:186905 ..... N90-26503* #
NAS 1.55:3077 ..... N90-26744* #
NAS 1.55:3081 ..... N90-25980* #
NAS 1.55:10046 ..... N90-26075* #
NAS 1.60:3007 ..... N90-26077* #
NAS 1.60:3019 ..... N90-26036* #
NAS 1.60:3031 ..... N90-26028* #
NAS 1.60:3036 ..... N90-25938* #
NAS 1.71:MFS-28425-1 ..... N90-26304* #
NAS 1.71:MSC-21469-1 ..... N90-26340* #
NAS 1.71:MSC-21502-1 ..... N90-26341* #
NAS 1.71:MSC-21540-1 ..... N90-26342* #
NAS 1.71:MSC-21542-1 ..... N90-26073* #
NAS 1.71:NPO-17204-1-CU ..... N90-26292* #
NAS 1.71:NPO-17480-1-CU ..... N90-26098* #
NAS 1.71:NPO-17569-1-CU ..... N90-26176* #
NAS 1.71:NPO-17723-1-CU ..... N90-26685* #
NAS 1.71:NPO-17917-1-CU ..... N90-26339* #
NAS 1.71:NPO-17939-1-CU ..... N90-26518* #
NAS 1.71:NPO-17949-1-CU ..... N90-26684* #
NAS 1.71:NPO-17954-1-CU ..... N90-26519* #
NAS 1.71:NPO-17970-1-CU ..... N90-26384* #

NASA-CASE-MFS-28425-1 ..... N90-26304* #
NASA-CASE-MFS-29491-1 ..... N90-26168*

NASA-CASE-MSC-21469-1 ..... N90-26340* #
NASA-CASE-MSC-21502-1 ..... N90-26341* #
NASA-CASE-MSC-21540-1 ..... N90-26342* #
NASA-CASE-MSC-21542-1 ..... N90-26073* #

NASA-CASE-NPO-17204-1-CU ..... N90-26292* #
NASA-CASE-NPO-17480-1-CU ..... N90-26098* #
NASA-CASE-NPO-17569-1-CU ..... N90-26176* #
NASA-CASE-NPO-17723-1-CU ..... N90-26685* #
NASA-CASE-NPO-17917-1-CU ..... N90-26339* #
NASA-CASE-NPO-17939-1-CU ..... N90-26518* #
NASA-CASE-NPO-17949-1-CU ..... N90-26684* #
NASA-CASE-NPO-17954-1-CU ..... N90-26519* #
NASA-CASE-NPO-17970-1-CU ..... N90-26384* #

NASA-CP-3077 ..... N90-26744* #
NASA-CP-3081 ..... N90-25980* #
NASA-CP-10046 ..... N90-26075* #

NASA-CR-4236 ..... N90-25966* #
NASA-CR-4294 ..... N90-26019* #
NASA-CR-4302 ..... N90-25940* #
NASA-CR-4310 ..... N90-26046* #
NASA-CR-4314 ..... N90-25939* #
NASA-CR-180701 ..... N90-26522* #
NASA-CR-180953 ..... N90-26378* #
NASA-CR-181917 ..... N90-25944* #
NASA-CR-182033 ..... N90-26632* #
NASA-CR-182039 ..... N90-26509* #
NASA-CR-182043 ..... N90-26577* #
NASA-CR-182057 ..... N90-26510* #
NASA-CR-182058 ..... N90-26527* #
NASA-CR-182061 ..... N90-26595* #
NASA-CR-182065 ..... N90-26061* #
NASA-CR-182068 ..... N90-26270* #
NASA-CR-182072 ..... N90-26533* #
NASA-CR-182247 ..... N90-26355* #
NASA-CR-182294 ..... N90-26320* #
NASA-CR-182557 ..... N90-26323* #
NASA-CR-182756 ..... N90-26322* #
NASA-CR-182843 ..... N90-26735* #
NASA-CR-183072 ..... N90-26321* #
NASA-CR-183944 ..... N90-26064* #
NASA-CR-183957 ..... N90-26325* #
NASA-CR-183958 ..... N90-26324* #
NASA-CR-183979 ..... N90-26067* #
NASA-CR-183986 ..... N90-26095* #
NASA-CR-183992 ..... N90-26108* #
NASA-CR-183993 ..... N90-26271* #
NASA-CR-184915 ..... N90-26737* #
NASA-CR-184918 ..... N90-26740* #
NASA-CR-184927 ..... N90-26165* #
NASA-CR-185151 ..... N90-26581* #
NASA-CR-185200 ..... N90-26171* #
NASA-CR-185240 ..... N90-26728* #
NASA-CR-185241 ..... N90-26633* #
NASA-CR-185252 ..... N90-26269* #
NASA-CR-185256 ..... N90-26063* #
NASA-CR-185265 ..... N90-26372* #
NASA-CR-185267 ..... N90-26142* #
NASA-CR-185280 ..... N90-26272* #
NASA-CR-185311 ..... N90-26649* #
NASA-CR-185630 ..... N90-26033* #
NASA-CR-185878 ..... N90-26582* #
NASA-CR-186137 ..... N90-26512* #
NASA-CR-186243 ..... N90-26663* #
NASA-CR-186459 ..... N90-26354* #
NASA-CR-186509 ..... N90-26391* #
NASA-CR-186520 ..... N90-26052* #
NASA-CR-186553 ..... N90-26558* #
NASA-CR-186575 ..... N90-26739* #
NASA-CR-186581 ..... N90-25934* #
NASA-CR-186606 ..... N90-26734* #
NASA-CR-186627 ..... N90-26535* #
NASA-CR-186629 ..... N90-26705* #
NASA-CR-186630 ..... N90-25943* #
NASA-CR-186631 ..... N90-26437* #
NASA-CR-186634 ..... N90-26306* #
NASA-CR-186636 ..... N90-26731* #
NASA-CR-186641 ..... N90-26213* #
NASA-CR-186642 ..... N90-26344* #
NASA-CR-186645 ..... N90-26524* #
NASA-CR-186648 ..... N90-26376* #
NASA-CR-186649 ..... N90-26375* #
NASA-CR-186654 ..... N90-26045* #
NASA-CR-186655 ..... N90-26479* #
NASA-CR-186656 ..... N90-26490* #
NASA-CR-186664 ..... N90-25968* #
NASA-CR-186676 ..... N90-25967* #
NASA-CR-186677-VOL-1 ..... N90-26039* #
NASA-CR-186690 ..... N90-26128* #
NASA-CR-186691 ..... N90-26044* #
NASA-CR-186705 ..... N90-25970* #
NASA-CR-186706 ..... N90-26525* #
NASA-CR-186712 ..... N90-26308* #
NASA-CR-186714 ..... N90-26115* #
NASA-CR-186716 ..... N90-26254* #
NASA-CR-186717 ..... N90-26435* #
NASA-CR-186719 ..... N90-26534* #
NASA-CR-186720 ..... N90-26234* #
NASA-CR-186727 ..... N90-26784* #
NASA-CR-186730 ..... N90-26492* #
NASA-CR-186731 ..... N90-26664* #
NASA-CR-186732 ..... N90-26634* #
NASA-CR-186733 ..... N90-26526* #
NASA-CR-186736 ..... N90-26698* #
NASA-CR-186751 ..... N90-26047* #
NASA-CR-186755 ..... N90-26536* #
NASA-CR-186764 ..... N90-26358* #
NASA-CR-186770 ..... N90-26093* #
NASA-CR-186781 ..... N90-26513* #
NASA-CR-186788 ..... N90-26689* #
NASA-CR-186790 ..... N90-26048* #
NASA-CR-186791 ..... N90-26488* #
NASA-CR-186792 ..... N90-26448* #
NASA-CR-186797 ..... N90-25964* #
NASA-CR-186807 ..... N90-26329* #
NASA-CR-186809 ..... N90-26328* #
NASA-CR-186810 ..... N90-26377* #
NASA-CR-186812 ..... N90-26578* #
NASA-CR-186814 ..... N90-26449* #
NASA-CR-186815 ..... N90-26451* #
NASA-CR-186816 ..... N90-26051* #
NASA-CR-186817-VOL-1 ..... N90-26332* #
NASA-CR-186818 ..... N90-26501* #

NASA-CR-186819 ..... N90-26053* #
NASA-CR-186820-VOL-2 ..... N90-25971* #
NASA-CR-186821 ..... N90-26436* #
NASA-CR-186822 ..... N90-26042* #
NASA-CR-186823 ..... N90-26050* #
NASA-CR-186829 ..... N90-26049* #
NASA-CR-186830 ..... N90-26161* #
NASA-CR-186831 ..... N90-26499* #
NASA-CR-186832 ..... N90-26330* #
NASA-CR-186833-VOL-2 ..... N90-26333* #
NASA-CR-186834 ..... N90-26500* #
NASA-CR-186835 ..... N90-26162* #
NASA-CR-186836 ..... N90-26026* #
NASA-CR-186838 ..... N90-26027* #
NASA-CR-186839 ..... N90-26331* #
NASA-CR-186845 ..... N90-26563* #
NASA-CR-186847 ..... N90-26216* #
NASA-CR-186852 ..... N90-26217* #
NASA-CR-186855 ..... N90-26701* #
NASA-CR-186863 ..... N90-26526* #
NASA-CR-186864 ..... N90-26498* #
NASA-CR-186867 ..... N90-26497* #
NASA-CR-186871 ..... N90-26233* #
NASA-CR-186872 ..... N90-26515* #
NASA-CR-186874 ..... N90-26738* #
NASA-CR-186878 ..... N90-26013* #
NASA-CR-186882 ..... N90-26652* #
NASA-CR-186883 ..... N90-26235* #
NASA-CR-186887 ..... N90-26281* #
NASA-CR-186886 ..... N90-26382* #
NASA-CR-186900 ..... N90-26017* #
NASA-CR-186903 ..... N90-25954* #
NASA-CR-186905 ..... N90-26503* #

NASA-SP-7039(37)-SECT-2 ..... N90-26700*
NASA-SP-7046(22) N90-26056*
NASA-SP-7084 ..... N90-26710* #

NASA-TM-4197 ..... N90-26296* #
NASA-TM-4205 ..... N90-26730* #
NASA-TM-4211 ..... N90-26743* #
NASA-TM-89715 ..... N90-26693* #
NASA-TM-100405 ..... N90-26741* #
NASA-TM-101344 ..... N90-26172* #
NASA-TM-101644 ..... N90-26167* #
NASA-TM-101718 ..... N90-25973* #
NASA-TM-101719 ..... N90-26564* #
NASA-TM-101800 ..... N90-26083* #
NASA-TM-101886 ..... N90-25972* #
NASA-TM-101914 ..... N90-26132* #
NASA-TM-102254 ..... N90-26452* #
NASA-TM-102369 ..... N90-26359* #
NASA-TM-102402 ..... N90-25948* #
NASA-TM-102486 ..... N90-26054* #
NASA-TM-102488 ..... N90-26373* #
NASA-TM-102592 ..... N90-26076* #
NASA-TM-102629 ..... N90-25981* #
NASA-TM-102654 ..... N90-26361* #
NASA-TM-102685 ..... N90-26511* #
NASA-TM-102694 ..... N90-26082* #
NASA-TM-102695 ..... N90-26362* #
NASA-TM-102697 ..... N90-26363* #
NASA-TM-102700 ..... N90-26032* #
NASA-TM-102790 ..... N90-26040* #
NASA-TM-102822 ..... N90-26274* #
NASA-TM-102827 ..... N90-25933* #
NASA-TM-102834 ..... N90-25945* #
NASA-TM-103104 ..... N90-26275* #
NASA-TM-103105 ..... N90-25982* #
NASA-TM-103106 ..... N90-26334* #
NASA-TM-103124 ..... N90-26279* #
NASA-TM-103135 ..... N90-26070* #
NASA-TM-103137 ..... N90-26635* #
NASA-TM-103147 ..... N90-26250* #
NASA-TM-103155 ..... N90-26278* #
NASA-TM-103159 ..... N90-26262* #
NASA-TM-103173 ..... N90-26170* #
NASA-TM-103178 ..... N90-26338* #
NASA-TM-103187 ..... N90-26030* #
NASA-TM-103188 ..... N90-26729* #
NASA-TM-103189 ..... N90-26163* #
NASA-TM-103198 ..... N90-26011* #
NASA-TM-103202 ..... N90-26065* #
NASA-TM-103203 ..... N90-26074* #
NASA-TM-103205 ..... N90-26068* #
NASA-TM-103207 ..... N90-26789* #
NASA-TM-103208 ..... N90-26299* #
NASA-TM-103209 ..... N90-26276* #
NASA-TM-103210 ..... N90-26396* #
NASA-TM-103212 ..... N90-26009* #
NASA-TM-103213 ..... N90-26069* #
NASA-TM-103215 ..... N90-26273* #
NASA-TM-103217 ..... N90-26160* #
NASA-TM-103220 ..... N90-26055* #
NASA-TM-103223 ..... N90-26682* #
NASA-TM-103225 ..... N90-26364* #
NASA-TM-103229 ..... N90-26614* #
NASA-TM-103231 ..... N90-26615* #
NASA-TM-103237 ..... N90-26397* #
NASA-TM-103240 ..... N90-26616* #
NASA-TM-103241 ..... N90-26071* #
NASA-TM-103246 ..... N90-26683* #
NASA-TM-103249 ..... N90-25946* #
NASA-TM-103465 ..... N90-26432* #
NASA-TM-103466 ..... N90-26619* #
NASA-TM-103467 ..... N90-26129* #
NASA-TM-103468 ..... N90-26445* #
NASA-TM-103469 ..... N90-26447* #
NASA-TM-103470 ..... N90-26399* #
NASA-TM-103471 ..... N90-26485* #
NASA-TM-103472 ..... N90-26080* #
NASA-TM-103473 ..... N90-26130* #
NASA-TM-103475 ..... N90-26651* #
NASA-TM-103476 ..... N90-26400* #
NASA-TM-103477 ..... N90-26401* #
NASA-TM-103478 ..... N90-26402* #
NASA-TM-103479 ..... N90-26214* #
NASA-TM-103480 ..... N90-26094* #
NASA-TM-103481 ..... N90-26433* #
NASA-TM-103482 ..... N90-26640* #
NASA-TM-103484 ..... N90-26131* #
NASA-TM-103486 ..... N90-25957* #
NASA-TM-103487 ..... N90-26309* #
NASA-TM-103493 ..... N90-26785* #
NASA-TM-103496 ..... N90-26480* #

NASA-TP-3007 ..... N90-26077* #
NASA-TP-3019 ..... N90-26036* #
NASA-TP-3031 ..... N90-26028* #
NASA-TP-3036 ..... N90-25938* #

NCSC-CR-20C-1-90 ..... N90-26504 #

NEDO-P-8819 ..... N90-26336 #

NEDU-2-90 ..... N90-26487 #

NEMO-13 ..... N90-26388 #

NIAR-90-5 ..... N90-26694 #
NIAR-90-6 ..... N90-26494 #
NIAR-90-7 ..... N90-26495 #
NIAR-90-9 ..... N90-26346 #
NIAR-90-12 ..... N90-26166 #
NIAR-90-14 ..... N90-26356 #
NIAR-90-17 ..... N90-25937 #
NIAR-90-18 ..... N90-26496 #
NIAR-90-20 ..... N90-26327 #

NLR-MP-88033-U ..... N90-25950 #
NLR-MP-88037-U ..... N90-26290 #
NLR-MP-88052-U ..... N90-25951 #
NLR-MP-88062-U ..... N90-26175 #
NLR-MP-88066-U ..... N90-26238 #
NLR-MP-88068-U ..... N90-26350 #
NLR-MP-88072-U ..... N90-25952 #

NLR-TR-88008-U ..... N90-26285 #
NLR-TR-88036-U ..... N90-26370 #

NOSC/TD-1781 ..... N90-26576 #

NOSC/TR-1332-PT-1 ..... N90-26617 #

NPS-PAPER-44 ..... N90-26277 #

NPS55-90-08 ..... N90-26557 #
NPS55-90-09 ..... N90-26590 #
NPS55-90-10 ..... N90-26623 #
NPS55-90-11 ..... N90-26624 #

ODU-TR-PTR-90-2 ..... N90-26308* #

ONERA-NT-1989-3 ..... N90-26123 #

ORNL/FTR-3618 ..... N90-26699 #
ORNL/FTR-3630 ..... N90-26136 #

ORNL/M-1121 ..... N90-26529 #

ORNL/SUB-84-00214/1 ..... N90-26084 #

ORNL/TM-11159 ..... N90-26671 #

OTA-O-412 ..... N90-26398 #

PB90-130451 ..... N90-26398 #
PB90-146838 ..... N90-26443 #
PB90-146846 ..... N90-26444 #
PB90-146853 ..... N90-26445 #

PD-CF-9005 ..... N90-25938 #

PD-FC-9003 ..... N90-26010 #

PD-MT-9001 ..... N90-26092 #

PNL-7247 ..... N90-26707 #

PNR90605 ..... N90-26654 #
PNR90611 ..... N90-26544 #
PNR90617 ..... N90-26087 #
PNR90618 ..... N90-26695 #
PNR90619 ..... N90-26696 #
PNR90622 ..... N90-26301 #
PNR90625 ..... N90-26150 #
PNR90628 ..... N90-26348 #
PNR90629 ..... N90-26349 #
PNR90632 ..... N90-26120 #
PNR90636 ..... N90-25977 #
PNR90639 ..... N90-26174 #
PNR90640 ..... N90-25999 #
PNR90642 ..... N90-26637 #
PNR90646 ..... N90-26000 #
PNR90650 ..... N90-26001 #
PNR90663 ..... N90-26367 #
PNR90665 ..... N90-26709 #
PNR90667 ..... N90-26002 #
PNR90669 ..... N90-26302 #
PNR90670 ..... N90-26303 #
PNR90671 ..... N90-26003 #
PNR90675 ..... N90-26004 #
PNR90676 ..... N90-26005 #

PTR-90-4 ..... N90-26316 #

R/D-5679-EN-01 ..... N90-26385 #
R/D-6176-EN-02 ..... N90-26431 #

RADC-TR-89-382 ..... N90-26631 #
RADC-TR-90-27 ..... N90-26243 #
RADC-TR-90-47 ..... N90-26560 #
RADC-TR-90-49 ..... N90-26559 #

RAE-TM-AERO-2171 ..... N90-26288 #

RAE-TM-P-1171 ..... N90-26121 #
RAE-TM-P-1179 ..... N90-26007 #
RAE-TM-P-1182 ..... N90-26122 #

RAE-TM-SPACE-374 ..... N90-26662 #

RAE-TM-SS-9 ..... N90-25953 #

REPT-2 ..... N90-26643 #
REPT-32 ..... N90-26158 #
REPT-89-3 ..... N90-26269* #
REPT-90B00106 ..... N90-26744* #
REPT-7114-01-PHASE-1 ..... N90-26037 #
REPT-7114-02-PHASE-2 ..... N90-26038 #

RFP-ASE274L-S90 ..... N90-26045* #

RI/RD89-171-PT-3 ..... N90-26320* #

RIACS-TR-87.29 ..... N90-26522* #

RICE-COMP-TR90-107 ..... N90-26622 #

RR-784-I-IMAG-94-LIFIA ..... N90-26383 #
RR-788-I-IMAG-97-LIFIA ..... N90-26551 #
RR-789-I-IMAG-98-LIFIA ..... N90-26571 #

RSRE-MEMO-4341 ..... N90-26579 #
RSRE-MEMO-4342 ..... N90-26580 #

RSRE-89017 ..... N90-26548 #

R89AEB-325 ..... N90-26355* #
R90-1 ..... N90-26499* #
R9003-3 ..... N90-26248 #
R9003-4 ..... N90-26247 #

SAND-89-2787C ..... N90-26145 #
SAND-89-2795C ..... N90-26144 #
SAND-89-2857C ..... N90-26669 #
SAND-89-2860C ..... N90-26311 #
SAND-89-2928C ..... N90-26031 #
SAND-89-7043 ..... N90-26396 #
SAND-89-7044 ..... N90-26387 #
SAND-90-0008 ..... N90-25941 #
SAND-90-0117C ..... N90-26135 #
SAND-90-0217 ..... N90-26134 #
SAND-90-0247 ..... N90-26531 #
SAND-90-0826C ..... N90-26143 #
SAND-90-1139C ..... N90-26251 #
SAND-90-1203C ..... N90-26097 #
SAND-90-1314C ..... N90-26133 #
SAND-90-1534C ..... N90-26681 #

SAND-90-1560C ..... N90-26389 #
SAND-90-1620C ..... N90-26146 #
SAND-90-8203 ..... N90-26530 #
SAND-90-8217 ..... N90-26112 #

SERI/TR-213-3624 ..... N90-26392 #

SU-CMR-90-5 ..... N90-26663* #

SU-SLAC-PUB-5241 ..... N90-26532 #
SU-SLAC-PUB-5244 ..... N90-26514 #

SUSSEX-AST-90/7-1-2 ..... N90-26735* #

TEX-4312 ..... N90-26128* #

TR-EE-89-23 ..... N90-26375* #
TR-EE-89-49 ..... N90-26376* #

TR-2 ..... N90-26103 #
TR-3 ..... N90-26687 #
TR-3-ONR ..... N90-26102 #
TR-4 ..... N90-26688 #
TR-7 ..... N90-26157 #
TR-12 ..... N90-26448* #
TR-39-ONR ..... N90-26265 #
TR-40-ONR ..... N90-26630 #
TR-90-28 ..... N90-26582* #
TR-90-007 ..... N90-26374 #
TR-90-1136 ..... N90-26535* #
TR-90-1139 ..... N90-26703 #
TR-90-1141 ..... N90-26254* #
TR-95 ..... N90-26441 #
TR-97 ..... N90-26101 #
TR-051190-357OP ..... N90-26448* #

TSG0478 ..... N90-26001 #

TWR-17272-VOL-6 ..... N90-26325* #
TWR-17546-1 ..... N90-26067* #
TWR-17548-10 ..... N90-26064* #
TWR-17591-VOL-4 ..... N90-26324* #

UCRL-ID-103139 ..... N90-26313 #
UCRL-ID-103669 ..... N90-26626 #

UCRL-JC-103406 ..... N90-26786 #
UCRL-JC-103666 ..... N90-26110 #
UCRL-JC-104010 ..... N90-26538 #
UCRL-JC-104223 ..... N90-26787 #

UCRL-101767 ..... N90-26315 #
UCRL-101921 ..... N90-26300 #
UCRL-102154 ..... N90-26114 #
UCRL-102205 ..... N90-26314 #

UDR-TR-90-04 ..... N90-26125 #

UILU-ENG-89-1773 ..... N90-26689* #
UILU-ENG-90-2214 ..... N90-26558* #

UIUCDCS-R-89-1554 ..... N90-26689* #

UM-AERO-90-27 ..... N90-26027* #
UM-AERO-90-28 ..... N90-26026* #

UMIACS-TR-90-58 ..... N90-26625 #
UMIACS-TR-90-78 ..... N90-26526* #

UMR-FDB-16 ..... N90-26099 #

US-PATENT-APPL-SN-266955 ..... N90-26491
US-PATENT-APPL-SN-279677 ..... N90-26168*
US-PATENT-APPL-SN-370965 ..... N90-26305
US-PATENT-APPL-SN-470480 ..... N90-26073* #
US-PATENT-APPL-SN-470663 ..... N90-26341* #
US-PATENT-APPL-SN-473242 ..... N90-26292* #
US-PATENT-APPL-SN-486458 ..... N90-26340* #
US-PATENT-APPL-SN-495553 ..... N90-26209 #
US-PATENT-APPL-SN-502968 ..... N90-26249 #
US-PATENT-APPL-SN-503015 ..... N90-26297 #
US-PATENT-APPL-SN-506137 ..... N90-26685* #
US-PATENT-APPL-SN-508386 ..... N90-26098* #
US-PATENT-APPL-SN-527462 ..... N90-26304* #
US-PATENT-APPL-SN-527508 ..... N90-26342* #
US-PATENT-APPL-SN-543915 ..... N90-26518* #
US-PATENT-APPL-SN-545014 ..... N90-26384* #
US-PATENT-APPL-SN-545015 ..... N90-26339* #
US-PATENT-APPL-SN-545016 ..... N90-26684* #
US-PATENT-APPL-SN-545019 ..... N90-26519* #
US-PATENT-APPL-SN-545236 ..... N90-26176* #

US-PATENT-CLASS-219-75 ..... N90-26168*
US-PATENT-CLASS-219-136 ..... N90-26168*
US-PATENT-CLASS-372-32 ..... N90-26305

US-PATENT-4,907,238 ..... N90-26305
US-PATENT-4,909,459 ..... N90-26491
US-PATENT-4,924,053 ..... N90-26168*

USAFSAM-JA-89-62 ..... N90-26657 #

USAFSAM-TR-89-26 ..... N90-26505 #

USCG-M-3-90 ..... N90-26177 #

USCG-MFSRD-74 ..... N90-26177 #

UTIAS-332 ..... N90-26650
UTIAS-335 ..... N90-25935

UVA/525398/MS90/104 ..... N90-26089 #

VDM00109 ..... N90-26301 #

VKI-LS-1990-02-VOL-1 ..... N90-25985 #
VKI-LS-1990-02-VOL-2 ..... N90-25995 #

VPI-E-90-11 ..... N90-26083* #

VTT-RR-623 ..... N90-26253 #

WBS-HQ302-10-10 ..... N90-26324* #

WBS-4B102-10-03 ..... N90-26325* #

WRDC-TR-90-0001 ..... N90-26020 #
WRDC-TR-90-1079 ..... N90-26246 #
WRDC-TR-90-2005 ..... N90-25979 #
WRDC-TR-90-4013 ..... N90-26125 #

Appendix—About STAR

Scientific and Technical Aerospace Reports (STAR) is a major component of a comprehensive National Aeronautics and Space Administration information system covering aeronautics, space, and supporting disciplines. *STAR* is issued on the 8th and 23rd of each month and announces current publications of the following types:

- NASA, NASA contractor, and NASA grantee reports
- Reports issued by other U.S. Government agencies, domestic and foreign institutions, universities, and private firms
- Translations in report form
- NASA-owned patents and patent applications
- Other U.S. Government agency and foreign patents and patent applications
- Domestic and foreign dissertations and theses

Journal, book, and conference literature, cover-to-cover journal translations, and certain foreign dissertations are announced in a companion journal, *International Aerospace Abstracts (IAA),* available on subscription from the American Institute of Aeronautics and Astronautics, Technical Information Service, 555 West 57th Street, 12th Floor, New York, NY 10019.

SUBJECT SCOPE

The subject scope of *STAR* and *IAA* includes all aspects of aeronautics and space research and development, supporting basic and applied research, and applications. Aerospace aspects of earth resources, energy development, conservation, oceanography, environmental protection, urban transportation, and other topics of high national priority are also covered.

OTHER NASA PUBLICATIONS

Other NASA publications and information services are described in the publication, *The NASA Scientific and Technical Information System ... and How to Use It,* available without charge from the NASA Scientific and Technical Information Facility, P.O. Box 8757, BWI Airport, MD 21240.

HOW TO USE *STAR* SUBJECT CATEGORIES

STAR is categorized by 10 major subject divisions broken down further into 76 specific subject categories and one general division/category. The major subject divisions are listed on page ii in the Table of Contents, together with a note for each that defines its scope and provides any cross-references. For example:

AERONAUTICS

Includes aeronautics (general); aerodynamics; air transportation and safety; aircraft communications and navigation; aircraft design, testing and performance; aircraft instrumentation; aircraft propulsion and power; aircraft stability and control; and research and support facilities (air).

For related information see also *Astronautics.*

Each major division is further divided into as many as nine specific categories, which are identified by category numbers.

Abstracts in *STAR* are grouped by subject category, the categories appearing in sequential order. Category breaks in the abstract section are identified by the category number and title, and a scope note. Cross-references to other categories are provided as appropriate. For example:

02 AERODYNAMICS

Includes aerodynamics of bodies, combinations, wings, rotors, and control surfaces; and internal flow in ducts and turbomachinery.

For related information see also *34 Fluid Mechanics and Heat Transfer.*

CROSS-REFERENCES

Individual *STAR* abstracts are not ordinarily cross-referenced, except for certain conference reports or book translations that have had separate abstracts written for their component papers or chapters. Citations and abstracts of the components follow immediately after those of the parent document. When the subject content of a component differs sufficiently from the general content of the parent, a cross-reference citation also is printed at the end of the category to which it normally would have been assigned if it were independent.

DOCUMENTS ON MICROFICHE

Documents on microfiche[1] are designated by a pound sign (#) following the accession number. The pound sign is used without regard to the source or quality of the microfiche.

LIMITED REPRODUCIBILITY

A Note of Limited Reproducibility appears in the citation, if one or a combination of the following factors affect the reproducibility of more than 20% of the document. These factors include: faint or broken type, color photographs, black and white photographs, foldouts, dot matrix print, charts/graphs with script notation, non-Roman alphabet, or some other factor that limits the reproducibility of that document. This notation also appears on the microfiche header, with the specific causing factor checked off on a list visible in the second frame.

COLOR COPIES

An increasing number of NASA scientific and technical reports are being produced with color graphs, charts, illustrations, and photographs. A message indicating that a document has color pages follows the Sales and Pricing (SAP) information in the *STAR* citation.

Registered users of the NASA Scientific and Technical Information System will receive ordered documents with color at no *additional* cost, as long as stock copies of that document are available. Otherwise, an additional fee of $2.00 per color page, over and above the standard document price will be charged. The NASA STI Facility staff will work with registered users over the telephone to inform and meet each individual's ordering needs.

AVAILABILITIES

One or more sources from which a document announced in *STAR* is available to the public is given in each citation. The most commonly indicated sources and their acronyms or abbreviations are listed below. If the publication is available from a source other than those listed, the publisher and his address will be displayed on the availability line or in combination with the corporate source line.

Avail: NTIS. Sold by the National Technical Information Service. Prices for hard copy (HC) and microfiche (MF) are indicated by a price code following the letters HC or MF in the *STAR* citation. Current values for the price codes are given in the tables on page A-7.

(1) A microfiche is a transparent sheet of film, 105 by 148 mm in size, containing as many as 60 to 98 pages of information reduced to micro images (not to exceed 26:1 reduction).

Initially distributed microfiche under the NTIS SRIM (Selected Research in Microfiche) is available at greatly reduced unit prices. For this service and for information concerning subscription to NASA printed reports, consult the NTIS Subscription Section, Springfield, VA 22161.

NOTE ON ORDERING DOCUMENTS: When ordering NASA publications (those followed by the * symbol), use the N accession number. NASA patent applications (only the specifications are offered) should be ordered by the US-Patent-Appl-SN number. Non-NASA publications (no asterisk) should be ordered by the AD, PB, or other *report number* shown on the last line of the citation, not by the N accession number. It is also advisable to cite the title and other bibliographic identification.

Avail: SOD (or GPO). Sold by the Superintendent of Documents, U.S. Government Printing Office, in hard copy. The current price and order number are given following the availability line. (NTIS will fill microfiche requests, as indicated above, for those documents identified by a # symbol.)

Avail: BLL (formerly NLL): British Library Lending Division, Boston Spa, Wetherby, Yorkshire, England. Photocopies available from this organization at the price shown. (If none is given, address inquiry to the BLL.)

Avail: DOE Depository Libraries. Organizations in U.S. cities and abroad that maintain collections of Department of Energy reports, usually in microfiche form, are listed in *Energy Research Abstracts.* Services available from the DOE and its depositories are described in a booklet, *DOE Technical Information Center - Its Functions and Services* (TID-4660), which may be obtained without charge from the DOE Technical Information Center.

Avail: ESDU. Pricing information on specific data, computer programs, and details on Engineering Sciences Data Unit (ESDU) topic categories can be obtained from ESDU International Ltd. Requesters in North America should use the Virginia address while all other requesters should use the London address, both of which are on page A-6.

Avail: Fachinformationszentrum, Karlsruhe. Sold by the Fachinformationszentrum Energie, Physik, Mathematik GMBH, Eggenstein Leopoldshafen, Federal Republic of Germany, at the price shown in deutschmarks (DM).

Avail: HMSO. Publications of Her Majesty's Stationery Office are sold in the U.S. by Pendragon House, Inc. (PHI), Redwood City, CA. The U.S. price (including a service and mailing charge) is given, or a conversion table may be obtained from PHI.

Avail: NASA Public Document Rooms. Documents so indicated may be examined at or purchased from the National Aeronautics and Space Administration, Public Documents Room (Room 126), 600 Independence Ave., S.W., Washington, DC 20546, or public document rooms located at NASA installations, and the NASA Pasadena Office at the Jet Propulsion Laboratory.

Avail: Univ. Microfilms. Documents so indicated are dissertations selected from *Dissertation Abstracts* and are sold by University Microfilms as xerographic copy (HC) and microfilm. All requests should cite the author and the Order Number as they appear in the citation.

Avail: US Patent and Trademark Office. Sold by Commissioner of Patents and Trademarks, U.S. Patent and Trademark Office, at the standard price of

$1.50 each, postage free. (See discussion of NASA patents and patent applications below.)

Avail: (US Sales Only). These foreign documents are available to users within the United States from the National Technical Information Service (NTIS). They are available to users outside the United States through the International Nuclear Information Service (INIS) representative in their country, or by applying directly to the issuing organization.

Avail: USGS. Originals of many reports from the U.S. Geological Survey, which may contain color illustrations, or otherwise may not have the quality of illustrations preserved in the microfiche or facsimile reproduction, may be examined by the public at the libraries of the USGS field offices whose addresses are listed in this Introduction. The libraries may be queried concerning the availability of specific documents and the possible utilization of local copying services, such as color reproduction.

Avail: Issuing Activity, or Corporate Author, or no indication of availability. Inquiries as to the availability of these documents should be addressed to the organization shown in the citation as the corporate author of the document.

NASA PATENTS AND PATENT APPLICATIONS

Patents and patent applications owned by NASA are announced in *STAR* under appropriate subject categories and are referenced in the *STAR* indexes. In the Report/Accession Number Index, patents are indexed by the NASA Case Number (which appears in lieu of the report number in other indexes), the U.S. Patent Number, the U.S. Patent Application Serial Number, and the U.S. Patent Class. Patent applications for which patents have not yet been issued are indexed by the NASA Case Number and the U.S. Patent Application Serial Number.

NASA *patent application specifications* are sold in paper copy and microfiche by the National Technical Information Service (NTIS). The US-Patent-Appl-SN- number should be used in ordering either paper copy or microfiche from NTIS. Printed copies of *patents* (which are not microfiched) are available for purchase from:

Commissioner of Patents and Trademarks
U.S. Patent and Trademark Office
Washington, DC 20231

When ordering patents, the U.S. Patent Number should be used, and payment must be remitted in advance, by money order or check payable to the Commissioner of Patents and Trademarks. Prepaid purchase coupons for ordering are also available from the Patent and Trademark Office. The patents and patent applications announced in *STAR* are owned by NASA and are available for royalty-free licensing. Requests for licensing terms and further information should be addressed to:

Associate General Counsel for Intellectual Property/Code GP
National Aeronautics and Space Administration
Washington, DC 20546

ELIGIBILITY AND REGISTRATION FOR NASA INFORMATION PRODUCTS AND SERVICES

A variety of services is available to organizations of the following types that have registered with NASA to receive specific services or products:

1. NASA offices and installations, contractors, subcontractors, grantees, and consultants;
2. Other U.S. Government agencies and their contractors;
3. Libraries in the United States that have arrangements with NASA to maintain collections of NASA documents for public reference;
4. Other organizations in the United States having a need for NASA documents in work related to aeronautics and space research;
5. Organizations abroad that have established reciprocal document exchange arrangements with NASA.

Only the central service points or central points of document acquisition and control within qualified organizations are eligible to register for NASA products and services. Domestic organizations that may be eligible to receive various classes of NASA publications and services should address their requests for registration or for further information to:

NASA Scientific and Technical Information Facility
ATTN: Registration Services
P.O. Box 8757
BWI Airport, MD 21240
301-621-0153

Organizations abroad should direct requests to Manager, International STI Activities, NTT, NASA Headquarters, Washington, DC 20546.

AVAILABILITY OF *STAR* ABSTRACTS ON MICROFICHE

Microfiche of the abstract sections of this issue and other issues of *STAR* are available on annual subscription from NTIS as PB90-911300, Attn: Subscriptions, 5285 Port Royal Road, Springfield, VA 22161. Annual subscription rates are $75.50 North America; $151.00 foreign. Abstract sections for previous years retroactive to 1964 are available at the current rates. Microfiche for individual *STAR* issue abstract sections are not available.

PUBLIC COLLECTIONS OF NASA DOCUMENTS

DOMESTIC: NASA and NASA-sponsored documents and a large number of aerospace publications are available to the public for reference purposes at the library maintained by the American Institute of Aeronautics and Astronautics, Technical Information Service, 555 West 57th Street, 12th Floor, New York, NY 10019.

EUROPEAN: An extensive collection of NASA and NASA-sponsored publications is maintained by the British Library Lending Division, Boston Spa, Wetherby, Yorkshire, England, for public access. The British Library Lending Division also has available many of the non-NASA publications cited in *STAR*. European requesters may purchase facsimile copy or microfiche of NASA and NASA-sponsored documents, those identified by both the symbols # and * from ESA - Information Retrieval Service, European Space Agency, 8-10 rue Mario-Nikis, 75738 Paris CEDEX 15, France.

FEDERAL DEPOSITORY LIBRARY PROGRAM

In order to provide the general public with greater access to U.S. Government publications, Congress established the Federal Depository Library Program under the Government Printing Office (GPO), with 51 regional depositories responsible for permanent retention of material, inter-library loan, and reference services. At least one copy of nearly every NASA and NASA-sponsored publication, either in printed or microfiche format, is received and retained by the 51 regional depositories. A list of the regional GPO libraries, arranged alphabetically by state, appears on the inside back cover. These libraries are *not* sales outlets. A local library can contact a Regional Depository to help locate specific reports, or direct contact may be made by an individual.

ADDRESSES OF ORGANIZATIONS

American Institute of Aeronautics and Astronautics
Technical Information Service
555 West 57th Street, 12th Floor
New York, New York 10019

British Library Lending Division,
Boston Spa, Wetherby, Yorkshire,
England

Commissioner of Patents and Trademarks
U.S. Patent and Trademark Office
Washington, DC 20231

Department of Energy
Technical Information Center
P.O. Box 62
Oak Ridge, Tennessee 37830

European Space Agency-Information Retrieval Service
ESRIN
Via Galileo Galilei
00044 Frascati (Rome) Italy

Engineering Sciences Data Unit International
P.O. Box 1633
Manassas, Virginia 22110

Engineering Sciences Data Unit International, Ltd.
251-259 Regent Street
London, W1R 7AD, England

Fachinformationszentrum Energie, Physik, Mathematik
GMBH
7514 Eggenstein Leopoldshafen
Federal Republic of Germany

Her Majesty's Stationery Office
P.O. Box 569, S.E. 1
London, England

NASA Scientific and Technical Information Facility
P.O. Box 8757
BWI Airport, Maryland 21240

National Aeronautics and Space Administration
Scientific and Technical Information Division (NTT)
Washington, DC 20546

National Technical Information Service
5285 Port Royal Road
Springfield, Virginia 22161

Pendragon House, Inc.
899 Broadway Avenue
Redwood City, California 94063

Superintendent of Documents
U.S. Government Printing Office
Washington, DC 20402

University Microfilms
A Xerox Company
300 North Zeeb Road
Ann Arbor, Michigan 48106

University Microfilms, Ltd.
Tylers Green
London, England

U.S. Geological Survey Library National Center
MS 950
12201 Sunrise Valley Drive
Reston, Virginia 22092

U.S. Geological Survey Library
2255 North Gemini Drive
Flagstaff, Arizona 86001

U.S. Geological Survey
345 Middlefield Road
Menlo Park, California 94025

U.S. Geological Survey Library
Box 25046
Denver Federal Center, MS914
Denver, Colorado 80225

NTIS PRICE SCHEDULES

(Effective January 1, 1990)

Schedule A
STANDARD PRICE DOCUMENTS AND MICROFICHE

PRICE CODE	NORTH AMERICAN PRICE	FOREIGN PRICE
A01	$ 8.00	$ 16.00
A02	11.00	22.00
A03	15.00	30.00
A04-A05	17.00	34.00
A06-A09	23.00	46.00
A10-A13	31.00	62.00
A14-A17	39.00	78.00
A18-A21	45.00	90.00
A22-A25	53.00	106.00
A99	*	*
N01	60.00	120.00
N02	59.00	118.00
N03	20.00	40.00

Schedule E
EXCEPTION PRICE DOCUMENTS AND MICROFICHE

PRICE CODE	NORTH AMERICAN PRICE	FOREIGN PRICE
E01	$10.00	$ 20.00
E02	12.00	24.00
E03	14.00	28.00
E04	16.50	33.00
E05	18.50	37.00
E06	21.50	43.00
E07	24.00	48.00
E08	27.00	54.00
E09	29.50	59.00
E10	32.50	65.00
E11	35.00	70.00
E12	38.50	77.00
E13	41.00	82.00
E14	45.00	90.00
E15	48.50	97.00
E16	53.00	106.00
E17	57.50	115.00
E18	62.00	124.00
E19	69.00	138.00
E20	80.00	160.00
E99	*	

* Contact NTIS for price quote.

IMPORTANT NOTICE

NTIS Shipping and Handling Charges

U.S., Canada, Mexico — ADD $3.00 per TOTAL ORDER

All Other Countries — ADD $4.00 per TOTAL ORDER

Exceptions — Does NOT apply to:

ORDERS REQUESTING NTIS RUSH HANDLING

ORDERS FOR SUBSCRIPTION OR STANDING ORDER PRODUCTS *ONLY*

NOTE: Each additional delivery address on an order requires a separate shipping and handling charge.

FEDERAL REGIONAL DEPOSITORY LIBRARIES

ALABAMA

AUBURN UNIV. AT MONTGOMERY LIBRARY
Documents Department
Montgomery, AL 36193
(205) 279-9110 ext.253

UNIV. OF ALABAMA LIBRARY
Reference Department/Documents
Box S
Tuscaloosa, AL 35486
(205) 348-6046

ARIZONA

DEPT. OF LIBRARY, ARCHIVES, AND PUBLIC RECORDS
Third Floor State Capitol
1700 West Washington
Phoenix, AZ 85007
(602) 255-4121

ARKANSAS

ARKANSAS STATE LIBRARY
Documents Service Section
One Capitol Mall
Little Rock, AR 72201
(501) 371-2090

CALIFORNIA

CALIFORNIA STATE LIBRARY
Govt. Publications Section
914 Capitol Mall
Sacramento, CA 95814
(916) 322-4572

COLORADO

UNIV. OF COLORADO
Norlin Library
Government Publications Division
Campus Box 184
Boulder, CO 80309
(303) 492-8834

DENVER PUBLIC LIBRARY
Govt. Pub. Department
1357 Broadway
Denver, CO 80203
(303) 571-2346

CONNECTICUT

CONNECTICUT STATE LIBRARY
231 Capitol Avenue
Hartford, CT 06106
(203) 566-4971

FLORIDA

UNIV. OF FLORIDA LIBRARIES
Documents Department
Library West
Gainesville, FL 32611
(904) 392-0367

GEORGIA

UNIV. OF GEORGIA LIBRARIES
Government Documents Dept.
Athens, GA 30602
(404) 542-8949

HAWAII

UNIV. OF HAWAII
Hamilton Library
Government Documents Collection
2550 The Mall
Honolulu, HI 96822
(808) 948-8230

IDAHO

UNIV. OF IDAHO LIBRARY
Documents Section
Moscow, ID 83843
(208) 885-6344

ILLINOIS

ILLINOIS STATE LIBRARY
Federal Documents
Centennial Building
Springfield, IL 62756
(217) 782-5012

INDIANA

INDIANA STATE LIBRARY
Serials Section
140 North Senate Avenue
Indianapolis, IN 46204
(317) 232-3686

IOWA

UNIV. OF IOWA LIBRARIES
Government Publications Dept.
Iowa City, IA 52242
(319) 335-5926

KANSAS

UNIVERSITY OF KANSAS
Spencer Research Library
Government Documents
Lawrence, KS 66045
(913) 864-4662

KENTUCKY

UNIV. OF KENTUCKY LIBRARIES
Government Publications/Maps Dept.
Lexington, KY 40506
(606) 257-8400

LOUISIANA

LOUISIANA STATE UNIVERSITY
Middleton Library
Government Documents Dept.
Baton Rouge, LA 70803
(504) 388-2570

LOUISIANA TECHNICAL UNIV.
Prescott Memorial Library
Government Documents Dept.
Ruston, LA 71272
(318) 257-4962

MAINE

UNIVERSITY OF MAINE
Raymond H. Fogler Library
Govt. Documents & Microforms Dept.
Orono, ME 04469
(207) 581-1680

MARYLAND

UNIVERSITY OF MARYLAND
McKeldin Library
Documents/Maps Room
College Park, MD 20742
(301) 454-3034

MASSACHUSETTS

BOSTON PUBLIC LIBRARY
Government Documents Dept.
666 Boylston Street
Boston, MA 02117
(617) 536-5400 ext.226

MICHIGAN

DETROIT PUBLIC LIBRARY
5201 Woodward Avenue
Detroit, MI 48202
(313) 833-1409

LIBRARY OF MICHIGAN
Government Documents
P.O. Box 30007
735 E. Michigan Avenue
Lansing, MI 48909
(517) 373-1593

MINNESOTA

UNIVERSITY OF MINNESOTA
Wilson Library
Government Publications
309 Nineteenth Avenue South
Minneapolis, MN 55455
(612) 373-7813

MISSISSIPPI

UNIV. OF MISSISSIPPI LIB.
Government Documents Dept.
106 Old Gym Bldg.
University, MS 38677
(601) 232-5857

MISSOURI

University of Missouri at Columbia Library
Government Documents
Columbia, MO 65201
(314) 882-6733

MONTANA

UNIV. OF MONTANA
Mansfield Library
Documents Division
Missoula, MT 59812
(406) 243-6700

NEBRASKA

UNIVERSITY OF NEBRASKA - LINCOLN
Love Memorial Library
Documents Department
Lincoln, NE 68588
(402) 472-2562

NEVADA

UNIV. OF NEVADA-RENO LIB.
Govt. Pub. Department
Reno, NV 89557
(702) 784-6579

NEW JERSEY

NEWARK PUBLIC LIBRARY
U.S. Documents Division
5 Washington Street
P.O. Box 630
Newark, NJ 07101
(201) 733-7812

NEW MEXICO

UNIVERSITY OF NEW MEXICO
General Library
Government Publications/Maps Dept.
Albuquerque, NM 87131
(505) 277-5441

NEW MEXICO STATE LIBRARY
325 Don Gaspar Avenue
Santa Fe, NM 87501
(505) 827-3826

NEW YORK

NEW YORK STATE LIBRARY
Documents Sect. Cultural Educ. Ctr.
Empire State Plaza
Albany, NY 12230
(518) 474-5563

NORTH CAROLINA

UNIVERSITY OF NORTH CAROLINA AT CHAPEL HILL
Davis Library 080A
BA/SS Department Documents
Chapel Hill, NC 27514
(919) 962-1151

NORTH DAKOTA

NORTH DAKOTA STATE UNIVERSITY LIBRARY
Government Documents Dept.
Fargo, ND 58105
(701) 237-8352
In cooperation with Univ. of North Dakota, Chester Fritz Library
Grand Forks

OHIO

STATE LIBRARY OF OHIO
Documents Section
65 South Front Street
Columbus, OH 43266
(614) 644-7051

OKLAHOMA

OKLAHOMA DEPT. OF LIBRARIES
Government Documents
200 NE 18th Street
Oklahoma City, OK 73105
(405) 521-2502, ext. 252

OKLAHOMA STATE UNIV. LIB.
Documents Department
Stillwater, OK 74078
(405) 624-0489

OREGON

PORTLAND STATE UNIV.
Millar Library
934 SW Harrison - P.O. Box 1151
Portland, OR 97207
(503) 229-3673

PENNSYLVANIA

STATE LIBRARY OF PENN.
Government Publications Section
Box 1601
Walnut St. & Commonwealth Ave.
Harrisburg, PA 17105
(717) 787-3752

SOUTH CAROLINA

CLEMSON UNIV. COOPER LIB.
Documents Department
Clemson, SC 29634
(803) 656-5174
In cooperation with Univ. of South Carolina, Thomas Cooper Library, Columbia

TEXAS

TEXAS STATE LIBRARY
Public Services Department
P.O. Box 12927 - 1201 Brazos
Austin, TX 78711
(512) 463-5455

TEXAS TECH. UNIV. LIBRARY
Documents Department
Lubbock, TX 79409
(806) 742-2268

UTAH

UTAH STATE UNIVERSITY
Merrill Library & Learning Resources Center, UMC-30
Documents Department
Logan, UT 84322
(801) 750-2682

VIRGINIA

UNIVERSITY OF VIRGINIA
Alderman Library
Government Documents
Charlottesville, VA 22903
(804) 924-3133

WASHINGTON

WASHINGTON STATE LIBRARY
Document Section
Olympia, WA 98504
(206) 753-4027

WEST VIRGINIA

WEST VIRGINIA UNIV. LIB.
Government Documents Section
P.O. Box 6069
Morgantown, WV 26506
(304) 293-3640

WISCONSIN

ST. HIST SOC. OF WISCONSIN LIB.
Government Pub. Section
816 State Street
Madison, WI 53706
(608) 262-2781
In cooperation with Univ. of Wisconsin-Madison, Memorial Library

MILWAUKEE PUBLIC LIBRARY
Documents Division
814 West Wisconsin Avenue
Milwaukee, WI 53233
(414) 278-3065

WYOMING

WYOMING STATE LIBRARY
Supreme Court & Library Bldg.
Cheyenne, WY 82002
(307) 777-5919

National Aeronautics and
Space Administration
Code NTT
Washington, D.C.
20546

Official Business

Penalty for Private Use, $300

SPECIAL FOURTH-CLASS RATE
POSTAGE & FEES PAID
NASA
PERMIT No. G27

NASA

POSTMASTER: If Undeliverable (Section 158 Postal Manual) Do Not Return